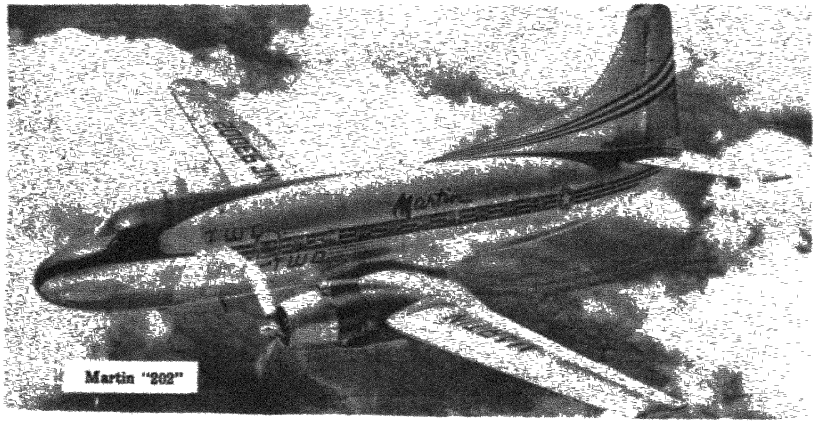
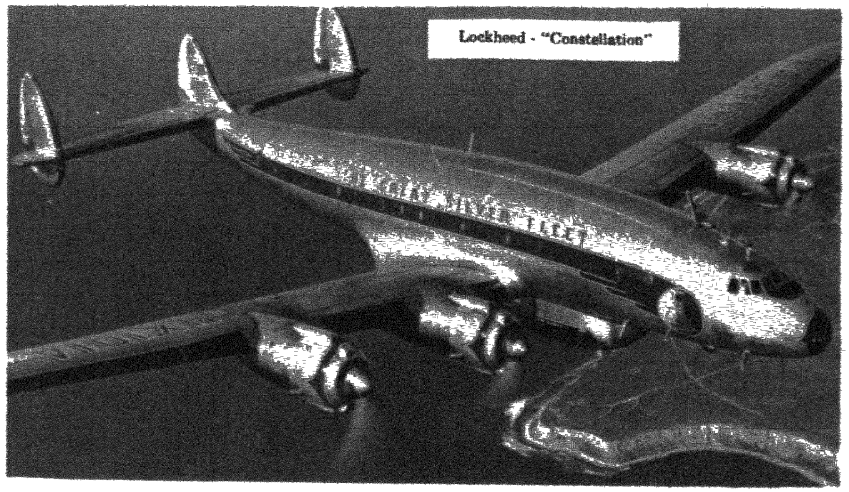
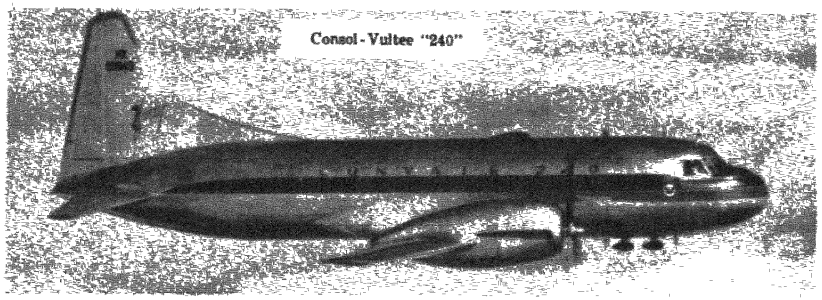
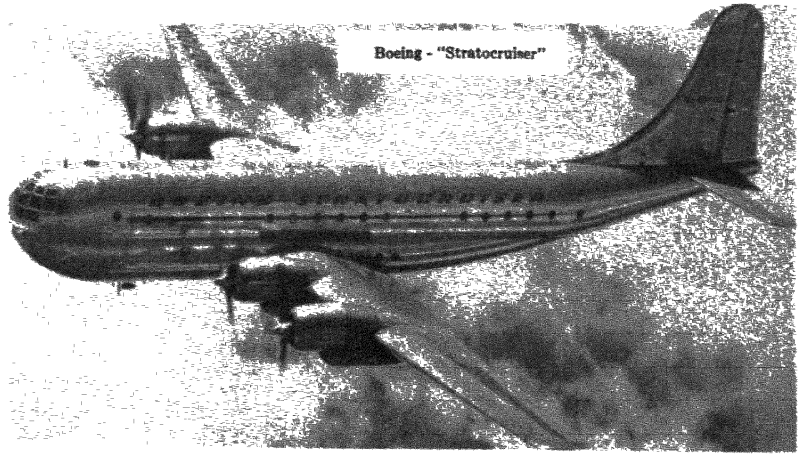
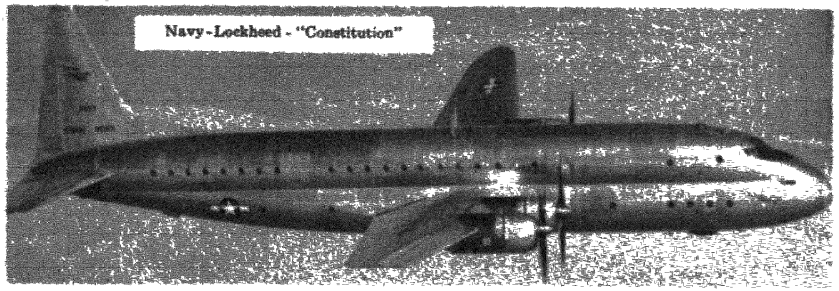
ANALYSIS AND DESIGN OF AIRPLANE STRUCTURES













MODERN AIR TRANSPORTS

Such large Airplanes present many new problems to the structural designer and stress analyst

ANALYSIS AND DESIGN OF AIRPLANE STRUCTURES

By

E. F. BRUHN, B.S., M.S., C.E.

Associate Fellow, I. Ae.S.

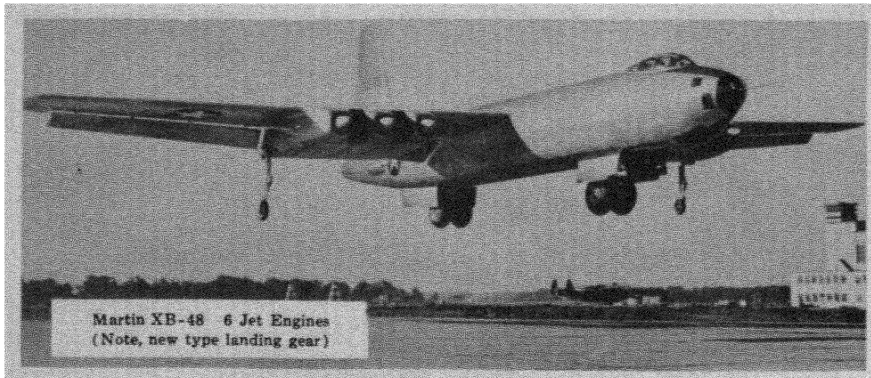
Professor of Aeronautical Engineering

Purdue University

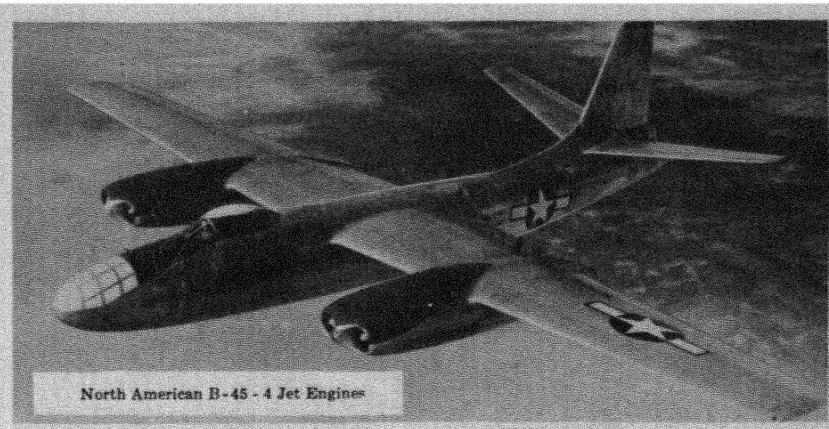
Copyright 1943, 1945, 1947, 1949
by
E. F. Bruhn

1949 REVISED EDITION
JANUARY, 1952

REPRODUCED BY PHOTO-OFFSET
DISTRIBUTED BY TRI-STATE OFFSET COMPANY
CINCINNATI 2, OHIO - - - - PRINTED IN U. S. A.



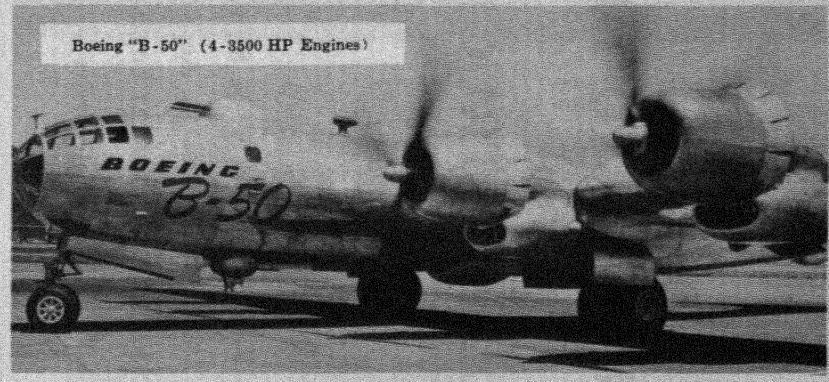
Martin XB-48 6 Jet Engines
(Note, new type landing gear)



North American B-45 - 4 Jet Engines



Consolidated-Vultee XB-46 - 4 Jet Engines



Boeing "B-50" (4-3500 HP Engines)



Martin XP4M
(2 Jet Engines and 2-Radial Aircooled Engines)



Consolidated-Vultee "B-36"
Six-28 Cylinder Radial Aircooled Engines

SOME LATE MILITARY AIRPLANES OF THE BOMBER TYPE

PREFACE

The initial issue of this book came out in April 1943 and the sixth printing was issued in October 1947. The wide acceptance of this volume both as a university or college textbook and as a reference for analysis and design by engineers in the aeronautical industry, has been very gratifying to the author. This seventh issue incorporates two major changes, namely, the book has been completely prepared using near-normal textbook type size in place of the admittedly too small type in the previous printings, and secondly, answers have been given to most of the problems which are presented, at the end of each chapter.

Considerable new material has been added to a number of chapters. Continued use is made of design information from the latest issue of the government publication ANC-5, including the Amendment - 2 of August 1946.

In the preface of the initial issue of this book in 1943 it was stated that, "No textbook on airplane structural analysis could be written without data and information from the various government publications, particularly, the publications of the National Advisory Committee for Aeronautics (N.A.C.A.)." In this seventh semi-revised edition, new information based on the investigations and researches of the N.A.C.A. has been added, as for example in the chapter dealing with diagonal tension field beams.

Dozens of new problems for student homework have been added to this new edition. A considerable number of these new problems were taken by permission from a publication, PROBLEMS IN AIRPLANE STRUCTURES, by I. R. Jensen and published by the W. C. Brown Company of Dubuque, Iowa. This publication, containing around three hundred problems, is recommended to instructors as a problem source.

For the benefit of new or beginning instructors using this textbook, the author has found the following sequence of chapters as satisfactory in teaching undergraduate courses in airplane structures:

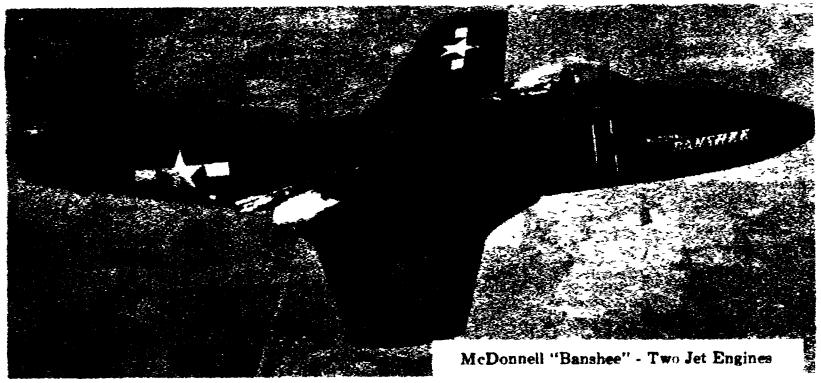
Beginning Course - 3 or 4 - one-hour periods per week for one 17 week semester.
Chapters: A1 through A8, A12, A10, C1 through C5, A11, A13.

Second Course - 3 or 4 - one-hour periods per week for one 17 week semester.
Chapters: A14, A15, B1 through B5, C6, C7, D1, D2, C9, C10, C11, A9, C8.

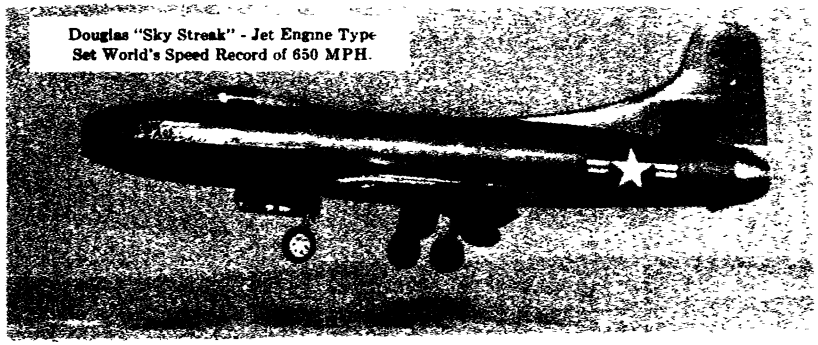
The writer wishes to acknowledge the many constructive suggestions and comments of his colleague, Professor Thomas J. Herrick of the School of Aeronautics of Purdue University.

E. F. Bruhn

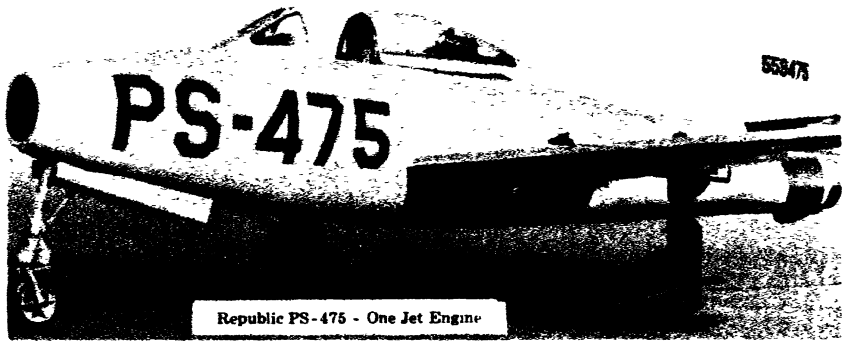
January 1, 1949



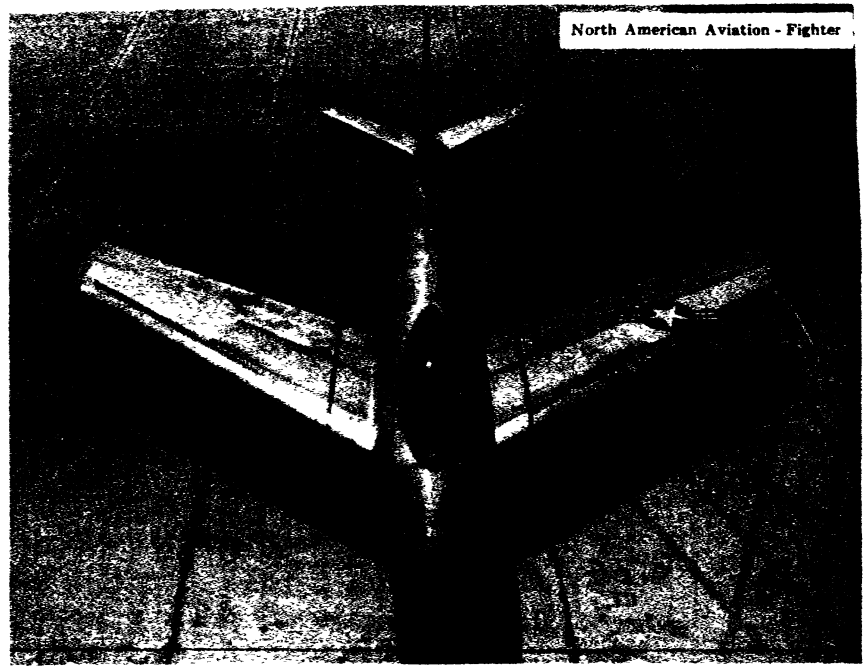
McDonnell "Banshee" - Two Jet Engines



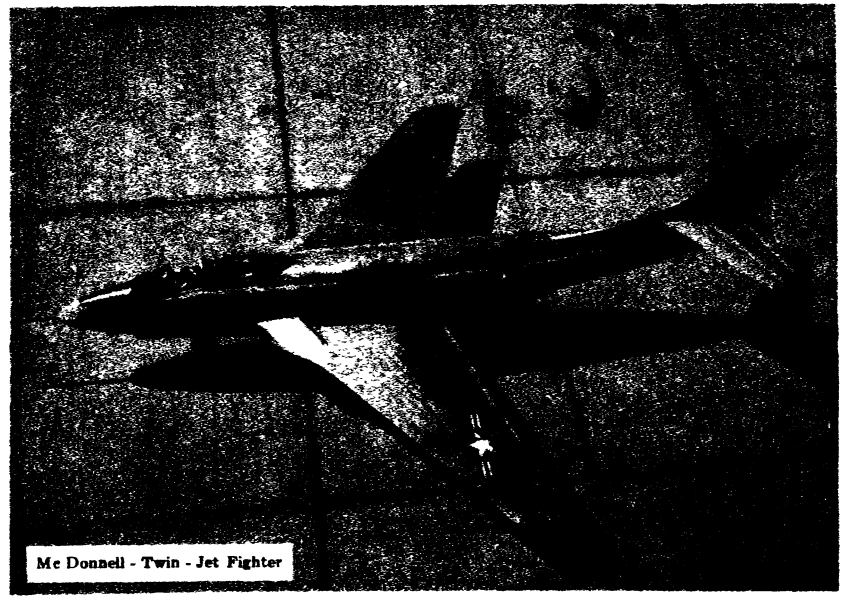
Douglas "Sky Streak" - Jet Engine Type
Set World's Speed Record of 650 MPH.



Republic PS-475 - One Jet Engine



North American Aviation - Fighter



Mc Donnell - Twin - Jet Fighter

SOME LATE AIRPLANES OF THE FIGHTER,
PURSUIT OR HIGH SPEED TYPE

CONTENTS

PART A

GENERAL THEORY OF STRESS AND STRAIN CALCULATION

Chapter Number	CHAPTER TITLE
A1	Review of the Principles of Equilibrium
A2	Truss Stress Analysis
A3	Properties of Sections - Centroids - Moments of Inertia Etc.
A4	Stress- Strain Relationships - Combined Stresses
A5	Torsional Stresses and Deflections
A6	Shear and Bending Forces
A7	Deflections of Beams and Trusses
A8	Statically Indeterminate Trusses
A9	Analysis of Rings and Frames
A10	Beam - Column Members
A11	Moment Distribution Method - Successive Corrections
A12	Bending and Shear Distribution
A13	Unsymmetrical Bending
A14	Shear Flow - Bending of Open Sections
A15	Shear Flow - Closed Sections

PART B

COLUMN THEORY. SUMMARY OF INFORMATION ON THE BUCKLING AND ULTIMATE STRENGTH OF THIN SHEET UNITS.

B1	Column Theory - Columns With Stable Cross Sections
B2	Buckling Stresses For Flat Sheet
B3	Buckling Strength of Thin Walled Cylinders and Curved Panels
B4	Ultimate Compressive Strength of Stiffened Flat and Curved Sheet
B5	Columns With Thin Walls: Crippling Stresses: Open and Closed Sections
B6	Compressive Strength of Sheet-Stiffener Units

PART C

PRACTICAL APPLICATIONS TO AIRPLANE STRUCTURAL ANALYSIS AND DESIGN

C1	Properties of Aircraft Materials
C2	Practical Design of Steel and Aluminum Alloy Tubes As Column and Tension Members
C3	Design of Round Tubes For Bending, Torsion and For Combined Loadings
C4	Airplane Fitting Analysis - Riveted and Bolted
C5	Airplane Welded Joints and Fittings
C6	Design of Metal Beams: Web Shear Resistant
C7	Design of Metal Beams: Semi-Tension Field Web
C8	Design of Wood Beams and Columns
C9	Analysis and Design of the Various Types of Wing Stressed-Skin Structures
C10	Analysis and Design of Metal Covered Fuselage and Hull Structures
C11	Bulkhead and Frame Analysis

PART D

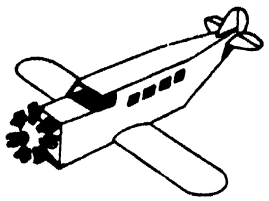
THE LOADS ON THE AIRPLANE

D1	The Loads on the Wing
D2	The Loads on the Body

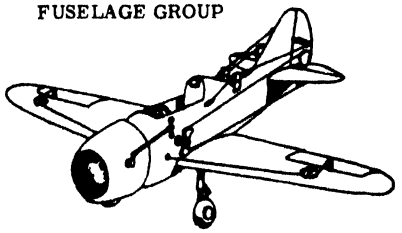
PART E

Answers to Problems
Index

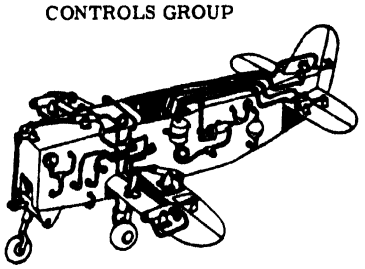
DREAM AIRPLANES



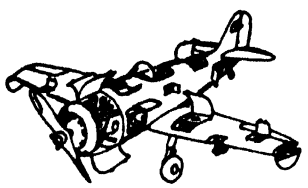
FUSELAGE GROUP



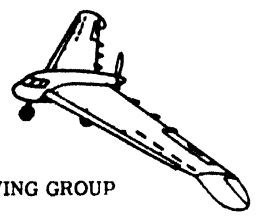
CONTROLS GROUP



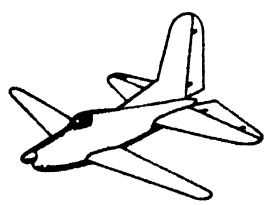
HYDRAULICS GROUP



SERVICE GROUP



WING GROUP

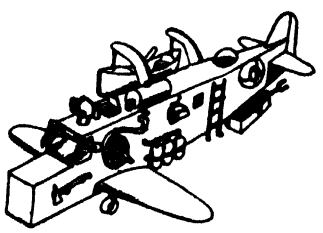


EMPENNAGE GROUP

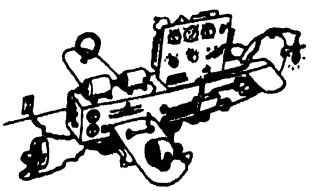
A completed airplane in many ways is a compromise of the knowledge, experience and desires of the many engineers that make up the various design and production groups of an airplane company.

It is only being human to understand why the engineers of the various groups feel that their part in the design of an airplane is of greater importance and that the headaches in design are due to the requirements of the other less important groups.

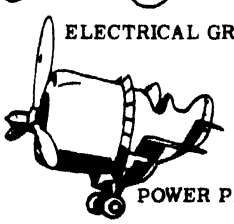
This cartoon "Dream Airplanes" by Mr. C. W. Miller, design engineer, indicates what might happen if each design or production group were allowed to take itself too seriously.



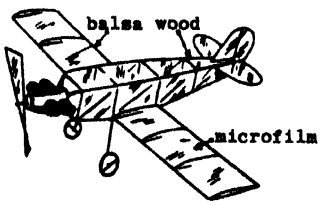
EQUIPMENT GROUP



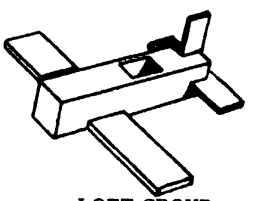
ELECTRICAL GROUP



POWER PLANT GROUP



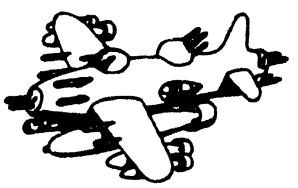
WEIGHT GROUP



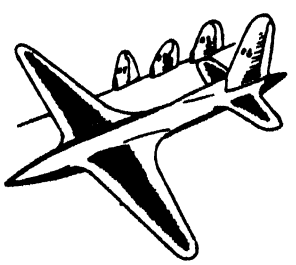
LOFT GROUP



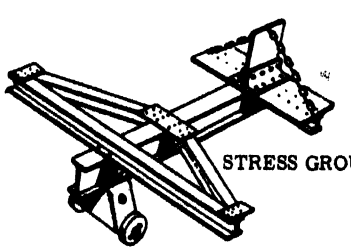
PRODUCTION ENGINEERING GROUP



ARMAMENT GROUP



AERODYNAMICS GROUP



STRESS GROUP

CHAPTER A1
REVIEW OF THE PRINCIPLES OF EQUILIBRIUM

A1.1 Introduction

It is realized that a student starting his first course in Airplane Structures has completed the regular college courses in Dynamics and Strength of Materials and therefore should have a good fundamental understanding of these basic engineering subjects. These fundamentals of engineering mechanics form the foundation or background for the study of airplane structures, thus a review of Statics and the Mechanics of Materials usually proves advisable before going on to new or more advanced work in the theory of structures as applied to airplane structures. The first several chapters therefore deal in general with a brief review of mechanics. The importance of these chapters cannot be overemphasized.

A1.2 Characteristics or Elements of a force

To completely define a force, that is, to determine its effect upon a body, the following three elements must be known:-

1. The magnitude of the force.
2. The direction of the force.
3. Point of application of the force or its location.

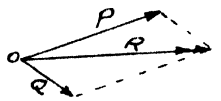
The sense in which a force acts along a given direction is indicated in the algebraic solution by the signs + and - in connection with the magnitude and in the graphical solution the sense of a force is indicated by an arrow head. Thus the sense of a force is not an element as it requires no separate equation for its determination.

A1.3 Definition of a Few Common Terms

A force system is any number of forces treated as a group. A force system is said to be concurrent if the action lines of all forces intersect in a common point and non-concurrent if the action lines do not intersect at a point. The resultant of a force system is the simplest equivalent system to which the given system will reduce. The process of reducing a force system to a simpler equivalent system is called composition. The process of expanding a force or a force system into a less simple equivalent system is called resolution. A component of a force is one of the two or more forces into which a given force may be resolved.

A1.4 Parallelogram Law

The law states if two coplaner concurrent forces are represented in magnitude and direction by the adjacent sides of a parallelogram, so constructed that the sense of each force is the same with respect to the point of concurrency; then the resultant of these two forces is represented in magnitude and direction by the diagonal of the parallelogram through the point of intersection of the two forces. The sense of the resultant is away from the point of intersection if the sense of the two forces is away from the point and vice versa. Thus in the figure the two concurrent forces OP and OQ intersect at O. Complete the parallelogram as shown by the dashed lines. Then the diagonal from point O or R represents the magnitude and direction of the resultant of the forces OP and OQ.



A1.5 The Law of the Triangle of Forces

The triangle law states that three concurrent coplanar forces in equilibrium may be represented in magnitude, direction and sense by the three sides of a triangle taken in continuous order. Any one of the three forces if the sense is reversed represents the resultant of the other two. Thus in (Fig. a) R is the resultant of the forces P and Q in magnitude and direction.

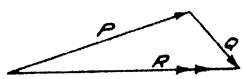


Fig. a

A1.6 Force (Magnitude - Direction Diagram)

When the resultant of several concurrent forces is required, the resultant of any two may be found by the force triangle. This resultant may be combined with a third force to obtain the resultant of the 3 forces and so on until all forces have been combined. (Fig. b) shows a concurrent coplanar force system of 5 forces. Fig. c shows the magnitude - direction polygon starting at some point o and considering the forces F_1 to F_5 in order. In the figure, oa represents the resultant of F_1 and F_2; of the resultant of F_1, F_2 and F_3, etc. and finally R represents resultant of the five forces in magnitude, direction and sense. It should be realized that the magnitude-direction diagram does not give the third element of the forces namely location unless as a special case the diagram is started from the point of concurrency of the force system.

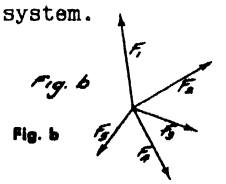


Fig. b

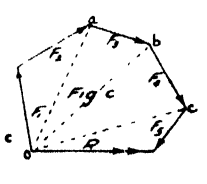


Fig. c

Fig. d shows a second magnitude - direction force polygon in which the laying off of the forces from the point o is in the following order: F_1, F_5, F_3, F_4, F_2.

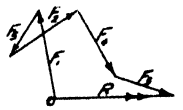


Fig. d

A1.7 Moment of a Force

Physically the moment of a force expresses the tendency of the force to turn the body on which it acts about a given axis. Thus the moment of force F (Fig. e) about a point o is Fa. The point about which the moment is taken is called the moment center and the distance (a) the moment arm. The moment of a force with respect to a point may also be regarded as the moment of the force with respect to the line which passes through the point and is perpendicular to the plane determined by the point and the action line of the force. Thus Fa also represents the moment of F about axis YY.

A1.8 Principle of Moments

The general principle of moments is of great importance in mechanics. In general terms the principle states that the moment of the resultant of a force system is equal to the algebraic sum of the moments of the forces of the system. This principle applies to lines, areas, volumes, masses, etc. as well as to forces and is therefore fundamental in determining centroids, center of gravity etc.

A1.9 Couple. General Facts Regarding Couples

Two equal parallel forces which are opposite in sense and not co-linear are called a couple. A couple cannot be reduced to a simpler system. A couple produces only a tendency to produce or prevent turning of a body. The turning effort or moment of a couple about any point in the plane of the couple (or axis perpendicular to its plane) is the product of the magnitude of either force of the couple and the perpendicular distance (moment arm) between the action lines of the two forces. The characteristics of a couple are: (1) Magnitude of the moment (2) Sense or direction of rotation of the couple (3) The aspect of the plane of the couple, that is, the direction or slope of the plane of the couple.

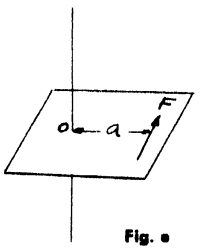


Fig. e

A couple may be translated into any parallel position in its own plane or into any parallel plane without changing its external effect on the body on which it acts.

A couple may be rotated through any angle in its plane without changing its external effect on the body on which it acts.

The resultant of any number of couples in a plane is a couple and the moment of this resultant couple equals the algebraic sum of the original couples.

Any two couples in the same plane which have the same sense and moment value are equivalent.

A1.9a Vector Representation of A Couple. Resolution of Couples

It is convenient in dealing with couples to represent them by means of a vector. The vector must show all the characteristics of the couple. Thus the length of the vector represents the magnitude of the moment of the couple. The aspect of the couple may be represented by drawing the vector perpendicular to the plane of the couple and thus parallel to the axis of the couple. The sense of the couple can be represented by an arrow head on the vector, the usual convention being to direct the arrow head away from the plane of the couple in the direction from which the rotation of the couple appears counter-clockwise, or toward the plane if the couple tends to produce clockwise rotation. This method of denoting the sense corresponds to the convention of the right-handed screw, since a right-handed screw having an axis perpendicular to the plane of the couple would move in the direction of the arrow if rotated in the direction or sense of the given couple.

In (Fig. f) the vector OA completely represents the couple Pd. The magnitude of the moment of the couple Pa is represented by the length of OA to scale.

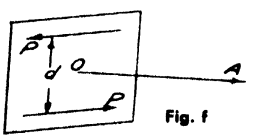


Fig. f

Example Problem

Fig. g shows a cantilever box beam subjected to two couples applied at free end as shown. Determine the resultant moment about rectangular axes 1-1 and 2-2 which make an angle of 10^0 with the x and y axes.

Fig. h shows the graphical solution. From an origin such as point O lay off vector OA parallel to y axis equal to 200"# and likewise a vector OB parallel to x axis equal to $M_x = 1000$"#. The diagonal of the parallelogram whose sides are OA and OB is resultant couple or vector OC. The vector OC is now resolved into vectors along axes 1-1 and 2-2 which make angles of 10^0 with X and Y. Erecting perpendiculars to 1-1 and 2-2 from C we obtain D and E.

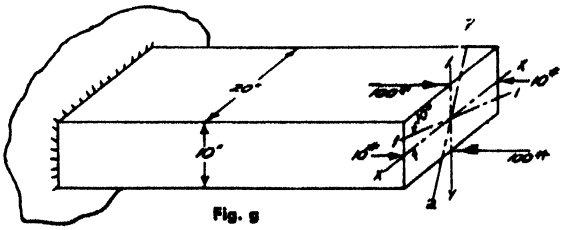


Fig. g

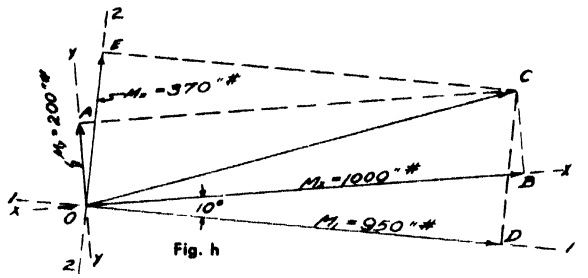


Fig. h

The vector OE which scales 370"# is the resultant moment about axis 2-2 and vector OD = 950"# is the resultant moment about the 1-1 axis.

Solution #2

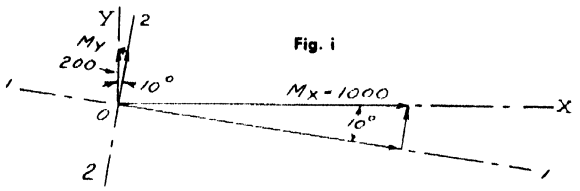


Fig. i

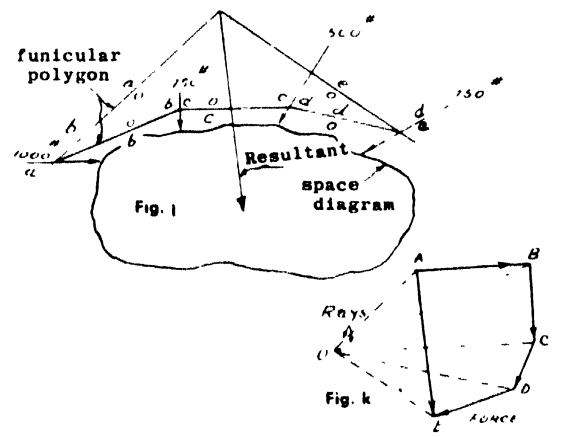
In Fig. i lay off vectors M_x and M_y. Then the projection of these vectors on the axis 1-1 and 2-2 give the moments about these axes.

$M_{1-1} = -200 \sin 10^0 + 1000 \cos 10^0 = 950"\#$

$M_{2-2} = -200 \cos 10^0 + 1000 \sin 10^0 = 370"\#$

A1.10 The Funicular Polygon or the "Location-Direction" polygon

As explained in article A1.6 the force or magnitude direction polygon gives the magnitude and direction of the resultant of a force system. A graphical construction for determining the other necessary element of the resultant namely location, is commonly referred to as the funicular polygon, but more appropriately should be called the location-direction polygon since the magnitude of the forces is not shown in this particular diagram. The principal of the funicular polygon can best be illustrated by an example.



(Magnitude & Direction) Polygon

Fig. j shows a body acted upon by 4 forces. It is desired to determine the resultant for this force system graphically. We first draw the force polygon (magnitude direction) as shown in Fig. K, by starting at some point A. Lay off the vectors representing the magnitude and direction of the four forces AB, BC, CD, and DE as shown. The resultant of these 4 forces in magnitude and direction is represented by the closing vector AE of the polygon. The sense of the resultant is opposite to the sense of the other forces. This resultant force is not completely defined, however, until its true location in Fig. J is known.

The graphical construction for determining this third element of line of action is as follows: In Fig. K, we select any point o, commonly referred to as the pole, and draw in the dashed lines OA, OB, OC, OD and OE, which are referred to as the rays of the force polygon. From the triangle law of Art. A1:5, it follows that the force AB can be resolved into the two components AO and OB; likewise BC into the components BO and OC; CD into CO and OD and finally DE into DO and OE. These vector rays represent only the magnitude and direction of these components. Our given system ABCDE has now been replaced by another system of 8 forces represented by the rays. We notice that rays OB and BO, OC and CO, OD and DO, are equal in magnitude, opposite in sense and parallel in direction. If we can make the third element, line of action of OB coincide with BO, (OC with CO) etc., then these 6 ray forces will completely cancel and we will have left the rays AO and OE, which are the components of the resultant R or AE and the line of action of the resultant R will act thru the intersection of the lines of action of its components AO and OE.

To determine the line of action of these two components it is necessary to draw another polygon commonly referred to as the funicular polygon but more appropriately a location-direction polygon since it shows only these two elements of a force. This polygon is drawn on the space diagram of Fig. J.

The sides of funicular polygon are commonly referred to as strings and are parallel to rays of the force polygon. The funicular polygon is constructed as follows: In Fig. J, from any point on the line of action ab of the force AB, strings ao and ob are drawn parallel to the rays AO and OB. From the point of intersection of ob and bc, the string bo (which will coincide with string ob) and the string oc are drawn. In like manner from the point of intersection of oc and cd, strings co and od are drawn, and do and oe from the intersection of od and de. Therefore OB will cancel BO, OC will cancel CO and OD will cancel DO since their lines of action are colinear and their magnitudes are equal and opposite in sense.

Our original system is now reduced to two forces represented in magnitude and direction by vectors AO and OE and lines of action by ao and

oe. The resultant of these two forces and therefore of the original force system will pass thru the intersection of the strings ao and oe in Fig. J. The resultant is thus completely defined, the magnitude and direction by the force polygon of Fig. K., and the line of action by the funicular polygon in Fig. J.

If the force polygon closes, which means that E coincides with A, the rays AO and OE represents two forces which are equal in magnitude and which have parallel action lines and opposite senses. If the funicular polygon does not close, the resultant will be a couple, but if the funicular polygon closes, (that is ao and oe coincide), the two forces AO and OE will balance each other and the resultant of the original force system will be zero, or the system is in equilibrium.

A1.11 Equilibrium of Force Systems

If a force system which is in equilibrium acts on a body, the body is either at rest or in a state of uniform motion. The independent equations which must be satisfied by the force system which maintains a body in equilibrium are referred to as the equations of equilibrium.

An airplane, actually, is in equilibrium only in steady unaccelerated flight. In accelerated conditions both linear and angular accelerations act to change the velocity and attitude of the airplane. In the field of stress analysis of airplanes it is customary to represent this dynamic condition as a static condition by the expedient of assigning to each item of mass the increased force with which it resists acceleration. Thus for example if the total air load on an airplane in a certain direction is "n" times the total weight of the airplane, each item of mass in the entire airplane is assumed to act on the airplane structure in the opposite direction of the applied air load and with an intensity equal to "n" times its weight. In considering the equilibrium of the airplane as a whole or of some of its parts, there may be certain elements of the forces acting which are unknown as for example the magnitude, direction or location of one or more of the forces. These unknown elements can be found if their number is not greater than the number of equations available for the particular force system involved. Such force systems are said to be statically determinate. If the unknowns are greater in number than the number of equilibrium equations available, the force system is said to be statically indeterminate.

If a force system has a resultant it must be a force or a couple. If a force system is in equilibrium then the equations of equilibrium must in general provide the conditions which make it impossible to have an unbalanced force or a couple. Thus the algebraic conditions of equilibrium are:-

(1) The algebraic sum of the components of all forces of the system in any direction must equal zero. If this fact is true it means the resultant if any could not be a force.

(2) The algebraic sum of the moments of all the forces of the system about any axis must equal zero. If this fact is true it means that the resultant if any can not be a couple.

The graphical conditions which express the above algebraic conditions for equilibrium are:-

(1) The force or (magnitude-direction) polygon must close.

(2) The funicular or (location-direction) polygon must close.

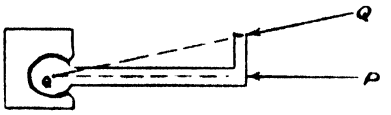
The number of independent equilibrium equations is different for the different types of force systems. These facts are listed in the following articles.

A1.12 Mechanical Methods of Fixing Elements of Forces or Reactions

Problems in statics in general deal with the determination of unknown elements of forces, that is, the magnitude, direction, or location of forces. The engineer frequently makes use of certain types of mechanical fittings or supports which definitely define certain elements of an unknown force or reaction, thus decreasing the number of unknowns below that, if these devices were not used.

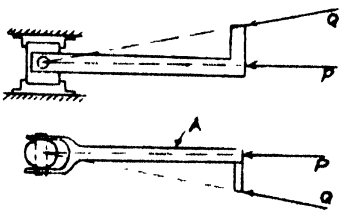
The figures which follow illustrate some of the mechanical methods.

Ball and Socket Joints



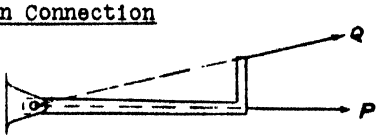
For equilibrium, the line of action of a force such as P or Q acting on bar A must pass thru center of ball joint at O or bar A will rotate about O since ball and socket joint has no resistance to rotation.

Universal Joint



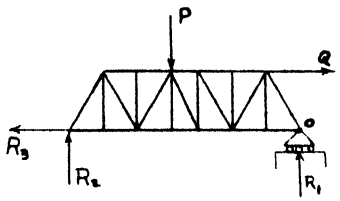
For equilibrium the line of action of a force such as P or Q acting on bar A in planes at right angles to each other must pass thru center of universal joint or rotation will take place. It should be noted however that this type of joint or fitting can transmit a torsional moment on bar A.

Single Pin Connection



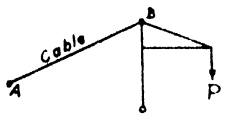
The line of action of a force such as P or Q in a plane normal to axis of pin must pass thru the pin center or rotation of bar will take place. Thus, a pin is used to determine the element of location of a force or reaction.

Rollers



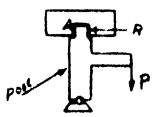
The reaction on the truss R must be vertical since the rollers have no resistance against a horizontal force. The line of action must be thru pin O. Thus, two elements of the reaction R_1 namely, direction and location, are fixed by this type of support.

Cables, Tie Rods



Since a cable has negligible resistance to bending, the reaction at B on the crane structure must lie along the line AB, or the direction and line of action of the reaction at B is known if a cable AB is used to support the crane.

Slot or Groove



Reaction at A must be horizontal since the lubricated slot offers no resistance to a vertical reaction between support and post. Thus, element of direction of reaction R is fixed by type of support.

ALGEBRAIC AND GRAPHICAL CONDITIONS FOR EQUILIBRIUM

A1.13 Coplanar Concurrent Force Systems

The following equations must be satisfied for equilibrium.

$\Sigma F_x = 0$ and $\Sigma F_y = 0$ where x and y denote any two non-parallel lines in the plane of the force system. For simplicity, a set of rectangular axes with the point of concurrence as the origin is used.

Another set of equations which insure equilibrium are:-

$\Sigma F_y = 0$ and $\Sigma M_A = 0$, where y denotes any line in a plane (usually taken for convenience as one of two rectangular axes thru the point of concurrency of the forces) and A is any point in the plane of the forces not on the x-axis.

A third set of equilibrium equations which may be used are:-

$\Sigma M_A = 0$ and $\Sigma M_B = 0$, where A and B are any two points in the plane of the forces, provided that a line joining A and B does not pass thru the point of concurrency of the given force system.

The element of location or point of application is known for all forces of a concurrent system, hence the unknown elements to be found will be either magnitudes or directions and the unknown elements can not be determined if more than two in number.

The graphical requirement for equilibrium is that the force (magnitude-direction) polygon must close.

Example Problem 1

Determine the magnitude of the two forces P and Q as shown in Fig. A1:1 to hold the 4000# load in equilibrium.

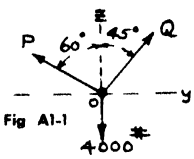


Fig A1-1

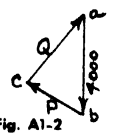


Fig. A1-2

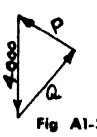


Fig A1-3

Algebraic Solution:-

For equilibrium, ΣF_Z and ΣF_y must equal zero.

$\Sigma F_Z = P \cos 60^\circ + Q \cos 45^\circ - 4000 = 0$ - - - -(1)

$\Sigma F_y = -P \sin 60^\circ + Q \sin 45^\circ = 0$ - - - - - -(2)

From (2) $P = \frac{.707Q}{.866} = .815Q$- - - - - - - - - -(3)

Substituting value of $P = .815Q$ in equation (1) we obtain,

$(.815 \times .5)Q + .707Q - 4000 = 0$, hence

$Q = 4000/1.115 = 3600\#$ (Same sense as assumed)

Substitute in equation (3) to obtain P,

$P = .815 \times 3600 = 2840\#$.

Graphical Solutions

Fig. A1.2 shows the force (magnitude-direction) polygon for the given force system. The polygon is constructed by starting at some point (a) and laying off the known force of 4000# to scale with the given direction and sense. Proceeding around the point (o) in a clockwise direction the other two forces P and Q of Fig. A1.1 whose directions are known must cause the force polygon to close on point (a). Thus from point (b) drawing a vector parallel to force P in Fig. A1.1 and from point (a) vector parallel to force Q, these two vectors will intersect at point (c). The true magnitudes of P and Q are then equal to the length of the sides bc and ca of the force polygon. Fig. A1.3 shows the force polygon when the forces P and Q are layed off when proceeding counter-clockwise around point o of the force system. The sense of the arrow heads on the vectors must be continuous around the polygon.

Example Problem 2

In Fig. A1.4, five forces are in equilibrium. Find the magnitude and direction of the force P_6 not shown in the Figure.

Algebraic Solution:-

Considering the forces P_1 to P_4 in order, $\Sigma F_x = 100 \times \frac{2}{\sqrt{13}} + 0 + 150 - 200 \times \frac{1}{\sqrt{2}}$ hence, $\Sigma F_x = 64.1\#$ and for equilibrium P_{6x} must $= -64.1\#$

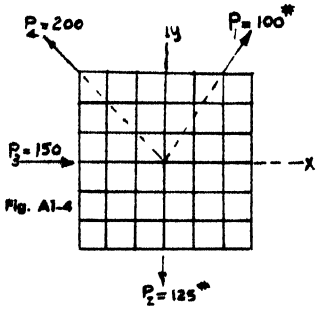


Fig. A1-4

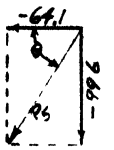


Fig. A1-4a

$\Sigma F_y = 100 \times \frac{3}{\sqrt{13}} - 125 + 0 + 200 \frac{1}{\sqrt{2}} = 99.6\#$

hence, $P_{6y} = -99.6\#$ for equilibrium to make $\Sigma F_y = 0$. Magnitude of $P_6 = \sqrt{64.1^2 + 99.6^2} = 118\#$.

The direction of P_6 with respect to horizontal thru point of concurrency $= \tan \theta = \frac{99.6}{64.1} = 1.55$

$\theta = 57^\circ - 10'$ (See Fig. A1.4a)

Thus the force P required for equilibrium = 118# acting at angle $\theta = 57^\circ - 10'$ as shown in Fig. A1.4a and it must pass thru point of concurrency O of Fig. A1.4. Note: The student should solve problem making use of other combinations of the equilibrium equations, e.g., $\Sigma F_x = 0$ and $\Sigma M_A = 0$.

Graphical Solution

Fig. A1.5 shows the force (magnitude-direction) polygon for the given force system. Starting with some point such as O the forces P_1 to P_4 are laid off to scale and parallel to their true directions as given in Fig. A1.4. Any other order of laying off the known forces could have been selected. The condition for equilibrium is that the force polygon must close. Thus the closing line from a to O gives the magnitude and direction of the unknown force P_6. The sense is shown by the arrow.

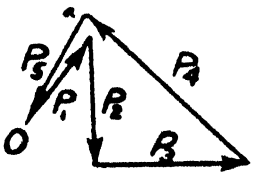


Fig. A1-5

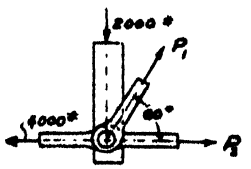


Fig. A1-6

A13.a Problems

(1) Fig. A1.6 shows a typical truss joint using a pin for the connecting medium. The loads in two of the members are given as shown. Find the loads P_1 and P_6 in the other members. Solve both algebraically and analytically.

(2) In Fig. A1.4 if force $P_4 = 100\#$ and acts in opposite direction find magnitude and direction of the fifth force P_6 required for equilibrium.

(3) Fig. A1.6a shows a pulley bracket fitting. For the cable loads as shown, determine the resultant load on the pulley hinge bolt and also the forces along the axes y and x which hold the bracket to the adjacent structure.

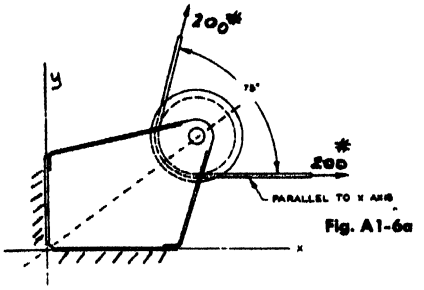


Fig. A1-6a

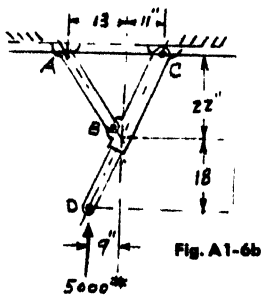


Fig. A1-6b

(4) Determine the reactions at the pin points A and C due to the 5000# load at D for the structure in Fig. A1.6b. Note that member AB is pinned at both ends. Solve both analytically and graphically.

A1.14 Coplanar - Parallel Force System

The following equations must be satisfied for equilibrium:

$\Sigma F = 0$ and $\Sigma M_A = 0$ { Where A is any point in plane of force system

or

$\Sigma M_A = 0$ and $\Sigma M_B = 0$ { Where A and B are any two points not on a line parallel to the forces of the force system.

Thus no more than 2 unknowns can exist in a parallel force system, and remain solvable with the available equations of equilibrium.

The graphical conditions for equilibrium are:-

(1) The force (magnitude - direction) polygon must close.

(2) The funicular (location - direction) polygon must close.

Example Problem 1

Fig. A1.7 shows an airplane resting on ground. Determine ground reactions at points 1 and 2.

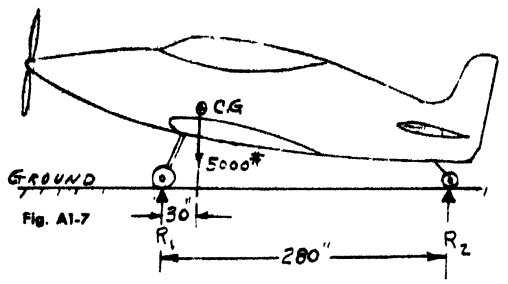


Fig. A1-7

Solution

Let R_1 and R_2 be unknown ground reactions. Taking moments about point (1) $\Sigma M_1 = 5000 \times 30 - 280\ R_2 = 0$. Hence $R_2 = 537\#$ (the sense is as assumed because algebraic sign of R_2 comes out plus. $\Sigma V = -5000 + 537 + R_1 = 0$, Hence $R_1 = 4463\#$. Check results by taking moments about point (2)

$\Sigma M_2 = -5000 \times 250 + 4463 \times 280 = 0$ (check)

A1.14a Problems

(1) Determine the reactions R_1 and R_2 for the beam in Fig. A1.8.

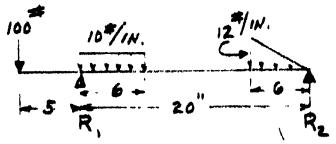


Fig. A1-8

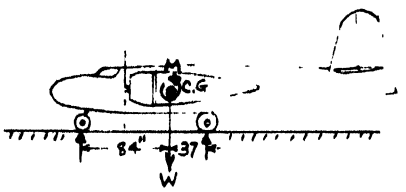


Fig. A1-8a

(2) Find the vertical reactions at each wheel for W = 40,000# and M = 65000"#. (See Fig. A1.8a)

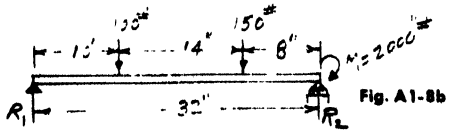


Fig. A1-8b

(3) Find the reactions for the loaded beam in Fig. A1.8b.

A1.15. Coplanar Non-concurrent - Non-parallel Force Systems

For equilibrium the following equations must be satisfied:

$\Sigma F_x = 0$, $\Sigma F_y = 0$, $\Sigma M_A = 0$ } Where x and y represent a set of rectangular axes and A is any point in the plane of the force system.

or

$\Sigma F_x = 0$, $\Sigma M_A = 0$, $\Sigma M_B = 0$ } Where x denotes any line in plane of force system and A and B are any two points in the plane, provided that the line AB is not perpendicular to X line.

or

$\Sigma M_A = 0$, $\Sigma M_B = 0$, $\Sigma M_C = 0$ } Where A, B and C are any three points in the plane of the forces not on a straight line.

Therefore in this type of force system three unknown elements of the force system may be determined since three equations of equilibrium are available.

The graphical conditions for equilibrium are:-

(1) The force (magnitude-direction) polygon must close.

(2) The funicular (location-direction) polygon must close.

Example Problem 1

Fig. A1.9 shows a loaded wing beam supported by a pin fitting at point A and an external strut BC pinned at point B. Determine the reactions on beam at points A and B and load in strut BC.

Solution:

There are three unknown elements in the reactions at A and B, namely, magnitude and direction of reaction at A and magnitude of the reaction at B. The direction of the reaction at B is along the strut BC since strut is pinned at B and C. Three equations of statics are available, thus the reactions can be determined. Fig. A1.10 shows free body diagram of beam AB. The distributed loads have been replaced by a single load acting thru center of gravity of the corresponding distributed load. The reactions have been resolved in to their x and y components for simplicity.

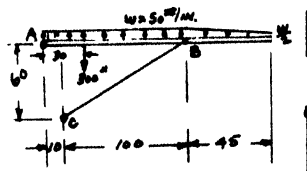


Fig. A1-9

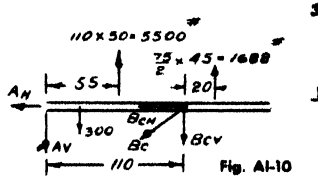


Fig. A1-10

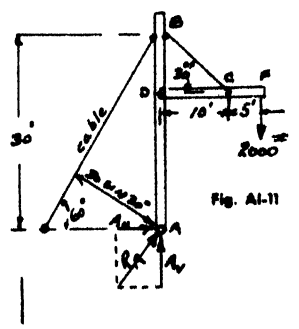


Fig. A1-11

$\Sigma M_A = -5500 \times 55 - 1688 \times 130 + 30 \times 300 + 110\ BC_V = 0$

Hence, $BC_V = 512700/110 = 4660$

Then $BC_H = 4660 \times 100/60 = 7760$

Hence load in strut BC = $\sqrt{7760^2 + 4660^2}$ = 9040 tension.

$\Sigma V = 5500 + 1688 - 4660 - 300 - A_V = 0$, hence $A_V = 2228$ acting down as assumed.

$\Sigma H = -7760 - A_H = 0$ hence $A_H = -7760$. The minus sign indicates that A_H is acting opposite to that assumed in Fig. A1.10. Having the H and V components of the reaction at point A, the reaction is completely defined. Check results by taking $\Sigma M_B = 0$

$\Sigma M_B = -2228 \times 110 - 300 \times 80 + 5500 \times 55 - 1688 \times 20 = 0$ (check)

Example Problem 2

Determine the forces acting on the members of the crane as shown in Fig. A1.11.

Solution

To find the load in the cable BE and the reaction at A, the crane as a whole can be treated as a free body, as shown in Fig. A1.11. There are three unknowns, the magnitude of the load in the cable BE, its direction and location being known. At A there are two unknowns namely the magnitude and the direction of the reaction. Three equations for equilibrium are available.

$\Sigma M_A = 2000 \times 15 - BE \times 30 \sin 30^0 = 0$. Hence BE = 2000# (tension as assumed)

$\Sigma H = -2000 \sin 30^0 + A_H = 0$. Hence A_H = 1000#

$\Sigma V = -2000 \cos 30^0 - 2000 + A_V = 0$. Hence A_V = 3773#

Resultant magnitude of reaction at A = $R_A = \sqrt{1000^2 + 3773^2} = 3900\#$

For direction of R_A, $\theta_A = \tan \frac{3773}{1000} = 75^0 - 10'$.

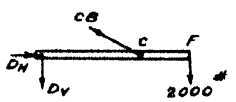


Fig. A1-12

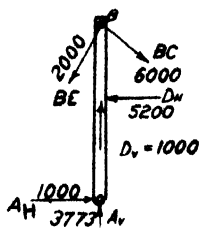


Fig. A1-13

Fig. A1.12 shows a free body diagram of the bar DCF. The unknown reaction at D is resolved into its H and V components.

$\Sigma M_D = 2000 \times 15 - 5\,CB = 0$

Hence CB = $2000 \times 15/3 = 6000\#$

$\Sigma V = -2000 + 6000 \sin 30^0 - D_V = 0$. D_V = 1000#

$\Sigma H = -6000 \times \cos 30^0 + D_H = 0$. $D_H = 5200\#$

The algebraic signs of the unknowns all come out positive thus indicating that the assumed sense of the forces was correct. To check work student should take moments about some other point to see if $\Sigma M = 0$.

Fig. A1.13shows a free body diagram of post AB with the forces as calculated. The student should check to see if post is in equilibrium under these forces.

Example Problem 3

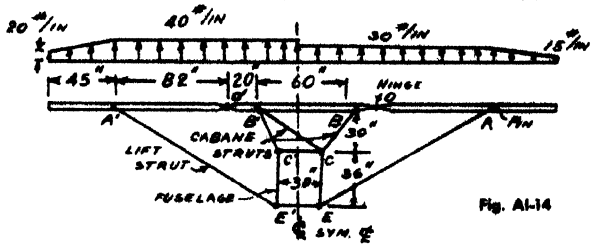


Fig. A1-14

Fig. A1.14 shows an externally braced wing beam. The beam carries the unsymetrical distributed air load as shown. The beam is held to the fuselage by the three cabane struts and the two lift struts. Each of the outer panels of the wing are hinged to the center panels at points O and O'. All struts are pinned at each end. Determine the reactions of the struts upon the wing beam.

Solution:

First are the reactions statically determinate. There are five unknowns namely, the magnitude of the forces in the five struts, since the direction and line of action or location of each strut reaction is known as struts are pinned at each end. For equilibrium of the beam as a whole we have three equations of equilibrium available, namely ΣV, ΣH, and $\Sigma M = 0$. However, we have two other additional facts due to the type of construction, namely the pin connection in the beam at points O and O' which tell us that the resultant of the forces on the beam outboard of this hinge point must pass thru the hinge points. This condition gives us two additional facts regarding equilibrium of the outer panels and we can then solve for the five strut reactions. Fig. A1.15 shows a free body of the beam outer panel. The distributed air load has been replaced by the two resultant forces as shown.

$\Sigma M_O = -2460 \times 41 - 1013 \times 102 + A_V \times 82 = 0$

$A_V = \frac{204000}{82} = 2480\#$

Hence $A_H = \frac{117}{66} \times 2480 = 4400\#$

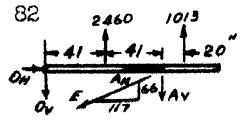


Fig. A1-15

Load in strut AE = $\sqrt{4400^2 + 2480^2} = 5050\#$ (tension)

$\Sigma H = -4400 + O_H = 0$. whence $O_H = 4400\#$

$\Sigma V = +2460 + 1013 - 2480 - O_V = 0$. whence O_V = 993#

Check by $\Sigma M_A = 0 = 2460 \times 41 - 1013 \times 20 - 993 \times 82 = 0$.

On the outer panel O'D', the strut reactions are obviously proportional to the increase in air-load or by the ratio $\frac{40.}{30}$

Hence A'E' = 6750, O'_H = 5880, O'_V = 1325.

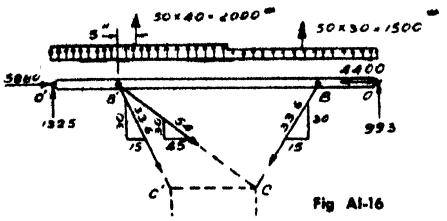


Fig A1-16

Fig. A1.16 shows a free body of the center beam panel O O'. To find reaction BC take moments about B'.

$$\Sigma M_{B'} = 1325 \times 20 - 2000 \times 5 - 1500 \times 55 - 993 \times 80 + 60\ BC_Y = 0$$

$$\text{therefore } BC_Y = \frac{145500}{60} = 2425\#$$

$$\text{Hence } BC = \frac{33.6}{30} \times 2425\# = 2720\#.$$

To find B'C' take moments about point C.

$$\Sigma M_C = 1325 \times 65 + 2000 \times 40 + (5880 - 4400)\ 30 - 1500 \times 10 - 993 \times 35 - B'C'_Y \times 30 = 0$$

$$\text{therefore } B'C'_Y = \frac{160700}{30} = 5357. \text{ Hence } B'C' = \frac{33.6}{30} \times 5357 = 6000\#$$

To find vertical or Y component of reaction B'C' take summation of vertical forces:

$$\Sigma V = +1325 + 2000 + 1500 + 993 - 2425 - 5357 - B'C_Y = 0$$

$$\text{therefore } B''C_Y = -1964. \text{ Hence } B'C = \frac{54}{30} \times -1964 = -3535$$

and the reaction acts opposite to the sense shown in Fig. A1.16 since algebraic sign comes out minus. The three unknown reactions on the center panel beam have now been determined.

The student should check the results by determining whether the results make $\Sigma M = 0$ about some other point and also $\Sigma H = 0$.

A1.15a Problems

(1) For the simplified airplane structure in Fig. A1.17 determine the load in the lift strut BC and the beam reaction at point A.

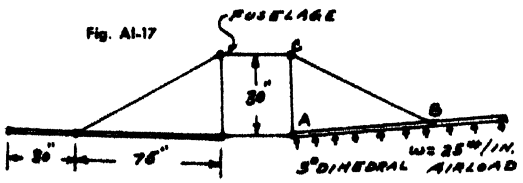


Fig. A1-17

(2) Fig. A1.18 shows a simplified biplane wing structure. The wing beam, wires and struts all are in the same plane. Under the distributed air load shown, find reactions on beams and loads in all wires and struts. Draw complete free body diagrams. Suggestion:- Start solution by considering lower beam first.

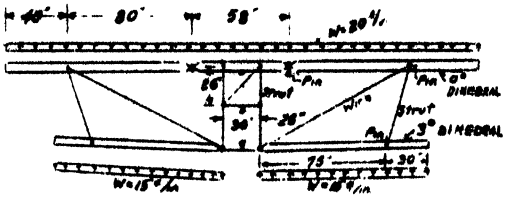


Fig. A1-18

(3) In Fig. A1.19 the load of 5000# is held by a cable load T passing over the sheaves A and B as shown. Find the reactions at C and G assuming no vertical component for reaction at C. Find also reactions at points D, E and F.

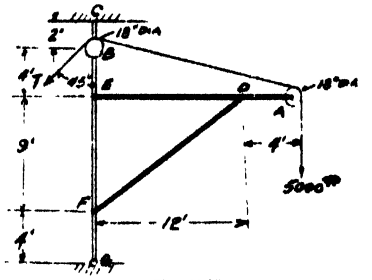


Fig. A1-19

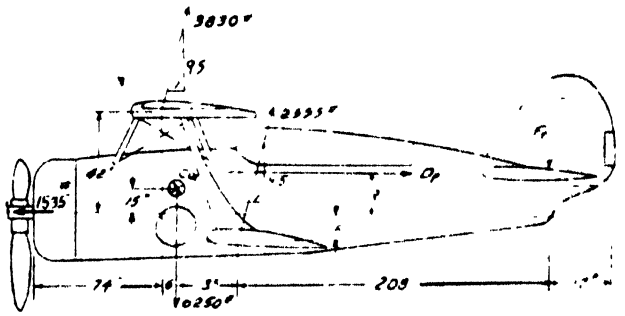


Fig. A1-19a

(4) Given the airplane in flight as shown in Fig. A1.19a. All forces are known except fuselage drag D_p and Tail Load F_t. Determine value of D_p and F_t for equilibrium. Solve both analytically and graphically.

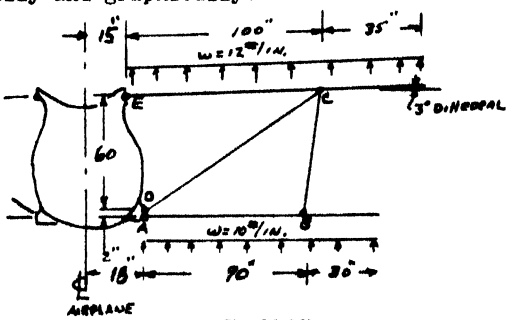


Fig. A1-19b

(5) Determine the axial loads in members AB, BC, DC, and CE of the wing truss in Fig. A1.19b due to the distributed wing beam loads as shown.

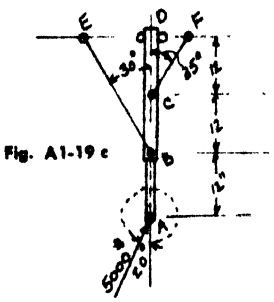


Fig. A1-19 c

(6) In Fig. A1.19c, the landing gear member AD is braced by the members BE and CF which are pinned at each end. The support at D is such that only a horizontal reaction can be set up. Determine the loads in the members BE and CF and the reaction at D for the 5000# load acting at A as shown.

A1.16 Non-Coplanar Con-Current Force System

A non-coplanar concurrent force system is in equilibrium if the algebraic sums of the components of all the forces along any three non-coplanar lines thru the point of concurrence are equal to zero. If the reference lines are taken as the rectangular axes, the general equations of equilibrium can be written,

$$\Sigma F_X = 0;\ \Sigma F_Y = 0;\ \Sigma F_Z = 0$$

Thus for a space concurrent force system three unknown loads or forces may exist which can be found by the available equations of equilibrium.

Example Problem:

Fig. A1.20 shows a tripod frame used for hoisting the propeller on large high wing airplanes. Assuming a vertical load on tripod at point O equal to 1000#, determine axial load in each member of the tripod frame.

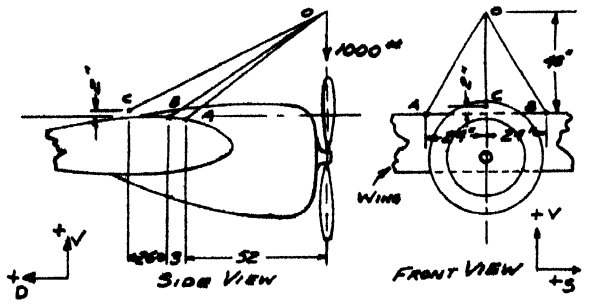


Fig A1-20

Solution

Table A1.1 shows the calculation of the member lengths and the V, D, and S direction cosines.

Table A1.1

Member	V	D	S	L	V/L	D/L	S/L
AO	48	52	24	74.6	.643	.696	.322
BO	48	55	24	76.8	.625	.716	.313
CO	48	81	0	93.0	.495	.871	0

$L = \sqrt{V^2 + D^2 + S^2}$ As a check the sum of the squares of the direction cosines must equal 1.

Considering joint O as a free body the 3 equations of equilibrium will be written. In writing the equations the axial load in each of the three members will be assumed as tension. For algebraic signs plus is up, aft and outboard.

$$\Sigma V = -.643\,AO - .625\,BO - .495CO - 1000 = 0$$

$$\Sigma D = +.696\,AO + .716\,BO + .871CO = 0$$

$$\Sigma S = -.322\,AO + .312\,BO = 0$$

Solving the above three equations gives,

AO = -2100# (compression)
BO = -2170# "
CO = 3460# (tension)

As a check on the solution of the equations, the sum of the V, D, and S components of the member loads will be checked against the applied load at joint (O) as illustrated in the following table.

Member	Load	V	D	S
AO	-2100	1355	-1462	678
BO	-2170	1360	-1558	-678
CO	3460	-1715	3020	0
	Σ	1000	0	0
		check	check	check

A1.17 Non-Coplanar - Non Concurrent - Non-Parallel Force Systems.

This type of force system is in equilibrium if the algebraic sum of the components of the forces in three directions at right angles to each other is equal to zero and the algebraic sum of their moments about any axis is equal to zero.

These conditions permit the writing of 6 equations of equilibrium or six unknowns can be determined for this type of force system.

Sometimes it is convenient to take the coordinate axes as the axes for resolution and moments in which case the equations of equilibrium can be written.

$$\Sigma F_X = 0 \qquad \Sigma M_X = 0$$

$$\Sigma F_Y = 0 \qquad \Sigma M_Y = 0$$

$$\Sigma F_Z = 0 \qquad \Sigma M_Z = 0$$

Example Problem 1

Fig. A1.21 shows the dimensional diagram of a landing gear for an actual airplane. The chassis is of the split-axle type; each half consisting of an axle strut (B), a shock-absorbing (oleo type) strut (A), and a cross strut (C). The axle-strut and the cross strut lie in the same plane, and both have pins at their upper ends perpendicular to the plane of symmetry allowing the chassis to swing fore and aft as well as up and down. The cross strut has a universal joint at its upper end and one pin at its lower end. The shock absorbing strut has universal joints at both ends. The axle strut is fixed at its lower end and has one pin, perpendicular to the symmetry plane at its upper end. The wheels are canted inwards 3.1°.

Unknowns. For the member end connections present in this landing gear there are six unknown forces as follows:

A = the axial load in member (A), the oleo strut
B = the axial load in member (B), the axle strut
C = the axial load in member (C), the rear cross strut
S_p = the shear reaction at the upper pin of the axle strut (B) in the plane of the rear struts
S_n = the shear reaction at the upper pin of the axle strut (B) perpendicular to the plane of the rear struts
T = a torsional moment in the axle strut (B).

To solve for these six unknowns, the following equations will be set up:

$\Sigma V = 0$ $\quad \Sigma M_n = 0$
$\Sigma D = 0$ $\quad \Sigma M_1 = 0$
$\Sigma S = 0$ $\quad \Sigma M_p = 0$ where,

V = a vertical force parallel to the plane of symmetry. It is (+) if acting upward.
D = a drag force parallel to the propeller axis (thrust line). It is (+) if acting aft.
S = a side force perpendicular to the plane of symmetry, or perpendicular to V & D plane. It is (+) if acting outboard from the plane of symmetry.
M_p = a moment about the axis (P) which is perpendicular to the plane of the rear struts. It is (+) if it appears clockwise when viewed from a position in front of the chassis.
M_n = a moment about the axis (N) which is in the plane of the rear struts and perpendicular to the axle strut (B). It is (+) if it appears clockwise when viewed from a position outboard of the chassis.
M_1 = a moment about the axis (1) which is in the plane of rear struts and parallel to the axle strut (B), or perpendicular to the axis (N) and (P). It is (+) if clockwise when viewed from a position below the chassis. The (1) axis passes thru the intersection of oleo strut (A) with the axle spindle.

Figs. A1.21 and A1.22 show the location of the three moment axes which have been selected for the solution of this problem.

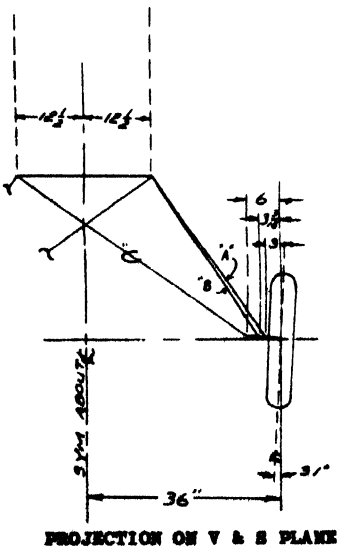
Table A1.2 gives the direction cosines of the members and the shear reactions S_n and S_p. The student should refer to figures A1.21 and A1.22 to check the values in this table.

Table A1.2 Direction Cosines of Members and Shear Reactions.

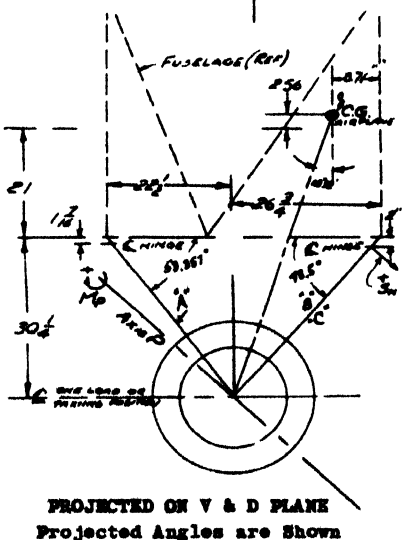
Member or Reaction	V	D	S	L Length	V/L	D/L	S/L
A	30.087	22.50	20.504	42.80	.7030	.5257	.4791
B	30.043	28.75	19.693	44.80	.6706	.5971	.4396
C	29.925	26.75	42.509	58.47	.5118	.4575	.7270
S_p					.3282	.2923	.6982
S_n					.6650	.7488	.0000

$L = \sqrt{V^2 + D^2 + S^2}$

NOTE: The distances have been calculated from fuselage joints to axle. To design members the actual pin ended lengths should be used.

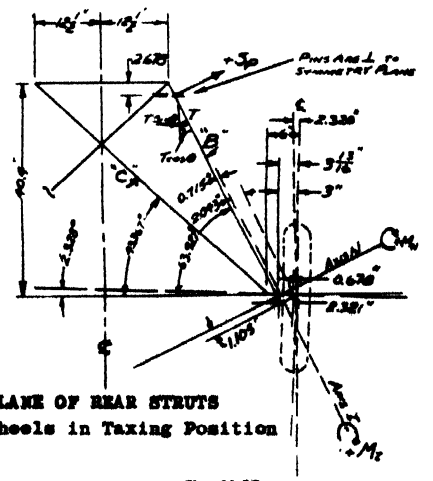


PROJECTION ON V & S PLANE



PROJECTED ON V & D PLANE
Projected Angles are Shown

Fig. A1-21



PLANE OF REAR STRUTS
Wheels in Taxing Position

Fig. A1-22

Assumption of Member Signs in Writing Equilibrium Equations:

(1) Tension axial loads are assumed in members (A), (B), and (C).

(2) A positive torsional moment (T) is assumed in the axle strut (B). This is reacted by a negative torsional moment about the axis (1) and due to the direction of the pin at the upper end of the axle-strut by a positive bending moment due to torque about the (N) axis.

(3) A positive value for shear reaction (S_p)

(4) A positive value for shear reaction (S_n)

Load Conditions

The loads in the chassis members will be

determined for the following three conditions of loading:

(1) A unit vertical load acting thru point of contact of the one-half deflected tire and the ground and applied at the axle spindle.

(2) A unit drag load applied to the axle spindle at the point of application of the unit vertical load. (condition 1.)

(3) A unit side load applied at the point of contact of the one-half deflected tire and the ground.

After the loads in the chassis members for the applied unit loads are determined the true design wheel loads for the various landing conditions can be found by simple multiplication.

Equations of Equilibrium (Refer to Table A1.2 and Figs. A1.21 and A1.22)

Condition 1. Unit upward vertical load:

$\Sigma V = +.7030\,A + .6706B + .5118C + .3282\,S_p - .6650\,S_n + 1.000 = 0$

$\Sigma D = -.5257\,A + .5971\,B + .4575C + .2922\,S_p + .7468\,S_n = 0$

$\Sigma S = -.4791\,A - .4396\,B - .7270C + .8982\,S_p = 0$

$\Sigma M_n = +T(\cot 63.927^\circ) + 1(1.105)(\cos 48.50) + S_n(41.82 + .3863) = 0$

$\Sigma M_1 = -S_n(0.715) - 1(\cos 48.5^\circ)(2.043) - T = 0$

$\Sigma M_p = S_p(41.82 + .3863 + C(\sin 41.039)(3) + .715B - 1(2.321)(\sin 48.5) = 0$

Solving the six equations gives,

A = -0.7723 lb.	S_n = -0.0017 lb.
B = -1.9774 lb.	S_p = -0.0046 lb.
C = +1.6989 lb.	T = -1.3524 in. lb.

Condition II Unit Drag Load Applied Aft.

$\Sigma V = +.7030A + .6706B + .5118C + .3282\,S_p - .6650\,S_n = 0$

$\Sigma D = -.5257A + .5971B + .4575C + .2922\,S_p + .7468\,S_n + 1.000 = 0$

$\Sigma S = -.4791A - .4396B - .7270\,C + .89288_p = 0$

$\Sigma M_n = S_n(42.2063) + T(\cot. 63.927^\circ)\,1(\sin 48.5\,(1.105) = 0$

$\Sigma M_1 = -S_n(0.175) - T + 1(\sin 48.5)(2.043) = 0$

$\Sigma M_p = S_p(42.2063) + C(1.9698) + B(0.715) - (\cos 48.5)(2.321) = 0$

Solving the six equations gives,

A = 0.8706 lb.	S_n = 0.0019 lb.
B = -1.0088 lb.	S_p = 0.0490 lb.
C = 0.0969 lb.	T = 1.5290 in. lb.

Condition III Unit Side Load Applied Outboard.

$\Sigma V = +.7030A + .6706B + .5118C + .3282\,S_p - .6650\,S_n = 0$

$\Sigma D = -.5257A + .5971B + .4575C + .2922\,S_p + .7468\,S_n = 0$

$\Sigma S = -.4791A - .4396B - .7270C - .8982\,S_p + 1.000 = 0$

$\Sigma M_n = S_n(42.2063) + T(\cot. 63.927^\circ) + 1(\cos 62.927)(12.5\cos 3.1^\circ + 3\sin 3.1^\circ)\cos 48.5 = 0$

$\Sigma M_1 = -S_n(0.715) - T - 1(\sin 63.927)(12.5\cos 3.1^\circ + 3.01\sin 3.1^\circ)(\cos 48.5^\circ) = 0$

$\Sigma M_p = S_p(42.2063) + 1.9698C + 0.715B - 1(\sin 48.5^\circ)(12.5\cos 3.1^\circ + 3\sin 3.1^\circ) = 0$

Solving the six equations gives,

A = .0042 lb.	S_n = 0
B = -2.2923 lb.	S_p = .1271 lb.
C = 2.9161 lb.	T = -7.5248 in. lb.

Example Problem 2

Fig. A1.23 shows another common arrangement for members of a airplane landing chassis. Member (A) incorporates the shock-absorbing mechanism. The fitting for member (A) at the lower end at "O" is such that only axial load can be taken by member (A). Member (C) is likewise connected to point O in such a manner that no torsion or bending can be transmitted by member (C). Member (B) is welded to the axle spindle, thus member (B) resists all applied couples by torsion and bending.

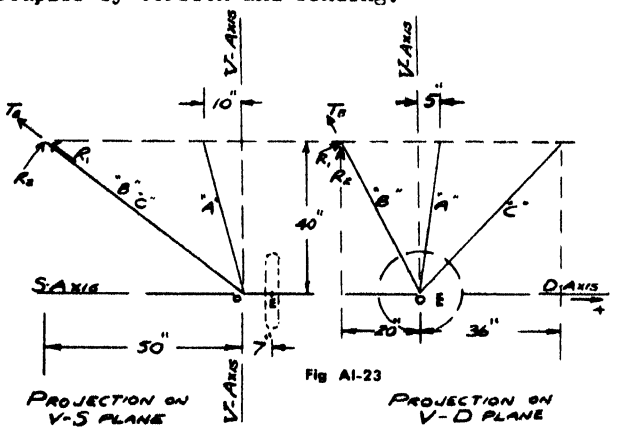


Fig A1-23

Coordinate Axes. In this chassis the three members intersect at point (O), thus this apex of the tripod is a good place for the origin of coordinates for the three axes (V), (D), and (S). The (D) axis is parallel to a line joining the upper ends of members (B) and (C) which line is parallel to propeller axis. The (V) axis is parallel to plane of symmetry and perpendicular to propeller axis. The (S) axis is perpendicular to the (V) and (D) axes.

Table A1.3 gives the direction cosines of the members.

Table A1.3 Direction Cosines of Members and Shear Reactions.

Member or Reaction	V	D	S	L	V/L	D/L	S/L
A	40	5	10	41.5	.964	.1204	.241
B	40	20	50	87.0	.597	.298	.746
C	40	38	50	73.5	.544	.490	.680
R1					.1862	.956	.2330
R2					.7809	0	.6247

$L = \sqrt{V^2 + D^2 + S^2}$

Symbols and Signs For Unknown Reaction.

For the given conditions, there are six unknowns as follows:
(A), (B), and (C), the direct or axial reaction on members A, B, and C respectively. It is plus if it produces tension in members.
T_B = torsional reaction at end of member (B). This couple is represented by a vector parallel to member B. The sense of the vector is determined by the conventional right hand screw.
R_1 = a shear reaction lying in plane of members (B) and (C) perpendicular to member (B) and acting at upper end of (B).
R_2 = a shear reaction perpendicular to the plane of the members B and C and acting at upper end of member (B). If R_1 and R_2 slope upward they are assumed positive.

Load Condition.

The values of the six upward reactions will be determined for a unit 1 lb. vertical force applied upward at point E on the axle.

In example problem 1, six equilibrium equations were written and solved for the six unknowns a procedure quite tedious because of the number of equations.

In this chassis arrangement all three members intersect at a common point, thus it is possible to select reference moment axes so that all six unknowns can be solved for progressively with a single independent equation for each unknown.

Equations of Equilibrium.

Since all three members intersect at O, and R_1 and R_2 pass thru centerline of member B, it is convenient to start the solution by taking moments about an axis coinciding with the axis of member (B) since all unknown forces have zero moment arms from this axis, which leaves the torque reaction T_B as the only unknown.

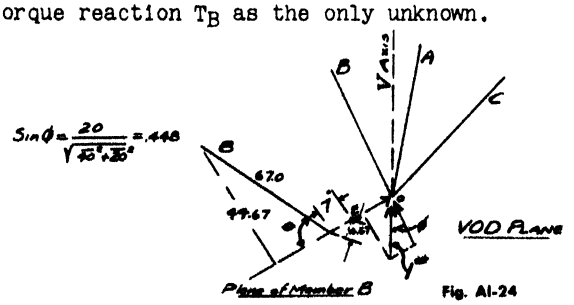


Fig. A1-24

From Fig. A1.24, the component of the 1# applied V load normal to member (B) equals 1 x sin Θ = 1 x .448 = .448# and the arm from axis of (B) equals 4.67", hence,

$M_b = .448 \times 4.67 + T_B = 0$ or $T_B = -2.092$ in. lb.

Now if we take moment about the (D) axis, all unknowns are eliminated except R_2 and T_B, but T_B is known from previous computations, hence.

$$\Sigma M_D = -T_B \times \frac{D_B}{L_B} - 1 \times 7 + 64.03\, R_2 = 0$$

$$= 2.092 \times .298 - 7 + 64.03\, R_2 = 0$$

$$R_2 = 0.100 \text{ lb.}$$

Now taking moments about the (S) axis all unknowns except R_2, R_1 and T_B drop out due to zero moment arms, but R_2 and T_B have been already determined, hence

$$\Sigma M_S = R_2 \times \frac{V}{L} \times D_B + T_B \times \frac{S_B}{L_B} + R_1 \times \frac{D}{L} \times V_B + R_1 \times \frac{V}{L} \times D_B = 0$$

$$= 0.100 \times .7809 \times 20 - 2.092 \times .746 + R_1 \times .956 \times 40 + R_1 \times .1862 \times 20 = 0$$

Solving $R_1 = 0$

The three remaining unknowns are the direct reactions in members (A), (B), and (C), thus a moment axis other than one thru the point of concurrency O must be used.

Take moments about an axis thru the upper ends of members (B) and (C).

$$\Sigma M_{bc} = -1(S_B + 7) - T_B \times \frac{D_B}{L_B} - A \times \frac{V}{L} \times 40 + A \times \frac{S}{L} \times 0 = 0 = -1(50 + 7) + 2.092 \times .298 + A \times .964 \times 40 + 0 = 0$$

$$A = -1.462 \text{ lb.}$$

To find direct reaction (C) take moments about an axis thru the upper end of member (B) and parallel to the (S) axis.

$$\Sigma M_{BS} = T_B \times \frac{S_B}{L_B} - A \times \frac{V}{L} \times 25 - A \times \frac{D_A}{L_A} \times 0 - 1 \times D_B - C \times \frac{V}{L} \times 56 = 0$$

$$= -2.092 \times .746 + 1.462 \times .964 \times 25 - 0 - 20 - C \times .544 \times 56 = 0$$

$$C = 0.448 \text{ lb.}$$

To find the remaining unknown (B) the direct reaction on member (B) take moments about an axis through the upper end of member C and parallel to S axis.

$$\Sigma M_{CS} = T_B \times \frac{S_B}{L_B} + A \times \frac{V}{L} \times 31 + R_2 \times \frac{V}{L}(36 + 20) + R_1 \times \frac{V}{L}(36 + 20) + 1 \times 36 + B \times \frac{V}{L}(36 + 20) = 0$$

$$= -2.092 \times .746 - 1.462 \times .964 \times 31 + .100 \times .7809 \times 56 + 0 + 36 + B \times .597 \times 56 = 0$$

$$B = 0.1582 \text{ lb.}$$

In a similar manner, the values of the six unknown reactions can be found for unit drag and side loads on landing gear. The student should carry through the solution for such external loads.

A1.18 Problems

(1) Determine the axial loads in the three landing gear members of Fig. A1.25 for the loading as shown. From the results calculate the V, D and S components of the fuselage reactions and check against the applied chassis load.

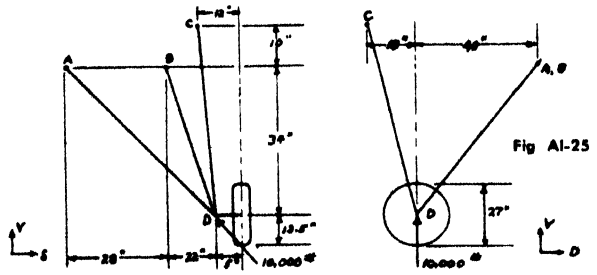


Fig A1-25

(2) Determine the axial loads in the tripod frame of Fig. A1.26 for the loading as shown.

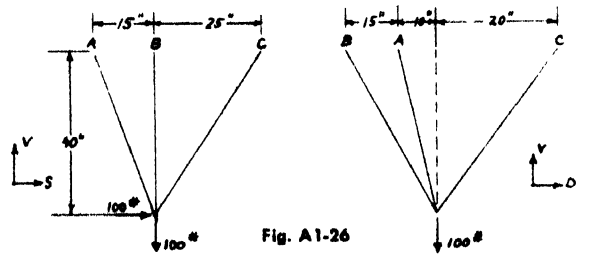


Fig. A1-26

(3) In the landing gear structure of Fig. A1.27, members AO and CO have such end fittings that they can resist only axial loads. Member BO is welded to axle OD. The fitting at B is capable of providing torsional resistance.

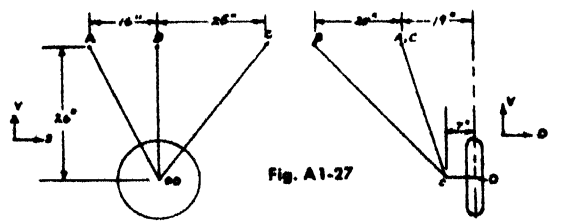


Fig. A1-27

(a) For unit vertical, drag and side load acting separately at point D on the landing gear find complete reactions at points A, B and C. Solve by both methods as illustrated in example problems (1) and (2).

(b) If the chassis is subjected to a simultaneous V, D and S loads at point D of 4000, 1000 and 800 lbs., respectively determine the resulting axial loads in the members and the shear and torque reactions on member BO at B.

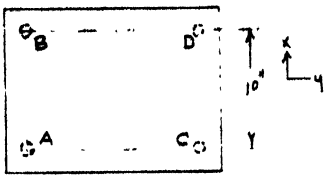
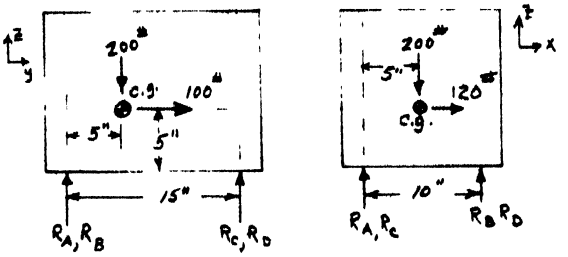


Fig. A1-28



(4) A box containing a radio installation is attached to fuselage supporting members at four points A, B, C and D as shown in Fig. A1.28 The C.g. of the box and its contents is located as shown. The inertia design loads acting through the c.g. in the Z, X and y directions are given on the figure. To design the supporting members the reactions at A, B, C and D must be known. Find these reactions for the given loads through the c.g.

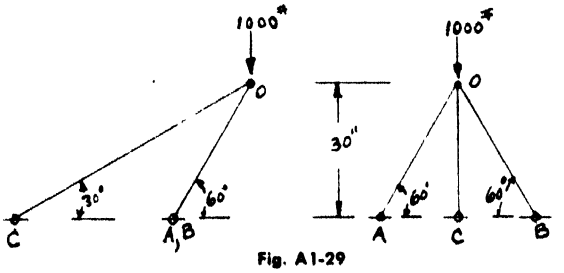


Fig. A1-29

(5) Determine the axial loads in the frame of Fig. A1.29. Solve by taking moments.

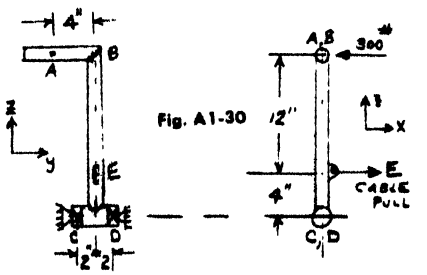


Fig. A1-30

(6) Fig. A1.30 illustrates a rudder pedal in an airplane. A foot pressure or load of 300# is applied at point A. Determine the reactions to the pedal load, namely the cable pull at E and the bearing reactions at C and D.

CHAPTER A2
TRUSS STRESS ANALYSIS

A2.0 Introduction. In aircraft construction, the truss type of construction is quite common. The most common is the tubular steel welded trusses that make up the fuselage frame, and less frequently, the aluminum alloy tubular truss. Trussed type beams composed of closed and open type sections are also frequently used in wing beam construction. The stresses or loads in the members of a truss are commonly referred to as "primary" and "secondary" stresses. The stresses which are found under the following assumptions are referred to as primary stresses.

(1) The members of the truss are straight, weightless and lie in one plane.

(2) The members of a truss meeting at a point are considered as joined together by a common frictionless pin and all member axes intersect at the pin center.

(3) All external loads are applied to the truss only at the joints and in the plane of the truss. Thus all loads or stresses produced in members are either axial tension or compression without bending or torsion.

Those stresses produced in the truss members due to the non-fulfillment of the above assumptions are referred to as secondary stresses. Most steel tubular trusses are welded together at their ends and in other truss types, the members are riveted or bolted together. This restraint at the joints may cause secondary stresses in some members greater than the primary stresses. Likewise it is common in actual practical design to apply forces to the truss members between their ends by supporting many equipment installations on these truss members. However regardless of the magnitude of these so-called secondary loads it is common practice to first find the primary stresses under the assumptions outlined above.

A2.1 Stability, Statically Determinate and Indeterminate Trusses.

The simplest truss that can be constructed is the triangle which has three members m and three joints j. A more elaborate truss consists of additional triangular frames, so arranged that each triangle adds one joint and two members. Hence the number of members to insure stability under any loading is:

$$m = 2j - 3 \qquad (1)$$

A truss having fewer members than required by Eq. (1) is in a state of unstable equilibrium and will collapse except under certain conditions of loading. The loads in the members of a truss with the number of members shown in equation (1) can be found with the available equations of statics, since the forces in the members acting at a point intersect at a common point or form a concurrent force system. For this type of force system there are two static equilibrium equations available, (see Art. A1.3)

Thus for j number of joints there are 2j equations available. However three independent equations are necessary to determine the external reactions, thus the number of equations necessary to solve for all the loads in the members is 2j - 3. Hence if the number of truss members is that given by equation (1) the truss is statically determinate relative to the primary loads in the truss members and the truss is also stable.

If the truss has more members than indicated by equation (1) the truss is considered redundant and statically indeterminate since the member loads can not be found in all the members by the laws of statics. Such redundant structures if the members are properly placed are stable and will support loads of any arrangement.

There are three analytical methods for determining the primary stresses in trusses, namely, the methods of joints, moments and shears.

A2.2 Method of Joints

If the truss as a whole is in equilibrium then each member or joint in the truss must likewise be in equilibrium. The forces in the members at a truss joint intersect in a common point, thus the forces on each joint form a concurrent-coplanar force system. The method of joints consists in cutting out or isolating a joint as a free body and applying the laws of equilibrium for a concurrent force system. (See Art. A1.3) Since only two independent equations are available for this type of system only two unknowns can exist at any joint. Thus the procedure is to start at the joint where only two unknowns exist and continue progressively throughout the truss joint by joint. To illustrate the method consider the cantilever truss of Figure A2.1. From observation there are only two members with internal stresses unknown at joint L_3. Fig. A2.2 shows a free body of joint L_3. The stresses in the members $L_3 L_2$ and $L_3 U_2$ have been assumed as tension, as indicated by the arrows pulling away from the joint L_3.

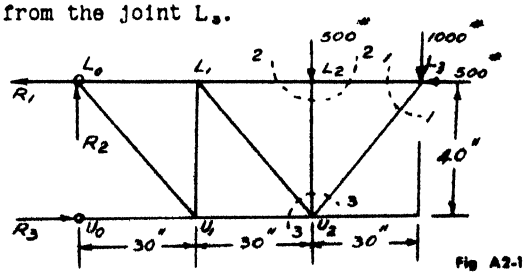


Fig A2.1

The equations of equilibrium are ΣH and ΣV = 0. Thus

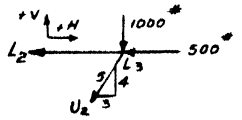
$\Sigma V = -1000 - \frac{40}{50} L_3U_3 = 0$ - - - - - - - - - - (1)

Hence $L_3U_3 = -1000 \times \frac{50}{40} = -1250\#$. Thus the stress in member L_3U_3 is compression or opposite to that shown in Fig. A2.2.

$\Sigma H = -500 - (\frac{-30}{50} \times 1250) - L_2L_3 = 0$ - - - - (2)

Hence $L_2L_3 = 250\#$ (tension as assumed in Fig. A2.2)

Fig. A2-2



In equation (2) the load of 1250 in L_3L_3 is substituted as a minus value since it was found to act opposite to the sense shown in Fig. A2.2. Possibly a better procedure would be to change the sense of the arrow in the free body diagram for any solved members before writing further equilibrium equations. We must proceed to joint L_3 instead of joint U_3, as three unknown members still exist at joint U_3 whereas only two at joint L_3. Fig. A2.3 shows free body of joint L_2 cut out by section 2-2 (see Fig. A2.1). The sense of the unknown member stress L_2U_2 has been assumed as compression (pushing toward joint) as it is obviously acting this way to balance the 500#.

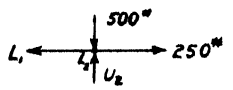


Fig. A2-3

$\Sigma V = -500 + L_2U_2 = 0$, therefore $L_2U_2 = 500\#$ compression or acting as assumed in Fig. A2.3 since the algebraic sign comes out + thus indicating that assumed sense of the stress was correct. $\Sigma H = +250 - L_2L_1 = 0$, therefore $L_2L_1 = 250\#$ (tension as assumed in Fig. A2.3). Next consider joint U_2 as a free body as cut out by section 3-3 of Fig. A2.1 and shown in Fig. A2.3a. The known member stresses are shown with their true sense as previously found. The two unknown member loads U_2L_1 and U_2U_1 have been assumed as tension.

$\Sigma V = -500 - 1250 \times \frac{40}{50} + U_2L_1 \times \frac{40}{50} = 0$. Hence

$U_2L_1 = 1875\#$ (tension as assumed)

$\Sigma H = -1250 \times \frac{30}{50} = 1875 \times \frac{30}{50} - U_2U_1 = 0$. Hence

$U_2U_1 = -1875\#$ comp. (opposite to that assumed in Fig. A2.3)

Note: The student should continue with succeeding joints. In this example involving a cantilever truss it was not necessary to find the reactions, as it was possible to select joint L_2 as a joint involving only two unknowns. In trusses such as illustrated in Fig. A2.4 it is necessary to first find reactions R_1 or R_2 which then provides a joint at the reaction point involving only two unknown forces.

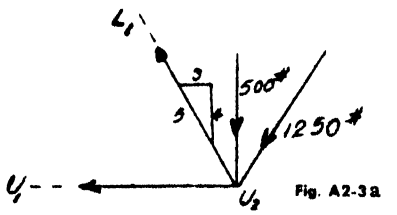


Fig. A2-3a

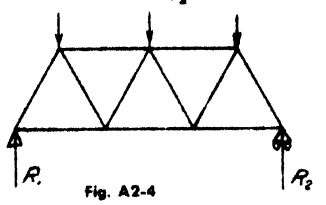
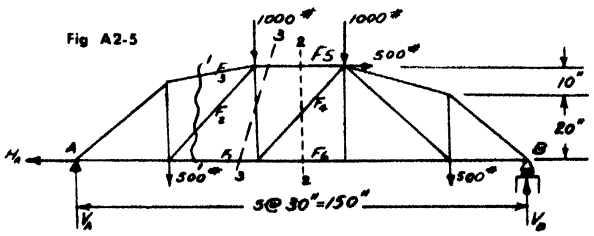


Fig. A2-4

A2.3 Method of Moments

For a co-planar-non concurrent force system there are three equations of statics available (see Art. A1.5). These three equations may be taken as moments about three different points must equal zero. Fig. A2.5 shows a typical truss. Let it be required to find the loads in the members F_1, F_2, F_3, F_4, F_5 and F_6.

Fig A2-5



The first step in the solution is to find the reactions at points A and B. Due to the roller type of support at B the only unknown element of the reaction force at B is magnitude. At point A, magnitude and direction of the reaction are unknown giving a total of three unknowns with three equations of statics available. For convenience the unknown reaction at A has been replaced by its unknown H and V components

Taking moments about point A,

$\Sigma M_A = 500 \times 30 + 1000 \times 60 + 1000 \times 90 + 500 \times 30 + 500 \times 120 - 150\ V_B = 0$

Hence $V_B = 1600\#$

Take ΣV = 0

$\Sigma V = V_A - 1000 - 1000 - 500 - 500 + 1600 = 0$ therefore $V_A = 1400\#$

Take ΣH = 0

$\Sigma H = 500 - H_A = 0$, therefore $H_A = 500\#$

The algebraic sign of all unknowns came out positive, thus the assumed direction as shown on Fig. A2.5 was correct.

Check results by taking $\Sigma M_B = 0$

$\Sigma M_B = 1400 \times 150 + 500 \times 30 - 500 \times 120 - 500 \times 30 - 1000 \times 90 - 1000 \times 60 = 0$ (Check)

To determine the stress in member F_1, F_2 and F_3

we cut the section 1-1 thru the truss (Fig. A2.5). Fig. A2.6 shows a free body diagram of the portion of the truss to the left of this section.

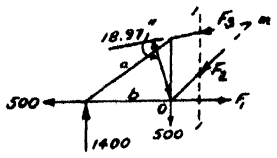


Fig A2-6

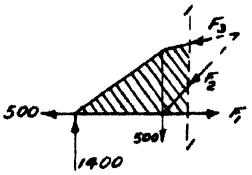


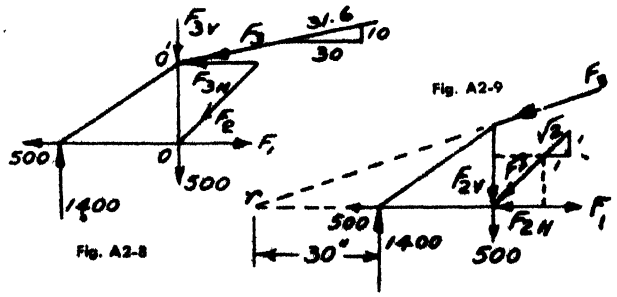
Fig. A2-7

The truss as a whole was in equilibrium therefore any portion must be in equilibrium. In Fig. A2.6 the internal stresses in the members F_1, F_2 and F_3 which existed in the truss as a whole now are considered external forces in holding the portion of the truss to the left of section 1-1 in equilibrium in combination with the other loads and reactions. Since the members a and b in Fig. A2.6 have not been cut the loads in these members remain as internal stresses and have no influence on the equilibrium of the portion of the truss shown. Thus the portion of the truss to left of section 1-1 could be considered as a solid block as shown in Fig. A2.7 without affecting the values of F_1, F_2 and F_3. The method of moments as the name implies involves the operation of taking moments about a point to find the load in a particular member. Since there are three unknowns a moment center must be selected such that the moment of each of the two unknown stresses will have zero moment about the selected moment center, thus leaving only one unknown force or stress to enter into the equation for moments. For example to determine load F_3 in Fig. A2.6 we take moments about the intersection of forces F_1 and F_2 or point 0.

Thus $\Sigma M_0 = 1400 \times 30 - 18.97\, F_3 = 0$

Hence $F_3 = \frac{42000}{18.97} = 2215\#$ compression (or acting as assumed)

To find the arm of the force F_3 from the moment center 0 involves a small amount of calculation, thus in general it is simpler to resolve the unknown force into H and V components at a point on its line of action such that one of these components passes thru the moment center and the arm of the other component can usually be determined by inspection. Thus in Fig. A2.8 the force F_3 is resolved into its component F_{3V} and F_{3H} at point 0'.



Then taking moments about point 0 as before $\Sigma M_0 = 1400 \times 30 - 20\, F_{3H} = 0$ whence

$F_{3H} = \frac{42000}{20} = 2100\#$. Hence $F_3 = \frac{31.6}{30} \times 2100 = 2215\#$ as previously determined. Determine the load F_1 assuming that F_2 and F_3 are also unknown. We take the moments about point "m" (see Fig. A2.6) the intersection of forces F_2 and F_3. Then $\Sigma M_m = 1400 \times 60 - 500 \times 30 - 500 \times 30 - 30F_1 = 0$. Hence $F_1 = \frac{84000}{30} = 2800\#$ tension as assumed, since algebraic sign comes out positive.

To find force F_2 with one equation we take moments about point "r" the intersection of forces F_1 and F_3 (see Fig. A2.9).

To eliminate the solving for the arm from point r to line of action of F_2, the force F_2 has been resolved into its V and H components at point 0 on its line of action.

Then $\Sigma M_r = -1400 \times 30 + 500 \times 60 + 60\, F_{2V} = 0$

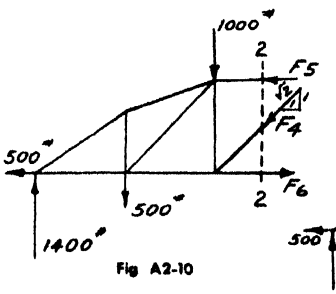
Hence $F_{2V} = \frac{12000}{60} = 200\#$ compression as assummed.

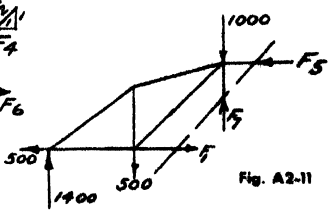
Then $F_2 = 200 \times \sqrt{2} = 282\#$ compression.

A2.4 Method of Shears

In Fig. A2.5 to find the stress in member F_4 we cut the section 2-2 giving the free body for the left portion as shown in Fig. A2.10.

The method of moments is not sufficient to solve for member F_4 because the intersection of the other two unknowns F_5 and F_6 lies at infinity. Thus for conditions where two of the 3 cut members are parallel we have a method of solving for the web member of the truss commonly referred to as the method of shears, or the summation of all the forces normal to the two parallel unknown chord members must equal zero. Since the parallel chord members have no component in a direction normal to their line of action, they do not enter the above equation of equilibrium.





Thus in Fig. A2.10

$\Sigma V = 1400 - 500 - 1000 - \frac{1}{\sqrt{2}} F_4 = 0$

Hence $F_4 = -141\#$ (tension or opposite to sense assumed in Fig. A2.10) Find the stress in member F_7 by the method of shears. In Fig. A2.5 we cut the section 3-3 giving the free body of the left portion as shown in Fig. A2.11

$\Sigma V = 1400 - 500 - 1000 + F_7 = 0$

$F_7 = 100\#$ (compression as assumed)

Note: The student should solve this example illustrating the methods of moments and shears using as a free body the portion of the truss to the right of the cut sections instead of the left portion as used in these illustrative examples. In order to solve for the stresses in the members of a truss most advantageously, one usually makes use of more than one of the above three methods, as each has its advantages for certain cases or members. It is important to realize that each is a method of sections and in a great many cases, such as trusses with parallel chords, the stresses can practically be found mentally without writing down equations of equilibrium. The following statements in general are true for parallel chord trusses:

(1) The vertical component of the stress in the panel diagonal members equals the vertical shear (algebraic sum of external forces to one side of the panel) on the panel, since the chord members are horizontal and thus have zero vertical component.

(2) The truss verticals in general resist the vertical component of the diagonals plus any external loads applied to the end joints of the vertical.

(3) The load in the chord members is due to the horizontal components of the diagonal members and in general equals the summation of these horizontal components.

To illustrate the simplicity of determining stresses in the members of a parallel chord truss, consider the cantilever truss of Fig. A2.12 with supporting reactions at points A and J.

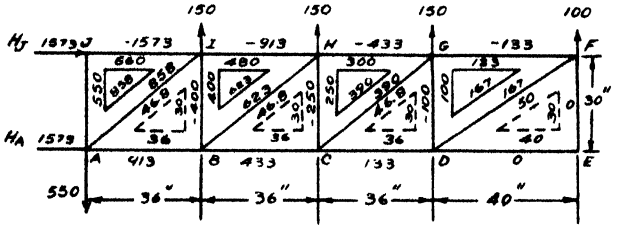


Fig. A2-12

First, compute the length triangles in each panel of the truss as shown by the dashed triangles in each panel. The other triangles in each panel are referred to as load or index triangles and their sides are directly proportional to the length triangles.

The shear load in each panel is first written on the vertical side of each index triangle. Thus, in panel EFGD, considering forces to the right of a vertical section cut thru the panel, the shear is 100#, which is recorded on the vertical side of the index triangle.

For the second panel from the free end, the shear is 100 + 150 = 250 and for the third panel 100 + 150 + 150 = 400#, and in like manner 550 for fourth panel.

The loads in the diagonals as well as their horizontal components are directly proportional to the lengths of the diagonal and horizontal side of the length triangles. Thus, the load in diagonal DF = $\frac{50}{30}$ x 100 = 167 and CG = $\frac{46.8}{30}$ x 250 = 390.

The horizontal component of the load in diagonal DF = $\frac{40}{30}$ x 100 = 133 and for CG = $\frac{36}{30}$ x 250 = 300. These values are shown on the index triangles for all panels. We start our analysis proper for the loads in the members of the truss by considering joint E first.

Using $\Sigma V = 0$ gives EF = 0 by observation, since no external vertical load exists at joint E. Similarly, by the same reasoning for $\Sigma H = 0$, load in DE = 0. The load in the diagonal FD equals the value on the diagonal of the panel index triangle or 167#. It is tension by observation since the shear in the panel to the right is up and the vertical component of the diagonal FD must pull down for equilibrium.

Considering Joint F. $\Sigma H = -FG - FD_H = 0$, which means that the horizontal component of the load in the diagonal DF equals the load in FG, or is equal to the value of the horizontal side in the index triangle or - 133#. It is negative because the horizontal component of DF pulls on Joint F and therefore FG must push against the joint for equilibrium.

Considering Joint D:-

$\Sigma V = DF_V + DG = 0$. But DF_V = 100 (vertical side of index triangle)

$\therefore$ DG = -100

$\Sigma H = DE + DF_H - DC = 0$, but DE = 0 and DF_H = 133 (from index triangle)

$\therefore$ DC = 133

Considering Joint G:-

$\Sigma H = GH - GF - GC_H = 0$. But GF = - 133, and GC_H = 300 from index triangle in the second panel. Hence GH = - 433#. Proceeding in this manner, we obtain the stress in all the members as shown in Fig. A2.12. All the equilibrium equations can be solved mentally and with the calculations being done on the slide rule, all member loads can be written directly on the truss diagram.

Observation of the results of Fig. A2.12 show that the loads in the truss verticals equal the values of the vertical sides of the index load triangle, and the loads in the truss diagonals equal the values of the index triangle diagonal side and in general the loads in the top and bottom horizontal truss members equal the summation of the values of the horizontal sides of the index triangles.

The reactions at A and J are found when the above general procedure reaches joints A and J. As a check on the work the reactions should be determined treating the truss as a whole.

Fig. A2.13 shows the solution for the stresses in the members of a simply supported Pratt Truss, symmetrically loaded. Since all panels have the same width and height, only one length triangle is drawn as shown in Fig. A2.14. Due to symmetry, the index triangles are drawn for panels to only one side of the truss center line. First, the vertical shear in each panel

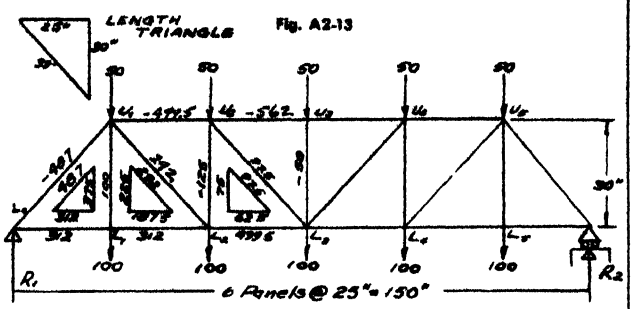


Fig. A2-13

is written on the vertical side of each index triangle. Due to the symmetry of the truss and loading, we know that one half of the external loads at joints U_3 and L_3 is supported at reaction R_1 and 1/2 at reaction R_2, or shear in center panel = (100 + 50) 1/2 = 75. The vertical shear in panel $U_1U_2L_1L_2$ equals 75 plus the external loads at U_2 and L_2 or a total of 225# and similarly for the end panel shear = 225 + 50 + 100 = 375#. With these values known, the other two sides of the index triangles are directly proportional to the sides of the length triangles for each panel, and the results are as shown in Fig. A2.13.

The general procedure from this point is to find the loads in the diagonals, then in the verticals, and finally in the horizontal chord members.

The loads in the diagonals are equal to the values on the hypotenuse of the index triangles. The sense, whether tension or compression, is determined by inspection by cutting mental sections thru the truss and noting the direction of the external shear load which must be balanced by the vertical component of the diagonals.

The loads in the verticals are determined by the method of joints and the sequence of joints is so selected that the stress in the vertical member is the only unknown in the equation $\Sigma V = 0$ for the joint in question.

Thus for joint U_2, $\Sigma V = -50 - U_2L_2 = 0$ or $U_2L_2 = -50$.

For joint U_2, $\Sigma V = -50 - U_2L_{2V} - U_2L_2 = 0$, but $U_2L_{2V} = 75$, the vertical component of U_2L_2 from index triangle. $\therefore U_2L_2 = -50 - 75 = -125$. For joint L_1, $\Sigma V = -100 + L_1U_1 = 0$, hence $L_1U_1 = 100$.

Since the horizontal chord members receive their loads at the joints due to horizontal components of the diagonal members of the truss, we can start at L_0 and add up these horizontal components to obtain the chord stresses. Thus, $L_0L_1 = 312$ (from index triangle). $L_1L_2 = 312$ from $\Sigma H = 0$ for joint L_1. At joint U_1, the horizontal components of diagonal members = 312 + 187.5 = 499.5. Therefore, load in $U_1U_2 = -499.5$. Similarly at joint L_2, $L_2L_3 = 312 + 187.5 = 499.5$#. At joint U_2, the horizontal components of U_1U_2 and $U_2U_3 = 499.5 + 62.5 = 562$ which must be balanced by - 562 in member U_2U_3.

The reaction R equals the value on the vertical side of our index triangle in the end panel, or 375#. This should be checked using the truss as a whole and taking moments about R_2.

If a truss is loaded unsymetrically, the reactions should be determined first, after which the index triangles can be drawn, starting with the end panels, since the panel shear is then readily calculated.

A2.4a Problems

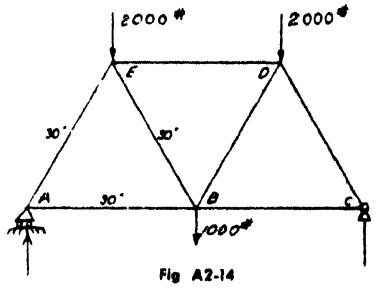


Fig A2-14

(1) Determine the primary stresses in the members of the Warren Truss shown in Fig. A2.14.

(2) Find the stresses in the members of the Pratt Truss shown in Fig. A2.15. P = 800#. Use method of index stresses.

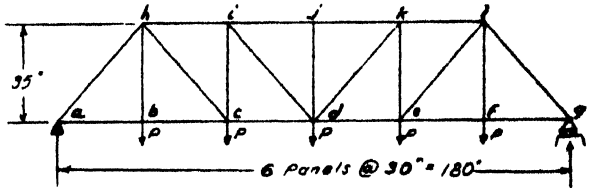


Fig A2-15

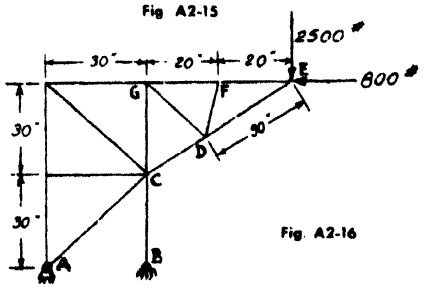


Fig. A2-16

(3) Determine the stresses in the members of the truss shown in Fig. A2.16.

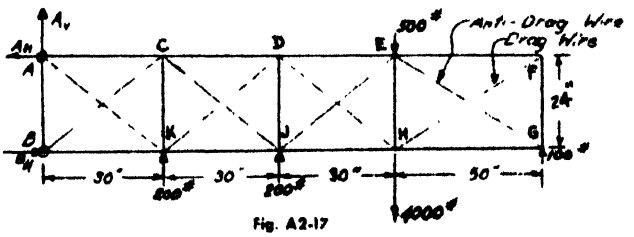


Fig. A2-17

(4) Determine the loads in the members of the wing drag truss of Fig. A2.17. Wires in compression are assumed out of action. Use method of index stresses.

(5) Determine the stresses in members, a, b, c, d, e, and f, of the fuselage truss shown in Fig. A2.18.

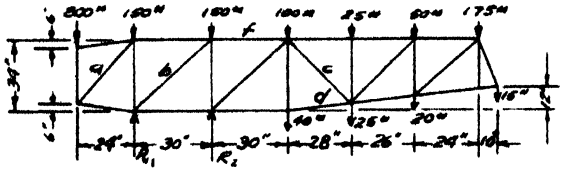


Fig. A2-18

Graphical Truss Analysis

A2.5 Introduction. For truss structures of one or two panels and for parallel chord trusses with any number of panels, it is usually best to solve for the stresses in the truss members by the analytical methods as explained in the previous pages. In airplane construction, the fuselage in many instances, consists of a rectangular frame composed of four trussed type beams and these trusses usually consist of non-parallel chord members and incorporate a large number of panels. In general a graphical solution for the truss member stresses is more convenient and rapid for this type of truss. Thus, the graphical method will be explained by the application to the solution of a simple truss.

Example Solution. Fig. A2.19 shows a Fink truss with a given loading. The first step is to determine the unknown reactions. This may be done graphically, however, for parallel force systems, the analytical solution for the reactions saves time. Taking moments about R_1:-

$\Sigma M_{R_1} = 2000x20 + 4000 \times 40 + 2500 \times 60 + 1000 \times 80 - 80R_2 = 0$

$\therefore R_2 = 5375\#$

$\Sigma V = 5375 - 10000 + R_1 = 0 \quad \therefore R_1 = 4625\#$

Check by taking moments about R_2:

$\Sigma M_{R_2} = 4625x80 - 500x80 - 2000x60 - 4000x40 - 2500x20 = 370000 - 370000 = 0$ (check)

Beginning with the number 1, we place a numeral between each of the external forces and reactions (see numbers 1 to 8 on Fig. A2.19). In each triangle of the truss, we place a letter (a to d in Fig. A2.19). Any external load or reaction is designated by the number on each side of its action line, and a truss member is designated by the number and letters on each side of the member. For example, R_1 is designated by 8-1 and the load at the top point of the truss by 3-4. Similarly, the lower chord members of the truss are denoted by a-8 and d-7. Since airplane fuselage trusses are subjected to a large number of panel point loads, it is better to use numbers for designating external loads and reactions and letters for the truss triangles, which will very seldom exceed the number of letters in the alphabet. An additional convenience of this system of designation is the obvious distinction between external loads and truss members, since external loads are designated only by numbers, whereas the truss members by letters or a combination of a letter with a number.

The loads in the truss members at any joint, together with any external forces at that joint, form a concurrent force system. The graphical solution involves the drawing of a magnitude-direction polygon for each joint. For equilibrium, this polygon must close and since the directions of all the loads on the joints are known, the unknowns are magnitudes. For a concurrent system, only two unknowns can be determined, thus, to start the graphical solution, a joint must be selected which has only two unknown forces. In the given truss, either of the two end joints could be selected as a starting point, since only two unknowns exist. In general, it is customary to start at the left end and work to the right, proceeding clockwise around each joint in drawing the magnitude-direction polygons.

Thus, starting with the joint at the left end, and treating it as a free body, we have four forces, 8-1, 1-2, 2-a, and a-8. The magnitudes and directions of 8-1 and 1-2 are laid off first in Fig. A2.20 in the order named. From point 2 a line parallel to member 2-a of Fig. A2.19 is drawn without any definite length, since its magnitude is unknown. For equilibrium, this magnitude-direction polygon must close, thus we draw a line thru point 8 parallel to member a-8 in Fig. A2.19. This line intersects the line just previously drawn thru point 2 at point a in our polygon of Fig. A2.20. The magnitude of the load or stress in members 2-a and a-8 equals the scaled length of the sides 2-a and a-8 in the polygon of Fig. A2.20 and which scale 9260 and 8300. The sense of the forces in the polygon of Fig. A2.20 must be continuous from start to end. To determine whether the stress in the members is tension or compression, imagine the line representing the magnitude-direction of a member in Fig. A2.20 to be made to coincide with the member of the truss in Fig. A2.19. Then, if the direction of the arrow as found in Fig. A2.20 pushes toward the joint under consideration, the member is in compression; if the arrow is pulling away from the joint, the member is in tension. The numerical values, with the signs plus or minus to indicate tension or compression, are usually indicated or written adjacent to the members of the truss, as illustrated in Fig. A2.27.

We now proceed to an adjacent joint which has only two unknowns. The upper adjacent joint has two unknowns, namely 3-b and b-a. The load in a-2 is known by the solution in Fig. A2.20. Figure. A2.21 shows the magnitude-direction polygon for this joint. Themagnitudes and directions of a-2 and 2-3 are laid off and the polygon is closed by drawing the directions of 3-b and b-a, which locates point b in Fig. A2.21. The magnitude of 3-b and b-a scale -7000 and -2270, with the sense as noted.

At the lower middle joint, the magnitudes of members b-c, c-d and d-7 are unknown, and thus, the solution of this joint is not possible as yet because of more than 2 unknowns. However, at the upper center joint, only two unknowns exist, namely, 4-c and c-b. Fig. A2.22 shows the magnitude-direction polygon for this joint, from

which the magnitudes of 4-c and c-b are obtained.

There are but two unknowns at each of the three remaining joints and they can be drawn in any order. Figures A2.23, A2.24, and A2.25 show the magnitude-direction polygons for these three joints. Polygon A2.25 is not necessary, since the loads in all members are known, however it is drawn using the known magnitudes to see if the polygon will close, which gives a check on the accuracy of drawing the previous polygons.

Since any two adjacent joints in a truss have one side in common, the magnitude-direction polygons for these adjacent joints will have one side in common, hence in our example problems, any one of our joint diagrams could have been added to the preceding or following diagram. If this process is followed, one complete figure referred to as the stress polygon is drawn, which gives all the magnitudes and directions of all members and external loads on the truss. This stress polygon is shown in Fig. A2.26 and is the diagram that would be obtained if the diagrams for the individual joints were superimposed on each other in the proper manner.

The general procedure of drawing the stress polygon as illustrated in Fig. A2.26 is as follows:- First draw the magnitude-directions of all external forces. In our example truss all external loads are parallel, hence the forces 1-2, 2-3, 3-4, 4-5, 5-6, 6-7, 7-8, and 8-1, which are laid off in this clockwise order, form a straight line as shown. In drawing the last force 8-1, the beginning point of force 1-2 should be reached, which shows that ΣV for the external forces equal zero. Now starting with the joint at the left end and going clockwise around the joint, the knowns 8-1 and 1-2 are already drawn on our "load line"; from point 2 on our stress polygon, we draw a line parallel to member 2-a of Fig. A2.19 and from point 8 on our stress diagram a line parallel to member a-8 of the truss. Their intersection gives point a in our stress polygon, and the magnitudes of 2-a and a-8 are found by scaling these lengths. The sense is determined as explained previously. Considering the upper adjacent joint next, a-2 is already known as is 2-3, and both of these forces have already been drawn in our stress polygon. Thus, starting at point 3, draw a line parallel to 3-b of Fig. A2.19 and from point a in the stress diagram draw a line parallel to b-a of Fig. A2.19; their intersection gives point b, which determines the magnitude of 3-b and b-a. For the top joint, we read b-3 and 3-4 on our stress diagram and draw 4-c and c-b, which locates point c. For the lower center joint, we read 7-8, 8-a, a-b, b-c and draw c-d and d-7, which locates point d in the stress diagram. Then considering the joint under the 2500# load, we read d-c, d-4, 4-5 in our stress polygon and draw 5-d. If this line 5-d in our stress polygon which is drawn parallel to the member 5-d in Fig. A2.19 and from point 5 in our stress diagram passes through point d, we have a

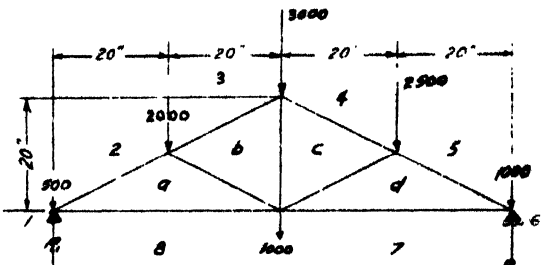
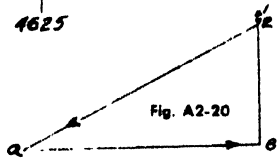
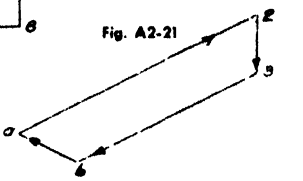
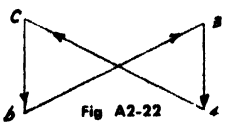
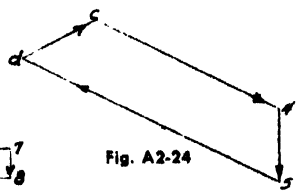


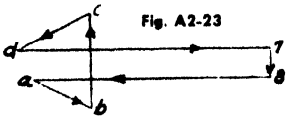
Fig. A2-19

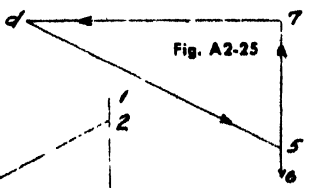

Fig. A2-20

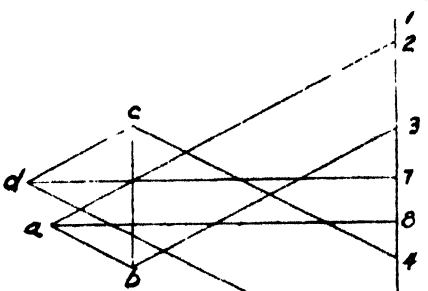

Fig. A2-21


Fig A2-22


Fig. A2-24


Fig. A2-23


Fig. A2-25


Fig. A2-26

STRESS DIAGRAM or combined magnitude-direction polygon.

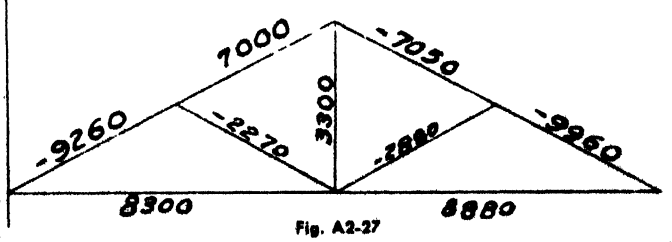


Fig. A2-27

check on the accuracy of the drawing of the stress diagram, since the direction of 5-d should go through point d on our stress polygon.

After the complete stress polygon is drawn, and a closure has been obtained the magnitudes of all members are scaled from the stress diagram and recorded with their proper sense (tension and compression) on the truss members as illustrated in Fig. A2.27.

It is always a good policy, before starting a stress polygon to be sure that the external load system is in equilibrium by taking moments algebraically about some point to see if they are zero.

In drawing a stress diagram, consistency must be followed in drawing the magnitude-directions for each joint by either proceeding clockwise about all joints or counter-clockwise, otherwise a confusion in the designating of the members will result.

A2.6 The Use of Auxiliary or Phantom Members

Figs. A2.28 and A2.29 illustrate the member arrangement of two common trusses. Fig. A2.28 represents the conventional Fink roof truss. In drawing the stress diagram for this truss, we start at joint L_0 and follow with joints U_1 and L_1. This is possible because only two unknows exist at each joint. However, in proceeding to either joint U_2 or L_2 , we find 3 unknowns, thus the stress diagram for these joints can not be drawn. To get around this difficulty members de and ef are replaced temporarily by the phantom member connecting the joints L_2and U_2 (shown dashed in Fig. A2.28. The member stresses at joint U_2 can now be found by drawing the stress

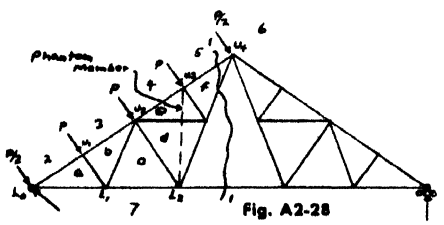


Fig. A2-28

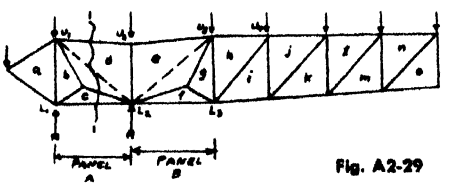


Fig. A2-29

diagram of joint U_2. Next the stress diagram of joint U_2 can be drawn since only two unknown members stresses exist and thus the stress in member U_2 U_4 is obtained. This stress in U_2 U_4 is the true stress since the insertion of the phantom member will not change the load in this member. This is evident if a section 1-1 is drawn as indicated in Fig. A2.28. To find the load in U_2 U_4 analytically, we take moments about L_2 the intersection of the other two members cut by the section 1-1. In this moment equation the loads in the web members de and ef or the phantom member will not enter, thus the web member arrangement can not effect the load in U_2 U_4. Having found the true load in U_2 U_4 the phantom member is removed, and stress diagrams of joints U_2 and U_2 and L_2 can be drawn since only two unknowns will exist at any one joint.

Fig. A2.29 illustrates a typical fuselage tubular truss condition. In order to obtain space to remove large items thru the side of the fuselage such as fuel tanks or in some cases to install a passenger door the web member arrangement as illustrated in panels A and B may be necessary. If the stress diagram for this truss is started difficulty is soon encountered in the form of 3 unknowns at joints L_1, U_1 etc. Thus an auxiliary construction making useof one of the phantom members as shown must be used. For example, members bc, bd and cd are replaced by the phantom diagonal U_1 L_2. With this arrangement stress diagrams can be drawn for joints L_0, L_1 and U_1. In the solution of joint U , the stress in U_1 U_2 will be the true stress regardless of the change in the web members. This is evident by cutting a truss section 1-1. To find the load in the member U_1 U_2 we take moments about L_2 and the load in U_1 U_2 will be the same for either web arrangement. Thus after the load in member U_1 U_2 is found using the phantom web member, the original web members are replaced and now joint U_1 can be solved since only two unknowns exist.

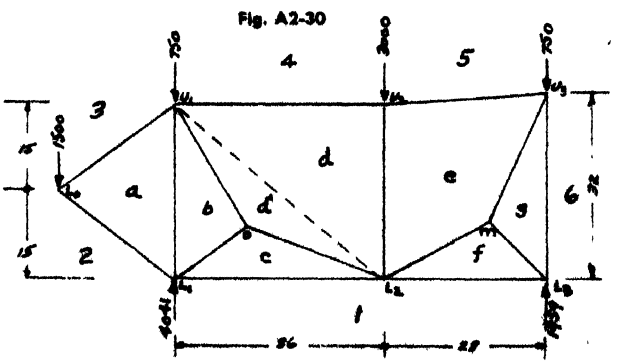
Example Problem of Use of Phantom Members.

Fig. A2.30 shows a truss in which the web members in two of the panels have been so arranged as to give greater open space compared to the general truss where single diagonal panel members are used. Let it be required to draw the stress diagram for the truss when subjected to the given loading.

Solution.

The first step is to calculate the truss reactions at points L_1 and L_2. This is generally done analytically and the results are as shown on Fig. A2.30. Fig. A2.31 shows the complete stress diagram for the truss. Since all loads and reactions are vertical they are laid off to scale as a single vertical line starting

Fig. A2-30



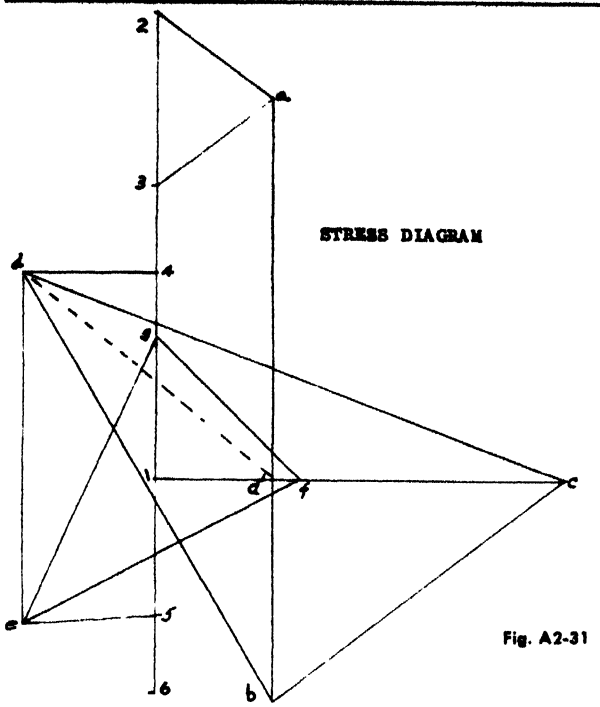


Fig. A2-31

with load 2-3 of 1500#, thus giving the line 2-3, 3-4, 5-6, 6-1 and 1-2 which closes on the beginning point 2. Joint L_0 is first eonsidered since 3 unknown member loads exist at all other joints. Starting at point 2 on stress diagram, the force 2-3 is already laid off. From point 3, a ray parallel to member 3a of Fig. A2.30 is drawn. From point 2, a ray is drawn parallel to member a-2. The intersection of these two rays locates point a and determines the magnitudes of the members a-2 and 3-a.

In going to either truss joint L_1 or U_1 we find that three unknown member loads exist, thus joints can not be solved since two unknowns is the maximum number. To get around this difficulty, the truss members b-d, b-c and c-d are replaced by the auxiliary or phantom diagonal member d-d' shown dashed in Fig. A2.30. With this modification, we have only two unknown member stresses at joint L_1, namely ad' and 1-d'. The stress polygon for this joint is now laid off in Fig. A2.31 starting at point 1. The magnitudes of 1-2 and 2-a are already drawn from previous construction. From point a, a ray is drawn parallel to member ad' and from point 1, a ray parallel to member d-1 is drawn, the intersection of which locates point d. Now considering joint U_1,d'a, a-3 and 3-4 are knowns, leaving 4-d and d-d' as unknowns. Starting stress polygon for this joint at point d', the three known loads are already drawn from previous construction. The polygon for the joint is closed by drawing rays parallel to members 4-d and d-d' from points 4 and d' respectively, the intersection of which locates point d. The length of the line 4-d in Fig. A2.31 is the true magnitude of the load in truss member 4-d since the replacing of the three web members by the phantom diagonal will not change the final load in member 4-d as explained in the previous article.

We now remove the phantom member and replace the original three web members. Now at joint U_1, are known a-3, 3-4 and 4-d leaving only two unknowns d-b and b-a. A new stress polygon is drawn for this joint by starting at point b in Fig. A2.31. We find rays representing members b-a, a-3, 3-4 and 4-d already drawn. The polygon for the joint is closed by drawing rays from d and a parallel to members d-b and b-a respectively, the intersection of which locates point b.

The balance of the stress diagram is constructed considering the remaining joints in the following order: L_1,0, U_2, L_2, m, U_3 and L_3. No difficulty is encountered because only two unknowns or less are found at any of the remaining joints.

If the stress diagram were constructed starting at right end of truss, then a phantom diagonal in the right end panel would be necessary in making a solution.

Phantom Members for Trusses With Loads Applied At Internal Panel Joints

Fig. A2.32 shows a truss with a load applied at the internal panel joint O. To avoid confusion in lettering, a simple solution is to move the load at O along its line of action until it lies outside the truss and is then treated as an external load and lettered accordingly as shown in Fig. A2.33. The line of action of the force is replaced by a phantom member extending from point O' to point O (Fig. A2.33). This phantom member is lettered and is treated as an actual member in the stress diagram. The load in the phantom member will be found to equal the applied load at O and will not influence the loads in any of the other truss members.

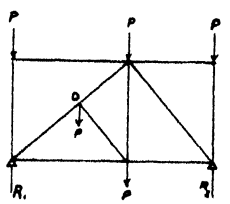


Fig. A2-32

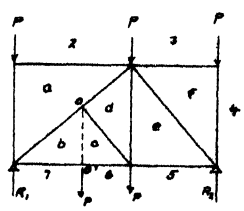


Fig. A2-33

Problems

(1) Solve graphically for the axial loads in the members of the truss in Figs. A2.14, A2.16, and A2.18.

(2) Draw the stress diagram for the truss and loading of Fig. A2.34.

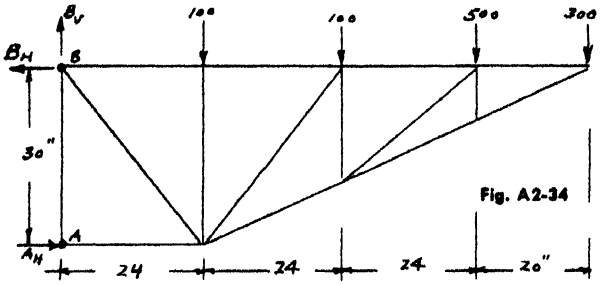


Fig. A2-34

(3) Draw the stress diagram for the truss and loading of Fig. A2.35.

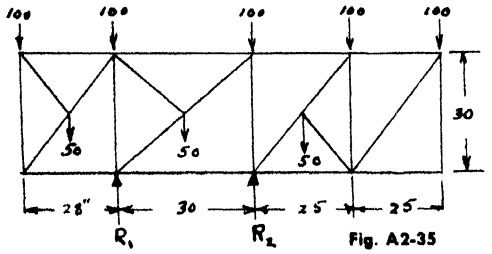


Fig. A2-35

(4) Draw the stress diagram for the engine nacelle truss and loading of Fig. A2.36.

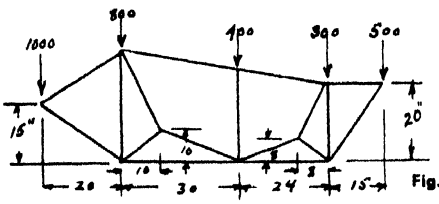


Fig. A2-36

(5) Draw the stress diagram for the Fink truss and loading of Fig. A2.36a

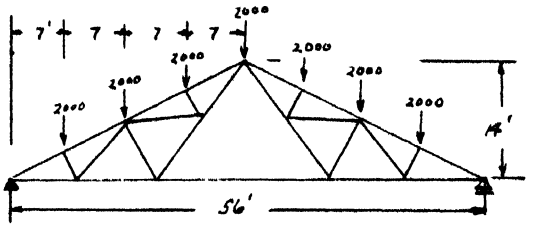


Fig. A2-36a

(6) Draw the stress diagram for the truss and loading of Fig. A2.36b. Solve analytically for the stresses in members a, b, c, d, and e.

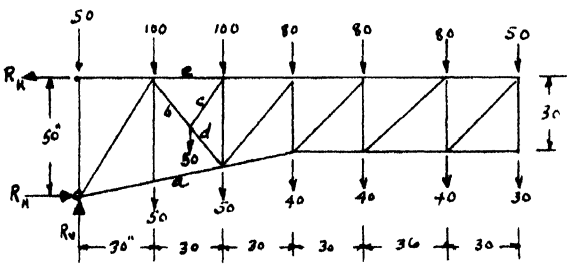
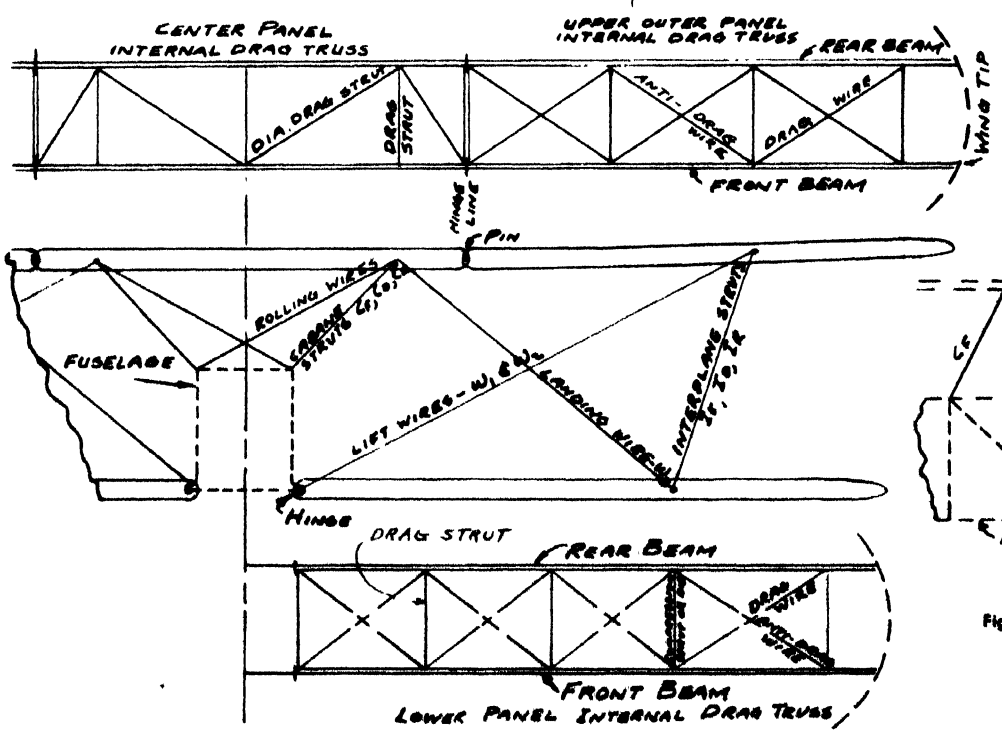


Fig. A2-36b



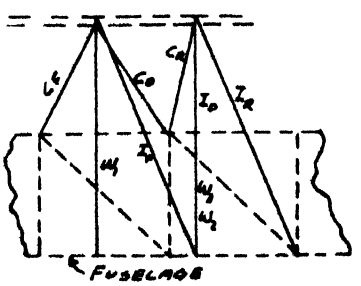


Fig. A2-37

A2.7 Analysis of Truss Systems for Externally Braced Monoplanes and Biplanes

The metal covered cantilever wing with its over-all better aerodynamic efficiency together with its sufficient torsional rigidity has gradually replaced the externally braced monoplane and biplane in the last 10 years. However, for small commercial planes and such military airplanes as trainers, the externally braced wing is still being used in airplane structural design.

Fig. A2.37 (on opposite page) shows the structural layout of a conventional externally braced biplane. The upper wing consists of two sections, an outer panel and a center panel, and the lower wing consists of a single panel. A drag truss consisting of the wing beams, drag struts, and drag wires is incorporated in each wing panel. These trusses will resist loads parallel to the wing chord direction. See Fig. A2.38 and 39 for typical drag truss construction. To resist loads in a direction normal to the drag trusses, the wings are tied together with lift wires, landing wires and interplane and cabane struts. The lift wires act when the resultant load on the wings is up and the landing wires act when the wing load is down as in a landing condition or a flight negative accelerated condition. In general the front beams of the upper outer panel and the lower panel together with the front lift wires, the front cabane strut and the front interplane strut form the front lift truss; the rear wing beams, wires and struts the rear lift truss. In addition to the lift and drag trusses there are two "stagger" or "incidence" trusses, one in the plane of the interplane struts and one in the plane of the cabane struts. The interplane struts tend to equalize the deflection of the front and rear lift trusses. Fig. A2.40 illustrates various types of interplane strut arrangements. The cabane wires, generally referred to as "rolling" wires are primarily for resisting unsymmetrical wing loads.

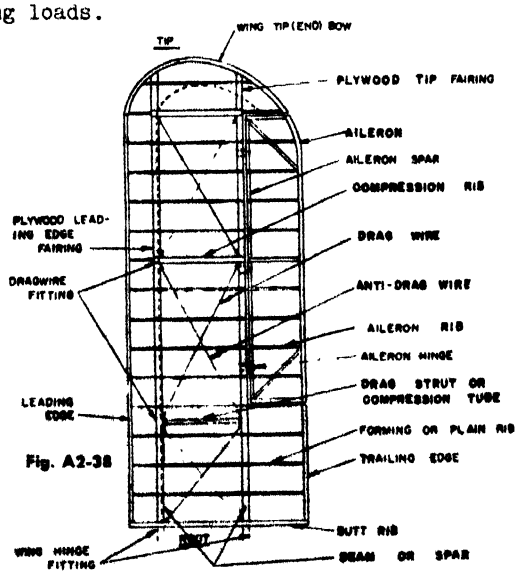


Fig. A2-38

To illustrate the stress solution for wing cellule structures several example problems will be carried thru for only one loading condition.

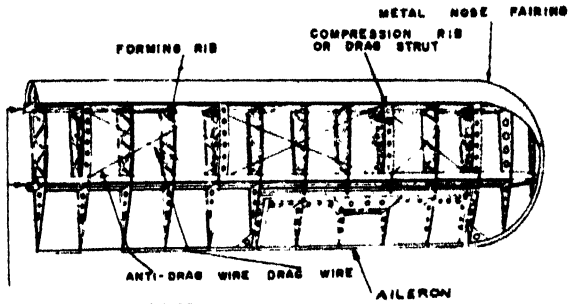


Fig. A2-39


Types of interplane struts.
Fig. A2-40

A2.8 Illustrative Problems

Example #1

Fig. A2.41 shows the structural dimensional diagram of a externally braced monoplane wing. The axial load in the members that form the lift and drag trusses will be determined. A simplified air loading will be used, as the purpose of this chapter is to give student practice in solving trusses. Questions regarding the calculation of the magnitudes and the distribution of air loads will be considered in other chapters.

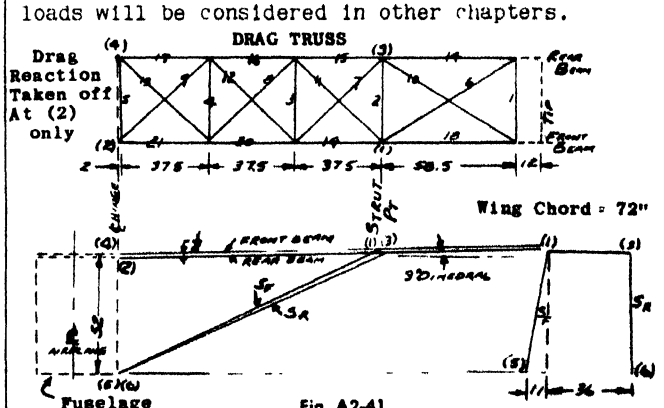


Fig. A2-41

Assumed Air Loading:

(1) A constant spanwise lift load of 45#/in. from hinge to strut point and then tapering to 22.5#/in. at wing tip.

(2) A forward uniform distributed drag load of 6#/in.

Solution

Calculation of running loads on front and rear beams due to lift: For our particular loading the center of pressure will be assumed as shown in Fig. A2.42, hence running load on front beam = 45 x 24.21/36 = 30.26#/in. And for the rear beam the running load equals 45 - 30.26 = 14.74#/in.

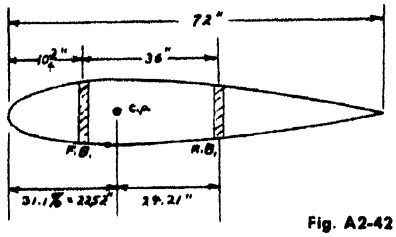
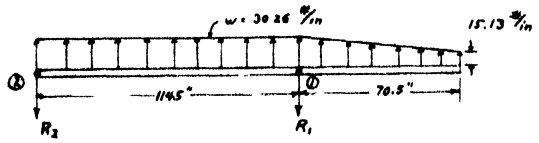


Fig. A2-42

Calculation of beam reactions at hinge and strut points due to lift load:

Front Beam



Taking moments about point (2)

$114.5R_1 - 114.5 \times 30.26 \times 114.5/2 - 15.13 \times 70.5 \times 149.75 - 15.13 \times 35.25 \times 138 = 0.$

hence

$R_1 = 3770\#$

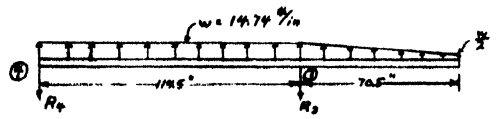
Take $\Sigma V = 0$ where V direction is taken normal to beam

$$\Sigma V = -R_2 - 3770 + 30.26 \times 114.5 + \frac{(30.26 + 15.13)}{2} 70.5 = 0$$

hence $R_2 = 1295\#$

(The student should always check results by taking moments about point (1) to see if $\Sigma M_1 = 0$)

Rear Beam



The rear beam has the same span dimensions but the loading is 14.74#/in. Hence beam reactions R_4 and R_3 will be 14.74/30.26 = .4875 times those for front beam.

hence $R_3 = .4875 \times 3770 = 1838\#$

$R_4 = .4875 \times 1295 = 631\#$

Solution of axial loads in lift truss members at strut point joints (1) and (3):

Table A2.1 gives the V, D and S projections of the lift truss members as determined from the information on Fig. A2.41. The true lengths L and the component ratios then follow by simple calculation.

Table A2.1

Member	Sym.	V	D	S	L	V/L	D/L	S/L
Front Beam	FB	5.99	0	114.34	114.50	.0523	0	.9986
Rear Beam	RB	5.99	0	114.34	114.50	.0523	0	.9986
Front Strut	S_F	57.99	11	114.34	128.79	.4501	.0854	.8878
Rear Strut	S_R	57.49	0	114.34	128.00	.4486	0	.8930

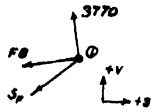
V = vertical direction,

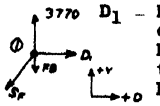
D = drag direction,

S = side direction,

$L = \sqrt{V^2 + D^2 + S^2}$

Joint 1 (Equations of equilibrium)





Drag Truss Reaction on Pin (1)-assume Drag Truss parallel to Drag direction. Error is negligible

$\Sigma V = 3770 \times .9986 - .0523\ FB - .4501\ S_F = 0$ -(1)

$\Sigma S = -3770 \times .0523 - .9986\ FB - .8878\ S_F = 0$-(2)

$\Sigma D = -.0854\ S_F + D_1 = 0$- - - - - - - - - - -(3)

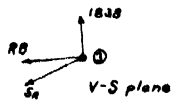
Solving equations 1, 2 and 3, we obtain

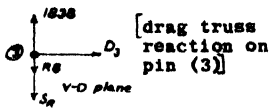
FB = -8513# (compression)

S_F = 9333# (tension)

D_1 = 798# (aft)

Joint (3) (Equations of equilibrium)





[drag truss reaction on pin (3)]

$\Sigma V = 1838 \times .9986 - .0523\ RB - .4486\ S_R = 0$ -(4)

$\Sigma S = -1838 \times .0523 - .9986\ RB - .8930\ S_R = 0$ -(5)

$\Sigma D = D_3 + 0 = 0$ - - - - - - - - - - - - - - - - -(6)

Solving equations 4, 5 and 6, we obtain

RB = -4189# (compression)

S_R = 4579# (tension)

D_3 = 0

Fig. A2.43 shows the reactions of the lift struts on the drag truss at joints (1) and (3) as found above.

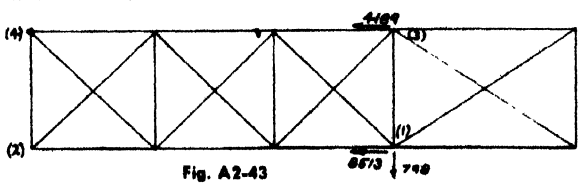


Fig. A2-43

Drag Truss Panel Point Loads Due to Air Drag Load.

It was assumed that the air load components in the drag direction were 6#/in. of wing acting forward.

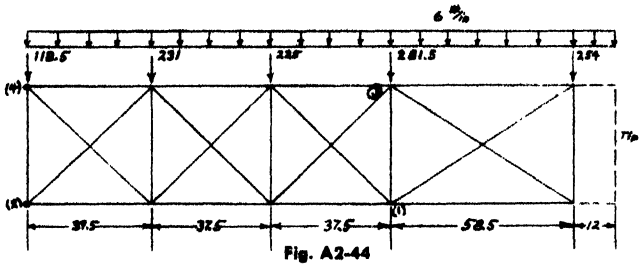


Fig. A2-44

The distributed load of 6#/in. is replaced by concentrated loads at the panel points as shown in Fig. A2.44. Each panel point takes one half the distributed load to the adjacent panel point, except for the two outboard panel points which are affected by the overhang tip portion.

Thus the outboard panel point concentration of 254# is determined by taking moments about (3) of the drag load outboard of (3) as follows:

$$P = 70.5 \times 6 \times 35.25/58.5 = 254\#$$

To simplify the drag truss solution, the drag strut and drag wires in the inboard drag truss panel have been modified to intersect at hinge points (2) and (4). In the design of the beam and fittings at this point, the effect of the actual conditions of eccentricity should of course be considered.

Combined Loads on Drag Truss

Adding the two load systems of Figs. A2.43 and A2.44, the total drag truss loading is obtained as shown in Fig. A2.45. The resulting member axial stresses are then solved for by the method of index stresses (Ref. Art. A2.4). The values are indicated on the truss diagram. It is customary to make one of the fittings attaching wing to fuselage incapable of transferring drag reaction to fuselage, so that the entire drag reaction from wing panel on fuselage is definitely confined to one point. In this example point (2) has been assumed as point where drag is resisted. Those drag wires which would be in compression are assumed out of action.

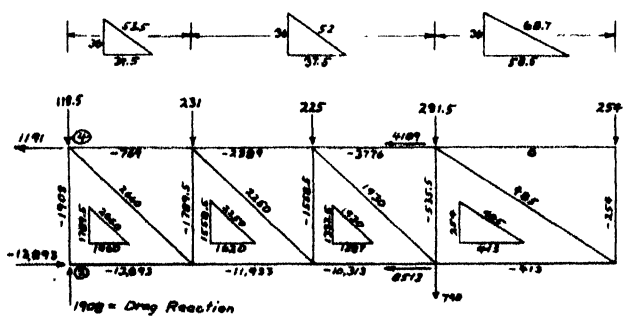


Fig. A2-45

Fuselage Reactions

As a check on the work as well as to obtain reference loads on fuselage from wing structure, the fuselage reactions will be checked against the externally applied air loads. Table A2.2 gives the calculations in table form.

Table A2.2

Point	Member	Load	V	D	S
2	FB Drag Reaction R_2(Reaction)	-13893 - 1908 - 1295	- 726 0 1294	0 -1908 0	-13870 0 - 67
4	RB R_4(Reaction)	1191 - 631	62 630	0 0	1190 - 33
5	F_S	9333	4205	798	8290
6	R_S	4579	2055	0	4090
Totals			7520	-1110	- 400

Applied Air Loads:

V component = (3770 + 1295 + 1838 + 631) .9986 = 753# (error 3#)

D component = -185 x 6 = 1110# (error = 0)

S component = -(3770 + 1295 + 1838 + 631) .0523 = - 394# (error 6#)

Example #2. 3 Bay Externally Braced Monoplane Wing.

Fig. A2.46 shows a high wing externally braced wing structure. The wing outer panel has been made identical to the wing panel of example problem 1. This outer panel attached to the center panel by single pin fittings at points (2) and (4). Placing pins at these points make the structure statically determinate, whereas if the beams were made continuous through all 3 panels, the reactions of the lift and cabane struts on the wing beams would be statically indeterminate since we would have a 3-span continuous beam resting on settling supports due to strut deformation. The fitting pin at points (2) and (4) can be made eccentric with the neutral axis of the beams, hence very little is gained by making beams continuous for the purpose of decreasing the lateral beam bending moments. For assembly, stowage and shipping it is convenient to build such a wing in 3 portions. If a multiple bolt fitting is used at points (2) and (4) to obtain a continuous beam, not much is gained because the design requirements of the various governmental agencies specify that the wing beams must also be analyzed on the assumption that a multiple bolt fitting provides only 50% of the full continuity.

The air loads on the outer panel are taken identical to those in example problem 1. Likewise the dihedral and direction of the lift struts S_F and S_R have been made the same as in example problem 1. Therefore the analysis for the loads in the outer panel drag and lift trusses is identical to that in problem 1. The solution will be continued assuming the running lift load on center panel of 45#/in. and a forward drag load of 6#/in.

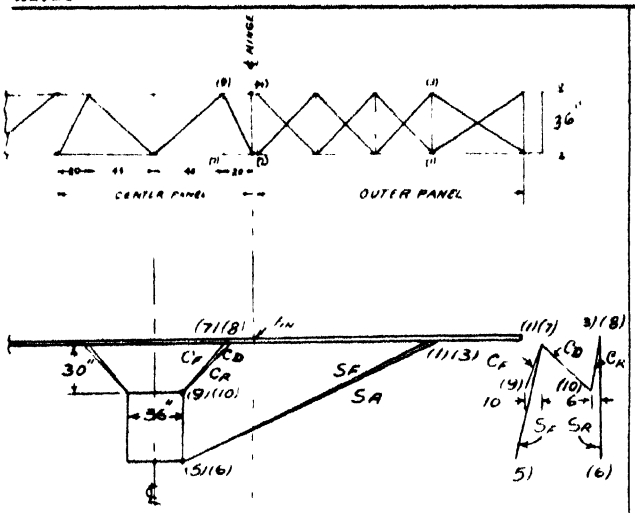


Fig. A2-46

Lengths & Directional Components of Cabane Struts

Member	Sym.	V	D	S	L	V/L	D/L	S/L
Front Cabane	C_F	30	10	27	41.59	.721	.240	.648
Diagonal Cabane Strut	C_D	30	30	27	50.17	.597	.597	.538
Rear Cabane Strut	C_R	29.5	6	27	40.42	.731	.1485	.668
$L = \sqrt{V^2 + D^2 + S^2}$								

Solution of Center Panel

Center Rear Beam

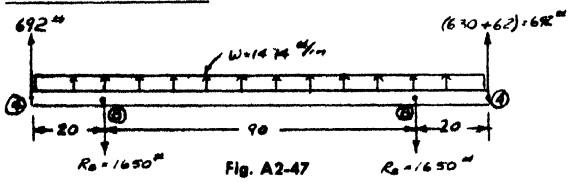


Fig. A2-47

Fig. A2.47 shows the lateral loads on the center rear beam. The loads consist of the distributed air load and the vertical component of the forces exerted by outer panel on center panel at pin point (4). From Table A2.2 of example problem 1, this resultant V reaction equals 630 + 62 = 692#.

The vertical component of the cabane reaction at joint (8) equalsone half the total beam load due to symmetry of loading or 65 x 14.74 + 692 = 1650#.

Solution of Force System at Joint 8



$$\Sigma V = 1650 - .731\ C_R = 0$$

hence

$$C_R = 1650/.731 = 2260\#\ \text{(tension)}$$

$$\Sigma S = -\ CRB - 2260 \times .668 = 0$$

hence

$$CRB = -\ 1510\#\ \text{(compression)}$$

$$\Sigma D = D_8 - 2260 \times .1485 = 0$$

hence

$$D_8 = 336\#\ \text{drag truss reaction}$$

Center Front Beam

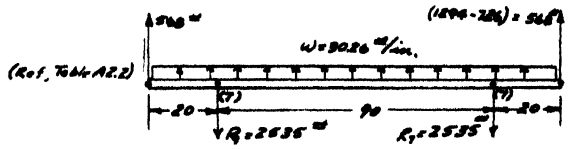
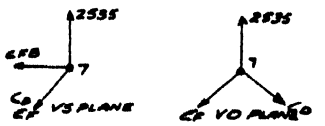


Fig. A2-48

Fig. A2.48 shows the V loads on the center front beam and the resulting V component of the cabane reaction at joint (7).

Solution of Force System at Joint 7



$$\Sigma V = 2535 - .721\ C_F - .597\ C_D = 0$$

$$\Sigma S = -\ CFB - .648\ C_F - .538\ C_D = 0$$

$$\Sigma D = -\ .240\ C_F + .597\ C_D = 0$$

Solving the three equations, we obtain

$$CFB = -2281\ \text{(compression}$$

$$C_F = 2635$$

$$C_D = 1058$$

Solution for Loads in Drag Truss Members

Fig. A2.49 shows all the loads applied to the center panel drag truss. The S and D reactions from the outer panel at joints (2) and (4)

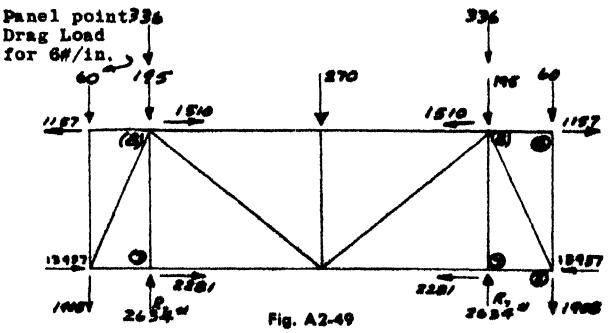


Fig. A2-49

are taken from Table A2.2 of problem 1. The drag load of 336# at (8) is due to the rear cabane strut, as is likewise the beam axial load of - 1510 at (8). The axial beam load of - 2281# at (7) is due to reaction of front cabane truss. The panel point loads are due to the given running drag load of 6#/in. acting forward.

The reaction which holds all these drag truss loads in equilibrium is supplied by the cabane truss at point (7) since the front and diagonal

cabane struts intersect to form a rigid triangle. Thus the drag reaction R_7 equals one half the total drag loads or 2634#.

Solving the truss for the loading of Fig. A2.49 we obtain the member axial loads of Fig. A2.50.

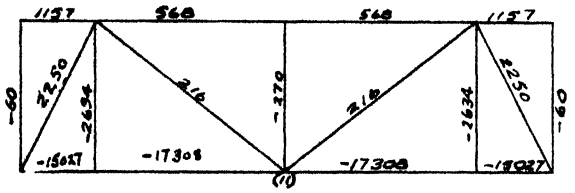


Fig. A2-50

Loads in Cabane Struts Due to Drag Reaction at Point 7



$\Sigma D = -2634 - .240\ C_F + .597\ C_D = 0$

$\Sigma V = -.721\ C_F - .597\ C_D = 0$

Solving for C_F and C_D, we obtain

$C_F = -2740\#$ (compression)

$C_D = 3310$ (tension)

adding these loads to those previously calculated for lift loads:

$C_F = -2740 + 2635 = -105$

$C_D = 1058 + 3310 = 4368\#$

$C_R = 2260\#$

Fuselage Reactions

As a check on the work the fuselage reactions will be checked against the applied loads. Table A2.3 gives the V, D and S components of the fuselage reactions.

Table A2.3

Point	Member	Load	V	D	S
9	Front Strut C_F	-105	-76	-25	-68
10	Rear Strut C_R Dia. Strut C_D	2260 4368	1650 2610	335 -2610	1510 2356
5	Front Lift Strut S_F	9333	4205	798	8290
6	Rear Lift Strut S_R	4579	2055	0	4090
Totals			10444	-1502	16178

Applied Air Loads

V component = 7523 (outer panel) + 65 x 45 = 10448 (check)

D component = -1110 (outer panel) - 65 x 6 = -1500 (error 2#)

The total side load on a vertical plane thru centerline of airplane should equal the S component of the applied loads. The applied side loads = - 394# (see problem 1). The air load on center panel is vertical and thus has zero S component.

From Table A2.3 for fuselage reactions we have $\Sigma S = 16178$. From Fig. A2.50 the load in the front beam at ℄ of airplane equals - 17308 and 568 for rear beam. The horizontal component of the diagonal drag strut at joints 11 equals 216 x 45/57.6 = 169#.

Then total S components = 16178 - 17308 + 568 + 169 = - 393# which checks the side component of the applied air loads.

Example Problem #3 Externally Braced Biplane.

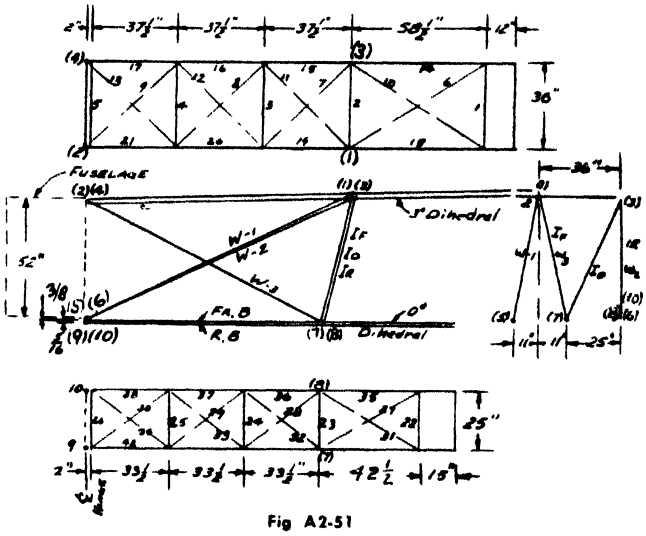


Fig A2-51

Fig. A2.51 shows a typical biplane wing structure. The upper wing panel is identical to the wing in example problem 1. A lower wing panel connected to the upper wing by the interplane struts IF, ID, and IR has been added. The lift struts have been replaced by the lift wires W-1 and W-2. A single landing wire W-3 is also added.

The lift and drag load on the upper wing is the same as in example problem 1. The air loads on the lower panel will be assumed as follows.

Running lift load = 25#/in. of wing span.
Running drag load = -3#/in. of wing span.

Solution

Table A2.4 gives the lengths and component ratios of the lift truss members.

Table A2.4

Member	Symb.	V	D	S	L	V/L	D/L	S/L
Upper Fr. B.	UF	5.99	0	114.34	114.50	.0523	0	.9986
Upper Rear B.	UR	5.99	0	114.34	114.50	.0523	0	.9986
Lower FR. B.	LF	0	0	102.5	102.5	0	0	1.00
Lower Rear B.	LR	0	0	102.5	102.5	0	0	1.00
Fr. Lift Wire	W_1	57.99	11	114.34	128.79	.4501	.0854	.8876
Rear Lift Wire	W_2	57.49	0	114.34	128.00	.4486	0	.8930
Fr. Int. Strut	IF	58.37	11	12	60.60	.9620	.1820	.1980
Dia. Int. Strut	ID	57.87	25	12	64.16	.9015	.3896	.1870
Rear Int. Strut	IR	58.18	0	12	59.40	.9810	0	.2017

$L = \sqrt{V^2 + D^2 + S^2}$

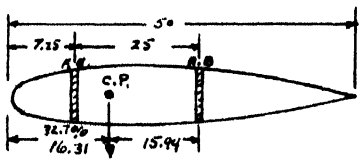
Beam Lift Load Reactions.

The beam reactions on the upper panel beams at points (1) (2) (3) and (4) due to distributed

lift load are identical to those of problem 1, thus the calculations will not be repeated here. The results are:

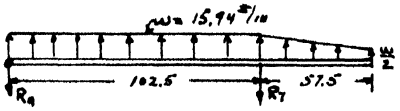
$R_1 = 3770\#$, $R_3 = 1838$
$R_2 = 1295\#$, $R_4 = 631$

Lower Panel Beams:



The running spanwise lift load on lower wing is given as 25#/in. Hence running load on front wing beams equals 25 x 15.94/25 = 15.94#/in. Rear beam = 25 - 15.94 = 9.06#/in.

Front Beams:

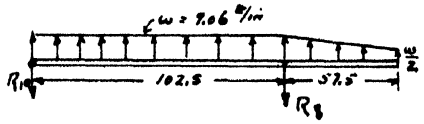


Taking moments about R_8,

$102.5\ R_7 - \frac{102.5^2}{2} \times 15.94 - 7.97 \times 57.5 \times 131.25 - 7.97 \times 28.75 \times 121.67 = 0$ hence $R_7 = 1678\#$.

$\Sigma V = -1678 - R_8 + 102.5 \times 15.94 + 7.97 \times 57.5 + 7.97 \times 28.75 = 0$. hence $R_8 = 644\#$

Rear Beam:



$R_8 = R_7\ (9.06/15.94) = 953\#$

$R_{10} = R_8\ (9.06/15.94) = 366\#$

Solution for Axial Loads in Lift Truss Members.

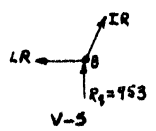
Referring to Fig. A2.51 we find the front lift truss composed of the upper and lower front beams, lift wire W-1 and front incidence strut IF and the rear lift truss composed of the upper and lower rear beams, rear lift wire W-2 and rear strut IR are tied together by the diagonal interplane strut ID. This strut tends to equalize the deflections of the front and rear lift truss by transferring load from the heavily loaded side to the lightly loaded truss. The wing structure would be stable with out this diagonal strut, thus incorporating such a strut makes the wing structure statically indeterminate.

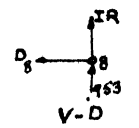
For landing conditions or negative accelerated flight conditions, wires W-1 and W-2 are out of action and a single lift truss wire W-3 is in action. For this condition strut ID is necessary to tie rear beam loads to the single front lift truss. For negative accelerated conditions, the wing structure is statically determinate, because no more than 3 unknown member axial loads exist at any one joint of the lift trusses. For normal flight conditions (W-1 and W-2 in action), we can solve only joint 8 by statics. In proceeding to the other joints we find more than 3 unknown members whereas only 3 equations of statics for a non-coplanar concurrent force system are available. Thus to solve this wing structure it is necessary to consider the relative regidities of the lift and drag trusses, but before this can be done the required member cross-sectional areas must be known, which in turn are determined by the true loads on the members. The design process is therefore in general a trial and error method. To make the wing structure statically determinate one member is removed which is referred to as the rebundant member and loads in all members are calculated under this assumption. Preliminary member sizes are then determined on the basis of these loads. With the member sizes known the load in the rebundant member can be found by a consideration of member axial deformations. In biplanes with a strut for the diagonal interplane strut it is customary to assume either the front or the diagonal strut as the redundant member. If diagonal wires are used, the wires are usually taken as the redundant members.

In this example problem the diagonal interplane strut ID will be assumed as the redundant member. The axial loads for the given air loading will therefore be determined in all members of the lift and drag trusses assuming member ID removed. Example problem #2 of Chapter A8 gives the detailed solution for the load in the redundant member as well as the true load in all the members for the same airplane wing cellule and loading as used in this example.

Solution For Loads in Lift Trusses. Member ID Out.

Joint (8) Equations of Equilibrium





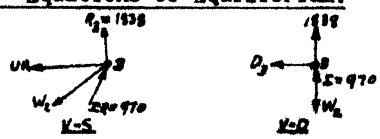
(The drag truss will be assumed horizontal. The error is negligible.)

$\Sigma V = 953 + .981\ IR = 0$, hence $IR = -970\#$

$\Sigma S = -LR - 970 \times .2017 = 0$, hence $LR = -196\#$

$\Sigma D = -D_8 + 0 = 0$, hence $D_8 = 0$, (D_8 = drag truss reaction)

Joint (3) Equations of Equilibrium.



$\Sigma V = 1838 \times .9986 - .0523\ UR - .4486\ W_2 + 970 \times .981 = 0$

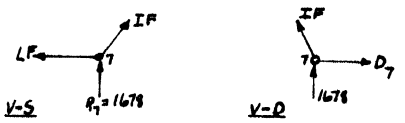
$\Sigma S = -1838 \times .0523 - .9986\ UR - .893\ W_2 + 970 \times .2017 = 0$

$\Sigma D = -D_2 + 0 = 0$, (D_2 = Drag truss reaction)

Solving the three equations we obtain,

$UR = -6160$
$W_2 = 6930$
$D_2 = 0$

Joint (7) Equations of Equilibrium.

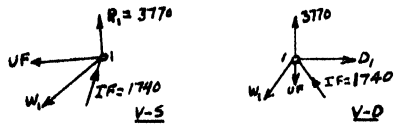


$\Sigma V = 1678 + .962\ IF = 0$, hence $IF = -1740$

$\Sigma S = -LF - 1740 \times .198 = 0$, hence $LF = -344$

$\Sigma D = D_7 + 1740 \times .182 = 0$, $D_7 = -317$

Joint (1) Equations of Equilibrium.



$\Sigma V = 3770 \times .9986 + 1740 \times .962 - .0523\ UF - .4501\ W_1 = 0$

$\Sigma S = -3770 \times .0523 + 1740 \times .198 - .9986\ UF - .8878\ W_1 = 0$

$\Sigma D = -1740 \times .182 - .0854\ W_1 + D_1 = 0$ (D_1 = drag truss reaction)

Solving the three equations we obtain,

$UF = -11780$
$W_1 = 13480$
$D_1 = 1464$

Figs. A2.52, 53 show the loads that are applied to the drag truss at joints 1, 3, 7, and 8, by the lift truss members as determined in the joint solutions.

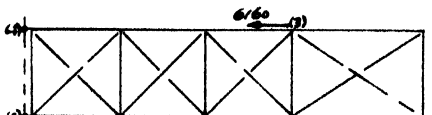


Fig. A2-52

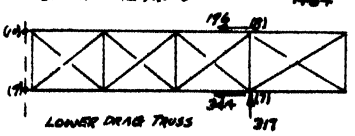


Fig. A2-53

Distributed Drag Loads On Drag Trusses

The air drag loads on the upper panel drag truss are identical to those in example problem 1 since the drag load of -6#/in. is the same. Fig. A2.54 repeats the results of Fig. A2.44 plus those of Fig. A2.52.

The running drag load on lower wing was given as -3#/in. Fig. A2.55 gives the results of replacing the distributed load by a resultant drag truss panel point loading. The loads from Fig. A2.53 also have been added.

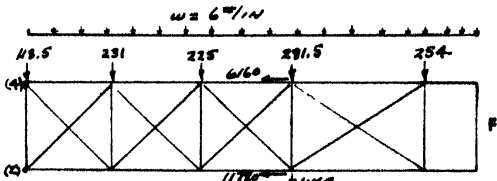


Fig. A2-54

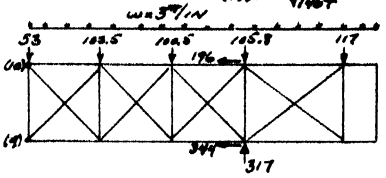


Fig. A2-55

Solution for Loads in Upper and Lower Drag Truss Members.

Figs. A2.56 and A2.57 give the resulting member stresses for the loadings of Figs. A2.54 and A2.55. The student should verify these stresses by writing the index stresses as in previous solutions. The drag reaction on fuselage has been assumed at the front beam points on both panels. Those drag wires which would be in compression in resisting the applied loads are assumed out of action.

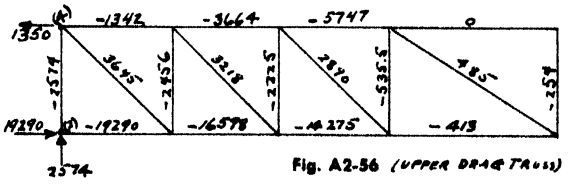


Fig. A2-56 (UPPER DRAG TRUSS)

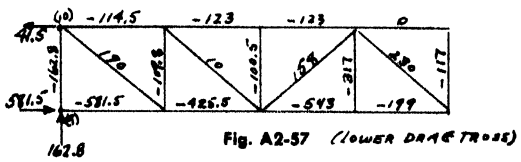


Fig. A2-57 (LOWER DRAG TRUSS)

Fuselage Reactions as A Check On Calculations.

Table A2.5 gives the V D and S components of the fuselage reactions.

Table A2.5

Joint	Member	Load	V	D	S
2	UF. Axial Load	-19290	- 1009	0	-19263
	Beam Air Reaction R_2	1295	1294	0	- 68
	Drag Reaction	2574	0	-2574	0
4	UR. Axial Load	1350	70.5	0	1348
	Beam Air Reaction R_4	631	631.0	0	- 33
9	LF-Beam Axial Load	581.5	0	0	-581. .5
	Beam Reaction R_9	644	644	0	0
	Drag Reaction R_9	162.8	0	- 162.8	0
10	LR Beam Axial Load	41.5	0	0	41.5
	Beam Reaction R_{10}	366	366	0	0
5	Wire W-1	13480	6050	1150	11960
6	Wire W-2	6930	3117	0	6190
		TOTALS	11163	-1590	- 405

Applied Air Loads.

V component = (3770 + 1295 + 1838 + 631) .9986 + 1678 + 644 + 953 + 366 = 11164 (check)

D component = -185 x 6 -160 x 3 = -1590 (check)

S component = -(3770 + 1295 + 1838 + 631) .0523 = -394 (error = - 9#)

PROBLEMS

(1) Fig. A2.58 shows the wing structure of a externally braced monoplane. Determine the axial loads in all members of the lift and drag trusses for the following loads.

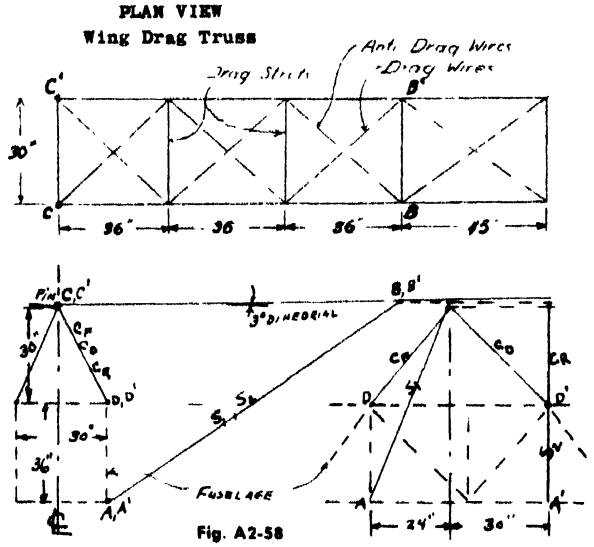


Fig. A2-58

Front beam lift load = 40#/in. (upward)
Rear beam lift load = 25#/in. (upward)
Wing drag load = -10#/in. of wing forward)

(2) For the biplane of Fig. A2.59 determine the axial loads in all members of the lift and drag trusses, assuming the diagonal interplane strut (1D) removed. The running beam and drag loads are as follows:

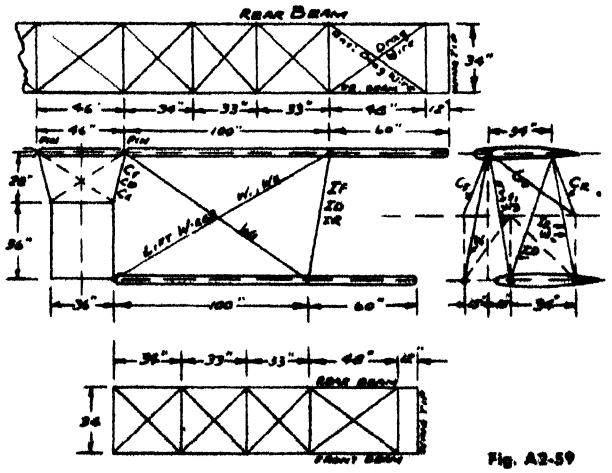


Fig. A2-59

Upper wing - Front Beam = 35#/in. (upward)
Rear Beam = 30#/in. (upward)
Lower wing - Front Beam = 30#/in. (upward)
Rear Beam = 27#/in. (upward)

Drag Loads:
Upper Wing = 8#/in. aft.
Lower Wing = 7#/in. aft.

(3) The inverted flight beam and drag loads for the wing structure of Fig. A2.59 are as follows:

Upper Wing:
Front beam lift load = -20#/in. (downward)
Rear beam lift load = -15#/in. (downward)
Drag load = -5#/in. of wing (forward)

Lower Wing:
Front beam lift load = -18#/in. (downward)
Rear beam lift load = -14#/in. (downward)
Drag = -4#/in. of wing (forward)

Determine the axial loads in all members. (Note:- lift wires w_1 and w_2 are out of action and w_3 is acting, thus member ID does not need to be removed to make structure statically determinate.)

(4) For the airplane in Fig. A2.58 assume the airloads on the left wing structure equal to 80 percent of that on the right side which would simulate a rolling condition. Determine the resultant loads on the cabane struts C_F, C_D and C_R.

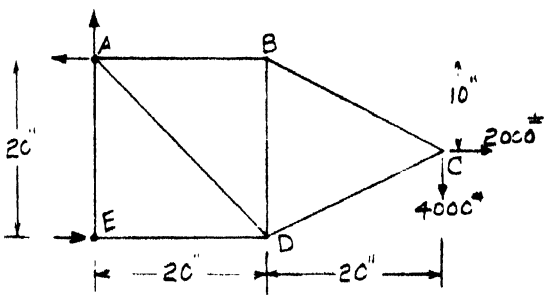


Fig. A2-18a

(6) Calculate the stresses for the loaded truss in Fig. A2.18a.

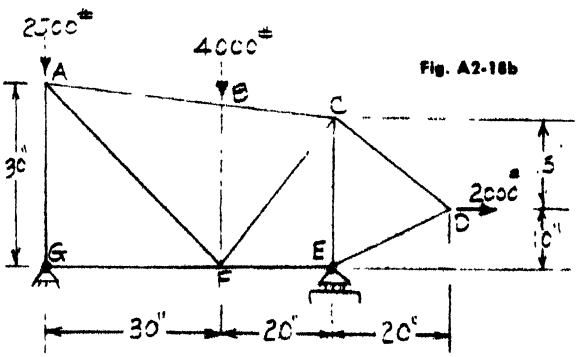


Fig. A2-18b

(7) Calculate the stresses in the members of the truss in Fig. A2.18b.

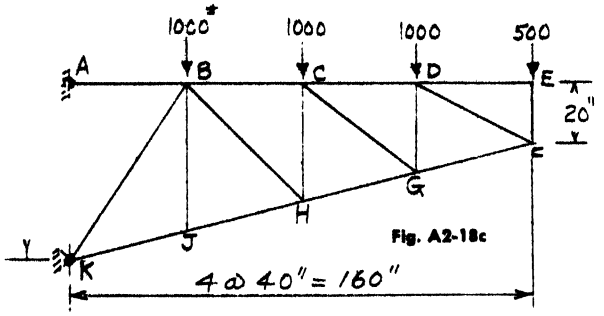


Fig. A2-18c

(8) Calculate the stresses in the members of the cantilever truss of Fig. A2.18c.

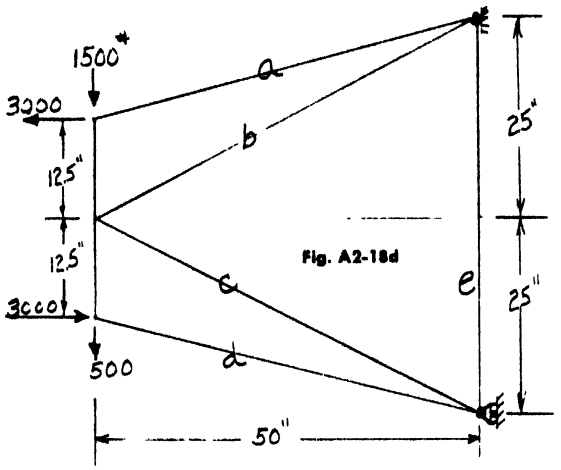


Fig. A2-18d

(9) Fig. A2.18d shows the side truss of an engine mount structure. Calculate the loads in the truss members.

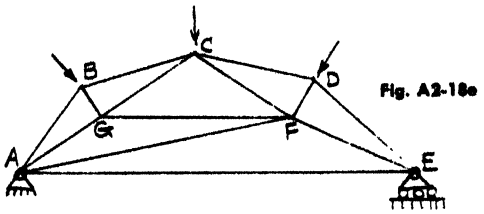


Fig. A2-18e

(10) Fig. A2.18e shows a pin jointed truss
- (a) Is the truss statically determinate?
- (b) If member AE is removed is structure stable and statically determinate?
- (c) If both members AE and AF are removed will structure collapse. Is it statically determinate?

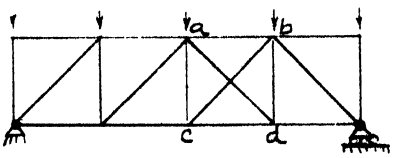


Fig. A2-18f

(11) Is the structure in Fig. A2.18f statically determinate relative to member stresses?

CHAPTER A3

PROPERTIES OF SECTIONS - CENTROIDS MOMENTS OF INERTIA ETC.

A3.1 Introduction In engineering calculations, two terms, center of gravity and moment of inertia, are constantly being used. Thus, a brief review of these terms is in order.

A3.2 Centroids, Center of Gravity. The centroid of a line, area, volume, or mass is that point at which the whole line, area, volume, or mass may be conceived to be concentrated and have the same moment with respect to an axis as when distributed in its true or natural way. This general relationship can be expressed by the principle of moments, as follows:

Lines:- $\bar{x}L = \Sigma Lx$, hence $\bar{x} = \frac{\Sigma Lx}{L} = \frac{\int x dL}{L}$

Areas:- $\bar{x}A = \Sigma ax$, hence $\bar{x} = \frac{\Sigma ax}{A} = \frac{\int x dA}{A}$

Volumes:- $\bar{x}V = \Sigma Vx$, hence $\bar{x} = \frac{\Sigma Vx}{V} = \frac{\int x dV}{V}$

Masses:- $\bar{x}M = \Sigma xm$, hence $\bar{x} = \frac{\Sigma mx}{M} = \frac{\int x dM}{M}$

If a geometrical figure is symmetrical with respect to a line or plane, the centroid of the figure lies in the given line or plane. This is obvious from the fact that the moments of the parts of the figure on the opposite sides of the line or plane are numerically equal but of opposite sign. If a figure is symmetrical to two lines or planes, the centroid of the figure lies at the intersection of the two lines or the two planes, and likewise, if the figure has 3 planes of symmetry, the centroid lies at the intersection of the 3 planes.

A3.3 Moment of Inertia The term moment of inertia is applied in mechanics to a number of mathematical expressions which represents second moments of areas, volumes and masses, such as

$\int y^2 dA$, $\int r^2 dV$, $\int r^2 dy$, etc.

A3.4 Moment of Inertia of an Area . As applied to an area, the term moment of inertia has no physical significance, but represents a quantity entering into a large number of engineering problems or calculations. However, it may be considered as a factor which indicates the influence of the area itself in determining the total rotating moment of uniformly varying forces applied over an area.

Let Fig. A3.1 be any plane area referred to three coordinate axes, ox, oy and oz; ox and oy being the plane of area.

Let dA represent an elementary area, with coordinates x, y, and r as shown.

Then

$$I_X = \int y^2 dA,\ I_Y = \int x^2 dA,\ I_Z = \int r^2 dA$$

where I_X, I_Y and I_Z are moments of inertia of the area about the axes xx, yy and zz respectively.

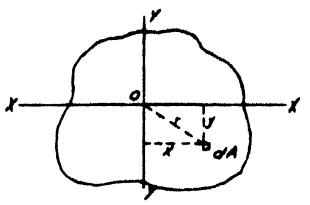


Fig. A3-1

A3.5 Polar Moment of Inertia . In Fig. A3.1, the moment of inertia $I_Z = \int r^2 dA$ about the Z axis is referred to as the polar moment of inertia and can be defined as the moment of inertia of an area with respect to a point in its surface.
Since $r^2 = x^2 + y^2$ (Fig. A3.1)
$I_Z = \int (y^2 + x^2)\, dA = I_X + I_Y$ or; the polar moment of inertia is equal to the sum of the moments of inertia with respect to any two axes in the plane of the area, at right angles to each other and passing thru the point of intersection of the polar axis with the plane.

A3.6 Radius of Gyration The radius of gyration of a solid is the distance from the inertia axis to that point in the solid at which, if its entire mass could be concentrated, its moment of inertia would remain the same.

Thus, $\int r^2 dM = \rho^2 M$, where ρ is the radius of gyration

Since, $\int r^2 dM = I$, then $I = \rho^2 M$ or $\rho = \sqrt{\frac{I}{M}}$

By analogy, in the case of an area,

$$I = \rho^2 A \text{ or } \rho = \sqrt{\frac{I}{A}}$$

A3.7 Parallel Axis Theorem In Fig. A3.2 let I_y be the moment of inertia of the area referred to the centroidal axis y-y, and let the moment of inertia about axis y_1y_1 be required. y_1y_1 is parallel to yy. Consider the elementary area dA with distance x + d from y_1y_1.

Then, $I_{y_1} = \int (d + x)^2 dA$

$= \int x^2 dA + 2d^2 \int x dA + d^2 \int dA$

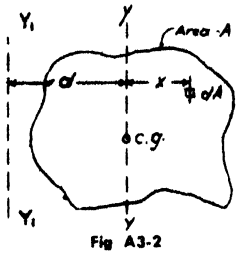


Fig A3-2

The first term, $\int x^2 dA$, represents the moment of inertia of the body about its centroidal axis y-y and will be given the symbol $\bar{I}$. The second term is zero because $\int x dA$ is zero since yy is the centroidal axis of the body. The last term, $d^2 \int dA = Ad^2$ or, area of body times the square of the distance between axes yy and $y_1 y_1$.

Thus in general,

$I = \bar{I} + Ad^2$

This expression states that the amount of inertia of an area with respect to any axis in the plane of the area is equal to the moment of inertia of the area with respect to a parallel centroidal axis plus the product of the area and the square of the distance between the two axes.

Parallel Axis Theorem For Masses. If instead of area the mass of the body is considered, the parallel axis can be written:

$I = \bar{I} + Md^2$, where M refers to the mass of the body.

A3.7a Mass Moments of Inertia The product of the mass of a particle and the square of its distance from a line or plane is referred to as the moment of inertia of the mass of the particle with respect to the line or plane. Hence,

$I = \Sigma Mr^2$. If the summation can be expressed by a definite integral, the expression may be written $I = \int r^2 dM$

Moments of Inertia of Airplanes. In both flying and landing conditions the airplane may be subjected to angular accelerations. To determine the magnitude of the accelerations as well as the distribution and magnitude of the mass inertia resisting forces, the moment of inertia of the airplane about the three coordinate axes is generally required in making a stress analysis of a particular airplane.

The mass moments of inertia of the airplane about the coordinate X, Y and Z axes through the center of gravity of the airplane can be expressed as follows:

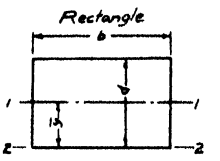
$$I_X = \Sigma wy^2 + \Sigma wz^2 + \Sigma \Delta I_X$$

$$I_Y = \Sigma wx^2 + \Sigma wz^2 + \Sigma \Delta I_Y$$

$$I_Z = \Sigma wx^2 + \Sigma wy^2 + \Sigma \Delta I_Z$$

TABLE 1

Section Properties of Areas



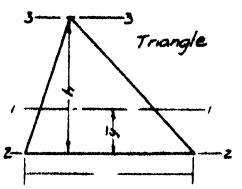
Area = bd

$\bar{y} = \frac{d}{2}$

$I_{1-1} = bd^3/12$

$I_{2-2} = \frac{bd^3}{3}$

$\rho_{1-1} = .289\ d$



Area = $\frac{bh}{2}$

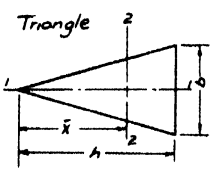
$\bar{y} = h/3$

$I_{1-1} = \frac{bh^3}{36}$

$I_{2-2} = \frac{bh^3}{12}$

$I_{3-3} = \frac{bh^3}{4}$

$\rho_{1-1} = .236\ h$

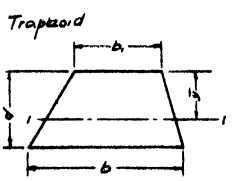


Area = $\frac{bh}{2}$

$\bar{x} = 2/3\ h$

$I_{1-1} = \frac{bh^3}{48}$

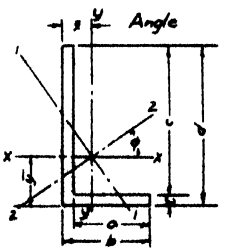
$\rho_{1-1} = .204\ h$



Area = $\frac{d(b + b_1)}{2}$

$\bar{y} = \frac{d(2b + b_1)}{3(b + b_1)}$

$I_{1-1} = d^3 \frac{(b^2 + 4bb_1 + b_1^2)}{36\ (b + b_1)}$



Area = t(b + c)

$\bar{x} = \frac{b^2 + ct}{2(b + c)}$ $\bar{y} = \frac{d^2 + at}{2(b + c)}$

$I_x = \frac{1}{3}\left[t(d-y)^3 + by^3 - a(y - t)^3\right]$

$I_y = \frac{1}{3}\left[t(b - x)^3 + dx^3 - c(x-t)^3\right]$

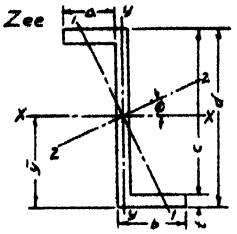
$\tan 2\phi = \frac{2\ I_{xy}}{I_y - I_x}$, where $I_{xy} = \frac{abcdt}{4(b+c)}$

$I_{1-1} = I_x \sin^2\phi + I_y \cos^2\phi + I_{xy} \sin 2\phi$

$I_{2-2} = I_x \cos^2\phi + I_y \sin^2\phi - I_{xy} \sin 2\phi$

TABLE 1 - Continued

Zee



$$\text{Area} = t(d + 2a)$$

$$\bar{y} = d/2$$

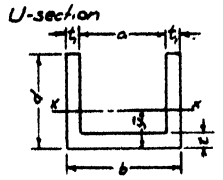
$$I_X = \frac{bd^3 - a(d - 2t)^3}{12}$$

$$I_y = d(b + a)^3 - 2a^3c - 6ab^2c$$

$$\tan 2\phi = \frac{(dt - t^2)(b^2 - bt)}{I_X - I_y}$$

For I_{1-1} and I_{2-2} see equations as given for angle.

U-section

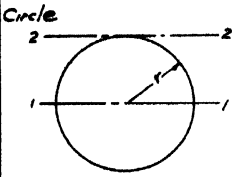


$$\text{Area } A = 2dt_1 + at$$

$$\bar{y} = \frac{d^2t_1 + .5t^2a}{A}$$

$$I_X = \frac{2t_1d^3 + at^3}{3} - A\bar{y}^2$$

Circle



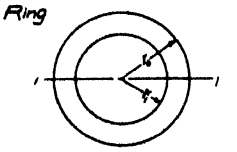
$$\text{Area} = \pi r^2$$

$$I_{1-1} = \frac{\pi r^4}{4}$$

$$I_{2-2} = \frac{5}{4}\pi r^4$$

$$\rho_{1-1} = \frac{r}{2}$$

Ring

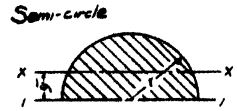


$$\text{Area} = \pi (r_o^2 - r_i^2)$$

$$I_{1-1} = \frac{\pi}{4}(r_o^4 - r_i^4)$$

$$\rho_{1-1} = \sqrt{\frac{r_o^2 + r_i^2}{2}}$$

Semi-circle



$$\text{Area} = \frac{\pi r^2}{2}$$

$$\bar{y} = .424\ r$$

$$I_X = .1098\ r^4$$

$$\rho_X = .264\ r$$

Semi-circular Ring



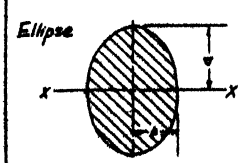
$$\text{Area} = \frac{\pi}{2}(R^2 - r^2)$$

$$y = \frac{4}{3\pi}\frac{(R^2 + Rr + r^2)}{R + r}, \text{approx. } \bar{y} = \frac{2r}{\pi}$$

$$I_X = .1098(R^4 - r^4) - \frac{.283R^2r^2(R - r)}{R + r}$$

$$I_X(\text{approx}) = \frac{.3t(r + R)^3}{2} \text{ when } \frac{t}{r} \text{ is small}$$

Ellipse

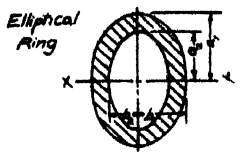


$$\text{Area} = \pi ab$$

$$I_X = \frac{\pi a^3 b}{4}$$

$$\rho_X = \frac{a}{2}$$

Elliptical Ring

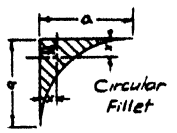


$$\text{Area} = \pi (a_1b_1 - a_2b_2)$$

$$I_X = \frac{\pi}{4}(a_1^3b_1 - a_2^3b_2)$$

$$\rho_X = \sqrt{\frac{I}{\text{Area}}}$$

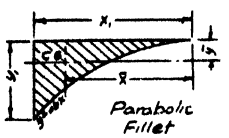
Circular Fillet



$$\text{Area} = .215\ a^2$$

$$\bar{x} = .223\ a$$

Parabolic Fillet

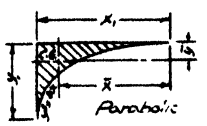


$$\text{Area} = \frac{x_1y_1}{3}$$

$$\bar{x} = \frac{3}{4}x_1$$

$$\bar{y} = .3\ y_1$$

Parabolic



$$\text{Area} = x_1y_1/4$$

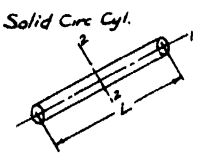
$$\bar{x} = \frac{4}{5}x_1$$

$$\bar{y} = \frac{2}{7}y_1$$

TABLE 2

Properties of Solids

Solid Circ Cyl.



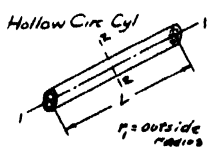
$$\text{Vol.} = \pi r^2L \text{ (r = radius)}$$

$$M = \frac{W}{g} \text{ (Total wt.)}$$

$$I_{1-1} = \frac{Mr^2}{2}$$

$$I_{2-2} = M\left[r^2 + (L^2/3)\right]1/4$$

Hollow Circ Cyl



$$\text{Vol.} = \pi L(r_1^2 - r_2^2)$$

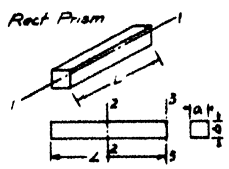
$$I_{1-1} = M(r_1^2 + r_2^2)/2$$

$$I_{2-2} = M(r_1^2 + r_2^2 + L^2/3)/4$$

For thin hollow circ. cyl.

$$I_{1-1} = Mr^2$$

Rect Prism



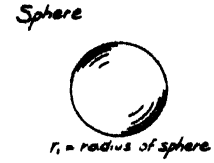
$$\text{Vol.} = abL,\ M = \frac{W}{g}$$

$$I_{1-1} = M(a^2 + b^2)/12$$

$$I_{2-2} = ML^2/12$$

$$I_{3-3} = ML^2/3$$

Sphere



Solid Sphere

$$\text{Vol.} = (4\pi r^3)/3$$

$$I_{\text{about axis}} = 2Mr^2/5$$

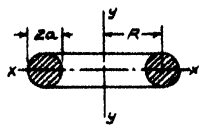
Thin Hollow Sphere

$$\text{Vol.} = \frac{4\pi}{3}(r_1^3 - r_2^3)$$

$$I_{\text{about dia.}} = \frac{2Mr_1^2}{3}$$

TABLE 2 - Continued

Ring with Circular Section



$M = \frac{w}{g}$ = mass per unit volume of body.

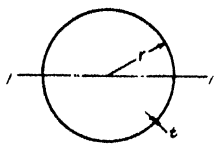
$I_{xx} = m\pi^2 Ra^2\left[R^2 + (5a^2/4)\right]$

$I_{yy} = \frac{1}{2} m\pi^2 Ra^2 (4R^2 + 3a^2)$

TABLE 3

Section Properties of Lines
(t is small in comparison to radius)

Circular Arc



Area = $2\pi rt$

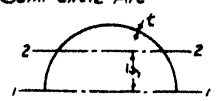
$I_{1-1} = \pi r^2 t$

$I_{polar} = 2\pi r^2 t$

$\rho_x = .707r$

$\rho_{polar} = r$

Semi-circle Arc



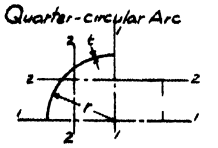
$A = \pi rt$

$\bar{y} = .6366\ r$

$I_{1-1} = \frac{\pi r^2 t}{2}$

$I_{2-2} = .2978\ r^2 t$

Quarter-circular Arc



Area = $\frac{\pi rt}{2}$

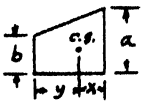
$\bar{y} = .6366\ r$

$I_{1-1} = \frac{\pi r^2 t}{4}$

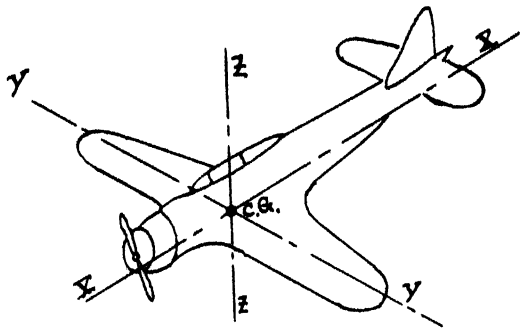
$I_{2-2} = .149\ r^2 t$

TABLE 4

Centroids of Trapizoidal Areas



Ratio $\frac{a}{b}$	Distance x	Distance y
1.01	0.4992	0.5008
1.02	0.4984	0.5016
1.03	0.4976	0.5024
1.04	0.4968	0.5032
1.05	0.4960	0.5040
1.06	0.4952	0.5048
1.07	0.4944	0.5056
1.08	0.4936	0.5064
1.09	0.4928	0.5072
1.10	0.4920	0.5080
1.11	0.4912	0.5088
1.12	0.4905	0.5095
1.13	0.4898	0.5102
1.14	0.4890	0.5110
1.15	0.4883	0.5117
1.16	0.4877	0.5123
1.17	0.4870	0.5130
1.18	0.4862	0.5138
1.19	0.4855	0.5145
1.20	0.4849	0.5151
1.22	0.4835	0.5165
1.24	0.4822	0.5178
1.26	0.4809	0.5191
1.28	0.4795	0.5205
1.30	0.4782	0.5218
1.32	0.4770	0.5230
1.34	0.4758	0.5242
1.36	0.4746	0.5254
1.38	0.4733	0.5267
1.40	0.4721	0.5279
1.45	0.4693	0.5307
1.50	0.4667	0.5333
1.55	0.4641	0.5359
1.60	0.4616	0.5384
1.65	0.4592	0.5408
1.70	0.4568	0.5432
1.75	0.4545	0.5455
1.80	0.4523	0.5477
1.85	0.4502	0.5498
1.90	0.4482	0.5518
1.95	0.4462	0.5538
2.00	0.4443	0.5557
2.10	0.4409	0.5591
2.20	0.4375	0.5625
2.30	0.4343	0.5657
2.40	0.4312	0.5688
2.50	0.4284	0.5716
2.60	0.4259	0.5741
2.70	0.4233	0.5767
2.80	0.4209	0.5791
2.90	0.4188	0.5812
3.00	0.4168	0.5832
3.20	0.4128	0.5872
3.40	0.4090	0.5910
3.60	0.4060	0.5940
3.80	0.4030	0.5970
4.00	0.4000	0.6000
4.20	0.3975	0.6025
4.40	0.3950	0.6050
4.60	0.3928	0.6072
4.80	0.3908	0.6092
5.00	0.3889	0.6111
5.50	0.3848	0.6152
6.00	0.3810	0.6190
6.50	0.3778	0.6222
7.00	0.3750	0.6250
7.50	0.3725	0.6275
8.00	0.3702	0.6298
9.00	0.3668	0.6332
10.00	0.3636	0.6364



where I_x, I_y, and I_z are generally referred to as the rolling, pitching and yawing moments of inertia of the airplane.

w = weight of the items in the airplane

x, y and z equal the distances from the axes thru the center of gravity of the airplane and the weights w. The last term in each equation is the summation of the moments of inertia of the various items about their own X, Y and Z centroidal axes.

If w is expressed in pounds and the distances in inches, the moment of inertia is expressed in units of pound-inches squared, which can be converted into slug feet squared by multiplying by 1/32.16 x 144.

Example Problem 1. Determine the gross weight of gravity of the airplane shown in Fig. A3.3. The airplane weight has been broken down into the 10 items or weight groups, with their individual c.g. locations denoted by the symbol +.

Solution. The airplane center of gravity will be located with respect to two rectangular axes. In this example, a vertical axis thru the centerline of the propeller will be selected as a reference axis for horizontal distances, and the thrust line as a reference axis for vertical distances. The general expressions to be solved are:-

$\bar{x} = \frac{\Sigma wx}{\Sigma w}$ = distance to airplane c.g. from ref. axis Z-Z

$\bar{y} = \frac{\Sigma wy}{\Sigma w}$ = distance to airplane c.g. from ref. axis X-X

Table 4 gives the necessary calculations, whence

$\bar{x} = \frac{417180}{3150} = 133.3$" aft of ℄ propeller

$\bar{y} = \frac{5480}{3150} = -1.74$" (below thrust line)

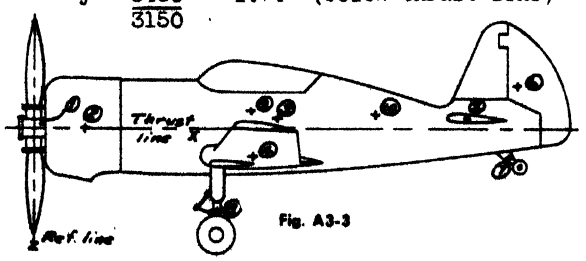


Fig. A3-3

Table 4

Item No.	Name	Weight W#	Horizontal Arm = x	Horizontal Moment = Wx	Vertical Arm = y	Vertical Moment = Wy
1	Propeller	180	0 in.	0	0	0
2	Engine Group	820	46	37720	0	0
3	Fuselage Group	800	182	145600	4	3200
4	Wing Group	600	158	94800	-18	-10800
5	Hori. Tail	60	296	17760	8	480
6	Vert. Tail	40	335	13400	26	1040
7	Tail Wheel	50	328	16400	-20	-1000
8	Front Land.Gear	300	115	34500	-30	- 900
9	Pilot	200	165	33000	10	2000
10	Radio	100	240	24000	5	500
Totals		3150		417180		-5480

Example Problem 2. Determine the moment of inertia about the horizontal centroidal axis for the area shown in Fig. A3.4

Solution. We first find the moment of inertia about a horizontal reference axis. In this solution, this arbitrary axis has been taken as axis x'x' thru the base as shown. Having this moment of inertia, a transfer to the centroidal axis can be made. Table 5 gives the detailed calculations for the moment of inertia about axis x'x'. For simplicity, the cross-section has been divided into the five parts, namely, A, B,C,D, and E.

I_{cx} is moment of inertia about centroidal x axis of the particular part being considered. Distance from axis x'x' to centroidal horizontal axis = $\bar{y} = \frac{\Sigma Av}{\Sigma A} = \frac{17.97}{6.182} = 2.91$"

By parallel axis theorem, we transfer the moment of inertia from axis x'x' to centroidal axis xx.

$I_{XX} = I_{x'x'} - A\bar{y}^2 = 79.47 - 6.18 \times 2.91^2 =$

27.2 in^4

Radius of Gyration, $\rho_{XX} = \sqrt{\frac{I_{XX}}{A}} = \sqrt{\frac{27.2}{6.18}} = 2.1$"

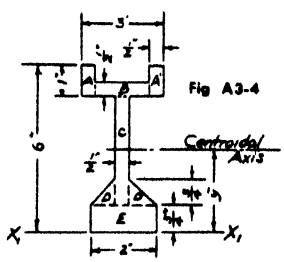


Fig A3-4

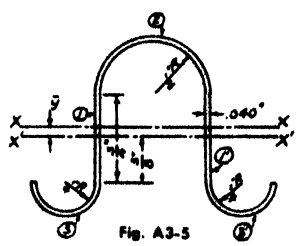


Fig. A3-5

Example Problem #3. Determine the moment of inertia of the stringer cross section shown in Fig. A3.5 about the horizontal centroidal axis.

Solution. A horizontal reference axis x'x' is assumed as shown. The moment of inertia is first calculated about this axis and then transferred to the centroidal axis xx. See Table 6.

Table 5

Portion	Area A	y	Ay	Ay^2	I_{c_x} = moment of inertia of portion about centroidal x axis.	$I_{x'x'} = I_{c_x} + Ay^2$
A	0.50	5.5	2.75	15.13	1/12 x .5 x 1^3 = .04	15.17
A^1	0.50	5.5	2.75	15.13	" = .04	15.17
B	1.00	5.25	5.25	27.50	1/12 x 2 x $.5^3$ = .02	27.52
C	2.12	2.875	6.10	17.56	1/12 x .5 x 4.25^3 = 3.19	20.75
D	0.281	1.00	0.28	0.28	bh ^{3}/36 - .75 ^{4}/36 = 0.01	0.29
D^1	0.281	1.00	0.28	0.28	" = 0.01	0.29
E	1.50	0.375	0.56	0.21	1/12 x 2 x $.75^3$ = 0.07	0.28
Sum	6.182		17.97			79.47 in^4

Table 6

Portion	Area	y	Ay	Ay^2	I_{c_x}	$I_{x'x'} = I_{c_x} + Ay^2$
1 + 1'	.06	0	0	0	.00281	.00281
2	.0654	.706	.04617	.0326	.00168	.03428
3 + 3'	.0679	-.547	-.0371	.0203	.000475	.02078
Sum	.1933		.009			.05787

$$\bar{y} = \frac{\Sigma Av}{\Sigma A} = \frac{.009}{.1933} = .0465"$$

$$I_{xx} = I_{x'x'} - A\bar{y}^2 = .05787 - .1933 \times (.0465)^2 = .05745 \text{ in}^4$$

Radius of gyration $\rho_{x-x} = \sqrt{\frac{.05745}{.1933}} = .55"$

Detailed explanation of Table 6:-

Portion 1 + 1'

$$I_{cx} = \frac{1}{12} bd^3 = \left(\frac{.04 \times .75^3}{12}\right) \times 2 = .00281 \text{ in}^4.$$

Portion 2 (ref. table 1)

$$y = .375 + \frac{4}{3\pi} \frac{R^2 + Rr + r^2}{R + r} = .375 + \frac{4}{3\pi} \frac{(.5^2 + .5 \times .54 + .54^2)}{(.5 + .54)} = .375 + 331 = .706"$$

By approx. method see Table 1.

$$y = .375 + \frac{2}{\pi} r_1 = .375 + \frac{2}{\pi} \times (.52) = .706"$$

$$I_{cx} = .1098 \times (R^4 + r^4)\, t\, (R + r) - \frac{.283\, R^4 + r^4 t}{R + r}$$

$$= .1098(.2916 + .25) \times .04 \times 1.04 - \frac{.283 \times .2916 \times .25 \times .04}{1.04}$$

$$= .002475 - .000793 = .001682 \text{ in}^4.$$

Approx. $I_{cx} = .3 t r_1^3 = .3 \times .04 \times .52^3 = .001688 \text{ in}^4.$

Portion 3 + 3' (ref. Table 1)

$$y = .375 + \frac{4}{3\pi} \times \frac{(.0841 + .0725 + .0625)}{.54} = .375 + .172 = .547"$$

approx. $y = .375 + \frac{2}{\pi} r_1 = .375 + .172 = 547"$

$$I_{cx} = \left[.1098(.0841 + .0625) + .04 \times .54 - \frac{.283 \times .0841 \times .0625 \times .04}{.54} \right] = .002375$$

approx. $I_{cx} = .3 \times .04 \times .27^3 = .002365 \text{ in}^4$

Problem #4, Determine the moment of inertia of the flywheel in Fig. A3.5a about axis of rotation. The material is aluminum alloy casting (weight = .1 lb. per cu. inch.)

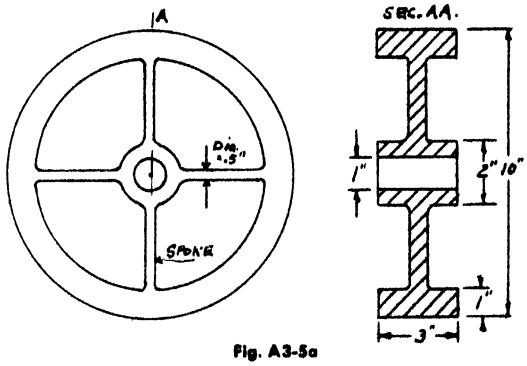


Fig. A3-5a

Solution: The spokes may be treated as slender round rods and the rim and hub as hollow cylinders. (Refer to Table 2)

Rim,

weight $W = \pi(R^2 - r^2) \times 3 \times .1 = \pi(5^2 - 4^2) .3 = 8.48$ lb.

$I = .5W(R^2 + r^2) = .5 \times 8.48\ (5^2 + 4^2) = 173.7$ lb. in^2

Hub,

$W = \pi(1^2 - .5^2) \times 3 \times .1 = .707\#$

$I = .5 \times .707\ (1^2 + .5^2) = .44$ lb. in^2

Spokes,

Length of spoke = 3"

Weight of spoke = 3 x $.25^2$ x .1 = .588#

I of one spoke = $WL^2/12 + W\bar{r}^2 = .588 \times 3^2/12 + .588 \times 2.5^2 = 4.10$ lb. in^2

I for 4 spokes = 4 x 4.10 = 16.40

Total I of wheel = 16.40 + .44 + 173.7 = 190.54 lb. in^2

$I = 190.54/32.16 \times 144 = .0411$ slug ft^2

Example Problem #5. Moment of Inertia of an Airplane.

To calculate the moment of inertia of an airplane about the coordinate axes through the gross weight center of gravity, a break down of the airplane weight and its distribution is

necessary, which is available in the weight and balance estimate of the airplane.

Table 6a shows the complete calculation of the moments of inertia of an airplane. This table is reproduced from N.A.C.A. Technical note #575, "Estimation of moments of inertia of airplanes from Design Data."

Explanation of Table

Fig. A3.5b shows the reference of planes and axes which were selected. After the moments of inertia have been determined relative to these axes the values about parallel axes through the center of gravity of the airplane are found by use of the parallel axis theorem.

Column (1) of Table 6a gives breakdown of airplane units or items.
Column (2) gives the weight of each item.
Columns (3), (4) and (5) give the distance of the c.g. of the items from the references planes or axes.
Columns (6) and (7) give the first moments of the item weights about the Y' and X' reference axes.
Columns (8), (9) and (10) give the moment of inertia of the item weights about the reference axes.
Columns (11), (12) and (13) give the moments of inertia of each item about its own centroidal axis parallel to the reference axes. Such items as the fuselage skeleton, wing panels and engine have relatively large values for their centroidal moments of inertia.

The last values in Columns (3) and (5) give the distances from the reference planes to the center of gravity of the airplane.

$$\bar{x}_{c.g.} = \frac{\Sigma wx}{\Sigma w} = \frac{617.024 \text{ (col. 6)}}{5325.3 \text{ (col. 2)}} = 115.9 \text{ in.}$$

$$\bar{z}_{c.g.} = \frac{\Sigma wz}{\Sigma w} = \frac{414.848 \text{ (col. 7)}}{5325.3} = 77.8 \text{ in.}$$

The last values in columns (8), (9) and (10) were obtained by use of the parallel axis theorem, as follows:-

$\Sigma w x^2$ about c.g. of airplane = 97,891,595 - 5325.3 x 115.9^2 = 26,691,595.

$\Sigma wz^2 = 33,252,035 - 5325.3 \times 77.8^2 = 992,035$

The third from the last value in columns (11), (12) and (13) give the moments of inertia of the airplane about the x, y and z axes through the c.g. of airplane. The values are obtained as follows:

$I_y = \Sigma wx^2 + \Sigma wz^2 + \Sigma \Delta I_y = 26,691,595 + 999,035 + 3,120,384 = 30,804,014$ lb. in^2

$I_x = \Sigma wy^2 + \Sigma wz^2 + \Sigma \Delta I_x = 10,287,522 + 992,023 + 2,899,470 = 14,179,027$ lb. $in.^2$

$I_z = \Sigma wy^2 + \Sigma wz^2 + \Sigma \Delta I_z = 10,287,522 + 26,691,595 + 5,157,186 = 42,136,303$ lb. $in.^2$

In order to determine the principal inertia axes, the product of inertia of the weight about the reference axes is necessary. Column (14) gives the values about the reference axes. To transfer the product of inertia to the c.g. axes of the airplane, we make use of the parallel axis theorem. Thus

$\Sigma wxz_{c.g.} = \Sigma wxz_{(Ref.\ axes)} - \Sigma w \bar{x} \bar{z} = 48,857,589 - 5325.3 \times 115.9 \times 77.8 = 839,253$ lb. $in.^2$

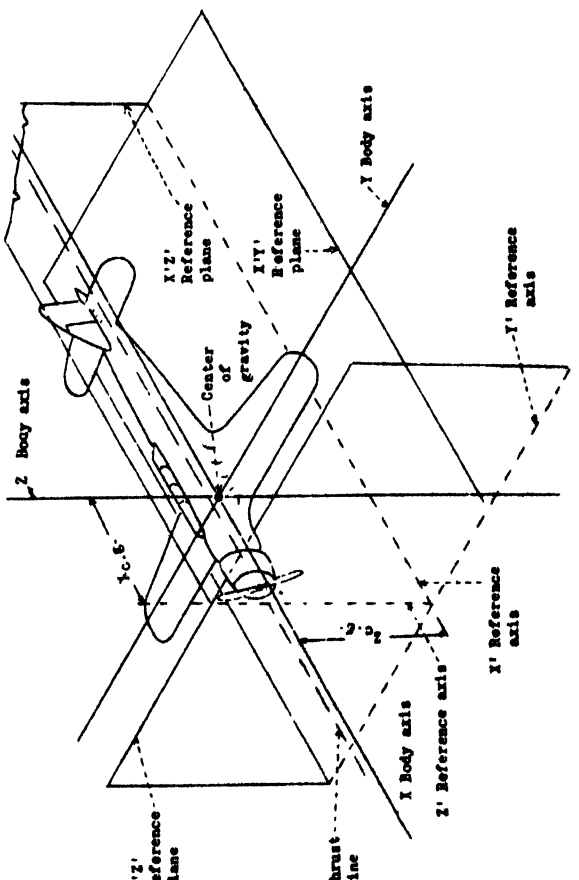
To reduce all values to slug $ft.^2$ multiply $\frac{1}{32.17} \times \frac{1}{144}$.

Hence $I_x = 3061$, $I_y = 6680$, $I_z = 9096$, $I_{xz} = 181$

Having the inertia properties about the coordinate c.g. axes, the moments of inertia bout the principal axes are determined in a manner as explained for areas. (See A3.13).

The angle ϕ between the X and Z axes and the principal axes is given by,

$$\tan 2\phi = \frac{2I_{xz}}{I_z - I_x} = \frac{2 \times 181}{9096 - 3061} = .05998 \text{ hence } \phi = 1^0\ 43''$$



(REF. N.A.C.A. TECH. NOTE No. 575)

Fig. A3-5b

Table 6a

COMPUTATIONS OF MOMENTS OF INERTIA

1.	2.	3.	4.	5.	6.	7.	8.	9.	10.	11.	12.	13.	14.
Item	Weight	x	y	z	wx	wz	wx^2	wy^2	wz^2	ΔI_x	ΔI_y	ΔI_z	wxz
Center section nose assembly	108.8	102	-	57	11,098	6,202	1,131,955	-	353,491	261,239	-	261,229	633,563
Center section beam, etc	204.6	121	-	57	24,757	11,662	2,995,549	-	664,745	491,245	-	491,245	1,411,126
Center section ribs, etc.	84.2	148	-	55	12,462	4,631	1,844,317	-	254,705	202,164	33,660	235,844	685,388
Flap	22.0	180	-	53	3,960	1,166	713,800	-	61,798	48,598	-	48,598	209,880
Outer panel nose	104.6	105	156	65	10,983	6,799	1,153,215	2,545,546	441,935	184,514	-	184,514	713,895
Outer panel beam	155.8	120	156	65	18,672	10,114	2,240,640	3,786,682	657,410	274,478	-	274,478	1,213,680
Outer panel ribs	69.8	139	156	64	12,482	5,747	1,735,026	2,185,373	367,821	158,407	17,601	176,008	798,861
Ailerons	31.4	172	156	62	5,401	1,947	928,936	764,150	120,702	55,390	-	55,390	334,850
Horizontal tail	87.1	367	-	96.7	31,966	8,423	11,731,412	-	814,463	178,378	-	176,378	3,091,083
Vertical tail	31.4	352	-	125	11,053	3,925	3,890,586	-	490,625	110,200	10,174	31	1,381,600
Fuselage skeleton	314.0	176	-	81	55,264	25,434	9,726,464	-	2,060,154	69,394	1,576,594	1,570,000	4,476,384
Engine mount	40.5	60	-	80	2,430	3,240	145,800	-	259,200	5,184	5,184	5,184	194,400
Turtleback (fairing)	48.5	254	-	80	12,319	3,880	3,129,026	-	310,400	15,181	57,861	56,648	985,520
Firewall	11.0	70	-	80	770	880	53,900	-	70,400	2,200	1,100	1,100	61,600
Steps	2.0	170	20	70	340	140	57,800	800	9,800	-	-	-	23,800
N.A.C.A. cowling	70.0	50	-	80	3,500	5,600	175,000	-	448,000	16,940	15,470	15,470	280,000
Cabin and windshield	66.5	146	-	108	9,709	7,182	1,417,514	-	775,656	2,394	106,400	108,794	1,048,572
Foot troughs	2.0	77	5	68	154	136	11,858	50	9,248	-	-	-	10,472
Floor, rear	9.5	210	-	86	1,995	827	418,950	-	41,382	608	1,368	1,976	131,670
Wing fillets	18.5	142	20	58	2,627	1,073	373,034	7,400	62,234	-	18,944	18,944	152,366
Bottom cowling and side frames	27.0	140	11	75	3,780	2,025	529,200	3,267	151,875	-	24,300	24,300	283,500
Arresting door	1.3	284	-	63	369	82	104,853	-	5,160	5	-	5	23,260
Tail-wheel pan, etc.	4.0	365	-	84	1,460	336	532,900	-	28,224	100	-	100	122,640
Side doors	17.0	143	18	82	2,431	1,394	347,633	5,508	114,308	1,088	28,288	27,200	199,342
Baggage door	1.8	165	-	63	297	113	49,005	-	7,144	720	-	720	18,711
Fabric and dope	13.0	254	-	80	3,302	1,040	838,708	-	83,200	4,394	15,509	15,509	264,160
Tail cone	7.5	385	-	91	2,888	683	1,111,688	-	62,108	120	-	120	262,763
Cowling, stations 1-2	12.0	110	-	95	1,320	1,140	145,200	-	108,300	1,200	-	1,200	125,400
Chassis (retracted)	232.4	115	54	51	26,726	11,852	3,073,490	677,678	604,472	-	23,240	23,240	1,363,026
Retracting mechanism	28.6	110	25	67	3,146	1,916	346,060	17,875	128,385	-	-	-	210,782
Wheels, etc.	91.0	141	54	56	12,831	5,096	1,809,171	265,356	285,376	-	-	-	718,536
Tail wheel	26.0	360	-	74	9,360	1,924	3,369,600	-	142,376	26	-	26	692,640
Engine	1049.0	33	-	80	34,617	83,920	1,142,361	-	6,713,600	253,858	253,858	253,858	2,769,360
Engine accessories	90.6	52	-	83	4,711	7,520	244,982	-	624,143	9,060	-	9,060	391,030
Engine controls	11.0	103	10	76	1,133	836	116,699	1,100	63,536	-	-	-	86,108
Propeller	222.0	9.3	-	80	2,065	17,760	19,201	-	1,420,300	177,600	89,300	89,300	165,168
Starting system	37.0	58	-	85	2,072	3,145	116,032	-	267,325	148	333	481	176,120
Lubricating system	26.0	69	-	82	1,794	2,132	123,786	-	174,824	1,274	-	1,274	147,108
Fuel system	82.0	128	-	80	10,496	6,560	1,343,488	-	524,300	22,056	20,006	25,666	839,680
Instruments	38.0	102	-	92	3,876	3,496	395,352	-	321,632	2,432	60,800	63,232	356,992
Surface controls	81.5	160	-	71	13,040	5,787	2,086,400	-	410,842	123,962	130,400	254,362	925,840
Furnishings	160.0	156	-	80	24,960	12,800	3,893,760	-	1,024,000	108,160	400,000	508,160	1,996,800
Electrical equipment	100.7	128	15	81	12,890	8,157	1,649,869	28,658	660,693	-	-	-	1,044,086
Hoist sling	6.0	115	-	102	690	612	79,350	-	62,424	864	-	864	70,380
AIRPLANE EMPTY	3867.4	106.8	0	74.8	412,196	289,138	67,342,573	10,283,443	22,263,736	2,681,572	2,890,404	4,980,908	31,090,714
Pilot	200.0	105	-	90	21,000	18,000	2,205,000	-	1,620,000	33,800	28,800	5,000	1,890,000
Observer	200.0	205	-	89	41,000	17,800	8,405,000	-	1,584,200	33,800	28,600	5,000	3,649,000
Fuel	780.0	132	-	85.5	102,960	66,690	13,590,720	-	5,701,995	141,180	178,380	157,560	8,803,080
Oil	75.0	71	-	85	5,325	6,375	378,075	-	541,875	3,675	-	3,675	452,625
Very Pistol	3.9	195	14	75	761	293	148,398	784	21,938	-	-	-	57,038
Smoke candles	4.0	184	14	96	736	384	135,424	784	36,864	-	-	-	70,656
Float lights	9.0	190	14	72	1,710	648	324,900	1,764	46,656	-	-	-	123,120
Radio	142.7	178	-	85	25,401	12,130	4,521,307	-	1,031,008	5,137	-	5,137	2,159,051
Chart board, etc.	3.7	80	3	94	296	348	23,680	33	32,693	-	-	-	27,824
Drift sight	1.6	222	14	84	355	134	78,854	314	11,290	-	-	-	29,837
First aid	4.0	165	10	57	660	228	108,900	400	12,996	-	-	-	37,620
Life raft	34.0	138	-	101	4,624	3,434	638,864	-	348,834	306	-	306	467,084
USEFUL LOAD	1467.9	140.5	0	86.7	204,838	136,464	30,549,032	4,078	10,998,298	317,898	239,980	176,678	17,766,875
TOTALS	5325.3				617,034	414,848	97,891,595	10,287,522	33,252,035	2,999,470	3,130,384	5,157,186	48,857,589
CORRECTION	5325.3	115.9	0	77.8			71,200,000	0	32,260,000				48,018,126
							26,691,595	10,287,522	992,035				839,463
										10,287,522	26,691,595	26,691,595	
										992,035	992,035	10,287,522	
										14,178,027	30,804,014	42,156,303	
I_x =										2,662	5,784	7,912	
k^2 =										51.6	78.1	88	
k =													
		$x_{c.g.}$		$z_{c.g.}$			$-Wx_{c.g.}^2$		$-Wz_{c.g.}^2$	I_X	I_Y	I_Z	H
													$Wx_{c.g.}z_{c.g.}$

(Table 6a From N.A.C.A. Tech. Note #575)

The principal moments of inertia are given by following equation.

$I_{xp} = I_x \cos^2 \phi + I_z \sin^2 \phi - I_{xz} \sin 2\phi$. (See Art. A3.11)

$I_{yp} = I_y$

$I_z = I_x \sin^2 \phi + I_z \cos^2 \phi + I_{xz} \sin 2\phi$

Substituting

$I_{xp} = 3061 \times (0.9996)^2 + 9096 \times (0.0300)^2 - 181 \times .0599 = 3056$

$I_{zp} = 3061 \times (0.0300)^2 + 9096 \times (0.9996)^2 + 181 \times .0599 = 9102$

$I_{yp} = 6680$

A3.7b Problems

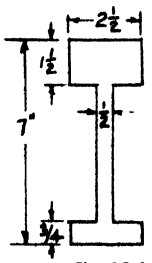


Fig. A3-6

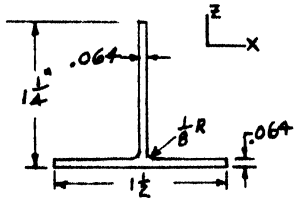


Fig. A3-7

(1) Determine the moment of inertia about the horizontal centroidal axis for the beam section shown in Fig. A3.6.

(2) For the section as shown in Fig. A3.7 calculate the moment of inertia about the centroidal Z and X axes.

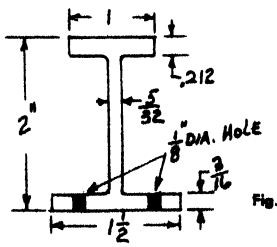


Fig. A3-8

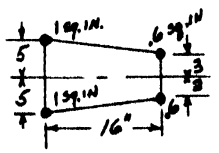


Fig. A3-9

(3) Determine the moment of inertia about the horizontal centroidal axis for the section shown in Fig. A3.8.

(4) In the beam cross-section of Fig. A3.9 assume that the four corner members are the only effective material. Calculate the centroidal moments of inertia about the vertical and horizontal axes.

A3.8 Product of Inertia

In various engineering problems, particularly those involving the calculation of the moments of inertia of unsymmetrical sections, the expression $\int xy\,dA$ is used. This expression is referred to as the product of inertia of the area with respect to the rectangular axes x and y. The term, product of inertia of an area, will be given the symbol I_{xy}, hence

$$I_{xy} = \int xydA \quad \text{----------(1)}$$

The unit, like that of moment of inertia, is expressed as inches or feet to the 4th power. Since x and y may be either positive or negative, the term I_{xy} may be zero or either positive or negative.

Product of Inertia of a Solid. The product of inertia of a solid is the sum of the products obtained by multiplying the weight of each small portion in which it may be assumed to be divided by the product of its distances from two of the three coordinate planes through a given point.

Thus with respect to planes X and Y

$$I_{xy} = \int xy\,dW$$

$$I_{xz} = \int xz\,dW$$

$$I_{yz} = \int yz\,dW$$

A3.9 Product of Inertia for Axes of Symmetry.

If an area is symmetrical about two rectangular axes, the product of inertia about these axes is zero. This follows from the fact that symmetrical axes are centroidal x and y axes.

If an area is symmetrical about only one of two rectangular axes, the product of inertia, $\int xydA$, is zero because for each product xydA for an element on one side of the axis of symmetry, there is an equal product of opposite sign for the corresponding element dA on the opposite side of the axis, thus making the expression $\int ydA$ equal to zero.

A3.10 Parallel Axis Theorem

The theorem states that, "the product of inertia of an area with respect to any pair of co-planar rectangular axes is equal to the product of inertia of the area with respect to a pair of parallel centroidal axes plus the product of the area and the distances of the centroid of the total area from the given pair.of axes". Or, expressed as an equation,

$$I_{xy} = \bar{I}_{xy} + A\bar{x}\bar{y} \quad \text{----------(2)}$$

This equation is readily derivable by referring to Fig. A3.10. $\bar{Y}\bar{Y}$ and $\bar{X}\bar{X}$ are centroidal axes for a given area. YY and XX are parallel axes passing through point O.

The product of inertia about axes YY and XX is $I_{xy} = \int (x + \bar{x})(y + \bar{y})\,dA$

$= \int xydA + \bar{x}\bar{y} \int dA + \bar{x} \int y\,dA + \bar{y} \int xdA$

The last two integrals are each equal to zero, since $\int ydA$ and $\int xdA$ refer to centroidal axes. Hence, $I_{xy} = \int xydA + \bar{x}\bar{y} \int dA$, which can be written in the form of equation (2).

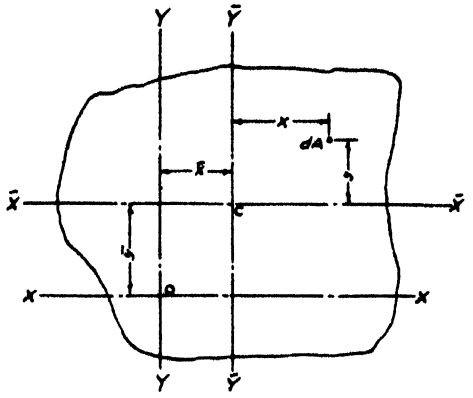


Fig. A3-10

A3.11 Moments of Inertia with Respect of Inclined Axes

Unsymmetrical beam sections are very common in aircraft structure, because the airfoil shape is generally unsymmetrical. Thus, the general procedure with such sections is to first find the moment of inertia about some set of rectangular axes and then transfer to other inclined axes. Thus, in Fig. A3.11 the moment of inertia of the area with respect to axis X_1X_1 is,

$$I_{X_1} = \int y_1^2\, dA = \int (y\cos\phi - x\sin\phi)^2 dA$$

$$= \cos^2\phi \int y^2 dA + \sin^2\phi \int x^2 dA - 2\sin\phi\cos\phi \int xy dA$$

$$= I_X \cos^2\phi + I_y \sin^2\phi - 2 I_{xy} \sin\phi\cos\phi \quad (3)$$

and likewise in a similar manner, the following equation can be derived:

$$I_{y_1} = I_X \sin^2\phi + I_y \cos^2\phi + 2 I_{xy} \sin\phi\cos\phi \quad -(4)$$

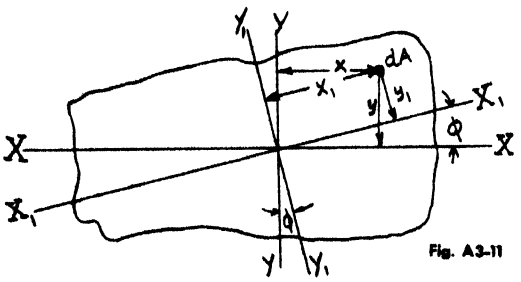


Fig. A3-11

By adding equations (3) and (4), we obtain $I_{x_1} + I_{y_1} = I_X + I_y$ -(5)

or the sum of the moments of inertia of an area with respect to all pairs of rectangular axes, thru a common point of intersection, is constant.

A3.12 Location of Axes for which Product of Inertia is Zero.

In Fig. A3.11

$$I_{x_1y_1} = \int x_1 y_1\, dA = \int (x\cos\phi + y\sin\phi)(y\cos\phi - x\sin\phi) dA$$

$$= (\cos^2\phi - \sin^2\phi \int xy dA + \cos\phi\sin\phi \int (y^2 - x^2)\, dA$$

$$= I_{xy}\cos 2\phi + \frac{1}{2}(I_X - I_y)\sin 2\phi$$

Therefore, $I_{x_1y_1}$ is zero when

$$\tan 2\phi = \frac{2I_{xy}}{I_y - I_X} \quad - - - - - - - - - - - - -(6)$$

A3.13 Principal Axes.

In problems involving unsymmetrical bending, the moment of an area is frequently used with respect to a certain axis called the principal axis. A principal axis of an area is an axis about which the moment of inertia of the area is either greater or less than for any other axis passing thru the centroid of the area.

Axes for which the product of inertia is zero are principal axes.

Since the product of inertia is zero about symmetrical axes, it follows that symmetrical axes are principal axes.

The angle between a set of rectangular centroidal axes and the principal axes is given by equation (6).

Example Problem 4.

Determine the moment of inertia of the angle as shown in Fig. A3.12 about the principal axes passing through the centroid. Solution: Reference axes X and Y are assumed as shown in Fig. A3.12 and the moment of inertia is first calculated about these axes. Table 8 gives the calculations. The angle is divided into the two portions (1) and (2).

			Table 8									
Part	Area A	x	y	Ay	Ax	Ay^2	Ax^2	Axy	I_{c_x}	I_{c_y}	I_x	I_y
1	.375	.75	.125	.0469	.281	.0058	.211	.0351	$\frac{1}{12}\times 1.5\left(\frac{1}{4}\right)^3 = .0018$	$\frac{1}{12}\times\frac{1}{4}\times 1.5^3 = .070$	.0077	.281
2	.500	.125	1.25	.625	.0625	.7800	.0078	.0781	$\frac{1}{12}\times\frac{1}{4}\times 2^3 = .167$	$\frac{1}{12}\times 2\times .25^3 = .0026$	.9470	.010
	.875			.6719	.3435	.7858	.2188	.1132			.9547	.291

*I_{cx} and I_{cy} = moment of inertia of each portion about their own X and Y centroidal axes.

Location of centroidal axes:-

$$\bar{y} = \frac{\Sigma Ay}{\Sigma A} = \frac{.6719}{.875} = .767"$$

$$\bar{x} = \frac{\Sigma Ax}{\Sigma A} = \frac{.3435}{.875} = .392"$$

Transfer moment of inertia and product of inertia from reference X and Y axes to parallel centroidal axes:-

$$\bar{I}_x = I_x - A\bar{y}^2 = .955 - .875 \times .\overline{767}^2 = .440$$

$$\bar{I}_y = I_y - A\bar{x}^2 = .291 - .875 \times .\overline{392}^2 = .157$$

$$\bar{I}_{xy} = \Sigma A_{xy} - A\bar{x}\bar{y} = .1132 - .875 \times .767 \times .392 = -.150$$

Calculate angle between centroidal X and Y axes and principal axes through centroidal as follows:-

$$\tan 2\phi = \frac{2\bar{I}_{xy}}{\bar{I}_y - \bar{I}_x} = \frac{2(-.150}{.157-.440} = \frac{-.30}{-.283} = 1.06$$

$$2\phi = 46^0 - 40' \qquad \phi = 23^0 - 20'$$

Calculate moments of inertia about centroidal principal axes as follows:-

$$\bar{I}_{xp} = \bar{I}_x \cos^2\phi + \bar{I}_y \sin^2\phi - 2\bar{I}_{xy} \sin\phi \cos\phi$$

$$= .44 \times .\overline{918}^2 + .157 \times .\overline{3965}^2 - 2(-.150) \times .3965 \times .918 = 504 \text{ in.}^4$$

$$\bar{I}_{yp} = \bar{I}_x \sin^2\phi + \bar{I}_y \cos^2\phi + 2\bar{I}_{xy} \sin\phi \cos\phi$$

$$= .44 \times .3965 + .157 \times .\overline{918}^2 + 2(-.150) \times .3965 \times .918 = .092 \text{ in.}^4$$

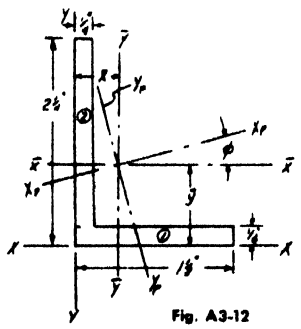


Fig. A3-12

Example Problem 5.

Fig. A3.13 shows a typical distributed flange - 2 cell - wing beam section. The upper and lower surface is stiffened by Z and bulb angle sections. Determine the moment of inertia of the section about the principal axes.

Solution:

The properties of the cross-section depend upon the effective material which can develop resisting axial stresses. The question of effective material is taken up in later chapter. Table 9 shows the calculations for the moment of inertia about the assumed rectangular reference axes XX and YY (see Fig. A3.13). The cross-section has been broken down into 16 stringers as listed in column 1. For the top surface, a width of 30 thicknesses of the .032 skin is assumed to act with the stringers and a width of 25 thicknesses of the .04 skin (see Col. 3). On the lower surface, the skin half way to adjacent stringers is assumed acting with each stringer, or the entire skin is effective. Column 4 gives the combined area of each stringer unit and is considered as concentrated at the centroid of the stringer and effective skin. All distances, x and y, columns 5 and 8, have been scaled from a large drawing.

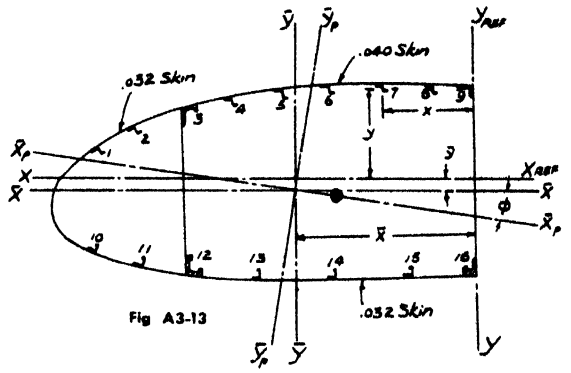


Fig A3-13

Table 9

1	2	3	4	5	6	7	8	9	10	11
Portion	Stringer Area	Area: Effective Skin	Area: Total Area A	y	Ay	Ay^2	x	Ax	Ax^2	Ixy = Axy
1	.11	.03	.14	4.00	0.560	2.240	-33.15	-4.641	153.83	-18.56
2	.11	.03	.14	6.05	0.847	5.124	-29.28	-4.099	120.02	-24.80
3	.30	.08	.38	7.00	2.660	18.620	-24.85	-9.443	234.66	-66.10
4	.13	.04	.17	7.37	1.253	9.234	-21.18	-3.600	76.25	-26.53
5	.13	.04	.17	7.55	1.288	9.687	-16.60	-2.822	46.84	-21.31
6	.13	.04	.17	7.50	1.275	9.563	-12.60	-2.142	26.99	-16.06
7	.13	.04	.17	7.30	1.241	9.059	- 8.60	-1.462	12.57	-10.67
8	.13	.04	.17	6.90	1.171	8.080	- 4.00	-0.680	2.72	- 4.69
9	.24	.05	.29	6.50	1.885	12.252	- 0.35	-0.100	0.04	-00.65
10	.07	.10	.17	-3.30	-0.561	1.851	-33.25	-5.653	187.96	18.65
11	.07	.10	.17	-4.90	-0.833	4.082	-29.28	-4.978	145.78	24.39
12	.13	.15	.28	-5.95	-1.666	9.913	-24.85	-6.958	172.90	41.40
13	.11	.20	.31	-7.40	-2.294	16.976	-18.70	-5.797	108.40	42.90
14	.11	.20	.31	-8.13	-2.520	20.487	-12.42	-2.850	47.82	31.30
15	.11	.20	.31	-8.62	-2.672	22.432	- 6.10	-1.891	11.54	16.30
16	.24	.11	.35	-8.87	-3.094	27.444	-00.35	-0.122	0.04	1.08
Totals			3.70		-1.465	187.04		-58.238	1348.36	-13.35

Location of centroidal axes with respect to ref. axes, -

$$\bar{y} = \frac{\Sigma Ay}{\Sigma A} = -\frac{1.465}{3.70} = -.396"$$

$$\bar{x} = \frac{\Sigma Ax}{\Sigma A} = -\frac{58.238}{3.70} = -15.74"$$

$$\bar{I}_x = 187.04 - 3.70 \times .\overline{396}^2 = 186.5 \text{ in.}^4$$

$$\bar{I}_y = 1348.36 - 3.70 \times \overline{15.74}^2 = .431.7 \text{ in.}^4$$

$$\bar{I}_{xy} = -13.35 - (3.70 \times .396 \times 15.74) = 36.41 \text{ in.}^4$$

$$\tan 2\phi = \frac{2\bar{I}_{xy}}{\bar{I}_y - \bar{I}_x} = \frac{2(-36.41)}{431.7-186.5} = -.29696$$

$$2\phi = 16^0 - 32.5', \quad \phi = 8^0 - 16.25'$$

$$\bar{I}_{xp} = \bar{I}_x \cos^2\phi + \bar{I}_y \sin^2\phi - 2\bar{I}_{xy} \sin\phi \cos\phi$$

$$= 186.46 \times .9896^2 + 431.7 \times .1438^2 - 2[-36.41 \times .9896 \times (-.1438)] = 181.2 \text{ in.}^4$$

$$\bar{I}_{yp} = \bar{I}_x \sin^2 \phi + \bar{I}_y \cos^2 \phi + 2\,\bar{I}_{xy} \sin \phi \cos \phi = 186.46 \times .14382^2 + 431.7 \times .9896^2 + 2\left[-36.41 \times .9896 \times (-.1438)\right] = 437 \text{ in.}^4$$

A3.14 Problems

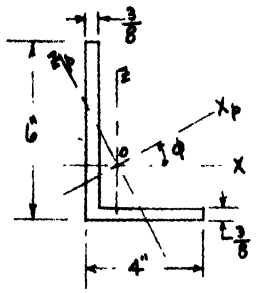


Fig. A3-14

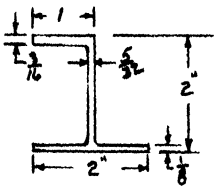


Fig. A3-15

(1) For the section of Fig. A3.14 determine the moment of inertia about each of the principal axes X_p and Z_p.

(2) Calculate the moment of inertia of the section in Fig. A3.15 about the principal axes.

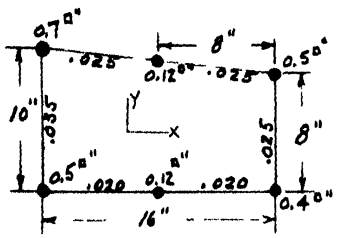


Fig. A3-16

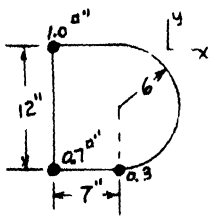


Fig. A3-17

(3) Fig. A3.16 illustrates a box type beam section with six longitudinal stringers. Determine the moment of inertia of the beam section about the principal axes for the following assumptions:-

(a) Assume the beam is bending upward putting the top portion in compression and the lower portion in tension. Therefore, neglect sheet on the top side since it has very little resistance to compressive stresses. The sheet on the bottom side is effective since it is in tension. For simplicity neglect the vertical webs in the calculations.

(b) Reverse the conditions in (a) thus placing top side in tension and lower side in compression.

(4) For the three stringer single cell box beam section in Fig. A3.17, calculate the moments of inertia about the principal axes. Assume all web or wall material ineffective.

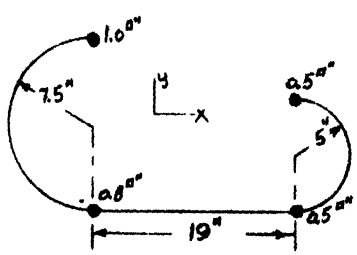


Fig. A3-18

(5) For the beam section in Fig. A3.18, calculate the moment of inertia about the principal axes assuming the four stringers as the only effective material.

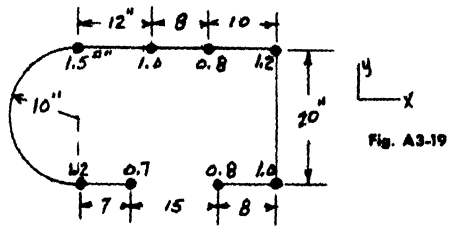


Fig. A3-19

(6) Fig. A3.19 shows a wing beam section with a cut-out on the lower surface. Determine the moments of inertia about the principal axes assuming the eight stringers are the only effective material.

CHAPTER A4
STRESS-STRAIN RELATIONSHIPS-COMBINED STRESSES

A4.1 Introduction. Stress Symbols

To properly design members which are subjected to loads which produce normal and shearing stresses it is usually necessary to determine the maximum value of the normal and shear stresses. This chapter will deal only briefly with this subject. The student should refer to any good textbook on mechanics for comprehensive treatment on this subject.

It is conventional practice to use Greek letters to represent stresses. The direction or plane of the stress is then noted by subscripts.

The letter sigma (σ) represents a normal stress.

The letter tau (τ) represents a shear stress.

A4.2 Shearing Stresses on Planes at Right Angles.

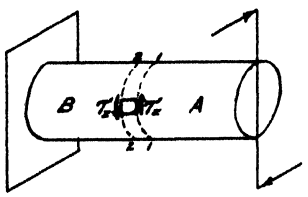


Fig. A4.1

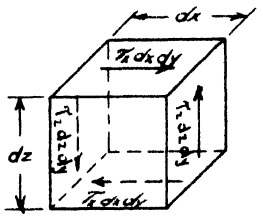


Fig A4-2

Fig. A4.1 shows a circular solid shaft subjected to a torsional moment. The portion (A) of the shaft exerts a shearing stress τ_z on section (1-1) and portion (B) exerts a resisting shearing stress τ_z on section (2-2). Fig. A4.2 illustrates a differential cube cut from shaft between sections (1-1) and (2-2). For equilibrium a resisting couple must exist on top and bottom face of cube. Taking moments about lower left edge of cube:

$$\tau_x \, dxdy \cdot dz - \tau_z \, dzdy \cdot dx = 0$$

hence, $\tau_x = \tau_z$ ----------(1)

Thus if a shearing unit stress occurs on one plane at a point in a body, a shearing unit stress of same intensity exists on planes at right angles to the first plane.

A4.3 Simple Shear Produces Tensile and Comprehensive Stresses.

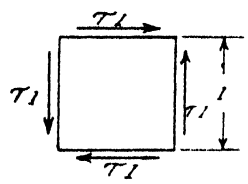


Fig A4-3

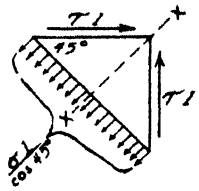


Fig A4-4

Fig. A4.3 shows an elementary block of unit thickness subjected to the pure shearing stresses τ_1. Fig. A4.4 shows a free body after the block has been cut along a diagonal section.

For equilibrium the sum of the forces along the x-x axis equals zero.

$$\Sigma F_x = -\frac{\sigma \, 1}{\cos 45} + 2\,(\tau_1 \cos 45^0) = 0$$

$$\text{hence, } \sigma = \frac{2(\tau_1 \cos 45^0)\cos 45^0}{1} = \tau \quad ----(2)$$

Therefore when a point in a body is subjected to pure shear stresses of intensity τ, normal stresses of the same intensity as the shear stresses are produced on a plane at 45^0 with the shearing planes.

A4.4 Principal Stresses

For a body subjected to any combination of stresses 3 mutually perpendicular planes can be found on which the shear stresses are zero. The normal stresses on these planes of zero shear stress are referred to as principal stresses.

A4.5 Shearing Stresses Resulting From Principal Stresses.

In Fig. A4.5 the differential block is subjected to tensile principal stresses σ_x and σ_z with zero principal stress σ_y. The block is cut along a diagonal section giving the free body of Fig. A4.6. The stresses on the diagonal section have been resolved into stress components parallel and normal to the section as shown. For equilibrium the summation of the stresses along the axes (1-1) and (2-2) must equal zero.

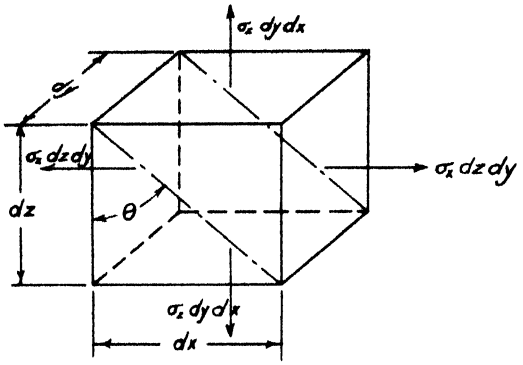


Fig A4-5

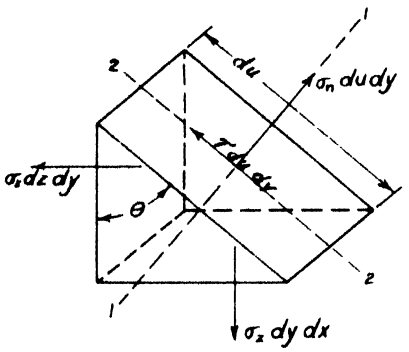


Fig A4-6

$\Sigma F_{s-s} = 0$

$-\tau\, dudy - \sigma_x\, dzdy \sin\theta + \sigma_z\, dydx \cos\theta = 0$

But $\frac{dzdy}{dudy} = \cos\theta$ and $\frac{dydx}{dudy} = \sin\theta$

hence, $\tau = \sigma_z \sin\theta \cos\theta - \sigma_x \cos\theta \sin\theta$

or, $\tau = = (\sigma_z - \sigma_x) \sin\theta \cos\theta$

$\tau = 1/2(\sigma_z - \sigma_x) \sin 2\theta$ where σ_z is maximum principal stress and σ_x is minimum principal stress.

Since $\sin 2\theta$ is maximum when $\theta = 45^0$,

$$\tau = 1/2(\sigma_{max} - \sigma_{min}) \text{ - - - - - - - - - -(3)}$$

Stated in words, the maximum value of the shearing unit stress at a point in a stressed body is one-half the algebraic differences of the maximum and minimum principal unit stresses.

A4.6 Combined Stress Equations.

Fig. A4.7 shows a differential block subjected to normal stresses on two planes at right angles to each other and with shearing forces on the same planes. The maximum normal and shearing unit stresses will be determined.

Fig. A4.8 shows a free body diagram of a portion cut by a diagonal plane at angle θ as shown.

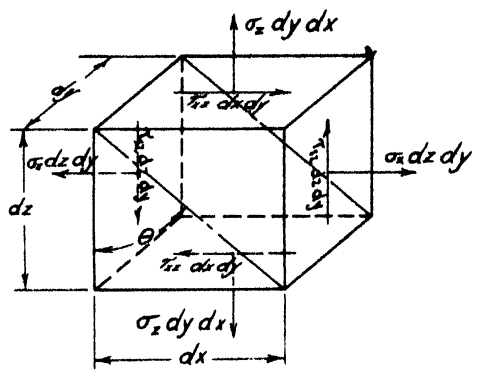


Fig A4-7

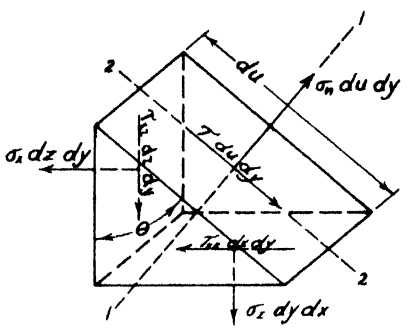


Fig A4-8

For equilibrium the sum of the forces in the z and x directions must equal zero.

$$\Sigma F_X = 0$$

$$\sigma_n\, dudy \cos\theta + \tau\, dudy \sin\theta - \sigma_x\, dzdy - \tau_{xz}\, dxdy = 0 \text{ - - - - - - - - - - - - - - - - - - -(4)}$$

$$\Sigma F_Z = 0$$

$$\sigma_n\, dudy \sin\theta - \tau\, dudy \cos\theta - \sigma_z\, dydx - \tau_{xz}\, dzdy = 0 \text{ - - - - - - - - - - - - - - - - - - -(5)}$$

By dividing each equation by du and noting that $\frac{dzdy}{dudy} = \cos\theta$ and $\frac{dydx}{dudy} = \sin\theta$, we obtain:

$$(\sigma_n - \sigma_x) \cos\theta + (\tau - \tau_{xz}) \sin\theta = 0 \text{ - - - - - -(6)}$$

$$(\sigma_n - \sigma_z) \sin\theta - (\tau - \tau_{xz}) \cos\theta = 0 \text{ - - - - - -(7)}$$

The maximum normal stress σ_n will be maximum when θ equals such angle θ' as to make τ = zero. Thus if $\tau = 0$ and $\theta = \theta'$ in equations (6) and (7), we obtain,

$$(\sigma_n - \sigma_x) \cos\theta' - \tau_{xz} \sin\theta' \text{ - - - - - - - - -(8)}$$

$$(\sigma_n - \sigma_z) \sin\theta' - \tau_{xz} \cos\theta' = 0 \text{ - - - - - - -(9)}$$

In equations (8) and (9) σ_n represents the principal stress. Dividing one equation by another to eliminate θ',

$$\frac{\sigma_n - \sigma_x}{\tau_{xz}} = \frac{\tau_{xz}}{\sigma_n - \sigma_z}$$

$$\sigma_n^2 - (\sigma_x - \sigma_z)\sigma_n + \sigma_x\sigma_z = \tau_{xz}^2$$

$$\sigma_n = \frac{\sigma_x + \sigma_z}{2} \pm \sqrt{\left(\frac{\sigma_x - \sigma_z}{2}\right)^2 + \tau_{xz}^2} \quad - - - - \quad (10)$$

In equation (10) tensile normal stress is plus and compression minus. For maximum σ_n use plus sign before radical and minus sign for minimum σ_n.

To find the plane of the principal stresses, the value of θ' may be solved for from equations (8) and (9), which gives:

$$\tan 2\theta' = \frac{2\tau_{xz}}{\sigma_x - \sigma_z} \quad - - - - - - - - - - - - - - - \quad (11)$$

θ' is measured from the plane of the largest normal stress σ_x or σ_z. The direction of rotation of θ' from this plane is best determined by inspection. Thus if only the shearing stresses τ_{xz} were acting, the maximum principal stress would be one of the 45° planes, the particular 45° plane being easily determined by inspection of the sense of the shear stresses. Furthermore if only the largest normal stress were acting it would be the maximum principal stress and θ' would equal zero. Thus if both σ and τ act, the plane of the principal stress will be between the plane on which σ acts and the 45° plane. As stated before σ refers to either σ_x or σ_z which ever is the largest.

Maximum Value of Shearing Stress. ($\tau_{max.}$)

The maximum value of τ from equation (3) equals,

$$\tau_{max.} = 1/2(\sigma_{n(max.)} - \sigma_{n(min.)}) - - - - - - \quad (12)$$

Substituting the maximum and minimum values of σ_n from (10) in (11), we obtain maximum shearing stress as follows:

$$\tau_{max.} = \pm\sqrt{\left(\frac{\sigma_x - \sigma_z}{2}\right)^2 + \tau_{xz}^2} \quad - - - - - \quad (13)$$

A4.7 Mohr's Circle for Determination of Principal Stresses.

It is sometimes convenient to solve graphically for the principal stresses and the maximum shear stress. Mohr's circle furnishes a graphical solution. (Fig. A4.9a). In the Mohr method, two rectangular axes x and z are chosen to represent the normal and shearing stresses respectively. Taking point O as the origin lay off to scale the normal stresses σ_x and σ_z equal to OB and OA respectively. If tension, they are laid off to right of point O and to the left if compression. From B the shear stress τ_{xz} is laid off parallel to Oz and with the sense of the shear stress on the face DC of Fig. A4.9b), thus locating point C. With point E the midpoint ofAB as the center and with radius EC describe acircle cutting OB at F and G. AD will equal BC and will represent the shear on face AB of Fig. b. It can be proven that OF and OG are the principal stresses $\sigma_{max.}$ and $\sigma_{min.}$ respectively and EC is the maximum shear stress $\tau_{max.}$. The principal stresses occur on planes that are parallel to CF and CG. (See Figs. c and d). The maximum shear stress occurs on two sections parallel to CH and CI where HEI is perpendicular to OB. If σ_x should equal zero then O would coincide with A.

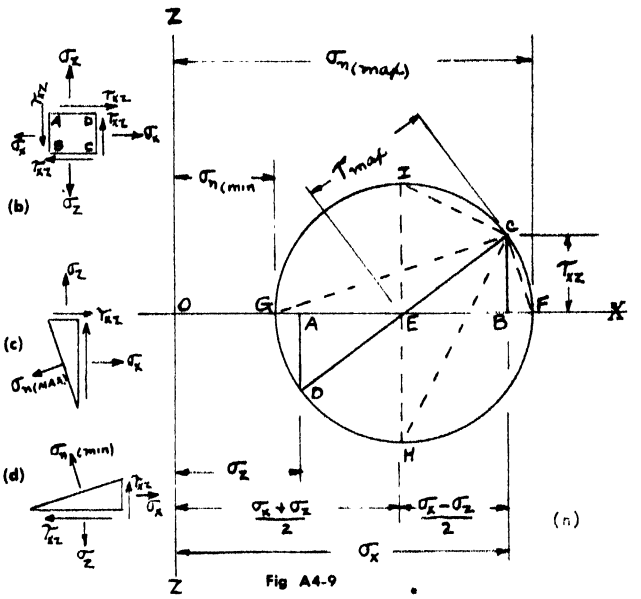


Fig A4-9

A4.8 Components of Stress From Principal Stresses by Mohr's Circle.

In certain problems the principal stresses may be known as in Fig. A4.10 and it is desired to find the stress components on other planes designated by angle θ. In Fig. A4.11 the axes x and z represent the normal and shear stresses respectively. The principal stresses are laid off to scale on ox giving points D and E respectively. Construct a circle with A the midpoint of DE and with diameter ED. Draw angle CAB equal to 2θ. It can be proven that OB represents the normal stress on the plane defc of Fig. A4.10, and CB represents the shear stress τ on this plane.

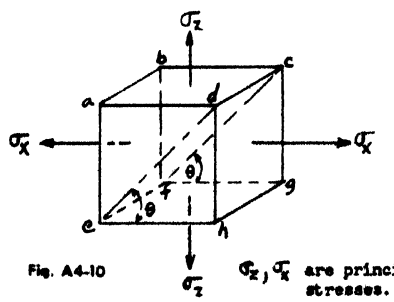


Fig. A4-10 σ_z, σ_x are principal stresses.

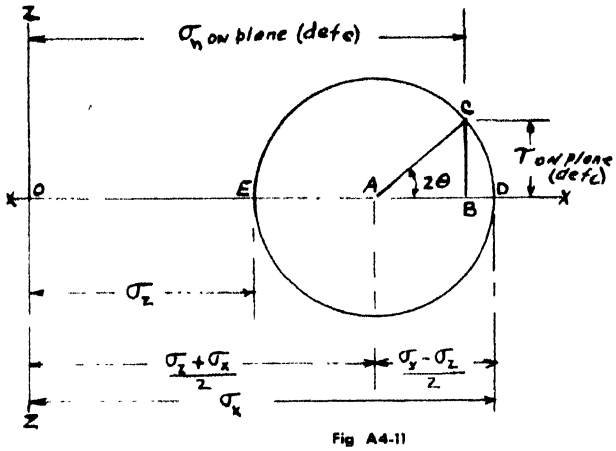


Fig A4-11

Example Problem #1

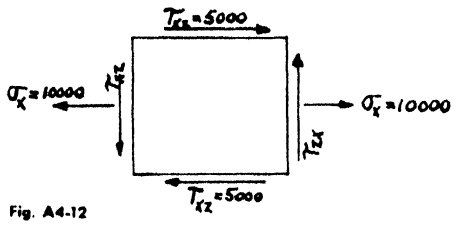


Fig. A4-12

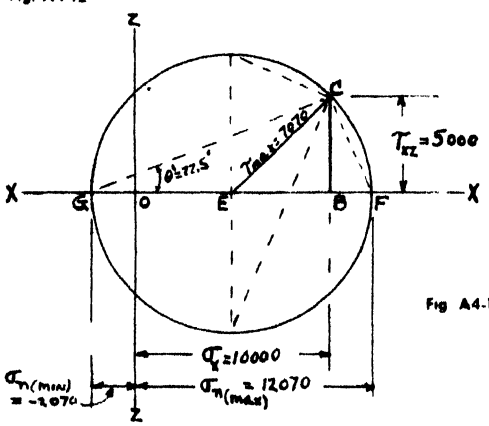


Fig A4-13

The maximum normal and shear stresses will be determined for the block loaded as shown in Fig. A4.12.

The graphical solution making use of Mohr's circle is shown in Fig. A4.13. From reference axes x and z thru point O, the given normal stress σ_x = 10000 is laid off to scale on ox and toward the right giving point B. From B the shear stress τ_{xz} = 5000 is laid off parallel to oz to locate point C. With E the midpoint of OB as the center of the circle and with radius EC a circle is drawn which cuts the Ox axis at F and G. The maximum and minimum principal stresses are then equal to oF and oG which equals 12070 and -2070 respectively. The maximum shear stress equals EC or 7070.

Algebraic Solution:

$$\sigma_n = \frac{\sigma_x + \sigma_z}{2} \pm \sqrt{\left(\frac{\sigma_x - \sigma_z}{2}\right)^2 + \tau_{xz}^2}$$

Substituting Values,

$$\sigma_n = \frac{10000 + 0}{2} \pm \sqrt{\left(\frac{10000 + 0}{2}\right)^2 + 50002} = 5000 + 7070$$

hence, $\sigma_{n(max.)} = 5000 + 7070 = 12070$ psi

$\sigma_{n(min.)} = 5000 - 7070 = -2070$ psi

$\tau_{max.} = 1/2\left(\sigma_{n(max.)} - \sigma_{n(min.)}\right)$ (Ref. Eq. 12)

$= 1/2\ \left(12070 - (-2070)\right) = 7070$ psi

$\tau_{max.}$ can also be computed by equation (13), whence

$$\tau_{max.} = \pm\sqrt{\left(\frac{10000 + 0}{2}\right)^2 + 5000^2} = \updownarrow 7070 \text{ psi}$$

$$\tan 2\theta' = \frac{2\,\tau_{xz}}{\sigma_x - \sigma_z} = \frac{2 \times 5000}{10000 - 0} = 1$$

hence, $\theta' = 22.5^\circ$.

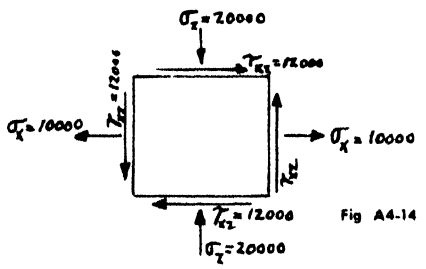


Fig A4-14

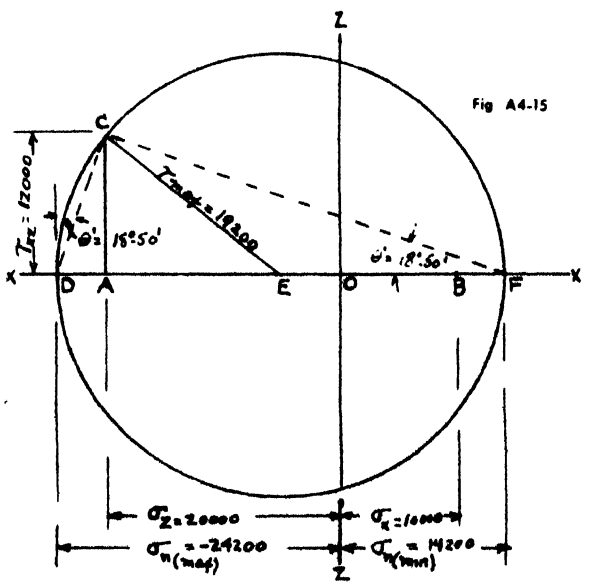


Fig A4-15

Example Problem #2

The maximum normal and shear stresses will be determined for the block loaded as shown in Fig. A4.14.

Fig. A4.15 shows the graphical soluting using Mohr's circle. From point 0, $\sigma_X = 10000$ and $\sigma_Z = -20000$ are laid off equal to OB and OA respectively. τ_{XZ} equal to 12000 is liad off parallel to OZ at A locating C. With E the midpoint of AB as the center of a circle of radius EC a circle is drawn which cuts the ox axis at F and D. The maximum normal and shear stresses are indicated on the figure.

Algebraic Solution

$$\sigma_n = \frac{\sigma_X + \sigma_Z}{2} \pm \sqrt{\left(\frac{\sigma_X - \sigma_Z}{2}\right)^2 + \tau_{XZ}^2}$$

$$= \frac{10000 - 20000}{2} \pm \sqrt{\left(\frac{10000 - (-20000)}{2}\right)^2 + 12000^2}$$

$$= -5000 \pm 19200$$

hence, $\sigma_{n(max.)} = -5000 - 19200 = -24200$ psi

$\sigma_{n(min.)} = -5000 + 19200 = 14200$

$\tau_{max.} = \pm 19200$, $\tan 2\theta' \frac{2 \times 12000}{10000 - (-20000)} = .8$

$\theta' = 18^\circ - .50'$

PROBLEMS

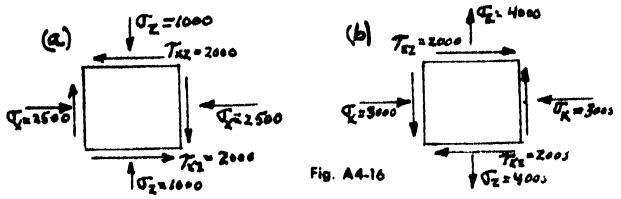


Fig. A4-16

(1) Determine both analytically and graphically the magnitudes of principal stresses and the direction of the plane on which each acts. Also determine the maximum shearing stress. See Fig. A4.16(a) for load system on block.

(2) Same as problem (1) but for stress system of Fig. A4.16(b)

A4.9 Stress Equilibrium - Varying Stress Intensities.

The previous discussion and the equations which were developed assumed a uniform distribution of stress over the given element. Since bending and torsion usually produce normal and shear stresses which are not uniform over an element the stress equations previously derived do not strictly apply.

Fig. A4.17 shows an element on which the stresses vary from one edge of the element to the other for a two dimensional case. The stresses on the element must be in equilibrium.

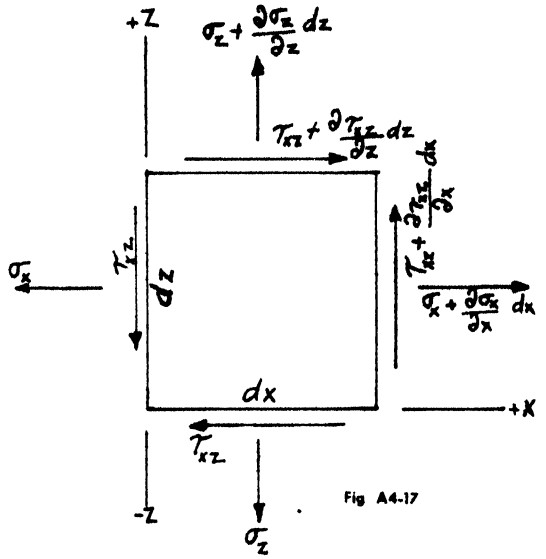


Fig A4-17

For equilibrium in the X direction, $\Sigma F_X = 0$, which gives:

$$\left(\sigma_X + \frac{\partial \sigma_X}{\partial x} dx\right) dz - \sigma_X dz + \left(\tau_{XZ} + \frac{\partial \tau_{XZ}}{\partial z} dz\right) dx - \tau_{XZ} dx = 0$$

which will reduce to,

$$\frac{\partial \sigma_X}{\partial x} + \frac{\partial \tau_{XZ}}{\partial z} = 0 \quad \text{- - - - - - - - - - - - - - (14)}$$

Likewise $\Sigma F_Z = 0$, which gives,

$$\left(\sigma_Z + \frac{\partial \sigma_Z}{\partial z} dz\right) dx - \sigma_Z dx + \left(\tau_{XZ} + \frac{\partial \tau_{XZ}}{\partial x} dx\right) dz - \tau_{XZ} dz = 0$$

which gives,

$$\frac{\partial \tau_{XZ}}{\partial x} + \frac{\partial \sigma_Z}{\partial z} = 0 \quad \text{- - - - - - - - - - - - - - (15)}$$

Similar equations can be derived for the 3 dimensional case of stresses.

CHAPTER A5
TORSIONAL STRESSES AND DEFLECTIONS

A5.1 Introduction. Problems involving torsion of tubular shapes are common in aircraft construction. For example, the metal covered wing and fuselage structure are basically thin walled tubular structures, and are subjected to large torsional forces in normal flight and landing loads. This chapter reviews the theory of torsional stresses, particularly the stresses in thin-wall cellular tubes.

A5.2 Torsion Formula - For Cylindrical Solid and Hollow Shafts and Tubes

The following conditions are assumed in the derivation of the formula:-

(1) The shaft is a circular, solid or hollow, cylinder.
(2) The unit shearing stress does not exceed the shearing proportional limit of the material.
(3) The loads lie in a plane or planes perpendicular to the axis of the cylinder or shaft.

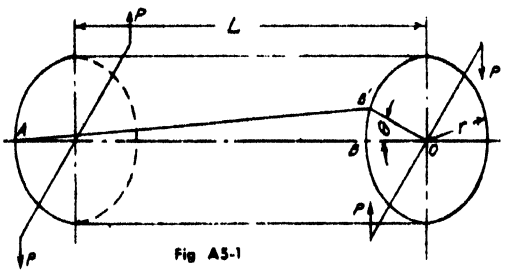


Fig A5-1

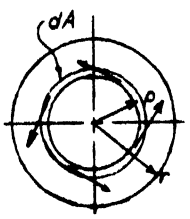


Fig. A5-2

Fig. A5.1 shows a straight cylindrical bar subjected to two equal but opposite torsional couples. The bar twists and each section is subjected to a shearing stress. Assuming the left end as stationary relative to the rest of the bar a line AB on the surface will move to AB' under these shearing stresses and this rotation at any section will be proportional to the distance from the fixed support. It is assumed that any radial line undergoes angular displacement only, or OB remains straight when moving to OB'.

The unit shearing strain in a distance $L = \varepsilon_s = \frac{BB'}{\overline{AB}} = \frac{r\theta}{L}$. Let G = modulus of rigidity.

Let f_s equal the unit stress intensity at the extreme fiber. $f_s = \varepsilon_s G = \frac{r\theta G}{L}$ ---------(A)

In Fig. A5.2, let $f_{s\rho}$ represent the unit shearing stress on a circular strip dA at a distance ρ from O.

$$f_{s\rho} = \frac{\rho}{r} f_s = \frac{\rho}{r}\frac{r\theta G}{L} = \frac{\rho\theta G}{L}$$

The moment of the shearing stress on the circular strip dA about the axis of the bar is equal to,

$dM = f_{s\rho}\rho dA = \frac{\rho^2\theta G\, dA}{L}$ and the total internal resisting moment $M = \int \frac{G\rho^2\theta\, dA}{L}$

For equilibrium, the internal resisting moment equals the external torsional moment or T, and since $\frac{G\theta}{L}$ is a constant,

$$\therefore T = M = \frac{G\theta}{L}\int \rho^2 dA = \frac{G\theta I_p}{L} \text{ ---------(B)}$$

where I_p = polar of inertia of the bar cross-section = $\int \rho^2 dA$ and equals twice that taken about a diameter.

From (A), $\frac{G\theta}{L} = \frac{f_s}{r}$

$$\therefore T = \frac{f_s I_p}{r} \text{ ----------(C)}$$

A5.4 Torsional Deflection of Cylindrical Shaft

Solving for θ from (B):

$\theta = \frac{TL}{GI_p}$ where θ is measured in radians- - - -(D)

A5.5 Transmission of Power by a Cylindrical Shaft

The work done by a twisting couple T in moving thru an angular displacement is equal to the product of the magnitude of the couple and the angular displacement in radians. If the angular displacement is one revolution, the work done equals $2\pi T$. If T is expressed in inch-pounds and N is the angular velocity in revolutions per minute, then the horsepower transmitted by a rotating shaft may be written,

$$H.P. = \frac{2\pi N T}{396000} \text{ ----------(E)}$$

where 396000 represents inch pounds of work of one horsepower for one minute. Equation (E) may be written

$$T = \frac{H.P. \times 396000}{2\pi N} = \frac{63025\ H.P.}{N} \text{ -----(F)}$$

A5.6 Example Problems

(1) Fig. A5.4 shows a conventional control stick-torque tube operating unit. For a side load of 150 lbs. on stick grip, determine the shearing stress on aileron torque tube and the angle of twist between points A and B.

Solution:

Torsional moment on tube AB due to side stick force of 150# = 150 x 26 = 3900 in. lb. The resistance to this torque is provided by the

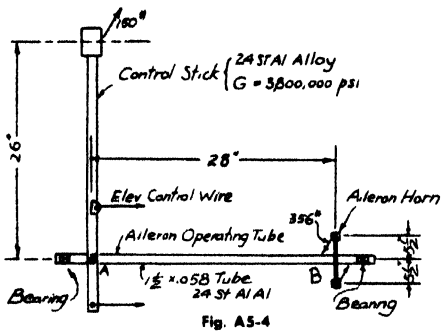


Fig. A5-4

aileron operating system attached to aileron horn and equals $\frac{3900}{11}$ = 356#. The polar moment of inertia of a 1-1/2 - .058 tube = .1368 in. hence, maximum shearing stress = $f_s = \frac{Tr}{I_p}$ = $\frac{3900 \times .75}{.1368}$ = 21400#/in.^{2} The angular twist between points A and B = $\theta = \frac{TL}{GI_p} = \frac{3900 \times 28}{3,800,000 \times .1368}$ = .21 radians = .21 x 57.3 = 12 degrees.

(2) Fig. A5.5 illustrates an aileron control surface, consisting of a circular torque tube (1-1/4 - .049 in size) supported on three hinge brackets and with the control rod fitting attached to the torque tube above the center support bracket. Find the maximum torsional shearing stress in the tube if the air load on the aileron is as indicated in Fig. A5.5, and also compute the angle of twist of tube between horn section and end of aileron.

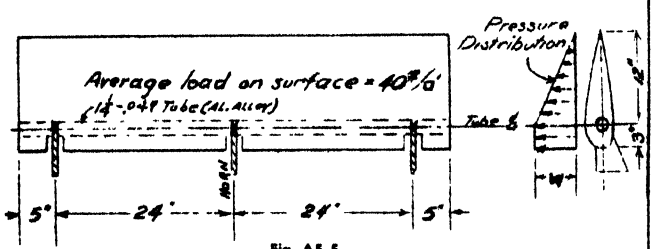
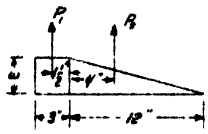


Fig A5-5

Solution

The airload on the surface tends to rotate the aileron around the torque tube, but movement is prevented or created by a control rod attached to the torque tube over the center supporting bracket. Total air load on a strip of aileron one inch wide = 40(15 x 1/144) = 4.16 lb. Let W = intensity per inch of aileron span at the leading edge point of the aileron, (see pressure diagram. $\therefore$ 3W + $\frac{W}{2}$ x 12 = 4.16.

Hence 9W = 4.16, or W = .463 lb. Total load P_1 forward of the ℄ of the torque tube = .463 x 3 = 1.389# and P_2 or load aft of the hinge line = $\frac{.463}{2}$ x 12 = 2.778 lb.



Torsional moment per running inch of torque tube: = - 1.389 x 1.5 + 2.778 x 4 = 9.0 in. lb. Hence, the maximum torque, which occurs at the center of the aileron, equals 9.0 x 29 = 261 in. lb.

The polar moment of inertia for a 1-1/4" diameter - .049" thick tube is .06678 in.^{4} = I_p

$\therefore$ f_s (max.) = $\frac{Tr}{I_p} = \frac{261 \times .625}{.06678}$ = 2450 lb/sq. in.

Since the tube section is constant and the torque varies directly as the distance from the end of the ailerons, the angle of twist θ can be computed by using the average torque as acting on entire length of the tube to one side of horn or a distant L = 29", hence

$\theta = \frac{TL}{GI_p} = \frac{261 \times 29}{2 \times 3800,000 \times .06678} \times 57.3$ = .86 degree

A5.7 Torsional Stresses for Single Cell Thin-Walled Closed Sections

The thin-wall closed tubular or box structure is quite common in aircraft construction. Close approximation to the shear stress distribution is given by Prandtl's formula (Eq.3), the derivation of which follows:-

Fig. A5.6 illustrates a thin-walled tube acted upon by an external torque T. The external torque is held in equilibrium by the internal shear stresses at the cut section as shown. It is assumed that the section is free to warp, thus there are no longitudinal stresses in the direction which tend to resist any warping of the section. Furthermore, the general shape of any cross section is assumed to remain the same as it warps.

To satisfy the equation of equilibrium at the cut section, namely $\Sigma F_x = 0$, $\Sigma F_y = 0$ and $\Sigma M = 0$, it is evident that the shear flow must be constant around the contour of the tube; or $q = tf_s$ - - - - - - - - - - - - - - - - (1) where t is the wall thickness and f_s = unit shear stress and q is positive when acting in a clockwise direction around cell. The moment of the internal shear system about any point such as O must equal the external torque T. Consider the shear force dq on a small portion dp of the wall

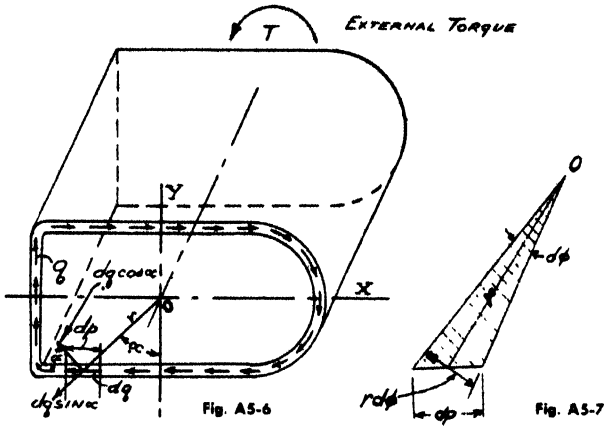


Fig. A5-6

Fig. A5-7

at a distance r from the moment center O. Resolve the force dq into components perpendicular and parallel to the arm r. The moment of dq about O then equals.

$dM = r\, dq \cos \alpha$

But $dq = f_s\, t\, dp$

Hence $dM = (r \quad f_s\, t \cos \alpha)\, dp$

But from Fig. A5.7

$dp = \dfrac{r\ d\phi}{\cos \alpha}$

Hence $dM = r^2 f_s\, t\, d\phi$ ----------(2)

In Fig. A5.7, the area dA of the triangle formed by the radii to the portion dp equals $\dfrac{r(rd\phi)}{2} = \dfrac{r^2\, d\phi}{2} = dA$, or $r^2 d\phi = 2\, dA$

Substituting the value of r d ϕ in (2), we obtain,

$dM = f_s t\ 2\, dA$, or $M = 2 f_s t \int dA = 2 f_s t A$, (A = enclosed area formed by ℄ of contour walls).

For equilibrium ΣM = 0, hence M-T = 0 or M = T, therefore,

$T = 2 f_s t A$ or

$$f_s = \frac{T}{2At} \text{ ----------(3)}$$

$$\text{or } q = \frac{T}{2A} \text{ ----------(3)}$$

Equation (3) has been found to check experimental results reasonably well if the wall thicknesses are small and sharp corners are avoided.

A5.8 Twist of Thin-Walled-Single Cell-Closed Sections

Consider a unit square cut from the wall of Fig. A5.6, adjacent to the cut section. Let Fig. A5.8 represent the small wall portion.

Shear force on the edge of the square:

$q = f_s t \times 1 = f_s t$

The shear deformation of the square:

$= \delta = \dfrac{f_s}{G} \times 1 = \dfrac{f_s}{G}$, where G is the modulus of rigidity work done by the shear force:

$$W = \frac{f_s t}{2} \times \delta = \frac{f_s^2 t}{2G} \text{ ----------(4)}$$

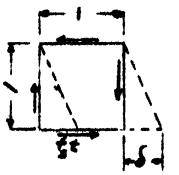


Fig. A5-8

Substituting the value of f_s from Eq. (3) in (4)

$$W = \frac{T^2}{8A^2 G t}$$

The total work for the entire cross-section and length of the tube, then, equals

$W = \dfrac{T^2 L p}{8A^2 t G}$, where p is the perimenter of the section. But, work is also $= \dfrac{T\theta}{2}$, where θ = angle of twist,

hence $\dfrac{T\theta}{2} = \dfrac{T^2 L p}{8A^2 t G}$, from which

$\theta = \dfrac{TLp}{4A^2 tG}$. The term $\dfrac{4A^2 t}{p}$ is generally referred to as the torsion constant since it is a function only of the geometrical shape. For a section where t varies for different parts of the section, this expression then becomes $\dfrac{4A^2}{\oint \frac{dp}{t}}$

Hence, $\theta = \dfrac{TL \oint \frac{dp}{t}}{4A^2 G}$ ----------(5)

If L is taken as unity,

$$\theta = \frac{T \oint \frac{dp}{t}}{4A^2 G} \text{ ----------(6)}$$

which may be written as follows, if the value of 2Aq is substituted for T (Eq. 3)

$$\theta = \frac{q \oint \frac{dp}{t}}{2AG} \text{ ----------(7)}$$

A5.9 Expression for Torsional Moment in Terms of Internal Shear Flow Systems for Multiple Cell Closed Sections

Fig. A5.9 shows the internal shear flow pattern for a 2-cell thin-walled tube, when the tube is subjected to an external torque. q_1, q_2 and q_3 represent the shear load per inch on the three different portions of the cell walls.

For equilibrium of shear forces at the junction point of the interior web with the outside wall, we know that

$$q_1 = q_3 + q_2 \text{ ----------(8)}$$

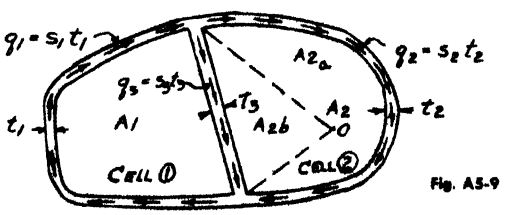


Fig. A5-9

Choose any moment axis, as point O in Fig. A5.9. From Fig. A5.7 we found that the moment of a shear force of constant intensity acting along a certain length dp of the cell wall about a point O wasequal to twice the area of the geometrical shape formed by radii from the moment center to the extremity of the wall portion dp times the intensity per inch of the shear force on this particular portion.

Therefore, in Fig. A5.9, the moment of the shear system about point O $= T_O = 2q_1 (A_1 + A_{2b}) + 2 q_2 A_{2a} - 2q_2 A_{2b} = 2q_2 A_2 + 2q_1 A_{2b} + 2q_2 A_{2a} - 2q_2 A_{2b}$ - (9)

But from (8) $q_2 = q_1 - q_2$

Substituting the value of q in (9)

$$T_O = 2q_1 A_1 + 2q_1 A_{2b} + 2q_2 A_{2a} - 2q_1 A_{2b} + 2q_2 A_{2b}$$

But $A_2 = A_{2a} + A_{2b}$

Hence, $T_O = 2q_1 A_1 + 2q_2 A_2$ - - - - - - - - - - (10)

where A_1 = area of cell (1) and A_2 = area of cell (2)

Therefore, the moment of the internal shear system of a multiple cell tube carrying pure torsional shear stresses is equal to the sum of twice the enclosed area of each cell times the shear load per inch which exists in the outside wall of that cell. (Note: The web mn is referred to as an inside wall of either cell).

A5.10 Distribution of Torsional Shear Stresses In a Multiple-Cell Thin-Walled Closed Section. Angle of Twist

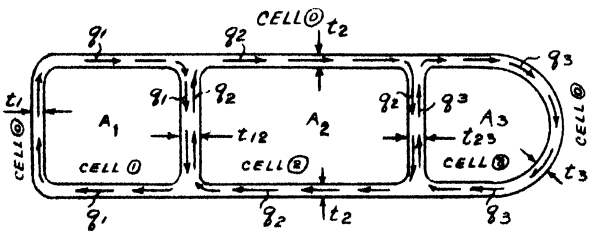


Fig. A5-10

Fig. A5.10 shows in general the internal shear flow pattern on a 3-cell tube produced by a pure torque load on the tube. The cells are numbered (1) (2) and (3), and the area outside the tube is designated as cell (0). Thus, to designate the outside wall of cell (1), we refer to it as lying between cells 1-0; for the outside wall of cell 2, as 2-0; for the web between cells (1) and (2) as 1-2, etc.

q_1 = shear load per inch = $f_{s_1} t_1$ in the outside wall of cell (1), where f_{s_1} equals the unit stress and t_1 = wall thickness. Likewise, $q_2 = f_{s_2} t_2$ and $q_3 = f_{s_3} t_3$ = shear load per inch in outside walls of cells (2) and (3) respectively. For equilibrium of shear forces at the junction points of interior webs with the outside walls, we have $(q_1 - q_2)$ equal to the shear load per inch in the web 1-2 and $(q_2 - q_3)$ for web 2-3.

For equilibrium, the torsional moment of the internal shear system must equal the external torque on the tube at this particular section. Thus, from the conclusions of article A5.9, we can write:

$$T = 2q_1 A_1 + 2q_2 A_2 + 2q_3 A_3 \text{ - - - - - - - (11)}$$

For elastic continuity, the twist of each cell must be equal, or $\theta_1 = \theta_2 = \theta_3$, etc.

From equation (7), the angular twist of a cell is

$$\theta = \frac{q \oint \frac{dp}{t}}{2AG} \quad \text{or}$$

$$2G\theta = \frac{q \oint \frac{dp}{t}}{A} \text{ - - - - - - - - - - - - - (12)}$$

Thus, for each cell of a multiple cell structure an expression

$\frac{q \oint \frac{dp}{t}}{A}$ can be written and equated to the constant value $2G\theta$. Let a_{10}, represent a line integral $\oint \frac{dp}{t}$ for cell wall 1-0, and a_{12}, a_{20}, a_{23} and a_{30} the line integrals $\oint \frac{dp}{t}$ for the other outside wall and interior web portions of the 3-cell tube. Let clockwise direction of wall shear stresses in any cell be positive in sign. Now, substituting in Eq. (12), we have:

$$\text{cell (1)} \quad \frac{1}{A_1}\left[q_1 a_{10} + (q_1 - q_2) a_{12}\right] = 2G\theta \text{ - - (13)}$$

$$\text{cell (2)} \quad \frac{1}{A_2}\left[(q_2 - q_1) a_{12} + q_2 a_{20} + (q_2 - q_3) a_{23}\right] = 2G\theta \text{ - - - - - - - - - - - - - - (14)}$$

$$\text{cell (3)} \quad \frac{1}{A_3}\left[(q_3 - q_2) a_{23} + q_3 a_{30}\right] = 2G\theta \text{ - - - (15)}$$

Equations (11, 13, 14 and 15) are sufficient to determine the true values of q_1, q_2, q_3 and θ

Thus, to determine the torsional stress distribution in a multiple cell structure, we write equation (12) for each cell and these equations together with the general torque equation, similar to equation (11), provides sufficient conditions for the solution of the shear stresses and the angle of twist.

A5.11 Stress Distribution and Angle of Twist for 2-cell Thin Wall Closed Section.

For a two cell tube, the equations can be simplified to give the values of q_1, q_2 and θ directly. For tubes with more than two cells, the equations become to complicated, and thus the equations should be solved simultaneously. Equations for two-cell tube (Fig. A5.11):-

$$q_1 = \frac{1}{2}\left[\frac{(a_{20}A_1 + a_{12}A)}{a_{20}A_1^2 + a_{12}A^2 + a_{01}A_2^2}\right] T \text{ - - (16)}$$

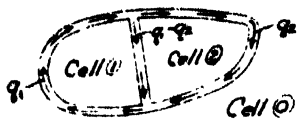


Fig A5-11

$$q_2 = \frac{1}{2}\left[\frac{a_{01}A_2 + a_{12}A}{a_{20}A_1^2 + a_{12}A^2 + a_{01}A_2^2}\right] T \quad - - - (17)$$

$$J = 4\left[\frac{a_{20}A_1^2 + a_{12}A^2 + a_{01}A_2^2}{a_{01}a_{12} + a_{12}a_{20} + a_{20}a_{01}}\right] \quad - - - - (18)$$

$$\theta = \frac{T}{G\,J} \quad - - - - - - - - - - - - - - - - (19)$$

where $A = A_1 + A_2$

Example Problems of Torsional Stresses in Multiple-Cell-Thin-Walled Tubes.

A5.12 Example 1 - Torsional Stresses in Un-symmetrical Two-Cell-Tube.

Fig. A5.12 shows a typical 2-cell tubular section as formed by a conventional airfoil shape, and having one interior web. An external applied torque T of 83450"# is assumed acting as shown. The internal shear resisting pattern is required.

Calculation of Cell Constants

Cell areas:- $A_1 = 105.8\square"$ $A_2 = 387.4\square"$
$A = 493.2\square"$

Line integrals $a = \oint \frac{dp}{t}$:-

$$a_{10} = \frac{26.9}{.025} = 1075; \quad a_{12} = \frac{13.4}{.04} = 335$$

$$a_{20} = \frac{25.25}{.04} + \frac{15.1}{.05} + \frac{25.3}{.032} = 1735$$

Solution by Equating Angular Twist of each cell.
General equation $2G\theta = q \oint \frac{dp}{t} \Big/ A$. Clockwise flow of q is positive.

Cell #1 Subt. in general equation

$$2G\theta = \frac{1}{105.8}\left[-q_1 \times 1075 + (-q_1 + q_2)\,335\right] =$$

$$- 13.33\,q_1 + 3.165\,q_2 \quad - - - - - - - - (20)$$

Cell #2

$$2G\theta = \frac{1}{387.4}\left[-(q_2 - q_1)335 - 1735q_2\right] = .865q_1 - 5.34q_2 \quad - - - - - - (21)$$

Equating (20) and (21)

$$-14.195\,q_1 + 8.505\,q_2 = 0 \quad - - - - - - - - (22)$$

The summation of the external and internal resisting torque must equal zero.

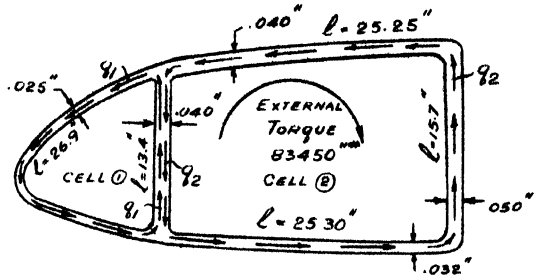


Fig. A5-12

$$83450 - 2 \times 105.8q_1 - 2 \times 387.4q_2 = 0 \quad - - - - - (23)$$

Solving equations (22) and (23) $q_1 = 55.6\#/in.$

$q_2 = 92.5\#/in.$ Since results come out positive, the assumed direction of counter-clockwise was correct for q_1 and q_2 or true signs are $q_1 = -55.6$ and $q_2 = -92.5$.

$q_{12} = -55.6 + 92.5 = 36.9\#/in.$ (as viewed from Cell 1)

Fig. A5.13 shows the resulting shear pattern. The angular twist of the complete cell can be found by substituting values of q_1 and q_2 in equations (20) and (21), since twist of each cell must be the same and equal to twist of tube as a whole. Solution by substituting in equations of Art. A5.11:-

$$q_1 = \frac{1}{2}\left[\frac{a_{20}A_1 + a_{12}A}{a_{20}A_1^2 + a_{12}A^2 + a_{10}A_2^2}\right] T$$

$$= \frac{1}{2}\left[\frac{1735 \times 105.8 + 335 \times 493.2}{1735 \times 105.8^2 + 335 \times 493.2^2 + 1075 \times 387.4^2}\right] T =$$

$$.000665\,T = .000665 \times 83450 = 55.6\#/in.$$

$$q_2 = \frac{1}{2}\left[\frac{a_{10}A_2 + a_{12}A}{a_{20}A_1^2 + a_{12}A^2 + a_{10}A_2^2}\right] T$$

$$= \frac{1}{2}\left[\frac{1075 \times 387.4 + 335 \times 493.2}{1735 \times 105.8^2 + 335 \times 493.2^2 + 1075 \times 387.4^2}\right] T$$

$$= .001107\,T = .001107 \times 83450 = 92.5\#/in.$$

A5.13 Example Problem 2

Determine the torsional shear stresses in the symmetrical 2 cell section of Fig. A5.14 when subjected to a torque T. Neglect any resistance of stringers in resisting torsional moment.

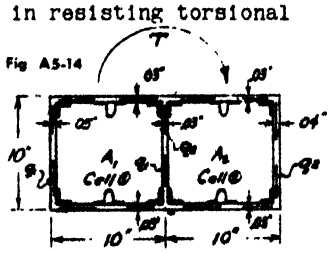


Fig A5-14

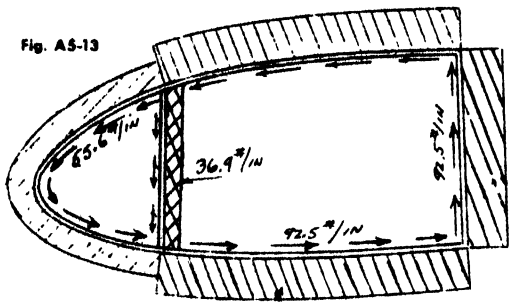
Solution:-
Calculation of terms
Area of cells:-
$A_1 = 100$ $A_2 = 100$
$A = A_1 + A_2 = 200$
Line integrals $a = \oint \frac{dp}{t}$:-

$$a_{10} = \frac{10}{.05} + \frac{20}{.03} = 866.7$$

$$a_{12} = \frac{10}{.03} = 333.3$$

$$a_{20} = \frac{20}{.03} + \frac{10}{.04} = 916.7$$

Fig. A5-13



Solution of Equations from Article A6.5:-

$$q_1 = \frac{1}{2}\left[\frac{a_{20}A_1 + a_{12}A}{a_{20}A_1^2 + a_{12}A^2 + a_{10}A_2^2}\right] T$$

$$q_1 = \frac{1}{2}\left[\frac{916.7 \times 100 + 333.3 \times 200}{916.7 \times 100^2 + 333.3 \times 200^2 + 866.7 \times 100^2}\right] T$$

$$= .002540T$$

$$q_2 = \frac{1}{2}\left[\frac{a_{10}A_2 + a_{12}A}{a_{20}A_1^2 + a_{12}A_2^2 + a_{01}A_2^2}\right] T$$

$$= \frac{1}{2}\left[\frac{866.7 \times 100 + 333.3 \times 200}{916.7 \times 100^2 + 333.3 \times 200^2 + 866.7 \times 100^2}\right] T$$

$$= .002456T$$

$$J = 4\left[\frac{a_{20}A_1^2 + a_{12}A^2 + a_{10}A_2^2}{a_{10}a_{12} + a_{12}a_{20} + a_{20}a_{10}}\right]$$

$$= 4\left[\frac{916.7 \times 100^2 + 333.3 \times 200^2 + 866.7 \times 100^2}{866.7 \times 333.3 + 333.3 \times 916.7 + 916.7 \times 866.7}\right]$$

$$= 89.76$$

$$\theta = \frac{T}{JG} = \frac{T}{G \times 89.76} = .01116\frac{T}{G} \text{ (rad.) per unit length of cell.}$$

A5.14 Example 3 - Three-cell-tube

Fig. A5.15 shows a thin-walled tubular section composed of three cells. The internal shear flow pattern will be determined in resisting the external torque of 100,000"# as shown.

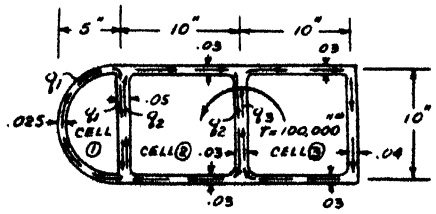


Fig. A5-15

Solution:-

Calculation of cell constants

Cell areas:-

$A_1 = 39.3$ $A_2 = 100$ $A_3 = 100$

Line integrals $a = \oint \frac{dp}{t}$.-

$$a_{10} = \frac{\pi \times 10}{2 \times .025} = 629 \quad a_{12} = \frac{10}{.05} = 200 \quad a_{20} = \frac{20}{.03} = 667$$

$$a_{23} = \frac{10}{.03} = 333 \quad a_{30} = \frac{20}{.03} + \frac{10}{.04} = 917$$

Equating the external torque to the internal resisting torque:-

$$2q_1A_1 + 2q_2A_2 + 2q_3A_3 + T = 0$$

Substituting:

$$78.6q_1 + 200q_2 + 200q_3 - 100{,}000 = 0 \quad - - - \quad (24)$$

Writing the expression for the angular twist of each cell:-

Cell (1)

$$2G\theta = \frac{1}{A_1}\left[q_1a_{10} + (q_1 - q_2)\, a_{12}\right]$$

Substituting:

$$2G\theta = \frac{1}{39.3}\left[629q_1 + 200q_1 - 200q_2\right] \quad - - - - \quad (25)$$

Cell (2)

$$2G\theta = \frac{1}{A_2}\left[(q_2 - q_1)\, a_{12} + q_2a_{20} + (q_2 - q_3)\, a_{23}\right]$$

Substituting:

$$2G\theta = \frac{1}{100}\left[200q_2 - 200q_1 + 667q_2 + 333q_2 - 333q_3\right] \quad - - - - - - - - - - \quad (26)$$

Cell (3)

$$2G\theta = \frac{1}{A_3}\left[(q_3 - q_2)\, a_{23} + q_3a_{30}\right]$$

Substituting:

$$2G\theta = \frac{1}{100}\left[333q_3 - 333q_2 + 917q_3\right] \quad - - - - \quad (27)$$

Solving equations (24) to (27), we obtain,

$q_1 = 143.4\#/\text{in.}$

$q_2 = 234.1\#/\text{in.}$

$q_3 = 208.8\#/\text{in.}$

$q_2 - q_1 = 90.7\#/\text{in.}$

$q_2 - q_3 = 25.3\#/\text{in.}$

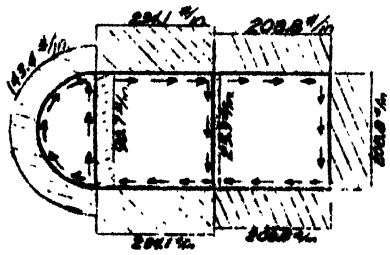


Fig. A5-16

Fig. A5.16 shows the resulting internal shear flow pattern. The angle of twist, if desired,

can be found by substituting values of shear stresses in any of the equations (25) to (27).

A5.15 Problems

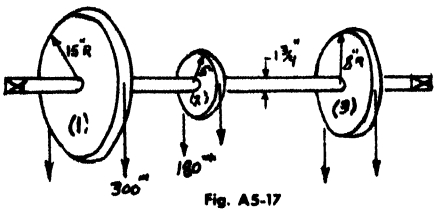


Fig. A5-17

(1) In Fig. A5.17 pully (1) is the driving pulley and (2) and (3) are the driven pulleys. The shaft rotates at constant speed, The difference in belt pull on two sides of a pulley are shown on the figure. Calculate the maximum torsional shearing stress in the 1-3/4 inch shaft between pulleys (1) and (2) and between (2) and (3).

(2) A 1/2 HP. motor operating at 1000 RPM rotates a 3/4 - .035 aluminum alloy torque tube 30 inches long which drives the gear mechanism for operating a wing flap. Determine the maximum torsional stress in the torque shaft under full power and RPM. Find the angular deflection of shaft in the 30 inch length. Polar moment of inertia of tube = .01 in. Modulus of rigidity G = 3800,000 psi.

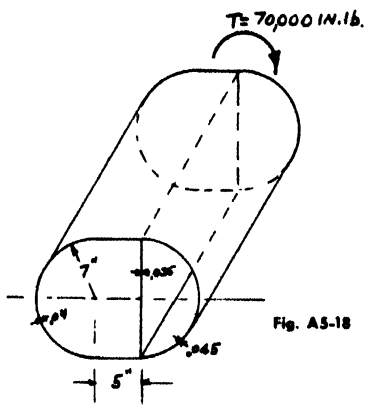


Fig. A5-18

(3) In the cellular section of Fig. A5.18 determine the torsional shear flow in resisting the external torque of 70000 in. lb. Web and wall thickness are given on the figure. Assume the tube is 100 in. long and find the torsional deflection. Material is aluminum alloy. (G = 3800,000 psi.)

(4) In Fig. A5.18 remove the interior .035 web and compute torsional shear flow and deflections.

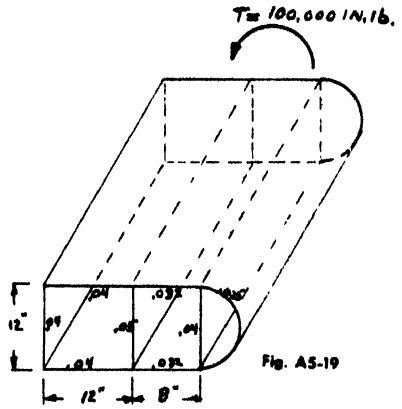


Fig. A5-19

(5) In the 3-cell structure of Fig. A5.19 determine the internal resisting shear flow due to external torque of 100,000 in. lb. For a length of 100 inches calculate twist of cellular structure if G is assumed 3,800,000 psi.

(6) Remove the .05 interior web of Fig. A5.19 and calculate shear flow and twist.

(7) Remove both interior webs of Fig. A5.19 and calculate shear flow and twist.

REFERENCES

"The Initial Torsional Stiffness of Shells With Interior Webs", by Kuhn; N.A.C.A. T.N. #542.

"Torsion in Thin Cylinders", by Atkin; Flight. Sept. 25, 1931

"The Torsion and Flexure of Cylinders and Tubes", by Duncan; R and M. #1444.

"Torsional Stiffness of Thin Duralumin Shells Subjected to Large Torques", by Kuhn; N.A.C.A., T.N. #500.

"Strength of Materials", Part II by Timoshenko; D. Van Nostrand.

"Structural Design of Metal Airplanes", by Younger; McGraw-Hill.

A15.16 Torsional Shear Flow by Method of Successive Corrections.

The method of successive corrections as explained and illustrated in Chapter A11 avoids the solution of a series of equations as presented in this chapter and therefore for cases of two or more cells the method in chapter A11 is more rapid in obtaining the desired shear flow results.

CHAPTER A6
SHEAR AND BENDING FORCES

A6.1 Introduction. As in other fields of structural engineering, the beam is a very important member in aircraft construction. In general, it no doubt can be truthfully said that the airplane structural designer goes into more detail in the analysis and design of beams than those engineers in other fields of structural engineering. This is due in part to two conditions, namely, that weight saving and aerodynamic cleanness is of primary importance in airplane design, and secondly, the factor of safety in airplane design, because of the effect of weight on performance, is generally not as high as in other fields of engineering structures.

Before we can proportion a beam to resist external loads, a thorough knowledge of the manner in which external loads on a beam tend to deform the beam is necessary. This chapter deals with the external influences for statically determinate beams, while a following chapter deals with indeterminate beams. The study of the internal relationships which resist these external influences is likewise taken up in following chapters.

A6.2 Beam Shear and Bending Forces. Fig. A6.1 shows a simply supported beam carrying a single concentrated load. The beam as a whole is in equilibrium under the load of 100# and the two reactions of 75 and 25 lbs., therefore, any portion of the beam must be in equilibrium. Consider the beam to be cut at section a-a.

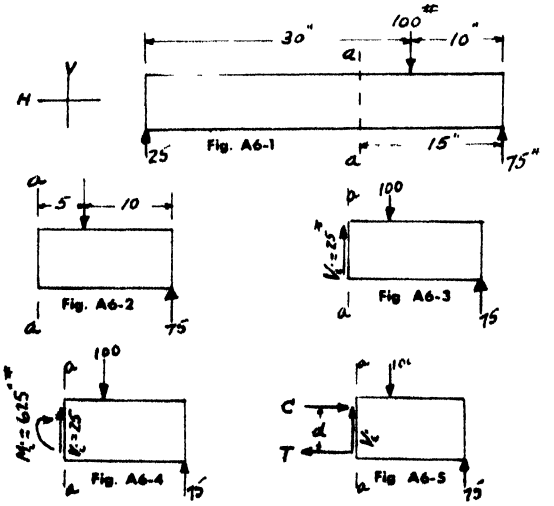


Fig. A6.2 shows a free body sketch of the portion of the beam to the right of the section with only the external load and reaction shown.

For equilibrium, the three equations ΣV, ΣH and ΣM must equal zero. Considering $\Sigma V = 0$ in Fig. A6.3.

$$\Sigma V = 75 - 100 = -25 \text{ lb} \quad \text{- - - - - - - - - - - - (1)}$$

thus, under the forces shown, the force system is unbalanced in the V direction, and therefore an internal resisting force V_1 equal to 25# must have existed on section a-a to produce equilibrium of forces in the V direction. Fig. A6.3 shows the resisting shear force, $V_1 = 25\#$, which must exist for equilibrium.

Considering $\Sigma M = 0$ in Fig. A6.3, take moments about some point O on section a-a,

$$\Sigma M_O = -75 \times 15 + 100 \times 5 = -625 \text{ in. lb.} \quad \text{- - - (2)}$$

or an unbalanced moment of -625# tends to rotate the portion of the beam about section a-a. A counteracting resisting moment $M = 625\#$ must exist on section a-a to provide equilibrium. Fig. A6.4 shows the free body with the V_1 and M_1 acting.

Now ΣH must equal zero. The external forces as well as the internal resisting shear V_1 have no horizontal components. Therefore, the internal forces producing the resisting moment M_1 must be such as to have no horizontal unbalanced force, which means that the resisting moment M_1 in the form of a couple, as shown in Fig. A6.5, or, $M_1 = Cd$ or Td and T must equal C to make $\Sigma H = 0$.

The tendency of the loads and reactions acting on a beam to shear or move one portion of a beam up or down relative to the adjacent portion of the beam is called the External Vertical Shear, or commonly referred to as the beam Vertical Shear and is represented by the term V.

From equation (1), the Vertical Shear at any section of a beam can be defined as the algebraic sum of all the forces and reactions acting to one side of the section at which the shear is desired. If the portion of the beam to the left of the section tends to move up relative to the right portion, the sign of the Vertical Shear is taken as positive shear and negative if the tendency is opposite. Or in other words, if the algebraic sum of the forces is up on the left or down on the right side, then the Vertical Shear is positive, and negative for down on the left and up on the right.

From equation (2), the Bending Moment at any section of a beam can be defined as the algebraic sum of the moments of all the forces acting to either side of the section about the section. If this bending moment tends to produce compression (shortening) of the upper fibers and tension (stretching) of the lower fibers of the beam, the bending moment is classed as a

positive bending moment, and negative for the reverse condition.

A6.3 Shear and Moment Diagrams. In aircraft design, a large proportion of the beams are tapered in depth and section, and also carry a variable distributed load. Thus, to design or check the various sections of such beams, it is necessary to have a complete picture as to the value of the vertical shear and bending moment at all sections along the beam. If these values are plotted as ordinates from a base line, the resulting curves are referred to as Shear and Moment diagrams. A few example Shear and Moment diagrams will be plotted, to refresh the students knowledge regarding these diagrams.

Example Problem 1

Draw a shear and bending moment diagram for the beam shown in Fig. A6.6. Neglect the weight of the beam.

In general, the first step is to determine the reactions.

To find R_B, take moments about point A.

$\Sigma M_A = -4 \times 500 + 1000 \times 5 + 300 \times 13 - 10 R_B = 0$.·. $R_B = 690\#$

$\Sigma V = -500 + R_A - 1000 - 300 + 690 = 0$.·. $R_A = 1110\#$

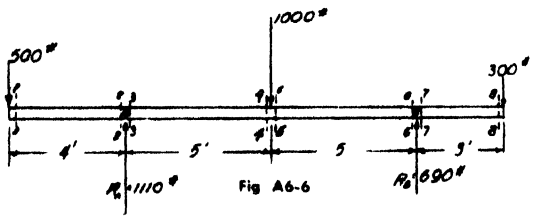


Fig A6-6

Calculations for Shear Diagram:-

We start at the left end of the beam. Considering a section just to the right of the 500# load, or section 1-1, and considering the portion to the left of the section, the Vertical Shear at 1-1 = $\Sigma V = -500\#$ (negative, down on left.)

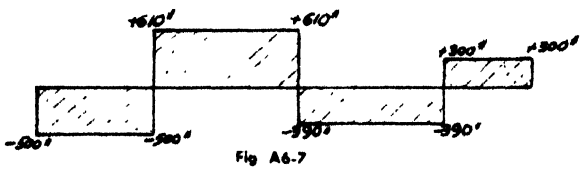


Fig A6-7

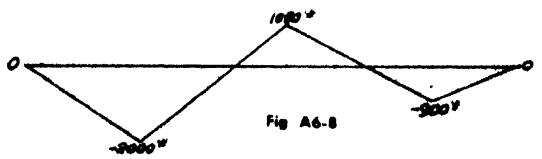


Fig A6-8

Next, consider section 2-2, just to left of reaction R_A.

$\Sigma V = -500\#$, or same as at section 1-1

Next, consider section 3-3, just to right of R_A

$\Sigma V = -500 + 1110 = 610\#$ (positive, up on left side of section)

Next, consider section 4-4, just to left of 1000# load.

$\Sigma V = -500 + 1110 = 610$ (same as at section 3-3)

Section 5-5, to right of 1000# load:

$\Sigma V = -500 + 1110 - 1000 = -390\#$ (down on left)

Check this shear at section 5-5 by using the portion of the beam to the right of 5-5 as a free body.

$\Sigma V = -300 + 690 = 390\#$, which checks (sign of shear is minus, because ΣV is up on right).

Section 6-6, use the portion to right as a free body:

$\Sigma V = -300 + 690 = 390$ (minus shear)

Section 7-7

$\Sigma V = -300$ (positive shear, down on right)

Section 8-8

$\Sigma V = -300$ (positive shear)

Fig. A6.7 shows the plotted values on the shear diagram.

Calculation of the Moment Diagram.

Start at section 1-1, and consider the forces to the left only:

$\Sigma M = -500 \times 0 = 0$

Since sections 2-2 and 3-3 are only a differential distance apart, assume a section just above R_A and consider the forces on the left side only:

$\Sigma M = -500 \times 4 = -2000"\#$ (Negative moment, because of tension in the top fibers). Consider the section under the 1000# load:

ΣM to left $= -500 \times 9 + 1110 \times 5 = 1050"\#$ (positive moment, compressing the top fibers).

Check by considering the forces to the right:

ΣM right $= 300 \times 8 - 690 \times 5 = -1050\#$

Next, consider a section over R_B:

ΣM right $= 300 \times 3 = 900\#$. (Negative moment, tension in top fibers).

At Section 8-8:

ΣM right $= 300 \times 0 = 0$

Fig. A6.8 shows the plotted values.

From the above results it may be noticed that when the bending moment is obtained from the forces that lie to the left of any section, the bending moment is positive when it is clockwise. If obtained from the forces to the right, it is positive, when counter-clockwise. The student should sketch in the approximate shape of the deflected structure and determine the signs from whether tension or compression exists in the upper and lower fibers.

Example Problem 2

Calculate and draw the shear and moment diagrams for the beam and loading as shown in Fig. A6.9.

First, determine the reactions, R_A and R_B:-

$\Sigma M_A = 36 \times 10 \times 18 + 120 \times 9 - 36 R_B = 0$. .·. $R_B = 210\#$

$\Sigma V = -120 - 36 \times 10 + 210 + R_A = 0$. .·. $R_A = 270\#$

Shear Diagram:-

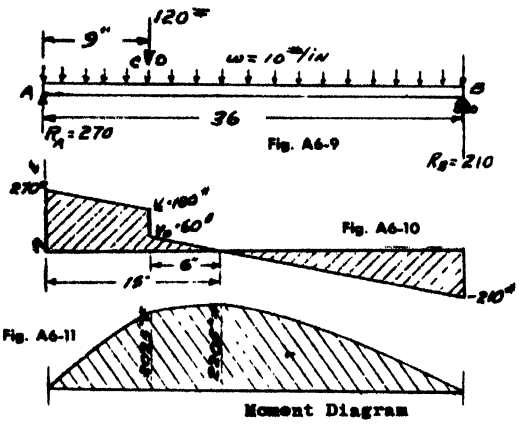
The vertical shear just to the right of the reaction at A is equal to 270# up, or positive. This is plotted as line AE in Fig. 6.10. The vertical shear at section C just to the left of the load P, considering the forces to the left of the section = 270 - 9 x 10 = 180# up, or positive. The vertical shear for any section between A and

C at a distance x from A is:

$V_x = 270 - 10x$, and hence, the shear decreases at a constant rate of 10#/in. from 270# at A to 180# at C.

The vertical shear at section D, just to the right of load P, is

$V_D = \Sigma V_{left} = 270 - 10 \times 9 - 120 = 60\#$ up, or positive.



The vertical shear between points D and B, when x is the distance of any section between D and B from A:

$$V_{DB} = 270 - 120 - 10x \quad \text{- - - - - - - - - - - (1)}$$

At point B, x = 36:

$\therefore V_B = 270 - 120 - 10 \times 36 = -210\#$, which checks the reaction R_B.

Since the Vertical Shear decreases at a rate of 10#/in. from D to B, it will be 6" from D to a point where the shear is zero, since the shear at D is 60#.

This point could also be located by equating equation (1) to zero and solving for x as follows:

$0 = 270 - 120 - 10x$, or $x = \frac{150}{10} = 15"$ from A.

If the shear diagram has passed thru zero under the concentrated load, then the method of equating the shear equation to zero and solving for x could not be used, thus in general, it is best to draw a shear diagram to find when shear is zero. Fig. A6.10 shows the plotted shear diagram.

Moment Diagram

At section A just to the right of reaction R_A the bending moment, considering the forces to the left, is zero, since the arm of R_A is zero.

The bending moment at any section between A and C, at a distance x from the left reaction R_A, is,

$$M_x = R_A x - \frac{wx^2}{2} \quad \text{- - - - - - - - - - - - - - (2)}$$

In equation (2), x can not be greater than 9.

The equation for the bending moment between D and B (x greater than 9) is

$$M_x = R_A x - P(x-9) - \frac{wx^2}{2} \quad \text{- - - - - - - - (3)}$$

$$= 270x - 120(x-9) - \frac{10x^2}{2} \text{ - - -}$$

$$= 1080 + 150x - 5x^2 \quad \text{- - - - - - - - - - - - - (4)}$$

At section C, x = 9", substitute in equation (4)

$M_C = 1080 + 150 \times 9 - 5 \times 9^2 = 2025"\#$ (positive, compression in top fibers)

At the point of zero shear, x = 15"

$M = 1080 + 150 \times 15 - 5 \times 15^2 = 2205"\#$

Thus, by substituting in equation (2) and (4) the moment diagram as plotted in Fig. A6.11 is obtained.

A6.5 Section of Maximum Bending Moment

The general expression for the bending moment on the beam of example problem 2 is from equation (3)

$$M_x = R_A x - P(x-9) - \frac{wx^2}{2}$$

Now, the value of x that will make M_x a maximum is the value that will make the first derivative of M_x with respect to x equal to zero, or

$$\frac{dM_x}{dx} = R_A - P - wx \quad \text{- - - - - - - - - - - - - (5)}$$

Therefore, the value of x that will make M_x a maximum may be found from the equation

$$R_A - P - wx = 0$$

But, observation of this equation indicates that the term $R_a - P - wx$ is the shear for the section at a distance x from the left reaction. Therefore, where the shear is zero, the bending moment is maximum. Thus, the shear diagram which shows where the shear is zero is a convenient medium for locating the points of maximum bending moment.

A6.6 Relation Between Shear and Bending Moment

Equation (5) can also be written

$\frac{dM}{dx} = V$, since the right hand portion of equation (5) is equal to the shear.

Hence, $dM = Vdx$ - - - - - - - - - - - - - - (6)

Which means that the difference dM between the bending moments at two sections that are a distance dx apart, is equal to the area Vdx under the shear curve between the two sections. Thus, for two sections x_1 and x_2,

$$\int_{M_1}^{M_2} dM = \int_{x_1}^{x_2} Vdx$$

Thus, the area of the shear diagram between any two points equals the change in bending moment between these two points.

To illustrate this relationship, consider the shear diagram in example problem 2 (Fig. A6.10). The change in bending moment between the left reaction R_A and the load is equal to the area of the shear diagram between these two points, or

$\frac{270 + 180}{2} \times 9 = 2025"\#$. Since the bending moment at the left support is zero, this change therefore equals the true moment at a section under the load P.

Adding to this the area of the small triangle between point D and the point of zero shear, or $\frac{60 \times 6}{2} = 180$, we obtain 2205"# as the maximum moment. This can be checked by taking the area of the shear diagram between the point of zero shear and point B = $\frac{210 \times 21}{2} = 2205$"#.

A6.7 Shears and Bending Moments for Cantilever Beam With Varying Load

Cantilever wing and tail surfaces are usually tapered in plan form, thus, the spanwise running load will be variable. Fig. A6.12 shows a cantilever beam loaded with a variable distributed load acting upward plus a single concentrated load acting down as shown. Table 1

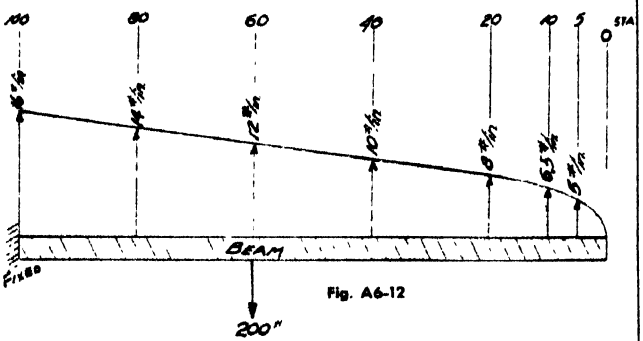


Fig. A6-12

shows the calculations for determining the shear and bending moments at various stations along the beam. The first step as indicated in Column 1 of Table 1 is to divide the load curve into small enough segments to give enough values of the shear and moment values, so that an accurate shear and moment curve can be drawn. Column 1 shows the widths selected. Near the free end of the beam, due to the rapid change in the load intensity, the load segments have been decreased in width from 10 to 5 inches. Columns 2,3,4 and 5 are self explanatory and give the calculations for determining the weight of the loads on each of the selected segments. Column 6 gives the arm a, to the centroid of the load on a segment from the left edge of the segment. A slightly conservative arm would be to take the center line point of each load segment. The values given in the table are exact, use having been made of Table 2 of Chapter A3 which gives the centroids of trapezoidal areas. The values in column 11 equal the sum of columns 7 and 10, and the value of M in column 11 at the station previous to that station being considered. This summation can be explained by referring to Fig. A6.13. $M_b = M_a + V_a x + P_a$ or in general, the bending moment at a particular station is equal to the bending moment at the previous station, plus the shear at the previous station times the distance between the two stations plus the moment of any forces acting on the beam between the two stations.

In column 1, it should be noticed that the concentrated load of 200# has been entered as a segment which extends from a differential distance to the right of the force or - 60 station to a differential distance to the left of the forces or station + 60, thus, a concentrated load is treated as a segment of zero width.

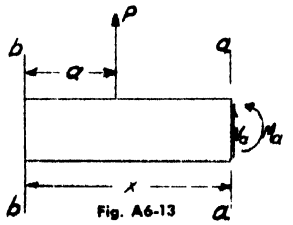


Fig. A6-13

A6.8 Problems

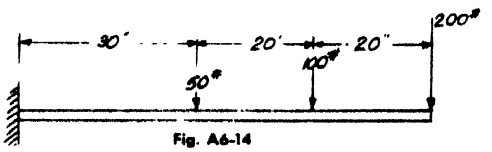


Fig. A6-14

(1) Draw vertical shear and bending moment diagrams for the cantilever beam shown in Fig. A6.14. Neglect the weight of the beam.

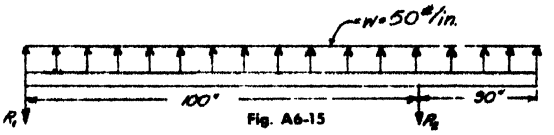


Fig. A6-15

Table I

1 Station	2 W = load/ inch	3 W_a = aver. load/ inch	4 X dist. between station	5 P = load between station	6 a = arm to centroid	7 P_a = moment M_1	8 V = ΣP = shear	9 dist. between station	10 Vx	11 Bend. moment = M
0	0						0			
		2.5	5.0	12.5	1.67			5.0		
5	5					20.9	12.5			20.9
		5.75	5.0	28.75	2.39			5.00		
10	6.5					68.80	41.25		62.5	132.2
		7.25	10.0	72.50	4.83			10.0		
20	8.0					350.00	113.75		412.5	914.7
		9.00	20.0	180.00	9.63			20.		
40	10.0					1735	293.75		2275	4925
		11.00	20.0	220.00	9.70			20		
+60	12.0					2130	513.75		5875	12930
			0	-200.00	0			0		
-60	12.0					0	313.75		0	13930
		13.0	20.0	260.0	9.75			20		
80	14.0					2540	573.75		6275	21745

(2) Draw vertical shear and bending moment diagrams for the beam shown in Fig. A6.15. Neglect the weight of the beam.

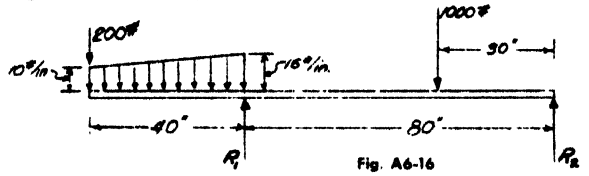


Fig. A6-16

(3) Draw shear and bending moment diagrams for the beam shown in Fig. A6.16. Neglect the weight of the beam.

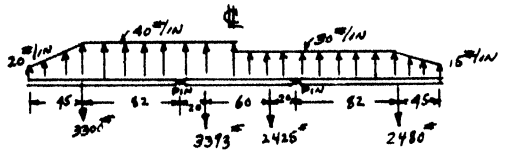


Fig A6-17

(4) Draw the shear and bending moment diagrams for the loaded biplane wing shown in Fig. A6.17. This beam is identical to the beam used in example 3 in Chapter A1 and the reactions are taken from that solution.

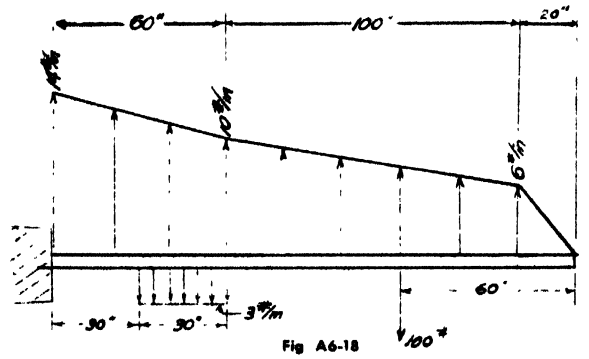


Fig A6-18

(5) Fig. A6.18 shows a cantilever beam loaded with a varying distributed upward load and a uniform distributed downward load and one concentrated downward load. In table form, calculate the shear and bending moments at various stations along the spar.

(6) Fig. A6.19 shows a plan view of a cantilever wing. The spanwise distribution of the normal lift load is constant. Taking the average normal lift wing loading as 100 lb./sq. ft., write expressions for shear and bending moment on wing and plot shear and bending moment diagrams.

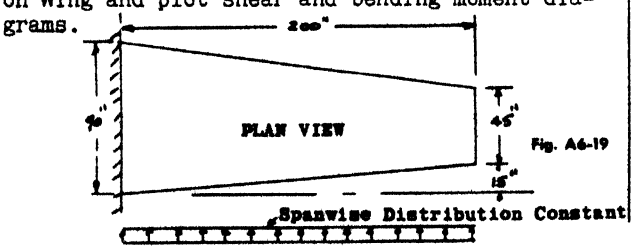


Fig. A6-19

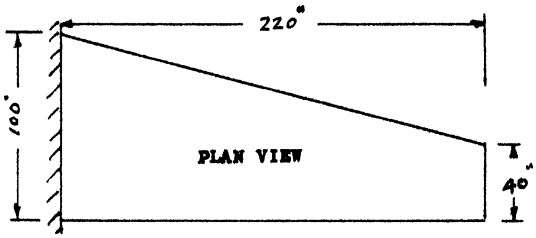


Fig. A6-20

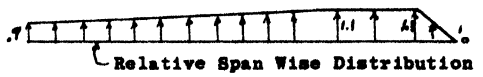


Fig. A6-21

(7) Fig. A6.20 shows a plan view of a cantilever wing. The relative spanwise distribution of the lift air load is shown in Fig. A6.21. For a total lift load on wing panel normal to wing of 12000#, calculate and plot the shear and bending moment diagrams.

(8) Fig. A6.22 shows an externally braced monoplane wing. Take an average wing lift load of 90 lb./sq. ft. normal to wing with center of pressure at 27 percent of the chord from leading edge of wing and calculate and draw the front and rear beam primary shears and bending moment diagrams.

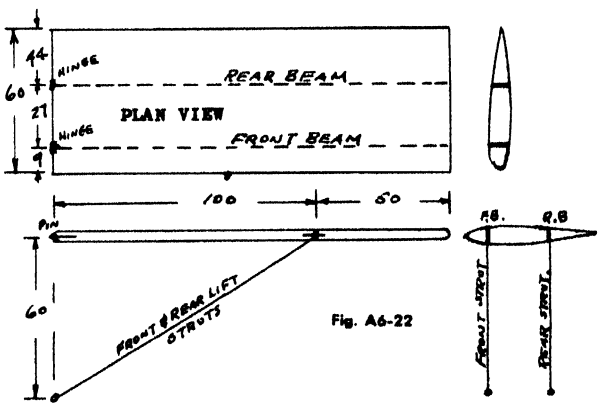


Fig. A6-22

(9) For the tapered externally braced monoplane of Fig. A6.23 draw the primary shear and bending moment diagrams for the front and rear wing beams for an average wing loading of 100 lb. per sq. ft. and with center of pressure of lift at 30% of chord from leading edge.

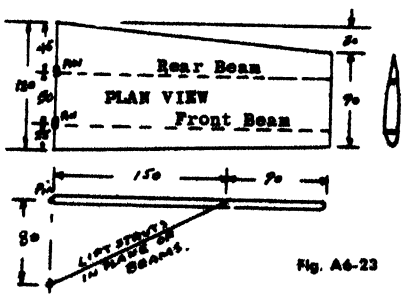


Fig. A6-23

CHAPTER A7
DEFLECTIONS OF BEAMS AND TRUSSES

A7.1 Introduction. A consideration of deflections or distortions plays an important part in the theory of structures because it provides the additional facts and means for determining such external reactions or internal forces on a structure which cannot be found completely with the laws of statics. For statically determinate structures, the magnitude and shape of the elastic curve is important in analysis of many aircraft structural problems, and questions of rigidity, flutter etc., also involve a consideration of deflections.

The subject of deflections can be treated by many variations of attack in writing the fundamental relationships of equilibrium and continuity. It is felt that the several methods reviewed in this chapter cover the most useful methods for most common aircraft structures.

A7.2 Deflection of Trusses by Virtual Work Method.

INTRODUCTION. The principle of virtual work is widely used in structural analysis as it is considered one of the most powerful tools in this field. The method has been credited to various persons and the method has been called by names other than virtual work. It appears that the first introduction in the United States was in a paper by Professor George F. Swain.① Many papers have been written regarding the method and some of them are presented in a highly mathematical and rigorous form. The rather brief and elementary presentation which follows is believed adequate for understanding the use of the method.

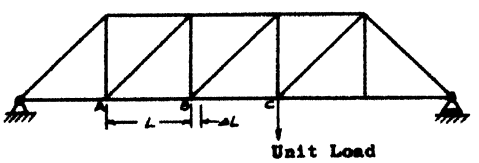


Fig. A7-1

Figure A7.1 shows a simple truss. Let it be required to find the vertical deflection of joint C due to lengthening ΔL of member AB. Now assume for analysis purpose that before the member AB is lengthened a load is applied at joint C in the direction of the desired deflection. For simplicity this load has been taken as one or unity. This assumed unit load at C will produce a certain axial load or stress u in member AB. Now let member AB be lengthened a distance ΔL, all other members of the truss being assumed as rigid. This ΔL lengthening of AB will cause joint C to move a distance δ in a vertical direction. Therefore our unit applied load at C will do external work equal to 1 x δ (force x distance) and the internal stress u in member AB due to the unit load at C will move through a distance ΔL and does internal work equal to uΔL, which becomes potential energy if the elastic limit of material is not exceeded. Since the truss comes to rest after member AB is lengthened ΔL, no kinetic energy is absorbed by the truss, and therefore the external work 1 x δ equals the internal work uΔL or, δ = uΔL and for length changes in any or all members

$$\text{Total } \delta = \Sigma u \Delta L \qquad \text{----------(1)}$$

It should be understood that this work equation is due to our assumed or imaginary force system, namely a unit load at joint C, thus the name virtual work, as this method of derivation has nothing to do with internal work in the structure which is produced by the forces causing the length changes in the members of the truss. The virtual work equation (Eq. 1) given above involves no work due to the reactions to our imaginary unit load, therefore the reactions of the truss to our imaginary or hypothetical unit load must not move if they do no work. The reactions of this unit imaginary load thus fix the direction and a point on the line of reference for the described displacement. For illustration if we want the deflection of point O (Fig. A7.2) due to some force system ΣP with reference to a line adjoining the true reactions A and B, then the reactions to our hypothetical unit load corresponds to these same supports. However, if the deflection of point O is wanted, with respect to a line joining BC and the point B on this line, then the reactions to the unit load at O are at C and B (See Fig. A7.3). A second example is illustrated by Figs. A7.4 and A7.5. If the deflection of joint A with respect to joint B in the direction of the line AB is required due to some external load system ΣP, a unit hypothetical load is applied at A with the reaction at joint B as shown in Fig. A7.5. A third example is illustrated in Figs. A7.6 and A7.7 where points A, B and C might represent points of attachment of aileron to wing beam and it is desired to know the deflection of point B relative to points A and C, due to load system ΣP on wing beam, since this deflection influences the design of the aileron structure and supporting brackets.

①"On the Application of the Principle of Virtual Velocities to the Determination of the Deflection and Stresses of Frames", by George F. Swain, Jr. of the Franklin Institute, Vol. 115, 1883

Fig. A7.7 shows the reactions A and C to the hypothetical unit load at B.

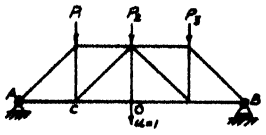


Fig. A7-2

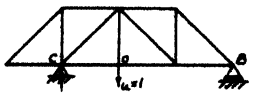


Fig. A7-3

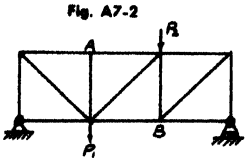


Fig. A7-4

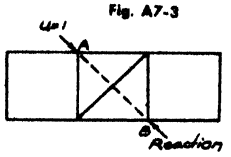


Fig. A7-5

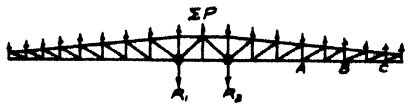


Fig. A7-6



Fig. A7-7 **Reactions at A and C for Unit Load at B**

Since in general the members of a truss carry axial loads and the cross section is usually constant, the term ΔL is equal to $\frac{SL}{AE}$, where S = total axial load or stress on member, L = length, A = cross-sectional area and E modulus of elasticity. Hence the deflection formula for a truss is:-

$$\delta = \sum \frac{SuL}{AE} \quad \text{----------(2)}$$

Summarizing, to find the deflection of any joint of a truss in any given direction under any set of load conditions, proceed as follows:-

(1) Compute the axial stresses "S" in the members of the given truss due to the given loading calling tensile stress plus and compressive stress minus.

(2) Place an auxiliary hypothetical unit load at the panel point where the deflection is required and acting in the direction of the desired deflection.

(3) Compute the stresses "u" in each member of the truss due to this unit hypothetical load, remembering that the reactions to this unit load fix the line of reference for the desired deflection.

(4) Compute for each member of the truss, the length L and the cross-sectional area "A".

(5) The desired deflection is given by the expression $\delta = \sum \frac{SuL}{AE}$. If the result comes out negative, it indicates that the true movement of the joint is opposite in sense to that assumed for the unit hypothetical load.

In order to determine the deflection of the joint completely, the method must be carried out twice for directions at right angles to each other.

The principle of virtual work does not depend on a consideration of true internal work. The internal distortions of the truss members may be elastic or plastic, or due to temperature or play in joints or faulty workmanship.

A7.3 Example Problems

Problem 1.

Fig. A7.8 shows a 2 bay truss supported at C and D and with external loads applied at joints A and E as shown. Required the vertical and horizontal deflection of joint E under the given loading. The members are made from steel with modulus of elasticity E = 29 x 10^6#/in.^{2} Cross-sectional areas of members are given in table A7.1

Solution:- First compute the member stresses due to the given load system. Fig. A7.9 shows the results of these calculations, the stresses being written on each member. To find the vertical deflection of Joint E, apply a unit vertical load u_v = 1# acting down as shown in Fig. A7.10 and calculate stresses in all members due to this unit load with reactions at C and D. The results are tabulated on the truss in Fig. A7.10. In like manner for horizontal deflection of Joint E apply a unit horizontal load u_h = 1# at E as shown in Fig. A7.11 and compute member stresses due to this loading. The results are shown in Fig. A7.11.

The remainder of the solution consists in substituting in equation $\delta = \sum \frac{SuL}{AE}$. Table A7.1 shows the detailed calculations.

Table A7.1

1	2	3	4	5	6	7	8	9
Member	Length	Area Sq. In.	$\frac{L}{AE}$ E-29x10^6	S	u_v	u_h	$Su_v \frac{L}{AE}$	$Su_h \frac{L}{AE}$
AB	40	.694	.0000147	-1000	0	0	0	0
AC	30	.052	.0000198	0	0	0	0	0
BC	50	.12	.0000144	2918	1.67	.625	.0700	.0262
BD	30	.106	.00000875	-2250	-1.50	-.563	.0330	.0123
BE	42.6	.106	.0000138	1420	1.42	.534	.0278	.0105
CD	40	.12	.0000115	-1332	-1.33	.500	.0204	-.0077
DE	42.6	.12	.0000122	-1420	-1.42	.534	.0246	-.0092
						Σ	.1758	.0321

The summation of column 8 equals .1758" = vertical deflection of Joint E.

The summation of column 9 equals .0321" = horizontal deflection of Joint E. Both values come out plus, thus deflection of E is in the direction as assumed for the unit hypothetical loads. If the values had come out minus then deflection would have been opposite to that assumed for the unit load.

Example Problem #2.

Given the cantilever truss as shown in Fig. A7.12. Determine the vertical deflection of Joint G due to the truss loading as shown.

Solution:- Compute the member axial stresses due to the given external loading. These resulting stresses are shown marked on truss members of Fig. A7.12.

Place a unit vertical load acting downward at Joint G as shown, in Fig. A7.13 and find

stresses in members due to this unit load. The results are noted on the members of Fig. A7.13. Table A7.2 gives the detailed calculations for term $\Sigma SuL/AE$.

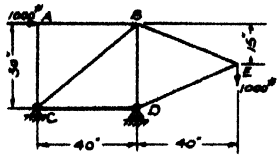


Fig. A7-8

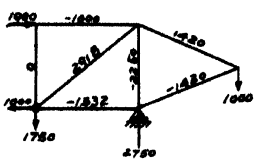


Fig. A7-9

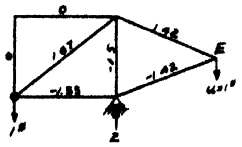


Fig. A7-10

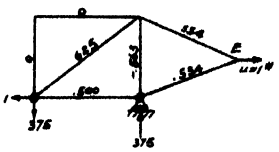


Fig. A7-11

Table A7.2

Member	Length in.	area sq.in.	$\frac{L}{\frac{A\,E}{10000}}$ $E=29\times10^6$	S	u	$(\frac{SuL}{AE})\frac{1}{10,000}$
AB	30	.165	.0626	10500	1.5	.0985
BC	30	.106	.0973	2250	0	0
CD	30	.106	.0973	2250	0	0
EF	30	.185	.0590	-5250	-0.75	.0232
FG	30	.185	.0590	-5250	-0.75	.0232
GH	30	.12	.0860	0	0	0
BE	50	.35	.0482	-8750	-1.25	.0527
BG	50	.12	.1435	5000	1.25	.0895
DG	50	.185	.0930	-3750	0	0
BF	40	.106	.130	2000	0	0
CG	40	.106	.130	-1000	0	0
DH	40	.106	.130	2000	0	0
						Σ 0.287

Therefore deflection of Joint G is .287" downward.

Example Problem #3. For the same truss and loading as shown in Fig. A7.12 determine the deflection of Joint G normal to a line joining points F and H.

The only change in the solution from that in Example #2 is the calculation of the u stresses. Since deflections are wanted relative to line FH, the truss reactions to the unit hypothetical load at point G are placed at Joints F and H (See Fig. A7.14) and stresses due to this system are calculated. The resulting values are shown adjacent to members on Fig. A7.14. Table A7.3 shows the remaining calculations for obtaining the desired deflection.

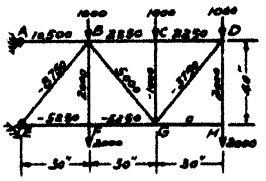


Fig. A7-12

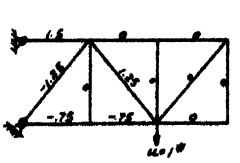


Fig. A7-13

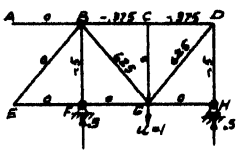


Fig. A7-14

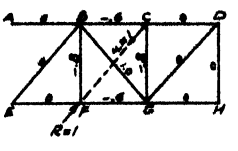


Fig. A7-15

Table A7.3

	Example Problem 3				Example Problem 4	
1	2	3	4	5	6	7
Member	$\frac{L}{\frac{A\,E}{10000}}$	S	u	$\frac{SuL}{AE}$	u	$\frac{SuL}{AE}$
AB	.0626	10500	0	0	0	0
BC	.0973	2250	-.375	-.0082	-.60	-.0131
CD	.0973	2250	-.375	-.0082	0	0
EF	.0590	-5250	0	0	0	0
FG	.0590	-5250	0	0	-.60	.0186
GH	.0860	0	0	0	0	0
BE	.0482	-8750	0	0	0	0
BG	.1435	5000	.625	.0448	1.0	.0717
DG	.0930	-3750	.625	-.0218	0	0
BF	.130	2000	-.50	-.0130	-.80	-.0208
CG	.130	-1000	0	0	-.80	.0104
DH	.130	2000	-.50	-.0130	0	0
				-.0198		.0668"
Deflection of joint G relative to line FH equals .0198" upward since $\frac{SuL}{AE}$ comes out negative.					.'.Deflection of C toward F = .0668"	

Example Problem #4.

For the same truss and loading shown in Fig. A7.12 determine the movement of Joint C relative to Joint F along a diagonal line CF. As in example #3 the only change in the solution is the calculation of the u stresses. Fig. A7.15 shows the unit load applied at joint C and the reaction is placed at F in the direction FC. For this loading the u stresses are calculated. The resulting stresses are shown on Fig. A7.15. Columns 6 and 7 of Table A7.3 show the remaining calculations.

A7.4 Angular Displacement of Truss Members by Virtual Work

In some problems it may be of importance to know the angular displacement of a given line or member in a certain frame work. The principle of virtual work is readily applied to a derivation of an expression for such displacement. Consider the truss in Fig. A7.16 or A7.17 and let it be required to determine the angular displacement of member AB due to a shortening ΔL of member AC.

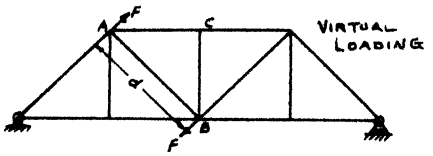


Fig. A7-17

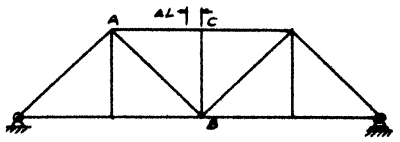


Fig. A7-16

Before the shortening of member AC takes place assume a unit hypothetical couple acting at the ends of the member AB. This unit couple will produce an axial stress u in the member AC. Now assume that member AC is shortened an amount ΔL, all other members being assumed rigid. This shortening ΔL of AC will cause the member AB to rotate thru a small angle δ. Then equating the external and internal work of the hypothetical force system, we obtain.

$$1 \times \delta = u\,\Delta L \quad \text{(Since Fd = unit moment = 1)}$$

Hence for length changes in any or all truss members total $\measuredangle$ (angular displ.) = $\Sigma u\,\Delta L$ and if $\Delta L = \frac{SL}{AE}$, we obtain

$$\delta = \sum \frac{SuL}{AE} \qquad \text{----------(3)}$$

If the angular displacement of member AB is wanted with respect to member EB due to some external load system ΣP (Fig. A7.18) the reactions to the hypothetical unit couple will be at the ends of member EB since it is the reference line for the desired deflection (See Fig. A7.19), the dashed part of the truss would not enter into the calculations.

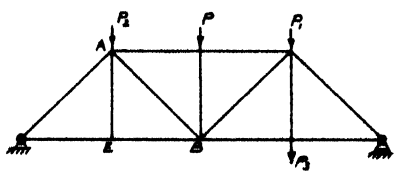


Fig A7-18

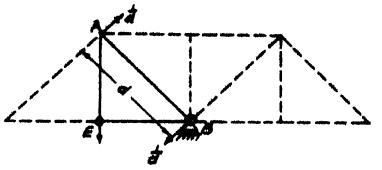


Fig A7-19

Summarizing to find the angular displacement of a member of a truss:-

(1) Compute the axial stresses "S" in the truss members due to the given loading, calling tensile stresses plus.

(2) Apply a unit hypothetical couple to the ends of the member of the truss whose displacement is wanted.

(3) Compute the stresses "u" in each member of the truss due to unit hypothetical couple, remembering that the reactions to this unit couple fix the line of reference for the desired angular deflection.

(4) Compute length "L" and area "A" of each member.

(5) The desired angular deflection is given by the expression $\delta = \sum \frac{SuL}{AE}$. If the result comes out negative, the rotation of the desired member is opposite to that assumed for the unit couple.

A7.5 Example Problems

Problem #5

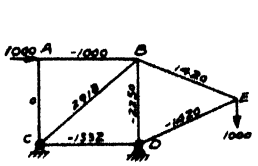


Fig. A7-20

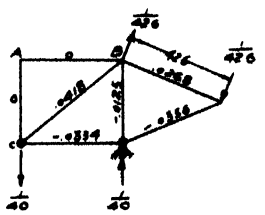


Fig A7-21

Find the angular rotation of member BE for truss of Fig. A7.20 (same truss and loading as in Problem #1 (Fig. A7.8)

Solution:- Compute member axial stresses due to given loading. The results are given on Fig. A7.20. Apply a unit couple to member BE and compute member axial stresses due to this couple loading. (See Fig. A7.21 for applied unit couple

and the stresses produced by the couple). Table A7.4 gives the remainder of the calculations.

Table A7.4

Member	Length in.	Area sq.in.	L/AE E=29x10⁶	S	u	SuL/AE
AB	40	.094	.0000147	-1000	0	0
AC	30	.052	.0000198	0	0	0
BC	50	.12	.0000144	2918	.0418	.00176
BD	30	.106	.00000975	-2250	-.0125	.000274
BE	42.6	.106	.0000138	1420	.0268	.000525
CD	40	.12	.0000115	-1332	-.0334	.000512
DE	42.6	.12	.0000122	-1420	-.0356	.000617
					Σ	.003688

Angular deflection δ of member BE = .003688 x 57.3 = .21° in a clockwise direction since result is positive.

Example Problem #6. Find the angular deflection of member BE of Fig. A7.20 with respect to member BD.

Solution:- Since angular deflection is wanted relative to member BD, the reactions to the unit applied hypothetical couple on member BE are placed at Joints B and D as shown in Fig. A7.22. The stresses in the members due to this hypothetical system are also shown in Fig. A7.22. Table A7.5 gives the detailed calculations for determining the required angular deflection.

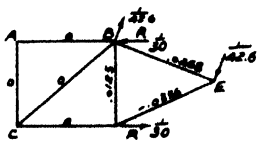


Fig A7-22

Table A7.5

Member	Length in.	Area sq.in.	L/AE E=29x10⁶	S	u	SuL/AE
AB	40	.094	.0000147	-1000	0	0
AC	30	.052	.0000198	0	0	0
BC	50	.12	.0000144	2918	0	0
BD	30	.106	.00000975	-2250	.0125	-.000274
BE	42.6	.106	.0000138	1420	.0268	.000525
CD	40	.12	.0000115	-1332	0	0
DE	426	.12	.0000122	-1420	-0356	.000617
					Σ	.000870

∴ angular deflection δ of member BE with respect to member BD = .0089 x 57.3 = .05° in clockwise direction.

A7.6 Deflection of Beams by Virtual Work

The method of virtual work is likewise easily applied in deriving an expression for the deflection of beams. In pin connected trusses the stress was uniform over the cross-section and uniform thru-out the length of the member, whereas for beams the fiber stress varies as the bending moment which generally varies along the span and furthermore the stresses on a cross-section are not uniform.

The fundamental theory of bending assumes that plane sections remain plane after bending or the fiber strains vary directly as the distance from the neutral axis. Let it be required to determine the vertical deflection of point O (Fig. A7.23), due to bending of a small element dx of the beam thru an angle dθ. Before the bending of this element takes place assume a unit hypothetical vertical load applied at O. This imaginary load will cause a bending moment m on the element dx. Now assume that the element dx is bent as shown thru an angle dθ, the remainder of the beam being rigid. This bending of dx causes the point O to move a vertical distance δ. The external work due to the hypothetical unit load = 1 x δ and the internal work of the hypothetical moment m due to this unit load = mdθ. Equating the internal and external virtual work δ = mdθ.

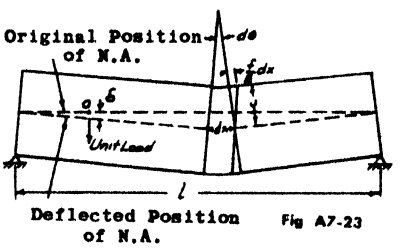


Fig A7-23

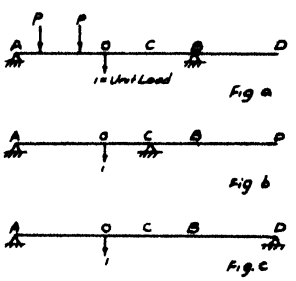


Fig A7-24

From Fig. A7.23 $cd\theta = \frac{f}{E}\,dx$, but $f = \frac{Mc}{I}$ (flexure formula)

hence

$d\theta = \frac{Mdx}{EI}$, where M = bending moment on dx due to any loading. Making a summation for all elements of the beam, we obtain

$$\text{Total } \delta = \int_0^L \frac{Mmdx}{EI} \qquad \text{----------(4)}$$

where,

M = bending moment at any section due to applied loads on beam.

m = bending moment at any point due to a unit load applied at the point at which the deflection of the beam is desired and acting in the direction of the desired deflection. The reactions to the hypothetical unit applied force fixes the

line of reference for the deflection. For example if the vertical deflection of point O due to load system ΣP is wanted relative to a line joining the true reactions at A and B then the reactions to the unit hypothetical load at O are also at these same points A and B (Fig. A7.24a). If the deflection of point O is wanted with respect to line joining A and C, then reactions to unit load are at A and C (Fig. b) and similarly if deflection of O with respect to AD is required place reactions to unit load at A and D.

Tension in the bottom fibers of a beam is considered positive moment. If the results of Eq. (4) come out negative it means the deflection is opposite that assumed for the unit hypothetical load.

E = modulus of elasticity of the material.
I = moment of inertia of beam cross-section.

A7.7 Angular Displacement of Beams due to Bending

The angular displacement of a point on a beam or of a line between any two points on a beam is determined in a similar manner except the hypothetical unit load is replaced by a unit couple. The virtual work equation of the hypothetical load system than becomes

$$\alpha = \int_0^L \frac{Mmdx}{EI} \quad \text{----------(5)}$$

where α is the angular displacement of a given point or a line joining two given points.

M = bending moment at any point due to loads, temperature etc., m is the bending moment at any point due to a unit couple applied at a point at which the angular displacement is wanted or at the ends of a line whose angular displacement is wanted, The reactions to this hypothetical unit couple fix the line of reference for the angular displacement.

Tension on the beam bottom fibers is positive bending moment. The unit couple may be applied with either a clockwise or anti-clockwise direction.. If α in Eq. (5) comes out positive, it means that the given load system produces a rotation in the same direction as that assumed for the applied unit couple.

A7.8 Example Problems of Beam Deflections by Virtual Work

Problem #7.

Determine the vertical deflection at the midpoint C for beam and loading of Fig. A7.25. EI is constant.

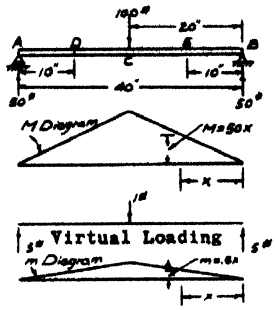


Fig. A7-25

Solution:-

$$\delta_C = \int_A^B \frac{Mmdx}{EI}$$

Take origin at B

M = 50 x If x < 20
m = .5 x If x < 20

Origin at A

M = 50 x If x < 20
m = .5 x If x < 20

$$\delta_C = 2\int_0^{20} \frac{(50x \cdot .5x)dx}{EI} = 2\int_0^{20} \frac{25\,x^2\,dx}{EI} =$$

$$2\left[\frac{25\,x^3}{3EI}\right]^{20} = \frac{133300}{EI}$$

(Due to symmetry integrate for one half and multiply by 2)

Find the deflection of C with respect to line joining points D and E.

Fig. A7.26 shows the virtual loading.

Origin at B

m = .5 (x - 10) = .5 x - 5 when x > 10 and < 20

hence, $\delta_C(DE) = 2\int_{10}^{20} \frac{50\,x\,(.5x - 5)dx}{EI}$

$$= \frac{2}{EI}\left[\frac{25\,x^3}{3} - \frac{250\,x^2}{2}\right]_{10}^{20} = \frac{2}{EI}\left[\left(\frac{25 \times 20^3}{3} - \frac{250 \times 20^2}{2}\right)\right.$$

$$\left. - \left(\frac{25 \times 10^3}{3} - \frac{250 \times 10^2}{2}\right)\right] = \frac{2}{EI}(66667 - 50000 -$$

$$8333 + 12500) = \frac{41668}{EI}$$

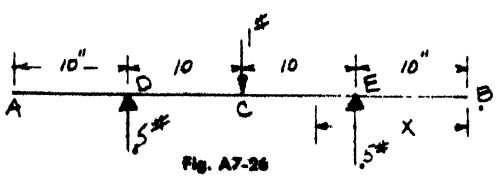


Fig. A7-26

Example Problem #8. Find the vertical deflection of point C for the cantilever beam of Fig. A7.27 carrying a concentrated load P at its end. Also find slope of elastic curve at C.

Solution:-

$$\delta_C = \int \frac{Mmdx}{EI}$$

With origin at B

$M = -Px$ (Fig. A7.27)

For virtual loading (Fig. A7.28)

$m = 0$, for $x < b$

$m = -1\,(x - b)$, for $x > b$

Hence $Mmdx = -Px(-x + b)dx = (Px^2 - Pbx)dx$

Whence $\delta_C = \frac{P}{EI}\int_b^L (x^2 - bx)dx = \frac{P}{EI}\left[\frac{x^3}{3} - \frac{bx^2}{2}\right]_b^L$

$$= \frac{P}{3EI}\left[L^3 - \frac{3L^2b}{2} + \frac{b^3}{2}\right],$$

If b = zero, then $\delta_B = PL^3/3EI$

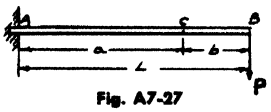


Fig. A7-27

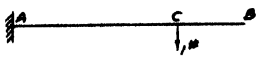


Fig. A7-28

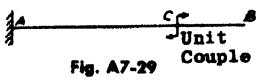


Fig. A7-29

$$\alpha_C = \int \frac{Mmdx}{EI}$$

For virtual loading see Fig. A7.29

$m = 0$, $x < b$, $m = -1$, $x > b$

Hence $Mmdx = (-Px.-1)\,dx = Px\,dx$

$$\therefore \alpha_C = \int \frac{Mmdx}{EI} = \frac{P}{EI}\int_b^L x\,dx = \frac{P}{2EI}(L^2 - b^2)$$

If $b = 0$, $\alpha_B = \frac{PL^2}{2EI}$

Example Problem #9

For the uniformly loaded cantilever beam of Fig. A7.30, find the deflection of point D relative to the line joining points C and E on the elastic curve of the beam. This is representative of a practical problem in aeronautics, in that AB might represent a rear wing beam and points C, D, E, the attachment points of an aileron or a flap. The wing beam deflection bends the aileron or flap structure by applying a load at D thru aileron supporting bracket. To know this force the deflection of the wing beam at D relative to line CE must be known.

Solution:-

Origin at B:-

$$M = 30x \cdot \frac{x}{2} = 15x^2$$

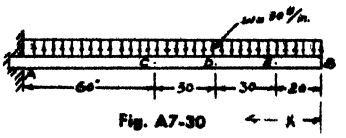


Fig. A7-30

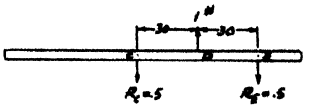


Fig. A7-31

Virtual Loading

$m = 0$, $x < 20$

$m = -.5\,(x - 20) = -.5x + 10$, when $x = 20$ to 50

$m = -.5\,(x - 20) + 1\,(x - 50) = .5x - 40$, when $x = 50$ to 80

$$\delta_{D(CE)} = \int \frac{Mmdx}{EI}$$

$$= \frac{1}{EI}\int_{20}^{50} 15x^2\,(-.5x + 10)dx + \frac{1}{EI}\int_{50}^{80} 15x^2\,(.5x - 40)\,dx$$

$$= \frac{1}{EI}\left[\frac{-7.5x^4}{4} + \frac{150x^3}{3}\right]_{20}^{50} + \frac{1}{EI}\left[\frac{7.5x4}{4} - \frac{600x^3}{3}\right]_{50}^{80}$$

$$= \frac{1}{EI}\Big[=11{,}718{,}750 + 6250000 + 300000 - 400000 + 76800000 - 102400000 - 11718750 + 25000{,}000\Big] = \frac{17888000}{EI}$$

Therefore deflection of point D relative to line joining CE is down because result comes out negative and therefore opposite to direction of virtual load.

Example Problem #10

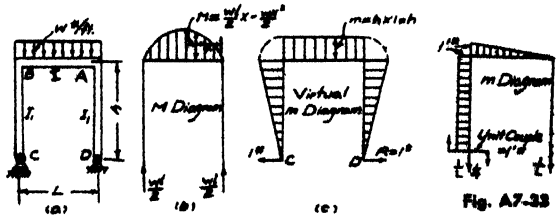


Fig. A7-32

Find the horizontal deflection of point C for the frame and loading of Fig. A7.32. Also angular deflection of C with respect to line CD. Solution:- Fig. b shows the static moment curve for the given loading and Fig. c the moment diagram for the virtual loading of a unit horizontal

load applied at C and resisted at D.

$$\delta_{C(H)} = \int \frac{Mmdx}{EI} \; ; \quad M = \frac{wLx}{2} - \frac{wx^2}{2} \; ; \; m = h$$

hence

$$\delta_C = \int_0^L \frac{\left(\frac{wLx}{2} - \frac{wx^2}{2}\right)}{EI} h dx = \left[\left(\frac{wLx^2}{4} - \frac{wx^3}{6}\right)\frac{h}{EI}\right]_0^L =$$

$$\frac{1}{12} \frac{whL^3}{EI}$$

To find angular deflection at C apply a unit imaginary couple at C with reactions at C and D. Fig. A7.33 show the virtual m diagram.

$$\alpha_C = \int_0^L \frac{Mmdx}{EI} = \frac{1}{EI}\int_0^L \left(\frac{wLx}{2} - \frac{wx^2}{2}\right)\frac{xdx}{L} = \frac{1}{EI}\int_0^L$$

$$\left(\frac{wLx^2}{2L} - \frac{wx^3}{2L}\right) dx = \frac{1}{EI}\left[\frac{wx^3}{6} - \frac{wx^4}{8L}\right]_0^L =$$

$$\frac{1}{24} \frac{wL^3}{EI}$$

A7.9 Linear Deflection of Beams Due to Shear by Virtual Work

Generally speaking, shear deflections in beams are small compared to that due to bending except for comparatively short beams and therefore are usually neglected in deflection calculations. A close approximation is sometimes made by using a modulus of elasticity slightly less than that for bending and using the bending deflection equations.

The expression for shear deflection of a beam is derived from the same reasoning as in previous derivations. The virtual work equation for the hypothetical unit load system for a shear detrusion dy (Fig. A7.34) considering only dx elastic is 1 x δ=vdy where v is shear on section due to unit hypothetical load at point O, and dy is the shear detrusion of the element dx due to any given load system or any other cause.

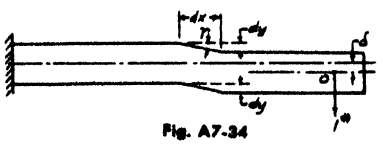


Fig. A7.34

dy = γ dx and $\gamma = \frac{V}{AE_S}$, where A = cross sectional area of beam at section and E_S = modulus of rigidity, and assuming that the shearing stress V is uniform over the cross-section.

Therefore 1 x δ = $\frac{Vvdx}{AE_S}$. Then the total deflection for the shear slips of all elements of the beam equals

$$\delta \text{ total} = \int_0^L \frac{Vvdx}{AE_S} \quad \text{----------} \quad (6)$$

where V is the shear at any section due to given loads. v = shear at any section due to unit hypothetical load at the point where the deflection is wanted and acting in the desired direction of the deflection. The reactions to the hypothetical unit load fix the line of reference for the deflection.

A is the cross-sectional area and E_S the modulus of rigidity. Equation (6) is slightly in error as the shearing stress is not uniform over the cross-section, e.g. being parabolic for a rectangular section. However, the average shearing stress gives close results.

For a uniform load of w per unit length, the center deflection on a simply supported beam is:-

$$\delta_{center} = 2\int_0^{\frac{L}{2}} \frac{Vvdx}{AE_S} = 2\int_0^{\frac{L}{2}} \frac{\left(\frac{wL}{2} - wx\right)}{AE_S} \cdot \frac{1}{2} dx =$$

$$= \frac{wL^2}{8AE_S}$$

For bending deflection for a simply supported beam uniformly loaded the center deflection is

$$\frac{5}{384} \frac{wL^4}{EI}$$

Hence $\frac{\frac{wL^2}{8AE_S}}{\frac{5wL^4}{384EI}} = 24 \left(\frac{r}{L}\right)^2$, using $E_S = .4E$

r = radius of gyration

For I beams and channels r is approximately $\frac{1}{2}d$.

and for rectangular sections $r = \frac{d}{\sqrt{12}}$

In aircraft structures a ratio of $\frac{d}{L}$ is seldom greater than $\frac{1}{12}$.

Thus the shearing deflection in percent of the bending deflection equals 4.1% for a $\frac{d}{L}$ ratio of $\frac{1}{12}$ for I-beam sections and 1.4 percent for rectangular sections.

Example Problem 11.

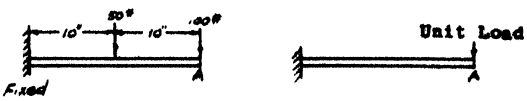


Fig. A7-35

Find the vertical deflection of free end A due to shear deformation for beam of Fig. A7.35 assuming shearing stress uniform over cross-section, and AE_S constant.

$$\delta_A = \int \frac{Vvdx}{AE_S}$$

V = 100# for x = 0 to 10
V = 150 for x = 10 to 20
v = 1 for x = 0 to 20

hence

$$\delta_A = \frac{1}{AE_S}\int_0^{10} 100 \cdot 1 \, dx + \frac{1}{AE_S}\int_{10}^{20} 150 \cdot 1 \, dx$$

$$= \frac{1}{AE_S}\left[100x\right]_0^{10} \frac{1}{AE_S}\left[150x\right]_{10}^{20} = \frac{2500}{AE_S}$$

A7.10 Method of Virtual Work Applied to Torsion of Cylindrical Bars

The angle of twist of a circular shaft due to a torsional moment may be found by similar reasoning as used in previous articles for finding deflection due to bending or shear forces. The resulting expressions are:-

$$\delta = \int \frac{Tm_t dx}{E_S J} \quad \text{- - - - - - - - - - - - - - - - -(A)}$$

$$\theta = \int \frac{Ttdx}{E_S J} \quad \text{- - - - - - - - - - - - - - - - -(B)}$$

In equation (A)

- T = twisting moment at any section due to applied twisting forces.
- m_t = torsional moment at any section due to a virtual unit 1 lb. force applied at the point where deflection is wanted and applied in the direction of the desired displacement.
- E_S = shearing modulus of elasticity for the material.
- J = polar moment of inertia of the circular cross-section.

In equation (B)

- θ = angle in twist at any section due to the applied twisting moments in planes perpendicular to the shaft axis. Angle in radians.
- t = torsional moment at any section due to a unit virtual couple acting at section where angle of twist is desired and acting in the plane of the desired deflection.

A7.11 Example Problem

Problem 12.

Fig. A7.36 shows a cantilever landing gear strut-axle unit ABC lying in XY plane. A load of 1000# is applied to axle at point A normal to XY plane. Find the deflection of point A normal to XY plane. Assume strut and axle are tubular and of constant section.

Solution:- The loading shown causes both bending and twisting of the strut axle unit. First find bending and torsional moments on axle and strut due to 1000# load.

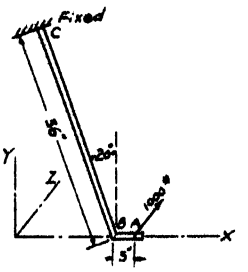


Fig. A7-36

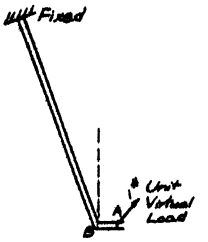


Fig. A7-37

$$\delta = \int \frac{Mmdx}{EI} + \frac{Tm_t dx}{E_S J}$$

Member AB $M = 1000\,x$, (for x = 0 to 3)
$T = 0$

Member BC $M_{BC} = 3000 \sin 20^\circ + 1000\,x$, (for x = 0 to 36)
$T_{BC} = 3000 \cos 20^\circ$ constant between B and C.

Now apply a unit 1# force at A normal to xy plane as shown in Fig. A7.37 and find bending and torsional moments due to this 1# force.

Member AB
$m = 1 \cdot x = x$, (for x = 0 to 3)
$m_t = 0$

Member BC
$m = 3 \sin 20^\circ + 1 \cdot x$ (for x = 0 to 36)
$m_t = 3 \cos 20^\circ$ constant between B and C.
Subt.

$$\delta = \int \frac{Mmdx}{EI} + \int \frac{Tm_t dx}{E_S J}$$

$$= \frac{1}{EI}\int_0^3 1000\,x \cdot x \, dx + \frac{1}{EI}\int_0^{36} \left[(1000\,x + 1026)(x + 1.026)\right] dx + \frac{1}{E_S J}\int_0^{36} (2820)(2.82)dx$$

$$= \frac{1}{EI}\left(\left[333\,x^3\right]_0^3 + \left[333\,x^3 + 1026\,x^2 + 1050\,x\right]_0^{36}\right) + \frac{1}{E_S J}\left[7952\right]_0^{36} = \frac{1}{EI}(16{,}92500) + \frac{1}{E_S J}(286200)$$

Note: A practical landing gear strut would involve a tapered or reinforced section involving a variable I and J and the integration would have to be done graphically.

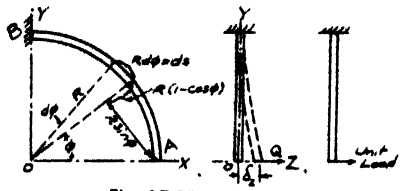


Fig. A7-38 Fig. A7-39

Example Problem 13

In Fig. A7.38 a round rod in the shape of a 90° arc of a circle with radius R, which is large relative to radius of bar is fixed at point B and subjected to a load Q at free end A normal to the xy plane. Find the deflection of A normal to xy plane.

$$\delta_g = \int \frac{Mmds}{EI} + \int \frac{Tm_t ds}{E_s J}$$

From Fig. A7.38 and A7.39

$M = QR \sin \phi$
$m = R \sin \phi$
$T = QR (1 - \cos \phi)$
$m_t = R (1 - \cos \phi)$

Substituting in the above equation.

$$\delta_g = \int_0^{\frac{\pi}{2}} \frac{QR^2 \sin^2 \phi \, Rd\phi}{EI} + \int_0^{\frac{\pi}{2}} \frac{QR^2 (1-\cos \phi)^2 Rd\phi}{E_s J}$$

$$= \frac{QR^3}{EI}\left[\frac{\phi}{2} - \frac{\sin 2\phi}{4}\right]_0^{\frac{\pi}{2}} + \frac{QR^3}{E_s J}\left[\phi - 2 \sin \phi + \frac{\phi}{2} + \frac{\sin 2\phi}{4}\right]_0^{\frac{\pi}{2}} = \frac{\pi QR^3}{4EI} + \frac{3\pi - 8}{4}\frac{(QR^3)}{E_s J}$$

A7.12 Deflection and Angular Change of Elastic Curve of Simple Beams by Method of "Elastic Weights", Mohr's Method.

The method of virtual work as illustrated in the previous articles is advantageous when the deflection of one or only a few points is desired. If the complete deflected elastic curve or the deflection of several points are required then other methods such as "Area Moments" and elastic weights are generally more advantageous. This article will deal with the method of "Elastic Weights".

For finding the deflection of a simply supported beam relative to a line joining the supports, the method of elastic weights, states "The deflection at any point "A" on the elastic curve of a simple beam is equal to the bending moment at point A due to the $\frac{M}{EI}$ diagram acting as a distributed beam load". The $\frac{M}{EI}$ diagram is due to given external loads or influences which produce bending on the beam. If EI is constant the elastic weight loading is identical to beam moment diagram.



Fig. A



Fig. B

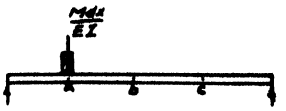


Fig. C

Fig. A7-40



Fig. D

m_b Moment Diagram for Unit Imaginary Load Acting Down at b

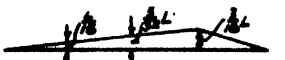


Fig. E

m_c Moment Diagram for Unit Load Acting Down at c



Fig. F

Fig. a of Fig. A7.40 shows a simply supported beam supporting a system P_1 and P_2. Fig. b shows the resulting M/EI diagram assuming assuming EI constant. Now consider only the portion of the $\frac{M}{EI}$ diagram acting on a small element dx of the beam at point A, and let it be required to find the deflection of points b and c due to the bending of element dx.

From the virtual work equation previously derived:-

For point b

$$\delta_b = \frac{Mdx\, m_b}{EI}$$

For a unit load at point b, Fig. d shows the m diagram. The value of m at the midpoint of dx (point a) = L/8. Hence

$$\delta_b = \frac{Mdx}{EI} \cdot \frac{L}{8} = \frac{MLdx}{8\,EI}$$

For deflection of point c, draw m diagram for a unit load at C (see Fig. e). Value of m on element dx = $\frac{L}{16}$

Hence

$$\delta_c = \frac{Mdx}{EI} \cdot \frac{L}{16} = \frac{MLdx}{16EI}$$

In Fig. f consider $\frac{Mdx}{EI}$ as a load on a simply supported beam and determine the bending moment at points b and c due to $\frac{Mdx}{EI}$ acting at point a.

$$M_b = \frac{Mdx}{4EI} \cdot \frac{L}{2} = \frac{MLdx}{8EI}$$

$$M_c = \frac{Mdx}{4EI} \cdot \frac{L}{4} = \frac{MLdx}{16EI}$$

These values of the beam bending moments at points b and c are identical to the deflections at b and c by the virtual work equations. The moment diagram m for a unit load at b and c (Figs. d and e) is numerically precisely the same as the influence line for moment at points b and c.

Therefore deflections of a simple beam can be determined by considering the $\frac{M}{EI}$ curve as an imaginary beam loading. The bending moment at any point due to this $\frac{M}{EI}$ loading equals the deflection of the beam under the given loads.

Likewise it is easily proved that the angular change at any section of a simply supported beam is equal to the shear at that section due to the $\frac{M}{EI}$ diagram acting as a beam load.

A7.13 Example Problems

Example Problem #14. Find the vertical deflection and slope of points a and b for beam and loading shown in Fig. A7.41. The lower Fig. shows the moment diagram for load P acting at center of a simple beam.

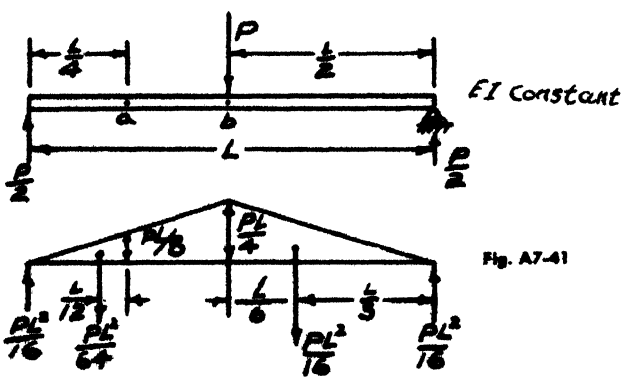


Fig. A7-41

Deflection at point a equals bending moment due to M diagram as a load divided by EI. (See lower Fig. of Fig. A1.41)

$$\delta_a = \left(\frac{PL^2}{16} \cdot \frac{L}{4} - \frac{PL^2}{64} \cdot \frac{L}{12}\right)\frac{1}{EI} = \frac{11}{768}\frac{PL^3}{EI}$$

$$\delta_b = \left(\frac{PL^2}{16} \cdot \frac{L}{2} - \frac{PL^2}{16} \cdot \frac{L}{6}\right)\frac{1}{EI} = \frac{1}{48}\frac{PL^3}{EI}$$

The angular change of any point equals the shear due to M/EI diagram as a load.

$$\alpha_a = \left(\frac{PL^2}{16} - \frac{PL^2}{64}\right)\frac{1}{EI} = \frac{3\,PL^2}{64\,EI}$$

$$\alpha_b = \left(\frac{PL^2}{16} - \frac{PL^2}{16}\right)\frac{1}{EI} = 0$$ (Slope is horizontal or no change from original direction of beam axis.)

Example Problem #14a. Determine the deflection of a simple beam loaded uniformly as shown in Fig. A7.42. The bending moment expression for a uniform load $M = \frac{wlx}{2} - \frac{wx^2}{2}$ or parabolic as shown in Fig. A7.42a. The deflection at midpoint equals the bending moment due to M diagram as a load.

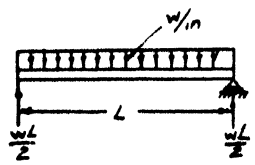


Fig. A7-42

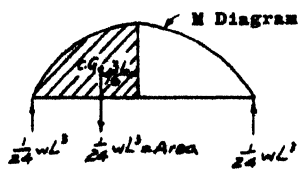


Fig. A7-42a

$$\delta_{center} = \left(\frac{1}{24}wL^3 \cdot \frac{L}{2} - \frac{1}{24}wL^3 \cdot \frac{3}{8}\frac{L}{2}\right)\frac{1}{EI} = \frac{5}{384}\frac{wL^4}{EI}$$

$$\alpha_{center} = \left(\frac{1}{24}wL^3 - \frac{1}{24}wL^3\right)\frac{1}{EI} = 0$$

Slope at supports = the reaction = $\frac{1}{24}\frac{wL^3}{EI}$.

Example Problem #15.

Fig. A7.43 shows the plan view of one-half of a cantilever wing. The aileron is supported on brackets at points D, E and F with self-aligning bearings. The brackets are attached to the wing rear beam at points A, B,and C. When the wing bends under the air load the aileron must likewise bend since it is connected to wing at three points. In the design of the aileron beam and similarly for cases of wihg flaps this deflection produces critical bending moments. Assuming that the running load distributed to the rear beam as the wing bends as a unit is as shown in the Fig., find the deflection of point B with respect to straight line joining points A and C, which will be the deflection of E with respect to

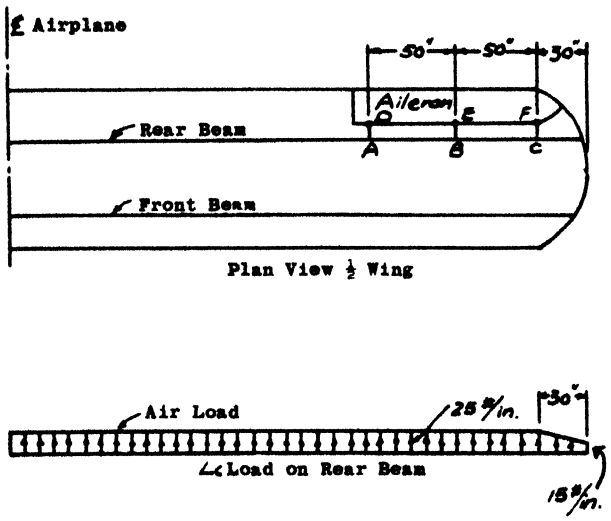


Fig. A7-43

line joining D and F if bracket deflection is neglected. The moment of inertia of the rear beam between A and C varies as indicated in the Table A7.6

Solution:- Due to the beam variable moment of inertia the beam length between A and C will be divided into 10 equal strips of 10 inches each. The bending moment M at the midpoint of each will be calculated. The elastic weight for each strip will equal $\frac{Mds}{I}$, where ds = 10" and I the moment of inertia at midpoint of the strip. These elastic loads are then considered at loads on an imaginary beam of length AC and simply supported at A and C. The bending moment on this imaginary beam will equal the deflection of B with respect to line joining AC.

The bending moment at C = 15 x 30 x 15 + 10 x 15 x 10 = 8250"#

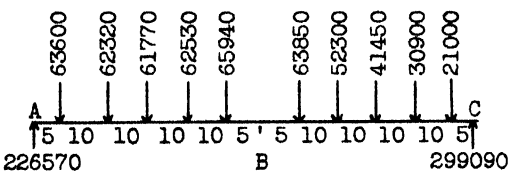
The shear load at C = $\frac{(15+25)}{2} \times 30 = 600\#$

Bending moment expression between points C and A equals, $M = 8250 + 600x + 12.5x^2$, where x = 0 to 100.

Table A7.6 gives the detailed calculations for the strip elastic loads. The I values assumed are typical values for a aluminum alloy beam carrying the given load. The modulus of elasticity E = 10 x 10^6 is constant and thus can be omitted until the final calculations. The figure below the table shows the elastic loads on the imaginary beam.

Table A7.6

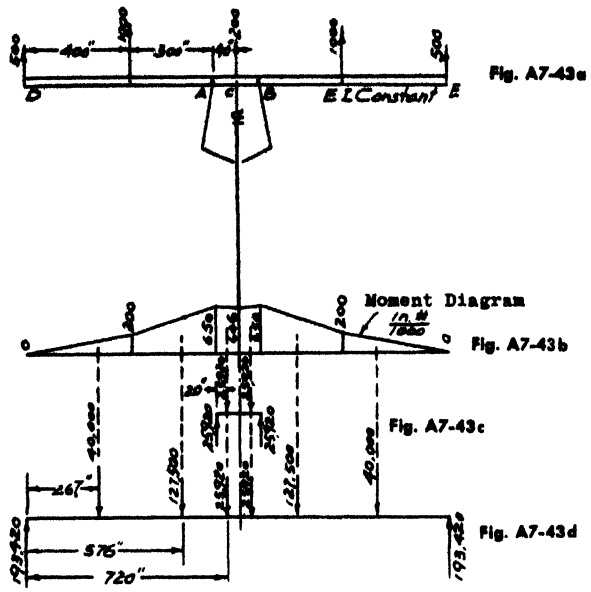
Strip No.	ds in.	M = moment at mid-point	I at mid-point	Elastic load $\frac{Mds}{I}$
1	10	11563	5.5	21000
2	10	20063	6.5	30900
3	10	31063	7.5	41450
4	10	44580	8.5	52300
5	10	60580	9.5	63850
6	10	79050	12.0	65940
7	10	100050	16.0	62530
8	10	123550	20.0	61770
9	10	149550	24.0	62320
10	10	178150	28.0	63600



Bending moment at point B due to above elastic loading = 7,100,000 .˙. deflection at B relative to line AC = $\frac{7,100,000}{E=10,000,000}$ = .71 inch

Example Problem 15-A

Fig. A7.43a shows a section of a cantilever wing sea plane. The wing beams are attached to the hull at points A and B. Due to wing loads the wing will deflect vertically relative to attachment points AB. Thus installations such as piping, controls, etc., must be so located as not to interfere with the wing deflections between A and B. For illustrative purposes a simplified loading has been assumed as shown in the figure. EI has been assumed as constant whereas the practical case would involve variable I. For the given loading determine the deflection of point C with respect to the support points A and B. Also determine the vertical deflection of the tip points D and E.



Solution:- Fig. A7.43b shows the bending moment diagram for the given wing loading. To find the deflection of C normal to line joining AB we treat the moment diagram as a load on a imaginary beam of length AB and simply supported at A and B. (See Fig. A7.43c.) The deflection of C is equal numerically to the bending moment on this fictitious beam.

Hence $EI\delta_C = 25920 - 40 = 25920 \times 20$

$$\text{or } \delta_C = \frac{518000}{EI}$$

To find the tip deflection, we place the elastic loads (area of moment diagram) on an imaginary beam simply supported at the tip D and E (See Fig. A7.43d). The bending moment on this imaginary beam at points A or B will equal numerically the deflection of these points with respect to the tip points D and E and since points A and B actually do not move this deflection will be the movement of the tip points with respect to the beam support points.

Bending moment at A = $193420 \times 700 - 40000 \times 433 - 127500 \times 124 = 102200000$. $\therefore \delta_{tip} = \frac{102,200,000}{EI}$.

A7.14 Deflections of Beams by Moment Area Method

For certain types of beam problems the method of moment areas has advantages and this method is frequently used in routine analysis.

Angular Change Principle. Fig. A7.44 shows a cantilever beam. Let it be required to determine the angular change of the elastic line between the points A and B due to any given loading. From the equation of virtual work, we have

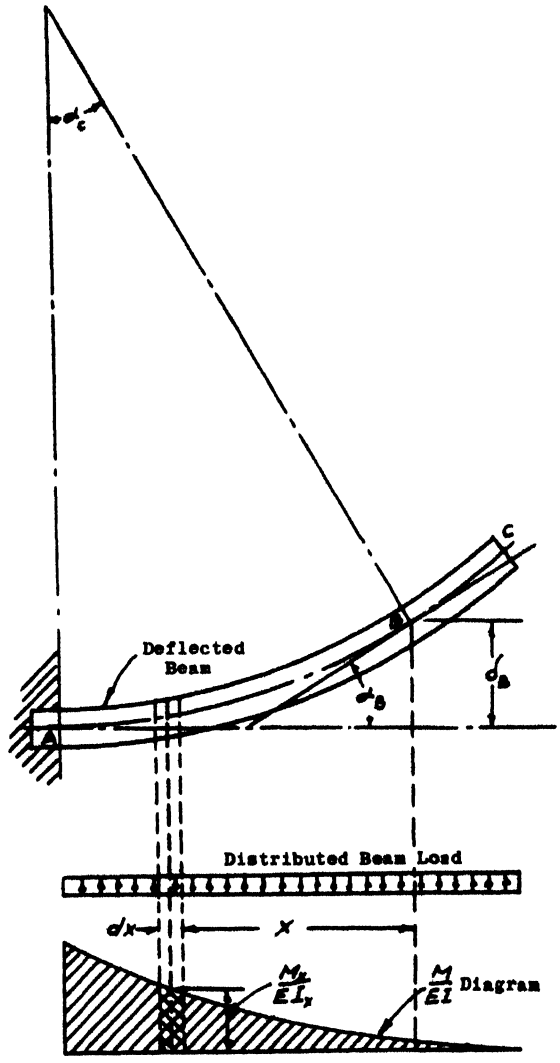


Fig. A7-44

$\alpha_b = \int_B^A \frac{Mdx}{EI} m$, where m is the moment at any section, distant x from B due to unit hypothetical couple applied at B. But m = unity at all points between B and A.

Therefore $\alpha_B = \int_B^A \frac{Mdx}{EI}$ - - - - - - - - - -(8)

(*Moment area first developed by Prof. Greene in 1874)

Referring to Fig. A7.44, this expression represents the area of the $\frac{M}{EI}$ diagram between points B and A. Thus the first principle:- "The change in slope of the elastic line of a beam between any two points A and B is numerically equal to the area of the $\frac{M}{EI}$ diagram between these two points."

Deflection Principle

In Fig. A7.44 determine the deflection of point B normal to tangent of elastic curve at A. In Fig. A7.44 this deflection would be vertical since tangent to elastic line at A is horizontal.

From virtual work expression $\delta_B = \int_B^A \frac{Mdx}{EI} m$,

where m is the moment at any section A distance x from B due to a unit hypothetical vertical load acting at B. Hence m = 1.x = x for any point between B and A.

Hence

$$\delta_B = \int_B^A \frac{Mdx}{EI} \cdot x \text{ - - - - - - - - - - - - - - (9)}$$

Expression (9) represents the 1st moment of the $\frac{M}{ED}$ diagram about a vertical thru B. Thus the deflection principle of the moment area method can be stated as follows:- "The deflection of a point A on the elastic line of a beam in bending normal to the tangent of the elastic line at a point B is equal numerically to the statical moment of the $\frac{M}{EI}$ area between points "A" and "B" about point A".

Illustrative Problems

Example Problem #16. Determine the slope and vertical deflection at the free end B of the cantilever beam shown in Fig. A7.45. EI is constant.

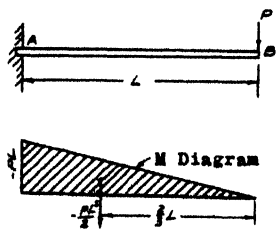


Fig. A7-45

Solution:- The moment diagram for given load is triangular as shown in Fig. A7.45. Since the beam is fixed at A, the elastic line at A is horizontal or slope is zero. Therefore true slope at B equals angular change between A and B which equals area of moment diagram between A and B divided by EI.

Hence

$$\delta_B = (-PL.\ L/2)\ \frac{1}{EI} = -\frac{PL^2}{2EI}$$

The vertical deflection at B is equal to the 1st moment of the moment diagram about point B divided by EI, since tangent to elastic curve at A is horizontal due to fixed support.

Hence

$$\delta_B = \left(-\frac{PL^2}{2} \cdot \frac{2}{3} L\right) \frac{1}{EI} = -\frac{PL^3}{3EI}$$

Example Problem #17

Fig. A7.46 illustrates the same simplified wing and loading as used in example problem 15a. Find the deflection of point C normal to line joining the support points A and B. Also find the deflection of the tip points D and E relative to support points A and B.

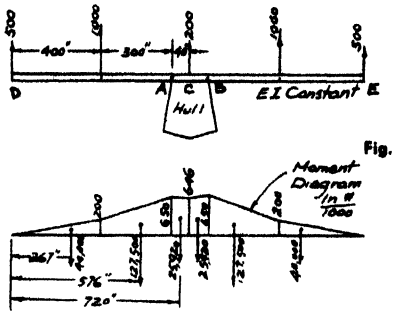


Fig. A7-46

Solution:-

Due to symmetry of loading, the tangent to the deflected elastic line at the center line of airplane is horizontal. Therefore, we will find the deflection of points A or B away from the horizontal tangent of the deflected beam at point C which is equivalent to vertical deflection of C with respect to line AB.

Thus to find vertical deflection of A with respect to horizontal tangent at C take moments of the $\frac{M}{EI}$ diagram as a load between points A and C about point A.

Whence

$$\frac{\delta_A}{1000} \text{ (tangent at C)} = \frac{1}{EI}\left(\frac{650 + 646}{2}\right)^{\text{(area)}} 40 \times 20^{\text{(arm)}} =$$

$$\frac{1}{EI}\ (518400) = \text{deflection of C normal to AB.}$$

To find the vertical deflection of the tip point D with respect to line AB, first find deflection of D with respect to horizontal tangent at C and subtract deflection of A with respect to tangent at C.

$$\frac{\delta_D}{1000} \text{ (respect to tangent at C)} = \frac{1}{EI}\ (40000 \times 267 + 127500 \times 576 + 25920 \times 720) = \frac{1}{EI}\ (102700{,}000)$$

(See Fig. A7.46 for areas and arms of M/EI diagram). Subtracting the deflection of A with respect to C as found above we obtain

$$\frac{\delta_D}{1000} \text{ (respect to line AB)} = \frac{1}{EI}\ (102{,}700{,}000 - 518400) = \frac{1}{EI}\ (102{,}180{,}000)$$

A7.15 Beam Fixed End Moments by Method of Area Moments

From the two principles of area moments as given in Art. A7.14, it is evident that the deflection and slope of the elastic curve depend on the amount of bending moment area and its location or its center of gravity.

Fig. A7.47 shows a beam fixed at the ends and carrying a single load P as shown. The bending moment shown in (c) can be considered as made up of two parts, namely that for a load P acting on a simply supported beam which gives the triangular diagram with value Pa (L-a)/L for the moment at the load point, and secondly a trapizoidal moment diagram of negative sign with values of M_A and M_B and of such magnitude as to make the slope of the beam elastic curve zero or horizontal at the support points A and B, since the beam is considered fixed at A and B.

The end moments M_A and M_B are statically indeterminate, however, with the use of the two moment area principles they are easily determined. In Fig. b the slope of elastic curve at A and B is zero or horizontal, thus the change in slope between A and B is zero. By the 1st

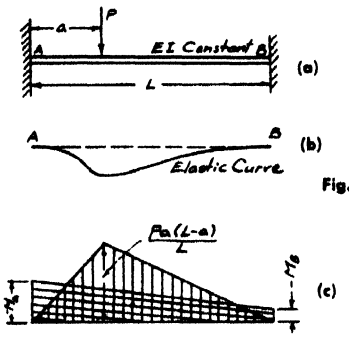


Fig. A7-47

principle of area moments, this means that the algebraic sum of the moment areas between A and B equal zero. Hence in Fig. c

$$\frac{(-M_A - M_b)}{2} L + \frac{(Pa\ (L-a)}{L} \cdot \frac{L}{2} = 0 \text{ - - - - - - - -(A)}$$

In Fib. b the deflection of B away from a tangent to elastic curve at A is zero, and also deflection of A away from tangent to elastic curve at B is zero.

Thus by moment area principle, the moment of the moment diagrams of Fig. C about points A, or B is zero.

Taking moments about point A:-

$$\Sigma M_A = \frac{Pa^2(L-a)}{2L} \cdot \frac{2a}{3} + \frac{Pa(L-a)^2}{2L} \times \left(a + \frac{L-a}{3}\right) + \frac{M_A L}{2} \times \frac{L}{3} +$$

$$\frac{M_B L}{2} \times \frac{2}{3} L = 0 \text{ -(B) - - - - - - - - - - - - -(B)}$$

Solving equations A and B for M_A and M_B

$$M_A = -\frac{Pab^2}{L^2} \text{ and } M_B = -Pba^2/L^2 \text{ where } b = (L-a)$$

To find the fixed end moments for a beam with variable moment of inertia use the M/I diagrams in place of the moment diagrams.

Example Problem #18

Fig. A7.48 shows a fix-ended beam carrying two concentrated loads. Find the fixed-end moments M_A and M_B.

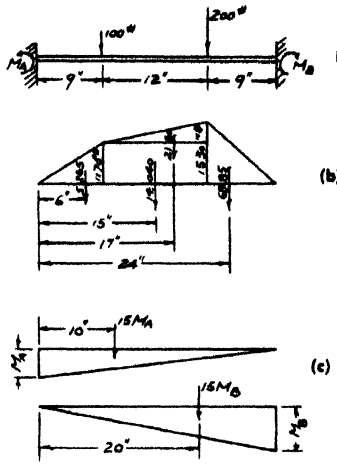


Fig. A7-48

Solution:- Fig. b shows the static moment diagram assuming the beam simply supported at A and B. For simplicity in finding areas and taking moments of the moment areas the moment diagram has been divided into the 4 simple shapes as shown. The centroid of each portion is shown together with the area which is shown as a concentrated load at the centroids.

Fig. C shows the moment diagrams due to unknown moments M_A and M_B. The area of these triangles is shown as a concentrated load at the centroids.

Since the change in slope of the elastic curve between A and B is zero, the area of these moment diagrams must equal zero, hence

$$5265 + 14040 + 2160 + 6885 + 15M_A + 15M_B = 0$$

or

$$15M_A + 15M_B + 28350 = 0 \text{ - - - - - - - - - - -(1)}$$

The deflection of point A away from tangent to elastic curve at B is zero, therefore the first moment of the moment diagrams about point A equals zero. Hence,

$5265 \times 6 + 15 \times 14040 + 17 \times 2160 + 24 \times 6885 + 150M_A + 300\ M_B = 0$ or $150\ M_A + 300\ M_B + 444600 = 0$- - - -(2)

Solving equations (1) and (2), we obtain

$M_A = -816$ in. lb.
$M_B = -1074$ in. lbs.

With the end moments known, the deflection or slope of any point on the elastic curve between A and B can be found by use of the 2 principles of area moments.

A7.16 Truss Deflection by Method of Elastic Weights

If the deflection of several or all the joints of a trussed structure are required, the method of elastic weights may save considerable time over the method of virtual work used in previous articles of this chapter. The method in general consists of finding the magnitude and location of the elastic weight for each member of a truss due to a strain from a given truss loading or condition and applying these elastic weights as concentrated loads on an imaginary beam. The bending moment on this imaginary beam due to this elastic loading equals numerically the deflection of the given truss structure.

Consider the truss of diagram (1) of Fig. A7.49. Diagram (2) shows the deflection curve for the truss for a ΔL shortening of member bc, all other members considered rigid. This deflection diagram can be determined by the virtual work ex pression δ = uΔL. Thus for deflection of joint O, apply a unit vertical load acting down at joint O. The stress m in bar bc due to this unit load = $\frac{2}{3} \cdot \frac{2P}{r} = \frac{4P}{3r}$. Therefore

$$\delta_o = \Delta L_{bc} \cdot \frac{4P}{3r}$$

. The deflection at other lower chord joints could be found in a similar manner by placing a unit load at these joints. Diagram (2) shows the resulting deflection curve. This diagram is plainly the influence line for stress in bar bc multiplied by ΔL_{bc}.

Diagram (3) shows an imaginary beam loaded with an elastic load $\frac{\Delta L_{bc}}{r}$ acting along a vertical line thru joint O, the moment center for obtaining the stress in bar bc. The beam reactions for this elastic loading are also given. Diagram (4) shows the beam bending moment diagram due to the elastic load at point O. It is noticed that this moment diagram is identical to the deflection diagram for the truss as shown in diagram (2).

The elastic weight of a member is therefore equal to the member deformation divided by the arm r to its moment center. If this elastic load is applied to an imaginary beam corresponding to the truss lower chord, the bending moment on this imaginary beam will equal to the true truss deflection.

Diagram 5, 6 and 7 of Fig. A7.49 gives a similar study and the results for a ΔL lengthening of member CK. The stress moment center for this diagonal member lies at point O', which lies outside the truss. The elastic weight $\frac{\Delta L}{r_1}$ at point O' can be replaced by an equivalent system at points O and k on the imaginary beam as shown in Diagram (6). These elastic loads produce a bending moment diagram (Diagram 7) identical to the deflection diagram of diagram (5).

Table A7.7 gives a summary of the equations for the elastic weights of truss chord and web members together with their location and sign.

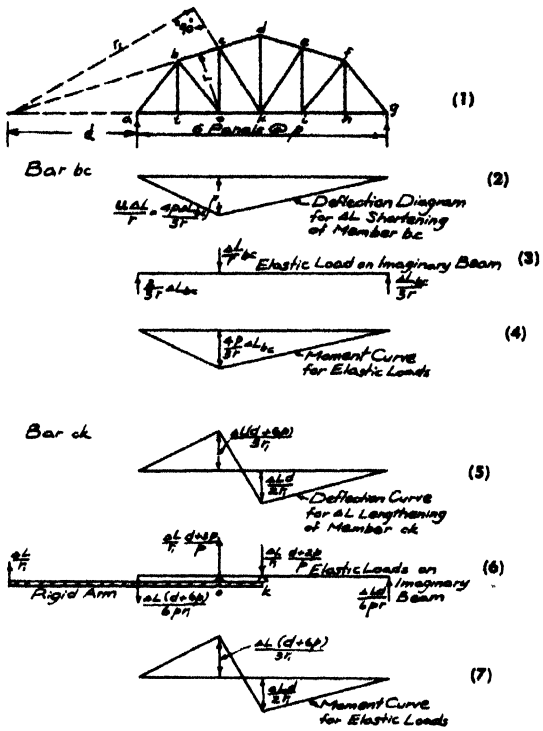
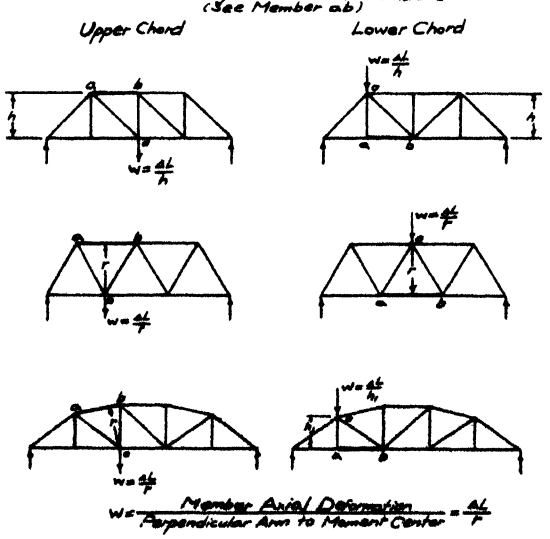


Fig. A7-49

Table A7.7 Equations for Elastic Weights

Elastic Weight for Chord Members (See Member ab)



The moment center O of a chord member is the intersection of the other two members cut by the section used in determining the load in that member by the method of moments

The sign of the elastic weight w for a chord member is plus if it tends to produce downward deflection of its point of application. Thus for a simple truss compression in top chord or tension in botton chord produces downward or positive elastic weight

Table A7.7 (continued)

WEB DIAGONAL MEMBERS (See Member ab)

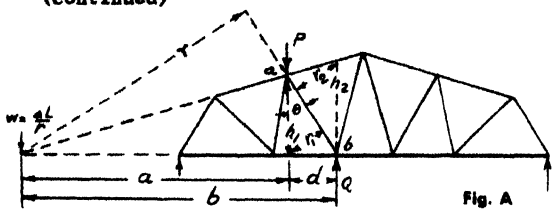


Fig. A

$$P = \frac{b}{d} w = \frac{\Delta L}{h_1 \sin\theta} = \frac{\Delta L}{r_1}$$

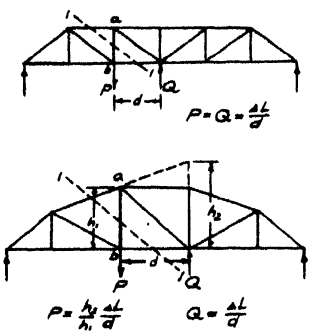
$$Q = \frac{a}{d} w = \frac{\Delta L}{h_2 \sin\theta} = \frac{\Delta L}{r_2}$$



For a truss diagonal member the elastic weights P & Q have opposite signs and are assumed to be directed toward each other or away according as the member is in compression or tension. In fig. a, P is greater than Q and P is located at the end of the diagonal nearest the moment center O. Downward elastic weights are plus.

TABLE A7.7 (CONTINUED)

Truss Verticals (See Member ab)



The elastic weight P acts at foot of vertical and downward if vertical is in tension. Q acts opposite to P at far end of chord member cut by index section 1-1 used in finding stress in ab by method of sections.

A7.17 Solution of Example Problems.

The method of elastic weights as applied to truss deflection can be best explained by the solution of several simple typical trusses.

Example Problem #21

Fig. A7.50 shows a simply supported truss symmetrically loaded. Since the axial deformations in all the members must be found, the first step is to find the loads in all the members due to the given loading. The results of

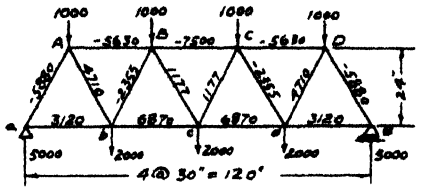


Fig. A7.50

this step are given in the figure, the stresses being written adjacent to each member. The next step or steps is to compute the member elastic weights, their location and their sense or direction. Tables A7.8 and A7.9 gives these calculations.

Table A7.8

Member	Length L	Chord Member Elastic Weights: Area A	Load P	PL/AE = ΔL, E=29x10^6	Arm r	Elastic wt. w = ΔL/r	Point of application joint
AB	30	.2172	-5630	-.0268	24	.001117	b
BC	30	.2172	-7500	-.0357	24	.001487	c
CD	30	.2172	-5630	-.0268	24	.001117	d
ab	30	.1198	3120	.0269	24	.001117	A
bc	30	.1198	6870	.0592	24	.002465	B
cd	30	.1198	6870	.0592	24	.002465	C
de	30	.1198	3120	.0269	24	.001117	D

Table A7.9 Web Member Elastic Weights.

Member	Length L	Area A	Load P	ΔL = PL/AE	r_1	P = ΔL/r_1	Apply at	r_2	Q = ΔL/r_2	Apply at
aA	28.25	.242	-5880	-.0236	12.75	-.00185	a	12.75	.00185	A
Ab	"	.146	4710	.0314	"	-.00246	A	"	.00246	b
bB	"	.146	-2355	-.0157	"	-.00123	b	"	.00123	B
Bc	"	.093	1177	.0123	"	-.000965	B	"	.000965	c
cC	"	.093	1177	.0123	"	-.000965	C	"	.000965	c
Cd	"	.146	-2355	-.0157	"	-.00123	d	"	.00123	C
Dd	"	.146	4710	.0314	"	-.00246	D	"	.00246	d
De	"	.242	-5580	-.0236	"	-.00185	e	"	.00185	D

Fig. A7.51 shows the elastic weights obtained from Tables 8 and 9 applied to an imaginary beam whose span equals that of the given truss. These elastic weights are the algebraic sum of the elastic weights acting at each truss joint.

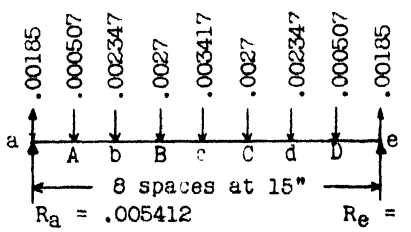


Fig. A7.51

The deflection at any joint equals the bending moment on the imaginary beam of Fig. A7.51.

Defl. at A = (.005412 + .00185)15 = .007262 x 15 = .109"

Defl. at b = .109 + (.007262 - .000507)15 = .109 + .006755 x 15 = .209"

Defl. at B = .209 + (.006755 - .002347)15 = .209 + .004408 x 15 = .275"

Defl. at c = .275 + (.004408 - .0027)15 = .301"
The slope of the elastic curve at the truss joint points equals the vertical shear at these points for the beam of Fig. A7.51.

Example Problem #22.

Find the vertical deflection of the joints of the Pratt truss as shown in Fig. A7.52. The member deformations ΔL for each member due to the given loading are written adjacent to each member. Table A7.10 gives the calculation of member elastic weights. Fig. A7.53 shows the imaginary beam loaded with the elastic weights from Table A7.10. The deflections are equal numerically to the bending moments on this beam.

δ_b = .01855 x 25 = .465"
δ_B = .465 + .053 (ΔL in Bar Bb) = .518"
δ_c = .01855 x 50 - .00387 x 25 - .833"
δ_C = .833 + .031 (ΔL of Cc) = .864
δ_D = .01855 x 75 - .00387 x 50 - .00623 x 25 = 1.03"

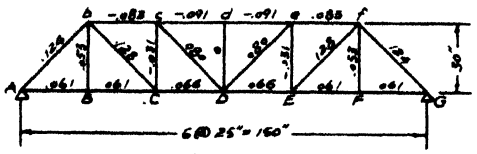


Fig. A7-52

Table A7.10

Elastic Weight Chord Members				
Member	Δ L	r	w = $\frac{\Delta L}{r}$	Joint
AB	.061	30	.00203	b
BC	.061	30	.00203	b
CD	.066	30	.0022	c
bc	-.083	30	.00277	C
Cd	-.091	30	.00304	D

Elastic Weight of Web Members							
Member	Δ L	P			Q		
		r_1	P = $\frac{\Delta L}{r_1}$	Joint	r_2	Q = $\frac{\Delta L}{r_2}$	Joint
Ab	.124	19.2	-.00648	A	19.2	.00648	b
Bb	.053	∞			∞		
bC	.128	19.2	-.00667	b	19.2	.00667	C
cC	-.031	25	-.00124	C	25	.00124	D
CD	.080	19.2	-.00417	c	19.2	.00417	D
Dd	0						

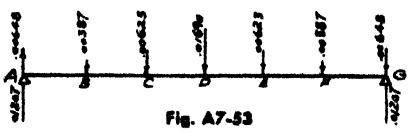


Fig. A7-53

Example Problem #23

Find the vertical joint deflections for the unsymmetrically loaded truss of Fig. A7.54. The ΔL deformations for all members are given on the Figure. Table A7.11 gives the calculation of the elastic weights, their signs and points of application. Fig. A7.55 shows the imaginary beam loaded with the elastic weights from Table A7.11. Table A7.12 gives the calculation for the joint deflections.

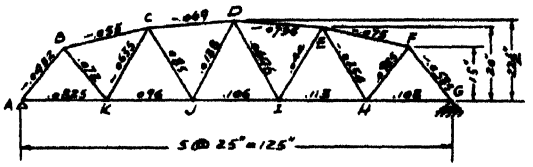


Fig. A7-54

Table A7.11

Elastic Weight of Chord Members				
Member	Δ L	r	w = $\frac{\Delta L}{r}$	Joint
AK	.0825	15.0	.00550	B
BC	-.055	17.17	.00320	K
KJ	.096	20.0	.00480	C
CD	-.069	21.14	.00322	J
JI	.106	22.50	.00471	D
DE	-.0736	21.14	.00348	I
IH	.113	20.0	.00565	E
EE	-.075	17.17	.00437	H
HG	.108	15.00	.00720	F

Elastic Weight of Web Members							
Member	Δ L	r_1	P = $\frac{\Delta L}{r_1}$	Joint	r_2	Q = $\frac{\Delta L}{r_2}$	Joint
AB	-.0432	9.60	-.00450	A	9.60	.00450	B
BK	.072	9.60	-.00748	B	11.20	.00643	K
KC	-.0635	9.27	-.00685	K	10.60	.00600	C
CJ	.085	10.60	-.00802	C	11.26	.00755	J
JD	.0138	10.33	.00134	J	10.93	-.00126	D
ID	.0496	10.33	.00480	I	10.93	-.00454	D
EI	.044	10.60	-.00415	E	11.26	.00891	I
HE	-.0254	9.27	-.00274	H	10.60	.00240	E
FH	.0985	9.60	-.01028	F	11.20	.00878	H
GF	-.0585	9.60	-.00610	G	9.60	.00610	F

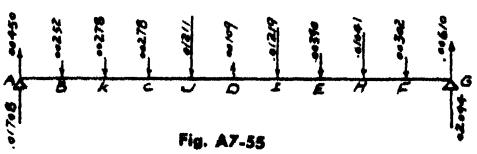


Fig. A7-55

Table A7.12

Panel	Panel Shear	Σ Shear	Moment = 12.5 x Shear = deflection	Point
		0	0	A
AB	.02158	.02158	.27	B
BK	.01906	.04064	.508	K
KC	.01628	.05692	.710	C
CJ	.01350	.07042	.881	J
JD	.00139	.07181	.900	D
DI	.00248	.07429	.930	I
IE	-.00971	.06458	.810	E
EH	-.01361	.05097	.638	H
HF	-.02402	.02695	.336	F
FG	-.02704	.00009*	0	G

*error

Example Problem #24

Fig. A7.56 shows a simply supported truss with cantilever overhang on each end. This simplified truss is representative of a cantilever wing beam the fuselage attachment points being

at e and e". The ΔL deformation in each truss member due to the given external loading is given on the figure. The complete truss elastic loading will be determined. With the elastic loading known the truss deflections from various reference lines are readily determined.

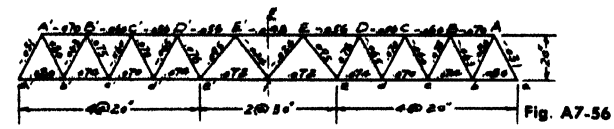
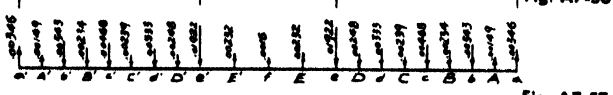


Fig. A7-56



Elastic Weight Loading

Fig. A7-57

Table A7.13

Elastic Weights of Chord Members

Member	ΔL	r	w = ΔL/r	Apply at Joint
ab	.080	20	.0040	A
AB	-.070	20	.0035	b
bc	.074	20	.0037	B
BC	-.060	k0	.0030	c
cd	.070	20	.0035	C
CD	-.056	20	.0028	d
de	.074	20	.0037	D
DE	-.056	20	.0028	e
ef	.072	20	.0036	E
EE	-.048	20	.0024	f

Elastic Weights of Web Members

Member	ΔL	r_1	P = ΔL/r_1	apply at joint	r_2	Q = ΔL/r_2	apply at joint
aA	-.031	8.95	-.00346	a	8.95	.00346	A
Ab	.080	8.95	-.00895	A	8.95	.00895	b
bB	-.063	8.95	-.00702	b	8.95	.00702	B
Bc	.075	8.95	-.00838	B	8.95	.00838	c
cC	-.060	8.95	-.00670	c	8.95	.00670	C
Cd	.070	8.95	-.00781	C	8.95	.00781	d
dD	-.065	8.95	-.00728	d	8.95	.00728	D
De	.076	8.95	-.00850	D	8.95	.00850	e
eE	.095	12.0	.00792	e	12.0	-.00792	E
Ef	.024	12.0	.0020	E	12.0	-.0020	f

Table A7.13 gives the calculations for the magnitude of the member elastic weights. The signs and also the joint locations for locating the elastic loads are also given. Combining algebraically the elastic weights for each joint from Table A7.13 the beam elastic loading as shown in Fig. A7.57 is obtained.

Let it first be required to determine the vertical deflection of Joint f relative to the truss support points at e and e'.

To determine the deflections of the truss between the supports e a d e' it is only necessary to consider the elastic weight loading between these points. Fig. A7.58 shows the portion of the imaginary beam of Fig. A7.57 between these points. The deflection at f relative to line ee' is equal to the bending moment at f for the portion of the imaginary beam between joints e and e' and simply supported at these points.

Hence deflection at f = - .00312 x 30 + .00232 x 15 = .0586" (upward since minus is up).

Find the vertical deflection of the cantilever over-hang portion of the truss relative to support points e and e'.

Since the cantilever portion is not fixed at e since the restraint is determined by the truss between e' and e, this fact must be taken into account in loading the cantilever portion. The reactions on the beam of Fig. A7.58 represent the slope at e due to the elastic loading between e and e'. This elastic reaction in acting in the reverse direction is therefore applied as a load to the imaginary beam between e and a as shown in Fig. A7.59.

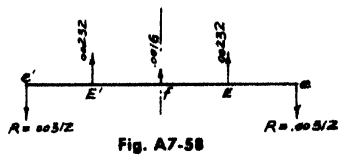


Fig. A7-58

In finding deflections this overhang elastically loaded portion is considered as fixed at a and free at e. The bending moment at any point on this beam equals the magnitude of the vertical deflection at that point.

Thus to find the deflection of the truss end (Joint a) we find the bending moment at point a of the imaginary beam of Fig. A7.59.

Hence

deflection at a = ΣM_a (calling counterclockwise positive). = (.01922 - .00312) 80 + .00248 x 70 + .00333 x 60 + .00239 x 50 + .00468 x 40 + .00234 x 30 + .00543 x 20 - .00149 x 10 = 2.13" upward. Due to symmetry of truss and loading of the truss we know the slope of the elastic curve at the center line of the truss is horizontal or zero. Thus to find the deflection of any point with reference to Joint f we can make use of the deflection principle of the moment area method. Thus in Fig. A7.60 the vertical deflection of any point for example joint a, relative to Joint f equals the moment of all elastic loads between a and f about a.

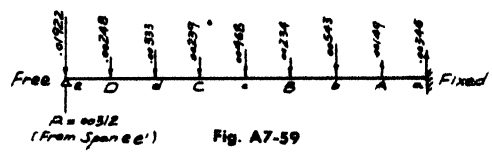


Fig. A7-59

ΣM_a = 2.077" (student should make calculations). Previously the deflection of f with respect to e was found to be -.0586". Thus deflection of a with respect to point e = 2.077 + .0586 = 2.135" which checks value found above. Let it be required to find the deflection of joint c relative to a line connecting joints b and d.

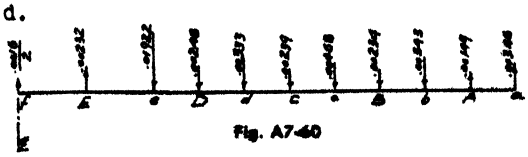


Fig. A7-60

For this problem we need only to consider the elastic loads between points b and d as loads on a simple beam supported at b and d (See Fig. A7.61) The deflection at C with respect to a line bd of the deflected truss equals the bending moment at point c for the loaded beam of Fig. A7.61.
hence

$$\delta_C = .004743 \times 20 - .00239 \times 10 = .07 \text{ inches}$$

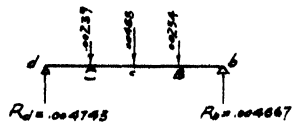


Fig. A7-61

A7.18 Problems

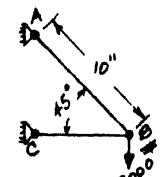


Fig. A7-62

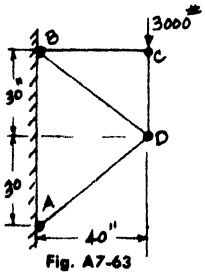


Fig. A7-63

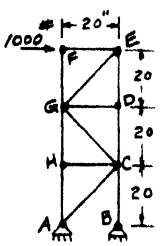


Fig. A7-64

(1) Find vertical and horizontal deflection of joint B for the structure in Fig. A7.62. Area of AB = 0.2 sq. in. and BC = 0.3. E = 10,000,000 psi.

(2) For the truss in Fig. A7.63, calculate the vertical deflection of joint C. Use AE for each member equal to 2 x 10^7.

(3) For the truss of Fig. A7.64 determine the horizontal deflection of joint E. Area of each truss member = 1 sq. in., E = 10,000,000 psi.

(4) Determine the vertical deflection of joint E of the truss in Fig. A7.64

(5) Determine the deflection of joint D normal to a line joining joint CE of the truss in Fig. A7.64.

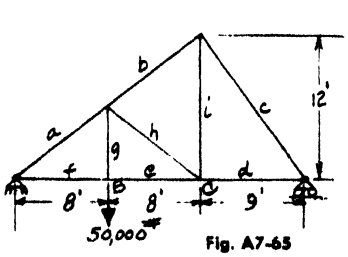


Fig. A7-65

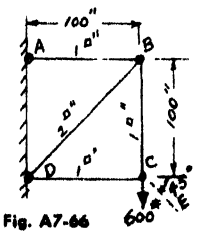


Fig. A7-66

(6) Calculate the vertical displacement of joint C for the truss in Fig. A7.65 due to the load at joint B. Members a, b, c and h have areas of 20 sq. in. each. Members d, e, f, g and i have areas of 2 sq. in. each. E = 30,000,000 psi.

(7) For the truss in Fig. A7.66 calculate the deflection of joint C along the direction CE. E = 30,000,000 psi.

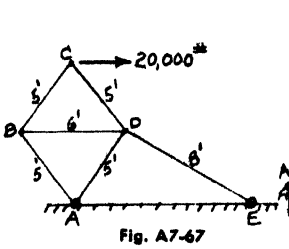


Fig. A7-67

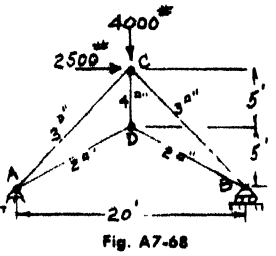


Fig. A7-68

(8) For the truss in Fig. A7.67, find the vertical and horizontal displacement of joints C and D. Take area of all members carrying tension as 2 sq. in. each and those carrying compression as 5 sq. in. each. E = 30,000,000 psi.

(9) For the truss in Fig. A7.68, determine the horizontal displacement of points C and B. E = 28,000,000 psi.

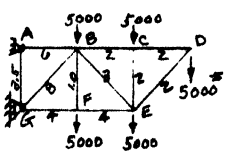


Fig. A7-69

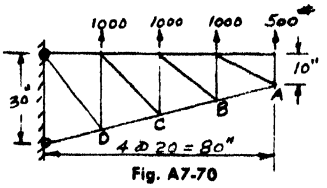


Fig. A7-70

(10) For the truss in Fig. A7.69, find the vertical deflection of joint D. Depth of truss = 180". Width of each panel is 180". The area of each truss member is indicated by the number on each bar in the figure. E = 30,000,000 psi. Also calculate the angular rotation of bar DE.

(11) For the truss in Fig. A7.70, calculate the vertical and horizontal displacement of joints A and B. Assume the cross-sectional area for members in tension as 1 sq. in. each and those in compression as 2 sq. in. E = 10,300,000 psi.

(12) For the truss in Fig. A7.70 calculate the angular rotation of member AB under the given truss loading.

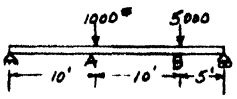


Fig. A7-71

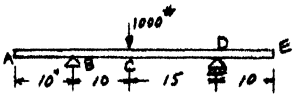


Fig. A-72

(13) For the beam in Fig. A7.71 determine the deflection at points A and B using method of elastic weights. Also determine the slopes of the elastic curve at these points. Take E = 1,000,000 psi and I = 1296 $in.^4$

(14) For the beam in Fig. A7.72 find the deflection at points A and E. Also the slope of the elastic curve at point C. Assume EI equals to 5,000,000 lb in. sq.

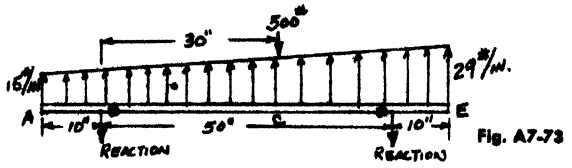


Fig. A7-73

(15) Fig. A7.73 illustrates the airloads on a flap beams ABCDE. The flap beams is supported at B and D and a horn load of 500# is applied at C. The beam is made from a 1"-.049 aluminum alloy round tube. I = .01659 in⁴; E = 10,300,000 psi. Compute the deflection at points C and E and the slope of the elastic curve at point B.

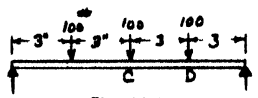


Fig. A7-74



Fig. A7-75

(16) For the beam of Fig. A7.74 determine the deflections at points C and D in terms of EI which is constant. Also determine slopes of the elastic curve at these same points.

(17) For the cantilever beam of Fig. A7.75 determine the deflections and slopes of the elastic curve at points A and B. Take EI as constant. Express results in terms of EI.

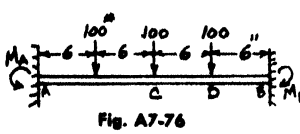


Fig. A7-76

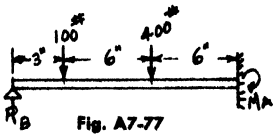


Fig. A7-77

(18) For the loaded beam in Fig. A7.76 determine the value of the fixed end moments M_A and M_B. EI is constant. Also find the deflection at points C and D in terms of EI.

(19) In Fig. A7.77 determine the magnitude of the fixed end moment M_A and the simple support R_B.

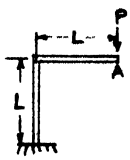


Fig. A7-78

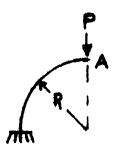


Fig. A7-79

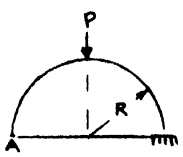


Fig. A7-80

(20) In Fig. A7.78 EI is constant throughout. Calculate the vertical deflection and the angular rotation of point A.

(21) For the curved beam in Fig. A7.79 find the vertical deflection and the angular rotation of point A. Take EI as constant.

(22) For the loaded curved beam of Fig. A7.80, determine the vertical deflection and the angular rotation of the point A. Take EI as constant.

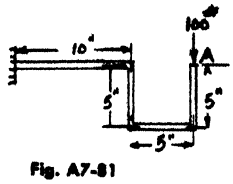


Fig. A7-81

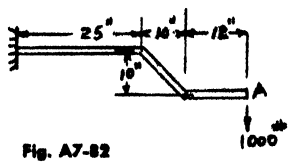


Fig. A7-82

(23) In Fig. A7.81 find the vertical movement and the angular rotation of point A. Take EI = 12,000,000.

(24) Determine the vertical deflection of point A for the structure in Fig. A7.82. EI = 14,000,000.

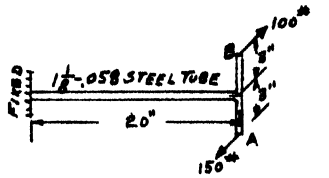


Fig. A7-83

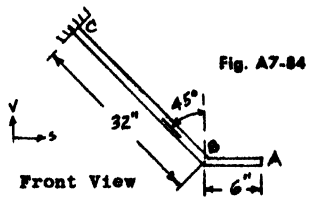
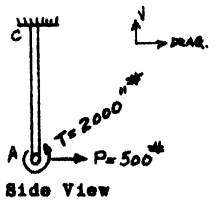


Fig. A7-84



(25) The cantilever beam of Fig. A7.83 is loaded normal to the plane of the paper by the two loads of 100# each as shown. Find the deflection of point A normal to the plane of the paper by the method of virtual work. The rectangular moment of inertia for the tube is 0.0277 in⁴. E = 29,000,000.

(26) The cantilever landing gear strut in Fig. A7.84 is subjected to the load of 500# in the drag direction at point A and also a torsional moment of 2000 in. lb. at A as shown. Determine the displacement of point A in the drag direction. The tube size for portion CB is 2"-.083 and for portion BA, 2"-.065 round tube. Material is steel with E = 29,000,000 psi.

A7.19 Deflection As The Partial Derivative Of The Internal Work of Deformation.

Introduction.

This method of calculating deflections of structures makes use of the consideration of internal work of deformation or the elastic strain energy in a member or structure.

Internal Work; Strain Energy

Work is equal to the product of a force and a distance. For a constant force P moving through a distance δ in the direction of the applied force P, the work done will be Pδ. If the force is not constant the work done will be given by the expression $\int P d\delta$.

Thus when a force is applied to a body it deforms the body in the direction of the applied force, or work is done on the body equal to the force times the displacement in line with the force. If the elastic limit stress of the material in the body is not exceeded this work done on the body is stored in the structure in the form of internal work or elastic energy. If the load or loads acting on the body are removed, this stored up elastic strain energy is entirely recoverable. Thus in general one can say that the work done in deforming an elastic body equals the elastic energy stored in the body.

A7.20 Elastic Strain Energy For a Body Under Axial Tension or Compression.

In stretching or shortening an element of length dx of a body under an axial tensile or compressive force P, the average applied force is $\frac{P}{2}$. Whence,

work = $w = \frac{P\delta}{2}$, when δ equals the deformation.

From elementary mechanics of materials, δ equals Pdx/EA, hence

$$w = \frac{P}{2}\left(\frac{Pdx}{EA}\right) = \frac{P^2dx}{2\,EA}$$

Then the total work for all elements dx of the body equals

$$W = \int \frac{P^2dx}{2\,EA}$$

But the external work equals the elastic energy. Let U represent total elastic energy. Then,

$$U = \int \frac{P^2dx}{2\,EA} \quad \text{- - - - - - - - - - - - - - - - -(1)}$$

A7.21 Elastic Energy in Bending

Fig. A7.84 shows a short element dx of a prismatic bar acted upon by a pure bending moment M. The element bends thru the angle dθ. The external work equals the product of the average moment and the angle through which it rotates, or

$w = \frac{Md\theta}{2}$, but from

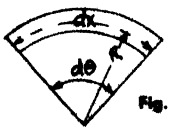


Fig. A7-84

elementary mechanics $\frac{1}{R} = \frac{M}{EI}$, hence $w = \frac{M^2dx}{2\,EI}$

The total elastic energy for the member which equals the external work, therefore equals

$$U = \int \frac{M^2dx}{2\,EI} \quad \text{- - - - - - - - - - - - - - - - -(2)}$$

A7.22 Elastic Energy in Torsion.

Fig. A7.85 shows a short element dx of a round bar or tube subjected to a pure torsional moment T, which causes one end of the rod to twist through angle dθ relative to the other end.

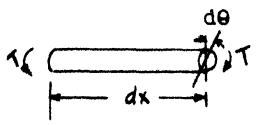


Fig. A7-85

$$w = \frac{Td\theta}{2},$$

but $d\theta = \frac{Tdx}{GJ}$, where G equals modulus of rigidity, and J = polar moment of inertia of the rod cross-section.

hence $w = \frac{T^2dx}{2GJ}$, then the total work or total elastic energy for all elements of a rod equals

$$U = \int \frac{T^2dx}{2GJ} \quad \text{- - - - - - - - - - - - - - - - -(3)}$$

A7.23 Elastic Energy in Pure Flexural Shear.

In Fig. A7.86, consider the element of length dx is subjected to the shear force V which produces a shearing strain or detrusion equal to δ. Then external work $w = \frac{V\delta}{2}$

But δ = Ødx, and from elementary mechanics $\emptyset = \frac{V}{AG}$ (where A equals area on which V acts)

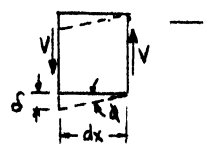


Fig. A7-86

Then

$$w = \frac{V^2dx}{2\,AG}$$, and therefore the total work or elastic energy for all elements equals

$$U = \int \frac{V^2dx}{2\,AG} \quad \text{- - - - - - - - - - - - - - - - -(4)}$$

Total Elastic Energy.

Many cases arise in which structures are subjected to axial bending, torsion and shear forces at the same time, thus the total elastic energy can be summed up as follows:-

$$U = \int \frac{P^2dx}{2\,EA}\ (\text{Tension or Comp.}) + \int \frac{M^2dx}{2\,EI}\ (\text{Bending}) + \int \frac{T^2dx}{2\,GJ}\ (\text{Torsion}) + \int \frac{V^2dx}{2\,GA}\ (\text{Shear})$$

- - - - - - - - - - -(5)

A7.24 *Castigliano's First Theorem.

Castigliano's first theorem states that the partial derivative of the elastic energy in a structure with respect to an applied force gives the deflection of the structure at the point of application of the applied force and in the direction of the applied force.

Consider a straight bar of length L subjected to a tensile axial load of P lbs.

From Equation (1)

$$U = \int_0^L \frac{P^2 dx}{2\,EA} = \frac{P^2 x}{2\,EA}\Big]_0^L = \frac{P^2 L}{2\,EA}$$

$\frac{dU}{dP} = \frac{2\,PL}{2\,EA} = \frac{PL}{AE}$, But $\frac{PL}{AE} = \delta$, the elongation of the bar or the movement of the load P in the direction of the load P. Therefore

$$\frac{dU}{dP} = \delta \text{ -(6)}$$

Equation (6) is a statement of Castigliano's first theorem. The above result was obtained from a consideration of a simple single bar in tension. The theorem will now be proved for a general case. Fig. A7.86a is considered to represent a beam or truss supported at A and B. Two external loads P_1 and P_2 are applied which produce the deflections δ_1 and δ_2. The work done by the two loads which are applied gradually from zero to full load will be equal to the internal work or elastic energy and will equal,

$$W = U = \frac{1}{2} P_1 \cdot \delta_1 + \frac{1}{2} P_2 \cdot \delta_2 \text{ - - - - - - - -(7)}$$

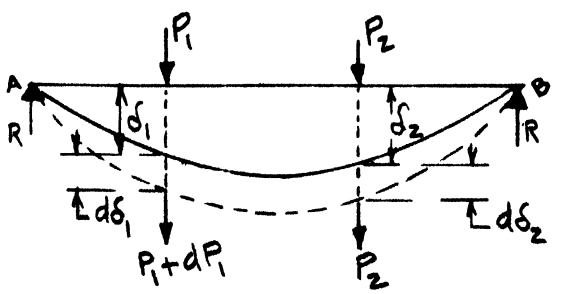


Fig. A7-86a

Now consider force P_1 is increased by a differential amount dP_1 which will produce a further deflection $d\delta_1$ under P_1 and $d\delta_2$ under the load P_2. The elastic energy will then equal,

$$U + dU = \frac{1}{2} P_1 \cdot \delta_1 + P_1 \cdot d\delta_1 + \frac{1}{2} dP_1 \cdot d\delta_1 + \frac{1}{2} P_2 \cdot \delta_2 + P_2 \cdot d\delta_2 \text{ - - - - - - - - - - - - - - - -(8)}$$

Note that the loads P_1 and P_2 act through the entire distances $d\delta_1$ and $d\delta_2$ respectively.

*Alberto Castigliano (1847-1884) a well known Italian Engineer.

Now subtract (7) from (8) and neglect the product of differentials,

$$dU = P_1 \cdot d\delta_1 + P_2 \cdot d\delta_2 \text{ - - - - - - - - - - -(9)}$$

Now consider $P_1 + dP_1$ and P_2 were increased gradually from zero to their full values, then

$$U + du = \frac{1}{2}(P_1 + dP_1)(\delta_1 + d\delta_1) + \frac{1}{2} P_2 (\delta_2 + d\delta_2)$$

$$= \frac{1}{2} P_1 \cdot \delta_1 + \frac{1}{2} P_1 \cdot d\delta_1 + \frac{1}{2} dP_1 \cdot \delta_1 + \frac{1}{2} dP_1 \cdot d\delta_1 + \frac{1}{2} P_2 \cdot \delta_2 + \frac{1}{2} P_2 \cdot d\delta_2 \text{ - - - - - - - - - (10)}$$

Subtracting (7) from (10) and neglecting products of differentials, we obtain

$$dU = \frac{1}{2} P_1 \cdot d\delta_1 + \frac{1}{2} dP_1 \cdot \delta_1 + \frac{1}{2} P_2 \cdot d\delta_2 \text{ - - - - - (11)}$$

Now multiply (11) by 2 and subtract from (9), we obtain,

$dU = dP_1 \cdot \delta_1$, or

$$\frac{dU}{dP_1} = \delta_1 \text{ - - - - - - - - - - - - - - - - - (12)}$$

Equation (12) is an expression of Castigliano's first theorem.

Angular Deflection or Rotation

For angular deflections, Castigliano's theorem can be stated as follows:-
The partial derivative of the elastic energy in a structure with respect to an applied moment gives the rotation of the structure at the point of application of the applied moment and in the direction of the applied moment.

Thus

$$\frac{\partial U}{\partial M} = \theta \text{ - - - - - - - - - - - - - - - - - (13)}$$

A7.25 General Deflection Equations.

General equations expressing Castigliano's first theorem can now be written for structures subjected to axial, bending, torsion or shear forces.

For the case of linear deflection at some point (r), we take the partial derivation of the elastic energy with respect to a force P_r applied at point r and acting in the direction of the desired deflection. Thus referring to equation (5)

$$\delta_r = \frac{\partial U}{\partial P_r} = \frac{\partial}{\partial P_r} \int \frac{P^2 dx}{2\,EA} + \frac{\partial}{\partial P_r} \int \frac{M^2 dx}{2\,EI} + \frac{\partial}{\partial P_r} \int \frac{T^2 dx}{2\,GJ} + \frac{\partial}{\partial P_r} \int \frac{V^2 dx}{2\,GA} \text{ - - - - - - - - - - - - - (14)}$$

Since the intregation in the above terms is with respect to X, it is permissible to differentiate with respect to P_r under the integral sign before the integration takes place. Equation (14) can therefore be modified as follows:

$$\delta_r = \int P \frac{\partial P}{\partial P_r} \frac{dx}{EA} + \int M \frac{\partial M}{\partial P_r} \frac{dx}{EI} + \int T \frac{\partial T}{\partial P_r} \frac{dx}{GJ} + \int V \frac{\partial V}{\partial P_r} \frac{dx}{GA}$$

- - - - - - - - - - (15)

For the case of angular deflection at a point (r) we take the partial derivation of the elastic energy with respect to a moment M_r applied at point (r).

$$\theta_r = \int P \frac{\partial P}{\partial M_r}\frac{dx}{EA} + \int M \frac{\partial M}{\partial M_r}\frac{dx}{EI} + \int T \frac{\partial T}{\partial M_r}\frac{dx}{GJ} + \int V \frac{\partial V}{\partial M_r}\frac{dx}{GA} \quad \text{- - - - - - - - - - (16)}$$

A7.26 Example Problem Solutions.

Problem #1

Fig. A7.87 shows a cantilever beam carrying two loads P_1 and P_2. Determine the deflection at point (1) due to bending only. EI is constant.

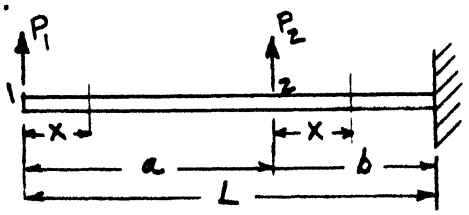


Fig. A7-87

From equation (15) using only the second term which applies to bending.

$$\delta_1 = \int M \frac{\partial M}{\partial P_1}\frac{dx}{EI} \quad \text{- - - - - - - - - - - - - - -(A)}$$

For portion (a) of beam,

$M = P_1 x$, limits $x = o$ to $x = a$

$$\frac{\partial M}{\partial P_1} = x$$

For portion (b) of beam,

$M = P_1 a + P_1 x + P_2 x$, limits, $x = 0$ to $x = b$

$$\frac{\partial M}{\partial P_1} = a + x$$

Substituting in equation (A),

$$\delta_1 = \frac{1}{EI}\int_0^a (P_1 x \cdot x)dx + \frac{1}{EI}\int_0^b (P_1 a + P_1 x + P_2 x)(a + x)dx$$

$$= \frac{1}{EI}\int_0^a P_1 x^2 dx + \frac{1}{EI}\int_0^b (P_1 a^2 + P_1 xa + P_2 xa + P_1 xa + P_1 x^2 + P_2 x^2)dx$$

$$= \frac{1}{EI}\left[\frac{P_1 x^3}{3}\right]_0^a + \frac{1}{EI}\left[P_1 a^2 x + \frac{P_1 x^2 a}{2} + \frac{P_2 x^2 a}{2} + \frac{P_1 x^2 a}{2} + \frac{P_1 x^3}{3} + \frac{P_2 x^3}{3}\right]_0^b$$

$$= \frac{1}{EI}\left(\frac{P_1 a^3}{3}\right) + \frac{1}{EI}\left(P_1 a^2 b + \frac{P_1 b_2 a}{2} + \frac{P_2 b^2 a}{2} + \frac{P_1 b^2 a}{2} + \frac{P_1 b^3}{3} + \frac{P_2 b^3}{3}\right)$$

Taking a = L - b, the above equation can be simplified to the following equations:-

$$\delta_1 = \frac{1}{EI}\left[\frac{P_1 L^3}{3} + P_2 b^2\left(\frac{L}{2} - \frac{b}{6}\right)\right]$$

Problem #2

Fig. A7.88 shows a cantilever beam with a load P at the end. Determine the deflection at point (r). EI is constant.

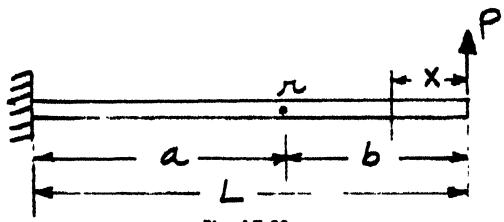


Fig. A7-88

Since the deflection at point (r) is required, there being no external load at point (r), an imaginary load P_r will be assumed acting as in Fig. A7.89.

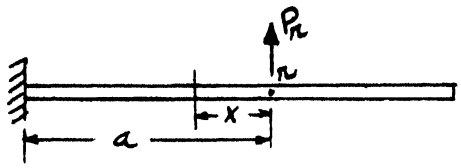


Fig. A7-89

The general expression for the deflection at point (r) equals

$$\delta_r = \int M \frac{\partial M}{\partial P_r}\frac{dx}{EI} \quad \text{- - - - - - - - - - - - - - -(B)}$$

For beam portion (b)

$M = Px$

$$\frac{\partial M}{\partial P_r} = 0 \qquad \text{hence } M\frac{\partial M}{\partial P_r} = 0$$

For beam portion (a)

$M = Pb + Px + P_r x$, from $x = o$ to $x = a$

$$\frac{\partial M}{\partial P_r} = x, \quad \text{Substituting in equation (B)}$$

$$\delta_r = 0 + \frac{1}{EI}\int_0^a (Pb + Px + P_r x)\,xdx$$

But P_r was imaginary so it will be dropped from the above equation, hence

$$\delta_r = \frac{1}{EI}\int_0^a (Pb + Px)xdx = \frac{1}{EI}\int_0^a (Pbx + Px^2)dx$$

$$= \frac{1}{EI}\left[\frac{Pbx^2}{2} + \frac{Px^3}{3}\right]_0^a = \frac{1}{EI}\left(\frac{Pba^2}{2} + \frac{Pa^3}{3}\right)$$

Since a = L - b, we can simplify,

$$\delta_r = \frac{P}{6EI}(2L^3 - 3L^2 b + b^3)$$

Problem #3

For the beam in Fig. A7.88, determine the angular rotation of the free end of the beam.

From equation (16)

$$\theta_1 = \int M \frac{\partial M}{\partial M_1} \frac{dx}{EI} \quad \text{----------(C)}$$

In Fig. a we apply a moment M_1 at point (1) the free end of the beam, since the rotation of this point is asked for.

Hence,

$$M = Px + M_1$$

$$\frac{\partial M}{\partial M_1} = 1$$

Substituting in equation (C)

$$\theta_1 = \frac{1}{EI} \int_0^L (Px + M_1)dx$$

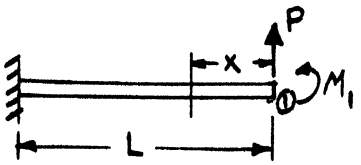


Fig. a

but M_1 is zero, since it was only imaginary and not an actual load on the beam. Therefore,

$$\theta_1 = \frac{1}{EI} \int_0^L Px\,dx = \frac{1}{EI} \left[\frac{Px^2}{2}\right]_0^L, \text{ whence}$$

$$\theta_1 = \frac{PL^2}{2\,EI}$$

Problem #4

Find the deflection at the free end of the beam in Fig. A7.88 due to shearing stresses only. Refer to the end of the beam as point (1)

From equation (15)

$$\delta_1 = \int V \frac{\partial V}{\partial P} \frac{dx}{GA} \quad \text{----------(D)}$$

$$V = P, \quad \frac{\partial V}{\partial P} = 1$$

Substituting in equation (D)

$$\delta_1 = \frac{1}{GA} \int_0^L Pdx = \frac{1}{GA} (Px)_0^L$$

hence $\delta_1 = \frac{PL}{GA}$

Problems

In order to become familiar with this method of finding the elastic deflections of structures, the student should solve a number of the problems given in Article A7.18.

A7.27 Maxwell's Law of Reciprocal Deflections.

Maxwell's Law of Reciprocal deflections often proves useful in solving statically indeterminate structures. A simple proof of this law or theorem will be given.

Fig. A7.90 shows a simply supported beam carrying the two loads P_a and P_b. The beam is in equilibrium and it is assumed that stresses are such that Hooke's law of deformation holds. In writing the subscripts to the forces, the first subscript is taken to designate the point at which the displacement occurs and the second subscript the load causing the displacement.

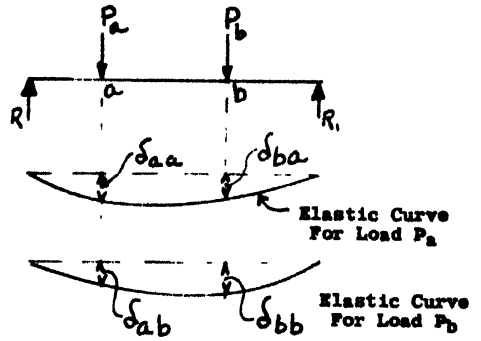


Fig. A7-90

In Fig. A7.90 consider that we apply load P_a first to the beam at point (a). The elastic curve due to P_a is shown. The external work done by $P_a = P_a\delta_{aa}/2$. The value 2 is due to the load P_a being applied gradually from zero to P_a, thus average load is P/2. The load P_a causes a deflection δ_{ba} at point (b), but since P_b is not considered as acting yet, there will be no external work due to P_b.

Now consider P_b as applied gradually to the beam. The elastic curve for load P_b is shown in Fig. A7.90. Then the external work done at point (b) equals $P_b\delta_{bb}/2$. As shown in Fig. A7.90, the load P_b produces a deflection δ_{ab} at point (a) and since the load P_a was already acting on beam, the external work done by P_a at point (a) due to the application of P_b equals $P_a\delta_{ab}$. Then the total work done in applying both loads in the order assumed equals

$$W_1 = \frac{P_a\delta_{aa}}{2} + \frac{P_b\delta_{bb}}{2} + P_a\delta_{ab} \quad \text{---------(A)}$$

If we repeat the loading but apply P_b first followed by P_a, the work done will equal

$$W_2 = \frac{P_b\delta_{bb}}{2} + \frac{P_a\delta_{aa}}{2} + P_b\delta_{ba} \quad \text{---------(B)}$$

Since the final work done must be the same W_1 must equal W_2, which means that,

$$P_a\delta_{ab} = P_b\delta_{ba}$$

This equation represents Maxwell's Reciprocal theorem of deflections and stated in words that equation says, "that the force P_a acting through the displacement at point (a) produced by the load P_b does the same amount of work as the force P_b acting through the displacement at point (b) due to the load P_a".

Maxwell's theorem likewise applies to moments and angular displacements. For angular displacements the theorem can be stated as follows:-

If M_a and M_b are moments applied to points (a) and (b) of a structure respectively, then the moment M_a acting through the angular displacement produced at point (a) by the moment M_b causes the same amount of work as the moment M_b acting through the angular displacement produced at point (b) by the moment M_a.

REFERENCES

"Statically Indeterminate Stresses", by Parcel and Maney; Publisher--John Wiley.

"Advanced Mechanics", by Seely; Publisher--John Wiley.

"Reinforced Concrete and Masonry Structures", by Hool and Kinne; Publisher--McGraw and Hill.

"Elastic Energy Theory", by Van Den Broek; Publisher--John Wiley.

"Continuous Frames of Reinforced Concrete", by Cross and Morgan; Publisher--John Wiley.

"Deflection of Structures by Method of Elastic Weights", by Kinne; Wisconsin Engineer--Feb. 1920.

"Statically Indeterminate Structures", by H. Cross; College Publishing Co. Champaign Ill. 1926.

"Airplane Structures", by Niles and Newell; Publisher--John Wiley.

"Airplane Structural Design" by Sechler & Dunn--Publisher--John Wiley.

"Fundamentals of Aircraft Structures" by Barton Publisher--Prentice-Hall.

"Strain Energy Methods of Stress Analysis" by Pippard; Publisher--Longman's.

CHAPTER A8
STATICALLY INDETERMINATE TRUSSES

A8.1 Introduction Several types of airplane structures involve trusses with redundant members. That is, the axial stresses in the members of the truss can not be determined with only the application of the laws of equilibrium. (See Chapter A2, Art. A2.1). To obtain additional relationships or equations, the equation of the continuity of the structure must be considered, which involves a study of the relative deflections of the truss. This chapter illustrates the application of the theory to the solution of several typical stress analytical problems.

A8.2 The Principle of Superposition

The general principle of superposition states that the resultant effect of a group of loadings or causes acting simultaneously is equal to the algebraic sum of the effects acting separately. This principle is restricted to the condition that the resultant effect of the several loadings or causes varies as a linear function. Thus, the principle does not apply when the member material is stressed above the proportional limit or when the member stresses or part of the member stresses are dependent upon member deflections or deformations, as, for example, the beam-column, a member carrying bending and axial loads at the same time.

A8.3 Stresses in a Truss Frame Work with One Redundant Member

Fig. A8.1 shows a truss with two diagonal members, both of which are capable of carrying compression loads. The reactions at A and B due to the external load P are statically determinate. However, when an attempt to find the member stresses is made, it is found that three unknowns exist at each joint with only two equations of statics, available for a concurrent force system. Thus, an additional equation is necessary if the member stresses are to be determined. In Fig. A8.2, member A has been selected as the redundant member. The truss is made statically determinate by cutting this redundant member A at section x-x' adjacent to one end of the member. Fig. A8.3 shows the truss with the unknown force X applied to each cut face x-x', where X equals the true load or stress in the redundant member A. Thus, the member stresses for the two systems in Figs. A8.2 and A8.3 equal the true member stresses of Fig. A8.1.

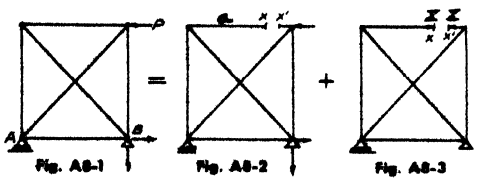


Fig. A8-1 Fig. A8-2 Fig. A8-3

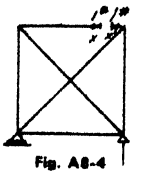


Fig. A8-4

Since the structure is continuous at the cut section x-x', the relative axial movement of the cut faces x-x' due to the two load systems of Figs. A8.2 and A8.3 must equal zero.

Let δ = axial movement of faces x-x' for the truss loading of Fig. A8.2.

From chapter A7,

$$\delta = \Sigma \frac{S\, u_x L}{A E}$$, where S equals the stress in the truss members which has been made statically determinate and is subjected to the given external loads. (Fig. A8.2)

u_x = member axial stresses due to virtual unit 1# axial forces applied at cut faces x-x' (see Fig. A8.4)

Let δ' = axial displacement of the cut faces x-x due to the load system of Fig. A8.3.

$$\delta' = \Sigma \frac{(X u_x)\, u_x L}{A E}$$

The term $(X\, u_x)$ is the stress in the truss members due to load X applied at cut faces, since u_x equals the stresses due to a 1# load applied at the same places.

For continuity at the cut faces, $\delta + \delta' = 0$

Hence, $$X\Sigma \frac{u_x^2 L}{A E} = -\Sigma \frac{S u_x L}{A E}$$

or $$X = -\frac{\Sigma \frac{S u_x L}{A E}}{\Sigma \frac{u_x^2 L}{A E}} \quad \text{----------(1)}$$

The stress S for the redundant member is always zero, hence, the numerator of the expression includes all members but the redundant member, whereas the term in the denominator includes all members. In determining the member stresses, tension is positive and compression negative.

A8.4 Example Problems - Trusses with Single Redundancy

Example Problem #1

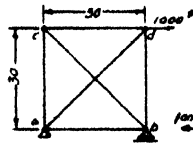


Fig. A8-5

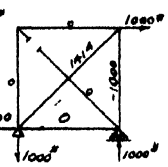


Fig. A8-6

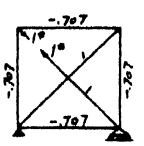


Fig. A8-7

Fig. A8.5 shows a single bay pin connected truss. The truss is statically determinate with respect to external reactions, but statically indeterminate with respect to internal member loads, since at any joint there are 3 unknowns with only two equations of statics available for a concurrent force system. The truss is therefore redundant to the first degree. The general procedure for solution is to make the truss statically determinate by cutting one of the members on Fig. A8.6, member bc has been selected as the redundant member, and it is cut as shown. The member stresses S for the truss of Fig. A8.6 are then determined, the results being recorded on the members and also entered in Table A8.1. In Fig. A8.7, a unit 1# tensile dummy load has been applied at the cut section of the redundant member bc, and the loads in all the members due to this unit load are calculated. The results are recorded on the figure and also in Table A8.1 under the head of u stresses. The solution for the redundant load X in the redundant member bc is given at the bottom of Table A8.1. The true load in any member equals the S stress plus X times its u stress.

Table A8.1

Member	L	A	S	u	$\frac{SuL}{A}$	$\frac{u^2L}{A}$	True Stress = S + Xu
ab	30	1	0	-.707	0	15	395
bd	30	1	-1000	-.707	21210	15	-605
dc	30	1	0	-.707	0	15	395
ca	30	1	0	-.707	0	15	395
cb	42.4	2	0	1.0	0	21.2	-559
ad	42.4	1.5	1414	1.0	40000	28.3	855
					Σ 61210	109.5	

X = true load in redundant member bc

$$X = -\frac{\Sigma \frac{SuL}{A}}{\Sigma \frac{u^2L}{A}} = \frac{-61210}{109.5} = -559\#$$

Example Problem #2 Biplane Wing Cellule.

Fig. A8.8 shows the wing structural layout of a externally braced biplane. This wing layout is identical to the wing structural arrangement of example problem #3 of Chapter A2. In that example problem the wing structure was analyzed for axial member loads for a given external air loading under the assumption that the diagonal interplane strut (ID) was removed. This was necessary because the wing structure is statically indeterminate to the first degree and to make it statically determinate the interplane strut was selected as the redundant member. The calculation for the member loads under this assumption are given in example problem #3 of Chapter A2. The results are tabulated in Fig. A8.9.

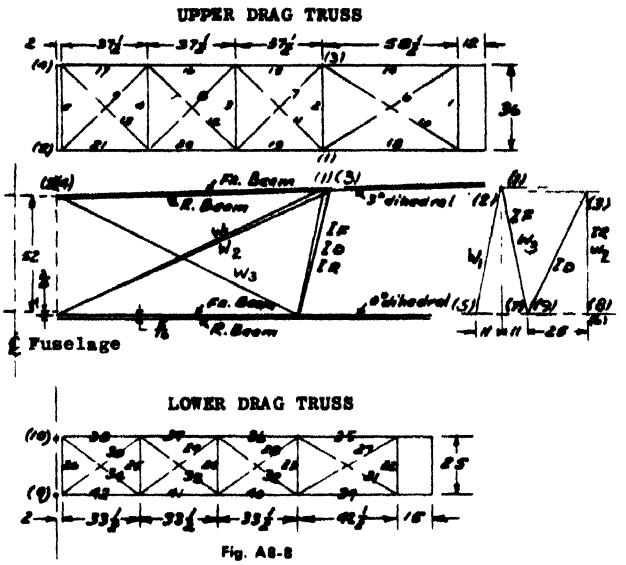


Fig. A8-8

Member	symb.	V	D	S	L	V/L	D/L	S/L
Up. Fr. Beam	UF	5.99	0	114.34	114.50	.0523	0	.9986
Up. R. Beam	UR	5.99	0	114.34	114.50	.0523	0	.9986
Low. Fr. Beam	LF	0	0	102.5	102.5	0	0	1.00
Low. R. Beam	LR	0	0	102.5	102.5	0	0	1.00
Fr. Lift Wire	W_1	57.99	11	114.34	128.79	.4501	.0854	.8878
R. Lift Wire	W_2	57.49	0	114.34	128.00	.4486	0	.8930
Fr. Int. Strut	IF	58.37	11	12	60.50	.9820	.1820	.1980
Dia. Int. Strut	ID	57.87	25	12	64.15	.9015	.3896	.1870
Rear Int. Strut	IR	58.18	0	12	59.40	.9810	0	.2017

$L = \sqrt{V^2 + D^2 + S^2}$

Summary of S Member loads, Member ID out.
(Ref. Problems3 Chapter A2)

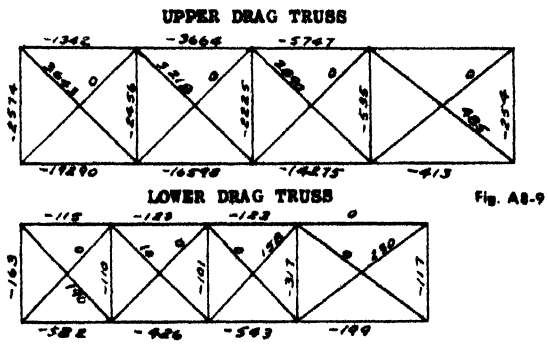


Fig. A8-9

Before we can solve the load in the assumed redundant member ID, we must know the final sizes for all other members in the wing lift and drag trusses. A preliminary design of the member sizes can be made using the member loads for the condition where member ID is out and for all

flight conditions. Since only one landing wire is used, inverted flight conditions are statically determinate and thus member ID need not be removed. More discussion on the preliminary design is given at the end of the problem. The member sizes which have been selected are shown in Table A8.2.

Solution for Load in the Redundant Strut ID.

Let X = true load in member ID, then

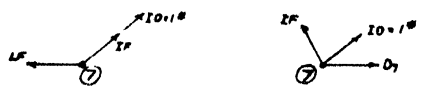
$$X = -\frac{\Sigma \frac{SuL}{AE}}{\Sigma \frac{u^2 L}{AE}} \quad \text{- (A)}$$

Where S = axial loads in truss members for given external wing loading and with diagonal interplane strut ID removed. (Values tabulated in Fig. A8.9) u = axial load in truss members due to a unit 1# tension load in the redundant member ID.

Determination of u Stresses in Members.

The loads in the lift truss members will be determined for a 1# tension load in member ID, by solving the concurrent force systems at joints 7, 8, 3, and 1.

Joint (7)



$\Sigma V = 1 \times .9015 + .962\ IF = 0$, hence $IF = -.938$

$\Sigma S = -LF - .938 \times .198 + 1 \times .187 = 0$ hence $LF = 0$

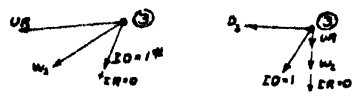
$\Sigma D = .938 \times .182 + 1 \times .3896 + D_7 = 0$, hence $D_7 = -.5614$

Joint (8)



$\Sigma V = .981\ IR + 0 = 0$ hence $IR = 0$ using ΣS and $\Sigma D = 0$, gives LR and $D_8 = 0$

Joint (3)



$\Sigma V = -.0523\ UR - .4486\ W_3 - 1 \times .9015 = 0$

$\Sigma S = -.9986\ UR - .8930\ W_3 - .1870 = 0$

$\Sigma D = -.3896 - D_3 = 0$

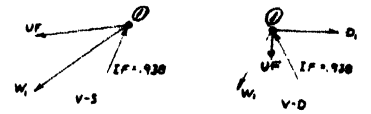
Solving the three equations, we obtain

$UR = 1.80$

$W_3 = -2.22$

$D_3 = D_3 = -.3896$

Joint (1)



$\Sigma V = -.0523\ UF - .4501\ W_1 + .938 \times .962 = 0$

$\Sigma S = -.9986\ UF - .8878\ W_1 + .938 \times .198 = 0$

$\Sigma D = -.0854\ W_1 - .938 \times .182 + D_1 = 0$

Solving the 3 equations, we obtain

$UF = -1.777$

$W_1 = 2.210$

$D_1 = .3595$

Figs. A8.10 and A8.11 show the lift truss reactions on drag truss at points 1, 3, 7, and 8 as found from the joint solutions.

Solving the drag trusses for these loadings the member axial loads or u stresses are recorded in Figs. A8.12 and A8.13.

It should be noticed that the same drag wires that were acting for the given external loading with member ID considered out of action are assumed acting for the u stresses, even though the u stresses are compression for the wire.

To check the numerical work the fuselage reactions should be calculated. The sum of the V, D, and S components should equal zero since the applied load of 1# in member ID will produce no resultant reaction on the fuselage.

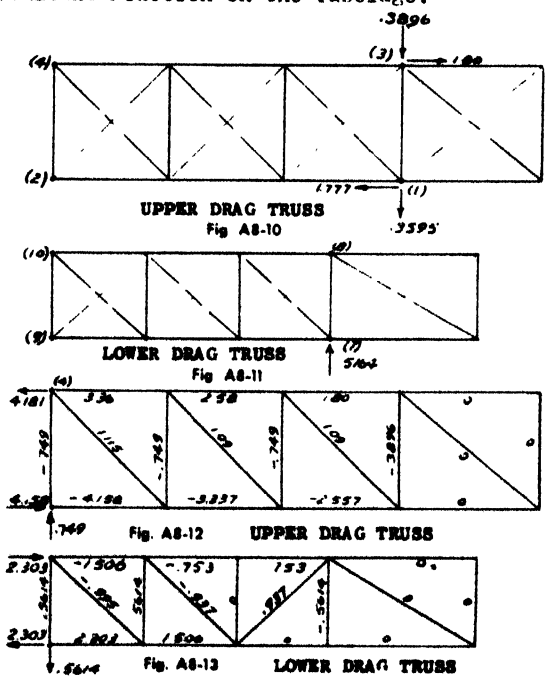


Table A8.2 gives the complete calculations for solving equation (A).

Column (2) gives the member sizes which must be known before deformations can be found.

Column (7) gives the member stresses (S stresses) for the given air loading with member ID considered out.

Column (8) gives the u stresses due to 1# load in member ID.

The load in the redundant member ID comes out -1660# and the final true load in any member equals S + Xu as shown in column (12).

General Discussion of the Results of Table A8.2

Investigating the drag wires, we find in column 12 of table A8.2 that member (28) is subjected to a compression load of 1402#. Obviously then, this wire is out of action and the counter wire (32) is in action. Thus to make the solution correct, the drag truss solutions for both the S and the u stresses should be recalculated for drag wire (32) acting instead of (28). The effect on the redundant member ID will be quite small as well as on the other members of the trusses. Thus in analyzing a wing cellule for various flight conditions different drag wires may act in different conditions and wires which may be in tension for the statically determinate condition may be in compression when redundant member is in action.

The air loading assumed in this example (See problem 2 of chapter A2) simulated a high angle of attack condition, that is pressure was forward. Thus the front lift truss would tend to be loaded heavier than the rear lift truss, which is indicated by the S loads in Table A8.2. The interplane strut ID which ties the front and rear lift trusses together should therefore tend to transfer some of the load from the front to the rear truss. This fact is shown in columns 11 and 12. It should be noticed that the front lift wire is relieved of 3660# and the rear wire increased 3670# over the statically determinate condition.

In comparing the member loads in columns 7 and 12, the student will notice a considerable change. The member sizes which were determined for use in this table should give small margins of the safety for the final loads in column 12. The student or stress analyst beginner will no doubt have to make several revisions in member sizes before the final sizes are obtained as he is inexperienced in allowing for transfer of loads when making the preliminary design for member sizes.

It is customary in actual design to multiply the values Xu in column 11 by .75 and 1.25 and add the result which will make the final value in column 12 the largest. This is done to compensate for the many unknowns that enter into the axial deformation calculations. For example E, the modulus of elasticity of the material may be slightly different than that used. Wing beams in many cases have filler blocks or tapered reinforcements at several points, thus the cross-sectional area is variable. End fittings likewise cause an error because of the change in cross-sectional areas. The clearances required in all bolt and pin fittings likewise produce an unknown amount of axial deformation. In this example the effect of deformation of the fuselage members was neglected. Thus the practice of increasing or decreasing the resulting XU stresses by 25 percent is a logical one.

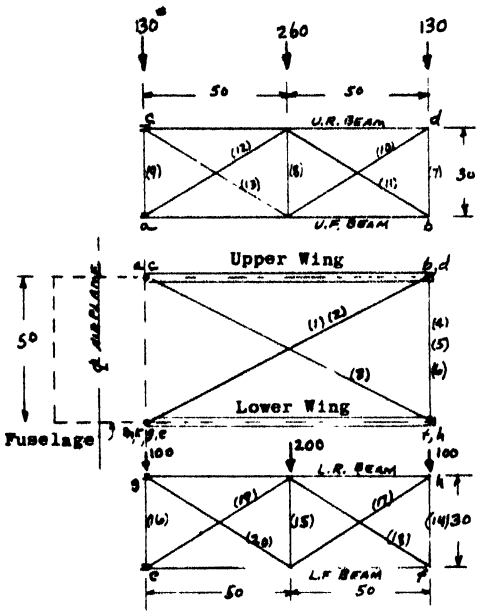
TABLE A8.2 SOLUTION FOR LOAD IN REDUNDANT ID

		1	2	3	4	5	6	7	8	9	10	11	12
Member		Member No.	Sizes and Material	Area A sq.in.	L Length in.	$\frac{E}{10^6}$	$\frac{L \times 10^6}{AE}$	S Member ID out.	u	$\frac{SuL}{AE}$	$\frac{u^2L}{AE}$	Xu	Final Load = S + Xu
UPPER PANEL	Front Beam	19	Al. Alloy I Sect	.70	37.5	10.3	5.20	-14275	-2.557	190000	34.00	4250	-10025
		20	Al. Alloy I Sect	.60	37.5	10.3	6.06	-16598	-3.337	315000	67.20	5550	-11048
		21	Al. Alloy I Sect	.60	39.5	10.3	6.40	-19290	-4.158	512000	111.00	6680	-12410
	Rear Beam	15	Al. Alloy I Sect	.55	37.5	10.3	6.62	- 5747	1.80	-68400	21.40	-2980	- 8727
		16	Al. Alloy I Sect	.50	37.5	10.3	7.28	- 3664	2.58	-68800	48.50	-4280	- 7944
		17	Al. Alloy I Sect	.50	39.5	10.3	7.68	- 1342	3.36	-34700	87.00	-5880	- 6922
	Drag Struts	2	1 3/8-.049 R.D. Al. Alloy	.304	36	10.3	17.20	- 535	- .3896	35700	2.60	645	110
		3	1 3/8-.049 R.D. Al. Alloy	.304	36	10.3	17.20	- 2225	- .749	28700	9.62	1245	- 980
		4	1 3/8-.049 R.D. Al. Alloy	.304	36	10.3	17.20	- 2456	- .749	31600	9.62	1245	- 1211
		5	1 3/8-.049 R.D. Al. Alloy	.304	36	10.3	17.20	- 2574	- .749	33200	9.62	1245	- 1329
	Drag Wires	11	5/16-24 Steel Tie Rod	.0404	52	29	44.40	2880	1.09	140000	53.00	-1800	1090
		12	5/16-24 Steel Tie Rod	.0404	52	29	44.40	3218	1.09	156000	53.00	-1800	1418
		13	5/16-24 Steel Tie Rod	.0404	53.4	29	45.30	3643	1.115	184000	56.60	-1840	1803
LOWER PANEL	Front Beam	40	Al. Alloy I Sect	.45	33.5	10.3	7.24	- 543	0	0	0	0	- 543
		41	Al. Alloy I Sect	.45	33.5	10.3	7.24	- 426	1.506	- 4650	16.40	-2500	- 2926
		42	Al. Alloy I Sect	.45	35.5	10.3	7.24	- 582	2.303	- 9720	38.50	-3800	- 4382
	Rear Beam	36	Al. Alloy I Sect	.40	33.5	10.3	8.15	- 123	- .753	757	4.62	1250	1127
		37	Al. Alloy I Sect	.40	33.5	10.3	8.15	- 123	.753	- 757	4.62	-1250	-1373
		38	Al. Alloy I Sect	.40	35.5	10.3	8.60	- 115	-1.506	1480	19.50	2500	2385
	Drag Struts	23	1 1/8-.049 Rd. Tube Al.	.165	25	10.3	14.70	- 317	- .5614	2820	4.64	930	613
		24	1 1/8-.049 Rd. Tube Al.	.165	25	10.3	14.70	- 101	0	0	0	0	- 101
		25	1 1/8-.049 Rd. Tube Al.	.165	25	10.3	14.70	- 110	.5614	- 912	4.64	- 930	- 1040
		26	1 1/8-.049 Rd. Tube Al.	.165	25	10.3	14.70	- 163	.5614	- 1342	4.64	- 930	1093
	Drag Wires	28	1/4-28 Steel Tie Rod	.024	41.8	29	60.0	158	.937	6900	52.80	-1560	- 1402
		33	1/4-28 Steel Tie Rod	.024	41.8	29	60.0	10	- .937	- 560	52.80	1560	1570
		34	1/4-28 Steel Tie Rod	.024	43.4	29	62.5	190	- .995	-11800	61.80	1650	1840
Front Lift Wire		W_1	2-7/16 S.L. Steel Wires	.156	128.6	29	28.50	13480	2.21	650000	138.50	-3680	9820
Rear Lift Wire		W_2	2-7/16 S.L. Steel Wires	.156	128.6	29	28.50	6980	-2.22	-436000	139.50	3670	10600
Front Int. Strut		IF	2 1/4-058 S.L. Al. Alloy	.399	60.8	10.3	14.80	- 1740	- .958	24100	13.65	1560	- 180
Dia. Int. Strut		ID	2 1/2-.065 S.L. Al. Alloy	.497	64.15	10.3	12.55	0	1.00	0	12.55	-1660	- 1660
TOTALS										1878400	1132.7		

$$X = \text{Load in redundant member ID} = -\frac{\Sigma \frac{SuL}{AE}}{\Sigma \frac{u^2L}{AE}} = \frac{\text{Col. 9}}{\text{Col. 10}} = -\frac{1878400}{1132.7} = -1660\#$$

Problems

(1) Fig. (D) shows a simplified biplane wing structure, the overhang at the outer strut point being omitted. Determine the axial loads in all the members of the lift and drag trusses for the given loading. Assume wire (3) out of action, and select either member (4) or (5) as the redundant member. Only one drag wire in each panel is assumed as in action. The drag reaction on fuselage is taken at points (a) and (e). Neglect influence of fuselage members on the truss deformations. Table (A) gives member sizes and kind of material.



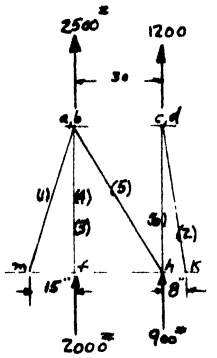


Fig. D

TABLE (A)

Member	Symbol	Material	E	Area Sq.In.
U.F. Beam		Alum. Al.	10.3×10^6	.60
U.R. Beam		Alum. Al.	10.3×10^6	.50
L.F. Beam		Alum. Al.	10.3×10^6	.45
L.R. Beam		Alum. Al.	10.3×10^6	.40
Drag Wires	10,11,12,13	Steel	29×10^6	.04
Drag Wires	17,18,19,20	Steel	29×10^6	.04
Drag Struts	7,8,9	Alum. Al.	10.3×10^6	.20
Drag Struts	14,15,16	Alum. Al.	10.3×10^6	.12
Lift Wire	1	Steel	29×10^6	.156
Lift Wire	2	Steel	29×10^6	.156
Front INT. S	4	Alum. Al.	10.3×10^6	.40
Dia. INT. S	5	Alum. Al.	10.3×10^6	.50
Rear INT. S	6	Alum. Al.	10.3×10^6	.40

(2) Determine the axial loads in lift and drag trusses if loading in Fig. (D) is reversed. (Note, lift wires (1) and (2) will be out of action).

A8.5 Stresses in Trusses with Multiple Redundancy

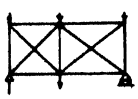


Fig A8-15

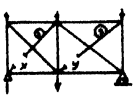


Fig A8-16

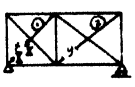


Fig. A8-17

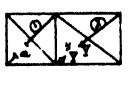


Fig A8-18

Fig. A8.15 shows a 2 panel truss. Relative to internal member stresses, the truss is redundant to the second degree because there are two more members than are necessary for stability. Thus, two additional equations based on continuity must be derived before the truss member loads can be determined. Fig. A8.16 shows the truss made statically determinate by cutting the two diagonals (1) and (2) at the points x and y respectively and carrying the given external loading. Fig. A8.17 shows the truss with only the load X applied to the cut faces x of the redundant member (1). The unknown load X is the true final load in the member (1). Fig. A8.18 shows the truss with only the load Y applied to the cut faces at y, where Y is the true final load in member (2).

By the principle of superposition, the true final loads in the members of the truss in Fig. A8.15 equals the algebraic sum of the member stresses due to the 3 loadings of Fig. 16, 17 and 18. Each of these 3 loadings produce a linear displacement of the cut faces at x and at y. However, the true condition is full continuity at these points, or the displacement between the cut faces at y and y due to the 3 loadings must equal zero. Thus, two additional equations involving the redundant loads X and Y can be obtained by writing the deflection at x and y and equating to zero.

Let δ_x = linear displacement between cut faces at x due to the three loadings of Fig. 16 to 18.

$$\delta_x = \sum \frac{S\, u_x\, L}{AF} + X \sum \frac{u_x^2\, L}{AE} + Y \sum \frac{u_x\, u_y\, L}{AE} = 0 \quad (2)$$

The first term represents the displacement at x for the loading of Fig. A8.16 where S equals the member loads due to the external truss loading and u_x the member loads due to a unit 1# tensile dummy load applied to the cut faces at point x; L = length of the members, A their cross-sectional area and E the modulus of elasticity.

The second term represents the displacement at x due to the truss loading of Fig. A8.17; that is, for a load of X applied at point x, u_x is the same as defined above. The member stresses due to load X equals Xu_x, since u_x equals the member stresses due to unit 1# tensile load at x. In other words, Xu_x corresponds to the value S in the first term of equation (2), and therefore to find the displacement at x due to these Xu_x member stresses, we apply another 1# load at x which produces u_x stresses, hence the resultant term u_x^2 in equation (2).

The third and last term of equation (2) represents the deflection at x due to the loading of Fig. A8.18, or due to a load Y acting at y.

u_y equals the member stresses due to a unit 1# tensile load applied to the cut faces at y, hence the member stresses due to Y equal Y u_y which corresponds to the term S in the first term of the equation, thus giving the term

$$\Sigma\, Y\, u_x u_y.$$

Similarly, the displacement of the cut faces y due to the three load systems must equal zero for continuity. Hence:

$$\delta_y = \sum \frac{S\, u_y\, L}{AE} + X \sum \frac{u_x\, u_y\, L}{AE} + y \sum \frac{u_y^2 L}{AE} = 0 \quad ---(3)$$

For trusses with additional redundants, equations similar to (2) and (3) can be written for each additional redundant member load.

X and Y can be found by solving equations (2) and (3). The true load in any member then equals the algebraic sum of the stresses for the three loadings, or:

$$\text{Final Member load} = S + Xu_x + Yu_y \quad -----(4)$$

In this example, two diagonal members were cut - but any two members consistent with stability could be chosen.

A8.6 Example Problem 2 - Two Redundant Members

Fig. A8.19 shows a structure composed of 4 co-planar members supporting a 2000# load. With only two equations of statics available, for a concurrent force system, the structure relative to loads in the members is redundant to the second degree. Fig. A8.20 shows the assumed statically determinate structure; the two members CE and DE are taken as the redundants and are cut at points x and y as shown. The member stresses for this structure and loading are recorded on the members. Figs. A8.21 and A8.22 give the u_x and u_y member stresses due to a unit 1# tensile load applied at the cut faces x and y. Table A8.3 gives the complete calculations for substituting in the deflection equations for the displacement at points x and y, with the loads in the redundant member CE designated X and that in DE as Y.

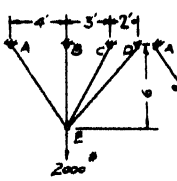


Fig A8.19

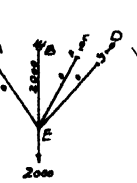


Fig A8.20

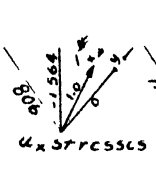


Fig. A8-21



Fig A8-22

Table A8.3

Member	Area	L	S	u_x	u_y	$\frac{S u_x L}{A}$	$\frac{S u_y L}{A}$	$\frac{u_x^2 L}{A}$	$\frac{u_y^2 L}{A}$	$\frac{u_x u_y L}{A}$	True Load $S + Xu_x + Yu_y$
AE	2	865	0	.866	1.154	0	0	2865	5765	462	900
BE	1	72	2000	-1.564	-1.729	-2,253,000	-2,488,000	1763	2150	1948	465
CE	2	865	0	1.00	0	0	0	4425	0	0	521
DE	.3	957	0	0	1.00	0	0	0	3125	0	416
Totals Σ						-2,253,000	-2,488,000	2446	5039	2350	

$$\delta_x = \sum \frac{S\, u_x\, L}{A} + X \sum \frac{u_x^2 L}{A} + Y \sum \frac{u_x\, u_y\, L}{A} = 0$$

Substituting values from table -2,253,000 + 2446X + 2350 Y = 0

$$\delta_y = \sum \frac{S\, u_x\, L}{A} + X \sum \frac{u_x\, u_y\, L}{A} + Y \sum \frac{u_y^2 L}{A} = 0$$

Substituting: -2,488,000 + 2350 X + 3039 Y = 0
Solving the two equations for X and Y, we obtain X = 521# and Y = 416#

The true load in any member = S + Xu_x + Xu_y which gives the values in the last column of the Table.

A8.7 Initial Stresses - Example Problem 3

Initial stresses are often produced in members of a pin connected redundant truss by erection or assembly operations. Thus, if the redundant member is not exactly the right length, it is often forced into place, which produces initial stresses in all members of a redundant truss, which must be added to the stresses produced by external loading.

In example problem #2, assume the redundant member CE is .01 inch too short, and is therefore stretched .01 inch in assembly of the structure. Find the resulting stresses in the bars due to this initial stretch in CE and also the 2000# load at E.

In the equation for deflection δ_x of problem #2, the deflection of the faces x of member CE will not equal zero, but .01 inch, since the member was initially stretched this amount in erection of the structure.

Thus;

δ_x = -2,253,000 + 2446 X + 2350 Y = .01 x 29,000,000

or -2,543,000 + 2446 X + 2350 Y = 0

The member material is assumed steel, or E = 29,000,000#/in.² The deflection equation for δ_y is the same as in problem 2.

$$\delta_y = -2{,}488{,}000 + 2350\, X + 3039\, Y = 0$$

Solving the equations for X and Y, we obtain

X = 985#, Y = 57#

Then, the load in BE = S + Xu_x + Yu_y = 2000 + 985 x (-1.564) + (57 x -1.729) = 358, and similarly, AE = 860#.

A8.8 Continuous Trusses

In airplane structures, a continuous truss is frequently used. Common examples are the center line keelson trusses of seaplane hulls, and wing beams of externally braced wing cellules. If a truss rests on more than two supports, it is statically indeterminate. The first general step in solving a continuous truss is to remove enough of the redundants to make it statically determinate. This may be done by removing all external supports except two. It may also be done by cutting certain members of the continuous truss as

the redundant members without modifying the truss supports. These two methods of solution can best be explained by the solution of a typical example.

Fig. A8.23 shows a continuous truss. Let it be required to determine the truss member stresses as well as the reactions for a load of 100# acting as shown.

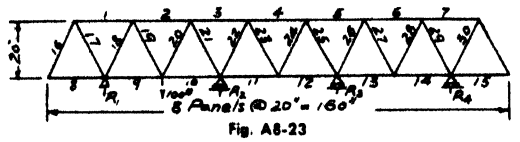


Fig. A8-23

Solution #1

In this solution, the truss is made statically determinate by cutting truss members #3 and #5. Fig. A8.24 shows the resulting truss together with all the truss member loads for this modified truss. The member loads are recorded adjacent to the truss members. The only members that are loaded lie between reactions R_1 and R_2.

Members #3 and #5 are the redundant members, the true load in #3 being X and Y in #5. The next step in the solution is to apply a unit one lb. tensile load to the cut faces x of member #3 and compute the loads in all truss members due to this unit loading. Fig. A8.25 shows the loaded truss together with the resulting member stresses which have been recorded on the members.

The next step is to apply a unit 1# tensile force to cut faces y of member #5 and compute the resulting member stresses. Fig. A8.26 shows the truss loading and resulting member stresses.

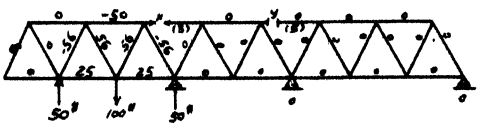


Fig. A8-24 **Cut Members (3) and (5) at x and y Resulting Member Stresses called S Stresses**

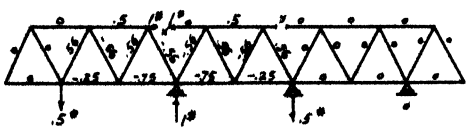


Fig. A8-25 *Member Loads u_x for 1# Load at x*

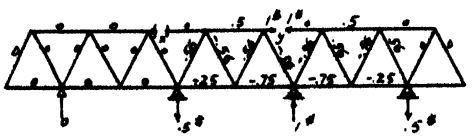


Fig. A8-26 *Member Load u_y for 1# Load at y*

To solve for the redundant member loads X and Y, we equate the displacement of the cut faces x and y for the load of Fig. A8.24 plus that due to X times the loading of Fig. A8.25 plus that due to Y times the loading of Fig. A8.26 and equate the sum of these three deflections for points x and y to zero, since full continuity at these three points actually exists.

Equating deflections at x to zero:

$$\delta_x = \sum \frac{S\ u_x\ L}{A} + X \sum \frac{u_x^2 L}{A} + Y \sum \frac{u_x\ u_y\ L}{A} = 0$$

Substituting values from table A8.4 - 1500 + 135.92 X - 7.96 Y = 0 - - - - - - - - - - - - -(1)

$$\delta_y = \sum \frac{S\ u_y\ L}{A} + X \sum \frac{u_x\ u_y\ L}{A} + Y \sum \frac{u_y^2 L}{A} = 0$$

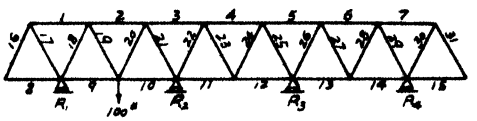


Table A8.4

Member	A	S	L	u_x	u_y	$\frac{S u_x L}{A}$	$\frac{S u_y L}{A}$	$\frac{u_x^2 L}{A}$	$\frac{u_y^2 L}{A}$	$\frac{u_x u_y L}{A}$	True load $= S + X u_x + Y u_y$
2	1	-50	20	.5	0	-500	0	5	0	0	-44.46
3	1	0	20	1.0	0	0	0	20	0	0	11.07
4	1	0	20	.5	.5	0	0	5	5	5	5.86
5	1	0	20	0	1.0	0	0	0	20	0	0.65
6	1	0	20	0	.5	0	0	0	5	0	0.32
9	5	25	20	-.25	0	-250.0	0	2.5	0	0	22.23
10	5	25	20	-.75	0	-750	0	22.5	0	0	16.70
11	.5	0	20	-.75	-.25	0	0	22.5	2.5	7.5	-8.48
12	.5	0	20	-.25	-.75	0	0	2.5	22.5	7.5	-3.25
13	.5	0	20	0	-.75	0	0	0	22.5	0	0.48
14	5	0	20	0	-.25	0	0	0	2.5	0	0.18
18	1	-559	22.36	.559	0	-6.99	0	6.99	0	0	-49.71
19	1	559	22.36	-.559	0	-6.99	0	6.99	0	0	-49.71
20	1	559	22.36	.559	0	6.99	0	6.99	0	0	62.09
21	1	-559	22.36	-.559	0	6.99	0	6.99	0	0	-62.09
22	1	0	22.36	-.559	.559	0	0	6.99	6.99	-6.99	-5.83
23	1	0	22.36	.559	-.559	0	0	6.99	6.99	-6.99	5.83
24	1	0	22.36	-.559	.559	0	0	6.99	6.99	-6.99	-5.83
25	1	0	22.36	.559	-.559	0	0	6.99	6.99	-6.99	5.83
26	1	0	22.36	0	-.559	0	0	0	6.99	0	-0.36
27	1	0	22.36	0	.559	0	0	0	6.99	0	0.36
28	1	0	22.36	0	-.559	0	0	0	6.99	0	-0.36
29	1	0	22.36	0	.559	0	0	0	6.99	0	0.36
TOTALS						-1500	0	135.92	135.92	-7.96	

Substituting:

0 - 7.96 X + 135.92 Y = 0 - - - - - - - - -(2)

Solving equations (1) and (2) for X and Y,

X = 11.074#, Y = .6485#

The true reactions can now be solved for:

$R_1 = 50 + 11.074 \times (-.5) + .64853 \times 0 = 44.463$

$R_3 = 50 + 11.074 \times 1 + .6485 \times (-.5) = 60.75$

$R_3 = 0 + 11.074 \times (-.5) + .6485 \times 1 = -4.889$

$R_4 = 0 + 11.074 \times 0 + .6485 \times (-.5) = -0.324$

Total = 100.00#

Solution #2

In this solution, the reactions R_3 and R_4 are selected as the redundants. In Fig. A8.27, these reactions are removed and the static member stresses are computed, the results being recorded on the truss members. Fig. A8.28 shows the assumed statically determinate truss subjected to a unit 1# reaction at reaction point R_3. The resulting member stresses are as shown. Similarly, Fig. A8.29 shows the results for a unit 1# reaction at R_4. The vertical deflection of the truss at the R_3 and R_4 reaction points due to the three loadings in Figs. 27, 28 and 29, must equal zero. Table A8.5 gives the necessary values for computing these deflections.

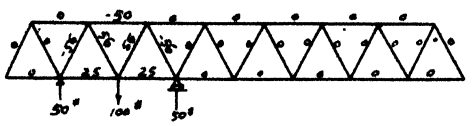


Fig. A8-27 Members Stresses S with Reactions R_3 and R_4 Removed

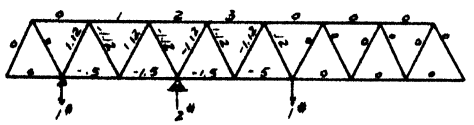


Fig. A8-28 Member Stresses U_3 for 1# Load at Reaction Point 3

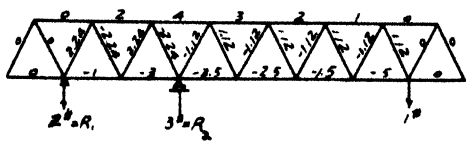


Fig. A8-29 Member stresses U_4 for 1# Load at Reaction Point R_4.

A8.9 Redundant Structures With Members Subjected to Both Axial and Bending Stresses.

If some of the members of a truss or framed structure are not pin ended, then in many cases the members of the structure may be subjected to both axial and bending stresses, thus a solution of such a truss involves a consideration of deflections due both to axial and bending stresses.

To illustrate, consider the structure in Fig. A8.30. The structure is statically indeterminate since the load at point B is held vertically by the wire BA and the bending stiffness of member BC which is built continuous with member AD at joint C. To solve this structure we first make the structure statically determinate by cutting wire AB at a-a' as shown in Fig. A8.31. The distortion of this structure will cause a deflection of (a) with respect to (a') in the line of action of the member AB. However since the member AB is continuous at a-a' there can be no movement between the cut forces a-a', therefore a load X must be added in the member AB which will cancel the deflection due to the stresses in Fig. A8.31. Thus Fig. A8.32 shows the unknown stress X which must be added to cause the distortion at a-a' to be zero. The solution therefore involves the writing of an equation expressing the deflection between the cut faces a-a' due to the load systems in Fig. A8.31 and Fig. A8.32 and equating this deflection to zero. The unknown is the true load in member AB which has been designated X. Once X is known, the true axial and bending forces on the other members can be found by statics.

Table A8.5

Member	A	L	S	u_3	u_4	Su_3L / A	Su_4L / A	u_3^2L / A	u_4^2L / A	u_3u_4L / A
2	1	20	-50	1	2	-1000	-2000	20	80	40
3	1	20		2	4	0	0	80	320	160
4	1	20		1	3	0	0	20	180	60
5	1	20			2	0	0	0	80	0
6	1	20			1	0	0	0	20	0
9	.5	20	25	- .5	-1	- 500	-1000	10	40	20
10	.5	20	25	-1.5	-3	-1500	-3000	90	360	180
11	.5	20		-1.5	-3.5	0	0	90	490	210
12	.5	20		- .5	-2.5	0	0	10	250	50
13	.5	20			-1.5	0	0	0	90	0
14	.5	20			-0.5	0	0	0	10	0
18	1	22.4	-55.9	1.118	2.236	-1397	-2795	27.95	111.8	55.9
19	1	22.4	55.9	-1.118	-2.236	-1397	-2795	27.95	111.8	55.9
20	1	22.4	55.9	1.118	2.236	1397	+2795	27.95	111.8	55.9
21	1	22.4	-55.9	-1.118	-2.236	1397	2795	27.95	111.8	55.9
22	1	22.4		-1.118	-1.118	0	0	27.95	27.95	27.95
23	1	22.4		1.118	1.118	0	0	27.95	27.95	27.95
24	1	22.4		-1.118	-1.118	0	0	27.95	27.95	27.95
25	1	22.4		1.118	1.118	0	0	27.95	27.95	27.95
26	1	22.4			-1.118	0	0	0	27.95	0
27	1	22.4			1.118	0	0	0	27.95	0
28	1	22.4			-1.118	0	0	0	27.95	0
29	1	22.4			1.118	0	0	0	27.95	0
Totals						-3000	-6000	543.6	2590.8	1055.4

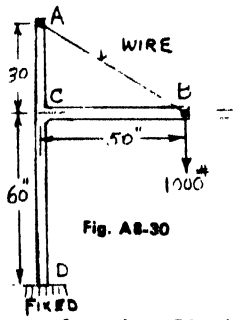


Fig. A8-30

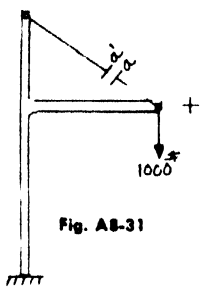


Fig. A8-31

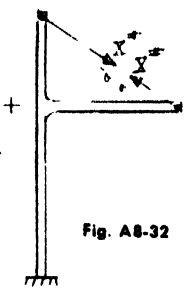


Fig. A8-32

Referring to Arts. A7.2 and A7.6, we can write the expression for deflection at a-a' as follows:-

$$\delta_{a\text{-}a'} = \sum \frac{Su\,L}{AE} + \int \frac{Mm\,dx}{EI} \qquad \text{- - - - - - - - - - - - (1)}$$

The terms u and m in equation (1) represent the axial and bending loads in the members due to the virtual loading which is a unit one pound force applied at the cut faces a-a' as shown in

Fig. A8.33. On this figure, the axial loads in the members are given in the () and the bending moment diagrams are sketched.

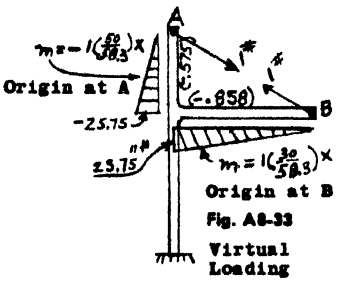


Fig. A8-33

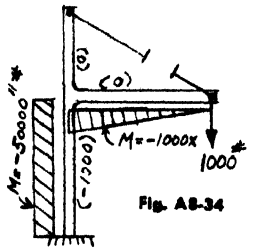


Fig. A8-34

In a similar manner Fig. A8.34 shows the stress S and the moments M for the loading of Fig. A8.31. The deflection at a-a' can now be written:-

$$\delta_{a-a'} = \sum\frac{SuL}{AE} + X\sum\frac{u^2L}{AE} + \int\frac{Mmdx}{EI} + X\int\frac{m^2dx}{EI} \quad ----(2)$$

(1) (2) (3) (4)

In equation (2) terms (1) and (3) are due to the loading in Fig. A8.34 and terms (2) and (4) are X times the values due to the 1# unit loading in Fig. A8.33. For explanation of the u^2 and m^2 terms refer to explanation in Art. A8.3.

Since $\delta_{a-a'}$ must equal zero, equation (2) is equated to zero and solved for X, which gives:-

$$X = -\frac{\sum\frac{SuL}{AE} + \int\frac{Mmdx}{EI}}{\sum\frac{u^2L}{AE} + \int\frac{m^2dx}{EI}} \quad ----------(3)$$

The calculations for solving equation (3) can best be made in table form as illustrated in Table A8.6. The member areas are assumed as shown. E is assumed the same for all members and thus is omitted from the calculations.

Table A8.6

Solution Of Equation (3)

Member	AB	AC	BC	CD	Total
Area sq.in.	0.025	3.0	2.5	3.5	
L - Length	58.3	30.0	50.0	60.0	
I, in^4	0	10.0	8.0	12.0	
S lbs.	0	0	0	-1000	
u lbs.	1.0	-0.575	-.858	0	
M	0	0	-1000x	-50000	
m	0	-0.858x	0.575x	0	
Σu L/A	0	0	0	0	0
$\int\frac{Mmdx}{100001}$	0	0	-299.6	0	-299.5
u^2 L/A	2332.	3.3	14.72	0	2350
m^2/I	0	$.0736x^2$	$.0412x^2$	0	
$\int m^2dx/I$		662	1723	0	2384

Solving for X by Subt. values in equation (3),

$$X = -\frac{0 + (-299.5 \times 10,000)}{2350 + 2384} = 634\#$$

Therefore the true load in AB is 634#. The true axial or bending moments on the other members then follow as a matter of statics, namely $P = S + Xu$, and $M_{true} = M + Xm$

A8.10 Problems

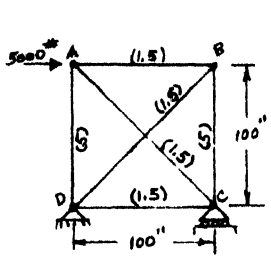


Fig. A

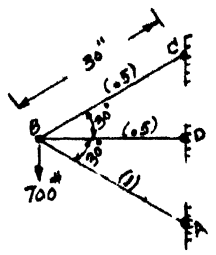


Fig. B

(1) Determine the load in all the members of the loaded truss shown in Fig. (a). Values in () on members represent the cross-sectional area in sq. in. for that member. All members of same material.

(2) For the structure in Fig. (b), determine the load in each member for a 700# load at joint B. Areas of members are given by the values in () on each member. All members made of same material.

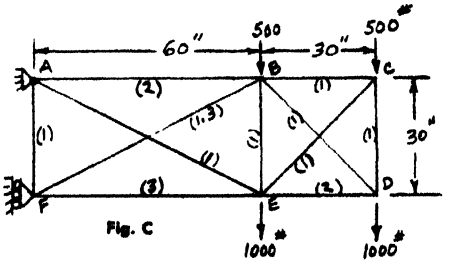


Fig. C

(3) For the loaded truss in Fig. c, determine the axial load in all members, Values in parenthesis adjacent to members represent relative areas. E is constant for all members.

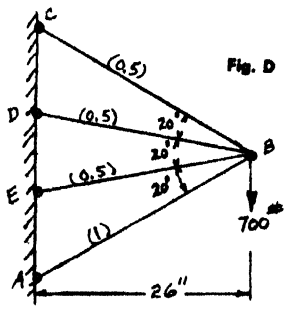


Fig. D

(4) For structure in Fig. d, calculate the axial loads in all the members. Values in parenthesis adjacent to each member represent relative areas. E is constant or same for all members.

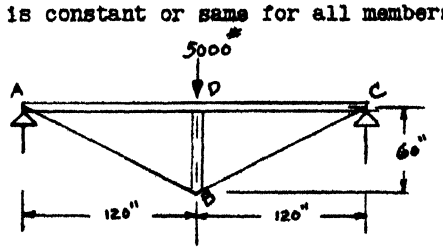


Fig. E

(5) For the "King post" truss in Fig. e, calculate the load in member BD. Members AB, BC and BD have area of 2 sq. in. each. The continuous member ADC has an area of 9.25 sq. in. and moment of inertia of 216 in^4. E is same for all members.

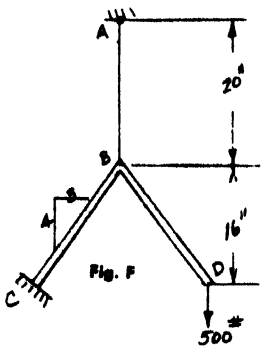


Fig. F

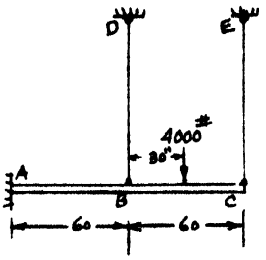


Fig. G

(6) In Fig. f, AB is a steel wire both 0.50 sq. in. area. The steel angle frame CBD has a 4 sq. in. cross section. Determine the load in member AB. E = 30,000,000 psi.

(7) In Fig. g find the loads in the two tie rods BD and CE. I_{ac} = 72 in.^{4}; A_{bd} = 0.05 sq. in. A_{ce} = 0.15 sq. in. E is same for all members.

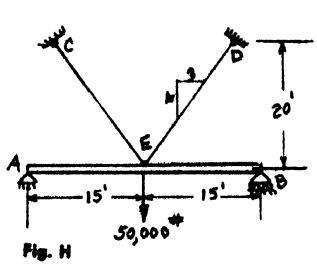


Fig. H

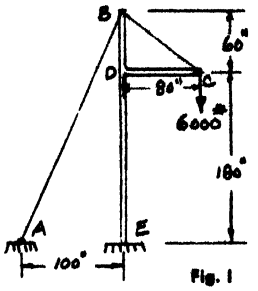


Fig. I

(8) For the structure in Fig. h, determine the reactions at points A, B. Members CE and ED are steel tie rods with areas of 1 sq. in. each. Member AB is a wood beam with 12" x 12" cross section. E_{steel} = 30,000,000 psi. E_{wood} = 1,300,000 psi.

(9) For the structure in Fig. i, determine the axial loads, bending moments and shears in the various members. The structure is continuous at joint D. Members AB, BC are wires. The member areas are AB = 1.2, BC = 0.6; CD = 6.0; BDE = 10.0. The moment of inertia for members CD = 60.0 in.^{4}; for BDE = 140 in.^{4}

CHAPTER A9
ANALYSIS OF RINGS AND FRAMES

A9.1 Introduction

In observing the inside of an airplane fuselage or seaplane hull one sees a large number of structural rings or closed frames. Some appear quite light and are essentially used to maintain the shape of the body metal shell and to provide stabilizing supports for the longitudinal shell stringers. At points where large load concentrations are transferred between body and tail, wing, power plant, landing gear, etc., relatively heavy frames will be observed. In hull construction, the bottom structural framing transfers the water pressure in landing to the bottom portion of the fuselage frames which in turn transfers the load to the fuselage shell.

In general the frames are of such shape and the load distribution of such character that these frames or rings under go bending forces in transferring the applied loads to the other resisting portions of the airplane body. These bending forces produce frame stresses in general which are of major importance in the strength proportioning of the frame, and thus a reasonable close approximation of such bending forces is necessary

Such frames are statically indeterminate relative to internal resisting stress and thus consideration must be given to section and physical properties to obtain a solution of the distribution of the internal resisting forces.

General Methods of Analysis.

There are many methods of applying the principles of continuity to obtain the solution for the redundant forces in closed rings or frames and bents. The author prefers the one which is generally referred to as the "Elastic Center" method and has used it for many years in routine airplane design. The method was originated by Muller-Breslau[@]. The main difference in this method as compared to most other methods of solution is that the redundant forces are assumed acting at a special point called the elastic center of the frame which gives resulting equations for the redundants which are independent of each other.

Assumptions.

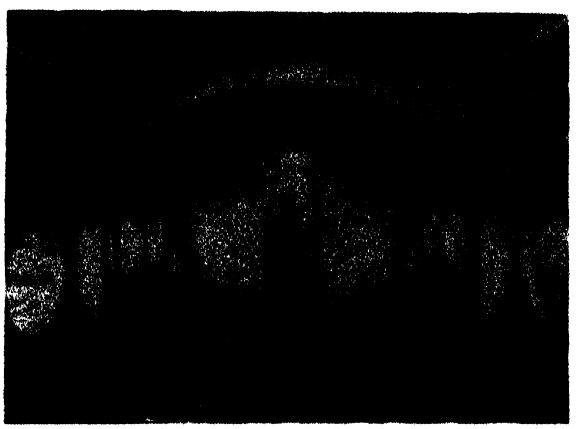
In the derivations which follow the distortions due to axial and shear forces are neglected. In general these distortions are small compared to frame bending distortions and thus the error is small. Since the distribution of the applied forces on a fuselage or hull shell are only known to an approximate degree in the present state of design knowledge, elaborate frame analyses are not justified.

In computing distortions plane sections are assumed to remain plane after bending. This is not strictly true because the curvature of the frame changes this linear distribution of bending stresses on a frame cross-section. (Corrections for curvature influence are given later in the chapter).

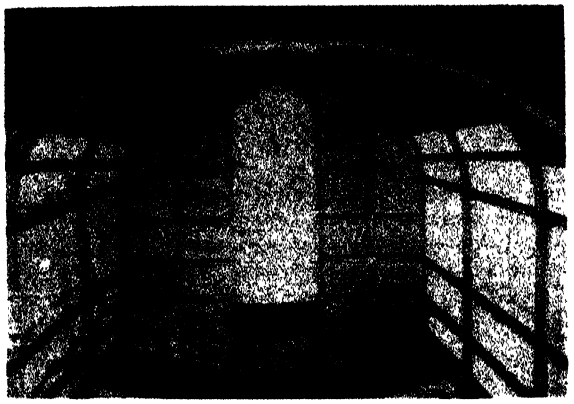
Furthermore it is assumed that stress is proportional to strain. Since the airplane stress analyst must calculate the ultimate strength of a frame, this assumption obviously does not hold with heavy frames where the rupturing stresses for the frame are above the proportional limit of the frame material.

This chapter will deal only with the theoretical analysis for bending moments in frames and rings by the elastic center method. Practical questions of body frame design are covered in a later chapter.

The following photographs of a portion of the structural framing of the hull of the Sikorsky S-43 airplane illustrate both light and heavy frames.



[@]Muller-Breslau, H., Die Neueren Methden der Festigkeitslehre und der Statik der Baukonstruktionen. Leipzig, 1886.



A9.2 Elastic Weight: Moment Weight

Fig. A9.1 shows a short section of a homogeneous elastic bar, which has been bent by some external agency. Assuming that plane sections remain plain after bending, we have the well-known flexural deformation of tension or elongation in the fibers below the neutral axis and compression or shortening of the fibers above the neutral axis. The fiber ab shortens the length

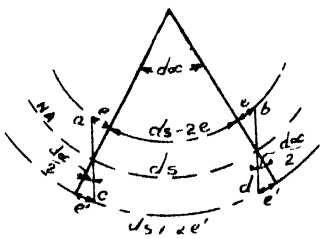


Fig. A9-1

2e in a length ds. From elementary mechanics, this shortening may be expressed as equal to (f/E)ds, where f equals the flexural fiber stress on the fiber and E the modulus of elasticity of the material. Then, from the geometry of small angles:-

$d\alpha = \frac{2e}{y} = \frac{fds}{Ey}$, where y is the distance from the neutral axis to the fiber ab. From the well known beam flexure formula we have: $f = \frac{My}{I}$.

Thus, we may write:

$$d\alpha = \frac{Myds}{EIy} = \frac{Mds}{EI} \quad \text{----------(1)}$$

The term $\frac{Mds}{EI}$ represents the angular change of the face ac of the element abcd relative to the other face bd. Actually, it is a small quantity in radians. For simplicity, this angle change on an element ds due to a certain moment will be called the moment weight of the element, and for simplicity in writing later equations, the symbol ϕ will be used to represent the moment weight of an element of an elastic bar. Thus:

$$\phi = \text{moment weight} = \frac{Mds}{EI} \quad \text{---------(2)}$$

If M is a unit moment, then $\phi = \frac{ds}{EI}$. The term $\frac{ds}{EI}$ is often referred to as the elastic weight of an element of an elastic bar. It represents the ability of the element to cause rotation when acted upon by a unit moment. Again for simplicity in writing later equations, we will let symbol w represent the elastic weight of an element of an elastic bar; or

$$w = \text{elastic weight} = \frac{ds}{EI} \quad \text{---------(3)}$$

A9.3 Deflections of a Cantilever Bar by Method of Moment and Angle Weights

Fig. A9.2 shows a curved cantilever beam. Assume that a bending moment acts only on the small element abcd of the beam. Due to the bending of this small element, the face ac will rotate through an angle $d\alpha$ relative to face bd and the portion of the beam between the free end B and face ac will move to the position B'.

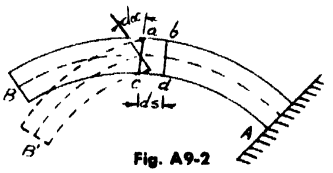


Fig. A9-2

Let it be required to determine the deflections of the terminal point B:- to avoid confusion of lines, Fig. A9.3 is drawn similar to Fig. A9.2 but showing only the neutral axis lines.

From Fig. A9.3, BB' is the arc of a circle where radius OB = r

Then $BB' = r d\alpha$

$dx = BB' (\cos \sphericalangle CBB') = r d\alpha (\cos \sphericalangle BOD) = r d\alpha \frac{(y)}{(r)} = d\alpha \cdot y$

From Eq. (1) Art. A9.2, $d\alpha = \frac{Mds}{EI}$

Substituting:

$dx = \left(\frac{Mds}{EI}\right) y$ and thus for bending on other elements:

$$\Delta x = \sum \frac{Mds}{EI} y$$

The term $\frac{Mds}{EI}$ has been given the name "moment weight" and the symbol ϕ (see Art. A9.2) Hence:

$$\Delta x = \Sigma \phi y \quad \text{----------(5)}$$

In like manner:

$dy = BB' (\sin \sphericalangle CBB') = r d\alpha \cdot (\sin \sphericalangle BOD)$

$= r d\alpha \cdot \frac{(x)}{r} = dx$

Hence,

$$\Delta y = \sum \frac{Mds}{EI} x \quad \text{or}$$

$$\Delta y = \sum \phi x \quad \text{----------(6)}$$

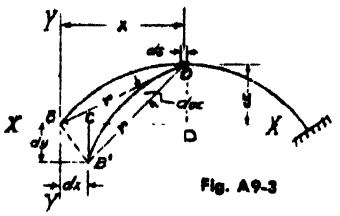


Fig. A9-3

Equations (5) and (6) state in general, that the deflection of the terminal point B in a certain desired direction due to bending of the beam equals the moment of the moment weights about a line through the terminal point and acting in the direction of the desired deflection.

Equations (5) and (6) express the relations for the translation of the terminal point B. The terminal point B also undergoes an angular displacement in moving to its final position B' For bending on the differential element abcd, the angular rotation of point B = $d\alpha$. Let $\Delta\alpha$ be the angular rotation of the terminal point B due to bending of the beam.

Then $\Delta\alpha = \Sigma\, d\alpha$. But, $d\alpha = \frac{Mds}{EI}$

Hence, $\Delta\alpha = \Sigma \frac{Mds}{EI}$. But $\frac{Mds}{EI}$ is the moment weight of any element which has been given for simplicity the symbol $\emptyset$. Therefore,

$$\Delta\alpha = \Sigma\emptyset \quad \text{- - - - - - - - - - - - - - - - - -(7)}$$

That is, the angular deflection of the terminal point B equals the total moment weight of the member.

To determine the proper signs, we note that to produce the deflection as shown in Fig. A9.2, a negative moment (Tension in the top fibers) must be applied to the cantilever beam. Hence, from the figure, M is negative, dx is positive, dy is negative. Then:

$$\Delta\alpha = -\Sigma\emptyset \quad \text{- - - - - - - - - - - - - - - - - -(I)}$$
$$\Delta y = \Sigma\emptyset\, x \quad \text{- - - - - - - - - - - - - - - - - (II)}$$
$$\Delta x = -\Sigma\emptyset\, y \quad \text{- - - - - - - - - - - - - - - - - -(III)}$$

A9.4 Equations for Redundant Internal Forces in a Closed Frame or Bent.

Fig. A9.4 shows two general types of frames. The internal stresses in these frames are statically indeterminate since we have 6

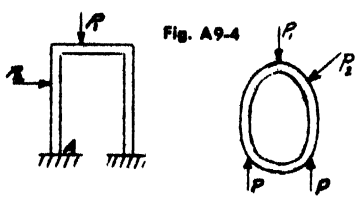


Fig. A9-4

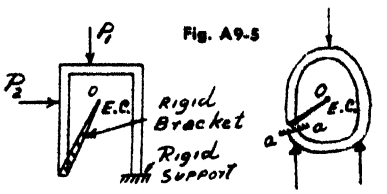


Fig. A9-5

unknowns and only 3 equations of statics available. Fig. A9.5 represents a modification of these frames which will be referred to as the "Residual Structure". In general, the residual structure is the original structure so modified as to be made statically determinate relative to internal stresses. In this treatment of frame analysis, the residual frame selected will be a cantilever structure as illustrated in Fig. A9.5. To simplify later deflection equations, the free end of the cantilever has been extended by an inelastic bracket to the point O, which coincides with the elastic center of the frame. The rigid bracket has zero elastic weight, since it is assumed as rigid or inelastic. The elastic center has been defined as a point coinciding with the centroid of the elastic weights $\frac{ds}{EI}$ of the structure. The residual frame and its loads satisfies the laws of statics but the true continuity of Fig. A9.4 has been altered. Thus, certain forces M_O, X_O, Y_O must be added to the residual frame at the terminal point O to give the true conditions of continuity relative to deformations of adjacent parts of the structure. Thus, Fig. A9.6 shows the force system which will satisfy both statics and continuity. The redundant forces are M_O, X_O and Y_O.

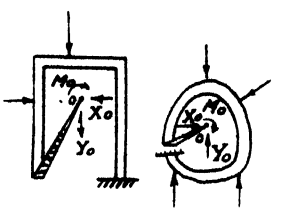


Fig. A9-6

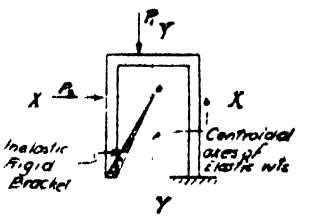


Fig. A9-7

Derivations of Expressions for Forces M_O, X_O and Y_O.

Consider the residual frame of Fig. A9.7 assumed symmetrical about the vertical axis. The point "O" which has been designated "elastic center" coincides with the centroid of the elastic weights of the frame. The reference axes through point O are the vertical symmetrical axis YY and XX which is perpendicular to YY. Considering only the effect of the external force system, we will write the expressions for the angular and translatory deflection of the point O. From equation I Article A9.3, angular deflection of point O,

$$\Delta\alpha_O = -\Sigma\emptyset_S \quad \text{- - - - - - - - - - - - - - - - - -(7)}$$

The subscript s has been added to the moment weight $\emptyset$ to signify that the moment is due to any static condition consistent with the given

loading. From Equation II, the deflection of point O in the Y-Y direction equals,

$$\Delta y_O = \Sigma\, \phi_S\, x \quad \text{- - - - - - - - - - - - - - - - (8)}$$

And similarly for deflection in the X-X direction from Equation III:

$$\Delta x_O = -\Sigma \phi_S y \quad \text{- - - - - - - - - - - - - - - - (9)}$$

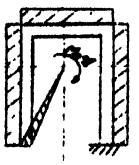


Fig. A9-8

Consider now only the redundant moment M_O at the elastic center O, and assume a unit value or $M_O = 1$. Fig. A9.8 shows the static moment diagram for $M_O = 1$. The angular rotation of point O due to a unit moment at O equals:

$$\Delta\alpha_O = -\Sigma\phi_S = -\Sigma \frac{Mds}{EI}$$

Since M is unity for every point on the frame,

$$\Delta\alpha_O = -\Sigma 1 \cdot \frac{ds}{EI} = -\Sigma \frac{ds}{EI} = -\Sigma w$$

Or, in other words, the angular rotation of point O due to the unit moment M_O equals the total elastic weight of the structure.

Thus, for a moment M_O other than zero,

$$\Delta\alpha_O(M_O \text{ at } {}_O) = -M_O\, \Sigma w \quad \text{- - - - - - - - - (10)}$$

Now, consider the translation of point O due to this unit moment M_O. The deflection of the elastic center O along the XX axis due to bending of the beam, from equation 9 is $\Delta x_O = -\Sigma\phi_S y$. Referring to the static moment curve of Fig. A9.8 it is observed that the XX axis is the centroidal axis of the moment weights ϕ_S (since M is constant) as well as being the centroidal axis of the elastic weights of the structure. Thus, the moment of the moment weights about axis XX is zero, hence:

$$\Delta x_O \text{ (due to } M_O) = -\Sigma\phi_S y = 0$$

For the same reason,

$$\Delta y_O \text{ (due to } M_O) = \Sigma\phi_S x = 0,$$

since the moment of the moment weights about the YY axis is zero. Thus, an external moment, applied at the elastic center, causes only rotation of the elastic center and no translation. Consider a force $X_O = 1$ acting on the residual frame as shown, in Fig. A9.9. The static moment curve due to this force is also shown. The bending moment on a differential element, as at point a = 1 . y = y. Then the moment weight of this element = $\frac{yds}{EI}$ = wy. The deflection of the point O along the XX axis due to bending of this element equals the moment of the moment weight of this element about axis XX = wy . y = wy^2. Hence,

$$\Delta x_O \text{ (due to } X_O = 1) = \Sigma wy^2$$

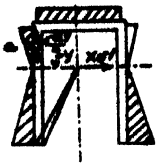


Fig. A9-9

The term Σwy^2 represents the moment of inertia of the elastic weights of the frame about the X axis. In other words, the deflection of the elastic center O along the XX axis due to a unit force at O acting along axis XX equals the elastic moment of inertia of the frame about the X-X axis. The term Σwy^2 will therefore be given the designation I_{XX}. Therefore, the deflection of point O along the XX axis due to a force X_O will equal:

$$\Delta x_O \text{ (due to } X_O) = X_O \Sigma wy^2 = X_O I_{XX} \quad \text{- - - - (11)}$$

The deflection of the point O along the Y-Y axis due to $X_O = 1$ equals the moment of the moment weights about the Y-Y axis, or:

$$\Delta y_O \text{ (due to } X_O = 1) = \Sigma wy \,.\, x = 0$$

The term Σ wyx represents the product of inertia of the elastic weights of the frame about the axes X and Y. This term is obviously zero, since the X and Y axes are principal axes.

The angular rotation of the point O, due to $X_O = 1$, equals the moment weight of the structure under this load, or in other words, the area of the $\frac{M}{EI}$ diagram. Total moment weight = $\Sigma \frac{Mds}{EI}$ = $\Sigma\frac{yds}{EI}$ = 0, because the axis XX is a centroidal axis, and thus $\Sigma \frac{yds}{EI}$ = 0. Thus summarizing, we can say that a force X_O produces pure translation of point O in the X direction, that is, no deflection in the Y direction and no rotation.

In a similar manner, it can be shown that a force Y_O acting at the elastic center O produces a translation of O along the Y axis equal to:-

$$\Delta y_O \text{ (due to } Y_O) = Y_O I_{yy} \quad \text{- - - - - - - (12)}$$

where I_{yy} = the elastic centroidal moment of inertia about the axis YY. Likewise, it can be shown that Y_O will produce no rotation of point O and no translation in the X direction.

We can now write three independent equations equating the displacement of the point O due to the external load system to the displacement due to the redundant forces M_O, X_O and Y_O. This must be so, since in Fig. A9.4, point A is a fixed support and thus does not suffer a displacement. Since point O is attached to A by an inelastic bracket, then O must not suffer any displacement, and thus, the effect of the external load system and the redundant system at O on the residual frame must produce zero movement of point O. For a closed frame as in Fig. A9.5, there can be no relative displacement between the cut faces at a-a (neglecting shear deformation), thus, point O which is attached to one face by an inelastic bracket, can suffer no displacement relative to

the other face at this cut section. Therefore:

$\Delta\alpha_O = -\Sigma\phi_S - M_O \Sigma w = 0$ (adding equations (7) and (10) or

$$M_O = -\Sigma \frac{\phi_S}{w}$$

$$= -\frac{\text{static moment weight of structure}}{\text{elastic weight of structure}} \quad \text{------(A)}$$

$$= -\frac{\text{Rotation of point "O" due to static moment}}{\text{Rotation of point "O" due to unit moment}}$$

and

$\Delta X_O = -\Sigma\phi_S y + X_O I_{XX} = 0$ (adding equations (9) and (11) or

$$X_O = \frac{\Sigma\phi_S y}{I_{XX}} \quad \text{------(B)}$$

$$= \frac{\text{moment of static moment weights about axis XX}}{\text{moment of inertia of elastic weights about axis XX}}$$

$$= \frac{\text{deflection of "O" along XX due to static moments}}{\text{deflection of "O" along XX due to } X_O = \text{unity}}$$

and

$\Delta Y_O = \Sigma\phi_S x + Y_O I_{yy} = 0$ (adding equations (8) and (12) or

$$Y_O = -\frac{\Sigma\phi_S x}{I_{yy}} \quad \text{------(C)}$$

$$= -\frac{\text{moment of static moment weights about axis YY}}{\text{moment of inertia of elastic weights about axis YY}}$$

$$= -\frac{\text{deflection of "O" along YY due to static moments}}{\text{deflection of "O" along YY due to } Y_O = 1}$$

Equations A, B and C give us three independent equations derived from the laws of elastic continuity, which, when used with the equations available from statics, permit the solution for stresses in a closed or restrained frame.

The particular reason for choosing a solution bringing in the elastic center is due to the fact that the resultant equations for the redundant forces are independent of each other, and thus the equations are simpler, eliminating the necessity of solving simultaneous equations.

It must be realized that the axes through the elastic center must be conjugate axes, that is, axes about which the product of inertia of the elastic weights is zero. For symmetrical frames, which is the case in practically all airplane problems, the symmetrical axes are, of course, conjugate axes.

Equations A, B and C consider only deformations due to bending. The effect of axial and shear deformation is not included.

Example problems 1 to 4 illustrate the application of the equations to symmetrical and unsymmetrical frames.

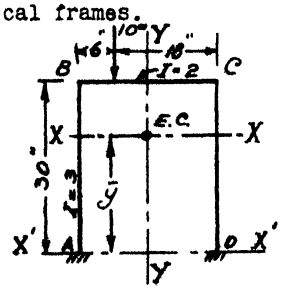


Fig. A9-10

A9.5 Application of Equations to Example Problems

Example Problem 1. To illustrate the use of equations A, B, and C, consider the fix-ended frame of Fig. A9.10 carrying a single external load. The relative moments of inertia of the top and side members are taken as 2 and 3 respectively. Let it be required to determine the bending moment diagram for this frame. The first step in the solution is to determine the location of the elastic center and the elastic moment of inertia of the frame about the X and Y axes through the elastic center. Table 1 shows the necessary calculations. Due to symmetry of the frame about a vertical axis, we know that the elastic center will lie on the vertical axis of symmetry. The vertical location of the elastic center is not evident from observation, so a reference axis X'X' is selected. Distances from reference axes to the elastic center:-

$$\text{From X'X'} = \bar{y} = \frac{\Sigma wy}{\Sigma w} = \frac{660}{32} = 20.63"$$

$$\text{From YY} = \bar{x} = \frac{\Sigma wx}{\Sigma w} = \frac{0}{32} = 0"$$

Transferring moment of inertia to the axes through the elastic center:-

$I_{XX} = 16{,}800 - 32 \times \overline{20.63}^2 = 3188$

$I_{yy} = 3456 - 0 = 3456$

The supporting medium at A and D are considered as fixed or rigid supports. Therefore, the supports have zero elastic weight; that is, a unit moment acting on a rigid support would cause zero rotation of support. The supports therefore, do not enter into the calculations.

Table 1

Portion	Elastic wt. $w=\frac{ds}{I}$	y=dist. from X'X'	x=dist. from YY	wx	wy	wy^2+i_x $i_x=\frac{(ds)^3}{(I)12}$	wx^2+i_y $i_y=\frac{(ds)^3}{(I)12}$
AB	$\frac{30}{3}=10$	15	-12	-120	150	$wy^2=2250$ $i_x=\frac{30^3}{3\times12}=750$	$wx^2=1440$ $i_y=0$
BC	$\frac{24}{2}=12$	30	0	0	360	$wy^2=10800$ $i_x=0$	$wx^2=0$ $i_y=\frac{24^3}{2\times12}=576$
CD	$\frac{30}{3}=10$	15	12	120	150	$wy^2=2250$ $i_x=750$	$wx^2=1440$ $i_y=0$
Totals	32			0	660	16800	3456

Note: i_x and i_y = moment of inertia of each portion about its own centroidal axis parallel to the X and Y reference axes respectively.

Solution #1

We first assume a condition for the frame that is statically determinate. Fig. A9.11 shows the static condition selected for solution #1. The frame has been broken at B and C and a hinge and rollers inserted. The static moment curve consists of a simple beam bending moment curve on member BC as shown and zero moment on the side members.

Due to bending of member BC, the elastic center of the residual structure of Fig. A9.12

will be displaced. In reality, the elastic center must suffer no displacement, thus certain forces M_o, X_o and Y_o are required to cancel the displacement due to the static moment on the residual frame. The equations for these forces are:

$$M_o = -\frac{\Sigma\phi_s}{\Sigma w}, \quad X_o = \frac{\Sigma\phi_s y}{I_{xx}}, \quad Y_o = -\frac{\Sigma\phi_s x}{I_{yy}}$$

$\Sigma\phi_s$ = static moment weight = area of static M/I curve = $\frac{45 \times 12}{2} = 270$

$\Sigma\phi_s y$ = moment of static $\frac{M}{I}$ curve about the XX axis

= 270 x 9.37 = 2534

Note:- Moments which cause tension on the inside of the frame are positive. In calculating the moment of the moment weights ϕ_s about the axes X and Y, the moment diagram should be considered as applied normal to the paper along the ℄ or neutral axis of the particular member.

$\Sigma\phi_s x$ = moment of the static moment weight about the YY axis = 270 x (-2) = - 540

Substituting in the general equations:-

$$M_o = -\frac{\Sigma\phi_s}{\Sigma w} = -\frac{270}{32} = -8.44 \text{ in. lb.}$$

$$X_o = \frac{\Sigma\phi_s y}{I_{xx}} = \frac{2534}{3188} = .796 \text{ lb.}$$

$$Y_o = -\frac{\Sigma\phi_s x}{I_{yy}} = -\frac{(-540)}{3456} = .1562 \text{ lb.}$$

Fig. A9.13 shows the bending moment on the residual frame due to these three forces. Fig. A9.14 gives the summation of the two moment curves of Figs. A9.11 and A9.13 which gives the true bending moment on the frame. With the bending moments on the frame known, shears and axial loads can be determined by statics.

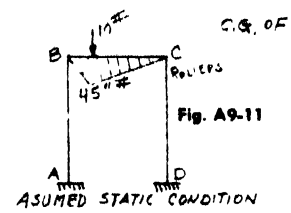


Fig. A9-11

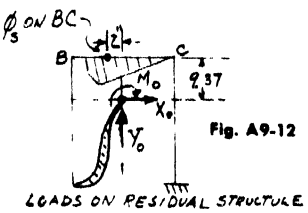


Fig. A9-12

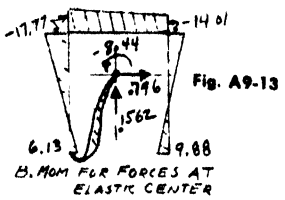


Fig. A9-13

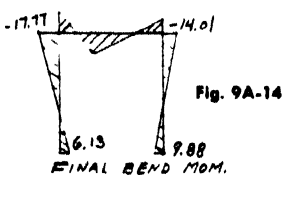


Fig. 9A-14

Solution #2

In this solution, the static condition assumed is two cantilevers (see Fig. A9.15). The frame is cut at the concentrated load point, and the load is assumed to act on the left cantilever. The static moment curve under this assumed condition is as shown. Fig. A9.16 shows the static moment load on the residual cantilever and the redundant forces at the elastic center which are required to give the true elastic action of the frame. Fig. A9.17 gives the bending moments due to the redundant forces only, and Fig. A9.18 the final moment value which equals the summation of Fig. A9.15 and A9.17. Table 2 gives the calculations for determining the redundant forces M_o, X_o and Y_o.

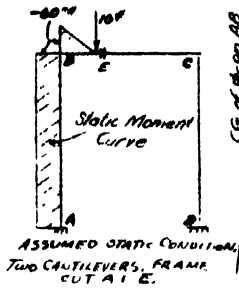


Fig. A9-15

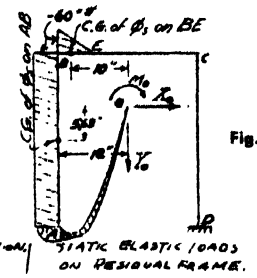


Fig. A9-16

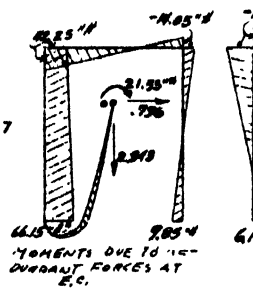


Fig. A9-17

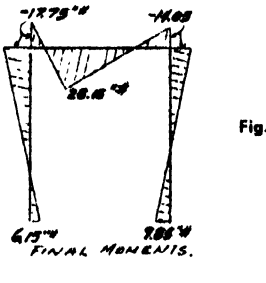


Fig. A9-18

Table 2

Portion	Static mom. Wt. $\phi_s = \frac{Mds}{I}$	x-dist. to axis YY	y-dist. to axis XX	$\phi_s x$	$\phi_s y$
AB	$\frac{-60x30}{3} = -600$	-12	-5.63	7200	3378
BE	$\frac{-30x6}{3} = -90$	-10	9.37	900	-843
EC	0	-		-0	0
CD	0	-		-0	0
Totals	-690			8100	2535

Calculation of redundant values.

$$M_o = -\frac{\Sigma\phi_s}{\Sigma w} = -\frac{(-690)}{32} = +21.55\text{"#}$$

$$X_o = \frac{\Sigma\phi_s y}{I_{xx}} = 2535/3180 = .796\#$$

$$Y_o = -\frac{\Sigma\phi_s x}{I_{yy}} = -8100/3456 = -2.343\#$$

The results in Fig, A9.18 are the same as in the first solution in Fig. A9.14. Any discrepancy is due to slide rule accuracy.

Example Problem2

Consider the same frame as in Problem #1, but with pin or hinge supports at A and D instead of rigid, fixed supports (see Fig. A9.19). Required the bending moment diagram.

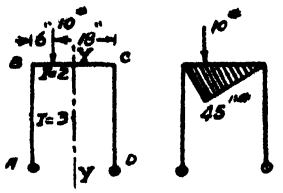


Fig. A9-19

Fig. A9-20

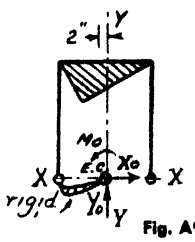


Fig. A9-21

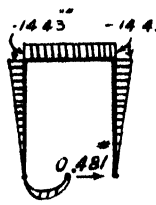


Fig. A9-22

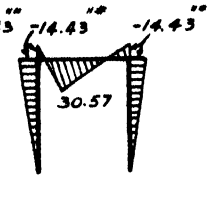


Fig. A9-23

The first step is to determine the location of the elastic center and the elastic moment of inertia about the X and Y axes through the elastic center. Due to symmetry the elastic center must be on the symmetrical axis Y-Y. In problem 1, the supports at A and D were fixed and thus, the supporting medium had zero elastic weight. In this example, the supporting mediums are hinges which have no resistance against rotation, which means they have infinite elastic weight that is, a unit moment on a hinge would cause infinite rotation. It is obvious therefore that the vertical location of the elastic center must be at point O on a line joining the two hinges, since the elastic weight of the hinges is infinitely large. Thus, the elastic weight of the frame is infinite, or $\Sigma w = \infty$. The elastic moment of inertia about axis YY is also infinite, due to the hinges or $I_{YY} = \infty$.

The elastic moment of inertia I_{XX} is as follows:-

Portion AB = 1/3 x 1/3 x $\overline{30}^3$ = 3000

Portion CD = 1/3 x 1/3 x $\overline{30}^3$ = 3000

Portion BC = 24 x 1/2 x 30^2 = 10800

I_{XX} = 16800

Fig. A9.20 shows the static condition assumed; that is, a pin at B and rollers at C. The static moment diagram is also shown. Fig. A9.21 shows the residual structure loaded with the static moment weight.

The static moment weight on the frame $\emptyset$ = area of the moment diagram on BC divided by I = 45 x 12 x 1/2 = 270

$\Sigma \emptyset_S x = 270 \times (-2) = -540$

$\Sigma \emptyset_S y = 270 \times 30 = 8100$

Solving for the redundants M_O, Y_O X_O,

$$M_O = -\frac{\Sigma \emptyset_S}{w} = -\frac{270}{\text{infinity}} = 0$$

$$Y_O = -\frac{\Sigma \emptyset_S x}{I_{yy}} = -\frac{(-540)}{\text{infinity}} = 0$$

$$X_O = \frac{\Sigma \emptyset_S y}{I_{xx}} = \frac{8100}{16800} = .481\#$$

Thus, the only redundant force required is X_O. It should be noted that if M_O or Y_O were other than zero the rigid bracket connecting the elastic center with hinge A would not be stable.

Fig. A9.22 shows the bending moment diagram on the residual frame due to the redundant force X_O = .481#. Adding these moments to the static moment assumed in Fig. A9.20, we obtain the final moment diagram in Fig. A9.23.

Example Problem 3 - Closed Frame

The bending moment diagram will be determined for the closed rectangular frame of Fig. A9.24. Table 3 gives the calculations for the location

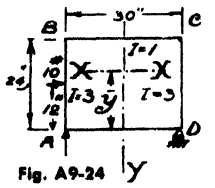


Fig. A9-24

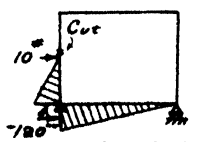


Fig. A9-25

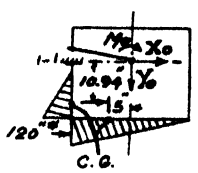


Fig. A9-26

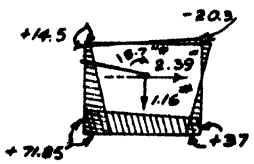
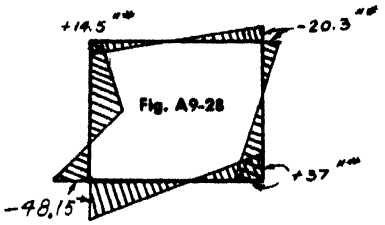


Fig. A9-27

of the elastic center and the elastic moment of inertia of the frame about axes X and Y through the elastic center. Due to symmetry about the vertical axis, the elastic center will lie on the vertical symmetrical axis. Thus, the X and Y axes through the elastic center will be conjugate axes. In Table 3, X'X' is taken as a reference axis in finding the desired properties. Fig. A9.25 shows the static condition assumed. The frame has been cut at the side load point, and the side load has been assumed to act on the lower portion at this point. The static moment curve for this assumed static condition is shown in Fig. A9.25. Fig. A9.26 shows the residual frame. The closed frame may be cut at any point as at section 1-1. One face is considered fixed. The other cut face is attached to the elastic center by an inelastic bracket. The static moment weight on this residual frame causes the elastic center O to move with respect to the cut face 1-1. However, since the frame is continuous at section 1-1, there can be no relative



displacement between the faces at this section. Thus, we find certain forces X_o, Y_o and M_o at the elastic center which will preserve continuity at section 1-1. Table 3 gives the calculations for these required forces and Fig. A9.27 shows the bending moments on the frame due to those forces. To obtain the final true moments, we add the moment diagram of Fig. A9.25 and A9.27 to get A9.28. (It is suggested that the student assume other static conditions and solve this problem).

Table 3

Portion	Elastic wt. $w=\frac{ds}{I}$	v = dist. to X'X'	x = dist. to Y'Y'	wy	wx	wy^2+i_x	wx^2+i_y
AB	$\frac{24}{3}=8$	12	-15	96	-120	$wy^2=1152$ $i_x=\frac{24^3}{12}=384$	$wx^2=1800$ $i_y=0$
BC	$\frac{30}{1}=30$	24	0	720	0	$wy^2=17280$ $i_x=0$	$wx^2=0$ $i_y=\frac{(30)^3}{12\times1}=2250$
CD	$\frac{24}{3}=8$	12	15	96	120	$wy^2=1152$ $i_x=384$	$wx^2=1800$ $i_y=0$
AD	$\frac{30}{2}=15$	0	0	0	0	$wy^2=0$ $i_x=0$	$wx^2=0$ $i_y=\frac{(30)^3}{2\times12}=1125$
Total	w=61			912	0	20352	6975

$\bar{y} = \Sigma wy/\Sigma w = 912/61 = 14.94"$

$I_{xx} = 20352 - 61 \times 14.94^2 = 6730$, $I_{yy} = 6975$

Static moment weight $\emptyset_S$ = area of static $\frac{M}{I}$ diagram:-

For member AB, $\emptyset_S = -\frac{120 \times 12}{2 \times 3} = -240$

For member AD, $\emptyset_S = -\frac{120 \times 30}{2 \times 2} = -900$,

Hence $\Sigma \emptyset_S = -1140$

The c.g. location of the static moment weight lies at the c.g. of the $\frac{M}{I}$ diagram for each portion or at the c.g. of each triangle on the N.A. or ℄ of the frame. Fig. A9.26 shows the distances to the c.g. of these static moment weights. Then

$\Sigma \emptyset_S x = -240 \times (-15) + [-900 \times (-5)] = 8100$

$\Sigma \emptyset_S y = -240\ (-10.94) - 900\ (-14.94) = 16075$

Substituting in equations for the required forces at the elastic centers:

$M_o = -\frac{\Sigma \emptyset_S}{\Sigma w} = -\frac{(-1140)}{61} = 18.7"\#$

$Y_o = -\frac{(\Sigma \emptyset_S x)}{I_{yy}} = -\frac{(8100)}{6975} = -1.16\#$

$X_o = \frac{\Sigma \emptyset_S y}{I_{xx}} = \frac{16075}{6730} = 2.39\#$

Example Problem 4 - Unsymmetrical Fame

Fig. A9.29 shows an unsymmetrical fix-ended bent, with a horizontal loading on one side. The procedure for determining the bending moments on the frame is the same as before with one exception. Due to the fact that the structure is not symmetrical about the X and Y axes, these two axis are therefore not conjugate axes; that is, axes about which the product of inertia of the elastic weights is zero. In the derivations of the simple equations A, B and C of article A9.4, it was necessary for the redundant forces at the elastic center to act along the axes which were conjugate to each other in order to be independent of each other. Table 4 gives the complete calculations for determining the conjugate axes and the properties about these axes. First, reference axes X'X' and Y'Y' are assumed. The elastic properties are determined about these axes and then transferred to parallel axes through the elastic center. The YY axis through the elastic center is taken as one conjugate axis. The direction of the other axis conjugate with this one is then determined.

Table 4

Portion	Elastic wt. $w=\frac{ds}{I}$	y = arm to X'X' axis	x = arm to Y'Y' axis	wx	wy	wx^2+i_y	wy^2+i_x	$wxy+i_{xy}$
AB	$\frac{15}{1}=15$	30	7.5	112.5	450	$wx^2=844$ $i_y=\frac{15^3}{12}=281$	$wy^2=13500$ $i_x=0$	$wxy=3375$ $i_{xy}=0$
BC	$\frac{30}{1.5}=20$	15	15	300.0	300	$wx^2=4500$ $i_y=0$	$wy^2=4500$ $i_x=\frac{30^3}{12}=1500$	$wxy=4500$ $i_{xy}=0$
AD	$\frac{20}{2}=10$	20	0	0	200	$wx^2=0$ $i_y=0$	$wy^2=4000$ $i_x=\frac{20^3}{24}=333$	$wxy=0$ $i_{xy}=0$
Σ	45			412.5	950	56250	23833	7875

Distances from reference axes to elastic center:-

$\bar{y} = \frac{\Sigma wy}{\Sigma w} = \frac{950}{45} = 21.11"$

$\bar{x} = \frac{\Sigma wx}{\Sigma w} = \frac{412.5}{45} = 9.166"$

Transferring values to parallel axes through the elastic center:-

$I_{xx} = 23833 - 45 \times \overline{21.11}^2 = 3780$

$I_{yy} = 5625 - 45 \times \overline{9.166}^2 = 1844$

$I_{xy} = 7875 - 45 \times 21.11 \times 9.166 = -832$

Let θ = angle between XX axis and axis X_oX_o which is conjugate with YY

$\theta = \tan^{-} \frac{I_{xy}}{I_{yy}} = -\frac{832}{1844} = -.4112$ or $\theta = 240 - 17"$

$I_{x_ox_o} = I_{xx}\cos^2\theta + I_{yy}\sin^2\theta - 2\, I_{xy}\sin\theta\cos\theta$

$I_{x_ox_o} = 3780 \times .\overline{9115}^2 + 1844 \times .\overline{4112}^2 - 2 \times (-832)$

$(-.4113) = 2648$

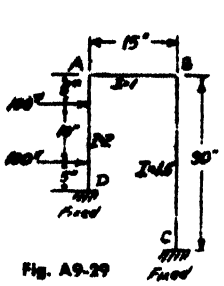
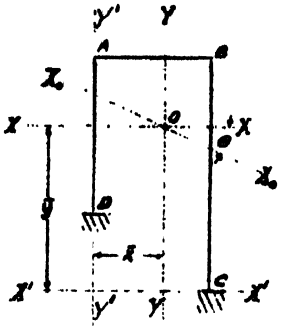


Fig. A9-29



The procedure from this point on is the same as in the previous examples. Fig. A9.30 shows the static condition assumed, namely, a cantilever, the frame being cut at A. The static moment curve is as shown. Fig. A9.31 shows the residual frame with the redundant forces acting at the elastic center.

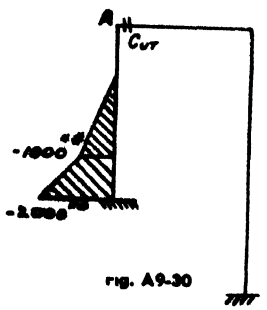


Fig. A9-30

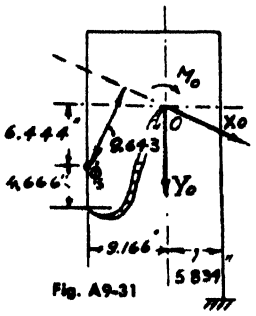


Fig. A9-31

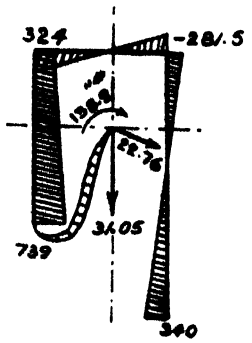


Fig. A9-32

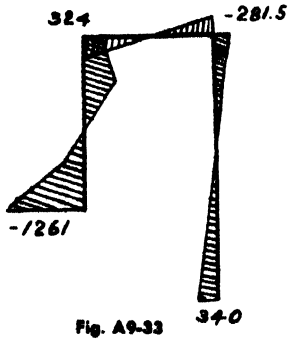


Fig. A9-33

X_0 acts along the conjugate axis X_0X_0. The static moment weight $\emptyset_s$ on the frame equals the area of the $\frac{M}{I}$ diagram:-

$$= \left[-1000 \times 5 + \frac{(1000 + 2000)}{2} 5 \right] \frac{1}{2} = -6250$$

This elastic static moment weight $\emptyset_s$ acts on the neutral axis of AD at the centroid of the $\frac{M}{I}$ diagram, which, by elementary arithmetic, falls at 4.666" from D.

We now substitute in our fundamental equations for the redundant forces at the elastic center.

$$M_0 = -\frac{\Sigma \emptyset_s}{\Sigma w} = -\frac{(-6250)}{45} = 138.9"\#$$

$$X_0 = \frac{\Sigma \emptyset_s y_0}{I_{x_0}} = -\frac{6250 \times (-9.643)}{2648} = 22.76\#$$

$$Y_0 = \frac{\Sigma \emptyset_s x}{I_y} = -\frac{6250 \times (-9.166)}{1844} = -31.05\#$$

Fig. A9.32 shows the bending moment on the residual frame due to the redundant forces acting at the elastic center. For example, for point D:-

M = 138.9 + 31.05 x 9.166 + 22.76 x .9115 x 11.11 + 22.76 x .4112 x 9.166 = 739"#.

The static bending moment under the assumed static condition at point D was -2000"# (see Fig. A9.30). Hence, the final moment at D = 739 - 2000 = - 1261"#.

Fig. A9.33 shows the final moment curve, which equals the summation of Figs. A9.30 and A9.32.

A9.6 Analysis of Frames Common to Airplane Structures

Open frames with a curved contour form one of the major units of semi-monocoque fuselage or hull structures. For such frames the general case is variable moment of inertia and concentrated as well as variable distributed loads. Some of the following example problems illustrate solutions of typical airplane frames. As stated before this chapter deals only with the analysis for the frame bending moments. Such questions as the design of frame sections and the true action of a frame as a unit in the airplane body are discussed in other chapters. In general airplane body frames are symmetrical structures about the vertical axis, thus the following example problems deal only with such symmetrical frames.

Example Problem 5

Fig. A9.34 shows a circular ring of constant cross-section subjected to the symmetrical loads as shown. The bending moment diagram on the frame will be determined.

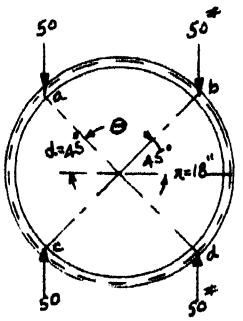


Fig. A9-34

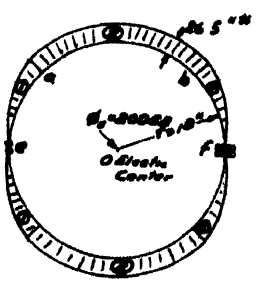


Fig. A9-35

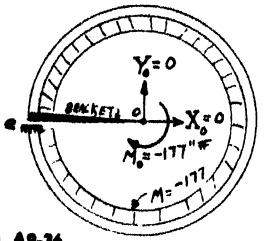


Fig. A9-36 Moments due to redundant forces.

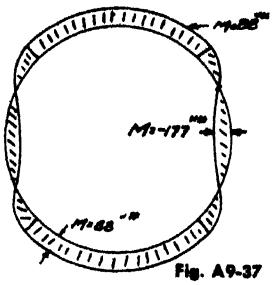


Fig. A9-37

Solution

Due to symmetry the elastic center of the frame coincides with the center of the circle. Since the moment of inertia of the cross-section of the ring has been assumed constant about its centerline axis, a relative value of 1 will be assumed. Thus total elastic weight of ring = $\Sigma w = \Sigma \frac{ds}{I}$ = perimenter of ring = $\pi \times 36$ = 113.1 since I is unity. The elastic moment of inertia of the ring about the X and Y diameters = $\pi r^3 = \pi \times \overline{18}^3 = 18300$.

Fig. A9.35 shows the bending moment diagram for the assumed statically determinate frame condition, namely, a pin at e and rollers at f. The static bending moment at points a, b, c and d = 50 x (18 - 18 cos 45°) = 265"#. (Tension on inside of a closed ring is positive moment). The moment is constant between a and b and between c and d. The next step is to determine the total static moment weights $\phi_s = \Sigma M\, ds/I$ which equals the area of the moment diagram since I is unity. Furthermore the centroid of this moment weight is required.

The area of portion (1) of the static moment curve is given by the equation

$$\text{Area} = Pr^2 (\alpha - \sin \alpha), \text{ where } P = 50\# \text{ and } \alpha = 45^\circ$$

Hence the elastic moment weight for the four portions (1) and equal

$$\phi_{s(1)} = 4 \left[50 \times \overline{18}^2 (.785 - .707)\right] = 5052$$

The elastic moment weight of the two portions marked (2) equal $2 \left[Pr^2 \theta (1 - \cos \alpha)\right]$

$$\phi_{s(2)} = 2 \left[50 \times \overline{18}^2 \times \frac{\pi}{2} (1 - .707)\right] = 15000$$

Hence total $\phi_s = 15000 + 5052 = 20052$. The sign is positive since M is positive.

Since the static moment curves are symmetrical with regard to the ring the centroid of the total moment weight ϕ_s is obviously at the center of the circle.

Fig. A9.36 shows one residual structure with the ring cut at e and a bracket extended to the elastic center O, where the redundant forces are applied. Substituting in the redundant equations.

$$M_o = -\frac{\Sigma \phi_s}{\Sigma w} = -\frac{(20052)}{113.1} = -177 \text{ in.lb.}$$

$$Y_o = -\frac{\Sigma \phi x}{I_{yy}} = -\frac{(20052 \times 0)}{1832} = 0\#$$

$$X_o = \frac{\Sigma \phi y}{I_{xx}} = \frac{20052 \times 0}{18320} = 0\#$$

Fig. A9.36 shows the moment diagram due to these redundants. It is a constant moment of -177"# since the redundants V_o and X_o equal zero. Adding the moment diagrams of Figs. 35 and 36 the final moment diagram of Fig. A9.37 is obtained.

Example Problem 6

Fig. A9.38 shows a simplified shape for an airplane body frame. The frame bending moments will be found for the given frame loading. The relative values of I as given for each portion of the frame.

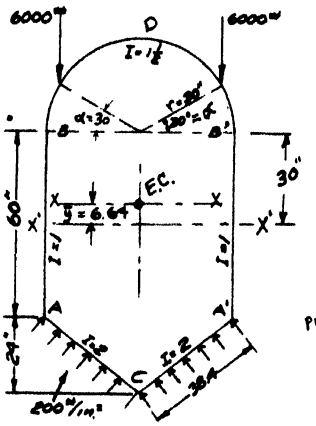


Fig. A9-38

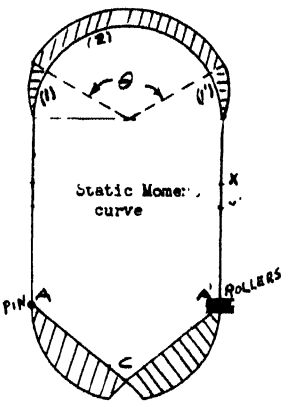


Fig. A9-39

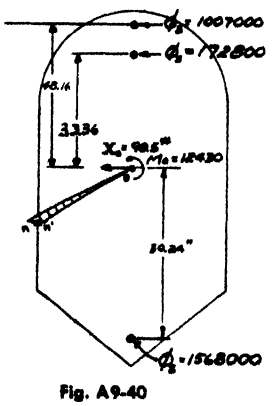


Fig. A9-40

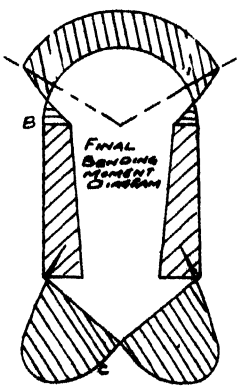


Fig. A9-41

Table A9.5
Take X'X' as reference axis.

Member	L	I	$w = \frac{L}{I}$	y	wy	$I_{X'X'} = i_{x'} + wy^2$
BDB'	94.25	1.5	62.8	$\frac{2r+30}{\pi} = 49.1$	3080	(1) 5400+151200 = 156600
AB	60.0	1.0	60.0	0	0	18000+0 = 18000
A'B'	60.0	1.0	60.0	0	0	18000+0 = 18000
AC	38.4	2.0	19.2	-42	-806	922+33850 = 34772
CA'	38.4	2.0	19.2	-42	-806	922+33850 = 34772
Totals			221.2		1468	262140

$\bar{y} = \frac{1468}{221.2} = 6.64"$ $I_{xx} = 262{,}140 - 221.2 \times \overline{6.64}^2 = 252400$

$C \curvearrowright C_{(1)} I_{cc} = .3r^3/I = .3 \times \overline{30}^3/1.5 = 5400$

$\bar{y}$ = distance from axis X'X' to Axis XX thru elastic center.

Solution

Table 5 gives the calculation of the frame elastic weight, the location of the elastic center and the elastic centroidal moment of inertia about the xx axis. Due to symmetry of external loading, I_{yy} is not required.

The next step in the solution is to compute the static moment elastic weights $\emptyset_s$ and their centroid locations. Fig. A9.39 shows the statically determinate frame condition which has been selected, namely a pin at point A and rollers at point A'. The static moment curves are shown on the figure.

Considering member BDB'

Static moment weight $\emptyset_s$ for portion (1) and (1'),

$$\emptyset_1 + \emptyset_1' = 2\left[\frac{Pr^2}{I}(\alpha - \sin\alpha)\right] =$$

$$2\left[\frac{6000 \times \overline{30}^2}{1.5}(.524 - .5)\right] = 172800$$

Vertical distance from line BB' to centroid of this moment load on portions (1) and (1') =

$$\bar{y} = \frac{r(1 - \cos\alpha - \frac{\sin^2\alpha}{2})}{\alpha - \sin\alpha} = \frac{30(1 - .867 - \frac{.5^2}{2})}{.524 - .5} = 10"$$

For portion (2) of moment diagram

$$\emptyset_2 = \frac{Pr^2\theta}{I}(1 - \cos\alpha) = \frac{6000 \times \overline{30}^2 \times 2.1}{1.5}(1 - .867 =$$

1,007,000

$\bar{y}$ from line BB' $= \frac{2r \sin\frac{\theta}{2}}{\theta} = \frac{2 \times 30 \times .867}{2.1} =$

24.8"

Considering Member AC:

From free body diagram of bottom portion of frame (Fig. A) the equation for bending moment

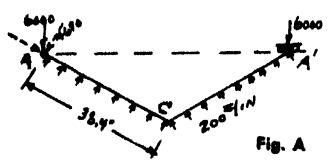


Fig. A

on member AC equals:

$M_x = 4690 \times -100 x^2$

Area of M/I curve between A and C =

$$1/2\int_0^{38.4}(4690 x - 100 x^2)dx$$

$$= 1/2\left[\frac{4690 x^2}{2} - \frac{100 x^3}{3}\right]_0^{38.4} = 784000$$

Distance to centroid of M/I curve along line AC from A.

$$\bar{X} = \frac{1/2\int_0^{38.4}(4690 \times 100 x^2)xdx}{78400}$$

$$= \frac{1/2\left[\frac{4690 x^3}{3} - \frac{100 x^4}{4}\right]_0^{38.4}}{78400} = 21.77"$$

Vertical distance from line AA' to centroid = 21.77 x 24/38.4 = 13.6". The static moment weight for A'C' is same as for AC, thus

$\emptyset_{AC} + \emptyset_{A'C'} = 2 \times 784000 = 1568000$

Fig. A9.40 shows the residual frame with the moment weights located at the centroids, together with the redundant forces M_o and X_o at the elastic center. It makes no difference where the frame is cut to form our residual cantilever, if one of the cut faces is attached to elastic center and the other is considered fixed. With the elastic properties and moment weights known the redundants can be solved for:

$$M_o = -\frac{\Sigma\emptyset_s}{\Sigma w} = -\frac{(1007000 + 172800 + 156800)}{221.2} =$$

12430"#

$$X_o = \frac{\Sigma\emptyset_s y}{I_{xx}} =$$

$$= \frac{1007000 \times 48.16 + 172800 \times 33.36 + 156800 \times -5.24}{252400}$$

$= -98.5$#

Y_o is zero because of the symmetrical frame and loading. The final or true bending moment at any point equals

$M = M_s + M_o - X_o y$

Thus for point B

$M_B = 0 + (-12430) - (-98.5 \times 23.36) = -10130"$

For point C

M_s at point C $= 4690 \times 38.4 - 200 \times (38.4)^2/2 =$ 32700

Hence $M_C = 32700 - 12430 - (-98.5 \times -60.64) = 14300"$#

Fig. A9.41 shows the general shape of the true frame bending moment diagram.

Example Problem No. 7 Analysis of Hull Frame.

Fig. A9.42 shows the general details of an intermediate hull frame taken from an actual large flying boat. The main external load on such frames is the water pressure on the hull bottom plating. The hull bottom stringers transfer the bottom pressure as concentrations on the frame bottom as shown. The resistance to this bottom upward load on the frame is provided by the hull metal covering which exerts tangential shear loads on the frame contour. The question as to the distribution of these shear resisting forces is discussed in later chapters. In this problem the resisting shear flow in the hull sheet has been assumed constant between the chine point and the upper heavy longeron. For analysis purposes the frame has been divided into 20 strips. The centroid of these strips located on the neutral axis of the frame sections are numbered 1 to 20 in Fig. A9.42. The tangential skin resisting forces are shown as concentrations on frame strips #6 to #16. On the figure these tangential loads have been replaced by their horizontal and vertical components. The sum of the vertical components should equal the vertical component of the bottom water pressure.

Table A9.6 shows the complete calculations for determining the bending moment on the frame. Columns 1 to 7 give the calculations for the elastic properties of the frame, namely the elastic weight of the frame; the elastic center location, and the elastic centroidal moment of inertia about the horizontal centroidal elastic axis. A reference horizontal axis X"X' has been selected as shown. All distance recorded in the table have been obtained by scaling from a large drawing of the frame.

Columns 8 to 13 of the Table, give the calculations necessary for determining the redundant M_o and X_o acting at the elastic center. Column 8 gives the static bending moments at the center of each frame strip when the frame is assumed cut at the crown point A and fixed at the keel section (see Fig. A9.43). Thus each side acts as a cantilever fixed at the keel section. Due to symmetry of frame and loading only one half of frame need be considered. The solution for the redundants is shown at the bottom of the Table. The final or true bending moment as given in column 13 and equals the static moment M_s plus that due to M_o and X_o acting at elastic center.

In the derivation of the equations for the redundant forces at the elastic centers, the summation from the elastic center around the frame was clockwise. In Fig. A9-42 the summation is counter-clockwise around the frame, thus the signs preceeding the expression for the three redundants is opposite to that given in equations A, B, and C on page A9.5. Fig. A9-44 shows the general shape of the resulting bending moment curve.

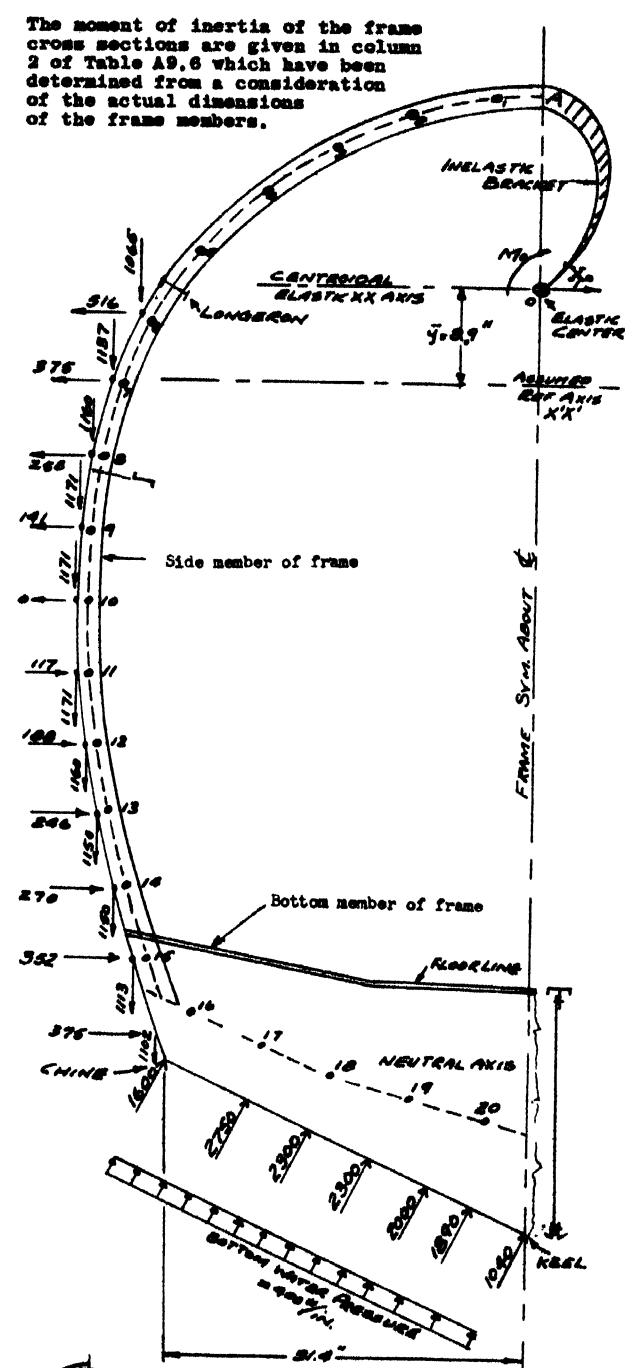


Fig. A9-42

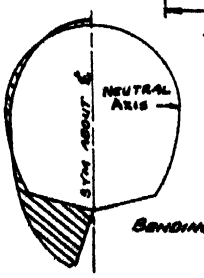


Fig. A9-44

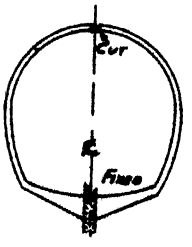


Fig. A9-43

Table A9.6

	Calculation of Frame Elastic Properties						Calculation of Moment Weights and Solution of Redundants							
Col.	1	2	3	4	5	6	7	8	9	10	11	12	13	14
Station	Strip length ds	Moment of Inertia I	Elastic Weight $w = \frac{ds}{I}$	Arm to Ref. Axis X'X' = y'	w y'	w y'^{2}	Arm to Axis XX = y	Static Moment M_S	Moment Weight $\phi = \frac{M_S w}{1000}$	ϕ_S y	M_O	X_Oy	*Total Moment M	
1	7.6	.065	117.00	26.1	3050	79700	17.2	0	0	0	+9020	16650	7630	
2	7.6	.065	117.00	24.4	2850	69500	15.5	0	0	0	"	15020	6000	
3	7.6	.065	117.00	21.4	2497	53300	12.5	0	0	0	"	12100	3080	
4	7.6	.065	117.00	17.3	2025	35020	8.4	0	0	0	"	8130	- 890	
5	7.6	.065	117.00	12.0	1403	16820	3.1	0	0	0	"	3000	-6020	
6	6.4	.25	25.60	5.9	151	892	- 3.0	1220	31.2	- 93.7	"	- 2910	-10710	
7	6.4	.25	25.60	0	0	0	- 8.9	2800	71.6	- 637	"	- 8610	-14840	
8	6.4	.25	25.60	- 6.3	-161	1017	-15.2	6230	159.3	- 2420	"	-14720	-17510	
9	6.4	.25	25.60	-12.6	-323	4060	-21.5	11260	286.5	- 6160	"	-20830	-18590	
10	6.4	.25	25.60	-19.1	-488	9320	-28.0	18470	473.0	- 13220	"	-27100	-17650	
11	6.4	.30	21.30	-25.5	-543	13850	-34.4	29020	618.0	- 21250	"	-33300	-13300	
12	6.4	.34	18.82	-32.0	-602	19250	-40.9	43180	814.0	- 33100	"	-39700	- 5540	
13	6.4	.34	18.82	-38.3	-720	27600	-47.2	58980	1110.0	- 52400	"	-45600	4360	
14	6.4	.34	18.82	-44.6	-840	37500	-53.5	77330	1455.0	- 77800	"	-51700	16610	
15	6.4	.34	18.82	-50.8	-959	48750	-59.9	99030	1865.0	-111300	"	-57900	32110	
Chine							-63.0	111700				-61100	41600	
16	7.0	12.0	0.58	-55.4	- 32	1780	-64.3	149700	86.7	- 5570	"	-62200	78500	
17	7.0	12.0	0.58	-58.4	- 34	1980	-67.3	221400	128.3	- 8650	"	-65100	147300	
18	7.0	18.0	0.39	-61.4	- 24	1470	-70.3	271200	105.8	- 7440	"	-68100	194100	
19	7.0	34.0	0.21	-63.2	- 13	840	-72.1	308600	64.9	- 4680	"	-70000	229600	
20	7.0	50.0	0.14	-64.8	- 9	588	-73.7	327900	45.9	- 3385	"	-71400	247500	
Keel							-75.0	332900			+9020	-72600	251300	
Totals			811.48		7228	423237			7315.0	-348106				

$\bar{y} = 7228/811.48 = 8.9"$

$I_{XX} = 423237 - 811.48 \times \overline{8.9}^2 = 358940$

$M_O = -\frac{\sum \phi_S}{\sum w} = + \frac{(7315.7 \times 1000)}{811.5} = +9020"\#$

$X_O = -\frac{\sum \phi_S}{I_{XX}} y = -\left[\frac{348106 \times 1000}{35894}\right] = +968\#$

*Total Moment M at any station = $M_S + X_O y - M_O$

Problems

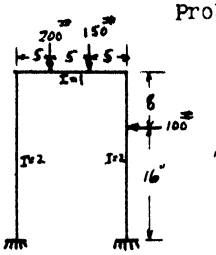


Fig. A9-45

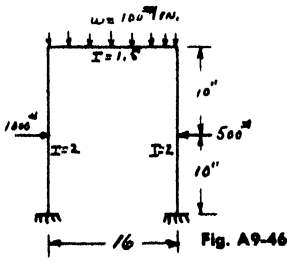


Fig. A9-46

(1) Determine the bending moment diagrams for the frames of Fig. A9.45 to A9.48. The relative moments of inertia (I) for each portion of the frames are shown on the figures.

(2) In Figs. A9.45 and A9.46 assume the frames pinned at bottom instead of fixed and determine frame bending moments.

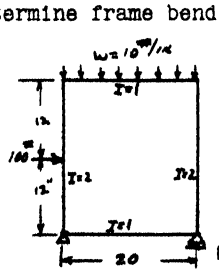


Fig. A9-47

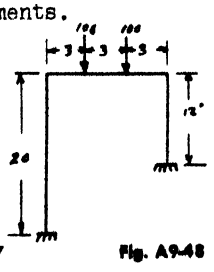
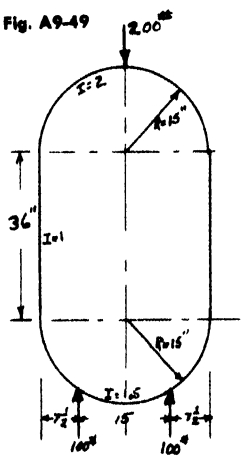


Fig. A9-48

Fig. A9-49



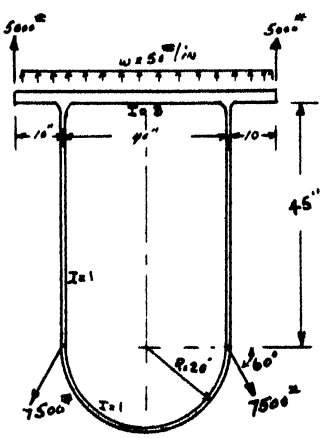


Fig. A9-50

(3) Determine the bending moment diagram for the closed frame of Fig. A9.49.

(4) Determine the bending moments on the frame of Fig. A9.50, for the given loading. Relative (I) values for the different portions of the frame are shown on the figure.

CHAPTER A10
BEAM - COLUMN MEMBERS

A10.1 Introduction

A beam-column is a member subjected to transverse loads or end moments plus axial loads. The transverse loading, or end moments, produces bending moments which, in turn, produce lateral bending deflection of the member. The axial loads produce secondary bending moments due to the axial load times this lateral deflection. Compressive axial loads tend to increase the primary transverse bending moments, where as tensile axial loads tend to decrease them.

Beam-column members are quite common in airplane structures. For example, the beams of externally braced wing and tail surfaces are typical examples, the air loads producing transverse beam loads and the struts introducing axial beam loads. In landing gears, one member is usually subjected to large bending and axial loads. In tubular fuselage trusses, lateral loads due to installations supported on members between truss joints produce beam-column action.

In general, beam column members in airplane structures are comparatively long and slender compared to those in buildings and bridges; thus, the secondary bending moments due to the axial loads are frequently of considerable proportion and need to be considered in the design of the members.

This chapter deals briefly on the theory of single span beam-column members. A summary of equations and design tables is included together with examples of their use. The information in this chapter is used frequently in other chapters where practical analysis and design of beam-column members is considered. For a completed and comprehensive treatment of beam-column theory and derivation of equations, see Niles and Newell-"Airplane Structures".

A10.2 General Action of a Member Subjected to Combined Axial and Transverse Loads.

Sub-figure a of Fig. A10.1 shows a member subjected to transverse loads W end axial compressive loads P. The transverse loads W produce a primary bending distribution on the member as shown in Fig. b. This bending will produce a transverse deflection curve as illustrated in Fig. c. The end loads P now produce an additional secondary bending moment due to the end load P times the deflection δ , or the bending moment diagram of Fig. d. This first secondary moment distribution produces the additional lateral deflection curve of Fig. e and the end load P will again produce further bending moments due to this deflection. If the axial load is not too large, these successive deflections will gradually converge and the member will reach a state of equilibrium. These secondary bending moments could be found by successive steps by the various deflection principles given in Chapter A7. However, for prismatic beams this convergency can be expressed as a mathematical series and thus save much time over the above successive step method. For members of variable moment of inertia, the secondary moments will usually have to be found by successive steps.

If the end loads P are tension, they will tend to decrease the primary moments; thus, in general, the case of axial compression is more important in practical design, since buckling and instability enter into the problem.

A10.3 Equations for a Compressive Axially Loaded Strut with Uniformly Distributed Side Load

Fig. A10.2 shows a prismatic beam of length L subjected to a concentric compressive load P and a uniformly transverse distributed load W, with the beam supported laterally at each end, and with end restraining moments M_1 and M_2. It is assumed that the general conditions for the beam theory hold, namely; that plane sections remain plane after bending; that stress is proportional to strain in both tension and compression.

At any point a distance x from the beam end, the moment expression is,

$$M = M_1 + \frac{(M_2 - M_1)}{L} x - \frac{WLx}{2} + \frac{WX^2}{2} - Py \text{ - - - - - } (10.1)$$

From applied mechanics, we know that

$M = EI \frac{d^2y}{dx^2}$ therefore, differentiating equation (10.1) twice with respect to x gives

$$\frac{d^2M}{dx^2} + \frac{P}{EI} M = w \text{ - - - - - - - - - - - - } (10.2)$$

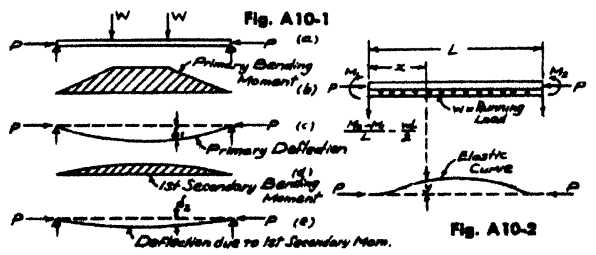


Fig. A10-1

Fig. A10-2

For simplification, let $j = \sqrt{\frac{EI}{P}}$; hence $\frac{P}{EI} = \frac{1}{j^2}$, which, substituted in (10.2), gives

$$\frac{d^2M}{dx^2} + \frac{1}{j^2} M = w$$

The solution of this differential equation gives.

$$M = C_1 \sin \frac{x}{j} + C_2 \cos \frac{x}{j} + wj^2 \text{ - - - - (10.3)}$$

where C_1 and C_2 are constants of integration and $\sin \frac{x}{j}$ and $\cos \frac{x}{j}$ are the limits of an infinite series of variable $\frac{x}{j}$. When x = o, M = M_1 and when x = L, M = M_2, therefore:

$$C_1 = \frac{M_2 - wj^2}{\sin \frac{L}{j}} - \frac{M_1 - wj^2}{\tan \frac{L}{j}}$$

$$= \frac{M_2 - wj^2 - (M_1 - wj^2) \cos \frac{L}{j}}{\sin \frac{L}{j}}$$

and $C_2 = M_1 - wj^2$

Let $D_1 = M_1 - wj^2$ and $D_2 = M_2 - wj^2$. Then, substituting in equation (10.3),

$$M = \frac{D_2 - D_1 \cos \frac{L}{j}}{\sin \frac{L}{j}} \sin \frac{x}{j} + D_1 \cos \frac{x}{j} + wj^2 \text{ (10.4)}$$

To find the location of the maximum moment, differentiate equation (10.3) and equate to zero.

$$\frac{dM}{dx} = o = \frac{C_1}{j} \cos \frac{x}{j} - \frac{C_2}{j} \sin \frac{x}{j}$$

whence

$$\tan \frac{x}{j} = \frac{C_1}{C_2} = \frac{D_2 - D_1 \cos \frac{L}{j}}{D_1 \sin \frac{L}{j}} \text{ - - - - - - -((10.5)}$$

The value of x must fall within x = O to x = l, otherwise M_1 or M_2 is the maximum value.

The value of the maximum span moment can be found by substituting the value from equation (10.5) in (10.4), which gives

$$M_{max} = \frac{D}{\cos \frac{x}{j}} + wj^2 \text{ - - - - - - - - - - (10.6)}$$

The moment M at any point x along the span can also be written:

$$M = D_1 \left[\left(\tan \frac{x_m}{j} \cdot \sin \frac{x}{j} \right) + \cos \frac{x}{j} \right] + wj^2 \text{ - (10.7)}$$

where x_m refers to the value of x where the span moment is maximum, or equation (10.5). Since it is customary to locate the point of maximum span bending moment and its value before investigating other span points, the value of $\tan \frac{x_m}{j}$ is known from equation (10.5) and thus is available to use in equation (10.7) for finding moments at other points along the span.

If the equation for the beam deflection is desired, it can be found by substituting the value of M from equation (10.3) in equation (10.1), which gives:

$$y = \frac{1}{P} \left(M_1 + \frac{M_2 - M_1}{L} x - \frac{WLX}{2} + \frac{WX^2}{2} \right.$$

$$\left. - \frac{D_2 - D_1 \cos \frac{L}{j}}{\sin \frac{L}{j}} \sin \frac{x}{j} - D_1 \cos \frac{x}{j} - wj^2 \right)$$

- - - - - - (10.7)

The slope of the elastic curve at any point is given by the first derivative of equation (10.7)

$$i = \frac{1}{P} \left(\frac{M_2 - M_1}{L} - \frac{WL}{2} + Wx - \frac{C_1}{j} \cos \frac{x}{j} + \frac{C_2}{j} \sin \frac{x}{j} \right) \text{ - (10.8)}$$

A10.4 Formulas for Other Single Span Loadings

In investigating other transverse loadings for a single span carrying axial compression, it is found that the expression for bending moment in the span always takes the form:

$$M = C_1 \sin \frac{x}{j} + C_2 \cos \frac{x}{j} + f(w) \text{ - - - (10.9)}$$

where f(w) is a term which does not include the axial load P or the end moments M_1 and M_2. The expressions for f(w), C_1 and C_2 depend on the type of the transverse load.

Table A10.1 gives the value of these 3 terms for types of transverse loading on a single span which are frequently encountered in airplane structures. The Table also gives equations for the point of maximum bending moment and its magnitude.

Table A10.2 is a table of sines, cosines, and tangents for L/j in radians which is more convenient to use than the usual type of trigonometric tables. This table is based on values given in Appendix I of Air Corps Information Circular #493. The Δ difference have been added to facilitate rapid use of the tables.

For single span beams, the critical value of L/j is π; that is, if the axial compressive load is such that the term L/j = π, the center region of the beam will tend to deflect until the combined stresses equal the failing stress of the material.

A10.5 Moments for Combinations of the Various Load Systems as Given in Table A10.1 Margins of Safety. Accuracy of Calculations.

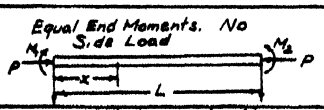
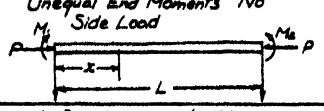
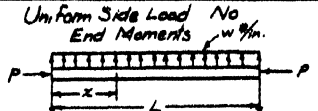
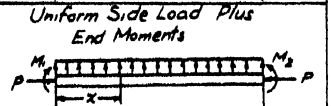
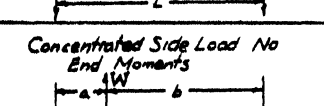
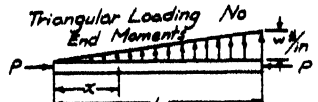
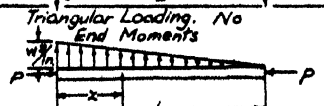
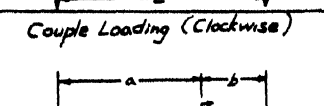
The principle of superposition does not apply to a beam-column, because the sum of the bending moments due to the transverse loads and the axial loads acting separately are not the same as the moments when they act simultaneously. In combining several transverse load systems with their accompanying axial loads, the principle of superposition can be said to apply if each transverse loading is used with the total axial load for the systems which are being combined. Thus, in Table A10.1, to find the moments for several combined loadings, add the values of C_1, C_2 and f(w) for the several loadings and use

Table A10.1

Values of Terms C_1, C_2, and f(w) in Equation

$$M = C_1 \sin \frac{x}{j} + C_2 \cos \frac{x}{j} + f(w)$$

Single Span - Axial Compression - Uniform Section

Loading	C_1	C_2	f(w)	Eq. for Point of Max Bending Moment	Eq. for Max. Span Bending Moment
Equal End Moments. No Side Load 	$M_1 \tan \frac{L}{2j}$	M_1	o	$x = \frac{L}{2}$	$M_{max} = \frac{M_1}{\cos \frac{L}{2j}}$
Unequal End Moments No Side Load 	$\frac{M_2 - M_1 \cos \frac{L}{j}}{\sin \frac{L}{j}}$	M_1	o	$\tan \frac{x}{j} = \frac{M_2 - M_1 \cos \frac{L}{j}}{M_1 \sin \frac{L}{j}}$	$M_{max} = \frac{M_1}{\cos \frac{x}{j}}$
Uniform Side Load No End Moments 	$\frac{wj^2 (\cos \frac{L}{j} - 1)}{\sin \frac{L}{j}}$	$-wj^2$	wj^2	$x = .5\ L$	$M_{max} = -wj^2 (1 - \sec \frac{L}{2j})$
Uniform Side Load Plus End Moments 	$\frac{D_2 - D_1 \cos L/j}{\sin L/j}$ where $D_1 = M_1 - wj^2$ $D_2 = M_2 - wj^2$	D_1	wj^2	$\tan \frac{x}{j} = \frac{D_2 - D_1 \cos \frac{L}{j}}{D_1 \sin \frac{L}{j}}$	$M_{max} = \frac{D_1}{\cos \frac{x}{j}} + wj^2$
Concentrated Side Load No End Moments 	$x < a$, $-\frac{Wj \sin \frac{b}{j}}{\sin \frac{L}{j}}$ $x > a$, $+\frac{Wj \sin \frac{a}{j}}{\tan \frac{L}{j}}$	o $-Wj \sin \frac{a}{j}$	o o	$\tan x/j = \frac{C_1}{C_2}$	$M_{max} = \frac{C_1^2 + C_2^2}{C_2} \cos \frac{x}{j}$
Triangular Loading No End Moments 	$-\frac{wj^2}{\sin \frac{L}{j}}$	o	$\frac{wj^2 x}{L}$	(NOTE A) To obtain Maximum Moment, compute moment at 3 or 4 points in span. Draw a smooth curve thru plotted results.	
Triangular Loading. No End Moments 	$\frac{wj^2}{\tan \frac{L}{j}}$	$-wj^2$	$wj^2 (1 - \frac{x}{L})$	(See Note A)	
Couple Loading (Clockwise) 	$x < a$, $-\frac{m \cos \frac{b}{j}}{\sin \frac{L}{j}}$ $x > a$, $-\frac{m \cos \frac{a}{j}}{\tan \frac{L}{j}}$	o $m \cos \frac{a}{j}$	o o	(See Note A)	

w or W is positive when upward.
M is positive when it tends to cause compression on the upper fibers of the beam at the section being considered.

Reference: ACIC #493; Niles, Airplane Design; Newell and Niles Airplane Structures.

TABLE A10.2

NATURAL SINES, COSINES, AND TANGENTS OF ANGLES IN RADIANS

$L/_j$ in Radians	Sin $L/_j$	Δ Sin $L/_j$	Cos $L/_j$	Δ Cos $L/_j$	Tan $L/_j$	Δ Tan $L/_j$
0.00	0.00000		1.00000		0.00000	
		0.01000		0.00005		0.01000
0.01	0.01000		0.99995		0.01000	
		0.01000		0.00015		0.01000
0.02	0.02000		0.99980		0.02000	
		0.01000		0.00025		0.01000
0.03	0.03000		0.99955		0.03000	
		0.00999		0.00035		0.01002
0.04	0.03999		0.99920		0.04002	
		0.00999		0.00045		0.01002
0.05	0.04998		0.99875		0.05004	
		0.00998		0.00055		0.01003
0.06	0.05998		0.99820		0.06007	
		0.00998		0.00065		0.01005
0.07	0.06994		0.99755		0.07012	
		0.00997		0.00075		0.01005
0.08	0.07991		0.99680		0.08017	
		0.00997		0.00085		0.01007
0.09	0.08988		0.99595		0.09024	
		0.00995		0.00095		0.01010
0.10	0.09983		0.99500		0.10034	
		0.00995		0.00104		0.0,011
0.11	0.10978		0.99396		0.11045	
		0.00993		0.00115		0.01012
0.12	0.11971		0.99281		0.12057	
		0.00992		0.00125		0.01016
0.13	0.12963		0.99156		0.13073	
		0.00991		0.00134		0.01019
0.14	0.13954		0.99022		0.14092	
		0.00990		0.00145		0.01022
0.15	0.14944		0.98877		0.15114	
		0.00988		0.00154		0.01024
0.16	0.15932		0.98723		0.16138	
		0.00986		0.00165		0.01027
0.17	0.16918		0.98558		0.17165	
		0.00985		0.00174		0.01032
0.18	0.17903		0.98384		0.18197	
		0.00983		0.00184		0.01036
0.19	0.18886		0.98200		0.19232	
		0.00981		0.00193		0.01039
0.20	0.19867		0.98007		0.20271	
		0.00979		0.00204		0.01043
0.21	0.20846		0.97803		0.21314	
		0.00977		0.00213		0.01048
0.22	0.21823		0.97590		0.22362	
		0.00975		0.00223		0.01052
0.23	0.22798		0.97367		0.23414	
		0.00972		0.00233		0.01058
0.24	0.23770		0.97134		0.24472	
		0.00970		0.00243		0.01062
0.25	0.24740		0.96891		0.25534	
		0.00968		0.00252		0.01068
0.26	0.25706		0.96639		0.27702	
		0.00965		0.00262		0.01074
0.27	0.26672		0.96377		0.27676	
		0.00963		0.00271		0.01080
0.28	0.27636		0.96106		0.28756	
		0.00959		0.00282		0.01085
0.29	0.28595		0.095824		0.29841	
		0.00957		0.00290		0.01093
0.30	0.29552		0.95534		0.30934	
		0.00954		0.00301		0.01098
0.31	0.30506		0.95233		0.32032	
		0.00951		0.00309		0.01107
0.32	0.31457		0.94924		0.33139	
		0.00947		0.00320		0.01114
0.33	0.32404		0.94604		0.34253	
		0.00945		0.00329		0.01121
0.34	0.33349		0.94275		0.35374	
		0.00941		0.00338		0.01129
0.35	0.34290		0.93937		0.36503	
		0.00937		0.00347		0.01137
0.36	0.36227		0.93590		0.37640	
		0.00935		0.00357		0.01146
0.37	0.36162		0.93233		0.38786	
		0.00930		0.00367		0.01155
0.38	0.37092		0.92866		0.39941	
		0.00927		0.00375		0.01164
0.39	0.38019		0.92491		0.41106	
		0.00923		0.00385		0.01174
0.40	0.38942		0.92106		0.42279	
		0.00919		0.00394		0.01184
0.41	0.39861		0.91712		0.43462	
		0.00915		0.00403		0.01194
0.42	0.40776		0.91309		0.44657	
		0.00911		0.00412		0.01205
0.43	0.41687		0.90897		0.45862	
		0.00907		0.00422		0.01216
0.44	0.42594		0.90475		0.47078	
		0.00906		0.00430		0.01228
0.45	0.43497		0.90045		0.48306	
		0.00898		0.00440		0.01239
0.46	0.44395		0.89605		0.49545	
		0.00894		0.00448		0.01251
0.47	0.45289		0.89157		0.50796	
		0.00889		0.00458		0.01265
0.48	0.46178		0.88699		0.52061	
		0.00885		0.00466		0.01278
0.49	0.47063		0.88233		0.53339	
		0.00880		0.00476		0.01301
0.50	0.47943		0.87758		0.54630	

$L/_j$ in Radians	Sin $L/_j$	Δ Sin $L/_j$	Cos $L/_j$	Δ Cos $L/_j$	Tan $L/_j$	Δ Tan $L/_j$
0.50	0.47943		0.87758		0.54630	
		0.00875		0.00484		0.01306
0.51	0.48818		0.87274		0.55936	
		0.00870		0.00496		0.01320
0.52	0.49688		0.86782		0.57256	
		0.00865		0.00501		0.01335
0.53	0.50553		0.86281		0.58591	
		0.00861		0.00510		0.01352
0.54	0.51414		0.85771		0.59943	
		0.00855		0.00519		0.01367
0.55	0.52269		0.85252		0.61310	
		0.00850		0.00526		0.01385
0.56	0.53119		0.84726		0.62695	
		0.00844		0.00536		0.01402
0.57	0.53963		0.84190		0.64097	
		0.00839		0.00544		0.01420
0.58	0.54802		0.83646		0.65517	
		0.00834		0.00552		0.01438
0.59	0.55636		0.83094		0.66955	
		0.00828		0.00506		0.01459
0.60	0.56464		0.82534		0.68414	
		0.00823		0.00569		0.01478
0.61	0.57287		0.81965		0.69892	
		0.00817		0.00577		0.01499
0.62	0.58104		0.81388		0.71391	
		0.00810		0.00585		0.01520
0.63	0.58914		0.80603		0.72911	
		0.00806		0.00593		0.01543
0.64	0.59720		0.80210		0.74454	
		0.00799		0.00602		0.01567
0.65	0.60519		0.79608		0.76021	
		0.00793		0.00609		0.01590
0.66	0.61312		0.78999		0.77611	
		0.00787		0.00617		0.01615
0.67	0.62099		0.78382		0.79226	
		0.00780		0.00625		0.01640
0.68	0.62879		0.77757		0.80866	
		0.00775		0.00632		0.01667
0.69	0.63654		0.77125		0.82533	
		0.00768		0.00641		0.01696
0.70	0.64422		0.76484		0.84229	
		0.00761		0.00648		0.01724
0.71	0.65183		0.75836		0.85953	
		0.00755		0.00655		0.01754
0.72	0.65938		0.75181		0.87707	
		0.00749		0.00664		0.01785
0.73	0.66687		0.74517		0.89492	
		0.00742		0.00670		0.01817
0.74	0.67429		0.73847		0.91309	
		0.00735		0.00678		0.01851
0.75	0.68164		0.73169		0.93160	
		0.00728		0.00685		0.01885
0.76	0.68892		0.72484		0.95045	
		0.00722		0.00693		0.01922
0.77	0.69614		0.71791		0.96967	
		0.00714		0.00700		0.01959
0.78	0.70328		0.71091		0.98926	
		0.00707		0.00706		0.01998
0.79	0.71035		0.70385		1.00924	
		0.00701		0.00714		0.02040
0.80	0.71736		0.69671		1.02964	
		0.00693		0.00721		0.02082
0.81	0.72429		0.68950		1.05046	
		0.00686		0.00728		0.02125
0.82	0.73116		0.68222		1.07171	
		0.00678		0.00734		0.02172
0.83	0.73793		0.67488		1.09343	
		0.00671		0.00742		0.02220
0.84	0.74464		0.66746		1.11563	
		0.00664		0.00748		0.02271
0.85	0.75128		0.65998		1.13834	
		0.00656		0.00754		0.02321
0.86	0.75784		0.65244		1.16155	
		0.00649		0.00761		0.02378
0.87	0.76433		0.64483		1.18533	
		0.00641		0.00768		0.02434
0.88	0.77074		0.63715		1.20967	
		0.00633		0.00774		0.02493
0.89	0.77707		0.62941		1.23460	
		0.00626		0.00780		0.02558
0.90	0.78333		0.62161		1.26018	
		0.00617		0.00786		0.02621
0.91	0.78950		0.61375		1.28637	
		0.00610		0.00793		0.02689
0.92	0.79560		0.60582		1.31326	
		0.00602		0.00799		0.02672
0.93	0.80162		0.59783		1.34088	
		0.00594		0.00804		0.02835
0.94	0.80756		0.58979		1.36923	
		0.00586		0.00811		0.02915
0.95	0.81342		0.58168		1.39838	
		0.00577		0.00816		0.02996
0.96	0.81919		0.57352		1.42836	
		0.00570		0.00822		0.03084
0.97	0.82489		0.56530		1.45920	
		0.00561		0.00828		0.03176
0.98	0.83050		0.55702		1.49096	
		0.00553		0.00833		0.03273
0.99	0.83603		0.54869		1.52369	
		0.00544		0.00838		0.03373
1.00	0.84147		0.54030		1.55741	

TABLE A10.2

NATURAL SINES, COSINES, AND TANGENTS OF ANGLES IN RADIANS

L_j in Radians	Sin L_j	Δ Sin L_j	Cos L_j	Δ Cos L_j	Tan L_j	Δ Tan L_j
1.00	0.84147		0.54030		1.55741	
		0.00538		0.00644		0.03480
1.01	0.84685		0.53386		1.59221	
		0.00528		0.00649		0.03592
1.02	0.85211		0.52737		1.62813	
		0.00519		0.00655		0.03712
1.03	0.85730		0.51482		1.66525	
		0.00510		0.00660		0.03836
1.04	0.86240		0.50822		1.70361	
		0.00502		0.00665		0.03971
1.05	0.86742		0.49787		1.74332	
		0.00494		0.00670		0.04110
1.06	0.87236		0.49887		1.78442	
		0.00484		0.00675		0.04261
1.07	0.87720		0.49012		1.82703	
		0.00476		0.00679		0.04419
1.08	0.88196		0.47133		1.87122	
		0.00467		0.00684		0.04588
1.09	0.88665		0.46249		1.91710	
		0.00458		0.00689		0.04766
1.10	0.89121		0.45360		1.96476	
		0.00449		0.00694		0.04958
1.11	0.89570		0.44466		2.01434	
		0.00440		0.00698		0.05161
1.12	0.90010		0.43568		2.06595	
		0.00431		0.00702		0.05380
1.13	0.90441		0.42666		2.11975	
		0.00422		0.00707		0.05613
1.14	0.90863		0.41759		2.17588	
		0.00413		0.00710		0.05861
1.15	0.91276		0.40849		2.23449	
		0.00404		0.00715		0.06131
1.16	0.91680		0.39934		2.29580	
		0.00395		0.00719		0.06418
1.17	0.92075		0.39015		2.35998	
		0.00386		0.00723		0.06728
1.18	0.92461		0.38092		2.42726	
		0.00376		0.00726		0.07064
1.19	0.92837		0.37166		2.49790	
		0.00367		0.00730		0.07425
1.20	0.93204		0.36236		2.57216	
		0.00358		0.00734		0.07818
1.21	0.93562		0.35302		2.65033	
		0.00348		0.00737		0.08243
1.22	0.93910		0.34365		2.73276	
		0.00339		0.00741		0.08706
1.23	0.94249		0.33424		2.81982	
		0.00329		0.00744		0.09212
1.24	0.94578		0.32480		2.91194	
		0.00320		0.00748		0.09763
1.25	0.94898		0.31532		3.00957	
		0.00311		0.00750		0.10371
1.26	0.95209		0.30582		3.11328	
		0.00301		0.00754		0.11035
1.27	0.95510		0.29628		3.22363	
		0.00292		0.00756		0.11772
1.28	0.95802		0.28672		3.34135	
		0.00282		0.00760		0.12586
1.29	0.96084		0.27712		3.46721	
		0.00272		0.00762		0.13489
1.30	0.96356		0.26760		3.60210	
		0.00262		0.00765		0.14498
1.31	0.96618		0.25785		3.74708	
		0.00254		0.00767		0.15627
1.32	0.96872		0.24818		3.90335	
		0.00243		0.00770		0.16896
1.33	0.97115		0.23848		4.07231	
		0.00233		0.00773		0.18331
1.34	0.97348		0.22875		4.25562	
		0.00224		0.00774		0.19961
1.35	0.97572		0.21901		4.45523	
		0.00214		0.00777		0.21821
1.36	0.97786		0.20924		4.67344	
		0.00205		0.00779		0.23962
1.37	0.97991		0.19945		4.91306	
		0.00194		0.00781		0.26438
1.38	0.98185		0.18964		5.17744	
		0.00185		0.00783		0.29326
1.39	0.98370		0.17981		5.47069	
		0.00175		0.00784		0.32719
1.40	0.98545		0.16997		5.79788	
		0.00165		0.00787		0.36749
1.41	0.98710		0.16010		6.16537	
		0.00155		0.00787		0.41573
1.42	0.98865		0.15023		6.58110	
		0.00145		0.00790		0.47436
1.43	0.99010		0.14033		7.05546	
		0.00136		0.00791		0.54636
1.44	0.99146		0.13042		7.60182	
		0.00125		0.00792		0.63528
1.45	0.99271		0.12050		8.23810	
		0.00116		0.00793		0.75052
1.46	0.99387		0.11057		8.98862	
		0.00105		0.00794		0.89878
1.47	0.99492		0.10063		9.88740	
		0.00096		0.00796		1.09698
1.48	0.99588		0.09067		10.98338	
		0.00086		0.00795		1.36653
1.49	0.99674		0.08771		12.34991	
		0.00075		0.00797		1.75151
1.50	0.99749		0.07074		14.10142	

L_j in Radians	Sin L_j	Δ Sin L_j	Cos L_j	Δ Cos L_j	Tan L_j	Δ Tan L_j
1.50	0.99749		0.07074		14.10142	
		0.00066		0.00998		8.32669
1.51	0.99815		0.06076		16.42811	
		0.00056		0.00999		3.2415
1.52	0.99871		0.05077		19.6696	
		0.00046		0.00998		4.8290
1.53	0.99917		0.04079		24.4986	
		0.00036		0.01000		7.9527
1.54	0.99953		0.03079		32.4513	
		0.00025		0.01000		15.8290
1.55	0.99978		0.02079		48.0803	
		0.00016		0.0999		44.5435
1.56	0.99996		0.01080		92.6238	
		0.00004		0.01000		1182.42
1.57	1.00000		0.00080		1275.04	
		0.00004		0.01000		1363.70
1.58	0.99996		-0.00920		-108.661	
		0.00014		0.01000		58.593
1.59	0.99982		-0.01920		-52.0676	
		0.00025		0.01000		17.8347
1.60	0.99957		-0.02920		-34.2329	
		0.00034		0.00999		8.7379
1.61	0.99923		-0.03919		-25.4950	
		0.00044		0.00999		5.1877
1.62	0.99879		-0.04918		-20.3073	
		0.00054		0.00999		3.4361
1.63	0.99825		-0.05917		-16.8712	
		0.00065		0.00998		2.4442
1.64	0.99760		-0.06915		-14.4270	
		0.00073		0.00997		1.8278
1.65	0.99687		-0.07912		-12.59926	
		0.00085		0.00997		1.41887
1.66	0.99602		-0.08909		-11.18059	
		0.00094		0.00995		1.13335
1.67	0.99508		-0.09904		-10.04724	
		0.00104		0.00995		0.93648
1.68	0.99404		-0.10899		-9.12076	
		0.00114		0.00993		0.77151
1.69	0.99290		-0.11892		-8.34925	
		0.00123		0.00992		0.65265
1.70	0.99167		-0.12884		-7.69660	
		0.00134		0.00991		0.55937
1.71	0.99033		-0.13875		-7.13723	
		0.00144		0.00990		0.48478
1.72	0.98889		-0.14866		-6.65245	
		0.00153		0.00988		0.42436
1.73	0.98736		-0.15853		-6.22809	
		0.00164		0.00987		0.37455
1.74	0.98572		-0.16840		-5.85353	
		0.00173		0.00985		0.33316
1.75	0.98399		-0.17825		-5.52037	
		0.00184		0.00983		0.29828
1.76	0.98215		-0.18806		-5.22209	
		0.00192		0.00981		0.26859
1.77	0.98023		-0.19789		-4.95340	
		0.00204		0.00979		0.24330
1.78	0.97819		-0.20768		-4.71010	
		0.00212		0.00977		0.22144
1.79	0.97607		-0.21745		-4.48866	
		0.00222		0.00975		0.20230
1.80	0.97385		-0.22720		-4.28627	
		0.00233		0.00973		0.18577
1.81	0.97152		-0.23693		-4.10050	
		0.00241		0.00970		0.17113
1.82	0.96911		-0.24663		-3.92937	
		0.00252		0.00968		0.15819
1.83	0.96659		-0.25631		-3.77118	
		0.00261		0.00965		0.14668
1.84	0.96398		-0.26596		-3.62450	
		0.00271		0.00963		0.13644
1.85	0.96127		-0.27559		-3.48806	
		0.00280		0.00960		0.12723
1.86	0.95847		-0.28519		-3.36083	
		0.00290		0.00957		0.11895
1.87	0.95557		-0.29476		-3.24188	
		0.00300		0.00954		0.11149
1.88	0.95257		-0.30430		-3.13039	
		0.00308		0.00951		0.10473
1.89	0.94949		-0.31381		-3.02556	
		0.00319		0.00948		0.09856
1.90	0.94630		-0.32329		-2.92710	
		0.00328		0.00945		0.09296
1.91	0.94302		-0.33274		-2.83414	
		0.00336		0.00941		0.08784
1.92	0.93964		-0.34215		-2.74630	
		0.00346		0.00938		0.08314
1.93	0.93618		-0.35153		-2.66316	
		0.00356		0.00934		0.07883
1.94	0.93262		-0.36087		-2.58433	
		0.00366		0.00931		0.07486
1.95	0.92896		-0.37018		-2.50947	
		0.00375		0.00927		0.07119
1.96	0.92521		-0.37945		-2.43828	
		0.00384		0.00923		0.06779
1.97	0.92137		-0.38868		-2.37049	
		0.00393		0.00920		0.06467
1.98	0.91744		-0.39788		-2.30582	
		0.00403		0.00916		0.06534
1.99	0.91341		-0.40705		-2.24048	
		0.00411		0.00912		0.05904
2.00	0.90930		-0.41615		-2.18504	

TABLE A10.2

NATURAL SINES, COSINES, AND TANGENTS OF ANGLES IN RADIANS

L_j in Radians	Sin L_j	Δ Sin L_j	Cos L_j	Δ Cos L_j	Tan L_j	Δ Tan L_j
2.00	0.90930		-0.41615		-2.18504	
		0.00421		0.00907		0.05851
2.01	0.90509		-0.42522		-2.12653	
		0.00436		0.00903		0.05416
2.02	0.90079		-0.43425		-2.07437	
		0.00436		0.00898		0.05195
2.03	0.89641		-0.44323		-2.02242	
		0.00448		0.00895		0.04990
2.04	0.89193		-0.45218		-1.97252	
		0.00457		0.00889		0.04766
2.05	0.88736		-0.46107		-1.92456	
		0.00466		0.00885		0.04615
2.06	0.88270		-0.46992		-1.87841	
		0.00473		0.00881		0.04445
2.07	0.87797		-0.47873		-1.83396	
		0.00484		0.00875		0.04284
2.08	0.87313		-0.48748		-1.79112	
		0.00491		0.00871		0.04135
2.09	0.86822		-0.49619		-1.74977	
		0.00503		0.00866		0.03993
2.10	0.86319		-0.50485		-1.70984	
		0.00507		0.00860		0.03857
2.11	0.85812		-0.51345		-1.67127	
		0.00518		0.00856		0.03732
2.12	0.85294		-0.52201		-1.63395	
		0.00526		0.00850		0.03610
2.13	0.84768		-0.53051		-1.59785	
		0.00535		0.00845		0.03498
2.14	0.84233		-0.53896		-1.56287	
		0.00543		0.00840		0.03389
2.15	0.83690		-0.54736		-1.52898	
		0.00552		0.00834		0.03288
2.16	0.83138		-0.55570		-1.49610	
		0.00559		0.00828		0.03191
2.17	0.82579		-0.56398		-1.46419	
		0.00569		0.00823		0.03098
2.18	0.82010		-0.57221		-1.43321	
		0.00576		0.00818		0.03011
2.19	0.81434		-0.58039		-1.40310	
		0.00585		0.00811		0.02928
2.20	0.80849		-0.58850		-1.37382	
		0.00591		0.00806		0.02848
2.21	0.80258		-0.59656		-1.34534	
		0.00601		0.00799		0.02773
2.22	0.79657		-0.60455		-1.31761	
		0.00609		0.00794		0.02701
2.23	0.79048		-0.61249		-1.29060	
		0.00616		0.00787		0.02631
2.24	0.78432		-0.62036		-1.26429	
		0.00625		0.00781		0.02566
2.25	0.77807		-0.62817		-1.23863	
		0.00632		0.00775		0.02503
2.26	0.77175		-0.63592		-1.21360	
		0.00639		0.00769		0.02444
2.27	0.76536		-0.64361		-1.18916	
		0.00648		0.00762		0.02385
2.28	0.75888		-0.65123		-1.16531	
		0.00655		0.00756		0.02332
2.29	0.75233		-0.65879		-1.14199	
		0.00662		0.00749		0.02278
2.30	0.74571		-0.66628		-1.11921	
		0.00669		0.00742		0.02227
2.31	0.73902		-0.67370		-1.09694	
		0.00678		0.00736		0.02180
2.32	0.73224		-0.68104		-1.07514	
		0.00685		0.00728		0.02133
2.33	0.72539		-0.68834		-1.05381	
		0.00692		0.00722		0.02089
2.34	0.71847		-0.69556		-1.03292	
		0.00699		0.00715		0.02046
2.35	0.71148		-0.70271		-1.01247	
		0.00707		0.00708		0.02005
2.36	0.70441		-0.70979		-0.99242	
		0.00713		0.00701		0.01966
2.37	0.69728		-0.71680		-0.97276	
		0.00721		0.00694		0.01927
2.38	0.69007		-0.72374		-0.95349	
		0.00726		0.00688		0.01893
2.39	0.68281		-0.73060		-0.93457	
		0.00733		0.00679		0.01858
2.40	0.67547		-0.73739		-0.91602	
		0.00741		0.00672		0.01823
2.41	0.66806		-0.74411		-0.89779	
		0.00746		0.00665		0.01790
2.42	0.66059		-0.75076		-0.87989	
		0.00754		0.00656		0.01759
2.43	0.65304		-0.75732		-0.86230	
		0.00760		0.00651		0.01728
2.44	0.64544		-0.76383		-0.84502	
		0.00767		0.00640		0.01701
2.45	0.63777		-0.77023		-0.82801	
		0.00774		0.00634		0.01671
2.46	0.63003		-0.77657		-0.81130	
		0.00779		0.00626		0.01645
2.47	0.62224		-0.78283		-0.79485	
		0.00786		0.00618		0.01619
2.48	0.61438		-0.78901		-0.77866	
		0.00792		0.00611		0.01594
2.49	0.60646		-0.79512		-0.76272	
		0.00799		0.00602		0.01569
2.50	0.59847		-0.80114		-0.74703	

L_j in Radians	Sin L_j	Δ Sin L_j	Cos L_j	Δ Cos L_j	Tan L_j	Δ Tan L_j
2.50	0.59847		-0.80114		-0.74703	
		0.00804		0.00596		0.01548
2.51	0.59043		-0.80709		-0.73155	
		0.00810		0.00586		0.01523
2.52	0.58233		-0.81295		-0.71632	
		0.00818		0.00578		0.01503
2.53	0.57417		-0.81873		-0.70129	
		0.00821		0.00571		0.01482
2.54	0.56596		-0.82444		-0.68647	
		0.00827		0.00561		0.01461
2.55	0.55769		-0.83005		-0.67186	
		0.00833		0.00554		0.01442
2.56	0.54936		-0.83559		-0.65744	
		0.00839		0.00545		0.01422
2.57	0.54097		-0.84104		-0.64322	
		0.00844		0.00537		0.01405
2.58	0.53253		-0.84641		-0.62917	
		0.00848		0.00528		0.01387
2.59	0.52405		-0.85169		-0.61530	
		0.00855		0.00520		0.01370
2.60	0.51550		-0.85689		-0.60160	
		0.00859		0.00511		0.01354
2.61	0.50691		-0.86200		-0.58806	
		0.00864		0.00503		0.01338
2.62	0.49827		-0.86703		-0.57468	
		0.00870		0.00494		0.01323
2.63	0.48957		-0.87197		-0.56145	
		0.00875		0.00485		0.01308
2.64	0.48082		-0.87682		-0.54837	
		0.00878		0.00476		0.01293
2.65	0.47204		-0.88158		-0.53544	
		0.00885		0.00468		0.01280
2.66	0.46319		-0.88626		-0.52264	
		0.00885		0.00459		0.01267
2.67	0.45431		-0.89085		-0.50997	
		0.00893		0.00449		0.01253
2.68	0.44538		-0.89534		-0.49744	
		0.00898		0.00441		0.01243
2.69	0.43640		-0.89975		-0.48502	
		0.00902		0.00432		0.01229
2.70	0.42738		-0.90407		-0.47273	
		0.00907		0.00423		0.01218
2.71	0.41831		-0.90830		-0.46055	
		0.00909		0.00414		0.01208
2.72	0.40923		-0.91244		-0.44849	
		0.00915		0.00404		0.01196
2.73	0.40007		-0.91648		-0.43653	
		0.00918		0.00398		0.01186
2.74	0.39089		-0.92044		-0.42467	
		0.00922		0.00386		0.01175
2.75	0.38167		-0.92430		-0.41292	
		0.00927		0.00377		0.01166
2.76	0.37240		-0.92807		-0.40126	
		0.00930		0.00368		0.01156
2.77	0.36310		-0.93175		-0.38970	
		0.00933		0.00358		0.01148
2.78	0.35377		-0.93533		-0.37822	
		0.00937		0.00350		0.01138
2.79	0.34440		-0.93883		-0.36684	
		0.00941		0.00339		0.01131
2.80	0.33499		-0.94222		-0.35553	
		0.00944		0.00331		0.01122
2.81	0.32555		-0.94553		-0.34431	
		0.00947		0.00320		0.01115
2.82	0.31608		-0.94873		-0.33316	
		0.00950		0.00312		0.01107
2.83	0.30658		-0.95185		-0.32209	
		0.00954		0.00302		0.01100
2.84	0.29704		-0.95487		-0.31109	
		0.00956		0.00292		0.01095
2.85	0.28748		-0.95779		-0.30014	
		0.00960		0.00282		0.01088
2.86	0.27788		-0.96061		-0.28926	
		0.00961		0.00274		0.01081
2.87	0.26827		-0.96335		-0.27847	
		0.00965		0.00263		0.01074
2.88	0.25862		-0.96598		-0.26773	
		0.00967		0.00254		0.01069
2.89	0.24895		-0.96852		-0.25704	
		0.00970		0.00244		0.01063
2.90	0.23925		-0.97096		-0.24641	
		0.00973		0.00234		0.01058
2.91	0.22952		-0.97330		-0.23583	
		0.00973		0.00225		0.01054
2.92	0.21979		-0.97555		-0.22529	
		0.00977		0.00215		0.01048
2.93	0.21002		-0.97770		-0.21481	
		0.00979		0.00205		0.01044
2.94	0.20023		-0.97975		-0.20437	
		0.00981		0.00195		0.01040
2.95	0.19042		-0.98170		-0.19397	
		0.00982		0.00186		0.01035
2.96	0.18060		-0.98356		-0.18363	
		0.00984		0.00175		0.01032
2.97	0.17076		-0.98531		-0.17330	
		0.00987		0.00166		0.01029
2.98	0.16089		-0.98697		-0.16301	
		0.00988		0.00156		0.01025
2.99	0.15101		-0.98853		-0.15276	
		0.00989		0.00146		0.01022
3.00	0.14112		-0.98999		-0.14254	

TABLE A10.2

NATURAL SINES, COSINES, AND TANGENTS OF ANGLES IN RADIANS

L_j in Radians	Sin L_j	Δ Sin L_j	Cos L_j	Δ Cos L_j	Tan L_j	Δ Tan L_j
3.00	0.14112		-0.98999		-0.14254	
		0.00991		0.00136		0.01019
3.01	0.13121		-0.99135		-0.13235	
		0.00992		0.00127		0.01018
3.02	0.12129		-0.99262		-0.12219	
		0.00993		0.00116		0.01013
3.03	0.11136		-0.99378		-0.11206	
		0.00994		0.00106		0.01011
3.04	0.10142		-0.99484		-0.10195	
		0.00996		0.00097		0.01010
3.05	0.09146		-0.99581		-0.09185	
		0.00996		0.00086		0.01008
3.06	0.08150		-0.99667		-0.08177	
		0.00997		0.00077		0.01006
3.07	0.07153		-0.99744		-0.07171	
		0.00998		0.00066		0.01004
3.08	0.06155		-0.99810		-0.06167	
		0.00999		0.00057		0.01003
3.09	0.05156		-0.99867		-0.05164	
		0.00997		0.00046		0.01002
3.10	0.04159		-0.99913		-0.04162	
		0.01000		0.00047		0.01001
3.11	0.03159		-0.99950		-0.03161	
		0.00999		0.00027		0.01001
3.12	0.02160		-0.99977		-0.02160	
		0.01000		0.00016		0.01000
3.13	0.01160		-0.99993		-0.01160	
		0.01000		0.00007		0.01000
3.14	0.00160		-1.00000		-0.00160	
		0.01001		0.00003		0.01001
3.15	-0.00841		-0.99997		0.00841	
		0.01000		0.00014		0.01000
3.16	-0.01841		-0.99984		0.01841	
		0.00999		0.00023		0.01000
3.17	-0.02840		-0.99960		0.02841	
		0.01000		0.00034		0.01002
3.18	-0.03840		-0.99926		0.03843	
		0.00999		0.00043		0.01002
3.19	-0.04839		-0.99883		0.04845	
		0.00999		0.00053		0.01003
3.20	-0.05838		-0.99830		0.05848	
		0.00998		0.00064		0.01004
3.21	-0.06936		-0.99766		0.06852	
		0.00997		0.00073		0.01005
3.22	-0.07833		-0.99693		0.07857	
		0.00996		0.00084		0.01007
3.23	-0.08829		-0.99609		0.08864	
		0.00996		0.00093		0.01009
3.24	-0.09825		-0.99516		0.09873	
		0.00995		0.00103		0.01010
3.25	-0.10820		-0.99413		0.10883	

these values in the general expression for M as given at the top of the Table.

In a beam-column member, the bending moments do not vary directly as the load is increased. Thus, the student should realize that margins of safety based on direct proportion of moments to loads are incorrect and lie on the unsafe side.

It is recommended that four significant figures be used in computations, making use of the so-called precise equations, since the results in many cases involve small differences between large numbers.

A10.6 Example Problems

Example Problem #1

Fig. A10.4 illustrates a typical upper, outer panel wing beam of a biplane. Let it be required to determine the maximum negative bending moment between points (1) and (2), generally referred to as the maximum span moment. To obtain the true bending moments on the beam, the axial beam load as well as the end moments at (1) and (2) are necessary since they influence the deflection of the beam.

Solution:-

To obtain the horizontal component T_h of the lift strut load. we take moments about the

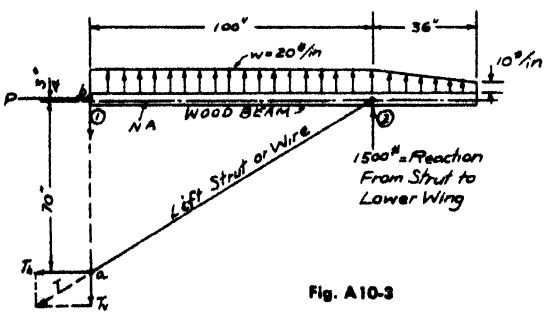


Fig. A10-3

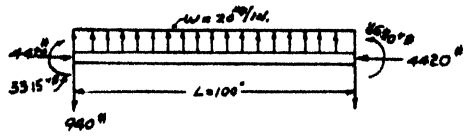


Fig. A10-4

hinge point at the left end.

$$\Sigma M_b = -2000 \times 50 - 540 \times 116 - 1500 \times 100 + 70.75\, T_h = 0$$

hence

$$T_h = 4420\#$$

The axial compressive load induced by the lift strut at point (2) then equals - 4420#.

Taking $\Sigma H = 0$ for the load system of Fig. A10.3 gives $P = -T_h = 4420\#$. The end moment on the beam at (1) equals the end load times the eccentricity of the hinge from the neutral axis of the beam, or 4420 x .75 = 3315"# positive because it produces compression in the top fibers. The moment at (2) due to the cantilever overhang equals $\frac{(20+10)}{2}\ 36 \times 16 = 8640"\#$. Fig. A10.4 shows the beam portion between points (1) and (2) as a free body.

From Art. A10.3, we have the following precise equations for a beam carrying a transverse uniform distributed load with end compressive loads.

$$\tan \frac{x}{j} = \frac{D_2 - D_1 \cos \frac{L}{j}}{D_1 \sin \frac{L}{j}} \qquad \text{----------(A)}$$

and

$$M_{max} = \frac{D_1}{\cos \frac{x}{j}} + wj^2 \qquad \text{----------(B)}$$

Evaluating terms for substitution in these equations, we obtain,

$M_1 = 3315"\#$

$M_2 = 8640"\#$

$P = 4420\#$ compression

$I = 10\ in^4$ given and assumed constant throughout the span.

$$j = \sqrt{\frac{1.3 \times 10^6 \times 10}{4420}} = \sqrt{2941} = 54.23$$

$wj^2 = 20 \times 2941 = 58820$

$D_1 = M_1 - wj^2 = 3315 - 58820 = -55505$

$D_2 = M_2 - wj^2 = 8640 - 58820 = -50180$

$$\frac{L}{j} = \frac{100}{54.23} = 1.844$$

From Table A10.2 $\sin \frac{L}{j} = .96290$ and $\cos \frac{L}{j} = -.26981$

Substituting in equation (A)

$$\tan \frac{x}{j} = \frac{D_2 - D_1 \cos \frac{L}{j}}{D_1 \sin \frac{L}{j}}$$

$$= -\frac{50180 - (-55505 \times -.26981)}{-55505 \times .96290} = \frac{-65156}{-53441} = 1.2192$$

$$\frac{x}{j} = \tan^{-1} 1.2192 = .88383$$

Hence, $x = .88383 \times 54.23 = 48"$, which equals the distance from the left end of the beam to the point of maximum span moment.

$$M_{max} = \frac{D_1}{\cos \frac{x}{j}} + wj^2, \quad \cos \frac{x}{j} = .63419 \text{ from Table A10.2}$$

Hence

$$M_{max} = -\frac{55505}{.63419} + 58820 = -28{,}700"\#$$

To obtain an idea as to the magnitude of the secondary bending moment, that is, the moment due to the axial load times the lateral beam deflection, the primary bending moment at a point 48"

from the left end will be computed.

$$M_{4.8} = 3315 + 48 \times 20 \times 24 - 940 \times 48 = -18765"\#$$

Thus the secondary bending moment equals - 28700 + 18765 = - 9935"# which is a large percentage of the primary moment. The transverse deflection of the beam at the point of max. span moment then equals $\frac{-9935}{-4420}$ = 2.25 inches upward.

Bending Moment at any Point Along Span

Let the moment at a point 10" from point (2) be required. In this case, x = 100 - 10 = 90

$$M = D_1\left[(\tan \frac{Xm}{j} \cdot \sin \frac{x}{j}) + \cos \frac{x}{j}\right] + wj^2 \text{ (Ref. Eq. 10.7)}$$

$$\frac{x}{j} = \frac{90}{54.23} = 1.6596 \quad \sin \frac{x}{j} = .99605$$

$$\cos \frac{x}{j} = - .08867$$

$\tan \frac{Xm}{j} = 1.2192$ = value for x at the point of maximum bending moment

Hence,

$$M = -55505\left[(1.2192 \times .99605) + -.08867\right] + 58820 = -3664"\#$$

Example Problem #2

Fig. A10.5 shows a simplified landing gear structure carrying a vertical load of 12000# on the axle. Member ABC is continuous thru B and pinned at C. Let it be required to determine the bending moment at the midpoint of member BC and its lateral deflection due to the 12000# vertical design load.

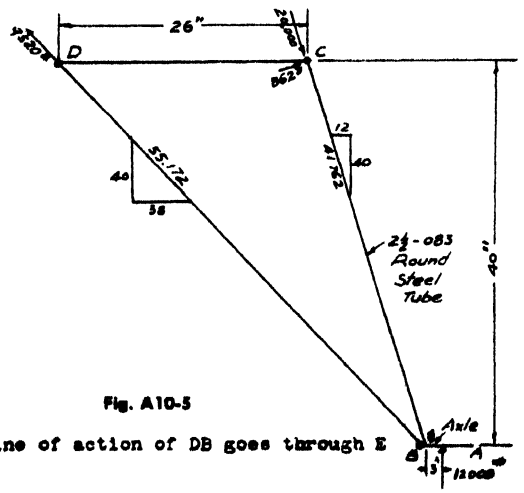


Fig. A10-5

Line of action of DB goes through E

Solution:-

Solving for reactions at C by statics, we obtain the axial load in BC = -20000. The bending moment at B due to 3" eccentricity of the wheel load = 3 x 12000 = 36000"#.

Fig. A10.6 shows a free body of portion BC of member ABC. From Table A10.1

$$M = C_1 \sin \frac{x}{j} + C_2 \cos \frac{x}{j} + f(w)$$

Substituting values of C_1 and C_2 and f(w) from Table A10.1 in the above equations:

$$M = \frac{(M_2 - M_1 \cos L/j) \sin x/j}{\sin L/j} + M_1 \cos x/j$$

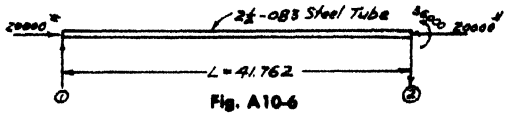


Fig. A10-6

But, $M_1 = 0$ in our problem, hence,

$$M = \frac{M_2 \sin x/j}{\sin L/j}$$

$$j = \sqrt{\frac{EI}{P}} = \sqrt{\frac{29 \times 10^6 \times .46}{20000}} = \sqrt{667} = 25.826$$

$$L/j = \frac{41.762}{25.826} = 1.617 \text{ - - - } \sin L/j = .99892$$

$$x = L/2 = 20.881$$

$$x/j = \frac{20.881}{25.80} = .8085 \text{ - - - } \sin x/j = .72327$$

Substituting in the above equations for M

$$M = \frac{36000 \times .72327}{.99892} = .26066"\#$$

This compares with a primary moment of 36000/2 = 18000"#. The deflection at the midpoint of BC = $\frac{26066 - 18000}{20000}$ = .403 in.

The maximum moment is given by the equation:

$$M_{max} = \frac{M_2}{\sin \frac{L}{j}}$$ and it occurs at $x = \frac{\pi j}{2}$ (See Table A10.1)

A10.7 Problems

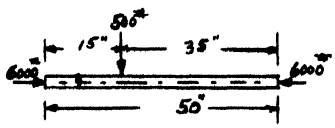


Fig. A10-7

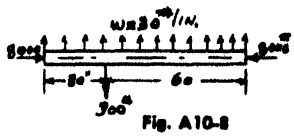


Fig. A10-8

(1) Fig. A10.7 shows a 1-1/2 - .065 steel tube subjected to both end and lateral loads. Determine the maximum bending moment on the tube. Compare the result with the bending moment due to the side load only. E = 29 x 10^6 psi. I of tube = .075 $in.^4$ Compute lateral deflection at point of maximum bending moment.

(2) The beam column member in Fig. A10.8 is made of 24ST aluminum alloy. Calculate and plot a curve of the bending moments on the member. Also plot bending moment due to lateral loads only. E = 10.3 x 10^6 psi. I = 5.0 $in.^4$

(3) Determine the maximum bending moment for the wood wing beam and loading of Fig. A10.9. I of beam section = 17 $in.^4$ E = 1.3 x 10^6.

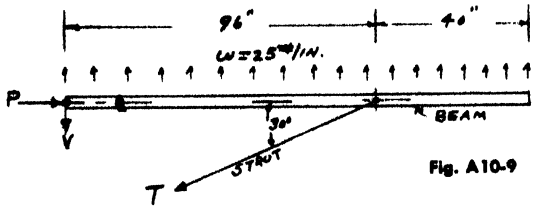


Fig. A10-9

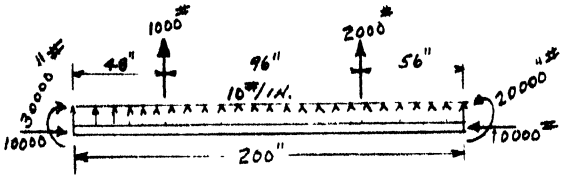


Fig. A10-10

(4) Determine the bending moment at the centerline of the beam-columns shown in Fig. A10.10. Assume EI = 64,000,000 lb. in. sq.

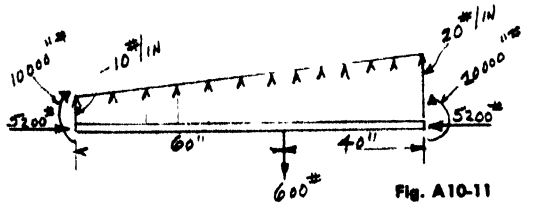


Fig. A10-11

(5) For the beam-column in Fig. A10.11 calculate the bending moment of the centerline of the member. Assume E = 1,300,000 psi. and I = 10 in.^{4}

CHAPTER A11
CONTINUOUS STRUCTURES - MOMENT DISTRIBUTION METHOD

A11.1 Introduction. The moment distribution method was originated by Professor Hardy Cross.* The method is simple, rapid and particularly adapted to the solution of continuous structures of a high degree of redundancy, where it avoids the usual tedious algebraic manipulations of numerous equations. Furthermore, it possesses the merit of giving one a better conception of the true physical action of the structure in carrying its loads, a fact which is usually quite obscure in some methods of solution.

The method of procedure in the Cross method is in general the reverse of that used in the usual methods where the continuous structure is first made statically determinate by removing the continuous feature and the value of the redundant then solved for which will provide the original continuity. In the Cross method each member of the structure is assumed in a definite restrained state. Continuity of the structure is thus maintained but the statics of the structure are unbalanced. The structure is then gradually released from its arbitrary assumed restrained state according to definite laws of continuity and statics until every part of the structure rests in its true state of equilibrium.

The general principles of the Cross method can best be explained by reference to a specific structure.

Fig. A11.1 shows a continuous 2 span beam. Let it be requited to determine the bending moment diagram. We first arbitrarily assume that each span is completely restrained against rotation at its ends. In the example selected ends A and C are already fixed so no restraint must be added to these points. Joint B is not fixed so this joint is imagained as locked so it cannot rotate. The bending moments which exist at the ends of each member under the assumed condition are then determined. Fig. A11.2 shows the moment curves for this condition. (For calculation and formulas for fixed end moments see following articles). Fig. A11.3 shows the general shape of the elastic curve under this assumed condition. It is noticed that continuity of the structure at B is maintained, however from the moment curves of Fig. A11.2 it is found that the internal bending moments in the beams over support B are not statically balanced, or specifically there is an unbalance of 270. The next step is to statically balance this joint, so it is unlocked from its imaginary locked state and obviously joint B will rotate (See Fig. A11.4) until equilibrium is established, that is, until resisting moments equal to 270 have been set up in the two beams at B. The question is how much of this moment is developed by each beam. The physical condition which establishes the ratio of this distribution to the two beams at B is the fact that the B end of both beams must rotate through the same angle and thus the unbalanced moment of 270 will be distributed between the two beams in proportion to their ability of resisting the rotation of their B end thru a common angle. This physical characteristic of a beam is referred to as its stiffness. Thus let it be considered that the stiffness factors of the beam BA and BC are such that 162 is distributed to BC and - 108 to BA as shown in Fig. A11.4. (The question of stiffness factors is discussed in a following article).

Referring to Fig. A11.4 again it is evident that when the elastic curve rotates over joint B that it tends to rotate the far ends of the beams at A and C, but since these joints are fixed, this rotation at A and C is prevented or moments at A and C are produced. These moments produced at A and C due to rotation at B are referred to as carry-over moments. As shown by the obvious curvature of the elastic curves (Fig. A11.4), the carry-over moment is of opposite sign to the distributed moment at the rotating end. The ratio of the carry-over moment to the distributed moment, referred to as the carry-over factor, depends on the physical properties of the beam and the degree of restraint of its far end. (Carry-over factors are discussed in a following article. For a beam of constant section and fixed at the far end, the carry-over factor is -1/2). In figure A11.4 a factor of -1/2 has been assumed which gives carry-over moments of 54 and -81 to A and C respectively. To obtain the final end moments we add the original fixed end moments, the distributed balancing moments and the carry-over moments as shown in Fig. A11.4. With the indeterminate moments thus determined, the question of shear, reactions and span moments follow as a matter of statics.

A11.2 Definitions and Derivations of Terms

1. Fixed-end moments:

By "fixed end moment" is meant the moment which would exist at the ends of a member if these ends were fixed against rotation.

2. Stiffness Factor:

The stiffness factor of a member is a value proportional to the magnitude of a couple that must be applied at one end of a member to cause unit rotation of that end, both ends of the member being assumed to have no movement of

(*Paper - A.S.C.E. Proceedings, May 1930)

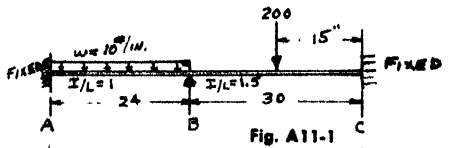


Fig. A11-1

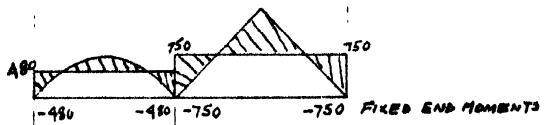


Fig. A11-2

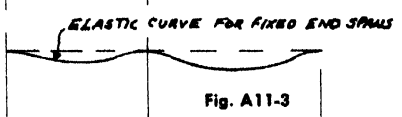


Fig. A11-3

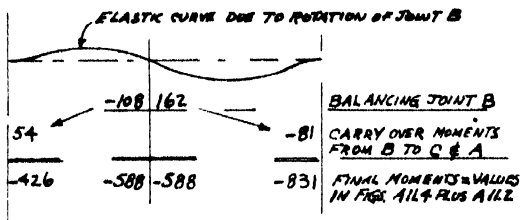
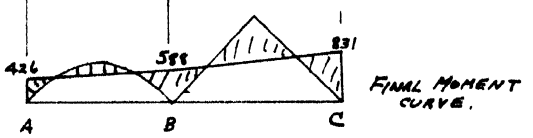


Fig. A11-4



translation. The value of the stiffness factor will depend in part on the restraint or degree of fixity of the opposite end of the member from which the couple is applied. The letter K is used as a symbol for stiffness factor.

3. Carry-over Factor:

If a beam is simply supported at one end and restrained to some degree at the other, and a moment is applied at the simply supported end, a moment is developed at the restrained end. The carry-over factor is the ratio of the moment at the restrained end to that at the simply supported end. For a prismatic beam without axial load the carry-over factor is 0.5 when far end is fixed. The letter C will be used to designate carry-over factor.

4. Distribution Factor:

If a moment is applied at a joint where two or more members are rigidly connected the distribution factor for each member is the proportional part of the applied moment that is resisted by that member. The distribution factor for any member which will be given the symbol D equals $K/\Sigma K$, where K equals stiffness factor of a particular member and ΣK equals the sum of K values for all the Joint members. The sum of the D values for any joint must equal unity.

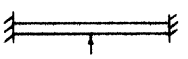
5. Sign Convention:

Due to the fact that in many problems where members come into a joint from all directions as is commonly found in airplane structure, the customary sign convention for moments may produce confusion in applying the moment distribution method. The following sign convention is used in this book: a clockwise moment acting on the end of a member is positive, a counterclockwise one is negative. It follows that a moment tending to rotate a joint clockwise is negative. It should be understood that when indeterminate continuity moments are determined by the moment distribution method using the above adopted sign convention, that they should be transferred into the convential signs before proceeding with the design of the member proper.

The following sketches illustrate the adapted sign convention.

Illustrations of Sign Conventions for End Moments.

Example 1



Fixed end beam with lateral loads.

Conventional + moment signs



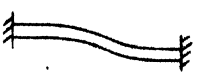
+ tension in bottom fibers is positive bending moment.

Adopted sign convention



moments which tend to rotate end of member clockwise are positive.

Example 2



Translation of supports of fixed ended beam.

Conventional moment signs



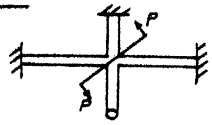
−

+

Adopted sign convention



Example 3



External applied moment at joint in structure

adopted sign

(+ joint, + moment) | Moments which tend to rotate joint counter-clockwise are positive.

A11.3 Calculation of Fixed End Moments

Since the fixed end moments are statically indeterminate, additional facts must be obtained from the laws of continuity in order to solve for them. In this book the theorem of area moments will be used to illustrate the calculation of the fixed end moments as well as the other terms which are used in the moment distribution method. (Ref. Chapter A7)

The following well known principles or theorem of area moments will be used:-

(1) The deflection of any point "A" on the elastic curve of a beam away from a tangent to the elastic curve at another point "B" is equal to the moment of the area of the $\frac{M}{EI}$ diagram between the points A and B about point "A".

(2) The change in slope between two points "A" and "B" on the elastic curve of a beam is equal to the area of the $\frac{M}{EI}$ diagram between the two points "A" and "B".

The "area moment" theorems will be illustrated by the applications to the solution of a simple problem. Fig. A11.5 shows a simply supported beam of constant moment of inertia and modulus of elasticity carrying a single concentrated load. Figs. A11.6 and A11.7 show the static moment curve and the shape of the beam elastic curve. Now assume that the ends are fixed as shown in Fig. A11.8 and let the value of the fixed end moments be required. Fig. A11.9 shows the shape of the final moment curves made up of the static moment curve and the unknown trapizoidal moment curve formed by the unknown end moments. Fig. A11.10 shows the shape of the elastic curve, the slope at the two supports being made zero by fixity at these points.

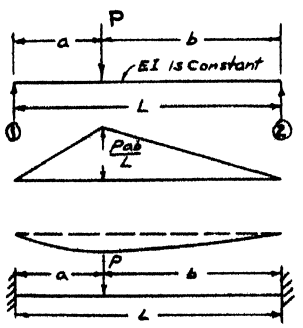


Fig. A11-5

Fig. A11-6

Fig. A11-7

Fig. A11-8

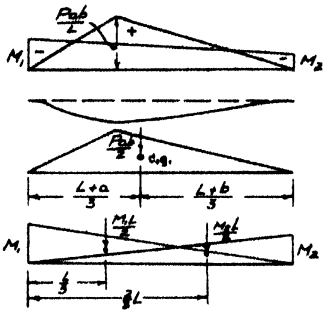


Fig. A11-9

Fig. A11-10

Fig. A11-11

Fig. A11-12

Since the change in slope of the elastic curve between ends (1) and (2) is zero, theorem (2) as applying to fixed end beams can be restated as follows.

The sum of the areas of the moment diagram must equal zero. And from theorem (1) the static moment of the areas of the moment diagram about any point must equal zero or in equation form:

$$\Sigma M = 0 \quad \text{----------(1)}$$

$$\Sigma Mx = 0 \quad \text{----------(2)}$$

For a beam with variable moment of inertia the conditions for fixity are:-

$$\int Mdx/EI = 0$$

$$\int Mxdx/EI = 0$$

Figs. A11.11 and A11.12 show the static and continuity moment areas, the total area of each portion and its c.g. location.

Substituting in Equation (1)

$$M = \frac{Pab}{2} + \frac{M_1 L}{2} + \frac{M_2 L}{2} = 0 \quad \text{---------(3)}$$

and from equation (2)

$$M_x \text{ about left end} = \frac{Pab}{2} \cdot \frac{L+a}{3} + \frac{M_1 L}{2} \cdot \frac{L}{3} + \frac{M_2 L}{2} \cdot \frac{2L}{3} = 0 \quad \text{------(4)}$$

The values of M_1 and M_2 for any value of a or b can now be found by solving equations (3) and (4)

Table A11.1 gives a summary of beam fixed end moments for most of the loadings encountered in routine design and analysis.

TABLE A11.1

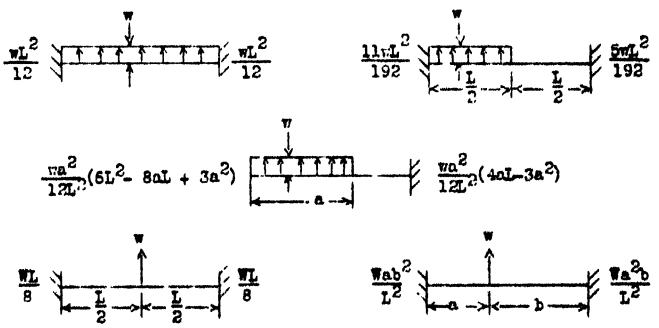
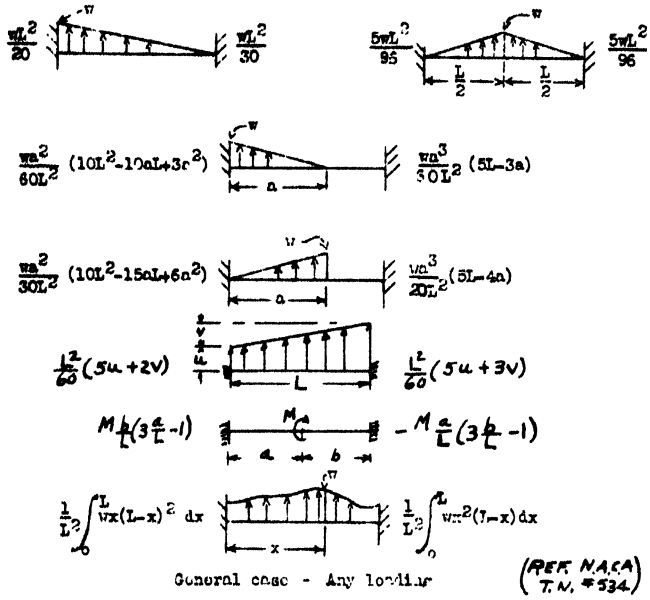


Table A11.1 - Continued



A11.4 Stiffness Factor; Carry over Factor: - Derivation of:

(For definitions of these terms see page A11.2)

Consider the beam of Figure A11.13. By Mohr's theorem (see Art. A7.12), the slope of a tangent to the elastic curve at point A relative to a line AB is equal to the shear at A on a simply supported beam AB due to the $\frac{M}{EI}$ curve between A and B acting as a load.

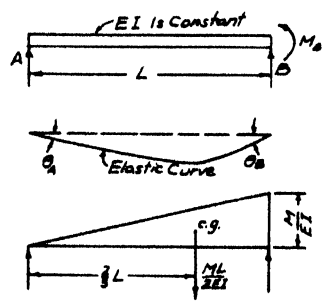


Fig. A11-13

Thus

$$\theta_A = -\frac{(\frac{ML}{2EI} \times 1/3)}{} = -\frac{ML}{6EI} \quad \text{(Positive Shear = Neg. Slope)}$$

$$\theta_B = \frac{ML}{2EI} \times 2/3 = \frac{ML}{3EI}$$

Let θ_B = unity

Then $1 = \frac{ML}{3EI}$ or $M_B = \frac{3EI}{L}$ = stiffness Factor of Beam BA of Fig. A11.13. A moment applied at B produces no moment at A since end A is freely supported. Thus the carry-over factor for a beam freely supported at its far end is obviously zero. Consider the beam of Fig. A11.14. Due to complete fixity at end A, the slope of the elastic curve at A is zero.

$$\theta_A = \frac{M_B L}{2EI} \cdot 1/3 + \frac{M_A L}{2EI} \cdot 2/3 = 0$$

or

$$M_A = -\frac{M_B}{2}$$

Thus the carry over factor for a beam fixed at its far end is 1/2. Using the conventional moment signs, the carry over moment is of the opposite sign as shown by the above equation, However, for our adopted sign convention inspection of the shape of the elastic curve as shown in Fig. A11.14 tells us that the sign of the carry-over moment is of the same sign as the rotating moment at the near end. That is, the moment acting on each end of the member is in the same direction, and therefore of the same sign.

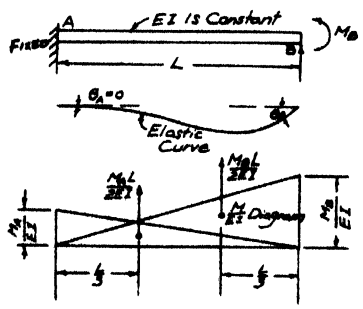


Fig. A11-14

$$\theta_B = \frac{M_B L}{2EI} \cdot 2/3 + \frac{M_A L}{2EI} \cdot 1/3 = \frac{M_B L}{3EI} + \frac{M_A L}{6EI}, \text{ but } M_A = -\frac{M_B}{2}$$

Then $\theta_B = \frac{M_B L}{3EI} - \frac{M_B L}{12EI} = \frac{M_B L}{4EI}$

Let θ_B = unity, then $M_B = \frac{4EI}{L}$ = stiffness factor of beam BA of Fig. A11.14.

A comparison of the stiffness factor of this beam to that of Fig. A11.13 shows that the stiff-

ness factor of a beam freely supported at its far end is 3/4 as great as one fixed at its far end. Furthermore in one case the carry-over factor is zero and in the other case it is 1/2. It is therefore obvious that the values of these two terms depends in part upon the restraint or degree of fixation of the far end of the beam.

A11.5 General Expressions for Stiffness and Carry-over Factor in Terms of Fixation Factor (F) at Far End of a Beam

In the beam of Fig. A11.14 (F) fixation factor at A was unity since beam had been taken as completely fixed at A. It was found that:-

$$M_B = \frac{4EI\theta_B}{L} \quad \text{and} \quad M_A = -\frac{2\,EI\,\theta_B}{L}$$

Take θ_B = unity and let $\frac{EI}{L} = K$ for simplicity.

Then $M_B = 4K$

$M_A = -2K$

Likewise the results for the beam of Fig. A11.13 give

$M_B = 3K$

$M_A = 0$

Figs. A11.15 and A11.16 show these results. Fig. A11.17 shows the general case, the fixation factor at A being F. The difference between Figs. A11.15 and A11.17 is that the slope at end A has changed but θ_B the slope at end B remains the same.



Fig. A11-15

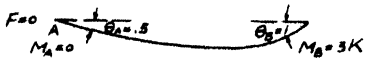


Fig. A11-16

The change in moment at end A when changing beam A11.15 to that of A11.17 = 2K - 2KF = 2K(1-F). Since θ_B is kept the same value, one-half of the moment change at end A appears at end B but of opposite sign, or

$$M_B = 4K - 1/2 \quad 2K(1-F) = 3K - KF = K\,(3+F) = \frac{EI}{L}\,(3+F)$$



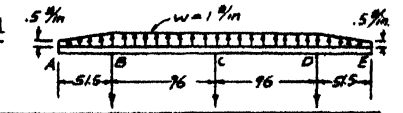
Fig. A11-17

Thus the general expression for the stiffness factor of a beam of constant section equals $\frac{EI}{L}$ (3+F). The carry-over factor from B to A = $\frac{M_A}{M_B} = -\frac{2KF}{K(3+F)} = -\frac{2F}{3+F}$ which is the general expression for carry-over factor for a degree of fixation F.

A11.5a Example Problems

To obtain a definite conception of the true mechanics of the "Cross" method, the reader is advised to follow thru the detailed solution of the following simple problems. In these problems, the moment of inertia in any span has been taken as constant and all joints have been assumed to undergo no translation. Problems involving variable I and joint translation will be considered later.

Example Problem #1



Stiffness Factor $\frac{EI}{L} = K$	0	1	1	1	0	
Distribution Factor $K/\Sigma K$	0	1	.5	.5	0	
Carry Over Factor	0	.5	.5	.5	0	
Fixed End Moments	*-8.83	7.68-4.83=+2.85	-7.68+4.83=-2.85	7.68-4.83=+2.85	8.83	
1st Balancing	0	1.15	0	0	-1.15	
Carry Over ½		0	-.575	-.575	0	
2nd Balancing	0	0	0	0	0	
Final Moments	-8.83	8.83	-7.105	7.10.5	-8.85	8.85
Coventional Moment Signs	+	+	+	+	+	+

*Overhang Moment = .5 x 5.15 x 2.575 + 2.5 x 5.16 x 1.717 = 8.83

Example Problem 1 shows a two-span continuous beam with over-hanging ends. We first assume all the joints B, C and D to be locked against rotation or the beams BC and CD are arbitrarily assumed in a fixed-end condition.

The first line in the solution gives the stiffness factor of each beam. From Art. A11.5 the general expression for stiffness factor is EI(3+F)/L, where F = fixation factor of far end, which equals 1, since all joints have been considered fixed. Thus, stiffness factor K = EI (3+1)/L = 4 EI/L. Since EI/L is the same for each span BC and CD, the stiffness factor has been written as one since it is only the relative values that are necessary. The cantilever BA has zero stiffness.

The second row gives the member distribution factor D at each joint or D = K/ΣK. For example at joint B, the distribution factor to BA = 0/(1 + 0) = 0 and to BC = 1/(1 + 0) = 1. At joint C, the distribution factor to CB = 1/(1 + 1) = .5 and likewise to CD.

The third row gives the carry-over factors. From Art. A11.5, the carry-over factor C = 2F/(3 + F) = 2 x 1/(3 + 1) = .5 assuming the far end fixed or F = 1 for each member.

The next step as shown by the 4th horizontal row is the calculation of the fixed end moments. The signs of the moments are according to our adopted sign convention, that is an internal resisting moment which tends to rotate the

end of a member clockwise is positive.

We now begin the solution proper by first unlocking joint B from its assumed fixed state. We find a moment of +883 on one side and 768 on the other side of joint or a static unbalance of -115. Joint B therefore will rotate until a resisting moment of 115 is set up in the members BA and BC.

The resistance of these members to a rotation of Joint B is proportional to their stiffness. The distribution factor based on the stiffness factors is 0 for BA and 1 for BC. Thus 1 x 115 = 115 is distributed to BC at B and 0 x 115 = 0 to BA. Joint B is now imagined as again locked against rotation and we proceed to Joint C, which is now released from its assumed locked state. Since the joint is already statically balanced, no rotation takes place and the distributing balancing moment to each span is zero. Next proceed to joint D, and release it. The unbalanced moment is, 115 so the joint is balanced by distributing -115 between DE and DC as explained above for joint B.

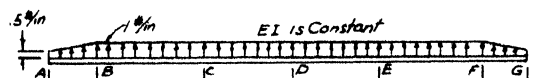
As pointed out in Art. A11.5, when we rotate one end of a beam it tends to rotate the far fixed end of the beam by exerting a moment equal to some proportion of the moment causing rotation at the near end. For beams of constant section and fixed at their far ends, the carry over factor is 1/2 as explained before. Thus the distributing balancing moments in line 4 produce the carry-over moments as shown in line 5 of the table. This completes one cycle of the moment distribution method, which is repeated until there is nothing to balance or carry-over, or in other words until all artificial restraints have been removed and the structure rests in its true state of equilibrium.

To continue with the second cycle, go back to joint B and release it again from its assumed locked state. There is no unbalance since the carry over moment from point C was zero, thus there is nothing to distribute or carry-over. Proceed to point C, releasing the joint, we find it balanced under the carry-over moments of 57.5 and -57.5. Thus the distributing balancing moments are zero. Joint D is likewise in balance since the carry-over moment from C is zero. All joints can now be released without any rotation since all joints are in equilibrium. To obtain the final moments we add the original fixed end moments plus all distributed balancing and carry over moments.

A11.6 General Summary of Proceedure

1. All computations should be written on, or adjacent to the diagram of the structure.
2. Determine the stiffness factor K for each end of each member. K = (3 + F) EI/L, where F is the degree of fixity at far end of member. If all members are assumed fixed at far end than K is proportional to I/L assuming E as constant.
3. Determine the distribution factor D for each member at each joint of structure. D = K/ΣK.
4. Calculate the carry-over factor C for each end of all members C = 2F/(3 + F). Thus for beams fixed at far end F = 1 and thus C = 1/2. For pinned at far end F = 0, hence C = 0.
5. Calculate the fixed end moments (f) for given transverse member loadings or support deflections, using equations in summary Table A11.1. End moments which tend to rotate end of beam clockwise are positive moments. (See Art. A11.2)
6. Considering one joint at a time, unlock it from its assumed fixed state, all other joints remaining locked. If an unbalanced moment exists balance it statically by distributing a counter acting moment of opposite sign among the connecting members according to their D or distribution factors.
7. These distributed balancing moments produce, carry over moments at far-end of members equal to the distributed moment times the carry-over factor C and of the same sign as the distributed moment. Record these carry-over moments at far ends for all distributed moments.
8. Repeat the proceedure of unlocking each joint, distributing, and carrying over moments until the desired precision is obtained, stopping the solution after a distribution. The final moment at the end of any member equals the algebraic sum of the original fixed end moments and all distributed and carry over moments.

Example Problem #2



Stiffness Factor $\frac{EI}{L}\cdot K$	0	.0104 = $\frac{1}{96}$ = .0104	.0139 = $\frac{1}{72}$ = .0139	.0139 = $\frac{1}{72}$ = .0139	.0139 = $\frac{1}{72}$ = .0139	.0104 = $\frac{1}{96}$ = .0104				
Distribution Factor $D=\frac{K}{\Sigma K}$	0	1	.428	.572	.5	.5	.572	.428	1	0
Carry-Over Factor C	0	.5	.5	.5	.5	.5	.5	.5	.5	0
Fixed End Moments	-883	768 = $\frac{1}{12}wL^2$ = 768	-432 = $\frac{1}{12}wL^2$ = -432	432 = $\frac{1}{12}wL^2$ = 432	-768 = $\frac{1}{12}wL^2$ = -768	883				
1st Balancing	0	115	144	192	0	0	-192	-144	+115	0
Carry-Over		72	57.5	0	96	-96	0	-57.5	-72	
2nd Balancing	0	-72	-24.6	-32.9	0	0	32.9	24.6	72	0
Carry-Over		-12.3	-36	0	-16.5	16.5	0	36	12.3	
3rd Balancing	0	12.3	15.4	20.6	0	0	-20.6	-15.4	-12.3	0
Carry-Over		7.7	6.1	0	10.3	-10.3	0	-6.1	-7.7	
4th Balancing	0	-7.7	-2.6	-3.5	0	0	3.5	2.6	7.7	0
Carry-Over		-1.3	-3.9	0	-7.8	1.8	0	3.9	1.3	
5th Balancing	0	1.8	1.7	2.2	0	0	-2.2	-1.7	-1.8	0
Final Moments	-883	883	-614	614	-344	344	-614	614	-883	883
Conventional Signs	+	+	+	+	+	+	+	+	+	+

Example Problem 2 is similar to problem 1 but two spans have been added. We first assume all joints locked against rotation. The stiffness factor of each span is proportional to EI/L or 1/L since EI is constant. The carry-over factor is 1/2 as in previous example. Fixed end moments are calculated as shown. Unlock joint B, the unbalanced moment is -115. Balance the joint by distributing 1 x 115 to BC and zero to BA. Proceed to joint C,

and unlock, all other joints remaining fixed against rotation. The unbalanced moment is (-768 + 432) = - 336. Balance by distributing .428 x 336 = 144 to CB and .572 x 336 = 192 to CD. Proceed to joint D, and release. The unbalanced moment is zero which means that joint D is in equilibrium, thus no distribution is necessary. Proceed to joint E and F and balance in a similar manner. The distributed moments will be the same as the values for joints B and C due to symmetry of structure and loading, however, the signs will be opposite under our adopted sign conventions. The next step is the carry-over moments which are equal to 1/2 the distributed balancing moments. This operation is shown clearly in the table. Values of all moments are given only to first decimal place. The first cycle has now been completed. Cycle two is started by again releasing joint B. We find the joint has been unbalanced by the carry-over moment of 72. Balance the joint by distributing - 72 x 1 = - 72 to BC and zero to BA. Proceed to joint C. The unbalanced moment is 57.5. Balance by distributing - 57.5 x .428 = - 24.6 to CB and the remainder - 32.9 to CD. Proceed to joint D. There is no unbalance at this joint since the carry-over moments are in balance, thus no distribution is necessary. Proceed to joints E and F in a similar manner.

The carry over moments equal to 1/2 of the 2nd set of balancing distributed moments are now carried over as shown in the table. The second cycle has now been completed. This operation has been repeated five times in the solution shown, or until the values of the balancing and carry over moments are quite small or negligible. The final moments equal the algebraic summation of the original fixed end moments plus all distributed and carry over moments. One requirement of the final end moments at any joint is that the algebraic sum must equal zero. The other requirement consistant with the common slope to all members at any joint is given by equation (5) of Art. A11.8. The results at joint C will be checked using this equation.

$$\frac{\Delta M_{cd} - .5\,\Delta M_{dc}}{\Delta M_{cb} - .5\,\Delta M_{bc}} = \frac{K_{cd}}{K_{cb}}$$

Subt. values

$$\frac{(610.4 - 432) - .5\,[344 - (-432)]}{[-610.4 - (-768)] - .5\,(883 - 768)} = \frac{178.6 - 44}{157.6 - 57.3} = 1.343$$

Ratio of stiffness factors = $\frac{K_{cd}}{K_{cb}} = \frac{.0139}{.0104} = 1.34$. Thus the distribution is according to the K ratios of the adjacent members.

Simplifying Modifications - Example Problem #3

The solution as given in Problem #2 represents the "Cross" method in its fundamental and most elementary detailed form. Many modifications of the general method have been presented, in the most part for the purpose of eliminating part of the arithmetic or the number of cycles necessary. These modifications usually involve rather long expressions for expressing the stiffness and carry over factors of a member in terms of the fixation given by adjacent members. It is felt that it is best to keep the method in its simplest form which means that very little is to be remembered and then the method can be used infrequently without refreshing ones mind as to many required formulas or equations.

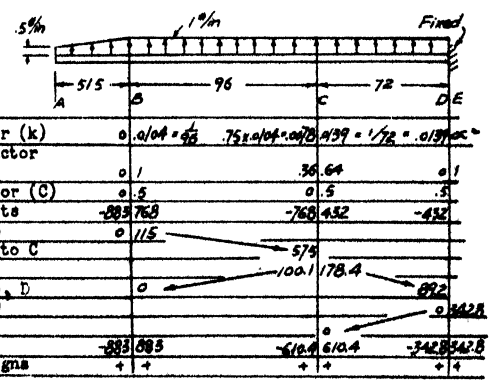
There are however several quite simple modifications which are easily understood and remembered and which reduce the amount of arithmetic required considerably.

For example in Problem #2, joints B and F are in reality freely supported, thus it is needless arithmetic to continue locking and unlocking a joint which is definitely free to rotate. Likewise due to symmetry of structure and loading it is only necessary to solve one half of the structure. Due to symmetry joint D does not rotate and thus can be considered fixed, which eliminates the repeated locking and unlocking of this joint.

A second solution of Problem #2 is given in Example Problem #3. As before we assume each joint locked and calculate the fixed end moments. Now release or unlock joint B and balance as explained in previous example #2. Before proceeding to joint C, carry over to C from B the carry over moment equal to 115 x 1/2 = 57.5. Joint B is now left free to rotate or in its natural condition. Proceed to joint C and unlock. The unbalanced moment = (-768 + 432 + 57.5) = - 278.5 or 278.5 is necessary for equilibrium. This moment is distributed between two beams, CD which is fixed at its far end D and CB which is freely supported at the far end B. The stiffness factor is equal to (3 + F) EI/L (See Art. A11.5).

Hence for CD stiffness factor = (3 + 1) EI/L = 4 EI/L. For CB stiffness factor = (3 + 0) EI/L = 3 EI/L or in other words the stiffness of a beam freely supported at its far end is 3/4 as great as when fixed at its far end. Thus the stiffness factor of CB at C is .75 x .0104 = .0078. The carry-over factor C to B is zero since B is left free to rotate. (See Art. A11.5)

Example Problem #3. Simplified Solution of Problem #2



Stiffness Factor (k)	0	.0104 = 1/96	.75 x .0104 = .0078	.439 = 1/72 = .0139	
Distribution Factor D = K/Σ K	0	1	.36 .64		0 1
Carry-over factor (C)	0	.5	0 .5		.5
Fixed end moments	-883	768	-768	432	-432
Balance joint B	0	115			
Carry-over 1/2 to C			57.5		
Balance joint C			-100.1	178.4	
Carry-over to B, D		0			89.2
Balance joint D					0 342.8
Carry-over to C			0		
Final moments	-883	883	-610.4	610.4	-342.8 342.8
Conventional signs	+	+	+	+	+ +

The stiffness factor of the fixed support is infinity, that is a rigid support has infinite resistance to rotation.

Joint C is now balanced by distributing 278.5 x .36 = 100.1 to CB and 278.5 x .64 = 178.4 to CD. Now carry over to joint B, 0 x 100.1 = 0 and 0.5 x 178.4 = 89.2 to D. Proceed to joint D and release it from its assumed locked state. The unbalanced moment is -432 + 89.2 = - 342.8, we balance by distributing 342.8 between DC which has a stiffness of 0.139 and the support E which has an infinite stiffness or zero goes to DC and 342.8 goes to rigid support. The carry over moment to C from D is zero since 0.5 x 0 = 0. The final moments thus equals the summations as shown which of course are equal to the results shown in Problem #2.

Example Problem #4

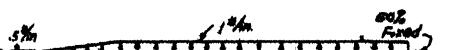
Problem 4 is similar to Problem #2 and #3, except that the support at D is assumed as having 50 percent fixity. Thus 50 percent of any moment at this point produces rotation of the member DC at D.

In continuous wing beams, which fasten together by fittings on a support, it is commonly required that the beam be considered as being fully continuous and also that the degree of continuity be taken as 50 percent. Solution 1 of Problem 4 is a detailed solution. The only change that has been made is in the stiffness factor of the support E, which has been taken as equal to the beam DC, thus any unbalanced moment at this point is equally divided between the beam and the support.

Solution 2 is a modified solution which eliminates considerable arithmetic. Thus it is unnecessary to lock and unlock joint B and D since we know definitely that one is freely supported and the other 50 percent fixed. Therefore, once we have released these joints from their assumed fixed end state, we leave them in their natural state. The stiffness and carry-over factors for beams CB and CD must then be determined for these beams with their modified end conditions.

By reference to the fundamental equations for stiffness and carry over factors in Art. A11.5, it is readily seen that the stiffness factor for CB is 3/4 as much as when fixed at its far end B and the carry over moment is zero. For beam CD the stiffness is 7/8 as much as when fixed at end D, and the carry over factor is 2F/3 + F = (2 x .5)/3 + .5 = .286. With these modifications the solution is carried thru with a relatively small number of steps. Thus in solution #2, joint B is unlocked. The unbalanced moment of -115 is balanced statically by distributing 115 to BC. The carry-over moment of .5 x 115 = 57.5 is carried over to C as shown. Joint B is now left unlocked or free to rotate. Joint D is unlocked next. The unbalanced moment is -432. It is balanced by distributing 216 to DC and 216 to E since support at E is considered to give 50% fixity. The carry-over moment of

Solution #1
Example Problem #4



	A	B	C	D	E	
Stiffness Factor k	0	.104 = 1/96 = .104	.139 = 1/72 = .139	.139		
Distribution Factor D=F/Σ	0	1	.428	.572	.5	.5
Carry-Over Factor	0	.5	.5	.5	.5	
Fixed End Moments	-888	768	-768	432	-432	
1st Balancing	0	115	144	192	216	216
Carry-Over		72	57.5	108	96	
2nd Balancing	0	-72	-78.7	-94.8	-48	-48
Carry-Over		-35.3	-36.0	-24.0	-47.4	
3rd Balancing	0	35.3	25.7	34.3	25.7	23.7
Carry-Over		12.9	17.6	11.8	17.2	
4th Balancing	0	-12.9	-12.6	-16.8	-8.6	-8.6
Carry-Over		-6.3	-6.4	-4.3	-8.4	
5th Balancing	0	6.3	4.6	6.1	4.2	4.2
Final Moments	-888	883	-644.3	644.5	-187.3	187.3
Conventional Signs	+	+	+	+	+	+

.5 x 216 = 108 is carried over to C. Joint D is left unlocked or in its true state of restraint. Joint C is now unlocked. The unbalanced moment

Solution #2
Example Problem #4



	A	B	C	D	E	
Stiffness Factor K	0	.104=1/96	.25-.104=.146	.071=1/8×1/2	1/2×.139=.070	.0139
Distribution Factor=F/Σ	0	1	.392	.608	.50	
Carry-over Factor		1/2	0	.286	1/2	
Fixed end Moments	-888	768	-768	432	-432	
Balance joint B	0	115				
Carry-over to C			57.5			
Balance joint D					216	216
Carry-over to C				108		
Balance joint C			66.0	103.7		
Carry over to D					29.6	
Balance D						29.6
Final Moments	-888	883	-643.7	643.7	-186.4	186.4

equals (-768 + 432 + 57.5 + 108) = - 170.5, or 170.5 is necessary for equilibrium. Joint C is balanced by distributing .392 x 170.5 = 66.8 to CB and the remainder of 103.7 to CD. The carry-over moment to B is zero and to D it equals 103.7 x .286 = 29.6. The final moments in solution #2 are slightly different than solution #1. If another cycle had been added in solution #1 the descrepancy would be considerably smaller.

A11.7 Continuous Beams with Yielding or Deflected Supports

In wing, elevator and rudder beams the support points usually deflect due to the deformation of the supporting struts or wires in the case of a wing, or to the deflection of the stabilizer or fin in the case of elevator and rudder beams. If these beams are continuous this deflection of their support points causes additional bending moments in the beams. The moment distribution method can of course be used to find the additional moments due to this deflection. Thus Example Problem #5, shows a solution illustrating a problem which involves the deflecting of the supports of a continuous beam. Due to symmetry of structure and loading, the slope at D is zero or the beam may be considered fixed at

Joint D. Since the moment of inertia is constant and the spans are constant, the relative stiffness factor of the beam is 1. In the solution shown since beam is freely supported at B this joint is left free to rotate after releasing and thus the stiffness factor of beam CB is 3/4 x 1 = 3/4, when compared to one having full fixity at B.

Since the first step in the solution proper is to assume the joints fixed against rotation, it is evident that deflecting one support relative to an adjacent support will produce moments at the ends which are assumed fixed against rotation.

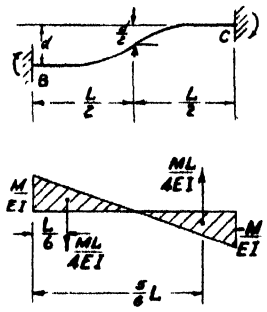


Fig. A11-18

A11.8 Fixed End Moments Due to Support Deflections

Fig. A11.18 shows a fixed end beam. The support B is deflected a distance d relative to the support point C. If the member is of constant cross-section the point of inflection will fall at the beam midpoint and $M_B = -M_C$.

By moment area principal deflection

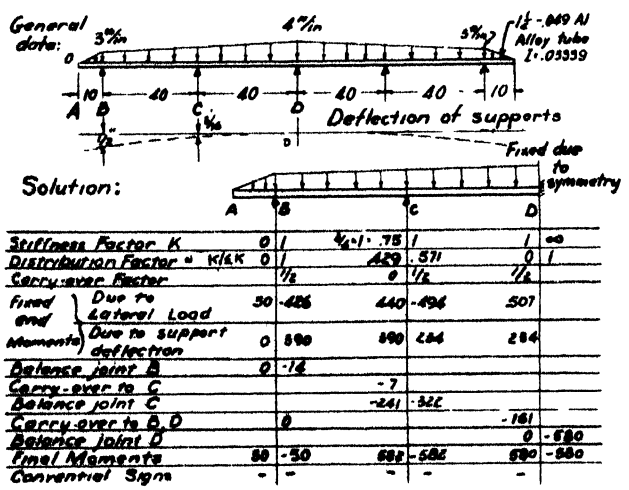
$$-d = \frac{ML}{4EI} \cdot \frac{L}{6} - \frac{ML}{4EI} \cdot \frac{5}{6} L$$

or $$d = \frac{ML^2}{6EI}$$

hence

$$M = \frac{6EId}{L^2}$$ the magnitude for the fixed end moment due to a transverse support settlement of d.

Example Problem #5. Continuous beam with deflected supports.



Stiffness Factor K		0	1	¾=1 · .75	1	1	∞
Distribution Factor = K/ΣK		0	1	.429	.571	0	1
Carry-over Factor			½	0	½	½	
Fixed end Moments	Due to Lateral Load	50	-426	440	-494	507	
	Due to support deflection	0	390	390	234	234	
Balance joint B		0	-14				
Carry-over to C				-7			
Balance joint C				-241	-322		
Carry-over to B, D			0			-161	
Balance joint D						0	-580
Final Moments		50	-50	582	-582	580	-580
Conventional Signs		+	−	+	−	−	

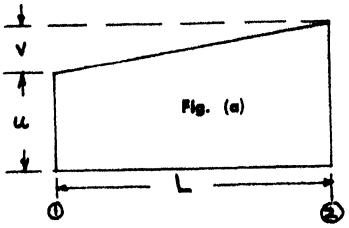
Since the fixed end moments are due to both lateral loads and support deflection, the values as listed in the solution table will be explained in detail.

Fixed End Moment For Lateral Beam Loading

The distributed airload is trapezoidal in shape. The fixed-end moments for a trapezoidal loading from Table A11.4 are:

$$M_{1-2} = \frac{L^2}{60}(5u + 2v) \quad \text{(See Fig. (a))}$$

$$M_{2-1} = \frac{L^2}{60}(5u + 3v) \quad \text{(See Fig. (a))}$$



For Span BC:

$$M_{bc} = \frac{40^2}{60}(5 \times 3 + 1) = 426 \text{ in. lb.}$$

$$M_{cb} = \frac{40^2}{60}(5 \times 3 + 1.5) = 440 \text{ in. lb.}$$

For Span CD:

$$M_{cd} = \frac{40^2}{60}(5 \times 3.5 + 1) = 494 \text{ in. lb.}$$

$$M_{dc} = \frac{40^2}{60}(5 \times 3.5 + 1.5) = 507 \text{ in. lb.}$$

Fixed End Moments Due to Support Movement

From Art. A11.8 $M = 6EId/L^2$

For Span BC:

Deflection of B relative to C = 5/16 inch. Hence,

$M_{bc} = M_{cb} = 6 \times 10{,}000{,}000 \times .03339 \times .3125/40^2 = 390$ in. lb.

For Span CD:

$M_{cd} = M_{dc} = 6 \times 10{,}000{,}000 \times .03339 \times .1875/40^2 = 234$ in. lb.

For signs of the moments due to these deflections see Art A11.2. Having determined the fixed end moments the general distributing and carrying over process follows as indicated in the solution table. Thus at joint B, the unbalanced moment = (50-426 + 390) = 14. Balance by distributing - 14 x 1 = - 14 to BC and zero to BA. Carry over .5 x -14 = - 7 to C. Considering joint C, the unbalanced moment = (440 + 390 + 234 - 494 - 7) = 563. Balance bydistributing - 563 x .571 = - 322 to CD and -563 x .429 = - 241 to CB. Carry over .5 x -322 = - 161 to D. At joint D the unbalanced moment = (507 + 234 - 161) = 580. This is balanced by distributing zero to DC and -580 to the fixed support.

A11.8 Check on Final Moments

To satisfy statics, the algebraic sum of the moments in all the members at a joint must equal zero. This requirement alone will not prove that the final moments are correct, as errors could have been made in the various distributing and carry over moments. Continuity tells us that the final slope of the elastic curve at any joint is common to all members meeting at that joint, thus for a complete check it is necessary to prove that the final moments are consistent with equal slopes for the various members. The rotation of the joints from their original assumed fixed or locked condition is due entirely to the distributed and carry over moments. The actual rotation will therefore equal the rotation of the end of a simply supported beam when subjected to end moments equal to those produced by the algebraic sum of the distributed and carry over moments. These end moments equal the final moments minus the original fixed end moments and will be referred to as ΔM moments.

From Chapter A7, the slope at any point on a simply supported beam equals the shear due to the M/EI diagrams as a loading.

The slope θ_A from Fig. a' equals the beam shear at A or equals the reaction at A.

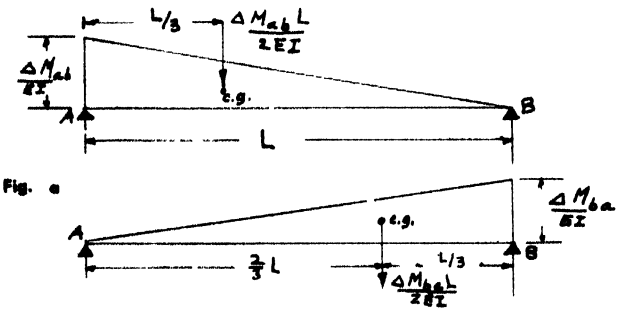


Fig. a

$$\theta_A = -\frac{\Delta M_{ab} L}{2EI} \cdot 2/3 - \frac{\Delta M_{ba} L}{2EI} \cdot \frac{1}{3}$$

$$= -\frac{(\Delta M_{ab} + .5\ \Delta M_{ba})}{3EK_{ab}}$$

where

$$K_{ab} = \frac{I}{L} \text{ of AB}$$

Since the angle θ_A must be the same for members meeting at A, the general relation between the moment increments of any two members such as AB and AC must be,

$$\frac{\Delta M_{ab} + .5\ \Delta M_{ba}}{\Delta M_{ac} + .5\ \Delta M_{ca}} = \frac{K_{ab}}{K_{ac}}$$

To make this equation consistent with the assumed sign convention, that is, the carry over moment has the same sign as the balancing distributed moment, the above equation must be modified as follows:-

$$\frac{\Delta M_{ab} - .5\Delta M_{ba}}{\Delta M_{ac} - .5\Delta M_{ca}} = \frac{K_{ab}}{K_{ac}} \quad \text{----------(5)}$$

If equation (5) is satisfied the accuracy of the moment distributions is established.

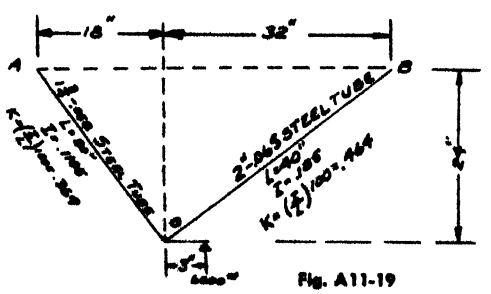
A11.9 End Moments for Continuous Frameworks Whose Members are not in a Straight Line. Joint Rotation Only

Continuous truss frame works are quite common in aircraft construction. Welded steel tubular fuselages are composed of members which maintain continuity thru the joints due to the welding. Landing gears frequently have two members which are made continuous at their points of connection. The members of such structures usually carry high axial stresses which cause joint translation which in turn produces bending of the members since the joints are rigid. These moments produce lateral deflection of the members which introduces additional secondary moments due to member axial loads times the lateral member deflections. These influences are treated in later articles. In this article to further familiarize the student with the moment distribution procedure, the effect of joint translation and secondary moments will be neglected.

Example Problem #6

Fig. A11.19 illustrates a simplified landing gear chassis problem. Let it be required to determine the bending moments in the two members due to the vertical load on the axle. The problem has been solved using three different degrees of restraint at ends A and B. Joint O is a welded joint and full continuity is assumed thru this joint. The solutions as given in Fig. A11.20 give only the moments due to joint rotation under primary bending moments. The effect of axial deformation and secondary moments due to member deflections is omitted in these solutions. These factors are treated in later articles.

In a practical problem the degree of restraint at points A and B would be determined by the type of fitting used and also on the rigidity of the adjacent fuselage or wing structure. As illustrated in later examples, the moment distribution method permits the consideration of the rigidity of the adjacent structure without adding any difficulty, while such methods as least work



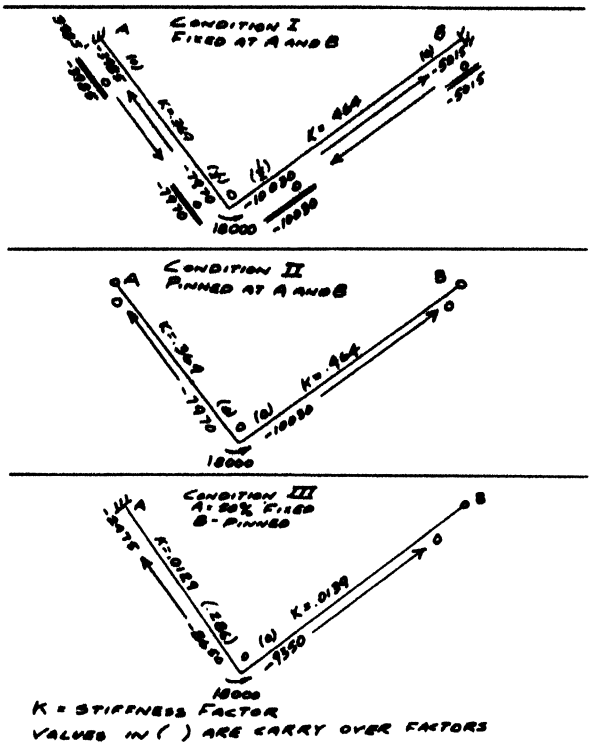


Fig. A11-20

are not practicable because of the large number of equations that must be solved to obtain values for the many unknowns.

Solution for Condition I, Fixed at Ends A and B

Referring to Fig. A11.20, all joints are assumed locked against rotation or fixed. The vertical axle load of 6000# produces a counter-clockwise moment of 3 x 6000 = 18000 in. lb. about joint O. The sign is positive (See Art. A11.2). Release or unlock joint O, the unbalanced moment is 18000 or - 18000 is required for static equilibrium of joint O. Joint O is balanced by distributing - 18000(.464/.464 + .369) =-10030 to member OB and the remainder or or -18000(.369/.464 + .369) = -7970 to OA. These distributed balancing moments at O produce carry over moments at A and B.

Thus carry over to B, .5 x - 10030 = - 5015

and carry over to A, .5 x - 7970 = - 3985

Proceeding to joint A which is a fixed joint, the unbalanced moment of -3985 is balanced entirely by the rigid support, or no rotation takes place when joint is released from its imaginary fixed state. Similar action takes place at joint B. The final end moments are as shown in the Figure.

Solution for Condition II. End A and B Pinned

For this condition the ends A and B are freely supported. Instead of locking and unlocking these joints which are definitely known to be free to be freely supported, they will be left in their true state. Thus the carry over moments from end O will be zero. Since A and B are both pinned, the relation between the relative stiffness factors of members OA and OB remain the same as in condition I, thus the same K or stiffness factors that were used in condition I can be used in distributing moments at joint O. Joint O is balanced in same manner as condition I but with zero carry over moments to A and B.

Solution for Condition III. A is 50% Fixed and B is Pinned.

Since each member has a different degree of fixity at its upper end, the stiffness and carry over factors will be considered in detail. In condition I since both members were fixed at their upper ends the relative stiffness factor of each member was proportional to I/L for the member and this ratio was used. The general expression for stiffness factor is K = EI (3 + F)/L; carry over factor = $\frac{2F}{3+F}$. For member OA, F equals .5 since A is 50% fixed, and for member OB, F is zero since B is freely supported. Hence for member OA

$$K = \frac{EI}{L}(3 + .5) = \frac{3.5\ EI}{L} = \frac{3.5 \times .1105\ E}{30} = .0129\ E$$

$$\text{C.O. Factor from O to A} = \frac{2 \times .5}{3 + .5} = .286$$

For member OB

$$K = \frac{EI}{L}(3 + 0) = \frac{3 \times .185 \times E}{40} = .0139E$$

$$\text{C.O. Factor From O to B} = \frac{2 \times 0}{3 + 0} = 0$$

Considering joint O in Fig. A11.20 the external moment of 18000 in.lb. is balanced by distributing - 18000 between the two members in proportion to their stiffness factors. Hence - 18000 (.0129/.0129 + .0139) = -8650 in lbs. is resisted by OA and the remainder of -18000 (.0139/.0129 + .0139)= -9350 to OB. The carry over moment from O to A = .286 x -8650 = -2475 and zero from O to B. (See Fig. A11.20)

Example Problem #7

Fig. A11.21 shows a structure composed of 3 members. Member AO is subjected to a transverse load of 120#. Joint A is fixed, B is freely supported C is 25 percent fixed and joint O is considered to maintain continuity between all members at O. The end moments on the three members due to the transverse loading on member AO will be determined.

Solution #1. Fig. A11.21 gives a solution using the "Cross" method in its fundamental unmodified state. The solution is started by assuming all three members as fix-ended. The relative stiffness factor K of each member is therefore proportional to I/L of each member. These K values are listed in Fig. A11.21. The distribution

factor D for each member at each joint which equal K/ΣK is recorded in □ on each member around each joint. Thus any balancing moment is distributed between the joint members as per these distribution factors. The carry over factors for all members is 1/2. The fixed end moments due to external loading are computed for the three members. For member AO, the fixed end moments equal PL/8 = 120 x 20/8 = 300 in. lb. The other two members having no transverse loading, the fixed end moments are zero.

In this solution the order of joint consideration has been AOBC and repeat. Starting with joint A the joint is released but since the member AO is actually held by a fixed support, no rotation takes place and the balancing moment of 300 is provided entirely by the support and zero by the member AO. The carry over moment C, to O is zero. Releasing joint O, the unbalanced moment of 300 is balanced by distributing - 300 between the three members according to their D values, thus - 300 x .416 = - 125 to OA; - 300 x .168 = - 50 to OC and - 125 to OB. To prevent confusion it is recommended that a line be drawn under all distributed balancing moments, thus any values above these lines need not be given further consideration and only values below the lines need be considered in later balancing of the joints. Immediately after distributing the moments at joint O the proper carry over moments should be taken over to the far end of each member, thus - 62.5 to A, - 62.5 to B and - 25 to C. Joint B is next considered. The unbalanced moment is -62.5 and it is balanced by distributing 62.5 to BO since the pin support has zero stiffness, or no resistance to rotation. A line is drawn under the 62.5 and the carry over moment of 31.25 is placed at O. Joint C is considered next. The unbalanced moment of -25 is balanced

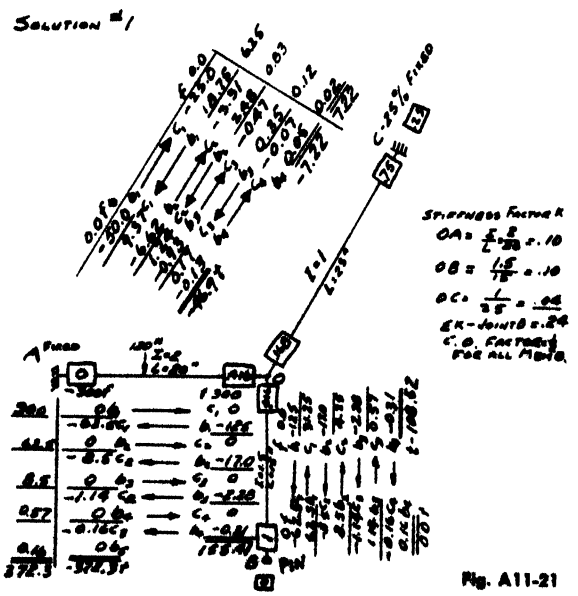


Fig. A11-21

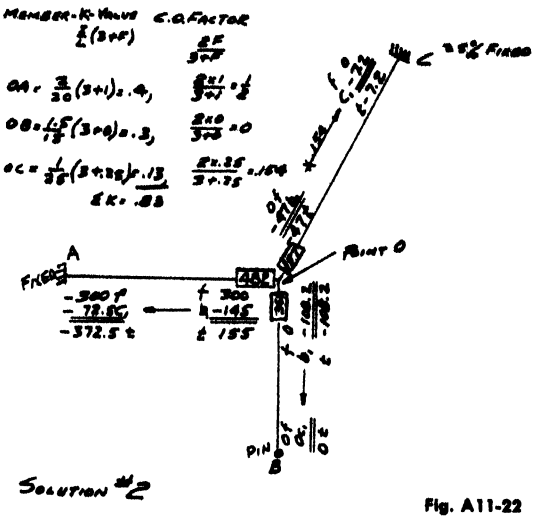


Fig. A11-22

by distributing .75 x 25 = 18.75 to CO and the remainder of 6.25 to the support, since the fixity of the support at C has been assumed as 25 percent. A line is drawn under the 18.75 and the carry over moment of 9.37 is taken over to O. One cycle has now been completed. Returning to joint A, we find -62.5 below the line. This is balanced by distributing zero to OA and 62.5 to the fixed support. A line is drawn under the zero distributed moment to AO and the carry over moment of zero is placed at O. Considering joint O for the second time the unbalanced moment is 9.37 + 31.25 + 0 = 40.62 or the sum of all values below the column horizontal lines. The joint is balanced by distributing - 17 to OA and OB and -6.62 to OC. Lines are drawn under these balancing moments as shown in Fig. A11.21 and the carry over moments are taken over to the far ends before proceeding to joint B.

This general process is repeated until joint A has been balanced 5 times and the other joints 4 times each, as indicated in the figure the distributing values have become quite small and it is evident that a high degree of accuracy has been obtained. The final end moments at each joint equal the algebraic sum of the values in each column. A double line is placed above the final moments as a distinguishing symbol. In the figure the letters b and c refer to balancing and carry over moments, the subscripts referring to the member of the balancing or carry over operation. Any order of joint consideration can be used in reaching the same result.

Solution #2 of Problem 7

Fig. A11.22 gives a second solution. With the end conditions known at A, B and C, the modified stiffness factors of the members can be found together with the modified carry over factors, thus making it necessary to balance joint O only once and carry over this final far end

moments of each member. The figure gives the calculation of the modified or actual stiffness and carry over factors. With these known the solution is started as before by computing the fixed end moments due to transverse loading on member AO. Joints B and C are released and since no fixed end moments exist, no balancing is required and the joints are left in their true state of restraint instead of locking and unlocking as in solution #1. Releasing joint O from its imaginary fixed state the unbalanced moment is 300 which is balanced by distributing - 300 between the 3 connecting members according to the new distribution factors at joint O. Thus - 300 x .482 = - 145 to OA; - 300 x .361 = - 108.2 to OB and - 300 x .157 = - 47 to OC. The carry over moment to A = - 145 x .5 = - 72.5 to B = - 108.2 x 0 = 0 and -47 x .154 = - 7.2 to C.

Example Problem #8

Figure A11.23 shows the forward portion of a fuselage side truss. Due to eccentricity of engine mount and landing gear members, external moments are produced on joints A, B and D as shown. Furthermore lateral loads due to equipment installation are shown acting on members BE and CD. Assuming the fuselage welded joints produce rigid continuity of members thru the joint, the problem is to find the end moments in all the members due to the eccentric joint moments and two lateral loads. The effect of joint translation and secondary moments due to deflections and axial loads is to be neglected in this example.

Solution:

Table A11.2 gives the calculation of the stiffness factor for each truss member. The fuselage truss aft of joints I and H have been assumed to give 50% fixity to these joints. In Table A11.2 a modified stiffness factor is calculated for members GI, FI, and FH using a 50 percent fixity at their far ends. The last column of Table A11.2 gives the summation of the member stiffness factors for members intersecting at each joint.

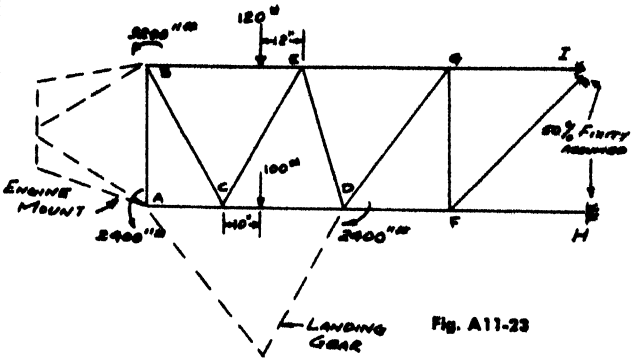


Fig. A11-23

TABLE A11.2

Member	Size Tube	Length L	I	$\frac{I}{L}$ x 1000 Stiffness K Factor	$\Sigma\frac{I}{L}$ for each joint: Joint	$\Sigma\frac{I}{L}$ Stiffness
BE	1-1/8 - .049	41.25"	.0240	0.582	A	5.80
BG	1-1/8 - .049	38.75	.0240	0.619	B	4.61
GI	1-1/8 - .049	34.0	.0240	.619*	C	4.98
AC	1-1/2 - .049	19.25	.0588	3.06	D	5.14
CD	1-1/2 - .049	30.0	.0588	1.96	E	3.81
DF	1-1/2 - .049	30.0	.0588	1.96	F	4.44
FH	1-3/8 - .049	34.0	.0448	1.16*	G	3.21
AB	1-3/4 - .049	34.5	.0947	2.74		
BD	1-1/4 - .049	35.4	.03339	0.944		
BC	1-1/8 - .049	34.5	.0240	0.695		
EC	1-1/2 - .049	39.5	.0588	1.49		
CD	1-1/8 - .035	41.0	.0176	0.434		
DG	1-1/2 - .049	46.0	.0588	1.28		
FI	1-1/4 - .049	48.5	.03339	0.602*		

(E is constant for all members)

(*stiffness factor - 7/8 $\frac{I}{L}$ because of 50% fixity)

Fig. A11-24

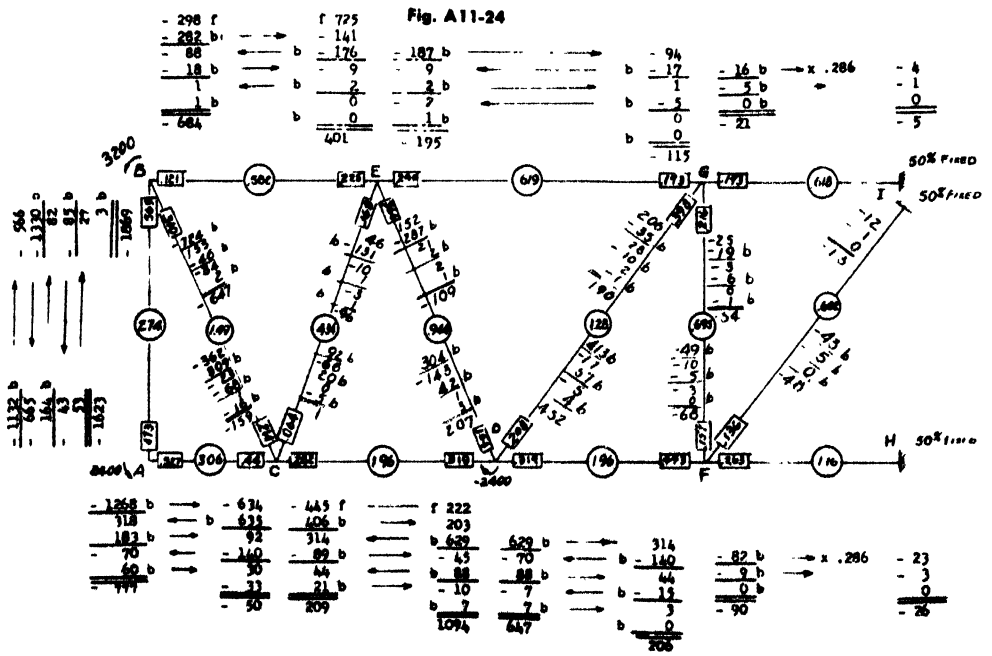


Fig. A11.24 gives the solution of the problem. The procedure in this solution was as follows:

The stiffness factor K for each member as computed in Table A11.2 is recorded in the circles adjacent to each truss member. The carry over factors for all members is 1/2 except for modified members GI, FI and FH for which the carry over factor to the 50% fixed ends is .286. The distribution factor for each member at each joint is recorded at the end of each member, and equals $K/\Sigma K$.

The next step in the solution is to compute the fixed end moments due to the transverse loads on members.

For member BE

$M_{BE} = Pab^2/L^2 = 120 \times 29.25 \times 12^2/41.25^2 = -298"\#$

$M_{EB} = 120 \times 29.25^2 \times 12/41.25^2 = 725"\#$

$M_{CD} = 100 \times 20^2 \times 10/30^2 = -445$

$M_{DC} = 100 \times 10^2 \times 20/30^2 = 222$

These moments are placed at the ends of the members on Fig. A11.23 together with the eccentric joint moments. The process of unlocking the joints, distributing and carrying over moments can now be started. In the solution as given the order of joint consideration is ABCDEFG and repeat, and each joint has been balanced three times.

Consider joint A:-

Unbalanced moment = 2400. Balance by distributing - 2400 as follows:-

To AC = - 2400 x .527 = -1268. Carry over to C = -634

To AB = - 2400 x .473 = -1132. Carry over to B = -566

Proceed to Joint B:-

Unbalanced moment = (-566 + 3200 - 298) = 2336. Joint is balanced by distributing - 2336 to connecting members as follows:-

To BA = - 2336 x .569 = - 1330. Carry over to A = - 665

To BC = - 2336 x .310 = - 724. Carry over to C = - 362

To BE = - 2336 x .121 = - 282. Carry over to E = - 141

The convenient device of drawing a line under all balancing moments is used to prevent confusion in later balances of the joint.

Proceed to Joint C:-

Unbalanced moment = (-634 - 362 - 445) = -1441. The joint is balanced by distributing 1441 as follows:-

To CA = 1441 x .44 = 635. Carry over to A = 318

CB = 1441 x .214 = 309. Carry over to B = 155

CE = 1441 x .064 = 92. Carry over to E = 46

CD = 1441 x .282 = 406. Carry over to D = 203

This process is continued for the remainder of the truss joints. After all joints has been balanced once, on returning to joint A we find below the lines an unbalanced moment of (318 - 665) = -347. The joint is balanced a second time by distributing 183 to AC and 164 to AB with carry over moments of half these values to ends C and B respectively.

The student should now be able to check the rest of the solution as given on Fig. A11.24.

The solution could be made with any order of joint consideration. If any particular joint appears to be nearly balanced, it is best to skip it for the time being and consider those joints which are considerably unbalanced.

The final moments at the end of each member are given below the double lines.

Example Problem #9

Fig. A11.25 represents a cross section of a welded tubular steel fuselage. The top and bottom members which are web members in the top and bottom fuselage trusses are subjected to the equipment installation transverse loads as shown. Let it be required to determine the end bending moments in the rectangular frame due to these transverse loads assuming full continuity thru joints.

Solution:

Fig. A11.26 shows the solution. The distribution factors based on the member stiffness factors are shown in □ at ends of each member. The first step is to compute the fixed end moments due to transverse loads, on members AB and CD using equations from Table A11.1. The magnitudes are 1890"# for AB and 2025"# for CD.

Joint B is now released from its assumed fixed state. The unbalanced moment of 1890 is balanced by distributing - 1890 x .247 = - 467 to BA and the remainder of -1423 to BD. The carry over moment to A = - 465 x .5 = - 233. Due to symmetry of structure and loading only one half of frame need be considered and hence these carry over moments to A are not recorded. However, in balancing joint A it will throw over to B the same magnitude of carry over moments as thrown over to A from B but of opposite sign since the original fixed end moment at B is minus. Thus 233 comes to B from first balance of A as shown in the figure. The distributing moment to B of -1423 produces a carry over moment of -1423 x .5= -712 at D.

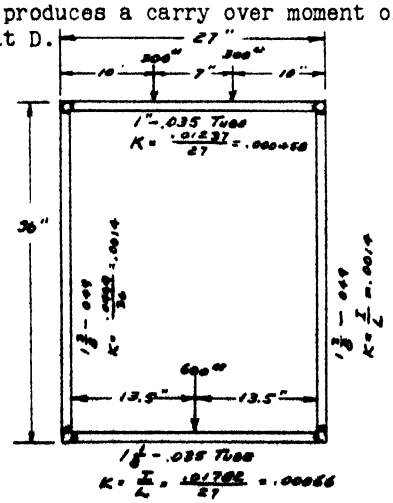


Fig. A11-25

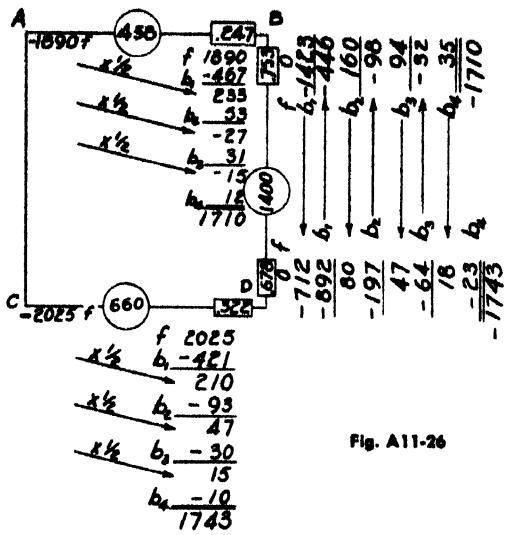


Fig. A11-26

Joint D is considered next: The unbalanced moment of (2025 - 712) = 1313 is balanced by distributing - 1313 to the connecting members.

To member DB = - 1313 x .678 = - 892 and the remainder of -421 to DC. The carry-over moment to B is - 446. The carry over from C to D is one-half the balancing moment B = - 421 but of opposite sign or 210, due to symmetry as explained before for member AB.

Returning to joint B, the unbalanced as recorded below the single lines is (233 - 446) = - 213. To balance 160 is distributed to BD and 53 to BA. Carry over 80 to D and bring over from A to B .5 x -53 = - 27. Continue this process until joints A and D have been balanced 4 times or 4 cycles have been completed. The final moments are shown below the double lines. Fig. A11.26a shows the resulting moment diagram on frame.

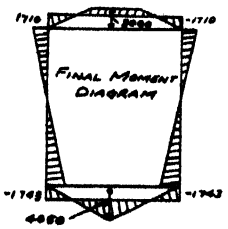


Fig. A11-26 a

A11.10 Continuous Structures with Members of Variable Moment of Inertia

In Arts. A11.3, 4 and 5 consideration was given to the derivation of expressions for fixed end moments, stiffness and carry over factors for beams of uniform cross-section. Many cases occur in routine design where members have a variable cross section. This article will illustrate the calculation of the fixed end moments, stiffness and carry over factor for a beam with variable moment of inertia. The effect of axial load on these factors will not be considered here but will be treated in a later article.

(A) Calculation of Fixed End Moments for a Given Beam Load

Fig. A11.27 shows a fixed end beam with a variable moment of inertia and carrying a single concentrated load of 100#. The beam moment diagram for this load is considered in three parts. Fig. A11.28 shows the static moment curve assuming the beam simply supported at A and B and carrying the load of 100#. Fig. A11.29 shows the other two parts, namely the triangular moment diagram due to the unknown moments M_A and M_B which produce fixity at the two ends. In this figure M_A and M_B have arbitrarily been taken as 100, instead of unity.

Fig. A11.30 shows the M/I diagram for the 3 moment diagrams of Fig. A11.29. The beam is divided into ten equal strips, and the M/I curves are obtained by dividing the moment values at the end of each strip or portion by the corresponding I value from Fig. A11.27.

From the conditions of fixity at the beam ends, we know that the slope of the beam elastic curve is zero at each end. Likewise the deflection of one end of the beam away from a tangent at the other end is zero. Stating these facts in terms of the moment area principles, we obtain

$$\int_0^L \frac{M dx}{I} = 0 \quad -(5)$$ (Area of M/I diagrams equal zero)

$$\int_0^L \frac{M x dx}{I} = 0 \quad -(6)$$ (Moment of the M/I diagram as a load about either end equals zero)

(Note: Since E is usually considered constant it has been omitted from denominator of the above equations).

TABLE A11.3

Beam Portion	Static M/I curve			Trial $\frac{M_A}{I}$ curve			Trial $\frac{M_B}{I}$ curve		
	Av. Ord. = y	Mom. arm left end = x	Mom. about left end = yx	Av. Ord. (y)	Mom. arm left end x	yx	Av. Ord. = y	Arm x	Mom. yx
1	107	2.67	286	110	2.06	227	6.7	2.67	18
2	397	6.31	2510	133	6.07	807	24.9	6.27	156
3	770	10.16	7800	143	10.0	1430	48.2	10.16	488
4	1120	14.10	15800	130	13.94	1810	70.0	14.10	990
5	1440	18.07	26000	110	17.96	1976	90.0	18.06	1630
6	1760	22.06	38900	90	21.92	1970	110.0	22.05	2430
7	1815	25.88	41600	67.3	25.88	1740	123.5	26.04	3480
8	975	29.77	29000	40.7	29.76	1215	117.0	29.94	3490
9	420	33.65	14180	17.5	33.68	590	91.0	33.88	3080
10	100	37.33	3733	4.2	37.33	157	62.5	37.86	2360
Σy	8504			845.7			743.8		
Σyx			179809			11922			18132

$\bar{x} = \frac{\Sigma yx}{\Sigma y} = \frac{179809}{8504} = 21.15"$ $\quad \bar{x} = \frac{11922}{845.7} = 14.1"$ $\quad \bar{x} = \frac{18132}{743.8} = 24.4"$

* Actual area is 4 times the results shown. For calculation of fixed end moments & c.o. factors only relative values are necessary.

Fig. A11-27

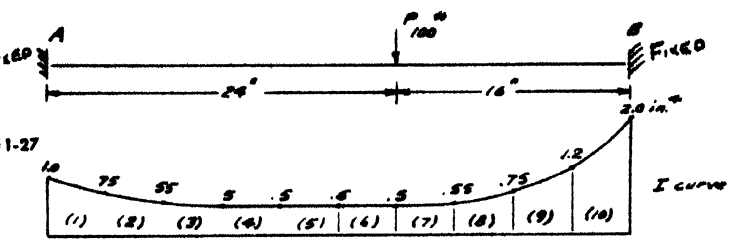


Fig. A11-28

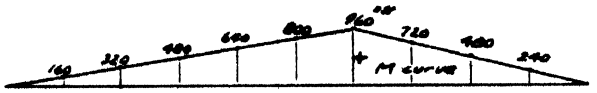


Fig. A11-29

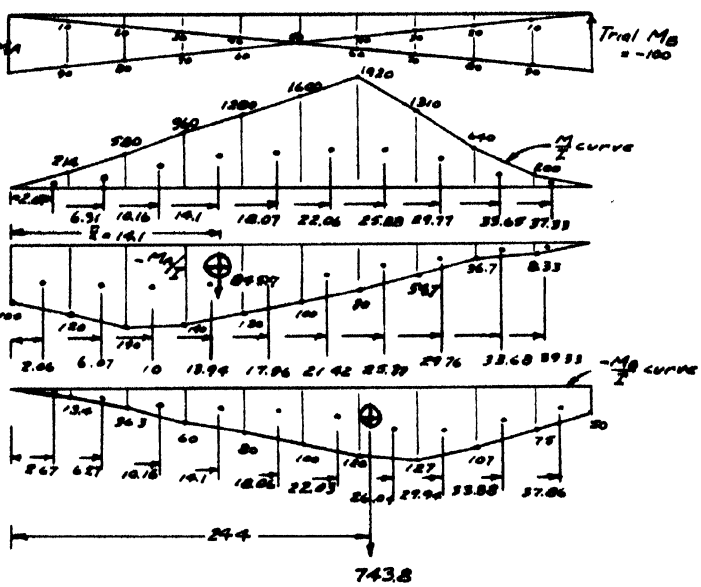


Fig. A11-30

Table A11.3 shows the calculations for computing the areas and the centroids of the three M/I diagrams of Fig. A11.30. Substituting values from Table in equations (5) and (6).

$$\frac{845.7}{100} M_A + \frac{743.8}{100} M_B + 8504 = 0 \text{ - - - - - -(7)}$$

$$\frac{11922}{100} M_A + \frac{18122}{100} M_B + 179809 = 0 \text{ - - - - - -(8)}$$

The value 100 in the denominators is due to the fact that trial values of 100 were assumed for M_A and M_B. Solving equations (7) and (8) we obtain;

M_A = - 315"# and M_B = - 785"#.

(B) Calculation of Carry Over Factors

To determine the carry over factor from A to B consider end A as freely supported and B as fixed. A moment M_A = 100 is applied at A which produces the M/I curve of Fig. A11.30b. Due to the deflection of the beam under this loading a restraining moment at B to cause tangent of elastic curve to remain horizontal will exist. This unknown fixed moment at B has arbitrarily been taken as 100, thus producing a M/I curve identical to Fig. A11.30c. For the conditions of support assumed, the deflection of A away from a tangent to the elastic curve at B is zero. Thus by the deflection principle of area moments, the moment of the M/I diagrams of Figs. A11.30 (a and b) about end A equals zero. Thus,

$$845.7 \times 14.1 + \frac{743.8}{100} M_B \times 24.4 = 0$$

or

M_B = - 66"#

Since M_A was assumed 100, then carry over factor from A to B = $\frac{-66}{100}$ = - .66.

To find carry over factor from B to A, take moments about B and equate to zero.

Hence

$$743.8 \times 15.6 + \frac{845.7}{100} M_A \times 25.9 = 0$$

whence

M_A = - 53.2"#

Therefore carry over factor B to A = $-\frac{53.2}{100}$ = - .532

(Note: For the moment sign convention used in this book carry over factor would be plus.)

(C) Calculation of Beam Stiffness Factors

When a beam is freely supported at one end A and fixed at the far end B, the stiffness factor at the A end is measured by the moment necessary at A to produce unit rotation of the elastic curve at A.

In Art. A11.4 it was proved for beams of uniform section that $E\Theta_A = M_A L/4I$ or $M_A = 4EI\Theta_A/L$. In a continuous structure at any joint all members have the same Θ, thus $4E\Theta$ is constant and the stiffness K of any prismatic beam is proportional to I/L. For beams of variable section the stiffness factor K may be written:-

$$K = cI_o/L \text{ - - - - - - - - - - - - - - - - - -(9)}$$

where I_o is the moment of inertia at a particular reference section and c is a constant to be found for each non-uniform member. Thus for non-uniform members

$$E\Theta_A = M_A L/4cI_o \text{ - - - - - - - - - - - - - (10)}$$

By the moment area slope principle, the slope at A when B is fixed equals the area of the M/I diagram between A and B.

Taking M_A = 100, M_B was found to equal -66"#. Thus $E\Theta_A = 4(845.7 - .66 \times 743.8) = 1419$. The value 4 is due to the strip width since true area is wanted and only average ordinate was used in Table A11.3.

Equating this result to Equation (10)

$1419 = \frac{100 \times 40}{4c \times 1}$, whence c = .707

I_0 was taken as the value at the A end or 1. (See Fig. A11.27).
Therefore $K_{AB} = .707\ I_A/L$

Similarly for end B:-

$E\theta_B = 4(743.8 - .532 \times 845.7) = \frac{100 \times 40}{4c \times 1}$

whence

c = .85 and $K_{BA} = .85\ I_A/L$

A11.11 Frames with Unknown Joint Deflections Due to Sidesway

In the example problems so far treated the joints of the particular structure were assumed to rotate without translation or with a definite amount of translatory movement. Translation of the joints may however, be produced by shortening and lengthening of the members due to axial loads and by lateral sway due to lack of diagonal shear members. The problem relative to the effect of joint translation due to axial stresses is treated in a later article. In this article only the effect of sidesway of rectangular frames on the frame bending moments will be considered.

Fig. A11.31 illustrates cases of frames where only rotation of joints takes place (neglecting axial deformation) whereas Fig. A11.32 illustrates conditions in which sidesway takes place and the joints suffer translation as well as rotation.

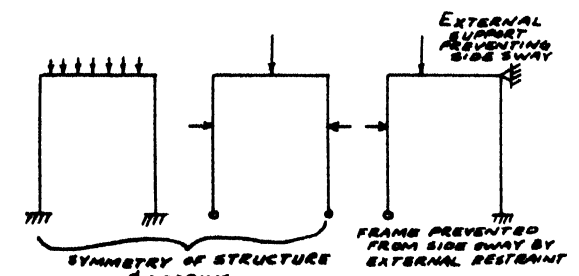


Fig. A11-31

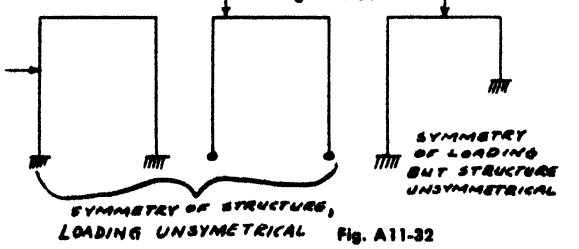


Fig. A11-32

There are several methods of determining the bending moments due to sidesway. Only one method will be presented here and it can best be explained by the solution of example problems. (For comprehensive treatment, see Prof. Cross's textbook)

Example Problem #10 (Rectangular Frame with Sidesway)

Fig. A11.33 shows a single bay rectangular bent carrying a distributed side load on one leg as shown. The K or I/L valves for each member of frame are assumed as indicated.

The first step in the solution is to determine the frame bending moments assuming only rotation of frame joints takes place. In other words sidesway of frame for given loading is assumed as zero. Fig. A11.34 shows the solution for bending moments under this assumption. The solution begins with computing the fixed end moments on member AB = $1/12\ wL^2 = 1/12 \times 300 \times 25^2 =$ 15.63 thousands of foot lbs. This value with the proper sign is written at the head of the column of figures on member AB as shown in Fig. A11.34.

Now considering Joint B, the unbalanced joint moment of 15.63 is distributed as follows:- To Member BA = - 15.63 (40/190) = - 3.27. Carry over to Joint A = - 3.27/2 = - 1.63

To Member BC = - 15.63 (150/190) = - 12.36. Carry over to Joint C = - 12.36/2 = - 6.18

Now consider Joint C:-

The unbalanced moment is -6.18. To balance we distribute to CB = 6.18 x 150/190 = 4.88. Carry over to B = 2.44; to CD = 6.18 x 40/190 = 1.30. Carry over to D = 0.65

The balancing and carry over procedure is now repeated for joints B and C, until the unbalanced moments become of negligible magnitude. Fig. A11.34 shows that 4 cycles have been carried thru by keeping the ratio 150/190 set on the slide rule the unbalanced moments at joints B and C are distributed and chased back and forth as rapidly as one can write them down. Since joints A and D are assumed fixed, they absorb moments but do not give out any.

Fig. A11.35 shows the vertical legs of the frame as free bodies with the external side load and the end moments as found in Fig. A11.34. Taking moments about a point on line AD the unbalanced side shear force at top of columns.

$$= -\frac{25 \times 300 \times 12.5}{25} + \frac{17570 - 11750}{25} - \frac{1530 - 770}{25} =$$

- 3609#

To balance this force the columns create a resisting shear reaction due to lateral bending of the legs which produces deflection or sidesway of the frame. Thus the next step is to determine the frame moments necessary to produce a resisting side shear of 3609# at upper end of vertical legs. These frame moments are determined as follows:- Assume the structure sways sideways as illustrated in Fig. A11.36, but with no rotation of the upper joints. It was proven in Art. A11.8 that the end moments produced by the lateral movement of one end of a beam whose ends are fixed against rotation are equal to $\frac{6EId}{L^2}$ where d is the lateral movement. In Fig. A11.36 both columns suffer the same lateral displacement at their upper ends, hence their end moments due to side sway are proportional to $\frac{EI}{L^2}$.

In our example problem EI and L are the same for each column. Hence for convenience we will assume that a moment of 10,000 ft. lbs. is produced at each end of the columns due to side sway. The signs are determined by inspection of Fig. d. We now permit the joints to progressively rotate and distribute the moments as illustrated in Fig. A11.37. The procedure is similar to that in Fig. A11.34. For example, we start by considering Joint B. The unbalanced

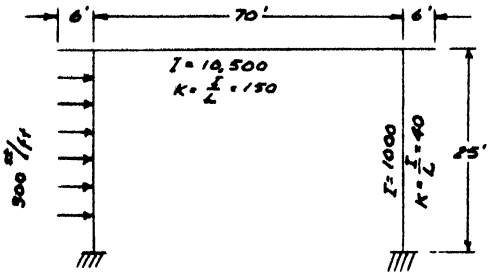


Fig. A11-33

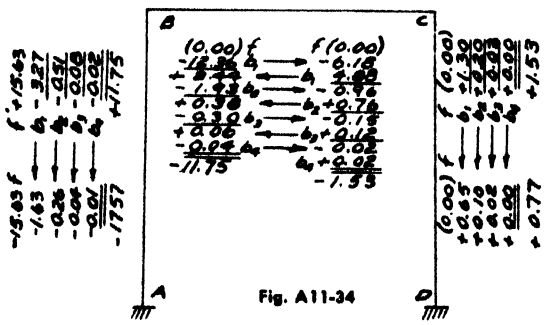


Fig. A11-34

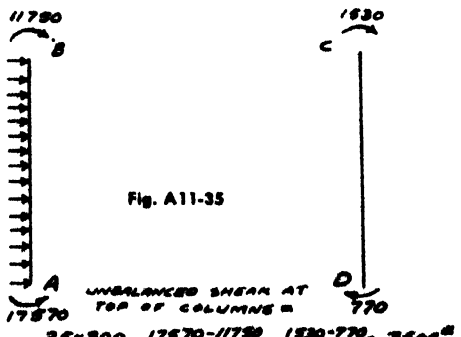


Fig. A11-35

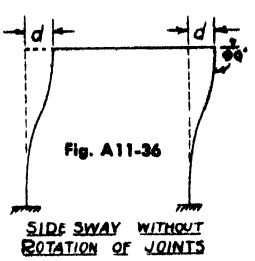


Fig. A11-36

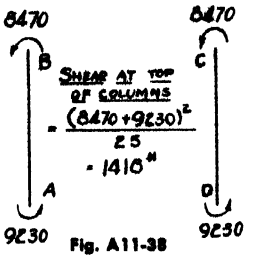
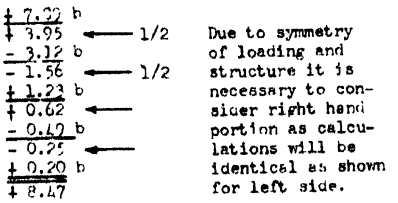


Fig. A11-38



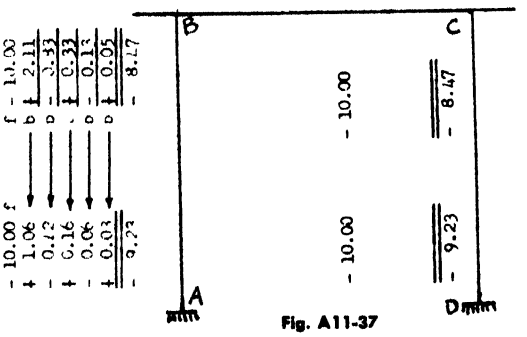


Fig. A11-37

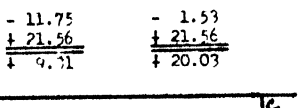


Fig. A11-39

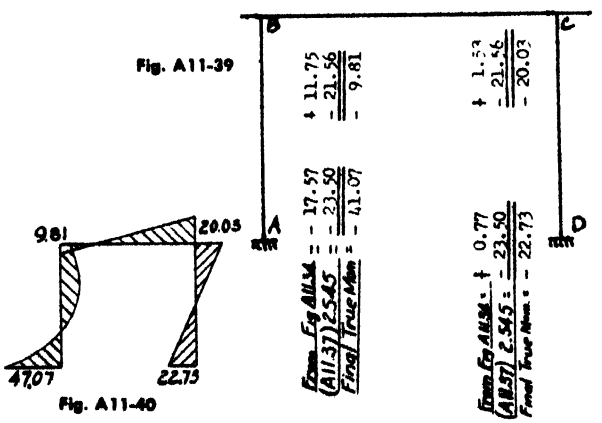


Fig. A11-40

moment is -10. This is balanced by distributing 10 x 150/190 = 7.89 to BC and the remainder of 2.11 to BA. The carry over moments are 7.89/2 = 3.95 to C and 2.11/2 = 1.06 to A. Due to symmetry of loading and structure, the distributing and carry over moments at joint C will be same as at joint B, hence it is needless work to show calculations at these joints. The carry over moments from C to B will be identical to those from B to C. Fig. A11.37 shows the 5 cycles have been

carried out to obtain the final end moments as shown below the double lines. Fig. A11.38 shows the free body of side members with end moments as found in Fig. A11.37. The unbalanced shear force at top of columns due to these end moments equals (8470 + 9230)2/25 = 1418#. In Fig. A11.35 we had an unbalanced shear of -3609#. Since the shear at column top must be zero for equilibrium, the moments produced by side sway in our problem are equal to 3609/1418 = 2.545 times those shown in Fig. A11.37. Adding these to those of Fig. A11.34 (due only to joint rotation) we obtain the final end moments as shown in Fig. A11.39 which gives to moment diagram of Fig. A11.40

Example Problem #11

Fig. A11.41 shows the same frame as used in Problem #10 but with a vertical load system added. The first step in the solution is to compute the fixed end moments, as follows:-

$M_{AB} = M_{BA} = 1/12\ wL^2 = 1/12 \times 300 \times 25^2 = 15620$ ft. lb.

$M_{BC} = M_{CB} = 1/12\ wL^2 = 1/12 \times 500 \times 70^2 = 204000$

$PL/8 = 60000 \times 70/8 = 525000$

729000 ft. lb.

Cantilever static moment at B and C

$= 6 \times 40000 + 3000 \times 3 = 249000$ ft. lb.

These values in units of thousands of ft. lb. are shown with the proper sign at the head of the columns of figures on Fig. A11.42. Then assuming that only rotation of the joints take place the end moments on the frame members are found by the moment distribution method as shown in Fig. A11.42. Thus starting with joint B the unbalanced moment equals (15.62 + 249 - 729) = -464.38. Joint B is balanced by distributing:-

To BA = 464.38 (40/190) = 98.18. Carry over to A = 49.09

To BC = 464.38 (150/190) = 366.2. Carry over to C = 183.1

Next consider Joint C:-

The unbalanced moment equals (729 + 183.1 - 249) = 663.1.

Joint B is balanced by distributing

to CB=-663.1 (150/190) = - 523. Carry over to B = -261.5

to CD=-663.1 (40/190) = - 140.1. Carry over to D = -70.05

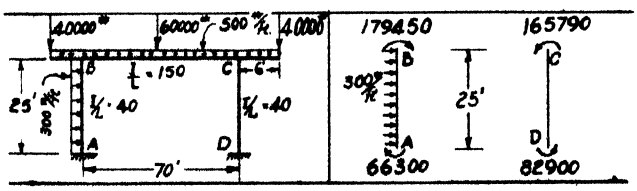


Fig. A11-41

Fig. A11-43

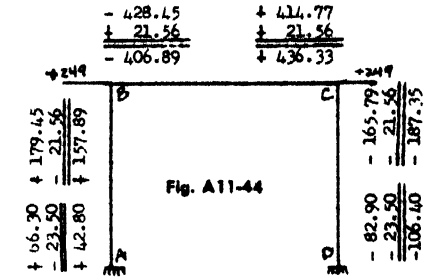


Fig. A11-44

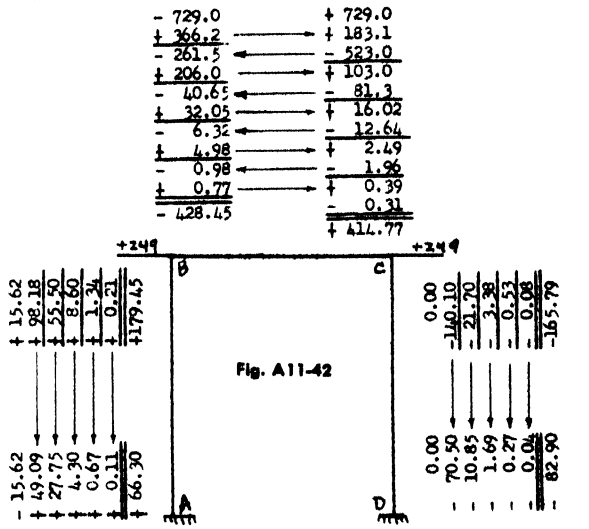


Fig. A11-42

Returning to Joint B, we find an unbalanced moment of -261.5. This is balanced as before by distributing 206 to BC and the remainder of 55.5 to BA. The carry over moments to C and A are 103 and 27.75 respectively. This process is repeated until joints B and C have been balanced 5 times. The final moments equal the summation of values in each column and are noted below the double lines.

In Fig. A11.43 these end moments are shown on the side members as free bodies. Taking moments about a point on line AD the unbalanced shear at top of side members equals

$$-\frac{7500}{2} - \frac{(179450 + 66300)}{25} + \frac{(165790 + 82900)}{25} =$$

$- 3610\#$

From Figures A11.37 and 38 of problem #10 the shear at top of side members for arbitrary side deflection equals 1418#. Our correction factor equals 3610/1418 = 2.545 as in previous example #10. This is true because the additional external load system which has been included as a symmetrical system and thus causes no side sway of frame. The final end moments therefore equal those of Fig. A11.42 plus 2.545 times those of Fig. A11.37 which give the results of Fig. A11.44.

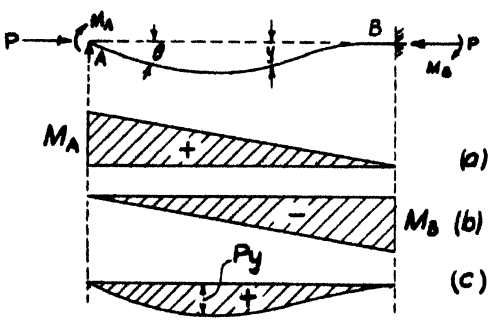
In this example problem the members at points A and D were assumed as fixed. For cases of pins or partial fixity at these points no difficulty arises in the solutions since the stiffness and carry over factors are modified accordingly.

In airplane structures problems involving side sway of trusses are frequently encountered in fuselage construction where large openings are necessary which prevents use of diagonal truss members.

A11.12 Effect of Axial Load on Moment Distribution

In the previous articles the effect of axial loads upon the member end moments of a continuous structure was neglected. The axial loads produce bending in the members of a continuous structure in two ways. (1) The shortening or lengthening of the various members due to axial loads produces translation of the joints of the structure. Since the angles between the members at a joint remain the same due to continuity, this translation of joints bends the members between joints. (2) The bending moments on the members due to external joint or lateral loads or those due to joint rotation produce lateral deflection of the members between joints. The member axial loads times these lateral deflections produce secondary moments. These secondary moments can be handled by the general method of moment distribution however the stiffness and carry over factors and the fixed end moments are not constant but become functions of the axial loads.

Fig. A11.45 shows a prismatic beam simply supported at A and fixed at B, with a moment M_A applied at A and carrying an axial compressive load P. Sub. Figure a, b and c show the 3 parts which make up the moment diagram on the beam. Without the axial load P the portion (c) would be omitted.



MOMENT DIAGRAMS

Fig. A11-45

By definition the stiffness factor of beam AB is measured by the necessary moment M_A to produce unit rotation ($\theta = 1$) for elastic line at point A. By the moment area principles, the slope at A equals the shear at A due to the moment diagrams acting as a load on a simply supported beam at A and B. For a given unit slope at A it is obvious that the required M_A is less when the load P is acting as it produces a moment load in (Fig. c) of the same sign as the moment load due to M_A. Thus the stiffness of AB is less when carrying an axial compressive load compared to that without it. For a tension axial load diagram C becomes a negative moment diagram and thus M_A must become larger to give unit slope at A. Or in other words a member carrying a tensile axial load has a greater stiffness than one without axial loads. It is evident that the moment diagram due to P will also effect the magnitude of any fixed end moments and also the carry over factor.

A11.13 Fixed End Moments, Stiffness and Carry over Factors for Beam Columns of Constant Section

In deriving expressions for fixed end moments, stiffness and carry over factors the beam columns formulas of chapter A10, must be used in finding slopes, deflection and moments.

Mr. B. W. James in an excellent thesis at Stanford University and later published by N.A.C.A. as Technical Note #534 has derived expressions for these factors and has provided graphs of these factors for use in routine design. Figures A11.46 to A11.56 inclusive are taken from this thesis. The use of these Figures can best be illustrated by the solution of several problems.

A11.14 Illustrative Problems

Example Problem #12

Fig. A11.57 shows the same continuous beam as used in Example Problem #4 (and solution #2). For this example it has been assumed that such axial compression loads exist in spans BC and CD as to make the term L/j = 2.5 and 2.0 for these spans respectively, where $j = \sqrt{EI/P}$. Due to the axial loads, new values of stiffness and carry over moments as well as fixed end moments must be determined as follows.

Span BC

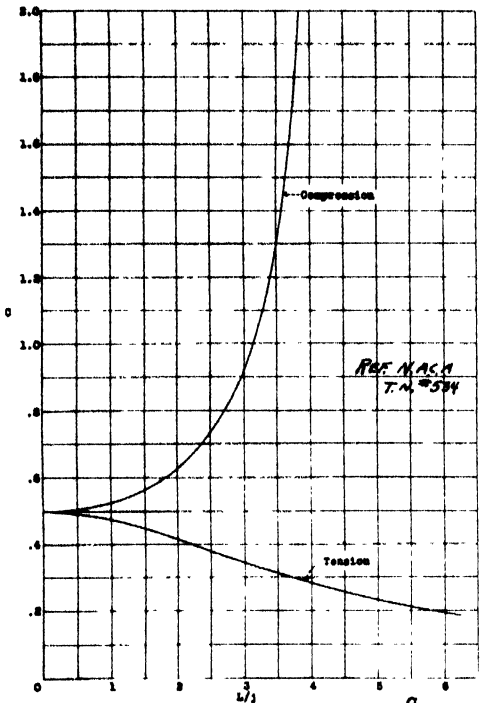
$$K = \frac{I}{L} = \frac{1}{96} = .0104$$

From Fig. A11.47 when L/j = 2.5, correction factor for stiffness factor = .775 when far end is fixed and .36 when far end is pinned. Hence,

$$K_{BC} = .0104 \times .775 = .00806$$

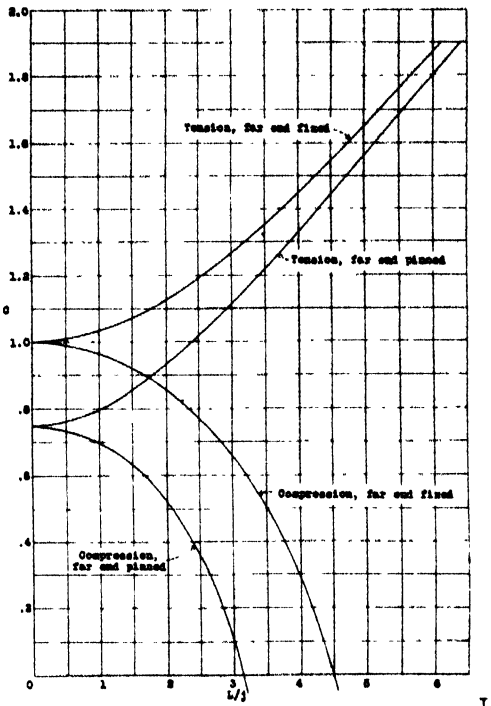
$$K_{CB} = .0104 \times .36 = .00374$$

From Fig. A11.46, when L/j = 2.5 the carry over factors are $C_{BC} = .73$ and $C_{CB} = 0$ if B is considered freely supported.



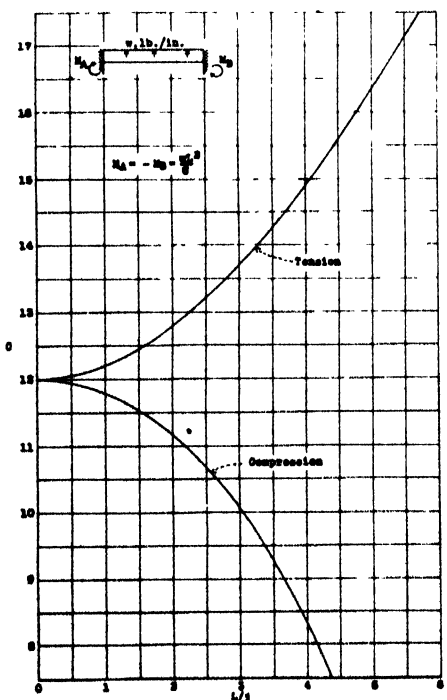
Carry-over factor. $C = \frac{\alpha}{2\beta}$

Fig. A11-46



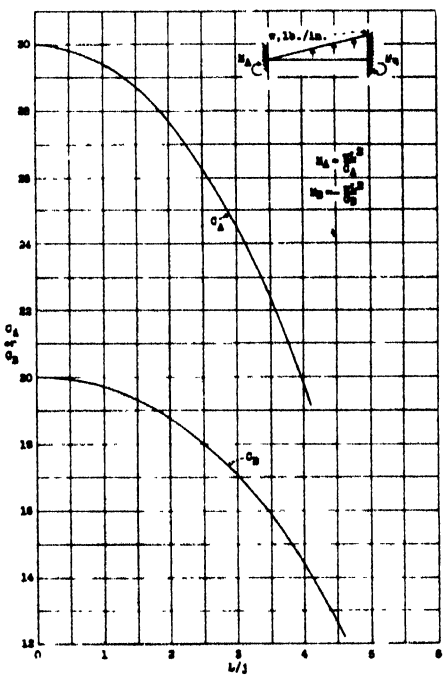
Stiffness factor coefficient. $K = C \frac{I}{L}$

Fig. A11-47



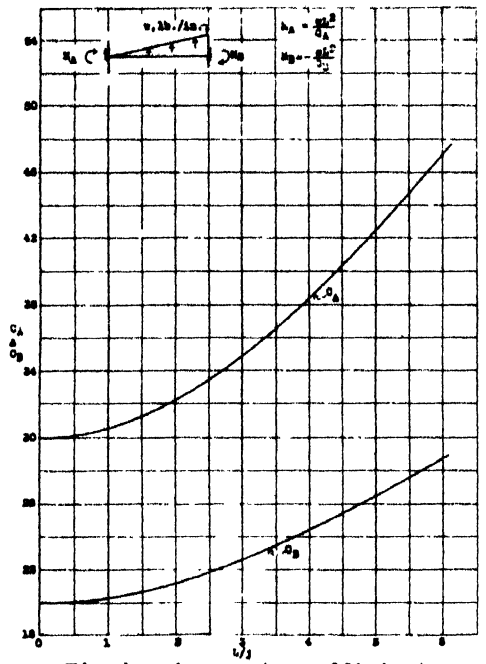
Fixed-end moment coefficient.
Uniform Load.

Fig. A11-48



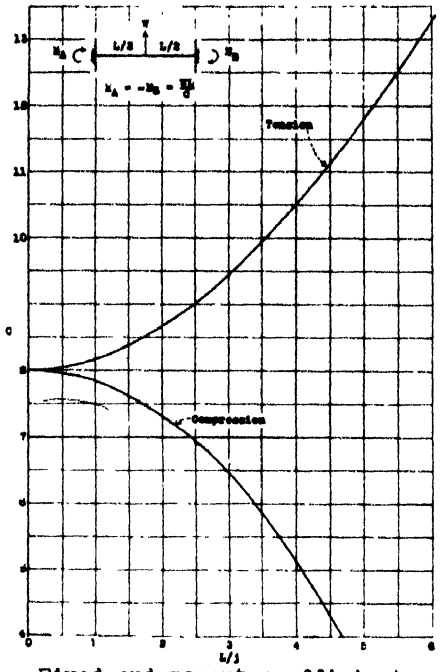
Fixed-end moment coefficient.
Uniformly varying load.
Axial compression.

Fig. A11-49



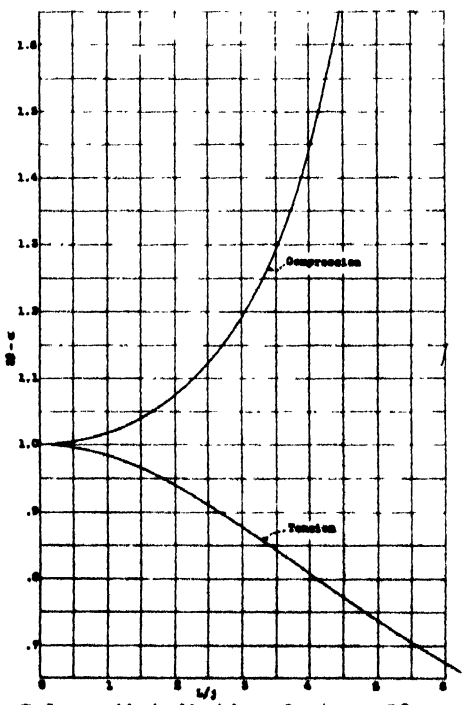
Fixed-end moment coefficient.
Uniformly varying load.
Axial tension.

Fig. A11-50



Fixed-end moment coefficient.
Concentrated load at mid-span.

Fig. A11-51



Column distribution factor. $2\beta - \alpha$.

Fig. A11-54

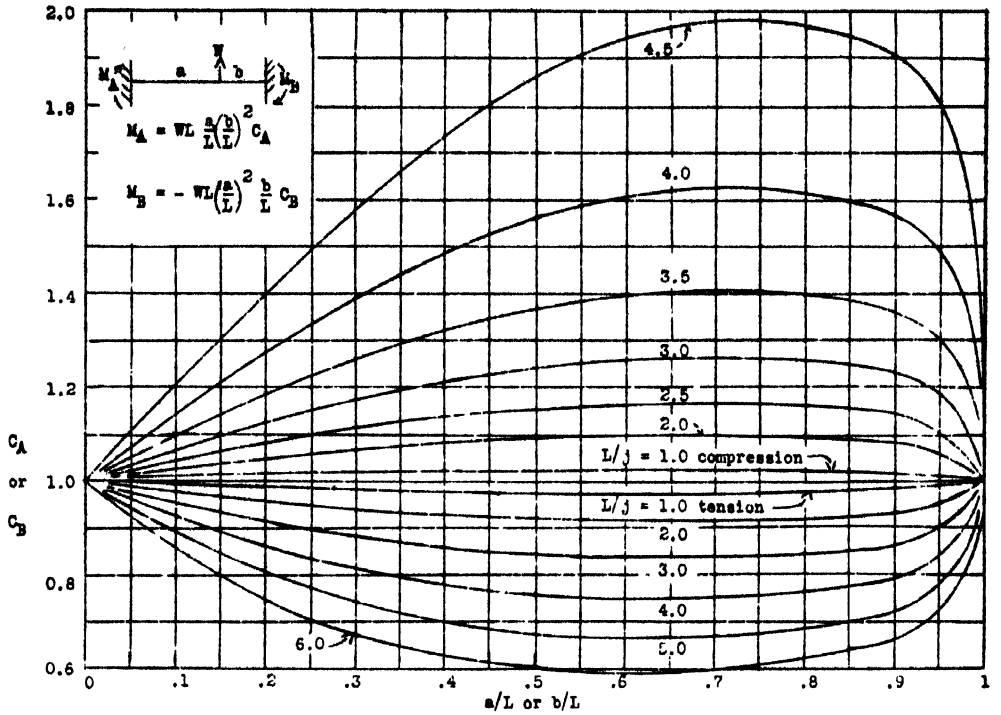


Fig. A11-52 Fixed-end moment coefficient. Concentrated load. REF. NACA T.N. 934

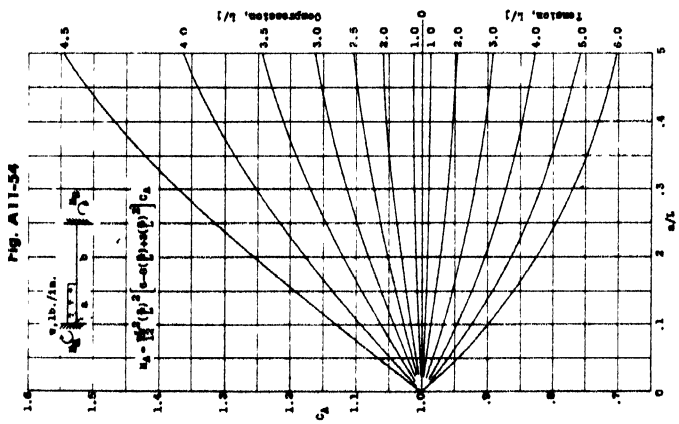


Fig. A11-54 Fixed-end moment coefficient for M_A. Uniform load over part of the span.

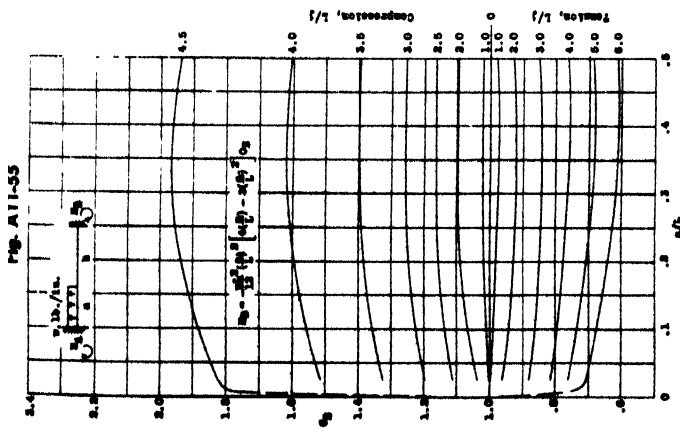


Fig. A11-55 Fixed-end moment coefficient for M_B. Uniform load over part of the span.

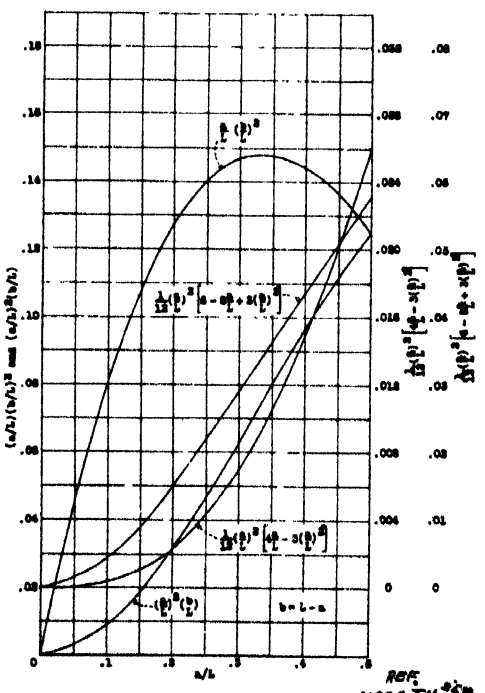


Fig. A11-53 REF. NACA T.N. 838

From Fig. A11.48 when L/j = 2.5 fixed end moments for uniform load = $wL^2/10.67$ = 1 x 96^2/10.67 = 865 in. lb.

Span CD

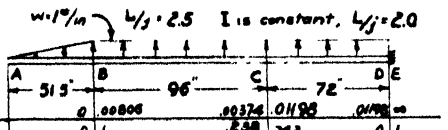
K = I/L = 1/72 = .0139, L/j = 2.0

From Fig. A11.47 correction factor = .86, hence $K_{CD} = K_{DC}$ = .86 x .0139 = .01198. Carry over factor from Fig. A11.46 = .62. Fixed end moments from Fig. A11.48 = $wL^2/11.2$ = 1 x 72^2/11.2 = 462

The distribution factor at joint C equals (.00374/.00374 + .01198) = .238 to CB and the remainder .762 to CD.

The balancing and carry over process is similar to that in Example Problem #4.

Fig. A11-57



Stiff. Fact. K	0	.00806	.00374	.01198	.01198	∞
Distribution Fac.	0	1	.238	.762	0	1
C.O. Factor	0	78	0	.62	.62	
Fixed End Mom.	-865	865	-865	462	-462	
Balance Joint B	0	48				
C.O. to C			13.2			
Bal. Joint C			146.0	243.8		
Carry-over		0			148	
Balance D					0	314
Carry over				0		
Final Mom.	-865	865	-705.8	705.8	-314	314

Comparing these results with those of Problem #3 we find moment at C is increased 15.7 percent and that at D is decreased 8.5 percent. For larger values of L/j the difference would be greater.

Example Problem #13

Fig. A11.58 shows the upper wing of a biplane. The wing beams are continuous over 3 spans. The distributed air loads on the front beam are shown in the figure, also the axial loads on front beam induced by the lift and drag truss. The bay sections of the spruce are shown in Fig. A11.58. The moment of inertia in each span will be assumed constant, neglecting the influence of tapered filler blocks at strut points.

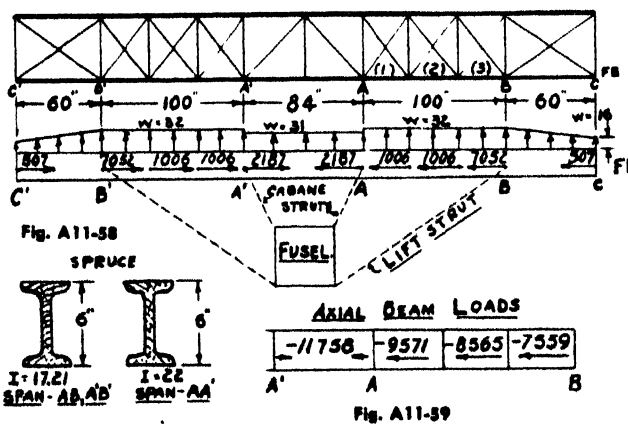


Fig. A11-58

Fig. A11-59

Fig. A11.59 shows the total beam axial loads in the various portions of the beam by adding the values shown in Fig. A11.58. The outer span AB due to the axial loads induced by drag wires of drag truss is subjected to a varying load. As is customary in design of such wing beams the axial load in span AB will be taken as equal to the average load or (-9571-8565-7559)/3=-8565#.

The beam bending moments at the support points will be determined by the moment distribution method.

Calculation of Factors:-

Span AB

I = 17.21, L = 100, I/L = .172

E = 1300,000, P = 8565

$$j = \sqrt{\frac{EI}{P}} = \sqrt{\frac{1300{,}000 \times 17.21}{8565}} = 51.1$$

L/j = 100/51.1 = 1.96

From Fig. A11.47 when L/j = 1.96, correction factor = .86 for fixed far end and .52 for pinned far end. Therefore

K_{AB} = .52 x .172 = .0895

K_{BA} = .86 x .172 = .148

From Fig. A11.46, when L/j = 1.96, the carry over factors are:-

$C.O._{BA}$ = .62, and zero from A to B since B is considered in its true state or freely supported. From Fig. A11.48 when L/j = 1.96 equation for fixed end moment for uniform load = $wL^2/11.25$ = 32 x $\overline{100}^2/11.25$ = 28420"#.

The overhand moment M_{BC} = 60 x 26.6 x (32 + 16)/2 = 38300"#.

Center Span AA':-

I = 22, I/L = 22/84 = .262, P = - 11758

$$j = \sqrt{\frac{1{,}300{,}000 \times 22}{11758}} = 49.4$$

L/j = 84/49.4 = 1.70

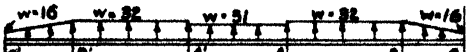
$K_{AA'} = K_{A'A}$ = .262 x .895 = .234

C.O. Factor = .585

Fixed end moment = $wL^2/11.35$ = 31 x $\overline{84}^2/11.35$ = 19300"#

The moment distribution process is given in Fig. A11.60. If the axial loads were neglected, the bending moment, at support A and A' would be 19480, thus the axial influence increases the moment at A approximately 7.5 percent.

Fig. A11-60



K Value	0	.148	.0095	.234	.234	.0095	.148	0
Distri. Factor	0	1	.276	.724				
C.O.Factor	0	.62	0	.362	.362	0	.62	0
F.E. Mom.	-58300	20420	-20420	19300	-19300	20420	-20420	58300
Bal. B' & B	0	9980					-9980	0
C.O.			6125			6125		
Bal. A' & A			868	2167	-2167	-868		
C.O.		0		-1265	1265		0	
Bal. A' & A			347	918	-918	-347		
C.O.		0		-536	536		0	
Bal. A' & A			148	390	-390	-148		
C.O.		0		-228	228		0	
Bal.			63	165	-165			
Final. Mom.	-58300	58300	-20909	20909	-20909	20909	-58300	58300

Example Problem #14

Fig. A11.61 shows a triangular truss composed of two members fixed at A and B and rigidly joined at C to the axle bar. Let it be required to determine the end moments on the two members considering the effect of axial loads on joint rotation and translation.

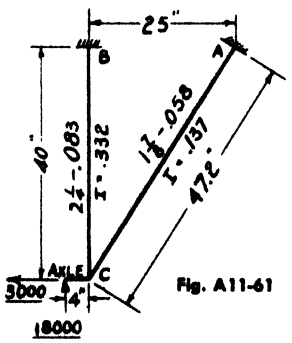


Fig. A11-61

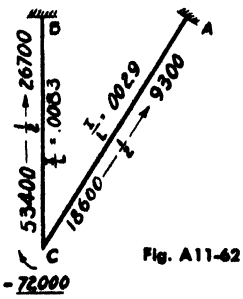


Fig. A11-62

Solution:-

The magnitude of the axial loads in the members is influenced by the unknown restraining moments at A and B. To obtain a close approximation of the axial loads, the end moments in the two members will be determined without consideration of axial loads. Thus the external joint moment of 4 x 18000 = 72000 in. lb. at C is distributed between the two members as shown in Fig. All.62. With the member end moments known the axial loads and shear reactions at A and B can be found by statics. The resulting axial loads are

P_{AC} = 10400# and P_{BC} = - 27150# and the shear reactions, S_A = 590# and S_B = 2000#.

With the axial loads known the modified beam factors can be determined.

For member BC

P = - 27150, I/L = .0083, I = .332

$$j = \left(\frac{29{,}000{,}000 \times .332}{27150}\right)^{1/2} = 18.82, \quad L/j = \frac{40}{18.82} = 2.12$$

From Fig. All.47, stiffness factor = .82 x .0083 = .00681

From Fig. All.46 C.O. Factor = .66

For Member AC

P = 10400#, I/L = .0029, I = .137

$$j = \sqrt{\frac{29{,}000{,}000 \times .137}{10400}} = 19.58, \quad \frac{L}{j} = \frac{47.20}{19.58} = 2.42$$

Stiffness factor = .0029 x 1.18 = .00342

C.O. factor = .39

Fig. All.63 shows the moment distribution solution which includes the effect of axial loads on joint rotation. Comparing the results in Figs. All.62 and 63, the moment M_{CA} of 24050 is 29 percent larger than that in Fig. 62, and the moment at B is 18 percent larger. The effect on the axial loads of these new final moments will be quite small, and thus further revision is unnecessary.

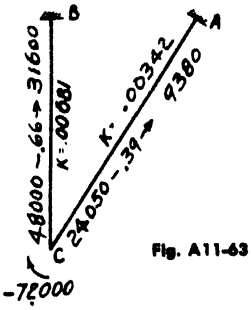


Fig. A11-63

Effect on End Moments Due to Translation of Joint C Due to Axial Loads.

The movement of joint C normal to each member will be calculated by virtual work. (Reference Chapter A7). Fig. All.64 shows the virtual loading of 1# normal to each member at C. The Table shows the calculation of the normal deflections at C.

Table

Mem.	L/AE	S	U_a	$\frac{S_{u_a} L}{AE}$	U_b	$\frac{S_{u_b} L}{AE}$
AC	.0000049	10400	1.89	.0962	1.6	.0816
BC	.00000244	-27150	-1.60	.1060	-1.89	.1250
				.202		.207

Thus the deflection of joint C normal to BC equals .168" in the direction assumed for the unit load, and the deflection of C normal to AC = .1778".

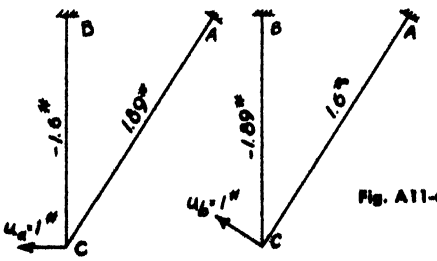


Fig. A11-64

The fixed end moments due to support deflection equals $M = 6EId/L^2$ as derived in Art. A11.7. However, the secondary moments due to axial loads times lateral deflection modify this equation. "James" has shown that the modified equation is,

$$M_{\text{fixed end}} = \frac{6EId}{L^2(2\beta-\alpha)}, \text{ if } K = \frac{I}{L} \text{ and } R = \frac{d}{L}, \text{ than}$$

$$M = \frac{6KER}{2\beta-\alpha},$$

Fig. A11.56 shows a plot of $2\beta-\alpha$ against L/j. For Member BC:-

$R = .202/40 = .00505 \quad K = I/L = .0083,$

$2\beta-\alpha = 1.08$ for $L/j = 2.12$.

Hence, fixed end moments due to translation of joint C equals-

$$M_{BC} = M_{CB} = \frac{6 \times .0083 \times .00505 \times 29{,}000{,}000}{1.08} = -6750''\#$$

For Member AC

$R = .207/47.2 = .00438 \quad K = .0029, \quad 2\beta-\alpha = .92$ when $L/j = 2.42$ and member is in tension. hence

$$M_{AC} = M_{CA} = \frac{6 \times .00438 \times .0029 \times 29{,}000{,}000}{.92} =$$

$$-2400''\#$$

The signs are minus because inspection shows that the moments tend to rotate ends of members counter clockwise. (Ref. Art. A11.2)

Fig. A11.65 shows the moment distribution for these moments. The magnitude of the moment at B is 6.7 percent of that in Fig. A11.63 and 10.4 percent at Joint C, however, it is relieving in this example.

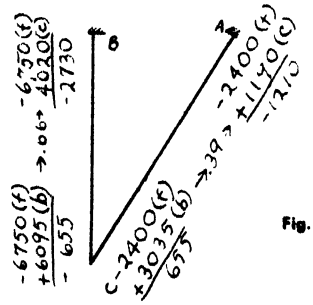


Fig. A11-65

For a truss involving many members, joint translations can be found more conveniently by use of the "Williot" diagram.

Generally speaking the effect of joint translation in trussed rigid joint structures is of secondary importance and is usually neglected.

A11.15 Problems

(1) By the moment distribution method, determine the beam bending moments at support points B, C and D for the beam and loading of Fig. A11.66. Beam section is constant thru-out. Draw beam bending moment diagram.
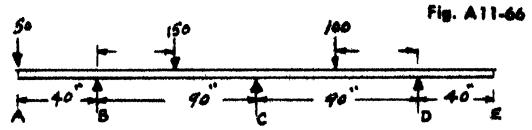


Fig. A11-66

(2) In Fig. A11.66 take free end (E) as fixed and determine complete bending moment diagram.

(3) In Fig, A1.66 take free end (E) as 50% fixed and free end (A) as freely supported and determine beam bending moment diagram.

(4) For the beam and loading of Fig. A11.67 determine the beam bending moment at points A, B and C, D. The moment of inertia is different in each span as shown.

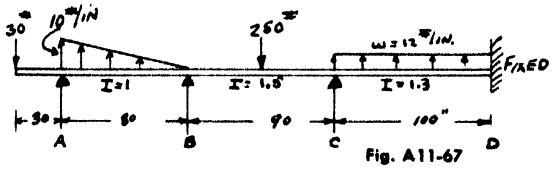


Fig. A11-67

(5) Fig. A11.68 shows a 1-1/4 - .058 round 24ST aluminum alloy tube supported on five supports and carrying the distributed load as shown. Supports B and D settle .20 inch and supports A and E settle .60 inch. Determine the beam bending moments over the five support points. I of tube equals .038 in and E = 10 x 10 psi.

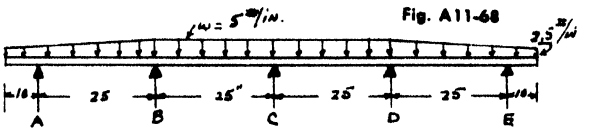


Fig. A11-68

(6) Determine the bending moment diagram for the truss and loading of Fig. A11.69. Points A and B are fixed and C is a rigid joint. Neglect effect of joint translation due to member axial loads. Also neglect effect of axial load on values of stiffness and carry over factors and magnitude of fixed end moments.

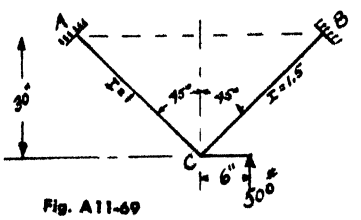


Fig. A11-69

(7) Same as problem (6) but consider point B as pinned.

(8) Same as problem (6) but consider point A is pinned and B is 50 percent fixed.

(9) Draw the bending moment diagram for the structure and loading of Fig. A11.70. The lateral loads are applied at the midpoint of each member. Neglect effect of joint translation due

to member axial loads, or effect of axial load on beam stiffness and carry over factors and the fixed end moments.

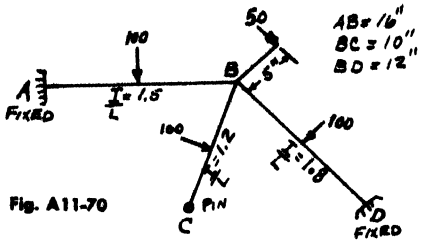


Fig. A11-70

(10) Same as Problem (9) but assume C is fixed and D is pinned.

(11) The cantilever truss of Fig. A11.71 is subjected to the panel point loading as shown. In addition two intermediate loads are applied to the members in the end panel and an external joint moment at joint (A) of 2500 in lb. Determine end moments on all members, neglecting effect of axial load in members.

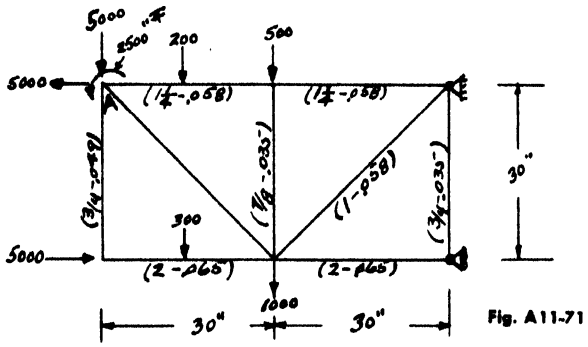


Fig. A11-71

(12) Same as (11) but consider effect of primary axial member loads on values of stiffness and carry-over factors and the values of the fixed-end moments.

(13) Fig. All.72 illustrates a continuous 3 span wing beam, carrying a uniform air load of 20#/in. Determine the beam bending moments at a strut points A and B. Take

$I_{AB} = 17$ in. , $I_{AA'} = 20$ in. and $E = 1.3 \times 10^6$ in.^{4}

Neglect effect of support deflection due to strut axial deformation.

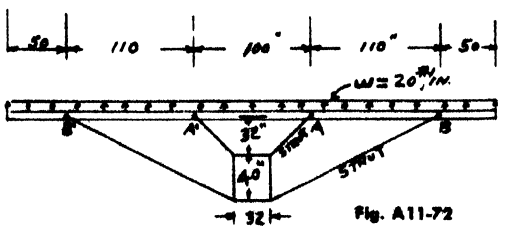


Fig. A11-72

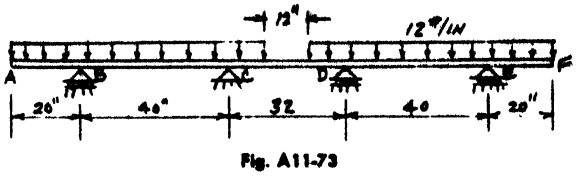


Fig. A11-73

(14) In the loaded beam of Fig. All.73, the supports B and E of the elevator beam deflect 0.1 inch more than supports C and D. Compute the resultant bending moments at the supports and find reactions. EI = 320,000 lb. in. sq.

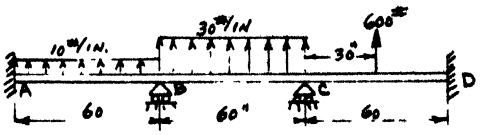


Fig. A11-74

(15) For the loaded beam of Fig. All.74, calculate support bending moments and beam reactions. EI is constant.

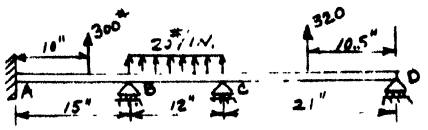


Fig. A11-75

(16) For the loaded beam in Fig. All.75 find bending moments at support points and draw final bending moment and shear diagrams. EI is constant.

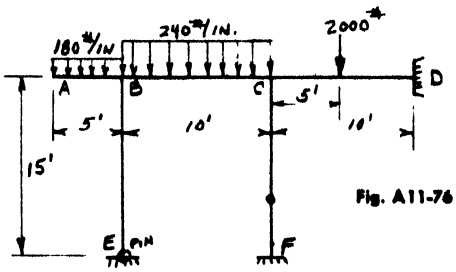


Fig. A11-76

(17) Calculate and draw the bending moment diagram for the loaded structure in Fig. All.76. EI is constant.

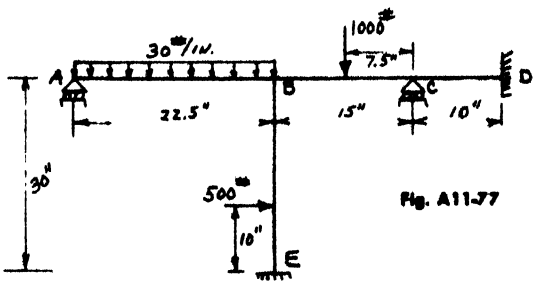


Fig. A11-77

(18) Calculate and draw the bending moment diagram for the loaded structure in Fig. A11.77. EI is constant.

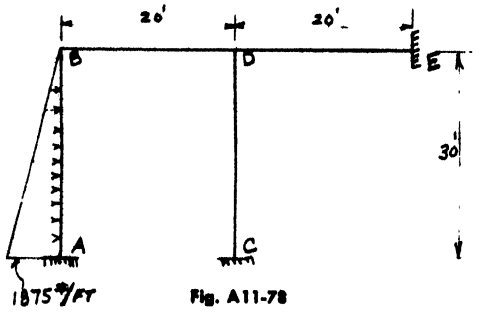


Fig. A11-78

(19) Calculate bending moments at points A B C D and E of the structure in Fig. A11.78. I_{BE} = 60, I_{CD} = 60, I_{AB} = 120 in.⁴

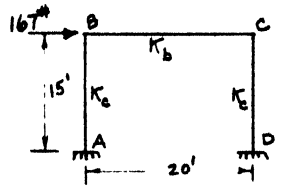


Fig. A11-79

(20) For the loaded structure in Fig. A11.79 locate points of contraflexure in the columns for the following three cases of relative stiffners of the members.

(a) $K_b = 2K_c$; (b) $K_b = K_c$; (c) $K_b = K_c/2$.

A11.16 Torsional Shear Flow in Multiple Cell Beams By Method of Successive Corrections.

Introduction. In Chapter A5, the shear flow distribution between the cells of a multiple cell beam structure under pure torque was determined by writing certain equations based on the following facts:-

(1) The summation of the external torsional moment and the internal resisting shear flow force system about an axis normal to the plane of the torsional moment must equal zero.

(2) The angular twist θ for each cell of the structure must be the same.

Equations expressing these facts were written in terms of the unknown constant shear flows q in each cell. Thus for a two cell structure, two equations involving two unknowns q_1 and q_2 could be written. Likewise for a three cell structure, three equations could be written involving three unknowns q_1, q_2 and q_3 and so on for any number of cells.

For a structure of three or more cells, the numerical work in solving a number of equations become appreciable, thus the method of *Successive Corrections to be explained provides a simple method as well as a rapid method for solving structures involving a number of cells. Since the method of successive corrections is similar in nature or method of procedure to the well-known "Moment Distribution" method explained in detail in the previous part of this chapter, the student should obtain a good understanding of the moment distribution process before studying the method to be presented here on the shear flow distribution in multiple cell structures.

*Based on Paper, "Numerical Transformation Procedures for Shear Flow Calculations" by S.U. Benscoter. Journal, Institute of Aeronautical Sciences, Aug. 1946.

Single Cell Formulas. (Ref. Chapter A5)

The following equations are taken from Chapter A5.

From $\Sigma M_x = 0$, (Fig. 1)

$T - 2Aq = 0$, whence

$$T = 2Aq \quad \text{--------(1)}$$

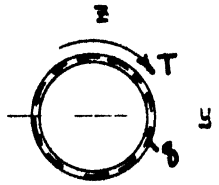


Fig. 1

where T = external torque (in.lbs.)

q = constant internal resisting shear flow. (lbs./in.)

A = area of cell interior. (in.²)

Equation (1) can be written,

$$q = \frac{T}{2A} \quad \text{--------(2)}$$

The relationship between the shear flow and the angular rate of twist θ per unit length of the cell is expressed by the following equation if q is constant around cell.

$$q = \frac{2AG\theta}{\Sigma L/t} \quad \text{--------((3)}$$

where,

G = modulus of rigidity
L = length of any cell wall portion of constant thickness
t = thickness of any cell wall portion
θ = twist per unit length of cell in radians

Equation (3) can be written,

$$2A\theta = \frac{1}{G} q \Sigma \frac{L}{t} \quad \text{--------(4)}$$

The right hand side of equation (4) represents the total shearing strain around the cell wall due to the shear flow q.

If it was assumed that the shear flow q was such as to produce a unit rate of twist or G θ = 1, then equation (4) could be written

$$2A = q \Sigma \frac{L}{t} \quad \text{--------(5)}$$

or

$$q = \frac{2A}{\Sigma \frac{L}{t}} \quad \text{--------(6)}$$

A11.17 Explanation of Successive Correction Method.

Consider a two cell tube as shown in Fig. a. To begin with assume each cell as acting inde-

pendently, and subject cell (1) to such a shear flow q_1 as to make $G\Theta_1 = 1$.

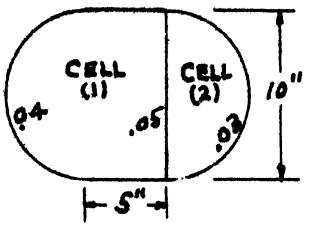


Fig. a

Then from equation (6),

$$q_1 = \frac{2A_1}{\Sigma \frac{L}{t}} = \frac{2 \times 89.3}{\frac{25.7}{.04} + \frac{10}{.05}} =$$

$$\frac{178.6}{842} = 0.212\#/\text{in.}$$

Fig. b. shows the results.

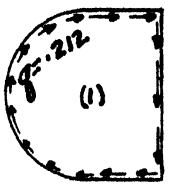


Fig. b

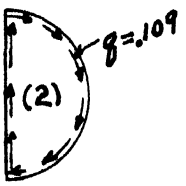


Fig. c

In a similar manner assume cell (2) subjected to a shear flow q_2 to produce a unit rate of twist of $G\Theta_2 = 1$. Then,

$$q_2 = \frac{2A_2}{\Sigma \frac{L}{t}} = \frac{2 \times 39.3}{\frac{10}{.05} + \frac{15.7}{.03}} = \frac{78.6}{723} = 0.109\#/\text{in.}$$

Fig. c shows the results.

Now assume the two cells are joined together with the interior web (1-2) as a common part of both cells. See Fig. d. The interior web is now subjected to a resultant shear flow of $q_1 - q_2 = (.212 - .109) = .103\#/\text{in.}$ Obviously this change of shear flow on the interior web will cause the cell twist to be different for each cell instead of the same when the cells were considered acting separately. To verify this conclusion the twist measured by the term $G\Theta$ will be computed for each cell.

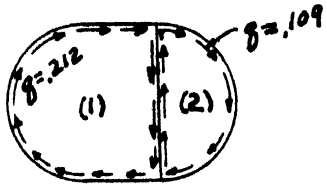


Fig. d)

Cell (1), $G\Theta_1 = \frac{1}{2A_1} \Sigma q \frac{L}{t} =$

$$= \frac{1}{2 \times 89.3} \left[.212 \times \frac{25.7}{.04} + (.212 - .109) \frac{10}{.05} \right] = 0.875$$

Cell (2), $G\Theta_2 = \frac{1}{2A_2} \Sigma q \frac{L}{t} =$

$$= \frac{1}{2 \times 39.3} \left[.109 \times \frac{15.7}{.03} - (.212 - .109) \frac{10}{.05} \right] = 0.4375$$

Since Θ_1 must equal Θ_2 if the cross-section is not to distort from its original shape, it is evident that the above shear flows are not the true ones when the two cells act together as a unit.

Now consider cell (1) in Fig. d. In bringing up andattaching cell (2) the common web (1-2) is subjected to a shear flow $q_2 = -.109\#/\text{in.}$ (counterclockwise with respect to cell (1) and therefore negative), in addition to the shear flow $q_1 = .212$ of cell (1). The negative shear flow $q_2 = -.109$ on web 1-2 decreases the twist of cell (1) as calculated above with the resulting value for $G\Theta_1 = 0.875$ instead of 1.0 as started with.

Thus in order to make $G\Theta_1 = 1$ again, we will have to add a constant shear flow q' to cell (1) which will cancel the negative twist due to q_2 acting on web (1-2). Since we are considering only cell (1) we can compare cell wall strains instead of cell twist since in equation 4, the term 2A is constant.

Thus adding a constant shear flow q'_1 to cancel influences of q_2 on web 1-2, we can write:

$$q'_1 \left(\Sigma \frac{L}{t}\right) \text{ cell (1)} - q_2 \left(\frac{L}{t}\right)_{\text{web 1-2}} = 0$$

hence

$$q'_1 = q_2 \left[\frac{\left(\frac{L}{t}\right) \text{ web 1-2}}{\left(\Sigma \frac{L}{t}\right) \text{ cell (1)}} \right] \text{ - - - - - - - - -(7)}$$

Substituting values in equation (7)

$$q'_1 = q_2 \left[\frac{\frac{10}{.05}}{\frac{25.7}{.04} + \frac{10}{.05}} \right] = \frac{200}{842} q_2 = .237\, q_2$$

Thus to make $G\Theta_1$ equal to 1 we must correct the shear flow in cell (1) by adding a constant shear flow equal to .237 times the shear flow q_2 in cell (2) which equals .237 x .109 = .0258#/in. Since this shear flow is in terms of the shear flow q_2 of the adjacent cell it will be referred to as a correction carry over shear flow, and will consist of a carry over correction factor times q_2.

Thus the carry over factor from cell (2) to cell (1) can be written as

$$\text{C.O.F.}_{(2 \text{ to } 1)} = \frac{\left(\frac{L}{t}\right) \text{ web (1-2)}}{\left(\Sigma \frac{L}{t}\right) \text{ cell (1)}} \text{ which equals .237}$$

as found above in substitution in equation (7)

Now consider cell (2) in Fig. d. In bringing up and attaching cell (1), the commom web (2-1) is subjected to a shear flow of $q_1 = -0.212\#/\text{in.}$ (counterclockwise as viewed from cell 2 and therefore negative). This additional shear flow changes $G\Theta_2$ twist of cell (2) to a relative value of 0.4375 instead of 1.0 (see previous $G\Theta_2$ calculations). Therefore to make $G\Theta_2$ equal to 1.0 again, a corrective constant shear flow q'_2 must be added to cell (2) to cancel the twist effect of $q_1 = 0.212$ on web (2-1). Therefore we can write,

$$q_2' \left(\Sigma \frac{L}{t}\right) \text{ cell (2)} - q_1 \left(\frac{L}{t}\right) \text{ web (2-1)} = 0$$

hence

$$q_2' = \frac{q_1 \left(\frac{L}{t}\right) \text{web (2-1)}}{\left(\Sigma \frac{L}{t}\right) \text{ cell (2)}} \qquad \text{-----------(8)}$$

Substituting in equation (8):-

$$q_2' = q_1 \left(\frac{200}{723}\right) = .277 q_1 = .277 \times .212 = .0587\#/\text{in.}$$

Thus the carry over factor from cell (1) to cell (2) in terms of q_1 to make $G\theta_2 = 1$ again can be written

$$\text{C.O.F.}_{(1 \text{ to } 2)} = \frac{\left(\frac{L}{t}\right) \text{ web (2-1)}}{\left(\Sigma \frac{L}{t}\right) \text{ cell (2)}} = \frac{200}{723} = .277$$

Fig. e shows the constant shear flows q_2' and q_1' that were added to make $G\theta = 1$ for each cell. However these corrective shear flows were added assuming the cells were again independent of each other or did not have the common web (1-2). Thus in bringing the cells together again the interior web is subjected to be resultant shear flow of $q_1' - q_2'$. In other words if we were to add the shear flows of Fig. e to those of Fig. d, we would not have $G\theta_1$ and $G\theta_2$ equal to 1. The resulting values would be closer to 1.0 then were found for the shear flow system of Fig. d.

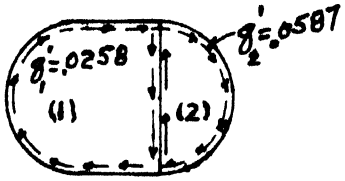


Fig. e

Considering Fig. e, we will now add a second set of corrective shear flows q_1'' and q_2'' to cells (1) and (2) respectively to make $G\theta_1$ and $G\theta_2 = 1$ for cells acting independently.

Considering cell (1), and proceeding with same reasoning as before,

$$q_1'' \left(\Sigma \frac{L}{t}\right) \text{ cell (1)} - q_2' \left(\frac{L}{t}\right) \text{ web 1-2} = 0$$

hence

$$q_1'' = \frac{q_2' \left(\frac{L}{t}\right) \text{1-2}}{\Sigma \left(\frac{L}{t}\right) \text{ cell(1)}} = .0587 \times .237 = .0139\#/\text{in.}$$

or

$$q_1'' = (\text{C.O.F.})_{2 \text{ to } 1} \text{ times } q_2' = .237 \times .0587 = .0139$$

Considering Cell (2)

$$q_2'' = q_1' (\text{C.O.F.})_{1 \text{ to } 2} = .0258 \times .277 = .00717\#/\text{in.}$$

Fig. f shows the resulting second set of corrective constant shear flows for each cell.

Since our corrective shears flows are rapidly getting smaller, the continuation of the process depends on the degree of accuracy we wish for the final results. Suppose we add one more set of corrective constant shear flows q_1''' and q_2'''. Using the carry over correction factors previously found we obtain,

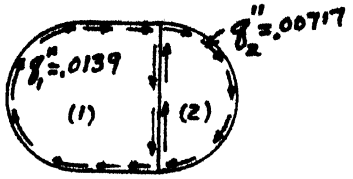


Fig. f

$$q_1''' = .237 \times .00717 = .0017\#/\text{in.}$$

$$q_2''' = .277 \times .0139 = .00385\#/\text{in.}$$

Fig. g shows the results

The final or resulting cell shear flows then equal the original shear flows plus all corrective cell shear flows, or

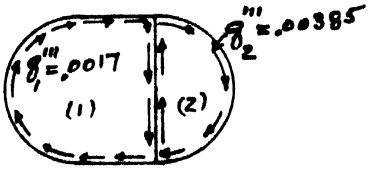


Fig. g

$$q_1(\text{final}) = q_1 + q_1' + q_1'' + q_1'''$$

$$q_2(\text{final}) = q_2 + q_2' + q_2'' + q_2'''$$

Fig. h shows the final results.

To check the final twist of each cell the value $G\theta$ will be computed for each cell using the q values in Fig. h.

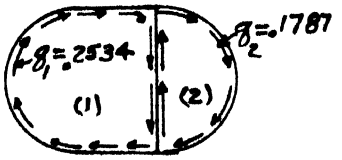


Fig. h)

Cell (1)

$$G\theta_1 = \frac{1}{2 \times 39.3}\left[.2534 \times \frac{25.7}{.04} + .0747 \times \frac{10}{.05}\right] = .997$$

$$G\theta_2 = \frac{1}{2 \times 39.3}\left[.1787 \times \frac{15.7}{.03} - .0747 \times \frac{10}{.05}\right] = .997$$

A11.18 Use of Operations Table to Organize Solution by Successive Corrections.

Operations Table 1 arranges the calculations so that the steps dealing with the corrective shear flows can be carried out rapidly and with a minimum of thought.

OPERATIONS TABLE 1

		Cell 1	Cell 2
1	C.O. Factor	.277	.237
2	Assumed q	.212	.109
3	C.O. q	.0258	.0587
4	C.O. q	.0139	.00717
5	C.O. q	.0017	.00385
6	Final q = Σ	.2534	.1787
7	T = 2Aq	45.2"#	14.1"#
8	Total T	59.3"#	

Explanation of Table 1

Line 1 gives the carry over factors for each cell, computed as explained before. Line 2 gives the necessary constant shear flow q in each cell to give unit rate of twist to each cell acting independently. ($G\theta = 1$). Line 3 gives the first set of constant corrective shear flows to add to each cell. The corrective q referred to as the carry over q or C.O.q in the table consists of the q in the adjacent cell times the C.O. factor of that cell.

Thus .237 x .109 = .0258 is carry over from cell (2) to cell (1) and .277 x .212 = .0587 is carry over from cell (1) to cell (2).

Line 4 gives the second set of corrective carry over shear flows, namely .277 x .0258 = .00717 to cell (2) and .237 x .0587 = .0139 to cell (1). Line 5 repeats the corrective carry over process once more. Line 6 gives the final q values which equal the original q plus all carry over q values.

Example Problem #1 (2 Cells)

Determine the internal shear flow system for the two cell tube in Fig. A11.80 when subjected to a torque of 20,000 in.lbs.

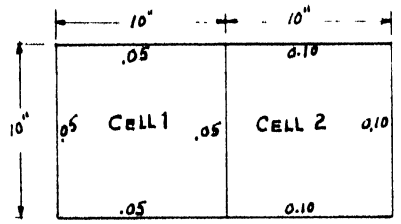


Fig. A11-80

OPERATIONS TABLE 2

		Cell 1	Cell 2
1	C.O. Factor	0.4	0.25
2	Assumed q	25.0	40.0
3	C.O. q	10	10
4	C.O. q	2.5	4
5	C.O.oq	1.0	1
6	C.O. q	0.25	0.4
7	C.O. q	0.10	0.1
8	Final q = Σ	38.85	55.5
9	2Aq	7770	11100
10	T (Total)	18870	
11	q for T=20,000	41.2	58.9

Explanation of solution as given in Table (2):

Line 1 gives the values of the carry over factors. The values are calculated as follows:

C.O. factor cell (1) to cell (2):

$$C.O._{(1-2)} = \frac{(\frac{L}{t}) \text{ web } 1\text{-}2}{\Sigma\,(\frac{L}{t}) \text{ cell } 2} = \frac{\frac{10}{.05}}{\frac{10}{.05}+\frac{30}{0.1}} = .40$$

$$C.O._{(2-1)} = \frac{(\frac{L}{t}) \text{ web } 2\text{-}1}{\Sigma\,(\frac{L}{t}) \text{ cell } 1} = \frac{\frac{10}{.05}}{\frac{40}{.05}} = .25$$

Line 2 gives the shear flow q in each cell, when it is assumed each cell is acting separately and is subjected to a unit rate of twist or $G\theta = 1$.

The calculations for the q values are as follows:-

For cell (1)

$$q_1 = \frac{2A_1}{\Sigma\,(\frac{L}{t}) \text{ cell } 1} = \frac{2 \times 100}{\frac{40}{.05}} = .25$$

For cell (2)

$$q_2 = \frac{2A_2}{\Sigma\,(\frac{L}{t}) \text{ cell } 2} = \frac{2 \times 100}{\frac{10}{.05}+\frac{30}{0.1}} = .4$$

A_1 and A_2 equal cell area of cells (1) and (2) respectively. L = length of wall element and t its corresponding thickness.

In order not to start out with decimal values of q, the values above will arbitrarily be multiplied by 100 to make q_1 = 25#/in. and q_2 = 40#/in. Since we want only relative values of terms this is permissible. These values are shown in line 2 of Table (2). The corrective carry over process proper is started in line 3 of table (2). In cell (1) the amount carried over of q = 25 to cell (2) equals the C.O. factor times 25 or 0.4 x 25 = 10 which is written along the vertical line under cell (2). Likewise in cell (2) the amount of q_2 = 40 that is carried over to cell (1) equals the C.O. factor times q_2 or .25 x 40 = 10, which is written along the vertical line under cell (1).

The second set of corrective carry over constant shear flows are given in line 4 of Table (2), thus, .4 of the q_1 = 10 = 4.0 is carried over to cell (2) and .25 x value of q_1 = 10 = 2.5 is carried over to cell (1). Line 5 repeats the process namely 0.4 x 2.5 = 1 to cell (2) and .25 x 4 = 1.0 to cell (1).

This process of carrying over values of q is continued until the values are small or negligible. Line 8 gives the final q values in each cell as the summation of the assumed q value plus all carry over values of q. Thus in cell (1) q = 38.85#/in. and for cell (2) q = 55.5. Line 9 gives the torque that these values of cell shear flow can produce.

$$T = 2Aq$$

For cell (1) T = 2 x 100 x 38.85 = 7770 in. lb.
For cell (2) T = 2 x 100 x 55.5 = 11100 in. lb.

Line 10 gives the sum of the above two values which equals 18870 in. lb.

The original requirement of the problem was the shear flow system for a torque of 20,000"#. Therefore the required q values follow by direct proportion, whence

$$q_1 = \frac{20000}{18870} \times 38.85 = 41.2\#/\text{in.}$$

$$q_2 = \frac{20000}{18870} \times 55.5 = 58.9\#/\text{in.}$$

These values are shown in line 11 of Table 2.

Check on twist of cells under final q values.

The relative total strain around each cell boundary is given by the term $\frac{1}{A} \Sigma q \frac{L}{t}$ for the cell

Thus for cell (1)

$$\frac{1}{A_1} \Sigma q \frac{L}{t} = \frac{1}{100}\left[41.2\ (\frac{30}{.05}) + (41.2 - 58.9)\ \frac{10}{.05}\right] = 212$$

For cell (2),

$$\frac{1}{A_2} \Sigma q \frac{L}{t} = \frac{1}{100}\left[(58.9 - 41.2)\ \frac{10}{.05} + 58.9 \times (\frac{30}{0.1})\right] = 212$$

Thus both cells have the same twist.

In the above calculations q_1 and q_2 act clockwise in each cell, hence the shear flow on the interior common web is the difference of the two q values.

Example Problem #2. Three cells

The three cell structure in Fig. A11.81 is subjected to an external torque of -100,000 in. lb. Determine the internal resisting shear flow pattern.

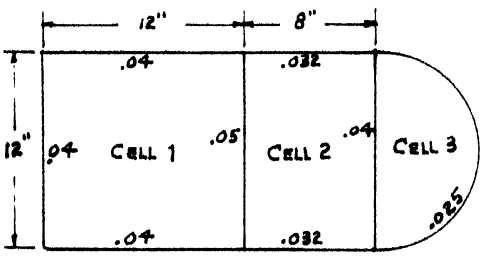


Fig. A11-81

OPERATIONS TABLE 3

		Cell 1	Cell 2	Cell 3
1	C.O. Factor	.23	.21 .284	.288
2	Assumed q	25.30	18.45	10.70
3	C.O. q	3.88	5.82 3.08	5.25
4	C.O. q	1.87	0.894 1.51	2.53
5	C.O. q	0.506	0.430 0.73	0.685
6	C.O. q	0.244	0.116 0.197	0.330
7	C.O. q	0.072	0.056 0.095	0.088
8	Final q = Σ	31.87	31.37	19.58
9	2Aq	9200	6020	2215
10	T (Total) =	9000 + 6020 + 2215 = 17435"#		
11	q - for T = 100,000	183	180	112.5

Explanation of Solution as given in Table 3:-

Cell (1)	Cell (2)	Cell (3)
$A_1 = 144$	$A_2 = 96$	$A_3 = 56.5$
$\Sigma \frac{L}{t} = 1140$	$\Sigma \frac{L}{t} = 1040$	$\Sigma \frac{L}{t} = 1055$

Shear flow q for $G\theta = 1$ for each cell acting independently:-

Cell (1) $q = \frac{2A_1}{\Sigma \frac{L}{t}} = \frac{288}{1140} = .253$

Cell (2) $q = \frac{2A_2}{\Sigma \frac{L}{t}} = \frac{192}{1040} = .1845$

Cell (3) $q = \frac{2A_3}{\Sigma \frac{L}{t}} = \frac{113}{1055} = .107$

To avoid small numbers these values of q are multiplied by 100 and entered on line 2 of the table. Calculation of carry factors as given in line 1 of Table 3.

Cell (1) to (2)

$$C.O._{(1-2)} = \frac{(\frac{L}{t}) \text{ web } 1\text{-}2}{\Sigma\ (\frac{L}{t}) \text{ cell } 2} = \frac{240}{1040} = .23$$

Cell (2) to (1)

$$C.O._{(2-1)} = \frac{(\frac{L}{t}) \text{ web } 2\text{-}1}{\Sigma\ (\frac{L}{t}) \text{ cell } 1} = \frac{240}{1140} = .21$$

Cell (2) to (3)

$$C.O._{(2-3)} = \frac{(\frac{L}{t}) \text{ web } 2\text{-}3}{\Sigma\ (\frac{L}{t}) \text{ cell } 3} = \frac{300}{1055} = .284$$

Cell (3) to (2)

$$C.O._{(3-2)} = \frac{(\frac{L}{t}) \text{ web } 2\text{-}3}{\Sigma\ (\frac{L}{t}) \text{ cell } 2} = \frac{300}{1040} = .288$$

The balance of the solution or procedure in Table 3 is the same as explained for Problem 1 in Table (2). It should be noticed that cell (2) being between two cells receives carry over q values from both adjacent cells and these two values are added together before being distributed or carried over again to adjacent cells. For example consider line 3 in Table (3) and cell (2). The q value 5.82 representing .23 x 25.3 is brought over from cell (1) and the q value 3.08 = .288 x 10.70 from cell (3). These two values are added together or 5.82 + 3.08 = 8.90. The carry over q to cell (1) is then .21 x 8.90 = 1.87 and to cell (3) is .284 x 8.90 = 2.53.

In line 8, the final q in cell (2) equals the original q of 18.45 plus all carry over q values from each adjacent cell.

Line 10 in Table (3) shows the total torque developed by the resultant internal shear flow is 17435"#. Since the problem was to find the shear flow system for a torque of -100,000 in. lb., the values of q in line 8 must be multiplied by the factor 100,000/17435.

Line 11 shows the final q values.

Example Problem 3. Four cells.

Determine the internal shear flow system for the four cell structure in Fig. A11.82 when

subjected to a torsional moment of -100,000 in. lb.

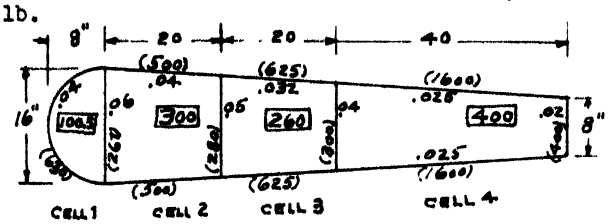


Fig. A11-82

OPERATIONS TABLE 4

		Cell 1	Cell 2	Cell 3	Cell 4		
1	C.O.F.	.173	.298	.153	.181	.078	.164
2	q	22.4	38.8	28.4	20.50		
3	C.O.	11.64	3.88	5.14	5.94	3.36	2.22
4	C.O.	2.69	2.00	1.68	1.38	0.36	0.73
5	C.O.	1.10	0.47	0.32	0.57	0.12	0.13
6	C.O.	0.15	0.19	0.12	0.08	0.02	0.15
7	Σq	37.95	52.60	40.23	23.83		
8	$2Aq$	7620	31560	22550	18900		
9	Total T = 80630						
10	q	47.1	65.3	49.9	29.41		

In Fig. A11.82 the values in the rectangles represent the cell areas. The values in () represent the L/t values for the particular wall or web. After studying example problems 1 and 2 one should have no trouble checking the values as given in Table 4. Line 10 shows the correction of q values to develop a resisting torque of 100,000"#. The multiplying factor is 100,000/80630.

A11.18 Problems

(1) Solve Problems 3 and 5 at the end of Chapter A5.

(2) The three box beam in Fig. A11.83 is subjected to an external torque of 600,000"#. Determine the internal shear flow distribution.

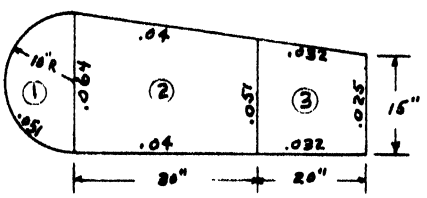


Fig. A11-83

(3) The two cell tube in Fig. A11.84 carries an external torque of -200,000"#. Determine the internal shear flow system.

(4) The 5-cell beam in Fig. A11.85 carries an external torque of 750,000"#. Calculate the internal shear flow system.

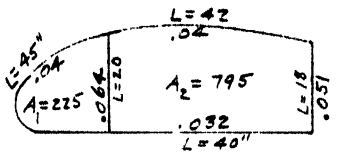


Fig. A11-84

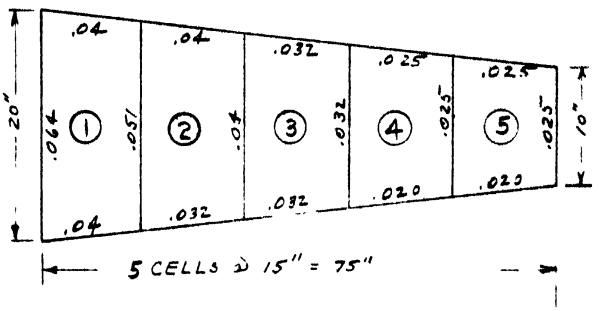


Fig. A11-85

CHAPTER A12
BENDING AND SHEAR DISTRIBUTION

A12.1 Introduction. In chapters A6 and A8 the magnitude and sense of the tendency of the external loads to shear or bend a beam were considered in detail. In this chapter, the manner in which the internal stresses resist these external applied loads is considered. Before the internal stress picture can be obtained, two facts must be known, namely,

(1) The manner in which the strain (shortening or lengthening) of a beam fiber varies with the location of the fiber in the beam when the beam bends in resisting the external loads.

(2) The stress-strain relationship or character of the material being used. Information concerning these two points comes chiefly from the results of tests and experiments. These experiments show that if a straight beam carries loads which lie in a plane which is also the plane of symmetry of the beam (see Fig. A12.1), the fibers on the upper portion of the beam will shorten, and those on the lower portion will lengthen and at some plane in between the beam fibers will suffer no strain or deformation. Thus, if two straight lines AB and CD are drawn on the beam side before the beam is bent, these lines will still be straight lines A"B' and C'D' after the beam is bent (if shearing deformation is neglected). This means that the unit strain of any fiber is directly proportional to the distance from the plane of zero stress (commonly referred to as the neutral plane or surface).

Furthermore, if the beam material is such that it possesses a straight stress-strain curve for the range of stresses which the external loads produce on the beam and the stress-strain curve is the same for both tension and compression, then the stress intensity will likewise vary directly as the distance from the neutral axis or plane.

With these conditions present, it is quite simple to obtain a true picture of the internal bending resisting forces and obtain an expression for the internal resisting moment in terms of the stress intensity and the geometrical properties of the beam cross-section.

Fig. A12-1

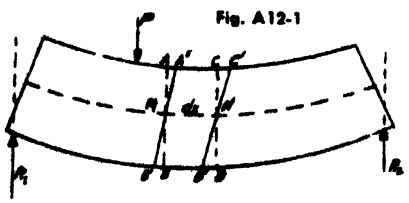
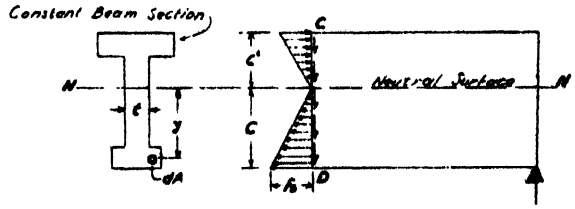


Fig. A12-2



A12.2 Neutral Axis Location - Beam Formula

Fig. A12.2 shows the free body of the right hand portion after the beam of Fig. A12-1 has been cut at section CD. The beam cross-section has been taken as shown. Let the neutral surface (plane of zero stress) be NN, the location of which is unknown as yet. Let the tension and compression forces on the face CD be represented by the arrows as shown. Let f_b represent the largest of these unit stresses and let dA be a differential area of the cross-section a distance y from the neutral surface, and let f_y represent the unit stress on this small area, dA. From similar triangles,

$$f_b : f_y = c : y \quad \text{or} \quad f_b y = f_y c \qquad \text{---------(1)}$$

hence, the unit stress on a fiber a distance y from the neutral surface.

$= f_y = f_b \frac{y}{c}$ and the total stress on the element dA is

$$\frac{f_b}{c} y \, dA \qquad \text{----------(2)}$$

The total tensile stress on the section below NN is

$$\frac{f_b}{c} \int_0^c y dA \qquad \text{----------(3)}$$

and the total compressive stress above NN is

$$\frac{f_b}{c} \int_0^{c'} y dA \qquad \text{----------(4)}$$

now, for equilibrium of the free body in the horizontal direction,

$$\Sigma H = 0 \text{ or } (3) = (4) \text{ or } \frac{f_b}{c} \int_0^c y dA = \frac{f_b}{c} \int_0^{c'} y dA$$

This means that $\int y dA$ above the neutral plane equals $\int y dA$ below NN, but since y is negative for all values below NN, it follows that $\int y dA$ for the entire section must be zero. This is the same relationship that locates the centroidal axis of the cross-section, and therefore, <u>the neutral plane or axis coincides with the centroidal axis of the cross-section.</u>

With the neutral axis located, an expression can now be obtained for the stress intensity.

The moment of the stress on the element dA, about the neutral axis NN is y times equation (2) or $y \frac{f_b}{c} ydA$, and the total resisting moment of all the stresses on the cross-section referred to the neutral axis NN, is $\int \frac{f_b}{c} y^2 dA$, since $\frac{f_b}{c}$ is constant, we can write: Resisting moment $= \frac{f_b}{c} \int y^2 dA$, but the term $\int y^2 dA$ equals the moment of intertia about the neutral axis and will be given the symbol I. Hence, resisting moment $= \frac{f_b}{c} I$. But, resisting moment = bending moment M, hence

$$M = f_b \frac{I}{c} \text{ - - - - - - - - - - - - - - - - - -(5)}$$

which is the well-known flexure formula, where M = bending moment at section in inch pounds.

I = moment of inertia about neutral axis

f_b= max. unit bending stress, which occurs on the most remote fiber at a distance c from the neutral axis. For the stress at any distance y from the neutral axis, replace c in formula (5) by term y.

The term $\frac{I}{c}$ in equation (5) is referred to as the section modulus and is a function of the size and shape of the cross-section.

A12.3 Flexural Shear Stress Distribution

Fig. A12.3 shows the same beam as in Fig. A12.1 with a notch cut out of the lower section of the beam as shown and treated as a free body in Fig. A12.4. The total pull on side CD = $\frac{f_b}{c} \int_{y_o}^{c} ydA$. The total pull on side EF = $\frac{f_b'}{c} \int_{o}^{c} ydA$. From the beam formula previously derived, $f_b = \frac{Mc}{I}$. Let M and M' equal external bending moment at beam sections CD and EF respectively and I and I' the moment of inertia of the beam sections at these same points. Hence, the total pull load on side

$$CD = \frac{M}{I} \int_{y_o}^{c} ydA \text{ - - - - - - - - - - - - - -(6)}$$

and similarly, total pull on side $EF = \frac{M'}{I'} \int_{y_o}^{c} ydA$

$$\text{- - - - - - - - - - - - - -(7)}$$

For equilibrium, ΣH for forces on block in Fig. A12.4 must = 0. Therefore total shear stress on section CE equals the difference between the values given by equations (6) and (7).

If the beam is of uniform section, that is, I = I' and c and y_o are the same in both expressions, then the resultant horizontal pull on block CDEF = $\frac{M - M'}{I} \int_{y_o}^{c} ydA$; writing ΣH = 0 for block, $f_s b\,dx = \frac{M - M'}{I} \int_{y_o}^{c} ydA$ or $f_s = \frac{M - M'}{Ibdx} \int_{y_o}^{c} ydA$.

But $\frac{M-M'}{dx} = \frac{dM}{dx} = V$ (external shear on section)

Therefore $f_s = \frac{V}{Ib} \int_{y_o}^{c} ydA$ - - - - - - - - -(8)

where f_s is the horizontal shearing unit stress (also vertical unit stress) on the cross section of a beam at a point distance y_o from neutral axis where the width is b and the external shear is V.

It is important to note that equation (8) applies only to beams of uniform section (constant I). In airplane wing and fuselage construction, the general case is for beams to taper in section, thus equation (8) cannot be used and resort must be made to the relationships expressed by equations (6) and (7).

A12.4 Example Problems Illustrating Application of Flexure Formula and Theory

Example Problem 1

Determine the maximum bending and shearing stress for the beam and loading as shown in Fig. A12.5. The cross-section of the beam is given in Fig. A12.6 and is constant through out the length of the beam. In general, the procedure is to calculate the reactions and draw shear and moment diagrams in order to obtain a complete picture of the shear and bending forces. This beam and loading is identical to that of Fig. A6.6. Since complete calculations for reactions, shear and moment diagrams were given there, the calculations are not repeated here, but the resulting shear and moment diagrams are re-drawn.

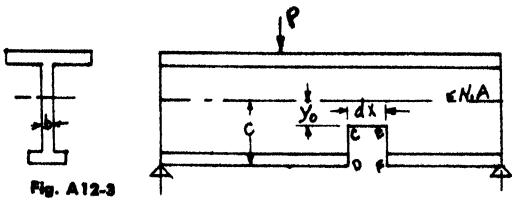


Fig. A12-3

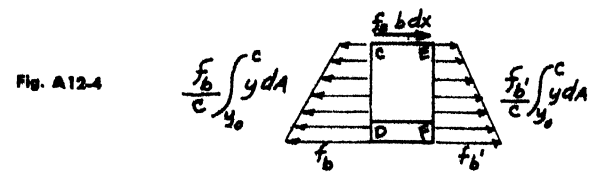


Fig. A12-4

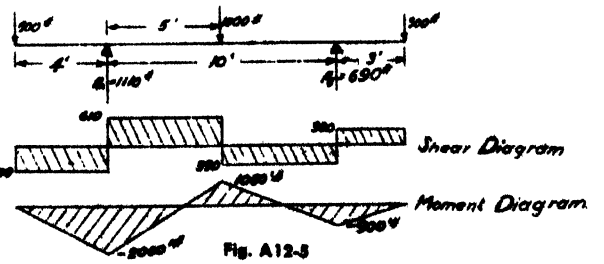


Fig. A12-5

Solution for Bending Stress

Method I - Using flexure formula $M = f_b I/c$. The maximum moment occurs over support R_A and equals -24000"#. Due to symmetry of beam section (Fig. A12.6) the neutral axis lies at mid-point of beam.

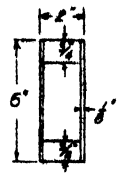


Fig. A12-6

Calculation of Moment of Inertia about neutral axis:

For flange: $I_{NA} = (1.75 \times .75 \times \overline{2.625}^2)2 + (1.75 \times .75^3)2/12 = 18.26$ in.^{4}

For webs: $I_{NA} = (6^3 \times .125)2/12 = 4.50$ in.^{4}. Total $I_{NA} = 22.76$ $f_b = Mc/I$. $c = 3$" for top and bottom fibers. Hence, $f_b = (24000 \times 3)/22.76 = 3170$#/in.^{2} tension on top fibers and compression on lower fibers.

Stress intensity at inside edge of flange block:

$y = 3 - .75 = 2.25$"
$f_b = My/I = (24000 \times 2.25)/22.76 = \pm 2380$#/in.^{2}

Method II (Without Use of Beam Formula)

In Fig. A12.5, cut a section through the beam at point 1-1, just to the left of the reaction R_A, which is the section of maximum bending moment. Fig. A12.7 shows the free body of the beam to the left of this section.

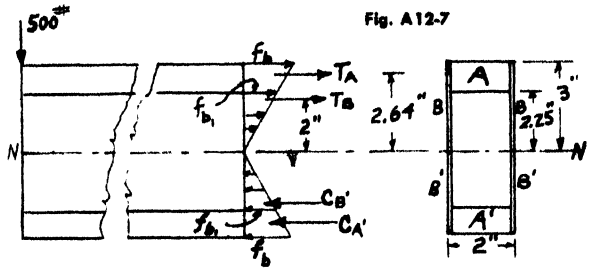


Fig. A12-7

Due to symmetry, the neutral axis NN is at the midpoint of the section. Since plane sections remain plane after bending and stress is assumed proportional to strain, the stress intensity diagram on the cut section will take the triangular shape shown by the arrow. Let f_b = stress intensity on outer fibers; due to symmetry, it will be the same on both the top and bottom fibers. Let f_{b_1} be the stress intensity at the inside edge of portion A. Then $f_{b_1} = \frac{2.25}{3.00} f_b = .75\, f_b$. Let T_A be the total tensile stress on A and $C_{A'}$ be the total compressive stress on portion A'.

$$T_A = C_{A'} = \frac{f_b + .75 f_b}{2} \times 1.75 \times .75 = 1.15\, f_b$$

average stress x area). The distance from N.A. to the loads T_A or $C_{A'}$ = 2.64" (T_A and $C_{A'}$ act thru the centroid of the trapezoidal stress load on portion A and A'). Let T_B = total tensile stress on the web above the N.A. and $C_{B'}$ = total compression on the web below the N.A.

$$T_B = C_{B'} = \frac{f_b}{2} \times 3 \times .25 = .375\, f_b$$

The distance from the N.A. to T_B or $C_{B'}$ = 2/3 x 3 = 2", since the stress pattern over these portions is triangular. We now equate the moment of these internal resisting forces to the external bending moment.

$T_A \times 2.64 + C_{A'} \times 2.64 + T_B \times 2 + C_{B'} \times 2 = M$

Substitute values for T and C in terms of f_b as found above:

$(1.15\, f_b + 1.15\, f_b)\, 2.64 + (.375\, f_b + .375\, f_b)2 = 24000$

Hence, $f_b = \frac{24000}{7.58} = \pm 3170$#/sq.in. as in the first solution.

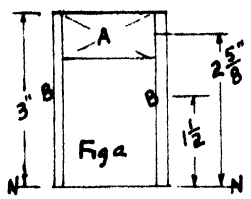
Solution for Shear Stresses

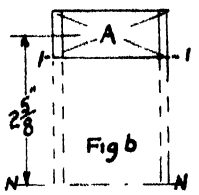
Method 1 = Using Formula $f_s = \frac{V}{Ib} \int ydA$

From the shear diagram Fig. A12.5 maximum external shear load = 610#, and is constant between the left reaction and the 1000# load. The maximum intensity of the shear stress will occur at the neutral axis since the term $\int ydA$ is maximum about the neutral axis.

$$f_s = \frac{V \int_0^3 ydA}{Ib} = \frac{610 \times 4.57^*}{22.76 \times 2 \times .125} = 490\text{#/in.}^2$$

* $\int_0^3 ydA$ = area of each portion A and B in Fig. a times arm from centroid to neutral axis.
= 1.75 x .75 x 2.625 + .25 x 3 x 1.5 = 4.57





Determine shear stress on section 1-1, 3/4" from top surface.

$$f_s = \frac{610 \times 3.94^*}{22.76 \times 2 \times .125} = 423\text{#/in.}^2$$

* $\int_{2.25}^3 ydA = 2.0 \times .75 \times 2.625 = 3.94$ (See Fig.b)

Method II Solution - (Difference of Bending Stresses)

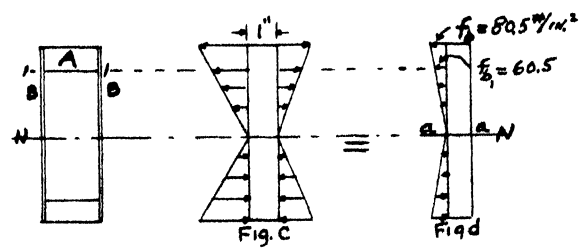


Fig. c shows a length of beam 1 inch long cut from the beam of Fig. A12.5 beginning at left reaction and extending 1 inch toward 100# load. The bending moment at left end of strip is - 24000"# and at right end = - 24000 + 610 = 23390"#, or a difference of 610"#. Thus the difference of the horizontal tension and compressive stresses on the strip forces in Fig. c equals that due to 610"# of moment as shown in Fig. d., where f_b for

outer fiber = $\frac{610 \times 3}{22.76}$ = 80.5#/in.² and f_b for point 3/4" from top of beam = $\frac{2.25}{3.00} \times 80.5$ = 60.05#/in.² The horizontal shear load on section a-a at neutral axis (Fig. d) equals the total pull on a strip face between neutral axis and extreme fiber. Hence,

Load on Portion A = area x average stress
= $1.75 \times .75 \times \frac{80.5 + 60.05}{2}$
= 92#

Load on Portion B = $3 \times .25 \times \frac{80.5}{2}$ = 30.15#

Total load above neutral axis = 92 + 30.15 = 122.15#, therefore f_s at neutral axis = $\frac{122.15}{2 \times .125}$ = 490#/in.² (checks solution 1)

For section 3/4" from top of beam:-

f_s = load on portion A plus load on web above section 1-1/shear area.

$$f_s = \frac{92 + 92\ (.25/1.75)}{2 \times .125 \times 1} = 423\ /in.^2$$

Example Problem 2

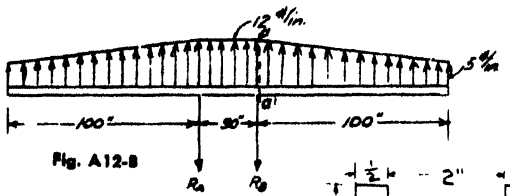


Fig. A12-8

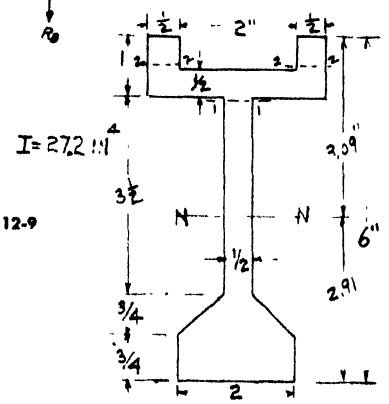


Fig A12-9

Given the double cantilever beam carrying a distributed load as shown in Fig. A12.8. (1) Let it be required to determine the maximum bending stress on the beam section at section a-a, just adjacent to support R_B. Fig. A12.9 shows a cross-section of the beam at point a-a on the beam. (2) Also, determine the shearing stress intensity at points 1-1 and 2-2 on the cross section of Fig. A12.9 and also the maximum shearing stress.

Solution 1 By Use of Flexure and Shear Formulas:

Bending moment at section, a-a: $M_{a-a} = 500 \times 50 + 350 \times 33.3 = 36670$"#.

Note: The distributed trapezoidal load has been replaced by two resultant forces. See Fig.A12.10

Shear at a-a = V_a = 350 + 500 = 850#. The calculations for the neutral axis and the moment of inertia have been calculated in Table 4 of Chapter A3 and thus will not be repeated here. The results are given in Fig. A12.9. Bending stress on the extreme upper fibers:

$$f_b = \frac{Mc}{I} = -\frac{36670 \times 3.09}{27.2} = -4160\#/sq.in.\ (compression)$$

Bending stress on the extreme lower fibers:

$$f_b = \frac{My}{I} = -\frac{36670 \times -2.91}{27.2} = 3920\#/sq.in.\ (tension)$$

The maximum shear stress occurs at the neutral axis:

$$f_{s\ (N.A.)} = \frac{V \int_0^{3.09} ydA}{I\ b}$$

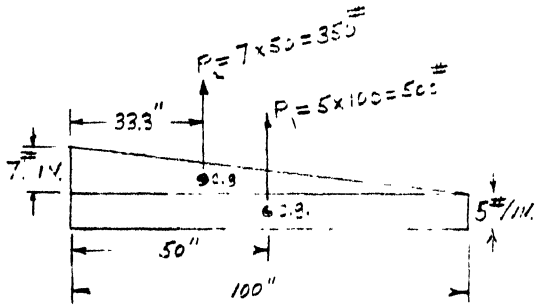


Fig. A12-10

Table A shows the calculation of term $\int_0^{3.09} ydA$ = 6.03

therefore $f_{s(N.A.)} = \frac{850 \times 6.03}{27.2 \times .5}$ = 377#/sq. in.

Shear stress at section 1-1: $f_{s(1-1)} = V \int_{2.09}^{3.09} \frac{ydA}{Ib}$

$\int_{2.08}^{3.09} ydA = 234 + (1.295)2 = 4.93$ (see Table A. Portion 1 drops out)

therefore $f_{s(1-1)} = \frac{850 \times 4.93}{27.2 \times .5}$ = 308#/sq.in.

Shear stress at section 2-2

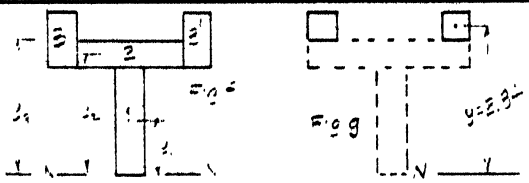
$$f_{s(2-2)} = V \frac{\int_{2.59}^{3.09} ydA}{Ib},$$

where $\int_{2.59}^{3.09} ydA = 2(.5 \times .5 \times 2.84) = 1.42$ (See Fig.g)

therefore $f_{s(2-2)} = \frac{850 \times 1.42}{27.2 \times (.5 + .5)}$ = 44.4#/sq. in.

Table A (See Figs. f, g)

Portion	A = Area	y	Ay
1	2.09 x .5 = 1.045	1.045	1.096
2	2 x .5 = 1.0	2.34	2.340
3	1 x .5 = 0.5	2.59	1.295
3'	1 x .5 = 0.5	2.59	1.295
Sum			6.026



Second Method of Solution Equilibrium of Bending Stresses

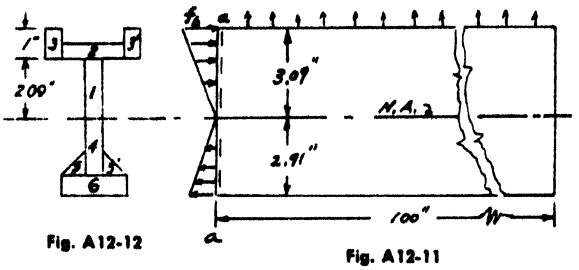


Fig. A12-12

Fig. A12-11

Fig. A12.11 shows a free body of the portion of the beam to the right of section a-a. The bending stress intensity diagram is shown by the horizontal arrows acting on the beam face at section a-a. Fig. A12.12 shows the cross-section of the beam at section a-a.

The general procedure will be to determine the total bending stress load on each portion, 1 to 6, of the cross-section and then the moment of each of these loads about the neutral axis, the summation of which must equal the external bending moment.

This method of solution involves more calculations than Method 1, where formulas are used, however, the student should obtain a better understanding of the internal force action by this second method of solution which will be valuable in later considerations when dealing with the design of aircraft beams, stressed above the proportional limit, a condition for which the beam formulas, as derived, do not apply.

In Fig. A12.11, let f_b be the intensity on the most remote fiber, or 3.09" above the neutral axis. Table B shows the calculations of the total stress on each of the portions of the cross-section and their moment about the neutral axis, all in terms of the unknown stress, f_b.

Table B

1	2	3	4	5	6
Portion See Fig. A12.12	Area A	Average Stress in terms of f_b	Total Load = (2) x (3)	y - arm to N.A.	Resisting moment -(4)x(5)
1	1.045	$-.337f_b$	$-.353f_b$	1.39	$-.490\ f_b$
2	1.00	-.757	-.757	2.35	-1.780
3 + 3'	1.00	-.837	-.837	2.62	-2.190
4	1.09	.350	.387	-1.44	-0.557
5 + 5'	0.56	.578	.323	-1.93	-0.622
6	1.50	$.821f_b$	$1.237f_b$	-2.57	$-3.180\ f_b$
Totals	6.19		$0.000f_b$		$-8.82\ f_b$

Explanation:-

Column #3 gives the average stress on each of the 6 portions. For example, the stress on portion (1) varies from zero at the neutral axis to $\frac{2.09}{3.09} f_b = .674\ f_b$ at the upper edge of (1). Thus, the average stress = $\frac{.674\ f_b + 0}{2} = .337\ f_b$.

On part 3 or 3', the stress on the lower edge = $.674\ f_b$ and f_b on the upper edge. Then, the average stress = $\frac{(1 + .674)}{2} f_b = .837\ f_b$. Column #5 is the distance from the neutral axis to the centroid of the load on each of the blocks. For portion (1) the stress pattern is triangular, and y = 2/3 x 2.09 = 1.39". On portions (2), (3), (5) and (6) the bending stress distribution is trapezoidal, and the arm is to the centroid of this trapezoid.

The total internal resisting moment of $-8.82\ f_b$ from Table B equals the external bending moment of 36670"#.

Thus, $f_b = \frac{-36670}{8.82} = -4160$#/in.², which checks solution (1).

For equilibrium, the total compressive stresses on the cross-section of the beam must be equal to the total tensile stresses, or ΣH must equal zero. Column 4 of Table B gives the total load on each portion of the cross-section and the total of this column is zero.

The bending stress on the lower fiber of the cross section is directly proportional to the distance from the neutral axis or, $f_{b_{lower}} = \frac{2.91}{3.09} \times 4160 = 3930$#/in.²

Shear Stresses

Fig. A12.13 shows a free body of a strip one inch wide. Section a-a is taken as one face and the other face b-b is taken one inch away.

The external bending moment at section b-b is less than at a-a thus, the arrows are shown of shorter length. The difference between these bending forces on each face of the beam strip is the horizontal shearing force tending to shear this beam strip which is 1" long.

The difference in bending moment between the two faces which are 1" apart equals 850 x 1 = 850"# (see Fig. A12.10). Thus, if we multiply the values of column 4 of Table B by $\frac{850}{36670} = .0231$, we obtain the difference in the loads on each portion, (1) to (6) of the cross section of Fig. A12.12, hence:

For Portion (1) Load = .0231 x (-.353) x 4160 = -34#
" (2) " = " x (-.757) x 4160 = -73#
" (3 3') " = " x (-.837) x 4160 = -80#
" (4) " = " x (.387) x 4160 = +37
" (5 5') " = " x (.323) x 4160 = +31
" (6) " = " x 1.237 x 4160 = 119#

Fig. A12.14 shows these forces applied to the 1 inch beam length. The horizontal shearing

force at any section equals the summation of the forces above or below the particular horizontal section being considered.

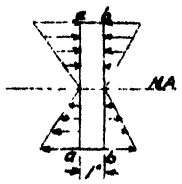


Fig. A12-13

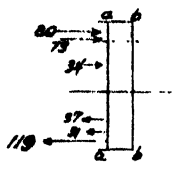


Fig. A12-14

Thus, for a section at the neutral axis, shear force = 80 + 73 + 34 = 187#; shear area = 1 x .5 = .5 sq. in. hence, $f_S = \frac{187}{.5}$ = 374#/sq. in.

At section 1-1, shear force = 80 + 73 = 153#. $f_S = \frac{153}{1 \times .5}$ = 306#/sq.in., which checks solution #1.

Example Problem 3. Beam With Variable Moment Of Inertia.

Fig. A12.15 shows a cantilever beam loaded with a single concentrated load of 600#. The beam cross-section at stations 132, 175 and 218 are as shown. The complete picture of the bending and shear stresses on these three cross sections will be determined.

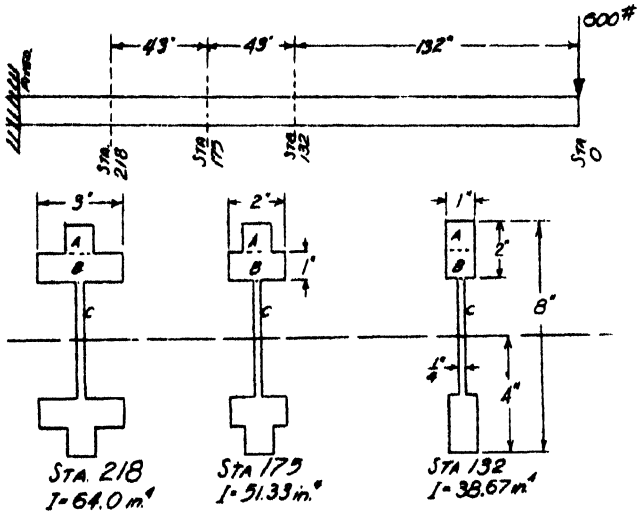


Fig. A12-15

Bending Moments:-

M_{132} = -600 x 132 = -79,200"#

M_{175} = -600 x 175 = -105,000"#

M_{218} = -600 x 218 = -130,800"#

Table C

1	2	3	4	5	6	7	8
Beam Station	Bending Moment M	Bend. Stress f_b = My/I			Total Bending Stress Load on:-		
		On Top or Bottom Fiber y =4"	Point 1" From Top or Bottom y = 3"	Point 2" From Top or Bottom y = 2"	Portion "A"	Portion "B"	Portion "C"
132	79,200"#	±8180	±6135	±4090	7157#	5112#	1023#
175	105,000"#	±8180	±6135	±4090	7157	10224	1023
218	130,800"#	±8180	±6135	±4090	7157	15336	1023

Table C shows the results of the calculation of the bending stresses at 3 points on each side of the neutral axis, for the three stations. For example, for station 132,

$f_b = \pm \frac{79100 \times 4}{38.66} = \pm$ 8180#/in.² for the top or bottom edge of the beam.

f_b for a point 1" from the edge = 3/4 x 8180 = ± 6135"/in.²

f_b for a point 2" from the edge = 1/2 x 8180 = 4090#/in.²

From the results in Table C, it should be noticed that the change in moment of inertia between the three stations is directly proportional to the change in bending moment, hence the same value for the bending stresses for all three stations. Columns 6, 7 and 8 give the total bending stress load on portions A, B and C of the three cross-sections (See Fig. A11.15). These values equal the average stress on the portions times the area of the portion; for example, for station 132, the load on portion A:

load = $\frac{8180 + 6135}{2}$ x 1 x 1 = 7157#, and for portion C:

load = $\frac{4090 + 0}{2}$ x 2 x .25 = 1023#

Fig. A12.16 shows the tension and compressive stresses acting on a portion of the beam between stations 175 and 218. Fig. A12.18 shows the resulting horizontal shear stress pattern resulting from the loads in Fig. A12.16. For example, if we take a section along the beam 1" from the top or bottom edge of the beam and treat this portion as a free body as shown in Fig. A12.21 applying ΣH = 0,

ΣH = -7157 + 7157 + f_S x 43 x .1 = 0 ∴ f_S = 0

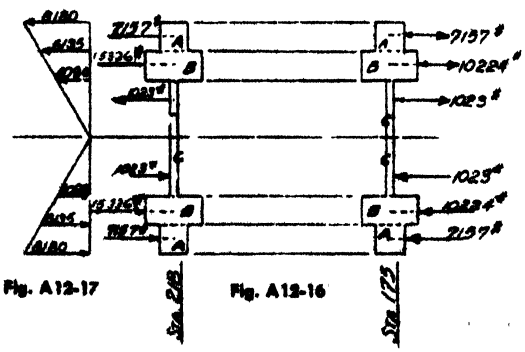
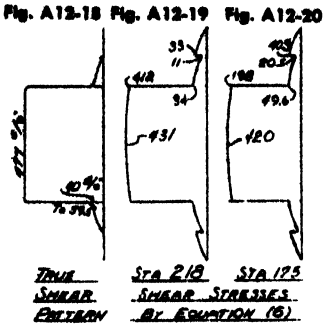


Fig. A12-17

Fig. A12-16

Fig. A12-18 Fig. A12-19 Fig. A12-20



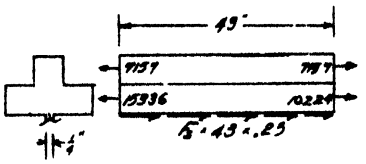


Fig. A12-22

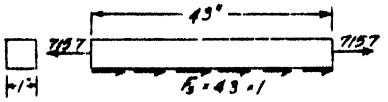


Fig. A12-21

and similarly, treating the portion between the edge of the beam and a point 2" from the edge as a free body diagram as shown in Fig. A12.22,

$$\Sigma H = -7157 + 7157 - 15336 + 10224 + f_s \times 43 \times .25 = 0, \text{ therefore } f_s = 477\#/\text{in}.$$

Obviously, the shear stress on portion C is constant, since the end load on this portion at both stations is the same, or 1023#.

Fig. A12.18 shows the general shape of the shear stress distribution on the beam section at any point between stations 175 and 218. The shear stresses between stations 132 and 175 would be the same, since the change in bending moment and moment of inertia have been made the same as between stations 175 and 218.

Figs. A12.19 and A12.20 show the shear stress patterns if the formula $f_s = \frac{V \int ydA}{Ib}$ be used for each station. The discrepancy is considerable as the equation does not apply to beams of varying section.

A12.5 Problems

Problem (1)

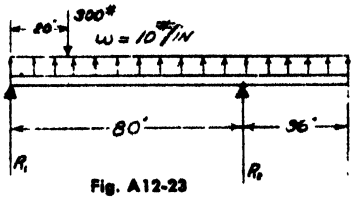


Fig. A12-23

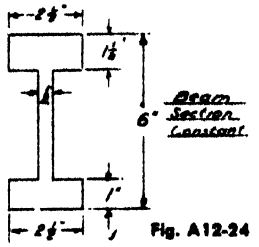


Fig. A12-24

For the beam shown in Fig. A12.23 and A12.24 determine the following:

(1) Shear diagram
(2) Value of maximum positive and negative bending moment.
(3) Maximum tensile and compressive stress by two methods.
(4) Maximum shearing stresses by two methods.
(5) Shearing stress intensity at section 1" from bottom edge of beam.

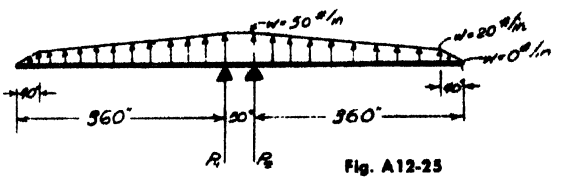


Fig. A12-25

Problem (2)

Fig. A12.25 shows a cantilever wing beam. The beam cross-section at the support points R_1 and R_2 is shown in Fig. A12.26. The Tee section and all flange plates are 1/8" thick. The plates are spot welded to Tee. Determine the following:

(1) Maximum bending tensile and compressive stresses.
(2) Maximum shearing stress.
(3) Shear load per inch of span on spot welds at sections 1-1 and 2-2 (See Fig. A12.26)

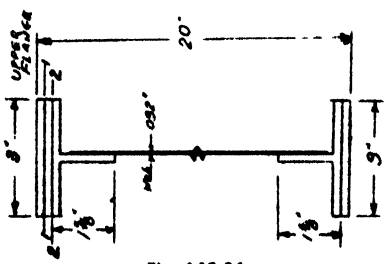


Fig. A12-26

(NOTE) Neglect web area in computing beam section properties. Neglect any effect of taper of beam in depth or section on bending and shearing stresses. Solve without use of flexure and shear formulas.

CHAPTER A13
UNSYMMETRICAL BENDING

A13.1 General. Aircraft structures present many beams whose cross-sections are unsymmetrical. A common case is the wing box beam since the airfoil shape is generally an unsymmetrical one. This chapter reviews the various equations and methods for determining the bending stresses in the bending of unsymmetrical sections.

Fig. A13.0 illustrates a box beam consisting of four corner flange members connected by sheet webs and walls. The axial loads in the stringers at beam section ABCD will be determined using the flexure formula $f = \frac{Mc}{I}$

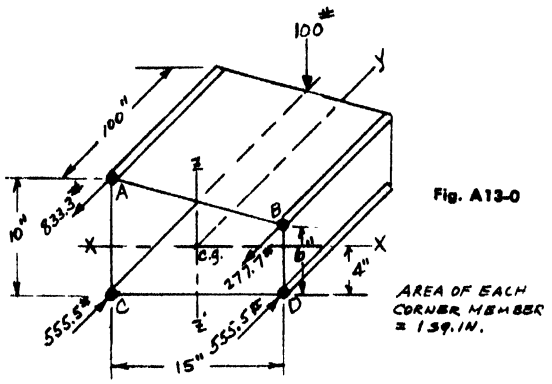


Fig. A13-0

M_X = bending moment about x axis = 100 x 100 = 10,000"#

$M_Z = 0$

$I_{XX} = 1\ (4^2 + 6^2 + 4^2 + 2^2) = 72$ in. (Neglects webs and walls)

Flange member A:-

$$f = \frac{Mc}{I} = \frac{10{,}000 \times 6}{72} = 833.3 \text{ psi.}$$

Total load on member A = f times area of A = 833.3 x 1 = 833.3#

By similar calculations, the total loads in the other corner members B, C, and D equal 277.7#, -555.5# and -555.5# respectively. Fig. A13.0 shows these resulting internal resisting loads on the four corner members.

The entire beam will now be checked for static equilibrium of moments.

M_X of internal forces = 833.3 x 6 + 277.7 x 2 + 555.5 (4 x 2) = 10,000 in.lb. This equals the external M_X of 10,000 in.lb.

M_Z of internal forces = (833.3 - 277.7) 7.5 = 4170 in. lb. However the external $M_Z = 0$. Thus there is an unbalanced moment in the xy plane of 4170"#. This result means that the beam section is not bending about the axis xx in resisting the given external loads as shown but must bend about some other axis which will develop internal stresses which will produce internal resisting moments which will balance the external bending moments.

Since the beam formula $f = \frac{Mc}{I}$ must be modified to give the true stresses in the bending of unsymmetrical sections, the modifications or derivations will be taken up in detail. Since this chapter makes use of such terms as Principal Axes, Product of Inertia etc., reference should be made to Chapter A3.

A13.2 Derivation of Equation for Bending Stress

In the following derivations, it will be assumed that the plane of the external loads contains the flexural axis of the beam and hence, thebeam is not subjected to torsional forces which, if present, would produce bending stresses if free warping of the beam sections was restrained, as occurs at points of support. The questions of flexural axes and torsional effects are taken up in later chapters.

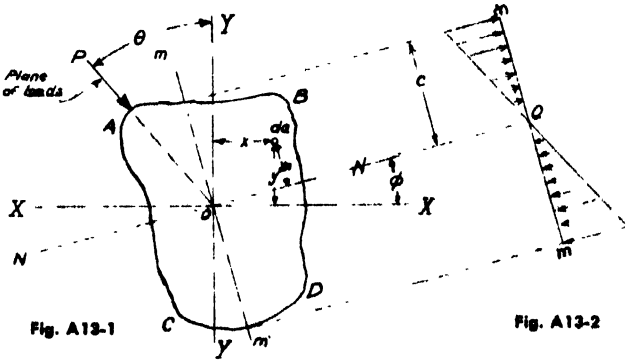


Fig. A13-1

Fig. A13-2

Fig. A13.1 represents a cross-section of a straight cantilever beam with a constant cross-section, subjected to external loads which lie in a plane making an angle θ with axis Y-Y through the centroid O. To simplify the figure, the flexural axis has been assumed to coincide with the centroidal axis, which in general is not true.

Let NN represent the neutral axis under the given loading, and let ø be the angle between the neutral axis and the axis X-X. The problem is to find the location of the neutral axis and the bending stress f at any point on the section.

In the fundamental beam theory, it is assumed that the unit stress varies directly as the distance from the neutral axis, within the proportional limit of the material. Thus, Fig. A13.2

illustrates how the stress varies along a line such as mm perpendicular to the neutral axis N-N.

Let f represent unit bending stress at any point a distance y_n from the neutral axis. Then the stress f on da is

$$f = ky_n \quad \text{----------(1)}$$

where k is a constant. Since the position of the neutral axis is unknown, y_n will be expressed for convenience in terms of rectangular coordinates with respect to the axes X-X and Y-Y Thus, $y_n = (y - x \tan \phi) \cos \phi$ ---------

$$= y \cos \phi - x \sin \phi \quad \text{----------(2)}$$

Then Eq. (1) becomes

$$f = k (y \cos \phi - x \sin \phi) \quad \text{----------(3)}$$

This equation contains three unknowns, f, k, and Ø. For solution, two additional equations are furnished by conditions of equilibrium namely, that the sum of the moments of the external forces that lie on one side of the section ABCD about each of the rectangular axes X-X and Y-Y must be equal and opposite, respectively, to the sum of the moments of the internal stresses on the section about the same axes.

Let M represent the bending moment in the plane of the loads; then the moment about axis X-X and Y-Y is $M_x = M \cos \theta$ and $M_y = M \sin \theta$. The moment of the stresses on the beam section about axis X-X is $\int f\, da\, y$. Hence, taking moments about axis X-X, we obtain for equilibrium,

$$M \cos \theta = \int f\, da\, y$$

$$= \int k (\cos \phi\, y^2 da - \sin \phi\, xyda)$$

$$- k \cos \phi \int y^2 da - k \sin \phi \int xyda \quad \text{---(4)}$$

A13.3 Method 1. Stresses from Moments about the Principle Axes

In equation (4), the term $\int y^2 da$ is the moment of inertia of the cross-sectional area about the X-X, which we will denote by I_x, and the term $\int xyda$ represents the product of inertia about axes X-X and Y-Y. We know, however, that the product of inertia with respect to the principal axes is zero. Therefore, if we select XX and YY in such a way as to make them coincide with the principal axes, we can write equation (4):

$$M \cos \theta = k \cos \phi\, I_{x_p} \quad \text{----------(5)}$$

In like manner, if moments are equated about the Y_p-Y_p axis, we obtain

$$M \sin \theta = - k \sin \phi\, I_{y_p} \quad \text{----------(6)}$$

To find the unit stress f at any point on the cross-section, we solve equation (5) for cos Ø and equation (6) for sin Ø, and then substituting these values in (3), we obtain the following expression, giving f the subscript b to represent bending stress:-

$$f_b = \frac{M \cos \theta\, y_p}{I_{x_p}} + \frac{M \sin \theta\, x_p}{I_{y_p}}$$

whence

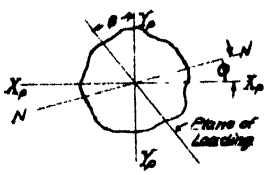
$$f_b = - \frac{M_{x_p} y_p}{I_{x_p}} - \frac{M_{y_p} x_p}{I_{y_p}} \quad \text{---------(7)}$$

The minus signs have been placed before each term in order to give a negative value for f when we have a positive bending moment, or M_{xp} is the moment of a couple acting about X_p-X_p, positive when it produces compression in the upper right hand quadrant. M_{yp} is the moment about the Y_p-Y_p axis, and is also positive when it produces compression in the upper right hand quadrant.

A13.4 Method 2. Stresses by use of Neutral Axis for Given Plane of Loading

The direction of the neutral axis NN, measured from the XX_p principal axis is given by dividing equation (6) by (5).

$$\text{Tan } \phi = - \frac{I_{x_p}}{I_{y_p}} \tan \theta \quad \text{----------(8)}$$



The negative sign arises from the fact that θ is measured from one principal axis and Ø is measured in the same direction from the other principal axis.

Since equation (8) gives us the location of the neutral axis for a particular plane of loading the stress at any point can be found by resolving the external moment into a plane perpendicular to the neutral axis N-N and using the moment of inertia about the neutral axis, hence

$$f_b = \frac{[M \cos (\theta - \phi)]\, y_n}{I_n} = \frac{M_n y_n}{I_n} \quad \text{------(9)}$$

I_n can be determined from the relationship expressed in Chapter A3, namely,

$$I_n = I_x \cos^2 \phi + I_y \sin^2 \phi \quad \text{-------(10)}$$

A13.5 Method 3. Stresses from Moments, Section Properties and Distances Referred to any Pair of Rectangular Axes through the Centroid of the Section

The fiber stresses can be found without resort to principal axes or to the neutral axis.

Equation (4) can be written:

$$M_x = k \cos \phi\, I_x - k \sin \phi\, I_{xy} \quad \text{-----(11)}$$

where $I_x = \int y^2 da$ and $I_{xy} = \int xyda$, and $M_x = M \cos \theta$

In like manner, if moments are equated about the Y-Y axis:

$$M_y = -k \sin \phi\, I_y + k \cos \phi\, I_{xy} \quad - - - - - \quad (12)$$

Solving equations (11) and (12) for sin ϕ and cos ϕ and substituting their values in equation (3), we obtain the following expression for the fiber stress f_b:

$$f_b = -\frac{(M_y I_x - M_x I_{xy})}{I_x I_y - I_{xy}^2} x - \frac{M_x I_y - M_y I_{xy})}{I_x I_y - I_{xy}^2} y \quad (13)$$

For simplification, let

$$k_1 = I_{xy}/(I_x I_y - I^2_{xy})$$

$$k_2 = I_y/(I_x I_y - I^2_{xy})$$

$$k_3 = I_x/(I_x I_y - I^2_{xy})$$

Substituting these values in Equation (13):

$$f_b = -(k_2 M_y - k_1 M_x)\, x - (k_3 M_x - k_1 M_y) y - \quad (14)$$

In Method 2, equation (8) was used to find the position of the neutral axis for a given plane of loading. The location of the neutral axis can also be found relative to any pair of rectangular centroidal axes X and Y as follows: since the stress at any point on the neutral axis must be zero, we can write from equation (14) that:

$(k_2 M_y - k_1 M_x)x = -(k_3 M_x - k_1 M_y)\, y$ for all points located on the neutral axis. From Fig. A13.1 $\tan \phi = \frac{y}{x}$

Thus $$\tan \phi = -\frac{(k_2 M_y - k_1 M_x)}{(k_3 M_x - k_1 M_y)} \quad - - - - - - - - - \quad (15)$$

It frequently happens that the plane of the bending moment coincides with either the X-X or the Y-Y axis, thus making either M_x or M_y equal to zero. In this case, equation (15) can be simplified. For example if $M_y = 0$

$$\tan \phi = \frac{I_{xy}}{I_y} \quad - - - - - - - - - - - - - - \quad (16)$$

and if $M_x = 0$

$$\tan \phi = \frac{I_x}{I_{xy}} \quad - - - - - - - - - - - - - - \quad (17)$$

A13.6 Advantages and Disadvantages of the Three Methods

Method 2 (Bending about the neutral axis for a given plane of loading) no doubt gives a better picture of the true action of the beam relative to its bending as a whole. The point of maximum fiber stress is easily determined by placing a scale perpendicular to the neutral axis and moving it along the neutral axis to find the point on the beam section farthest away from the neutral axis. In airplane design, there are many design conditions, which change the direction of the plane of loading, thus, several neutral axes must be computed for each beam section, which is a disadvantage as compared to the other two methods.

In determining the bending moments and shears on a wing due to air loads, it is customary to resolve the loads for all conditions into two rectangular planes, as for example, parallel and perpendicular to the thrust line. Then, if the section properties are computed about centroidal axes parallel to these reference wing axes, method (3) can be used without further resolution of the wing bending moments, whereas, if method (1) was used, the wing bending moments about the wing reference axes would have to be further resolved about the principal axes at each beam section.

Since bending moments about one principal axis produces no bending about the other principal axis, the principal axes are convenient axes to use when calculating internal shear flow distribution.

A13.7 Deflections

The deflection can be found by using the beam section properties about the neutral axis for the given plane of loading and the bending moment resolved in a plane normal to the neutral axis. The deflection can also be found by resolving the bending moment into the two principal planes and then using the properties about the principal axes. The resultant deflection is the vector sum of the deflections in the direction of the principal planes.

A13.8 Illustrative Problems

Example Problem #1

Fig. A13.3 shows a unsymmetrical one cell box beam with four corner flange members a, b, c and d. Let it be required to determine the bending axial stress in the four corner members due to the loads P_x and P_y acting 50" from the section abcd.

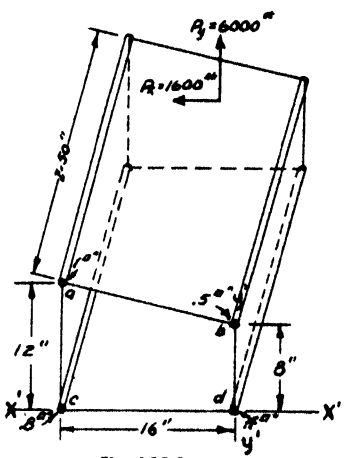


Fig. A13-3

In this example solution the sheet connecting the corner members will be considered ineffective in bending. The stresses will be determined by each of the three methods as presented in this chapter.

Solution #1

The first step common to all three methods is the calculation of the moments of inertia about the centroidal X and Y axis. Table A13.1 gives the detailed calculations. The properties are first calculated about the reference axes x'x' and y'y' and then transferred to the parallel centroidal axes.

Table A13.1

Mem.	Area "A"	y'	x'	Ay'	Ax'	Ay'²	Ax'²	Ax'y'
a	1.0	12	-16	12	-16	144.0	256.0	-192
b	0.5	8	0	4	00	32.0	0	0
c	0.8	0	-16	0	-12.8	0	204.8	0
d	0.4	0	0	0	0	0	0	0
Totals	2.7			16	-28.8	176.0	460.8	-192

Calculation of Centroid of Section:

$$\bar{x} = \frac{\Sigma Ax'}{\Sigma A} = \frac{-28.8}{2.7} = -10.667"$$

$$\bar{y} = \frac{\Sigma Ay'}{\Sigma A} = \frac{16}{2.7} = 5.926"$$

$$I_x = 176 - 2.7 \times \overline{5.926}^2 = 81.18$$

$$I_y = 460.8 - 2.7 \times \overline{10.667}^2 = 153.58$$

$$I_{xy} = -192 - (2.7 \times -10.667 \times 5.926) = -21.33$$

Solution by Method I (bending about principal axes)

The angle ϕ between the x axis and the principal axes is given by the equation,

$$\tan 2\phi = \frac{2\,I_{xy}}{I_y - I_x} = \frac{2\,(-21.33)}{153.58 - 81.18} = \frac{-42.66}{72.40} = -.589$$

$2\phi = 30^0 - 30'$, $\phi = 15^0 - 15'$

$$I_{x_p} = I_x \cos^2\phi + I_y \sin^2\phi - 2\,I_{xy} \sin\phi \cos\phi$$

$$= 81.18 \times \overline{.9648}^2 + 153.58 \times \overline{.2636}^2 - (-21.33 \times -.2636 \times .9648)2$$

$$= 75.56 + 10.67 - 10.85 = 75.38 \text{ in.}^4$$

$$I_{y_p} = I_x \sin^2\phi + I_y \cos^2\phi + 2\,I_{xy} \sin\phi \cos\phi$$

$$= 81.18 \times \overline{.2636}^2 + 153.58 \times \overline{.9647}^2 + 10.85 =$$

$$159.34 \text{ in.}^4$$

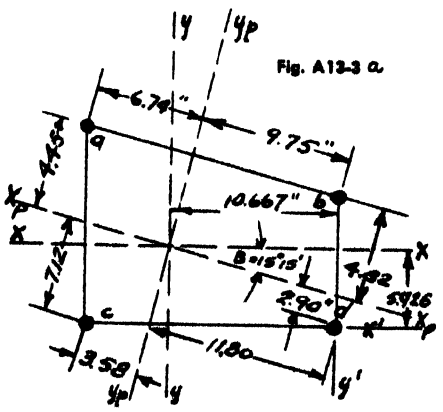


Fig. A13-3 a.

Fig. A13.3a shows the location of the principal axes, as well as the perpendicular distances from each corner member to each of the principal axes. These distances are readily determined from elementary trigonometry.

The external bending moment about the X and Y axes equal,

$$M_X = 6000 \times 50 = 300{,}000"\#$$

$$M_y = -1600 \times 50 = -80{,}000"\#$$

These moments will be resolved into bending moments about the x_p and y_p principal axes.

$$M_{x_p} = 300{,}000 \times \cos 15^0\text{-}15' - 80000 \times \sin 15^0\text{-}15'$$

$$= 289700 - 21000 = 268700"\#$$

$$M_{y_p} = -300000 \times \sin 15^0\text{-}15' - 80000 \times \cos 15^0\text{-}15'$$

$$= -79000 - 77200 = -156200"\#$$

(Positive moments produce compression in upper right hand quadrant)

Calculation of Stresses

$$f_b = -\frac{M_{xp}\,y_p}{I_{xp}} - \frac{M_{yp}\,x_p}{I_{yp}}$$

Stringer a

$x_p = -6.74$, $y_p = 4.45$

$$\text{hence } f_b = -\frac{268700 \times 4.45}{75.38} - \frac{-156200 \times -6.74}{159.34}$$

$$= -15900 - 6600 = -22500\#/\text{in.}^2$$

Stringer b

$x_p = 9.75'$, $y_p = 4.82$

$$f_b = -\frac{268700 \times 4.82}{75.38} - \frac{-156200 \times 9.75}{159.34}$$

$$= -17180 + 9570 = -7610\#/\text{in.}^2$$

Stringer c

$x_p = -3.58$, $y_p = -7.12$

$$f_b = \frac{-268700 \times -7.12}{75.38} - \frac{-156200 \times -3.58}{159.34}$$

$$= 25400 - 3520 = 21880$$

and similarly for stringer d, $f_b = 21900$

Solution by Method #2 (Neutral Axis Method)

Let θ' = angle between yy axis and plane of loading.

$$\tan\theta' = \frac{-80000}{300000} = -.2667$$

hence $\theta' = 14^0\text{-}56'$ $\therefore$ $\theta = 14^0\text{-}56' + 15^0\text{-}15' = 30^0\text{-}11'$

Let α = angle between neutral axis NN and the X_p axis

$$\tan\alpha = -\frac{I_{x_p} \tan\theta}{I_{y_p}} = \frac{-75.38 \times -0.5816}{159.34} = .275$$

hence $\alpha = 15^0\text{-}24'$ (see Fig. A13.3b)

Since the angle between the X axis and the neutral axis is only 9', we can say $I_N = I_X = 81.18$

Resolving the external bending moments normal to neutral axis, we obtain

$M_N = 300000 \times .9999 + 80000 \times \sin 0^0\text{-}9' = 300200$"#. The bending stress at any point is given by,

$$f_b = \frac{M_n Y_n}{I_n}$$

Stringer A

$y_n = 6.074 + 5.33 \times .0025 = 6.087$"

$$f_b = \frac{-300\,200 \times 6.087}{81.18} = -22500\#/\text{in.}^2$$

Stringer b

$y_n = 2.055$"

$$f_b = \frac{-300\,200 \times 2.05}{81.18} = -7570$$

Stringer c

$y_n = -5.92$

$$f_b = \frac{-300\,200 \times -5.92}{81.18} = 21850$$

Stringer d

$y = -5.95$

$$f_b = \frac{-300\,200 \times -5.95}{81.18} = 22000$$

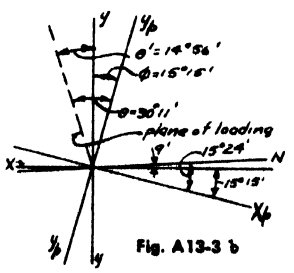


Fig. A13-3 b

Solution by Method #3 (Method Using Properties About X and Y Axes).

$M_x = 300000$, $M_y = -80000$

$I_x = 81.18$, $I_y = 153.58$,

$I_{xy} = -21.33$

$$K_1 = I_{xy}/(I_x I_y - I^2_{xy}) = \frac{-21.33}{81.18 \times 153.58 - 21.33^2} =$$

$$\frac{-21.33}{12016} = -.00177$$

$K_2 = I_y/(I_x I_y - I^2_{xy}) = 153.58/12016 = .012794$

$K_3 = I_x/(I_x I_y - I^2_{xy}) = 81.18/12016 = .00674$

$f_b = -(K_2 M_y - K_1 M_x)\,x - (K_2 M_x - K_1 M_y)y$

Stringer a

$x = -5.333$", $y = 6.074$"

$f_b = -(.00674 \times -80000 + .00177 \times 300000)x - (.012794 \times 300000 - .00177 \times -80000)y$ hence $f_b = (8) \times -(3697)y$ hence $f_b = 8 \times -5.33 - 3697 \times 6.074 = -22450$

Stringer b

$x = 10.667$, $y = 2.074$

$f_b = 8 \times 10.667 - (3697)\ 2.074 = 85 - 7660 = -7575$

Stringer c

$x = -5.333$, $y = -5.926$

$f_b = 8 \times -5.333 - (3697 \times -5.926) = -42 + 21900 = 21862$

Stringer d

$x = 10.667$, $y = -5.926$

$f_b = 8 \times 10.667 - (3697 \times -5.926) = 85 + 21900 = 21985$

NOTE: The stresses f_b by the three methods were calculated by 10" slide rule, hence the small discrepancy between the results for the three methods

Error is Stresses Due to Assumption That Section Bends About X and Y Centroidal Axes Due to M_x and M_y.

$$f_b = -\frac{M_x y}{I_x} - \frac{M_y x}{I_y}$$

Stringer a

$y = 6.074$, $x = -5.33$

$$f_b = -\frac{300000 \times 6.074}{81.18} - \frac{-80000 \times -5.33}{153.58} = -25190$$

Stringer b

$y = 2.07$, $x = 10.667$

$$f_b = -\frac{300000 \times 2.07}{81.18} - \frac{-80000 \times 10.667}{153.58} = -2110$$

In like manner for stringers c, and d

$f_{b(c)} = 19130$ and $f_{b(d)} = 27440$

Comparing these results with the previous results it is noticed that considerable error exists. Under these eroneous stresses the internal resisting moment does not equal the external bending moments about the X and Y axis.

Example Problem 2

Fig. A13.4 shows a portion of a cantilever 2-cell stressed skin wing box beam. In this example, the beam section is considered constant, and the section is identical to that used in

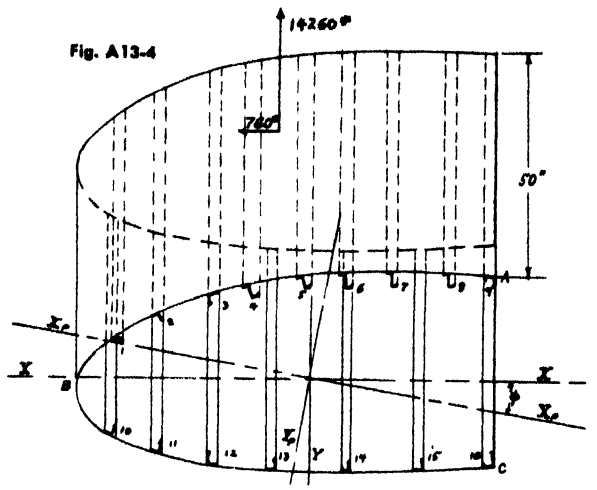


Fig. A13-4

Fig. A3.13 of Chapter A3 for which the section properties were computed and are as follows:

$I_x = 186.5$ in.^{4} $I_y = 431.7$ in.^{4} $I_{xy} = 36.41$ in.^{4}

$\phi = 8^0 - 16.25'$ $I_{x_p} = 181.2$ $I_{y_p} = 437$

The resultant air load on the wing outboard of section ABC is 14260# acting up in the Y direction and 760# acting forward in the X direction, and the location of these resultant loads is 50" from section ABC (Fig. A13.4)

The bending stress intensity at the centroids of stringers number (1), (9) and (12) will be calculated using all three methods.

Solution by Method #1 (Bending about Principal Axes)

The bending moment at section ABC about the X and Y axes is,

$M_X = 14260 \times 50 = 713{,}000$"#

$M_y = -760 \times 50 = -38000$"#

These moments are resolved into bending moments about the principal axes, as follows:-

$M_{x_p} = 713000 \times \cos \phi - 38000 \times \sin \phi = 700{,}000$"#

$M_{y_p} = -71300 \times \sin \phi - 38000 \times \cos \phi - 140000$"#

From equation (7), the general formula for f_b is:

$$f_b = -\frac{M_{x_p} y_p}{I_{x_p}} - \frac{M_{y_p} x_p}{I_{y_p}}$$

Stress on Stringer #1:

$y_p = 1.85$" and $x_p = -17.86$" (scaled from full size drawing)

$$f_b = -\frac{(700000 \times 1.85)}{181.17} - \frac{-140000 \times (-17.86)}{437}$$

$= -7150 - 5700 = -12850$#/sq. in.

Stress on Stringer #9

$y_p = 9.04'$, $x_p = 14.24$"

$$f_b = -\frac{(700000 \times 9.04)}{181.17} - \frac{-140000 \times 14.24}{437}$$

$= -34{,}900 + 4560 = -30340$#/sq. in.

Stress on Stringer #12

$y_p = -6.80$", $x_p = -8.22$"

$$f_b = -\frac{700000 \times (-6.80)}{181.17} - \frac{-140000 \times (-8.22)}{437} = 26200 +$$

$+ 2630 = -23570$ #/sq.in.

Solution by Method 2 (Neutral Axis Method)

In Fig. A13.5 let θ' be the angle between the Y-Y axis and the plane of the resultant bending moment. Resultant bending moment,

$M = \sqrt{713000^2 + 38000^2} = 714600$"

$\tan \theta' = \frac{-38000}{713000} = -.0533$ $\theta' = -3^0 - 3'$

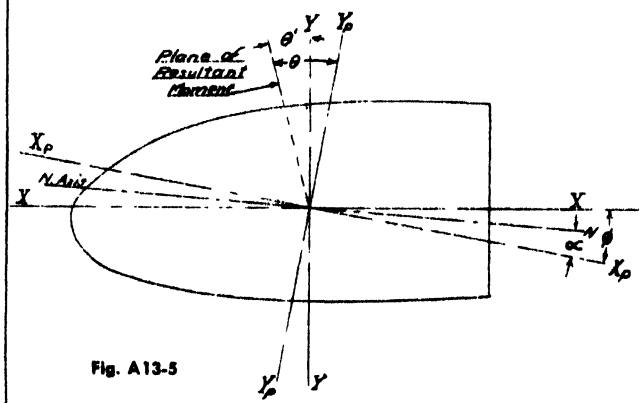


Fig. A13-5

Let θ equal the angle between the plane of the resultant moment and the Y_p axis.

$\therefore \theta = \theta' + \phi = 3^0 - 3' + 8^0 - 16' = 11^0 - 19'$

From equation (8), the angle between the X_p axis and the neutral axis = α, and $\tan \alpha = -\frac{I_{xp} \tan \theta}{I_{yp}}$

$= -\frac{181.17 \times (-.200)}{437} = .083$. Hence, $\alpha = 4^0 - 45'$

Fig. A13.5 shows the relative positions of the neutral axis, principal axes, and plane of loading.

The component of the external resultant moment about the neutral axis N equals:

$M_N = 714060 \times \sin 83^0 - 26' = 709350$ in.lb.

$I_N = I_{xp} \cos^2 \alpha + I_{yp} \sin^2 \alpha$

$= 181.17 \times .9966^2 + 437 \times .0878^2 = 183.37$ in.^{4}

Stress on Stringer (1):

$Y_{n_1} = (y_p + x_p \tan \alpha) \cos \alpha = (1.85 + 17.86 \times .083) .9966 = 3.32$"

$$f_b = -\frac{M_n y_n}{I_n} = -\frac{709350 \times 3.32}{183.37} = -12850\text{\#/sq.in.}$$

Stress on Stringer (9)

$$yn_9 = (9.04 - 14.24 \times .083)\ .9966 = 7.84"$$

$$f_{b_9} = -\frac{709350 \times 7.84}{183.37} = -30300\#/\text{sq. in.}$$

Stress on Stringer #12

$$yn_{12} = (6.80 + 8.22 \times .083)\ .9966 = 6.10$$

$$f_{b_{12}} = \frac{-709350 \times -610}{183.37} = 23600\#/\text{sq.in.}$$

Solution by Method #3

$$M_X = 713000"\#, \quad M_Y = -38000"\#$$

$$I_X = 186.46 \qquad I_Y = 431.7 \qquad I_{XY} = -36.41$$

The constants K_1, K_2, and K_3 are first determined

$$K_1 = I_{XY}/(I_X I_Y - I^2_{XY}) = \frac{-36.41}{186.46 \times 431.7 - 36.41^2} =$$

$$-.00046$$

$$K_2 = I_Y/(I_X I_Y - I^2_{XY}) = \frac{431.7}{186.46 \times 431.7 - 36.41^2} =$$

$$\frac{431.7}{793000} = .00545$$

$$K_3 = I_X/(I_X I_Y - I^2_{XY}) = \frac{186.46}{793000} = .002355$$

Stress on Stringer #1:

$$y_1 = 4.39", \quad x_1 = -17.41"$$

$$f_b = -(k_2 M_Y - k_1 M_X)x - (k_3 M_X - k_1 M_Y)y$$

$$f_{b_1} = \left[.002355 \times (-38000) - (-.00046 \times 713000)\right] -17.41 - \left[.00545 \times 713000 - (-.00046 \times (-38000)\right] 4.39$$

$$= -(238.5) - 17.41 - (3868)\ 4.39$$

$$= 4150 - 17000 = -12850 \text{ psi.}$$

Stress on Stringer #9:

$$y_9 = 6.89", \quad x_9 = 15.39"$$

$$f_{b_9} = -\left[238.5\right] 15.39 = \left[3868\right]\ 6.89 = -30320\#/\text{in}^2$$

Stress on Stringer #12:

$$y_{12} = -5.55", \quad x_{12} = -9.11"$$

$$f_{b_{12}} = -\left[238.5\right](-9.11) - \left[3868\right](-5.55) = 23620\#/\text{in}^2$$

NOTE: in the three solutions, the distances from the axis in question to the stringers 1, 9, and 12 have been taken to the centroid of each stringer unit. Thus, the stresses obtained are average axial stresses on the stringers. If the maximum stress is desired, the arm should refer to the most remote part of the stringer or the skin surface.

Approximate Method

It is sometimes erroneously assumed that the external bending moments M_X and M_Y produce bending about the X and Y axes as though they were neutral axes. To show the error of this assumption, the stresses will be computed for stringers #1 and #9.

Stringer #1

$$y_1 = 4 + .39 = 4.39$$

$$x_1 = -33.15 + 15.74 = -17.41$$

$$f_b = -\frac{M_X y}{I_X} - \frac{M_Y x_1}{I_Y}$$

$$f_b = -\frac{713000 \times 4.39}{186.46} - \frac{(-38000 \times -17.41)}{431.7} =$$

$$-18330\#/\text{in}^2.$$

Stringer #9

$$y_9 = 6.89, \quad x_9 = 15.39$$

$$f_b = -\frac{713000 \times 6.89}{186.46} - \frac{(-38000 \times 15.39)}{431.7} =$$

$$-25000\#/\text{in}^2$$

A13.9 Problems

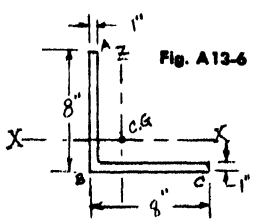


Fig. A13-6

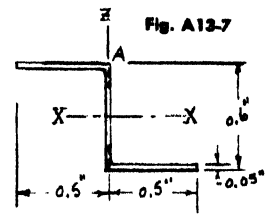


Fig. A13-7

(1) In Fig. A13.6 the angle section is subjected to a bending moment about the XX axis equal to 200,000 in.lb. Calculate the bending stresses at points A, B and C.

(2) The Z section in Fig. A13.7 is subjected to a bending moment of 80 in.lb. about axis XX and zero moment about ZZ. Find the bending stress at joint A by the three methods explained in this chapter.

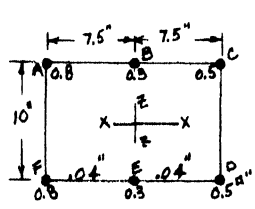


Fig. A13-8

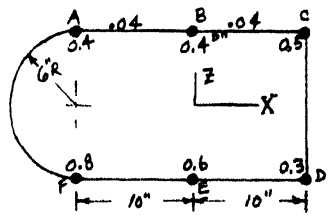


Fig. A13-9

(3) The beam section in Fig. A13.8 is subjected to $M_{XX} = 160{,}000"\#$ and $M_{ZZ} = 32000"\#$. Calculate the bending stress intensity at each of the six stringer points. Assume bottom skin effective in bending and all remaining skin ineffective in bending. Use two methods of calculation.

(4) The beam section in Fig. A13.9 is subjected to bending moments $M_X = -300{,}000"\#$ and

M_Z = -125000"#. Assume the lower skin, the curved side and the vertical webs as ineffective in bending. Calculate the bending stress intensity at the midpoint of the six stringers A to F.

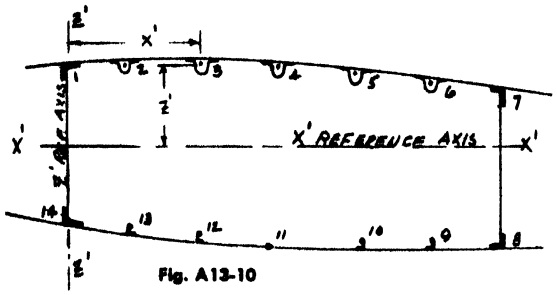


Fig. A13-10

(5) Fig. A13.10 shows a cross-section of a wing box type beam. The effective section is represented by the 14 flange and stringer units. Table A shows the area of each of these units and their centroid distances from the reference Z' and X' axes.

Compute the stresses at the centroid of each stringer due to the following bending moments:-

M_X = 500,000"#

M_Z = -107,500"#

TABLE A

Flange No.	Area A	Arm Z'	Arm X'
1	.476	5.60	-0.10
2	.318	5.83	4.40
3	.266	5.75	10.00
4	.266	5.42	15.60
5	.266	4.90	21.20
6	.318	4.30	26.70
7	.476	3.60	31.70
8	.553	-7.10	31.70
9	.235	-7.40	26.50
10	.235	-7.40	21.30
11	.125	-7.20	15.10
12	.235	-6.90	9.60
13	.235	-6.25	4.50
14	.605	-5.40	-0.10
TOTALS	4.61		

CHAPTER A14
SHEAR FLOW - BENDING OF OPEN SECTIONS

A14.1 Introduction. In many cases of beam design, it is important to know where to locate external loads so that the beam will bend without twisting. This chapter deals with bending of beams with open sections. Closed and cellular sections are treated in following chapters.

A14.2 Shear Center

When a beam bends without twisting, due to some external load system, shearing stresses are set up on the cross sections of the beam. The centroid of this internal shear force system is often referred to as the shear center for the particular section. The resultant external shear load at this section must pass through the shear center of the section if twist of the section is to be prevented. Thus, if the shear center is known, it is possible to represent the external load influences by two systems, one that causes flexure and the other which causes only twist.

A14.3 Equation for Internal Flexural Shear Stress Distribution for Prismatic Beams

The general expression for flexural shear distribution for beams of uniform section was derived in Chapter A12. A second derivation will be given to emphasize the fundamental relationships.

Fig. A14.1 shows a cantilever beam extending from the section ABCD and supporting the external load P, assumed as so located as to produce bending about the X-X axis as the neutral axis without twist of the beam. The direction of the coordinate axes have been taken as shown. Fig. A14.2 shows a free body of a small portion of differential length which has been cut out from the upper flange. Under the external load P it is evident that the upper flange is in compression.

In Fig. A14.2, C_y' = total compressive stress on the body at station Y' and C_y that at station Y. Obviously, C_y' is greater than C_y, since the cantilever bending moment is greater at station Y'. The other forces on the free body in the Y direction are the shearing forces on the sides at section a and b, represented by q_{yb} and q_{ya}.

For equilibrium in the Y direction, $\Sigma F_y = 0$, hence

$$-q_{yb}\,dy + q_{ya}\,dy + (C'_y - C_y) = 0$$

$$\text{or } q_{yb} = q_{ya} + \frac{C'_y - C_y}{dy}$$

$$\text{but } (C'_y - C_y) = \frac{M' - M}{I_x}\int_a^b z\,dA \quad \text{(Refer to Art. A12.3)}$$

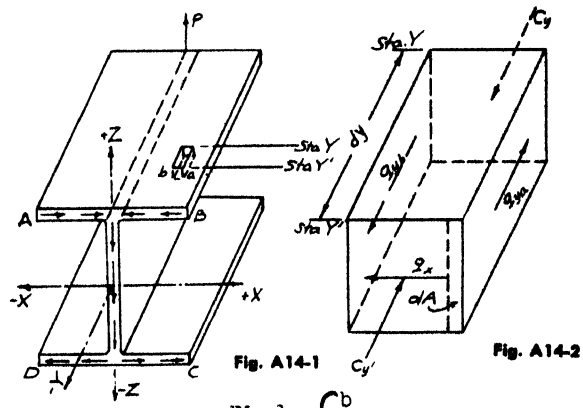


Fig. A14-1 Fig. A14-2

$$\text{hence } q_{yb} = q_{ya} + \frac{dM}{dy}\,\frac{1}{I_x}\int_a^b z\,dA$$

But $\frac{dM}{dy} = V$ = external shear in ZZ direction

$$\text{hence, } q_{yb} = q_{ya} + \frac{V}{I_x}\int_a^b z\,dA \quad \text{-------(1)}$$

Furthermore, we know from elementary mechanics that the intensities of shearing stresses on planes at right angles to each other at any point in a body are equal.

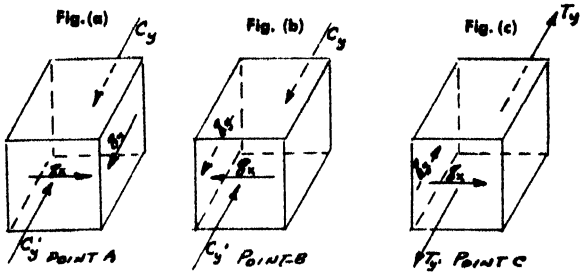
Thus at section b (Fig. 14.2), $-q_{y_b} = -q_{x_b}$ or in general $q_y = q_x$ ----------(2)

and in a similar manner, it can be shown that $q_y = q_z$ ----------(3)

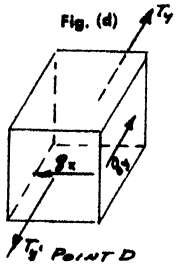
Thus, having determined the intensity and direction of the horizontal shear stress q_y from equation (1), the shear stress in a plane at right angles is of the same intensity.

A14.3a Sense of Shear Flow q in XZ Plane.

The sense of the shear flow in the XZ plane is easily determined from a consideration of the forces on a differential cube cut from the section at a point where the shear flow intensity has been computed. Figs. a, b, c and d illustrate the determination of the sense of q_x and q_z at the four points A, B, C and D on the cross-section of the beam of Fig. A14.1. The sense of a q_y is given by equation (1), however it is likewise obvious from the figures, since C'_y or T'_y is greater than C_y or T_y for the given beam and loading. For equilibrium of the cube, the shear flow q_x or q_z must act as shown which thus gives the sense of the shear flow as shown on the beam section in figure A14.1. In general when the sense of the shear flow is established at a point it will act continously in this direction until equation (1) reverses its sign.



The following general rules for establishing the sense of the shear flow on the cross-section of a beam in the xz plane are convenient. Rewriting equation on a modified form.



$$q = \frac{V_Z}{I_X} \Sigma zA \quad \text{- - - - - - - - - (4)}$$

when bending is about axis xx.

$$q = \frac{V_X}{I_Z} \Sigma xA \quad \text{- - - - - - - - - (5)}$$

when bending is about axis zz.

V_Z is positive when up.

V_X is positive when acting toward the right.

z is positive when measured above x axis.

x is positive when measured to the right of z axis.

If in equation (4) or (5) the summation ΣzA or ΣxA is carried out in a clockwise direction around the cross-section of the beam, then a resulting positive value of q means that the shear flow on section at the particular point is in a clockwise sense. If the summation is carried out in a counterclockwise direction, then the equations for q should be written

$q = -\frac{V}{I} \Sigma zA$, that is with a minus sign in order to make the above rule hold.

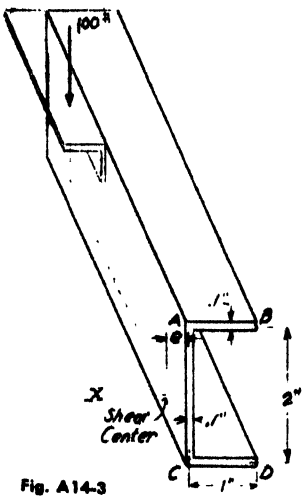
A14.4 Shear Center For Sections Possessing One Axis of Symmetry

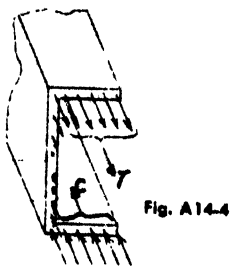
Fig. A14.3 shows a channel beam carrying a 100# load as a cantilever. The problem is to determine where the 100# load is to be placed laterally so as to cause the channel to bend about the symmetrical axis XX without twisting. The beam has been cut at section ABCD and we have from statics that the internal stress system must hold the external load in equilibrium. In other words, the following equations must be satisfied:

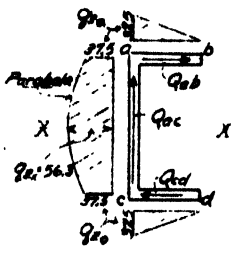
$$\Sigma F_Z = 0,\ \Sigma M_X = 0,\ \Sigma M_y = 0,\ \Sigma F_X = 0,\ \Sigma F_y = 0,$$

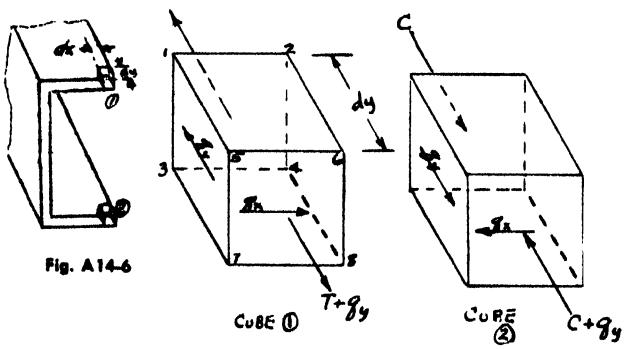
$$\Sigma M_Z = 0$$

From the fundamental beam theory, for bending about the neutral axis XX, the internal fiber stresses normal to the XZ plane form a couple TC (see Fig. A14.4) which equals the bending moment of the external load about the









XX axis. Thus, $\Sigma M_X = 0$ is satisfied. Since T = C, $\Sigma F_y = 0$ is also satisfied.

The internal shear stress pattern must now be determined before we can set up the remaining equations of equilibrium. From article A14.3, we have equations (1), (2) and (3) which provide the means of determining the internal shear system.

Fig. A14.5 shows the shear stress intensity diagram as well as the direction of the shear forces on the cross-section. The calculations, using Eq. (1) for determining this shear pattern, are as follows:

I_{XX} for the section = .2667 in.^{4}

Consider a point at the edge b of the upper flange. The longitudinal shear stress at this point is obviously zero, or

$\int zdA = 0$ since $dA = 0$

Consider point a (intersection of the center lines of flange and web). Substituting in Eq. (1)

$$q_a = q_b - \frac{V_Z}{I_X}\int_b^a zdA = 0 - \frac{(-100)}{.2667}\ (1 \times .1 \times 1) = 37.5\#/\text{in.}$$

(+) is clockwise)

At a point on the XX axis:

$$q_x = q_a - \frac{V_Z}{I_X}\int_x^a zdA = 37.5 - \frac{(-100)}{.2667}\ (1 \times .1 \times .5) =$$

56.3#/in.

Due to symmetry, it is obvious that q_{yc} = + 37.5 and q_{yd} = 0. The expression $\int zdA$ tells us that the shear intensity varies as a straight line between b and a, while from a to the axis XX, it varies as kz^n, or parabolic.

Since shear intensities in planes at right angles are equal at any point, the shear stress diagrams plotted in Fig. A14.5 also represent the intensities on the beam section in the XZ plane. Then, the total shear force on flange ab = Q_{ab} = $\frac{37.5}{2}$ x 1 = 18.75# and similarly Q_{cd} = 18.75#

$$Q_{ac} = 37.5 \times 2 + (56.3 - 37.5)\ .667 \times 2 = 100\#$$

The minus sign before the $\frac{V}{I}$ term in the above equations is due to the fact that $\int_b^a zda$ is carried out in a counterclockwise direction. (See rule in previous article). Fig. A14.6, cube (1) and (2) illustrate how the sense of q can be determined by considering equilibrium of cubes.

Having determined the internal shear pattern, the following equilibrium equations must still be satisfied.

ΣF_X = 0, Q_{ab} and Q_{cd} are the only x forces:

hence 18.75 - 18.75 = 0

ΣF_Z = 0. The external shear force and the internal force Q_{ac} are the only Z forces.

hence - 100 + 100 = 0

ΣM_Z = 0. This is true since no forces have moments about the Z-Z axis.

ΣM_y = 0. This expression says that the moment of the force forces about any axis perpendicular to the XZ plane must be zero. Assume a moment axis on the center line of the channel web at the neutral axis XX. The moment of the internal force system about this point equals 18.75 x 1 + 18.75 x 1 = 37.5"# (clockwise). Q_{ac} has no moment since it passes thru the moment axis. Since ΣM_y must equal zero, the external shear force must produce a moment of -37.5"#. To do this, the external shear force V_Z = -100# must act at a distance 37.5/100 = .375" to the rear of the channel web. Thus, the shear center for bending about the axis XX lies .375" back of the centerline of the web channel. (See distance e Fig. A14.3)

Therefore, we can state that for sections possessing one axis of symmetry, in bending about the symmetrical axis as the neutral axis, the shear center does not lie in a plane perpendicular to the neutral axis through the center of gravity of the section but lies at some distance from the C.G. of the section.

However, for bending loads parallel to the plane of the symmetrical axis, which causes bending about the other principal axis as the neutral axis, the shear center will lie in the plane of the symmetrical axis. This is evident from inspection of Fig. A14.7. If the internal stress pattern is determined by Eq. (1), it will give the results shown diagrammatically in Fig. A14.7. It is evident that the resulting position of the vertical components of the internal shear system lies on the symmetrical axis. Therefore, for equilibrium the external shear must lie in the plane of the symmetrical axis, or e must equal zero. Fig. A14.8 shows a symmetrical I section. For bending about axis XX

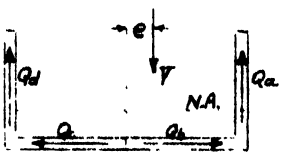


Fig. A14-7 Shear Center Symmetrical Axis

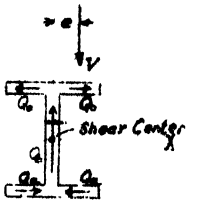


Fig. A14-8

without twisting, it is evident that the shear center lies on the Z-Z axis, since the resultant of the internal shear pattern lies on the Z-Z axis or e = 0 for location of the external shear load.

A14.5 Additional Illustrative Examples

Example #1 Equal Leg Angle Section for Bending About the Symmetrical Axis (see Fig. A14.9)

For bending about axis XX, the internal shear stress pattern from equation (1) will give that shown in Fig. A14.9. The vertical components of the two internal shear forces Q_a will equal V in magnitude. The horizontal component of the internal system equals zero, and the resultant of the internal system must pass through point O, since the moments of the separate internal forces about O is zero. The shear center is therefore at O and the external V load must act through the point O to prevent twisting when bending about axis X-X.

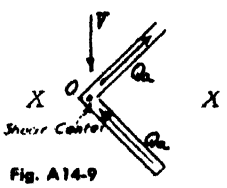


Fig. A14-9

Example #2 Unequal Flanges H Section

Problem:- To find where to place the external load V = 100 to cause bending about axis X-X with no twist. It will be assumed that the web takes no bending axial loads.

$$I_{XX} \text{ of Flange (1)} = \frac{1}{12} \times .2 \times 10^3 = 16.67$$

$$I_{XX} \text{ of Flange (2)} = \frac{1}{12} \times .3 \times 6^3 = \underline{5.40}$$

Total I_{XX} 22.07

Determination of the internal shear system:-

Flange (1)

Point at axis X-X

$$q_x = -\frac{V}{I_x}\int_a^o z\,da = -\frac{-100}{22.07} \times .2 \times 5 \times 2.5 = 11.35\#/in.$$

Points a and b

$q_a = q_b = 0$ since $\int z\,dA = 0$

Q_1 = area of shear intensity curve (see Fig. A14.11) = 2/3 x 11.35 x 10 = 75.5#

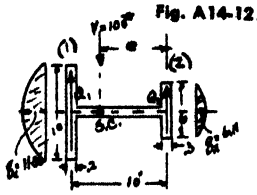


Fig. A14-12

Flange (2)

Point on axis x-x

Fig. A14-11 Fig. A14-10

$$q_x = -\frac{-100}{22.07} \times .3 \times 3 \times 1.5 = 6.11\#/in.$$ (see Fig. A14.12)

Then Q_2 = area of Fig. A14.12 = 2/3 x 6.11 x 6. = 24.5#

Now, $\Sigma F_z = 0 = 24.5 + 75.5 - 100 = 0$ satisfied.

$\Sigma M = 0$

Take moments about a point on Q_2

$$\Sigma M = -100e + 75.5 \times 10 = 0 \quad \therefore \quad e = \frac{75.5}{100} \times 10 = 7.55"$$

Hence the shear center lies at a distance of 7.55" from the center line of flange (2)

Example Problem #3

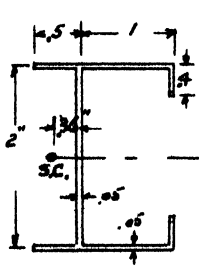


Fig. A14-13

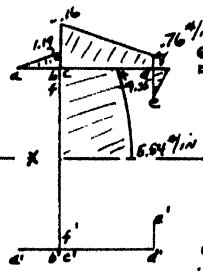


Fig. A14-14

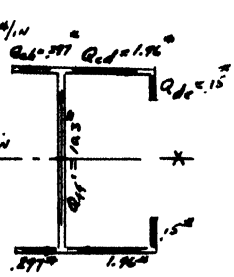


Fig. A14-15

Determine the shear center for bending about axis X-X for the section shown in Fig, A14.13

I_{xx} of section = .2094 (based on ℄ dimensions)

For convenience, we will assume a shear load of V = 10# acting down which causes tension in the upper half of the beam due to bending. Calculation of the internal shear pattern: See Fig. A14.14

Point e

$q_e = 0$ since $\int z\,dA = 0$

Point d

$$q_d = 0 - \frac{V}{I_x}\int_e^d z\,dA = -\frac{-10}{.2094} \times .4 \times .05 \times .8 = .76\#/in.$$

Point c

$$q_c = q_d - \frac{-10}{.2094}\int_d^c z\,dA = .76 - \frac{-10}{.2094} \times 1 \times .05 \times 1 = 3.16\#/in.$$

Point a

$q_a = 0$ since $\int z\,dA = 0$

Point b

$$q_b = +\frac{-10}{.2094}\int_a^b z\,dA = -\frac{-10}{.2094} \times .5 \times .05 \times 1 = -1.19\#/in.$$

Point f

$q_f = q_b + q_c = 1.19 + 3.16 = 4.35\#/in.$

Point x

$$q_x = q_f - \frac{-10}{.2094}\int_f^x z\,dA = 4.35 - \frac{-10}{.2094} \times 1 \times .05 \times .5 = 5.54\#/in.$$

Fig. A14.14 shows these values plotted on cross-section. The variation of stress between e and d has been drawn as a straight line which is approximately true. The stress intensity for the lower half is, of course, identical to that for the upper half.

The total internal shear force on each portion equals the area of the shear diagrams.

Hence

$$Q_{ab} = \frac{1.19}{2} \times .5 = .299\#$$

$$Q_{cd} = \frac{3.16 + .76}{2} \times 1 = 1.96\#$$

$$Q_{de} = .76 \times \frac{.4}{2} = .15\#$$

$$Q_{ff'} = 4.35 \times 2 + (5.54 - 4.35) \times .667 \times 2 = 10.30\#$$

Fig. A14.15 shows these forces acting on the section. The direction of these stresses is easily determined by a consideration of the forces on a differential cube as explained in article A14.3. Since we assumed a shear force of -10 acting on the section, we will check to see if ΣF_z of the internal stresses = 10

$$\Sigma F_z = 10.3 - .15 - .15 = 10$$

Take moments about the intersection of $Q_{ff'}$ and the XX axis of the internal system:

$$\Sigma M = +1.96 \times 1 \times 2 + .15 \times 1 \times 2 - .297 \times 1 \times 2 = 3.63"\# \text{ (clockwise)}$$

The external shear force must produce an opposite moment of this magnitude if no twisting is to take place. Therefore, the shear center lies $\frac{3.63}{10}$ = .36" to the left of the vertical leg web of the section. (See Fig. A14.13)

A14.6 Beams With Constant Flow Shear Webs

Fig. A14.16 shows a beam composed of heavy flange members and a curved thin web. For bending about axis X-X the web on the compressive side of the neutral axis absorbs very little compressive axial stress, since buckling will occur at low stresses, particularly when the curvature of the sheet is small. On the tension side, the web will be more effective, but if the flange areas are relatively large, the

proportion of the bending stresses carried by the web is very small and for all practical purposes, the flexural web shear stress is constant between flanges. In other words, in the formula $q = \frac{V}{I} \int zdA$, if the effect of the web is negligible, the term $\int zdA$ is constant and therefore q is constant.

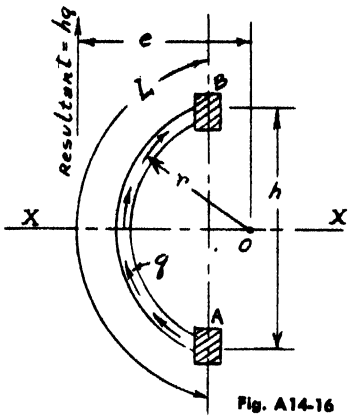


Fig. A14-16

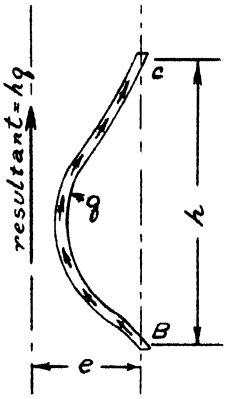


Fig. A14-17

Let q equal the shear stress per inch, and since it is constant, we will assume q = 1 for simplicity.

The direction of the resultant of the shear stresses on the web is obviously in a direction parallel to the line AB or a line joining the ends of the web, because the components of the shear stress normal to this line are zero. The magnitude of the resultant shear flow is qh or h since q = unity. Since the moment of the resultant about any point must equal the moment of the shear flow system, we will take moments for convenience about point O.

$$(1 \times h)e = L \times 1 \times r$$

hence $e = \frac{Lr}{h}$, where e is the distance from O to the resultant of the shear flow pattern. Thus, to prevent twisting in bending about axis X-X, the external shear load must act at a distance $e = \frac{Lr}{h}$ from the center of curvature of the circular web.

A14.7 General Relationships for Resultants of Constant Flow Shear Patterns

The following general relationships relative to the resultant of a constant flow shear pattern are useful in the solution of certain types of thin wall beams, as illustrated in later chapters.

Referring to Fig. A14.17: (1) The magnitude of the resultant of the shear flow pattern is equal to hq, where h is the length of the line joining the ends of the web and q is the shear stress intensity per running inch. (2) The direction of the resultant is parallel to the line BC, a line joining the ends of the web. (3) The line of action of the resultant with references to the line BC equals $e = \frac{2A}{h}$, where A is the enclosed area formed by the web and the closing line BC.

Example Problem #4

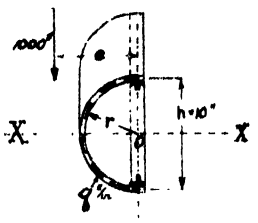


Fig. A14-18

For the beam with a curved web as shown in Fig. A14.18, determine the position of the external load of 1000# so that the beam will bend about axis XX without twist. Assume that the web takes no flexural axial loads.

For equilibrium:-

$\Sigma V = -1000 + 10q = 0 \therefore q = 100\#/\text{inch}$.

$\Sigma F_X = -q \times 5 + q \times 5 = -500 + 500 = 0$

$\Sigma M_O = -1000e + q\pi r \cdot r = 0$

$= -1000e + 100\pi \times 5^2 = 0$

$\therefore e = \frac{7870}{1000} = 7.87"$

Therefore, the shear center is 7.87" to the left of point O, on axis X-X, because axis X-X is an axis of symmetry. The distance e could also be solved for using the general relationship given in item (3), that is, $e = \frac{2A}{h}$, where A is the area between the web and line CD.

Hence, $e = \frac{2\pi 5^2}{2 \times 10} = 7.87"$ as found before

Example Problem #5

Fig. A14.19 shows an open beam section composed of eight flange members or stringers connected by thin sheet to form the webs and walls. The stringers are numbered a to h and the areas

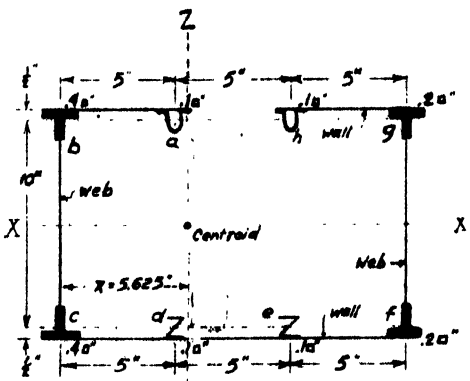


Fig. A14-19

of each are given on the figure. Assuming that the thin webs and walls do not take flexural bending loads, compute the shear center for the cross-section, assuming the beam section is constant spanwise.

Solution

Determine the centroidal principal axes.

The vertical position of the section centroid by observation, due to symmetry, is midway between the flange members.

To find the horizontal position of the section, take moments about the left end of the section on line bc.

$$\bar{x} = \frac{.4 \times 15 + .2 \times 10 + .2 \times 5}{1.6} = 5.625"$$

$$I_X = .8 \times 5^2 \times 2 = 40 \text{ in.}^4$$

$$I_Z = .8 \times \overline{5.625}^2 + .2 \times \overline{.625}^2 + .2 \times \overline{4.375}^2 + .4 \times \overline{9.375}^2 = 64.4 \text{ in.}^4$$

Horizontal Position of Shear Center:

To find the horizontal position of the shear center, we find the horizontal location of the centroid of the internal shear flow system due to bending about the principal axis X-X.

For convenience, to eliminate large decimal values for shear stress values, an external shear load of V = + 100# acting normal to XX will be assumed.

Calculation of Internal Shear Flow System:

Beginning with stringer a, the shear stress per inch along the section will be computed. Since the skin is considered ineffective in taking bending axial stresses, the shear stress will be constant between stringers. The general expression for the shear stress per inch = $q = \frac{V_Z}{I_X} \Sigma z A = \frac{100}{40} \Sigma z A = -2.5 \Sigma zA$.

(minus sign due to counter clockwise summation around section). $q_{ab} = -2.5 \Sigma z A = -2.5 (5x.1) = -1.25$#/in. (The subscript ab refers to the shear flow q adjacent to stringer a on the side toward b).

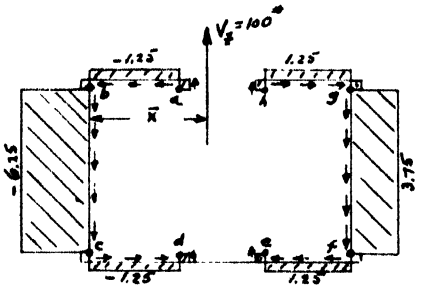


Fig. A14-20

$q_{ba} = -1.25$

$q_{bc} = -1.25 -2.5 (5x.4) = -6.25$#/in.

$q_{cb} = -6.25$

$q_{cd} = -6.25 -2.5 (-5x.4) = -1.25$#/in.

$q_{dc} = -1.25$

$q_{de} = -1.25 -2.5 (-5x.1) = 0$

$q_{ed} = 0$

$q_{ef} = 0 -2.5 (-5x.1) = 1.25$#/in.

$q_{fe} = 1.25$

$q_{fg} = 1.25 -2.5 (-5x.2) = 3.75$#/in.

$q_{gh} = 3.75 -2.5 (5x.2) = 1.25$

$q_{hg} = 1.25$

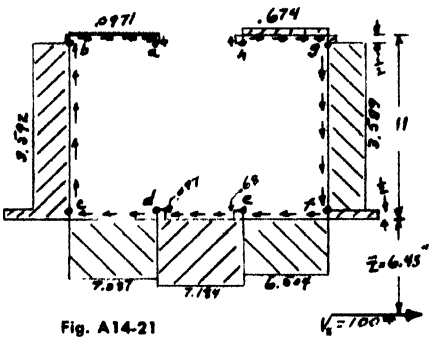


Fig. A14-21

Fig. A14.20 shows the results in graphical form. The circular dots represent centroids of the flange stringers. The shear flow values are assumed to change at these centroid points.

For equilibrium of the external and internal shear forces in the plane of the beam cross-section, ΣF_X, ΣF_Z and ΣM must equal zero.

$\Sigma F_X = -5 \times 1.25 + 5 \times 1.25 - 5 \times 1.25 + 5 \times 1.25 = 0$ (check)

$\Sigma F_Z = 100 - 10 \times 6.25 - 10 \times 3.75 + 1.25 \times .5 \times 4 - 1.25 \times .5 \times 4 = 0$ (check)

For $\Sigma M = 0$, take moments about some point such as C.

$\Sigma M_C = -100 \bar{x} + 10 \times 3.75 \times 15 - 1.25 \times .5 \times 2 \times 5 - 1.25 \times .5 \times 2 \times 10 + 1.25 \times .5 \times 2 \times 15 = 0$

Hence $\bar{x} = 562.5/100 = 5.625"$. Therefore to prevent twisting of the section, the external vertical shear load must act through a point 5.625" from side bc, which locates the horizontal position of the shear center.

Calculation for Vertical Position of Shear Center:

For convenience as before, we assume a shear load $V_X = 100$# acting normal to the principal axis ZZ, and compute the internal shear system to resist this external load assuming bending about axis ZZ without twist.

$$q = \frac{V_X}{I_Z} \Sigma x A = -(100/64.4) \Sigma x A = -1.55 \Sigma x A$$

Starting adjacent to stringer a and proceeding counterclockwise around the beam section:

$q_{ab} = -1.55 \Sigma x A = -1.55 (-.625 \times .1) = .0971$#/in. (clockwise)

$q_{ba} = .0971$

$q_{bc} = .0971 -1.55 (-5.625 \times .4) = 3.592$#/in.

$q_{cb} = 3.592$

$q_{cd} = 3.592 -1.55 (5.625 \times .4) = 7.087$#/in.

$q_{dc} = 7.087$

$q_{de} = 7.087 - 1.55\ (-.625 \times .1) = 7.184$#/in

$q_{ed} = 7.184$

$q_{ef} = 7.184 - 1.55\ (4.375 \times .1) = 6.504$

$q_{fe} = 6.504$

$q_{fg} = 6.504 - 1.55\ (9.375 \times .2) = 3.589$

$q_{gf} = 3.589$

$q_{gh} = 3.589 - 1.55\ (9.375 \times .2) = .674$

Fig. A14.21 shows the shear flow pattern in graphical form. The circular dots represent the centroids of the stringers.

Checking to see if $\Sigma F_Z = 0$,

$\Sigma F_Z = 3.592 \times 10 - 3.589 \times 10 + .5 \times .09\ 71 - .5 \times .09\ 71 + 5 \times .674 - .5 \times .674 + .5 \times .097 - .5 \times .68 - .5 \times 6.504 + .5 \times 7.087 = 0$ (check)

Check to see if $\Sigma F_X = 0$,

$\Sigma F_X = 100 + 5 \times .09\ 71 + 5 \times .674 - 5\ (7.087 + 7.184 + 6.504) = 0$ (check)

The resultant of the internal shear flow is a horizontal force of 100#. To find its location, take moments about point 1/2" below c.

$\Sigma M_C = 5\ (.09\ 71 + .674)\ 11 + 10 \times 3.589 \times 15 + (.5 \times .09\ 71 \times 5) - (.5 \times .674 \times 10) + (.5 \times .674 \times 15) + (.5 \times 6.504 \times 15) + .5 \times .68 \times 10 - (.5 \times .097 \times 5) - 100\ \bar{z} = 0$

$\therefore\ \bar{z} = \frac{643}{100} = 6.43$" below side cdef as shown.

Fig. A14.22 shows the resultant position of the shear center for the section.

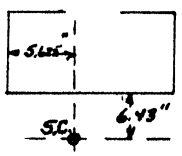


Fig. A14-22

A14.8 Shear Flow and Shear Center for Unsymmetrical Open Beam Sections

In the bending of unsymmetrical sections without twist the bending is referred to the principal axes, and thus the properties and distances to stringers must be in reference to the principal axes when substituting in the general shear flow equation. If shear flow is calculated by use of the ΔP axial loads in the stringers, as explained in the example problem which follows, then the ΔP loads must be found by flexural equations for unsymmetrical bending as given in chapter A13.

Example Problem #6

Fig. A14.23 shows an unsymmetrical channel section with four concentrated flange members a, b, c and d. The web members connecting these flanges will be neglected in computing the section properties or in other words the flanges provide the entire bending resistance.

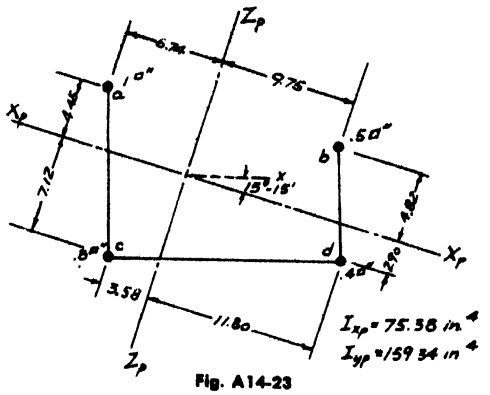


Fig. A14-23

The first step is the calculation of the position of the principal axes and the moment of inertia about the principal axes. As for as effective flange material is concerned the beam section is identical to the beam section of Fig. A13.3 of chapter A13, thus reference should be made to Art. A13.8 for the necessary calculations for the principal moments of inertia.

Solution Shear Center Locations for Bending About Xp Principal Axis.

For simplicity a shear load $V_{Z_p} = 100$# will be assumed.

$q = \frac{V_{Z_p}}{I_{X_p}} \Sigma\ z_p\ A = -(100/75.38)\ \Sigma\ z_p A = -1.328\ \Sigma z_p\ A$

$q_{ac} = -1.328\ (4.45 \times 1) = -5.91$#/in.

$q_{ca} = -5.91$

$q_{cd} = -5.91 - 1.328\ (-7.12 \times .8) = 1.65$#/in.

$q_{dc} = -1.65$

$q_{db} = 1.65 - 1.328\ (-2.90 \times .4) = 3.19$#/in.

Fig. A14.24 shows the shear flow diagram for bending about X_p axis for an external shear load of 100#

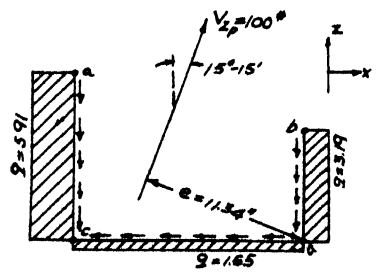


Fig. A14-24

Check ΣF_Z and $\Sigma F_X = 0$

$\Sigma F_Z = 100 \times \cos 15^0 - 15' - 12 \times 5.91 - 8 \times 3.19 = 96.47 - 70.97 - 25.5 = 0$

$\Sigma F_X = 100 \sin 15^0 - 15' - 16 \times 1.65 = 26.36 - 26.36 = 0$

The resultant of the internal shear flow pattern

equals - 100# acting parallel to the z_p axis. To find the location of the resultant take moments about some point such as d.

$\Sigma M_d = 100e - 12 \times 5.91 \times 16 = 0$
hence $e = 1134/100 = 11.34"$

Thus for bending about the x_p axis the shear center lies on a line parallel to the z_p axis and located a distance 11.34" from point d.

Shear Center for Bending About the z_p Principal Axis

$I_{z_p} = 159.34$. Assume $V_{x_p} = + 100\#$

Therefore $q = -\frac{100}{159.34} \Sigma x_p A = - .627 \Sigma x_p A$

$q_{ac} = - .627 (-6.74 \times 1) = 4.22\#/in.$ (clockwise)

$q_{cd} = 4.22 - .627 (-3.58 \times .8) = 6.02\#/in.$

$q_{db} = 6.02 - .627 (11.80 \times .4) = 3.05\#/in.$

Fig. A14.25 shows the resulting shear flow diagram.
Check ΣF_x and $\Sigma F_z = 0$

$\Sigma F_x = 100 \cos 15^0 - 15' - 16 \times 6.08 = 96.47 - 96.47 = 0$

$\Sigma F_z = -100 \sin 15^0 - 15' + 4.22 \times 12 + 8 \times 3.05 = 0$

The resultant of the internal system is -100# parallel to X_p axis. To find its location take moments about point d.

$\Sigma M_d = 100e + 4.22 \times 12 \times 16 = 0$ hence $e = 811/100 = 8.11"$ (see Fig. A14.25)

The shear center proper is therefore given by the two reference distances e in figures 24 and 25.

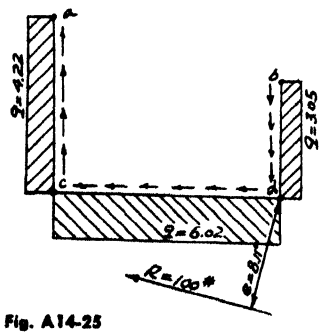


Fig. A14-25

A14.9 Solution By Considering Δ P loads In Flange Members

The equation $q = \frac{V_z}{I_x} \Sigma zA$ can be written

$q = \frac{dM}{dx} \frac{1}{I_x} \Sigma z A$. For a particular stringer or flange member of area A, this expression represents the change in the axial load on the stringer over a length dx and if dx is taken as 1", the change in axial load per inch of stringer due to bending of the entire beam section represents the change in shear flow in the connecting web or wall as you pass from one side of the stringer to the other.

To illustrate, the shear flow pattern for the first part of example problem #6 will be determined by considering the Δ P loads in the stringers:

The change in bending moment about the X_p axis per inch of beam = $\Delta M = 1 \times 100 = 100"\#$.

The change in the stringer axial loads due to this moment of 100"# equals $\Delta P = -\left(\frac{\Delta M_{x_p} z}{I_x}\right) A$,

where A is the area of a particular stringer and z is the distance from the X_p axis to this stringer. For stringer a (see Fig. A14.23).

$$\Delta P = -\left(\frac{100 \times 4.45}{75.38}\right) 1.0 = -5.91\#$$

For stringer c

$$\Delta P = -\left(\frac{100 \times -7.12}{75.38}\right) .8 = 7.56\#$$

For stringer d

$$\Delta P = -\left(\frac{100 \times -2.90}{75.38}\right) .4 = 1.54\#$$

For stringer b

$$\Delta P = -\left(\frac{100 \times 4.82}{75.38}\right) .5 = -3.19\#$$

Fig. A14.26 shows the resulting Δ P loads in the stringers. Starting with stringer a or d the horizontal shear in the connecting webs obviously equals Σ Δ P of all forces to one side of the section being considered.

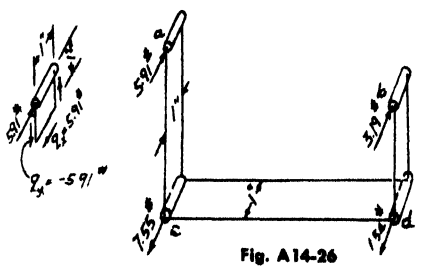


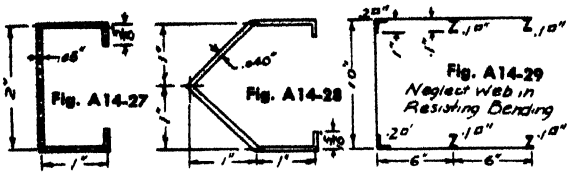
Fig. A14-26

Thus the shear q between a and c = 5.91#. Between c and d, q = 5.91 - 7.55 = - 1.65 and between b and d, q = 3.19#. The shear flow in the plane of the cross-section is of the same intensity and the direction is easily determined by inspection or by drawing a simple free body diagram as shown in Fig. A14.26 for the web portion between a and b.

The resulting shear flow diagram is of course identical to that of Fig. A14.24. This method making use of the Δ P loads is quite useful in dealing with tapered wing boxes and will be discussed in later articles.

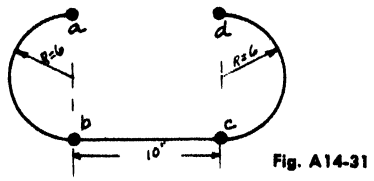
A14.10 Problems

(1) Determine the shear flow diagram and the shear center location for bending about the horizontal symmetrical axis for the section in Figs. A14.27 to A14.29.

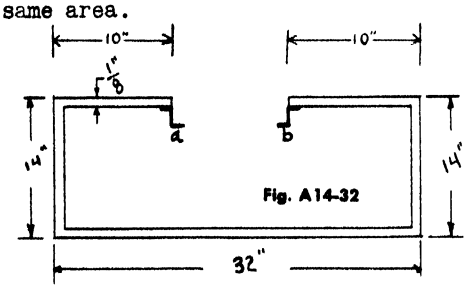


(2) Determine the shear center of the unsymmetrical section of Fig. A14.30. Consider the web as ineffective in resisting bending stresses.

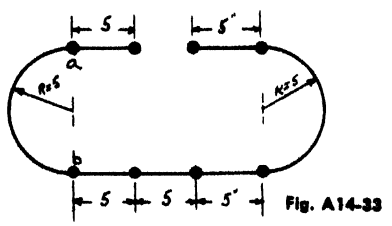




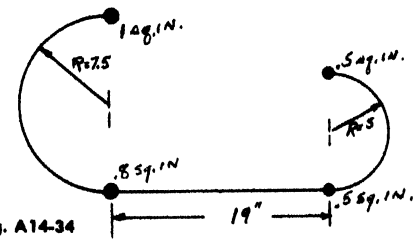
(3) Determine the shear center of the section of Fig. A14.31. Assume the flange members a, b, c and d as the only effective material in resisting bending loads. All four stringers have same area.



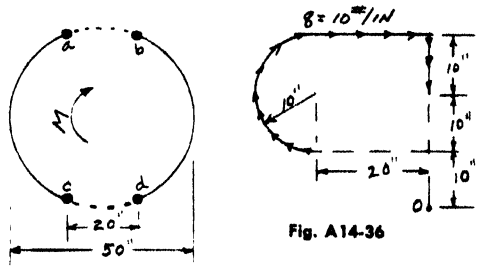
(4) Determine the shear center location beam section of Fig. A14.32. All material is effective. The Z stringers (a) and (b) are 1-1/2 inches deep and have an area of .5 sq. inches each.



(5) Determine the shear center for the beam section of Fig. A14.33. Assume only the 8 stringers as being effective in bending. Area of stringers (a) and (b) = 2 sq. in. each. All other stringers 1 sq. in. each.

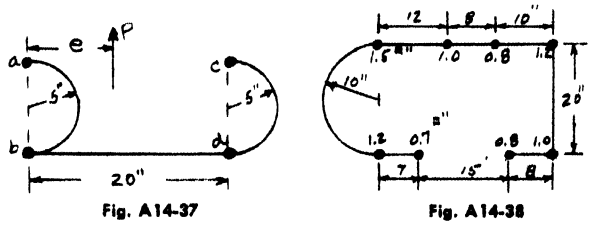


(6) Determine the shear center for the unsymmetrical beam section of Fig. A14.34. Assume sheet connecting the four stringers as ineffective. Areas of stringers shown on Fig.



(7) In Fig. A14.35, the shell structure is subjected to a torsional moment M = 50,000 in. lb. The shell skin shown dashed is cut out, thus the torsional moment is resisted by the constant shear flow on the two curved sheet elements ac, and bd. Determine the value of the shear flow.

(8) Determine the moment of the constant flow force system in Fig. A14.36 about point (O). Also find the resultant of this force system.



(9) In Fig. A14.37, the four stringers a, b, c and d have the same area. Assume the webs ineffective in resisting bending stresses. Determine the distance (e) to produce bending about the horizontal axis without twist.

(10) For the wing cell beam section in Fig. A14.38, determine the location of the shear center. Assume webs and walls ineffective in bending.

CHAPTER A15
SHEAR FLOW - CLOSED SECTIONS

A15.1 Introduction. The wing and fuselage of the present day metal covered airplane is essentially a single or multiple box beam. A stress analysis of such a structural unit involves consideration of the distribution of the internal resisting shear stresses. This chapter deals only with a simplified elementary treatment of shear flow in cellular beams in order to acquaint the student with the general principles. Later chapters will apply these general principles to practical airplane problems. Chapter A14 should be studied before undertaking this chapter.

A15.2 Single Cell - 2 Flange - Box Beam

Fig. 15.1 shows a single-cell-2 flange beam. The vertical web and leading edge skin is assumed ineffective in taking bending axial loads, or in other words, the two flange members A and B provide the bending resistance.

area of each flange = .5 sq.in.

area of cell = 80.52 sq.in.

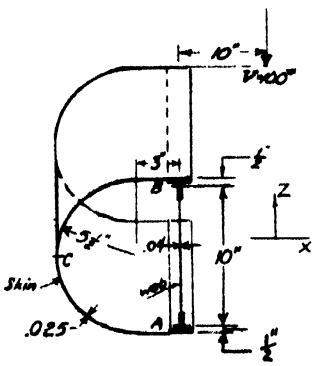


Fig. A15-1

It is obvious that the external loads must act in a vertical direction or parallel to AB as the two flanges have negligible bending resistance in the horizontal direction. The external loads, however, do not have to lie in the plane of AB, as the closed cell formed by the web and skin can resist torsional moments due to the external loads. Since the web and skin have been assumed to take no bending axial loads, the flexural shear flow on each part will be constant; however, the distribution between the web and skin cannot be found directly as in an open section because the point of zero-shear is not known. For equilibrium in the plane of the cross-section we know that ΣF_Z and ΣF_X for the internal shear system plus the external load system must equal zero. Likewise, ΣM about any axis normal to the beam section of all internal and external forces must equal zero.

Assumed static flexural shear flow. $\Sigma F_Z = 0$, $\Sigma F_X = 0$	plus constant shear flow to make $\Sigma M_y = 0$	gives the true shear

q is assumed zero at point C.

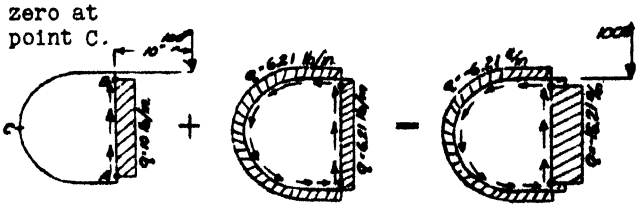


Fig. A15-2 Fig. A15-3 Fig. A15-4

q is assumed zero at point D

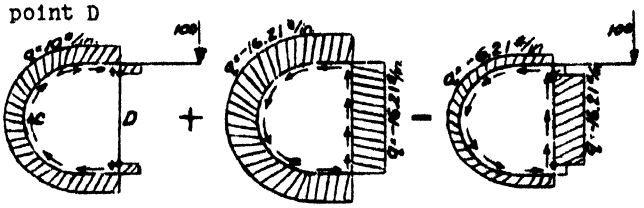


Fig. A15-5 Fig. A15-6 Fig. A15-7

q is assumed -5 at point C

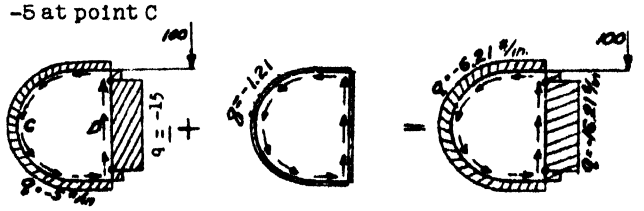


Fig. A15-8 Fig. A15-9 Fig. A15-10

Solution Method 1 (Internal Shear Flow For Cell of Fig. 15.1

Assume a value for the internal shear flow stress at some point and compute the balance of the internal flexural shear flow consistent with this assumption. For illustration Fig. 15.2 shows the flexural shear system if we assume the shear is zero at point C and Fig. 15.5 shows the results if the shear is assumed zero at a point midway between A and B and Fig. 15.8 shows the shear pattern if a shear flow of 5# acting counter clockwise is assumed at point C. The circular dots represent the centroids of the flange numbers A and B and the flange material is

assumed concentrated at this point in computing the shear flow.

In Fig. A15.2 if the internal shear at C is zero then the shear is also zero between C and B, and C and A, since the skin is ineffective in bending.

$$q_{ba} = 0 + \frac{V_z}{I_x} \Sigma Az = 0 + \frac{-100}{25} (.5 \times 5) = -10\#/in.$$

(- is counterclockwise flow)

Note: $I_x = .5 \times 5^2 \times 2 = 25$

Taking moments about a point on line AB of all shear forces both internal and external:

$\Sigma M_{AB} = 100 \times 10 = 1000"\#$, which means that an unbalanced moment of -1000"# exists, which can be balanced by adding a constant shear flow for the entire cell of intensity:-

$q = \frac{-M}{2A} = -\frac{1000}{2 \times 80.52} = -6.21\#/in.$ Adding this constant shear flow (Fig. A15.3), which still leaves ΣF_Z and $\Sigma F_X = 0$ to that of Fig. A15.2, we obtain the true shear flow as shown in Fig. A15.4.

In Fig. A15.5, it was assumed that the shear stress at a point D midway between A and B was zero. With that assumption, the flexural shear flow forACB is calculated as follows:

$$q_{acb} = 0 + \frac{V_z}{I_x} \Sigma Az = 0 + \frac{-100}{25} (.5x-5) = 10\#/in.$$

Taking moments about point D:

$\Sigma M_D = 100 \times 10 + 10 \times 2 \times 80.52 = 2612"\#$. This moment must be balanced by a constant internal shear flow of $q = -\frac{M}{2A} = -\frac{2612}{2 \times 80.52} = -16.21\#/in.$

(See Fig. A15.6)

Adding this constant shear flow to that of Fig. A15.5, we obtain the final shear flow of Fig. A15.7 which, of course, checks the first solution in Fig. 15.4.

In Fig. A15.8 an arbitrary value of q = -5# per inch was assumed on the skin BCA. With this assumption, the shear flow on BA = $q_{ba} = -5 + \frac{-100}{25} (.5 \times 5) = -15\#/in.$

Taking moments about the line AB:

$\Sigma M = 100 \times 10 - 5 \times 2 \times 80.52 = 194.8"\#$. For equilibrium, this moment must be balanced by an additional shear flow of $q = -\frac{194.8}{2 \times 80.52} =$ 1.21#/in. Adding this constant shear flow (Fig. A15.9) to that of Fig. A15.8, we obtain the true shear flow of Fig. A15.10 which is identical to Figs. A15.4 and A15.7.

Solution Method 2 (Equilibrium of Shear Flow Resultant Vectors)

Since the web and leading edge skin were assumed ineffective for resisting bending loads, the shear flow on each of these two portions will be constant. Let Q_{AB} be the resultant shear flow on web AB. Since the web is straight, the location and direction of this resultant shear force is obviously along AB. Let Q_{ACB} be the resultant of the shear flow on ACB. By the simple relationships given in Chapter A14, the direction and location of Q_{ACB} is readily determined. The direction of Q_{ACB} is parallel to the closing line of the leading edge ACB, or the line AB. The location of Q_{ACB} relative to the closing line AB equals

$\frac{2 \times \text{area}}{h} = \frac{2 \times 80.52}{10} = 16.10"$ (See Fig. A15.11)

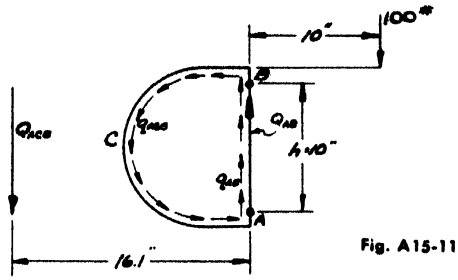


Fig. A15-11

The magnitudes of Q_{AB} and Q_{ACB} can be found by statics. Taking moments about a point on Q_{AB}, $\Sigma M_{AB} = 100 \times 10 - Q_{ACB} \times 16.10 = 0$ Hence, $Q_{ACB} = 62.1\#$ acting with sense as assumed.

The shear flow intensity $q_{acb} = \frac{-62.1}{10} =$ -6.21#/in.

$\Sigma F_Z = -100 - 62.1 + Q_{AB} = 0$, $Q_{AB} = 162.1\#$

$\therefore q_{ab} = \frac{-162.1}{10} = -16.21\#/in.$, which gives the same resulting shear flow system as found in previous solutions.

Solution Method 3 (Shear Center Method)

In this method, the shear flow system for bending of the cell without twist is first determined. The centroid of this shear flow system locates the so-called shear center. Then, any external torsional moment about this shear center must be resisted by a constant shear flow around the cell, the magnitude of which is $q = \frac{T}{2A}$ # per inch.

Due to the fact that the beam section is a closed one, the flexural shear flow is statically indeterminate, since the value of q is unknown at any point.

The general procedure is to assume a point of zero shear flow or assume a definite value for q at some point, as was done in solution method #1 and compute the flexural shear flow consistent with the given beam section. The assumed static flexural shear flow system will, in general, cause the beam cell to twist, but since we desire the shear flow system which will cause the beam to bend without twist, we must add a constant shear flow system which will cancel the torsional deflection due to the static shear flow system.

The centroid of these combined two shear flow systems locates the shear center for the beam section.

In this solution, we will assume a shear flow of q = 0 at point C. The resulting shear flow system will be identical to that in Fig. A15.2, since the same assumption was made. Fig. A15.12 repeats this system, and Fig. A15.13 shows the unknown constant shear flow system of q#/in. which must be added to make the total shearing strain around the perimeter of the cell equal to zero, or, in other words, make the twist zero.

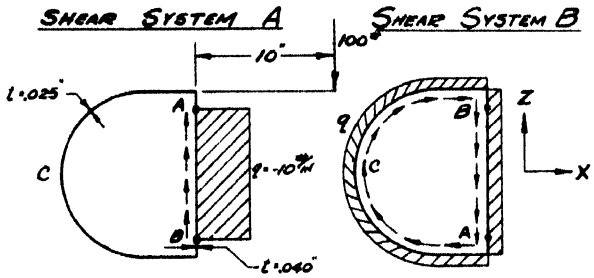


Fig. A15-12 Fig. A15-13

The shearing strain per inch of the perimeter = $\frac{q}{tG}$, where t = sheet thickness and G = modulus of rigidity. Since G is constant and only relative deflections are necessary, it may be omitted in calculations. The total shearing strain

δ around the perimeter of the cell equals:

$$\delta = \Sigma \frac{qL}{t} \quad \text{- - - - - - - - - - - - - - - - - -(1)}$$

Thus, the area of the shear flow diagrams in Figs. A15.12 and A15.13 divided by the corresponding skin thickness equals the total shearing strain.

For the shear flow system of Fig. A15.12,

$$\delta = \frac{-10 \times 10}{.04} \quad \text{- - - - - - - - - - - - - - - -(2)}$$

For the shear flow system of Fig. A15.13,

$$\delta = \frac{23.28\ q}{.025} + \frac{11\ q}{.04} \quad \text{- - - - - - - - - - -(3)}$$

(Note: 23.28 equals the length of .025 sheet)

Adding equations (2) and (3) and equating to zero, since the cell must bend without twist, and solving for value of q, we obtain, q = 2.08#/in. (positive and therefore in the direction assumed). Then adding the shear flow systems A and B to constant flow q of 2.08, we obtain the shear flow system C of Fig. A15.14, which is the shear flow system for bending about axis X-X without twist.

The location of the resultant of this shear flow system locates the horizontal position of the shear center of the cell.

$\Sigma F_Z = 10 \times 7.92 + 10 \times 2.08 = 100\#$

$\Sigma F_X = -2.08 \times 8.5 + 2.08 \times 8.5 = 0$

Therefore the resultant is a force and its location can be found by the principle of moments.

Taking moments about B,

$M_B = 10 \times 2.08 \times 16.1 = 335"\#$, hence distance from line AB to line of action of the resultant internal shear flow of 100# equals,

$$\bar{x} = \frac{335}{100} = 3.35" \text{ to left of AB.}$$ (Fig. A15.14 shows location).

Due to symmetry of the cell about the X axis the vertical location of the shear center is of course on the X axis.

The original 100# external load produces a moment of 100 x 13.35 = 1335 in lb. For equilibrium a resisting constant shear flow q which will produce a moment of - 1335 must exist, hence.

q = M/2A = -1335/161.04 = -8.29#/in. (See Fig. A15.15)

Adding shear flow systems "C" and "D" gives the final shear flow system "E" of Fig. A15.16.

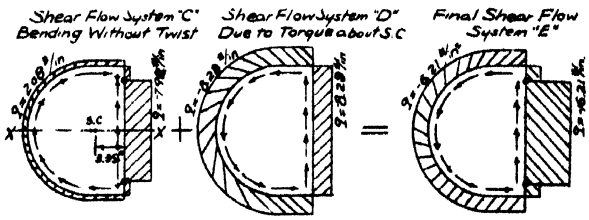


Fig. A15-14 Fig. A15-15 Fig. A15-16

It should be noticed that the web or skin thickness does not influence the magnitude of the shear flow system in a single cell beam. A change in thickness, however, effects the unit shearing stress and therefore the shearing strain and thus in computing angular twist of the cell, the web and wall thickness does influence the amount of twist for a given torsional load. In the shear center solution, it is known what portion of the shear flow is due to torque or pure twist, and also that due to bending without twist, which fact is sometimes of importance.

A15.3 Torsional Deflection of Cell in Example Problem

The resulting shear flow system as given in Fig. A15.16 should produce the same torsional deflection or twist of the cell section as the shear flow system of Fig. A15.15, which is due to torque about the shear center of the section, and furthermore, the shear flow system of Fig. A15.14 should produce no twist of the cell. To check these statements, the twist due to all

three shear flow systems will be computed.

From Chapter A5, $\theta = \dfrac{\Sigma\, q \frac{L}{t}}{2AG}$ or

$$2\theta AG = \Sigma\, q \frac{L}{t}$$

For the shear flow system of Fig. A15.16:-

(4) $$2\theta AG = \frac{6.21 \times 23.28}{.025} + \frac{6.21 \times 1}{.04} + \frac{16.21 \times 10}{.04} = 9990$$

For the shear flow system of Fig. A15.15:-

(5) $$2\theta AG = \frac{8.29 \times 23.28}{.025} + \frac{8.29 \times 11}{.04} = 9990$$

For the shear flow system of Fig. A15.14:-

$$2\theta AG = \frac{2.08 \times 23.28}{.025} + \frac{2.08 \times 1}{.04} - \frac{7.92 \times 10}{.04} = 0$$

If the actual angular twist is desired, solve equation (4) or (5) since A and G are known quantities. The result is the twist per unit length of beam.

A15.4 Single Cell-3 Flange-Unsymmetrical Beam Section

With 3 flange members not in a straight line the box beam can resist bending due to loads in any direction and torsional resistance is provided by the closed cell. This type of wing box beam is quite common in small and medium size airplanes.

Fig. A15.16a illustrates a 3-flange-unsymmetrical single cell beam subjected to an external load of 100# as shown. Let it be required to determine the internal shear flow resisting pattern assuming the web and walls are ineffective in resisting bending loads, which means the shear flow is constant between flange members.

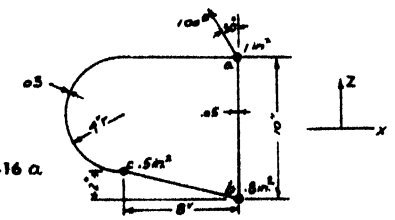


Fig. A15-16 a

Solution 1 (Equilibrium of Resultant Shear Vectors)

Fig. A15.17 shows the resultant shear vector on each portion of the cell wall. Since the portions ab and bc are straight, the line of action of the shear force on these portions coincides with the web or wall. The location of the constant shear flow on portion cda is parallel to line ac and acts at a distance of 2 A/L from line ca = 2 x 57.1/11.31 = 10.1".

The sense of the three unknown resultant shear vectors is assumed as indicated by the arrows.

To find Q_{cda} take moments about point (b),

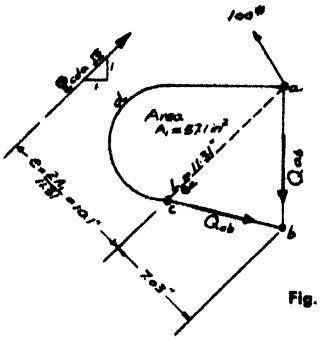


Fig. A15-17

$\Sigma M_b = (-100 \sin 30^0)\ 10 + 17.13\ Q_{cda} = 0.$

Therefore $Q_{cda} = 500/17.13 = 29.17\#$; and $q_{cda} = Q_{cda}/11.31 = 29.17/11.31 = 2.58\#/in.$

To find Q_{cb} use $\Sigma F_x = 0$.

$$\Sigma F_x = 29.17 \times \frac{1}{\sqrt{2}} - 100 \sin 30^0 + \frac{8}{8.25} Q_{cb} = 0$$

hence

$Q_{cb} = 30.2\#$, which gives $q_{cb} = -30.2/8.25 = 3.66\#/in.$

To find Q_{ab}, take $\Sigma F_z = 0$

$$\Sigma F_z = 100 \cos 30^0 + 29.17 \times \frac{1}{\sqrt{2}} - 30.2 \times \frac{2}{8.75} - Q_{ab} = 0$$

hence

$Q_{ab} = 100\#$ which gives $q_{ab} = 100/10 = 10\#/in.$

Fig. A15.17a shows the resulting shear flow diagram.

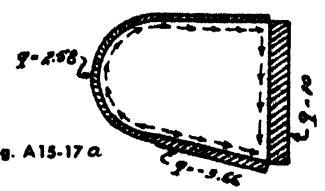


Fig. A15-17 a

It is of course not necessary to deal with the resultant vectors since the moment of the constant shear flows can be considered directly. Thus in Fig. A15.17b, assume the three unknown shear flows q_{cda}, q_{ab}, q_{bc} as acting in the clockwise direction. To find the value of q_{cda} we take moments about point (b).

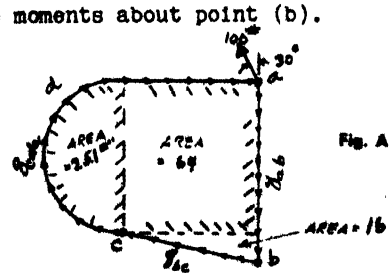


Fig. A15-17 b

$\Sigma M_b = 2\ (25.1 + 64 + 8)\ q_{cda} - 10 \times 50 = 0$

hence $q_{cda} = 2.58\#/in.$

In the above equation, the moment of the constant shear flow system q_{cda} about point b equal twice the cell area times q_{cda}.

Then to find q_{bc} take $\Sigma F_X = 0$

$$\Sigma F_X = 8 \times 2.58 - 100 \sin 30^0 - 8.25\ q_{bc}\ \frac{8}{8.25} = 0$$

hence $q_{bc} = -3.66\#/in.$

and in a similar manner by using $\Sigma F_Z = 0$, q_{ab} will be found equal to 10#/in.

Solution 2 (Shear Flow From Bending About Principal Axes)

Table A15.1a shows the calculations for the moments of inertia of the section about the principal axes.

Table A15.1a (Ref. Fig. 15.18)

Portion	Area A	x'	Z'	Ax'	Ax'^{2}	Az'	Az'^{2}	Ax'z'
A	1.0	0	10	0	0	10	100	0
B	0.8	0	0	0	0	0	0	0
C	0.5	-8	2	-4.0	32	1	2	-8
Totals	2.3			-4.0	32	11	102	-8

$z = 11/2.3 = 4.783$
$X = 4.0/2.3 = -1.739$
$I_{xx} = 102 - 2.3 \times 4.783^2 = 49.38\ in.^4$
$I_{zz} = 32 - 2.3 \times 1.739^2 = 25.04$
$I_{xz} = -8 - (2.3 \times 4.783 \times -1.739) = 11.13$

$$\tan 2\phi = \frac{2 I_{xz}}{I_z - I_x} = \frac{2 \times 11.13}{25.04 - 49.38} = \frac{22.26}{-24.34} = -.9105$$

$2\phi = 42^\circ - 19', \quad \phi = 21^\circ - 9.5'$

$I_{x_p} = I_x \cos^2\phi + I_z \sin^2\phi - 2 I_{xz} \sin\phi \cos\phi = 49.38$
$\times .9326^2 + 25.04 \times .3609^2 - 2 \times 11.13 \times -.3609 \times .9326$
$= 42.96 + 3.26 + 7.5 = 53.72$

$I_{z_p} = I_x \sin^2\phi + I_z \cos^2\phi + 2 I_{xz} \sin\phi \cos\phi = 6.42 + 21.78 - 7.5 = 20.70$

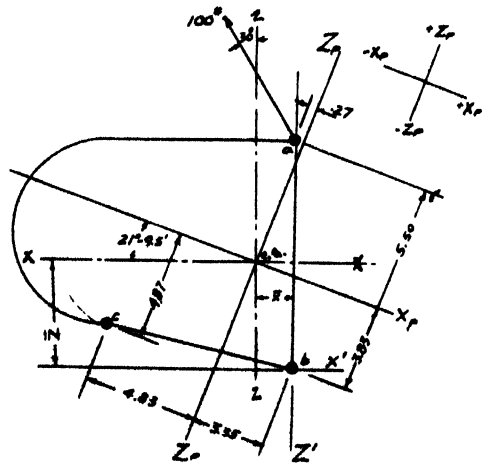


Fig. A15-18

The external shear load of 100# is resolved into components normal to each principal axis.

$V_{z_p} = 100 \sin 38^0 - 50.5' = 62.73\#$

$V_{x_p} = -100 \cos 38^0 - 50.5' = -77.87\#$

Calculation of internal shear flow assuming shear flow q between a and c equals zero. Due only to $V_{z_p} = 62.73\#$

$$q = \frac{V_{z_p}\ \Sigma A z_p}{I_{x_p}}$$

$$q_{ab} = \frac{62.73}{53.72}\ (1 \times 5.50) = 6.42\#/in.$$

$$q_{cb} = \frac{62.73}{53.72}\ (.5 \times -4.87) = 2.84\#/in.$$

Due to $V_{x_p} = -77.87\#$ $\quad q = \dfrac{V_{x_p}\ \Sigma A x_p}{I_{z_p}}$

$$q_{ab} = \frac{77.87}{20.70}\ (1 \times -.27) = 1.01\#/in.$$

$$q_{bc} = 1.01 - \frac{77.87}{20.70}\ (.8 \times 3.35) = -9.08\#/in.$$

Figs. A15.19 and A15.20 show the resulting shear flow diagrams in resisting the external shear loads as shown. Both of these force systems will satisfy ΣF_Z and $\Sigma F_X = 0$. To check $\Sigma M = 0$ take moments about point b.

$\Sigma M_b = -100 \sin 30^0 \times 10 = -500"\#$. Thus for equilibrium a constant shear flow producing a moment of 500"# is necessary.

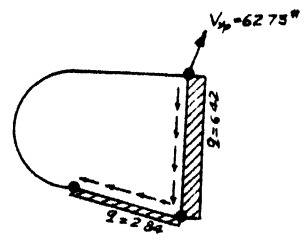


Fig. A15-19

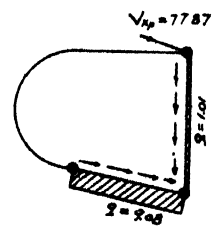


Fig. A15-20

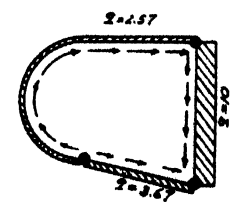


Fig. A15-21

hence balancing $q = \dfrac{T}{2A} = \dfrac{500}{2 \times 97.1} = 2.57\#/in.$

(97.1 equals enclosed area of cell)
Adding a constant shear flow of 2.57 to that of Figs. A15.19 and A15.20 we obtain the final shear flow of Fig. A15.21 which checks solution #1.

Solution 3 (Shear Center Method)

In this solution we find the shear flow system which causes the section to bend without twist. The resultant of this system passes thru the shear center of the section. Then the moment of the external forces about any point on the line of action of the resultant will produce pure torsion.

Assuming the shear flow q on portion ac as in Solution #2, we obtain the shear flow pattern of Fig.s A15.19 and A15.20.

The total shearing strain around perimeter of cell equals $\delta = \Sigma \frac{q\,L}{t\,G}$. Substituting, but omitting G, since it is constant.

$$\delta = \frac{6.42 \times 10}{.05} + \frac{2.84 \times 8.25}{.04} + \frac{1.01 \times 10}{.05} - \frac{9.08 \times 8.25}{.04} = 1285 + 587 + 201 - 1870 = 203$$

This total relative shearing strain of 203 must be canceled by a constant shear flow of q. Total shearing strain due to q = $\delta' = \frac{q \times 10}{.05} + \frac{q \times 8.25}{.04} + \frac{q \times 20.57}{.03} = 1090\ q$

$\delta + \delta' = 0$ or, $1090\ q + 203 = 0$

hence $q = -203/1090 = -.186$#/in.

Adding this constant shear flow to that of Figs. A15.19 and A15.20 we obtain the shear flow system of Fig. A15.22.

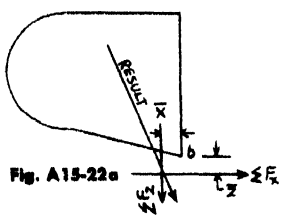


Fig. A15-22a

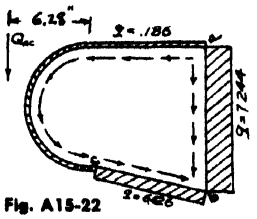


Fig. A15-22

The resultant of the shear force system in Fig. A15.22 will pass thru the shear center of the section. One point on the line of action of the resultant can be determined by finding the intersection of the Z and X components of the resultant. From Fig. A15.22:-

$\Sigma F_z = -0.186 \times 8 - 6.426 \times 2 - 7.244 \times 10 = -86.78$ lbs.

Take moments of z components about point (b)

$\Sigma M_b = 0.186 \times 114.2 = -21.23$ in.lbs.

$-86.78\ \bar{x} = -21.23$

hence, $\bar{x} = -21.23/86.78 = -0.245$" from b.

$\Sigma F_x = -0.186 \times 8 + 8 \times 6.426 = 50.0$ lbs.

Take moments of x components about (b)

$\Sigma M_b = -8 \times 0.186 \times 10 = -14.9$ in.lbs.

hence $\bar{z} = -14.9/50 = -0.298$" below b.

See Fig A15.22a for results.

The moment of the external load system about shear center equals $-50 \times 10.298 - 86.67 \times .245 = -536$"#. For equilibrium 536"# is necessary which is produced by a constant shear flow

$q = + \frac{536}{2 \times 97.1} = 2.75$#/in.

Adding this constant shear flow of 2.75#/in. to that of Fig. A15.22, we obtain the same resulting values as given by previous solutions.

Solution 4 (Shear flow by changes in flange axial loads)

Relative to flange loads a 3-flange single cell beam is statically determinate. Fig. A15.23 shows a one inch length of the beam, with the external load acting on the aft face of cantilever beam as shown.

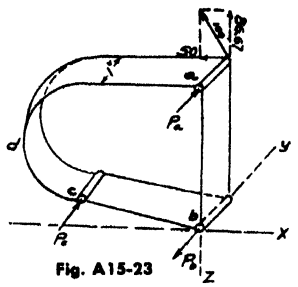


Fig. A15-23

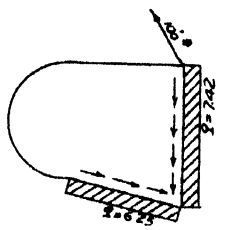


Fig. A15-24

For equilibrium of flange loads

$\Sigma M_x = 0$, $\Sigma M_z = 0$, and $\Sigma F_y = 0$

Selecting reference rectangular axes at stringer b, we obtain

$\Sigma M_x = 2\ P_c + 10\ P_a - 86.67 \times 1 = 0$ - - - - - - -1

$\Sigma M_z = 8\ P_c - 50 \times 1 = 0$ - - - - - - - - - - - - -2

$\Sigma F_y = P_a - P_b + P_c = 0$ - - - - - - - - - - - - -3

Solving the 3 equations we obtain

$P_c = 6.25$#

$P_a = 7.42$#

$P_b = 13.67$#

The sense of each flange load is as assumed in the figure namely compression in c and a and tension in b. For solution purposes assume that shear flow in portion a d c of cell wall is zero. Then the resisting shear flow q_y in the y direction between flange members a and b = $-P_a = -7.42$#/in. Hence $q_z = 7.42$#/in.

Similarly the shear flow q_y between c and b equals the load in flange c = $-P_c = -6.25$#/in.

and thus q in plane of cross section between c and a = 6.25#/in.

Fig. A15.24 shows the resulting shear flow diagram. Taking moments about any point such as b we find M_b = - 100 x sin 30° x 10 = - 500"# (The shear flow has zero moment about b)

For equilibrium 500"# is necessary which is given by a constant shear flow of q = $\frac{500}{2 \times 97.1}$ = 2.58#/in. adding this constant flow to that of Fig. A15.24 we obtain the final results as obtained in previous solutions.

If we had assumed in starting the shear flow calculation that the shear flow was zero between a and b instead of between a and c, than the shear flow due to change in flange loads over a beam length of one inch would be as indicated in Fig. A15.25.

Taking moments about any point as b.

$$\Sigma M_b = 100 \sin 30^\circ \times 10 - 7.42 \times 11.31 \times 17.13 = - 500 - 1444 = - 1944"\#$$

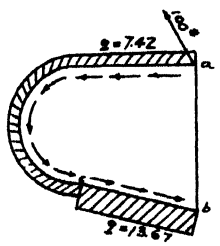


Fig. A15-25

For equilibrium a constant shear flow of q = $\frac{1944}{2 \times 97.1}$ = 10#/in. Adding this constant flow to that of Fig. A15.25 we obtain the final shear flow as previously found.

A15.5 Single Cell-Distributed & Multiple Flange

Example Problem #1

Fig. A15.26 shows a cantilever box beam supporting a load of 100# as shown. Determine the internal shear flow system on the cross-section abcd. In this example problem, the entire cross-section will be assumed as effective in resisting bending loads. The moment of inertia about the X axis = 62.5 in^4. Since XX is an axis of symmetry, the X and Z axes are principal axes.

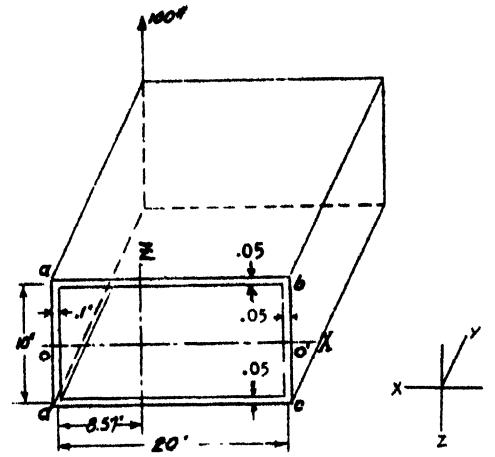


Fig. A15-26

Solution 1 The flexural shear flow is statically indeterminate, since the shear flow at any point is unknown. The flexural shear flow will be made statically determinate by assuming the shear flow at point O (intersection of X axis and ad) = zero.

Fig. A15.27 shows the static flexural shear flow for this assumed condition.

$$q_o = 0 \text{ (assumed)}, \quad \frac{V_Z}{I_X} = 100/62.5 = 1.6$$

$$q_a = 0 + \frac{V_Z}{I_X} \sum_{o}^{a} zA = 0 + 1.6 \times 5 \times .1 \times 2.5 = 2\#/\text{in.}$$

$$q_b = q_a + 1.6 \sum_{b}^{a} zA$$

$$= 2 + 1.6 \times 20 \times .05 \times 5 = 10\#/\text{in.}$$

$$q_{o'} = q_b + 1.6 \sum_{b}^{o'} zA$$

$$= 10 + 1.6 \times 5 \times .05 \times 2.5 = 11\#/\text{in.}$$

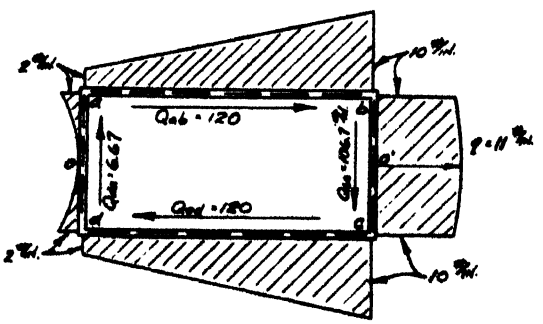


Fig. A15-27

Continuing around the cell wall, the balance of the static shear flow is obtained. Since the

section is symmetrical about axis XX, the shear flow will be symmetrical. The flexural shear flow as found satisfies the equations ΣF_Z and $\Sigma F_X = 0$ for equilibrium of internal and external shear loads. ΣM_y of external and internal shear forces about any point must also equal zero for equilibrium. Take moments about point d, using the resultant shear load Q_{ab}, Q_{bc} on each wall of the cell, which equal the area of the shear flow diagram in ab, and bc respectively:-

$\Sigma M_d = 120 \times 10 + 106.7 \times 20 = 3334$"# as an unbalanced moment. To make $\Sigma M_d = 0$ a constant internal shear flow must be added to create a resisting moment of -3334"#. Therefore, the resisting constant shear flow $q = \frac{M}{2A} = \frac{-3334}{2 \times 10 \times 20}$ -8.34# per in. Adding this constant shear flow to that of Fig. A15.27, we obtain the true internal shear flow of Fig. A15.28.

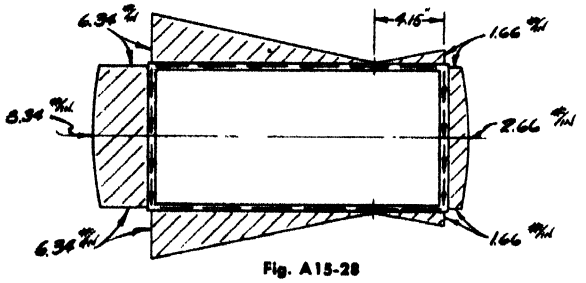


Fig. A15-28

Solution 2 Shear Center Method. In this solution, we determine the centroid of the internal shear flow system, which will exist if the beam bends about axis X-X without twist. The external shear load can then be resolved into a force acting thru this internal shear flow centroid or shear center plus a torsional moment about the shear center.

The solution is started by assuming a value for the flexural shear flow and computing the shear flow system, as for example, that in Fig. A15.27.

The total shearing strain around the box circumference due to this shear flow, assuming G as constant and unity as relative values of shearing strain only are needed, equals:

$$\delta = \frac{\Sigma qL}{t} = \left[\frac{2 \times 5}{3 \times .1} + \frac{(10+2)}{(2)}\frac{20}{.05} + \frac{10 \times 5}{.05} + \frac{(11-10)}{.05}\frac{.667 \times 5}{.05}\right] 2 = 7000$$

(Notes: The quantity above is written for the covering on one side of the X-X axis, hence the equation is multiplied by 2.) If the cell wall does not twist when bending, the relative value of 7000 must, therefore, be canceled by a constant shear flow of q#/in. which will create a total shearing strain of -7000. The shearing strain for a constant shear flow of q#/in, is:

$$\delta = \left[\frac{q \times 5}{.1} + \frac{q \times 20}{.05} + \frac{q \times 5}{.05}\right] 2 = -7000$$

hence, $q = \frac{-7000}{1100} = -6.36$#/in.

Fig. A15.29 shows the resultant shear flow pattern if a constant shear flow of q = - 6.36#/in. is added to the shear flow of Fig. A15.27.

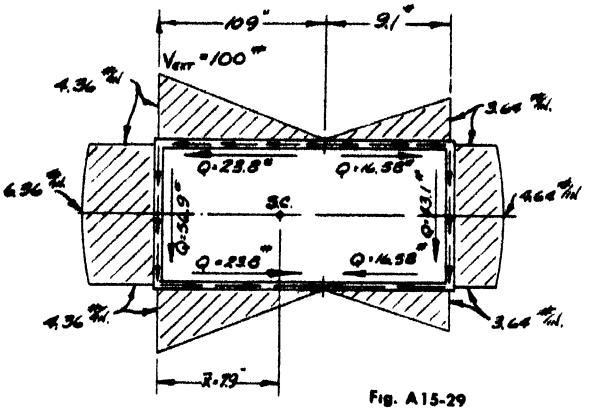


Fig. A15-29

The location of the resultant of this shear flow system will give the horizontal position of the shear center for the sectionl Due to symmetry of the section about the X axis, the vertical position of the shear center will be on the X axis, because for bending about the Z axis, the shear flow would be symmetrical and thus, the resultant would coincide with the X axis.

Fig. A15.29 also shows the resultant shear load Q on each portion of the cell wall which equals the area of the shear flow diagram for various portions as shown.

$\Sigma F_Z = -56.9 - 43.1 = -100$, which balances the external load of 100#

$\Sigma F_X = 0$ by observation. Take moments about point O, the intersection of axis XX and side ad

$$\bar{x} = \frac{\Sigma M_O}{\Sigma F_Z} = \frac{43.1 \times 20 + (-23.8 + 16.58)10}{100} = 7.90 \text{ in.}$$

Hence the shear center lies on the X axis, 7.9" from side ad.

The moment of the external shear load of 100# about the shear center = 100 x 7.90 = 790#. For equilibrium, $\Sigma M_y = 0$. Therefore, a constant shear flow q must be added to create a resisting moment of -790"#.

$$q = \frac{M}{2A} = \frac{-790}{2 \times 200} = -1.98\text{#/in.}$$

Adding this constant shear flow of -1.98#/in. to that of Fig. A15.29, we obtain the final shear flow system which is identical to that of Fig. A15.28.

Torsional Deflection. The torsional deflection per unit length of the cell can be computed by using a constant shear flow q = - 1.98#/in. which represents the pure torsion on the cell. Thus,

$$2A\Omega\theta = \Sigma \frac{qL}{t} = \frac{(20+10+20)1.98}{.05} + \frac{10 \times 1.98}{.10} = 2178$$

The student should check this result using the shear flow of Fig. A15.28

Fig. A15.30 shows the position of the shear center with respect to the center of gravity of the cross-section and also the centroid of the moment of inertia of the cross-section, that is,

$$\bar{x} = \frac{\Sigma xz^2 A}{\Sigma z^2 A} \quad \text{- - - - - - - - - - - - - - - (a)}$$

Sometimes it is assumed that the shear center lies at a point as given by equation (a) which in general is true only for special cases.

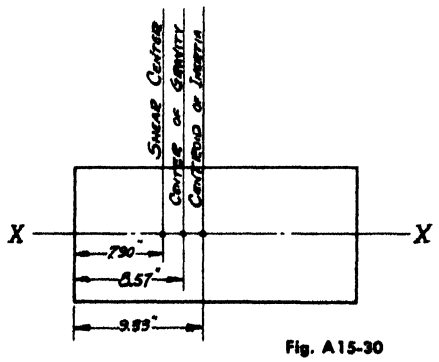


Fig. A15-30

Example Problem #2

Fig. A15.31 shows the cross-section of a single cell box beam. The section is identical to the beam section of Fig. A14.19 of Chapter A14, except that the top cover, or skin, is extended between stringers a and h, thus making the section a closed one. The problem is to find the internal shear flow system when resisting the external shear load of 100# acting as shown. As assumed in Chapter A14, the covering is considered ineffective in resisting bending flexural load.

In bending about the X axis, the flexural shear flow is statically indeterminate, since the value at any point is unknown. If we assume the shear flow q between a and h = zero, then the flexural shear flow consistent with the given loading and beam section will be identical to that of (Fig. A14.20 Chapter A14) and which is repeated in Fig. A15.32.

If ΣF_Z and ΣF_X are considered for the internal and external shear loads, they will be found to be zero.

To check $\Sigma M_y = 0$, take moments about point C.

$\Sigma M_C = -100 \times 7.5 + 10 \times 3.75 \times 15$
$- 1.25 \times 5 - 1.25 \times 10 + 1.25$
$\times 15 = -187.5$"#.

Therefore, to make $M_C = 0$, a constant resisting shear flow of $M = \frac{187.5}{2A} = \frac{187.5}{2 \times 11 \times 15} = .57$#/". must be added to the shear flow system of Fig. A15.32 to

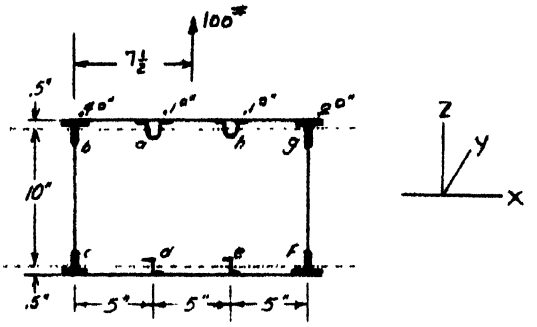


Fig. A15-31

give the final internal shear flow system of Fig. A15.33. The student should check these results by using the shear center method. The thickness of walls and webs can be assumed, since they have no effect on the shear flow system if the web is considered ineffective in bending. The amount of twist of the cell will of course, be affected by the web and wall thickness.

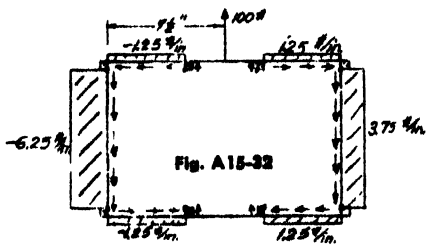


Fig. A15-32

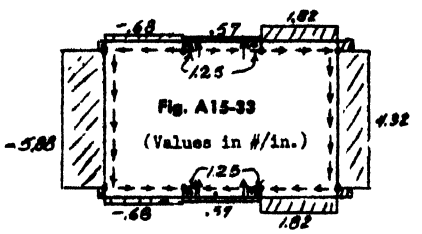


Fig. A15-33
(Values in #/in.)

A15.6 Unsymmetrical-Multiple Flange-Single Cell Beam.

Fig. A15.34 shows a 16 flange single cell box beam. This section is identical to the beam section of Fig. A13.13 which the section properties about the principal axes were calculated. In Fig. A15.34 two external loads of 100# are assumed acting at indicated.

The problem will be to calculate the internal shear flow system in resisting these two external loads. Table A15.1 gives most of the required calculations in tabular form. The shear flow between flange members (1) and (10) is assumed zero. Under this assumption the shear is computed for bending about the two principal axes.

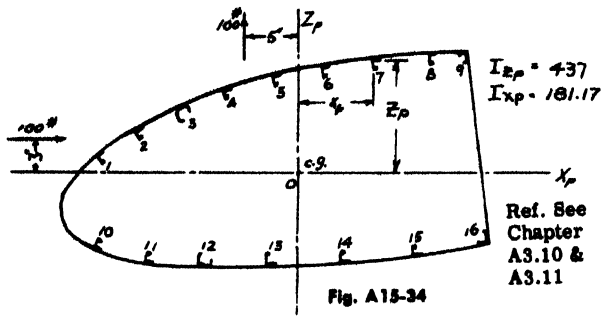


Fig. A15-34

$$q_1 = \frac{V_{x_p}}{I_{z_p}} \Sigma Ax_p = \frac{100}{437} \Sigma Ax_p = .229 \Sigma Ax_p$$

$$q_2 = \frac{V_{z_p}}{I_{x_p}} \Sigma Az_p = \frac{100}{181.17} \Sigma Az_p = .552 \Sigma Az_p$$

Columns 6 and 10 of Table A11.1 gives the values of q_1 and q_2. The next step is to check $\Sigma M_y = 0$ of the internal and external shear loads. Moments are taken about the centroid of the section.

The moment of the shear flow q_1 and q_2 on the cell wall between two adjacent flange members equals the shear flow times twice the area of the triangle formed by straight lines joining the moment center O and the extremities of the cell wall between the two stringers. Column 11 of Table A15.1 gives the double areas, which have been determined by use of a planimeter.

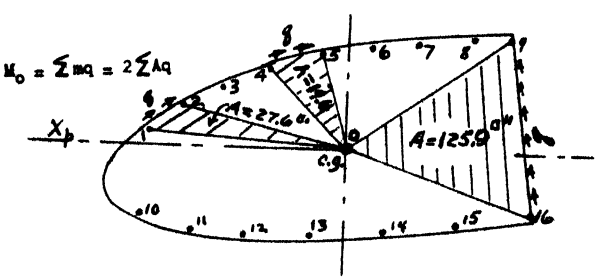
Columns 12 and 13 give the moment of the shear flow q_1 and q_2 about point O. Hence ΣM_O = -297.7 + 1766 + 5 x 100 + 100 x 3 = 2268 in.lb. For equilibrium ΣM_O must equal zero which means that a constant shear flow q must be added to create a balancing moment of - 2268 in.lb.

$$q = \frac{M}{2A} = \frac{-2268}{2 \times 493} = -2.3\#/in.$$ (Note 493 = total enclosed area of cell).

Adding q to q_1 and q_2 of table A15.1, the final shear flow system of Fig. A15.35 is obtained.

Table A15.1

1	2	3	4	5	6	7	8	9	10	11	12	13
Flange Member	Area A	x_p	Ax_p	ΣAx_p	q_1	z_p	Az_p	ΣAz_p	q_2	m	$q_1 m$	$q_2 m$
1	.14	-17.86	-2.50	-2.50	-0.572	1.85	.26	.26	0.142	55.2	-31.7	0.78
2	.14	-14.33	-2.01	-4.51	-1.035	4.44	.62	.88	0.485	44.2	-45.7	21.40
3	.38	-10.1	-3.84	-8.35	-1.915	6.01	2.29	3.17	1.750	32.0	-61.2	56.00
4	.17	- 6.48	-1.10	-9.45	-2.160	6.91	1.18	4.35	2.400	38.2	-82.5	91.80
5	.17	- 1.98	-0.34	-9.79	-2.240	7.75	1.32	5.67	3.130	33.0	-73.8	103.50
6	.17	2.00	0.34	-9.45	-2.162	8.27	1.40	7.07	3.900	33.2	-71.9	129.70
7	.17	6.00	1.02	-8.43	-1.936	8.65	1.47	8.54	4.720	40.2	-77.8	190.00
8	.17	10.31	1.75	-6.68	-1.530	8.93	1.52	10.06	5.550	32.6	-50.0	181.00
9	.29	14.30	4.15	-2.53	-0.580	9.06	2.62	12.68	7.001	251.8	146.0	176.20
16	.35	16.47	5.78	3.25	0.745	-6.18	-2.16	10.52	5.800	46.	34.2	267.00
15	.31	10.78	3.34	6.59	1.51	-6.80	-2.11	8.41	4.640	48.2	73.4	224.00
14	.31	4.40	1.36	7.95	1.82	-7.14	-2.21	6.20	3.420	46.4	84.6	158.40
13	.31	- 1.92	-0.59	7.36	1.685	-7.36	-2.28	3.92	2.162	47.6	80.2	103.52
12	.28	- 8.22	-2.31	5.05	1.157	-6.19	-1.90	2.02	1.115	36.6	42.4	40.80
11	.17	-12.78	-2.17	2.88	0.660	-6.41	-1.09	0.93	0.514	42.6	28.1	21.90
10	.17	-17.00	-2.89			-5.38	-0.91					
										Σ	-297.7	1766.0



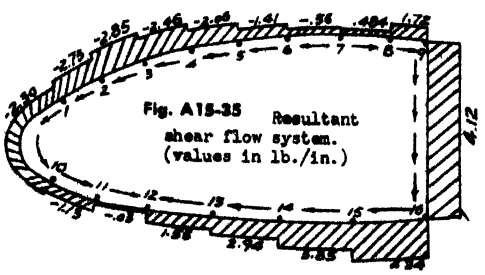


Fig. A15-35 Resultant shear flow system. (values in lb./in.)

A15.7 Two Cell-Multiple Flange Box Beams.

Fig. A15.36 shows a two cell cantilever beam with 10 flange stringers. The cross-section is constant. Let it be required to determine the internal shear flow in resisting the 1000# load acting as shown. For simplification, the top and bottom sheet covering and the three vertical webs will be considered ineffective in taking bending flexural loads. Since the beam section is symmetrical about the X axis, the beam will bend about this axis in resisting the given external load. The amount of inertia of the section about the X axis equals 250 in.⁴

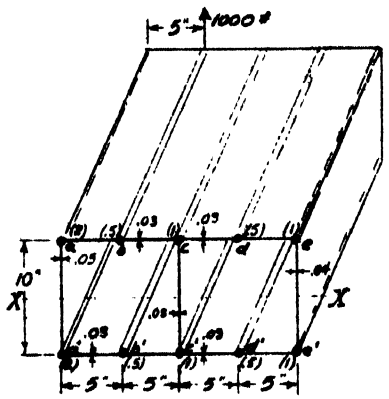


Fig. A15-36

Solution 1 (Without use of shear center)

The internal shear flow is statically indeterminate to the second degree, since the shear flow at any point in each cell is unknown. Therefore, to make the flexural shear flow statically determinate, a value for the shear flow q in each cell will be assumed at some point, and the flexural shear flow for each cell will then be calculated, consistent with the assumed conditions. These resulting static shear flow systems will, in general, produce a different total shearing strain around the perimeter of each cell, or in other words, produce a different cell twist. Since full continuity exists between cells, this condition cannot exist, and therefore an unknown constant shear flow of q_1 in cell (1) and q_2 in cell (2) must be added to make the twist of both cells identical. This fact gives us the basis for one equation and the other equation necessary for the solution of the two unknowns q_1 and q_2 is given by the requirement of equilibrium, namely, that the moment of the external and the internal shear forces about any point in the plane of the cross section must equal zero. In Fig. A15.37 the flexural shear flow has been assumed as zero just to the left of stringer c in cell (1) and just right of stringer c in cell (2). The balance of the flexural shear system consistent with this assumption is calculated as follows:

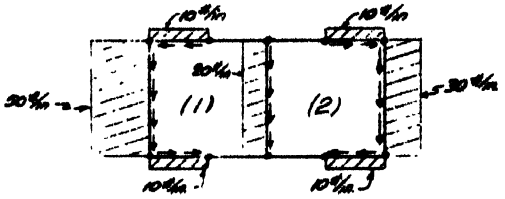


Fig. A15-37

Cell (1). (Starting with stringer c and going counterclockwise around cell)

$$q = -\frac{V_z}{I_x} \Sigma A z = -\frac{1000}{250} \Sigma A z = -4 \Sigma A z$$

hence, $q_{cb} = 0$

$q_{ba} = 0 - 4 \times .5 \times 5 = -10\#/in.$

$q_{aa'} = -10 - 4 \times 2 \times 5 = -50\#/in.$

$q_{a'b'} = -50 - 4 \times 2 \times -5 = -10\#/in.$

$q_{b'c'} = -10 - 4 \times .5 \times -5 = 0\#/in.$

To obtain q in web cc' integrate from c to c' or clockwise, which eliminates the minus sign before the equation. Thus

$q_{cc'} = 0 + 4(1 \times 5) = 20\#/in.$

Cell (2)

$q_{cd} = 0$

$q_{de} = 4(.5 \times 5) = 10\#/in.$

$q_{ee'} = 10 + 4(1 \times 5) = 30\#/in.$

$q_{e'd'} = 30 + 4(1 \times -5) = 10$

$q_{d'c'} = 10 + 4(.5 \times -5) = 0$

$q_{cc'} = 0 - 4(1 \times 5) = -20\#/in.$

Fig. A15.37 shows a plot of shear flow. Plus q is clockwise flow. Fig. A15.38 illustrates the unknown constant shear flow systems q_1 and q_2 which must act on cells (1) and (2) respectively to produce the same cell twist when added to the shear flow system of Fig. A15.37. The sense of q_1 and q_2 has been assumed clockwise or positive in each cell.

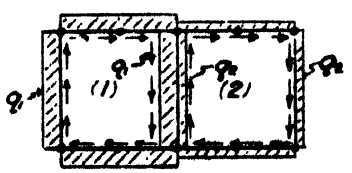


Fig. A15-38

The angular twist of a cell = $\frac{1}{2AG} \Sigma q L/t$ or

$2AG\theta = \Sigma q L/t$

For cell (1) (See Fig. A15.38)

$2A_1G\Theta_1 = \frac{-10 \times 5}{.03} - \frac{50 \times 10}{.05} - \frac{10 \times 5}{.03} + \frac{20 \times 10}{.03} + \frac{10}{.05}q_1 + \frac{3 \times 10}{.03}q_1 - \frac{10}{.03}q_2$. Hence, $2A_1G\Theta_1 = 1200q_1 - 333q_2 - 6670$ - (1)

For cell (2)

$2A_2G\Theta_2 = \frac{10 \times 5 \times 2}{.03} + \frac{30 \times 10}{.04} - \frac{20 \times 10}{.03} + \frac{3 \times 10}{.03}q_2 + \frac{10}{.04}q_2 - \frac{10}{.03}q_1$. Hence, $2A_2G\Theta_2 = -333q_1 + 1250q_2 + 4170$ - - - - - - - - - - - - - - (2)

Since there is continuity between cells, $\Theta_1 = \Theta_2$. Also since area of each cell is the same, $A_1 = A_2$. Equating (1) and (2),

$1533q_1 - 1583q_2 - 10840 = 0$ - - - - - - - - - - - - (3)

One other equation is necessary to solve for unknowns q_1 and q_2, and it is given by the moments of the external and internal shear forces about any point in the plane of the cross section, which must equal zero for equilibrium.

Take moments about point (b) of the shear flow system of Figs. A15.37 and A15.38 and also the external shear load of 1000#, which in this case has no moment about our assumed moment center.

$\Sigma M_b = -50 \times 10 \times 5 + 20 \times 10 \times 5 + 10 \times 30 \times 15 + 200q_1 + 200q_2 = 0$ hence, $200q_1 + 200q_2 + 3000 = 0$- - -(4)

Solving equations (3) and (4) for q_1 and q_2, we obtain

$q_1 = -4.07$#/in. $\qquad q_2 = -10.80$#/in.

The final or true internal shear flow system then equals that of Fig. A15.37 plus that of Fig. A15.38 when $q_1 = -4.07$ and $q_2 = -10.80$#/in., which gives the shear flow diagram of Fig.

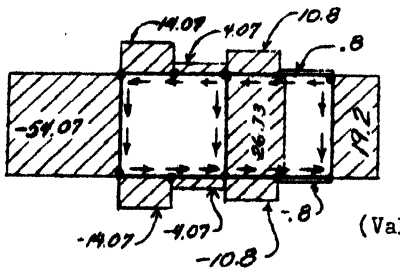


Fig. A15.39

Solution #2 (By use of shear center)

In this solution, we find the flexural shear flow for bending about axis X-X without twist. The centroid of this internal shear system locates the shear center. The moment of the external shear load about the shear center produces pure torsion on the 2 cell beam. Thus, adding the shear due to this pure torsion to that of pure bending, we obtain the final resisting internal shear flow.

In bending about axis X-X without twist, the shearing strain for each cell as given by equations (1) and (2) must equal zero. Hence:

$1200\,q_1 - 333q_2 - 6670 = 0$ - - - - - - - - -(5)

$-333q_1 + 1250q_2 + 4170 = 0$ - - - - - - - - -(6)

Solving equations (5) and (6) for q_1 and q_2, we obtain $q_2 = -2.0$#/in. $q_1 = 5.00$#/in. Therefore, taking these values of q_1 and q_2 in Fig. A15.38 and adding the results to that of Fig. A15.37, we obtain the shear flow pattern of Fig. A15.40 which is the shear flow system for bending without twist about X axis. The centroid of this shear system locates the shear center.

In Fig. A15.40, check:

$\Sigma V = 0 = -10 \times 45 - 10 \times 28 - 10 \times 27 = -1000$#, which checks the external shear of 1000#. $\Sigma H = 0$ by observation of Fig. A15.40.

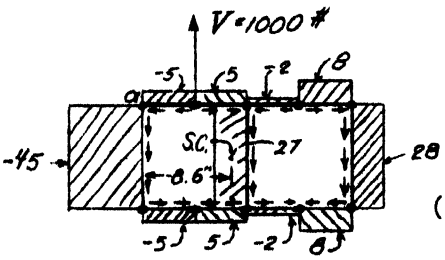


Fig. A15-40

To find the horizontal position of the centroid of the shear flow in Fig. A15.40, take moments about point a:

$\Sigma M_a = 10 \times 27 \times 10 + 10 \times 28 \times 20 + 5 \times 8 \times 10 - 5 \times 2 \times 10 = 8600$"#.

$\therefore \bar{X} = \frac{8600}{1000} = 8.6$" to the right of web aa'.

The external shear load of 1000# acts 5" to the right of aa', and therefore causes a moment about the shear center equal to $(8.6 - 5.0)\,1000 = 3600$"#. To resist this torsional moment, a constant torsional shear flow $q_{t(1)}$ and $q_{t(2)}$ must act on cells (1) and (2) respectively.

The values of $q_{t(1)}$ and $q_{t(2)}$ can be found by using equations (16) and (17) of Art. A5.11 of Chapter A5. Thus

$$q_{t(1)} = -\frac{1}{2}\left[\frac{a_{20}A_1 + a_{12}A)}{a_{20}A_1^2 + a_{12}A^2 + a_{01}A_2^2}\right]T$$

$$q_{t(1)} = -\frac{1}{2}\left[\frac{\left(\frac{10}{.03} + \frac{10}{.04} + \frac{10}{.03}\right)100 + \frac{10}{.03} \times 200}{\left(\frac{10}{.03} + \frac{10}{.04} + \frac{10}{.03}\right)100^2 + \frac{10}{.03} \times 200^2 + \left(\frac{10}{.03} + \frac{10}{.05} + \frac{10}{.03}\right)100^2}\right]T = \frac{1}{2}\left[\frac{158200}{31190000}\right]T = .00254\,T$$

$q_{t(1)} = .00254T$. But, $T = 3600$"#/in. and the resisting torque must therefore be -3600"#. hence:

$q_{t(1)} = .00254 \times (-3600) = -9.17$#/in.

$$q_{t(2)} = \frac{1}{2}\left[\frac{a_{o1}A_a + a_{1a}A}{31190000}\right] T$$

$$= \frac{1}{2}\left[\frac{\left(\frac{10}{.03} + \frac{10}{.03} + \frac{10}{.05}\right) 100 + \frac{10}{.03} \times 200}{31190000}\right] = .00245T$$

hence: $q_{t(2)} = .00245 \times -3600 = -8.85\#/in.$

Therefore, if we add to the shear flow system of Fig. A15.40, a constant shear flow of -9.17#/in. to cell (1) and -8.85#/in. to cell (2), we will obtain the true internal resisting shear flow of Fig. A15.41, which checks solution #1, any discrepancy being due to slide rule accuracy.

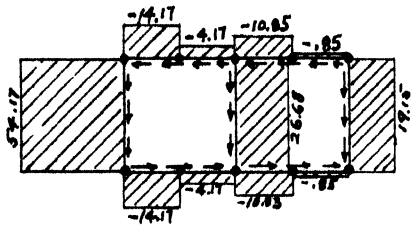


Fig. A15-41

Torsional Deflections

The angular twist of each cell is the same. The value of the angular twist θ per unit length of the beam can be found using the shear flow pattern of Fig. A15.41 which is the true resultant shear flow, or the pure torsional shear flows of $q_{t(1)} = -9.17\#/in.$ and $q_{t(2)} = -8.85\#/in.$ may be used if desired.

The results will, of course, be the same. For example:

For cell (1) due to $q_{t(1)} = -9.17\#/in.$ and $q_{t(2)} = -8.85\#/in.$

$$2\Theta GA_1 = \frac{\Sigma qL}{t} = \frac{(9.17 \times 10)}{.03} 3 + \frac{9.17 \times 10}{.05} - \frac{8.85 \times 10}{.03} =$$

$$8000$$

Cell (2)

$$2\Theta GA_a = \frac{\Sigma qL}{t} = \frac{(8.85 \times 10)}{.03} 3 + \frac{8.85 \times 10}{.04} - \frac{9.17 \times 10}{.03} =$$

$$8000$$

Cell (1) Final stresses - Fig. A15.41

$$2\Theta GA_1 = \frac{\Sigma qL}{t} = \frac{(14.17 \times 5)2}{.03} + \frac{(4.17 \times 5)2}{.03} + \frac{54.17 \times 10}{.05} -$$

$$\frac{26.68 \times 10}{.03} = 8000$$

Cell (2) Final stresses

$$2\Theta GA_a = \frac{\Sigma qL}{t} = \frac{(10.85 \times 5)2}{.03} + \frac{(0.85 \times 5)2}{.03} + \frac{26.68 \times 10}{.03}$$

$$- \frac{19.15 \times 10}{.04} = 8000$$

A15.8 Unsymmetrical-Multiple Flange-Two Cell Beam

Fig. A15.42 shows a two-cell wing beam with 16 flange members. This beam section is identical to the single cell beam of Fig. A15.34 of article A15.6 except that an .032 interior web has been added between stringers #3 and #12. The same external loads are used as in the example of Fig. A15.34.

The internal resisting shear flow is statically indeterminate to the second degree. The flexural shear flow for bending about the principal axes for the given loads will be computed based on an assumed value for q at two points, one in each cell. For this example the shear flow q at points c and c' will be assumed zero (see Fig. A15.42). Under this assumption the shear flow will be exactly the same as for the

Table A15.2

1	2	3	4	5	6	7	8	9	10	11	12	13	14
Stringer No.	q_1	q_2	m	q_1 m	q_2 m	L	t	q_1 L/t CELL A	q_1 L/t CELL B	q_2 L/t CELL A	q_2 L/t CELL B	q_2 L/t CELL A	q_2 L/t CELL B
1													
2	-0.572	0.142	55.2	-31.7	0.78	4.42	.025	177		-101.8		25.1	
3	-1.035	0.485	44.2	-45.7	21.40	4.30	.025	172		-178.0		83.5	
4	-1.915	1.750	32.0	-61.2	56.00	4.05	.04		101		-194.0		177.0
5	-2.160	2.400	38.2	-82.5	91.80	4.58	.04		115		-250.0		276.0
6	-2.240	3.130	33.0	-73.8	103.50	4.00	.04		100		-224.0		313.0
7	-2.162	3.900	33.2	-71.9	129.70	4.00	.04		100		-216.0		390.0
8	-1.936	4.720	40.2	-77.8	130.00	4.62	.04		116		-224.0		549.0
9	-1.530	5.550	32.6	-50.0	181.00	4.0	.04		100		-163.0		555.0
10	-0.580	7.001	251.8	-146.0	176.20	15.7	.05		314		-182.0		2190.0
16	0.745	5.800	46	34.2	267.00	6.10	.032		191		143.0		1103.0
15	1.51	4.640	48.2	73.4	224.00	6.35	.032		198		299.0		920.0
14	1.82	3.420	46.4	84.6	158.40	6.35	.032		198		360.0		678.0
13	1.685	2.162	47.8	80.2	103.52	6.55	.032		205		346.0		442.0
12	1.187	1.115	36.6	42.4	40.80	4.3	.025	172		198.0			192.0
11	0.660	0.514	42.6	28.1	21.90	4.3	.025	172		113.5			88.0
10	0	0	158.6	0	0	9.56	.025	382		0			
1													
web 3-12	0	0				13.3	.032	416	416	0	0	0	0
Sum				-297.7	1766			1491	2184	31.7	-295	108.6	7873

single cell of Fig. A15.34. The calculations will not be repeated here but the results will be copied direct from column 6 to 10 of table A15.1 and entered direct in table A15.2 of this article. The moment of this static shear flow about the section c.g. will be the same as the single cell, thus columns 11, 12, and 13 of table A15.1 are recopies in table A15.2 without further explanation. A constant shear flow q_A in cell A and q_B in cell B will be added to the static flexural shear flows q_1 and q_2 to make the twist of each cell the same and also to make the moments in the XZ plane equal to zero. Table A15.2 gives most of the calculations in tabular form.

The twist of each cell due to q_1, q_2, q_A and q_B will now be written.

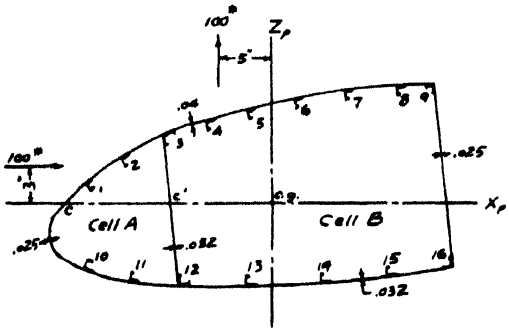


Fig. A15-42

$\theta = \Sigma \frac{q L}{\bar{t}} \frac{}{2AG}$ Since G is constant it will be omitted.

For Cell "A"

Enclosed area of cell "A" = 102.5 sq. in.

$$\theta_A = \frac{1}{2 \times 102.5} (31.7 + 108.6 + 1491\ q_A - 416\ q_B)$$

or $\theta_A = 7.27\ q_A - 2.03\ q_B + 6.85$ - - - - - - - -(7)

For Cell "B"

Enclosed area = 391 sq. in.

$$\theta_B = \frac{1}{2 \times 391} (-295 + 7873 + 2154\ q_B - 416\ q_A)$$

or $\theta_B = -.533\ q_A + 2.76\ q_B + 9.68$ - - - - - - - -(8)

But $\theta_A = \theta_B$, hence equating (7) and (8)

$7.803\ q_A - 4.97\ q_B - 9.00 = 0$ - - - - - - - - - -(9)

For equilibrium the moments of external and internal shear forces about the Y axis must equal zero. Take moments about c.g. of section:

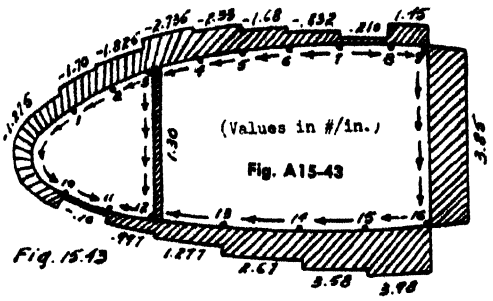
$-297.7 + 1766 + q_A\ (2 \times 102.5) + q_B\ (2 \times 391) + 100 \times 5 + 100 \times 3 = 0$ or

$205\ q_A + 782\ q_B + 2268.3 = 0$ - - - - - - - - - -(10)

Solving equations (9) and (10) for q_A and q_B

$q_A = -.55$#/in. $q_B = -2.76$#/in.

Adding these constant shear flows to q_1 and q_2 of table A15.2 we obtain the final shear flow as shown in Fig. A15.43. Comparing this figure with Fig. A15.35 we see the effect of adding the interior web on the shear flow.



A15.9 Three-Cell-Multiple Flange Box Beam.

Fig. A15.44 shows a 3-cell box beam subjected to an external shear load of 1000# as shown. The section is symmetrical about axis XX. The area of each stringer is shown in parenthesis at each stringer point. The internal shear flow system which resists the external load of 1000# will be calculated assuming that the webs and walls take no bending loads, or, the stringers are the only effective material in bending. The moment of inertia about the XX axis of effective material equals 250 in^4. (Note: this beam section is identical to the two cell beam of Fig. A15.36 plus the leading edge cell (3).

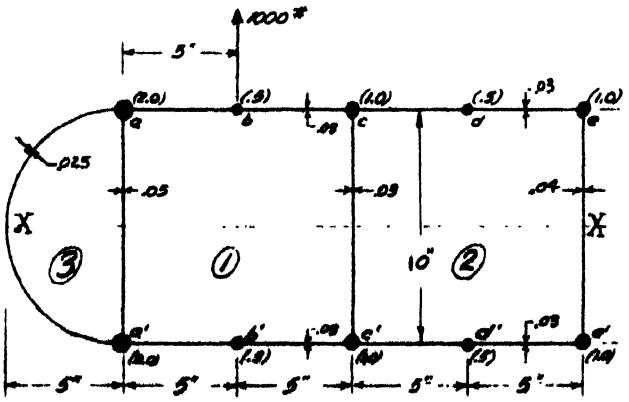


Fig. A15-44

Solution #1 (Without use of shear center)

The system is statically indeterminate, to the third degree, since the value of the shear flow q at any point in each cell is unknown.

The value of the shear flow will be assumed at a point in each cell and the flexural shear flow for bending about the XX axis will be determined consistent with this assumption. A

constant unknown shear flow q_1, q_2, and q_3 for cells (1) and (2) and (3) respectively will be added to the static flexural shear flow so as to make the angular twist θ of each cell the same, since if any twisting takes place, all cells must suffer the same amount. Furthermore, for equilibrium, the moment of the internal shear flow system plus the moment of the external shear load must equal zero. Thus, four equations are available to solve for the four unknowns q_1, q_2, q_3, and θ.

For bending about axis XX, the flexural shear flow will be assumed as zero at a point just to the left of stringer a in cell (3) and just to the left and right of stringer c in cells (1) and (2) respectively. One might consider the cells as cut at these three points. Fig. A15.45 shows the flexural shear flow under these assumptions. Since the leading edge cell (3) has no stringers and the covering is considered ineffective in bending, the shear flow will be zero on the leading edge portion since the shear flow was assumed zero just to the left of stringer a. The resulting flexural shear flow for the 3 cell section will therefore be identical to Fig. A15.37 and the calculations for the flexural shear flow will be identical to those in Art. A15.7.

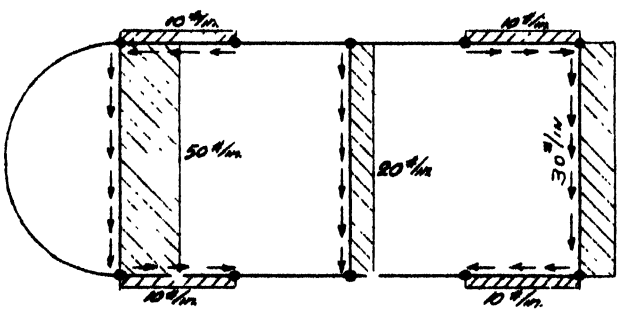


Fig. A15-45

Fig. A15.46 shows the unknown constant shear flows q_1, q_2, and q_3 which must be added to the flexural shear flow of Fig. A15.45 to make the twist θ of each cell the same. The sense of each has been assumed positive in each cell.

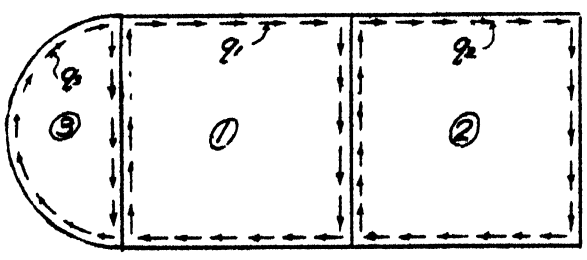


Fig. A15-46

The angular twist θ for each cell equals $\theta = \frac{1}{2AG} \Sigma\, q\, L/t$

The value θG will be computed for each cell.

Cell (3)

$$2\theta A_3 G = \frac{\Sigma\, qL}{t}$$

$$2\theta \times 39.4G = \frac{10 \times 50}{.05} + \frac{15.71}{.025}\, q_3 + \frac{10q_3}{.05} - \frac{10q_1}{.05}$$

$$\text{or } \theta G = 10.5q_3 - 2.55q_1 + 127 \text{ - - - - - - (11)}$$

Cell (1)

$$2\theta A_1 G = \frac{\Sigma\, qL}{t}$$

$$2\theta \times 100G = \frac{-50 \times 10}{.05} - \frac{2\,(10 \times 5)}{.03} + \frac{10 \times 20}{.03} + \frac{3(10q_1)}{.03}$$

$$+ \frac{10q_1}{.05} - \frac{10q_3}{.05} - \frac{10q_3}{.03} \text{ hence } \theta G = 6q_1 - q_3 - 1.67q_3 -$$

$$33.34 \text{ - - - - - - - - - - - - - - - - - (12)}$$

Cell (2)

$$2\theta A_2 G = \frac{\Sigma qL}{t}$$

$$2\theta \times 100 \times G = -\frac{20 \times 10}{.03} + \frac{2(10 \times 5)}{.03} + \frac{10 \times 30}{.040} +$$

$$\frac{3 \times 10 \times q_3}{.03} + \frac{10q_3}{.04} - \frac{10q_1}{.03}$$

$$\text{hence; } \theta G = 6.25q_3 - 1.67q_1 + 20.83 \text{ - - - (13)}$$

Taking moments of the internal shear flow systems of Fig. A15.45 and A15.46 and the external load of 1000# about stringer a and equating to zero:-

$$\Sigma M_a = 10 \times 20 \times 10 + 10 \times 30 \times 20 - 5 \times 1000 - 78.6q_3 + 200q_1 + 200q_3 = 0$$

$$= 3000 + 78.6q_3 + 200q_1 + 200q_3 = 0 \text{ - - (12.1)}$$

Solving equations (11) (12) (13) and 13.1) for the unknown q_1, q_2, q_3 and θG we obtain:

$q_1 = -2.12$#/in.

$q_2 = -7.09$#/in.

$q_3 = -14.5$#/in.

$\theta G = -19.9$

Adding these constant shear flows to the flexural shear flow of Fig. A15.45, we obtain the true internal resisting shear flow as shown in Fig. A15.47.

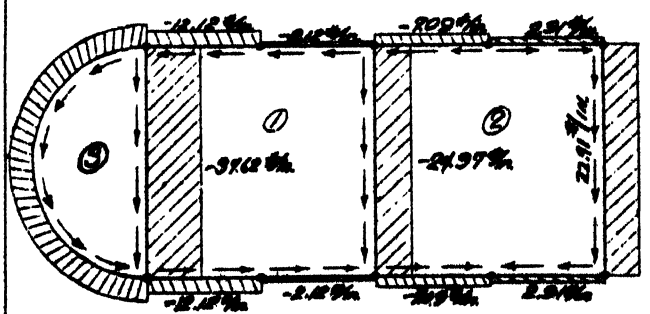


Fig. A15-47

Solution #2 (By use of the shear center)

In this solution we find the internal shear system for bending about the X axis without twist. The centroid of this shear system locates the horizontal position of the shear center. The given external load produces a moment about this shear center. The internal torsional resisting moments are determined by the method explained in Chapter A5.

If the beam bends without twist, then θG for each cell equals zero. Thus, equations (11) and (12) and (13) are equated to zero, giving the following three equations:

$$10.5q_3 - 2.54q_1 + 127 = 0 \quad \text{- - - - - - - - - (14)}$$

$$-q_3 + 6q_1 - 1.67q_2 - 33.34 = 0 \quad \text{- - - - - - - (15)}$$

$$-1.67q_1 + 6.25q_2 + 20.83 = 0 \quad \text{- - - - - - - (16)}$$

Solving for q_1, q_2 and q_3 we obtain,

$$q_1 = 3.03\#/in;\ q_2 = -2.53\#/in.\ q_3 = -11.36\#/in.$$

Adding these constant shear flow systems in each cell to that of Fig. A15.45, we obtain Fig. A15.48, the shear flow system for bending without twist. To find the centroid which locates the shear center, take moments about some point as stringer a.

$$\Sigma M_a = 25.56 \times 10 \times 10 + 27.47 \times 10 \times 20 + (3.03 + 7.47)\ 5 \times 10 - (6.99 + 2553)\ 5 \times 10 - 10 \times 11 \times 11.36 \times 7.88^* = 7205\text{"\#}$$

(*Location of resultant flow on curved portion $= \frac{2A}{10} = \frac{2 \times 39.4}{10} = 7.88$" from line aa")

Then $\bar{X} = \frac{7205}{1000} = 7.205$" to the right of a = horizontal location of the shear center for bending about axis XX.

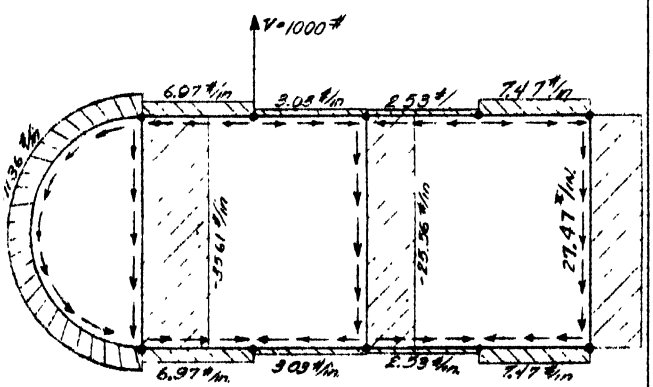


Fig. A15-48

The external load V = 1000# acts at a point 5" to the right of a. Therefore, the moment of the external load about the shear center = 1000 x (7.205 - 5) = 2205"#

This pure torsional moment is resisted by a constant flow torsional stress in each cell.

Example problem 3 of Art. A5.14 of chapter A5 shows the distribution of the resisting torsional stress for this identical 3-cell box for an external torque of -100,000"#. Thus, we will take $-\frac{2205}{100000} = -.02205$ times the result in that example problem, hence;

$$q_{1_t} = -.02205 \times 234.1 = -5.16\#/in.$$

$$q_{2_t} = -.02205 \times 208.8 = -4.60\#/in.$$

$$q_{3_t} = -.02205 \times 143.4 = -3.16\#/in.$$

Adding these constant shear flows to those of Fig. A15.48, we obtain the same values as in Fig. A15.47 by the first solution.

A15.10 Problems

(1) Figs. A15.49 and A15.50 illustrate single cell 2 flange beams. Assuming the webs and walls ineffective in resisting bending axial loads, determine the internal shear flow system for each section in resisting the given external loads. Solve by all three methods as illustrated in article A15.2.

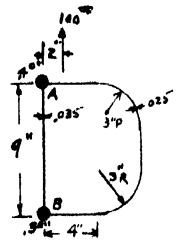


Fig. A15-49

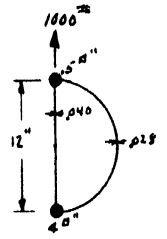


Fig. A15-50

(2) Figs. A15.51 and A15.52 illustrate single cell 3 flange beams. Assuming the web and wall skin as ineffective in bending determine the internal shear flow system in resisting the external loads as shown. Solve by the various methods of article A15.4

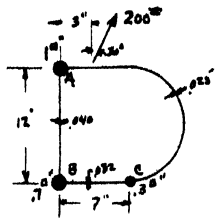


Fig. A15-51

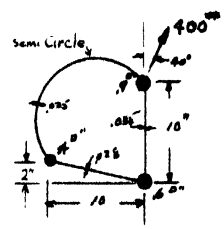


Fig. A15-52

(3) Fig. A15.53 shows a rectangular box beam supporting a 1000# load as a cantilever beam. Assuming all material effective determine the internal shear flow system. Solve by the two methods of article A15.5.

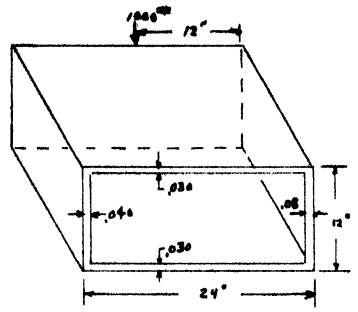


Fig. A15-53

(4) Fig. A15.54 shows a distributed flange single cell beam section. Assuming the eight stringers as effective only in resisting bending loads, determine the internal shear flow system in resisting the external load of 100# applied as shown. Determine the shear center for the section.

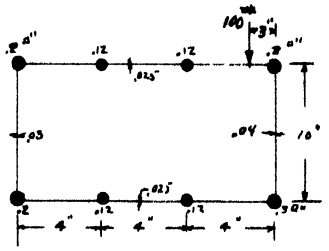


Fig. A15-54

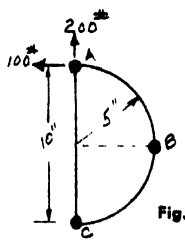


Fig. A15-55

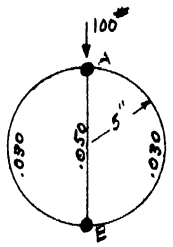


Fig. A15-56

(5) Determine the internal shear flow system for the loaded beam section in Fig. A15.55. Assume stringers A, B and C as the only effective material.

(6) For the two cell beam section in Fig. A15.56 determine the internal resisting shear flow system if the two flange members A and B take all the bending stresses.

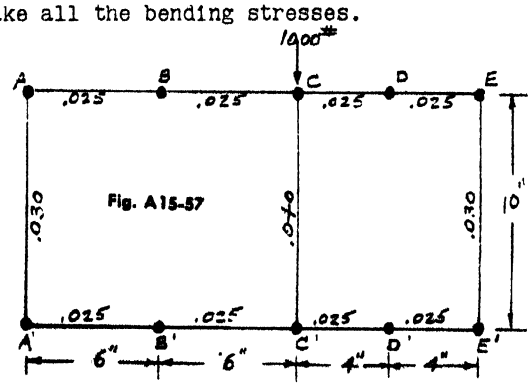


Fig. A15-57

(7) Determine the internal shear flow system for the two-cell-multiple flange beam section in Fig. A15.57. Assume all webs ineffective in bending. Area of each stringer = 1 sq. in.

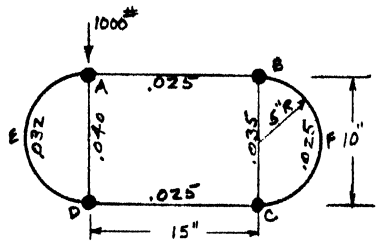


Fig. A15-58

(8) Determine the internal shear flow pattern for the beam section in Fig. A15.58. The four flange members have equal areas. Webs are ineffective.

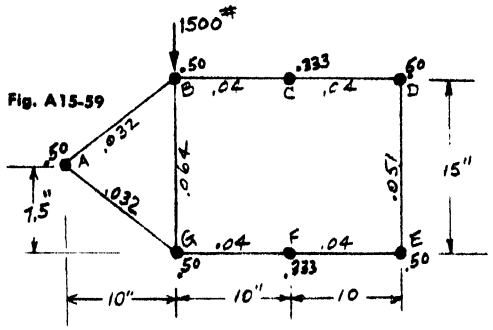


Fig. A15-59

(9) Calculate the internal shear flow pattern for the beam section in Fig. A15.59. Area of each flange member is given on the figure. Consider web members ineffective in bending.

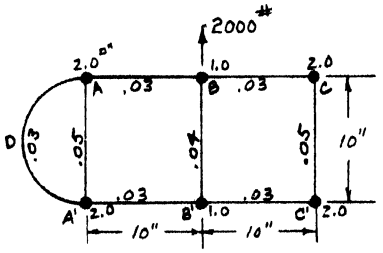


Fig. A15-60

(10) Assuming all webs ineffective in bending determine internal shear flow system for 3 cell beam section in Fig. A15.60.

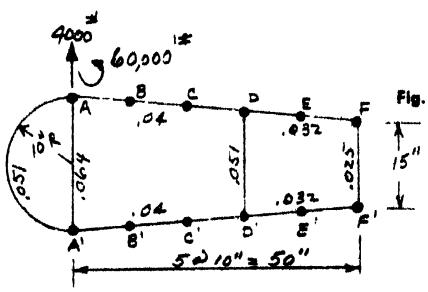


Fig. A15-60a

(11) The twelve flange members for the beam section in Fig. A15.60a have same area. Assuming all webs ineffective in bending, determine the internal shear flow system for the given external loading.

A15.11 Shear Flow For Single Cell Beams of Variable Moment of Inertia

The previous part of this chapter dealt entirely with beams of constant moment of inertia along the flange direction. In airplane wing and fuselage structures, the common case is a beam of non-uniform section in the flange direction. In cases where the change of the cross-sectional areas is fairly well distributed between the various flange members which make up the beam cross section, the shear flow results as given by the solution for beams of constant moment of inertia are not much in error. For beams where this is not the case, the shear flow results may be considerably different from the actual shear flows. This fact will be illustrated later by the solution of a few example problems.

A15.12 The Determination of the Web Shear Flow System By Considering Changes in Flange Load.

Fig. A15.61 shows a single cell distributed flange beam. Consider the beam acts as a cantilever beam with the bending moment existing at section (A) being greater than that existing at section (B) and that the bending moment produces compression on the upper surface. By the use of the flexural stress equations, the bending stress on each stringer can be found, which if multiplied by the stringer area gives the stringer axial load. Thus at beam section (B), let P_1, P_2, P_3, etc. represent the axial loads due to a bending moment M. The external bending

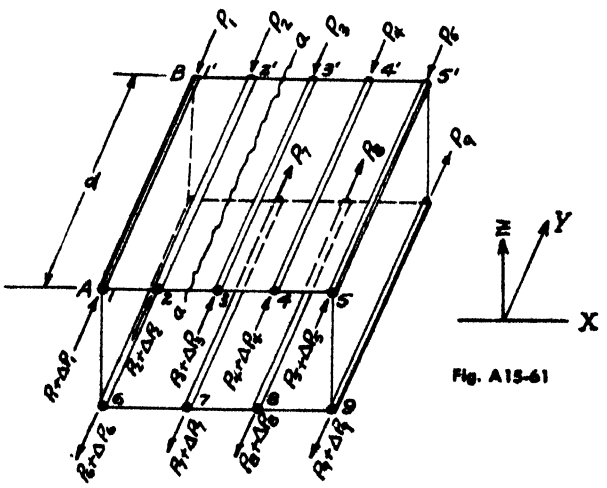


Fig. A15-61

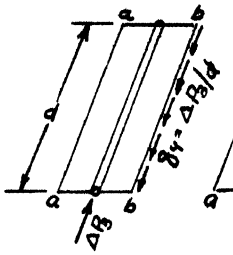


Fig. A15-62

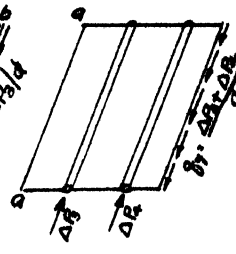


Fig. A15-63

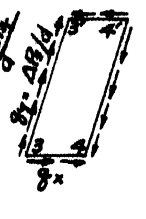


Fig. A15-64

moment at section (A) is M + ΔM, hence the stringer axial loads at section (A) will equal $P_1 + \Delta P_1$, $P_2 + \Delta P_2$, $P_3 + \Delta P_3$, etc. These stringer axial loads are shown on Fig. A15.61.

Imagine the upper sheet panel 2, 2' 3, 3' is cut along the line (a-a). The average shearing stress q_y in the Y direction along any section between flange stringers (3) and (4) equals the sum of the flange forces acting in the Y direction. Fig. A15.62 shows a free body for determining the q_y shear stresses on the sheet between stringers (3) and (4). Since ΣF_y must equal zero, the resisting shear force Q on the line bb must equal ΔP_3 and hence the average shear per inch equals $q_y = \Delta P_3/d$. In like manner for the shear stress in the panel between stringers (4) and (5), the average shear flow $q_y = (\Delta P_5 + \Delta P_4)/d$ (See Fig. A15.63).

Fig. A15.64 shows panel (3, 3', 4, 4') isolated as a free body. Taking moments about corner 4':

$$\Sigma M_{4'} = \frac{\Delta P_3 \times d}{d} \times b - q_x \, b \, d = 0, \text{ hence } q_x = \Delta P_3/d$$

Thus for rectangular sheet panels between stringers, the shear flow q_x or q_z equals the average shear q_y in the sheet parallel to the stringers. A general shear flow equation using the ΔP loads in the stringers over a beam length of d can thus be written as follows:

$$q_n = q_o + \Sigma_1^n \frac{\Delta P}{d} \text{ - - - - - - - - - - - - - (17)}$$

Example Problems:

Two example problems will be given to illustrate the difference between the results obtained by equation (17) and the general shear flow equation which applied only for beams of constant section.

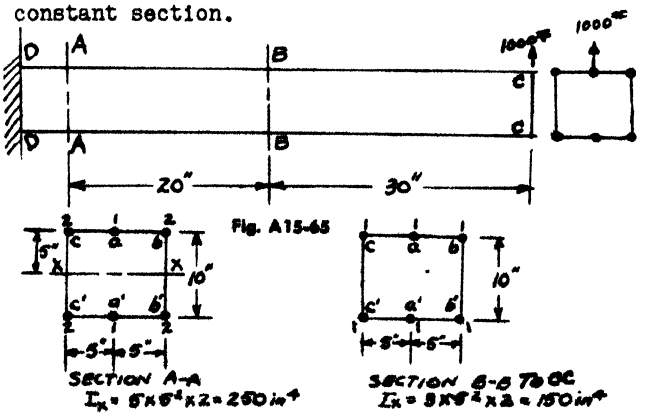


Fig. A15-65

Fig. A15.65 shows a square single cell beam with six flange stringers. Between points B and C, the beam has a constant flange section which is shown in Section B-B. The numerals beside each stringer represent the area of the stringer. Between points B and D, the flange material tapers uniformly with the flange material at point A as indicated in Section A-A. It should be noticed that the increase in flange area is obtained by increasing only corner stringers b and c. The shear flow on section A-A will be computed by the general equation for beams of constant sections and by equation (17) which deals with the change in flange loads.

Solution 1 - Using the Shear Flow Expression For Beams of Constant Section

It will be assumed that stringer (a) at section A-A is split in two with half the stringer area acting with web ab and half with web ac. If webs are considered ineffective in bending then

$$q_{ab} = \frac{V_z}{I_x} \Sigma\, z\, A = \frac{1000}{250} \times .5 \times 5 = 10\#/\text{in.}$$

$$q_{bb'} = 10 + \frac{1000}{250} \times 2 \times 5 = 50\#/\text{in.}$$

Proceeding around the cell the balance of the shear flow could be calculated, but due to symmetry enough values have been found for the shear flow to draw the complete shear flow picture for bending about the X axis when it is assumed that one half of the area of stringer (a) acts with each adjacent web. Fig. A15.66 shows the resulting shear flow diagram. The resultant of this shear flow pattern is a 1000# force in the Z direction and its location through the midpoint of the box since the flow is symmetrical. The external load of 1000# also acts through the midpoint of the cell hence the external load is in equilibrium with the shear flow system of Fig. A15.66, which therefore is the final shear flow system for this method of solution.

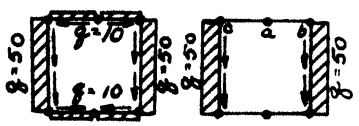


Fig. A15-66

Fig. A15-67

Solution No. 2 - Considering ΔP Loads in Flange Stringers.

Bending moment at section AA = 1000 x 50 = 50000 in. lb.

Bending moment at section BB = 1000 x 30 = 30000 in. lb.

Considering Section B-B:

Bending stress intensity at midpoint of stringers by the flexural formula:

$$f_b = \frac{Mz}{I_x} = \frac{30000 \times 5}{150} = 1000 \text{ psi.}$$

Axial load in each of the stringers a, b, and c = 1000 x 1 = 1000#

Considering Section A-A:

$$f_b = \frac{Mz}{I_x} = \frac{50000 \times 5}{250} = 1000 \text{ psi.}$$

Axial load in stringer (a) = 1000 x 1 = 1000#

Axial load in stringer (b) or (c) = 1000 x 2 = 2000#

These resulting axial loads are shown acting on the portion between points A and B in Fig. A15.68, which equals the results as shown in Fig. A15.69.

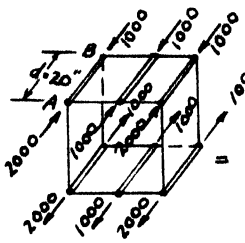


Fig. A15-68

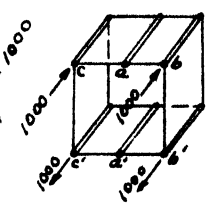


Fig. A15-69

Having found the ΔP flange loads over a length (d) of 20", the shear flow can be computed by equation (17).

It will be assumed that one half of the ΔP load in stringer (a) will flow to each adjacent web. However, there is no ΔP load in stringer (a) hence $q_{ab} = q_{ac} = 0$. Then

$$q_{bb'} = 0 + \Sigma \frac{\Delta P}{d} = 0 + \frac{1000}{20} = 50\#/\text{in.}$$

$$q_{b'a'} = 50 + \Sigma \frac{\Delta P}{d} = 50 + \frac{-1000}{20} = 0$$

Due to symmetry the left side of cell would give the same results. The results are plotted in Fig. A15.67. Since the increase in section moment of inertia between beam points B and A is increasing at the same rate as the external bending moment, the average shear of 50#/in. is constant between the two beam sections A and B. Comparing Figs. 66 and 67, we find the first method gives a shear flow of 10#/in. in the top and bottom webs, whereas actually it is zero. This seems reasonable since the entire increase of flange area was placed in stringers b and c.

Example Problem No. 2.

The same beam as in Problem 1 will be used except that the cross-sections at beam points B and A are as shown in Fig. A15.70. The increase in flange area between beam points B and A has been placed entirely in stringer (a) which changes from 1 sq. in. at B to 3 sq. in. at A.

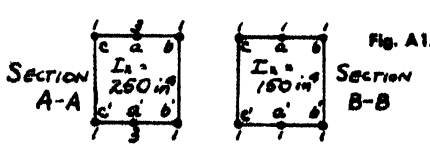


Fig. A15-70

Solution No. 1

The same assumptions will be made as in example problem 1, whence

$$q_{ab} = \frac{V_z}{I_x} \Sigma\, z\, A = \frac{1000}{250} \times 1.5 \times 5 = 30\#/\text{in.}$$

$$q_{bb'} = 30 + \frac{1000}{250} \times 1 \times 5 = 50\#/\text{in.}$$

Fig. A15.71 shows the plotted results.

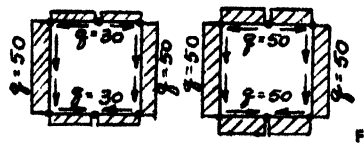


Fig. A15-71 Fig. A15-72

Solution No. 2

The axial loads in the stringers at section B-B are the same as in problem 1.

At station A-A

$$f_b = \frac{Mz}{I_x} = \frac{50000 \times 5}{250} = 1000 \text{ psi}$$

Axial load in stringer (a) = 1000 x 3 = 3000#

Axial load in stringer (b) or (c) = 1000 x 1 = 1000#

Fig. A15.73 shows the results, which gives the ΔP loads of Fig. A15.74. The web shear flow can now be calculated as in example problem 1. It will be assumed as before that one half of the ΔP load in stringer (a) will flow to each adjacent web, whence

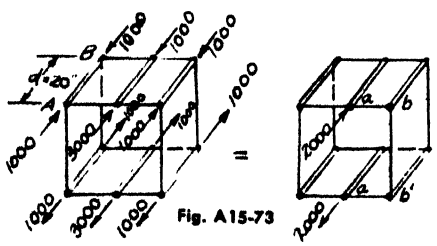


Fig. A15-73 Fig. A15-74

$$q_{ab} = \Sigma\, \frac{\Delta P}{d} = \frac{2000}{2 \times 20} = 50\#/\text{in.}$$

$$q_{bb'} = 50 + \Sigma\, \frac{\Delta P}{d} = 50 + 0 = 50\#/\text{in.}$$

$$q_{b'a'} = 50 + \Sigma\, \frac{\Delta P}{d} = 50 + 0 = 50\#/\text{in.}$$

$$q_{a'c'} = 50 + \Sigma\, \frac{\Delta P}{d} = 50 + \frac{-2000}{20} = -50\#/\text{in.}$$

$$q_{c'c'} = -50 + \Sigma\, \frac{\Delta P}{d} = -50 + 0 = -50\#/\text{in.}$$

Fig. A15.72 shows the plotted results. Positive shear flow means clockwise flow in cell. In this problem, the resulting shear in the top and bottom webs is 50#/in. instead of 30#/in. as given by the shear flow equation for beams of constant section. Likewise the true shear flow between stringers a and b is the same as between b and b'. This seems reasonable as all the area increase in the stringers was placed in stringer a.

These simple examples show that variation in the section moment of inertia can produce considerable change in shear flow as compared to that obtained by equation for constant section beams.

A15.13 Shear Flow in Tapered Web

Since the airplane wing and fuselage structures taper in section, the web panels between flange members are usually tapered in width. Fig. A15.75 shows a tapered cantilever beam carrying a load V at end. The flange reactions at the left end have been found by simple statics. A free body diagram of the web is shown in Fig. A15.76.

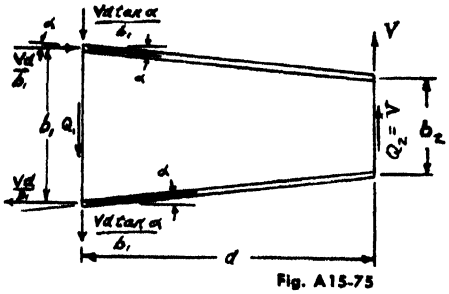


Fig. A15-75

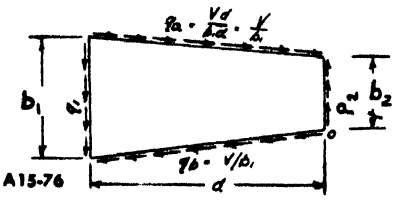


Fig. A15-76

Take moments about point (O):

$$\Sigma M_O = \frac{Vd}{b_1}\, b_2 - q_1\, b_1\, d = 0$$

hence

$$q = \frac{Vb_2}{b_1{}^2}$$

but

$V = q_2\, b_2$, whence

$$q = \left(\frac{b_2}{b_1}\right)^2 q_2 \quad \text{- - - - - - - - - - - - - - (18)}$$

$$q_2 = \frac{V}{b_1} = \frac{q_2\, b_2}{b_1}, \text{ hence } q_2 = \frac{b_1\, q_2}{b_2}$$

Substitute value of q_2 in (18), we obtain

$$q_1 = \left(\frac{b_2}{b_1}\right) q_2 \quad \text{- - - - - - - - - - - - - - (19)}$$

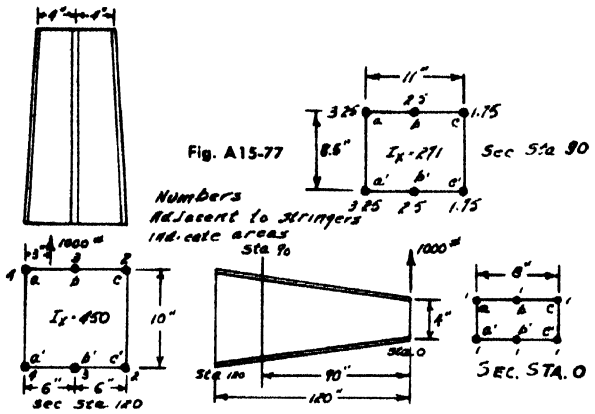
Thus having the average shear flow along the stringer side of the tapered web panel, the shear flow on the large end can be found by equation (19).

A15.14 Example Problem of Shear Flow in Tapered Multiple Flange Single Cell Beam.

Fig. A15.77 shows a tapered single cell beam with 6 spanwise stringers or flange members. The beam is loaded by a 1000# load located as

shown. Assuming the webs ineffective in bending the internal resisting shear flow pattern will be determined.

In this solution the shear flow at Station 120 will be determined by considering the ΔP flange loads over a length of 30" or between Stations 90 and 120.



Consider section at Station 120:

$$\text{Bending stress} = f_b \quad \frac{1000 \times 120 \times 5}{450} = 1333 \text{ psi.}$$

Horizontal component of axial load in stringers = f_b A (where A = area)

hence

$P_a = 4 \times 1333 = 5332\#$, $P_b = 3 \times 1333 = 3999\#$,

$P_c = 2 \times 1333 = 2666\#$

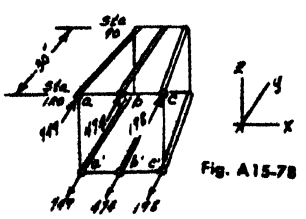
Consider section at Station 90:

$$f_b = \frac{1000 \times 90 \times 4.25}{271} = 1410 \text{ psi.}$$

$P_a = 3.25 \times 1410 = 4583\#$, $P_b = 2.5 \times 1410 = 3525$, $P_c = 1.75 \times 1410 = 2468$

The change in axial load ΔP in the stringers between stations 90 and 120 equals the difference of the above loads. Thus $\Delta P_a = 749$, $\Delta P_b = 474$, $\Delta P_c = 198$.

Fig. A15.78 shows these ΔP loads acting on the wing portion. Assume the shear flow in web aa' is zero. The average shear flow in each web panel over the length of 30" will be calculated by eq. (17).



$q_y = q_o + \Sigma \frac{\Delta P}{d}$, hence

$q_{y(ab)} = 0 + 749/30 = 24.97\#/\text{in.}$

Since panel ab is tapered in width from 6" at Station 120 to 5.5" at Station 90, the shear flow $q_{x(ab)}$ at Station 120 can be determined from Equation (19)

hence

$q_{x(ab)} = 24.97 \times 5.5/6 = 22.83\#/\text{in.}$

$q_{y(bc)} = 24.97 + 474/30 = 40.77\#/\text{in.}$

$q_{x(bc)} = 40.77 \times 5.5/6 = 37.4$

$q_{y(cc')} = 40.77 + 198/30 = 47.37\#/\text{in.}$

$q_{z(cc')} = 47.37 \times 8.5/10 = 40.2\#/\text{in.}$

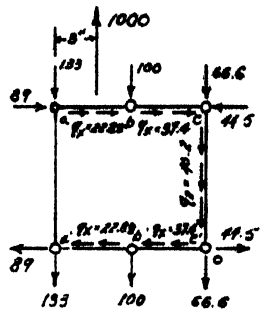


Fig. A15-79

$q_{y(c'b')} = 47.37 - 198/30 = 40.77$

$q_{x(c'b')} = 40.77 \times 5.5/6 = 37.4$

$q_{y(b'a')} = 40.77 - 474/30 = 24.97\#/\text{in.}$

$q_{x(b'a')} = 24.97 \times 5.5/6 = 22.83$ (See Fig. A15.79 for best results)

IN PLANE FORCES PRODUCED BY INCLINATION OF FLANGE MEMBERS

Since the box tapers in depth and width, the flange stringers are not normal to section 120, thus X and Z force components are produced on section by flange loads.

Stringer (a) $P_x = 5332 \times 2/120 = 89\#$, $P_z = 5332 \times 3/120 = 133\#$

Stringer (b) $P_x = 3999 \times 0 = 0$, $P_z = 3999 \times 3/120 = 100$

Stringer (c) $P_x = 2666 \times 2/120 = 44.5$, $P_z = 2666 \times 3/120 = 66.6\#$

These in plane forces induced by flange loads are also shown in Fig. A15.79.

The equilibrium of the loads in Fig. A15.79 will be checked:

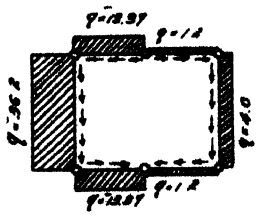
$\Sigma F_Z = 1000 - 266 - 200 - 133.2 - 10 \times 40.2 = 1000 - 1001.2$

$\Sigma F_X = 0$ by observation (Check)

Take moments about stringer (a):

$\Sigma M_a = -3 \times 1000 + 200 \times 6 + 133.2 \times 12 + 10 \times 40.2 \times 12 + 89 \times 10 - 44.5 \times 10 + 22.83 \times 6 \times 10 + 37.4 \times 6 \times 10 = 8688$ in. lb.

For equilibrium, a moment of -8688 is required, which can be produced by a constant shear flow $q = M/2A = -8688/240 = -36.2\#/\text{in.}$ Adding this constant shear flow to that of Fig. A15.79, we obtain the final shear flow at Station 120 as shown in Fig. A15.80



PART B

CHAPTER B1
COLUMN THEORY - COLUMNS WITH STABLE CROSS SECTIONS

The modern airplane structure is essentially a thin shell with or without stiffening units. The design of this general type of structure involves a consideration of instability in both elastic and plastic range of stresses. A considerable amount of theoretical and experimental work has been done in this special field of structures, but much still remains to be done before the many semi-empirical methods of design now being used can be eliminated.

Part B summarizes and discusses some of the theory and experimental results which are available and which form the basis of the various methods for the design of thin-wall aircraft structures. The application of the information in part B to the design of monocoque and semi-monocoque airplane structures is taken up in detail in several of the chapters of part C.

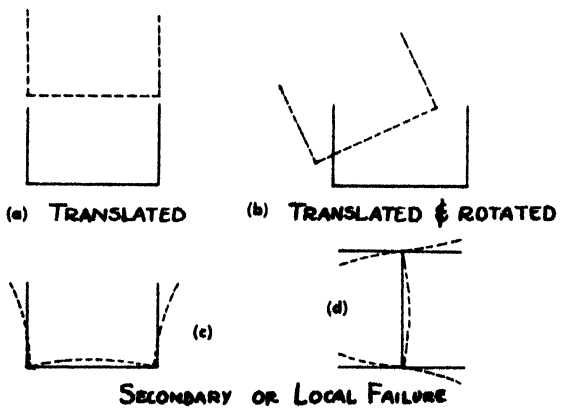
GENERAL COLUMN THEORY

B1.0 Methods of Column Failure

In general all types of column failures may be classed under two headings, (Ref. 4), namely,

(1) Primary or general failure of column as a whole.
(2) Secondary, or local failure.

Primary or general failure is any type of column failure in which the cross sections are translated, rotated, or both translated and rotated but not distorted in their own planes (Figs. (a) and (b). Secondary or local failure of a column is defined as any type of failure in which cross sections are distorted in their own planes but not translated or rotated. (Figs. (c) and (d).



Thus to determine the critical strength of a column section from short to long column lengths, the critical strengths in bending, twisting and local crippling must be found to obtain a complete picture as to the action of a particular section when used as a column. Fig. (e) illustrates how the strength of some sections may vary when loaded as a column.

For a slenderness ratio L/ρ between (o) and (a) the critical column strength will be determined by the local buckling or crippling strength. For longer column lengths between (a) and (b) column failure may be due to twisting and for still longer lengths (b) and (c) failure will be due to bending or translation of the sections without rotation.

This chapter deals mostly with the bending strength of columns. The twisting strength of columns is touched on lightly near the end of the chapter. The crippling or local strength of a column is discussed in detail in chapter B5.

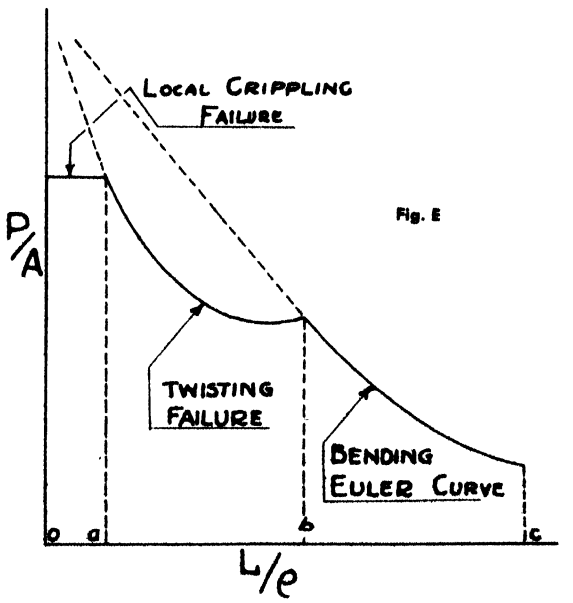


Fig. E

B1.1 Column Buckling

Fig. B1.1 shows a column subjected to an end load P and a side load F. If load P is very small it will take a certain load F to deflect the column the small distance Δ. If load P is

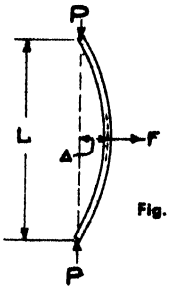


Fig. B1-1

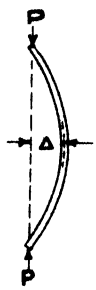


Fig. B1-2

increased it will take a smaller load F to deflect the column the same distance Δ, until finally as load P is increased it will take only an infinitesimal load F to deflect the column the distance Δ. This maximum load P is called the column critical load P_{cr}. The column will buckle or bend sideways if this P_{cr} load is increased a very small amount. This illustrates therefore that the buckling strength of columns is a function of their bending stiffness.

If the column of Fig. B1.2 is given an initial deflection Δ it will return to its original straight condition. If load P is slightly less than the critical load P_{cr}.

B1.2 Euler's Equation for Critical Column Load

Euler's equation is, for pin end columns,

$$P_{cr} = \frac{\pi^2 EI}{L^2}$$ where P_{cr} is the maximum column compressive load.

L = column length
E = Modulus of elasticity of the material
I = least moment of inertia of cross-section

For a column with end restraint or fixity, the coefficient C is added or

$$P_{cr} = C\pi^2 \ EI/L^2 - - - - - - - - - - - - - (1)$$

The equation was first derived by Euler many years ago. Derivations are given in practically every textbook on mechanics of materials, using a method involving a differential equation relating curvature to bending moment or by use of energy relationships.

If one knew the shape of the deflected column, the critical load P could be found by simple considerations of deflections, assuming the column in a sort of neutral equilibrium in the deflected position.

Suppose for example that the shape of the deflected column curve follows a sine curve relationship with deflection at midpoint equal to unity. See Fig. B1.3

The equation of the deflected column curve is $y = \sin \frac{\pi x}{L}$. If P is the end load, the bending moment at any point = $M = Py = P \sin \frac{\pi x}{L}$

By the well known "moment area" principle (see Chapter A7; art. A7.14), the deflection of a point (A) on the elastic curve away from a tangent to elastic curve (B) equals the first moment of the M/EI diagram between (A) and (B) about (A),

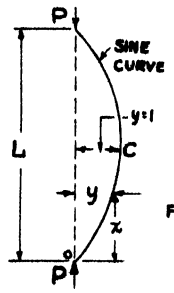


Fig. B1-3

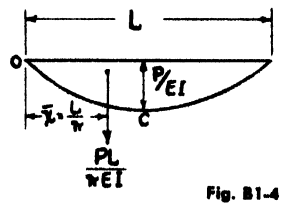


Fig. B1-4

Thus in Fig. B1.3, the deflection of point (O) away from tangent at midpoint c equals unity in our assumed conditions and it also equals the first moment of the area of the M/EI diagram between (O) and (C) about (O). (Fig. B1.4).

The value of the ordinate for M/EI diagram at any point x from O is $\frac{P}{EI} \sin \frac{\pi x}{L}$

The total area under the curve is,

$$\text{area} = \frac{P}{EI} \int_0^L \sin \frac{\pi}{L} x \, dx = \frac{P}{EI} \left[-\frac{L}{\pi} \cos \frac{\pi}{L} x \right]_0^L$$

$$= \frac{P}{EI} - \left\{ \left[\frac{L}{\pi} (-1) \right] - \left[\frac{L}{\pi} (1) \right] \right\} = \frac{P}{EI} \left(\frac{L}{\pi} + \frac{L}{\pi} \right)$$

hence area $= \frac{2PL}{\pi EI}$ and half area $= \frac{PL}{\pi EI}$

The center of gravity of the half area is

$$A\bar{x} = \int x \, da$$

$$\left(\frac{PL}{\pi EI}\right) \bar{x} = \frac{P}{EI} \int_0^{L/2} x \sin \frac{\pi}{L} x \, dx \ ,$$

$$\frac{L}{\pi} \bar{x} = \int_0^{L/2} x \sin \frac{\pi}{L} x \, dx$$

Integrating this simple expression and solving for x we obtain:

$$\bar{x} = L/\pi$$

Taking moments about point (O) of the M/EI diagram between O and C about O:

$$y_O = 1 = \frac{PL}{\pi EI} \cdot \frac{L}{\pi} = \frac{PL^2}{\pi^2 EI} \quad \text{hence,} \quad P = \frac{\pi^2 EI}{L^2}$$

which is the Euler equation, and thus the assumed sine curve was the proper one for the deflected elastic curve of the column.

Suppose that the elastic curve of deflected column had been assumed as a parabola with unit

deflection at midpoint. Fig. B1.5 shows the M/EI diagram.

The area of one half the diagram = $\frac{1}{2}\left(\frac{2}{3} L \times \frac{P}{EI}\right) = \frac{PL}{3EI}$

Taking moments about O of the area between O and C;

$$y_o = 1 = \frac{PL}{3EI} \cdot \frac{5}{16} L = \frac{5PL^3}{48EI} \quad \text{hence,}$$

$P = \frac{48EI}{5L^2} = \frac{9.6\ EI}{L^2}$, which compares with $P = 9.9EI/L^2$ of the Euler equation or an error of 3 percent.

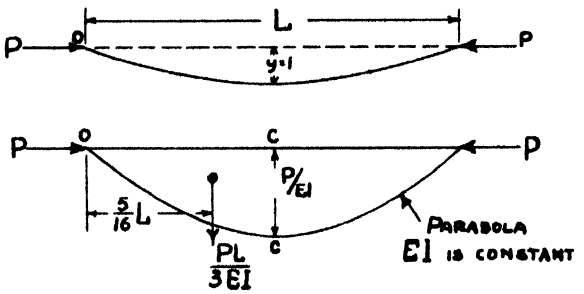


Fig. B1-5

This general method of attach is useful in solving columns with variable moment of inertia and variable E. That is, the shape of the deflected column curve is guessed, which gives a definite M/EI diagram, and if the resulting elastic curve checks the assumed one the problem is solved. Thus problems which are too complicated for strictly mathematical approach can be solved readily by this method although the procedure involves considerable arithmetic.

B1.3 Long and Short Columns. End Conditions.

Tests show that for column stresses below the proportional limit of the material, the column strength can be accurately calculated by the Euler equation. However,when the column stresses begin to exceed the proportional limit the Euler equation gives a column strength greater than that actually given by tests. The reason for this fact is because the stiffness of the material changes above the proportional limit, that is, E is less and is not constant. It is customary to call columns which fall in the Euler range long columns and those columns which do not follow the Euler curve as short columns. Empirical curves are then fitted to the test data and we obtain the many short column equations such as Johnson's parabolic equation and the straight line column equations. The student should refer to Fig. C2.2 of chapter C2 for a comparison of these curves. Chapter C2 gives information regarding the practical design of columns.

End Conditions

In the Euler equation the distance L refers to the free length. Any degree of end restraint effects only the free length. The degree of restraint is denoted by the letter C called the end fixity coefficient. Thus Eulers equation can be written,

$$P = \frac{C \pi^2 EI}{L^2}$$

For a column pinned at both ends, C = 1, hence $P = \pi^2 EI/L^2$.

For a column fixed at both ends, C = 4, hence $P = 4 \pi^2 EI/L^2$

For a column pinned at one end and fixed at the other C = 2.25, hence, $P = 2.25 \pi^2 EI/L^2$

For a column fixed at one end and free at other, C = 1/4 hence $P = .25 \pi^2 EI/L^2$

B1.4 Use of Euler's Equation for Stresses Above The Proportional Limit. Double Modulus and Tangent Modulus Theories.

When the stress in a column exceeds the proportional limit, E is not constant but varies with the stress, thus Eulers equation will only hold for the entire range of stress if an effective modulus E_e is used. Thus to make Eulers equation general it should be written.

$$P = C \pi^2 E_e I/L^2$$

There are two well known theories for determining a value for the effective modulus E_e, namely, the "Double Modulus" and the "Tangent Modulus" theories.

Double Modulus Theory

When the column stress exceeds the proportional limit and the column reaches its critical load it starts to bend, causing the fibers to stretch on one side and shorten on the other which in turn subtract and add to the direct column stresses. Since the modulus E varies with the stress above the proportional limit, we have a varying modulus on the column section due to this bending. An effective $\bar{E}$ to use for this condition is given by Engesser (Ref. 1 and 2) and is expressed as follows:

Rectangular Section	For I- section
$\bar{E} = \frac{4EE'}{(\sqrt{E} + \sqrt{E'})^2}$	$\bar{E} = \frac{2EE'}{E + E'}$

$\bar{E}$ is the effective or reduced modulus of elasticity

E' = tangent modulus of elasticity

E = modulus of elasticity (below proportional limit. Using this value of effective $\bar{E}$, Euler's equation can be used for columns throughout the stress-strain range, or

$$P = \pi^2 \bar{E}I/L^2$$

Tangent Modulus Theory

Engesser (Reg. 1 and 2) originally suggested that the strength of columns stressed above

the proportional limit could be closely estimated by substituting the tangent modulus E' for the initial modulus E of the material, or

$$P = c\pi^2 E' I/L^2 \quad \text{- - - - - - - - - - - - - -(2)}$$

which may be written in terms of area and radius of gyration as

$$\frac{P}{A} = \frac{c\pi^2 E'}{(L/\rho)^2} \quad \text{= = - - - - - - - - - - - - - -(3)}$$

For convenience in plotting this equation, it may be written,

$$L/\rho = \pi\sqrt{\frac{cE'}{P/A}}$$

The tangent modulus theory seems to check actual test results better than the double modulus theory which should be more correct if columns were perfect specimens.

Therefore if the stress strain curve of the material is known, the column strength throughout the range of stresses can be closely calculated by the tangent modulus theory. Stress strain curves of various airplane structural materials are given in chapter C1. Figs. B1.6, B1.7 and B1.8 taken from technical paper No. 1 of the Aluminum Research Laboratories give comparison of actual column strengths as determined by tests with the calculated strengths using the double modulus and tangent modulus theories. This report gives many other comparison curves all of which show a close agreement of the actual strength with that computed by the tangent modulus method.

Fig. B1.9 shows a further comparison for an I section of 24ST aluminum, as given in NACA report No. 656 (Ref. 3).

Thus for a column section for which there are no test data, the column strength curve can be calculated by the tangent modulus method and then only a couple of tests need be made to substitute the calculated curve in the region where column stresses are above the proportional limit of the material.

B1.5 Column Curves of Sections with Stable Cross Sections.

To obtain a complete picture of the column strength of a particular section from short to long lengths, the best way of course is to make a series of accurate tests covering the complete range of column lengths. A curve of the plotted results will show the true column strength regardless whether the failure is due to bending, twisting or local crippling. For many sections such as round tubes, streamline tubes etc., complete test information has been obtained. In the stress range above the proportional limit of the material the test results do not follow the Euler column formula with constant E and thus it has been conventional procedure to fit an empirical curve to the test data in the stress region above the proportional limit, which has given rise to the various straight line and parabolic short column formulas. (See chapter C2). The mechanical properties of materials are constantly being improved and new materials are being rapidly developed for which there is practically no column test data available. The column bending strength as calculated by the modified Euler formula using the tangent modulus is very useful in studying the column bending strength for new materials. It is always best to check such calculated curves by a couple of tests for column lengths where stresses are above the proportional limit of the material.

Figs. B1.10, to B1.11 show the bending column curves for stable cross sections for aluminum alloy and stainless steel materials. These curves do not show the local strength or the twisting strength for column sections which are unstable. The use of these column curves will be referred to in chapters B5 and B6. Table B1.1 illustrates calculations for obtaining these column curves.

Table B1.1

Calculations for determining column curve for 24 ST sheet material.

(For columns with stable cross-sections)

$f_c = \frac{P}{A}$	*E' x 10^6 (psi)	$L/\rho = \pi\sqrt{E'/f_c}$	**$K_1 K f_c$
5000	10.5	144	4900
10000	10.5	102	9800
20000	10.5	72	19300
27500	10.5	61.3	26000
30000	10	57.4	28300
31000	9.15	54.0	29400
32500	7.75	48.5	30600
35000	5.62	39.8	32900
37500	4.40	34.0	35000
40000	3.30	28.6	37500
42500	2.55	24.4	39600
45000	1.90	20.4	42200
47500	1.60	18.25	44600
50000	1.35	16.30	46500
55000	0.90	12.7	51500

* The tangent modulus for the column stresses in the first column are taken from the stress-modulus curves of Fig. C1.17 of chapter C1.

** The stress-modulus curves are for a material which has a yield strength of 43000 psi and E of 10.5 x 10^6 psi. These values are corrected to the standard values of 40000 and 10,300,000 by use of the material correction factors K_1 and K (as explained in ANC-5) L/ρ values are then plotted against these corrected stresses.

B1.6 Johnson-Euler Column Formula

As discussed in Art. B1.0 many columns fail due to local buckling or crippling. The question of local buckling of column sections is considered in detail in Chapter B5. The Johnson-Euler column formula (Eq. 5) has been widely used to cover both bending and local failure of columns. In this equation f is considered as the local crushing or crippling stress. For design convenience this equation has been plotted for aluminum alloy and stainless steel as shown in Figs. B1.12 and B1.13. The use of these curves is discussed in Chapters B5 and B6.

$$F_c = P/A = f - \frac{f^2 (L/\rho)^2}{4\,C\,\pi^2\,E} \quad \text{- - - - - - - - -} \quad (5)$$

Fig. B1-6

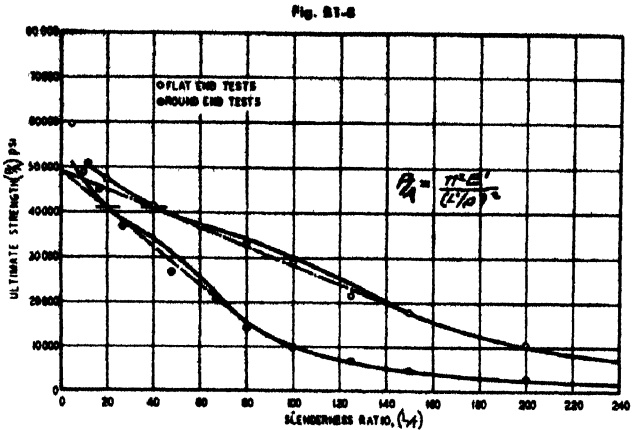
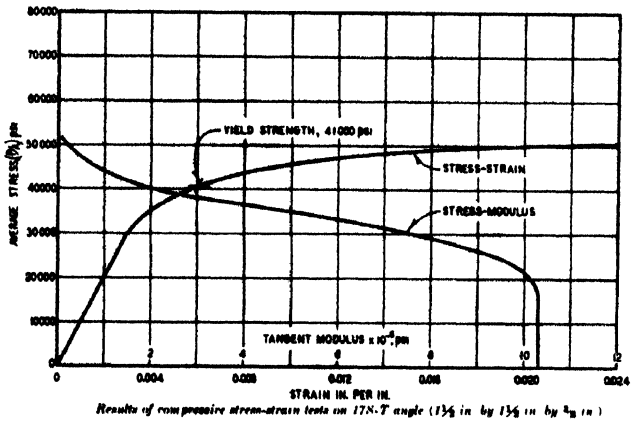
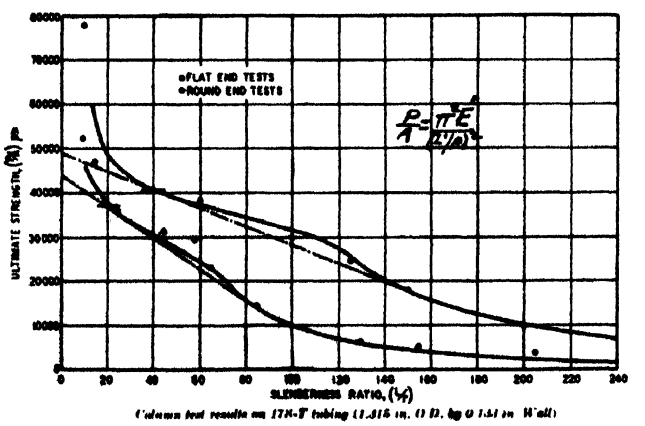


Figure 6. Column test results on 17S-T angle (1½ in. by 1½ in. by ⅛ in.)



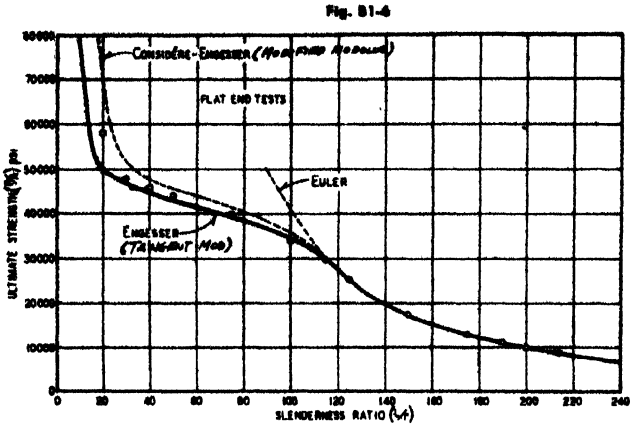
Results of compressive stress-strain tests on 17S-T angle (1½ in. by 1½ in. by ⅛ in.)

Fig. B1-7

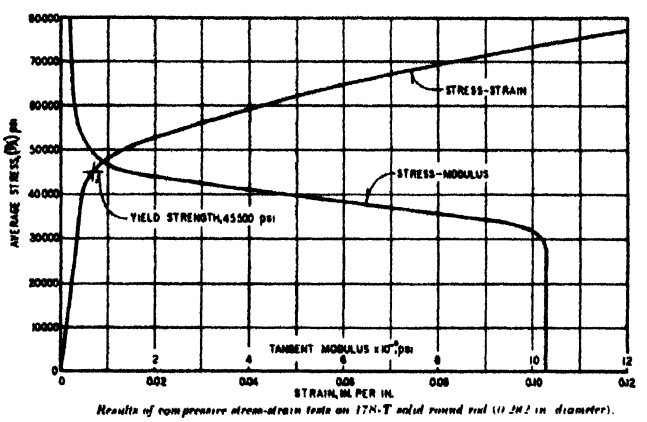


Column test results on 17S-T tubing (1.315 in. O.D. by 0.151 in. Wall)

Fig. B1-6

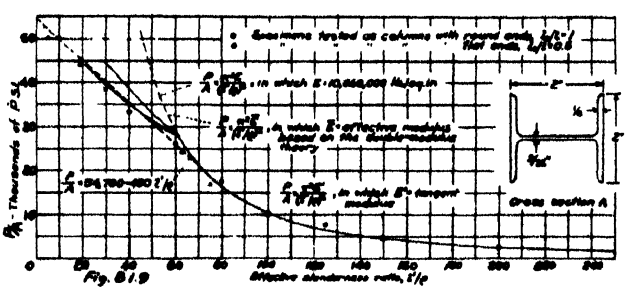


Column test results on 17S-T solid round rod (0.282 in. diameter).

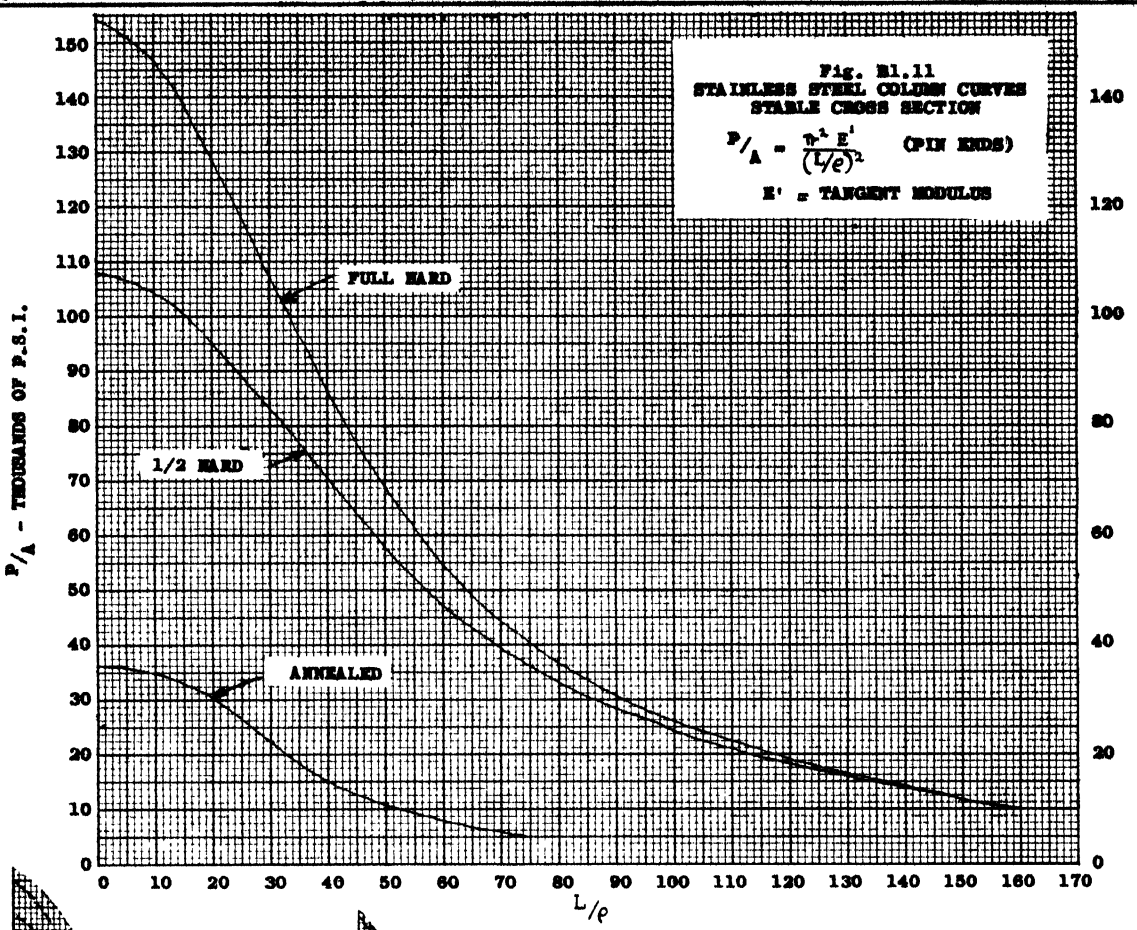


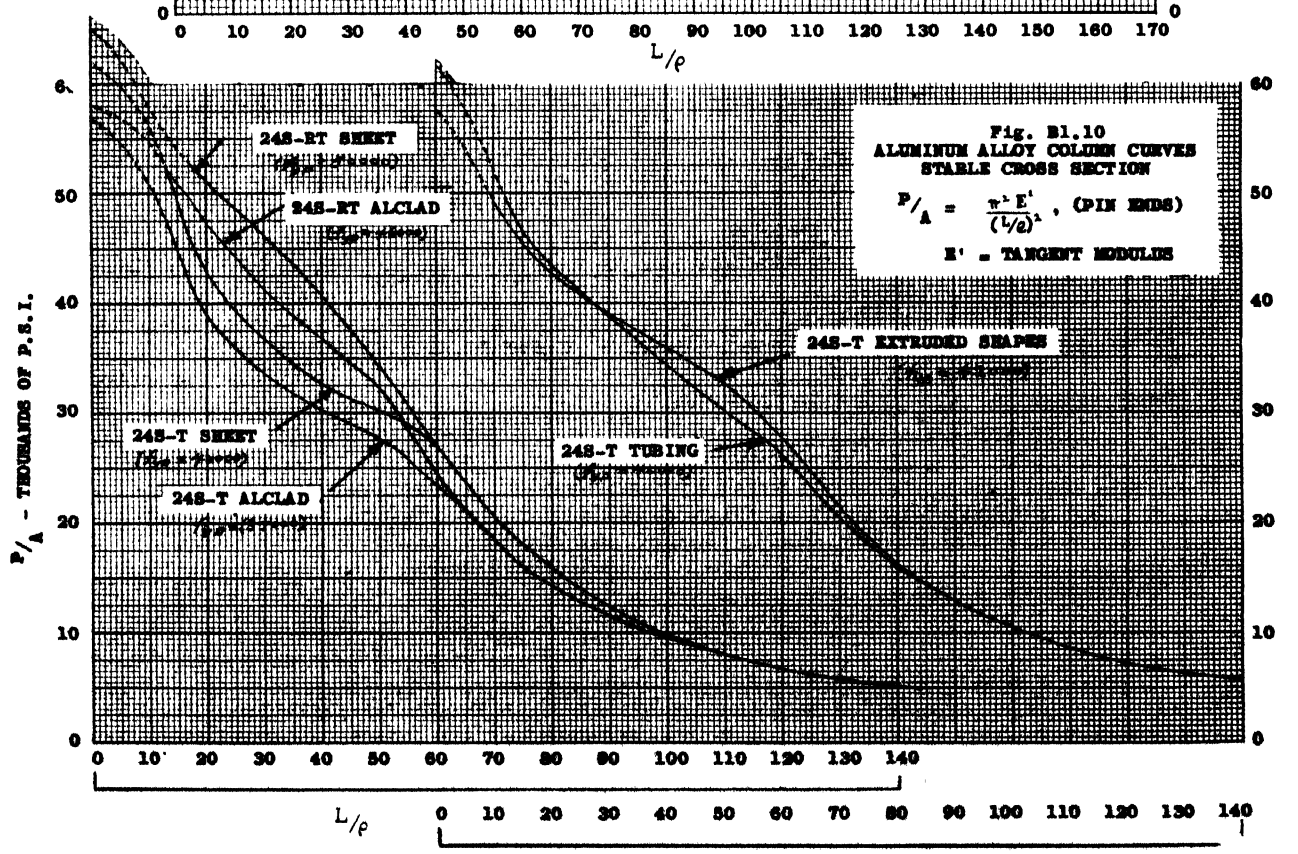
Results of compressive stress-strain tests on 17S-T solid round rod (0.282 in. diameter).

Fig. B1.9



Figs. 6, 7 & 8 from Technical Paper #1, of the Aluminum Research Laboratories.
Fig. 9 from NACA Tech., report #656.


Fig. B1.11
STAINLESS STEEL COLUMN CURVES
STABLE CROSS SECTION
$P/A = \frac{\pi^2 E'}{(L/\rho)^2}$ (PIN ENDS)
E' = TANGENT MODULUS
FULL HARD
1/2 HARD
ANNEALED
P/A - THOUSANDS OF P.S.I.
L/ρ


Fig. B1.10
ALUMINUM ALLOY COLUMN CURVES
STABLE CROSS SECTION
$P/A = \frac{\pi^2 E'}{(L/\rho)^2}$, (PIN ENDS)
E' = TANGENT MODULUS
24S-RT SHEET
24S-RT ALCLAD
24S-T EXTRUDED SHAPES
24S-T SHEET
24S-T TUBING
24S-T ALCLAD
P/A - THOUSANDS OF P.S.I.
L/ρ

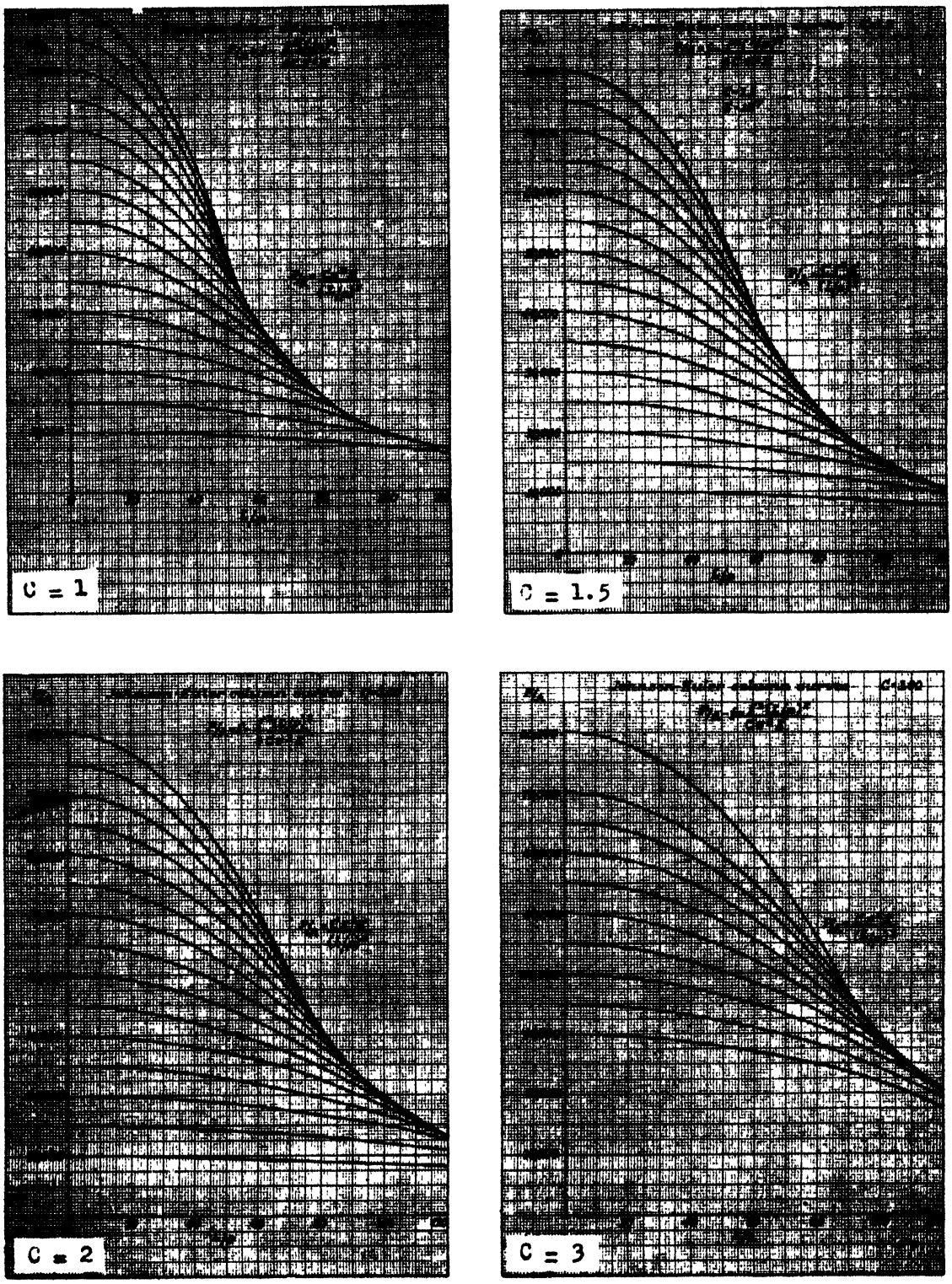


FIG. B1.12 (E = 10,000,000 psi.) (FROM REF. 5)

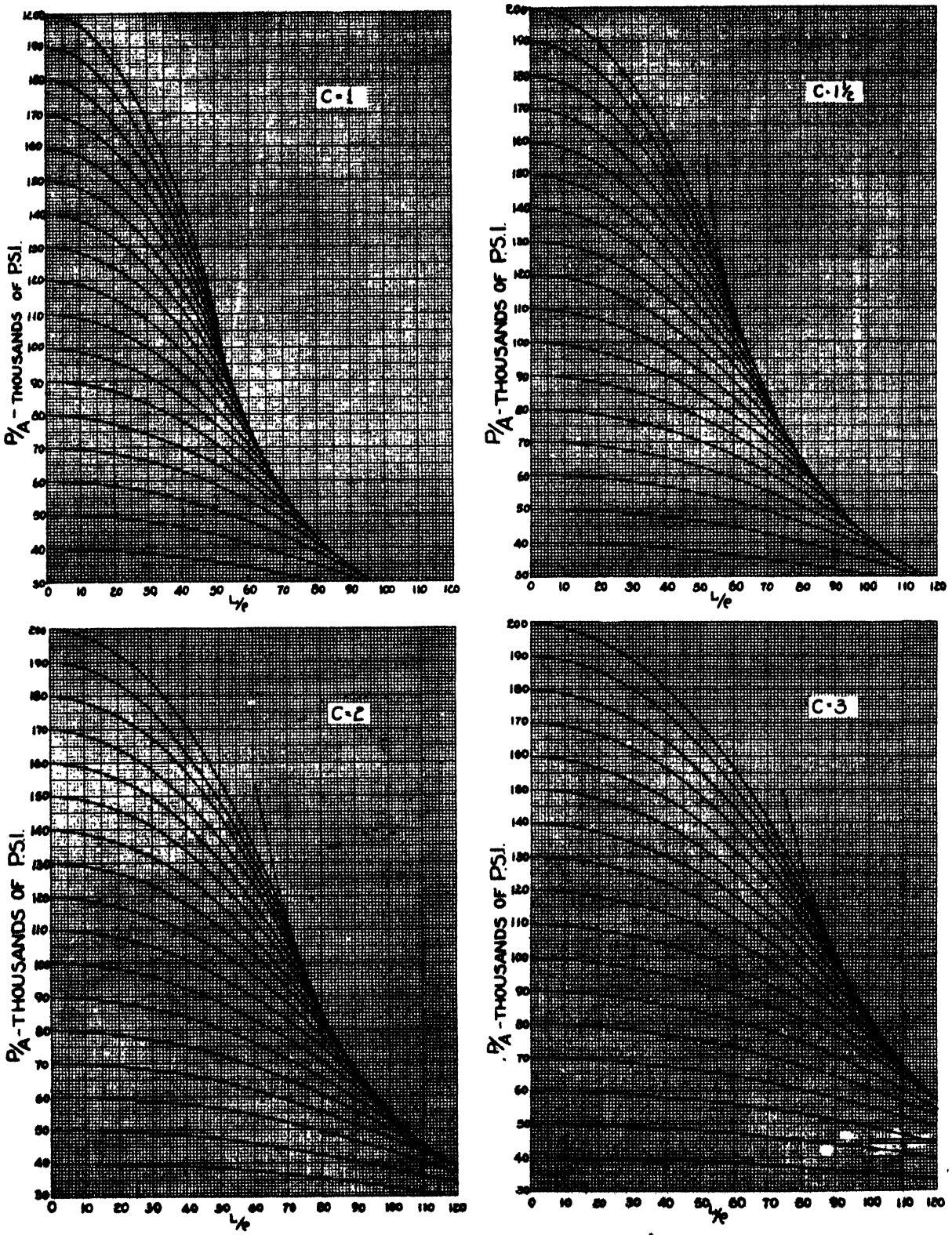


FIG B1.13 JOHNSON-EULER COLUMN CURVES: $P/A = f - \frac{f^2(L/\rho)^2}{4C\pi^2E}$ & $P/A = \frac{C\pi^2E}{(L/\rho)^2}$

E = 28,000,000

B1.7 Torsional Instability of Columns.

The calculation of the torsional instability of a column is more involved as compared to bending instability. Lundquist and Fligg (Ref. 4) give the general equation for the critical failing stress of a concentrically loaded column which is subject to a twisting failure as follows:

$$f_{crit.} = \frac{GJ}{I_p} + \frac{C_{BT}}{I_p} \times \frac{\pi^2 E}{L_o^2}$$

where GJ = torsional rigidity of the section

E = Young's modulus

I_p = polar moment of inertia of the cross-section

L_o = effective length of column

C_{BT} = torsion-bending constant, which is dependent upon the location of the axis of rotation and the dimensions of the cross-section.

The main difficulty in solving the above equation is the determination of the term C_{BT}. For columns acting alone, that is, not attached to sheet, twisting failure will occur by rotation of the column sections about the shear center of the cross-section. If the column is attached to a sheet, the center of rotation will move due to the restraint offered by the sheet.

A rather complete discussion of this problem of column twisting is given in (Ref. 4) and the student should refer to it.

For closed sections as columns, the torsional instability is not the critical factor. For open sections, particularly the angle or bulb angle section, the critical strength as a column may be due to torsional instability, particularly when attached to a sheet which tends to cause free leg to roll or weave.

As pointed out in (Ref. 5), the cross-section of a loaded column usually suffers a distortion, which may cause a shift in the axis of resistance of the member from the axis of loading. This shift causes the loading to be eccentric which produces a moment on the column which causes the member to deflect with the result that a shear is produced on the affected sections whose magnitude is P sin i, where i represents the slope of the bent section and P the axial load on the column. Such shear stresses produce forces on the elements of an open section which may cause it to rotate as a whole or may increase the bending of a deflected element.

Figure B1.14 illustrates the direction of shear forces acting on the sections of various open sections when the axial load is applied eccentrically. In Figure a, bending subjects one leg to compression and the other to tension, which tends to twist section as a whole. When the eccentricity is along the other axis, the tendency is to fail by bending the outstanding portions inward or outward due to the shear forces, as shown in Figures b to f, the direction depending on whether the point of loading is one side or the other of the centroid and on whether such flanges are bent inward or outward. Sketches (e) and (f) do not present a true picture of the acting shear forces since they are unsymmetrical sections and the axes considered are not principal axes, thus section would tend to deflect about both axes.

PROBLEMS

(1) Plot a column curve for 24 ST extruded material over 1/4 inch thick. Use tangent-modulus values from curve of Fig. C1.7 in Chapter C1.

(2) Compare the curve obtained in problem (1) with that obtained by using a reduced modulus E as given by the equations for E in Art. B1.4

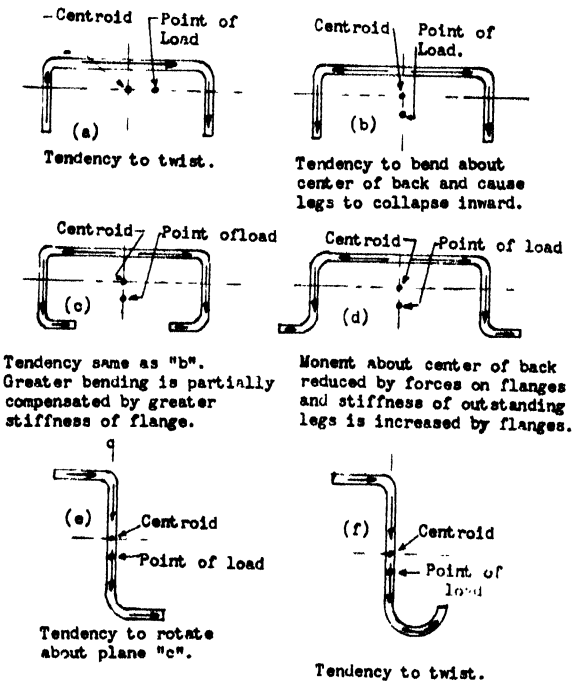


Fig. B1-14

References:

(1) Templin, Sturm, Hartman, and Holt, "Column Strength of Various Aluminum Alloys", Tech. Paper No. 1, by Aluminum Research Laboratories.

(2) Timoshenko, "Theory of Elastic Stability" by McGraw-Hill Book Company.

(3) Osgood, W. R., "The Double Modulus Theory", Civil Engineering, March 1935.

(4) Lundquist and Fligg, "A Theory For Primary Failure of Centrally Loaded Columns", N.A.C.A. Tech. Report #852.

(5) Progress Report on Methods of Analysis Applicable To Monocoque Aircraft Structures", Air Corps Tech. Report No. 4313 (1940).

(6) Osgood, W. R., "Column Curves and Stress-Strain Diagrams", Research Paper No. 492, Bureau of Standards Jour. Res. Vol. 9, October 1932, p. 571-582.

(7) Timoshenko, S. "Strength of Materials", Part II, D. Van Nostrand Company (1930).

(8) Templin and Sturm "Some Stress-Strain Studies of Metals", Journ. of Aeronautical Sciences, March 1940.

(9) Franks, R. and W. O. Binder, "Cold-Rolled Stainless Steels", Aero Digest, July 1942.

(10) Franks, R. and W. O. Binder, "Tension and Compression Stress-Strain Characteristics of Cold-Rolled Austenitic Chromium-Nickel Stainless Steels," Journ. of Aeronautical Sciences, Sept. 1942.

CHAPTER B2
BUCKLING STRESSES FOR FLAT SHEET

B2.1 Introduction.

In the major structural units, wing, tail and body of the modern metal covered airplane the flat or curved sheet is an important element. The structural designer requires information as to what stresses will cause a sheet to buckle at what stress will buckles become permanent and finally what ultimate load will the sheet carry. This chapter discusses the buckling strength of flat sheet. The following chapters discuss the other problems.

B2.2 Buckling Compressive Strength of a Flat Isotropic Sheet

Eulers equation for the critical column buckling load is $P_{cr} = \pi^2 EI/L^2$. In this equation the term EI is referred to as the flexural rigidity factor. Fig. B2.1a shows a beam in bending. The shortening of the upper fibers due to bending stresses produces transverse strains which tend to widen the beam, whereas the lengthening of the fibers on the lower side produces transverse strains which tend to decrease the beam width according to Poisson's ratio for the particular material. Fib. B2.1b shows the distorted cross section. The beam theory as generally used assumes this transverse distortion of the beam section can take place without restraint.

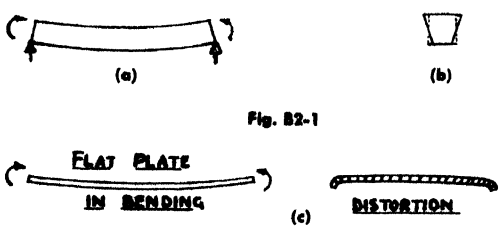


Fig. B2-1

Experiments on flat plates (width large compared to thickness) show that distortion of the cross section takes place only near the edges (Fig. B2.1c) (Ref. (1) and (5)). It can be shown that if the plate remains flat, (Ref. (1)) the flexural rigidity factor EI is increased by the term $1/(1-\mu^2)$, where μ is Poissons ratio, or the flexural rigidity factor becomes $EI/(1-\mu^2)$.

Thus Eulers equation for flat sheet can be written,

$$P_{cr} = \frac{\pi^2 EI}{(1-\mu^2) L^2} \quad \text{----------(1)}$$

or in terms of stress

$$F_{cr} = \frac{\pi^2 E}{(1-\mu^2)(L/\rho)^2}, \text{for a plate thickness}$$

t, $\rho = t/\sqrt{12}$, hence

$$F_{cr} = \frac{\pi^2}{12(1-\mu^2)} E \left(\frac{t}{L}\right)^2 \quad \text{----------(2)}$$

Equation (2) is for a plate simply supported at the loaded edges and free on the two sides (Fig. B2.2). Plates in practical structures very seldom occur with free side edges, the general condition usually ranging somewhere between freely supported and fixed edges. If the side edges in the direction of the loading are restrained against buckling, the plate as a whole will buckle or bend in two directions under the critical end load since the width of the plate as a whole will be considerably strengthened in its ability to carry a compressive load in one direction.

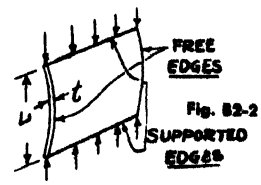


Fig. B2-2

The ratio of the length of the plate to its width when the sides are restrained influences the buckling strength. Thus in Fig. B2.3 if the side edges of the plate are freely supported are prevented from bowing normal to the paper and the rectangular plate tends to act as a series of square plates with buckles in each square, since it is prevented from buckling in a single long wave. Thus in equation (2) we can replace L by b the plate width.

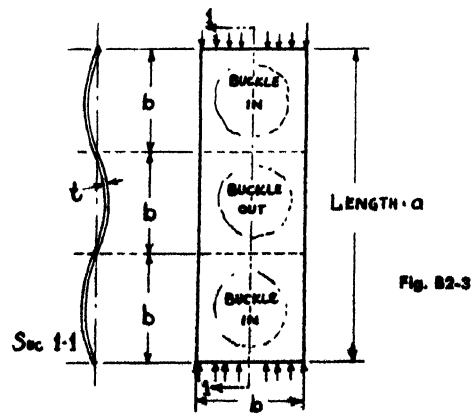
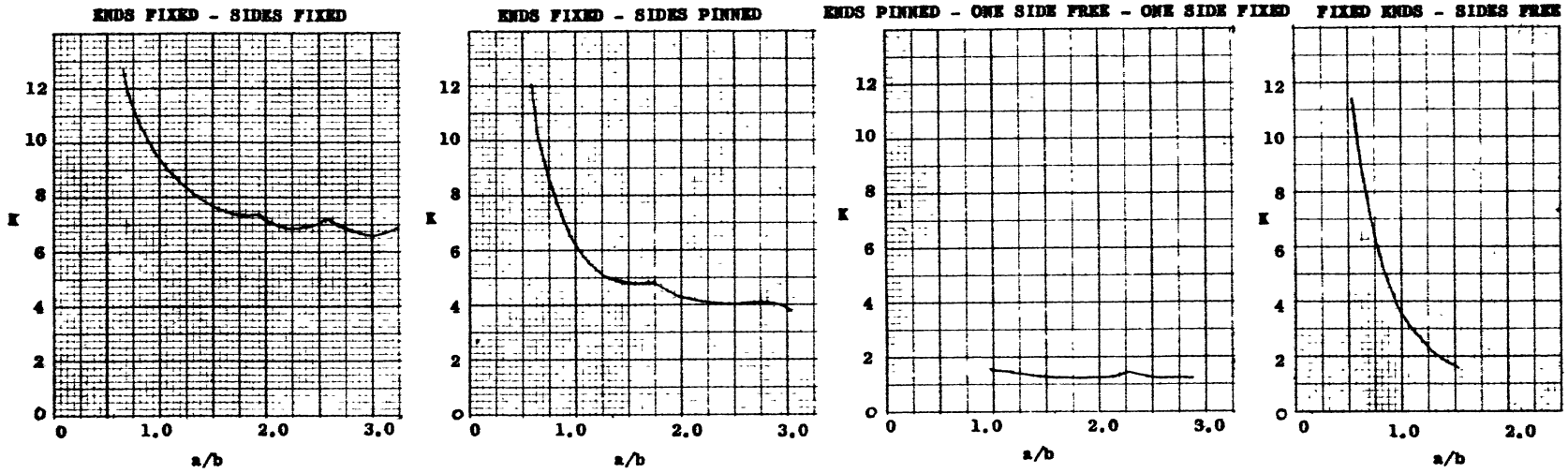
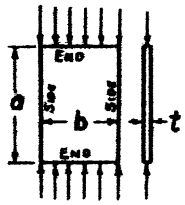


Fig. B2-3

Hence the general expression for critical buckling compressive stress can be written

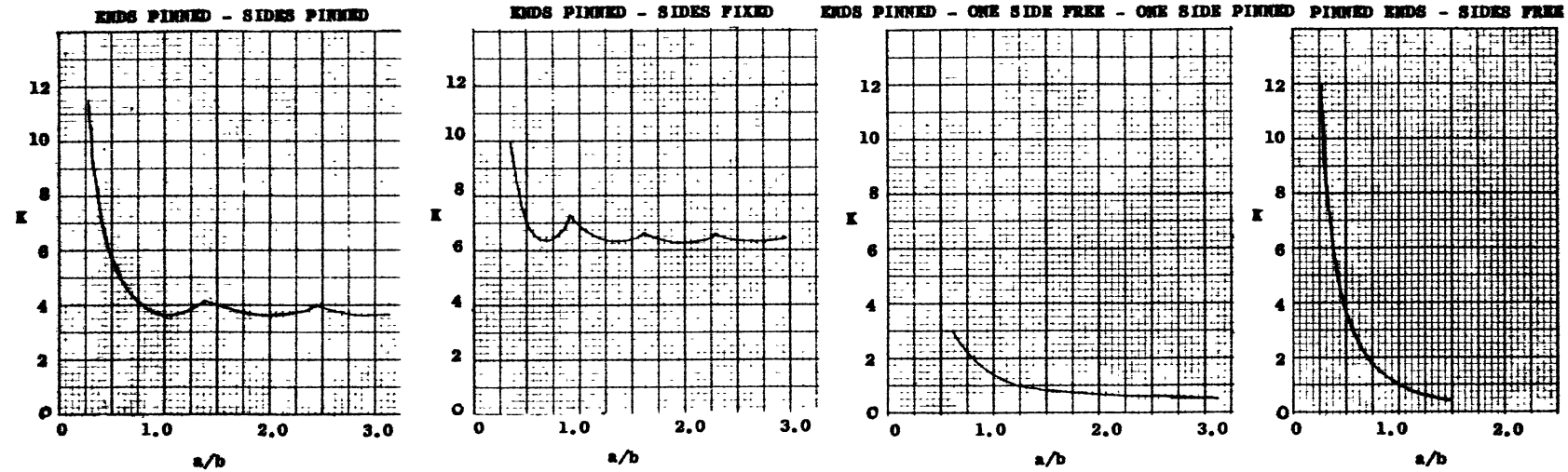
$$f_{cr} = K E \left(\frac{t}{b}\right)^2 \quad \text{----------(3)}$$





$$F_{ce} = KE\left(\frac{t}{b}\right)^2$$

Fig. B2-4



where K is a function of a/b and the degree of edge restraint.

Fig. B2.4 shows the plot of the factor K for various conditions of edge restraint versus values of the aspect ratio of the sheet a/b. The peaks in the various curves indicate a change in the number of buckles.

Equation (3) is often written,

$$f_{cr} = \frac{k\,\pi^2\,E t^2}{12\,(1-\mu^2)b^2} \quad \text{- - - - - - - - - - - - -(3a)}$$

when the term k does not include the values $\pi^2/12(1-\mu^2)$

In practical airplane structures with metal covering, the edge restraint on the sheet panels depends on the bending and torsional rigidity of the stiffeners which break the sheet up into panels. The problem of determining this true edge restraint has been studied by several persons. (Ref. 6 and 7).

In general for light stringers and formers it is usually assumed that all four edges of the sheet are simply supported.

B2.3 Buckling Shear Strength of Flat Isotropic Sheet.

In chapter A4 Art. A4.3, it was shown that an element of plate under a pure shear loading produces both tensile and compressive stresses on the plate element which act at an angle of 45 degrees from the direction of the shear stress and that the value of these tensile and compressive stresses along diagonal paths are equal to the intensity of the shear stresses.

Thus buckling of a plate subjected to a pure shearing load is due to the induced compressive stresses. The diagonal tensile stresses tend to restrain the buckles or folds due to the compressive stresses at right angles with the tensile stresses.

The general equation for the buckling shear stress thus takes the same form as that for sheet subjected to edge compression. (Ref. 1)

$$fs_{cr} = K\,\frac{\pi^2\,E}{12\,(1-\mu^2)}\left(\frac{t}{b}\right)^2 \quad \text{- - - - - - - - -(4)}$$

where,

Fs_{cr} = intensity of the uniformly distributed shear stress in psi at the point of initial buckling

μ = Poissons ratio, usually taken at .3 for metals.

b = Short dimension of sheet in inches.

t = Sheet thickness.

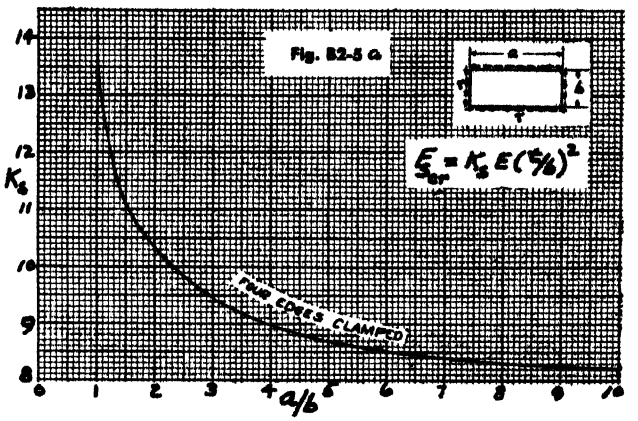
K = A factor depending on degree of restraint of sheet edges and also on the sheet aspect ratio a/b. where (a) is the long dimension of the sheet.

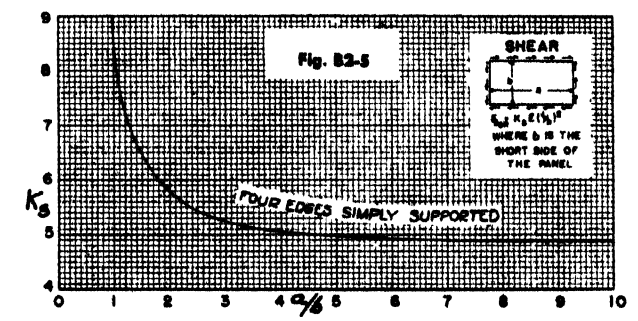
Equation (4) is usually simplified as follows:-

$$Fs_{cr} = K_s\,E\,(t/b)^2 \quad \text{- - - - - - - - - - - - -(4a)}$$

where $K_s = \frac{\pi^2 K}{12\,(1-\mu^2)}$

Figs. B2.5 and B2.5a give a plot of K_s values versus a/b values.



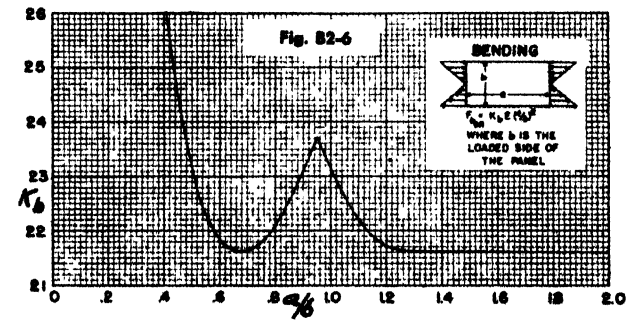


B2.4 Bending Buckling Strength of Flat Isotropic Sheet.

The buckling bending strength of flat sheet has also been theoretically determined. (Ref. 1). The critical buckling stress can be written,

$$F_{b(cr)} = K_b\,E\,(t/b^2 \quad \text{- - - - - - - - - - -(5)}$$

Fig. B2.6 gives a curve for the value K_b for a sheet simply supported on all four edges.



B2.5 Buckling Strength of Flat Isotropic Sheet Under Combined Loadings.

The following relations express the conditions of buckling under combined loading according to Ref. 8.

Compression and Bending

$$R_b^{1.75} + R_c = 1 \quad \text{----------(6)}$$

Compression and Shear

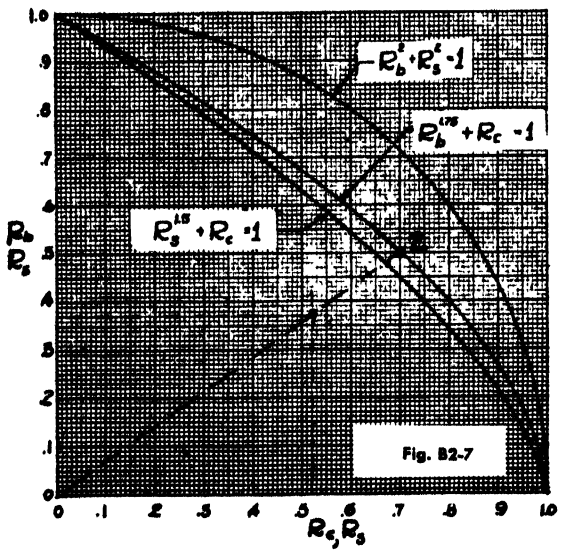
$$R_s^{1.5} + R_c = 1 \quad \text{----------(7)}$$

Bending and Shear

$$R_b^{2} + R_s^{2} = 1 \quad \text{----------(8)}$$

where $R_c = \frac{f_c}{F_{c(cr)}}$, $R_b = \frac{f_b}{F_{b(cr)}}$, $R_s = \frac{f_s}{F_{s(cr)}}$

Fig. B2.7 shows a plot of these interaction equations. (See chapter C3 for general discussion of theory of stress ratio and interaction curves).



B2.6 Margins of Safety For Combined Two Load Systems.

From (Ref. 8), when only two applied stress systems are involved and when these remain in constant proportion, the margin of safety may be determined from Fig. B2.7 by the following procedure:-

Consider the case of combined bending and compression, the interaction curve being defined by the equation

$$R_b^{1.75} + R_c = 1$$

(1) From the computed applied stress compute values of stress ratios R_b and R_c. Assume they are $R_b = .37$ and $R_c = .52$. Point (1) on Fig. B2.7 represent the intersection of these values.

(2) Draw straight line from origin (0) through point (1) and extend line until it intersects the proper interaction curve at point (2).

(3) Read the allowable R_{b_a} and R_{c_a}, the projected ordinate and obscissa values of point (2).

(4) The factor of utilization or strength ratio is obtained as the ratio of the applied to the allowable value of either stress ratio as follows:-

$$U = \frac{R_b}{R_{b_a}} = \frac{R_c}{R_{c_a}} \quad \text{----------(9)}$$

For our example,

$$U = \frac{.37}{.5} = \frac{.52}{.7} = .74$$

(5) The true margin of safety then can be computed from the following equation:-

$$M.S. = \frac{1}{U} - 1 \quad \text{----------(10)}$$

For our example,

$$M.S. = \frac{1}{.74} - 1 = .35$$

For the stress interaction relationship represented by the equation $R_b^2 + R_s^2 = 1$, the margin of safety can be expressed as follows:-

$$M.S. = \frac{1}{\sqrt{R_b^2 + R_s^2}} - 1 \quad \text{----------(11)}$$

B2.7 Combined Compression, Shear and Bending Loading.

From Ref. 8, the conditions for buckling are represented by the interaction curves of Fig. B2.8. This figure tells whether the sheet will buckle or not but will not give the margin of safety. Given the ratios R_c, R_s and R_b:- if the value of the R_c curve defined by the given value of R_b and R_s is greater numerically, than the given value of R_c, then the panel will buckle.

The margin of safety of elastically buckled flat panels may be determined from Fig. B2.9. The dashed lines indicate a typical application where $R_c = .161$, $R_s = .23$, and $R_b = .38$. Point 1 is first determined for the specific value of R_s and R_b. The dashed diagonal line from the origin 0 through point 1, intersecting the related R_c/R_s curve at point 2, yields the allowable shear and bending stresses for the desired margin of safety calculations. (Note when R_c is less than R_s use the right half of the figure; in other cases use the left half). (Ref. 8)

B2.8 Problems.

(1) A 24ST sheet 3" x 9" x .051" has the 3" sides simply supported and the 9" sides free. Determine the buckling load if the compressive load is applied normal to the 3" sides.

(2) In problem (1) if all edges were simply supported what would be the buckling load.

(3) In problem (1) if the 9" sides were fixed and the 3" sides freely supported or pinned

what would be the buckling load.

(4) Fig. B2.10 shows a 4" x 8" x .032 24ST sheet loaded by a test frame in pure shear. The frame provides groove supports thus giving a simply supported sheet edge condition. What value of P_1 and P_2 will cause initial buckling of the sheet.

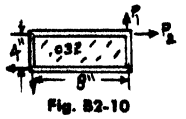


Fig. B2-10

(5) A sheet panel 5" x 12.5" x .051 of 24SRT material has all edges simply supported. The sheet is subjected to combined compression and shear loads which produce stresses as follows:-

f_c = 2400 psi., applied normal to 5" side and f_s = 2800 psi. Will the sheet buckle under the loads. If not what is the margin of safety.

(6) A 24ST sheet 3" x 12" x .040" has all edges simply supported. It is subjected to the following combined stresses:-

f_c = 3000 psi., f_b = 10000 psi., f_s = 8000 psi. The f_c and f_b stresses are normal to the 3" side. What is the M.S. on buckling strength under the given combined stresses?

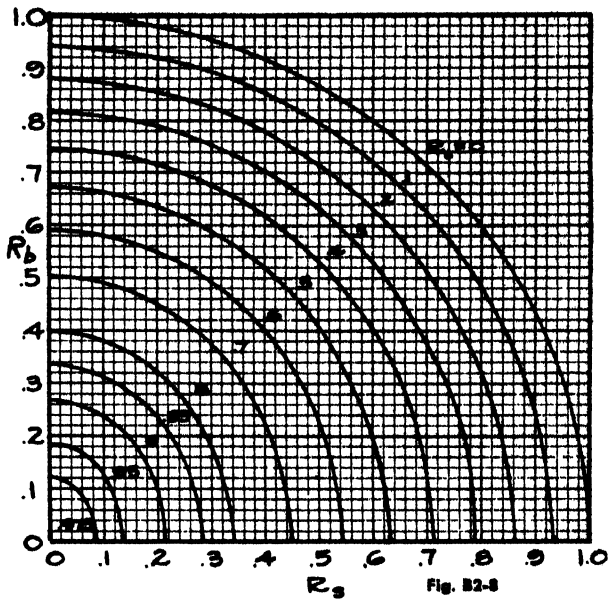


Fig. B2-8

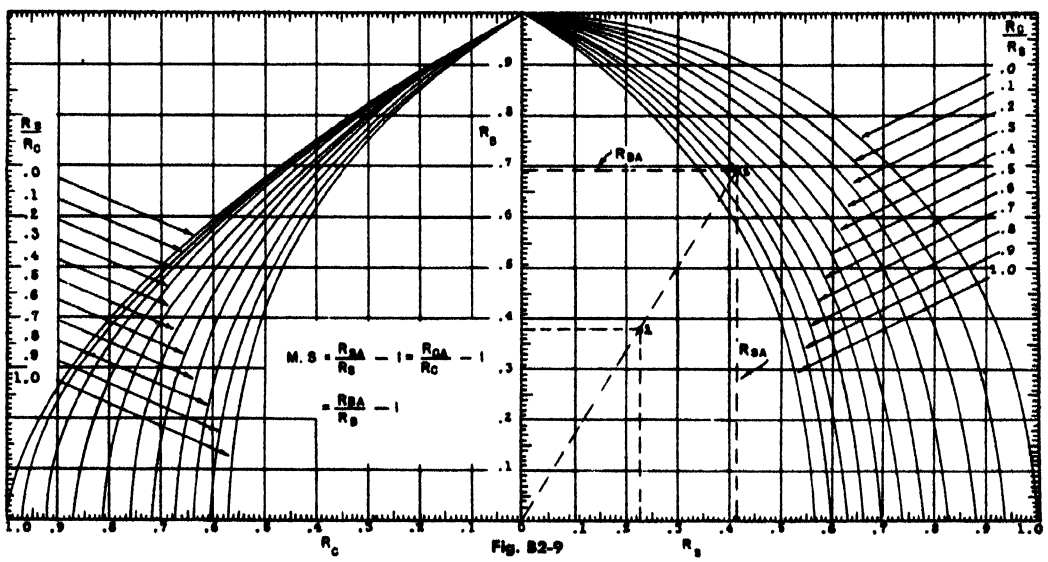


Fig. B2-9

INTERACTION CURVES TO DETERMINE THE MARGIN OF SAFETY IN ELASTICALLY BUCKLED FLAT PANELS.

REFERENCES

1. Timoshenko - "Strength of Materials" Vol. 1 and II.
2. Timoshenko and Lessells, "Applied Elasticity
3. Timoshenko, "Theory of Elastic Stability".
4. Heck and Ebner - " Methods and Formulas for calculating the strength of plate and shell construction as used in airplane design. N.A.C.A., T.M. No. 785
5. Curtiss - Wright Technical Institute Engineering Bulletin No. 1, "Engineering Aspects of Buckling Part I. Flat Plates. Author, Shanley.
6. Dunn, "An Investigation of Sheet-Stiffener Panels Subjected to Compression Loads with Particular Reference to Torsionally Weak Stiffeners". N.A.C.A. Techn. Note No. 752.
7. E. Chwolla. "Dos all Genuine Stabilitats Problem der ge druckten, dench Randwinkel verstarken Platte". In genieur, Vol. V. (1934)
8. ANC-5 Revision of 1942. "Strength of Aircraft Elements".

CHAPTER B3
BUCKLING STRENGTH OF THIN WALLED CYLINDERS AND CURVED PANELS

B3.1 General

The buckling critical stress for thin wall cylinders and large curved thin sheet panels is of considerable importance in airplane structural design since in general tests show that the critical buckling stress is equal or near the ultimate strength. This chapter gives a resume of available theory and experimental data on this subject. Application of the data in this chapter to practical design is given in part C of this book.

B3.2 Buckling Compressive Strength of Thin-Walled Circular Cylinders.

There is considerable experimental data available on the buckling compressive strength of thin-walled cylinders. (Ref. 1 and 2). A resumé of theoretical studies (Ref. 1) arrives at the following general form for the critical buckling stress,

$$f_{c(cr)} = K_c \, E \, t/r \quad \text{- - - - - - - - - - - - -(1)}$$

where,

t = wall thickness in inches
r = cylinder radius in inches
E = Young's modulus for the material
$f_{c(cr)}$ = critical buckling stress (psi)
K_c = a term which is constant for a given buckled wave form.

Experiments to determine the value of K have been made (Ref. 1 and 2) and the results show that K is a function of the r/t ratio of the cylinder, but that it is much less than the theoretical value for large values of r/t and approaching the theoretical value at low values of r/t.

Aluminum Alloy Cylinders

Fig. B3.1 shows the results of tests on aluminum alloy cylinders (Ref. 1). The curve C represents the lower limit of data for the most perfect cylinders. Care should be used in using curve C as a design allowable curve since the data as plotted does not show clearly how the buckling stress varies with the L/r ratio of the cylinder. Equation (2) is recommended as a more general basis for obtaining the allowable compressive buckling stress.

Steel Cylinders

Fig. B3.2 taken from (Ref. 1) shows results on circular cylinders of various materials including steel. Curve C is the same as on Fig. B3.1 for aluminum alloy cylinders. In Fig. B3.2 it is noted that curve C falls above most of the test results on steel cylinders. For preliminary conservative design the author has added curve D, the equation of which is,

$$f_{c(cr)} = \frac{0.09E}{r/t}$$

Empirical equation (2) is recommended as a better design value since it brings in the effect of cylinder length more definitely and has been obtained from a detail study of test data.

Kanenutsu and Nojima Formula

Kanenutsu and Nojima (Ref. 3) proposes the following empirical equation, which they find checks experimental values of the critical buckling compressive stress on brass, dural and steel cylinders for values of r/t between 500 and 3000 and values of L/r between 0.10 and 2.5, where L is the cylinder length.

$$\frac{f_{c(cr)}}{E} = 9\left(\frac{t}{r}\right)^{1.6} + 0.16\left(\frac{t}{L}\right)^{1.3} \quad \text{- - - - - - - -(2)}$$

Donnell's Equation

Donnell developed the following equation for the ultimate strength of circular cylinders in compression.

$$f_{c(ult)} = E\left[\frac{0.6\ t/r - 10^{-7}\ r/t}{1 + 0.004\ \frac{E}{f_{yp}}}\right] \quad \text{- - - - - - - -(2a)}$$

approximately this equation equals,

$$f_{c(ult)} = 0.3\ E\ t/r \quad \text{- - - - - - - - - - - - - -(2b)}$$

Equation (2b) has been widely used to estimate the compressive strength of thin-walled cylinders, however since the L/r ratio does not enter, the equation should be used with caution.

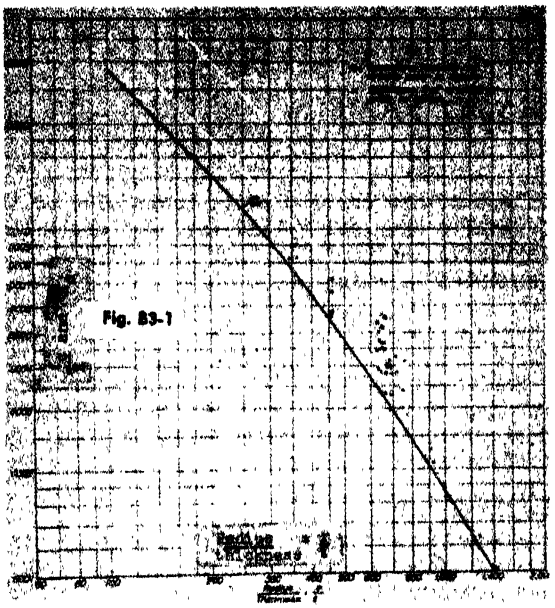
B3.3 Ultimate Compressive Strength of Thin-Walled Circular Cylinders.

Experiments with complete cylinders indicate that the buckling load is practically the same as the ultimate load, since large axial deformations take place suddenly at buckling loads. Thus for design purposes use curve C in Fig. B3.1 or equation (2) or (2b) preferably (2).

B3.4 Bending Buckling Strength of Thin-Walled, Circular Cylinders.

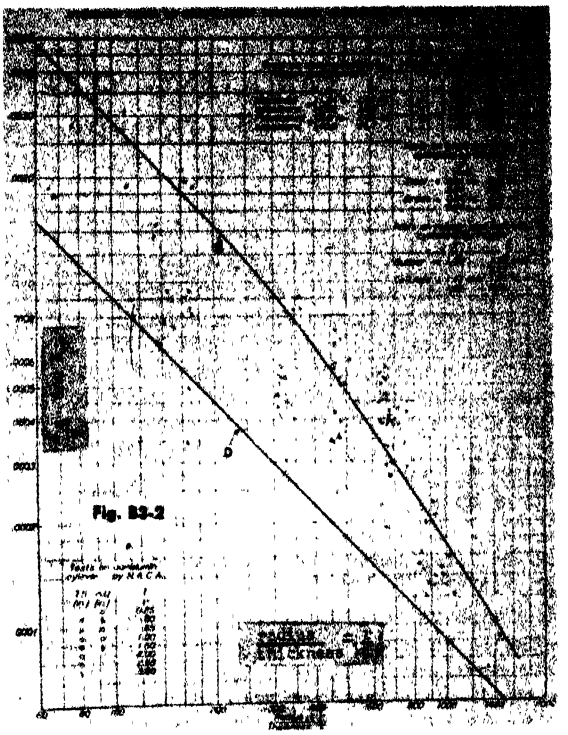
The pure bending stress in a thin-walled circular cylinder up to the point of buckling can be computed by the ordinary beam formula,

$$f_{b(c)} = \frac{Mr}{I}, \text{ where } I = \pi r^3 t$$



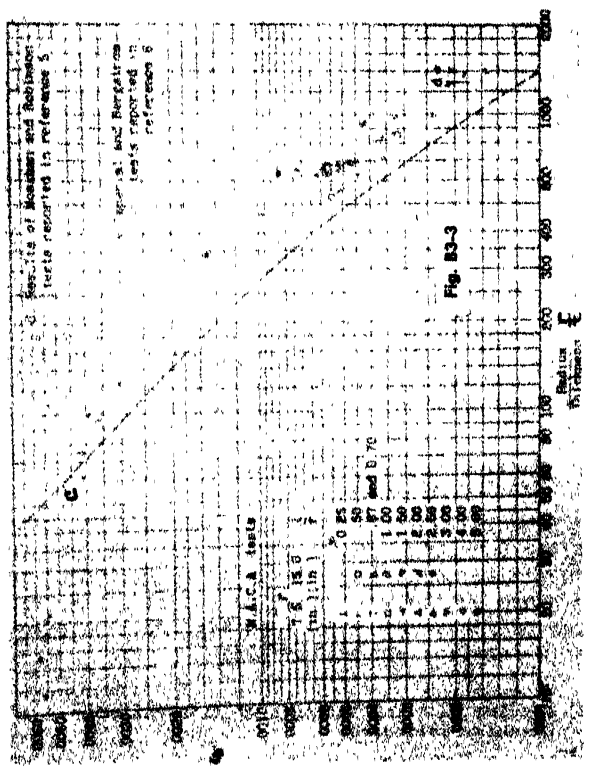
Compressive strength of aluminum alloy circular cylinders

(NACA T.R. 473)



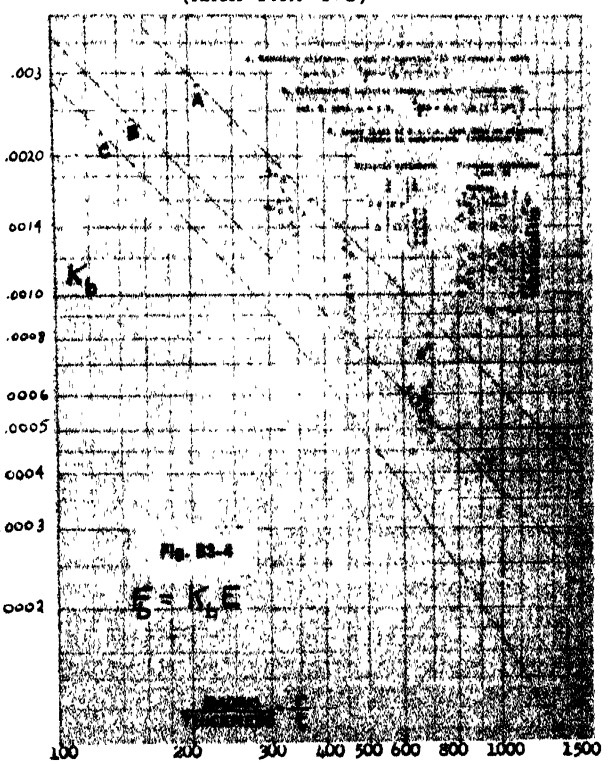
Compressive strength of circular cylinders of various materials.

(NACA T.R. 473)



Results of pure bending tests. Curve C same as in Fig. B3.2

(From NACA T.N. 479)



Pure bending tests on elliptical cylinders as compared to results on circulars cylinders

(NACA T.N. 527)

Experiments (Ref. 4) have shown that the bending modulus of rupture, that is the bending compressive stress at the buckling load can be expressed by an equation of the form

$$F_b = K_b E \quad \text{----------(3)}$$

Except for very short cylinders, the radius and thickness as expressed by the ratio r/t are the only dimensions that need be considered to establish the value of the term K_b. Fig. B3.3 taken from (Ref. 4) gives a resume of experimental values on aluminum alloy cylinders. Curve C can be taken as the allowable design curve for both buckling and ultimate buckling strength.

For r/t values less than 40 use allowable bending stress curves for aluminum alloy round tubes in chapter C3.

Very little experimental data is available on steel cylinders in bending, thus Fig. B3.3 can be used in preliminary studies and designs.

B3.4a Bending Buckling Strength of Thin-Walled Elliptical Cylinders.

Fig. B3.4 taken from (Ref. 5) gives the results from tests on aluminum alloy elliptical cylinders in pure bending. In the presentation of the results, it was assumed that the ordinary theory of bending applied and that the stress in compression on the extreme fiber was given by the equation,

$$f_b = \frac{Mc}{I} = \frac{M}{k_b a^2 t} \quad \text{----------(4)}$$

where M = bending moment applied in the plane of the major axis.
a = semi-major axis of the ellipse
k_b = a non-dimensional coefficient that varies with the eccentricity of the ellipse (See Fig. B3.5) which was taken from (Ref. 5). Thus in design, calculate the bending stress due to the given design bending moment from equation (4) and obtain allowable bending stress from curve B of Fig. B3.4 using r as the radius of curvature at the ends of the major axis. This buckling strength can be assumed as also being the ultimate strength of the cylinder in bending.

B3.5 Torsional Buckling Strength of Thin-Walled Circular Cylinders.

From chapter A5, the shearing stress f_s in the walls of a thin walled cylinder due to a torsional moment is given by the following equation,

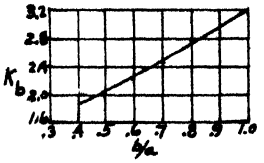
$$f_s = \frac{T}{2At} \quad \text{----------(5)}$$

where A = circumscribed area
t = skin thickness

In chapter A4 it was shown that pure shearing stresses produces compressive stresses of the same intensity on planes at 45° with the shearing planes. (See Fig. B3.6). Due to these compressive stresses, the thin walls fail by local instability.

Fig. B3.7 shows the results of tests on 17ST aluminum alloy cylinders (Ref. 6). The failing stress is shown as a function of r/t and L/r.

Fig. B3-5



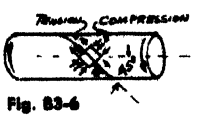


Fig. B3-6

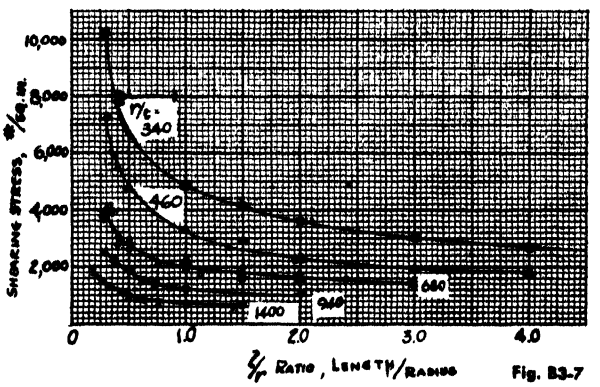


Fig. B3-7

In (Ref. 7) Donnell gives the results of both theoretical and experimental investigations of the torsional strength of circular thin walled cylinders.

The critical shear stress equations derived by Donnell are as follows:-

$$f_{s(cr)} = \frac{Et^2}{(1-\mu^2)L^2}\left[4.6 + \sqrt{7.8 + 1.67\left(\sqrt{1-\mu^2}\,\frac{L^2}{td}\right)^{3/}}\right.$$

----------(6)

For edges simply supported

$$f_{s(cr)} = \frac{Et^2}{(1-\mu^2)L^2}\left[2.8 + \sqrt{2.6 + 1.40\left(\sqrt{1-\mu^2}\,\frac{L^2}{td}\right)^{3/}}\right.$$

----------(7)

where μ = Poisson's ratio
t = wall thickness in inches
d = diameter in inches
L = cylinder length in inches
$f_{s(cr)}$ = critical buckling shear stress in psi.

Fig. B3.8 taken from (Ref. 7) shows how test data checks with these theoretical equations. The average actual test results are approximately 75 to 80 per cent of the theoretical results with a minimum of around 60%. For design purposes Donnell reduces equations (6) and (7) by multiplying them by 60 percent the resulting design curves being plotted on Fig. B3.8.

B3.6 Torsional Buckling Strength of Thin-Walled Elliptical Cylinders.

The shear stress is calculated by the general formula,

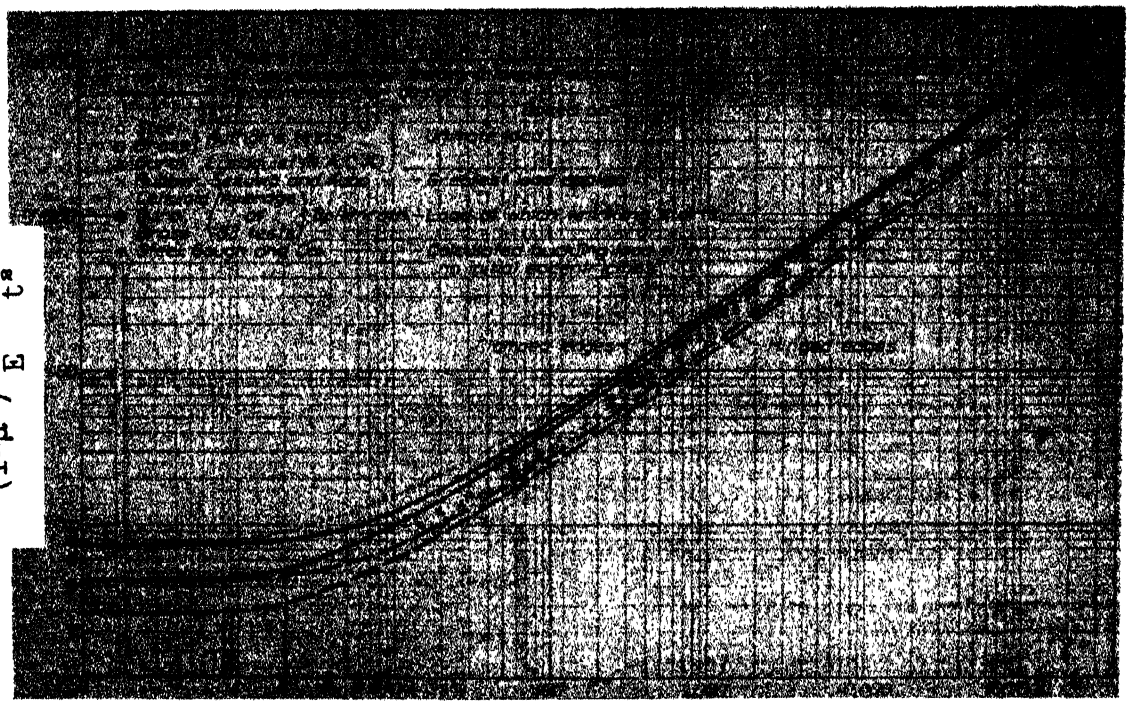


Fig. B3-8 CRITICAL TORSION STRESS FOR CIRCULAR CYLINDERS. (N.A.C.A.T.R. 479)
(Short and medium length cylinders)

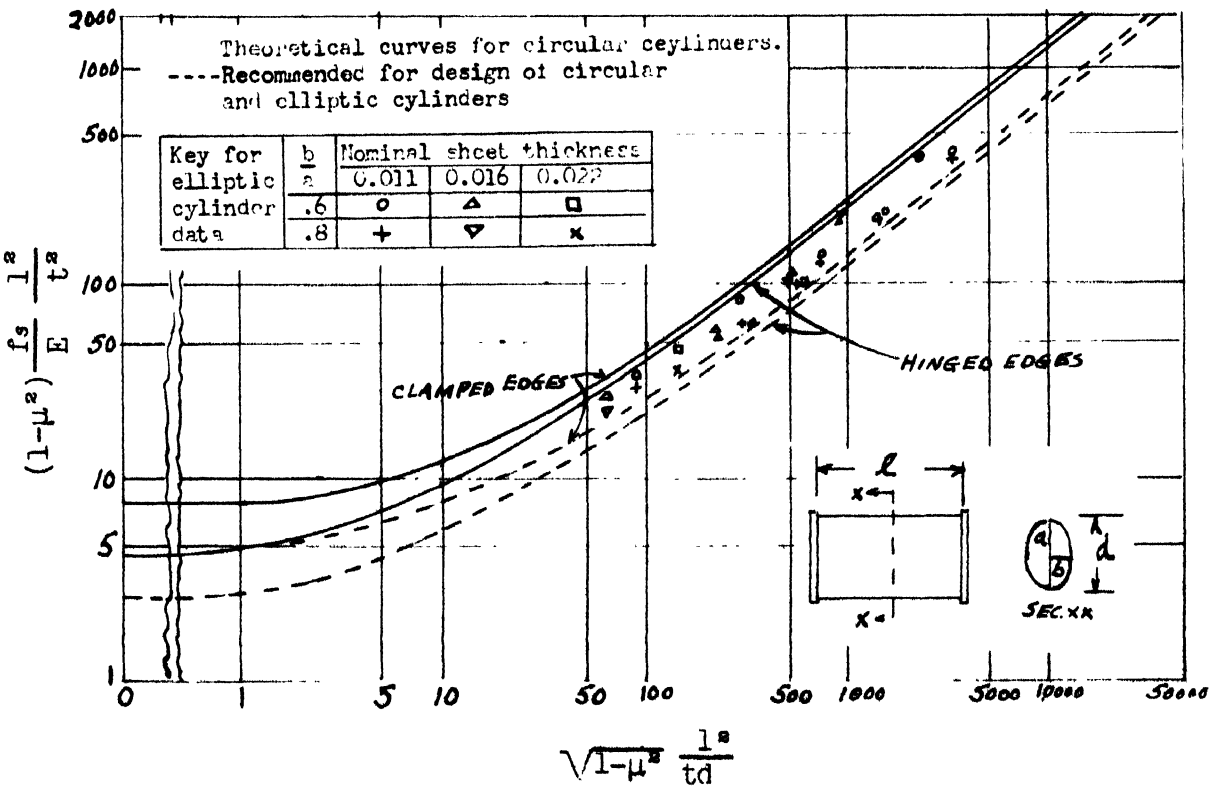


Fig. B3-9 TEST RESULTS OF ELLIPTIC CYLINDERS IN TORSION.

$$f_s = \frac{T}{2At} \quad \text{----------(8)}$$

T = torsional moment in inches lbs.
t = wall thickness in inches
A = area of ellipse = πab
f_s = shear stress in psi.

In tests of aluminum alloy elliptical cylinders (Ref. 5), the shearing stress as given by equation (8) were calculated for each test cylinder when first wrinkle appeared and at ultimate load. These stresses were plotted on a chart similar to Fig. B3.8 see Fig. B3.9 and it was found that the values fell below Donnell's equations for the shear strength of circular cylinders but above the recommended design curves. Thus it may be concluded that the shearing stress at ultimate load for an elliptic cylinder is the same as that for the circumscribed circular cylinder of the same sheet thickness and length.

B3.7 Strength of Circular Thin-Walled Cylinders Under Transverse Shear and Bending.

For circular cylinders, the equations for bending and shear stress according to the general beam theory are,

$$f_b = \frac{M}{\pi r^2 t} \quad \text{----------(9)}$$

$$f_s = \frac{V}{\pi rt} \quad \text{----------(10)}$$

where t = thickness of the cylinder wall
r = radius of cylinder.

In tests of aluminum alloy cylinders (Ref. 8) under transverse shear and bending, the results indicate that three general cases can be assumed to cover the entire field, (Ref. 9), namely,

(a) Bending predominating
(b) Shear predominating
(c) Intermediate conditions

In case (a) failure will take place at a stress approximately equal to that for pure bending as given in Fig. B3.3. In case (b) it was found that the allowable transverse shear stress appeared to be about 20 percent higher than the allowable shear stress for pure torsion as given in Fig. B3.8.

For intermediate conditions, the following relationship is given by (Ref. 9).

$$R_b^2 + R_s^2 = 1.0 \quad \text{----------(11)}$$

where,

$R_b = \frac{f_b}{F_b}$, F_b from Fig. B3.3)

$R_s = \frac{f_s}{F_s}$, F_s from Fig. B3.8 and increased 20%.

Margin of safety for a given loading,

$$M.S. = \frac{1}{\sqrt{R_b^2 + R_s^2}} - 1$$

Fig. B3.10 (Ref. 8) shows curves which express the strength of a cylinder under transverse shear and bending as a percentage of the strength in pure bending. In order to use the curve of Fig. B3.10 in design it is necessary to know the loading conditon M/rV and to be able to predict the values of f_b and f_s (due to V) for the cylinder. With these three quantities shown, the maximum allowable moments can be read from Fig. B3.10 as a percentage of that for pure bending as obtained from Fig. B3.3

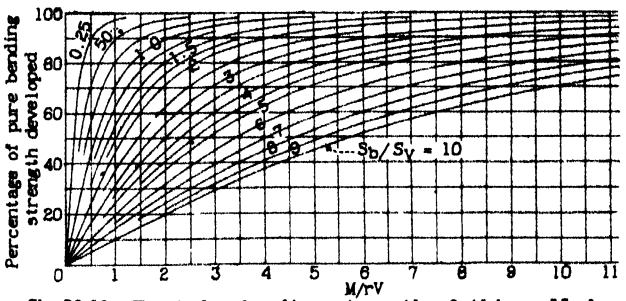


Fig. B3-10 Chart for bending strength of thin-walled cylinders subjected to combined transverse shear and bending.

B3.8 Strength of Elliptical Cylinders Under Combined Transverse Shear and Bending.

The strength of elliptical cylinders can be calculated in the same manner as given in Art. B3.7 for circular cylinders, with bending and shear stresses computed by the following equation,

$$f_b = \frac{M}{k_b a^2 t} \quad \text{----------(12)}$$

$$f_s = \frac{V}{k_v at} \quad \text{----------(13)}$$

k_v and k_b are obtained from Fig. B3.11

To use the curves of Fig. B3.10, the abscissa is taken as $\frac{M}{r' V}$, in which $r' = \frac{k_b a}{k_v}$ where a = semi-major axis of the ellipse.

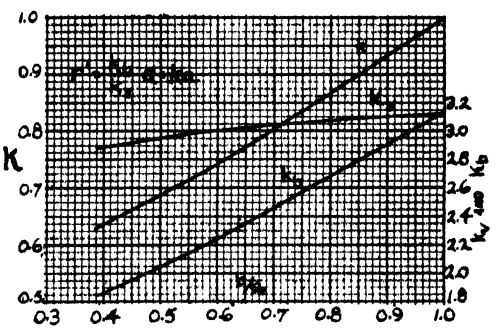


Fig. B3-11

B3.9 Strength of Circular and Elliptical Thin-Walled Cylinders in Combined Bending and Torsion.

Limited test data for thin walled cylinders in combined bending and torsion indicate the

following stress ratio equation is safe.

$$R_b^2 + R_s^2 = 1.0 \quad \text{- - - - - - - - - - - - - - (14)}$$

where $R_b = \frac{f_b}{F_b}$, F_b from Fig. B3.3 (Ref. 9)

$$R_s = \frac{f_s}{F_s}, \quad F_s \text{ from Fig. B3.8}$$

$$M.S. = \frac{1}{\sqrt{R_b^2 + R_s^2}} - 1$$

when transverse shear stresses exist in addition to the shear stresses due to torsion, Ref. 9 suggests as a safe procedure to add the values of R for torsion and transverse shear. Hence

$$R_b^2 + (R_s + R_{st})^2 = 1 \quad \text{- - - - - - - - - - - - (15)}$$

where R_s refers to transverse shear
R_{st} refers to torsional shear

B3.10 Strength of Thin-Walled Circular Cylinders in Combined Compression and Bending.

Limited test data indicates that the following relationship can be used. (Ref. 9).

$$R_c + R_b = 1.0 \quad \text{- - - - - - - - - - - - - - (16)}$$

where $R_c = \frac{f_c}{F_c}$, F_c obtained from Fig. B3.1

$$R_b = \frac{f_b}{F_b}, \quad F_b \text{ obtained from Fig. B3.3}$$

$$M.S. = \frac{1}{R_c + R_b} - 1$$

Buckling of Large Curved Sheet Panels

B3.11 Introduction

There is practically no published data on the buckling strength of large curved sheet panels. A common use of curved sheet sheet panels is in the small or medium size semi monocoque fuselages where the fuselage structures consists of metal skin supported by relatively closely spaced transverse frames with 3 or four fore and aft stringers or longerons. Fig. B3.12 illustrates this type of fuselage structure. To provide bending strength after the metal skin has buckled on the compressive side, longerons or stringers are used as illustrated in Sec. 1-1.

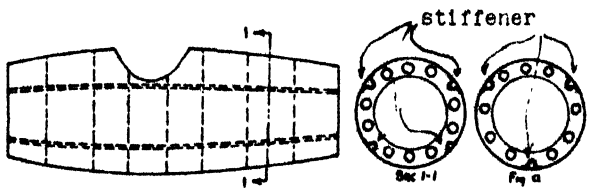


Fig. B3-12

At least 3 stringers are required since fuselage is subjected to loads in both vertical and side directions. The metal skin between the frames and the longitudinal stringers is broken up into large curved sheet panels. The stresses due to fuselage bending which produce compression and shear stresses on the sheet will cause the curved sheet to buckle under certain critical stresses and due to the large panel size in this type of construction, the initial buckles in general become permanent. The structural designer does not want permanent buckles under the applied loads, thus the curved sheet must be so designed by regulating its thickness and the frame spacing so as to keep the stresses below the buckling stresses. The practical application of the data in this chapter is applied to fuselage design in a later chapter.

B3.12 Buckling Compressive Strength of Large Curved Sheet Panels.

Timoshenko in "Theory of Elastic Stability" page 467 gives the following expression for the critical compressive buckling stress,

$$F_{c(cr)} = 0.6E\ t/r \quad \text{- - - - - - - - - - - (17)}$$

where t = plate thickness
r = radius of curvature.

He also states that equation (17) agrees with test data on aluminum alloy panels, provided the axial and circumferential dimensions for the panel are about equal and the central angle subtended by the panel is less than about 0.5 radian, and as the central angle increases to two radians the critical stress decreases to about one half that of equation (17)

One aircraft manufacturer in tests of a fuselage of the type described in Fig. B3.12 concludes that equation (17) should be multiplied by a correction factor C_c varying from .75 to 1.0 for various r/t ratios and fuselage frame spacing.

For preliminary design purposes, a constant curvature factor of .75 will be applied to equation (17), or

$$f_{c(cr)} = .60C_c\ E\ \frac{t}{r} = .6 \times .75\ E\ \frac{t}{r} = .45\ E\ \frac{t}{r} \quad \text{- - (18)}$$

Until more test data is available, we should be conservative in estimating the buckling stresses.

B3.13 Buckling Shear Strength of Curved Panels.

Very little experimental data on the buckling shear strength is available.

Younger (Ref. 10) gives the critical buckling stress

$$F_{s(cr)} = .06\ E\ t/r \quad \text{- - - - - - - - - - - (19)}$$

Wagner and Ballerstedt (Ref. 11) gives the buckling stress for a simply supported curved panel in shear as

$$F_{s(cr)} = 0.1\ E\ \frac{t}{r} + 5.3\ E\left(\frac{t}{b}\right)^2 \quad \text{- - - - - - - - (20)}$$

where t = sheet thickness

r = radius of curvature
b = distance measured along arc between stiffeners.

The writer believes that equations (18) and (19) are far too conservative, since they give a considerably less value for the critical shear stress than the value for a circular thin-walled cylinder as given by Donnell's.equation (Art. B3.5, Eq. 7) or

$$F_{s(cr)} = \frac{Et^2}{(1-\mu^2)L^2}\left[2.8 + \sqrt{2.6 + 1.40\sqrt{(1-\mu^2)\frac{L^4}{td}}}^{3/2}\right] \quad \text{- - - - - - - - - - - - - - - - (21)}$$

For design purposes this equation is multiplied by 60 percent. (See Fig. B3.8). Adding three or four longitudinal stringers should not decrease the critical shear stress below that of equation (20) times 60 percent, which is for a complete circular curved sheet without longitudinal stringers.

For comparison of the results of the above equations take t = .04", frame spacing L = 10", Distance b between stiffeners = 30" and r = 30".

By Eq. (19), F_s = 824 psi
By Eq. (20), F_s = 1470 psi
By Eq. (21), x 60% F_s = 2360 psi

For design of metal covered fuselages with closely spaced frames and only 3 or 4 longitudinal equation (21) multiplied by .6 or the design curve of Donnell on Fig. B3.8 is believed satisfactory and fairly close to the true conditions.

B3.14 Buckling Strength of Large Curved Panels in Combined Compression and Shearing Stresses.

For bending of a thin-walled cylinder combined with transverse shear and torsion, (Ref.) 12 gives the following relationships.

For compression and shear:

$$\left(\frac{f_s}{F_s}\right)^n + \frac{f_c}{F_c} = 1 \quad \text{- - - - - - - - - - - - - - - (22)}$$

For tension and shear:

$$\frac{f_s}{F_s} + \frac{1}{2}\left(\frac{f_c}{F_c}\right) = 1 \quad \text{- - - - - - - - - - - - - - - (23)}$$

According to Ballerstedt and Wagner n = 2 as the exponent in equation (22) whereas experiments by Lundquist (Ref. 6) indicate that n is nearer 3.

To be conservative n = 2 is recommended. In equation (22)

f_s = shear stress due to transverse shear plus torsion
F_s = critical buckling shear stress from Fig. B3.8
f_c = compressive stress due to bending and axial loads.
F_c = critical buckling compressive stress from equation (18) F_c = .45 t/r

Fig. B3.13 shows a plot of the interaction curves for equation (22) and (23) using n = 2.

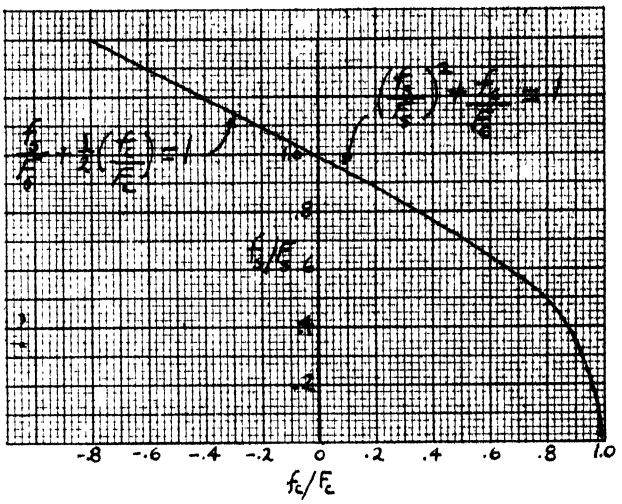


Fig. B3-13

References for Chapter B3

(1) E. Lundquist, "Strength of Thin-Walled Duralumin Cylinders in Compression", N.A.C.A. Tech. Rept. 473

(2) W. Wilson and N. Newmark, "The Strength of Thin Cylindrical Shells as Columns", Bull. 225 Eng. Exp. Sta. Univ. of Illinois, 1933

(3) S. Kanenutsu, and H. Nojima, "Axial Compression Tests of Thin Circular Cylinders," Thesis. Calif. Inst. of Tech. 1939

(4) E. Lundquist, "Strength Tests of Thin-Walled Duralumin Cylinders in Pure Bending", N.A.C.A. Tech. Note 479, 1933

(5) E. Lundquist, "Strength Tests of Thin-Walled Duralumin Cylinders of Elliptic Section", N.A.C,A. Tech. Note 527, 1935

(6) E. Lundquist, "Strength Tests of Thin-Walled Duralumin Cylinders in Torsion", N.A.C.A. Tech. Note 427, 1932

(7) L. H. Donnell, "Stability of Thin-Walled Tubes Under Torsion", N.A.C.A. Tech. Rep. 479, 1933

(8) E. Lundquist, "Strength Tests of Thin-Walled Duralumin Cylinders in Combined Transverse Shear and Bending". N.A.C.A. Tech. Note 523, 1935

(9) "Strength of Aircraft Elements", ANC-5 Handbook U.S. Government Printing Office Washington D.C. Revision of 1940

(10) Younger, "Structural Design of Metal Airplanes", McGraw-Hill Co.

(11) Wagner and Ballerstedt, "Tension Fields in Originally Curved Thin Sheets During Shear Stresses, N.A.C.A. T.M. No. 774 (1935)

(12) H. Ebner, "The Strength of Shell Bodies". N.A.C.A. T.M. No. 838 (1937)

B3.5 Problems

(1) A circular aluminum cylinder (E = 10,500,000 psi) is 16" long, 24" in diameter and made of .032" sheet. (a) Find allowable compressive stress from Equation (2) page B3.1 and from graph on page B3.2. (b) Find allowable bending stress from graph on Page B3.2. (c) Find allowable compressive load and allowable bending moment.

(2) Find the allowable torsional moment for the cylinder of Problem (1). Assume simply supported edges. Find allowable Moment M if T = .5M. Find margin of safety if M = 300 in. lb. and T = 150 150 in. 16.

(3) (a) Compute the allowable transverse shear load on the cylinder of Problem (1). (b) Compute the allowable bending moment if the transverse shear load is one half the allowable. (c) Compute the allowable torsion if the transverse shear and bending moment are each one half of the allowable.

CHAPTER B4
ULTIMATE COMPRESSIVE STRENGTH OF STIFFENED FLAT AND CURVED SHEET

B4.1 Introduction

The metal covering as commonly used in airplane wing and fuselage construction is relatively thin, thus the buckling compressive stresses are quite low unless the sheet is broken down into very small panels which is not practical. In general the common aircraft metal covered structure consists primarily of a stringer system capable of carrying relatively high compressive stresses, which causes to sheet covering to act in the buckled state since the sheet is fastened to the stringers. The question as to the effectiveness of this sheet in taking stress or load after buckling has brought forward many theories and considerable experimental data since information regarding this matter is important in the efficient design of sheet covered structures. The practical application of the results of this chapter are given in Part C of this book where the practical design of wings and fuselages are considered.

B4.2 The Ultimate Compression Strength of Isotropic Flat Plates

Fig. B4.1(a) illustrates a continuous flat thin plate fastened to stringers and the entire unit is subjected to a uniform compressive load. Up to the buckling strength of the sheet the compressive stress distribution is uniform over both stringers and sheet as in (Fig. b) assuming same material for sheet and stringers. As the load is increased the sheet buckles between the stiffeners and does not carry a greater stress than the buckling stress. However as the stringers are approached the skin bending stabilized by the stringers to which it is attached can take a higher stress and immediately over the stringer the sheet can take the same stress as the ultimate strength of the stiffener assuming that the sheet has a continuous connection to the stiffener. Fig. c shows the general stress distribution after the sheet has buckled. This distribution depends on the degree of restraint provided by the stiffeners and the panel dimension.

Various theoretical studies (Ref. 4.1) have been made to determine this stress distribution after buckling. In general they lead to long and complicated equations. To provide a simple basis for design purposes, an attempt has been made to find an effective width of sheet w which would be considered as taking a uniform stress (Fig. d) which would give the same total sheet strength as the sheet under the true non-uniform stress distribution of Fig. c.

Equations for Sheet Effective Width

The question of sheet effective width has been considered by many individuals. The names of Von Karaman, Sechler, Timoshenko, Newell, Frankland, Margurre and Fischel and many more are closely associated with the development of the present knowledge on sheet effective width.

The general expression for the critical compressive buckling stress is (Eq. 3 of Art. B2.2),

$$f_{cr} = KE\left(\frac{t}{b}\right)^2 \qquad \text{----------(1)}$$

If the four edges of the plate are considered simply supported K = 3.60 (Ref. Fig. B2.4 of chap. B2) hence,

$$F_{cr} = 3.60\,E\left(\frac{t}{b}\right)^2 \qquad \text{----------(2)}$$

The Von-Karman-Sechler method as first proposed consisted of solving equation (2) for the width w in place of the sheet width b when F_{cr} was equal to the yield point of the material, since experiments have shown that the ultimate

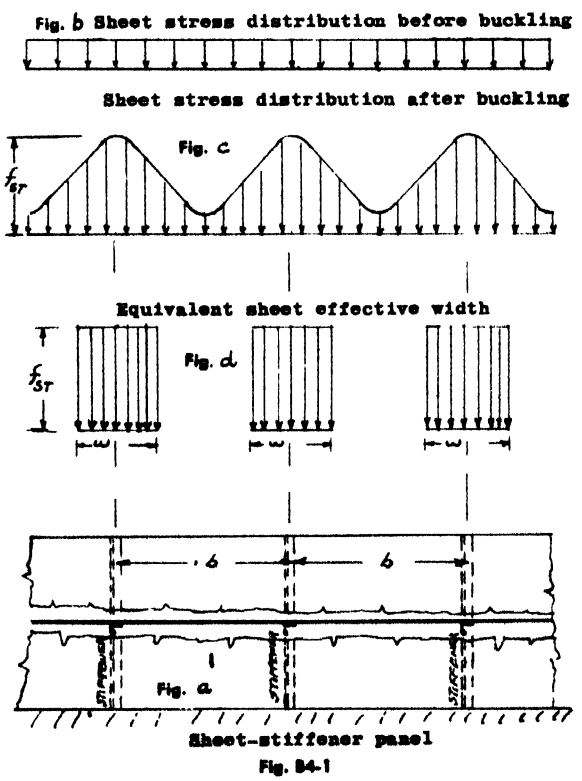


Fig. B4-1

strength of a sheet simply supported at the edges was independent of the width of the sheet.

hence, $f_{yp} = 3.60\ E\left(\frac{t}{w}\right)^2$ - - - - - - - - - - - -(3)

References:

(4.1) "Experimental Study of Deformation and of Effective Width in Axially Loaded Sheet-Stringer Panels", NACA Tech. No. 684, 1939.

(4.2) Niles and Newell, "Airplane Structures".

(4.3) Air Corps Information Circular No. 713, "Progress Report on Methods of Analysis Applicable to Aircraft Structures".

(4.4) J. R. Fischel, "Effective Widths in Stiffened Panels Under Compression", Jour. of Aeronautical Sciences, March 1940.

(4.5) Sechler, "Stress Distribution in Stiffened Panels Under Edge Compression", Journ. of Aeronautical Sciences, Vol. IV, No. 8, 1937.

(4.6) Howland, W. L., "Effect of Rivet Spacing on Stiffened Thin Sheet Under Compression", Journ. of Aeronautical Sciences, Vol. 3, No. 12, 1936.

(4.7) Newell, "Letter to Editor", Journ. of Aeronautical Sciences, Vol. 4, No. 6, 1937.

(4.8) Dickinson and Fischel, "Measurement of Stiffener Stresses and Effective Widths in Stiffened Panels", Journ. of Aeronautical Sciences, Vol. 6, No. 6, 1939.

(4.9) Sanderson and Fischel, "Corrugated Panels Under Combined Compression and Shear Load", Journ. of Aeronautical Sciences, Vol. 7, No. 4, Feb. 1940.

(4.10) J. R. Fischel, "The Compressive Strength of Thin Aluminum Alloy Sheet in the Plastic Region".

whence

$$w = 1.90\ t\sqrt{\frac{E}{f_{yp}}} \quad \text{- - - - - - - - - - - -(4)}$$

Later the yield point stress was replaced by the stiffener stress f_{st}, whence

$$w = 1.90\ t\sqrt{\frac{E}{f_{st}}} \quad \text{- - - - - - - - - - - -(5)}$$

Early experimental work by "Newell" indicated that the value 1.90 was too high as the tests indicated an average value of 1.70. Thus the equation

$$w = 1.70\ t\sqrt{\frac{E}{f_{st}}} \quad \text{- - - - - - - - - - - -(6)}$$

has been widely used and is recommended by ANC-5.

The effective width w can be expressed in terms of the actual plate width b as follows:

From (1)

$$f_{cr} = K\ E\left(\frac{t}{b}\right)^2 \quad \text{- - - - - - - - - - - -(7)}$$

From (5) replacing 1.90 by K

$$f_{st} = K\ E\left(\frac{t}{w}\right)^2 \quad \text{- - - - - - - - - - - -(8)}$$

Dividing (7) by (8)

$$\frac{w}{b} = \sqrt{\frac{f_{cr}}{f_{st}}} \quad \text{- - - - - - - - - - - -(9)}$$

The ratio $\frac{w}{b}$ gives the amount of sheet width which can be considered as fully effective or taking the same stress as the stiffener.

More recent experiments (Ref. 4.1) indicate that a closer approximation, to actual conditions is given by Marguerres equation, which is,

$$\frac{w}{b} = \sqrt[3]{\frac{f_{cr}}{f_{st}}} \quad \text{- - - - - - - - - - - -(10)}$$

Fig. B4.2 (from Ref. 4.1) gives a comparison of the several proposed equations for effective width as compared to actual test results.

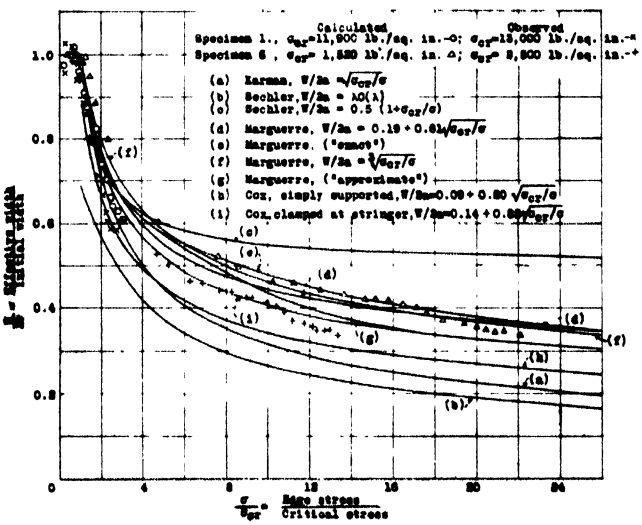


Fig. B4-2 Comparison of Calculated Effective Widths with Test Results.

B4.3 Fischel's Method for Effective Width

The following method proposed by Fischel (Ref. 4.4) appears to check experiments closely and takes into consideration such things as variation in the modulus of elasticity and effect of inter-rivet buckling.

Fischel states that experiments of sheet stringer sections common to monocoque construction produce edge conditions on sheet at stringer points which are more closely represented by a clamped condition instead of the freely supported edge condition as used in the Von-Karman equation.

Thus in the general buckling equation (1) the minimum value K for clamped edges is 6.35 (see Fig. B2.4 of Chapter B2).

$$f_{cr} = K E \left(\frac{t}{b}\right)^2 = 6.35 E \left(\frac{t}{b}\right)^2 \text{ - - - - - -}$$

let b = w the effective width when f_{cr} = stringer stress f_{st}

whence

$$w = 2.52\ t\sqrt{\frac{E}{f_{st}}} \quad \text{- - - - - - - - - - - (11)}$$

Equation (11) gives the effective width w at or above the initial buckling stress for the sheet.

Effect of Variation In Modulus of Elasticity on Effective Width.

Formula (11) assumes the same material for sheet and stringer and compressive stresses below the proportional limit of the material. In practical design, this is seldom true. It is common practice to use 24SRT sheet on 24ST extruded stringers. The compressive stress strain curve of these two materials is quite different above the proportional limit. Efficient stringer design, particularly closed sections or corregations permit ultimate design stresses above the proportional limit or in the plastic region where the modulus of elasticity is not constant. (Refer to Chapter C1 for stress-modulus curves of aluminum alloy). Therefore if the stiffener stress is above the proportional limit, the tangent modulus E' should be used in equation (11).

The stiffener and the effective width of sheet both have the same strain, but if the stringer and sheet have different stress-strain diagrams as illustrated in Fig. B4.3, this difference in stress for the same strain (points A and B in Fig. B4.3) must be compensated for in the formula. Since stiffener stress is of primary concern, it is necessary to express the effective width formula in terms of the stiffener stress and correct for the different strength of the sheet.

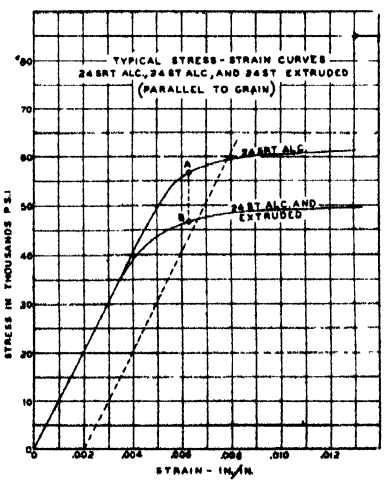


Fig. B4-3 Typical stress-strain curves for 24ST Alclad, 24ST extruded durel, and 24SRT Alclad.

Sechler (Ref. B4.5) has shown by strain measurements on a panel that at the higher stresses most of the load in the sheet is carried by the portion adjacent to the stiffener. By assuming all the stress is carried by a rectangular sheet adjacent to the stiffener equal in width to w_1 and acting at the stiffener stress, the load in the sheet will be $w_1\ t\ f_{sh}$, where f_{sh} is the sheet stress corresponding to the stiffener stress at the same unit strain (Points A and B, Fig. B4.3), and w is the uncorrected effective width corresponding to the stiffener stress. Expressing this load in terms of stiffener stress and correct effective width (w) acting at the stiffener stress,

$$P = f_{sh}\ t\ w_1 = f_{st}\ t\ w$$

whence

$$w = \frac{f_{sh}}{f_{st}} w_1 = 2.52\ t\ \frac{f_{sh}}{f_{st}}\sqrt{\frac{E}{f_{st}}}\ t \text{- - - - - (12)}$$

If sheet and stiffener have same stress-strain curve then f_{sh}/f_{st} equals unity and equation (11) is obtained. Equation (12) can thus be used for various combination of materials for the sheet and stringer if the stress strain curve of each is known.

Effect of Inter-Rivet Buckling on Effective Width

Fischel explains as follows how the strength of the sheet after inter-rivet buckling is treated in arriving at effective width for sheet. Inter-rivet buckling is a column failure of the sheet between rivets and since the total load in the sheet is assumed to be carried by an effective width at the stiffener, this effective width may be regarded as representing the column between rivets. When a column of any type is loaded axially in compression, it will sustain this maximum stress over a relatively large deflection before any large decrease is detected. Thus it may be assumed that after inter-rivet buckling occurs, the sheet stress at which it occurs will remain practically constant until the failure stress of the stiffener is reached. Thus proceeding as before, the effective width of the sheet at stiffener stresses above the inter-rivet buckling stress f_e will be given by,

$$w = 2.52\ t\ \frac{f_e}{f_{st}}\sqrt{\frac{E}{f_{st}}} \text{ - - - - - - - - - (13)}$$

Combining (13) with (12), the equation for dissimilar materials,

$$w = 2.52\ t\ \frac{f_e\ f_{sh}}{f_{st}^2}\sqrt{\frac{E}{f_{st}}}\ t \text{- - - - - - - (14)}$$

The inter-rivet buckling stress f_e, was originally determined by Howland (Ref. 6) and corrected by Newell (Ref. 7). Fischel has extended the curves in Fig. B4.4 to cover the entire range of stresses covered by the curves in Fig. B4.3. For stresses above 20,000 psi, the Euler formula with tangent modulus was used to determine the inter-rivet buckling stress. Two curves are given in Fig. B4.4, one for 24SRT alclad stiffeners and the other for 24ST alclad and extruded stiffeners. The inter-rivet buckling

stress must be taken from the curve corresponding to the stiffener material used and not the sheet material. Equation (14) applies only when stiffener stress is above the inter-rivet buckling stress, since for stresses below the inter-rivet buckling stress the value of f_e/f_{st} becomes unity.

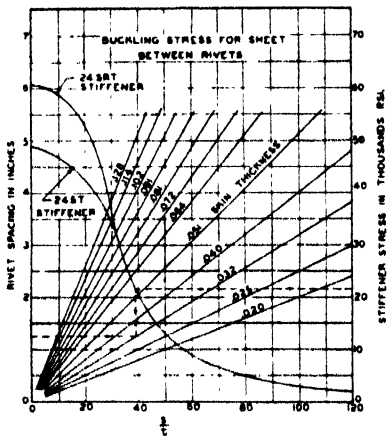


Fig. B4-4 Inter-rivet buckling curves for flat sheet attached to 24ST and 24SRT and stiffeners.

Application of Fischel's Theory to Design

In Fig. B4.5 Fischel (Ref. 4) has plotted curves of effective width of sheet against stiffener stress for various standard guages of 24ST alclad sheet commonly used in aircraft design. The curves are plotted for a rivet spacing S = 0, or a continuous attachment of sheet to stiffener and for two stiffener materials, 24ST alclad and 24SRT alclad, whose stress strain curves are shown in Fig. B4.3. It may also be assumed without serious error that extruded 24ST aluminum alloy has the same properties as the 24ST alclad. The limiting value of the effective width w is the stiffener spacing.

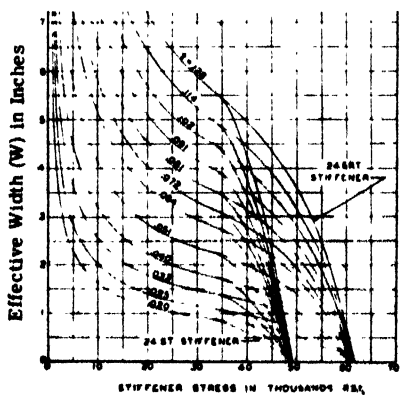


Fig. B4-5 Curves of effective width of skin versus stiffener stress for various standard sheet gages of 24ST alclad.

To use the curves for any rivet spacing above S = 0, determine the inter-rivet buckling stress, f_e from Fig. B4.4 for the proper stiffener material. If this is below the design stiffener stress f_{st}, determine the ratio f_e/f_{st} and multiply this by the effective width determined from Fig. B4.5 for S = 0. For any other combination of sheet and stiffener materials, the effective width must be found from equation (14).

The agreement of test data with the general theory is shown in Fig. B4.6. The test points given in Table 2 of (Ref. 8) are compared with the theoretical curve for .032 sheet. The rivet spacing on the test panel was one inch for which, from Fig. B4.4, the inter-rivet buckling stress is 34,000 psi. The theoretical curve is corrected for inter-rivet buckling and shows good agreement with the test data especially at high stresses where the experimental method of determining effective width was most accurate. Points taken from (Ref. 9) for .032 sheet attached to corrugations are also compared with the theoretical curve and show good agreement.

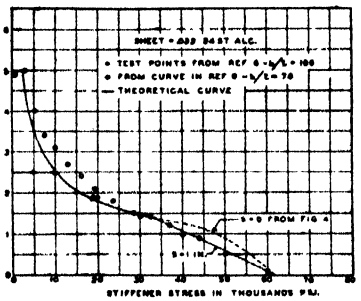


Fig. B4-6 Comparison of test data with general theory.

Exceptions have been found to the general theory in examining available test data. Test data on stiffened test panels with b/t less than 75, showed that the moments induced into the stiffeners by the sheet became of sufficient magnitude to alter the boundary conditions. A reduction factor of 0.76 for sheet stiffener combinations with a b/t below 75 gives a more nearly correct effective width w, that is, w as determined from Fig. B4.5 or equation (14) should be reduced 24 percent.

This reduction reduces the constant 2.52 to 1.90 which corresponds to an effective width for a simply supported edge.

Fischel in a later publication (Ref. 4.10) gives results of further study and test results which the student should refer to.

B4.4 Ultimate Compressive Strength of Curved Thin Sheet Panels

Very little theoretical or experimental data is available on the ultimate strength of curved sheet simply supported at edges, or restrained by stiffeners.

Sechler has proposed a general method for estimating the ultimate strength of curved sheet with simply supported edges, which is as follows:

(1) That the edges carry a stress equal to the yield point of the material over an effective width w determined by the equation for flat sheet simply supported at edges.

(2) That the remaining center portion of the sheet of width equal to (b - w) carries a critical buckling stress equal to that of a circular cylinder having the same thickness and radius as the panel.

Equation (4), $w = 1.90\ t\sqrt{\frac{E}{f_{yp}}}$, gives the effective width w.

The load P_1 on effective strip of width w =

$$P_1 = w\ t\ f_{yp} \quad \text{- - - - - - - - - - - - - - - (15)}$$

The stress on the remaining portion can be computed by either equation (2) or (2a) of Chapter B3, namely

$$f_{cr} = E\left[9\left(\frac{t}{r}\right)^{1.6} + 0.16\left(\frac{t}{L}\right)^{1.3}\right] \text{- - - (16)}$$

or by the simpler but more approximate equation

$$f_{cr} = 0.3\ E\ t/r \quad \text{- - - - - - - - - - - - - (17)}$$

Then load P_2 on center remaining portion is

$$P_2 = f_{cr}\ (b - w)\ t \quad \text{- - - - - - - - - - - - (18)}$$

Example Problem

The ultimate compressive load will be calculated for the following curved sheet panel of aluminum alloy. The resulting stress distribution is shown in Fig. B4.7

DATA: t = .020 b (panel width) = 3 in.

r (radius of curvature) = 20

L (sheet length) = 12 in.

Yield point of material = 36,000 psi.

Effective width $\frac{w}{2}$ at each edge:

$$w = 1.90\ t\sqrt{\frac{E}{f_{yp}}} = 1.90 \times .02\sqrt{\frac{10.3 \times 10^6}{36{,}000}} = .642 \text{ in}$$

Load on $w = P_1 = w\ t\ f_{yp} = .642 \times .02 \times 36{,}000 = 462$ lb

Buckling stress on center portion:

By equation (16)

$$f_{cr} = 10.3 \times 10^6\left[9\left(\frac{.02}{20}\right)^{1.6} + 0.16\left(\frac{.02}{12}\right)^{1.3}\right] = 1850$$

By equation (17)

$f_{cr} = 0.3 \times 10.3 \times 10^6 \times .02/20 = 3090$ psi.

Load P_2 on center portion = $f_{cr}\ t\ (b - w)$

$P_2 = 1850 \times .02(3 - .642) = 88$ (using f_{cr} from Eq.16)

$P_2 = 3090 \times .02(3 - .642) = 145$ (using f_{cr} from Eq.17)

Total net load on sheet = $P = P_1 + P_2$

P = 462 + 88 = 550 lb. or,

P = 462 + 145 = 607 lb.

The test result on this particular panel gave 540 lb.

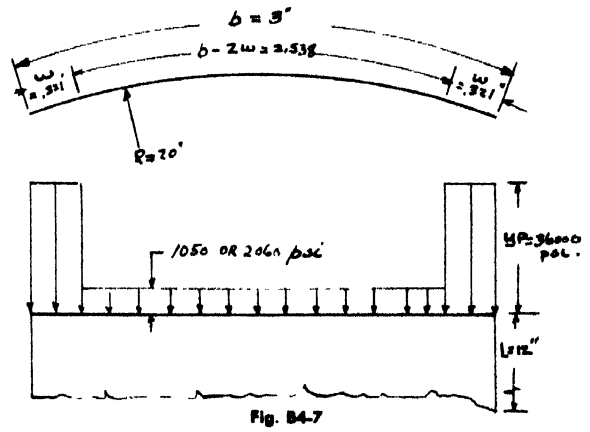


Fig. B4.7

PROBLEMS

(1) A 24ST sheet .04 inches in thickness is stiffened by 24SRT stiffeners spaced 5 inches apart with a single row of rivets at 1.25 inch spacing attaching each stiffener to the sheet. If the ultimate stiffener stress is 35,000 psi., calculate the effective sheet widths acting with each stringer by the various methods presented in this chapter.

(2) Repeat problem (1) with a stiffener stress of 40,000 psi.

(3) Repeat problem (1) with a stiffener stress of 25,000 psi.

(4) Determine the ultimate compressive load that the following curved sheet panel will carry. t = .040, b = 7, r = 30, L = 16. Material is 24ST aluminum alloy, E = 10,300,000 and yield strength is 40,000 psi.

(5) Same as (4) but with t = .051, b = 5, r = 20 and L = 20 inches.

(6) Same as (5) but use 24SRT material which has a yield strength of 50,000 psi.

CHAPTER B5
COLUMNS WITH THIN WALLS: CRIPPLING STRESSES: OPEN AND CLOSED SECTIONS

B5.1 Introduction

In aircraft structures, sections such as angles, zees, channels, tees, square tubes, etc. are used for members carrying compressive loads. In some cases columns fabricated from these sections will act as columns with stable cross sections, and in other cases, failure will be due to local buckling or crippling. Most of the methods in use for calculating the strength of such sections are semi-empirical in nature but appear to check actual test results reasonably well. The general methods given in this chapter have been checked against many test results, and it is believed in general that they are accurate to within 10 percent of the actual strengths, The methods can at least be used in preliminary design.

B5.2 Angle Sections - Bent-up and Extruded

The angle section is frequently used as a member for carrying compressive loads. Angle members are made by bending flat plates or by

Fig. B5-1

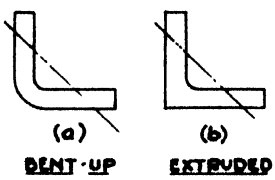
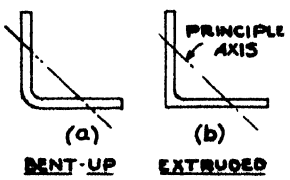


Fig. B5-2



extruding if the minimum thickness is approximately 1/16 inch. If the bent-up or extruded angle section has thick and short legs as in Fig. B5.1, the section when used as a column will act as a column with a stable cross section, and thus the methods of Chapter B1 can be used, using the section properties with respect to the principle axis, since the angle will bend about this axis as the moment of inertia is minimum about the principal axis as shown in Fig. B5.1 and B5.2.

However, if the angle section is composed of long thin legs as illustrated in Fig. B5.2, the legs may buckle or go into a wave state before the stress given by the Euler equation for stable sections is reached. The angle section however in the so-called short column range will carry a higher load than that which starts the legs to buckle. Very little data seems to be available on the shape of the column curve for equal leg angles in the plastic range or after the legs start to buckle. The following procedure seems to check meager test results reasonably well.

Each leg is considered as a plate simply supported on three sides and free on the fourth. The buckling stress is given by the equation,

$$F_{cr} = .452\,\bar{E}\left(\frac{t}{b}\right)^{a} \quad \text{(See Eq. 3 of Art. B5.4)}$$

This equation is plotted on Fig. B5.12 and B5.13 for various materials.

To make test results agree reasonably with the ultimate crippling stress and also with the initial buckling stress, the assumption for width b are given in Fig. B5.3.

To illustrate the use of these conclusions, two example problems will be given.

Example Problem 1

Determine the ultimate compressive strength of a 1 x 1 x 1/16 extruded 24ST angle 11 inches long if end fixity C = 1.0. (Fig. a)

Solution.

For the ultimate crippling stress, the effective width b of each leg equals,

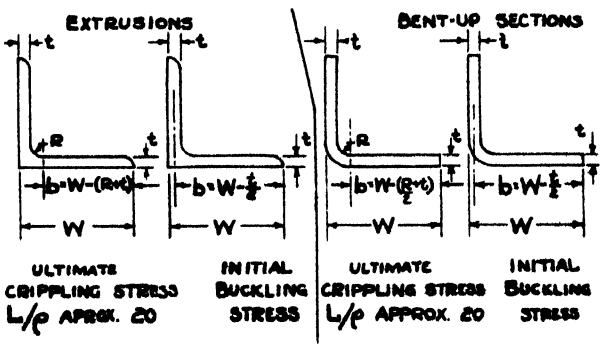
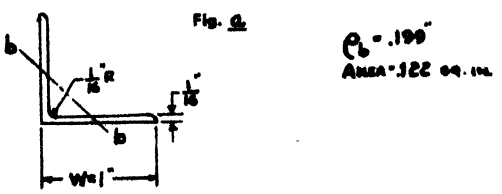


Fig. B5-3

$$b = W - (R + t) = 1 - (1/16 + 1/16) = 7/8$$



hence b/t = .875/.0625 = 14. From curve on Fig. B5.13 for 24ST extruded material and for a b/t = 14, we obtain an ultimate F_{cr} of 22,400 psi.

To determine the stress at which initital buckling of the legs start, we use a width b = w - t/2 = 1 - 1/32 = 31/32, hence b/t = .97/.0625 = 15.5.

From Fib. B5.13, we obtain a buckling stress F_{cr} of 19,200 psi. This stress is considered as the point where the column curve of the actual angle breaks away from the Euler column curve.

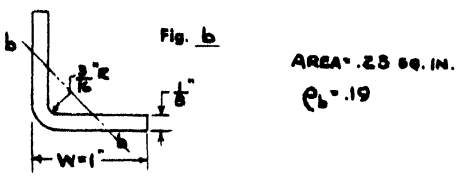
The Euler column strength assuming stable cross sections will now be calculated.

$L/\rho = 11/.199 = 55.3$

From column curve for 24ST extruded material (Fig. B1.10 of Chapter B1), we obtain F_c = 30,500 psi for L/ρ = 55.3. Since this is higher than our initial buckling stress of 19,200, the column strength for this angle is influenced by buckling of the legs. To obtain a so-called short column curve, we locate one point as the ultimate critical stress of 24,300 at L/ρ = 20, and a second point on the Euler curve at a stress equal to 19,200 and assume a straight line variation in between. Projecting up on Fig. B1.10 on a L/ρ value of 55.3, we obtain an allowable stress equal to 20,500 psi. Hence column strength = 20500 x .122 = 2500#.

Example Problem 2

The bent up angle in Fig. (b) is 24 inches long and is fabricated from 24ST alclad material.



Assuming end fixity C = 1.5, calculate the ultimate compressive strength of the angle member.

Solution

For ultimate crippling stress,

$$b/t = \frac{W - (.5R + t)}{t} = \frac{1 - (.093 + .125)}{.125} = \frac{.782}{.125} = 6.25$$

From Fig. B5.12, F_{cr} = 39400 psi.

For the initial buckling stress,

$b/t = (W - t/2)/t = (1 - .062)/.125 = 7.5$

From Fig. B5.12, F_{cr} = 35400 psi

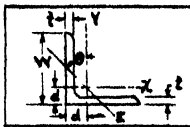
Euler column strength:

$$L'/\rho = \frac{24}{\sqrt{1.5 \times .19}} = 104$$

From Euler column curve for 24ST alclad on Fig. B1.10 of Chapter B1, we obtain F_c = 9000 psi, which is less than the values found above.

Hence compressive strength of given angle = 9000 x .23 = 2070#.

Table B5.1



Properties of Extruded Aluminum Alloy Equal Leg Angles. (Ref. 1938 Alcoa Handbook)

Dimensions			Area	Axis XX or YY			Axis ZZ		
W	t	R	sq.in.	I	ρ	d	I	ρ	θ
5/8	3/32	1/8	.111	0.004	0.183	0.187	.0015	0.117	45°
3/4	1/16	1/8	.089	0.004	0.220	0.199	.0018	0.142	45
3/4	3/32	1/8	.132	0.006	0.219	0.214	.0026	0.141	45
3/4	1/8	1/8	.171	0.008	0.217	0.227	.0034	0.141	45
1	1/16	1/16	.122	0.012	0.311	0.271	.0048	0.199	45
1	3/32	1/8	.178	0.016	0.301	0.276	.0066	0.193	45
1	1/8	1/8	.234	0.021	0.298	0.290	.0085	0.191	45
1	3/16	1/8	.339	0.029	0.293	0.314	.0124	0.192	45
1-1/4	3/32	3/32	.230	0.033	0.38	0.34	.014	0.24	45
1-1/4	1/8	3/16	.30	0.042	0.37	0.35	.017	0.24	45
1-1/4	3/16	3/16	.43	0.059	0.37	0.37	.025	0.24	45
1-1/4	1/4	3/16	.56	0.074	0.36	0.40	.032	0.24	45
1-1/2	3/32	3/16	.28	0.058	0.46	0.40	.024	0.30	45
1-1/2	1/8	3/16	.36	0.074	0.45	0.41	.031	0.29	45
1-1/2	3/16	3/16	.53	0.107	0.45	0.44	.044	0.29	45
1-1/2	1/4	3/16	.69	0.135	0.44	0.46	.057	0.29	45
1-3/4	3/32	3/32	.32	0.096	0.55	0.47	.039	0.35	45
1-3/4	1/8	3/16	.42	0.121	0.53	0.47	.050	0.34	45
1-3/4	3/16	3/16	.62	0.174	0.53	0.50	.072	0.34	45
1-3/4	1/4	3/16	.81	0.223	0.52	0.52	.093	0.34	45
2	1/8	1/4	.49	0.18	0.61	0.53	.08	0.40	45
2	3/16	1/4	.72	0.27	0.61	0.56	.11	0.39	45
2	1/4	1/4	.94	0.34	0.60	0.58	.14	0.39	45
2	5/16	1/4	1.16	0.41	0.60	0.61	.17	0.39	45

B5.3 Critical Local Strength of Chanel, I, and Zee Sections

Lundquist (Ref. 5.1) has presented a theoretical method for determining the local strength of channel, I and Zee sections which checks experimental results reasonably well, but tends toward the conservative side.

The method in general considers the section as made up of two basic plate elements and the buckling strength of these elements is determined taking into account the interacting stabilizing influence of one plate element upon the other.

The critical buckling compressive stress for a rectangular plate is given by equation 3a of Chapter B2.2, as follows:

$$f_{cr} = \frac{k\,\pi^2\,E\,t_F^{\,2}}{12\,(1-\mu^2)\,b^2}$$

As applied by Lundquist to channel, Zee and I sections, this buckling equation is written,

$$f_{cr} = \frac{k_F\,\pi^2\,E\,t_F^{\,2}}{12\,(1-\mu^2)\,b_F^{\,2}} \quad \text{----------(1)}$$

and

$$f_{cr} = \frac{k_W\,\pi^2\,E\,t_W^{\,2}}{12\,(1-\mu^2)\,b_W^{\,2}} \quad \text{----------(2)}$$

In these formulae, either of which may be used, t_F and t_W are the thicknesses of the flange and the web plates, respectively. b_F and b_W refer to flange and web widths as defined in the small figures of Figs. B5.5 to B5.8. k_F and k_W are non-dimensional coefficients dependent on the shape of the cross-section. The values of these terms were calculated by the energy method. They are plotted against b_W/b_F and b_F/b_W respectively to obtain the curves of Figs. B5.5 to B5.8.

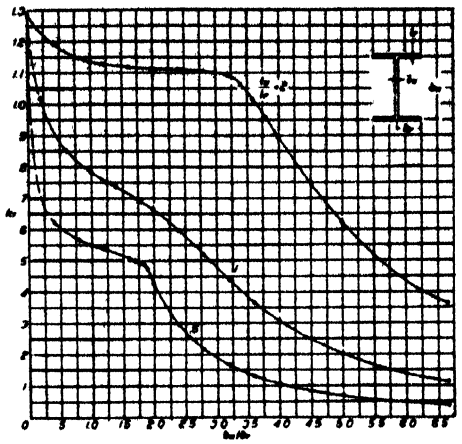


Fig. B5-5

Minimum values of k_F for centrally loaded columns of I-section ($\mu = 0.3$) $\frac{f_{cr}}{\eta} = \frac{k_F \pi^2 E t_F^2}{12(1-\mu^2) b_F^2}$

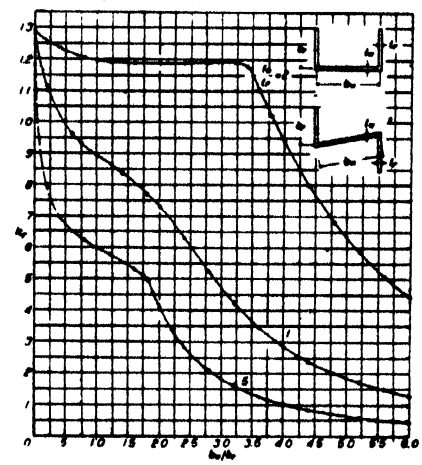


Fig. B5-7

Minimum values of k_F for centrally loaded columns of channel section and Z section ($\mu = 0.3$) $\frac{f_{cr}}{\eta} = \frac{k_F \pi^2 E t_F^2}{12(1-\mu^2) b_F^2}$

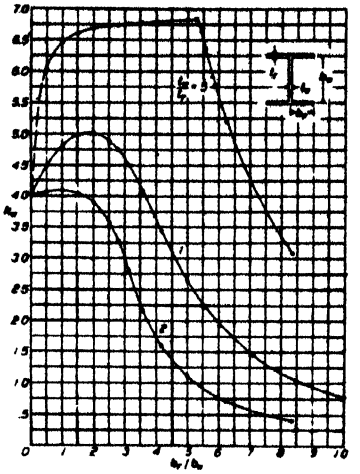


Fig. B5-6

Minimum values of k_W for centrally loaded columns of I-section ($\mu = 0.3$) $\frac{f_{cr}}{\eta} = \frac{k_W \pi^2 E t_W^2}{12(1-\mu^2) b_W^2}$

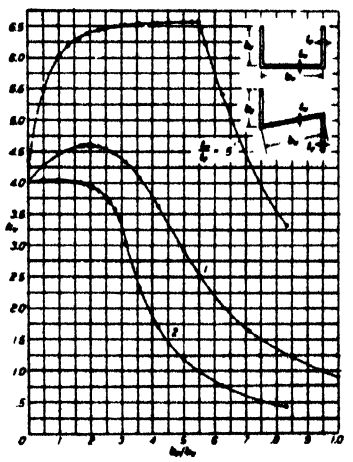


Fig. B5-8

Minimum values of k_W for centrally loaded columns of channel section and Z-section ($\mu = 0.3$) $\frac{f_{cr}}{\eta} = \frac{k_W \pi^2 E t_W^2}{12(1-\mu^2) b_W^2}$

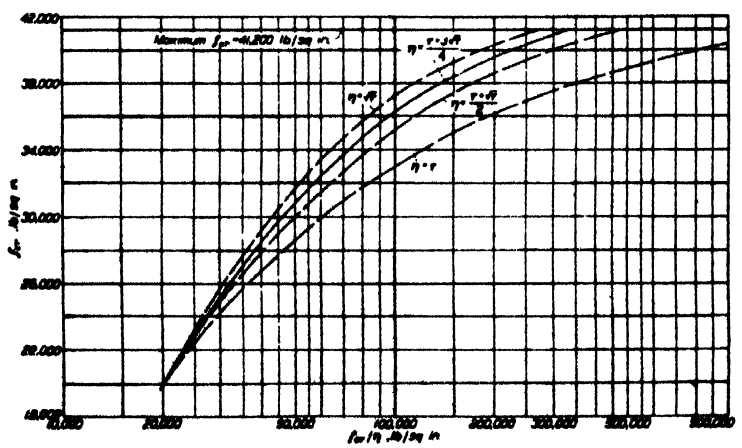


Fig. B5-9 Variation of f_{cr} with f_{cr}/η for 24 ST aluminum alloy. When $f_{cr} < 19{,}600$ lb/sq.in., $\eta=1$ and $f_{cr} = f_{cr}/\eta$

(All figures from NACA Tech. Note No. 743)

Equations (1) and (3) are as given on these figures with f_{cr} replaced by f_{cr}/η . The non-dimensional coefficient η allows for the effect of stress beyond the elastic range where E is not constant. See Fig. B5.9 for variation of f_{cr} with f_{cr}/η.

The use of the charts can best be explained by the solution of an example.

Example 1

Calculate the critical compressive stress at which cross sectional distortion begins in the I section of Fig. a

Dimensions: b_F = 1 in. b_W = 2 in.

t_F = 0.1 in. t_W = 0.1 in.

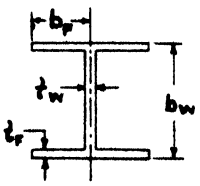


Fig. a

$E = 10.66 \times 10^6$

$\mu = 0.3$

Solution: $\frac{b_W}{b_F} = \frac{2}{1} = 2$

$\frac{t_W}{t_F} = \frac{0.1}{0.1} = 1$

From Fig. B5.5, $k_F = 0.662$

From Equation (1), but replacing f_{cr} by f_{cr}/η

$$\frac{f_{cr}}{\eta} = \frac{0.662 \times \pi^2 \times 10.66 \times 10^6 \times (0.1)^2}{12\,(1-.3^2) \times (1)^2} = 63800 \text{ psi}$$

From the solid curve of Fig. B5.9

f_{cr} = 33000 psi

This stress theoretically represents the stress at which cross sectional distortion takes place, and not the ultimate strength. As f_{cr} approaches the yield point of the material, the critical load or stress as found by this method and the ultimate strength approach the same value. Thus in general this method should be conservative. This critical local stress can be considered as the strength at zero L/ρ. For other values of L/ρ, the column strength can be estimated by substituting the crippling stress as the stress f_{cr} in the Johnson-Euler formula:

$$F_c = f_{cr} - \frac{f_{cr}\ (L/\rho)^2}{4\ C\ \pi^2\ E}$$

or more conveniently by using the plotted curves of this equation in Fig. B1.12 of Chapter B1.

B5.4 Ultimate Compressive Crippling Strength of Open Sections

Practically no theoretical information is available on the ultimate crippling strength of open sections composed of flat and curved segments. The treatment presented here is semi-empirical but the method appears to check experimental data quite well, and is similar to methods used by structures department of various airplane companies. The method in general consists of determining the buckling strength of the various plate elements and then adding them together to obtain the ultimate strength of the entire section in compression. Thus in Fig. B5.10 the element (a) is considered as a flat plate freely supported on all four sides, while

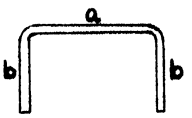


Fig. B5-10

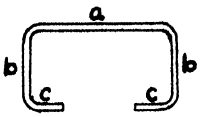


Fig. B5-11

plate element (b) is considered as a plate freely supported on three sides and free on the fourth. In the section of Fig. B5.11 plate elements (a) and (b) are considered as simply supported on four sides and element (c), simply supported on 3 sides and free on the fourth.

From Chapter B2 (Eq. 3), the buckling compressive stress for a flat plate is given by the equation,

$$F_{cr} = K\ E \left(\frac{t}{b}\right)^2$$

For a plate simply supported on 3 sides and free on the fourth, Fig. B2.4 of Chapter B2 gives a value of K = .452 when a/b = 3.

hence

$$F_{cr} = .452\ E \left(\frac{t}{b}\right)^2 \text{ - - - - - - - - - - - - -(3)}$$

For a plate simply supported on all four sides

K = 3.64 from Fig. B2.4.

hence

$$F_{cr} = 3.64\ E \left(\frac{t}{b}\right)^2 \text{ - - - - - - - - - - - - -(4)}$$

Equations (3) and (4) are for critical buckling stresses below the proportional limit of the material. As the values of b/t get smaller, the buckling stresses will exceed the proportional limit and thus a reduced modulus $\bar{E}$ is used in equation (3) and (4) in the plastic range.

Buckling Stress Curves

Figs. B5.12 and B5.13 give the buckling stress curves for aluminum alloy and stainless steel as determined by equations (3) and (4). Tables B5.1 and B5.2 illustrate the calculations and the values of the tangent and modified modulus of elasticity that were used.

Crippling Stress F_{cs} For Complete Sections.

The general method of determining the crippling stress for such sections as shown in Figs. B5.12 and B5.13, is to find the buckling stress for each plate element and then determine allowable crippling stress for the entire section

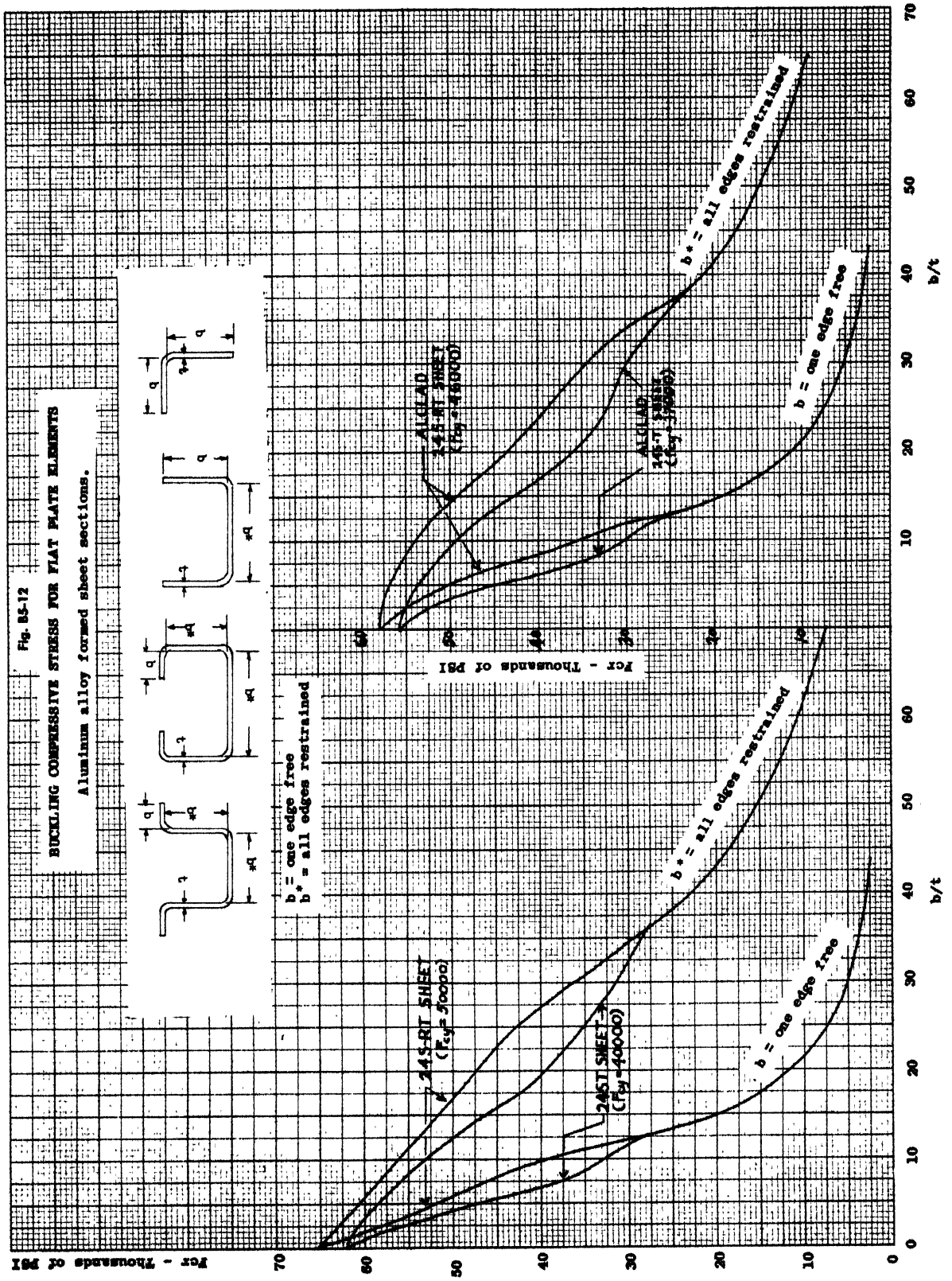
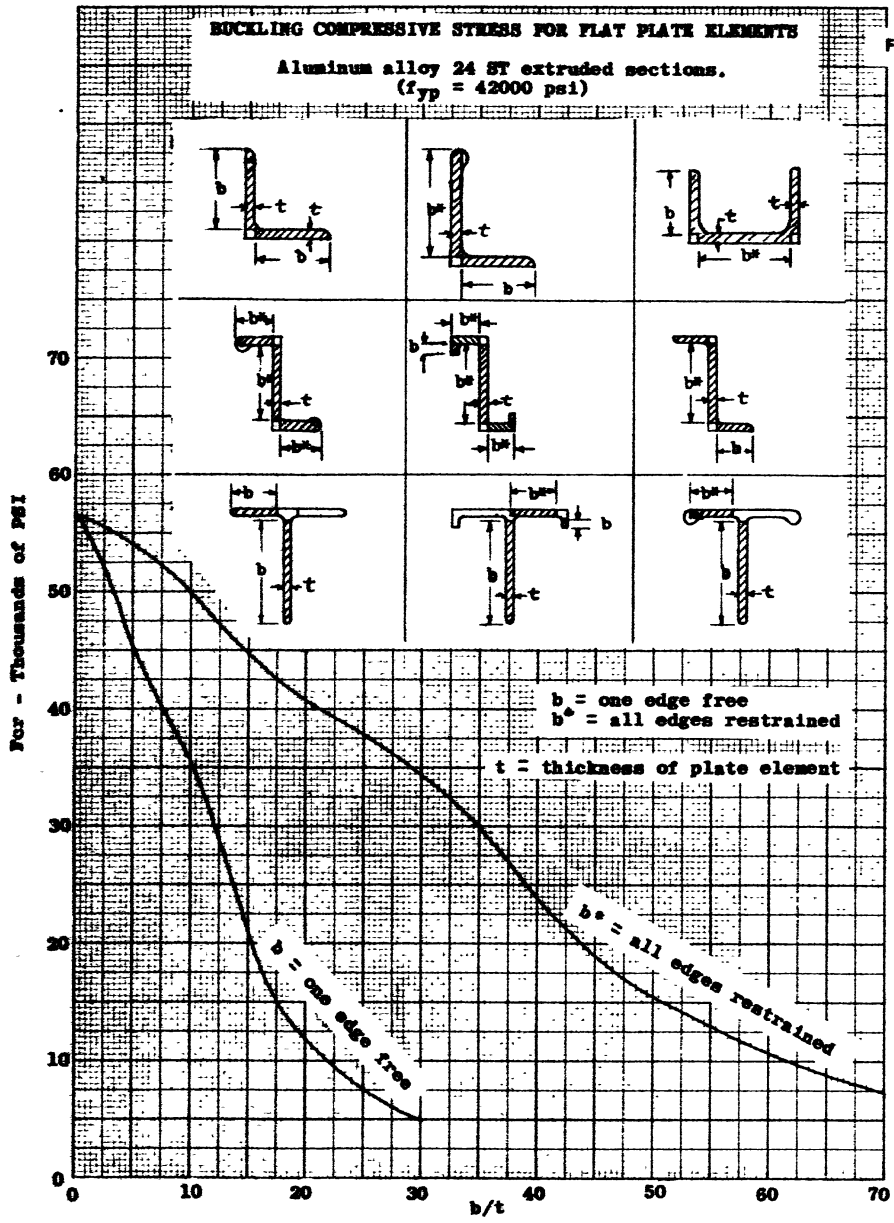
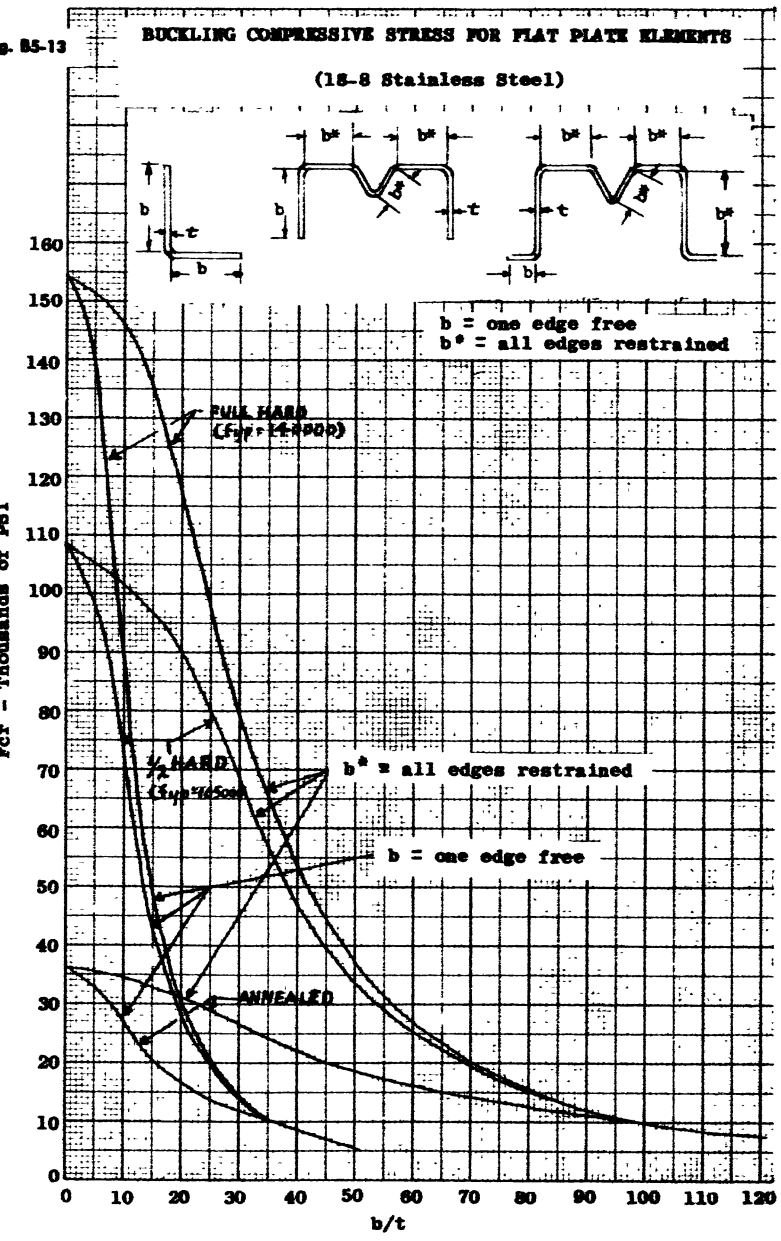

Fig. B5-12
BUCKLING COMPRESSIVE STRESS FOR FLAT PLATE ELEMENTS
Aluminum alloy formed sheet sections.
b = one edge free
b* = all edges restrained
Fcr - Thousands of PSI
b/t
ALCLAD 24S-RT SHEET (Fcy=46000)
ALCLAD 24S-T SHEET (Fcy=39000)
24S-RT SHEET (Fcy=50000)
24ST SHEET (Fcy=40000)
b* = all edges restrained
b = one edge free

Fig. B5-13


BUCKLING COMPRESSIVE STRESS FOR FLAT PLATE ELEMENTS
Aluminum alloy 24 ST extruded sections.
(f_{yp} = 42000 psi)
b = one edge free
b* = all edges restrained
t = thickness of plate element
b = one edge free
b* = all edges restrained
Fcr - Thousands of PSI
b/t
0
10
20
30
40
50
60
70


BUCKLING COMPRESSIVE STRESS FOR FLAT PLATE ELEMENTS
(18-8 Stainless Steel)
b = one edge free
b* = all edges restrained
FULL HARD
1/2 HARD
b* = all edges restrained
b = one edge free
ANNEALED
Fcr - Thousands of PSI
b/t
0
10
20
30
40
50
60
70
80
90
100
110
120
130
140
150
160

by the following equation:-

$$F_{cs} = \frac{\Sigma F_{cr}\, b\, t \text{ (of all plate elements)}}{\Sigma\, b\, t \text{ (of all plate elements)}}$$

$$= \frac{\Sigma\,(f_1 b_1 t_1 + f_2 b_2 t_2 + f_3 b_3 t_3 - - - \text{ etc.})}{\Sigma\,(b_1 t_1 + b_2 t_2 + b_3 t_3 - - - - - - \text{ etc.})}$$

- - - - - - - - - - - -(5)

If the thickness of the plate elements is the same, as is the usual case, then

$$F_{cs} = \frac{\Sigma\,(f_1 b_1 + f_2 b_2 + f_3 b_3 - - -)}{\Sigma\,(b_1 + b_2 + b_3 - - -)} \quad - - - -(6)$$

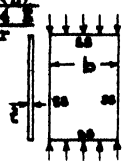
where f_1, f_2, b_1, b_2, t_1, and t_2 etc. refer to the buckling stress, effective width and thickness of plate elements (1) and (2) respectively.

Table B5.1a (24ST Sheet)

Sheet Simply Supported on all Four Sides.

$f_{cr} = 3.64\,\bar{E}\left(\frac{t}{b}\right)^2$

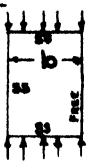
or $b/t = \sqrt{\frac{3.64\,\bar{E}}{f_{cr}}}$



Sheet Simply Supported on 3 Sides, Free on Other

$f_{cr} = .452\,\bar{E}\left(\frac{t}{b}\right)^2$

or $b/t = \sqrt{\frac{.452\,\bar{E}}{f_{cr}}}$



1	2	3	4	5	6	7
f_{cr}(psi)	E' (x10^6)	$\bar{E}$ (x10^6)	$\frac{b}{t}$	f_{cr}	$\bar{E}$	b/t
10000	10.5	10.5	61.8	10000	10.0	21.8
20000	10.5	10.5	43.7	20000	10.5	18.4
27500	10.5	10.5	37.4	27500	10.5	13.2
30000	10.0	10.25	35.3	30000	10.5	12.28
31000	9.15	9.8	33.9	31000	9.8	11.95
32500	7.75	8.97	31.7	32500	8.97	11.18
35000	5.62	7.48	27.9	35000	7.48	9.81
37500	4.40	6.48	25.1	37500	6.48	8.82
40000	3.30	5.42	22.2	40000	5.42	7.81
42500	2.55	4.57	19.8	42500	4.57	6.96
45000	1.90	3.73	17.4	45000	3.73	6.11
47500	1.60	3.31	15.9	47500	3.31	5.58
50000	1.35	2.92	14.6	50000	2.92	5.13
55000	0.90	2.14	12.0	55000	2.14	4.20

Column 2 - Tangent modulus E' obtained from curves in Chapter C1 for 24ST sheet.

Column 3 - $\bar{E}$ = reduced modulus = $\frac{4\,EE'}{(\sqrt{E} + \sqrt{E'})^2}$

where E = Youngs modulus = 10.5×10^6

E' = tangent modulus

The values of the tangent modulus as obtained from the stress-strain curves were for material with E = 10.5×10^6 psi. and yield point 43000 psi. Before plotting the above values of b/t versus f_{cr}, the material is corrected to E = 10.3×10^6 and F_{yp} = 40000 (which are the guaranteed minimum values) by use of correction tables of ANC-5.

Table B5.2

18-8 Stainless Steel - Full Hard Cond.

Sheet Simply Supported on all Four Sides.

$F_{cr} = 3.64\,\bar{E}\left(\frac{t}{b}\right)^2$

or $b/t = \sqrt{\frac{3.64\,\bar{E}}{F_{cr}}}$

Sheet Simply Supported on 3 Sides, Free on Fourth

$F_{cr} = .452\,\bar{E}\left(\frac{t}{b}\right)^2$

or $b/t = \sqrt{\frac{.452\,\bar{E}}{F_{cr}}}$

1	2	3	4	5	6
F_{cr}(psi)	E' (x10^6)	$\bar{E}$ (x10^6)	b/t	F_{cr}	b/t
10000	27	27	99.0	10000	34.8
20000	27	27	70.0	20000	24.6
30000	25.3	26.2	56.5	30000	19.9
40000	23.2	25.05	47.8	40000	16.8
50000	21.3	23.9	41.7	50000	14.7
60000	19.2	22.6	37.0	60000	13.0
70000	17.1	21.2	33.2	70000	11.7
80000	15.2	19.8	30.0	80000	10.56
90000	13.0	18.2	27.1	90000	9.53
100000	11.0	16.4	24.6	100000	8.65
110000	8.9	14.35	21.75	110000	7.65
120000	6.9	13.30	20.1	120000	7.06
130000	4.8	9.52	16.3	130000	5.73
140000	2.8	6.43	12.9	140000	4.53
150000	0.7	2.08	7.1	150000	2.5
154000	0	0	0	154000	0

The effective width is influenced to some unknown degree by the edge or corner condition of the section. Thus a section involving a bend radius would have a different restraining effect than one without a bend radius. Furthermore, many sections have bulb sections at their free ends which influence the effective width. The cross section details of various sections in Figures B5.12 and B5.13 show what has been taken as the effective width (b) for the plate elements in order to make the calculated results check closely with many test results of such sections.

If a plate element is labeled b* in the cross-section figures, it refers to a plate freely supported on all four edges and the buckling stress is determined from the curve for all edges simply supported. If it is labeled (b) it refers to a plate free at one edge and the buckling stress curve for a plate free at one edge is used.

B5.5 Example Problems in Calculating Column Strength of Columns with Open Sections

Example Problem 1

Figure B5.15 shows the cross-section of a column fabricated from 24ST sheet. If the length of the column is 12 inches, what is the

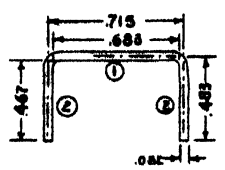


Fig. B5-15

ultimate strength if end fixity C = 1. Also if C = 2

Solution.

The local ultimate crippling strength will first be computed. Consider plate element (1),

$b/t = .683/.032 = 21.3$

From Figure B5.12, F_{cr} = 38400 psi

Plate element (2)

$b/t = .467/.032 = 14.6$

From Figure B5.12, F_{cr} = 20500 psi

Crippling stress for entire section,

$$F_{cs} = \frac{\Sigma F_{cr}\, b}{\Sigma b} = \frac{38400 \times .683 + 20500 \times .467 \times 2}{.683 + 2 + .467}$$

$$= 45380/1.617 = 28100 \text{ psi}.$$

Thus the column section will fail locally at a stress of 28100 psi. The next question is the strength for the given length of 12 inches for fixities of C = 1 and C = 2.

In general, test data show (Ref. 5.2) that the relation of the allowable column stress F_c to the slenderness ratio L/ρ can be expressed closely by Johnson's Parobolic Equation (see Art. B5.3) if the crippling stress F_{cs} is used as the stress at zero L/ρ hence

$$F_c = F_{cs} - \frac{F_{cs}^2\ (L/\rho)^2}{4\ C\ \pi^2\ E} \qquad \text{---------(7)}$$

ρ of our section = .16 inches, hence L/ρ = 12/.16 = 75, using C = 1 and substituting in Equation (7)

$$F_c = 28100 - \left(\frac{28100^2\ (75)^2}{4 \times 1 \times \pi^2 \times 10{,}300{,}000}\right) = 28100 -$$

$$10800 = 17300 \text{ psi}$$

This value F_c could more conveniently be read from the column curves of Figure B1.12. These curves are slightly conservative since E has been taken as 10,000,000. For a fixity of C = 2,

$F_c = 28100 - (1/2)(10800) = 22700$ psi.

Thus the maximum column load for C = 1 = 17300 x .053 = 917 lb. and 22700 x .053 = 1200 lb. for C = 2.

Another semi-empirical method which the author has used to obtain approximate column curve and which appears to check reasonably well with test data is as follows:

Take the calculated crippling stress F_{cs} as the allowable column stress at L/ρ = 20. Take the lowest buckling stress on any element of section as found when computing crippling stress of the section as the point where the true column curve breaks away for the Euler curve for columns with stable sections. Draw a straight line between these two points which is considered as the true column allowable stress curve between these points. Figure B5.16 illustrates this procedure.

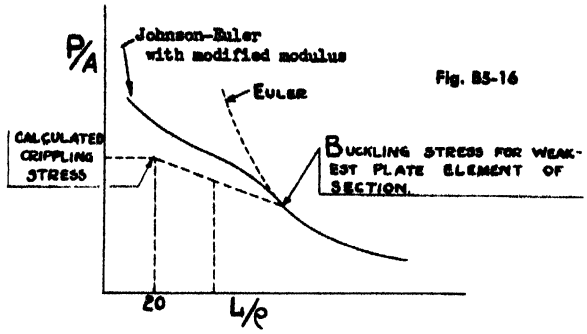


Fig. B5-16

The column strength for our given channel will now be calculated by this method.

Figure B1.10 in Chapter B1 shows the Euler column curve for columns with stable sections for various aluminum alloys. The calculated crippling stress of 28100 psi is located on a L/ρ value of 20. From the buckling stress calculations, plate element (2) was weakest and buckled at 20500 psi. This locates a point on the Euler curve for our given material of 24ST. A straight line is drawn between these two points. For C = 1 the value of L/ρ = 75 and for C = 2 the effective $L/\rho = \frac{12}{\sqrt{2} \times .16} = 53$. The value of 75 lies on the Euler curve and gives a value of 18000 psi. A value of L/ρ = 53 projected to the straight line gives 23000 psi. These allowable stresses are slightly higher than those given by the Johnson-Euler curves of Figure B1.12.

Example Problem 2

Figure B5.17 shows the cross-section of a column 30 inches long made from 24ST alclad sheet. If end fixity coefficient C is taken as 1.5,

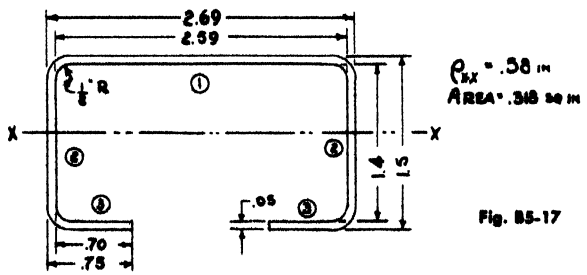


Fig. B5-17

calculate ultimate compressive load that member can carry.

Solution.

Calculation of section crippling strength:

Plate element (1)

$b/t = 2.59/.05 = 51.8$

F_{cr} (from Figure B5.12) = 13800 psi.

Plate element (2)

b/t = 1.4/.05 = 28

F_{cr} (from Figure B5.12) = 31000 psi.

Plate element (3)

b/t = .70/.05 = 14

F_{cr} (from Figure B5.12) = 21300 psi

Hence crippling stress for entire section is

$$F_{cs} = \frac{\Sigma F_{cr}\, b}{\Sigma b} = \frac{13800 \times 2.59 + 31000 \times 1.4 \times 2 + 21300 \times .70 \times 2}{2.59 + 1.4 \times 2 + .70 \times 2}$$

$$= \frac{152300}{6.79} = 22400 \text{ psi}$$

This stress will be used in the Johnson-Euler equation to determine allowable column stress for length of 30 inches with C = 1.5.

$L/\rho = 30/.58 = 51.7$

$$F_c = 22400 - \left(\frac{22400^2 \times (51.7)^2}{4 \times 1.5 \times 2 \times \pi^2 \times 10.3 \times 10^6}\right) = 20200 \text{ psi}$$

From the curves Figure B1.12 using F_c = 22400, C = 1.5 and L/ρ = 51.7, the allowable column stress = 20000 psi.

Calculation of allowable column stress by second empirical method:

$$\text{Effective } L/\rho = \frac{30}{\sqrt{1.5} \times .58} = 42.2$$

On Figure B1.10 for 24ST alclad locate the stress on the L/ρ = 20 line equal to the crippling stress of the section = 22400 psi. The buckling stress for the weakest plate element which is plate element (1) is 13800 psi. Locate this point on the column curve and draw a line between these two points. Taking L/ρ = 42.2 and projecting upward to this line, we obtain a corresponding column stress of 19400 psi as compared to 20200 psi by Johnson-Euler equation.

Column strength = $f_c A$ = 19400 x .318 = 6160 lbs.

Example Problem 3

Determine the ultimate crippling strength for the 24ST extruded zee section of Figure B5.18.

Solution.

Plate element (1)

b/t = 1.314/.093 = 14.1

F_{cr} from Figure B5.13 = 45600 psi.

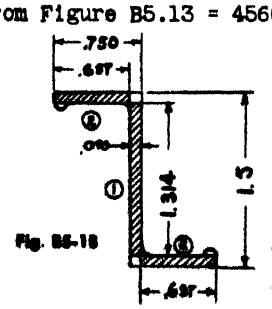


Fig. B5-18

Plate element (2)

Tests in general, show that a bulb at the plate edge does not produce a complete freely supported edge condition thus the effective width is taken to the outside edge of bulb as shown by the cross-hatched area in Figure B5.18.

b/t = .657/.093 = 7.05

F_{cr} from Figure B5.13 = 53000 psi.

$$\text{Section } F_{cs} = \frac{\Sigma F_{cr}\, b}{\Sigma b} = \frac{45600 \times 1.314 + 53000 \times .657 \times 2}{1.314 + .657 \times 2}$$

$$= \frac{129600}{2.628} = 49300 \text{ psi.}$$

Example Problem 4 (Stainless Steel Section)

Figure B5.19 shows the cross-section of a stainless steel column member. If the material is in full hard condition, and the member is 8

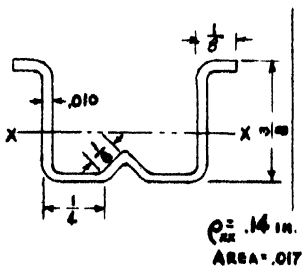


Fig. B5-19

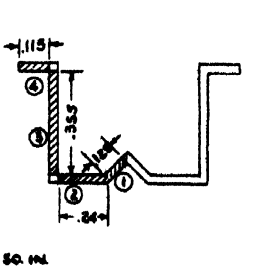


Fig. B5-20

inches long, calculate the ultimate conpressive strength if end fixity C = 2.

Solution.

The crippling stress for the entire section will be calculated first. The section is split up into the four plate elements as shown in Figure B5.20.

Consider plate element (1)

b/t = .125/.01 = 12.5

From Figure B5.13 for plate simply supported at all edges and for full hard condition,

F_{cr} = 141000 psi.

Plate element (2)

b/t = .24/.01 = 24

F_{cr} = 101500 psi

Plate element (3)

b/t = .355/.01 = 35.5

F_{cr} = 64000 psi.

Plate element (4)

b/t = .115/.01 = 11.5

From Figure B5.13, using curve for plate free at one edge,

F_{cr} = 71000 psi

Since this value is greater than the 64000 for plate element (3), no doubt element (4) would tend to buckle at the same stress as (3) since element (4) is only stabilized by element (3). Thus 64000 psi will be taken as F_{cr} of element (4).

Section crippling stress $F_{cs} = \frac{\Sigma F_{cr}\, b}{\Sigma b}$

hence

$$F_{cs} = \frac{141000x.125x2+101500x.24x2+64000x.355x2+64000x.115x2}{.125x2+.24x2+.355x2+.115x2}$$

$$= \frac{144100}{1.67} = 86300 \text{ psi.}$$

The length of the member is 8 inches and least radius of gyration is .14 inches hence $L/\rho = 8/.14 = 57$.

The only sure way of obtaining the column strength for the given section would be to make a series of tests on various lengths in order to obtain the complete column curve. Experience has shown that the use of the Johnson-Euler column equation, using the section crippling stress as the stress at $L/\rho = 0$, checks actual tests fairly well. Fig. B1.13 of Chapter B1 shows a plot of the Johnson-Euler equation for steel with a modulus of 28,000,000 psi. Using the curves which are plotted for C = 2, we obtain 75000 psi. as the allowable column stress for $L/\rho = 57$ for a curve which begins at $L/\rho = 0$ at a stress of 86300 psi, which equals the calculated section crippling stress.

The other empirical method is the same as that given in the previous examples, which gives the following result:

Effective column length $L' = 8/\sqrt{2} = 5.67$

$L'/\rho = 5.67/.14 = 40.4$

On the column curve of Figure B1.11 of Chapter B1, locate point on $L/\rho = 20$ line equal to 86300 psi (the calculated section crippling stress). The first plate element buckles at 64000 psi. This stress on the column curve is taken as the point where the column strength of our particular section begins to break away from the plotted curve. Draw a straight line between these two points. Using an L/ρ value of 40.4, this line is intersected at a stress of 72000 psi, which is the estimated column allowable stress.

The column strength equals f_c A or 75000 x .017 = 1275# in one case, and 72000 x .017 = 1221# in the other case.

B5.6 Members with Lightening Holes

For members with flanged lightening holes, a section should be used through the hole and the plate element with the hole can be considered as simply supported at each side. If the hole is unflanged, the strength of each element can be taken as the average between a plate freely supported and one that is free. This

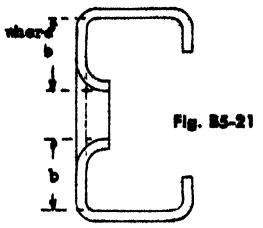


Fig. B5-21

empirical procedure compares well with tests. (Ref: 5.2).

B5.7 Ultimate Crippling Stress of Closed Sections

For an open section as explained in the previous article, the crippling strength of the entire section is obtained by adding up the buckling strengths of the various flat plate elements of the section. For a closed section that procedure is too conservative. The side of a square tube or a closed section composed of flat plate elements can buckle, but since the section is closed, a stabilizing influence on the section as a whole still remains and permits the material at the corner portions to continue to take load after the middle portion of the plate elements have buckled.

A close approximation of the ultimate crippling stress for a square tube or a closed section with flat sides can be found by a consideration of effective widths as discussed in Chapter B4.

From equation (4) of Chapter B4 and using a constant of 1.7 instead of 1.9 to be conservative, we obtain

$w = 1.70\, t \sqrt{E/f_{yp}}$, when effective width w is assumed stressed to yield point f_{yp}.

Total load on w, $P = f_{yp}\, t\, w$ ----------(a)

Let b = width of plate element and F_{cs} the average stress on plate element at which ultimate crippling occurs.

Thus P also equals $F_{cs}\, b\, t$ ----------(b)

Equating (a) to (b) and solving for F_{cs}

$$F_{cs} = \frac{1.7\sqrt{E\, f_{yp}}}{b/t} \text{ ----------(8)}$$

For stresses above the elastic limit, a reduced modulus $\bar{E}$ should be used, hence

$$F_{cs} = \frac{1.7\sqrt{\bar{E}\, f_{yp}}}{b/t} \text{ ----------(9)}$$

where $\bar{E} = \frac{4\, EE'}{(\sqrt{E} + \sqrt{E'})^2}$

E' = tangent modulus.

E = Young's modulus

Figure B5.22 shows a plot of equation (9) for aluminum alloy and stainless steel materials. The values of the tangent and the reduced modulus

Fig. B5-22

18-8 STAINLESS STEELS

Local crippling stress for square tubes

$$f_{cr} = \frac{1.7\sqrt{\bar{E} f_{cy}}}{b/t}$$

($\bar{E}$ = reduced modulus)

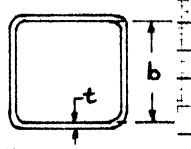


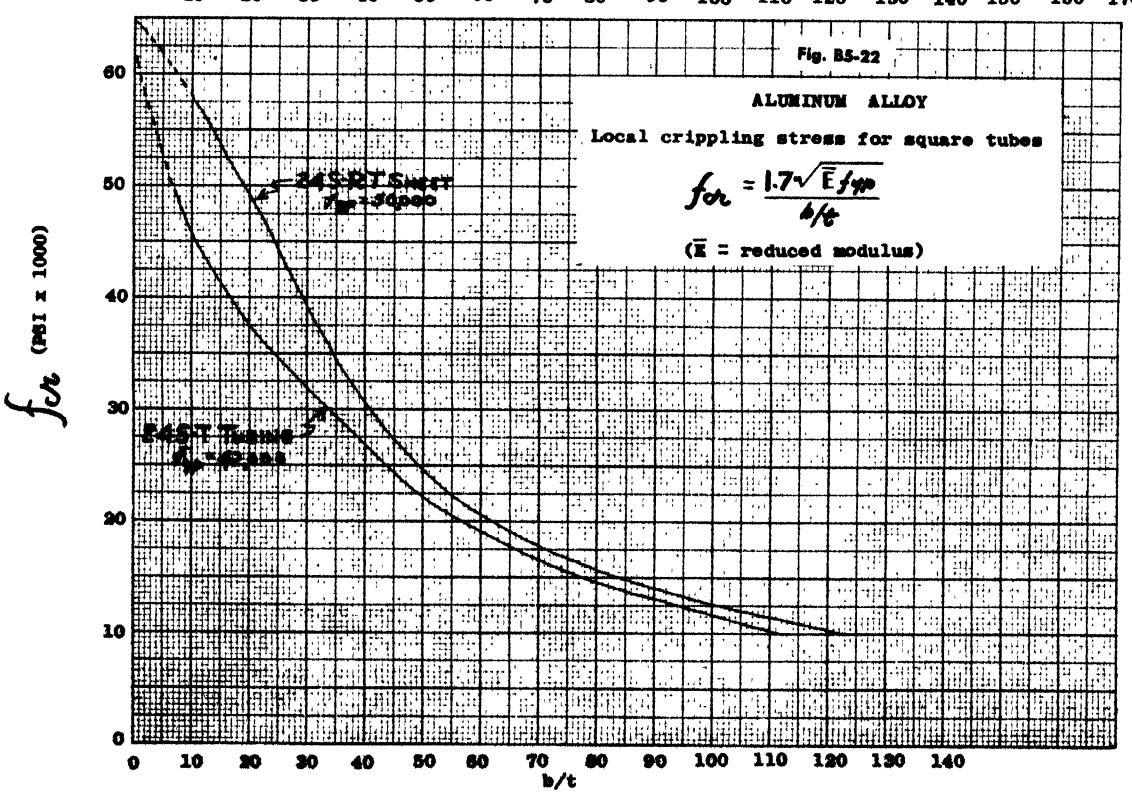
Fig. B5-22

ALUMINUM ALLOY

Local crippling stress for square tubes

$$f_{cr} = \frac{1.7\sqrt{\bar{E} f_{cy}}}{b/t}$$

($\bar{E}$ = reduced modulus)



$\bar{E}$ are the same as used in Art. B5.4.

To find the ultimate compressive strength of the entire closed section, a summation of the ultimate strengths of the various plate elements is made as explained for open sections. (See Art. B5.4 equations (5) and (6).)

ILLUSTRATIVE PROBLEMS

Example Problem 1.

Determine the ultimate column strength of a 1-1/4 - .035 24ST square tube 30 inches long if end fixity C = 1, also if C = 2.

Solution.

The local crippling stress will first be calculated.

b/t ratio for tube-side wall = $\frac{1.25 - .070}{.035} = 33.7$

From the crippling stress curve for 24ST tubing (Figure B5.22), we obtain F_{cs} = 29700 psi. as the local strength of the tube. For column strength, we refer to Figure B1.10 of Chapter B1.

$L/\rho = 30/.489 = 61.4$

hence

F_c = 25400 psi. which is less than the local crippling strength of 29700.

Area of tube = .1599

Therefore tube strength = .1599 x 25400 = 4060#

For end fixity of C = 2, the effective length = $30/\sqrt{2} = 21.2$. Then $L/\rho = 21.2/.489 = 43.3$.

From Figure B1.10, F_c = 33000 psi., which is greater than the local crippling strength, hence tube strength is equal to 29700 x .1599 = 4750#.

Example Problem 2.

Determine the column strength of a 5/8 - .022 stainless steel square tube (full hard condition) for a length of 20 inches when end fixity C = 1-1/2.

Solution.

b/t for tube side wall = (.625 - .044)/.022 = 26.4

From Figure B5.22 for full hard condition crippling stress = 98300 psi.

Effective column length for C = 1.5 = $L' = 20/\sqrt{1.5} = 16.3$

$L'/\rho = 16.3/.26 = 62.7$

From Figure B1.11, allowable column stress = 51300 psi.

Therefore column will fail by column instability instead of local crippling.

Column strength P = $F_c A$ = 51300 x .0483 = 2480#

Example Problem 3

Determine the ultimate crippling stress for the closed stainless steel section of Figure B5.23. The material is in the full hard condition.

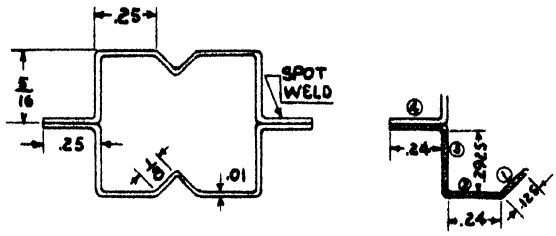


Fig. B5-23

Solution.

The section is considered as composed of the four plate elements as shown in Figure B5.23.

The ultimate crippling stress will be calculated for each plate element.

Plate element (1)

b/t = .125/.01 = 12.5

F_{cs} from Figure B5.22 = 138000 psi.

Plate element (2)

b/t = .24/.01 = 24

F_{cs} = 104500 psi.

Plate element (3)

b/t = .2925/.01 = 29.25

F_{cs} = 91700 psi

Plate element (4)

The two legs are spot welded together thus they will be considered as one plate with .02 thickness.

The buckling strength of this element which has one edge free is taken from the curve on Fig. B5.13 for a b/t = .24/.02 = 12 and equals 68000 psi.

The crippling stress for entire section is

$$F_{cs} = \frac{\Sigma F_{cs}\, b\, t}{\Sigma\, bt}$$

$$F_{cs} = \frac{4(138000x.125+104500x.24+91700x.2925).01+68000x.24x2x.02}{4(.125+.24+.2925).01+.24x2x.02}$$

$$= 3420/.0359 = 95300 \text{ psi}$$

For a given column length, the column strength could be found as illustrated in the previous two examples.

B5.8 Crippling Stress of Sections With Combined Curved and Flat Plate Elements

It is common practice to use stiffener sections as illustrated in Figure B5.24 which involve

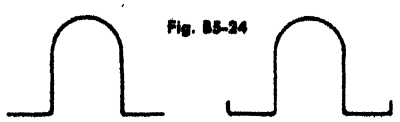


Fig. B5-24

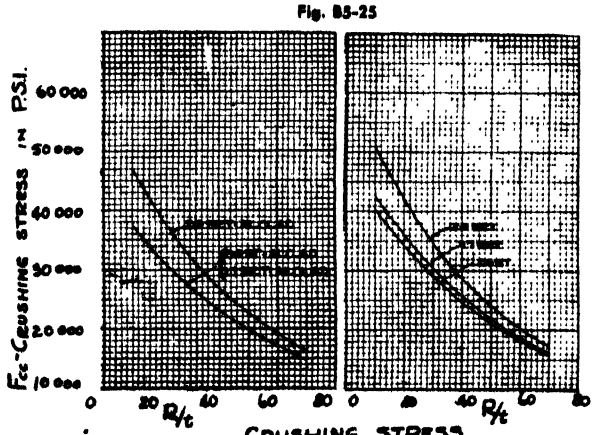
both flat and curved plate elements. Test on curved panels tend to indicate that the buckling stress and the ultimate stress are practically the same. The following empirical procedure seems to check reasonably well with the meager test results which are available and is satisfactory for preliminary design but should be checked by tests for final design.

(1) If the critical buckling stress of no flat plate element of the section is reached before the buckling stress of the curved element is reached, than the crippling stress for the entire section is taken equal to the buckling stress of the curved element.

(2) If the critical buckling stress of any of the flat plate elements is below the buckling stress of the curved plate element, then the maximum load carried by the section equals the buckling loads on the flat plate elements which have buckled, plus the buckling stress of the weakest curved portion, times the remaining area of the elements which have buckling stresses above that calculated above.

For practical aluminum alloy stiffeners as illustrated in Figure B5.24, the r/t values are usually relatively small, very seldom over 30, thus it seems appropriate to use the crippling stresses for aluminum alloy circular corrugations as given in ANC.5, and which are given in Figure B5.25.

Fig. B5-25



CRUSHING STRESS FOR CORRUGATED ALUMINUM ALLOY SHEET

Example Problem.

Figure B5.26 shows a typical stringer section. If the material is 24SRT aluminum alloy, calculate the ultimate crippling stress for the section.

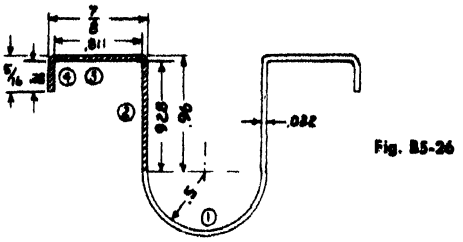


Fig. B5-26

Solution.

Consider curved plate element (1)

$r/t = .516/.032 = 16.1$

From curve Figure B5.25

$F_{cr} = 45000$

Flat plate element (2)

$b/t = .928/.032 = 29.1$

From curve Figure B5.12

$F_{cr} = 37500$ psi.

Flat plate element (3)

$b/t = .811/.032 = 25.4$

$F_{cr} = 42000$ psi.

Flat plate element (4)

$b/t = .28/.032 = 8.75$

From Figure B5.12, use curve for plate with one edge free.

$F_{cr} = 42500$ psi.

Crippling stress for section

$$F_{cs} = \frac{\Sigma F_{cr}\, b}{\Sigma\, b}$$

$$= \frac{45000x\pi x.516+37500x.928x2+42000x.811x2+42500x.28x2}{\pi x.516+.928x2+.811x2+.28x2}$$

$$= \frac{234400}{5.66} = 41400 \text{ psi.}$$

For any given length the column strength can be found as illustrated in previous examples.

PROBLEMS

(1) Determine the column strength of a 1-1/4 x 1-1/4 x 3/32 24ST extruded angle 28 inches long if end fixity C = 1.5. Find strength also for C = 2.

(2) The channel section in Fig. B5.27 is 16 inches long and is fabricated from 24ST alclad. Determine the column strength if C = 1. Also if C = 2.0.

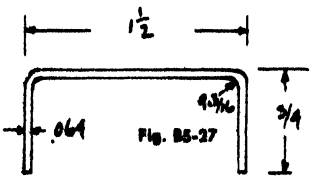


Fig. B5-27

(3) The section of B5.28 is 32 inches long. Calculate the ultimate compressive strength if C = 2. The material is 24ST aluminum alloy.

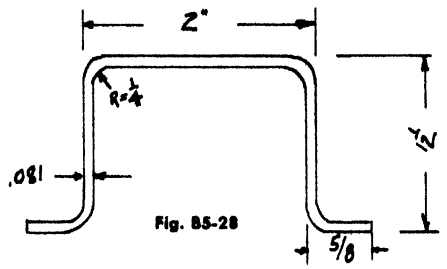


Fig. B5-28

(4) Determine the crippling stress for the extruded 24ST bulb angle section of Fig. B5.29.

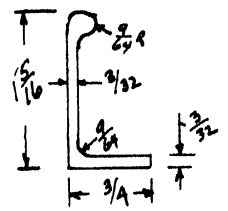


Fig. B5-29

AREA = .231 □"

(5) Determine the crippling stress for the extruded T section of Fig. B5.30.

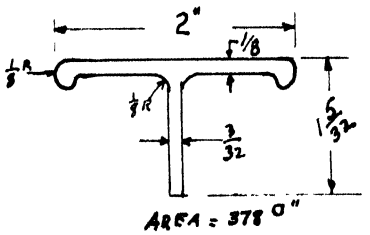


Fig. B5-30

AREA = .378 □"

(6) Determine the crippling stress for the stainless steel section of Fig. B5.31, if material is in the full hard condition. If length is 18 inches and C = 2 what is the column strength.

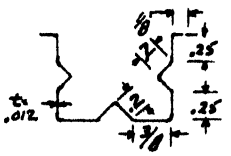


Fig. B5-31

(7) Determine the strength of a 24ST square tube 27 inches if C = 1.5. The outside dimensions of the tube is 1-1/4 inches and the wall thickness is .058 inches.

(8) Determine the crippling stresses for the two sections of Figs. B5.32 and B5.33 if material is 24SRT alclad.

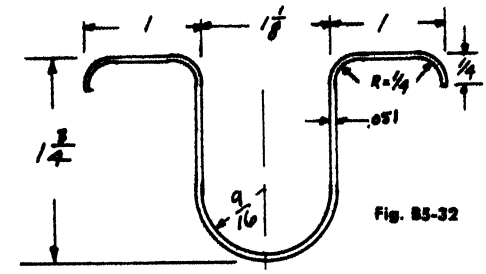


Fig. B5-32

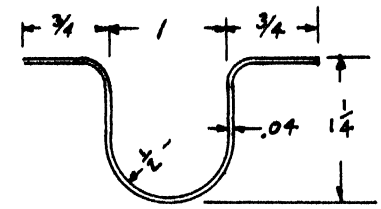


Fig. B5-33

REFERENCES

(5.1) Stowell and Lundquist, "local instability of Columns with I, Z, Channel and Rectangular Tube Sections". NACA Tech. Note No. 743.

(5.2) "Progress Report on Methods of Analysis Applicable to Monocoque Aircraft Structures" Air Corps Information Circular No. 713 (1939)

CHAPTER B6
COMPRESSIVE STRENGTH OF SHEET-STIFFENER UNITS

B6.1 Introduction

Possibly the most common type of metal airplane structural design is the use of flat or curved sheet as the surface covering which is stiffened by attached stringers running parallel to the bending stresses. Figure B6.1 illustrates such types of structures.

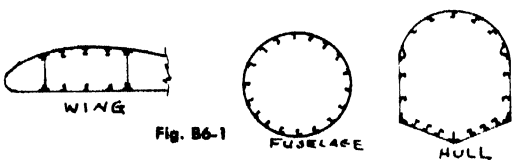


Fig. B6-1

In tension the sheet and stiffeners are equally effective, however, under compressive stresses, the sheet and stiffeners are not equally effective under all stress intensities. The determination of this combined effective strength of a sheet stiffener unit is thus a necessary consideration in the design of a large proportion of the so-called stressed-skin structures.

Chapter B1 considered the column strength of stiffeners with stable cross-sections. Chapter B4 considered sheet effective widths and Chapter B5 considered the crushing or local crippling strength of stiffener sections. This chapter makes use of this information in considering the compressive strength of the combined sheet-stiffener unit.

B6.2 Sheet Effective Widths

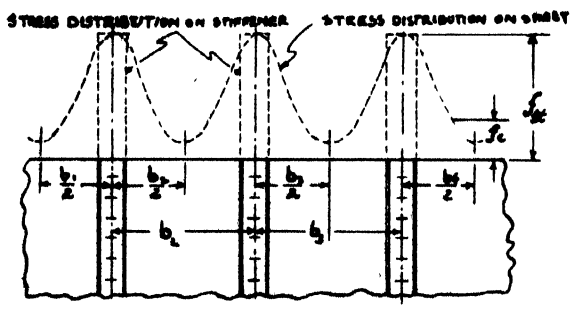


Fig. B6-2

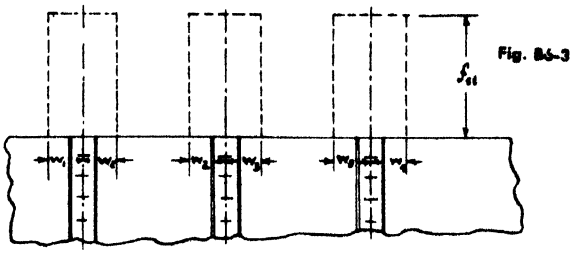


Fig. B6-3

Figure B6.2 shows the compressive stress distribution on a flat sheet stiffened with stringers parallel to the applied compressive load. Over the stiffeners, the sheet and the stiffener have the same stress intensity but between stiffeners the sheet stress falls off in the general manner as indicated.

Figure B6.3 shows a convenient assumption in which the variable compressive stress on the sheet is replaced by an effective width w_1, w_2, etc., which carries the same stress intensity as the stiffener and whose widths w are such as to make the total sheet load equal to the original sheet with its varying compressive stress distribution as shown in Figure B6.2. Chapter B4 should be referred to for the various expressions which have been derived for calculating the effective width w_e.

The total compressive load P on a stiffener plus its effective sheet width then equals

$$P = f_{st} (A_{st} + w_e t) \text{ - - - - - - - - - - - -(1)}$$

where

f_{st} = stress in stiffener in psi.

A_{st} = area of stiffener in square inches.

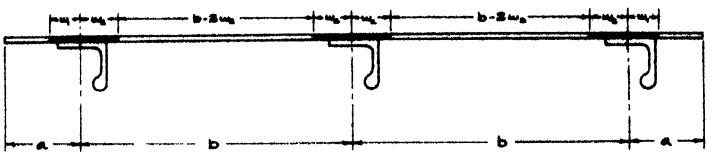
t = sheet thickness in inches.

w_e = effective width of sheet acting with stiffener.

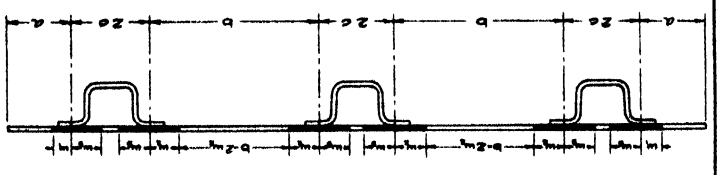
Figure B6.4 and Table B6.1 gives the recommendations of ANC-5 for sheet effective widths.

B6.3 Estimation of Compressive Strengths of Sheet-Stiffener Panels

If the axis for the least radius of gyration of the stiffener section is parallel to the panel sheet to which it is attached and the stiffener does not fail through torsional instability, the compressive strength of a sheet-stiffener panel can be calculated fairly well without resort to tests or sufficient information can be obtained for preliminary design. This is due to the fact that the stiffener tested alone fails in the same manner as when attached to the sheet.



(a) PANEL WITH STIFFENERS HAVING A SINGLE LINE OF CONNECTION TO THE SHEET



(b) PANEL WITH STIFFENERS HAVING A DOUBLE LINE OF CONNECTION TO THE SHEET

Fig. B6-4

Table B6.1

EFFECTIVE WIDTH CONSTANTS FOR ALUMINUM ALLOY SHEET

	Stiffener	w	*C for (Eq)	*Max (refer to Fig. B6.4)
Stiffeners Having Single Line of Connection	Edge	w_1	.60	a
	"	w_2	.85	b/2
	Intermediate	w_2	.85	b/2
Stiffeners Having Double Line of Connection	Edge	w_1	.60	a
	"	w_2	.85	b/2
	"	w_3	.85	c
	Intermediate	w_2	.85	b/2
	"	w_3	.85	c

NOTE: The above contents apply when the sheet remains unbuckled between rivets and when $\sqrt{\frac{E}{f_c}}\frac{t}{b}$ does not exceed 0.4.

* $w = Ct\sqrt{E/F_c}$ (Ref. ANC 5)

The general method to be used is essentially that proposed by Lundquist (Ref. 6.1). In this method, we need to know the complete column curve for the stiffener acting alone. This problem is considered in Chapters B1 and B5. The general procedure is a trial and error process. The author suggests the following procedure:

(1) Assume an effective width of sheet of 30t acting with each rivet line or attachment line of sheet to stiffener and calculate the column strength for the section. For pin end conditions use C = 1 and for flat ends use C from 2 to 3.

(2) Compute the effective sheet width for the column stress obtained in step (1). If this effective width is different than the width of 30t as assumed in (1), modify the effective width and compute the new section properties of stiffener with the new assumed effective sheet. Compute the column strength of this new section and the effective sheet due to this column strength. Repeat this process until the assumed effective sheet width equals the calculated width.

EXAMPLE PROBLEM NO. 1

Figure B6.5 shows a sheet stiffener panel 12" long. The details of the channel type stiffener are given in Figure 6.6. If all material is 24ST aluminum alloy and end fixity of panel is assumed as C = 2 what is the strength of an intermediate stiffener plus it effective sheet if rivet spacing is assumed small enough to prevent buckling of sheet between rivets at stresses below the stiffener column strength.

Solution.

The width of the effective sheet, which can be considered as carrying the same stress as the stringer, depends on the stringer stress. The stringer ultimate stress is determined by the column strength of the stringer plus its effective sheet width. Thus the method in general must be a trial and error method.

As discussed in Chapter B5, the column curve for a channel section follows the Johnson parabola quite well if the crippling stress is used as the column stress at $L/\rho = 0$.

In example Problem (1) of Art. B5.5, the crippling stress for this identical channel was computed and the results gave

F_{cs} = 28,100 psi.

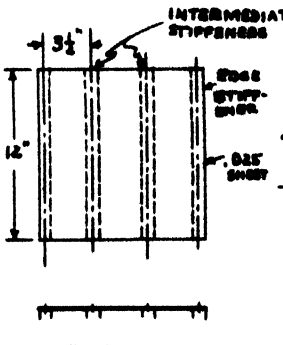


Fig. B6-5

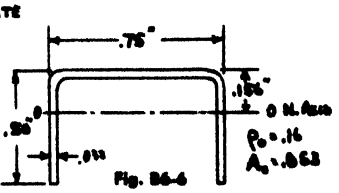


Fig. B6-6

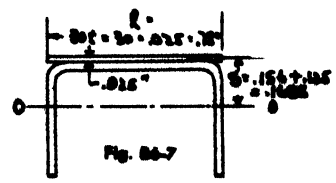


Fig. B6-7

The effective sheet width acting with an intermediate stiffener will be assumed as equal to 30t = 30 x .025 = .75 inches. Figure B6.7 shows the resulting section. To obtain the allowable column stress for this section the radius of gyration must be determined. Mr. R. J. White of C.I.T. (Ref. 6.3) has developed equation (2) which gives the variation in the radius of gyration in terms of the known variables for any stiffener cross-section. Since the failing stress of a column is directly proportional to

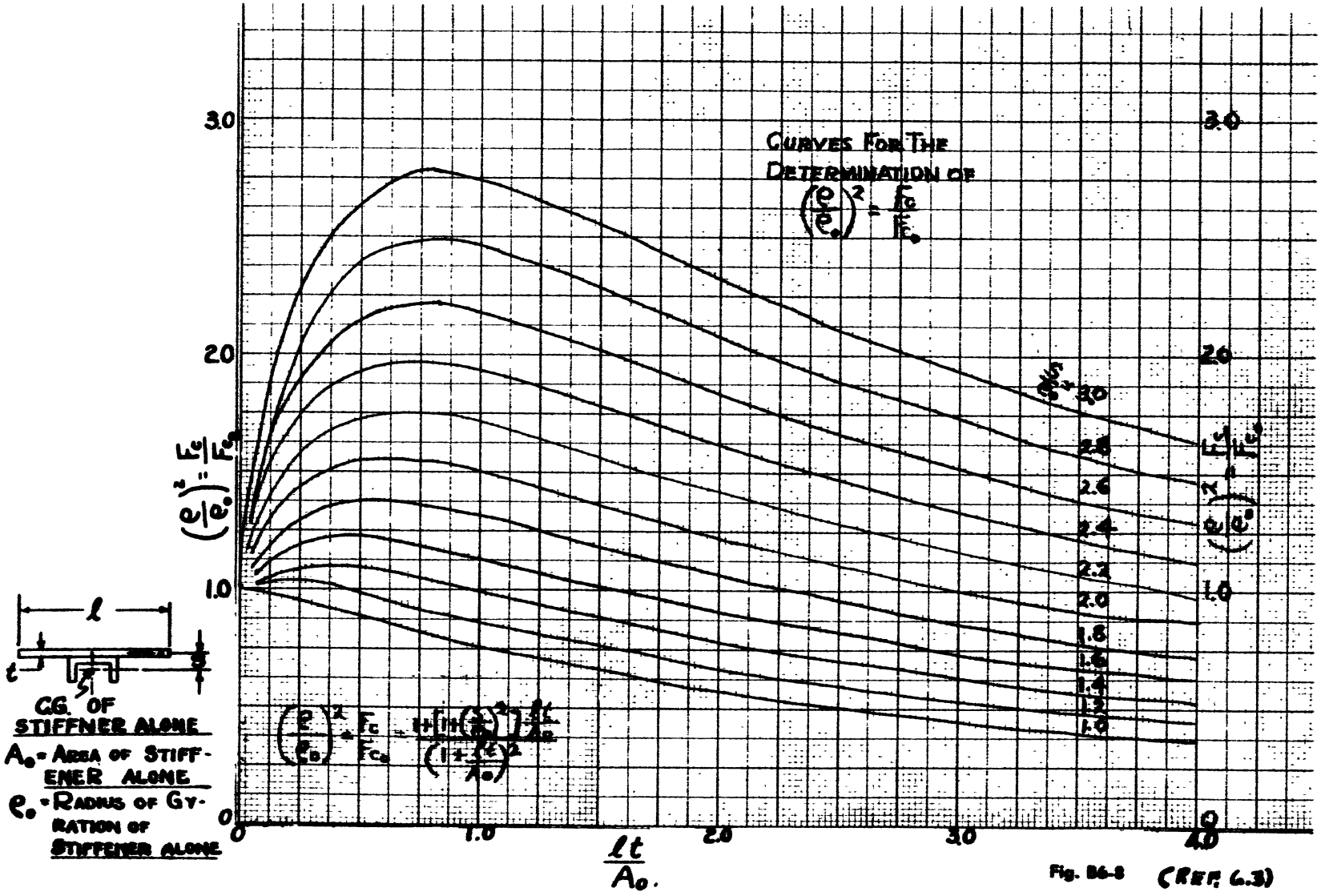


Fig. B6-8 (REF. 6.3)

the radius of gyration squared equation (2) can be equated to the ratio of the column stresses.

$$\left(\frac{\rho}{\rho_o}\right)^2 = \frac{F_c}{F_{co}} = \frac{1+\left[1+\left(\frac{S}{\rho_o}\right)^2 \frac{\ell t}{A_o}\right]}{\left(1+\frac{\ell t}{A_o}\right)^2} \quad \text{------(2)}$$

ρ_o = radius of gyration of stiffener alone.

ρ = radius of gyration of stiffener plus effective sheet

A_o = area of stiffener alone.

S = distance from center of sheet to neutral axis of stiffener.

t = thickness of sheet.

ℓ = total width of sheet assumed acting with stiffener.

Equation (2) has been put in curve form. (Figure B6.8).

The radius of gyration of the section of Figure B6.7 will now be calculated using the curves of Figure B6.8

S = .156 + .0125 = .1685 inches

ρ_o = .16 inches. (given in Figure B6.6), hence

$\frac{S}{\rho_o}$ = .1685/.16 = 1.052

ℓ = 30t = .75 inches, A_o = .053 (Fig. B6.6)

$\frac{\ell t}{A_o} = \frac{.75 \times .025}{.053} = .354$

From curves of Figure B6.8 for above values of S/ρ_o and $\frac{\ell t}{A_o}$, we obtain $\left(\frac{\rho}{\rho_o}\right)^2 = .925$, from which $\rho = .158$"

From Chapter B1, Johnson's parabolic column equation is,

$$F_c = F_{cs} - \frac{F_{cs}^2\left(\frac{L}{\rho}\right)^2}{4C\pi^2 E} \quad \text{----------(3)}$$

The crippling stress F_{cs} for our section is 28,100 psi. For a 12" panel length L/ρ = 12/.158 = 76. C is given as 2. Hence substituting in equation (3)

$$F_c = 28{,}100 - \frac{\overline{28{,}100}^2 \times 76^2}{4 \times 2 \times \pi^2 \times 10.3 \times 10^6}$$

$$= 28{,}100 - 5580 = 22{,}520 \text{ psi.}$$

The equation for sheet effective width as recommended by ANC-5 will be used in this example.

$w = 1.7t\sqrt{\frac{E}{F_c}}$ (See Table B6.1), hence

$$w = 1.7 \times .025 \times \sqrt{\frac{10300000}{22520}} = .91 \text{ inches}$$

This effective width is greater than the .75 inches which was assumed as acting with the stiffener. This greater width will change the radius of gyration of the section which in turn effects the column strength, thus a second guess for the effective sheet width must be made and the calculations repeated to see if the calculated effective width w checks the assumed width.

Take ℓ = .92"

$$\frac{\ell t}{A_o} = \frac{.92 \times .025}{.053} = .434$$

From curves Figure B6.8, $\left(\frac{\rho}{\rho_o}\right)^2 = .950$, hence $\rho = .156$

$L/\rho = 12/.156 = 77^2$

$$F_c = 28{,}100 - \frac{\overline{28100}^2 \times 77^2}{4 \times 2 \times \pi^2 \times 10.3 \times 10^6} = 22280 \text{ psi.}$$

$$w = 1.7 \times .025\sqrt{\frac{10300000}{22280}} = .915 \text{ inches which}$$

checks the assumed .92.

Therefore, the total allowable compressive load on a stiffener plus its effective sheet equals,

$$P_{total} = F_c (A_{st} + w\,t)$$

$$= 22280\ (.053 + .92 \times .025) = 1695\#$$

The student should solve the problem using the other expressions for sheet effective width as given by equations (5) and (10) of Chapter B4.

End Stiffeners of Sheet Stiffener Panel

Figure (A) illustrates the edge stiffener of the panel of Figure B6.5. The edge of the panel plate (ee of Figure A) represents a plate where one edge is free and the other 3 sides are restrained.

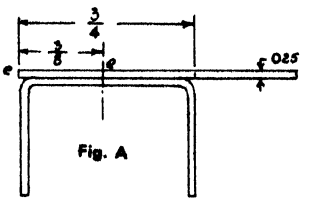


Fig. A

In Chapter B5 equation (3), the buckling stress for a flat plate free at one edge and simply supported on the other three sides is given by

$$F_{cr} = .452\ E\left(\frac{t}{b}\right)^2 \quad \text{----------(4)}$$

Therefore the crippling stress for the edge plate ee of Figure (A) is

$$F_{cr} = .452 \times 10{,}300{,}000 \times \left(\frac{.025}{.375}\right)^2 = 20{,}700 \text{ psi.}$$

If this buckling stress is greater than the column strength of the stiffener then the entire distance of 3/8 inch would be effective. If less than the column strength of the stiffener the effective width of the edge plate can be determined by the following equation:

$$w_{(edge)} = a\frac{F_{cr}}{F_c} \quad \text{----------(5)}$$

where

a = distance from rivet line to edge of sheet.

F_{cr} = buckling stress for sheet designated by (a) and computed by equation (4).

F_c = column strength of stiffener plus total effective sheet acting as a column unit.

In the foregoing example dealing with an intermediate stiffener the effective sheet width was found to be .92 inches which is more than is available for the edge stiffener. The column strength for an intermediate stiffener was 22,280 psi. The column strength F_c for the edge stiffener will be higher since less effective sheet area will increase the radius of gyration of the column unit. Thus it will be slightly conservative to use the column strength of an intermediate stiffener for the edge stiffener in computing effective width of edge plate (a) of Figure A, hence

$$w_{(edge)} = a\frac{F_{cr}}{F_c} = .375 \times \frac{20700}{22280} = .35 \text{ inches}$$

Thus the total sheet acting with edge stiffener is .35 + .92/2 = .81 inch as shown in Figure B. The total load carried by edge stiffener unit will equal 22280 (.053 + .81 x .025) = 1620#

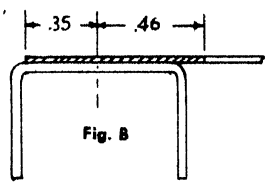


Fig. B

ANC-5 (See Table B6.1) recommends that the effective width of edge plate be calculated by equation

$$w = ct\sqrt{E/F_{co}}, \text{ where } C = .60$$

Substituting

$$w = .60 \times .025\sqrt{\frac{10300000}{22280}} = .32 \text{ inches as}$$

compared to .35 calculated above.

When the sheet and stiffener are made from different aluminum alloys and rivet spacing is such as to permit buckling of sheet between rivets, a method of approach as proposed by Fischel and illustrated in Example Problem 2 is recommended.

Example Problem 2

Figure B6.9 shows a sheet-stiffener panel 20 inches long. The sheet material is 24ST alclad and the stiffener material is 24SRT. Figure B6.10 gives details of the stiffener section. The sheet is attached to stiffeners with rivets at 1 inch spacing.

Let is be required to determine the effective width of sheet acting with the stiffener and the ultimate compressive strength of a stiffener unit for a length of 20 inches when the end fixity of panel is taken as C = 2.

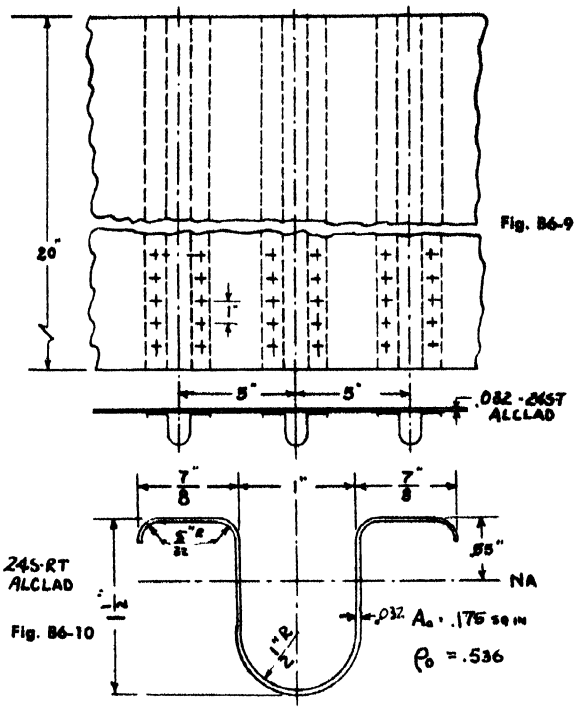


Fig. B6-9

Fig. B6-10

Solution.

In this solution, the method proposed by Fischel for determining the sheet effective width will be used. This method as explained by Fischel is given in detail in Chapter B4.

Since the effective sheet width is a function of the stiffener stress, the ultimate column strength of the stiffener must be calculated. This column strength depends on the radius of gyration of the section which in turn is influenced by the amount of effective sheet, thus the general solution falls in the trial and error category.

Tests have shown that a stiffener section of this type attached to sheet gives a column curve which follows the Johnson parabola if the crippling stress is taken as the column strength at $L/\rho = 0$.

In the example problem of Art. B5.8 of Chapter B5, the crippling stress of this same stiffener was computed and gave a result of F_{cs} = 41400 psi but for 24SRT material. If 24SRT alclad material is used the result would be 38500 psi. (Student should check this value).

As a trial effective sheet width, a length of sheet equal to 30t will be assumed acting with each rivet line (Figure B6.11).

The radius of gyration of this composite section will be computed using the curves of Figure B6.8.

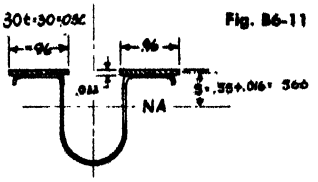


Fig. B6-11

$S = .566$

$\rho_0 = .536$ (Figure B6.10)

$\frac{S}{\rho_0} = .566/.536 = 1.058$

$\ell = .96 + .96 = 1.92$

$\frac{\ell t}{A_0} = \frac{1.92 \times .032}{.175} = .35$

From curve Figure B6.8 $\left(\frac{\rho}{\rho_0}\right)^* = 97$, hence $\rho = .528$

$\frac{L}{\rho}$ for 20 inch length stiffener unit $= \frac{20}{.528}$ = 37.8, using Johnson's column formula

$$F_c = F_{cs} - \frac{F_{cs}^* \left(\frac{L}{\rho}\right)^*}{4\ C\ \pi^*\ E}$$

$$F_c = 38500 - \frac{38500^* \times 37.8^*}{4 \times 2 \times \pi^* \times 10.3 \times 10^6} = 38500 - 2600$$

$= 35900$ psi.

From Fig. B4.5 of Chapter B4 we find that the effective width for .032 24ST alclad sheet with a 24SRT alclad stiffener stress of 35900 psi. equals 1.37 inches approximately. From Figure B4.4 of Chapter B4, we find that a rivet spacing of 1 inch on .032 sheet causes the sheet to buckle between rivets when the 24SRT stiffener stress is 35000 psi. Hence the corrected effective sheet width is $\frac{35000}{35900} \times 1.37 = 1.34$ inches.

This effective width is different than the value of .96 inches assumed, thus the above process will be repeated using an effective sheet width of 1.34 inches with each rivet line.

$\frac{\ell t}{A_0} = \frac{2 \times 1.34 \times .032}{.175} = .490$

$\frac{S}{\rho_0} = 1.058$ (as before)

From curves Fig. B6.8

$\left(\frac{\rho}{\rho_0}\right)^* = .925$, hence $\rho = .515$

$L/\rho = 20/.509 = 38.8$

$$F_c = 38500 - \frac{38500^* \times 38.8^*}{4 \times 2 \times \pi^* \times 10.3 \times 10^6} = 35800 \text{ psi.}$$

From Figure B4.5 for a stiffener stress of 35800 the effective width for .032 sheet is again 1.37 inches within the accuracy of reading the curves.

Correcting the effective width for buckling stress of sheet between rivets as before

$w = 1.37 \times 35000/35800 = 1.34$"



Thus the total area of stiffener and effective sheet equals .175 + 2 x 1.34 x .032 = .256 sq. in.

Total compressive load taken by one stiffener with effective sheet equal .256 x 35800 = 9160 lb.

B6.4 General Information on Design of Stiffeners and Sheet-Stiffener Units.

Stiffeners should be designed to take as high an allowable compressive stress as possible over the length to be used in order to make the effective sheet more efficient from a load carrying standpoint. To illustrate this fact, the load carried by the effective sheet will be calculated for a stiffener stress of 20000 and 40000 psi. using the equation

$w = 1.7t \sqrt{E/F_{st}}$

as recommended by ANC-5.

For $f_{st} = 20000$, $t = .04$ and $E = 10 \times 10^6$

$w = 1.7 \times .04 \sqrt{10{,}000{,}000/20000} = 1.52$ inches

hence load on effective sheet = 1.52 x .04 x 20000 = 1210#

For $f_{st} = 40000$, $t = .04$

$w = 1.7 \times .04 \sqrt{10{,}000{,}000/40000} = 1.075$". Load = 1.075 x .04 x 40000 = 1720#

There is an additional increment of strength in favor of the high strength stiffener and less effective width of sheet since in general adding sheet to the stiffener section decreases the radius of gyration of the composite section as compared to the stiffener alone which results in a lower column strength.

Stiffeners composed of closed sections as illustrated in Figure B6.12 in general offer greater resistance to local crippling and also stability against twisting failure as found in some open and unsymmetrical sections. For efficient column strength the radius of gyration should be as large as possible, that is, the material must be spread out. This requirement tends toward thin plate elements for the section. To increase the local crippling strength resort is made to grooves or lightening holes as illustrated in Figure B6.13. The chief objection to closed sections is the possibility of corrosion on the inside which cannot be inspected.

Fig. B6-12

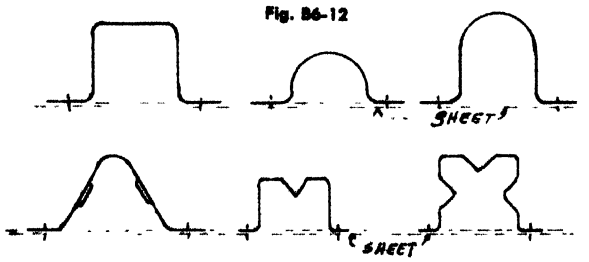


Fig. B6-13

Figure B6.14 illustrates sections of open type stiffeners which are in common use. These sections when they suffer distortion of their cross sections usually produce internal shear and compressive forces which tend to twist the section. The attachment of certain types of open

sections to sheet panels may produce a stabilizing influence on certain elements of the stiffener and thus may increase the stiffener strength over that of the stiffener acting alone. On the other hand the attachment of the sheet to open stiffeners may cause stiffener to bend as a column about a different axis than that which the stiffener bends about when acting alone. Thus for sheet stiffener panels using open section stiffeners, tests should usually be made to check calculated strengths.

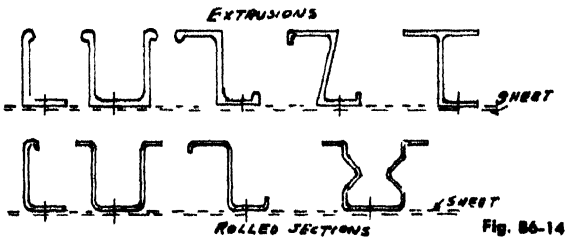


Fig. B6-14

B6.5 Rivet Spacing

If the attachment of the sheet to the stiffener is weakened in any way such as large rivet spacing which permits the sheet to buckle between rivets before the ultimate strength of the stiffener is reached, the effectiveness of the sheet is reduced as a load carrying medium. For high efficiency the rivet spacing should be such as to prevent buckling of the sheet between the rivets. Tests indicate that when such buckling of the sheet between rivets occurs, the plate between rivets can be considered as a fixed-ended column. From Euler's column equation, neglecting Poisson's ratio, which is conservative.

$$P = \frac{C \pi^2 EI}{L^2}, \text{ but } C = 4, \quad \rho^2 = I/A \text{ and}$$

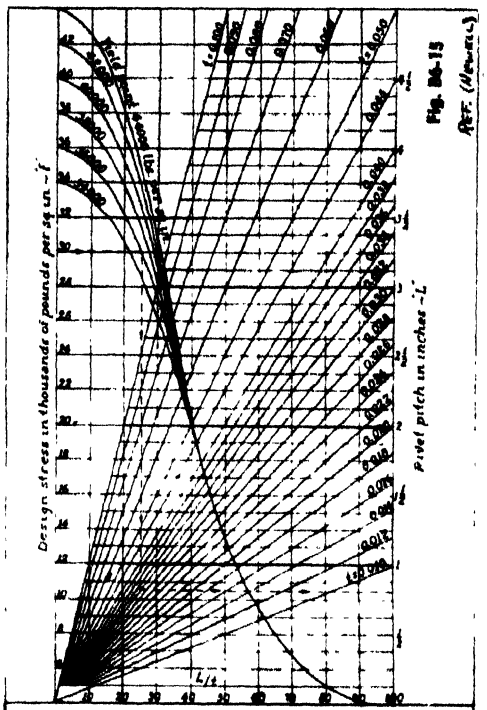
$$P = F_c/A$$

For a sheet of thickness t, $\rho^2 = t^2/12$

Substituting in Euler's equation and solving for L

$$L = 1.814\, t \sqrt{E/F_c} \quad \text{----------(5)}$$

Euler's equation holds only for stresses below the proportional limit, thus for stresses above the proportional limit a modified E must be used or a stress F_c given by a short column formula. This method of estimating rivet spacing was suggested by Howland and Newell (Ref: 6.4, 6.5). Figure B6.15 (From Ref. 6.2) represents the conditions where L is determined for various aluminum alloys for stresses below 20000 psi., and where it is reduced to accord with Johnson's parabola for stresses between 20000 and the material yield point. Since equation (5) is conservative because Poisson's ratio has been omitted, it is felt that the curves of Figure B6.15 can be safely used in design.



In using the above Figure enter at the left with the desired compressive stress and proceed horizontally to the curve representing the yield point of the material being used, thence vertically to the line representing the sheet thickness. A horizontal line from that point to the scale at the right gives the rivet pitch required to prevent buckling of sheet between rivets for the given compressive stress.

Figure B4.4 of Chapter B4 gives the inter-rivet buckling curves as proposed by Fischel in which the stress-strain diagrams of the material is considered and is therefore no doubt a better measure of the true conditions as to permissible rivet spacing for the particular materials which were considered.

B6.6 Tests of Sheet-Stiffener Panels to Obtain Design Allowables

The general method of estimating the ultimate strength of sheet-stiffener panels as given in this chapter is useful in comparative studies, and in most cases, will give results in close agreement with test results. To obtain actual design allowables, the best procedure is to make tests of sheet-stiffener panel specimens. A logical procedure in making such tests would be as follows:

(1) Obtain compressive stress-strain diagrams of short lengths of the stiffener acting alone.

(2) Place strain gages on one or all stiffeners of the test panel, and record the stiffener

strains as the complete panel is loaded in compression. Using the stress-strain diagrams obtained in (1), the stresses in the panel stringers under the panel loading are determined. These stresses times the stiffener areas gives the total load carried by the stiffeners. The difference between this load and the total panel test load gives the total load carried by the sheet. Hence, the actual effective width of the sheet can be written

$$w_e = \frac{P - f_{st} A_{st}}{f_{st} t} = \frac{1}{t}\left(\frac{P}{f_{st}} - A_{st}\right)$$

where P = total test load on panel

f_{st} = measured stress in stiffener

A_{st} = area of stiffeners

t = sheet thickness

(3) Determine the end fixity of the test panel with the results of (1) and (2).

Test panels are usually tested with flat ends. In actual design of wing and fuselage structures it is customary to use an end fixity C between 1.5 to 2.0. Thus, to correct the test panel end fixity to design values, it is necessary to know the fixity of the test panels in the tests. Most sheet-stiffener panels have a column curve which follows the Johnson-parabola closely. With the effective sheet width known as found in (2) the radius of gyration of a stiffener plus its effective sheet can be computed. If two lengths of test panels are tested, the terms f_{co} and C can be found by substituting in the following Johnson equation and solving the two equations for f_{co} and C (f_{co} = column stress at zero L/ρ).

$$f_{st} = f_{co} - \frac{f_{co}^2 \left(\frac{L}{\rho}\right)^2}{4\, C\, \pi^2 E}$$

The majority of tests indicate that flat ends on sheet-stiffener test panels gives a value of C of around 3 for end fixity.

(4) For design purposes the material properties of the test panel material should be corrected to the minimum guaranteed values for the material. Likewise, the test results must be corrected from the test panel end fixity to the design end fixities.

To correct results to the minimum guaranteed yield point, the value of f_{co} as found in (3) is corrected as explained in Chapter B1. To correct to design fixities, the procedure must be a trial and error one since the stiffener stress is changed for a given L/ρ, and ρ depends on the stiffener stress. Since the test results in (2) gives data from which a curve of f_{st} versus ρ can be plotted, the trial and error procedure for correcting the design end fixities is easily carried out.

Design Allowables From Tests Where Stiffener Strains are not Measured.

In this case the effective sheet width is calculated by one of the methods of Chapter B4 using an assumed trial stiffener stress f_{st}. If the assumed column stress times the area of the stiffeners plus the effective sheet equals the test panel load, then the correct stiffener stress f_{st} was assumed. With the effective sheet known the radius of gyration can be computed. At least two lengths of test panels should be used in order to obtain at least two values of L/ρ versus f_{st}. Many tests of sheet stiffener panels using a closed type stiffener indicate that the test results plot to give a curve which follows the Johnson parabola quite closely. Thus taking two tests values of f_{st} and L/ρ, one can solve for the test end fixity and the crushing stress f_{co} at zero L/ρ. This resulting equation representing the test data can then be modified for design purposes by correcting material and end fixities to permissible design values. The general procedure can best be explained by carrying thru and example illustration.

Example Problem.

Figure B6.16 shows the section of a sheet stiffener panel. Two test panels were tested, one 16 inches long and one 32 inches long. Ends of test panel were milled square and parallel and were tested in compression with flat end conditions. The 16 inch panel took an ultimate load of 80,000 pounds, and the 32 inch panel took an ultimate load of 70,000 pounds. The yield point of the material used in the test specimens was 55,000 psi. Let it be required to determine a design allowable stress curve for this sheet-stiffener combination using a yield point of 50,000 psi and an end fixity of C = 1.5.

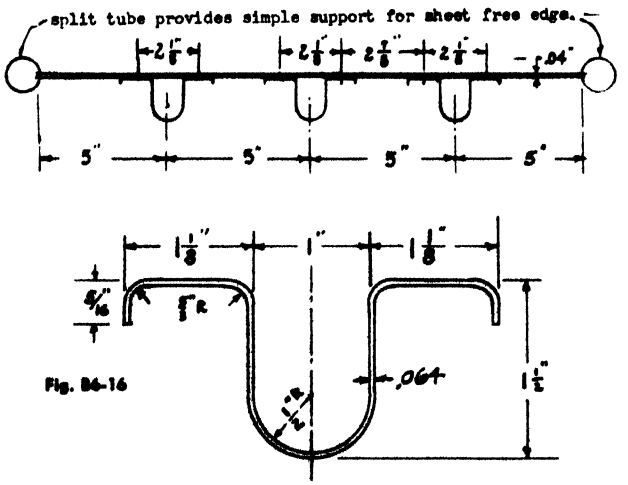


Fig. B6-16

General Data:

Area of stiffener = A_0 = .362 sq. in.
Radius of gyration of stiffener = ρ_0 = .524
Sheet thickness = t = .04 in.
All material 24SRT aluminum alloy.

Solution.

The beginning of the procedure will be to assume a stiffener stress. The effective sheet width for this assumed stiffener stress will then be computed. The total stiffener area plus total effective sheet area times the assumed stiffener stress must equal the test load on panel, if not, the process is repeated until a check is obtained.

In this solution, Marqueere's equation for sheet effective width will be used, since it has been found to check test results fairly well. (See Chapter B4).

The 16 inch specimen will be considered first:

The equation for effective sheet width according to Marquerre is:

$$\frac{w}{b} = \sqrt[3]{\frac{f_{cr}}{f_{st}}} \quad \text{----------(A)}$$

where: w = effective width

b = distance between rivet or attachment lines

f_{cr} = buckling stress of sheet between rivet lines considered simply supported on all 4 edges.

f_{st} = stringer stress

The first trial value of f_{st} will be assumed as 50,000 psi. Since our stringer type has a double rivet line, we have two sheet widths, to consider, namely 2-7/8 inch and 2-1/8 inch.

for b = 2.875

$$f_{cr} = 3.60\ E\ (\frac{t}{b})^2$$

$$= 3.60 \times 10{,}300{,}000 \times (.04/2.875)^2 =$$

7170 psi.

Subst. in equation (A)

$$\frac{w}{2.875} = \sqrt[3]{\frac{7170}{50{,}000}}$$

hence

w = .522 x 2.875 = 1.5 inch or 1.5/2 = .75 inch of sheet acting with each rivet line toward plate width b = 2-7/8.

For b = 2.125

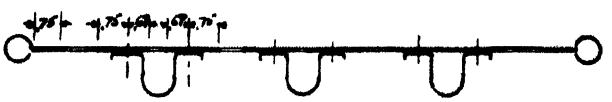
$f_{cr} = 3.60 \times 10{,}300{,}000 \times (.04/2.125)^2 = 13150$ psi.

$$\frac{w}{2.125} = \sqrt[3]{\frac{13150}{50{,}000}}$$

w = .632 x 2.125 = 1.34" or .67" per side.

Figure B6.17 shows the resulting effective sheet width

Fig. B6-17



Total stiffener area = 3 x .362 = 1.086 1.086

Total effective sheet = (8 x .75 + 6 x .67).04 = 0.403

Total = 1.489

Calculated panel load = 1.489 x 50,000 = 74,500 lb. The test load is 80,000 lb. Therefore the assumed trial values of 50,000 lb. for stiffener stress was too low.

As a second trial, assume f_{st} = 54,000 psi:

For b = 2.875

$$\frac{w}{2.875} = \sqrt[3]{\frac{7170}{54{,}000}}, \text{ or } w = .51 \times 2.875 = 1.465"$$

for b = 2.125

$$\frac{w}{2.175} = \sqrt[3]{\frac{13150}{54{,}000}}, \text{ or } w = .625 \times 2.125 = 1.33"$$

Total effective sheet area = (8 x .73 + 6 x .665) .04 = .392

Total area = 1.086 + .392 = 1.478 sq. in.

Calculated panel load = 1.478 x 54000 = 79,800 lb. which checks with the test load of 80,000 lb.

Consideration of Test Panel 32 Inches Long.

This panel should be treated in the same manner as the 16 inch specimen. The results are a stiffener stress f_{st} of 46,500 psi. which gives an effective sheet width with each stiffener as shown in Figure B6.18. The student should check this result.

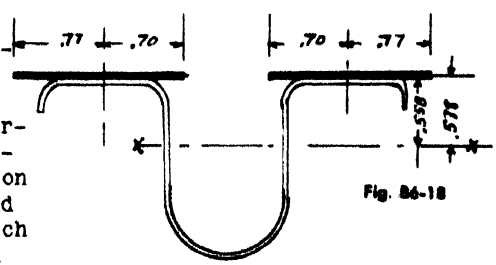


Fig. B6-18

The next step in the general solution will be to determine a column equation and the end fixity which existed in the panel tests. Tests of many panels with closed section stiffeners indicate that the column curve follows the Johnson-parabola closely. Therefore we will substitute in the Johnson column equation, which is as follows:

$$f_{st} = f_{co} - \frac{f_{co}^2\ (L/\rho)^2}{4\ \pi^2\ C\ E} \quad \text{------}$$

f_{st} has been found as 54,000 and 46,500 psi for the 16 and 32" length specimen respectively.

ρ = radius of gyration of stiffener plus the effective sheet.

From Figure B6.18

$$\frac{S}{\rho_o} = \frac{.578}{.524} = 1.1$$

$$\frac{\ell t}{A_o} = \frac{2.94 \times .04}{.362} = .325$$

From curves of Figure B6.8 $(P/\rho_o)^2 = .98$

hence

$$\rho = (.98)^{1/2} \times .524 = .518$$

therefore

$$L/\rho = 32/.518 = 61.8$$

The effective sheet for the 16 inch specimen is approximately the same as ρ can also be taken as .518. Hence $L/\rho = 16/.518 = 30.9$.

Substituting in the Johnson column equation:

$$54000 = f_{co} - \frac{f_{co}^2 (30.9)^2}{4\pi^2 C \times 10{,}300{,}000} \quad \text{(For 16" test panel)}$$

$$46500 = f_{co} - \frac{f_{co}^2 (61.8)^2}{4\pi^2 C \times 10{,}300{,}000} \quad \text{(For 32" test panel)}$$

Solving the two above equations simultaneously for f_{co} and C, we obtain

f_{co} = 56500 and C = 2.99.

Correction of Test Column Equation to Design Column Curve.

Design yield point of 24SRT material is 50,000 psi. Design end fixity is assumed as C = 1.5.

Thus the test results must be decreased from a yield point of 55,000 psi. and an end fixity of C = 2.99 to the above design values.

The crushing stress f_{co} = 56,500 psi which was for the material having a yield point equal to 55,000 can be corrected to the standard material yield point of 50,000 by the correction factor K of .918 obtained from ANC-5.

Therefore f_{co} corrected = .918 x 56,500 = 51900 psi.

The Johnson equation for the design C = 1.5 can therefore be written as follows:

$$f_{st} = 51900 - \frac{51900^2 (L/\rho)^2}{4 \times 1.5 \times \pi^2 \times 10{,}300{,}000}$$

hence

$$f_{st} = 51900 - 4.4 (L/\rho)^2 \text{ - - - - - - - - - - (B)}$$

Since the column stress f_{st} is influenced by ρ and since ρ is influenced by effective skin width, which in turn depends on the value of f_{st}, a column design curve of f_{st} versus panel length must be found by a trial and error process.

For example take a panel length of 24":

For stiffener alone, $A_o = .362$, $\rho_o = .524$, S = .578/.524 = 1.1

Assume ρ = .517 for stiffener plus effective sheet

Then $L/\rho = 24/.517 = 46.4$

Substitute in Equation (B)

$f_{st} = 51900 - 4.4 (46.4)^2 = 42400$ psi.

The effective sheet width will be computed for this stress of 42400 psi.

For b = 2.875

$$w = 2.875 \sqrt[3]{\frac{7170}{42400}} = 1.59"$$

For b = 2.125

$$w = 2.125 \sqrt[3]{\frac{13150}{42400}} = 1.44"$$

Total effective sheet width per stringer = ℓ = 1.59 + 1.44 = 3.03"

$$\frac{\ell t}{A_o} = \frac{3.03 \times .04}{.362} = .335$$

From curves of Figure B6.8

$\left(\frac{\rho}{\rho_o}\right)^2 = .978$, hence $\rho = .517$ which was the value that was assumed for ρ. Thus for a sheet-stiffener length of 24" the allowable column design stress is 42400 psi. The above process should be repeated for several lengths so that a design curve can be plotted as illustrated in Fig. B6.19

B6.7 Stiffened Curved Sheet in Compression

In wing sheet-stiffener construction, the radius of curvature of the sheet covering aft of the 15 percent of chord point is quite large, thus the slightly curved sheet with stiffeners for most wing structures can be analyzed by methods similar to those described for flat sheet with stiffeners.

When the radius of curvature is small as along the leading edge portion of the airfoil or for small circular fuselages, the load carried by the curved sheet between the effective widths as calculated for flat sheet becomes appreciable and should be added to the load carried by the stiffeners plus the effective flat sheet.

For the load on the curved sheet between the effective widths a compressive stress f_c = 0.3 E t/r can be used. (See Chapter B3 for additional expressions for compressive strength of curved sheet). Figure B6.20 illustrates the stress distribution that is usually assumed for stiffened curved sheets with rather sharp curvature.

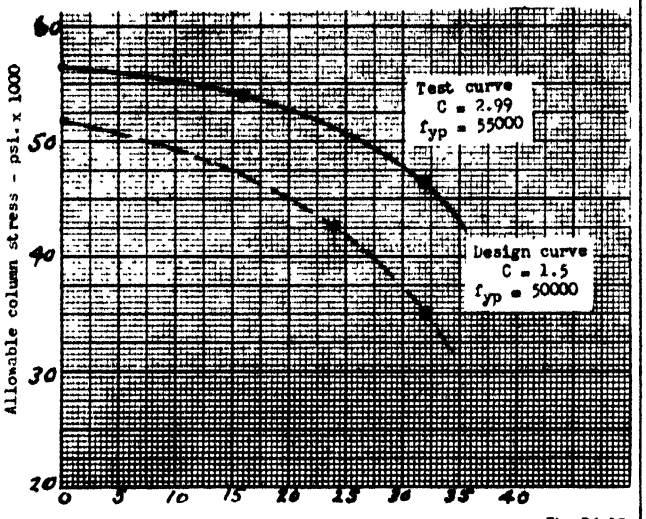


Fig. B6-19

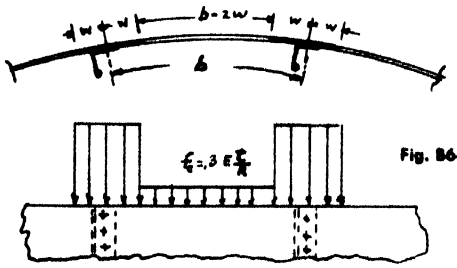


Fig. B6-20

B6.8 Corrugated Sheet as a Stiffening Element

Corrugated sheet is widely used as a sheet stiffening element. Since sheet is used in forming the corrugation, the highest strength aluminum alloy, namely, 24SRT, can be used thus giving an advantage over the common 24ST extruded stiffener sections. Corrugations being a continuous sheet, it is capable of carrying large shear loads, thus necessitating less skin or covering thickness. To obtain a smooth external surface, the corrugations must be covered with sheet which causes a closed section, a condition not good from a corrosion and inspection standpoint.

Circular Arc Corrugations

The most common form of corrugated sheet which has been used in the past is the corrugation made of a series of circular arcs. Figure B6.21 gives information regarding the standard corrugations which have used and also curves for calculating the section properties. Figures B6.22 and B6.23 (Ref. ANC-5) give allowable column and crushing stresses which can be used in design.

Modified Corrugated Shapes.

In circular corrugations due to the spring back of the material in forming, there is usually a short length of straight section near the tangency of the two arcs. This short flat section has a lower crushing stress than the curved portion and thus failure usually begins at this point. To eliminate this weakening effect, some designers have developed corrugation sections as illustrated in Figure B6.24. The local crippling strength of such sections can be estimated closely by the methods explained in Chapter B5, but tests should be made of test panels to obtain design allowables.

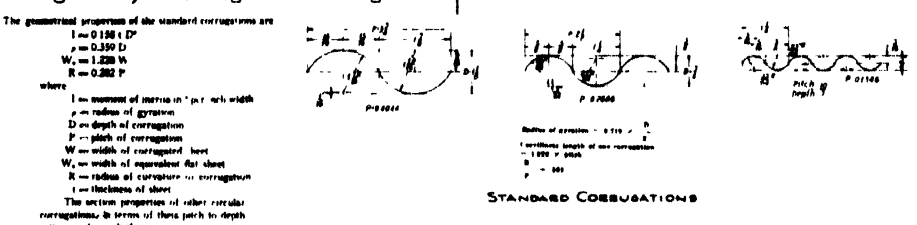
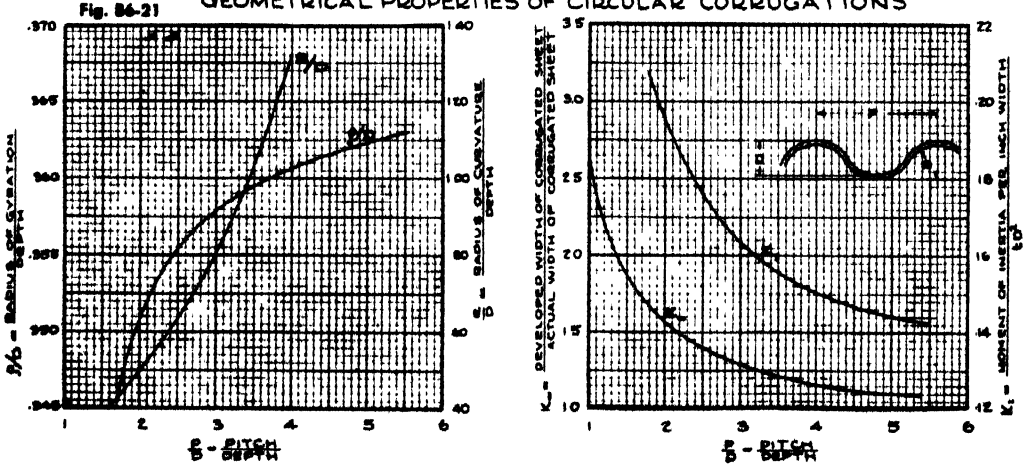


Fig. B6-21 GEOMETRICAL PROPERTIES OF CIRCULAR CORRUGATIONS



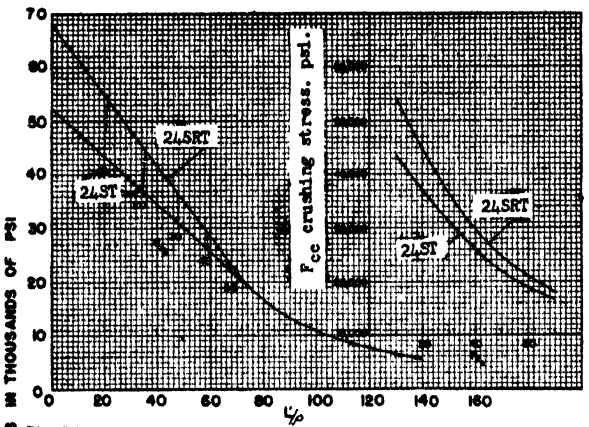


Fig. B6-22 ALLOWABLE COLUMN AND CRUSHING STRESSES
CORRUGATED ALUMINUM ALLOY SHEET-24ST, 24SRT
(CIRCULAR CORRUGATIONS)

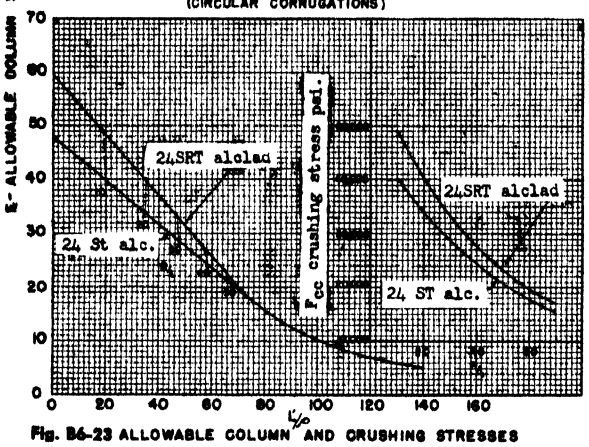


Fig. B6-23 ALLOWABLE COLUMN AND CRUSHING STRESSES
CORRUGATED ALUMINUM ALLOY SHEET
24ST ALCLAD, 24SRT ALCLAD
(CIRCULAR CORRUGATIONS)

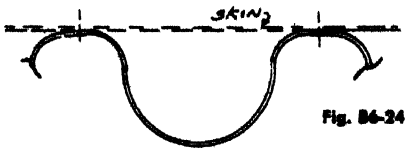


Fig. B6-24

PROBLEMS

(1) Solve example problem No. 1 on page B6.2 if stiffener thickness is .051 and sheet thickness is .04 in.

(2) Solve example No. 2 on page B6.5 if channel thickness is changed to .051 and sheet thickness to .04 inches.

REFERENCES

(6-1) E.E. Lundquist, "Comparison of three methods for calculating the compressive strength of flat and slightly curved sheet and stiffener combinations", NACA Tech. Note No. 455

(6-2) "Progress report on methods of analysis applicable to monocoque aircraft structures" Air Corps Information Circular No. 713

(6-3) E.E. Sechler, Thesis, "The Ultimate Compressive Strength of Thin Sheet Metals Panels". Appendix A, C.I.T. 1935.

(6-4) Niles & Newell. "Airplane Structures" p. 331. John Wiley & Sons.

(6-5) W.L. Howland, "Effect of Rivet Spacing on Stiffened Thin Sheet in Compression", Jr. Aero. Sci. Oct. 1936 p. 434.

PART C
CHAPTER C1
PROPERTIES OF AIRCRAFT MATERIALS

In general, the allowable properties of materials and the various allowable design charts and tables which are presented in Chapters C1, C2, C3, and C4 of Part C are taken from government publication ANC-5 (Strength of Aircraft Elements) revision of 1942 including admendment 2 of August, 1946. Since the issue of this book on January 1, 1949, a new government publication ANC-5a (Strength of Metal Aircraft Elements) dated May, 1949 has been issued. The student should use ANC-5a in conjunction with Part C in order to become acquainted with the latest government design information.

C1.1 Definitions of General Terms

Only those terms and general properties which the stress analyst or structural designer should be familiar with will be discussed in this chapter. For complete information on the materials of aircraft construction the student should refer to textbooks on this subject.

Density

The density of a material is the weight of a unit volume of the material. It is customary in aircraft weight calculations to deal with the weights per cubic inch of the material. Table C1.1 gives the weights for most metals common to aircraft design.

Conductivity (Electrical and Thermal)

Conductivity is the ability of the material for transmitting electricity or heat. Welding technique is influenced by the amount of thermal conductivity. Electrical conductivity is important in bonding airplanes to eliminate possible radio interference. Table C1.1 gives value of conductivity for aircraft metals.

Thermal Expansion and Contraction

Materials expand or contract with increase or decrease of temperature. Thermal deformation is important in the design of castings, welding jigs etc. Table C1.1 gives values of the thermal coefficient of expansion of aircraft materials.

Table C1.1

	Material	Wt. lb/ cu. in.	Electrical conductivity % of Annealed copper standard	Thermal Conductivity at 100°c C.G.S. units	Av. Coef Thermal Expansion per °F Range (68° - 212°F)
Wrought Alum. Alloys	25S	0.098	59	0.54	.0000133
	3s-½ H	0.099	41	0.38	.0000133
	14ST	0.101	40	0.37	.0000122
	17ST	0.101	30	0.28	.0000122
	24ST	0.100	30	0.28	.0000122
	52SH	0.096	40	0.37	.0000130
	53ST	0.097	40	0.37	.0000130
Alum. Cast	43	0.098	37	0.34	.0000122
	112	0.103	30	0.28	.0000122
	195-T4	0.100	35	0.33	.0000122
	BRASS	0.310	24-43	0.29-0.44	.000010
	COPPER	0.322	100		.0000093
	MAGNESIUM	.063	38.6	0.376	.0000143
Mag. Alloy	D.M.J.	.065		.19	.000016
	D.M.H.	.064		.30	.000016
	D.M.K.	.065			.000016
	Monel	0.318	4	0.06	.0000078
	Nickel	0.319	18	0.14	.0000073
	Steel	0.283	3-15		.0000070
	Stainless Steel	0.286		0.039	.0000096

C1.2 Physical Test Terms

Strain

Strain is the deformation of a material caused by a load or some other influence. Unit strain is usually recorded in inches per inch.

Stresses

The internal forces which resist the external forces are called stresses

Stress Strain Diagram

The stress strain diagram is a diagram showing the relationship between unit stress and unit strain for a member when it is loaded from zero stress to ultimate or breaking stress. The shape of the stress-strain curve is quite different for the various materials. Furthermore in general for the same material the stress strain curve is different for axial tensile stresses than for axial compressive stresses. Likewise the stress strain properties are influenced by the grain directions of the material.

The airplane structural designer must proportion his structural members so that no permanent deformation will be produced under the applied loads and must provide a certain ultimate strength (usually strength to carry 1.5 times the applied load). For the applied loads the stress strain relationships can in general be classed in the elastic range but for the ultimate or design load values, the stress strain range is usually in the plastic range, with several exceptions such as long columns or thin walled structures. Since the ultimate strength of a member must be given in all stress analyses of airplane structures, more and more consideration in being given to stress strain diagrams as the basis for calculating or estimating the strength of members.

Typical Stress Strain Curves and Definition of Terms.

Fig. C1.1 shows a typical tension stress-strain curve for low carbon or soft steel. Since the results of tests will vary somewhat with the dimensions of the test specimen, all tests should be made on standard size test specimens. Figs. C1.2 and C1.3 give dimensional data for test specimens for material sizes common in aircraft design.

In Fig. C1.1 between points (O) and (a) the curve is straight which means that stress is proportional to strain. The slope of this part of the curve gives the value of the modulus of elasticity for the material when stresses are

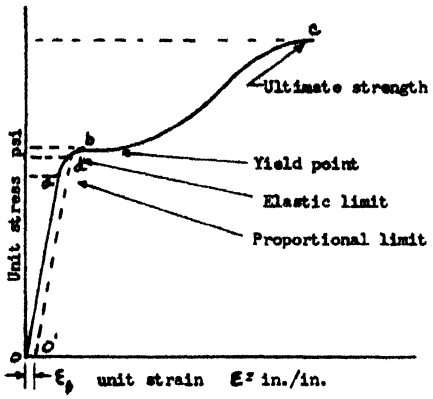


Fig. C1-1

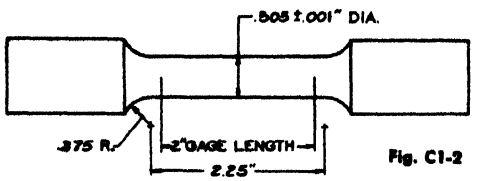


Fig. C1-2

ROUND TENSILE TEST SPECIMEN

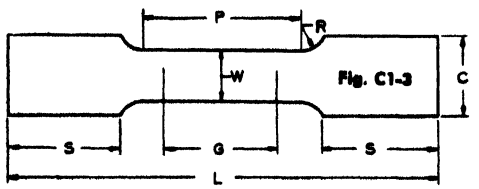


Fig. C1-3

FLAT TENSILE TEST SPECIMEN FOR MATERIAL ½ INCH THICK AND UNDER

DIMENSION	UP TO ½ INCH INCLUSIVE	½ TO ½ INCH INCLUSIVE
C (max.)	1.13 W	1.15 W
(grip length)	2 or 4	2 or 4
(approx.)	8 or 11	8 or 11
G (min.)	1½ C	1½ C
(min.)	W	W
S (approx.)	3	3
W	½ ± 0.010	½ ± 0.015

confined to this region. That is,

$$E = \frac{\text{unit stress}}{\text{unit strain}} = \frac{f}{\epsilon}$$

At point (a) the curve starts to diviate from a straight line, which means that stress is no longer directly proportional to strain. The unit stress at which the diviation begins is called the proportional limit of the material.

As the specimen is loaded to point (b) it will be found that the material continues to suffer deformation without increase of load or stress. The unit stress at which considerable deformation takes place without increase of load is called the yield point of the material.

After this yielding the material regains its ability to take more load or stress until the specimen finally ruptures at point (c) which is referred to as the ultimate strength of the material.

In loading the specimen if for any stress below the proportional limit the load is removed, the specimen deformation will return to zero. It load to a stress greater than the proportional limit such as to point (d) and then removed the strain will not return to zero but specimen will have a permanent set and the stress strain curve will follow (do') approximately parallel to (ao) as the load is removed thus giving a permanent set at zero load. The greatest unit stress that the material can take without permanent deformation is called the elastic limit of the material. This value will lie between the proportional limit and the yield point.

Certain materials like aluminum alloys and heat-treated steels do not possess a definite yield point, that is, there is no point on the stress strain curve at which the tangent to the curve is horizontal. Fig. C1.4 shows a stress strain curve typical of aluminum alloys. Since no definite yield point exists an arbitrary yield point or yield strength is set. In aircraft structural design the yield strength of a material is defined as that unit stress which produces a unit permanent set of 0.2 percent, or $\epsilon = .002$. On Fig. C1.4 a straight line $\epsilon = .002$ is drawn parallel to the straight part of the stress strain curve. The point of the intersection (b) locates the arbitrary yield strength of the material. The tangent modulus of elasticity at any stress equals the slope of the stress strain curve at that particular stress.

The student should realize that most of the stress-strain relationships used in developing equations and formulas in applied mechanics, machine design etc., assume that stress is directly proportional to strain, thus the equations are only strictly applicable for stresses below the proportional limit of the material. For ultimate strength design and ultimate deformation calculations the student should give careful consideration to the material stress strain diagrams. Figs. C1.5 and C1.6 give stress strain curves of materials common to airplane design.

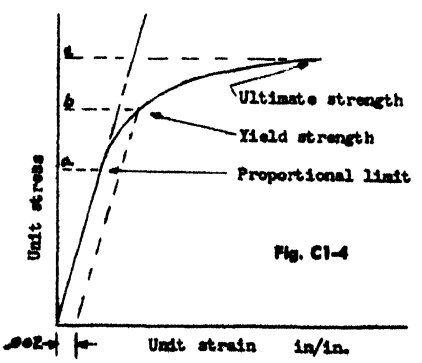


Fig. C1-4

Stiffness

Stiffness is a term which is commonly used to indicate the rigidity of the material in the elastic range. Stiffness is measured by the modulus of elasticity of the material. A high value of E indicates the material has a small deformation for a given stress.

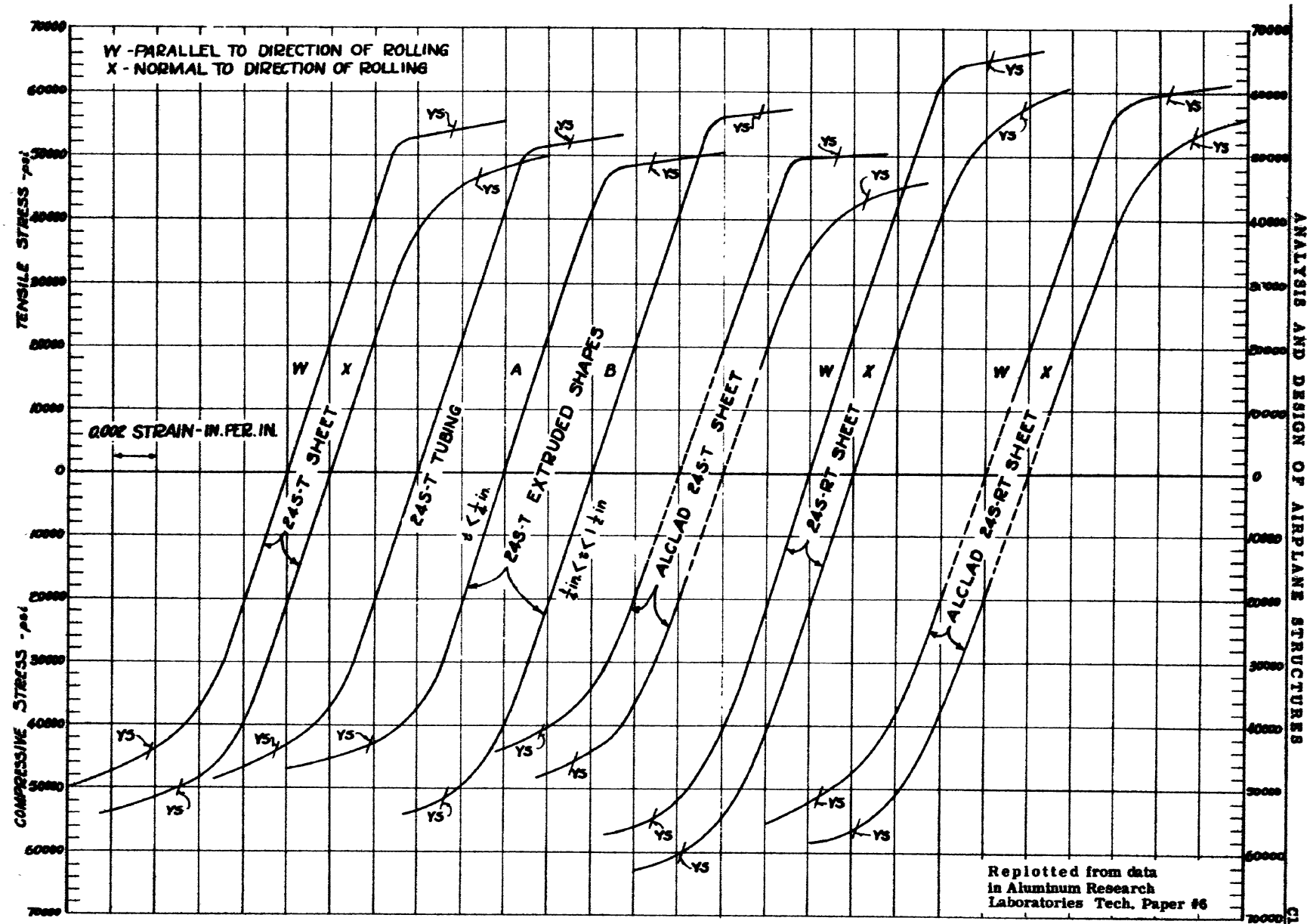
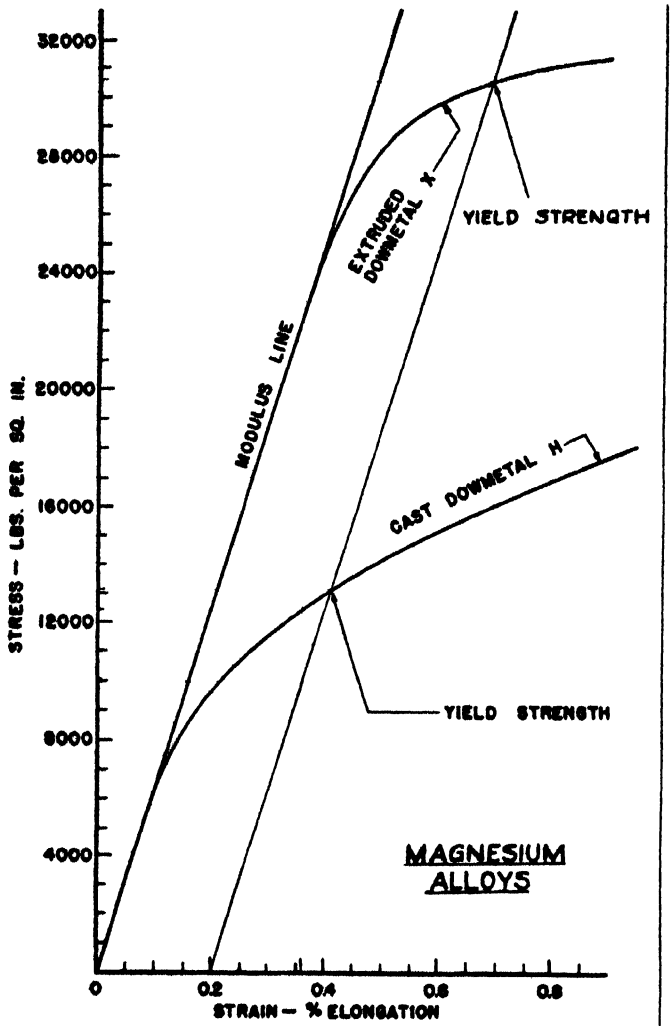
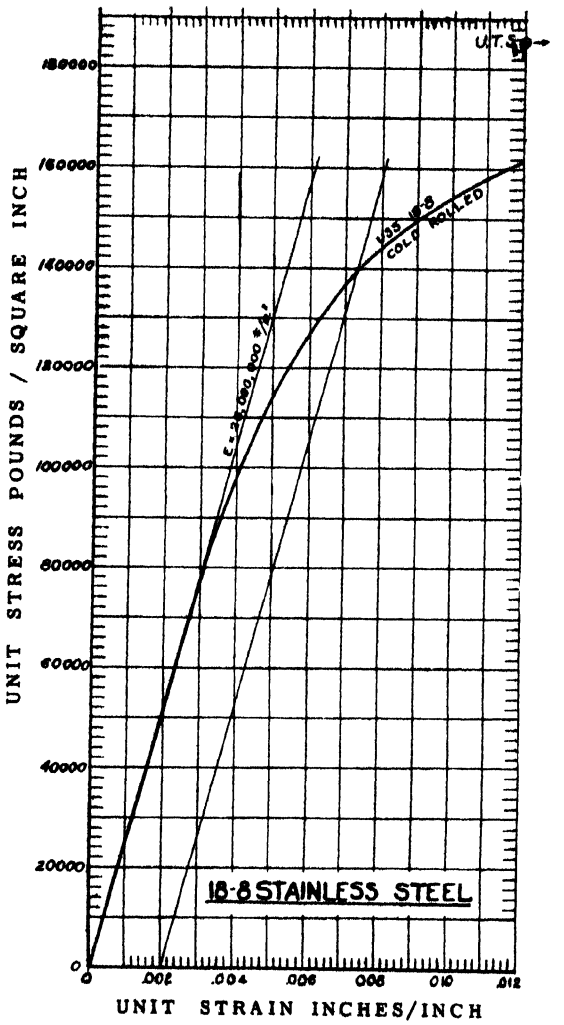
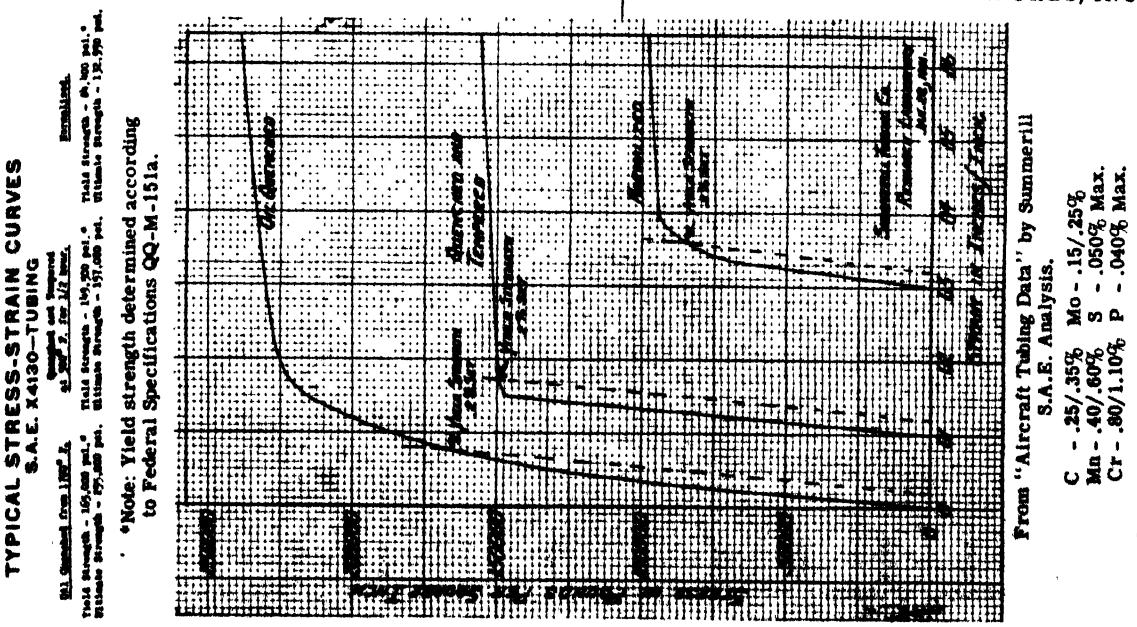


Fig. C1-6 STRESS — STRAIN CURVES FOR ALUMINUM ALLOYS

Fig. C1-6 Stress-Strain Diagrams For Various Aircraft Materials







From "Aircraft Tubing Data" by Summerill
S.A.E. Analysis.
C - .25/.35% Mo - .15/.25%
Mn - .40/.60% S - .050% Max.
Cr - .80/1.10% P - .040% Max.

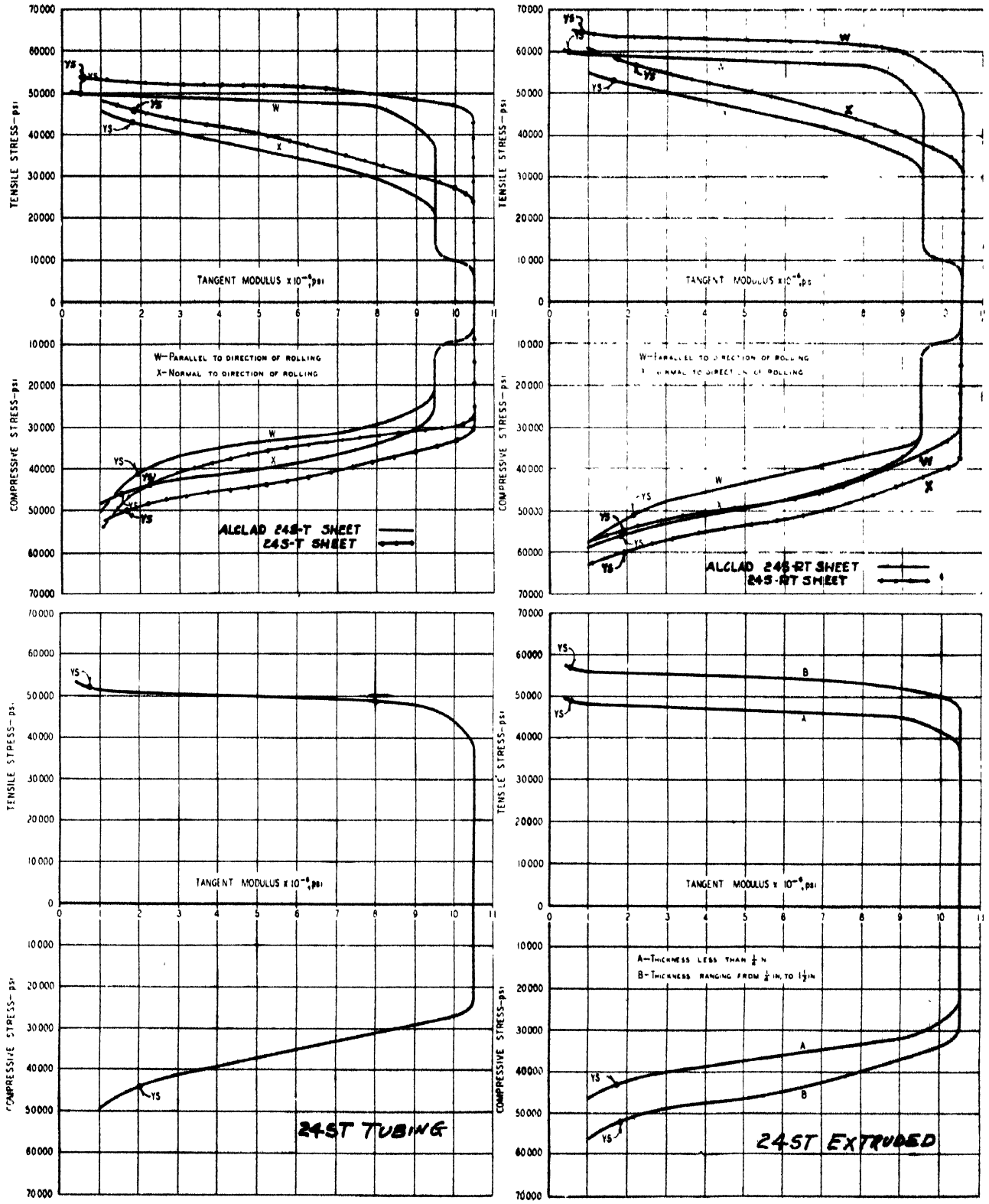


Fig. C1-7 Stress-Modulus Curves For 24st Aluminum Alloy

Reproduced by Permission from Aluminum Research Laboratories Technical Paper #6.

Ductility

Ductility is the property of materials which permits them to be drawn out without breaking. Ductility in a sense measures the stiffness of a material above the elastic range that is in the plastic range of stresses. There is no absolute measure of ductility. It is sometimes measured for comparative purposes by using the percent elongation of the specimen of certain gage length at the rupturing point.

Without ductility in a material, engineers would be faced with serious problems in design, because the property of ductility permits the material to absorb shocks and localized excessive stresses without failure of the member.

Resilience

Resilience of a material is the ability of the material to release energy as the stress is removed. The modulus of elastic resilience is the amount of energy released per unit volume when released from stresses equal to the elastic limit. In equation form, the modulus is

$$u = \frac{f_e^2}{2E}, \text{ where } f_e = \text{elastic limit stress.}$$

Graphically, the modulus of resilience can be represented by the area under the stress strain curve up to the elastic limit. For members subjected to energy loads, such as springs, connecting rods, etc., the material should have high value of elastic resilience.

Toughness

Toughness is a term used to indicate the ability of the material to absorb energy in the plastic range. Toughness is measured by the amount of energy absorbed per unit volume from zero to the breaking stress. Graphically this is the area under the stress strain curve. Toughness is a desirable property in shock resisting parts.

Hardness of a Material

Hardness is the property of a material to resist scratching, cutting or penetration. Experiment has shown that hardness is a good measure of the tensile strength of the material. Thus the tensile strength of a material can be closely estimated by making a simple hardness test. The principle involved in hardness tests is to sink a hardened steel ball under a definite load into the material being tested and to measure the amount of penetration or the size of the impression. Numbers are given to given amounts of penetration which are correlated with the tensile strength of the material.

Hardness tests are used in standard routine inspection practice in airplane factories to check up on materials which are received and to check materials for proper heat treatment.

C1.3 Stress-Modulus Curves

Structural designers are giving more and more consideration to stress-modulus relations in problems involving strength of columns and the buckling of sheets and shapes where the ultimate stresses fall within the plastic range. Fig. C1.7 shows the stress-modulus curves for 24ST aluminum alloys, which were obtained from the stress-strain curves of Fig. C1.5.

C1.4 Mechanical Properties of Aircraft Materials

The mechanical properties of aircraft materials is constantly changing and thus no textbook could be up-to-date on such information. The official reference for information on material properties to use in aircraft design is the government publication ANC-5. This reference manual is revised or amended quite frequently. The information on material properties as given in Tables C1.2 to C1.5 of this chapter is presented for convenience for general reference when presenting elementary design problems in the several chapters to follow.

Table C1.2 Mechanical Properties of Alloy Steels

		NOTE: Except as noted, the values in this Table apply to any of the structural alloy steels containing less than ½% carbon.	Annealed plate & Bar (over 1½ in. thick)	Annealed Plate Tube & Bar (1½" thick & under)	Normalized Plate, Tube & Bar, over .188 thick (x-4130)	Normalized Plate, Tube & Bar .188" thick and under (x-4130)	Heat-Treated to F_{tu} = 100,000	Heat-Treated to F_{tu} = 125,000	Heat-Treated to F_{tu} = 150,000	Heat-Treated to F_{tu} = 180,000	Heat-Treated to F_{tu} = 200,000
Tension	F_{tu}	Ultimate Stress	55000	65000	90000	95000	100000	125000	150000	180000	200000
	F_{ty}	Yield Stress	36000	45000	70000	75000	80000	100000	135000	165000	165000
	F_{tp}	Proportional Limit	25000	30000	50000	.	70000	90000	115000	140000	150000
	E	Modulus of Elasticity	29000000	29000000	29000000	29000000	29000000	29000000	29000000	29000000	29000000
Compress.	F_{cu}	Ultimate (Block Stress)	55000	65000	90000	95000	1000000	125000	150000	180000	200000
	F_{cy}	Yield Stress			70000	75000		100000	135000	165000	165000
	F_{ct}	Proportional Limit	25000	30000	50000		70000	90000	115000	140000	150000
	F_{co}	Column Yield Stress	36000	36000	74100	79500	80000	100000	135000	165000	165000
	E_c	Modulus of Elasticity	29000000	29000000	29000000	29000000	29000000	29000000	29000000	29000000	29000000
Shear	F_{su}	Ultimate Stress	35000	40000	55000	55000	65000	75000	90000	105000	115000
	F_{st}	Torsional Modulus Rup.	50000	55000	80000	80000	90000	110000	125000	145000	155000
	F_{sp}	Proportional Limit	20000	25000	40000	40000	55000	65000	80000	95000	105000
	G	Modulus of Regidity	11000000	11000000	11000000	11000000	11000000	11000000	11000000	11000000	11000000
	F_{br}	Ultimate Bearing Stress	90000	110000	140000	140000	140000	175000	190000	200000	
	F_{be}	Bending Endurance Limit 300 x 10^6 cycles	25000	30000	45000	45000	50000	65000	78000	85000	94000

For effect of welding on properties see Chapter C2 and C5.

All values in this table taken from ANC-5 Rivision of 1942

Table C1.3

STAINLESS STEEL SHEET - COLD ROLLED
TYPICAL PROPERTIES - PARALLEL TO GRAIN

Temper	F_{tu}	F_{ty}	F_{cy}	F_{su}	F_{st}	F_{br}
Annealed	75000	30000	35000	40000	45000	75000
1/4 Hard	125000	75000	65000	67500	80000	150000
1/2 Hard	150000	110000	85000	80000	90000	180000
3/4 Hard	175000	135000	95000	95000	110000	190000
Hard	185000	140000	105000	100000	115000	195000

See ANC-5 - Amendment 2 of 1946 for full information on stainless steel.

Table Cl.4 Mechanical Properties of Aluminum Alloys

	NOTE: All values in psi.	SHEET					TUBING		EXTRUSION	BAR	FORGINGS		CASTINGS	
		17ST Sheet & Plate	24ST Sheet	24ST Alclad Sheet	24SRT Sheet	24SRT Alclad Sheet	24ST Tubing After Stretching (As Received)	24SRT Tubing	24ST Extruded Shapes less 25" thick	24ST Bar up to 3" thick	Forging 14ST	Forging 25ST	Casting 195-T6	Casting 220-T4
Tension	F_{tu} Ultimate Stress	55000	62000	56000	68000	62000	62000	70000	57000	62000	65000	55000	32000	42000
	F_{ty} Yield Stress	32000	40000	37000	50000	46000	42000	58000	42000	40000	50000	30000	18000	22000
	F_{tp} Proportional Limit	25000	32000	27000				44000						
	E Modulus of Elasticity	10500000	10500000	1050000 (av)	10500000	10500000 (av)	10500000	10500000	10500000	10500000	10500000	10500000	10500000	10500000
Compression	F_{cu} Ultimate (block) Stress						62000	70000	57000	62000	65000	55000	62000	70000
	F_{cy} Yield Stress	34000	43000	40000	53000	48000	41000	54800	38000	40000	50000	30000	22000	23000
	F_{cp} Proportional Limit	25000												
	F_{co} Column Yield Stress						50000	70000						
	E_c Modulus of Elasticity	10500000	10500000	1020000 (av)	10500000	10200000 (av)	10500000	10500000	10500000	10500000	10500000	10500000	10500000	10500000
Shear	F_{su} Ultimate Stress	34000	38000	34000	42000	38000	38000	43000	35000	38000	40000	34000	29000	31000
	F_{st} Torsional Modulus of Rup.	50000											22000	
	F_{st} Proportional Limit (torsion)	15000												
	G Modulus of Regidity (torsion)	3800000	3900000		3900000		3900000	3900000	3900000	3900000	3900000	3900000	3800000	3800000
	F_{br} Ultimate Bearing Stress	75000	90000	82000	98000	90000	90000		83000	90000	93000	75000	45000	68000
	F_{be} Bending Endurange Limit (500,000,000 cylles)	16000	18000	12000	18000	13000	14000	16000	16000	16000	12000	12000	6500	7000

(All values in this table taken from ANC -5 Revision of 1942) Student should refer to latest issue of ANC-5 for changes.

Table C1.5
PROPERTIES OF MAGNESIUM ALLOYS

DESIGN MECHANICAL PROPERTIES (KIPS PER SQ. IN.), FOR MAGNESIUM ALLOYS

TYPE	BARS AND RODS						DIE CASTINGS	(3) SAND CASTINGS							FORGINGS				
ALLOY								AN-M-36											
SPECIFICATION	AN-M-24		AN-M-25		AN-M-26	AN-M-27	AN-M-16	COMP. A.			COMP.B.	COMP. C.			AN-M-20	AN-M-21		AN-M-22	AN-M-23
CONDITION	AS EXTRUDED	AS EXTRUDED	EXTRUDED AND AGED	EXTRUDED H.T. & A.	AS EXTRUDED	AS EXTRUDED	AS CAST	AS CAST	HEAT-TREATED	H.T. & AGED	AS CAST	AS CAST	HEAT-TREATED	H.T. & AGED	AS FORGED	AS FORGED	FORGED & AGED	AS FORGED	AS FORGED
THICKNESS	.250 TO 1.500																		
BASIS																			
F_{tu} (1)	40	43	45	48	30	35	30	24	32	34	12	20	32	34	38	42	42	30	36
F_{ty}	26	28	30	33	20	22	20	10	10	16	4	10	10	18	22	26	28	18	22
F_{cy}	16	18	27	30	8	14	20	10	10	16	4	10	10	18	14	18	25		16
F_{su}	19	19	20	23	14	16	18	16	16	19	10	16	16	20	19	20	20	14	15
F_{bru} (E/D - 1.5)(2)									38	41	14		38	41					
F_{bru} (E/D - 2.0)									51	54	19		51	54					
F_{bry} (E/D - 1.5)									20	32	8		20	36					
F_{bry} (E/D - 2.0)									25	40	10		25	45					
% E	11	9	5	4	3	10	2	4	7	3	3		6	1	6	5	2	3	7
E, E_c	6 500										6 500				6 500				
G	2 400										2 400				2 400				
ν	.0649	.0653			.0635	.0645	.0653	.0664			.0635	.0657			.0649	.0653		.0635	.0674
	J-1	O-1	O-1A	O-1HTA	M	FS-1	R	H-AC	H-HT	H-HTA	M-AC	C-AC	C-HT	C-HTA	J-1	O-1	O-1A	M	D-1
COMMERCIAL DESIGNATIONS	AM-C57S	AM-C58S	AM-C58S-T5		AM3S	AM-C52S	AM263-C	AM 265-C	AM 265-T4	AM 265-T6	AM 403-C	AM 260-C	AM 260-T4	AM 260-T6	AM C57S	AM C58S	AM S-T5	AM3S	AM 65S

NOTES:

1. Standard Structural Symbols are explained in Section 1.1, Chapter I.
2. D = hole diameter; e = edge distance measured from the hole centerline in the direction of stressing; use value of e/D = 2.0 for all larger values of edge distance; for ratios between 1.5 and 2.0, the bearing stress value should be obtained by linear interpolation; values for e/D less than 1.5 must be substantiated by adequate tests prior to approval by the procuring or certificating agency.
3. The sand casting properties are minimum values obtained from cast test bars. Reference should be made to the specific requirements of the procuring or certificating agency with regard to the use of the above values in the design of castings.
4. Properties given in this column are typical properties from material specification.

CHAPTER C2

PRACTICAL DESIGN OF STEEL AND ALUMINUM ALLOY TUBES AS COLUMN AND TENSION MEMBERS

Steel and aluminum alloy tubes of circular, streamline, elliptical and square cross-section are common units in the modern airplane structure. This chapter deals with the practical design of such members. The theory of column action and failure is considered in detail in another chapter.

C2.1 Long Columns . The Euler formula for long columns, which fail by lateral bending is,

$$F_{ce} = \frac{c\pi^2 E}{(L/\varrho)^2} = \frac{\pi^2 E}{(L'/\varrho)^2} \text{ if } L' = \frac{L}{\sqrt{c}} \quad \text{------(1)}$$

where, F_{ce} = ultimate column unit compressive stress.

L = column length

c = column end fixity coefficient

ϱ = least radius of gyration of cross-section

E = Modulus of elasticity

L' = effective or free length of column, which is influenced by the amount of end restraint. Fig. C2.1 illustrates the effect of end restraint on the effective column length which is the distance between the column points of inflection.

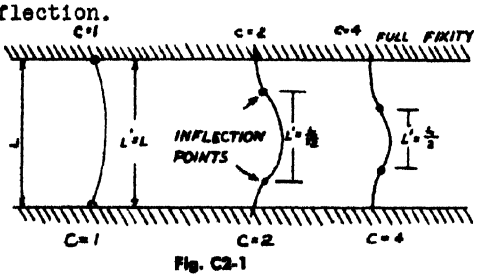


Fig. C2-1

C2.2 Short Columns. The stress-strain diagram of steel and aluminum alloy is not a straight line throughout the stress range, which means that E is not constant, but decreases in the higher stress range where elastic action transforms into plastic action. Test results of short columns give results which occur below those calculated by the Euler formula. To fit the test data use is made of formulas which express the equation of a curve which follows the test data closely.

C2.3 Summary of Column Formulas for Steel and Aluminum Alloy Round Tubes

Tables C2.1 and C2.2 give a summary of column formulas for steel and aluminum alloy tubes respectively as given in ANC-5a Revision of 1949.

The three basic column formulas for round tubes are:

(2) $F_c = F_{co}\left[1 - \frac{F_{co}\,(L'/\varrho)^2}{4\pi^2 E}\right]$ (Johnson-2.0 Parabola)

(3) $F_c = F_{co}\left[1 - .3027\,\frac{(L'/\varrho)^{1.5}}{\pi\sqrt{E/F_{co}}}\right]$ (1.5 Parabola)

(4) $F_c = F_{co}\left[1 - \frac{.385\,(L'/\varrho)}{\pi\sqrt{E/F_{co}}}\right]$ (1.0 Parabola - Straight Line)

Table C2-1 Colulm Formulas For Round Steel Tubes.

Material	F_{tu}-psi	F_{ty}-psi	F_{co}-psi	Short Columns Formula For F_c (psi)	Critical L'/ϱ	Long Column Formula F_c (psi)
1025	55000	36000	36000	$36000 - 1.172\,(L'/\varrho)^2$	124	$276 \times 10^6/(L'/\varrho)^2$
X-4130	95000	75000	79500	$79500 - 51.9\,(L'/\varrho)^{1.5}$	91.3	$286 \times 10^6/(L'/\varrho)^2$
X-4130	100000	85000	90100	* $90100 - 64.4\,(L'/\varrho)^{1.5}$	86.0	$286 \times 10^6/(L'/\varrho)^2$
Heat treated Alloy Steel	125000	100000	100000	$100000 - 8.74\,(L'/\varrho)^2$	75.6	$286 \times 10^6/(L'/\varrho)^2$
Heat treated Alloy Steel	150000	135000	135000	$135000 - 15.92\,(L'/\varrho)^2$	65.0	$286 \times 10^6/(L'/\varrho)^2$
Heat treated Alloy Steel	180000	165000	165000	$165000 - 23.78\,(L'/\varrho)^2$	58.9	$286 \times 10^6/(L'/\varrho)^2$

GENERAL NOTES: $L'/\varrho = L/\varrho\sqrt{c}$. L'/ϱ shall not exceed 150
Critical L'/ϱ is that above which columns are "long" and below which they are "short".
For values of $D/t' < 30$ investigation of local instability unnecessary.
*For use on civil airplanes only. Formula applies only to tubing "As Received." If annealed and reheat-treated, the column formula based on F_{ty} = 75000 psi must be used.

Table C2-2 Column Formulas For Round Aluminum Alloy Tubing.

Material	F_{cy}	F_{co}	Short Columns[a]	Critical L'/ρ[b]	Long Columns[a]	Local Failure
Aluminum Alloy General		$F_{cy}\left[\frac{1+F_{cy}}{200,000}\right]$	Equation 4	$1.732\pi\sqrt{E/F_{co}}$	$\frac{\pi^2 E}{(L'/\rho)^2}$	Note (c)
17ST (Re-heat-treated)	32,000	37,000	37,000-269.3 L'/ρ	92.0	$103.8\times10^6/(L'/\rho)^2$	Fig. C2.5
17ST (As received)	36,000	42,500	42,500-330.5 L'/ρ	85.7	$103.8\times10^6/(L'/\rho)^2$	Fig. C2.5
24ST	41,000	50,000	50,000-421.0 L'/ρ	79.2	$103.8\times10^6/(L'/\rho)^2$	Fig. C2.5
24SRT	54,800	70,000	70,000-700.0 L'/ρ	66.7	$103.8\times10^6/(L'/\rho)^2$	Fig. C2.5

Note (a). $L'/\rho = L/\rho\sqrt{c}$; L'/ρ shall not exceed 150 without specific authority from the procuring or certificating agency.

Note (b). Critical L'/ρ is that above which the columns are "long" and below which they are "short".

Note (c). Must be determined by test unless conservatively assumed. (Ref. ANC-5 1942)

C2.4 Column Yield Stress (F_{co}) The upper limit of the allowable column stress for primary failure is called the column yield stress and will be designated F_{co}. It can be determined by extending the "short-column" curve to a point corresponding to zero length, ignoring any tendency of the curve to rise rapidly or "pick-up" for very short lengths. The short-column curve used in determining F_{co} should be obtained from tests on specimens having geometrical proportions such that local failure is precluded except for very low values of L'/ρ.

When the column yield stress is reached, the walls of the column will tend to buckle unless restrained by extreme shortness, or by the application of lateral restraining forces. In some cases, however, if the specimen has not been allowed to buckle, the stress may be increased considerably above this value. Due to the danger of buckling when the column yield stress is approached, the latter should be considered as the limiting stress for all columns.

The column yield stress is mainly determined by the nature of the compressive stress-strain diagram of the material. When the material has a definite yield point in compression, this value may be assumed for the column yield stress. Few aircraft materials, however, have a sharply defined yield point. In such cases, it is usually possible to determine the column yield stress.

C2.5 Comparison of Column Curves A comparison of these column curves is given in Fig. C2.2 in which the column curves are plotted in non-dimensional form. The Johnson Parabola curve is tangent to Euler curve at a value of $R_a = .5$. The tangent points for the 1.5 parabolic formula and the straight line formula occur at values of R_a equal to .428 and .333 respectively.

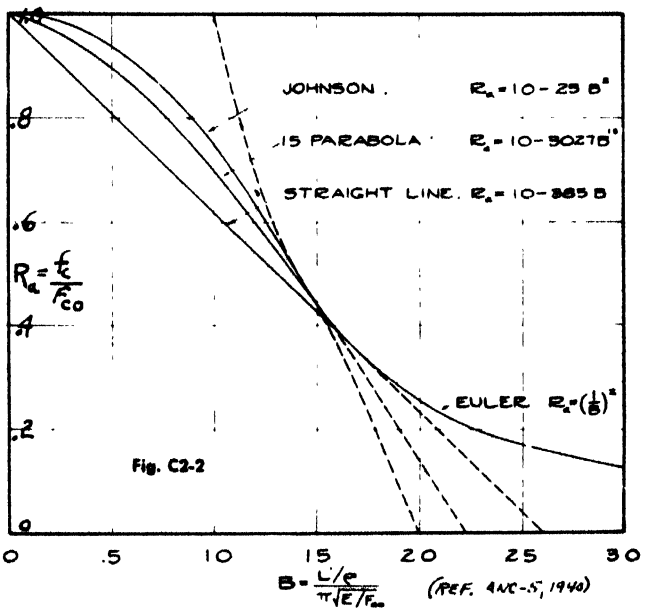


Fig. C2-2

C2.6 Design Column Charts. In designing a column for a given load the area and radius of gyration are unknown, thus in general a method of trial and error or guess and check is necessary. To eliminate the necessity of substituting in the column formulas and thus speed up the trial and error method curves of allowable column unit stress versus the effective slenderness ratio L'/ρ are plotted. Such curves are illustrated in Figs. C2.3, C2.4, and C2.5 which deal with steel and aluminum alloy tubing. To eliminate entirely the necessity of guessing and checking, complete column curves can be constructed as illustrated in Figs. C2.6, C2.7, and C2.8.

C2.7 Local Instability Failure. Crippling Stress (F_{cc})

Columns may fail by local buckling or crippling of the tube wall. The upper limit of the allowable column stress for local failure is referred to as the crippling stress and is designated by the term F_{cc}. If the cross-section is of such size that local collapse takes place at a stress above the proportional limit of the material, than the crippling action falls in the field of elastic buckling.

In the general notes of table C2.1 for steel tubes it states that for values of D/t less than 50 investigation of local instability is unnecessary. Since practically all the standard steel tubes which are used in primary structures have D/t values less than 50, this matter of local buckling is not important in steel tubes.

For aluminum alloy tubes the crippling stresses as a functfon of D/t are given in Fig. C2.5.

C2.8 Effects of Welding on Steel Tube Allowable Column Stresses

When steel tubes are used as members of a structure they are usually welded at their ends to form a tie or connection with other members or fittings. This welding of the tube ends will not effect the primary failure of the member as a column. Welding will however effect the local crippling strength since it decreases the physical strength properties of the material in the region of the weld. Thus the column stress should not exceed these decreased values of the local crippling strength. These values are indicated on the column curves by breaking the column curves by a horizontal line. For example in Fig. C2.3 the cut off stress due to welding is 76600 psi for a material of F_{ty} = 85000 psi. For tubes heat-treated after welding the ends should be checked for a crippling stress as given by the weld cut-off lines in Fig. C2.4.

C2.9 General Summary and Information Regarding Column Design Procedure

1. For a given area, the larger the tube diameter, the greater the column strength if failure due to local crippling is not critical.
2. The higher the D/t ratio of tube the lower the crippling or local failure strength.
3. If columns fall within the long column category, the use of higher strength alloy steel or aluminum alloy will not increase strength of column since E is practically constant for all chrome-moly steel alloys and likewise for all aluminum alloys. Failure is due to elastic buckling of the column as a whole and is therefore a function only of I, L' and E.
4. In the short column range the use of higher strength alloys of steel and aluminum increascreases the ultimate strength of the column, since failure is influenced by plastic action and raising the proportional limit of material likewise increases the stress at which plastic action begins.
5. For the design of chrome-moly steel round thbes of x-4130 material with U.T.S. of 95000 and 100000 use column charts of Figs. C2.6 and C2.7 respectively. For design of 24ST AL. ALLOY round tube columns use charts of Fig. C2.8. These charts give sizes direct without trial and check.
6. For design of columns of heat treated alloy steel, or from other aluminum alloys use column curves C2.4 and C2.5 respectively. A guess and check method is necessary in the use of these charts. A good procedure is first find the approximate size using column charts on Fig. C2.7 or C2.8. If this resulting size falls within the long column range, than changing to the specified material will not change the size as the strength will remain the same. If the resulting tube falls within the short column range, than using better material will in general permit decreasing tube thickness one gauge and increase it one gauge if weaker material is used. With these modified assumed sizes find allowable unit stress F_c from charts on Figs. C2.4 and C2.5 from which the column strength equals F_cA. Using this general method of procedure very little revision will be necessary in obtaining the lightest tube for carrying the load.
7. The column end restraint effects the necessary tube size. Consult the design requirements of the Army, Navy, and C.A.A. in this matter. In general with welded steel tubular trusses a coefficient of C = 2 is permissible except for engine mount and Nacelle structures. For trusses with riveted joints a value of not over 1.5 is generally permissible.
8. The student should realize that practical limitations such as clearance requirements may determine the diameter of the tube instead of strength/weight considerations. Thus design can consist of checking the tubes available under the given restrictions.

C2.10 Steel and Aluminum Alloy Tubes as Tension Members

The ultimate tensile strength of a tube in tension which is loaded concentrically equals the area of the cross-section of the tube times the ultimate tensile strength of the material. However to join a tension member to another member or a fitting requires welding or a joint involving rivets or bolts. If welding is used the ultimate tensile strength of the material is reduced near the weld point. If the rivet or

bolts are used, tube area is cut away, thus tensile strength of tube depends on net area.

For chrome-moly steel tubes of 100,000 and 95000 U.T.S., ANC-5 specifies that the allowable tensile strength near the weld of tubes joined by tapered welds at angles of 30 degrees or less to the center line or fishmouth welds formed by cuts of 60 degrees or less shall be .947 times the U.T.S. of the material. For all other types of welds it recommends an allowable tensile strength near the weld equal to .841 times the U.T.S.

For steel tube members heat-treated after welding, the tensile strength F_{tu} is reduced by the factors as given in Table C2.3a

In welded tabular steel structures where 7 or more members converge ANC-5 specifies that the allowable stress shall be determined by dividing the normal allowable stress by a material factor of 1.5 unless the joint is reinforced in a satisfactory manner. A tube that is continuous through a joint is assumed as 2 members.

In designing a tension member, the designer must give consideration to the ratio of the U.T.S. of the material to the yield strength of the material. The general design criterion states that the members of a structure must not be stressed above the yield point under the applied loads and that the member shall not break or collapse under a load 1.5 times the applied loads. Thus if the ratio of the U.T.S. to the yield strength of a material is more than 1.5, a member in tension must be designed on the basis of the yield strength and the applied loads or a reduced U.T.S. under the ultimate design loads. A study of tables C2.1 and C2.2 indicates that when using 17ST and 24ST aluminum alloy with yield strength of 30000 and 40000 psi respectively it is necessary to reduce the U.T.S. in order that yield strength is not exceeded under applied loads when factor of safety on applied loads is 1.5

C2.11 Example Problems in the Design of Steel and Alluminum Alloy Tubes as Columns and Tension Members

Example Problem #1

Fig. C2.8a shows a steel tubular engine mount structure for a 1050 H.P. radial engine. The ultimate design tension and compressive load in each member as determined from a stress analysis for the various flying and landing conditions are shown in () adjacent to each member. The true length L of each member is also shown. Using chrome-moly steel tubes, U.T.S. = 95000, select tube sizes for the given loads. It is common practice to assume the column end fixity c = 1 for engine mount members, since the mount is subjected to considerable vibration as well as complex or involved loadings.

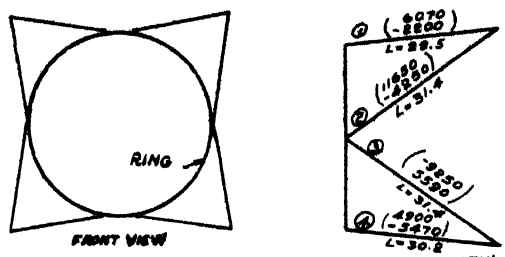


Fig. C2-8a.

Consider member (3). Ultimate design load = - 9250#. Referring to the column charts of Fig. C2.6, we find for C = 1 and L = 31.4 the following tube sizes for a strength near - 9250#.

1-1/2 - .035, Pa = 8850 (weak). (Note - Pa = allowable load).

1-3/8 - .049, Pa = -10350, weight = 5.78#/100", M.S. = (10350/9250) - 1 = .12

1-1/4 - .058, Pa = -10000, weight = 6.15, M.S. = 10000/9250) - 1 = .08

Thus use 1-3/8 - .049 since it is the lightest as well as the strongest.
Consider member (4), Load = - 5470, L = 30, c = 1

From Fig. C2.6:

1-1/8 - .049, Pa = -7100, wt. = 4.68, M.S. = .30

1-1/4 - .035, Pa = -6500, wt. = 3.78, M.S. = .19

1" - .058, Pa = -6000, wt. = 4.86, M.S. = .10

The results show that 1-1/4 - .035 is the lightest. Since there is danger in welding .035 thickness to the other heavier tube gauges particularly the engine mount ring which is usually relatively heavy for this size engine, a minimum tube thickness of .049 will be used, hence the 1-1/8 - .049 tube will be selected.

Consider Member (2)

Design loads 11650 tension and 4250 compresson. Since the tension load appears critical, the tube will be designed for the tension load and then checked for the compressive load. The U.T.S. of the material equals 95000 psi. Since the engine mount in a welded structure, the strength of the tube adjacent to the end welds must be reduced to .841 x 95000 = 80000 psi. (Ref. Art. C2.10)
Hence tube area required = 11650/80000 = 0.146 sq. in. From table C2.3 which gives the section properties of round tubes we select the following results:

1 - .049, Area = .146, M.S. = (.146/.146) - 1 = 0

1 - .058, Area = .172, M.S. = (.172/.146) - 1 = .19

1-1/8 - .049, Area = .166, M.S. = .14

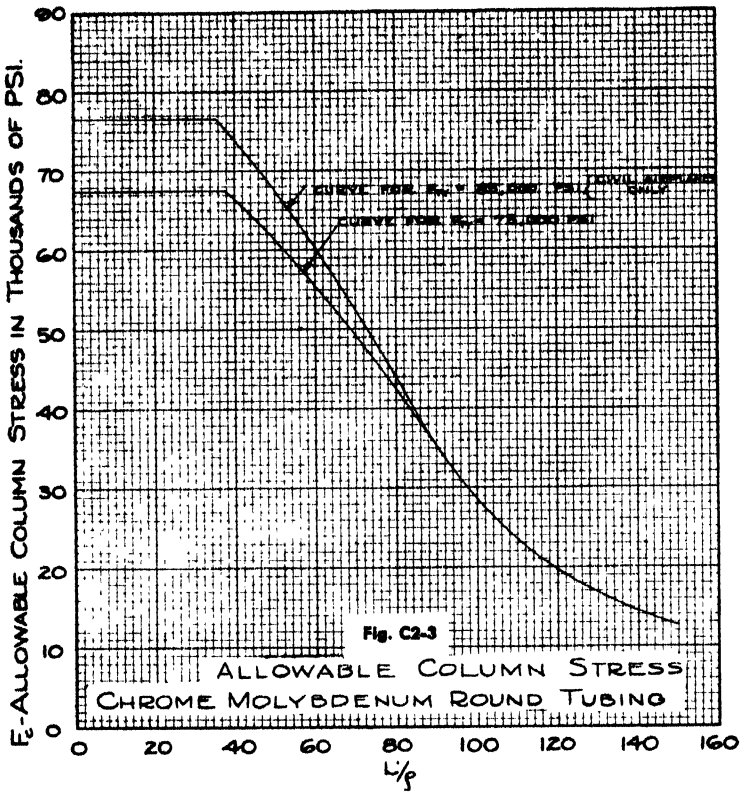
1-3/8 - .035, Area = .147, M.S. = 0

To obtain a reasonable margin of safety, the 1-1/8 - .049 will be selected.

Table C2.3 PROPERTIES OF ROUND TUBING

Dia.	Gage	A	ρ	I	I/Y	D/t	Weight Lb/100 ins. Steel	Weight Lb/100 ins. Dural
1/4	.022	.01576	.0810	.000103	.000825	11.38	.45	.16
	.028	.01953	.0791	.000122	.000978	8.33	.55	.20
3/8	.028	.03063	.1231	.000462	.002466	13.39	.86*	.31
	.035	.03739	.1208	.000546	.002912	10.72	1.06	.38
	.049	.06018	.1166	.000682	.003636	7.65	1.43	.51
1/2	.028	.04152	.1672	.001160	.004641	17.85	1.17	.42
	.035	.06113	.1649	.001390	.005559	14.28	1.45*	.52*
	.040	.06943	.1576	.001788	.007144	10.20	1.96	.70
5/8	.028	.05252	.2113	.002345	.007503	22.30	1.49	.54
	.035	.06487	.2090	.002833	.009065	17.85	1.84*	.66*
	.049	.08867	.2044	.003704	.011852	12.77	2.51	.90
	.058	.10331	.2016	.004195	.013425	10.79	2.93	1.05
3/4	.028	.06351	.2555	.004145	.011052	26.80	1.80	.65
	.035	.07862	.2531	.005036	.013429	21.42	2.23*	.80*
	.049	.10791	.2485	.006661	.017762	15.30	3.06	1.09
	.058	.12609	.2455	.007601	.02027	12.94	3.57	1.28
	.065	.13988	.2433	.008278	.02208	11.53	3.96	1.42
7/8	.028	.07451	.2996	.006689	.015289	31.23	2.11	.76
	.035	.09236	.2973	.008161	.018653	25.00	2.62*	.94*
	.049	.12715	.2925	.010882	.02487	17.85	3.60	1.29
	.058	.14887	.2896	.012484	.02853	15.10	4.22	1.51
	.065	.16541	.2865	.013653	.03121	13.47	4.66	1.68
1	.035	.10611	.3414	.012368	.02474	28.56	3.01*	1.07*
	.049	.14640	.3367	.016594	.03319	20.40	4.15	1.48
	.058	.17164	.3337	.019111	.03822	17.25	4.86	1.74
	.065	.19093	.3314	.020970	.04193	15.38	5.41	1.93
1 1/8	.035	.11985	.3856	.01782	.03168	32.10	3.40*	1.21
	.049	.16564	.3808	.02402	.04270	22.95	4.68*	1.68
	.058	.19442	.3780	.02775	.04933	19.40	5.51	1.37
	.065	.21650	.3755	.03052	.05425	17.30	6.14	2.20
1 1/4	.035	.13360	.4297	.02467	.03948	35.70	3.78*	1.35*
	.049	.18488	.4250	.03339	.05342	25.50	5.23*	1.87*
	.058	.2172	.4219	.03867	.06187	21.55	6.15	2.20
	.065	.2420	.4196	.04260	.06816	19.22	6.86	2.45
1 3/8	.035	.1473	.4739	.03309	.04814	39.25	4.17	1.49
	.049	.2041	.4691	.04492	.06534	28.05	5.78*	2.07
	.058	.2400	.4661	.05213	.07583	23.70	6.80	2.43
	.065	.2675	.4638	.05753	.08367	21.15	7.58	2.70
1 1/2	.035	.1611	.5181	.04324	.05765	42.80	4.56	1.63
	.049	.2234	.5132	.05885	.07847	30.60	6.32*	2.26*
	.058	.2628	.5102	.06841	.09121	25.85	7.45	2.66
	.065	.2930	.5079	.07558	.10079	23.05	8.30	2.97
	.083	.3695	.5018	.09305	.12407	18.08	10.47	3.74
1 5/8	.035	.1748	.5622	.05528	.06803	46.40	4.95	1.77
	.049	.2426	.5575	.07540	.09279	33.15	6.87*	2.46
	.058	.2855	.5544	.08776	.10801	28.00	8.09	2.89
	.065	.3186	.5520	.09707	.11948	25.00	9.05	3.23
	.083	.4021	.5459	.11985	.14751	19.58	11.40	4.06
1 3/4	.035	.1885	.6065	.06936	.07927	50.00	5.32	1.91
	.049	.2618	.6017	.09478	.10832	35.70	7.42*	2.65*
	.058	.3083	.5986	.11046	.12624	30.20	8.73*	3.12
	.065	.3441	.5962	.12230	.13977	26.90	9.75	3.48
	.083	.4347	.5901	.15136	.17299	21.10	12.32	4.40
1 7/8	.035	.2023	.6507	.08565	.09136	53.60	5.73	2.04
	.049	.2811	.6458	.11720	.12500	38.25	7.95	2.84
	.058	.3311	.6427	.13677	.14589	32.30	9.38	3.35
	.065	.3696	.6404	.15156	.16166	28.80	10.47	3.74
	.083	.4673	.6342	.18797	.20050	22.60	13.25	4.73
2	.049	.3003	.6900	.14299	.14299	40.80	.50	3.04
	.058	.3539	.6869	.16696	.16696	34.45	10.03*	3.58*
	.065	.3951	.6845	.18514	.18514	30.75	11.19	4.00
	.083	.4999	.8783	.2300	.2301	24.10	14.16	5.06
	.095	.5885	.6744	.2586	.2586	21.05	16.11	5.76
2 1/4	.049	.3388	.7783	.2052	.1824	45.90	9.59	3.43
	.058	.3994	.7753	.2401	.2134	38.80	11.30*	4.03*
	.065	.4462	.7728	.2665	.2369	34.60	12.64	4.52
	.083	.5651	.7667	.3322	.2953	27.15	16.01	5.72
	.095	.6432	.7626	.3741	.3325	23.70	18.22	6.51
2 1/2	.049	.3773	.8667	.2834	.2267	51.00	10.68	3.82
	.058	.4450	.8635	.3318	.2655	43.10	12.60	4.50
	.065	.4972	.8613	.3688	.2950	38.45	14.09*	5.03*
	.083	.6302	.8550	.4607	.3686	30.10	17.85	6.38
	.095	.7178	.8509	.5197	.4158	26.30	20.34	7.27
2 3/4	.049	.4158	.9551	.3793	.2759	56.10	11.78	4.20
	.058	.4905	.0521	.4446	.3233	47.40	13.90	4.96
	.065	.5483	.9496	.4944	.3596	42.30	15.50*	5.55*
	.083	.6954	.9434	.6189	.4501	33.15	19.70*	7.04
	.095	.7924	.9393	.6991	.5084	28.95	22.48	8.03
3	.058	.5361	1.0403	.5802	.3868	51.70	16.18	5.42
	.065	.5993	1.0380	.6457	.4305	46.20	16.95	6.06
	.083	.7606	1.0318	.8097	.5398	36.15	21.55*	7.70*
	.095	.8670	1.0276	.9156	.6104	31.58	24.56	8.78
	.120	1.0857	1.0191	1.1276	.7518	25.00	30.76	11.00
3 1/4	.058	.5816	1.1287	.7410	.4560	56.10	16.47	5.89
	.065	.6504	1.1263	.8251	.5077	50.00	18.40	6.58
	.083	.8258	1.1201	1.0361	.6376	39.15	23.38*	8.35*
	.095	.9416	1.1160	1.1727	.7217	34.20	26.66	9.52
	.120	1.1800	1.1074	1.4472	.8906	27.10	33.43	11.95
3 1/2	.065	.7014	1.2147	1.0349	.5914	53.80	19.85	7.09
	.083	.8910	1.2085	1.3012	.7435	42.20	25.20	9.01
	.095	1.0162	1.2043	1.4739	.8422	36.85	28.70*	10.25*
	.120	1.2742	1.1958	1.8220	1.0411	29.15	36.00	12.89
3 3/4	.065	.7525	1.3031	1.2777	.6814	57.60	21.30	7.60
	.083	.9562	1.2968	1.6080	.8576	45.20	27.06	9.67
	.095	1.0908	1.2927	1.8228	.9722	39.50	30.84*	11.04*
	.120	1.3685	1.2841	2.2565	1.2035	31.25	38.70	13.82
4	.065	.8035	1.3915	1.5557	.7779	61.50	22.75	8.12
	.083	1.0214	1.3852	1.9597	.9799	42.20	28.95	10.32
	.095	1.1655	1.3810	2.2228	1.1114	42.10	32.95	11.78
	.120	1.4627	1.3725	2.7552	1.3776	33.33	41.40*	14.80*
4 1/4	.134	1.7327	1.4557	3.6732	1.7408	31.75	49.10*	17.55*
4 1/2	.156	2.1289	1.5369	5.0282	2.2347	28.80	60.40*	21.55*
4 3/4	.188	2.6944	1.6143	7.0213	2.9563	25.25	76.25*	27.20*

* AN STANDARD TUBING



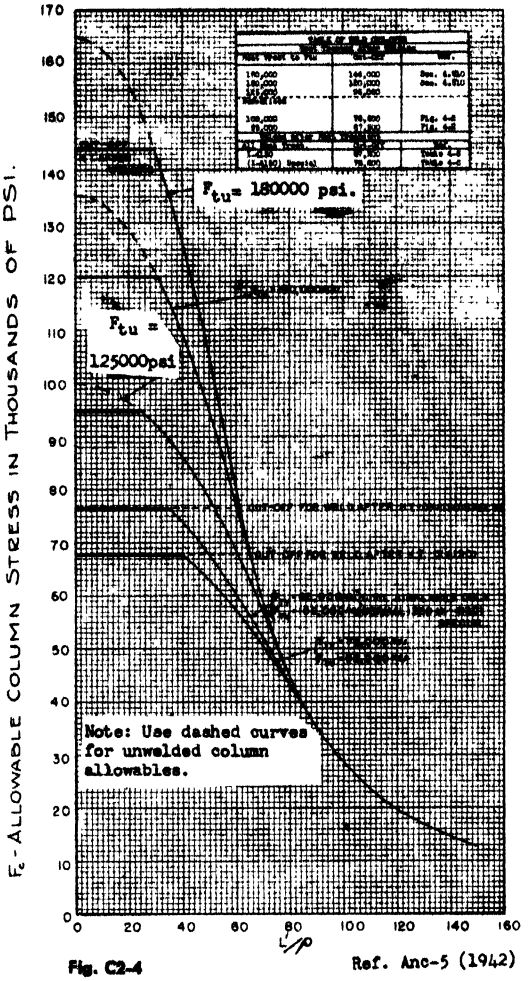


Fig. C2-4 Ref. Anc-5 (1942)

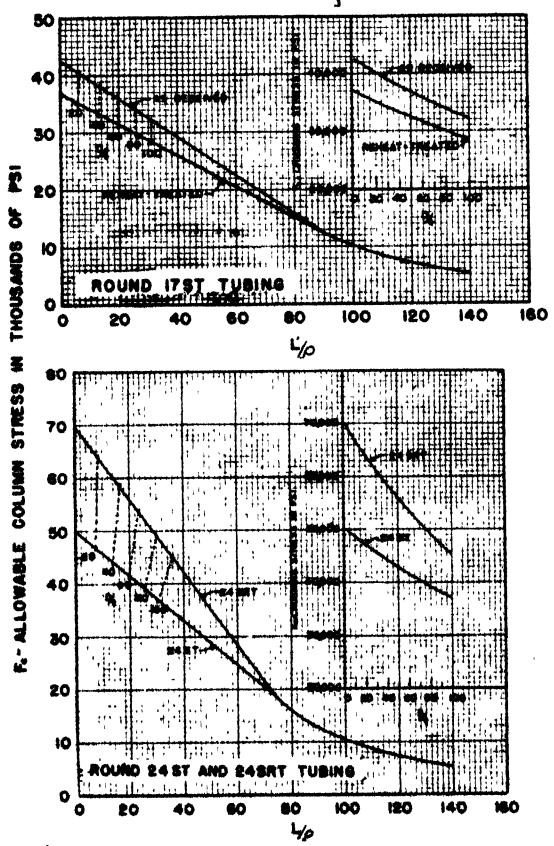


Fig. C2-5 ALLOWABLE COLUMN AND CRUSHING STRESSES ALUMINUM ALLOY TUBING - 17ST

Table C2.3a

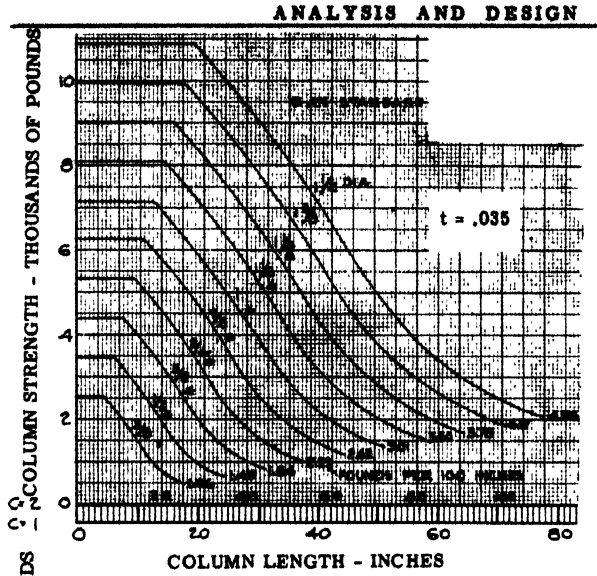
TENSION ALLOWABLES NEAR WELDS IN STEEL TUBING (X-4130)

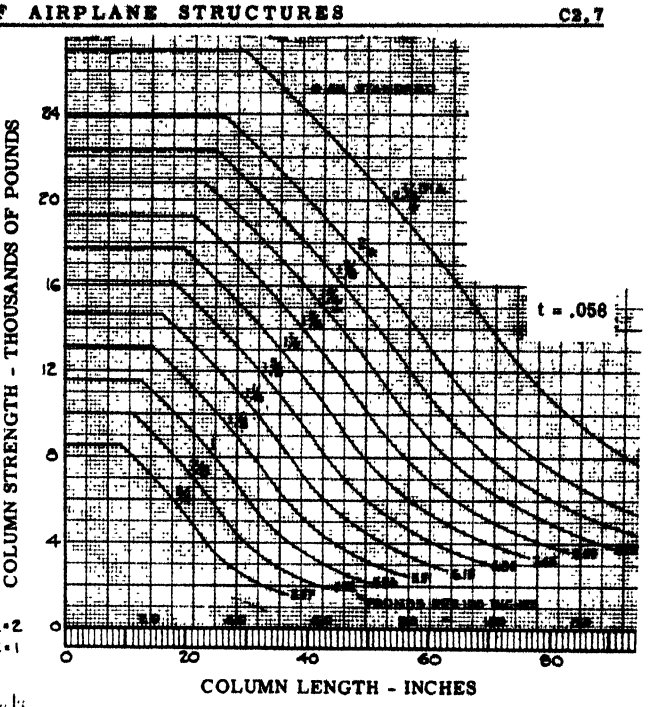
Type of Weld	Normalized Tube Welded	Welded after HT or Norm. after Weld	HT after Welding
*Tapered Welds of 30° or Less	.947 Ftu	90,000 psi	.90 Ftu
All others	.841 Ftu	80,000 psi	.80 Ftu

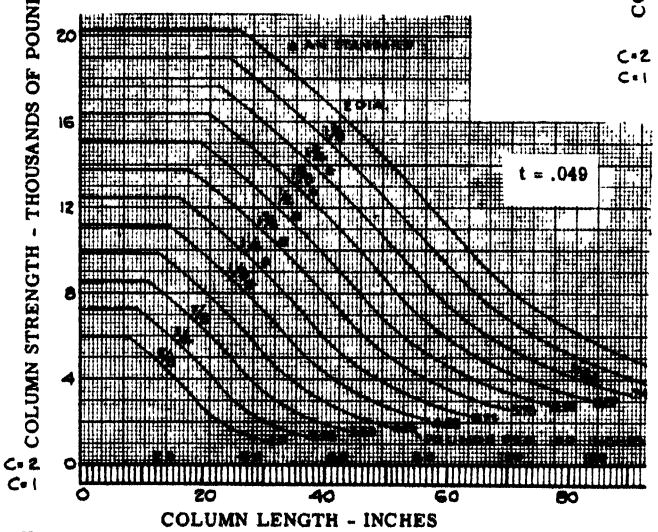
* Note: Gussets or plate inserts considered 0° "taper" with ℄.

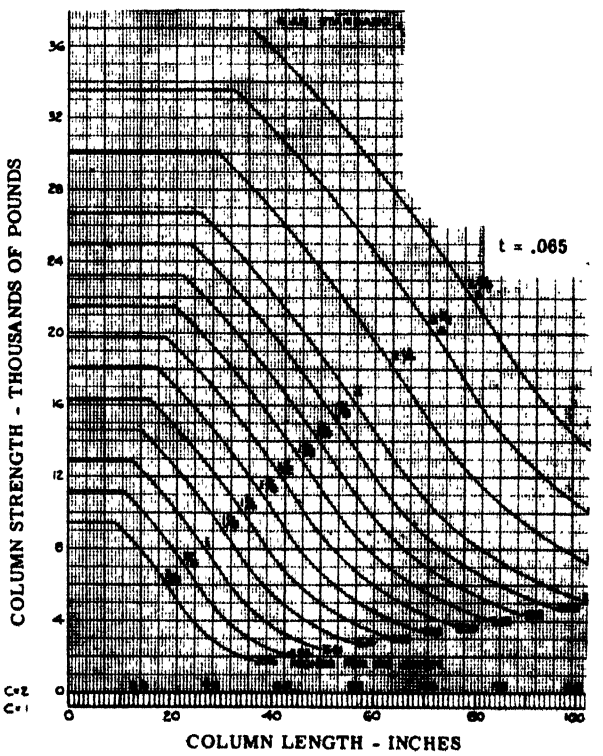
** For (X-4130) Special, comparable, values to the F_{tu}, equal to 90,000 and 80,000, are stresses 94,500, and 84,100 psi, respectively.

Ref. Anc-5 (1942)









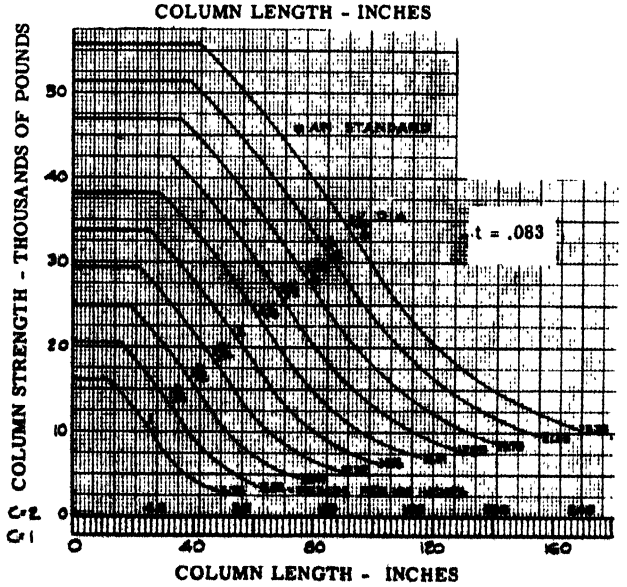


Fig. C2-6

STRENGTH OF CHROME MOLY ROUND STEEL TUBES

F_{TY} = 75,000 PSI F_{TU} = 95,000 PSI

(Curves in this page reproduced from A N C-5, Revised 1942)

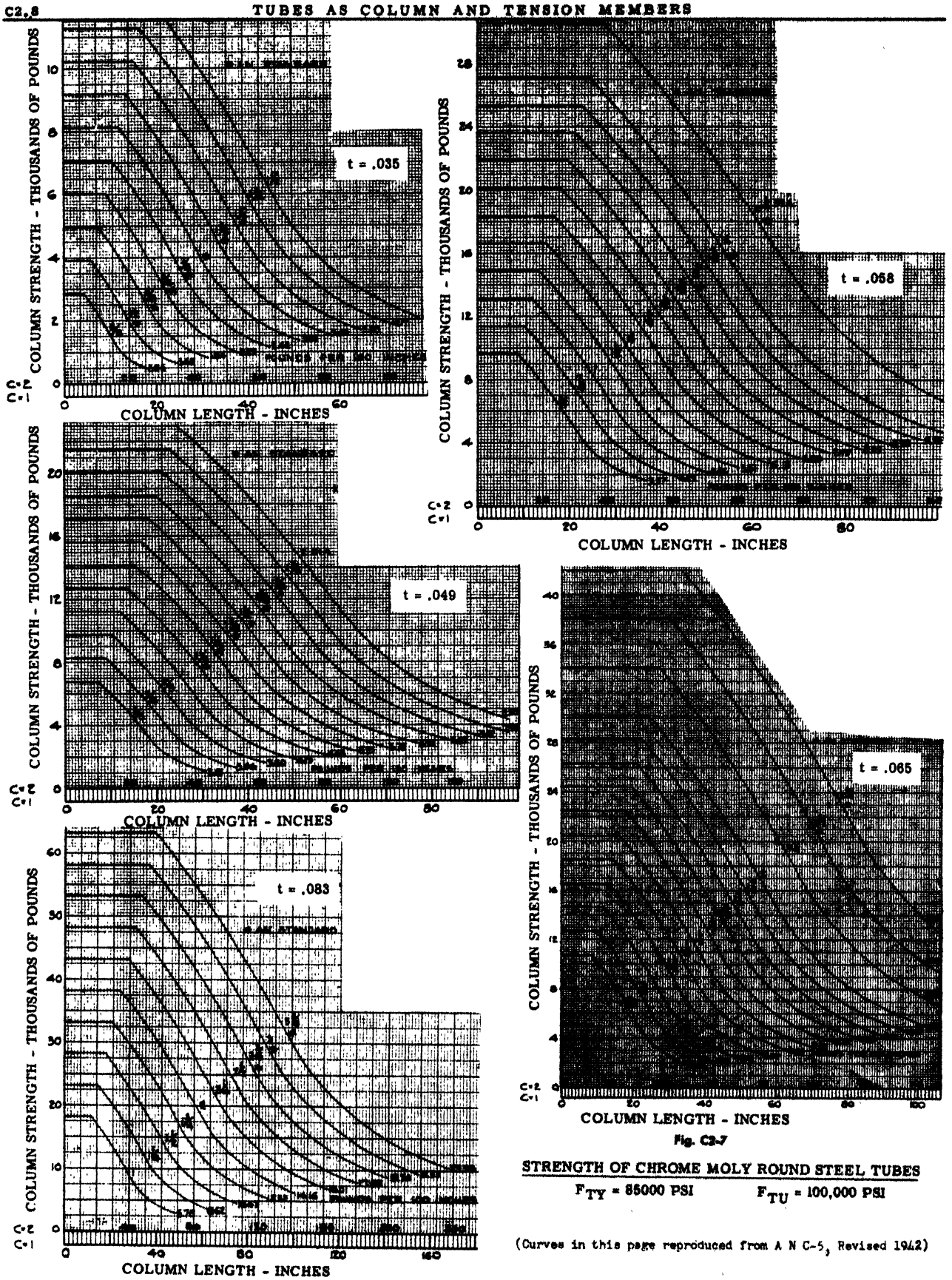


Fig. C2-7

STRENGTH OF CHROME MOLY ROUND STEEL TUBES

F_{TY} = 85000 PSI F_{TU} = 100,000 PSI

(Curves in this page reproduced from A N C-5, Revised 1942)

Fig. C2-8

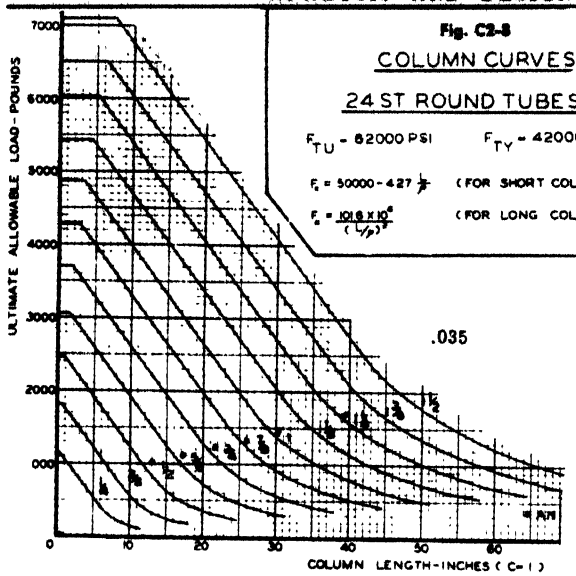
COLUMN CURVES

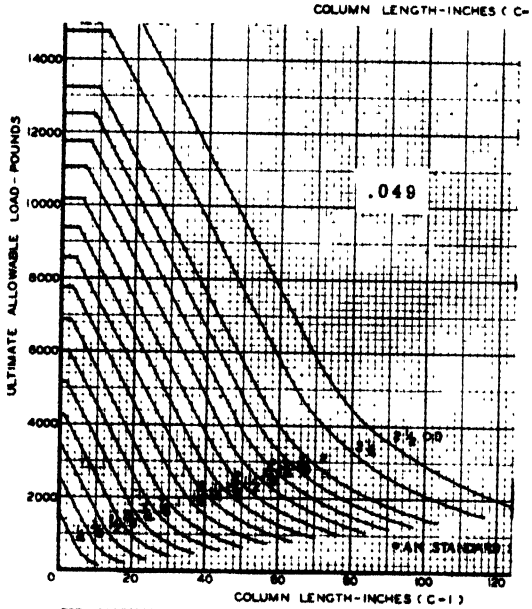
24 ST ROUND TUBES

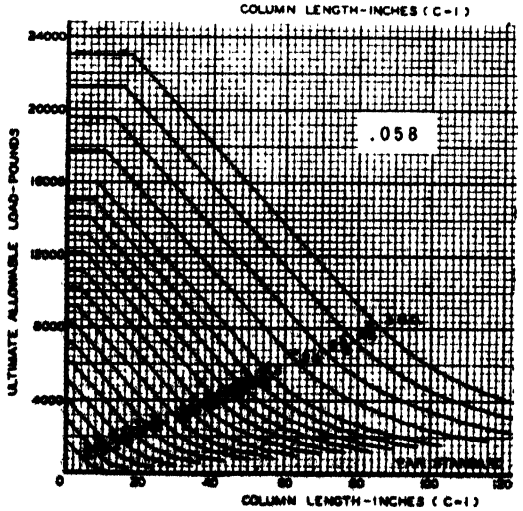
F_{TU} = 62000 PSI F_{TY} = 42000 PSI

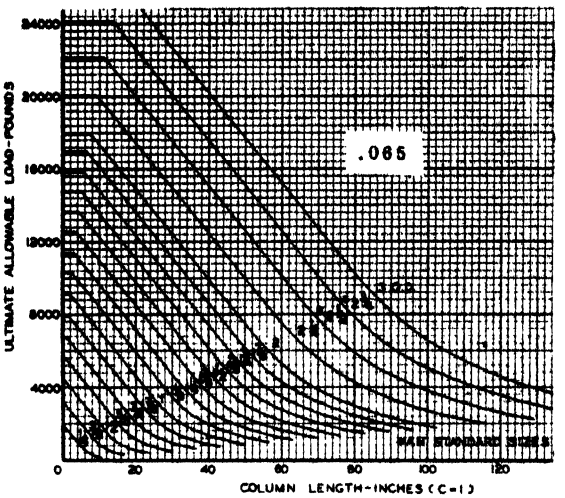
$F_c = 50000 - 427\frac{l}{\rho}$ (FOR SHORT COLUMNS)

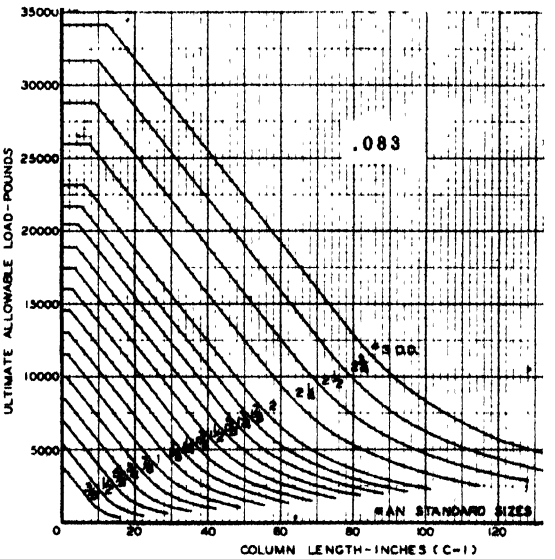
$F_c = \frac{10.8 \times 10^6}{(l/\rho)^2}$ (FOR LONG COLUMNS)

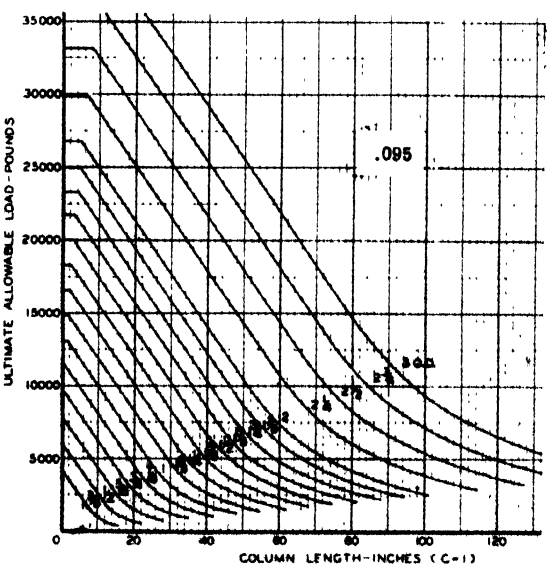












Many structural designers prefer to have large margins of safety on engine mount members as considerable trouble has been encountered in the failure or cracking of engine mount members.

The strength of the 1-1/8 - .049 tube as a column for length = 31.4 and c = 1 equals - 6700# (Fig. C2.6) which gives a margin of safety of (6700/4250) - 1 = .58 on the maximum compressive load. The student should select a tube size for member (1).

Example Problem #2.

Fig. C2.9 shows a welded steel tubular truss representative of the center section portion of a wing beam. The design loads are shown adjacent to each member. The truss member tube sizes for steel with an U.T.S. of 100,000 have been determined and are recorded on the truss.

(1) Determine the margins of safety for the given tube sizes.

(2) Redesign truss considering that truss is heat treated to 150000 U.T.S. after welding.

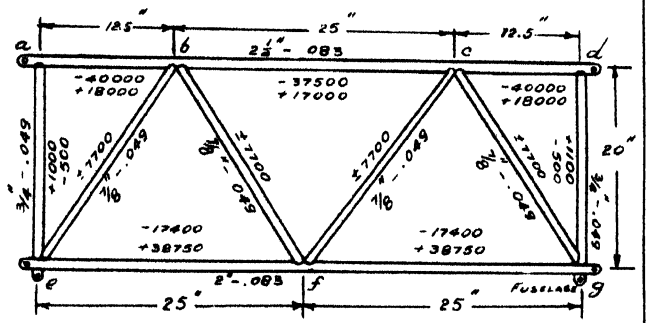


Fig. C2-9

(1) Solution for Margins of Safety for Given Truss:

Since the members of the truss are welded together at the panel joints each member has a certain amount of restraint at each end, that is the fixity coefficient is greater than 1, however it cannot reach a value of c = 4 which is full fixity. Experience of the industry over many years has indicated a fixity coefficient of c = 2 is reasonable for welded steel tubular fuselage trusses and this value is generally used. A more rigorous investigation of member stability is discussed in another chapter.

Consider the Upper Longeron abcd:

This member is composed of one continuous tube, size 2-1/4 .083. For portion bc a fixity coefficient of c = 2 will be used. For the portion ab or cd a value of 1.5 for c will be assumed since only one member (ae) joins ab at a and it is relatively light compared to longeron ab. Considering member bc, whose length is 25" we find in referring to the column curves of Fig. C2.7 that for a 2-1/4 - .083 tube, 25" long when c = 2, the ultimate compressive strength is -43200#. Thus margin of safety is (43200/37500) - 1 = .15. The student should notice that the allowable load falls in the weld cutoff region, (Horizontal line on curves). The effective length of our member using c = 2 is comparatively small thus giving a high allowable column unit stress which exceeds the unit stress allowed on the tube adjacent to the end welding. The strength of bc for the given tension load of 17000 obviously gives a large margin of safety.

Considering member ab, a value of c = 1.5 will be used. The column curves in Fig. C2.7 give base scales for values c = 1 and c = 2 only. Thus we will find the effective length of ab for c = 1.5 and use the result with the c = 1 scale of Fig. C2.7. Effective length $L' = L/\sqrt{c} = 12.5/\sqrt{1.5} = 10.4"$. Referring to Fig. C2.7 for a 2-1/4 - .083 tube when L = 10 we obtain an allowable load of -43200# as before. M.S. = 43200/40000 - 1 = .07.

Consider Lower Longeron efg:

The allowable U.T. stress correcting for welding = .841 x 100000 = 84100 psi. Since the tube is continuous between e and g and the fittings at e and g would be welded to tubes with fishmouth welds, it would be permissible to use a correction factor of .941 instead of .841 (See article C2.9). However to be conservative the value of 84100 psi will be used.

Area of 2 - .083 tube = .500 (See table C2.3)
Allowable tensile strength = .5 x 84100 = 42050# M.S. = (42050/38750) - 1 = .08

The column strength for a length of 25" and c = 2 from Fig. C2.7 equals - 38200#. M.S. = (38200/17400) - 1 = 1.19.

Consider Truss Diagonals:

Size = 7/8 - .049 L = 23.4, c = 2 Load = ±7700
From Fig. C2.7 allowable compressive load = 7900, M.S. = (7900/7700) - 1 = .03.
Allowable tensile strength = 100,000 x .841 x .127 = 10700# (not critical).

The end verticals which carry only a small load are obviously far over strength.

(2) Redesign of tube sizes considering that truss is head treated to 150000 U.T.S. after truss is welded together.

In general heat treating of trusses to high tensile strengths after welding is done only for trusses whose members are short and carry relatively large loads and thus fall definitely in the short column class. Since there is considerable practical difficulty in holding the original shape when being heat treated due to warping etc., the heat treatment of tubular trusses is usually confined to small units and for cases where the weight allowance is very tight. Another disadvantage is that in case of repair the heat treated properties of the tubes are decreased in the vicinity of the welds.

Column charts for 150000 steel similar to those of Fig. C2.7 are not available thus those of Fig. C2.4 must be used or the original column equations of table C2.1.

Design of Upper Longeron abcd:

In Fig. C2.4 we find the allowable column unit stress F_c for heat treated alloy steel plotted against the effective column slenderness ration L'/ρ. The general procedure in selecting a tube to carry a given compressive load is to assume a tube size, which gives a preliminary L/ρ value from which the preliminary allowable stress F_c is obtained. Multiplying F_c by the tube area we get its column strength for the given length. If the resulting strength is too large or small the tube sizes is changed and the checking process repeated. Common sense should be used in guessing at a tube size instead of wild guessing without any logical thought.

Since portion ab carries the largest compressive load it will be considered first. For $c = 1.5$, $L' = L\sqrt{c} = 12.5\sqrt{1.5} = 10.4'$. Since this is a relatively small length, the tube will be designed for crippling stress at the tube ends adjacent to the welds. The tube size obtained from this consideration will be checked for column action.

From Fig. C2.4, the value for F_c as determined by the weld cut-off line for 150000 steel equals 120000 psi.

area required = 40000/120000 = .333 sq. in. From Table C2.3 we find that a 1-3/4 - .065 tube has an area of .3441 and ρ = .5962. The M.S. for local crushing near weld = (.3441/.333) - 1 = .03.

Check tube for column strength: L'/ρ = 10.4/.596 = 17.4

From Fig. C2.4 using dashed portion of curve, F_c = 130000 psi.

Hence $P_a = F_cA$ = 130000 x .3441 = 44800#. M.S. = (44800/40000) - 1 = .12.

Member bc

This member will be made the same size as (ab) namely, 1-3/4 - .065 since a continuous longeron for this short truss is desirable.

$L' = 25/\sqrt{2} = 17.8$, $L'/\rho = 17.8/.596 = 29.8$

From Fig. C2.4 when $L'/\rho = 29.8$, F_c = -120100 psi. The local crushing stress as shown by the weld cut-off line = -120000. Hence P_a = -120000 x .3441 = -41300#. M.S. = (41300/38750) - 1 = .06.

Diagonal Members (be)

Design load = - 7700 $L' = 23.4/\sqrt{2} = 16.6$

From column curves of Fig. C2.7 which is for 100,000 U.T.S. steel we select a 7/8 - .049 tube as necessary. However our material is 150000 U.T.S. so that decreasing the 7/8 - .049 to 7/8 - .035 appears reasonable as a trial size.

For 7/8 - .035, ρ = .297, A = .0924, L'/ρ = 16.6/.297 = 56. From Fig. C2.4, F_c = -88500 psi.

$\therefore$ tube strength = - 88500 x .0924 = - 8180#
M.S. = (8180/7700) - 1 = .06.

The crushing strength adjacent to weld is -120000 psi. (See Fig. C2.4). The allowable tensile stress adjacent to weld is .8 x 150000 = 120000 psi. (See Table C2.3a). Therefore $P_a = F_cA$ = 120000 x .0924 = 11100#. (not critical)

Bottom Longeron.

Design load = + 38750, - 17400#. Design for tension and check for compression. Net area required = $\frac{38750}{.8 \times 150000}$ = 0.324.

Area 1-3/4 - .065 = .344

Area 1-7/8 - .058 = .331

Use 1-7/8 - .058. M.S. = (.331/.324) - 1 = .02
Check column strength

ρ = .643, $L' = 24/\sqrt{2} = 17.8$, $L'/\rho = 17.8/.643 = 27.5$

From chart Fig. C2.4, F_c = 122500 psi. This is more than the crippling stress of .8 x -135000 = -108000 psi. Hence the column of the tube = .331 x 108000 = - 35800#. (not critical).

Since tension is the critical load by a large margin, there are various tubes that could be used. Thus smaller tubes of greater wall thickness would be satisfactory, however since the diagonal members are .035 it is not good practice to go much over .083 for longeron thickness because of danger of burning the thinner tube in welding.

Example Problem #3

A member is 50" long and carries a design load of -10400#. Design a round tube for the following conditions:

(1) Material - steel - F_{tu} = 180000 psi; c = 1

(2) Material - 24SRT Al. Alloy; c = 1.5

Solution

(1) P = -10400, L = 50, c = 1
To obtain preliminary approximate size use steel column curves of Fig. C2.7 which gives following results:

Size	Strength	ρ	L'/ρ	Critical L'/ρ for 180,000 steel (table C2.1)
1 3/4 - .049	-10800	.602	83	59
1 5/8 - .058	-10000	.554	90	59

Therefore the required column falls in the long column range and heat treating to 180000 does not increase the strength over that shown above for 100,000 steel.

Hence size required = 1-3/4 - .049. M.S. = (10800/10400) - 1 = .04

(2) Design of 24SRT round tube.

P = - 10400; L = 50; c = 1.5; L' = $50/\sqrt{1.5} = 40.8$

The column curves of Fig. C2.8 are for 24ST material, and time has not been taken to plot such curves for 24SRT tubes. However good use can be made of these curves for selecting a trial size for 24SRT.

From Fig. C2.8, the following 24ST tubes would be satisfactory.

Size	ρ	L'/ρ	Critical L'/ρ (See table C2.1)
2 1/4 - .058	.775	52.5	66
2 1/4 - .065	.773	52.5	66
2 1/2 - .049	.867	47	66

The results show that the approximate tube required falls definitely into the short column range. Since 24SRT has greater strength properties than 24ST (See Fig. C2.5) it is logical to decrease the above sizes one gauge and check the resulting strengths using 24SRT material. The results are as follows:

Size	Area	ρ	L'/ρ	F_c from Fig. C2.5	P = F_c A	M.S.
2 1/4 - .049	.339	.778	52.5	-32700	-11100	.06
2 1/4 - .058	.399	.775	52.6	-32700	-13000	.25

hence 2-1/4 - .049 is the required size.

If a 17ST material had been specified, the logical procedure would be to increase the preliminary sizes as determined by the 24ST curves by one gauge and check the resulting tubes.

Example Problem #4.

Determine the strength of a 2-3/4 - .049 24ST al. alloy round tube 10 inches long when c = 1.

Solution:

ρ for tube = .955, hence L/ρ = 10/.955 = 10.4
Area = .416
From Fig. C2.5 allowable column stress F_c = - 45500 psi.
The D/t ration of tube = 2.75/.049 = 56

From Fig. C2.5 the crippling stress for D/t = 56 = F_c = -42000. Hence local crippling is critical and P_c = .416 x 42000 = 17500#.

C2.12 Design of Streamline Steel and Aluminum Alloy Tubes as Columns

In the days of the externally braced wing and tail surface and the fixed landing gear, the streamline strut was a major unit of the airplane preliminary structure. However the metal covered cantilever wing and the retractable landing gear has eliminated the necessity of using streamline struts. At present the chief use of streamline struts is the attachment of main and auxiliary floats to the fuselage and wing in small seaplanes.

Table C2.4 gives the section properties of streamline tubes with 2.5 to 1 fineness ratio. In a streamline member acting as a column the member will fail by bending about the major axis unless restraint is provided by end fitting design.

Fig. C2.9 gives the allowable column and crushing stresses for aluminum alloy streamline tubing and Fig. C2.10 gives the same for chrome-molybdenum streamline tubing. Using these column curves the design of a column is a trial and error process. A good procedure to follow in making a guess at the first trial size is to find the size of round tube required from curves of Figs. C2.7 and C2.8 and select a streamline tube with a moment of inertia I about the major axis equal to the I of the required round tube. In general this will give a streamline tube size fairly close to the required size, thus requiring simple modification.

C2.13 Example Problems in Design of Streamline Struts

Fig. C2.12 diagram a shows the three struts that make up the interplane N-strut between the wings of a conventional biplane. The design loads as well as the pin to pin length are given in the figure. Diagram b illustrates the 3 members that form the cabane truss between the upper wing and the fuselage. Design loads and lengths are given in the figure.

The size of 24ST aluminum alloy streamline struts will be determined for the front interplane strut (member AC) and the front cabane strut (member FH.)

Member Ac

Design load = - 2950#, L = 65.6, c = 1

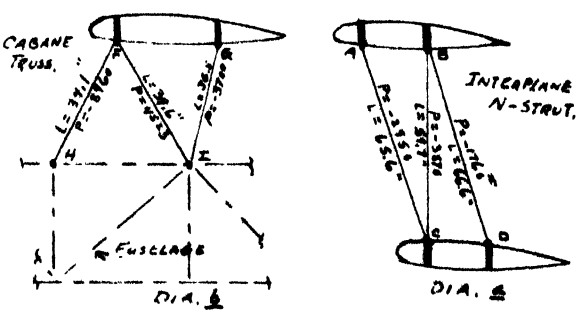


Fig. C2-12

*Streamline** TABLE C2.4 SECTION PROPERTIES OF STREAMLINE TUBING (Fineness Ratio 2.5 to 1)

Equiv. Round O.D.	Wall Dec'l	Wall Gage	Axes Major	Axes Minor	Area	Wt per ft	I Major	Z Major	ρ Major	I Minor	Z Minor	ρ Minor
¾	.035	20	1 0114	.4286	.0786	.2673	.0017	.0079	.1486	.0073	.0140	.3046
	.049	18	"	"	.1079	.3668	.0022	.0103	.1435	.0097	.0187	.2998
⅞	.035	20	1 1800	.5000	.0924	.3140	.0028	.0112	.1753	.0118	.0195	.3572
	.049	18	"	"	.1272	.4323	.0037	.0148	.1703	.0158	.0261	.3525
	.058	17	"	"	.1489	.5061	.0042	.0168	.1671	.0182	.0301	.3495
1	.035	20	1 3485	.5714	.1061	.3607	.0043	.0151	.2020	.0178	.0257	.4100
	.049	18	"	"	.1464	.4977	.0057	.0200	.1972	.0239	.0345	.4044
	.058	17	"	"	.1716	.5835	.0065	.0228	.1939	.0278	.0402	.4023
1⅛	.035	20	1 5170	.6428	.1199	.4074	.0063	.0195	.2292	.0257	.0329	.4626
	.049	18	"	"	.1656	.5631	.0083	.0258	.2240	.0347	.0445	.4573
	.058	17	"	"	.1944	.6609	.0094	.0292	.2205	.0402	.0516	.4549
	.065	16	"	"	.2165	.7359	.0103	.0320	.2182	.0443	.0569	.4525
1¼	.035	20	1 6857	.7143	.1336	.4542	.0088	.0246	.2559	.0355	.0409	.5154
	.049	18	"	"	.1849	.6285	.0116	.0325	.2509	.0482	.0557	.5107
	.058	17	"	"	.2172	.7384	.0133	.0372	.2477	.0560	.0647	.5077
	.065	16	"	"	.2420	.8226	.0145	.0406	.2451	.0618	.0714	.5053
1⅜	.035	20	1 8543	.7857	.1473	.5009	.0118	.0300	.2828	.0476	.0549	.5683
	.049	18	"	"	.2041	.6939	.0157	.0400	.2777	.0648	.0680	.5635
	.058	17	"	"	.2400	.8158	.0181	.0461	.2745	.0754	.0791	.5604
	.065	16	"	"	.2675	.9094	.0198	.0504	.2719	.0833	.0875	.5581
1½	.035	20	2 0228	.8571	.1611	.5476	.0154	.0359	.3096	.0621	.0597	.6209
	.049	18	"	"	.2234	.7593	.0207	.0483	.3045	.0848	.0815	.6162
	.058	17	"	"	.2627	.8932	.0239	.0555	.3014	.0988	.0951	.6131
	.065	16	"	"	.2934	.9962	.0262	.0611	.2989	.1093	.1052	.6108
	.083	14	"	"	.3695	1 256	.0316	.0737	.2923	.1351	.1302	.6047
1⅝	.035	20	2 1913	.9285	.1748	.5943	.0198	.0426	.3365	.0793	.0704	.6736
	.049	18	"	"	.2426	.8248	.0266	.0573	.3314	.1085	.0964	.6689
	.058	17	"	"	.2855	.9707	.0308	.0448	.3282	.1266	.1124	.6659
	.065	16	"	"	.3186	1 083	.0338	.0728	.3256	.1402	.1245	.6634
	.083	14	"	"	.4021	1 367	.0410	.0883	.3192	.1738	.1545	.6574
	.095	13	"	"	.4566	1 552	.0453	.0976	.3149	.1949	.1732	.6541
1¾	.035	20	2 3600	1 0000	.1886	.6411	.0249	.0498	.3633	.0995	.0820	.7263
	.049	18	"	"	.2618	.8902	.0336	.0672	.3583	.1363	.1123	.7216
	.058	17	"	"	.3083	1 048	.0389	.0778	.3551	.1592	.1312	.7186
	.065	16	"	"	.3441	1 170	.0428	.0856	.3525	.1765	.1455	.7163
	.083	14	"	"	.4347	1 478	.0521	.1042	.3461	.2192	.1809	.7101
	.095	13	"	"	.4939	1 679	.0577	.1154	.3418	.2463	.2034	.7061
1⅞	.035	20	2 5285	1 0714	.2023	.6878	.0308	.0575	.3902	.1227	.0943	.7789
	.049	18	"	"	.2811	.9556	.0417	.0779	.3851	.1685	.1296	.7743
	.058	17	"	"	.3311	1 126	.0482	.0900	.3815	.1969	.1515	.7712
	.065	16	"	"	.3696	1 257	.0532	.0993	.3794	.2186	.1683	.7690
	.083	14	"	"	.4673	1 589	.0650	.1214	.3729	.2719	.2093	.7624
	.095	13	"	"	.5312	1 806	.0722	.1348	.3687	.3098	.2770	.7523
2	.035	20	2 6970	1 1428	.2161	.7345	.0376	.0658	.4170	.1494	.1076	.8313
	.049	18	"	"	.3003	1 021	.0510	.0893	.4120	.2053	.1480	.8269
	.058	17	"	"	.3539	1 203	.0591	.1034	.4088	.2402	.1732	.8238
	.065	16	"	"	.3951	1 343	.0652	.1141	.4062	.2668	.1925	.8217
	.083	14	"	"	.4999	1 699	.0799	.1398	.3998	.3325	.2399	.8156
	.095	13	"	"	.5685	1 933	.0889	.1556	.3954	.3744	.2703	.8115
2¼	.049	18	3 0343	1 2857	.3388	1 152	.0735	.1144	.4657	.2946	.1887	.9325
	.058	17	"	"	.3994	1 358	.0854	.1329	.4625	.3450	.2212	.9294
	.065	16	"	"	.4462	1 517	.0944	.1469	.4600	.3835	.2458	.9271
	.083	14	"	"	.5650	1 921	.1161	.1807	.4531	.4794	.3075	.9123
	.095	13	"	"	.6432	2 186	.1298	.2020	.4492	.5409	.3470	.9170
	.120	11	"	"	.8030	2 730	.1558	.2421	.4402	.6629	.4255	.9086
2½	.049	18	3 3713	1 4285	.3773	1 283	.1018	.1425	.5194	.4063	.2343	1.0377
	.058	17	"	"	.4450	1 513	.1186	.1660	.5163	.4764	.2747	1.0348
	.065	16	"	"	.4972	1 690	.1312	.1837	.5137	.5300	.3057	1.0325
	.083	14	"	"	.6302	2 143	.1621	.2269	.5071	.6640	.3832	1.0265
	.095	13	"	"	.7178	2 440	.1815	.2541	.5028	.7504	.4333	1.0224
	.120	11	"	"	.8972	3 050	.2188	.3063	.4938	.9236	.5329	1.0141
2¾	.049	18	3 7085	1 5714	.4158	1 414	.1366	.1739	.5732	.5434	.2848	1.1432
	.058	17	"	"	.4905	1 668	.1593	.2028	.5699	.6372	.3340	1.1398
	.065	16	"	"	.5483	1 864	.1765	.2247	.5674	.7099	.3723	1.1379
	.083	14	"	"	.6954	2 364	.2188	.2785	.5609	.8907	.4673	1.1318
	.095	13	"	"	.7924	2 694	.2455	.3125	.5566	1.0081	.5299	1.1279
	.120	11	"	"	.9915	3 371	.2973	.3785	.5476	1.2427	.6523	1.1196
3	.058	17	4 0455	1 7142	.5361	1 822	.2085	.2433	.6236	.8118	.3997	1.2456
	.065	16	"	"	.5993	2 037	.2312	.2698	.6211	.9265	.4452	1.2434
	.083	14	"	"	.7606	2 586	.2872	.3352	.6145	1.1645	.5599	1.2373
	.095	13	"	"	.8670	2 947	.3229	.3768	.6103	1.3184	.6338	1.2332
	.120	11	"	"	1.0857	3 691	.3925	.4580	.6013	1.6289	.7839	1.2249
	.156	9/32	"	"	1.3959	4 746	.4824	.5630	.5879	2.0497	.9869	1.2118
3¼	.058	17	4 3828	1 8571	.5816	1 977	.2668	.2873	.6773	1.0617	.4708	1.3511
	.065	16	"	"	.6504	2 211	.2961	.3189	.6747	1.1830	.5248	1.3487
	.083	14	"	"	.8258	2 807	.3689	.3973	.6684	1.4886	.6604	1.3426
	.095	13	"	"	.9416	3 201	.4150	.4470	.6639	1.6873	.7449	1.3386
	.120	11	"	"	1.1800	4 011	.5062	.5452	.6549	2.0887	.9275	1.3304
	.156	5/32	"	"	1.5186	5 163	.6251	.6732	.6416	2.6353	1.1707	1.3173
3½	.065	16	4 7200	2 0000	.7014	2 385	.3723	.3723	.7286	1.4831	.6108	1.4541
	.083	14	"	"	.8910	3 029	.4645	.4645	.7220	1.8686	.7699	1.4481
	.095	13	"	"	1.0162	3 455	.5234	.5234	.7177	2.1194	.8733	1.4442
	.120	11	"	"	1.2742	4 332	.6400	.6400	.7087	2.6269	1.0828	1.4358
	.156	5/32	"	"	1.6414	5 580	.7934	.7934	.6952	3.3221	1.3705	1.4227
3¾	.065	16	5 0570	2 1428	.7525	2 558	.4604	.4297	.7822	1.8299	.7033	1.5594
	.083	14	"	"	.9562	3 251	.5754	.5371	.7757	2.3073	.8871	1.5534
	.095	13	"	"	1.0908	3 708	.6490	.5777	.7713	2.6195	1.0075	1.5497
	.120	11	"	"	1.3685	4 652	.7955	.7425	.7624	3.2505	1.2502	1.5412
	.156	5/32	"	"	1.7641	5 997	.9894	.9235	.7489	4.1192	1.5855	1.5281
4	.065	16	5 3940	2 2856	.8033	2 732	.5614	.4912	.8359	2.2270	.8025	1.6648
	.083	14	"	"	1.0214	3 472	.7024	.6146	.8293	2.8161	1.0148	1.6604
	.095	13	"	"	1.1655	3 962	.7933	.6941	.8250	3.1917	1.1506	1.6549
	.120	11	"	"	1.4627	4 973	.9739	.8522	.8160	3.9661	1.4303	1.6467
	.156	5/32	"	"	1.8867	6 414	1.2153	1.0634	.8026	5.0332	1.8164	1.6333
	.188	3/16	"	"	2.2457	7 635	1.4109	1.2345	.7926	5.9364	2.1431	1.6259
4¼	.065	16	5 7513	2 4285	.8546	2 905	.6761	.5568	.8895	2.6784	.9082	1.7704
	.083	14	"	"	1.0866	3 694	.8473	.6978	.8830	3.3817	1.1471	1.7641
	.095	13	"	"	1.2400	4 216	.9574	.7885	.8787	3.8426	1.3055	1.7604
	.120	11	"	"	1.5570	5 293	1.1779	.9701	.8698	4.7789	1.6216	1.7519
	.156	5/32	"	"	2.0095	6 832	1.4729	1.2131	.8573	6.0748	2.0628	1.7387
	.188	3/16	"	"	2.3930	8 135	1.7144	1.4120	.8464	7.1732	2.4365	1.7314
4½	.083	14	6 0683	2 5713	1.1517	3 915	1.0105	.7860	.9367	4.0256	1.2894	1.8696
	.095	13	"	"	1.3147	4 469	1.1429	.8889	.9324	4.5759	1.4662	1.8656
	.120	11	"	"	1.6512	5 613	1.4082	1.0953	.9235	5.6952	1.8254	1.8572
	.156	5/32	"	"	2.1322	7 249	1.7650	1.3728	.9098	7.2508	2.3247	1.8441
	.188	3/16	"	"	2.5403	8 636	2.0580	1.6007	.9001	8.5740	2.7498	1.8372
	.219	7/32	"	"	2.9421	10 01	2.3221	1.8061	.8884	9.8001	3.1451	1.8251

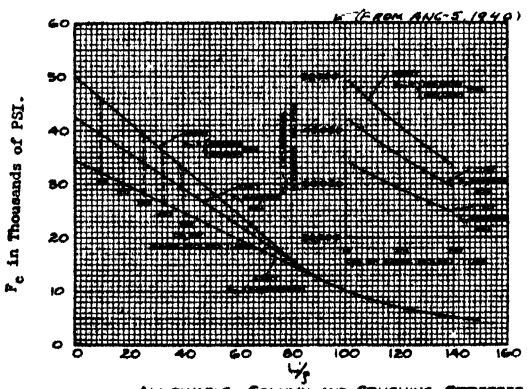
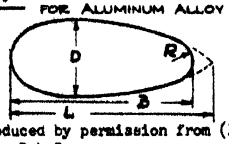


Fig. C2-9 ALLOWABLE COLUMN AND CRUSHING STRESSES FOR ALUMINUM ALLOY STREAMLINE TUBING



B·.944L R·.19 D

D·.5714d L·2.5D

d·Equiv Round Dia.

* Reproduced by permission from (1941) Summerill "Aircraft Tubing Data".

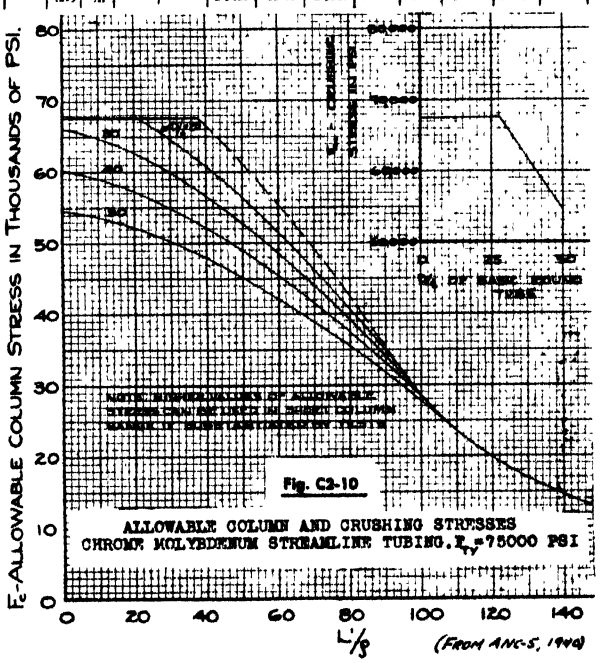


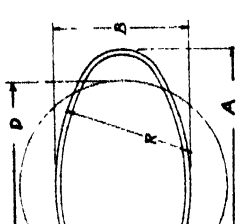
Fig. C2-10 ALLOWABLE COLUMN AND CRUSHING STRESSES CHROME MOLYBDENUM STREAMLINE TUBING. F_{ty}=75000 PSI

Squares *TABLE C2.5 SECTION PROPERTIES OF SQUARE TUBING

Size Dist. Across Flats	Wall Dec'l	Wall Gage	Area	Wt per ft	I	Z	ρ
½	.022	24	.0294	.0998	.0006	.0031	.1415
	.028	22	.0368	.1252	.0007	.0038	.1396
	.035	20	.0453	.1589	.0009	.0045	.1372
	.049	18	.0612	.2081	.0011	.0057	.1318
⅝	.022	24	.0386	.1348	.0016	.0065	.2023
	.028	22	.0499	.1697	.0020	.0079	.1991
	.035	20	.0616	.2096	.0024	.0094	.1956
	.049	18	.0841	.2861	.0030	.0120	.1892
	.058	17	.0980	.3330	.0033	.0134	.1853
	.065	16	.1084	.3684	.0035	.0141	.1804
¾	.022	24	.0483	.1641	.0033	.0104	.2600
	.028	22	.0630	.2143	.0040	.0129	.2526
	.035	20	.0780	.2652	.0048	.0155	.2489
	.049	18	.1071	.3640	.0063	.0201	.2420
	.058	17	.1251	.4253	.0071	.0227	.2379
	.065	16	.1388	.4717	.0077	.0245	.2348
⅞	.028	22	.0761	.2588	.0064	.0168	.2890
	.035	20	.0944	.3209	.0078	.0206	.2866
	.049	18	.1300	.4419	.0103	.0274	.2816
	.058	17	.1522	.5175	.0118	.0313	.2784
	.065	16	.1692	.5751	.0129	.0342	.2760
	.083	14	.2113	.7184	.0154	.0408	.2700
7/8	.028	22	.0892	.3033	.0103	.0236	.3390
	.035	20	.1108	.3766	.0125	.0288	.3364
	.049	18	.1528	.5193	.0168	.0386	.3320
	.058	17	.1794	.6098	.0193	.0445	.3283
	.065	16	.1996	.6785	.0212	.0487	.3528
	.083	14	.2502	.8504	.0255	.0588	.3194
1	.028	22	.1023	.3479	.0154	.0309	.3883
	.035	20	.1271	.4322	.0190	.0380	.3867
	.049	18	.1758	.5978	.0256	.0511	.3813
	.058	17	.2065	.7020	.0295	.0591	.3782
	.065	16	.2300	.7819	.0324	.0649	.3756
	.083	14	.2890	.9824	.0394	.0788	.3693
	.095	13	.3272	1.112	.0436	.0873	.3652
1¼	.035	20	.1435	.4878	.0275	.0489	.4340
	.049	18	.1988	.6757	.0369	.0657	.4311
	.058	17	.2336	.7942	.0427	.0759	.4265
	.065	16	.2604	.8852	.0471	.0838	.4241
	.083	14	.3278	1.114	.0576	.1024	.4191
	.095	13	.3716	1.263	.0640	.1138	.4151
	.120	11	.4600	1.564	.0760	.1351	.4064
1¼	.035	20	.1599	.5435	.0378	.0604	.4891
	.049	18	.2217	.7536	.0513	.0821	.4831
	.058	17	.2608	.8865	.0595	.0952	.4778
	.065	16	.2908	.9886	.0657	.1051	.4753
	.083	14	.3666	1.246	.0805	.1290	.4950
	.095	13	.4161	1.414	.0899	.1438	.4647
	.120	11	.5161	1.755	.1074	.1718	.4561
1⅜	.035	20	.1763	.5992	.0506	.0736	.5360
	.049	18	.2446	.8316	.0689	.1003	.5309
	.058	17	.2879	.9787	.0801	.1166	.5276
	.065	16	.3212	1.092	.0886	.1288	.5251
	.083	14	.4055	1.378	.1091	.1587	.5187
	.095	13	.4605	1.566	.1219	.1773	.5145
	.120	11	.5723	1.946	.1464	.2130	.5058

Side	Wall Dec'l	Wall Gage	Area	Wt per ft	I	Z	ρ
1½	.035	20	.1926	.6549	.0661	.0881	.5859
	.049	18	.2675	.9095	.0902	.1203	.5807
	.058	17	.3150	1.071	.1051	.1401	.5776
	.065	16	.3516	1.195	.1162	.1550	.5750
	.083	14	.4443	1.510	.1436	.1915	.5686
	.095	13	.5050	1.717	.1608	.2144	.5643
	.120	11	.6284	2.136	.1940	.2586	.5556
1¾	.049	18	.3134	1.065	.1451	.1658	.6804
	.058	17	.3693	1.255	.1691	.1932	.6766
	.065	16	.4124	1.402	.1877	.2146	.6747
	.083	14	.5220	1.774	.2331	.2663	.6682
	.095	13	.5938	2.019	.2618	.2992	.6640
	.120	11	.7307	2.484	.3175	.3628	.6592
2	.049	18	.3592	1.221	.2180	.2180	.7790
	.058	17	.4236	1.440	.2557	.2557	.7769
	.065	16	.4732	1.609	.2838	.2838	.7744
	.083	14	.5996	2.038	.3536	.3536	.7679
	.095	13	.6827	2.321	.3981	.3981	.7636
	.120	11	.8530	2.900	.4859	.4856	.7548
	.156	5/32	1.0912	3.710	.6010	.6010	.7422
2¼	.049	18	.4051	1.377	.3080	.2738	.8721
	.058	17	.4778	1.624	.3607	.3207	.8689
	.065	16	.5341	1.816	.4000	.3556	.8654
	.083	14	.6773	2.302	.5007	.4451	.8598
	.095	13	.7716	2.623	.5640	.5013	.8549
	.120	11	.9652	3.281	.6918	.6149	.8466
	.156	5/32	1.2372	4.206	.8765	.7791	.8418
2½	.058	17	.5321	1.809	.5074	.4035	.9757
	.065	16	.5949	2.022	.5643	.4488	.9739
	.083	14	.7549	2.566	.7071	.5625	.9678
	.095	13	.8605	2.925	.7981	.6530	.9631
	.120	11	1.0775	3.663	.9809	.7806	.9541
	.156	5/32	1.3831	4.702	1.2256	.9760	.9413
	.188	3/16	1.6479	5.602	1.4257	1.3183	.9301
2¾	.058	17	.5864	1.993	.6792	.4940	1.0763
	.065	16	.6557	2.229	.7559	.5497	1.0737
	.083	14	.8326	2.830	.9481	.6896	1.0671
	.095	13	.9494	3.227	1.0724	.7799	1.0628
	.120	11	1.1898	4.045	1.3213	.8653	1.0541
	.156	5/32	1.5291	5.198	1.6569	1.1121	1.0410
	.188	3/16	1.8238	6.200	1.9334	1.3264	1.0296
3	.065	16	.7166	2.436	.9860	.6573	1.1730
	.083	14	.9102	3.094	1.2394	.8263	1.1669
	.095	13	1.0383	3.530	1.4032	.9355	1.1625
	.120	11	1.3021	4.426	1.7325	1.1550	1.1544
	.156	5/32	1.6750	5.694	2.1793	1.4529	1.1406
	.188	3/16	1.9997	6.798	2.5503	1.7002	1.1381
	.219	7/32	2.3081	7.847	2.8873	1.9249	1.1184

Ovals *TABLE C2.5a. SECTION PROPERTIES OF OVAL TUBING



A = 2
B = 1.57 D
R = 1.100 D (approx.)
r = .206 D (approx.)
D = Equiv. Round Dia.

Equiv. Round O.D.	Wall Dec'l	Wall Gage	Axes Major	Axes Minor	Area	Wt. per ft.	I Minor	I Major	Z Minor	Z Major	ρ Minor	ρ Major
¾	.035	20	.9728	.4864	.0786	.2673	.0069	.0179	.0143	.0371	.2971	.4768
	.049	18	1.1348	.5674	.0924	.3140	.0112	.0198	.0185	.0485	.3485	.4628
1	.035	20	1.2972	.6486	.1222	.4323	.0150	.0265	.0265	.0652	.3437	.4659
	.049	18			.1464	.4977	.0179	.0314	.0262	.0771	.4003	.4633
	.058	17			.1599	.5607	.0197	.0329	.0353	.0824	.3954	.4539
	.065	16			.1696	.5631	.0211	.0345	.0335	.0853	.4518	.4469
1¼	.035	20	1.6212	.8106	.1536	.5242	.0318	.0536	.0418	.0957	.4554	.4886
	.049	18			.1849	.6285	.0359	.0599	.0657	.0957	.4657	.4952
	.058	17			.2172	.7384	.0513	.0631	.0453	.1092	.5546	.4906
1¼	.035	20	1.7824	.8912	.1473	.5009	.0354	.0607	.0568	.1092	.4992	.5463
	.049	18			.2041	.6939	.0238	.0464	.0716	.1804	.5463	.5182
	.058	17			.2400	.8158	.0535	.0415	.0804	.1359	.6038	.5151
1½	.035	20	1.9456	.9728	.1611	.5476	.0232	.0559	.0604	.1359	.6016	.5159
	.049	18			.2234	.7593	.0272	.0869	.0831	.1489	.5983	.5160
	.058	17			.2627	.8932	.0314	.0646	.0967	.1489	.5960	.5160
	.065	16			.2930	.9962	.0346	.0711	.1070	.1459	.5960	.5160
1⅝	.035	20	2.1076	1.0538	.2426	.8248	.0149	.0763	.0962	.1795	.6531	.5492
	.049	18			.2855	.9707	.0204	.0767	.1145	.2263	.6492	.5463
	.058	17			.3186	1.083	.0245	.0845	.1267	.2263	.6467	.5463
1⅝	.049	18	2.2200	1.1350	.3538	1.203	.0336	.0940	.1146	.2129	.7050	.5463
	.058	17			.3983	1.048	.0440	.0706	.1391	.2129	.7037	.5463
	.065	16			.3441	1.170	.0561	.0992	.1482	.4015	.6992	.5463
1⅝	.049	18	2.4320	1.2160	.2811	.9556	.0546	.0897	.1608	.4405	.7564	.5463
	.058	17			.3311	1.126	.0653	.1042	.1923	.4374	.7532	.5463
	.065	16			.3696	1.257	.0699	.1130	.2068	.4347	.7507	.5463
1¾	.049	18	2.5940	1.2970	.4673	1.589	.0899	.1413	.2129	.4287	.7445	.5463
	.058	17			.5003	1.021	.1021	.1027	.1512	.4710	.8180	.5463
	.065	16			.5539	1.203	.1194	.1961	.1767	.4681	.8047	.5463
	.083	14			.3951	1.343	.0856	.1320	.2543	.4658	.8023	.5463
	.095	13			.4999	1.699	.1054	.1625	.2441	.4591	.7958	.5463
	.120	11			.5685	1.935	.1177	.1815	.3166	.4551	.7917	.5463
1⅞	.058	17	2.9184	1.4592	.3994	1.358	.1117	.1531	.2747	.5289	.9080	.6096
	.065	16			.4462	1.517	.1237	.1695	.2993	.5266	.9055	.6096
	.083	14			.5650	1.921	.1529	.2095	.3658	.5202	.8991	.6096
	.095	13			.6432	2.186	.1713	.2348	.4568	.5160	.8948	.6096
2	.058	17	3.2428	1.6214	.4450	1.513	.1549	.1911	.3329	.5900	1.0112	.6768
	.065	16			.4972	1.690	.1716	.2117	.3729	.5875	1.0088	.6768
	.083	14			.6302	2.143	.2129	.2626	.4658	.5812	1.0024	.6768
	.095	13			.7178	2.440	.2390	.2948	.5285	.5771	.9981	.6768
	.120	11			.8972	3.050	.2900	.3577	.6488	.5685	.9895	.6768
2⅛	.065	16	3.5668	1.7834	.5483	1.864	.2306	.2586	.4516	.6412	1.1118	.7440
	.083	14			.6954	2.364	.2868	.3216	.5617	.6412	1.1054	.7440
	.095	13			.7924	2.694	.3225	.3617	.6380	.6412	1.1001	.7440
	.120	11			.9915	3.371	.3927	.4404	.7833	.6394	1.0923	.7440
	.156	5/32			1.2732	4.328	.4841	.5430	1.0789	.6167	1.0789	.7440
2¼	.065	16	3.9812	1.9456	.5993	2.037	.3019	.3105	.4548	.7097	1.2151	.8160
	.083	14			.7606	2.587	.3783	.3868	.5711	.7034	1.2086	.8160
	.095	13			.8670	2.949	.4238	.4357	.6464	.6992	1.2044	.8160
	.120	11			1.0857	3.691	.5176	.5321	.8179	.6905	1.1955	.8160
	.156	5/32			1.3959	4.746	.6409	.6589	1.0024	.6776	1.1820	.8160
	.188	3/16			1.6967	5.771	.7396	.7603	1.1721	2.2863	1.1732	.8160
2½	.065	16	4.2152	2.1076	.6504	2.211	.3862	.3664	.5242	.7705	1.3180	.8832
	.083	14			.8258	2.807	.4823	.4576	.6642	.7642	1.3117	.8832
	.095	13			.9416	3.201	.5438	.5161	.7460	.7600	1.3074	.8832
	.120	11			1.1800	4.011	.6660	.6320	.9441	.7513	1.2985	.8832
	.156	5/32			1.5186	5.163	.8239	.7856	1.1596	.7385	1.2849	.8832
	.188	3/16			1.8460	6.133	.9586	.9096	1.3521	.7221	1.2765	.8832
3	.065	16	4.8851	2.4274	.7014	2.385	.5504	.4172	.6244	.8116	1.4215	1.0176
	.083	14			.8910	3.029	.6868	.5217	.7859	.8055	1.4150	1.0176
	.095	13			1.0162	3.455	.7750	.6036	.9169	.8017	1.4107	1.0176
	.120	11			1.2742	4.332	.9699	.7408	1.1031	.7931	1.4017	1.0176
	.156	5/32			1.6414	5.580	1.2486	.9239	1.3931	.7993	1.3880	1.0176
	.188	3/16			1.9912	6.663	1.5117	1.0729	1.6361	.7900	1.3796	1.0176
3½	.065	16	5.5586	2.7698	.8024	2.727	.7955	.4778	.7146	.9528	1.6252	1.1520
	.083	14			1.0194	3.465	.9923	.5974	.8975	.9466	1.6187	1.1520
	.095	13			1.1628	3.952	1.1205	.6911	1.0473	.9424	1.6144	1.1520
	.120	11			1.4584	4.958	1.4030	.8486	1.2646	.9317	1.6054	1.1520
	.156	5/32			1.8869	6.414	1.8071	1.1016	1.6000	.9178	1.5918	1.1520
	.188	3/16			2.3047	7.835	2.1888	1.2337	1.9400	.9038	1.5834	1.1520

A = 2
B = 1.57 D
R = 1.100 D (approx.)
r = .206 D (approx.)
D = Equiv. Round Dia.

*Tables C2.5 and C2.5a reproduced by permission from Summerill "Aircraft Tubing Data", (1941).

To obtain a preliminary size, select a round 24ST tube for the given load and length from curves of Fig. C2.8. The results are 1-7/8 - .058 or 1-3/4 - .065 with moments of inertia of .136 and .122 respectively. A streamline tube size having a moment of inertia about the major axis equal approximately to the above values will be selected from table C2.4. The following sizes are selected:

Size	I_m	A	ρ	L/ρ	F_c, Fig. C2.9	$P_c = F_cA$
2 1/2 - .058	.1186	.445	.516	127	-6300	-2800
2 1/2 - .065	.1312	.497	.514	127	-6300	-3135
2 3/4 - .049	.1366	.416	.573	114.5	-7800	-3200

Thus lightest tube is 2-3/4 - .049 if available. Hence M.S. = (3200/2950) - 1 = .08

Design of Member FH

P = - 8960, L = 39.1, c = 1

To obtain a trial size, select necessary round tube from Fig. C2.8 which gives a 2" - .058 or 1-7/8 - .065 with I of .167 and .152 respectively. From table C2.4 we select a 2-3/4 - .058 streamline tube which has a I major = .159.

Size	A	ρ	L/ρ	F_c	P_c	M.S.
2 3/4 - .058	.49	.57	68.8	-20600	-10100	.13

A tube size of 2-3/4 - .049 is not available, thus the above size is the lightest available.

The D/t = .275/.058 = 47.5. From Fig. C2.9 the local crushing stress F_{cc} for D/t = 47.5 = - 33000, which is not critical when compared to the 20600 for F_c.

The student should design streamline struts of aluminum alloy and also steel for the other interplane and cabane struts.

C2.14 Design of Square and Elliptical Steel and Aluminum Alloy Tubes as Columns

Table C2.5 gives the section properties of oval and square tubes. The column charts of Figs. C2.9 and C2.10 can be used for the design of oval shaped tubes. The local crushing or crippling stress of oval tubes is no doubt greater than that of streamline tubes of the same basic round tube and gauge because the contour curvature is sharper. Thus using these curves is no doubt slightly conservative for crushing strength.

For square tubes as compression members primary column strength can be found by use of the curves of Figs. C2.3 and C2.5. However data on local crushing or crippling strength of square tubes is scarce so tests should be made to establish the shape of the transition curve from local to primary column failure. The student should refer to the chaper which covers the buckling and crippling of flat sheets as a means of estimating the local crushing strength of square tubes.

C2.15 Columns of Solid Sections

The primary instability column strength for sections where local instability is not critical can be calculated by the general column formulas

Example Problem.

Fig. C2.13 shows a forged (I) section member 30" long. It is to be used as a compression member. If the material is aluminum alloy (14ST) what is the ultimate column strength of the member.

Fig. C2-13

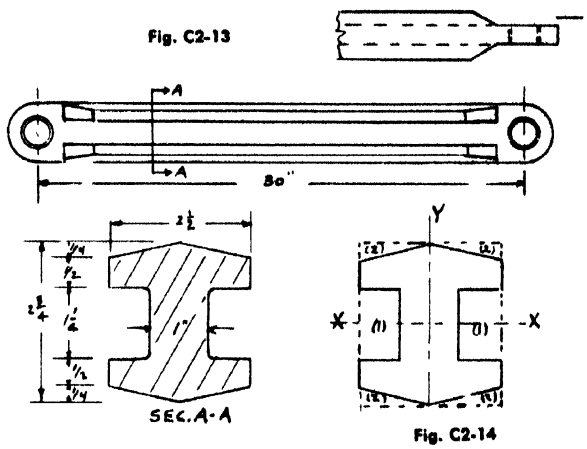


Fig. C2-14

Solution:

Since the column may fail by bending about either the X or Y axes, the column strength for bending about each of these axes will be calculated. Since the column strength is a function of the radius of gyration of the cross-section, the first step in the solution will be the calculation of I_x and I_y, from which ρ_x and ρ_y can be found.

Calculating I_x: In Fig. C2.14 the section will be first considered a solid rectangle 2.5 x 2.75 and then the properties of portions (1) and (2) will be subtracted.

$$I_x \text{ (rectangle)} = \frac{1}{12} \times 2.5 \times 2.75^3 = 4.32$$

Portions (1) and (2)

$$I_x = -\frac{1}{12} \times 1.5 \times 1.25^3 - 4(.625 \times .25 \times 1.292^2) = -1.29$$

(I_o of (2) about its x centroidal axis is negligible)

$$I_x = 4.32 - 1.29 = 3.03 \text{ in.}^4$$

$\rho_x = \sqrt{\frac{I_x}{A}}$, Area A = 2.5 x 2.75 - 2 x .75 x 1.25 - 4 x .25 x .625) = 4.375 sq. in.

$\rho_x = \sqrt{3.03/4.375} = .83$ in.

Calculation of Iy:

I_y (solid) $= \frac{1}{12} \times 2.75 \times 2.5^3 = 3.58$

Portion (1) $= -(1.25 \times .75 \times .875^2)2 - (1.25 \times .75^3/12)2 = -1.52$

Portion (2) $= -(.25 \times .625 \times .833^2)4 - 4(.25 \times 1.25^3/36) = -.488$

$I_y = 3.58 - 1.52 - .488 = 1.58$ in.^{4}

$\rho_y = \sqrt{1.58/4.375} = .60$"

Strength P_c in bending about axis XX:

$L = 30"$, $C = 1$, $\rho = .83$, $L'/\rho = 30/.83 = 36$

This is definitely in short column range.

$$F_c = F_{co}\left[1 - \frac{.385\ (L'/\rho)}{\pi\sqrt{E/F_{co}}}\right] \text{(Ref. Eq. 4 page C2.1)}$$

From Table C2.2, $F_{co} = F_{cy}\left(1 + \frac{F_{cy}}{200000}\right)$

For 14ST aluminum alloy

$$F_{co} = 50000\left(1 + \frac{50000}{200000}\right) = 62500 \text{ psi.}$$

$$F_c = 62500\left[1 - \frac{.385 \times 36}{\pi\sqrt{\frac{10.3 \times 10^6}{62500}}}\right] = 62500\ (1 - .344) = 41000 \text{ psi}$$

hence, $P_c = F_c A = 41000 \times 4.375 = 179500$ lb.

Strength P_c in bending about axis YY:

The end fitting on this strut is designed to fit into a female fitting. The hinge pin is perpendicular to the YY axis, thus a certain amount of end fixity is provided. For these calculations a value of C = 2 will be used.

$L' = L/\sqrt{C} = 30/\sqrt{2} = 21.2$, $L'/\rho = 21.2/.6 = 35.4$

$$F_c = 62500\left[1 - \frac{.385 \times 35.4}{\pi\sqrt{\frac{10.3 \times 10^6}{62500}}}\right] = 41300 \text{ psi}$$

hence, $P_c = 41300 \times 4.375 = 180800$ lb.

With the assumed end fixity of C = 2, the strut gives practically the same column strength about either axis. The tapering of the strut at the ends to provide fitting would reduce the column strength only a very small amount, since material near the ends effects the column bending strength as a whole very little.

PROBLEMS

(1) Fig. C2.15 shows the cross-section of a member 25" long which is to be used as a compression member. Calculate the maximum compressive concentric end load that member will carry for the following conditions.

(a) Material - 24ST aluminum alloy.
C = 1 for bending about xx axis.
C = 1.5 for bending about yy axis.
(b) Same as (a) but for 17ST material.
(c) Same as (a) but for Chrome-moly steel heat treated to 180000

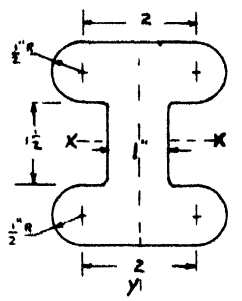


Fig. C2-15

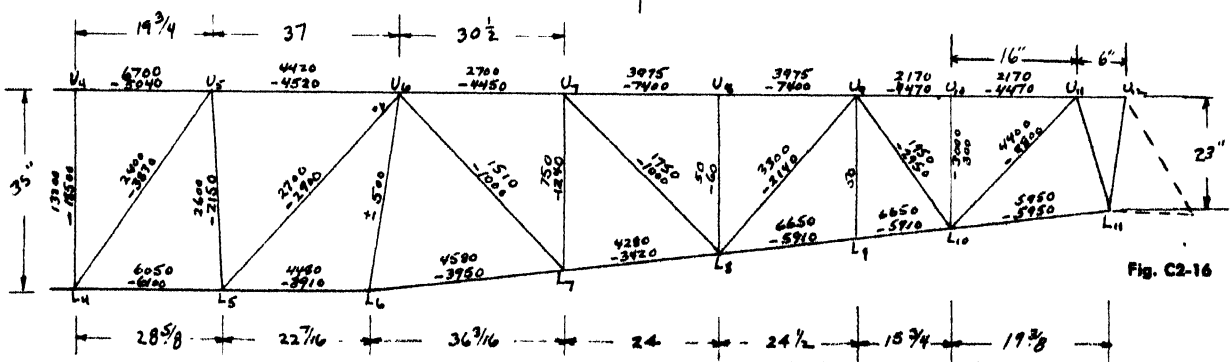


Fig. C2-16

Member	Length L	Design Load Tension	Design Load Comp.	C	Tube Size	P	Area A	Tube Strength Tens.	Tube Strength Compress	M. S.

(2) Fig. C2.16 shows the aft portion of the welded steel tubular fuselage of and actual airplane. The critical tension and compression load for each truss member as determined from a stress analysis involving consideration of all flying and landing condition are given adjacent to each member in the figure. Assuming a fixity of C = 2 for all members, select tube sizes for all members and fill in a table with the column headings as given above. Minimum size of any member to be 3/4 - .035. The top and bottom longerons should not be spliced more than twice. Material chrome-moly steel (F_{tu} = 95000 psi).

(3) For the cantilever welded steel tubular truss of Fig. C2.17, select the lightest members

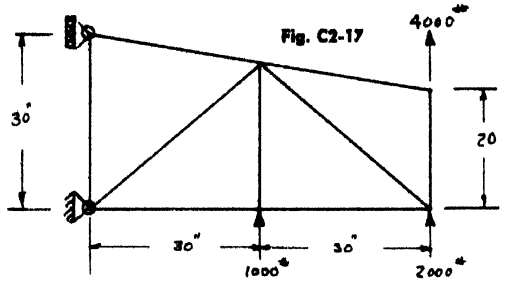


Fig. C2-17

for the truss loading as shown. The top and bottom longerons should be continuous members. Minimum size 3/4 - .035. Use C = 2 for web members and C = 1.5 for longerons. Material (chrome-moly steel F_{tu} = 100000 psi).

(4) If the truss of Fig. C2.17 is heat treated to 180000 psi after welding, how much weight could be saved over the results obtained in problem (3).

(5) Same as problem (3) but change material to 24ST aluminum alloy round tubes. Members to be fastened together by rivets and gusset plates. For design of tension members assume that rivet or bolt holes cutout 10% of tube area.

(6) Fig. C2.18 shows a typical tubular engine mount structure. The engine is supported at points A and B. For design purposes assume that engine torque is reacted 60% at A and 40% at B. Tube material is steel F_{tu} = 95000 psi. Use C = 1 for all members. Determine tube sizes for the followingdesign conditions:

Condition I Vertical Load factor = 10 (down)
Thrust Load factor 2 (forward)
Engine Torquw Load factor = 2

Condition II (Same as I except vertical load factor is 5 up.

General Data: Weight of power plant installation = 440#

Maximum engine thrust = 400# Engine H.P. = 120 at 2000 R.P.M.

(7) Fig. C2.19 illustrates an externally braced wing beam. Determine the axial load in the lift strut for a beam running lift load of 50#/in. acting up. Also for a negative or down lift load of -30#/in. of beam.

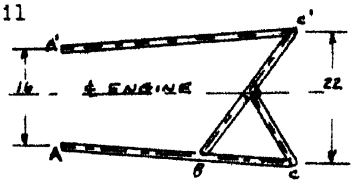
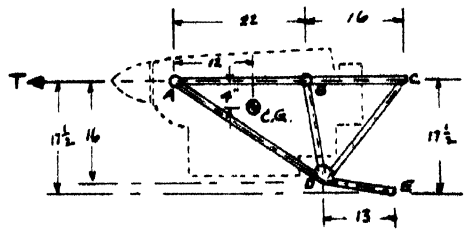


Fig. C2-18



(a) Determine the size of a steel streamline tube. (F_{tu} = 95000)

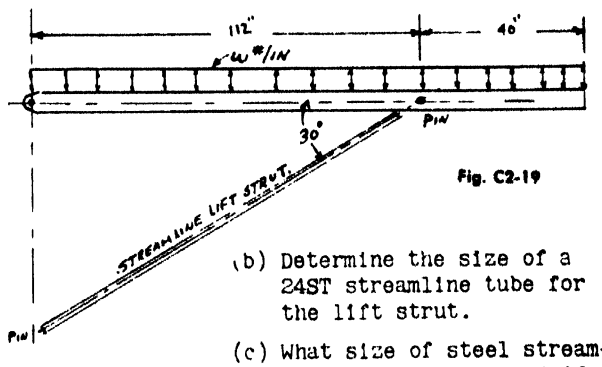


Fig. C2-19

(b) Determine the size of a 24ST streamline tube for the lift strut.

(c) What size of steel streamline tube is required if tubes are heat treated to 16500 psi.

(8) Fig. C2.20 illustrates the strut and wire bracing for attaching float to fuselage of seaplane. Determine the necessary sizes for the streamline struts AC and BD for the following loadings:

Condition I. V = -32000#, H = -8000#
Condition II. V = -8000, H = 28000 Material is 24ST. Use C = 1

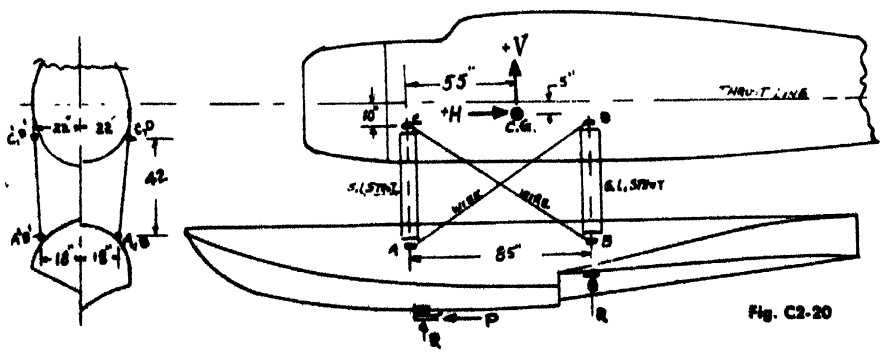


Fig. C2-20

CHAPTER C3
DESIGN OF ROUND TUBES FOR BENDING, TORSION AND FOR COMBINED LOADINGS

C3.1 Introduction

Steel and aluminum alloy tubes are a very common unit in the structure of the modern airplane. In many instances the tubes are loaded in such a manner as to produce compression, bending, or torsional stresses on the tube or a combination of these stresses. The airplane structural designer must usually provide a minimum ultimate strength which will carry loads 1.5 times the applied loads. In general the ultimate stresses may fall in the plastic range of the material and thus to determine the ultimate strength consideration must be given in the calculations to the stress-strain properties of the material above the proportional limit or tests must be run to establish the ultimate strength of the members.

C3.2 Modulus of Rupture in Bending.

The well known flexure formula $f_b = Mc/I$ (see chapter A12), assumes that Hookes' law holds, that is, stress is directly proportional to strain. Usually however a tube that fails in bending is stressed above the proportional limit, thus the above equation does not apply. To simplify bending design of steel and aluminum alloy tubes, bending tests have been run on a series of these tubes. The bending moment which causes the failure of these tubes in the tests is then used in the flexure formula to give a value of $F_b = Mc/I$. This ficticous stress F_b which is not the actual stress is referred to as the modulus of rupture in bending.

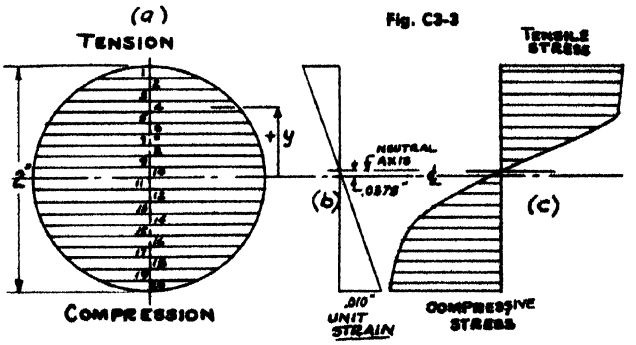
Fig. C3.1 gives curves for determining values of the modulus of rupture in bending for chrome-moly steel tubes of various heat treats. Fig. C3.2 gives curves for F_b for aluminum alloy tubes, and Fig. C3.2a the F_b values for magnesium alloy tubes. The values as plotted depend on the D/t ratio of the tubes. Making use of these allowable stress curves the bending strength of chrome-moly steel and 24ST aluminum alloy tubes have been calculated and the results are tabulated in table C3.1. This table is also valuable in estimating the required sizes for heat treated steel tubes and other aluminum alloys as will be illustrated in the example problems.

C3.3 Bending Modulus of Rupture Calculation from Stress-Strain Curves.

The modulus of rupture of rods, bars, and tubes which fail under stresses in the plastic range can be estimated quite closely by the use of the stress-strain curve of the material in the calculation of the ultimate internal resisting moment for the particular member in question. This procedure can best be illustrated by giving example calculations.

Example Problem 1 Bending Modulus of Rupture for Solid Round Rod of 24ST Aluminum Alloy.

Fig. C3.3(a) shows a rod with 2 inch diameter. In chapter C1, Fig. C1.5 a stress-strain curve is given for 24ST tubing material, which shows that the stress-strain curve for compression is different from that in tension. The assumption that plane sections remain plane after bending even in the plastic range will be made. Fig. C3.3(b) shows the strain diagram that has been assumed. Since the location of the neutral axis is unknown a trial and error method must be used. Considering that tension is produced on the upper portion of the rod the neutral axis is estimated or guessed to lie .0375" above center line of rod. It is toward the tension side because observation of the stress-strain curve of Fig. C1.5 shows that for a given strain in the plastic region the corresponding tensile stress is greater than the corresponding compressive stress. Table C3.2 gives the calculations for determining the internal ultimate resisting moment assuming the neutral axis as shown and with the maximum ultimate compressive unit strain equal to .010.



For equilibrium the total tension on section must equal the total compression. The summation of columns 6 is 740# which should be zero but is close enough for all practical purposes, and which shows that the neutral axis location is correct.

The total resisting moment when section is strained as assumed in Fig. C3.3(b) equals 56735 in. lb. (col. 7)

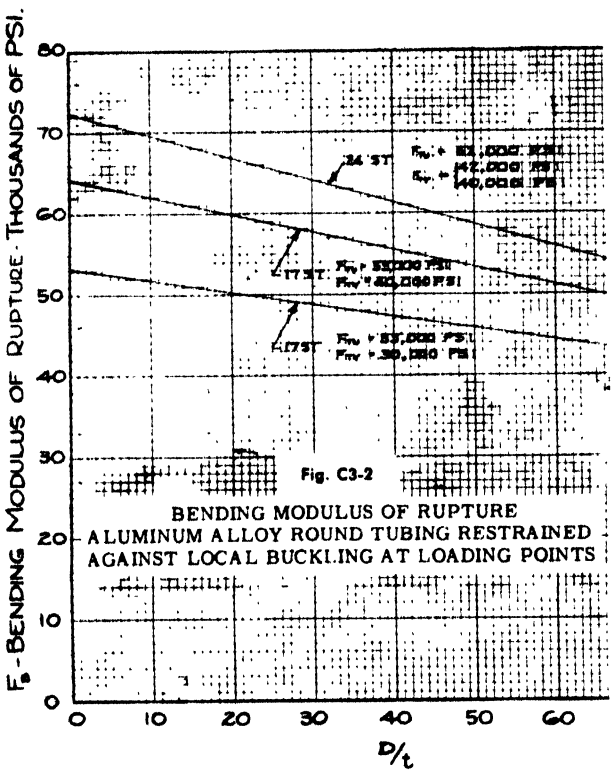
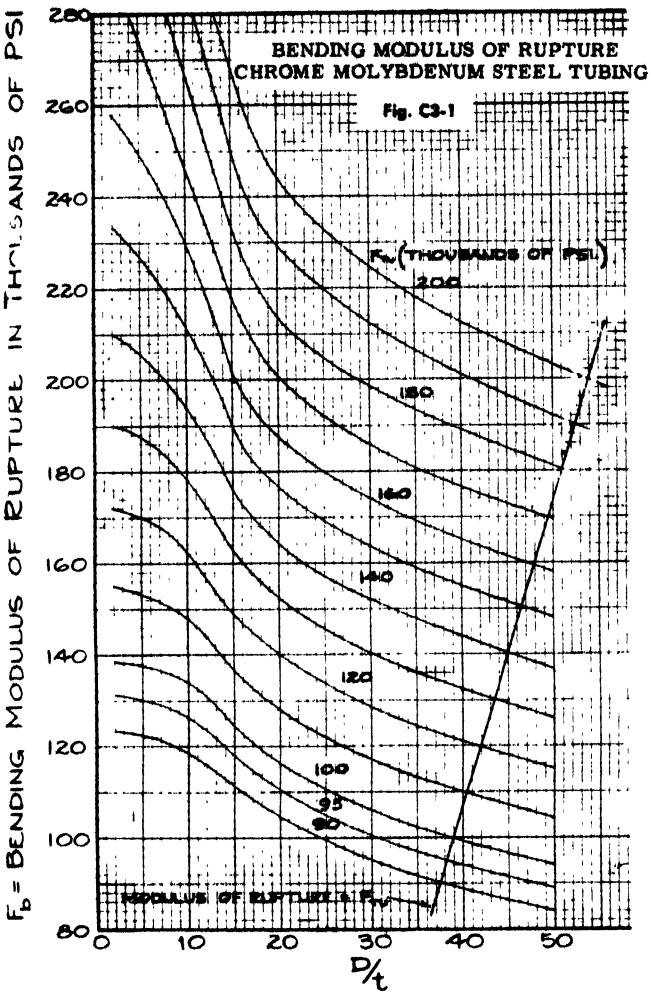
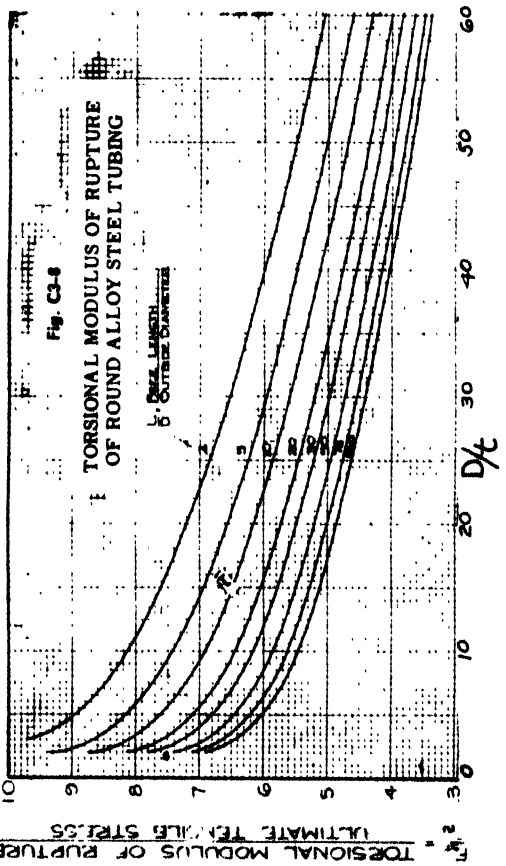
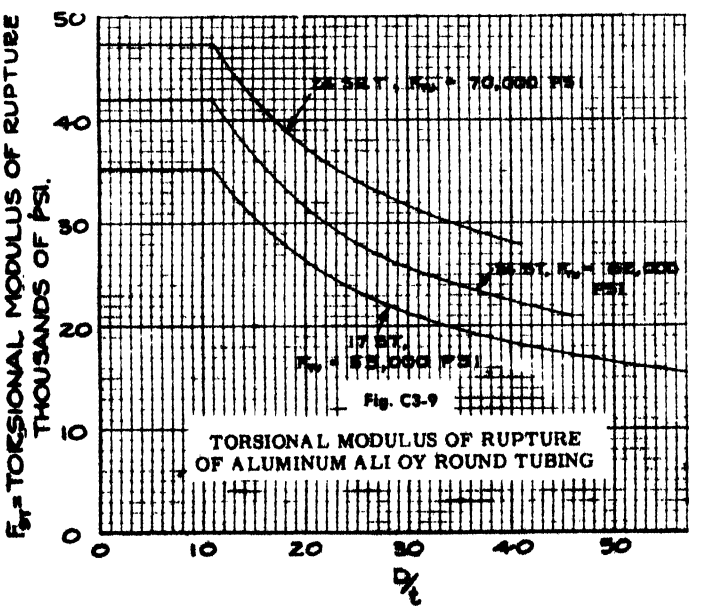


Fig. C3-2

BENDING MODULUS OF RUPTURE
ALUMINUM ALLOY ROUND TUBING RESTRAINED
AGAINST LOCAL BUCKLING AT LOADING POINTS







All curves on this page from ANC-5 Revision of 1941

(Ref. ANC-5, 1946)

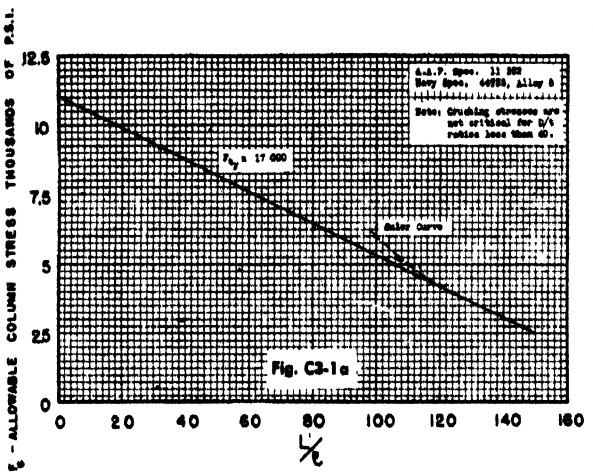


Fig. C3.1a Allowable Column Stresses For Magnesium Alloy Round Tubing

(Ref. ANC-5, 1946)

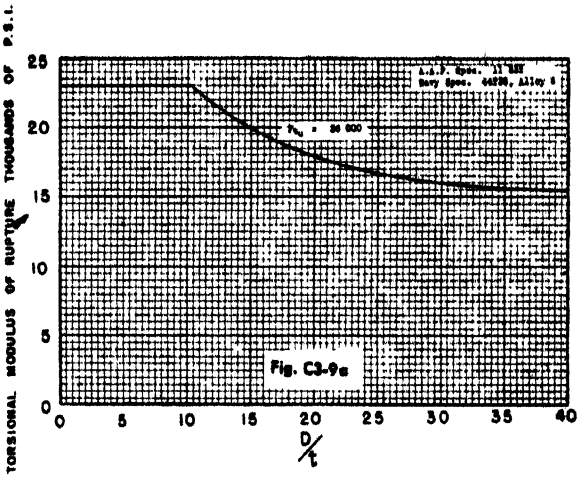


Fig. C3.9a Torsional Modulus of Rupture For Magnesium Alloy Round Tubing

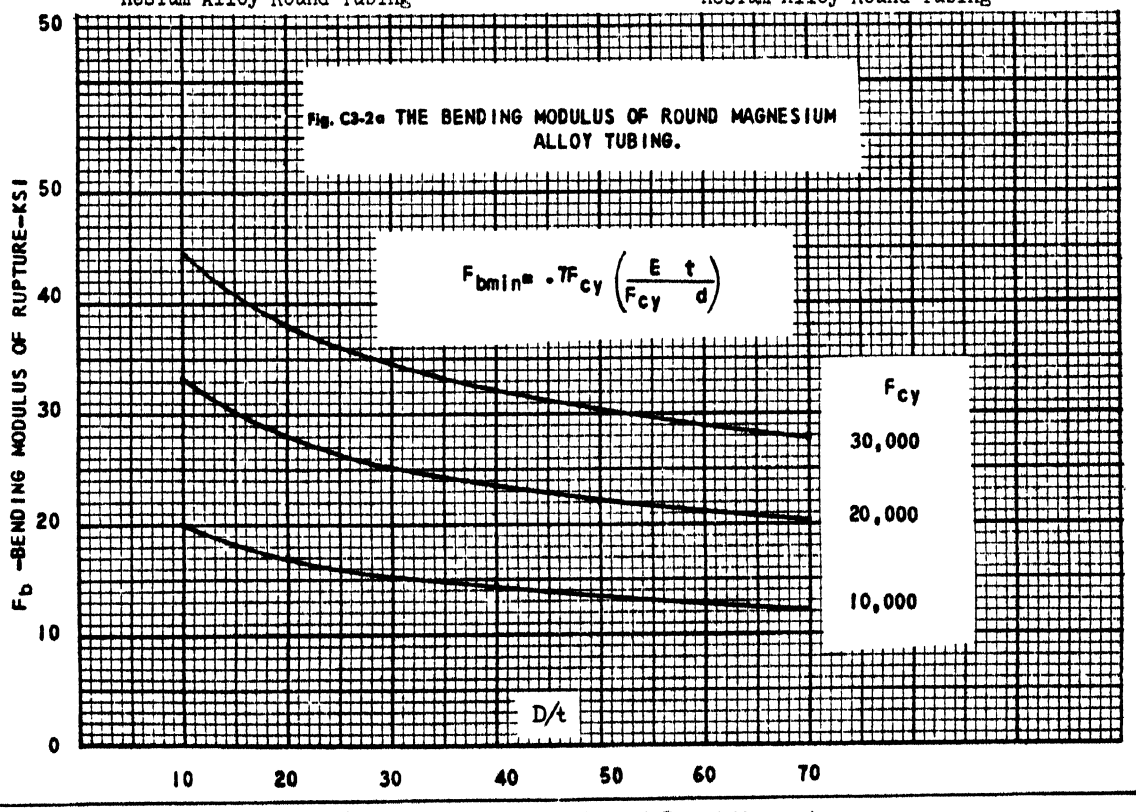


Fig. C3.2a The Bending Modulus of Round Magnesium Alloy Tubing.

The values in Fig. C3.2a were taken from an article in the journal of the Institute of Aeronautical Sciences of Nov. 1948, entitled, "The Bending Modulus of Rupture of Round Magnesium Tubing", by C. H. Mortenson of the Dow Chemical Co. Mr. Mortenson recommends the curves in Fig. C3.2a for preliminary design purposes. Tubes with a D/T value ≤ 38 fail by general flattening of the tubes together with excessive deflection and for the last ten percent of the load the deflection increases approximately 100 percent. For D/T values greater than 38 failure is by sudden instability of the tube walls.

Table C3.1 Bending and Torsional Strength of Round Tubes
(Values in Inch lbs.)

SECTION PROPERTIES							24ST AL. ALLOY			X4130 STEEL		
Dia.	t	A	ρ	I	I/y	D/t	Bend-ing	Tor-sion	wt 100"	Bend-ing	Tor-sion	wt 100"
1/2	.028	.04152	.167	.001160	.004641	17.85	313	311	.42	554	543	1.17
	.035	.05113	.165	.001390	.005559	14.28	379	417	.52*	705	679	1.45*
	.049	.06943	.160	.001786	.007144	10.20	495	600	.70	955	920	1.96
5/8	.028	.05252	.211	.002345	.007503	22.30	495	447	.54	854	842	1.49
	.035	.06487	.209	.002833	.009065	17.85	611	531	.66*	1080	1061	1.84*
	.049	.08867	.204	.003704	.011852	12.77	815	936	.90	1533	1473	2.51
	.058	.10331	.202	.004195	.013425	10.79	930	1130	1.05	1774	1700	2.93
3/4	.028	.06351	.255	.004145	.011052	26.80	716	596	.65	1195	1177	1.80
	.035	.07862	.253	.005036	.013429	21.42	890	817	.80*	1540	1520	2.23*
	.049	.10791	.248	.006661	.017762	15.30	1210	1280	1.09	2213	2150	3.06
	.058	.12609	.245	.007601	.02027	12.94	1390	1605	1.28	2618	2513	3.57
	.065	.13988	.243	.008278	.02208	11.53	1527	1820	1.42	2890	2770	3.96
7/8	.028	.07451	.299	.006689	.015289	31.23	975	770	.76	1610	1575	2.11
	.035	.09236	.297	.008161	.018653	25.00	1220	1010	.94*	2068	2038	2.62*
	.049	.12715	.292	.010882	.02487	17.85	1675	1610	1.29	2970	2913	3.60
	.058	.14887	.289	.012484	.02853	15.10	1935	2090	1.51	3540	3443	4.22
	.065	.16541	.286	.013653	.03121	13.47	2140	2400	1.68	3950	3813	4.66
1	.035	.10611	.341	.012368	.02474	28.56	1590	1300	1.07*	2640	2595	3.01*
	.049	.14640	.337	.016594	.03319	20.40	2215	2070	1.48	3860	3800	4.15
	.058	.17164	.334	.01911	.03822	17.25	2590	2600	1.74	4610	4515	4.86
	.065	.19093	.331	.02097	.04193	15.38	2855	3040	1.93	5210	5062	5.41
1 1/8	.035	.11985	.385	.01782	.03168	32.10	2020	1580	1.21*	3305	3240	3.40*
	.049	.16564	.381	.02402	.04270	22.95	2815	2500	1.68	4810	4748	4.68
	.058	.19442	.378	.02775	.04933	19.40	3300	3160	1.97	5810	5709	5.51
	.065	.21650	.375	.03052	.05425	17.30	3660	3690	2.20	6550	6418	6.14
1 1/4	.035	.13360	.429	.02467	.03948	35.70	2470	1870	1.35*	4015	3895	3.78*
	.049	.18488	.425	.03339	.05342	25.50	3490	2960	1.87*	5900	5821	5.23*
	.058	.2172	.422	.03867	.06187	21.55	4100	3750	2.20	7050	6945	6.15
	.065	.2420	.419	.04260	.06816	19.22	4560	4380	2.45	8040	7900	6.86
1 3/8	.035	.1473	.474	.03309	.04814	39.25	2970	2180	1.49	4810	4618	4.17
	.049	.2041	.469	.04492	.06534	28.05	4230	3460	2.07	7040	6922	5.78*
	.058	.2400	.466	.05213	.07583	23.70	4990	4520	2.43	8450	8338	6.80
	.065	.2675	.464	.05753	.08367	21.15	5570	5130	2.70	9620	9508	7.58
1 1/2	.035	.1611	.518	.04324	.05765	42.80	3495	2515	1.63	5630	5345	4.56
	.049	.2234	.513	.05885	.07847	30.60	5020	3980	2.26	8250	8085	6.32*
	.058	.2628	.510	.06841	.09121	25.85	5940	5030	2.66	10000	9850	7.45
	.065	.2930	.508	.07558	.10079	23.05	6650	5880	2.97	11380	11230	8.30
	.083	.3695	.502	.09305	.12407	18.08	8340	8200	3.74	14800	14510	10.47
1 5/8	.035	.1748	.562	.05526	.06803	46.40	4060	2840	1.77	6530	6120	4.95
	.049	.2426	.557	.07540	.09279	33.15	5850	4560	2.46	9630	9390	6.87*
	.058	.2855	.554	.08776	.10801	28.00	7000	5740	2.89	11640	11450	8.09
	.065	.3186	.552	.09707	.11948	25.00	7830	6690	3.23	13170	12970	9.05
	.083	.4021	.546	.11985	.14751	19.58	9880	9430	4.06	17200	16960	11.40
1 3/4	.035	.1885	.606	.06936	.07927	50.00	4650	3170	1.91	7450	6900	5.32
	.049	.2618	.602	.09478	.10832	35.70	6780	5120	2.65*	11010	10680	7.42*
	.058	.3083	.598	.11046	.12624	30.20	8070	6480	3.12	13360	13100	8.73*
	.065	.3441	.596	.12230	.13977	26.90	9070	7560	3.48	15200	14980	9.75
	.083	.4341	.590	.15136	.17299	21.10	11500	10600	4.40	19900	19650	12.32
1 7/8	.049	.2811	.6458	.11720	.12500	38.25	7740	5750	2.84	12580	12100	7.95
	.058	.3311	.6427	.13677	.14589	32.30	9230	7240	3.35	15190	14880	9.38
	.065	.3696	.6404	.15156	.16166	28.80	10380	8450	3.74	17300	17000	10.47
	.083	.4673	.6342	.18797	.2005	22.60	13210	11770	4.73	22700	22300	13.25
2	.049	.3003	.690	.14299	.14299	40.8	8740	6330	3.04	14120	13440	8.50
	.058	.3539	.687	.16696	.16696	34.45	10500	8050	3.58*	17200	16730	10.03*
	.065	.3951	.684	.18514	.18514	30.75	11830	9420	4.00	19460	19060	11.19
	.083	.4999	.678	.2300	.2301	24.10	15120	13200	5.06	25650	25300	14.16
	.095	.5685	.674	.2586	.2586	21.05	17170	15950	5.76	29800	29400	16.11
2 1/4	.049	.3388	.778	.2052	.1824	45.90	10600	7630	3.43	17480	16380	9.59
	.058	.3994	.775	2401	.2134	38.80	13150	9670	4.05*	21300	20450	11.30*
	.065	.4462	.773	2665	.2369	34.60	14900	11400	4.52	24220	23610	12.64
	.083	.5651	.767	3322	.2953	27.15	19120	15900	5.72	32060	31570	16.01
	.095	.6432	.762	3741	.3325	23.70	21850	19200	6.51	37140	36630	18.22
2 1/2	.049	.3773	.866	.2834	.2267	51.00	13200	8980	3.82	21220	19570	10.68
	.058	.4450	.863	.3318	.2655	43.10	16000	11500	4.50	25950	24630	12.60
	.065	.4972	.861	.3688	.2950	38.45	18200	13600	5.03*	29630	28560	14.09*
	.083	.6302	.855	.4607	.3686	30.10	23000	19000	6.38	39100	38380	17.85
	.095	.7178	.851	.5197	.4158	26.30	27000	23000	7.27	45600	44900	20.34

Bending and torsional tube strengths in table are based on Figs. C3.1, C3.2, C3.8 and C3.9 and are for materials with following mechanical properties.

X - 4130
Chrome-Moly Steel

Ftu = 100,000 psi

Fty = 85000 psi

Fsu = 65000 psi

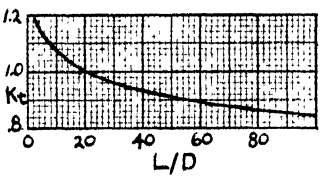
L/D ratio = 20 (see note "A")

24ST Aluminum Alloy

Ftu = 62000 psi

Fty = 42000 psi

Fsu = 37000 psi



Note "A"

Torsional strength of steel tubes in table C3.1 based on L/D = 20. For other values of L/D multiply by factor Kt from above graph.

* AN Standard

Table C3.2

1	2	3	4	5	6	7
Strip No.	Strip Area "A"	y	x	Unit Stress S	F = SA	Res. Moment M = Fr
1	.058	0.935	.00867	53000	3075	2760
2	.102	0.840	.00773	52500	5350	4300
3	.135	0.75	.00685	52100	7025	5040
4	.153	0.65	.00591	51500	7870	4820
5	.165	0.55	.00494	51000	8410	4310
6	.180	0.45	.00398	43000	7740	3200
7	.185	0.35	.00302	33200	6140	1920
8	.195	0.25	.00205	22800	4450	945
9	.197	0.15	.00108	12500	2460	280
10	.200	0.05	.00012	3200	640	10
11	.200	-0.05	-.00084	- 7250	-1450	130
12	.197	-0.15	-.00181	-17800	-3510	660
13	.195	-0.25	-.00276	-28500	-5780	1650
14	.185	-0.35	-.00374	-35500	-6560	2540
15	.180	-0.45	-.00470	-40000	-7200	3510
16	.165	-0.55	-.00566	-43000	-7100	4170
17	.153	-0.65	-.00663	-44800	-6850	4710
18	.135	-0.75	-.00759	-46000	-6210	4880
19	.102	-0.84	-.00846	-47200	-4810	4210
20	.058	-0.935	-.00937	-48000	-2780	2690
Total	3.140				740	56735

Col. 1 Rod divided into 20 strips .1" thick.
Col. 3 y = distance from centerline to strip c.g.
Col. 4 x = strain at midpoint = (y - .0375)/103.75
Col. 5 Unit stress for x strain from Fig. C15
Col. 6 Total stress on strip.
Col. 7 Moment about neutral axis. r = (y - .0375)

$$F_b = \frac{Mc}{I}$$

hence our calculated modulus of rupture F_b in bending is,

$$F_b = \frac{56735}{.785} = 72300 \text{ psi.}$$

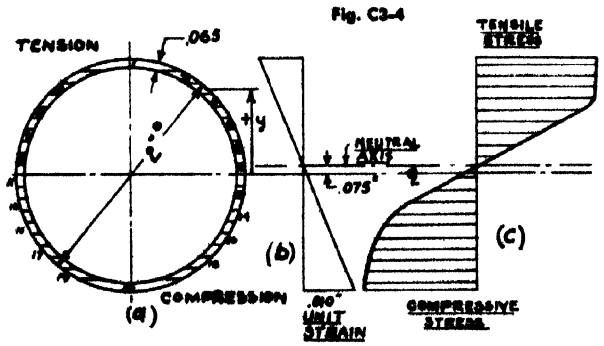
The allowable stress chart of Fig. C3.2 for 24ST material and D/t = 0, gives F_b = 72200 psi.

In assuming the unit strain curve of Fig. C3.3(b) it would make very little difference if maximum compression unit strain were .008 or .012 since curve is relatively flat in the plastic region.

Using the values in column 5, the stress distribution at ultimate strength is shown in Fig. C3.3(c).

Example Problem #2 Bending Modulus of Rupture for 2" - .065 Round 24ST Tube

Fig. C3-4



In Fig. C3.4 the tube section is divided into 20 sections as shown. The ultimate compressive unit strain is taken as .010 and the neutral axis is guessed at .075" above centerline. Table C3.3 gives the calculations for determining the ultimate internal resisting moment. The procedure is identical to that of example problem 1.

Table C3.3

Strip No.	Strip Area "A"	y	x = (y - .075)/107.5	Unit Stress "S"	F = SA	Resist Mom. M = Fr, r = y-.075
1	.0470	0.94	.00804	52800	2480	2150
2	.0290	0.85	.0073	52500	1520	1180
3	.0205	0.75	.00637	52000	1070	725
4	.0180	0.65	.00543	51700	930	535
5	.0160	0.55	.00452	47000	752	356
6	.0150	0.45	.00358	38000	570	215
7	.0142	0.352	.00265	27500	390	107
8	.0138	0.25	.00172	17000	235	40
9	.0133	0.15	.00079	8700	116	10
10	.0130	0.05	-.00005	- 1000	- 10	0
11	.0130	-0.05	-.00116	-12300	- 160	20
12	.0133	-0.15	-.00209	-22000	- 292	65
13	.0138	-0.25	-.00302	-31500	- 435	140
14	.0142	-0.35	-.00395	-37000	- 525	225
15	.0150	-0.45	-.00488	-41000	- 615	325
16	.0160	-0.55	-.00581	-43000	- 687	430
17	.0180	-0.65	-.00674	-45000	- 810	590
18	.0205	-0.75	-.00767	-46000	- 945	780
19	.0290	-0.85	-.00860	-47500	-1375	1275
20	.0470	-0.94	-.00945	-48700	-2280	2320
Total	.3998				70 error	11490

Ultimate internal resisting moment = 11470"#

hence, Modulus of rupture $F_b = \frac{Mc}{I} = \frac{11490}{.185} = 62000$ psi

which corresponds to 63600 from allowable stress chart of Fig. C3.2.

C3.4 Example Problems Tubes in Bending Use Allowable Curves.

Example Problem #1

Let it be required to determine the size of a round tube for the conditions illustrated in Fig. C3.5, if the material is (1) 24ST, (2) 17ST with F_{ty} = 30000 psi, and (3) if material is chrome-moly steel with F_{tu} = 10000 psi.

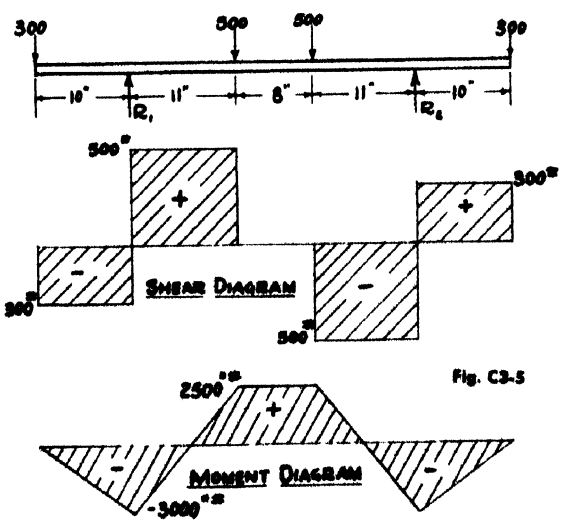


Fig. C3-5

Solution:

The maximum bending moment shouod first be determined. The moment diagram for the given load conditions shows that the maximum moment equals -3000 in. lb. and it occurs over the supports.

In selecting a tube size if we use the curves of Figs. C3.1 and C3.2, we must guess a size since the modulus of rupture as given on these curves is a function of the D/t value of the tube and then check the strength of the assumed trial size and repeat the guess and check method until the final proper size is obtained. Table C3.1 however eliminates this trial and error procedure for the two materials for which the table applies. The table is however very useful for selecting trial sizes for other materials thus saving time in the general guess and check method.

(1) Design of 24ST Round Tube:-

From table C3.1 the following sizes in table A give a bending strength near the required 3000 in. lb.

Table A

Tube size	Bending Strength	wt/100"	M.S. on 3000 in. lb.
1 1/8 - .058	3300	1.97	.10
1 1/4 - .049	3490	1.87	.16
1 3/8 - .035	2970	1.49	-.01
1 1/2 - .035	3495	1.63	.16

From the above table the lightest tube with a positive margin of safety is the 1-1/2 - .035, which has the same M.S. as the heavier 1-1/4 - .049 tube.

In many cases of practical design the structural designer must use AN standard sizes or he may be restricted to sizes stocked by the company. Furthermore installation clearances etc., may dictate the maximum tube diameter.

However no matter what the restrictions are it is easy to select the proper tube from table C3.1 or make use of it in selecting trial sizes for tube material for which it does not apply.

(2) Design of 17ST Round Tube, F_{ty} = 30000 psi:-

Table C3.1 does not apply for 17ST tubes and thus Fig. C3.2 must be used. However to obtain logical trial sizes time can be saved by finding the size required for 24ST material from table C3.1 which gives the sizes in table A. As shown by Fig. C3.2, the modulus of rupture for 17ST is lower than for 24ST tubes. Hence a logical tube size selection would be to increase the tube sizes in table A to the next gage and then compute the strength of these tubes using Fig. C3.2. Table B gives the results.

Table B

Tube size	D/t	F_b from Fig. C3.2	Moment Strength $M = F_b I/y$	M.S. on 3000"#	wt/100"
1 1/8 -.065	17.30	50700	2750	-.08	
1 1/4 -.058	21.55	50000	3090	.03	2.20
1 3/8 -.049	28.05	49000	3200	.065	2.07
1 1/2 -.049	30.60	48800	3840	.28	2.26

From table B, the 1-3/8 - .049 is the lightest tube and it has a greater margin of safety than the 1-1/4 - .058 which is a heavier tube.

In the design of tubes as beams consideration must be given to holes due to bolts or rivets. For the least detrimental effect the bolt or rivet holes should be located on neutral axis of tube in bending.

(3) Design of Chrome-moly Steel Tube, F_{tu} = 100,000 psi.

The bending strength of 100,000 U.T.S. chrome-moly tubes has been calculated and recorded in table C3.1. Thus tubes which give a bending strength close to 3000 in. lb. are quickly selected as given in table C.

Table C

Tube size	Bending Strength Table C3.1	wt/100"	M.S. on 3000"#
7/8 - .049	2970	3.60	-.01
1" - .049	3860	4.15	.28
1 1/8 - .035	3305	3.40	.10

The 1-1/8 - .035 size is the lightest tube.

Example Problem #2

Fig. C3.6 shows a welded steel tube rectangular frame, carrying a 2000# load at the midpoint of member AB. The material is chrome-moly steel, F_{tu} = 100,000 psi. Determine the margin of safety of the member AB in bending.

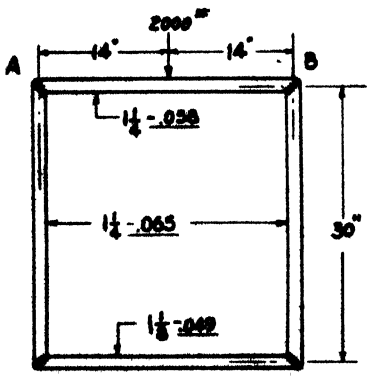
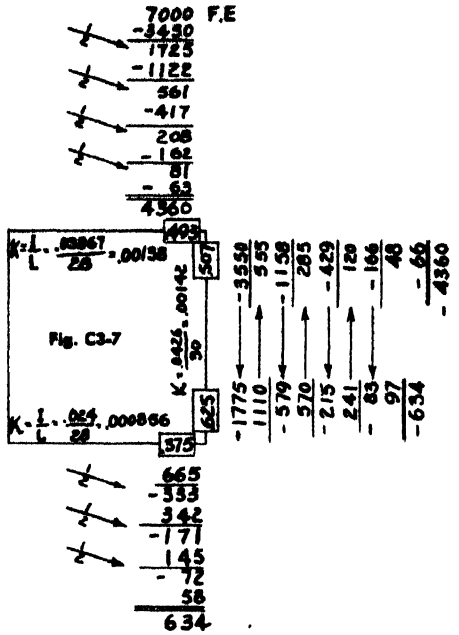


Fig. C3-6

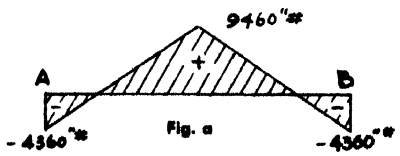
Solution

Since the members of the frame are welded together the bending moment on member AB is statically indeterminate since the degree of restraint at A and B is unknown. The joint bending moments

will therefore be determined by use of the "Cross" moment distribution method. (See chapter A11). Fig. C3.7 shows the moment distribution solution.



Due to symmetry of loading and structure only one half of the structure is considered in the distribution and carry-over process. The solution is started with the fixed end moments on AB = to PL/8 = 2000 x 28/8 = 7000 in. lb. The final moments at A and B are 4360 in. lb. giving the moment diagram for member AB as shown in Fig. a.



The maximum moment occurs at midpoint of AB and equals 9460"#.

From table C3.1, 1-1/4 - .058 tube will develop 7050 in. lb. Hence margin of safety = (7050/9460 -1 = - .25, thus member is understrength at midpoint.

At point (A) due to welding influence, the above allowable of 7050 will be reduced 20 per cent or .8 x 7050 = 5640"#. The tube bending strength is satisfactory at A and B since moment is 4360.

To make the frame show a positive margin of safety it will be heat-treated to 150,000 after welding.

From Fig. C3.1, for a tube with D/t = 21.6 and heat-treated to 150,000, the modulus of rupture F_b = 174,000 psi. I/y for 1-1/4 - .058 tube = .06187.

Hence bending strength = 174000 x .06187 = 10770 in. lb. M.S. = (10770/9460) -1 = .14

C3.5 Torsional Modulus of Rupture.

Tubes subjected to pure torsion fail due to plastic deformation or elastic instability of the tube walls or a combination of each action.

The well known torsional stress formula $f_s = Tr/J$ assumed stress proportional to strain. For tubes with low D/t values failure will occur in the plastic range, then the torsion formula will not give the true shearing stress since stress is not proportional to strain. However if we substitute the ultimate rupturing torsional moment as obtained from tests in the above formula we obtain a value for f_s which is referred to as the torsional modulus of rupture and is given the symbol F_{st}. This stress may not be the true shearing stress that exists at failure but the values serve as a measure of the ultimate torsional strength.

Figs. C3.8, C3.9 and C3.9a give the torsional modulus of rupture curves for steel, aluminum alloy and magnesium alloy respectively.

In table C3.1 the torsional bending strength has been computed for 24ST aluminum alloy round tubes and also for steel tubes whose F_{tu} = 100,000 psi. and whose L/D values = 20.

Example Problem

A round tube 30" long is subjected to a design torsional moment of 6600 in. lb. Select the lightest tube for the member using the following materials: (1) 24ST, (2) 24SRT, (3) x -4130 steel, F_{tu} = 100000 psi., (4) x -4130 steel heat treated to 160000 psi.

(1) Design of 24ST tube:-

Table C3.1 summarizes the torsional strength of 24ST round tubes. Selecting those sizes which have a strength close to 6600 in. lb., the values in table D are obtained.

Table D

Tube size	Torsional Strength Table C3.1	wt/100"	M.S. on 6600"#
1 5/8 - .065	6690	3.23	.01
1 7/8 - .058	7240	3.34	.10
1 1/2 - .083	8200	3.74	.24

The 1-5/8 - .065 tube is the lightest. The 1-7/8 - .058 tube is approximately 3 percent heavier but it will give a 9 percent greater margin of safety.

(2) Design of 24SRT Round Tube:-

Since 24SRT is stronger than 24ST, it will be logical to cut the tube sizes in table D one gage and check their strength. Table E gives the results.

Table E

Tube size	D/t	F_{st} from Fig. C3.9	wt/100"	Torsional Strength $T = F_{st}\frac{J}{r}$	M.S.
1 5/8 - .058	28	32800	2.88	7040	.07
1 7/8 - .049	38.2	28700	2.84	7170	.09
1 1/2 - .065	23.1	35100	2.97	7040	.07

The 1-7/8 - .049 is the lightest as well as the strongest.

(3) Design of x -4130 Steel Tube F_{tu} = 100000 psi:-

Fig. C3.8 shows that the torsional modulus for steel tubes is influenced by the L/D ratio of the tube. The torsional shear strength for the x -4130 tubes as given in table C3.1 is for an L/D ratio of 20. Thus for any other value of L/D the correction factor as obtained from the L/D correction curve must be used. The values in table C3.1 will however prove valuable in selecting trial sizes for checking purposes.

Table F shows the tube sizes taken from table C3.1, the necessary correction factors etc.

Table F

Tube size	Tor. Str.	L/D	Corr. Fac. K_t	Corr. $T_a = TK_t$	wt/100"	M.S. on 6600"#
1 3/8 - .049	6920	21.8	.99	6840	5.78	.03
1 3/4 - .035	6900	17.1	1.02	7050	5.32	.06

The lightest and the strongest is 1-3/4 = .035

(4) Design for Steel Tube Heat-treated to 160000 psi.

From the sizes required for 100,000 steel in table F it is logical to assume at least the next gage smaller for the 160,000 heat-treated steel tubes. Table G shows the assumed sizes and the calculations of the margin of safety.

Table G

Tube size	D/t	L/D	F_{st}/F_{tu} From Fig C3.8	F_{st}	$T_a = F_{st}\,J/r$	wt/100"	M.S. on 6600
1 1/4 - .035	35.7	24	.485	77600	6150		-.07
1 1/4 - .049	25.5	24	.53	84800	9060	5.23	.37
1 3/8 - .035	39.2	21.8	.478	76500	7350	4.17	.11

The required steel tube is therefore 1-3/8 - .035 when heat-treated to 160,000 psi.

C3.6 Failure Under Combined Loads.

A common condition in the use of tubes as structural members is the fact that loads exist which produce compressive, bending or shearing stresses acting simultaneously, thus the problem confronting the designer is the question of allowable stresses for conditions of combined loading since failure may be due to buckling or instability and there is no general theory which applies to all conditions of combined loadings.

A new method of approach referred to as the stress ratio method has been proposed by "Shanley" which appears to have excellent possibilities. This general method is constantly referred to in ANC-5. In this method the stress conditions are represented by "stress ratios" which can be considered as non-dimensional coefficients denoting the fraction of the allowable stress or strength for the member which can be developed under the given conditions of combined loading.

For a single simple stress, the stress ratio can be expressed as,

$$R = \text{stress ratio} = \frac{f}{F} \quad \text{----------(1)}$$

where f = applied stress and F = allowable stress. The margin of safety in terms of the stress ratio R can be written,

$$M.S. = \frac{1}{R} - 1.0 \quad \text{----------(2)}$$

For combined loadings the general conditions for failure are expressed by Shanley as follows:

$$R_1^x + R_2^y + R_3^z + \text{------} = 1.0 \quad \text{----(3)}$$

In this expression, R_1, R_2, and R_3 could refer to compression, bending and shear and the exponents x, y, and z gives the relationship for combined stresses. The equation states that the failure of a member under a combined loading will result only when the sum of the stress ratios is equal to or greater than 1.

Load ratios $R = P/P_a$, where P is the applied load and P_a the allowable load can be used for the stress ratios if desired.

C3.7 Combined Bending and Compression.

In tubes subjected to combined compression and bending the stress due to compression is uniform over the section whereas the stress due to bending is not unfform over the cross-section. The following stress ratio equation which is no doubt slightly conservative should be used in the design of tubes unless test data is available or tests are made which show that an exponent greater than one is permissible.

$$R_c + R_b = 1.0 \quad \text{----------(4)}$$

which can be written,

$$\frac{f_c}{F_c} + \frac{f_b'}{F_b} = 1.0 \quad \text{----------(5)}$$

where f_b' = maximum bending stress including effects of secondary bending.

F_b = bending modulus of rupture (Figs. C3.1 and C3.2)

f_c = compressive axial stress

F_c = allowable column stress

Equation (5) can also be written,

$$\frac{\text{Column load}}{\text{Column strength}} + \frac{\text{Design bending moment}}{\text{Bending Strength}} = 1 \quad \text{--(6)}$$

Fig. C3.10 shows a plot of equation (4).

Also the equation $R_c + R_b^{1.25} = 1.0$ is plotted which may be closer to actual conditions but should not be used unless substantiated by tests.

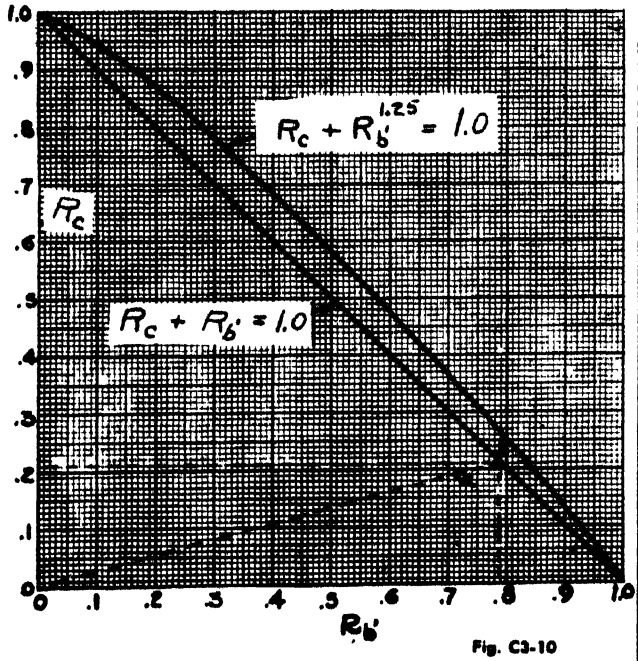


Fig. C3-10

Example Problem Involving Combined Bending And Compression

Fig. C3.11 shows a round 24ST tube acting as a beam-column. It is supported at pin A and by the inclined strut BC at point C. Let it be required to determine the margin of safety when carrying a uniform lateral load of 10#/in.

To find the axial load in tube AC, take moments about point (B).

$\Sigma M_B = -40 \times 10 \times 20 + 20\ R_{A_H} = 0$, hence R_{A_H} = 400#.

Thus axial load in tube is 400# compression

The column strength of a 24ST - 1-1/4 - .049 round tube 40 inches long with end fixity C = 1 is obtained from Fig. C2.8 of chapter C2 and equals -2100#, hence stress ratio

$$R_c = \frac{\text{Column load}}{\text{column strength}} = \frac{-400}{-2100} = .191$$

The bending moment will be maximum at the center of span because of symmetry of loading and the value of the moment is obtained from the following equation which includes the secondary moments due to deflection. (Reference table A10.1 of chapter A10).

$$M_{max.} = wj^2 \left(1 - \sec \frac{L}{2j}\right) \text{ - - - - - - - - - - - - (A)}$$

$$j = \sqrt{\frac{EI}{P}} = \sqrt{\frac{10{,}300{,}000 \times .0334}{400}} = \sqrt{860} = 29.3$$

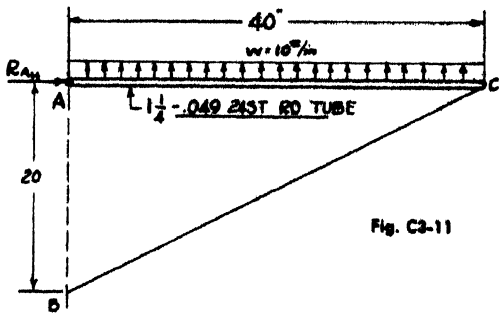


Fig. C3-11

$wj^2 = 10 \times 860 = 8600$

$\frac{L}{2j} = \frac{40}{58.6} = .683$ $\qquad \sec \frac{L}{2j} = \frac{1}{\cos \frac{L}{2j}}$

From table A10.2 of chapter A10 cos of .683 = .7757

hence $\frac{1}{\cos L/2j} = 1/.7757 = 1.29$

Substituting in equation (A)

$M_{max.} = 8600\ (1 - 1.29) = -2490$ in. lb.

From Fig. C3.2, the modulus of rupture F_b for a 24ST round tube which has D/t value of 25.5 equals 65300 psi. Therefore the bending strength M = $F_b I/y = 65300 \times .0534 = 3480$ in. lbs.

Stress ratio in bending $F_b = \frac{2490}{3480} = .715$

$R_c + R_b = .191 + .715 = .906$ which shows that member is not weak.

Margin of safety M.S. = $\left(\frac{1}{R_c + R_b}\right) - 1 = \left(\frac{1}{.191 + .715}\right) - 1 = .10$

The margin of safety could be determined from the interaction curve of Fig. C3.10 as follows. The intersection of lines normal to R_b and R_c base scale using values of R_b and R_c equal to .715 and .191 respectively, locates point (a) on the chart. A line drawn thru origin (0) and point (a) intersects interaction line at point (b). The values of $R_{b(b)}$ and $R_{c(b)}$ for point (b) equal .787 and .21 respectively.

The strength ratio or factor of utilization U

$= \frac{.191}{.21} = \frac{.715}{.787} = .907$ Hence M.S. $= \frac{1}{U} = \frac{1}{.907} - 1 = .10$

The student should notice that the maximum bending moment of 2490 in. lb. is 24 percent greater than the primary moment which equals $wL^2/8 = 10 \times 40^2/8 = 2000$. The lateral deflection at the midpoint of the tube thus equals 490/400 = 1.22 inch.

The secondary moments due to lateral deflection do not vary linearly so resulting values of margins of safety may be less than that calculated as above for certain conditions of loading.

C3.8 Combined Bending and Torsion.

This type of combined loading is probably the most common combined load system which is encountered in aircraft structural design.

Since shearing stresses due to torsion produce compressive stresses on planes at 45° with tube axis, the weakening effect on a tube carrying bending of a torsional moment should not be as great as the addition of more bending moment since the compressive stresses produced by torsion are not in the same direction as the bending compressive stresses. The same reasoning applies to the weakening effect of bending on the torsional strength.

Tests of round tubes in combined bending and torsion have shown that the ultimate interaction strength curve can be safely and closely expressed by the following equation:

$$R_b^2 + R_s^2 = 1.0 \quad \text{- - - - - - - - - - - - - -(7)}$$

Thus margin of safety equals,

$$M.S. = \frac{1}{\sqrt{R_b^2 + R_s^2}} - 1$$

Equation (7) is plotted in Fig. C3.12 and can be used for finding margins of safety if desired, but is particularly handy to determine if a selected tube is weak.

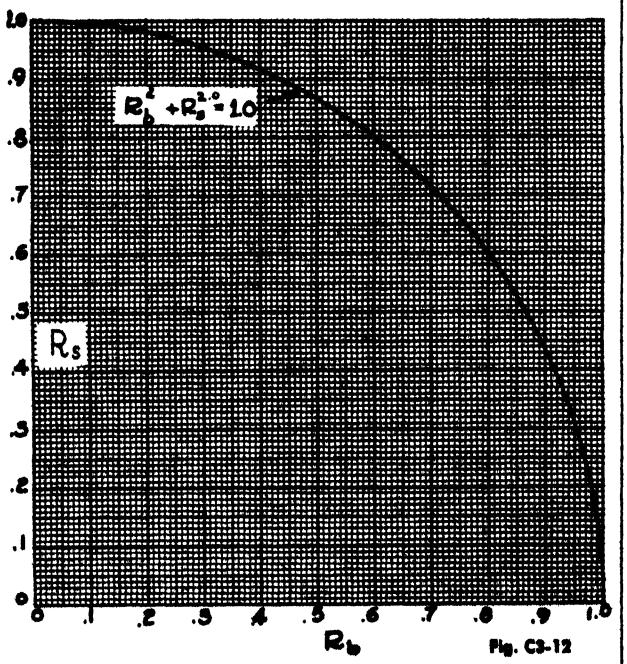


Fig. C3-12

Since the allowable bending and torsional moments are functions of the D/t values of the tube, the design process is in general a trial and error method.

A relationship making use of an equivalent torsional moment T_e which will produce the same torsional stress as produced by the combined bending and torsional loads is quite useful in reducing the error in the general trial and error method of solution.

$$\text{Let } f_{s(max.)} = T_e\, r/2I \quad \text{- - - - - - - - - -(8)}$$

From chapter A4, $f_{s_{max.}}$ can also be expressed as,

$$f_{s_{max.}} = \sqrt{f_s^2 + (f_b/2)^2} \quad \text{- - - - - - - - - -(9)}$$

$$\text{But } f_s = Tr/2I \quad \text{- - - - - - - - - - - - - - - - - (10)}$$

and

$$f_b = Mr/I \quad \text{- - - - - - - - - - - - - - - - - - - (11)}$$

Substituting equations (10) and (11) in (9), we obtain

$$f_{s_{max.}} = \frac{r}{2I}\left[M\sqrt{1 + (T/M)^2}\right] \quad \text{- - - - - - - - - (12)}$$

Equating (12) to (8) and solving for T_e,

$$T_e = M\sqrt{1 + (T/M)^2} \quad \text{- - - - - - - - - - - - - - - (13)}$$

C3.9 Example Problems in Combined Bending and Torsion.

Example Problem #1

Find the lightest 24ST aluminum alloy round tube which will carry a bending moment of 3000 in. lb. and a torsional moment of 2000 in. lb.

Solution

As a help for guessing tube sizes which will have a small margin of strength or weakness, we will make use of equation (13) and solve for the equivalent torque T_e. Hence

$$T_e = M\sqrt{1 + (T/M)^2} = 3000\sqrt{1 + \left(\frac{2000}{3000}\right)^2} = 3600 \text{ in. lb.}$$

From table C3.1 we select following tube sizes as having torsional strengths near 3600 but not over 3600. In general the bigger the tube diameter the more efficient the tube.

Tube size	wt/100"	M_a Table C3.1	T_a Table C3.1	$R_b = \frac{M}{M_a}$	$R_s = \frac{T}{T_a}$
1 3/8 - .049	2.07	4230	3460	.71	.578
1 3/4 - .035	1.91	4650	3170	.645	.631

Using the values of R_b and R_s on Fig. C3.12 it is quickly noticed that the b point of intersection of these values falls inside the $R_b^2 + R_s^2 = 1$ curve hence they have a positive margin of safety.

M.S. for 1-3/4 - .035 tube which is the lightest equals,

$$\frac{1}{\sqrt{.645^2 + .631^2}} - .1 = \frac{1}{.902} - 1 = .10$$

Example Problem #2

A steel tube (x - 4130, U.T.S. = 100000) 62.5 inches long is subjected to a bending moment of 20000 in. lb. and a torsional moment of 10,000 in. lb. Select the lightest tube if maximum permissible diameter equals 2-1/2 inches.

Solution

The equivalent torsional moment T_e will be computed for purposes of helping to make a close guess as to the proper tube size.

$$T_e = M\sqrt{1 + (T/M)^2} = 20000\sqrt{1 + \left(\frac{10}{20}\right)^2} = 22400 \text{ in.lb.}$$

From table C3.1 we select steel tubes which have a torsional strength near or slightly less than 22400. The following table gives the results.

Tube size	wt/100"	M_b Table C3.1	T_a Table C3.1	$R_b = \frac{M}{M_b}$	$R_s = \frac{T}{T_a}$
2 1/4 - .058	11.30	21300	20450	.94	.488
2 1/2 - .049	10.68	21220	19570	.94	.51
2 1/4 - .065	12.64	24220	23610	.824	.424
2 1/2 - .058	12.60	25950	24630	.771	.406

The first two tubes selected in the table are quickly found to be understrength when the values of R_b and R_c are projected on Fig. C3.12 and found to fall outside the interaction curve. The next tube thickness is then selected as shown in the table, and the values of R_b and R_s projected on Fig. C3.12 show that a positive margin of safety exists.

The 2-1/2 - .058 is slightly lighter and its margin of safety will be calculated.

The torsional strength T_a given in table C3.1 for steel tubes is for an L/D of 20, whereas the L/D ratio for our tube is 62.5/2.5 = 25.

The correction factor K_t from graph on table C3.1 is .98, hence corrected T_a = .98 x 24630 = 24200

$$R_s = \frac{10000}{24200} = .413, \text{ M.S.} = \frac{1}{\sqrt{.771^2 + .413^2}} - 1 = .14$$

For design of tubes of 17ST and 24SRT aluminum alloy or heat-treated steels, table C3.1 can be used to help guess a size near that required, remembering that better material than that on which table C3.1 is based would tend to decrease tube gage, whereas weaker material would tend to increase tube gage.

Example Problem 3 Elevator Beam

Fig. C3.13 shows the plan view of an elevator surface of an actual airplane. The elevator beam is a round tube 1-3/4 x .049, 17ST material. The critical design loading and distribution is given in Fig. C3.14. The strength of the elevator beam will be checked for the given design loading.

Area of elevator aft of hinge line = 9.15 sq.ft./side.
Area of elevator balance = 0.46 sq.ft./side.

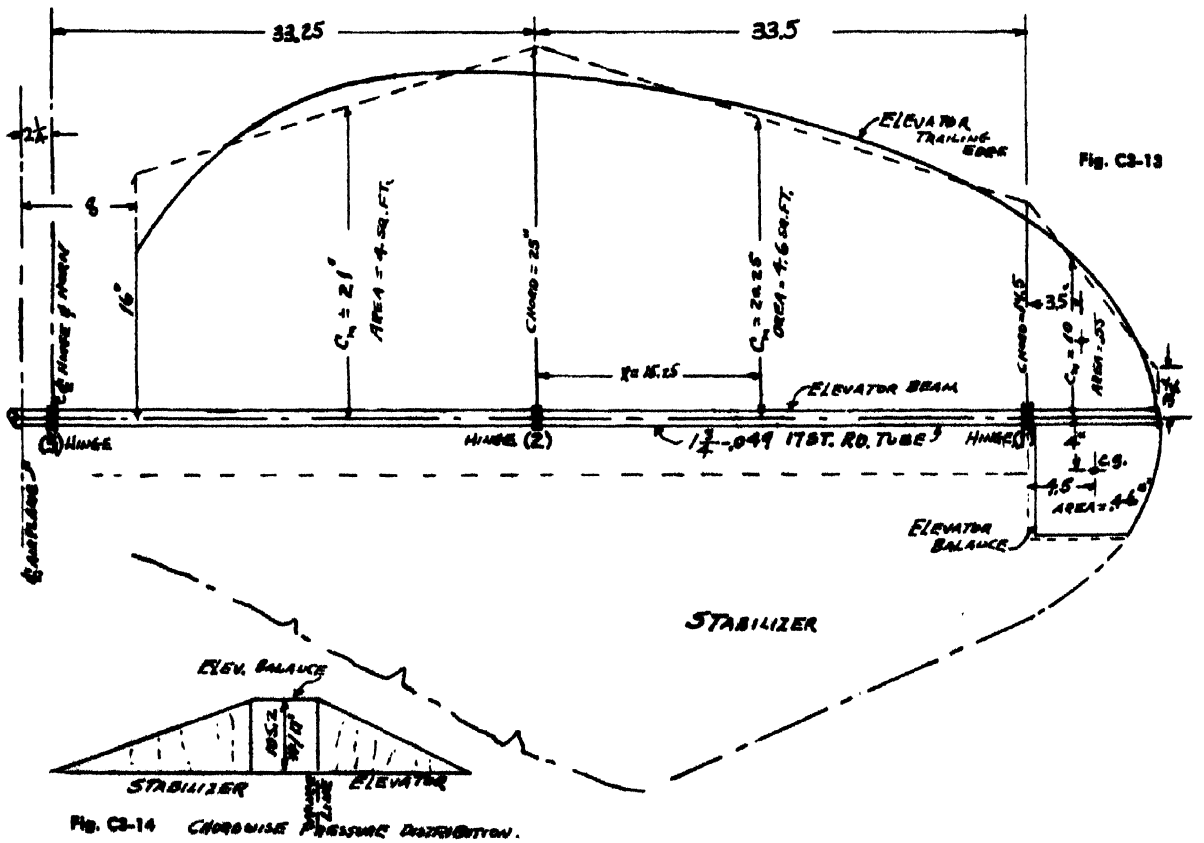


Fig. C3-13

Fig. C3-14 Chordwise Pressure Distribution.

Solution:

To simplify the calculations the elevator with its curved trailing edge will be changed to the equivalent system made up of 3 trapizoids as shown by the dashed line. The area of each trapizoid, its mean chord length and location are given on Fig. C3.13. For example, the portion between hinges number (1) and (2), the mean chord is 20.25" and its location is 15.25" from hinge #2., which was obtained as follows:

$$C_m = \frac{2}{3}\left[C + C_a - \frac{CC_a}{C + C_a}\right]$$

$$X = \frac{L\ (C + 2\ C_a)}{3\ (C + C_a)}$$

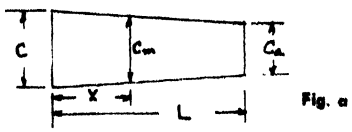


Fig. a

Fig. a explains the terms in the above equations. Substituting in the above equations,

$$C_m = \left[\frac{2}{3}\ 25 + 14.5 - \frac{25 \times 14.5}{25 + 14.5}\right] = 20.25"$$

$$X = \frac{33.5\ (25 + 29)}{3\ (25 + 14.5)} = 15.25$$

Calculation of Elevator Beam Running Loads.

Average air load per sq. ft. = 52.6"

Load w per running inch on beam = chord x 52.6/144 = .366 x chord.

At hinge #1, w = .366 x 14.5 = 5.3#/in.
At hinge #2, w = .366 x 25 = 9.15#/in.
At point 8" outboard of centerline of airplane, w = .366 x 16 = 5.85

Fig. C3.15 shows the resulting running beam load.

The cantilever shear and bending moment due to air loads outboard of hinge #1 will be calculated:

$M_1 = .55 \times 52.6 \times 3.5 + 105.2 \times .46 \times 4.5 = 319$ in. lb.
Shear = $.55 \times 52.6 + 105.2 \times .46 = 77.5$#

Since the elevator beam is continuous over several supports, the moments over the support points will be determined by the moment distribution method. Fig. C3.15 gives the solution. (Reference chapter A11)

The fixed end moments on each span are as follows:-
For equations see table A11.1 of chapter A11.

Span 1-2



$$M_{1-2} = \frac{33.5^2}{60}\ (5 \times 5.3 + 2(9.16 - 5.3)) = 640 \text{ in. lb.}$$

$$M_{2-1} = \frac{33.5^2}{60}\ (5 \times 5.3 + 3(9.16 - 5.3)) = 712 \text{ in. lb.}$$

Span 2-3

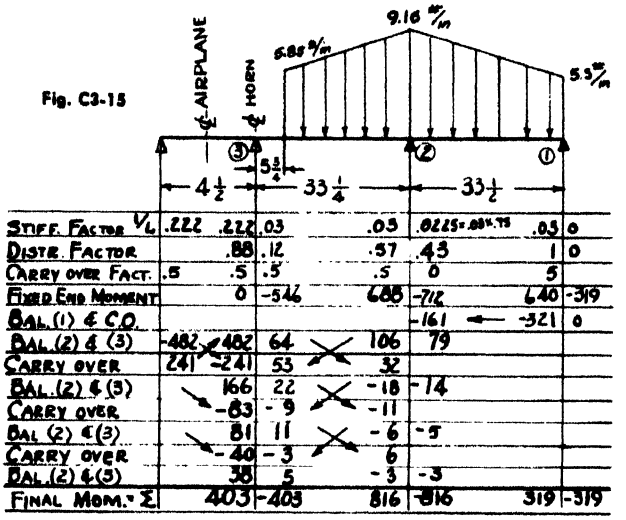


$$M_{2-3} = \frac{5.85 \times 2.75^2}{12 \times 33.25^2}\ (3 \times 27.5^2 - 8 \times 27.5 \times 33.25 + 6 \times 33.25^2) + \frac{3.31 \times .5 \times 27.5^2}{30 \times 33.62}\ (3 \times 27.5^2 - 10 \times 27.5 \times 33.25 + 10 \times 33.25^2) = 530 + 158 = 688 \text{ in. lb.}$$

$$M_{3-2} = \frac{5.85 \times 27.5^2}{12 \times 33.25}\ (4 \times 33.25 - 3 \times 27.5) + \frac{3.31 \times .5 \times 27.5^2}{30 \times 33.25^2}\ (5 \times 33.25 - 3 \times 27.5) = 460 + 86 = 546"\#$$

The moment signs in Fig. C3.15 are according to the adopted sign convention of chapter A11.

Fig. C3-15



STIFF. FACTOR V_L	.222	.222	.03	.03	.0225	.05	0
DISTR. FACTOR		.88	.12	.57	.43	1	0
CARRY OVER FACT.	.5	.5	.5	.5	0	5	
FIXED END MOMENT		0	-546	685	-712	640	-319
BAL (1) & CO.					-161	-321	0
BAL (2) & (3)	-482	482	64	106	79		
CARRY OVER	241	-241	53	32			
BAL (2) & (3)		166	22	-18	-14		
CARRY OVER		-83	-9	-11			
BAL (2) & (3)		81	11	-6	-5		
CARRY OVER		-40	-3	6			
BAL (2) & (3)		38	5	-3	-3		
FINAL MOM. Σ		403	-403	816	-816	319	-319

Calculation of Torsional Moments.

The bending moments are maximum over the hinge support points, therefore the torsional moment will only be calculated at the hinge points (1), (2), and (3). The air load distribution chordwise is triangular hence, c.g. is at 1/3 point of mean chord of each elevator area portion.

$T_1 = -.46 \times 105.2 \times 4 + .55 \times 52.6 \times 10/3 = -97$ in.lb.

$T_2 = -97 + 4.6 \times 52.6 \times 20.25/3 = 1538$ in. lb.

$T_3 = 1538 + 4 \times 52.6 \times 21/3 = 3010$ in. lb.

The results show that the bending moment is maximum over support (2) whereas the torsional moment is maximum over support (3), therefore the margin of safety of the tube will be checked at both points (2) and (3).

Check of Elevator Tube Over Support #2.

Fig. b shows a cross-section of the tube at this point. The tube section is pierced by 6 - 1/8 rivets for attaching bearing collar and elevator rib to tube.

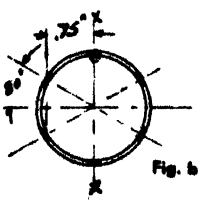


Fig. b

The moment of inertia of net section equals:

$$I_{xx} = .09478 - \left[4 \times .75^2\ (.125 \times .049)\right] = .081$$

Design bending moment = 816 in. lb.
Design torsional moment = 1538 in. lb.

$$f_b = \frac{Mc}{I} = \frac{816 \times .875}{.081} = 8820 \text{ psi.}$$

$$f_s = \frac{Mr}{2I} = \frac{1538 \times .875}{2 \times .081} = 8300 \text{ psi.}$$

F_b from Fig. C3.2 for 17ST material and D/t = 1.75/.049 = 35.7 equals 56500 psi.

F_{st} from Fig. C3.9 for D/t = 35.7 = 19400 psi.

$R_b = f_b/F_b = 8820/56500 = .156$

$R_s = f_s/F_{st} = 8300/19400 = .428$

$$M.S. = \frac{1}{\sqrt{R_b^2 + R_s^2}} - 1 = \frac{1}{\sqrt{.156^2 + .428^2}} - 1 = 1.19$$

Check of Section Over Hinge Support #3

Fig. C shows section of elevator tube at this point.

$$I_{xx} = .09478 - \left[4 \times .618^2 \ (.049 \times .156)\right] = .083$$

Design bending moment = 403 in. lb.
Design torsional moment = 3010 in. lb.

$$f_b = \frac{403 \times .875}{.083} = 4250 \text{ psi.}$$

$$f_s = \frac{3010 \times .875}{2 \times .083} = 16000 \text{ psi.}$$

$$R_b = \frac{4250}{56500} = .075 \quad R_s = \frac{16000}{19400} = .825$$

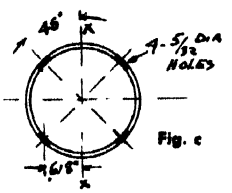


Fig. c

$$M.S. = \frac{1}{\sqrt{.075^2 + .825^2}} - 1 = .23$$

In general an elevator using a round tube as an elevator beam and torque tube, the tube is kept same size throughout to give sufficient torsional regidity, the tube thus being far over strength except near inner support or horn point where torque is maximum.

The approximate angle of twist of elevator beam under full design load is,

$$\theta = \frac{TL}{G I_p}$$

T = average torque = 3010/2 = 1505
L = 70", G = 3800,000 I_p = 2I

hence, $\theta = \frac{1505 \times 70}{3800,000 \times .1895} = .147$ radians = 8.3° (approx.)

It is usually customary to keep θ under 10 or 11 degrees.

The bending moments as found in the solution of Fig. C3.15 assume no settlement of the supports whereas in reality the hinge points move vertically because of the deflection of the stabilizer which is the supporting structure for the elevator. Thus the approximate deflection of the stabilizer structure should be calculated and these deflections used in finding additional bending moments on the elevator beam. (See chapter A11 for problem illustrating influence of support deflection on moments.)

C3.10 Combined Compression, Bending and Torsion.

Very little published test data on steel and aluminum round tubes in combined compression, bending and shear is available. ANC-5 recommends the following interaction equation for the design of steel and aluminum round tubes.

$$R_c + R_b' + R_s^2 = 1 \quad \text{- - - - - - - - - - - - - - (14)}$$

The bending stresses should include the effect of secondary bending due to compression.

The maximum normal stress should be computed and this stress should not exceed the compressive yield stress of the material.

For the interaction equation (14), the margin of safety can be written:

$$M.S. = \frac{2}{R_b' + R_c + \sqrt{(R_b' + R_c)^2 + 4 R_s^2}} - 1$$

The margin of safety equation assumes that all stresses vary linearly, which is not strictly true since the secondary moment in the term R_b' does not vary linearly.

Fig. C3.16 shows the interaction curves for equation (14). Fig. C3.17 gives the change in the interaction curves for increasing the exponent of R_b to 1.5. This curve may prove more suitable in the future when more test data is available but should not be used at this time.

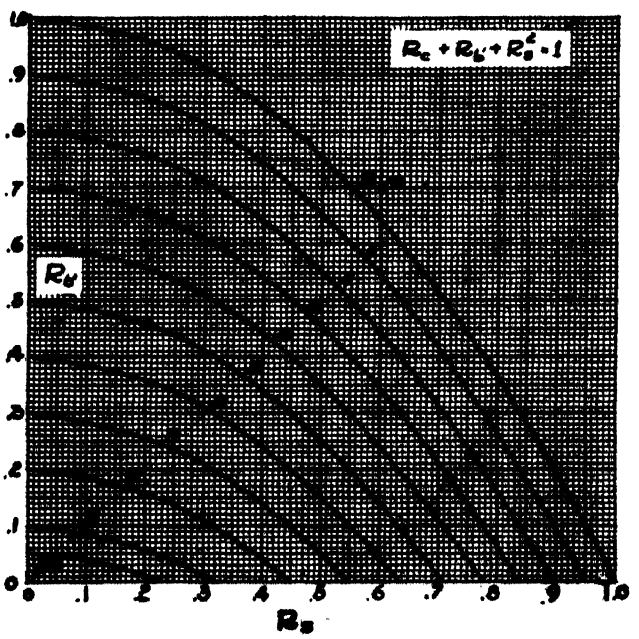


Fig. C3-16

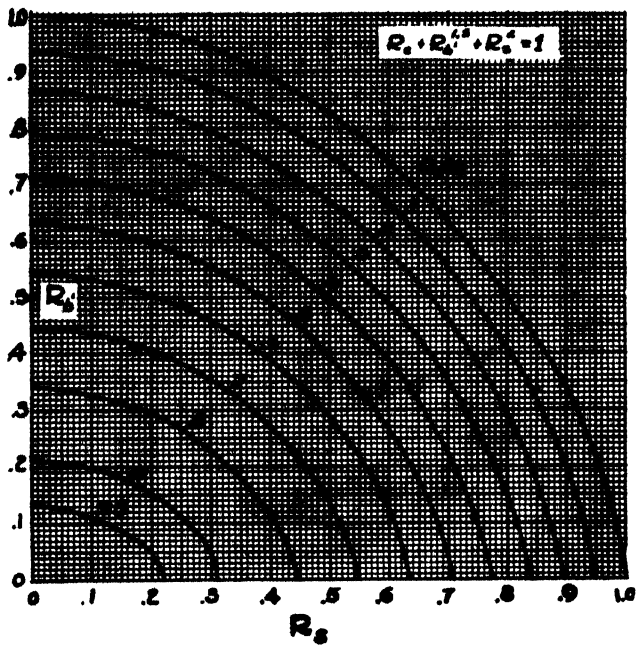


Fig. C3-17

Example Problem #1.

A 1-1/8 - .049 24ST round tube 25 inches long with pin ends is subjected to a compressive end load of 1600#, a constant torsional moment of 650 in. lb. and a uniform lateral load of 10#/in. (See Fig. C3.19). Determine margin of safety for tube under the given combined loading.

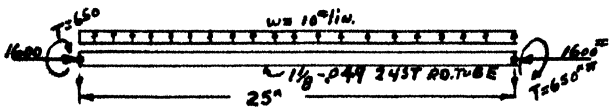


Fig. C3-19

Solution.

The maximum bending moment due to symmetry will occur at midpoint of tube. For a beam column carrying a uniform side load with no end moments, the maximum moment is given by the following expression. (See chapter A10, table A10.1)

$$M_{max.} = wj^2 \left(1 - \sec \frac{L}{2j}\right)$$

$$j = \sqrt{\frac{EI}{P}} = \sqrt{\frac{10{,}300{,}000 \times .0240}{1600}} = \sqrt{154.7} = 12.43$$

$$\frac{L}{2j} = \frac{25}{2 \times 12.43} = \frac{25}{24.86} = 1.005$$

$$\sec \frac{L}{2j} = \frac{1}{\cos L/2j} = \frac{1}{.5361} = 1.87 \text{ (See table A10.2)}$$

hence,

$$M_{max.} = 10 \times 154.7 \ (1 - 1.87) = -1347 \text{ in. lb.}$$

The bending strength of a 1-1/8 - .049 24ST tube from table C3.1 equals 2815 in. lb.

The column strength for the tube for a length of 25" and pin ends (C = 1) from column charts of Fig. C2.8 equals - 3700#.

The torsional strength of a 1-1/8 - .049 tube from table C3.1 = 2500 in. lb.

Calculation of Stress ratios:

$$R_c = \frac{1600}{3700} = .432$$

$$R_b = \frac{1347}{2815} = .479$$

$$R_s = \frac{650}{2500} = .26$$

$$M.S. = \frac{2}{R_b' + R_c + \sqrt{(R_b' + R_c)^2 + 4 R_s^2}} - 1$$

$$= \frac{2}{.479 + .432 + \sqrt{(.479 + .432)^2 + 4 \times .26^2}} - 1$$

$$= \frac{2}{1.96} - 1 = .02$$

Example Problem #2

In welded steel tubular fuselages, cases often occur where traverse loads due to various fuselage installations are applied to truss members between truss joints. Fig. C3.20 illustrates a portion of a fuselage truss with one member (AB) supporting a traverse concentrated load, which is also applied off center relative to tube. A so called accurate investigation of this member under the combined loading would involve a moment distribution of about 3 bays of the fuselage taking into account the effect of axial loads on the factors involved in the moment distribution method. (See chapter A11). An approximate solution will be made which should show if member is satisfactory for the combined loading. The transverse load of 200# is the design load and includes the factor of safety. An axial load of 9500# compression due to truss action exists simultaneously with the above load.

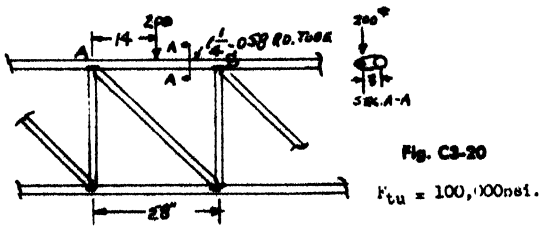


Fig. C3-20

F_{tu} = 100,000 psi.

Approximate Solution

Assuming the same torsional resistance at (A) and (B) the torsional moment on tube AB = 200 x 3/2 = 300 in. lb.

The bending moment on AB due to the transverse load depends on the restraint at joints A

and B. Since it is customary practice to use a end fixity coefficient of C = 2 in the column design of fuselage longeron members end moments will be assumed consistent with the points of inflection of a column with C = 2. Fig. C3.21 shows the results for primary moments.

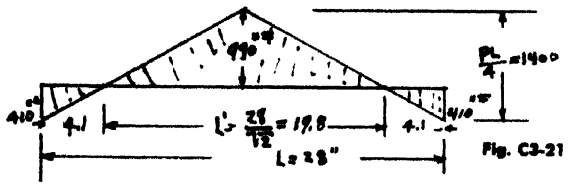


Fig. C3-21

End moments of 410"# will be assumed. Since the secondary moments due to axial load times deflection are usually appreciable in aircraft structures they will be computed. From table A10.1 of chapter A10, the expression for the maximum bending moment is as follows:

$$M_{max.} = \frac{M}{\cos L/2j} - \frac{Wj \sin^2 L/2j}{\sin L/j}$$

This expression is obtained by adding expressions for M of a beam with equal end moments and a axial compressive load P, to the case of a beam with lateral load W at midpoint plus same end load P.

Solving for terms in the above equation:

M_1 = end moments = - 410"#

$$j = \sqrt{\frac{EI}{P}} = \sqrt{\frac{29000{,}000 \times .03867}{9500}} = \sqrt{118} = 10.88$$

$$L/j = \frac{28}{10.88} = 2.573 \qquad \sin L/j = .5384$$

$$\cos L/2j = .2800$$

$$L/2j = 1.287 \qquad \sin L/2j = .9600$$

$$\sin^2 L/2j = .9216$$

Substituting:

$$M_{max.} = \frac{-410}{.2800} + \frac{-200 \times 10.88 \times .9216}{.5384}$$

$$= -1460 + 3720 = 2260"\#$$

Calculation of Stress Ratios:

$$R_c = \frac{\text{Column load}}{\text{Column strength}} = \frac{9500}{15000} = .633$$

The column strength of 15000 is obtained from curves on Fig. C2.7 of chapter C2 for end fixity C = 2 and L = 28.

$$R_b = \frac{2260}{7050} = .32$$

The bending strength of a 1-1/4 - .058 round tube is 7050 (see Table C3.1)

$$R_s = \frac{300}{6870} = .047, \text{ where 6870 is the torsional}$$

strength from Table C3.1 using K_t = .99.

$$M.S. = \frac{2}{R_b + R_c + \sqrt{(R_b + R_c)^2 + 4 \times R_s^2}} = 1$$

$$= \frac{2}{.32 + .633 + \sqrt{(.32 + .633)^2 + 4 \times .047^2}} - 1$$

$$= \frac{2}{1.91} - 1 = .05$$

The results indicate that the member would be satisfactory if the end restraints are as large as that assumed. Tentatively therefore the member can be assumed satisfactory until a more rigorus analysis for the end moments is made using the moment distribution method.

The ends of member AB will be checked for maximum combined normal stress which should not exceed .8 times the compressive yield point since member is welded, or .8 x 85000 = 68000 psi.

From chapter A4,

$$f_{n(max.)} = \frac{f_c}{2} \pm \sqrt{\left(\frac{f_c}{2}\right)^2 + f_s^2}$$

$$f_c = \text{axial stress} = \frac{P}{A} + \frac{My}{I} = \frac{9500}{.2172} + \frac{410}{.06187} = 49500 \text{ psi}$$

$$f_s = Tr/2I = 300/.1237 = 2430 \text{ psi.}$$

$$f_{n(max.)} = \frac{49500}{2} + \sqrt{\left(\frac{49500}{2}\right)^2 + 2430^2} = 49520 \text{ psi.}$$

M.S. = (68000/49520) - 1 = 0.37

C3.11 Problems.

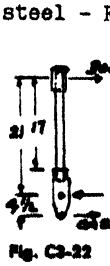
(1) Fig. C3.22 shows the dimensions of a conventional control stick. The design pull load on the grip is 300#. Determine the size of a 24ST round tube to take the grip pull of 300#.

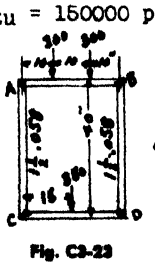
(2) In Fig. C3.23 determine the size of steel round tubes (F_{tu} = 95000 psi.) for the members AB and CD. Frame is welded. Loads are applied loads. Use factor of safety of 1.5.

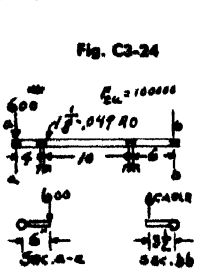
(3) In Fig. C3.24 determine the margin of safety of tube for the given loading.

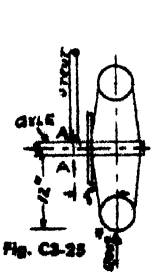
(4) Consider that the elevator of Fig. C3.13 is subjected to an average ultimate air load of 65#/sq. ft. with the distribution varying from a maximum at the hinge line to 1/3 the maximum at the trailing edge. Design a 24ST round tube elevator beam for this loading.

(5) In Fig. C3.25 determine the size of axle required at section A-A, for a braked landing condition, coefficient of friction between tire and ground = .5. Axle material-nickel steel - F_{tu} = 150000 psi.


Fig. C3-22


Fig. C3-23


Fig. C3-24


Fig. C3-25

(6) Determine the lightest 24ST aluminum alloy round tube which will carry a combined bending and torsional loading of 4500"# and 3000"# respectively.

(7) Same as for problem (6) but for a tube made from chrome-moly steel. (F_{tu} = 100,000 psi.

(8) A trim-tab control system torque tube is subjected to an ultimate torque of 300"#. The tube is 21" long and it is desired to restrict the outside diameter of the tube to 3/4 inch. The torsional deflection at limit load which is 2/3 the ultimate load must not exceed 5 degrees. Find the lightest 24ST round tube. Show its M.S. and torsional deflection.

(9) A 1-1/2 - .065 24ST round tube is subjected to a side load of 12#/in. The member is 50" long. It also carries an axial compressive load of 700#. What is the M.S. of the tube under these loads?

(10) If the tube in problem (9) is also subjected to atorsional moment of 1400"# in addition to the loads of problem (9), what would be the M.S. of the tube?

(11) A 2" - .049 round magnesium tube (F_{cy} = 30000 psi.) 30 inches long acts as a simple supported beam with a transverse load of 500# at the midpoint. What is the M.S. for this load?

(12) A 1-1/2 - .049 round magnesium tube (F_{tu} = 36000) is subjected to a torsional moment of 2200 in. lbs. What is the M.S. under this load?

CHAPTER C4
AIRPLANE FITTING ANALYSIS-RIVETED AND BOLTED

C4.1 Introduction. The ideal airplane structure would be the single complete unit of the same material involving one manufacturing operation. Unfortunately the present day types of materials and their method of working dictates a composite structure. Furthermore general requirements of repair, maintenance and stowage dictate a structure of several main units held to other units by main or primary fittings or connections, with each unit incorporating many primary and secondary connections involving fittings, bolts, rivets, welding etc. No doubt main or primary airplane fittings involve more weight and cost per unit volume than any other part of the airplane structure, and therefore fitting and joint design plays an important part in airplane structural design.

C4.2 Fitting Design Loads. Minimum Margins of Safety.

As discussed in chapter D1, Applied Loads represent the actual maximum loads that may be subjected to the airplane in a landing or flight maneuver. The combined resultant stresses on a fitting in the primary airplane structure should not exceed the yield point of the fitting material or in other words should not produce permanent set on any part of the fitting. The Design Loads, are the applied loads multiplied by a factor, generally 1.5 and the structure must carry these design loads without failure or collapse. Fittings under the design loads are required to show a certain minimum margin of safety. In general the required fitting margin of safety is 15% for military airplanes and 20% for commercial airplanes. The minimum blanket margin of safety on the design loads is specified because it is realized that many additional unknown factors may effect the strength of a fitting as compared to that of the primary member itself. The combined stress distribution and the allowable stresses for the common major fitting involving bolt holes, rather abrupt changes in section etc., is far less determinate than for the primary members to which the fittings attach. In fittings involving several bolts with matching plates perfect bearing of all bolts is seldom obtained. Material tolerances and the human element particularly in welded connections provide additional unknown factors. Thus to take care of these many unknowns it is logical to provide an additional reserve minimum margin of safety for fitting design.

C4.3 Special or Higher Fitting Margins of Safety.

A blanket margin of safety as specified above is not logical for all fittings. The manner under which the load it applied should be considered such as questions of shock, vibration, and relative movement of connected parts. Primary fittings like wing, fuselage, landing gear, and tail attachment fittings whose failure mean collapse of the airplane and possibly involving loss of human life should have greater margins of safety on the design loads than fittings which connect various structural parts of secondary units or installations whose failure would not be dangerous but would only cause expense and inconvenience.

The military and commercial design requirements specify various required fitting margins of safety and the beginning stressman should acquaint himself with these requirements.

C4.4 Economy in Fitting Design.

For structural economy the structural designer in the initial layout of the airplane should strive to use a minimum number of fittings particularly those fittings connecting units which carry large loads. Thus in a wing structure splicing the main beam flanges or introducing fittings near the centerline of the airplane are far more costly than splices or fittings placed farther outboard where member sizes and loads are considerably smaller. Avoid changes in direction of heavy members such as wing beams and fuselage longerons as these involve heavy fittings. If joints are necessary in continuous beams place them near points of inflection in order that the bending moments to be transferred through the joint be kept of small magnitude. In column design with end fittings avoid introducing eccentricities on the beam and on the other hand make use of the fitting to increase column end fixity thus compensating some of the weight increase due to fitting weight by saving in the weight of the beam.

For economy of fabrication, the structural designer should have a good knowledge of shop processes and operations. The cost of fitting fabrication and assembly varies greatly with the type of fitting, shape and the require tolerances. Poor layout of major fitting arrangement may require very expensive tools and jigs for shop fabrication and assembly.

Fittings likewise add considerably to the cost of inspection and rejections of costly fittings because of faulty workmanship or materials

are quite frequent thus adding greatly to the cost.

C4.5 Aircraft Rivets.

Rivet Types. From an airplane structural standpoint rivets may be placed into two general classifications, namely:-

(1) The Protruding Head type of rivet.

(2) The Flush type rivet.

Fig. C4.1 illustrates the protruding head type of rivet. Fig. C4.2 illustrates a number of modifications of the protruding head type of rivet that have been used in the past.



Fig. C4-1

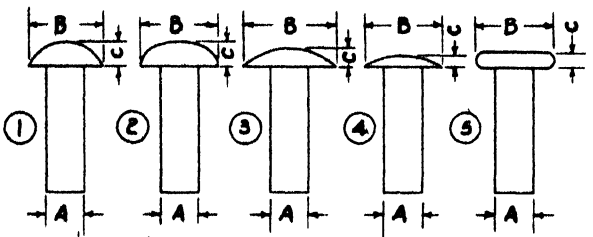


Fig. C4-2

NO	RIVET TYPES	B	C
1	ROUND HEAD	2A	.75A
2	MUSHROOM HEAD	2A	.625A
3	BRAZIER	2.5A	.50A
4	MODIFIED BRAZIER	2A	.25A
5	FLAT HEAD	2A	.4A
6	CTSK. HEAD	1.81A	.5A

For many years the round head rivet was used for all interior work and before the era of high speeds it was used as a surface rivet as well. When wind tunnel experiments showed that such rivets gave appreciable drag, designers turned to rivets with less head protrusion, thus the development of the Brazier and modified Brazier type of rivet head. Then as the age of relatively high airplane speeds arrived a flush surface was needed, particularly on certain sensitive portions of the airplane surface, thus various modifications of the countersunk head involving press and machine countersinking of the sheets were developed.

Fig. C4.3 illustrates the flush type of rivet. The government ANC-5 Manual gives strength information for three different rivet head angles, namely, 78, 100 and 115 degrees. The 100 degree angle head is possibly the best compromise between shear and tension strength values for the rivet. As illustrated in Fig. C4.3, this flush type rivet can be used in several different ways, thus the method shown in Fig. C4.3a is referred to as the machine countersunk type; that in Fig. C4.3b as the press countersunk double dimpled type; and that in Fig. C4.3c as the combined press and machine countersunk type or the dimpled machine countersunk type.



Fig. a

Machine Countersunk Type



Fig. b

Press Countersunk - Double Dimpled Type.



Fig. c

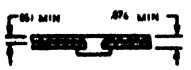
Combined Press and Machine Countersunk; or Dimpled Machine Countersunk Type.

Fig. C4-3

Fig. C4.4 is presented to give the student a general idea of flush riveting operations.

Fig. C4.5 illustrates the approximate sheet thickness limitations for the three methods of flush riveting.

Approx. Sheet Limitations For Machine Countersunk Rivets (AN-426)



1/8 Dia. Rivet.



5/32 Dia. Rivet



3/16 Dia. Rivet.

Approx. Limitations For Press Countersunk Or Double Dimpled Rivets (AN-426)



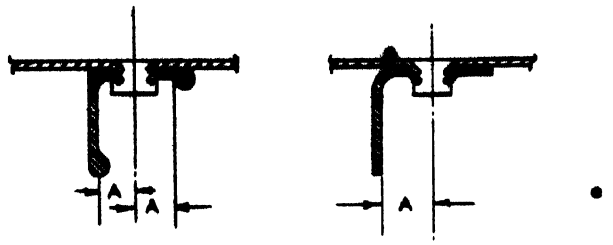
1/8 Dia. Rivet.



5/32 Dia. Rivet

Fig. C4-5

Flush Riveting Operations



RIVET DIAMETER	A
3/32	1/4
1/8	9/32
5/32	5/16
3/16	11/32

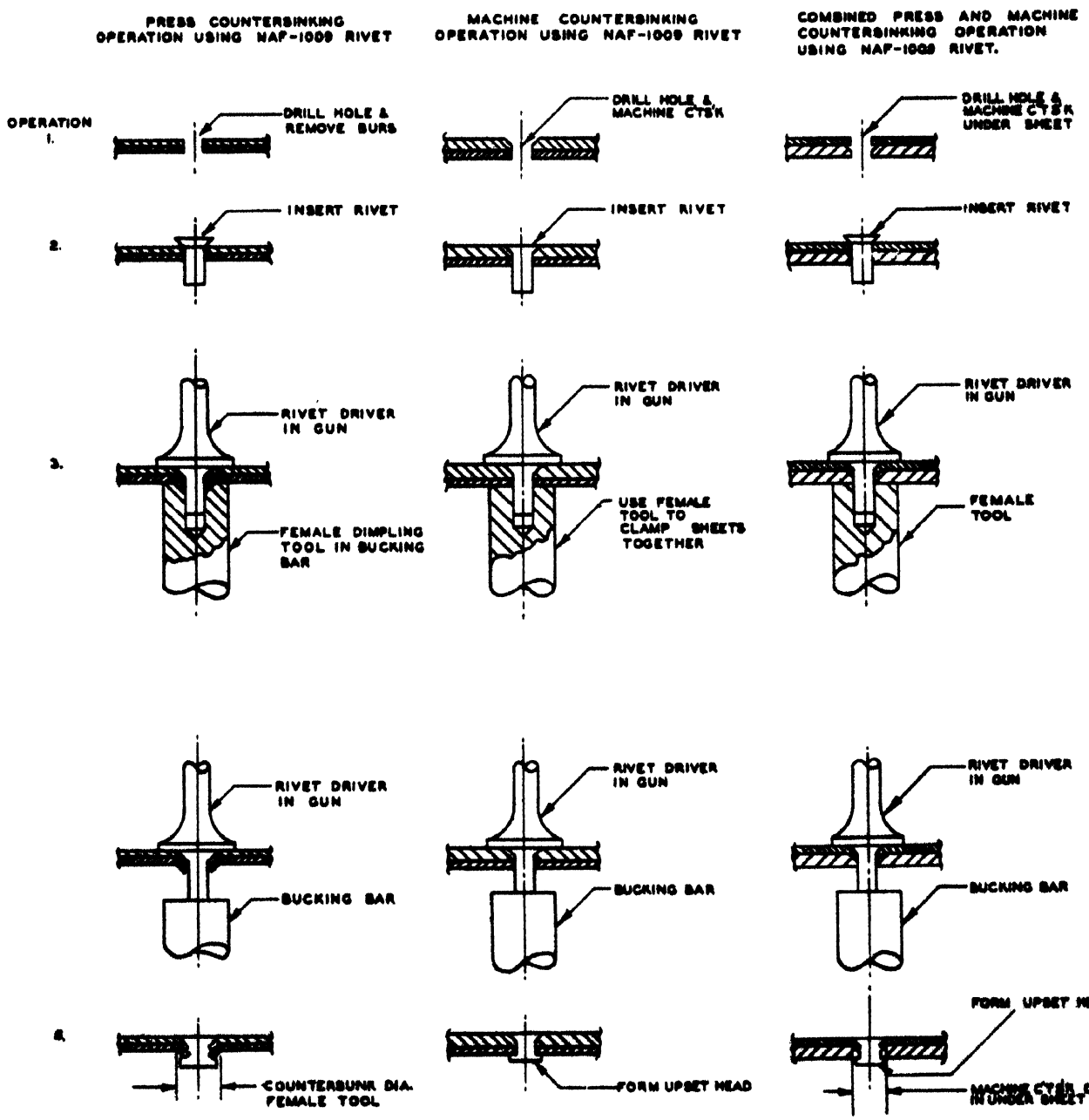


Fig. C4-4

(By permission from, Vought - Sikorsky Engineering Manual)

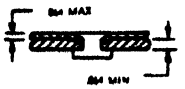


3/16 Dia. Rivet

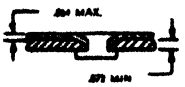
Approx. Limitations For Press-Machine Countersunk Rivets (AN-426)



1/8 Dia. Rivet



5/32 Dia Rivet



3/16 Dia. Rivet

Fig. C4-5

C4.6 Rivet Material. In general the structural rivets now in use are made from various aluminum alloys. The common aluminum alloys for structural rivets are:-

17ST Rivets (Made from 17ST alloy in the hard state).
A17ST Rivets (Made from 17ST alloy in the soft or annealed state).
24ST Rivets (Made from 24ST alloy in the hard state).

If the 17ST and the 24ST are driven in the hard state difficulty is encountered in the form of cracked rivet heads, hence it is common practice to heat treat the rivets and drive them within a half hour before they have age hardened. To delay the ageing period the rivets are kept in boxes with dry ice and distributed to the workmen as needed.

A17ST rivets are driven as received and no special handling is necessary. The disadvantage of this rivet is its weaker shear strength as compared to 17ST and 24ST rivets. The A17ST rivet is being widely used since it speeds up production and lowers fabrication cost. Fig. C4.6 shows the material identification mark which is incorporated on the rivet head. The critical strength of a good proportion of the rivets used in the surface plating of wings and fuselages as well as many other places where rivets are in single shear is determined by bearing of rivet on plate, hence nothing is lost from a overall strength standpoint in using the A17ST rivets as the smaller rivet shear strength is not the critical factor.

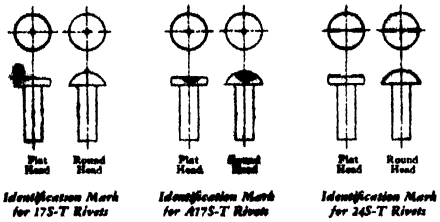


Fig. C4-6

C4.7 Strength of Rivets. Protruding Head Type.

Rivets are widely used in airplane structures to fasten or tie together two or more structural units. Standard methods of stress analyses of riveted joints consider two primary types of failure, namely, the shear of the shank of the rivet and the bearing or compressive failure of the metal at the point where the rivet bears against the connecting sheet or plate.

Fig. C4.7 illustrates the main forces on a rivet in transferring a load from one plate to another. The load is transferred to the rivet from the plate by bearing of the plate on the rivet. The load is then transferred along the rivet and resisted by bearing action on the other plate. Since the plate bearing forces on the rivet are not in the same line, the forces tend to shear and bend the rivet. Bending of the rivet is usually neglected if there are no intermediate filler plates. In Fig. (a) of C4.7, the rivet is in single shear, whereas in Fig. (b) the rivet is in double shear.

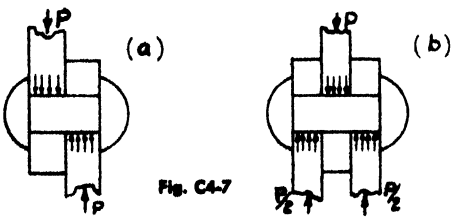


Fig. C4-7

The ultimate shear strength of a rivet is given by the following equation:-

$$P_a = F_{su} A n \text{ - - - - - - - - - - - - - - - -(1)}$$

where, P_a = ultimate shear strength of rivets. (lbs.)
F_{su} = ultimate allowable shear stress for rivet (psi.)
A = area of rivet cross-section = $\pi D^2/4$, where D equals the nominal rivet hole diameter.
n = number of shear areas per rivet.

Reference (1) shows that the shear strength of protruding head aluminum alloy rivets is affected by increasing D/t (Diameter of rivet over sheet thickness) ratios. The conclusions in Reference (1) are as follows:-

Rivets in Single Shear:-

For values of D/t up to 3:-
Sihgle shear strength = basic allowable single shear strength.

For values of D/t greater than 3:-
Single shear strength = basic allowable single shear strength times $[1 - 0.04\ (D/t - 3)]$

For Rivets in Double Shear:-

For values of D/t up to 1.5:-
Double shear strength = basic allowable double shear strength.

For values of D/t greater than 1.5:-
Double shear strength = basic allowable double shear strength times $[1 - 0.13\ (D/t - 1.5)]$

ANC-5 Amendment No. 2, August, 1946 incorporates the above results in presenting Tables of Shear Strengths of protruding head rivets. Table C4.1 gives the rivet information as taken from the ANC-5 amendment.

Bearing Strength of Protruding Head Rivets.

Tables C4.2 and C4.2a taken from (ANC-5 Amendment, No. 2 of August, 1946) gives the allowable bearing strengths between protruding head rivets and aluminum alloy sheets. The allowable bearing factors are given for rivet edge distances of 2D or 1.5D, where D is the diameter of the rivet. The edge distance is measured from the center of the rivet hole to the edge of the sheet in the direction of stressing. Any reduction of edge distance may cause bulging of the edge of the sheet due to the driving energy. The edge distance should never be less than 1.5D. No important gain in bearing strength is obtained with an edge distance over 2D.

C4.8 Strength of Rivets. Flush Type.

Since flush rivets have no protruding head on the flush end of the rivet and also since flush riveting involves machine countersinking or press countersinking or both, the strength of the flush type rivet is different than the common protruding head type.

Fig. C4.8 illustrates a machine countersunk rivet. Due to the pull P on the two sheets which are held together by the rivet and induced force P_1 is produced on the sloping side of the head of the rivet. This induced force tends to show and bend the portion 1-1 of the rivet head. The sharp edge of the countersunk sheet at point (a) tends to cut into the rivet. These combined influences tend to cause excessive deflections and finally failure as roughly illustrated in Fig, C4.9.

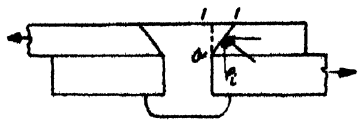


Fig. C4-8

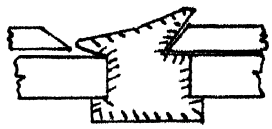


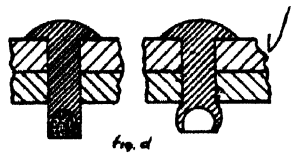
Fig. C4-9

In the press countersunk or dimpled type of flush rivet connection, see Fig. C4.3b and c, because of the interlocking of the sheets due to the dimple, the joint could transmit a load without a rivet if the sheets were held together. Since there is no clearly defined bearing or shear surface in this type of joint, the manner in which the loads are transferred is quite complex. As a result resort must be made to tests to establish design allowables. Tables C4.3, C4.4 and C4.5 give the allowable strength values for flush type rivets.

C4.9 Blind Rivets.

The name "Blind" rivet is given to that type of rivet which can be completely installed from one side of the joint, and is therefore almost exclusively used where it is impossible or impractical to drive the normal rivet, which requires access to both sides of the joint. There are two general types of blind rivets, namely where the inside or blind head is formed mechanically or where it is formed by an explosive force.

Explosive Rivet. Fig. C4.10 illustrates the first explosive type of rivet as developed by Heinkel of Germany. It was fired by holding a hot iron against its head. Fig. C4.11 illustrates the Du Pont extended cavity type of explosive rivet and it is available in both the protruding and flush type of head. When using this rivet



HEINKEL EXPLOSIVE RIVET

Fig. C4-10

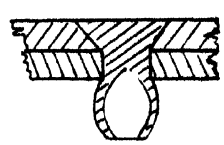


Fig. C4-11

the recommendations of the manufacturers should be strictly followed. Table C4.6 gives allowable strength values for the Du Pont explosive rivet.

The "Cherry" Blind Rivet. The cherry rivet, Fig. C4.12 is a self-plugging rivet which has a mandrel with an expanded section and head on the blind side. This expanded section is pulled into the hollow member, expands the shank and forms a tulip head in the back.

Table C4.1

SHEAR STRENGTHS OF PROTRUDING HEAD ALUMINUM ALLOY RIVETS (LBS)

(Ref. ANC-5-1946)

Dia. of Rivet or Pin	1/16	3/32	1/8	5/32	3/16	1/4	5/16	3/8
56S F_{su} = 27 ksi	95	195	350	536	774	1400	2210	3160
A17ST F_{su} = 30 ksi	106	217	388	596	862	1550	2460	3510
17ST F_{su} = 34 ksi	120	247	442	675	977	1760	2790	3970
17ST F_{su} = 38 ksi	135	275	494	755	1090	1970	3110	4450
24ST F_{su} = 41 ksi	145	296	531	815	1180	2120	3360	4800

Table (a)

STANDARD RIVET HOLE DRILL SIZES AND NOMINAL HOLE DIAMETERS								
Rivet Size	1/16	3/32	1/8	5/32	3/16	1/4	5/16	3/8
Drill No.	51	41	30	21	11	F	P	W
Nom. Hole Dia.	.067	.096	.1285	.159	.191	.257	.323	.386

SINGLE SHEAR RIVET STRENGTH FACTORS

Sheet thickness \ Dia. of Rivet or Pin	1/16	3/32	1/8	5/32	3/16	1/4	5/16	3/8
.014								
.016	.964							
.018	.984							
.020	.998							
.025	1.000	.972						
.032		1.000	.964					
.036			.980					
.040			.996	.964				
.045			1.000	.980				
.051				.996	.972			
.064				1.000	1.000	.964		
.072						.980	.964	
.081						.996	.974	
.091						1.000	.984	
.102							.996	.972
.128							1.000	1.000
.156								
.188								
.250								

DOUBLE SHEAR RIVET STRENGTH FACTORS

Sheet thickness \ Dia. of Rivet or Pin	1/16	3/32	1/8	5/32	3/16	1/4	5/16	3/8
.014								
.016	.688							
.018	.753							
.020	.792							
.025	.870	.714						
.032	.935	.818	.688					
.036	.974	.857	.740					
.040	.987	.896	.792	.688				
.045	1.000	.922	.831	.740				
.051		.961	.870	.792	.714			
.064		1.000	.935	.883	.818	.688		
.072			.974	.919	.857	.740		
.081			1.000	.948	.896	.792	.688	
.091				.974	.922	.831	.753	
.102				1.000	.961	.870	.792	.714
.128					1.000	.935	.883	.818
.156						.987	.935	.883
.188						1.000	.974	.935
.250							1.000	1.000

NOTES:
1. Values of shear strength should be multiplied by the factors given herein whenever the D/T ratio is large enough to require such a correction.
2. Shear values are based on areas corresponding to the nominal hole diameters specified in Table a above.
3. Shear stresses in Table 5/7a corresponding to 90% probability data are used wherever available. (See ANC-5)
4. Sheet thickness is that of the thinnest sheet in single shear joints and of the middle sheet in double shear joints.

Table C4.2

BEARING STRENGTHS OF ALUMINUM ALLOY SHEET (LBS.)

BEARING FACTORS FOR ALUMINUM ALLOY SHEETS

(Ratio of actual bearing strength to 100 ksi)

Material	Thickness Range	Kultimate e/d - 2.0	Kultimate e/d - 1.5	Kyield e/d - 2.0	Kyield e/d - 1.5
24 ST (HT by user)	all	1.18	.93	.64	.56
24ST	<.250	1.29	1.02	.80	.70
24SRT	<.500	1.35	1.06	1.00	.88
clad 24ST (HT by user)	<.064	1.06	.84	.59	.52
clad 24ST(HT by user)	.064-.500	1.14	.90	.61	.53
clad 24ST	.012-.063	1.16	.91	.76	.67
clad 24ST	.064-.500	1.25	.99	.78	.69
clad 24SRT	.020-.063	1.25	.99	.93	.81
clad 24SRT	.064-.500	1.29	1.02	.97	.84
clad 24ST (coiled)	<.064	1.16	.92	.61	.53
clad 24ST (coiled)	.064	1.22	.96	.64	.56
clad 24ST80	<.064	1.14	.90	.75	.66
clad 24ST80	>.064	1.18	.93	.78	.69
clad 24ST81	<.064	1.22	.96	.90	.78
clad 24ST81	>.064	1.27	1.00	.94	.83
clad 24ST84	<.064	1.27	1.00	1.01	.83
clad 24ST84	>.064	1.33	1.05	1.06	.92
clad 24ST86	<.064	1.33	1.05	1.04	.91
clad 24ST86	>.064	1.35	1.06	1.09	.95
clad 14SW, R301-W	.020-.039	1.06	.84	.59	.52
clad 14SW, R301-W	.040-.250	1.08	.85	.59	.52
clad 14ST, R301T	.020-.039	1.20	.94	.90	.78
clad 14ST, R301T	.040-.250	1.22	.96	.91	.80
clad 75ST	.016-.500	1.42	1.12	1.09	.95
75ST	.016-.500	1.54	1.21	1.19	1.04

Table C4.2a

SHEET ALLOWABLE BEARING STRENGTH (LB.) BASED ON F_{br} = 100,000 psi

Sheet thickness \ Dia. of Rivet or Pin	1/16	3/32	1/8	5/32	3/16	1/4	5/16	3/8
.014	44	134	180	223	267	360	452	540
.016	107	154	206	254	306	411	517	618
.018	121	173	231	286	344	463	581	695
.020	134	192	257	318	382	514	646	772
.025	168	240	321	398	478	643	808	965
.032	214	307	411	509	611	822	1030	1230
.036	241	346	463	572	688	925	1160	1390
.040	268	384	514	636	764	1030	1290	1540
.045	302	432	578	716	860	1160	1450	1740
.051	342	490	655	811	974	1310	1670	1970
.064	429	614	822	1020	1220	1640	2070	2470
.072	482	691	925	1140	1370	1850	2330	2780
.081	543	778	1040	1290	1550	2080	2620	3130
.091	610	874	1170	1450	1740	2340	2940	3510
.102	683	979	1310	1620	1910	2620	3290	3940
.128	858	1230	1640	2030	2410	3290	4130	4940
.156	1050	1500	2010	2480	2980	4010	5040	6030
.188	1250	1800	2410	2980	3580	4820	6060	7240
.250	1670	2400	3210	3970	4770	6420	8070	

NOTES:
1. Values of rivet bearing strength corresponding to a ratio of edge distance to rivet diameter of 1.5, 2.0, or greater, are obtained directly by multiplying the bearing strength for F_{br} - 100 ksi by the appropriate factor given in Table C4.2.
2. For e/D values between 1.5 and 2.0, the factor may be obtained by linear interpolation.
3. Bearing stresses for materials are based on unit bearing stresses corresponding to 90 per cent probability data whenever available.
4. Bearing values are based on areas corresponding to the nominal hole diameters specified in Table a.

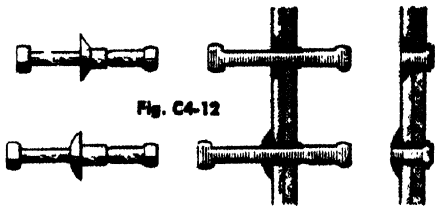


Fig. C4-12

Drawings of the self-plugging Cherry rivet assemblies in both the brazier and the countersunk types--before and after the heading-up operation.

The cherry rivet is available in both the protruding head and the 100 degree flush head type. Allowable strength values for this rivet are given in Table C4.6.

The Huck Blind Rivet. Fig. C4.13 illustrates the Huck rivet which consists of a sleeve and a pin. The sleeve is made of A17ST and the pin from 14SRT aluminum alloy material. The features of this rivet include expanding shank, positive pin lock and sheet clamping action. The installation recommendations of the manufacturer should be strictly followed. Allowable strength values for this rivet are given in Table C4.6.

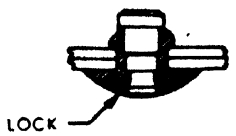
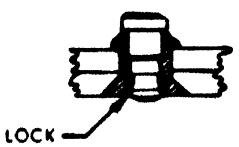


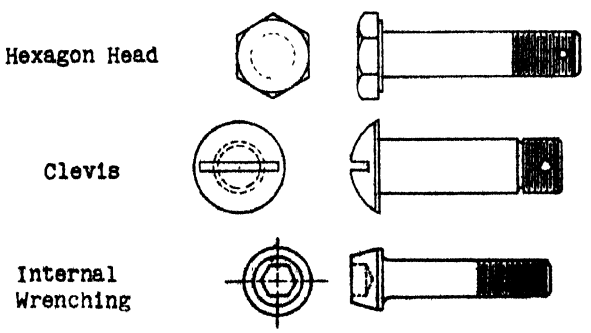
Fig. C4-13



C4.10 Aircraft Bolts.

The aircraft bolt is used primarily to transfer relatively large shear or tension loads from one structural unit to another. Fig. C4.14 shows the three standard aircraft bolts which are in common use.

Fig. C4-14



The hexagon head bolt is an Army-Navy standard bolt made from SAE 2330-3.5 percent nickel steel, heat treated to an ultimate tensile strength of 125,000 psi. The bolt head is of sufficient size as to develop the full tensile strength of the bolt.

The internal-wrenching bolt is a high strength steel bolt usually heat treated from 160,000 to 180,000 psi. It is especially suitable for main splice fittings because of its high strength and the relatively small space required for the bolt head.

The clevis bolt is referred to as a shear bolt because its head is not designed to develop the full tensile strength of the bolt. The clevis bolt is usually used when a group or cluster of bolts is required to transfer a load by shear loads on the bolts. The smaller bolt heads thus save weight and also provide greater bolt head clearances. The clevis bolt will develop about one half the tensile strength of the standard AN hexagon head bolt.

The three bolts are also made from aluminum alloy for diameters over 1/4 inch. In many fitting designs weight can be saved by using aluminum alloy bolts.

General Rules in Using Bolts.

Bolt threads should not be placed in bearing or shear. The length of the bolt shank should be such that not more than one thread extends below fitting surface, which can be done by the use of washers.

Bolts less than 3/8 diameter should not be used in major fittings. For steel bolts, 3/16 inch diameter should be the smallest size to be used in any fitting.

Bolts connecting parts having relative motion or stress reversal should have close tolerances to decrease shock loads.

For bolts connecting members having relative motion a lubricator should be incorporated in the surrounding parts of the fitting; the fitting should not be drilled to provide lubrication.

Bolts should be used in double or multiple shear if possible in order to increase strength efficiency in bolt shear and to decrease bending tendency on bolt.

It is not good practice to tap a fitting to save a nut.

C4.11 Bending of Bolts.

When a bolt in a fitting such as illustrated in Fig. C4.15 is loaded to failure, the failure seems to be a combination of shear crushing and bending. The magnitude of the actual bending forces are unknown, however it is logical to believe that a free fit bolt with a clearance between fitting lugs would suffer considerable more bending stress than a tight fit bolt with no

Table C4.3

ALLOWABLE STRENGTH OF FLUSH RIVETED JOINTS 78° HEAD ANGLE

I MACHINE COUNTERSUNK

ALLOWABLE SHEAR STRENGTH - LB. PER RIVET

Rivet Dia.		3/32	1/8	5/32	3/16
Rivet Alloy	A17ST	186	331	518	745
	17ST	206	368	574	828
	24ST	241	429	670	966

ALLOWABLE BEARING STRENGTH - LB. PER RIVET

Sheet Alloy		17ST Alclad				17ST				24ST Alclad				24ST			
Dia. of Rivet		3/32	1/8	5/32	3/16	3/32	1/8	5/32	3/16	3/32	1/8	5/32	3/16	3/32	1/8	5/32	3/16
Thickness of Thinnest Sheet	.020	92	113			105	129			122	150			131	162		
	.025	104	132			119	151			138	175			149	189		
	.032	120	158	257		138	181	294		160	210	340		172	226	366	
	.036	130	174	269		149	200	307		173	231	356		187	249	384	
	.040	139	189	283	347	160	217	324	397	185	251	375	460	199	271	405	495
	.045	151	209	300	409	173	239	344	468	201	277	398	542	217	299	430	585
	.051	166	232	319	446	190	266	365	510	220	308	423	590	237	332	456	635
	.064	197	284	364	525	225	325	416	601	241	376	482	695	241	405	520	750
	.072	215	315	391	573	241	360	448	655	241	417	518	758	241	429	558	815
	.081	237	350	421	627	241	400	481	717	241	429	557	830	241	429	600	895
	.091	241	389	455	687	241	429	520	787	241	429	602	910	241	429	650	966
	.102		429	492	756		429	563	865		429	652	966		429	670	966
	.128			582	922			666	966			670	966			670	966

II DIMPLED

ALLOWABLE SHEAR STRENGTH - LB. PER RIVET

Rivet Dia.		3/32	1/8	5/32	3/16
Rivet Alloy	A17ST	276	480	735	1020
	17ST	300	530	810	1130
	24ST	350	620	950	1325

ALLOWABLE BEARING STRENGTH - LB. PER RIVET

Sheet Alloy		17ST Alclad				17ST				24ST Alclad				24ST			
Dia. of Rivet		3/32	1/8	5/32	3/16	3/32	1/8	5/32	3/16	3/32	1/8	5/32	3/16	3/32	1/8	5/32	3/16
Thickness of Thinnest Sheet	.020	170	204			194	233			225	270			243	291		
	.025	185	238	388		212	272	444		246	315	514		265	340	555	
	.032	208	287	427	521	230	328	488	596	276	380	565	690	276	410	610	745
	.036	221	312	449	559	253	358	514	640	293	414	595	740	316	447	642	799
	.040	234	340	471	597	268	389	539	683	310	450	624	790	334	486	673	853
	.045	250	374	498	646	287	429	570	739	332	480	660	855	350	535	712	923
	.051	270	415	532	706	310	475	609	808	350	550	705	935	350	594	761	1009
	.064	314	503	604	831	350	576	692	951	350	620	735	1100	350	620	864	1188
	.072		560	650	910		620	743	1042		620	860	1205		620	928	1301
	.081			699	1000			800	1146			925	1325			950	1325
	.091				1103				1262				1325				1325
	.102				1210				1325				1325				1325
	.128																

Table C4.4

ALLOWABLE STRENGTH OF FLUSH RIVETED JOINTS - 100° HEAD ANGLE

100° MACHINE COUNTERSUNK RIVETS - DESIGN ULTIMATE STRENGTH

Sheet Alloy		Clad 24ST					
Rivet Alloy		A17ST				24ST	
Rivet Diameter		3/32	1/8	5/32	3/16	3/16	1/4
Sheet thickness	.025	120					
	.032	155	205				
	.040	190	255	310			
	.051	215	320	390	475	630	
	.064	215	390	495	600	795	1080
	.072	215	390	555	665	880	1220
	.081	215	390	595	750	1000	1375
	.091	215	390	595	860	1135	1540
	.102	215	390	595	860	1180	1740
	.128	215	390	595	860	1180	2130

100° DIMPLE COUNTERSUNK RIVETS - Design ULTIMATE STRENGTH

Sheet Alloy		Clad 24ST				
Rivet Alloy		A17ST				24ST
Rivet Diameter		3/32	1/8	5/32	3/16	3/16
Sheet thickness	.020	190	270			
	.025	245	320	415		
	.032	265	375	510	630	800
	.040	265	415	570	750	920
	.051	265	480	650	845	1060
	.064	265	480	735	960	1330
	.072	265	480	735	1030	1330

(Ref. ANC-5-1946)

Table C4.5

ALLOWABLE STRENGTH OF FLUSH RIVETED JOINTS
115° HEAD ANGLE

MACHINE COUNTERSUNK
ALLOWABLE SHEAR STRENGTH
- LB. PER RIVET

Rivet Alloy	Rivet Dia.	3/32	1/8	5/32	3/16
	A17ST	186	331	518	745
	17ST	206	368	574	828
	24ST	241	429	670	966

DIMPLED
ALLOWABLE SHEAR STRENGTH
- LB. PER RIVET

Rivet Alloy	Rivet Dia.	3/32	1/8	5/32	3/16
	A17ST	218	430	675	955
	17ST	240	478	740	1040
	24ST	280	555	870	1220

MACHINE COUNTERSUNK
ALLOWABLE BEARING STRENGTH
- LB. PER RIVET

Sheet Alloy		17ST Alclad				17ST				24ST Alclad				24ST			
Dia. of Rivet		3/32	1/8	5/32	3/16	3/32	1/8	5/32	3/16	3/32	1/8	5/32	3/16	3/32	1/8	5/32	3/16
Thickness of Thinnest Sheet	.020	73	75			83	86			97	100			104	108		
	.025	87	96			99	110			115	128			124	138		
	.032	105	124	174		120	141	198		139	164	230		150	177	248	
	.036	115	139	196		132	159	224		153	184	260		165	198	280	
	.040	126	154	218	252	144	176	250	288	167	204	289	333	180	220	312	360
	.045	140	174	244	293	160	200	279	335	185	231	323	388	200	249	348	418
	.051	154	197	277	342	176	225	317	391	204	261	367	452	220	281	396	488
	.064	189	250	348	451	216	286	398	516	241	331	460	597	241	357	496	645
	.072	209	280	392	518	239	320	447	592	241	370	518	685	241	400	559	740
	.081	233	314	421	593	241	360	482	678	241	416	558	785	241	429	601	845
	.091	241	355	455	675	241	405	520	772	241	429	602	894	241	429	650	966
	.102		398	493	756		429	563	865		429	651	966		429	670	966
	.128			582	922			665	966			670	966			670	966

DIMPLED
ALLOWABLE BEARING STRENGTH
- LB. PER RIVET

Sheet Alloy		17ST Alclad				17ST				24ST Alclad				24ST			
Rivet Dia.		3/32	1/8	5/32	3/16	3/32	1/8	5/32	3/16	3/32	1/8	5/32	3/16	3/32	1/8	5/32	3/16
Thickness of Thinnest Sheet	.020	147	204			168	233			195	270			210	291		
	.025	165	238	340		188	272	389		218	315	450		235	340	485	
	.032	188	287	378	484	215	328	432	554	249	380	500	640	268	410	540	690
	.036	202	301	400	520	231	345	458	596	267	399	530	690	280	430	570	745
	.040	215	317	423	566	246	363	484	648	280	420	560	750	280	453	604	810
	.045	232	340	450	612	265	389	515	700	280	450	596	810	280	485	643	874
	.051	252	363	484	673	280	415	553	770	280	480	640	890	280	518	690	960
	.064	280	415	555	800	280	475	635	915	280	550	735	1060	280	555	793	1140
	.072		448	600	880		512	687	1005		555	795	1165		555	858	1220
	.081			650	970			744	1110			860	1220			870	1220
	.091				1070				1220				1220				1220
	.102				1180				1220				1220				1220
	.128																

Table C4.6

Design Shear Strengths of Blind Rivets
(Protruding and Flush Heads)
Type A - Explosive Rivet
Type B, Class I Huck Rivet
Type B, Class II - Cherry Rivet

Type of Rivet	Rivet Diameter 1/8	5/32	3/16
Type A	465	725	1050
Type B, Class I	430	665	965
Type B, Class II	390	600	860

NOTES: (1) Higher shear values may be used in design if substantiated to the satisfaction of the procuring or licensing agency.

Type A - Du Pont Explosive Rivet
Type B - Class I - Huck Rivet
Type C - Class II - Cherry Rivet

Ultimate Bearing Strengths of Brazier Head Blind Rivets in Aluminum Alloy Sheet

TYPE A

Thickness		.025	.032	.040	.051	.064	.072
Rivet Diameter	1/8	270	355	420	465	465	465
	5/32		435	555	660	825	725
	3/16		460	665	840	960	1000

TYPE B, Class II

Thickness		.025	.032	.040	.051	.064	.072
Rivet Diameter	1/8	250	320	375	430	430	430
	5/32		400	500	585	665	665
	3/16		480	600	755	870	930

TYPE B, Class II

Thickness		.025	.032	.040	.051	.064	.072
Rivet Diameter	1/8	240	300	350	390	390	390
	5/32		380	465	555	600	600
	3/16		455	570	705	820	860

NOTE:
(1) Higher bearing values may be used in design if substantiated to the satisfaction of the procuring or licensing agency.

Yield Bearing Strengths of Brazier Head Rivets in Aluminum Alloy Sheet

TYPE B

Thickness		.025	.032	.040	.051	.064	.072
Rivet Diameter	1/8	210	275	325	355	360	
	5/32		335	430	510	550	575
	3/16		360	510	660	750	780

TYPE B, Class I

Thickness		.025	.032	.040	.051	.064	.072
Rivet Diameter	1/8	175	225	270	340	410	
	5/32		280	350	435	530	585
	3/16		340	425	530	645	720

TYPE B, Class II

Thickness		.025	.032	.040	.051	.064	.072
Rivet Diameter	1/8	220	255	290	325	360	
	5/32		345	400	460	510	540
	3/16		425	510	605	675	715

NOTE:
(1) Higher bearing values may be used in design if substantiated to the satisfaction of the procuring or licensing agency.

(Ref. ANC-5-1946)

clearance between lugs and with bolt nut drawn tight against fitting.

It is the author's opinion that free fit bolts in main fittings should not suffer a permanent bending deformation under the applied loads and Fig. C4.8 is offered as an approximate check on the bolt bending stresses. Some structural designers neglect bending in the fitting type #1 but consider it for the more obvious condition of type #2.

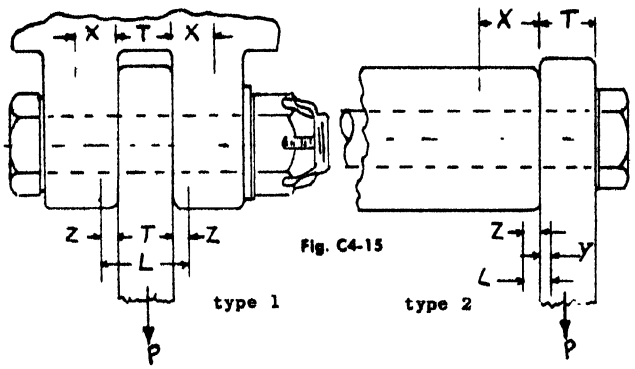


Fig. C4-15

Make X equal in bearing to T/2	Make X equal in bearing to T
Z = X/4	Y = T/4
L = T + 2Z + clearance	Z = X/4
Bolt B.M. = PL/4	L = Y + Z + clearance
	Bolt B.M. = PL

Taper Bolts. Where tight joints are required and expense is not a criterion taper bolts are used. (See Fig. C4.16). When service produces wear they can be taken up.

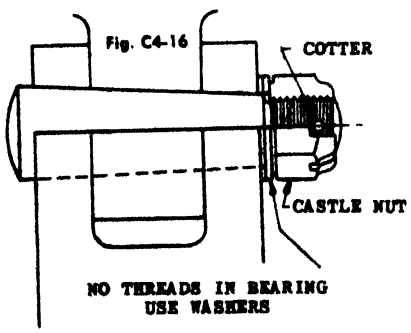


Fig. C4-16

C4.12 Strength of Aircraft Bolts.

Table C4.7 gives the ultimate strength of AN steel and aluminum alloy bolts in shear, tension, and bending.

Table C4.8 gives the allowable bearing strength of steel sheet on steel pins or bolts. Table C4.9 gives the shear and tension strengths of steel internal wrenching bolts.

Combined Tension and Shear on Steel Bolts.

In some parts of the airplane structure as for example the engine mount structure main fitting, bolts are used under high combined tension and shear loads. The allowable strength under this combined loading of tension and shear is given by the interaction equation $R_t^2 + R_s^2 = 1.0$. Fig. C4.17 shows a plot of this equation for standard steel AN bolts.

Table C4.7

Ultimate Strength of AN Bolts
Hexagonal Head Bolts

AN No	Nom. Diam	STEEL			2427		
		SHEAR F_{su}=75,000	tension F_{tu}=125,000	BENDING F_b=160,000	SHEAR F_{su}=35,000	TENSION F_{tu}=68,000	BENDING F_b=72,000
3	3/16	2128	2136	116	992	1659	46
4	1/4	3681	3982	276	1717	1975	110
5	5/16	5751	6439	539	2684	3189	216
6	3/8	8287	9953	932	3866	4937	373
7	7/16	11272	13433	1480	5261	6663	592
8	1/2	14722	18356	2210	6871	9104	884
9	9/16	18637	23313	3150	8697	11563	1260
10	5/8	23010	28676	4320	10738	14718	1730
12	3/4	33138	43494	7450	15463	21573	2980
14	7/8	45097	59515	11840	21046	29520	4740
16	1	58908	80159	17670	27489	38759	7070

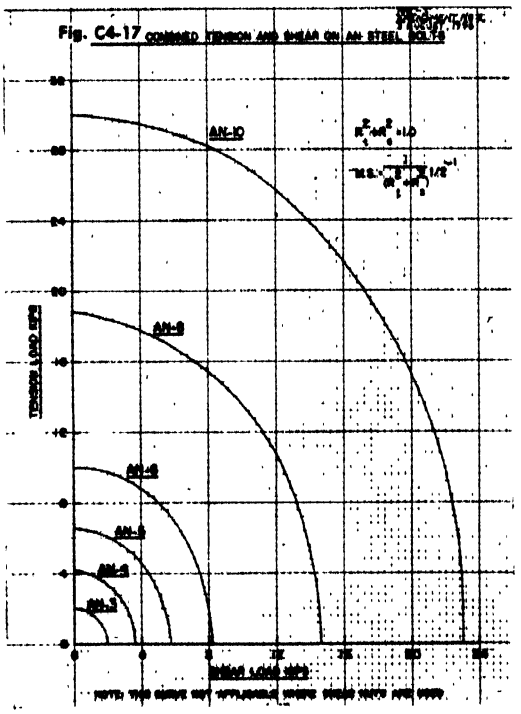


Fig. C4-17

C4.13 Special Bearing Factors.

The failure of a material in bearing may consist of crushing, splitting or progressive rapid yielding in the region where the load is applied. Such factors are reversal of stress, shape and size of surfaces in contact effect the allowable bearing pressures. Table C4.10 gives these special required bearing factors.

Table C4.8

BEARING STRENGTH OF STEEL SHEETS ON RIVETS, BOLTS AND PINS
NORMALIZED X-4130 SHEET (F_{br} = 110,000 PSI)

Size of Rivets	1/16	3/32	1/8	5/32	3/16	1/4	5/16	3/8	1/2	5/8	3/4	7/8	1
Plate Sizes	Bearing Strength of Plate												
.028	245	368	490										
.035	306	459	612	765	918								
.049	429	643	857	1072	1286	1714							
.058	507	761	1015	1269	1522	2030	2537						
.065	569	853	1137	1422	1706	2275	2844						
.072	630	945	1260	1575	1890	2520	3150	3780					
.083	726	1089	1452	1815	2178	2904	3630	4356					
.095	831	1247	1662	2078	2494	3325	4156	4988	6650				
.120	1050	1575	2100	2625	3150	4200	5250	6300	8400	10500			
3/16	1640	2460	3280	4100	4920	6560	8200	9840	13120	16400	19680	22960	26240
1/4	2188	3281	4375	5469	6563	8750	10938	13125	17500	21875	26250	30625	35000

F_{br} = 100,000 PSI
(FOR USE IN COMPUTING BEARING STRENGTH AT OTHER VALUES OF ALLOWABLE BEARING STRESS)

Size of Rivets	1/16	3/32	1/8	5/32	3/16	1/4	5/16	3/8	1/2	5/8	3/4	7/8	1
Plate Sizes	Bearing Strength of Plate												
.028	175	263	350										
.035	219	328	438	547	656								
.049	306	459	612	766	919	1225							
.058	362	544	725	906	1087	1450	1812						
.065	406	609	812	1016	1219	1625	2031						
.072	450	675	900	1125	1350	1800	2250	2700					
.083	519	778	1038	1297	1556	2075	2594	3112					
.095	594	891	1188	1484	1781	2375	2969	3563	4750				
.120	750	1125	1500	1875	2250	3000	3750	4500	6000	7500			
3/16	1172	1758	2344	2930	3516	4688	5859	7031	9375	11719	14063	16406	18750
1/4	1563	2344	3125	3906	4688	6250	7813	9375	12500	15625	18750	21875	25000

FOR D/t VALUES > 5.5 THE ALLOWABLE BEARING STRENGTHS MUST BE SUBSTANTIATED BY TESTS COVERING BOTH YIELD AND ULTIMATE OF THE JOINT.

Table C4.9

SHEAR AND TENSION STRENGTHS OF INTERNAL WRENCHING BOLTS

MATERIAL		HEAT TREATED ALLOY STEEL (160,000-180,000 psi)	
SPECIFICATION		AN-QQ-S-687, AN-S-16, and	AN-QQ-S-690 AN-QQ-S-756
SIZE	STANDARD	ULT. TENSILE STRENGTH (Min.lbs.)	DOUBLE SHEAR STRENGTH (Min.lbs.)
1/4	NAS 144	5,000	9,300
5/16	NAS 145	8,200	14,600
3/8	NAS 146	12,700	21,000
7/16	NAS 147	17,100	28,600
1/2	NAS 148	23,400	37,300
9/16	NAS 149	29,800	47,200
5/8	NAS 150	38,000	58,300
3/4	NAS 152	55,600	83,900
7/8	NAS 154	76,200	114,200
1	NAS 156	102,500	149,200
1-1/8	NAS 158	128,800	188,900
1-1/4	NAS 172	162,600	233,200
1-3/8	NAS 174	200,300	282,100
1-1/2	NAS 176	241,176	335,800

NOTES:

1. Navy contractors must obtain approval of structural applications involving internal wrenching bolts prior to their use in design.
2. Internal wrenching nuts should be used in applications wherein these internal wrenching bolts are specified.

Table C4.10(1)

BEARING FACTORS FOR PLAIN(2) BEARINGS(3) HAVING NO OR INFREQUENT(4) RELATIVE ROTATION UNDER DESIGN LOADS

Infrequent Relative Rotation under Design Loads	Shock(6) or Vibration	Factor(7)
None(5)	None	1.0
Yes	None	2.0
None(5)	Yes	2.0
Yes	Yes	2.5

NOTES:

(1) The factors given in this table are applicable to other materials as well as to steel.

(2) "Plain" bearings as against anti-friction bearings (ball bearings, etc.).

(3) Bearings are distinguished from fittings, in general, in that a bearing is a pin-jointed fitting which permits relative movement between the parts joined other than that due to deformation of the parts under load.

(4) For rotations in the order of 100 revolutions per hour, and up, see Table 4-3.

(5) No relative rotation under design loads; to illustrate, some landing gear joints have no relative rotation under landing loads, although they have relative rotation during retraction.

(6) Shock is considered to occur in such structures as landing gears, gun mounts, hoisting, towing and mooring connections.

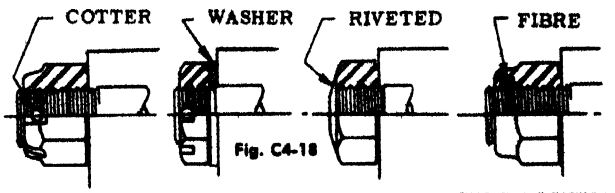
(7) It should be noted that the fitting factors specified by the procuring or certificating agency also apply to the bearing surfaces. If the applicable fitting factor exceeds the bearing factor, the former shall be used in lieu of (not in addition to) the latter, and vice-versa.

C4.14 Aircraft Nuts.

Fig. C4.18 illustrates the four standard steel aircraft nuts. Nut material is more ductile than bolt material, thus when the nut is tightened the threads will deflect to seat on the bolt threads.

The Castle nut is probably the most common aircraft nut. It develops the full rated strength of the bolts. The nut has slots milled in it so that nuts can be prevented from turning.

The Shear nut is only one half as thick as the Castle nut, and thus has only threads enough to develop one half of bolt tensile strength. It is used with a clevis bolt which has a screw driver slot to limit the torsion in tightening the nut. The nut is also castellated for cotter pin lock.



The Plain nut which is very seldom used in present design is used for permanent locations and is locked by "peening" or riveting the end of the bolt over the nut, an operation which destroys the bolt protective coating or finish.

Aluminum Alloy Nuts. Aluminum alloy nuts are not used on bolts designed for tension. Sometimes aluminum alloy nuts are used on steel bolts on land planes to save weight provided the bolts are cadmium plated. If the bolt is used in places where the nut is repeatedly removed, neither bolt or nut should be aluminum alloy because of the danger of injuring the relatively soft threads.

C4.15 Self Locking Nuts.

Elastic Stop Nut.

The elastic stop nut is widely used in the aircraft industry. The self locking means is provided by a fiber insert. (See Fig. C4.18). When the bolt reaches the fiber collar it tends to push the fiber up because the hole in the collar is smaller than the bolt, and is not threaded. The fiber ring thus sets up a heavy downward pressure on the bolt automatically throwing the load carrying sides of the nut and bolt threads into positive contact. Thus all play in the threads is eliminated and a friction is set up between every bolt and nut thread in constant. This constant pressure which is maintained on threads, provides the friction which prevents nut from moving under vibration. (See Fig. C4.19 for various types).

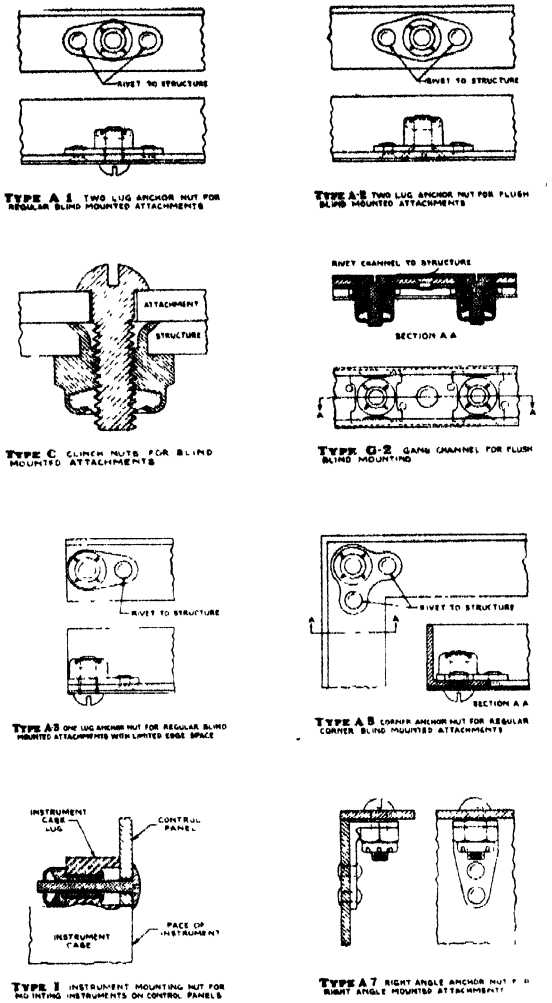
The use of the self locking nut reduces the assembly costs as it eliminates the bothersome cotter pin which takes extra operations of the mechanic and is very difficult to install on the nut in the many joints and corners of an airplane.

BOOTS Self Locking Nut.

The photographs below show samples of the Boots all metal locking nut. The locking force is provided by the spring action of the upper portion of nut.

The designer before using any type of stop nut should consult all military and governmental regulations to determine if any restrictions exist on their use.

Fig. C4-19 Self Locking Nut (Elastic Stop Nut)





Boots Self Locking Nut



Boots Floating Anchor Nuts are specifically designed for use where accommodation is desired for possible slight hole misalignment.

C4.16 Bushings.

It is customary to provide bushings in the lugs of single bolt or pin fittings subjected to reversal of stress or to slight rotation. Thus if wear and tear takes place a new bushing can be inserted in the lug fitting. Steel bushings are commonly used in aluminum alloy single bolt fitting lugs to increase the allowable bearing stress on the lug since the bushing increases the bearing diameter 1/8 inch since bushings are usually 1/16 inch in wall thickness. If bushings are not used on single bolt connections sufficient edge distance should be provided to ream hole for next size bolt in case of excessive wear of the unbushed hole. If considerable rotation occurs a lubricator should be provided for a plain bushing or a oil-impregnated bushing should be used.

C4.17 Standard Tie Rods, Lugs and Cables.

Tie rods and cables are tension structural units which are frequently used in aircraft structure or aircraft control systems. These units have been placed in the category of AN standard units. The rated strength of these standard tie rods and the size of the mating male lug to go with the female clevis terminal on the tie rod is given in Table C4.11.

The strength and stiffners factor of aircraft steel cable are given in Tables C4.12, and C4.12a.

Table C4.11

STEEL TIE RODS AND TENSION LUGS

Tie rods			Clevis			Lug					
1	2a.	2b.	3	4	5	6	7	8	9	10	11
Size	125000 lb. U T S. Alloy Steel and High Strength Steel Tubular Sections	180000 lb. U T S. Alloy Steel Tubular Sections	Gap G	Throat H	Hole D_1	Thick T	Hole D_1	90000 lb. U T S. Alloy Steel R	90000 lb. U T S. Alloy Steel W	125000 lb. U T S. H T Alloy Steel R	125000 lb. U T S. H T Alloy Steel W
			+.010 -.000		-.000 +.010	+.006 -.006	+.003 -.003	-.000	-.000	-.000	-.000
No. 6	1000	1250	1/8	3/8	1/8	3/32	13/64	9/32	3/16	7/32	1/4
No. 10	2100	2400	1/8	15/32	1/8	1/8	13/64	3/8	3/8	9/32	3/8
1/4	3400	4300	.252	5/8	1/4	3/16	17/64	13/32	9/16	3/8	1/2
5/16	6100	6800	.252	27/32	.275	3/16	25/64	29/32	13/16	9/16	5/8
3/8	8600	10800	.252	7/8	.275	1/4	25/64	29/32	7/8	9/16	5/8
7/16	11 800	13700	.344	1	.338	5/16	25/64	1	1	5/8	7/8
1/2	15700	18800	.406	1-3/16	.380	3/8	13/64	15/16	1-1/8	3/4	1
9/16	19300	24000	.406	1-3/8	.463	3/8	27/64	1-1/8	1-1/4	7/8	1-1/16
5/8	24 200	28000	.516	1-1/2	.588	7/16	41/64	1-1/8	1-1/8	15/16	1-1/8
3/4	43400	42000	.656	1-15/16	.709	1/2	29/32	1-1/2	2	1-1/8	1-3/8
7/8		55000	.781	2-5/16	.775	5/8	29/32	1 7/8	2-1/2	1 1/4	1-3/4
1		70000	.906	2-11/16	1 00	3/4	1.31	2-3/16	3	1-1/2	2

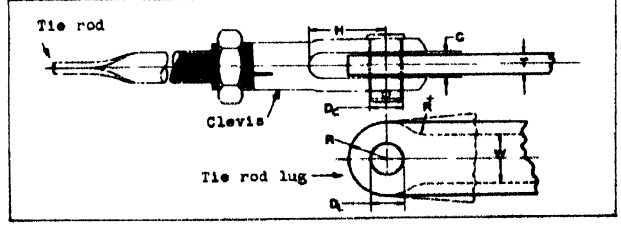


Table C4.12

STRENGTH OF STEEL CABLE

Preformed Flexible Cable (Corrosion Resisting) AN-RR-C-48 7 x 7, 7 x 19		
Diameter in inches	Approx. Wt. In lb. per 100 ft.	Breaking strength in lb. minimum
7 x 7 Flexible		
1/16	0.75	480
3/32	1.35	920
7 x 19 Flexible		
1/8	2.9	1900
5/32	4.44	2600
3/16	6.47	3800
7/32	9.50	5200
1/4	12.00	6600
9/32	14.56	8000
5/16	17.71	8200
3/8	26.46	12000

Table C4.12a

STRENGTH OF STEEL CABLE

Diameter in inches	Army Spec. 48-21 19 strands, non-flexible		EA**	Army Spec. 48-22 7 x 7 Flexible		EA**	AN-RR-C-43 7 x 19 Flexible		EA**
	Approx. Wt. in lbs. per 100 ft.	Breaking Strength in lb. minimum		Approx. Wt. in lbs. per 100 ft.	Breaking Strength in lb. minimum		Approx. Wt. in lbs. per 100 ft.	Breaking Strength in lb. minimum	
0.031 1/32	0.30	185	20,580						
0.062 1/16	0.78	500	52,810	0.81	480	47,990			
0.078 5/64	1.21	780	87,210*	0.83	550	54,990*			
0.094 3/32	1.75	1100	125,690*	1.45	920	83,900			
0.109 7/64	2.60	1600	176,540						
0.125 1/8	3.50	2100	227,730	2.45	1350	123,110*	2.90	2000	155,020
0.156 5/32	5.50	3200	359,120*	4.67	2600	270,700	4.44	2800	255,230
0.187 3/16	7.70	4600	528,910	5.80	3200	332,240*	6.47	4200	374,760
0.218 7/32	10.00	6100	737,760	8.30	4800	479,140*	9.50	5600	500,500*
0.250 1/4	13.50	8000	1,079,930*	10.50	5800	603,670*	12.00	7000	643,500*
0.281 9/32							14.56	8000	813,510
0.312 5/16	20.65	12500	1,687,350*	16.70	9200	958,290*	17.71	9800	1,026,230*
0.344 11/32							22.53	12500	1,309,140
0.375 3/8							26.45	14400	1,625,570*

* Computed using estimated values of A

** These values of EA should be used only if the cables are pre-stretched. It should be noted that the load deflection curves for cables, in general, are non-linear. The values of EA at low loads are less than those specified.

THE GENERAL DESIGN AND STRENGTH CHECKING OF AIRCRAFT FITTINGS.

C4.18 Single Bolt Fitting.

Possibly the simplest method of joining two members together is the use of a single bolt or pin connection. Such a joint can transmit relatively large loads and yet the joint is easily and quickly disconnected.

Fig. C4.20 illustrates the four general methods of connecting two members by a single bolt. First the connection is made symmetrical about the centerline of the load on the joint. Thus is Fig. C4.20a the load P on the male part of the fitting divides equally and symmetrically to the two female plates or units which make up part of the fitting unit. If the male and female parts of the connection are to be tied together by a single bolt it is evident that the connecting plates will be weakened due to the bolt hole unless extra material is added at the bolt hole section.

Fig. C4.20a shows a fitting consisting of three rectangular plates of uniform section throughout fastened together by a single bolt. Obviously the weak section for the plates in tension would be a section through the centerline of the hole. If this section is strong enough to carry the given loads, then the remaining part of the fitting members are considerably over strength. To avoid this overstrength which means extra weight of fitting units, a single bolt fitting unit is usually made like one of the examples indicated in Fig. b, c and d of Fig. C4.20.

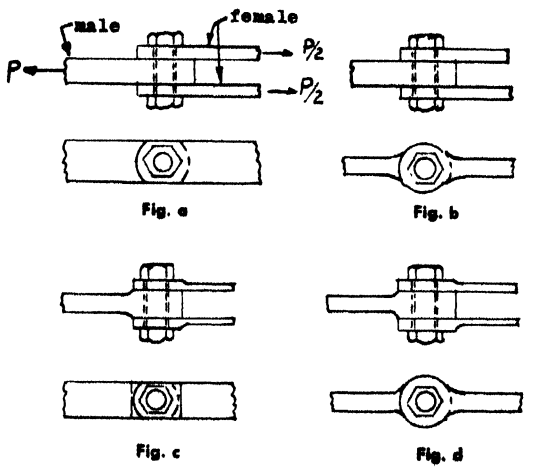


Fig. C4-20

In Fig. b, the plates are made constant thickness but increased in width in the vicinity of the hole section. In Fig. c, the width of the plates is kept constant but the thickness of the plates are increased in the vicinity of the hole section, and in Fig. d, both width and thickness of plates are changed.

C4.19 Methods of Failure of a Single Bolt Fitting.

As the load on a fitting is transferred from one side of the fitting to the other, internal stresses are produced which tend to cause the fitting to fail in several different ways.

Failure by Bolt Shear.

In Fig. C4.21 the bushing is not continuous between the plates, but each of the three plates have separate bushings. As the pull P is placed

on the fitting it tends to shear the bolt at sections (1-1) and (2-2), (Fig. C4.21a). Fig. C4.21b illustrates the forces or pressures on the bolt and the failure which can take place if the stresses are sufficient.

Let P_a represent the maximum or ultimate load on the fitting. This force P_a must be resisted by the shear strength of the bolt at the two sections (1-1) and (2-2). Hence,

$$P_{a(\text{bolt shear})} = F_{su} \cdot A \cdot 2 = F_{su}\, A \quad \text{- - - - -(1)}$$

where F_{su} = ultimate shearing stress for bolt material.
A = cross-sectional area of bolt.

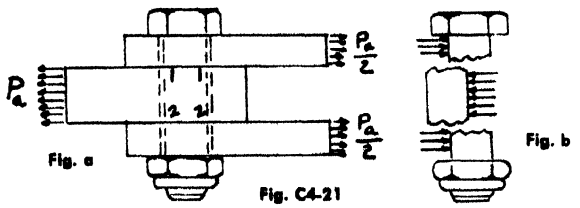
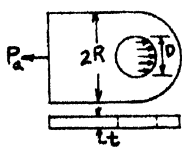


Fig. C4-21



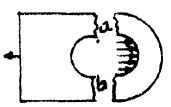
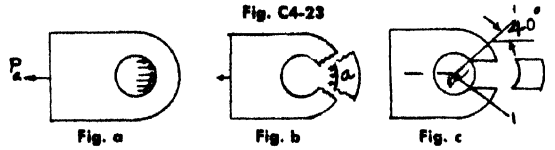


Fig. C4-22

Fig. C4-23



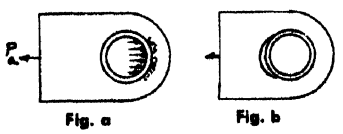


Fig. C4-24

Failure in Tension.

Fig. C4.22 indicates how a fitting plate can pull apart due to tension stresses on a section through the centerline of the bolt hole. Both the male and female parts of the fitting must transfer the load past the centerline of the hole, thus both parts must be considered in the design of a fitting. Equating the allowable load P_a to the ultimate resisting tensile stresses at points (a) and (b) Fig. C4.22, we obtain,

$$P_{a(\text{tension})} = F_{tu}\,(2R - D)t \quad \text{- - - - - - - -(2)}$$

where F_{tu} = ultimate tensile strength of plate material.

Failure by Shear Tear Out.

Fig. C4.23 illustrates the manner in which failure can occur by the shearing tear out of a plate sector in front of the bolt. In Fig. a, the load P causes the bolt (not shown) to press on the plate around the bolt hole edge. Stresses are produced which tend to cause the portion (a) in Fib. (b) to tear out as shown. Equating the load P_a to the ultimate shear resistance of the material times the area of the two shear out areas, we can write,

$$P_{a(\text{shear out})} = F_{su}\, A_s \quad \text{- - - - - - - - - -(3)}$$

where F_{su} = ultimate shearing strength of the plate material.
A_s = shear out area.

It is very common practice to take the shear out area A_s equal to the edge distance at the centerline of the hole times the thickness t of the plate times two since there are two shear areas. This is slightly conservative because the actual shear area is larger. The ANC-5 Manual permits one to use the area along line 1-1 which is limited by the 40 degree line as shown in Fig. C4.23c.

Failure by Bearing of Bushing on Plate.

In Fig. C4.24a, the pull P causes the bolt (not shown) to press against bushing wall which in turn presses against the plate wall. If the pressure is high enough the plate material adjacent to the hole will start to crush and flow thus allowing the bolt and bushing to move which results in the elongated hole as illustrated in Fig. b. Equating the load P_a to the ultimate bearing strength on the bearing surfaces we can write,

$$P_a = F_{br}\, D\, t \quad \text{- - - - - - - - - - - - - - -(4)}$$

where F_{br} = allowable bearing stress
D = diameter of bushing
t = plate thickness

Failure by Bearing of Bolt Bushing.

A bushing is pressed into the plate hole and thus it is considered as a tight fit. A fitting bolt is usually considered as removable therefore a certain tolerance between the bolt and bushing inside diameters is necessary in order to insert and remove bolt. If fitting is subjected to reversible loads the small slop in the fitting tends to cause shock on the fitting. Also the fitting may be such that slight rotation takes place on the bolt, which tends to cause wear between bolt and bushing. It is therefore customary to check the bearing pressure between the bolt and the bushing since failure of the bushing could take place in a manner explained in the previous article dealing with bearing of bushing on plate. Then as before,

$$P_a = F_{br}\, D\, t \quad \text{- - - - - - - - - - - - - - -(5)}$$

where D = bolt diameter

Problem 1

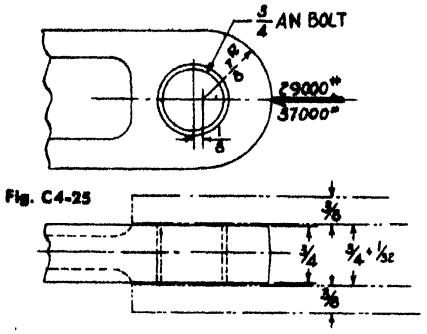


Fig. C4.25 shows a fitting link forged from 14ST aluminum alloy material. The design loads of 29000# and 37000# as shown include the fitting factor of safety of 1.2. The fitting is subjected to shock and vibration but no rotation. Let it be required to check the link for the given loads as well as the fitting bolt.

Let P_a = allowable load on fitting.

Consider bolt shear strength.

From observation bolt will be in double shear. From Table C4.7 the single shear strength of a 3/4" diameter AN bolt (F_{tu} = 125000) = 33100#

hence $P_a = 2 \times 33100 = 66200\#$

$$M.S. = \frac{P_a}{P} - 1 = (66200/37000) - 1 = .78$$

Consider shear out of link.

$$P_a = F_{su} A_s$$

Edge distance = (.875 + .125 - 4375) = .5625
Shear out area = 2 x .75 x .5625 = .843 sq. in.
In the above equation the value .75 is the link thickness and the term 2 represents the two shear out surfaces.

F_{su} = 39000 psi. (See Table C1.4)

Hence P_a = 39000 x .843 = 33000#

M.S. = (33000/29000) - 1 = .14

Note that the load of 37000# pushes inward on link and thus does not tend to cause shear out failure. Or in other words only tension on link will cause shear out failure.

Consider tension on section through hole.

$$P_a = F_{tu} A$$

A = tension area = (2 x .875 - .875).75 = .655 sq. in.
F_{tu} for 14ST material = 65000 psi. (See Table C1.4).

Hence P_a = 65000 x .655 = 42600#

M.S. = (42600/29000) - 1 = .47

Consider Bearing of Bushing on Link.

$$P_a = F_{br} A$$

A = bearing area = .875 x .75 = .655
F_{br} = 93000 psi.
Hence P_a = 93000 x .655 = 61000#
M.S. = (61000/37000) - 1 = .65

Consider Bearing of Bolt on Bushing.

For a free fit bolt subjected to shock and vibration but no relative rotation an additional bearing factor of 2.0 should be used. (See Table C4.10).

Therefore the allowable bearing pressure equals .5 F_{br} = .5 x 175000 = 87500 psi. The value 175000 represents the F_{br} for steel with F_{tu} = 125000 psi. Usually AN bolts and bushings are made from F_{tu} = 125000 material.

Bearing area = .75 x .75 = .562

hence P_a = 87500 x .562 = 49200#
M.S. = (49200/37000) - 1 = .33

Consider Bending of Bolt.

The true bending forces on the bolt are unknown. Since the clearance in a free fit condition permits the bolt to bend to some unknown degree, an approximate estimate of the bending stresses in the bolt will be made under the applied loads. If these stresses exceed the yield strength stresses of the material, the deformation of the bolt may be such as to make the bolt difficult to remove.

The bending stress $f_b = \frac{PL}{4S}$

Referring to Fig. C4 L = T + 22 + clearance or L = .75 + 2 x .0937 + .032 = .97"

The applied load on the fitting = $\frac{37000}{1.5 \times 1.2}$ = 20500#.

S = section modulus of 3/4 bolt = .041, hence

$$f_b = \frac{20500 \times .97}{4 \times .041} = 121000 \text{ psi.}$$

The modulus of rupture F_b for a solid round steel rod with F_{tu} = 125000 psi equals 180000 psi (See chapter C3). The tensile yield strength F_{ty} for this material = 100000 psi. Therefore a yield modulus of rupture of 180000 x 100000/125000 = 144000 psi will be assumed. Since the applied load bending stress f_b is 121000 the bolt appears satisfactory in bending.

Example Problem 2

Fig. C4.26 shows a forked steel fitting fastened to a double channel section made of 24ST aluminum alloy plate. Required, a completely strength check of the fitting portion as shown in Fig. C4.26. Fitting subjected to vibration and reversal of load.

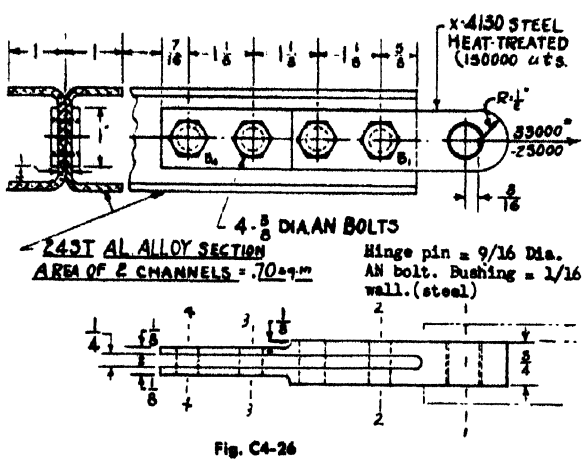


Fig. C4-26

Solution:-

Design fitting load = +33000#; - 25000#

Since these values include the fitting factor, the fitting must show a margin of safety of zero or greater to be satisfactory.

Let P_a = allowable load on fitting.

Check bolt shear strength:-

Single shear strength of 9/16 AN bolt = 18637#.

Bolt is in double shear, hence

$P_a = 2 \times 18637 = 37674\#$

M.S. = (37674/33000) - 1 = .14

Check bearing of bolt on bushing:-

Bolt bushing both have F_{tu} = 125000 psi.

Bearing area = .5625 x .75 = .422 sq. in.

F_{br} for 125000 steel equals 175000 psi.

Since fitting is subjected to shock and vibration an additional factor of safety on bearing stresses of 2 must be used. Hence allowable F_{br} = 175000/2 = 875000. Then,

P_a = .422 x 87500 = 36900#

M.S. = (36900/33000) - 1 = .12

The bearing of bushing on fitting is obviously satisfactory since bearing area is greater and fitting steel is 150,000 psi. material.

Check shear tear out of steel fitting:-

Shear out area = 2(.6875 - .3437).75 = .515 sq. in.

F_{su} for 150000 alloy steel = 90000 psi. (See Chapt. C1).

Hence, P_a = .515 x 90000 = 46100#

M.S. = (46100/33000) - 1 = .40

Check tensile strength steel fitting at ℄ bolt hole.

Net tension area = .75 (1 - .6875) = .234 sq. in.

F_{tu} = 150000 psi.

Hence, P_a = .234 x 150000 = 35100#

M.S. = (35100/33000) - 1 = .07

Check tensile strength section (2-2) Steel Fitting

From Fig. C4.26 it is noted that 4 - 3/8 dia. AN steel bolts transfer the load from the steel forked fitting to the two aluminum alloy channels. Thus it is reasonable to assume that each bolt transfers 1/4 of the total fitting load between the steal fitting and the channels. Fig. C4.27 shows the manner in which the load is transferred by the four bolts. The graph shows the load in the steel fitting and the channels at

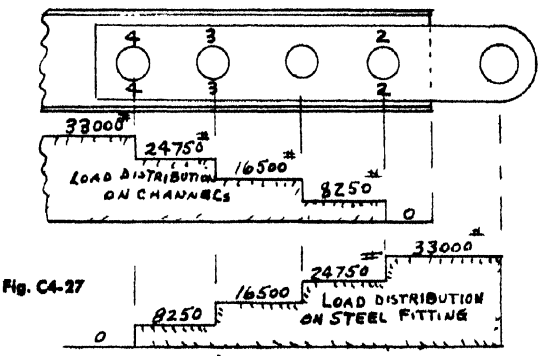


Fig. C4-27

the various sections. The total load of 33000# passes by section 2-2.

Net tension area = (1 - .375) (.75 - .25) = .3125 sq. in.

P_a = .3125 x 150000 = 47000#

M.S. = (47000/33000) - 1 = .42

Check tensile strength section (3-3) steel fitting.

Load on this section = 16500#

Net tension area = (1 - .375) (.5 - .25) = .1562 sq. in.

Hence P_a = .1562 x 150000 = 23500#

M.S. = (23500/16500) - 1 = .42

Check shear strength of the 4 -3/8 bolts.

Bolts are in double shear.

Single shear strength of 3/8 AN bolt = 8287#

Hence, P_a = 4 x 2 x 8287 = 66000#

M.S. = (66000/33000) - 1 = 1.0

Check bearing strength of 3/8 bolts on steel fitting.

Load per bolt = 8250#.

See (3-3) or (4-4) is critical since steel fitting thickness is less or 1/8 inch.

Bearing area one bolt = .375 x .25 = .09375 sq. in.

Hence P_a = 175000 x .09375 = 16400#

M.S. = (16400/8250) - 1 = .99

Check bearing of 3/8 bolts on 24ST channel Sections.

Bearing area per bolt = .375 x .25 = .0937 sq. in.
F_{br} = 90000 psi.
P_a for bolts = 4 x .0937 x 90000 = 33500#
M.S. = (33500/33000) - 1 = .02

Check tensile strength of channels at Sec. (4-4).

Load on this section = 33000# (See Fig. C4.27)
Net tension area = .70 - (.25 x .375) = .60 sq. in.
Note:- .70 = area of two channels (See Fig. C4.26)
F_{tu} = 62000 psi. for 24ST material
hence, P_a = .60 x 62000 = 37200#
M.S. = (37200/33000) - 1 = .12

Check shear tear out for channels at bolt B_1.

Centerline edge distance = (.625 - .875) = .4375
Shear out area = 2 x .4375 x .25 = .218 sq. in.
F_{su} = 38000 psi.
Hence, P_a = .218 x 38000 = 8300#
Load on bolt B_1 = 8250#
M.S. = (8300/8250) - 1 = .01

The shear out area is conservative. It is permissible to take shear out distance to a 40 degree line thru center line of hole. This change would add .044 inches to shear out length, hence
P_a = 2 x (.4375 + .044) .25 x 38000 = 9150#
M.S. = (9150/8250) - 1 = .11

Check shear tear out strength of steel fitting at bolt B_4.

Edge distance = (.4375 - .1875) = .25"
Shear out area = 2 x .25 x .25 = .125 sq. in.
F_{su} = 90000 psi.
P_a = 90000 x .125 = 11250#.
M.S. = (11250/8250) - 1 = .36

Check shear strength of channels between bolts.

Edge distance between 3/8 dia. bolts = (1.125 - .375) = .75 in.
P_a = .75 x .25 x 2 x 38000 = 14200#
Bolt load = 8250. Not critical.

Conclusions:

Since the strength check of the fitting shows no negative margins of safety, the strength is satisfactory.

C4.20 Design of Single Bolt Fittings.

The example problems given above dealt with fittings that were already designed and a strength check was made. The usual case however is given certain definite design loads, proportion or design a connection to transfer these loads efficiently. There are usually two or more designs that will carry and transfer the loads efficiently. Also in many cases external requirements such as clearance between fitting parts and other parts of the airplane may dictate certain dimensions for the fitting. Thus example problems of fitting design usually prove rather difficult to present in a textbook where space is limited. The author believes that if a student can strength check any type of fitting, he should be able to design a fitting without too much difficulty.

In the designing of a single bolt fitting, three primary things must be determined namely, the diameter of the bolt or pin and the dimensions of the male and female parts of the fitting unit. In general each dimension of a part of a fitting has an influence on the dimension of another unit of the fitting. The following general order of procedure in designing a single bolt fitting will usually eliminate the trial and error or guess and check method.

Step 1 To establish bolt diameter, select bolt for shear failure.

Step 2 To establish thickness of male fitting, that is the dimension of male fitting parallel to bolt axis, consider bearing of bolt on the bushing in the male fitting and the bearing of the bolt on the bushing. Since the bearing area consists of the diameter of the bolt or bushing times the thickness of the male fitting, the only unknown is this thickness since the loads and allowable bearing stresses are known.

Step 3 To establish the width of the male fitting at the bolt centerline, consider tension failure at this section. The only unknown is the width dimension.

Step 4 To establish the shear tear out dimension of the male fitting, consider tear out failure. Again only one value is missing in the equation $P = F_{su} A$, namely, the one shear out dimension of the shear area A.

Step 5 To establish the size of the base of the male fitting, consider tension or any other type of failure for this part of the fitting.

Step 6 Repeat the above general steps for the female part of the fitting unit.

C4.21 Bolt Loads for Multiple Bolt Fitting, Concentrically Loaded.

In designing or strength checking a multiple bolt fitting, the question arises as to what proportion of the total fitting load does each bolt transfer. This distribution could be affected by many things such as bolt fit or bolt tightness in the hole; bearing deformation or elongation of the bolt hole; shear deformation of the bolt or pin; tension or compressive axial deformation of the fitting members and the member being connected, and a number of other minor influences.

Since aircraft materials have a considerable degree of ductility, if the fitting is properly designed, the loads on the bolts when the loads on the fitting approach their maximum value, will tend to be in proportion to the shear strength of the bolt. That is, if the combined shear strength of the bolts is the critical strength, the yielding of the fitting material in bearing, shear and tension will tend to equalize the load on the bolts in proportion to their shear strengths. For stresses below the elastic limit of the fitting plates the bolt load distribution no doubt is more closely proportional to the bearing area of each bolt. Since the primary interest is failing strength, the bolt load distribution in proportion to the bolt shear strengths is usually assumed.

Let:-

P = design load on fitting.
P_s = allowable shear strength of any bolt.
P_n = load on bolt n
P_{sn} = allowable shear strength of bolt n.

Therefore we can write,

$$P_n = P\left(\frac{P_{sn}}{\Sigma P_s}\right) \text{ - - - - - - - - - - - - - - (A)}$$

Example Problem of bolt load distribution.

Fig. C4.28 shows a multiple bolt fitting unit subjected to a concentric load of 100,000#. Determine the load transferred by each bolt.

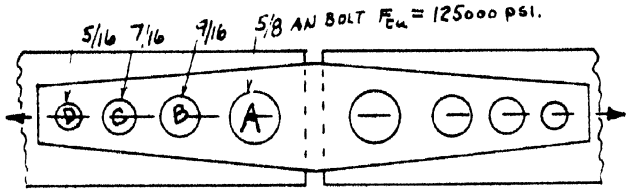


Fig. C4-28

Bolt Sym.	Bolt Dia.	Double Shear Strength = P_s
A	5/8	23010 x 2 = 46020
B	9/16	18637 x 2 = 37274
C	7/16	11272 x 2 = 22544
D	5/16	5751 x 2 = 11502
		ΣP_s = 117340

Distribution of loads to each bolt:-

$$P_a = P\left(\frac{P_{sa}}{\Sigma P_s}\right) = 100{,}000 \times \frac{46020}{117340} = 39200\#$$

$P_b = 100{,}000 \times 37274 / 117340 = 31800\#$

$P_c = 100{,}000 \times 22544 / 117340 = 19200\#$

$P_d = 100{,}000 \times 11502 / 117340 = 9800\#$

Total load on the four bolts adds up to 100,000#.

C4.22 **Example Problem - Rudder Torque Tube - Rudder Horn Connection.**

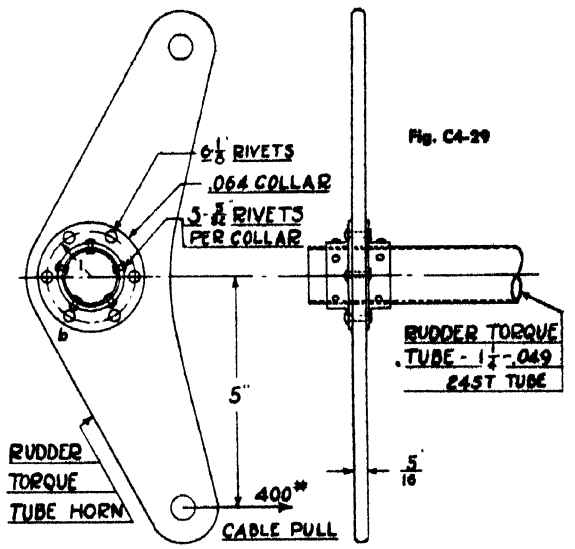


Fig. C4-29

Fig. C4.29 illustrates a rudder horn attached to the lower end of a rudder torque tube. The horn is attached to the tube by two collars riveted to the horn and likewise to the tube. For the design cable pull of 400# determine the margin of safety of the riveted connection.

Solution

The horizontal cable pull of 400# can be replaced by an equivalent force system at centerline of tube consisting of a torsional moment of 400 x 5 = 2000"# and a horizontal force of 400#.

Consider Attachment of Collars to Horn:

6 - 1/8 diameter rivets are used.

Load per rivet due to torque = $\frac{2000}{6 \times 1}$ = 334#

Load per rivet due to horizontal force = $\frac{400}{6}$ = 67#

Rivet b will be critical as both load components are practically horizontal.

Resultant load on rivet b = 334 + 67 = 401#

Take the rivets as A17ST material, the double shear strength of a 1/8 diameter rivet from Table C4.1 is 388 x 2 = 776#. M.S. = (776/401) - 1 = .93.

The bearing strength on the 25ST - .064 collar with edge distance assumed as 1.5 rivet diameters is obtained from Table C4.2.

P_b = 2 x .93 x 822 = 1530#

Consider attachment of collars to torque tube:-

10 - 5/32 diameter A17ST rivets are used.

Load on each rivet due to torque

= $\frac{2000}{10 \times .6}$ = 334#

The horizontal component of the 400# acting through the center of the tube can be taken by direct bearing of collars on tube. Single shear strength of 5/32 - A17ST rivet bearing on .049 tube wall equals 596# from Table C4.1.

Bearing strength on .049 tube wall using value for edge distance equal two or greater, we obrain from Table C4.2

$P_b = 1.18 \times 100{,}000 \times .049 \times 5/32 = 903\#$

Shear strength of rivet is critical.

M.S. = (596/334) - 1 = .78

C4.23 Multiple Riveted or Bolted Joints Subjected to Eccentric Loads.

Fig. C4.30 shows a plate fitting attached to another member by means of four bolts or rivets. (The circles represent the bolts). The fitting plate is subjected to the loads P_H and P_V acting as shown. Let it be required to find the resultant loads on the bolt group due to the given loads.

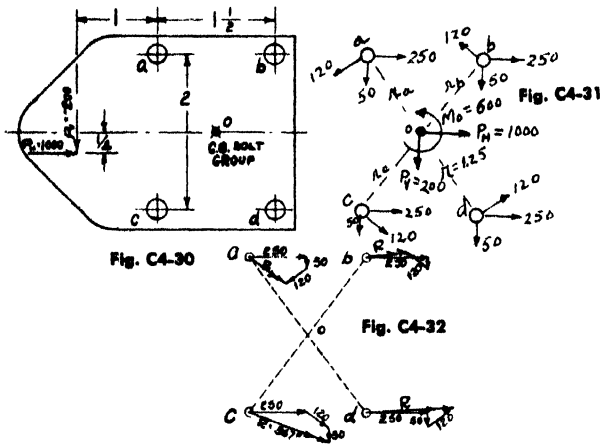


Fig. C4-30

Fig. C4-31

Fig. C4-32

The centroid of resistance for the bolt group will then correspond to the centroid of the bolt areas. Fig. C4.31 shows the fitting unit with the force P_H and P_V replaced by an equivalent force system at the bolt group centroid point (O). This equivalent force system will be:-

$P_V = -200\#, \qquad P_H = 1000\#$

and $M_O = -200 \times 1.75 - 1000 \times .25 = -600$ in.lb.

Since P_V and P_H act through the bolt centroid they will be reacted equally by each bolt, hence V load on each bolt due to $P_V = -200/4 = -50\#$; H load on each bolt due to $P_H = 1000/4 = 250\#$.

The load produced on each bolt due to the moment load $M_O = -600"\#$ will vary directly as the distance of the b

the distance of the bolt from the center of resistance which coincides with the bolt group centroid.

Let r_a equal the distance from the bolt group centroid to bolt (a). Then the resisting moment developed by bolt (a) equals $F_a r_a$, where F_a equal the load on bolt (a). Since the bolt loads are proportional to their distance from O, the resisting moment M_b developed by bolt (b) will equal

$\left(F_a \frac{r_b}{r_a}\right) r_b$ or $F_a \frac{r_b^2}{r_a}$, and similarly for bolt (c) $M_c = F_a \frac{r_c^2}{r_a}$ and for bolt d = $F_a \frac{r_d^2}{r_a}$.

The total moment resistance of the bolt group therefore equals,

$$M = \frac{F_a r_a^2 + F_a r_b^2 + F_a r_c^2 + F_a r_d^2}{r_a} \quad \text{-----(1)}$$

hence,

$$F_a = \frac{M r_a}{r_a^2 + r_b^2 + r_c^2 + r_d^2} = \frac{M r_a}{I} \quad \text{------(2)}$$

where $I = \Sigma r^2$ of bolt group.

Therefore for the loads on the other bolts,

$$F_b = \frac{M r_b}{I}; \quad F_c = \frac{M r_c}{I}; \quad F_d = \frac{M r_d}{I}$$

For the bolt group of Fig. C4.31 $r_a = r_b = r_c = r_d = 1.25"$.

hence $I = \Sigma r^2 = 4 \times 1.25^2 = 6.25$ in.

Therefore the moment load on each bolt will equal

$$\frac{Mr}{I} = \frac{-600 \times 1.25}{6.25} = 120\#$$

Fig. C4.31 shows the resulting H, V and moment loads applied to each bolt. The resultant load can be found graphically by drawing the force polygons as shown in Fig. C4.32. The resultant bolt loads can likewise be determined analytically. For example consider bolt (c)

$$\Sigma H = 250 + 120 \times \frac{1}{1.25} + 0 = 346\#$$

$$\Sigma V = -50 - 120 \times \frac{.75}{1.25} + 0 = -122\#$$

Hence $R = \sqrt{\Sigma H^2 + \Sigma V^2} = \sqrt{346^2 + 122^2} = 367\#$

Case where bolts or rivets are of Different diameters.

When the joint bolts or rivets are not all the same size, the moment load on each bolt is proportional to the bolt area times its distance to the bolt group centroid. Thus the bolt areas must enter equation (2).

hence,

$$F_a = \frac{M A_a r_a}{n_a A_a r_a^2 + n_b A_b r_b^2 + n_c A_c r_c^2 + n_d A_d r_d^2} \quad \text{---------(3)}$$

where n_a = number of (a) bolts.
n_b = number of (b) bolts, etc.
A_a = area of an (a) bolt.
A_b = area of an (b) bolt, etc.

Example Problem 1. Eccentric Loading

Fig. C4.33 illustrates a fitting plate attached to a double channel section by 6-1/4" dia. rivets. The margin of safety on the given loads for the riveted connection will be determined.

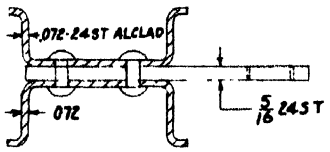


Fig. C4-33

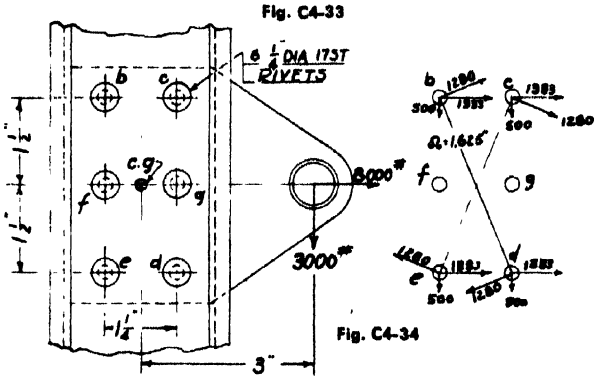


Fig. C4-34

Solution

The given fitting force system will be replaced by an equivalent system acting at the center of gravity of the rivet group at point O. This system will consist of:

H_O = 8000#
V_O = -3000#
M_O a moment = 8000 x 0 + 3000 x 3 = 9000"#

All rivets are assumed to share equally in resisting the H and V loads.

Load on each rivet due to H_O = 8000/6 = 1333# in H direction to right.
Load on each rivet due to H_O = -3000/6 = -500# in V direction and down.

From equation (2) load on a rivet due to a moment M_O on rivet group equals F = Mr/I, where

$I = \Sigma r^2 = 1.625^2 \times 4 + .625^2 \times 2 = 11.4$

Consider rivet C:

r = 1.625 = arm to c.g. of rivet group, hence

$$F_c = \frac{9000 \times 1.625}{11.4} = 1280\#$$

Since rivet b, d, and e are the same distance as rivet c from the rivet group centroid, the moment load on these rivets will also equal 1280# each. Fig. C4.34 shows the H, V and M loads on rivets b, c, d and e. Since the arm r to the rivets f and g is only .625", the moment load will be considerably smaller and these rivets will not be critical. Observation of Fig. C4.34 shows that rivet (c) is critical. The resultant load on this rivet equals,

$R_c = \sqrt{\Sigma F_H^2 + \Sigma F_V^2}$

$\Sigma F_H = 1333 + 1280 \times 1.5/1.625 = 2513\#$

$\Sigma F_V = -500 - 1280 \times .625/1.625 = -992\#$

Hence, $R = \sqrt{2513^2 + 992^2} = 2700\#$

The rivets are in double shear. Double shear strength of 1/4 diameter 17ST rivet equals 22 x 1760 = 3520#.

Bearing strength on .072 24ST alclad channel sections is 4625#.

Hence shear is critical. M.S. = $(\frac{3520}{2700})-1 = .30$

Example Problem - Eccentric Loading - Rivets With Different Diameters.

Take same fitting as in Fig. C4.33 but change rivets (f) and (g) to 3/16 diameter rivets. Required the resultant loads on the rivets.

Solution

In this example we have two rivet sizes making up the rivet pattern. Thus in this case the assumption that the load on any rivet is proportional to its distance from the bolt pattern center of resistance does not hold. However for rivets of the same material, the stress on the rivets remains proportional to the distance from the group center of gravity. (See equation (3).

Let area of 1/4 diameter rivet equal unity. Then equivalent area of 3/16 diameter rivet = $(3^2/4^2)$ 1 = 9/16. Hence moment of inertia of bolt group about bolt group c.g. which remains at same location as before equals:

$I = \Sigma nAr^2 = 4 \times 1 \times 1.625^2 + 2 \times .5625 \times .625^2 = 11.00$
Total equivalent 1/4 diameter rivets = 4 +2 x 9/16 = 5.125
Load on each 1/4 rivet due to H_O = 8000/5.125 = 1560 lb.
Hence H load on 3/16 rivet = .5625 x 1560 = 877 lb.
Load on each 1/4 rivet due to V_O = -3000/5.125 = -585 lb.
Hence V load on each 3/16 rivet = .5625 x - 585 = -329 lb.

Consider rivet C: Load due to moment,

$$F_c = \frac{90000 \times 1 \times 1.625}{11.00} = 1330$$

$\Sigma F_H = 1560 + 1330 \times 1.5/1.625 = 2790$

$\Sigma F_V = -585 - 1330 \times .625/1.625 = -1095$

Hence $R = (2790^2 + 1095^2)^{1/2} = 3000$ lb.

M.S. = (3520/3000) - 1 = .17

Consider rivet (g).

Moment load $F_g = \frac{9000 \times .5625 \times .625}{11.0} = 288$ lb.

$\Sigma F_H = 877 + 0 = 877$ lb.

$\Sigma F_V = -329 - 288 = -617$ lb.

Hence $R = (877^2 + 617^2)^{1/2} = 1065$ lb.

Double shear strength = 1954
Bearing strength on .072 channels = 3520
M.S. = (1954/1065) - 1 = .83

C4.24 Strength Check and Design of Sheet Splices or Attachments.

In splicing or connecting two sheets together by means of rivets or bolts, the joint or connection may fail in the various ways as explained in detail for single and multiple bolt fitting units. Thus one must check the shear strength of the rivets; bearing of rivets on the sheets; tear out of the sheet edges and tension on sections through the rivet holes.

Types of Sheet Splices or Connections.

Fig. C4.35 illustrates the various types of sheet splices. In the offset lap splice between two sheets of different guages, the offset should be in the heavier material. For a single shear butt splice, the butt splice plate should be equal to the thinnest of the two sheets being spliced and likewise in the double shear butt splice the splice plates should be of the same thickness and should be equal to the thinnest plate being spliced.

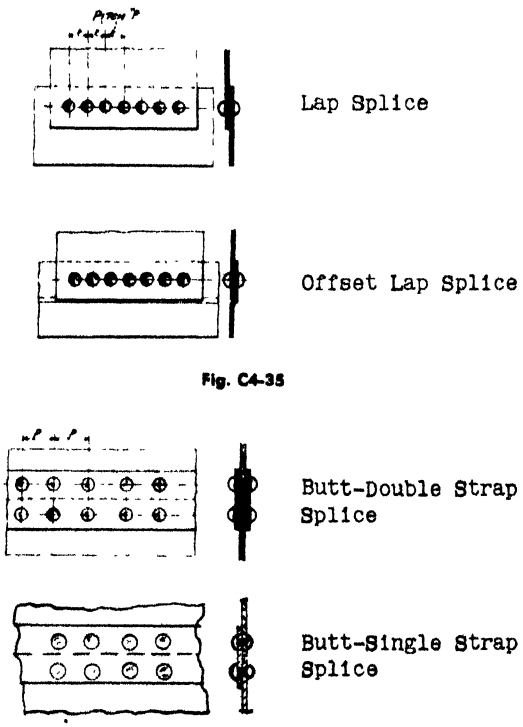


Fig. C4-35

Proper Rivet Size to use.

No exact rules can be given relative to the optimum rivet for a given splice, because a number of practical considerations usually enter into the design of a sheet splice. Small rivets, namely 1/16 and 3/32 diameters are hard to handle and are seldom used as structural rivets. The common size of rivets are 1/8, 5/32, 3/16 and 1/4 inch diameters. The larger sizes should not be used in sheet splices unless there is a backing up structure as the sheet may buckle under the driving of the large rivets. From a structural design standpoint, the optimum joint is one in which the allowable rivet shear strength and bearing strength of the given sheets are practically the same for the largest practical size rivet.

Rivet Spacing. Sheet Edge Distance.

The allowable rivet-sheet bearing loads as given in ANC-5 are based on an edge distance of two diameters. Therefore in general no edge distance in a joint should be less than 2 rivet diameters for protruding head rivets, and 2-1/2 diameters for press and machine countersunk flush rivets.

The minimum pitch (distance between centerline of rivets in the same row) for a given size rivet should not be less than that given in Tables A and B.

Table A

PROTUDING HEAD RIVET NORMAL MINIMUM SPACING				
Rivet Diameter	1/8	5/32	3/16	1/4
Normal Minimum Spacing	1/2	9/16	11/16	7/8

Table B

NORMAL MINIMUM SPACING PRESS AND MACHINE COUNTERSUNK FLUSH RIVETS				
Rivet Diameter	1/8	5/32	3/16	1/4
Normal Minimum Spacing	11/16	27/32	1 1/32	1 1/4

In general the minimum rivet row spacing should be such as to make the distance between any two rivets in the two rows not less than the minimum rivet spacing for the rivet size being used.

Splice Sheet Tension Efficiency.

When a sheet is spliced by means of rivets or bolts it means the sheet is weakened since the rivet holes cut away a part of the sheet material. The ratio of the tension strength of the spliced sheet to the unspliced sheet is called the sheet tension efficiency of the joint. If the minimum rivet spacing is used and only one row of rivets the sheet efficiency,

will be around 70 to 75 percent. The designer should strive for a higher efficiency.

C4.24 Example Problems In Strength Checking Sheet Splices.

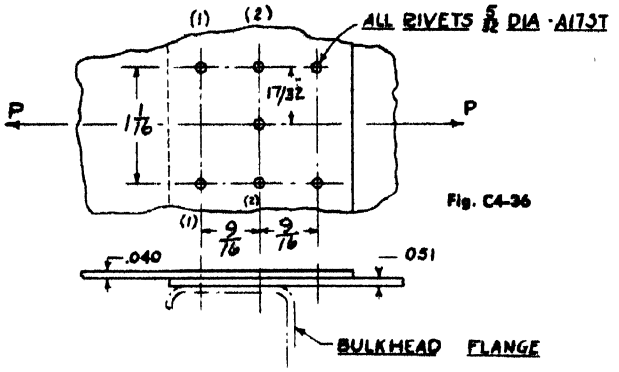


Fig. C4-36

Problem 1.

Fig. C4.36 shows a sheet lap riveted joint. The maximum applied tensile stress on the .040 sheet is 27500 psi. The sheet material is 24ST alclad. Using a design ultimate factor of safety of 1.5 and a fitting factor of 1.15, check the strength of the sheet splice.

Solution:-

Design load P per 1-1/16" length of joint = 27,500 x 1.0625 x .040 x 1.15 = 2015#.

Check Shear Strength of Rivets:-

Effective rivets per 1-1/16" length of joint = 4 in single shear.

Allowable shear strength 5/32 dia. A17ST rivet = .964 x 596 = 575# (See Table C4.1)

Hence allowable P_a = 4 x 575 = 2300#

M.S. = (2300/2015) - 1 = .14

Check Bearing Strength of Rivets on .040 Sheet.

Allowable bearing of 5/32 rivet on 24ST alclad .04 sheet = 1.16 x 636 = 737#

Hence P_a = 4 x 737 = 2948#

M.S. = (2948/2015) -1 = .45

Check Tension on .040 sheet at section (1-1)

Net area = (1.0625 - .1562) .04 = .0362 sq.in.

F_{tu} for 24ST alclad = 56000 psi.

Hence P_a = 56000 x .0362 = 2030#

M.S. = (2030/2015) - 1 = .01

Check Tension on .04 Sheet at Section (2-2)

Net area = $\left[1.0625 - (2 \times .1562)\right]$.04 = .03 sq. in.

P_a = 56000 x .03 = 1680#

Load on this section = .75 x 2015 = 1510#, since the rivet at section 1-1 has transferred 1/4 of load.

M.S. = (1680/1510) - 1 = .11

The student should notice that if the rivet spacing at sections 1-1 and 2-2 had been reversed, the margin of safety would be negative since the strength in tension would have been 1680# at section (1-1) and the load 2015# or a negative M.S. of -.16

Example Problem 2

Design a butt splice joint using 17ST rivets for the .072 24ST sheet carrying a fitting design load of 2400#/in. See Fig. C4.37.

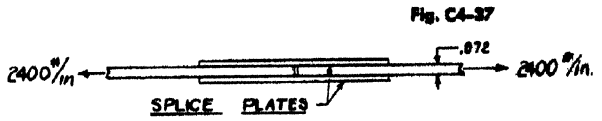


Fig. C4-37

Solution:

The splice plates will be made .036 each, thus they will be as strong as the main plate. Using table C4.1 and 2 the shear and bearing strengths of 1/8 and 5/32, 17ST rivets on 24ST sheet are as follows:-

Rivetsize	Double Shear Str.	Bearing On .072
1/8	2 x 442 = 884#	1.18 x 925 = 1090#
5/32	2 x 675 = 1350#	1.18 x 1140 = 1345#

To obtain highest efficiency the 5/32 rivet is best since shear and bearing strengths are practically the same.

Number of 5/32 rivets required per inch = (2400/1345) = 1.78.

If one row of rivets was used on each side of the splice the spacing would be 1/1.78 = .5625 = 9/16 inch! Since this is the minimum normal spacing for 5/32 dia. rivets, one row of rivets at 9/16 spacing could be used. With this spacing the sheet strength will be checked. Net area over a rivet pitch = (9/16 - 5/32) .072 = .0293 sq. in.

Load on 9/16" joint width = 9/16 x 2400 = 1350#.

Tension stress = $\frac{1350}{.0293}$ = 46000 psi. which leaves a considerable margin of safety.

If two rows of rivets were used the spacing could be 1-1/8 inches and the rows could be staggered or in line since tension in the sheet would not be critical. Edge distances on sheet and splice plates should be 5/16" or two rivet diameters.

C4.25 Problems.

(1) Strength check the male fitting end as shown in Fig. C4.38. Design fitting load is 65000# tension. Hinge bolt is 3/4 diameter AN bolt. F_{tu} = 125000 psi. Steel bushing has 1/16" wall and is heat treated to F_{tu} = 125000 psi. Fitting material is 14ST aluminum alloy.

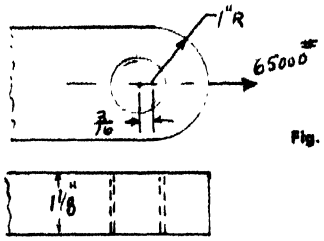


Fig. C4-38

(2) The female hinge fitting in Fig. C4.39 is made of X-4130 steel heat treated to F_{tu} = 180000 psi. The 1/2" diameter steel hinge pin is heat treated to 150,000 psi, as is also the steel bushing. Strength check the fitting for the design fitting loads as shown.

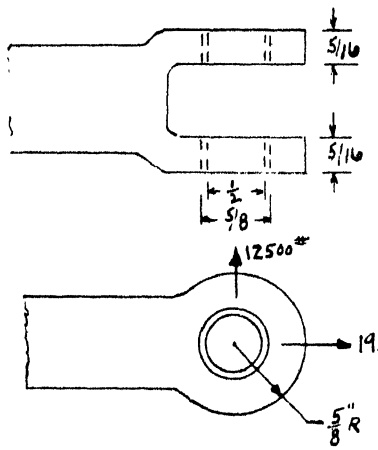


Fig. C4-39

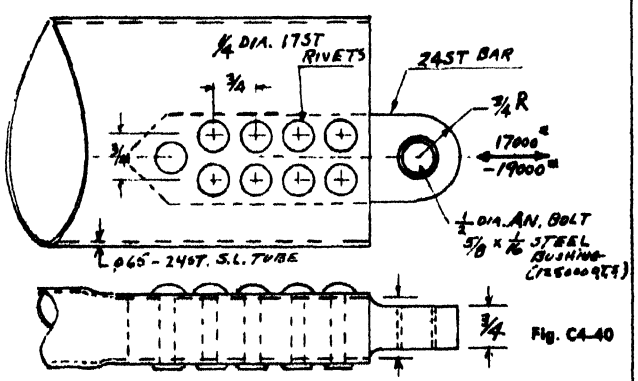
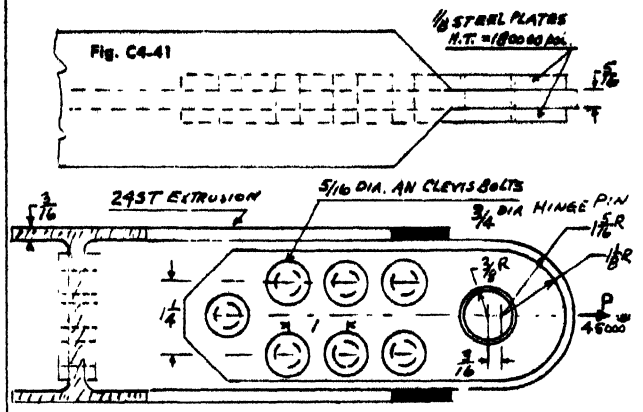
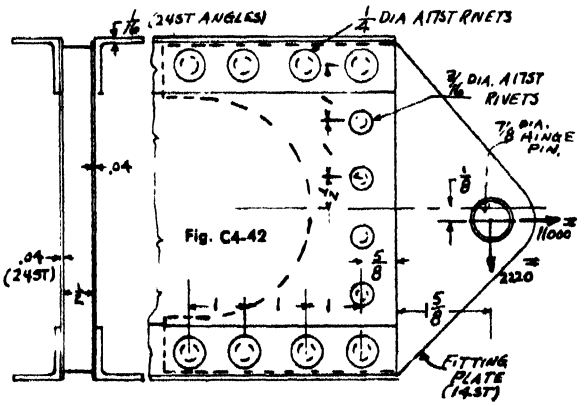


Fig. C4-40

(3) Fig. C4.40 illustrates an end fitting for a streamline strut. The tube is flattened slightly at the end to fit a simple block fitting. Loads shown are design strut loads. Using a fitting factor of 1.20, check the strength of the entire fitting unit. Assume no shock or vibration.

(4) Fig. C4.41 illustrates a fitting unit on the end of an extruded (I) section. The web on the (I) section extends out to form part of the fitting lug, which is reinforced by steel fitting plates. Strength check the fitting for a design load of 45000 lb. Use fitting factor of 1.15.





(5) Fig. C4.42 shows a typical beam end-single pin fitting unit. The fitting plate is attached to beam section by the rivet pattern as shown. The loads shown on figure are applied loads. Using a factor of safety on applied loads of 1.5 and a fitting factor of 1.2 determine the margin of safety of the rivet attachment of fittng plate to beam section.

(6) Fig. C4.43 shows a flap hinge fitting attached to supporting structure by 4 -1/4" dia. AN steel bolts. The bolts are in double shear. Check the most critical bolt in shear and bearing for load of 3500# acting as shown. Fitting material is 24ST.

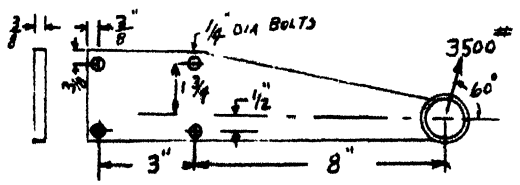


Fig. C4-43

(7) In the eccentrically loaded multiple bolt fitting of Fig. C4.44, determine the resultant load on each of the five AN steel bolts in resisting the 24000# load acting as shown.

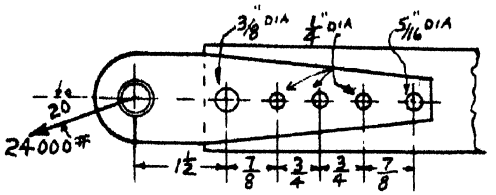


Fig. C4-44

(8) Strength check the riveted lap splice shown in Fig. C4.45 if the maximum applied tensile stress on the .051 sheet is 25000 psi. The sheet material is 24ST alclad and the rivets are 3/16 dia. A17ST. Use a design factor of safety = 1.5 and a fitting factor of 1.15.

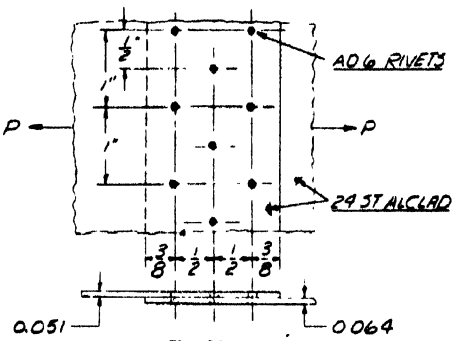


Fig. C4-45

(9) What would be the maximum allowable applied stress in the 0.91 25ST alclad sheet which is shown butt spliced in Fig. C4.46. The fitting margin of safety of 15 percent must be maintained.

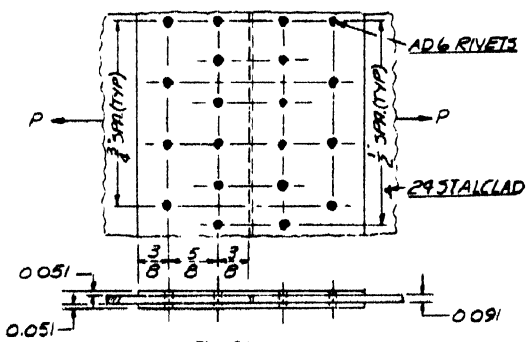


Fig. C4-46

(10) The shear flow along a wing sheet splice of .025 and .032 24ST sheet is 460# per inch. This value includes all factors. Design a butt-single strap plate splice joint to carry this shear flow load.

(11) In Fig. C4.47 the fitting is attached to a fuselage frame by four 1/4 dia. AN steel bolts. The design fitting loads are as shown. Determine the margin of safety on the most critical bolt. Use Fig. C4.17 to obtain equation for combined tension and shear stresses.

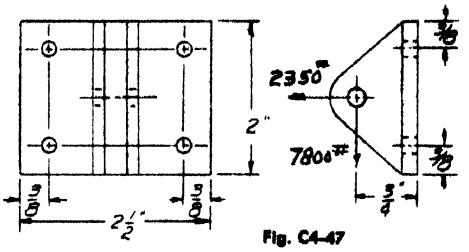


Fig. C4-47

(12) In Fig. C4.48 find the size of 17ST rivets necessary to carry the ultimate fitting design load of 3000# as shown. The fitting plate is X4130 steel 1/8 thick and the 24ST channel frame is .081 inch thick.

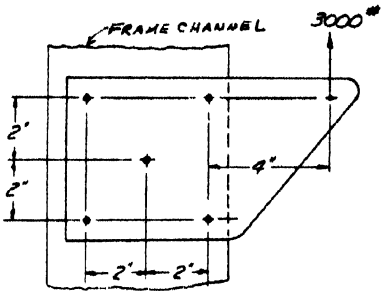


Fig. C4-48

(13) Design the lightest protruding head rivet offset lap splice in .051 24ST sheet carrying a tension load of 2350#/in. Determine rivet diameter, number of rivet rows, rivet spacing, edge distances and splice overlap width.

(14) Rework the splice of Problem (13) using flush type dimpled rivets.

(15) Same as (13) but use flush machine countersunk rivets.

REFERENCES

(1) NACA Tech. Note No. 942. "The Shear Strength of Aluminum Alloy Driven Rivets as affected By Increasing D/t Ratios". By Hartman and Wescoat.

(2) NACA Tech. Note No. 981. "Bearing Strengths of 24ST Aluminum Alloy Plate" by Moore and Wescoat.

(3) ANC-5 - 1946

CHAPTER C5
AIRPLANE WELDED JOINTS AND FITTINGS

C5.1 Gas Welding.

There are two types of gas welding, namely, oxyacetylene and oxyhydrogen. Practically all gas welding in aircraft work is oxyacetylene. Some welders prefer the oxydrogen flame in welding aluminum alloys because the flame is not so hot. The major aircraft structural units in which gas welding plays an important part are welded steel tubular fuselages, engine mounts, and landing gears and the attachment of plate and machined fittings to such structure. Aircraft welding in steel is generally limited to low carbon (SAE 1020) and chrome-molybdenum (x 4130).

C5.2 General Notes on the Practical Design of Welded Joints.

The designer of welded structures in steel can greatly help the welder obtain good joints or connections by adherring to the following general rules.

(1) It is much easier to obtain a good weld when the parts being welded together are of equal thickness. It is general design practice to try and keep thickness ratio between the two welded parts less than 3 to 1. Some designers try to keep within a 2 to 1 ratio in order to eliminate possibilities of welders burning the thinner sheet.

(2) Designers usually consider .035 as the minimum thickness to be welded in general practical structural joints as there is considerable danger that the average welder might burn a thinner guage.

(3) In general avoid welds in tension since they produce a weakening effect. In some connections it is difficult to avoid all tension loads on welds, thus weld stresses should be kept low and if possible incorporate a fishmouth joint or finger patch to put part of weld in shear.

(4) A weld should not encircle a tube in a plane perpendicular to the tube length. Standard splices or joints for over lapping tubes, and end socket fittings in tubes have been developed, which require no strength check. These are the diagonal weld and the fishmouth welds as illustrated in Fig. C5.1

(5) Tapered gusset plates should be incorporated in all important welded joints to insure gradual change in stress intensity in members. These gussets lessen the danger of fatigue failure by reducing stress intensity.



BUTT WELD FISHMOUTH WELD

Fig. C5-1

(6) A weld over a weld should not be made.

(7) To prevent burning of sheet welds should not be made on both sides of a thin sheet.

(8) If two welds are placed close together lack of shrinkage space may cause cracking.

(9) Cracks usually develop if welding is done on bends.

(10) When tubes are spliced by welding locate splice near one end of the tube, to avoid effecting column properties. In general it is not good practice to weld brackets to the middle of column members. Clamps are preferable.

(11) In welding members together local internal stresses are set up. On most weld assemblies it is therefore customary to "normalize" the assemblies after welding. This heating permits the equalization of the internal localized stresses thus preventing cracking in service.

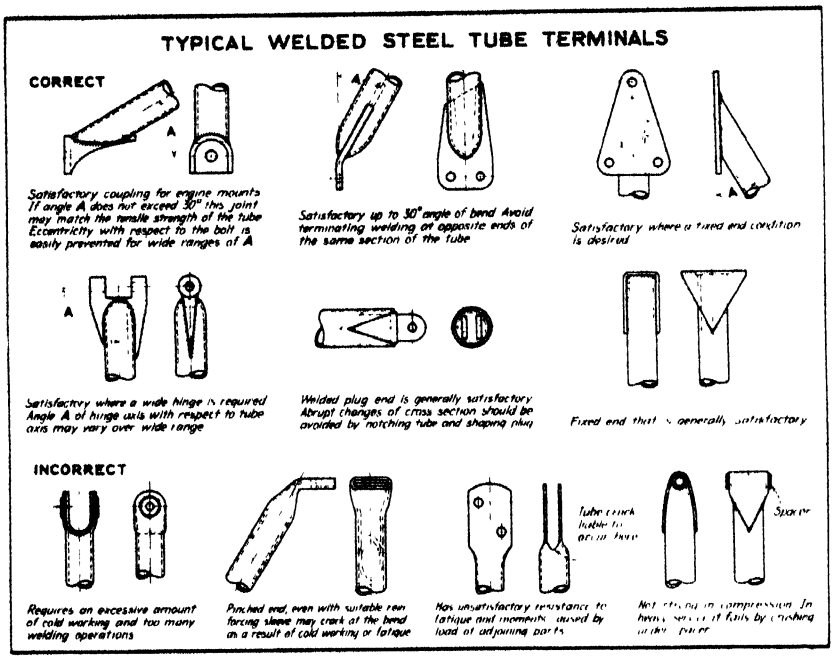
(12) Standard aircraft bolts should not be welded in place since they are made of nicket steel and therefore cannot be satisfactorily welded. Since standard aircraft nuts are made of 1025 steel they can be welded in place if desired.

C5.3 General Types of Welded Steel Fitting Units.

Fig. C5.2 taken from aircraft tubing handbook of the Summerill Tubing Company summarizes the common types of tube terminals and discusses their structural merit. Fig. C5.3 illustrates the conventional concentric butt welded fuselage joint which tests show is satisfactory where vibration is not present. Tests have shown that the fatigue strength of a welded joint as illustrated in Fig. C5.3 when the members are subjected to reverse bending is reduced considerably, thus it is common practice to add additional joint reinforcement such as finger plates or insert gussets as illustrated in Figs. C5.4 and C5.5 to joints subjected to vibration.

Figs. C5.6 to C5.8 illustrate methods of splicing a longeron at a truss joint. The

Fig. C5-2



Reproduced by permission from Summerill "Aircraft Tubing Data"

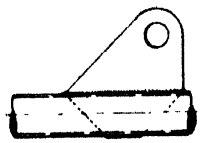


Fig. C5-9

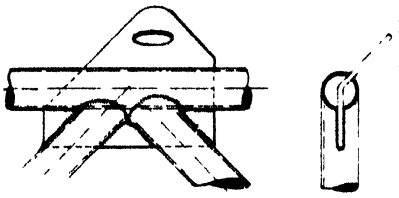


Fig. C5-10

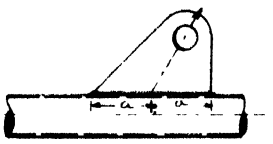


Fig. C5-11

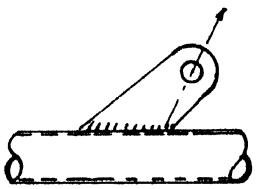


Fig. C5-12

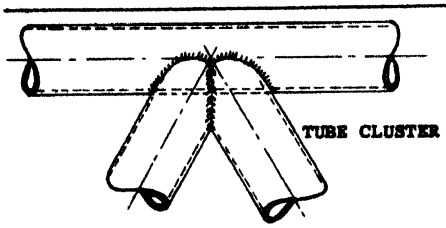


Fig. C5-3

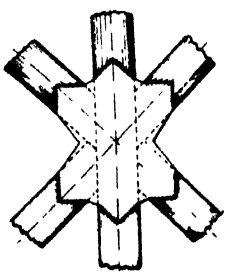


Fig. C5-4

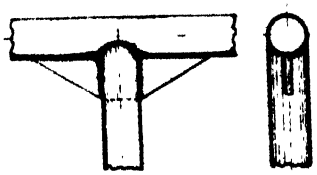


Fig. C5-5

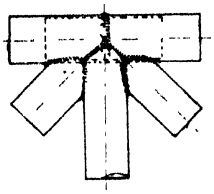


Fig. C5-6

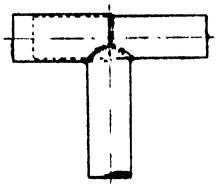


Fig. C5-7

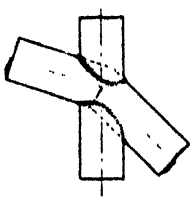


Fig. C5-8

bending on tube tends to out lower weld in tension

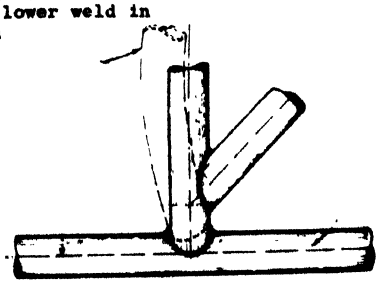


Fig. C5-13

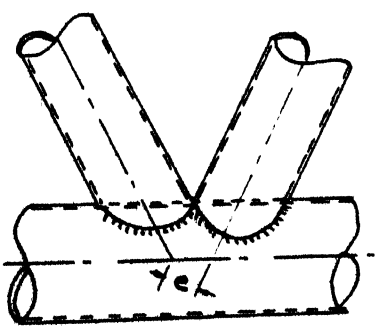
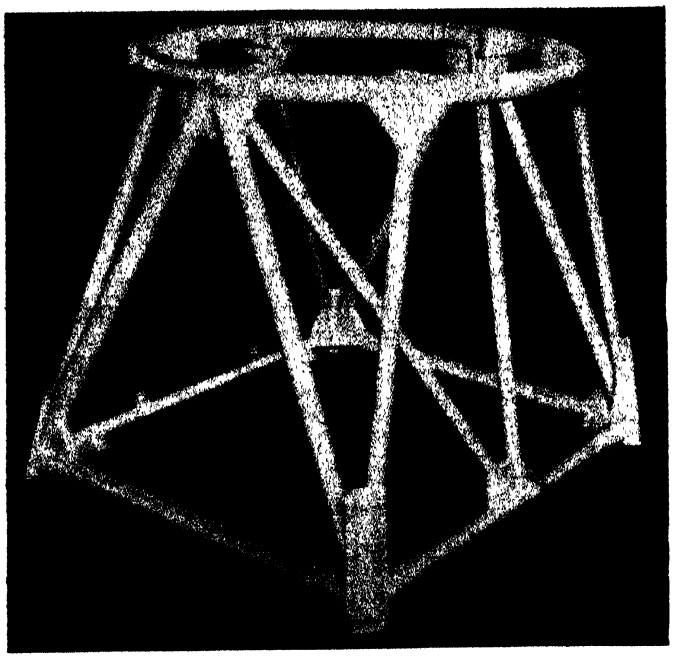
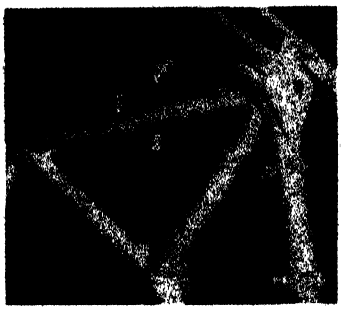


Fig. C5-14



COURTESY GLENN L. MARTIN CO

Engine Mount for Martin Bomber, one of the latest designs for modern high power radial engines. Note re-enforcements at joints and extra-diagonal tubes



Close-up of a section of finished tubular structure to show types of welded joints.



Good example of welded joint design with special fitting at cluster for controls.

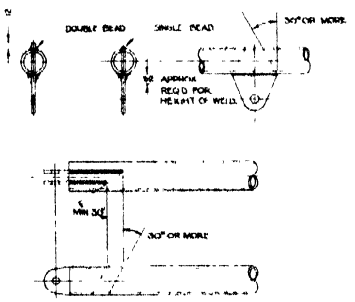


Fig. C5-15

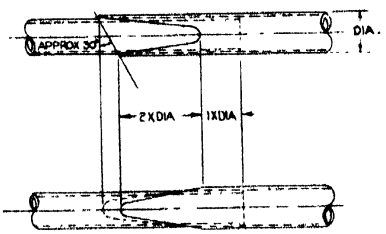


Fig. C5-16

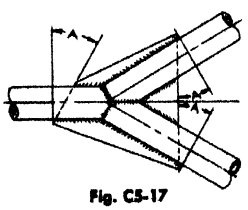


Fig. C5-17

angle "A" to be not less than 30°

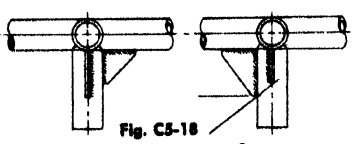


Fig. C5-18

30° or more

Photographs and figures reproduced by permission from Summerill "Aircraft Tubing Data"

vertical and diagonal members strengthen the butt weld on the spliced member.

Figs. C5.9 and C5.10 illustrate fitting plate attachments to tubes. Except for light fitting loads, the fitting plate should extend thru to both sides of tube or to the adjoining members. The fitting type illustrated in Fig. C5.11 is only used for secondary conditions where loads or plate are relatively light.

Since eccentricity of member forces on a joint produce bending in the connecting members which may lower the fatigue strength of the joint, such cases of joint eccentricity as illustrated in Figs. C5.12 to C5.14 should be eliminated in joint design.

The photographs illustrate welded joint design of tubular structures.

C5.4 Electric Arc Welding.

This method of welding is based upon the heat generated in an electric arc. Arc welding to a limited extent has been used for many years in aircraft fabrication. No doubt the flexibility and general all around good results obtained with gas welding retarded its extensive use, however in recent years its use is increasing rapidly as its economies and advantages become apparent to the designer. One large aircraft manufacturer making use of recently developed welding equipment is using electric arc welding on mass production of steel tubular fuselage.

In arc welding the applied heat is more concentrated and quicker welding results with less expansion and warning as compared to gas welding. In the design of tubular joints, care should be taken to make all welds as accessible as possible. To secure proper stress distribution in arc welded joints the designer should follow the recommendations as illustrated in Figs. C5.15 to C5.17.

The fact that less expansion and warping takes place since the heat is concentrated makes it possible to hold to closer tolerances on parts requiring machining after welding an allowance of 1/16 inch is generally sufficient on most assemblies.

New electric arc welding and control equipment is constantly being developed. This new equipment makes it possible to weld sections as thin as .016.*

C5.5 Effect of Welding on Base Metal.

Tests show that plain carbon and chrome-molybdenum steels suffer very little in loss of tensile strength due to welding. For cold rolled sheet or tubing the refinement in grain due to cold working is lost in the material adjacent to the weld which lowers strength to a small degree. Welding however does produce a more brittle material which has lower resistance to shock, vibration and reversal of stress, thus it is customary to assume an efficiency of welded joints less than 100 percent. Table C5.1 gives the decreased values as permitted in ANC-5.

For steels heat-treated after welding, the allowable stresses should be reduced to 80 percent of the standard heat-treated values.

C5.6 Allowable Loads for Welded Seams.

The allowable load on the weld metal in welded seams can be computed from the following formulas: (Ref. ANC-5)

Low carbon steel - - - - - P = 32000 Lt.

Chrom-molybdenum steel - - P = .48 Lts.

where P = allowable load in lbs.

L = length of welded seams.

t = thickness of thinnest material joined by the weld in the case of lap welds between two steel plates or between plates and tubes. (inches)

t = average thickness in inches of the weld metal in the case of tube assemblies, but not to be greater than 1.25 times the thickness of the welded stock.

s = 90000 psi for material not heat-treated after welding.

s = ultimate tensile stress of material heat-treated after welding but not to exceed 150000 psi.

C5.7 Brazing.

Brazing as applied to aircraft work is a process of uniting steel parts by means of a copper-zinc mixture, which is applied by melting with an air-gas flame or by dipping into the molten mixture. The strength of the joint depends on the surface areas of contact and the clearance between the parts to be joined.

Although the brazing mixture may develop a shearing strength of 40000 psi, a general allowable value of 10000 psi is used in aircraft work because many factors particularly the skill of the workman effects the strength of a brazed joint.

The requirements of the procuring or government agencies should be noted before using brazing in aircraft work.

C5.8 Welding of Aluminum Alloys.

The heat-treatable alloys, commonly referred to as the strength alloys, namely 17S, 24S, cannot be welded with the oxyacetylene torch without destroying their mechanical properties, which are

*See Arc Welding in Design, Manufacture, and Construction published by J. E. Lincoln, Arc Welding Foundation, Cleveland, Ohio

not restored even if heat-treated after welding. These alloys are difficult to weld and are thus generally classed as unweldable.

The strain-hardened alloys, namely 2S, 3S, 4S and 5S are readily joined by gas welding. Either a oxyacetylene or a oxyhydrogen flame is used and sheet thicknesses as low as .020 are successfully welded. After welding the material on either side of the weld is in the annealed condition and the weld itself in a cast structure. It is common practice to weld fuel and oil tanks fabricated from aluminum alloy sheets.

C5.8 Example Problems. Strength Check of Fittings.

Problem 1

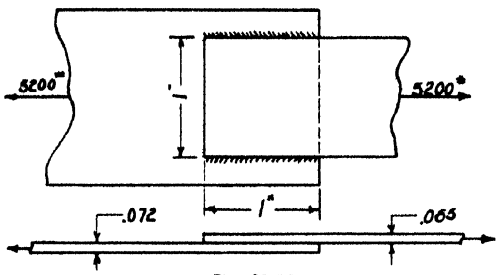


Fig. C5-19

Fig. C5.19 shows a welded lap plate joint. The material is chrome-moly (x-4130) steel, U.T.S. = 95000 psi. Find the margin of safety for weld strength.

Allowable weld strength P_a = .48Lts

L = 2 x 1 = 2"

t = .065

s = 90000 for x 4130 steel

Hence, P_a = .48 x 2 x .065 x 90000 = 5620#

M.S. = (5620/5200) - 1 = .08

Tensile strength of .065 plate using reduced allowable tensile stress = 1 x .065 x 80000 = 5200#. M.S. = 0. This is no doubt conservative since weld is along edge of sheet and thus should not effect material near middle of sheet.

Problem 2

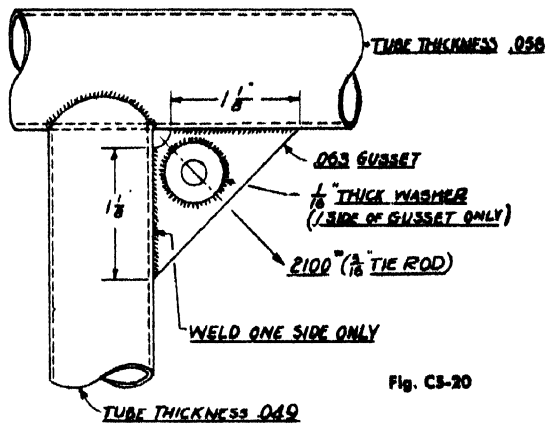


Fig. C5-20

Fig. C5.20 shows a gusset plate inserted between the ends of two tubes of a truss. The gusset is used as a fitting to take the pull from a 3/16 dia. steel tie rod. Determine the margin of safety of connection of gusset to tubes. All material x - 4130 U. T. S. 95000.

Resolving the wire pull into components parallel to the tubes we obtain P = 2100 x sin 45° = 1480# x 1.2 (fitting factor = 1780#. The allowable weld load is governed by thinnest material or .049 of the vertical tube.

Allowable load on vertical weld seam = P_a = .48Lts = .48 x 1.125 x .049 x 90000 = 2400 M.S. = (2400=1780)-1 = .35.

Problem 3

In general welded fittings involving plates and tubes present conditions for which it is difficult to determine the actual stress flow through the joint, thus the general procedure is to make conservative assumptions regarding the stress flow

Table C5.1

Allowable Steel Stresses Before And After Welding

Sym.	Ultimate Properties	Normalized Plate Tube & bar over .188" thick (x-4130)	Normalized Plate tube & bar .188" thick and under (x - 4130)	Near Weld, when welded after heat treatment (x-4130)	Normalized Tubes .188" & under (x-4130 Special) (2)	Nearweld when welded after heat treatment (x-4130 Special) (2)	Stainless Steel cold worked bar & sheet	Stainless Steel near weld
F_{tu}	Ult. Tens. Str.	90000	95000	80000 (1)	100000	84100	125000-185000	80000
F_{cu}	Ult. Comp. Block	90000	95000	67500	100000	78600	125000-185000	80000
F_{su}	Ult. Shear Str.	55000	55000	50000	58000	52500	90000-125000	70000
Fbr	Ult. Bear. Str.	140000	140000	125000	147000	130000		

Notes:

(1) Where joints with tapered welds at angles of 30 degrees or less to the center line, or fishmouth welds formed by cuts of 60 degrees or less are used, the allowable tensile stress near the welding can be assumed to be 90,000 psi.

(2) Properties in these columns are for use in civil aircraft only. Their use is permitted provided that tensile stresses stated are guaranteed by manufacturer. These properties apply to tubing "as received".

distribution and check the fitting units for these conservative assumptions. The following example illustrates this approximate procedure of strength checking a welded fitting joint.

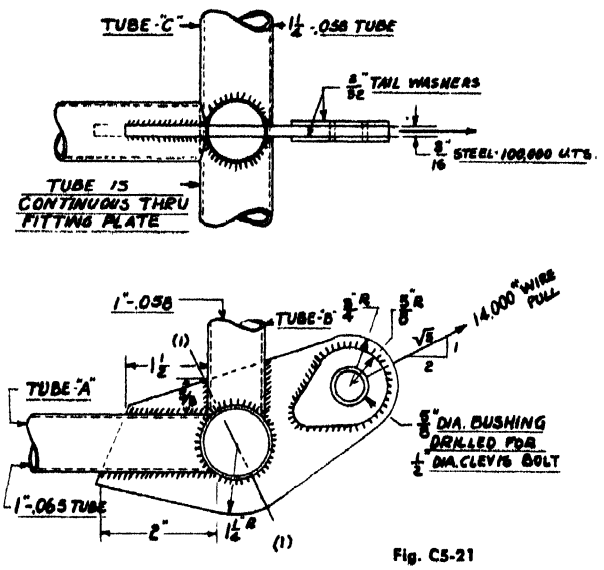


Fig. C5-21

In Fig. C5.21 the fitting plate which is welded to the three steel tubes is subjected to a tension load of 14000 lb. as shown. The fitting will be investigated for possible weakness.

Solution

Shear Strength of Clevis Pin:

Load on pin = 14000#

Double shear strength of 1/2 diameter AN clevis bolt = 2 x 14722 = 29444# M.S. = (294444/14000) -1 = 1.1

Bearing of Clevis bolt on Bushing:

Bearing stress $f_b = \frac{14000}{.5 \times .375} = 59500$ psi

Ultimate bearing stress = 175000 psi. Thus a large margin of safety is available to take care of wear due to slight rotation or shock.

Bearing Stress Bushing on Lug:

$f_b = \frac{14000}{.625 \times .375} = 59500$ psi

Allowable bearing stress F_{br} = 125000 psi (See Table C5.1)

The result shows that bearing on lug is not at all critical.

Shear Out Strength of Fitting Plate:

Shear area Main plate = (.75 - .3125) .1875 x 2 = .164
Washers = (.625 - .3125).1875 x 2 = .118
Total shear out area = .282 sq.in.

f_s = 14000/.282 = 49700 psi
F_{su} = 50000 psi (See Table C5.1)
M.S. = (50000/49700) - 1 = .01 (Conservative)

Tension Stress on Section Thru Bolt Hole:

area of section thru hole:

Main plate = (1.5 - .625).1875 = .164
Washers = (1.25 - .675).1875 = .118
Total net area = .282 sq.in.

f_t = 14000/.282 = 49700 psi.
F_{tu} = 80000 psi M.S. = .60

Tension stress on fitting plate at section 1-1 (See Fig. C5.21)
Net area = (2.5 - 1.25).1875 = .235 sq.in.
The entire load of 14000 will be assumed to pass this section, which is no doubt conservative.

f_t = 14000/.235 = 59500, F_t = 80000 psi. o.k.

Check of Weld Strength:

Connection of fitting plate to tube "A":
Load = 14000 x $2/\sqrt{5}$ = 12500#

The weld length between tube and plate is 1.5 inch on the upper tube surface and 2" on the lower surface. To be conservative a weld length of 2 x 1.5 = 3" will be taken. The weld strength P_a = .48 Lts where t = .065 (Tube thickness is critical)

L = 2 x 3 = 6 (plate is welded to tube on both sides and since twice .065 is less than thickness of fitting plate the weld length of 3 is multiplied by two since tube thickness is critical. s = 90000 psi hence, P_a = .48 x 6 x .065 x 90000 = 16800#, which gives considerable reserve strength over the load of 12500#

Connection of fitting plate to tube "B":

Load = 14000 x $1/\sqrt{5}$ = 6250#. Part of this load will be transferred first to the tube "C" by the weld between the plate and the bottom and right side of tube "C". Tube "C" than transfers it to tube "B" by butt action on the weld between tubes "B" and "C". Additional strength is provided by the weld between plate and tube "C", which is 5/8" long on one side and 1" on the other. To be conservative take a total weld length twice the shorter length or 2 x .625 = 1.25"
hence strength of this weld connection = P_a = .48 x 1.25 x .058 x 2 x 90000 = 6250 . Thus joint appears to have plenty of strength for transferring the 6250# load from plate to tube "B".

C5.10 Spot Welding of Aluminum Alloys.

After many years of research and experiment, spot welding of aluminum alloy sheets had developed to the point that today it is an established reliable method of joining many parts or units of the metal airplane.

Most of the design information which follows is based on or taken directly from an article by

Mr. C. W. Dodge and published in the June (1941) issue of "Aviation". Figures and photographs are reproduced by courtesy of "Aviation".

Spot Welding Process

According to Mr. Dodge, "spot welding is accomplished by clamping two or more sheets of metal between copper or copper alloy electrodes, under comparatively high pressure and causing an electric current of low voltage to flow between the electrodes for a predetermined interval. The current creates an intense heat at point "A" (See Fig. a) which melts the metal locally due to the resistance set up by the sheets. As soon as the metal is molten to the extent shown at "B", the predetermined time of current flow is completed and the sheets are forged together by the pressure on the electrodes "P". This pressure depends on the thickness of the sheet".

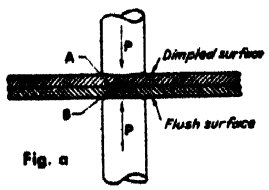
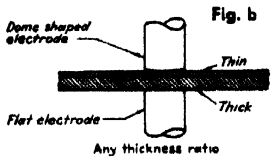
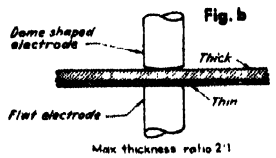


Fig. a

Aluminum Alloys Best Suited for Spot Welding

In general all the aluminum alloys can be spot welded, however best results are obtained with 24ST, 24SRT and 17ST alclad alloys. If alclad sheets are not used, the spot welding must be done before anadizing of the material.





General Design Considerations

For successful spot welding results, the structural designer should give consideration to proper shapes and sections, possible sheet thicknesses, edge distances, etc. Fig. b and Table C5.2 gives this general information.

Spot Strength Design Data

The strength of spot welds is influenced by the edge distance as well as the spacing of the spot welds. In general a minimum spacing should be eight times the sheet thickness. Table (A) gives the recommendation of Mr. Dodge.

Table A

Spotweld Spacing

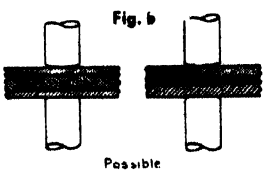
Condition	*Secondary Structures	*Primary Structures	
		Below .051	Above .051
Single Row "S"	5/8 ± 1/8	1/2 ± 1/8	5/8 ± 1/8
Double Row "S"	1 ± 1/8	3/8 ± 1/8	1 ± 1/8
Normal Distance Between Rows "D"	5/8	5/8	5/8

* As determined by structures department.

Table C5.3 from ANC-5 gives the maximum design shear strength standards for aluminum alloys.

C5.10a Problems.

(1) Fig. C5.22 illustrates a welded plate fitting unit fastened to a round steel tube. If all material is chrome-moly steel F_{ut} = 95000 psi, what is the maximum design tensile load (P)



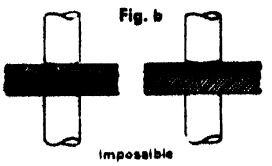


Table C5.2

Spot Diameters			Minimum Edge Distance			Practical Limits				
Thickness of Dimpled Sheet	aprox. Spotweld Dia. in inches		Single Sheet Thickness	Minimum Edge Distance		T	24ST Alclad "A"		Soft Alloys "A"	
	Alc. 24ST	Softer Alloy		Alc. 24ST	Soft Alloys		in.	Desired	Min.	Desired
.016	1/8	3/32	.016	3/16	3/16	.016	3/8	1	7/16	1/2
.020	9/64	11/64	.020	3/16	3/16	.020	3/8	1/2	7/16	1/2
.025	5/32	3/16	.025	3/16	1/4	.025	3/8	1/2	1/2	1/2
.032	5/16	7/32	.032	1/4	1/4	.032	1/2	5/8	9/16	5/8
.040	7/32	1/4	.040	1/4	5/16	.042	1/2	5/8	5/8	5/8
.051	15/64	17/64	.045	1/4	5/16	.045	9/16	5/8	5/8	5/8
.051	1/4	9/32	.051	5/16	5/16	.051	5/8	5/8	11/16	3/4
.064	9/32	5/16	.064	5/16	3/8	.064	5/8	5/8	3/4	3/4
.072	19/64	11/32	.072	3/8	3/8	.072	11/16	3/4	13/16	3/4
.081	5/16	23/64	.081	3/8	7/16	.081	3/4	3/4	7/8	7/8
.091	11/32	3/8	.091	3/8	7/16	.091	3/4	3/4	7/8	7/8

Table C5.3

Spotweld Maximum Design Shear Strength Standards for Unclad And Clad Aluminum Alloys* (Ref.) ANC-5

NOMINAL THICKNESS OF THINNER SHEET	ULTIMATE TENSILE STRENGTH 56 ksi and above	ULTIMATE TENSILE STRENGTH 28 ksi to 56 ksi	ULTIMATE TENSILE STRENGTH 19.5 ksi to 28 ksi	ULTIMATE TENSILE STRENGTH 19.5 ksi and below
INCHES	POUNDS	POUNDS	POUNDS	POUNDS
.012	60	52	24	16
.016	86	78	56	40
.020	112	106	80	62
.025	148	140	116	88
.032	208	188	168	132
.040	276	248	240	180
.051	384	354	329	240
.064	552	500	451	320
.072	678	589	524	364
.081	842	691	620	424
.091	1020	810	703	484
.102	1230	960	760	548
.114	1465	1085	803	591
.125	1698	1300	840	629
.156	2400			

*Spotwelding of aluminum alloy combinations conforming to AN-A-11, AN-A-12 and AN-A-22 may be accomplished providing specific approval is obtained from the procuring or certificating agency.

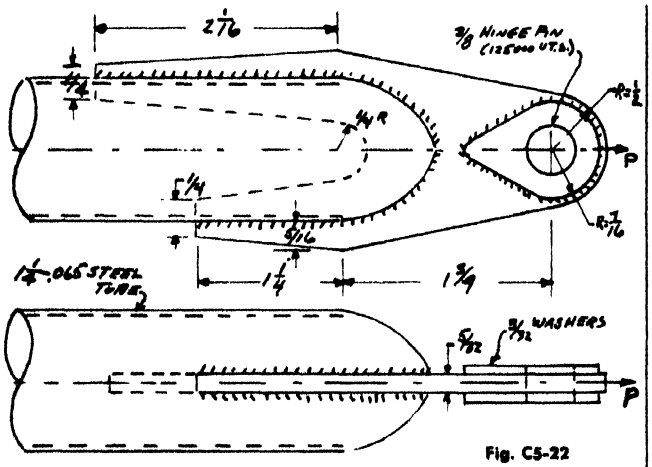


Fig. C5-22

which the fitting can be subjected to if a fitting factor of 1.2 is used. Fitting is not subjected vibration and no relative rotation of hinge pin.

(2) Same as problem (1) but tube and fitting unit is heat treated to 150000 psi after welding.

(3) A .032 24ST alclad sheet is joined to a .025 sheet by means of a lap joint and spot welds. If the applied tension load on .032 sheet is 20000 psi, design a spot welded joint using a design factor of safety of 1.5 and a fitting factor of 1.15

C5.11 Resistance Welding of Magnesium Alloys.

Resistance welding (spot, seam and butt) of magnesium alloys is increasing in use because the operations are rapid and economical. Since no flux is required corrosion possibilities are greatly eliminated. As with aluminum good spot welding depends on accurate control of current, time and electrode pressure. The power consumption in welding magnesium is considerably lower than for aluminum, however the spot welding equipment designed for aluminum can be used for magnesium. The various sheet and extruded alloys of magnesium can be spot welded together but it is preferable to use the same alloys. To obtain best results the dichromate coating should be removed by wire brushing before welding, after welding the spots should be scrubbed with hot water to remove copper deposits.

Strength of Spot Welds.

Very little information is available on the strength of spot welds for magnesium alloys. Table C5.4 reproduced by permission from the "Resistance Welding Data Book" published by the P. R. Mallory and Company of Indianapolis gives information on spot weld strength and proper spacing.

Strength of Seam and Butt Welding.

Tables C5.5 and C5.6 give values for the strength of seam and butt welds in magnesium alloys.

C5.12 Resistance Welding of Stainless Steel.

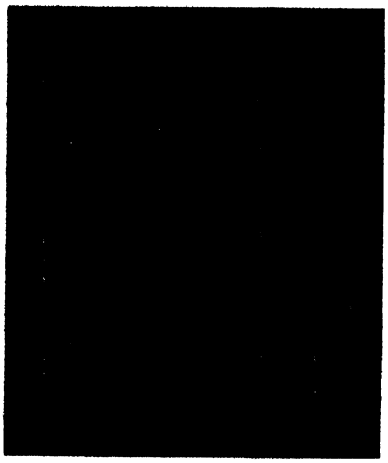
Stainless steel 18-8 (18% chromium, 8% nickel) has an electrical resistance several times that of carbon steel, thus the heat generated in a spot welding operation is much greater with stainless steel as compared to the ordinary carbon steels. Stainless steel furthermore has a low value of heat conductivity, thus it poses-ses the properties to provide good spot welding.

Table C5.4

Spot welds of Magnesium alloy sheet welded to each other (single-spot lap welds) have been found to have the following approximate mechanical strengths:

Alloy and Temper	Sheet Thickness .040"	.051"	.081"	.125"
	Average Breaking Load in Pounds per Spot			
AM3S'T	270	320	710	820
AM3S-RT	270	320	710	820
AM53S-O	340	450	900	1450
AM53S-H	390	530	1200	1750

Definition of letter designations: O - Annealed; H - Hard rolled; T - Soft (heat treated); RT - Hard (rolled after heat training).



Minimum and Recommended Dimensions for Placement of Spot Welds in Magnesium Alloys

Thickness (In.)	S	E	W	L
.016	1/4 - 1/2	3/16 - 5/16	3/8 - 5/8	1/2 - 5/8
.020	1/4 - 1/2	3/16 - 5/16	3/8 - 5/8	1/2 - 5/8
.025	1/4 - 1/2	3/16 - 5/16	3/8 - 5/8	1/2 - 5/8
.032	1/4 - 1/2	3/16 - 5/16	3/8 - 5/8	1/2 - 5/8
.040	3/8 - 3/4	3/16 - 5/16	3/8 - 5/8	1/2 - 5/8
.051	3/8 - 3/4	3/16 - 3/16	3/8 - 5/8	1/2 - 5/8
.064	1/2 - 1	1/4 - 3/8	1/2 - 3/4	9/16 - 3/4
.081	5/8 - 1 1/4	5/16 - 3/8	5/8 - 3/4	5/8 - 3/4
.102	3/4 - 1 1/2	3/8 - 1/2	1 - 1 1/2	1 -1 1/4

Courtesy P.R. Mallory Co.

Table C5.5

The following breaking loads were obtained in continuous seam welds (lap welded sheet of 1" width):

Strength of Seam Welds in Magnesium Alloys

Alloy and Temper	Sheet Thickness .040"	.051"	.081"	.125"
	Average Breaking Load Lbs. per Linear Inch of Welded Seam			
AM3S-T	750	800	900	1460
AM3S-RT	750	800	980	1460
AM53S-O	1200	1400	1750	2100
AM53S-H	1270	1480	1750	2100

Table C5.6

Depending on the size and shape of the welded section and on the alloy, tensile strengths of about 26,000 to 43,000 lbs. per sq. in. with 3 to 8% elongation can be obtained. Mechanical properties obtained in welds of 1/2" diameter rod after trimming off the excess metal are approximately as follows:

Strength of Electric Butt Welds in Magnesium Alloys

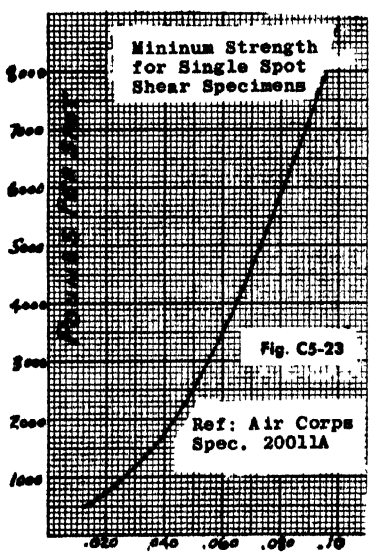
Alloy	Tensile Strength Lb./Sq. In.	Yield Strength Lb./Sq. In.	Elongation %
AM53S	35,000	21,000	4
AM5?S	41,000	22,500	6
AM58S	36,000	24,000	3

The low current requirements compared to that required for aluminum makes it possible to develop long secondary leads for portable hand spot welding tools.

In the act of spot welding the heat developed by the current flow causes the metal between the adjacent pieces at the point of contact between the electrodes to become molten and fuse together. When the current flow is stopped, the fused metal is chilled by the surrounding metal forming a small ingot on button.

Strength of Spot Welds.

Fig. C5.23 gives the minimum required values for spot welds in single shear.



CHAPTER C6

DESIGN OF METAL BEAMS: WEB SHEAR RESISTANT

C6.1 Introduction.

The analysis and design of a metal beam composed of flange members riveted or spot-welded to web members is a frequent problem in airplane structural design. In this chapter, the general theory for beams with non-buckling webs is considered. In Chapter C7, the more common case where the beam web wrinkles and goes over into a semi-tension field condition is considered. The advantages and disadvantages of the non-buckling and the buckling or semi-tension field web are discussed in Chapter C7. The general beam theory as given in this chapter is basic to that given in Chapter C7, thus the student should study this chapter before C7.

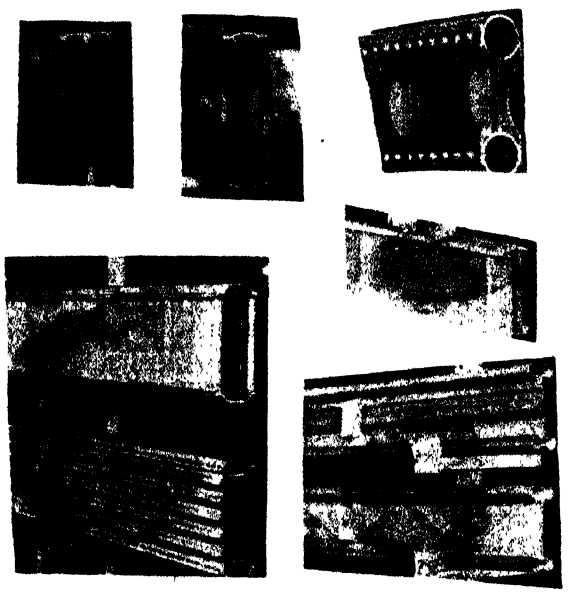


Fig. C6-1 (From ACI Circular No. 622)



Fig. 6 Truss type of beam with channel section flange member.

C6.2 Flange Design

For strength/weight efficiency, the beam flange should be designed to make the radius of gyration of the beam section as large as possible, and at the same time maintain a flange section which will have a high local crippling or crushing stress. Furthermore, the flange sections for large cantilever beams which are frequently used in wing design should be of such shape as to permit efficient tapering or reducing of the section as the beam extends outboard. This tapering of section should also be considered from a fabrication or machining standpoint. The most efficient flange from a strength/weight standpoint might be very costly or entirely impractical from a fabrication and assembly standpoint.

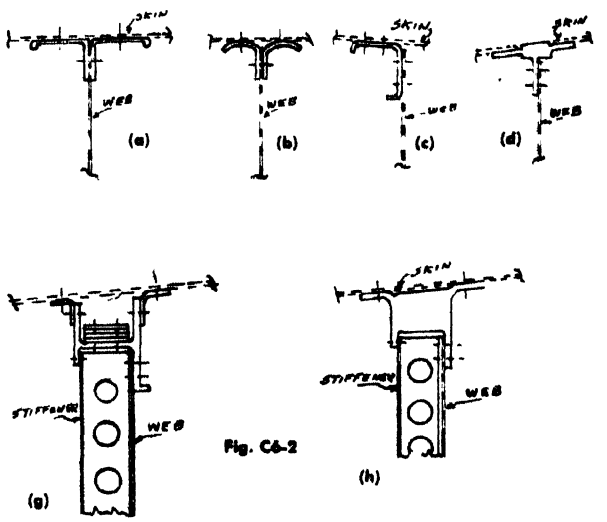


Fig. C6-2



Fig. 7 Wing beam of Boeing "Clipper" flying boat. Basic flange section is square tube.

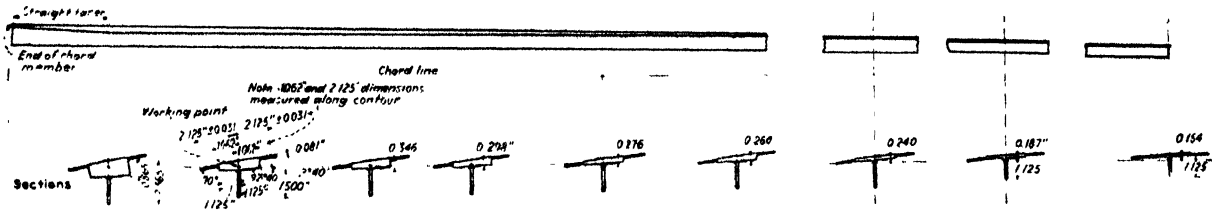


Fig. (i). Flange section of wing beam for Bell Aircraft "Airacobra" airplane. Tapering of section as shown accomplished by only two passes thru a special milling machine.



Fig. (j). Basic wing section of outer panel wing beam of Vought-Sikorsky VS-44 airplane showing gradual taper of flange section as wing tip is approached. Basic section B-B is further increased by adding reinforcing plates.

Fig. C6.1 shows a few typical metal beam sections for externally braced wings. Such beams must carry large axial compressive loads as well as bending loads. Fig. C6.2 shows typical beam flange sections for cantilever metal covered wing construction. Sections (a), (b), (c) and (d) are typical beam flange sections for wide box beams where additional stringers or skin stiffeners are also used to provide bending resistance. These flange sections are generally of the extruded type although such sections as (b) and (c) are frequently made from sheet stock. These flange sections are almost always used with a beam web composed of flat sheet, which is stiffened by vertical stiffeners riveted or spot-welded to the web or stiffened by beads or flanged lightening holes.

Figs. (e) and (f) illustrate two types of flange sections used in truss beams which lend themselves readily to connection with truss web members. Beam flange sections (g) and (h) are typical sections for wing construction in which no additional spanwise stringers are used. In section (g) tapering of sectional area is provided by first omitting the reinforcing plates, and then gradually decreasing the extruded shape by machining until only a small angle remains. In section (h) a gradual decrease in section area is produced by milling out the center portion to form a π section and then cutting this section down finally to a simple angle. Figs. (i) and (k) show actual examples of tapering of the flange sections of wing beams.

Allowable Flange Design Stresses

The calculating of the stresses in the beam flanges is in general not a difficult procedure if the usual assumptions are made in the flexure theory. The question as to what flange stresses will cause failure is the difficult one from a theoretical standpoint. The only sure way to determine the design allowable is to make sufficient static tests of specially designed test beams.

For beam sections as illustrated in Fig. C6.1, the following tests are usually necessary for forming the basis of design alllwable stresses.

(1) A test subjecting the beam to pure bending.

(2) A test of a short length of beam in bending so that failure will occur in web instead of flange.

(3) A test of a short length of beam in pure compression to obtain local crippling strength.

(4) Several tests of beams in combined bending and compression, using different ratios of bending to compressive loads.

Enough data from the above tests can usually be obtained to give rather complete allowable stress curves for the design of the beam. For the approximate design of beam flanges, the method given in this chapter can be used.

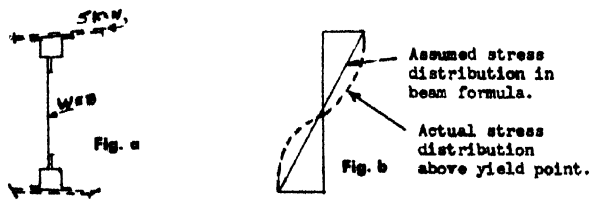
The beam flange sections (a), (b), (c), and (d) of Fig. C6.2 are stabilized by the sheet covering and also by the beam web; thus compressive tests of short lengths to obtain crippling stress, and a test of a length equal to the wing rib spacing should give sufficient information on which to base design allowables. Several lengths of the flange section for the truss type of beam should be tested in compression to obtain the column curve since the distance between panel points of the truss will vary.

Before designing any test beams, the structural designer would like to know approximately what his proposed beam flange sections will carry from a stress standpoint, since it is desirable to make test specimens closely approximate to the sections to be finally used in the completed structure. For most of the sections of Fig. C6.2, the ultimate stresses can be calculated approximately by the methods of Part B, Chapters B1 and B5. For heavy sections similar to

(g) and (h) of Fig. C6.2, where the ultimate stresses fall far above the yield strength of the material, and where some parts of the section buckle before other parts, and also where two different kinds of material are used in the same flange section, a logical procedure in trying to calculate ultimate strength of the section would be to make use of the stress-strain diagrams of the materials.

C6.3 Use of Stress-Strain Diagrams in Computing Beam Flange Bending Allowable Design Stresses.

In the beam type of wing construction, where the flange material is concentrated over the web members instead of distributed over the surface in the form of stringers, the allowable ultimate compressive stress which can be developed is considerably above the yield strength of the material since the flange is composed of a section with thick elements which promotes a high crippling stress and since the beam flange is stabilized in both vertical and horizontal directions by the web and skin covering respectively, the influence of column action is negligible. Fig. (A) illustrates this type of beam. The general flexure formula assumes that stress is proportional to strain which is correct for stresses below the proportional limit of the beam material, but the ultimate resisting stresses for the flange of a beam such as in Fig. (A) is far above the proportional limit, thus the actual stress distribution is more like



the dashed line in Fig. (B) instead of the triangular distribution as assumed in the common beam theory. Thus to obtain beam fiber stresses above the proportional limit, it is necessary to consider strain and the stress which accompanies such a strain which relationship can be obtained from the stress-strain diagram of the material. A straight line distribution for strain, that is, plane sections remains plane after bending is a reasonable one.

In a beam in bending one side is in tension and the other in compression. The tensile and compressive stress-strain diagrams for materials like aluminum alloy are different above the proportional limit, and the same unit strain will cause different stresses on the two sides of the beam. In frequent cases of large beam design, the beam flange may be composed of two kinds of material and certain portions for attaching to skin or web make buckle before the ultimate strength of the section as a whole is obtained. The solution for the ultimate internal resisting moment for such a beam requires that consideration be given to the stress-strain diagram of the various materials and units making up the beam section. This general method of approach in studying the ultimate internal resisting moment of a beam section can best be explained by an example problem.

Example Problem

Fig. C6.3 shows the cross-section of a beam in a metal covered wing. The main flange members are composed of heavy 24ST extruded shapes. The extrusions are reinforced by 24SRT sheet strips. The beam web is made from 24ST alclad material. The problem is to calculate the ultimate internal resisting moment for this beam section.

Fig. C6.4 shows the stress-strain diagram for these various materials. The 1/8 inch thick outstanding legs of the extrusions, act as a plate stiffened on three sides and free on the fourth. These legs will buckle at a stress of 35,000 psi in compression as determined by the methods given in Chapter B5. The stress-strain diagram of the two outstanding legs will be horizontal at 35,000 psi as shown in Fig. C6.4. Although the legs buckles, they will tend to hold the buckling stress under farther flange strain. In Fig. C6.5, each beam section has been broken down into narrow horizontal strips designated from (a) to (w). Only that portion of the web in way of flange has been considered in this example. Fig. C6.5a shows the strain distribution assumed for the trial solution. A heavy aluminum alloy section in compression will usually fail at a strain between .008 to .01 inch per inch if column failure is prevented. In Fig. C6.5a, the compressive unit strain at the upper beam fiber has been taken as .008"/". The neutral axis of the section has been assumed at 1.25" above center line of beam. Taking zero strain at this point the beam section strain diagram is as shown in Fig. C6.5a.

For equilibrium the total compressive bending stresses above the neutral axis must equal the total tensile bending stresses below the neutral axis.

Tables C6.1 and C6.2 give the detail calculations for calculating the resisting moment. The bending unit stress in column (5) is obtained from Fig. C6.4 using the unit strain in column (4). If the summation of column (6) in each Table is the same, the assumed location of the neutral axis is correct. The total ultimate resisting moment for this section equals 1032000 + 1360110 = 2393000 in. lb. Using the ordinary beam formula with properties about the geometric neutral axis as given in Fig. C6.3 and taking extreme fiber stresses of 46000 and 52000 psi which correspond to stresses as per strain diagram of Fig. C6.5a, the internal resisting moment would equal, $M = f\ I/c = 46000 \times 436/969 = 2070000$ in. lb. as compared to 2392000 in. lb.

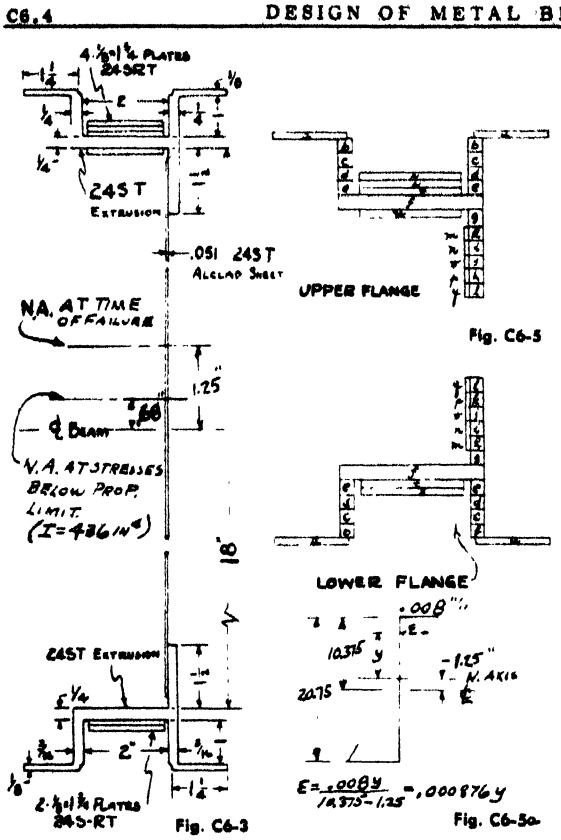


Fig. C6-3

Fig. C6-5

Fig. C6-5a

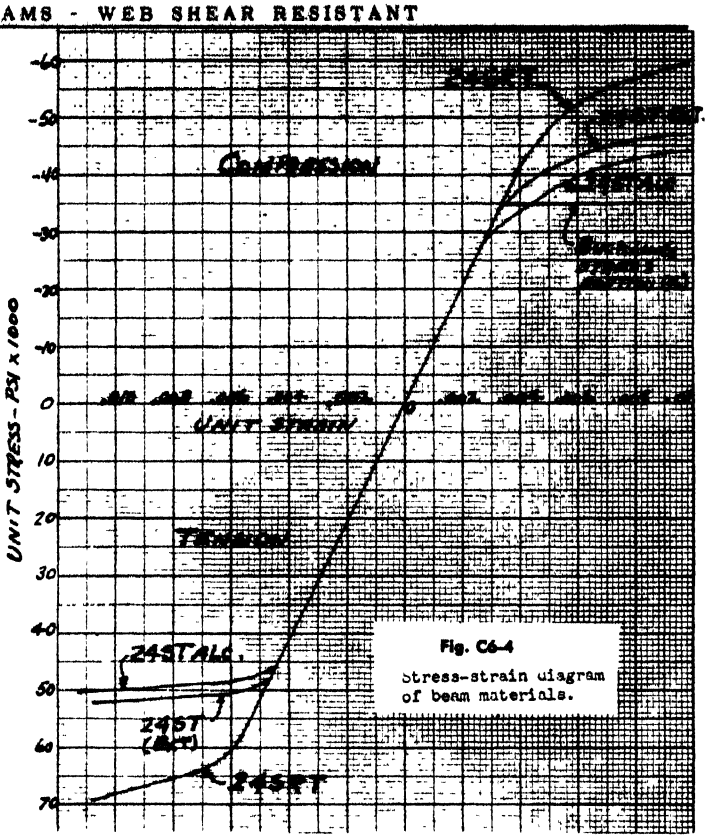


Fig. C6-4
Stress-strain diagram of beam materials.

Table C6.1

Resisting Moment of Comp. Bending Stresses about Neutral Axis

	Strip Port.	A = area of strip	y = area to strip from N.A.	Unit strain ε = .00876y	f_c=unit stress	Load on Strip = f_c A	Mom. about N.A. = f_c A y
24S T Extru.	a	.3125	9.0625	.00795	-35000*	10940	99200
	b	.1250	8.875	.00778	-45800	5725	50800
	c	.1250	8.625	.00756	-45400	5660	48900
	d	.1250	8.375	.00734	-45150	5640	47200
	e	.1250	8.125	.00712	-45000	5620	45700
	f	.6250	7.875	.00691	-44700	27900	220000
	g	.0625	7.625	.00668	-44300	2770	21150
	h	.0625	7.375	.00646	-44000	2750	20300
	i	.0625	7.125	.00625	-43300	2710	19300
	j	.0625	6.875	.00603	-43100	2695	18610
	k	.0625	6.625	.00581	-42700	2670	17700
	l	.0625	6.375	.00559	-42000	2625	16720
24S T Alc	m	.01275	7.375	.00646	-40700	519	3830
	n	.01275	7.125	.00625	-40100	511	3640
	o	.01275	6.875	.00603	-39700	506	3480
	p	.01275	6.625	.00581	-39000	497	3290
	q	.01275	6.375	.00559	-38600	492	3130
24S-RT	r	.21875	8.3125	.00728	-55500	12230	101800
	s	.21875	8.1875	.00718	-55200	12080	98700
	t	.21875	8.0625	.00706	-55100	12050	97100
	u	.21875	7.6875	.00674	-54400	11900	91450
TOTALS						128490	1032000

*Buckling stress

Table C6.2

Resisting Moment of Tensile Bend. Stresses about Neutral Axis

	Strip Port.	A = area of strip	y = arm to strip	Unit strain ε = .000876y	f_t=unit stress	Load on Strip = f_t A	Mom. about N.A. = f_t A y
24S T Extru.	a	.31250	11.5625	.01014	52050	16280	188000
	b	.09375	11.375	.00997	52000	4870	55450
	c	.09375	11.125	.00976	51950	4865	54100
	d	.09375	10.875	.00954	51900	4860	52900
	e	.09375	10.625	.00931	51800	4855	51600
	f	.59375	10.375	.00910	51750	30700	318000
	g	.0469	10.125	.00887	51700	2425	24550
	h	.0469	9.875	.00866	51600	2420	23900
	i	.0469	9.625	.00844	51500	2415	23250
	j	.0469	9.375	.00822	51400	2410	22600
	k	.0469	9.125	.00800	51300	2405	21950
	l	.0469	8.875	.00778	51200	2400	21300
24S T Alc	m	.01275	9.875	.00866	49600	633	6250
	n	.01275	9.625	.00844	49400	629	6050
	o	.01275	9.375	.00822	49300	628	5890
	p	.01275	9.125	.00800	49200	627	5720
	q	.01275	8.875	.00778	49100	625	5500
24 SRT	r	.21875	10.8125	.00948	67500	14770	159600
	s	.21875	10.6875	.00936	67300	14720	157200
	t	.21875	10.5625	.00926	67100	14700	156300
TOTALS						128237	1360110

by the more logical solution, which is a difference of 16 percent. The descrepancy would still be larger if the outstanding leg (a) did not buckle, since the more exact solution only allowed 35000 psi on this element whereas the general beam formula stresses it to 46000 psi.

Trial and Error Approach

The location of the neutral axis is unknown, thus the calculations in Tables C6.1 and 2 are for the final assumption which is the true location of the neutral axis. The general procedure would be as follows: Assume neutral axis as center line axis of beam, and find total axial load on each side of axis. The results will usually show excess load on one flange. For the next trial move neutral axis so as to give excess load on other flange. Plot the

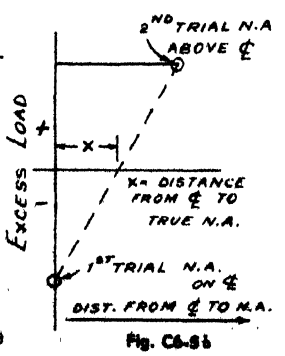


Fig. C6-5b

results as indicated in Fig. C6.5b to obtain true location of neutral axis and then make final calculations as illustrated in Tables C6.1 and 2.

C6.3a. Flange Discontinuities.

From a weight saving standpoint, it is necessary to taper flange sections in order to approach a beam of constant strength relative to the applied loads. Figs. (i) and (j) of Fig. C6.2 illustrated how this was done in the case of two actual wing beams.

Fig. A illustrates how such tapering of the flange section may produce local eccentric flange loads. Between sections (1) and (2) the upper flange tapers in side view as shown which

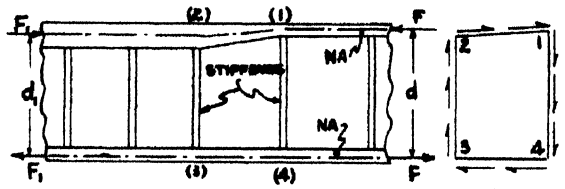


Fig. a Fig. b

displaces the flange neutral axis as shown. Assuming there is no change in bending moment over the beam portion as shown, the force F_1 must be greater than F since resisting arm d_1 is less than d. For equilibrium this moment due to F_1 and F not being colinear must be balanced in some manner. If the flanges are rigidly connected to web and stiffeners, this moment can be balanced by an additional shear stress on the web panel between points (1, 2, 3 and 4) as illustrated in Fig. B. Thus in cases of rather abrupt changes in flange sections which produce the eccentricity as illustrated the web and stiffeners should be checked for the additional shear flow load on the web. If such displacements in the flange neutral axis occur in the plan view, the skin covering should be investigated for the additional shearing stresses.

C6.4 Web Design

In this chapter only, the shear resistant web is being considered. From elementary mechancis (see Art. A4.3 of Chapter A4) it was proven that when a point in a body was subjected to pure shear stresses, normal stresses of the same intensity as the shear stresses were produced on planes at 45 degrees with the shearing planes, one normal stress being compressive and the other tension. Therefore, if a thin sheet is subjected to shearing stresses, the first evidence of distortion will be the buckling of the sheet along diagonal lines due to the diagonal compressive stresses which are caused by the shearing stresses.

In Chapter B2, Art. B2.3, the equation for the critical shearing stress which produced diagonal buckling due to compressive stresses is

$$F_{s(cr)} = K \frac{\pi^2 E}{12(1-\mu^2)} \left(\frac{t}{b}\right)^2 \text{ - - - - - - - - -(1)}$$

Since the web of a beam is subjected to shear stresses, the web shear stresses must be found in order to compare it with the critical buckling shear stress of equation (1).

In Art. A12.3 of Chapter A12, the well-known flexural shear stress equation was derived, namely

$$f_s = \frac{V}{Ib} \int ydA \text{ - - - - - - - - - - - - - -(2)}$$

Since the term $\int ydA$ is maximum for a section at the neutral axis, the shearing stress in a beam will be maximum at the neutral axis. In general, the webs of aircraft beams are relatively thin; thus the term $\int ydA$ for the web is quite small so that the shearing stress intensity over the web is approximately uniform. Thus a simple formula $f_s = V/hb$ has been widely used for calculating the maximum web shearing stress. In this equation h is a distance which will make the shear stress f_s check the maximum value of the shear stress as given by equation (2).

A simple consideration of the internal stresses on a small element cut from a beam in bending and shear will indicate what value of h to use in the simplified shear equation $f_s = V/hb$.

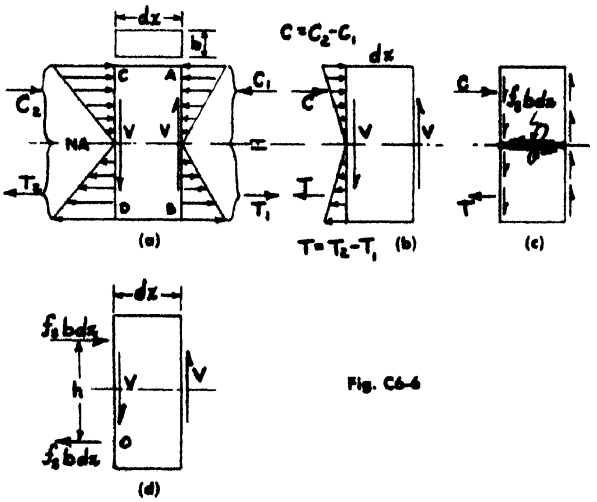


Fig. C6-6

Fig. C6.6a shows a beam element of length dx cut from a beam which is subjected to a bending moment which produces compression on the upper portion. The bending moment on section (AB) is M and on section (CD) M + ΔM, thus the vectors representing the stress on face (CD) are drawn longer than on face (AB). The beam element is also subjected to a total shear force V on each face. C_2 and C_1 represent the resultant of the total compressive forces on each face and T_2 and T_1 the resultant of the tensile stresses. Fig. (b) shows the same free body but with the tensile

and compressive stresses on each face replaced by a simple force C and T which tends to move the block with the same results as the system of Fig. (a). In Fig. (c) the beam element of Fig. (b) has been cut along the neutral axis, and a force applied to the cut faces equal to f_s bdx, where f_s equals the horizontal shear stress intensity.

Writing the equilibrium equation, that the sum of the horizontal forces on the upper portion must equal zero, we obtain

$$C - f_s\ bdx = 0, \text{ hence } C = f_s\ bdx$$

and likewise for the lower - $T + f_s\ bdx = 0$, hence $T = f_s\ bdx$.

Fig. (d) shows the free body of Fig. (b), but with C and T replaced by their above equivalent values.

Taking moments about point (O)

$$M_O = f_s\ bdx \cdot h - Vdx = 0, \text{ hence}$$

$$f_s = \frac{V}{bh} \quad \text{- - - - - - - - - - - - - - - - - (2a)}$$

Thus to obtain a value f_s equal to the maximum value given by equation (2) use an effective arm (h) equal to the distance between the bending stress centroids. For a rectangular section the effective arm is obviously equal to 2/3 the beam height, but for the common beam sections as illustrated in Figs. C6.11 or C6.12, the distance between bending stress centroids is not so obvious particularly, if the web is considered effective in bending. A close approximation of the effective arm (h) and a procedure which is common practice is to assume (h) equal to the distance between the centroids of the web-flange rivets. The student should take several example beam sections and check this assumption for (h) using Eq. (2a) against the exact values by Eq. (2).

Some structural designers make assumptions as to the proportion of the total vertical beam shear which is carried by the beam web. For example, it is sometimes assumed that the web takes the entire beam shear, or it may take only 90 percent. The percentage of the shear load carried by the web depends of course upon the size of the flange sections and the form of the web section. For example in Fig. C6.7, the same flange is connected by a web which is attached to the flanges in two ways as illustrated in Figs. (a) and (b). In Fig. (a), the shear flow on portions (AB) and (CD) help resist the external shear, whereas the shear flow on these portions in Fig. (b) act in the same direction as the external shear load; thus causing the shear load on the web to be greater than the external shear load. (See Chapter A14 and A15 for general discussion of shear flow in open and closed sections).

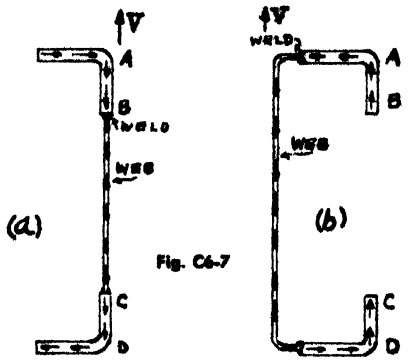


Fig. C6-7

C6.5 Shear Resistance Provided by Sloping Flanges.

A large majority of the beams in airplane wing and tail surfaces have sloping flanges because of the taper of the structure in both planform and thickness. This sloping of the beam flanges relieves the beam web of considering shear load and should not be neglected. Fig. C6.8 shows a beam (abcd) carrying a load system P_1, P_2, etc. The top flange is sloping

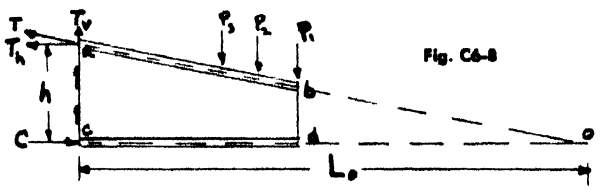


Fig. C6-8

as shown. If both flanges were extended, they would intersect at point (O).

Let M = bending moment at section (ac)

Then $C = T_h = M/h$ (h = distance between flange stress centroids)

The vertical component T_v of the load T in the upper flange equals $T_h\ h/L_O$, but $T_h = M/h$, hence

$$T_v = \frac{M}{h}\frac{h}{L_O} = \frac{M}{L_O}$$

Let V_F = shear load carried by beam flanges

Then $V_F = M/L_O$ - - - - - - - - - - - - - - - - -(3)

Thus the shear component carried by the axial loads in the sloping flange members equals the bending moment at the section being considered divided by the distance from the section to the point of intersection (O) of the flanges.

The above derivation was based on the assumption that the entire resisting moment M was developed by the flanges. With the web effective in bending, the moment developed by the web should be subtracted from the total bending moment M.

Let $I = I_{Fl.} + I_{Web}$

The moment developed by web = $M\frac{I_{Web}}{I}$, where

M = total bending moment on section

In airplane construction the cantilever beam with sloping flange members is the common case, and the shear resistance by the flange axial loads is an important factor which should not be neglected if an efficient structure is desired from a strength-weight standpoint.

C6.6 Effect of Variable Moment of Inertia on Flexural Shear Stress Distribution.

The fundamental shear stress equation (2) as derived in Chapter A12 applies strictly to beams of constant moment of inertia. For airplane beams the common case is one with variable moment of inertia; thus the stresses obtained by equation (2) are incorrect, although the descrepancy in most cases is not large. The student should realize this fact in studying the shear flow picture in tapered wing structures.

C6.7 Critical Shear Stresses for Shear Resistant Webs.

Chapter C7 considers beam design in which the web acts in a semi-tension field condition, and which is a more general type of web design than the one dealt with in this Chapter where the web is considered as a complete shear resistant member, that is, the web does not buckle due to the compressive stresses on diagonal planes due to the shear stresses. As given in Chapter B2, the critical shear stress which produces the diagonal buckling is given by the equation,

$$F_{s(cr)} = \frac{K\pi^2 E}{12(1-\mu^2)} \left(\frac{t}{b}\right)^2 \text{ - - - - - - - - - -(4)}$$

The value of K depends on the edge conditions of the flat sheet and the ratio of its width to length, and can be obtained from Fig. B2.5 of Chapter B2. To increase the critical buckling shear stress F_s, the sheet thickness t must be increased or the size of the flat sheet panel must be decreased, which is done in a beam by decreasing the vertical stiffener spacing.

C6.8 Stiffener Size to Use with Shear Resistant Web.

A web stiffener is used to decrease the size of web panel; thus when buckling of the web starts, the stiffener tends to keep buckles from extending across the stiffener or causes the sheet to buckle in two panels instead of one. Mr. H. Wagner in a paper presented before a meeting of the A.S.M.E. in 1930 offered the following expression as the required moment of inertia of a stiffener to be used with a shear resistant web.

$$I_{st} = \frac{2.29d}{t} \left(\frac{V h_w}{33 E}\right)^{4/3} \text{ - - - - - - - - - -(5)}$$

where

I_{st} = moment of inertia of stiffener

d = center line distance between stiffeners

h_w = depth of web plate

V = vertical shear at section

t = web thickness

E = modulus of elasticity

C6.9 Critical Bending Buckling Stress of Web Plate.

A shear resistant beam web is also subjected to tensile and compression stress parallel to the beam axis due to bending stresses. These compressive stresses acting with diagonal compressive stresses due to web shear stresses tend to reduce the critical shearing stresses as determined by equation (4). Chapter B2, Art. B2.4 and B2.5, gives information on the bending critical buckling stresses for flat sheet panels as well as combined stress relationships.

C6.10 Notes on Rivet Design.

Except for very small beam sections which may be extruded as one piece, the usual beam consists of separate web and flange members, fastened together by rivets, bolts, spot welding or continuous welding. In the design of such beams it is thus necessary to know what loads the rivets, bolts, etc. are subjected to in order to provide the proper connective strength. It is quite easy to substitute in simple formulas to find the loads on beam flange rivets, however, the student should be sure that he understands the fundamental beam action behind these formulas.

Fig. C6.9 illustrates a beam portion equal in length to the flange rivet pitch p. The beam section at (AA') is subjected to a bending moment M and M + ΔM at section (CC'). The bending stress distribution on the beam faces is indicated by the stress triangles. In this example section it will be assumed that the web takes no bending stresses.

Let P_F equal the total pull on the flange angles due to bending stresses at section AB due to bending moment M. Then total pull on flange angles at section CD due to a moment M + ΔM on beam section CC' equals $P_F + \Delta P_F$.

Under the action of these two forces the flange angles would move to the left, but this movement is prevented by the rivet which ties the flange angles to the web. Thus load on rivet equals ΔP_F The same reasoning applies to the rivet holding the bottom flange angles to the web.

The beam portion of Fig. C6.9 as a whole is in equilibrium under the bending stresses and the shear load V on each face.

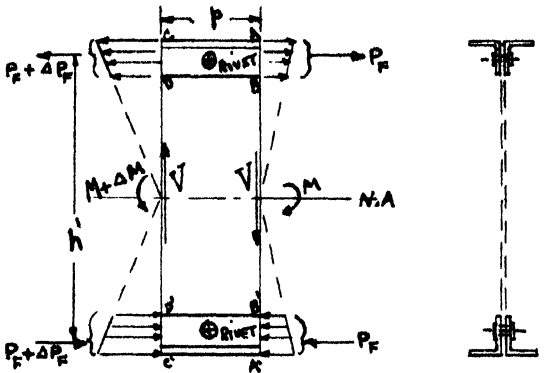


Fig. C6-9

Taking moments about the intersection of the lower flange bending load and the beam face CC',

$$\left[P_F - (P_F + \Delta P_F)\right] h' + Vp = 0 \quad \text{--------(5)}$$

hence

$$\Delta P_F = \frac{Vp}{h'} \quad \text{----------(6)}$$

Equation (6) says that the change in flange axial load in a distance p equals the vertical shear on beam times rivet pitch p divided by the distance between flange bending stress centroids. ΔP_F is also the horizontal shear flow produced by flange angles over a length of p. The horizontal shear (q) per inch due to flange would be

$$q = V/h' \quad \text{----------(7)}$$

The general expression for shear flow (see chapters A12 and A14) is,

$$q = \frac{V}{I}\int ydA \quad \text{----------(8)}$$

Equation (7) is easier to use since the terms I and $\int ydA$ of Eq. (8) are not required, and the distance h can be estimated closely without calculation, and will be greater than the distance between the centroids of the flange areas.

Equation (7) wasderived on the assumption that the beam web took no bending stresses. In general this is not true or only partially true. With the web taking bending, equation (5) would be wrong because the moment of the bending stresses on the web about our moment center is not included. Thus to make the simplified equation (7), check the exact result as given by equation (8), the distance (h) would have to be greater than the distance between the flange stress centroids. In fact, taking (h) equal to beam depth would not be far off from the results of equation (8)

C6.11 Loads on Rivets Attaching Reinforcing Plates to Flange Angles.

The beam flange is commonly composed of a main unit plus several reinforcing plates or parts which are held to the main unit by rivets or spot welds. Fig. C6.10 illustrates typical beam flanges. The basic section of the upper flange is reinforced by the plates (a) and (b), and the lower flange by the plates (c) and (d). The purpose of the rivets is to keep the reinforcing plates from sliding along the flange tee section due to the bending of the beam; thus making the plates effective in bending. This horizontal force tending to slide reinforcing plates and which is prevented by the rivets in shear is given by the fundamental shear flow equation (8), namely

$$q = \frac{V}{I}\int ydA, \text{ which}$$

equals the horizontal shear per inch along the beam. To find the load or rivet section 1-1 of the upper flange of Fig. C6.10, the term $\int ydA$ equals the area of the plate (a) times the distance from its centroid to the neutral axis. For shear load on rivet at section (2-2), the term $\int ydA$ equals the area of plate (b) times distance to neutral axis. On the lower flange rivet section (3-3) is critical since both reinforcing plates are on same side, and the entire shear flow produced by plates (c) and (d) must be resisted by rivet section (3-3). The term $\int ydA$ would thus equal area of both plates times the distance to the neutral axis of the beam.

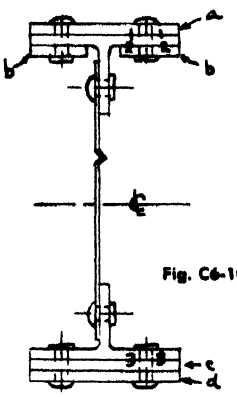


Fig. C6-10

A simplified method which yields good results is based on the relative areas of the units of the total flange. To design connection of flange to beam web, the total horizontal shear q produced by entire flange is always necessary and involves the use of the entire flange area in the shear flow calculation

$$q = \frac{V}{I}\int ydA.$$

The shear flow produced by a reinforcing plate is then taken as proportional to the area of the plate over the total flange area times the total flange shear flow. Using simplified equation (7), we can write

$$q = \frac{V}{h'}\,\frac{a_p}{A_F} \quad \text{----------(9)}$$

where

a_p = area of plates under consideration

A_F = total area of flange

q = load per inch on rivet

V and h same as explained before

For rivet loads in beams with sloping flanges the shear V is the net shear as explained before in disuussing web shear stresses.

C6.12 Web Splices.

Usually in designing a sheet girder beam, it is necessary from a weight saving standpoint to use several web sheet thicknesses, which means web splices. Fig. C6.11 illustrates typical web splices. Fig. (a) is typical for a

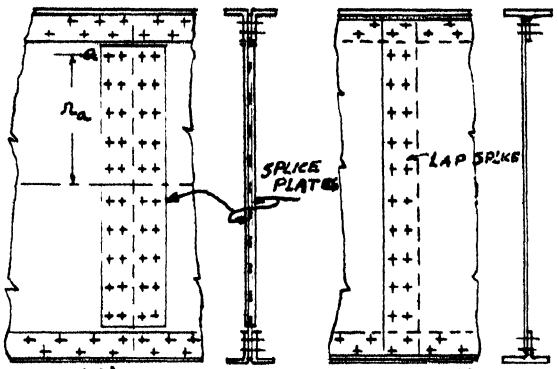


Fig. C6-11

comparatively heavy web which prevents joggling of web as in the case of Fig. (b). In the case of Fig. (b), the lap is usually made under a web stiffener which provides a support for the web in driving the rivets thru the thin web sheets.

Loads on Web Splice Rivets

The web is subjected to shear loads and for stable webs, the web undergoes bending stresses.

For rivet design it is usually assumed that the web shearstress is constant over the depth. Thus the vertical component of load on each web splice rivet is the same or

$$R_V = \frac{V}{n} \qquad (10)$$

where

V = net web shear

n = number of rivets in splice. If butt splice, n, equals the number of rivets on one side of splice.

In bending the splice rivets must transfer the bending moment due to the bending moment M developed by the web. The largest rivet load on a rivet due to bending will be on the most remote rivet, e.g., rivet (a) at distance r_a from center of rotation of the rivet group. Then load on this rivet due to web moment equals

$$R_{m_a} = \frac{M_W r_a}{\Sigma r^2} \qquad (11)$$

where

Σr^2 = moment of rivet group which equals the sum of the squares of the distances of the rivets from the center of rotation of bolt group.

The resultant load on the critical rivet will equal the vector sum of the values of equations (10) and (11).

Since in most cases only two rows of rivets are used in a web splice, a close approximation for the moment load on critical rivet can be written by using the vertical distances (y) to the rivets instead of the radial distances (r), the resulting force acting in the horizontal direction. Hence

$$R_{m_a} = \frac{M_W y_a}{\Sigma y^2} \qquad (12)$$

The resultant combined load on critical rivet is

$$R = \sqrt{R_{V_a}^2 + R_{m_a}^2}$$

The student should review Chapter C4 for more detailed information on rivet loads due to moment loads on riveted connections.

C6.13 Example Problems.

Example Problem #1

Fig. C6.12 shows the cross-section of a riveted beam. If the design vertical shear on the section is 3000#, check the strength of the riveted connection.

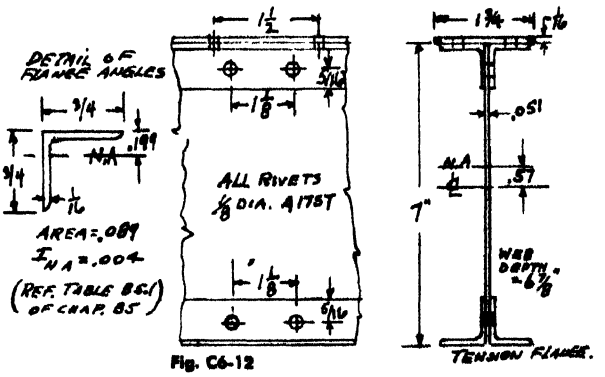


Fig. C6-12

Solution:

The loads on the rivets will be calculated by the "exact" and also by the simplified approximate equations.

The exact shear flow equation is

$$q = \frac{V}{I} \int y dA$$

The first step will be the calculation of the moment of inertia of the beam section about the neutral axis. The bending loads are such as to put the upper flange in compression.

The moment of inertia will be calculated about the centerline axis of the beam section and then transferred to the neutral axis. Table C6.2 gives the detailed calculations.

Table C6.2

Part	Area (A)	y	Ay	Ay^2	I_o*	$I = Ay^2 + I_o$
Upper angles	.1780	3.301	.588	1.94	.008	1.948
Upper reinforcing plate	.1093	3.531	.386	1.36	negl.	1.360
Web	.3510	0	0	0	$1/12 \times .051 \times 6.875^3 = 1.38$	1.380
Lower angles	.1780	-3.301	-.588	1.94	.008	1.948
Rivet hole lower flange	-.022	-3.062	.067	- .206	-	-0.206
SUM =	.7943		.453			6.43

$\bar{y} = \frac{\xi Ay}{\xi A} = \frac{.453}{.7943} = .57"$

$I_{N.A.} = 6.43 - .7943 \times .57^2 = 6.17$ in.^{4}

* I_o = moment of inertia about its own centroidal axis.

Rivet load on upper flange rivets which attach angles to web:

Rivet pitch = 1-1/8 inch

Horizontal shear load per 1-1/8 inch distance equals

$$q = 1.125 \frac{V}{I} \int ydA \quad \text{----------(A)}$$

$\int ydA$ = first moment of flange area about N.A.

= angles = 2 x .089 x 2.731 = .486

Reinforcing plate = 1.75 x .0625 x 2.961 = .324

Total .810

Substituting in equation (A)

$$q = 1.125 \times \frac{3000}{6.17} \times .810 = 443\#$$

Shear flow by simplified equation $q = \frac{V}{h'}$

h' = beam depth = 7.062" (see Art. C6.10)

hence

$$q = 1.125 \times \frac{3000}{7.062} = 478\#$$ which is conservative compared to 443 by exact expression.

The web is attached to angles by 1/8 diameter A17ST aluminum alloy rivets and are acting in double shear.

From Table C4.1 of Chapter C4:

Double shear strength of 1/8 - A17ST rivet = 2 x 331 = 662#.

Bearing strength on 24ST - .051 web plate = 573#, thus bearing is critical and

Margin of safety = $\frac{573}{443} - 1 = .29$ and with the approximate method the Margin of safety would equal (573/478) - .1 = .20

Check on rivets attaching reinforcing plate to angles:

Rivet spacing = 1.5" with two rows of rivets.

By exact equation, load on two rivets

$$q = 1.5 \frac{V}{I} \int ydA$$

$$= 1.5 \times \frac{3000}{6.17} \times .1093 \times 2.961 = 236\#$$

Load per unit = 236/2 = 118#

By simplified formula:

$$q = \left(\frac{V}{h'} \frac{a_{plate}}{a_{flange}}\right) 1.5 = \left(\frac{3000}{7.062} \times \frac{.1093}{.2873}\right) 1.5 =$$

243# = 122#/rivet

The rivets are in single shear which is critical and equals 331# as given above.

Hence Margin of safety = $\frac{331}{118} - 1 = 1.8$

Example Problem #2

Fig. C6.13 shows a built up (I) section beam simply supported and carrying a uniform ultimate design load of 75#/in. The beam will be strength checked for the design load.

Check on Bending Strength

Since the beam cross-section is constant, the critical section in bending occurs at mid-span.

$$M_{max.} = 1/8\ w\ L^2 = 75 \times 100^2/8 = 94{,}000"\#$$

As indicated in Fig. C6.13, the beam is riveted to the sheet covering. On the upper flange which is in compression under the given loading, a certain effective sheet width will act with the beam flange. This effective sheet width depends upon the beam flange stress which is unknown as yet. As a preliminary value,

Table C6.3

Part	Area A	y	Ay	Ay^2	I_o	$I_o + Ay^2$
Upper angles	.264	3.786	1.000	3.786	.012	3.798
Upper skin	.0375	4.012	0.1504	0.604	-	0.604
Web	.2520	0	0		$1/12 \times .032 \times 7.875 = 1.30$	1.300
Lower angles	.1780	-3.801	-0.676	2.570	.008	2.578
Lower skin	.080	-4.01	-0.321	1.290	-	1.290
Skin rivet holes	-.0206	-3.969	0.082	-0.323	-	-0.323
Web flange rivet holes	-.0196	-3.562	0.070	-0.249	-	-0.249
SUM	.771		0.305			8.988

$\bar{y} = .305/.771 = .40$

$I_{N.A.} = 8.988 - .771 \times .4^2 = 8.86$ in.^{4}

I/y upper flange = 8.86/3.6 = 2.46, I/y lower flange = $\frac{8.86}{4.41} = 2.005$

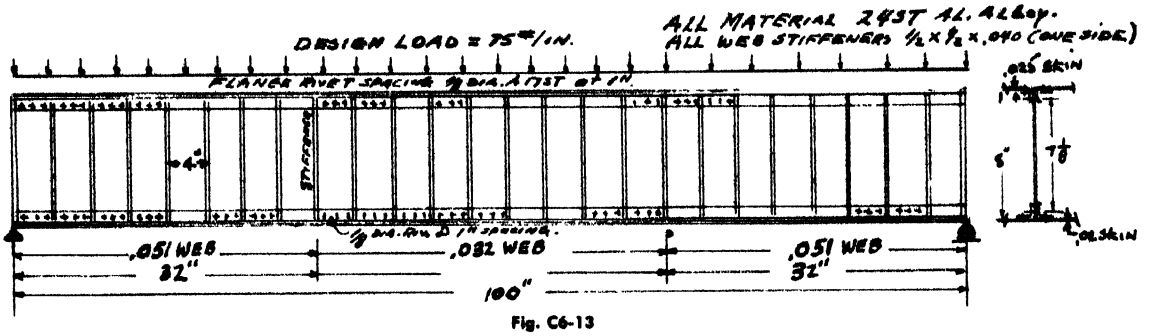


Fig. C6-13

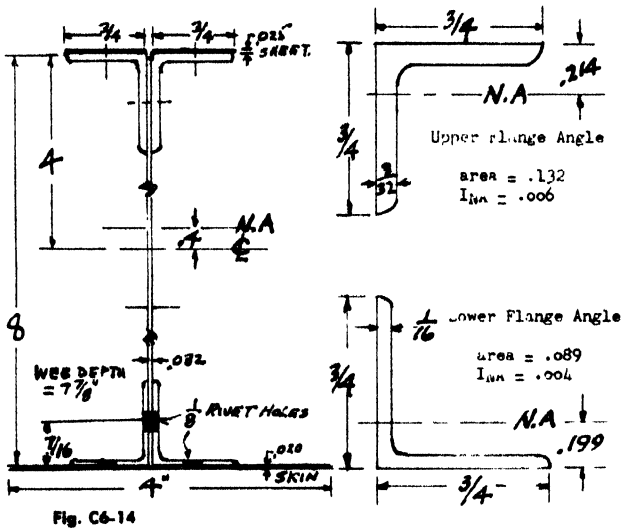


Fig. C6-14

the assumption that a width of skin sheet equal to 30 t as acting with each rivet line is a reasonable one. On the tension or bottom side the entire skin sheet is effective or 2 inches to each side of the beam which is the distance half way to the first skin stiffener on each side.

Fig. C6.14 shows the details of the effective cross-section at midspan of the beam. Three rivet holes are assumed in the tension flange. Table C6.3 shows the calculations for the section properties, first about centerline reference axis, then transferred to the neutral axis.

Maximum bending stress at top edge of the upper flange angles:

$$f_{b(upper)} = \frac{My}{I} = -94{,}000/2.46 = 38{,}300 \text{ psi.}$$

At the midpoint of the outstanding leg of the angles

$$f_b = \frac{-94{,}000 \times 3.55}{8.86} = -37{,}600 \text{ psi.}$$

The assumption of 30 t for effective width of sheet used will now be checked.

From Chapter B4, von Karman-Sechler gives the effective sheet width as $w = 1.90\ t\ \sqrt{E/f_{st}}$, where

f_{st} = stiffener stress. Taking f_{st} = 38,300 psi.

$$w = 1.90 \times .025 \times \sqrt{\frac{10{,}300{,}000}{38{,}300}} = .78".$$ Since 30 t or .75" was assumed, the error is negligible, and also the accurate expression for effective width is still unknown.

The difficult question now is the question of the allowable stress at this point. Since the flange angles are prevented from buckling as a column due to skin and web, a reasonable estimate of the allowable stress would be the crippling stress for the onstanding leg of the angle. This crippling stress can be estimated closely by the methods of Art. B5.4 of Chapter B5.

Thus b/t of leg = (.75 - .093)/.093 = 7.1

From Fig. B5.13 the crippling stress for 24ST extruded material would be 40,400 psi., using a plate element with one edge free. The vertical legs of the angles are riveted together and are stabilized to some extend by the web, thus the crippling stress of this portion would be higher, and after the outstanding leg had buckled this portion could still keep on taking load thus increasing the ultimate internal resisting moment. Thus the apparent stress as computed in equation (c) could no doubt be a few percent higher than the allowable crippling stress of 40,400 psi. The student should realize that the computed bending stress is by the flexure formula derived on the assumption that the stresses are in the elastic range while our stresses are in the plastic range.

The conclusion then is that the beam is safe in bending stresses on the upper flange since the apparent stress is around 38,000 psi and the allowable should be somewhat higher than 40,400 psi.

Tension Flange

f_b = 94,000/2.005 = 46,900 psi.

The allowable tensile stress for 24ST extrusions is 58,000 (see Chapter C1). Hence margin of safety = (58,000/46,900) = .23

The student should try to find the ultimate internal resisting moment of this section by using the method of attack illustrated in Art. C6.3.

Check of Web Buckling Strength

The maximum shear occurs at the support and equals 75 x 50 = 3750#. The web thickness is .051, and the web is stiffened by stiffeners at 4 inch spacing. The maximum shearing stress on web using the simplified equation is

$$f_s = \frac{V}{ht} = \frac{3750}{7.125 \times .051} = 10350 \text{ psi.}$$

(Student should check this value using exact Eq. 2).

The critical shear stress at which buckling occurs is given by the following equation. (See Equation 4, page B2.3)

$$F_{s(cr)} = \frac{K \pi^2 E}{12 (1-\mu^2)} \left(\frac{t}{b}\right)^2$$

To be conservative the four edges of the web panels will be assumed simply supported. With web stiffeners at 4 inch spacing the size of panels between rivet lines will be 7.125 x 4. With a/b = 7.125/4 = 1.78 and using the curve of Fig. B2.5, we obtain K = 6.85, hence

$$F_{s(cr)} = \frac{6.85 \times \pi^2 \times 10{,}300{,}000}{12 (1-.3^2)} \times \left(\frac{.051}{4}\right)^2 =$$

10,000 psi.

The margin of safety on buckling strength of web = (10000/10350) - 1 = - .04. This is not serious since panel edges were assumed freely supported.

Check of .032 Web Portion

Vertical shear at midpoint of first .032 web panel or 34" from end = 3750 - 34 x 75 = 1200#.

$f_s = V/ht = 1200/7.125 \times .032 = 5275$ psi.

$$F_{s(cr)} = \frac{6.85 \pi^2 \times 10{,}300{,}000}{12 (1-.3^2)} \times \left(\frac{.032}{4}\right)^2 =$$

4100 psi.

Thus for buckling strength of the web at this point the web appears weak since the shear stress is 5275. The student should notice that if the edges of the web panel were assumed clamped (see Fig. B2.5) the value of K would be 11.5 thus making F_s = (11.5/6.85) 4100 = 6880 psi. Using an average value for freely supported and clamped edges K = 9.17 and $F_{s(cr)}$ = 5470, which should show a margin of safety.

Check on Rivets Attaching Web to Flange Angles

Rivets for .051 web

$$q = \frac{V}{d'} = \frac{3750}{8} = 468\# \text{ per inch.}$$

Since rivet pitch is 1", load per rivet = 468#.

Load per rivet due to beam distributed load of 75#/in. equals 75#.

Resultant load on rivet at bean end = $\sqrt{468^2 + 75^2} = 475\#$.

Double shear strength 1/8, A17ST rivet = 2 x 331 = 662.

Bearing strength on .051 24ST web = 573#

Margin of safety = (573/475) - 1 = .20

The student should check rivets for .032 web.

Check of Web Stiffener Size

The web is stiffened by 1/2 x 1/2 x .040 angles on one side of web.

From equation (5), moment of inertia required of stiffener to prevent web buckles equals

$$I_{st} = \frac{2.29d}{t} \left(\frac{V h_w}{33 E}\right)^{4/3}$$

$$= \frac{2.29 \times 4}{.051} \left(\frac{3750 \times 7.875}{33 \times 10{,}300{,}000}\right)^{4/3} = .00062$$

Moment of inertia of stiffener = .00094. Thus stiffener is satisfactory.

Example Problem #3

Fig. C6.15 shows a tapered cantilever beam carrying the trapezoidal distributed load as shown. Determine the bending and shearing stresses at section (A-A), and estimate the margin of safety of this section for carrying the given loading. All material is 24ST, and the skin and web is spot welded to the flange.

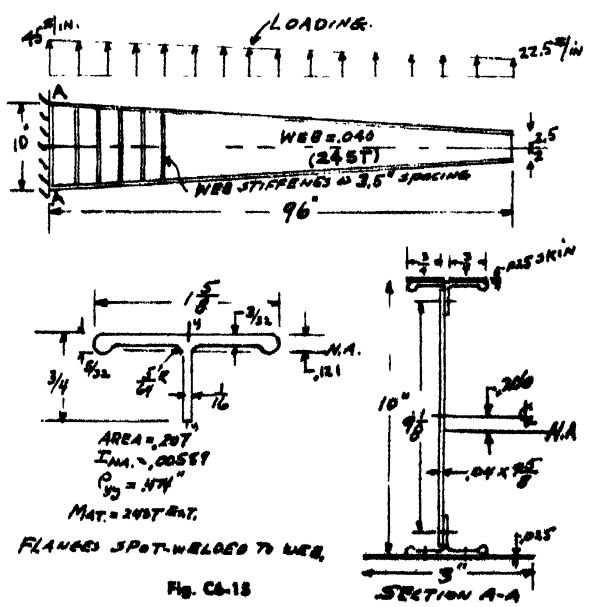


Fig. C6.15

Solution

Bending moment at section A-A:

$M = 22.5 \times 96 \times 48 + 96 \times 11.25 \times 32 = 138,400$ in. lb.

Shear $V = 96 \times 33.75 = 3,240\#$

Calculation of Section Properties at Section A-A

On the compression flange an effective width of skin equal to 30 t will be assumed acting with each row of spot welds. On the tension flange, the full skin width of 3" will be taken, which is the distance midway to adjacent skin stiffener.

Effective width of top skin = $2 \times 30 \times .025 = .75 \times 2 = 1.5$ inches.

Area of section:

Top flange angle = .207

Top skin = $1.5 \times .025 = .0375$

Web = $9.625 \times .04 = .385$

Lower flange angle = .207

Lower skin = $3 \times .025 = .075$

Total = .911 sq. in.

Moment of inertia about center line axis of section:

Angles = $(.00589 + .207 \times \overline{4.879}^2) \; 2 = 9.89$

Skin = $4.5 \times .025 \times 5.0125^2 = 2.84$

Web = $.04 \times 9.625^3/12 = 2.98$

15.71 in.^{4}

Distance to neutral axis from center line axis equals

$$\bar{y} = \frac{1.5 \times .025 \times (-5.0125)}{.911} = -.206"$$

$$I_{N.A.} = 15.71 - .911 \times .206^2 = 15.67 \text{ in.}^4$$

$Q = \int ydA = 5.02 \times .04 \times 2.51 + .207 \times 5.08 + .0375 \times 5.22 = 1.75$ (about N.A.)

Bending Stresses

Tension (lower flange)

$y = 5 - .206 + .025 = 4.819"$

$$f_b = \frac{138,400 \times 4.819}{15.67} = 42,600 \text{ psi.}$$

Since the flange has a slope, the above stress represents the horizontal component of the flange stress at this point. However, this angle is only 1.24 degrees, thus correction $1/\cos 1.24^0$ is negligible. Since the allowable tensile stress of 24ST sheet is 62,000 and 58,000 psi for extrusions, the calculated stress of 42,600 gives a large margin of safety.

Compressive Stress (upper flange)

$y = 5 + .206 - .046 = 5.16$

$$f_b = \frac{-138,400 \times 5.16}{15.67} = -45,600 \text{ psi.}$$

(y has been taken to the midpoint of the horizontal leg of the tee section)

The difficult question now is the allowable ultimate compressive stress.

To obtain a close approximation of the crippling stress of the elements of the T section, the method of Chapters B5, Art. B5.4, will be used.

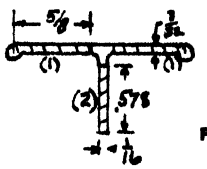


Fig. C6-16

Considering plate element (1) of Fig. C6.16:

$b/t = .625/.0937 = 6.7$

From Fig. B5.13:

$F_{cr} = 53,000$ psi

Plate element (2)

$b/t = .578/.0625 = 9.25$

$F_{cr} = 37,000$ psi

Crippling section for section as a whole:

$$F_{cs} = \frac{\Sigma F_{cr}\, bt}{\Sigma\, bt} = \frac{53,000 \times .625 \times .0937 \times 2 + 37,000 \times .578 \times .0625}{.625 \times .0937 \times 2 + .578 \times .0625}$$

$F_{cs} = -49,200$ psi.

A reasonable allowable bending crippling stress would appear to be somewhere between -49,200 and -53,000; -51,000 will be selected. The question of column action of the flange in the sideways direction should also be considered. The flange is stabilized by the skin to an unknown degree and by transverse ribs at 10.5 inch spacing. To be conservative the lateral column strength of the tee section for a length of 10.5" and end fixity coefficient C = 1.5 will be determined.

$\rho_y = .474"$, $L/\rho = 10.5/.474 = 22$

Using the Johnson-Euler curve for C = 1.5 on page B1.7 of Chapter B1, an allowable column stress of -49,000 psi is obtained when the crippling stress of 51,000 is used for $L/\rho = 0$.

Thus an estimation of the margin of safety for the compressive flange for the given loading is $(49,000/45,600) - 1 = .07$.

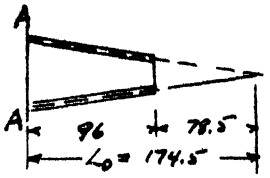
To determine the error of this estimated strength a static test of the section in bending should be made.

Web Stresses

External shear adjacent to section A-A = 3,240#. Since the beam flanges slope they carry part of the beam shear.

From equation (3)

$V_{flange} = M/L_o$



M is the bending moment developed by the flange members at section A-A. Since the web was considered fully effective in resisting bending, the moment developed by the web will be subtracted from the total moment of 138,400 in.#.

$$\text{Moment developed by flanges} = \frac{I_{flange}}{I_{total}} \times M$$

$$= \left(\frac{15.71 - 2.98}{15.71}\right) 138{,}400 = 112{,}000\text{"\#}$$

(The moment of inertia about ℄ axis was used since there is very little difference from that about N.A.)

Therefore shear taken by flange equals 112,000/174.5 = 642 lbs.

Net shear load on web = 3,240 - 642 = 2,598#

$$\text{Maximum shear stress on web, } f_s = \frac{V}{ht} = \frac{2598}{9.125 \times .04}$$

$$= 7120$$

$$\text{By exact formula, } f_s = VQ/It = \frac{2598 \times 1.75}{15.67 \times .04} = 7250 \text{ psi.}$$

Web stiffener spacing = 3.5"

Depth of web panel between spot weld lines = 9.25"

Panel ratio a/b = 9.25/3.5 = 2.64

From Fig. B2.5, K = 6.30

$$F_{s_{cr}} = \frac{K \pi^2 E}{12(1-\mu^2)} \left(\frac{t}{b}\right)^2$$

$$= \frac{6.30\ \pi^2 \times 10{,}300{,}000}{12(1 - .3^2)} \times \left(\frac{.04}{3.5}\right)^2 = 7700 \text{ psi.}$$

Therefore, the web will not buckle at section A-A for the given beam loads which produces a maximum shear stress of 7250 psi.

It is suggested that the student check other sections of the beam and recommend proper tapering of flange section and web gages in order to save weight for the given beam loading.

C6.14 Problems.

(1) Fig. C6.17 shows the cross section of a wing beam. Calculate the ultimate resisting moment for the section using the stress-strain diagram for 24ST extruded material from Fig. C6.4. Use .008 unit strain at extreme fiber of the compression flange. Compare the results with the resisting moment using the general beam formula.

(2) Solve problem (1) but use .009 unit strain on extreme fiber of the compressive flange.

(3) The beam section of Fig. C6.18 is subjected to a design ultimate shear load of 5000#. Determine the margin of safety of all riveted connections, assuming web does not buckle.

(4) Design a butt web splice for the beam section of Fig. C6.12 for a design shear load of V equals 3000# and a bending moment of 50000 in. lbs.

(5) Fig. C6.19 shows a tapered cantilever beam carrying a trapezoidal distributed load. Make a strength check of the beam at section A-A.

(6) A cantilever beam 120 inches long carries a design uniform lateral load of 40 pounds per inch. The depth of the beam at the supported end is 12 inches and 5 inches at the free end, the lower flange being horizontal. Make a complete design of the beam using 24ST extruded and 24ST sheet material. The beam is braced laterally by .025 skin riveted to the top and bottom flanges.

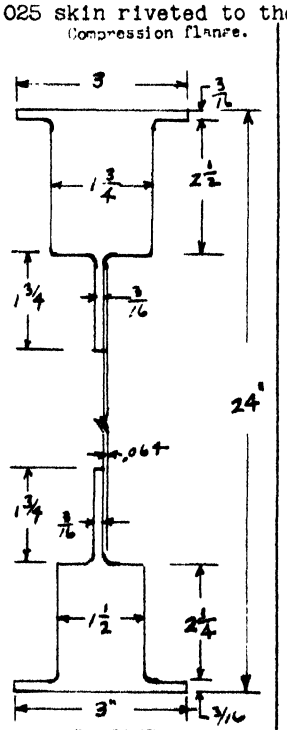


Fig. C6-17

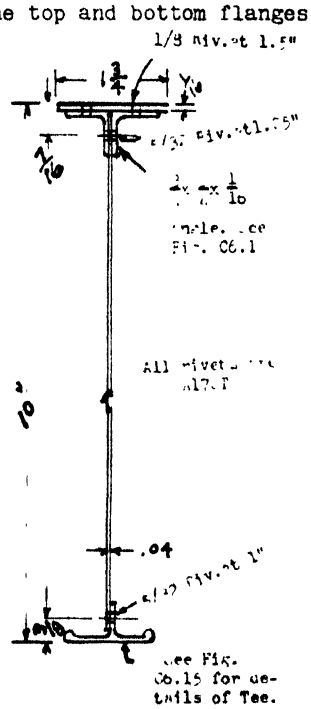


Fig. C6-18

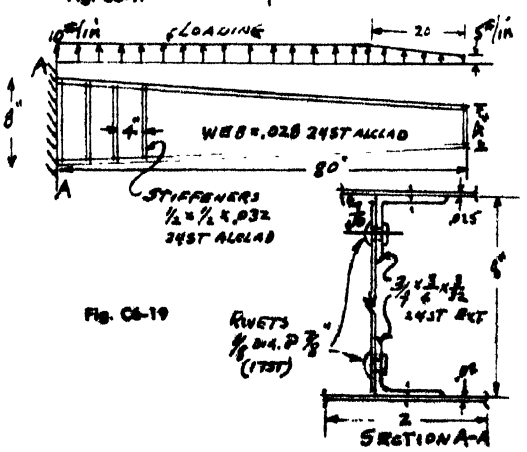
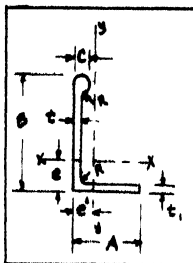
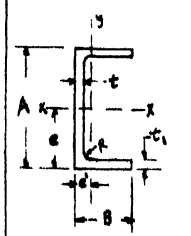
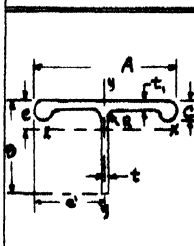
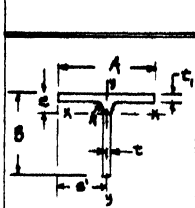
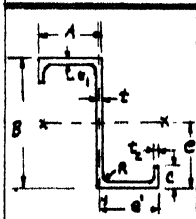
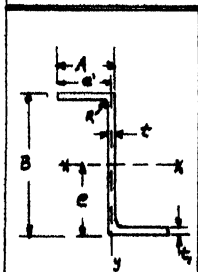


Fig. C6-19

Table C6.4

SECTION PROPERTIES OF TYPICAL AIRCRAFT EXTRUDED SECTIONS

	Sect. No.	Dimensions							Area, $in.^2$	Properties about X-X Axis			Properties about Y-Y Axis		
		A	B	C	t	t_1	t_2	R		I_{xx}	$\bar{c}_{xx}$	e	I_{yy}	$\bar{c}_{yy}$	e'
	1	17/32	13/16	1/8	.040	.050		1/16	.068	.00686	.317	.319	.00150	.148	.112
	2	1/2	1	7/32	.050	.050		.050	.113	.01515	.3665	.510	.00155	.117	.110
	3	1/2	7/8	3/16	1/16	1/16		3/32	.1025	.0100	.313	.383	.00162	.125	.116
	4	9/16	7/8	3/16	.060	.060		3/32	.1031	.0102	.313	.383	.00215	.114	.130
	5	9/16	7/8	3/16	.050	.078		3/32	.1061	.0120	.329	.345	.00302	.165	.133
	6	3/4	1-1/8	3/16	.075	.075		1/16	.1514	.0239	.397	.435	.00550	.190	.182
	7	3/4	1-5/16	9/32	3/32	3/32		9/64	.230	.0507	.471	.574	.0080	.187	.171
	8	7/8	3/8		1/16	1/16		1/16	.095	.0101	.326	.4375	.00111	.108	.108
	9	7/8	3/8		3/32	3/32		3/32	.1375	.0136	.314	.4375	.00148	.104	.118
	10	1	1/2		3/32	3/32		3/32	.1736	.0240	.371	.500	.00376	.147	.158
	11	1-1/4	11/16		3/32	3/32		3/32	.2320	.0536	.480	.625	.00992	.206	.210
	12	1-13/16	1		3/16	3/16		3/32	.644	.2920	.677	.906	.0555	.295	.326
	13	2-1/2	1		1/8	1/8		1/8	.581	.525	.950	1.25	.0662	.338	.323
	14	2-1/4	1-1/8		1/8	3/16		1/8	.666	.524	.888	1.125	.0872	.362	.375
	15	1-3/8	11/16	1/8	1/16	1/16		1/16	.137	.00425	.176	.133	.0178	.360	.687
	16	1-5/8	3/4	5/32	1/16	1/16		1/16	.168	.00580	.186	.133	.0335	.446	.812
	17	1-5/8	3/4	5/32	1/16	3/32		5/64	.206	.00589	.170	.121	.0458	.474	.812
	18	2	1-1/16	3/16	3/32	3/32		3/32	.306	.0252	.287	.201	.0791	.509	1.0
	19	2	1-1/4	3/16	1/8	3/32		3/32	.359	.0475	.364	.300	.0827	.479	1.0
	20	2	1-5/32	1/4	3/32	1/8		1/8	.378	.0291	.279	.217	.1095	.541	1.0
	21	2-5/16	1-1/2	5/16	5/32	5/32		5/32	.668	.1075	.401	.338	.2326	.590	1.156
	22	1-1/2	1-1/8		1/16	1/16		1/16	.161	.0186	.342	.255	.0171	.326	.750
	23	1-1/2	2		1/8	3/32		1/8	.384	.1562	.641	.658	.0346	.302	.750
	24	1-3/4	2		9/32	1/8		1/8	.760	.315	.643	.757	.0599	.281	.875
	25	1-3/4	2-9/16		1/4	5/32		5/32	.918	.600	.809	.959	.0730	.282	.875
	26	2	2-1/2		5/32	1/8		5/32	.605	.385	.800	.793	.159	.514	1.00
	27	11/16	1	1/8	.050	.050	.050	3/32	.135	.0218	.404	.500	.0163	.348	.6625
	28	13/16	1-1/8	3/16	.060	.060	.050	3/32	.180	.0375	.456	.562	.0295	.405	.7828
	29	5/8	1-1/2	3/16	.050	1/16	1/16	3/32	.166	.0603	.595	.75	.0151	.298	.600
	30	3/4	2	1/4	.050	1/16	1/16	3/32	.214	.1382	.793	1.00	.0281	.358	.725
	31	3/4	2	1/4	1/16	1/16	1/16	3/32	.2378	.1449	.773	1.00	.0282	.341	.719
	32	3/4	2	1/4	1/16	3/32	3/32	3/32	.2855	.1820	.795	1.00	.0365	.356	.719
	33	9/16	7/8		.050	.050		1/16	.099	.0120	.349	.437	.0056	.238	.537
	34	1/2	7/8		1/16	1/16		1/16	.115	.0135	.341	.437	.00446	.197	.469
	35	9/16	1		1/16	.080		3/32	.151	.0239	.397	.500	.00828	.234	.531
	36	9/16	1 1/4		.075	.075		3/32	.170	.0384	.475	.625	.00876	.227	.525
	37	11/16	1-1/4		1/16	.100		3/32	.213	.0550	.508	.625	.0194	.302	.655
	38	.825	1-1/2		.075	.120		3/32	.302	.110	.604	.750	.0391	.360	.787
	39	3/4	2		.072	.072		1/8	.249	.1446	.757	1.00	.0180	.267	.714
	40	3/4	2		.102	.102		3/32	.330	.1826	.750	1.00	.0228	.265	.700

CHAPTER C7
DESIGN OF METAL BEAMS: SEMI-TENSION FIELD WEB

C7.1 Introduction.

The aircraft structural engineer is constantly searching for types of structures which will save structural weight and yet be satisfactory from a fabrication and economic standpoint. The introduction and development of the semi-tension field beam or commonly referred to as the "Wagner" beam is an excellent example of the results of such a search.

In Chapter C6, the general beam principles dealing with the design of a beam with shear resistant web (one that does not buckle) was considered. In such a beam the only way the allowable web stresses can be increased is to either increase the web thickness or to decrease the panel web size by adding more web stiffeners. Such a procedure is inefficient from a weight saving standpoint; thus the semi-tension field web type of beam was introduced. (Reference 7.2) In this type of beam the web is permitted to buckle, but provision is made to prevent entire failure or collapse of the beam due to web wrinkling. Much research testing in recent years has been carried out by airplane companies and government agencies to obtain accurate information on which to base the design procedure of such beams, but this information in general is not available to the general public; thus the material in this chapter can be only general in character and cannot discuss the latest design information in this particular problem.

C7.2 Elementary Approximate Explanation of Tension-Field Beam.

Fig. C7.1 shows a single bay truss with double diagonal members (A) and (B) carrying an external load P. The load P will produce a compression on diagonal member (A) and tension in

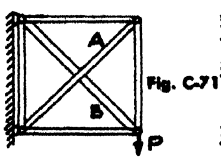


Fig. C-71

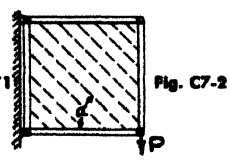


Fig. C7-2

member (B). If member (A) is quite flexible it will buckle under a relatively small load P. As the load P is increased above this value, the diagonal (A) will not take any more load than that which caused it to buckle; but member (B) being in tension is capable of taking any increase of panel shear due to an increase in the load P. Thus when P becomes large the proportion of the panel shear carried by the buckling strength of (A) is negligible.

Fig. C7.2 shows the same frame as in Fig. C7.1 but with the diagonal members replaced by a thin sheet. Under a small load P the web is shear resistant. The shearing stresses in the sheet produce compression stresses in a direction parallel to diagonal (A) and tensile stresses parallel to member (B). (Reference Art. A4.3 of Chapter A4). The web sheet being quite thin can carry only small compressive stresses in the (A) direction; thus the sheet buckles and folds into corrugations parallel to the lines in Fig. C7.2. In the direction parallel to the lines in Fig. C7.2, the sheet is in tension thus having the capacity to carry any increase of panel shear due to a further increase of load P; whereas, the compressive stresses normal to the folds remain practically at the same small stresses which caused the buckling of the sheet. Such a beam panel which carries its shear load by a diagonal tension field in the web after the web has wrinkled, constitutes the fundamental action in the "Wagner beam". Figs. C7.3, 4 and 5 show photographs of so-called Wagner beams under loadings which cause wrinkling of the web in to diagonal folds. Fig. C7.6 shows two photographs of a thin sheet panel subjected to shear loads. Fig. (a) shows the condition of the web for stresses slightly above the sheet buckling stress; whereas, Fig. (b) shows the web condition under stresses far above the critical buckling stress.

C7.3 Elementary Derivation of Approximate Tension-Field Beam Formulas.

In order to give the student a general picture of the influence of web tension field action upon the beam component parts, an elementary approximation of the beam equations will be given.

Fig. C7.7 shows a cantilever beam with parallel chords and vertical stiffeners subjected to a single shear load V at the free end. The dashed diagonal lines indicate the direction of the wrinkles as the thin sheet buckles under the load V.

Assuming that the flange angles develop all the bending resistance, the vertical and horizontal shearing stress is constant over the web and equals

$$f_s = \frac{V}{ht} \quad \text{- - - - - - - - - - - - - - - - - - (1)}$$

where

t is web thickness
h is taken as the distance between centroids of flange rivets.
V = vertical shear load.

(From Ref. 7.1)

Fig. C7-3

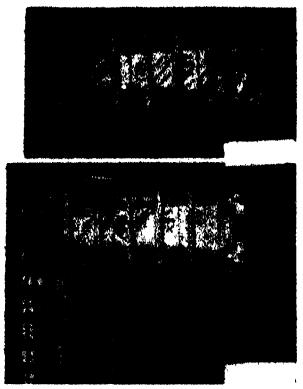


Fig. C7-4

(From Ref. 7.1)



Fig. C7-5

(From Ref. 7.1)



(a)

(b)

Fig. C7-6

(From Ref. 7.3)

Fig. C7.8 shows the free body diagram of a small triangular segment of the web cut from the upper portion of the beam.

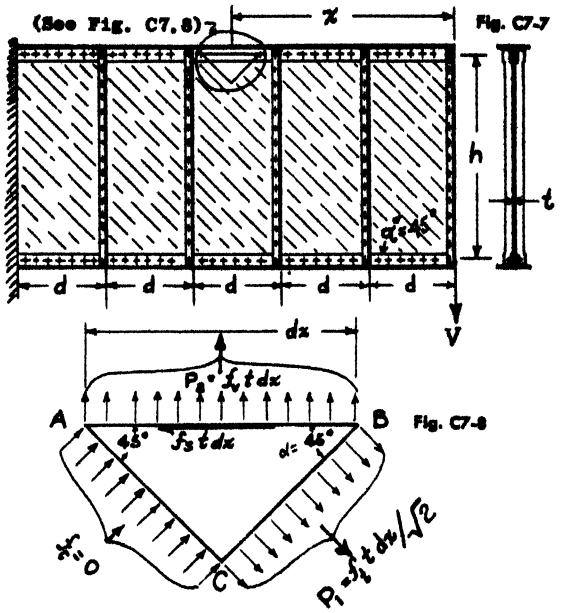


Fig. C7-8

From elementary mechanics (Reference Chapter A4) the horizontal and vertical shearing stresses produce compressive and tensile stresses on planes at 45° with the shearing planes.

The web, being very thin, can carry very little compression stress on the surface (AC) of Fig. C7.8 before buckling; thus this small stress which produces buckling on AC will be neglected or $f_c = 0$. The edge BC is subjected to tensile stresses which the sheet can carry effectively. The forces acting on the sheet element are shown in Fig. C7.8.

For equilibrium of the element:

$$\Sigma F_X = 0 \text{ or } -f_s\, tdx + f_t\, \frac{tdx}{\sqrt{2}} \cdot \frac{1}{\sqrt{2}} = 0$$

whence

$$f_t = 2\, f_s \quad \text{----------(2)}$$

or the web tensile stress equals twice the web shearing stress:

From (1) $f_s = V/ht$

whence

$$f_t = 2V/ht \quad \text{----------(3)}$$

Likewise for equilibrium:

$$\Sigma F_y = 0 \text{ or } f_v\, tdx - f_t\, t\, \frac{dx}{\sqrt{2}} \cdot \frac{1}{\sqrt{2}} = 0$$

whence

$$f_t = 2\, f_v \quad \text{----------(4)}$$

hence

$$f_v = f_s \quad \text{----------(5)}$$

Rivet Loads

The sheet element is held to the flange angles by the rivets along line (AB). The rivets are subjected to two loads, one parallel to AB and one normal to AB; and each force equals f_s tdx. The resultant rivet load therefore equals $\sqrt{2}\ f_s$ tdx; and if dx is taken as one inch, the resultant load will be $\sqrt{2}\ f_s$ t.

But $f_s = V/ht$, hence

Rivet load/inch = 1.41 V/h- - - - - - - -(6)

Web Stiffener Load

The tendency of the web is Fig. C7.7 which has broken down into the tension bands, is to pull the flanges together; this action is prevented by the vertical stiffeners which keep the flanges apart. Thus if a complete tension field is assumed, the axial compressive load P_s in the stiffeners from Fig. C7.9 equals the vertical component of the web tensile stresses over a distance (d), the stiffener spacing.

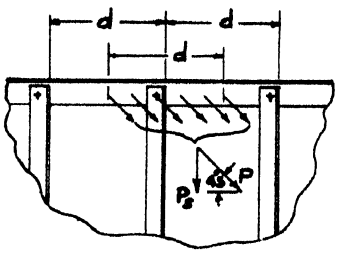


Fig. C7-9

whence

$$P_s = P \sin \theta$$

But

$$P = f_t\ dt\ 1/\sqrt{2}$$

hence

$$P_s = \frac{1}{\sqrt{2}}\ \frac{1}{\sqrt{2}}\ f_t\ dt = f_t\ dt/2$$

but

$$f_t = 2\ f_s \text{ and } f_s = V/ht$$

whence

Stiffener load P_s = Vd/h compression - -(7)

Flange Axial Loads

Fig. C7.10 shows a free body of the portions of the beam to the right of a section a distance x from the end of the beam.

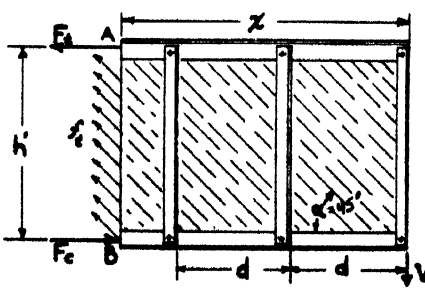


Fig. C7-10

Let M_x = external bending moment at Section AB. For equilibrium the internal resisting moment on Section AB must equal external bending moment M_x.

Taking moments about point B:

$$\Sigma M_B = M_x - F_t\ h' - f_t \cos 45^\circ\ h'\ t\ .\ \cos 45^\circ\ .\ \frac{h'}{2} = 0 \text{ - - - - - - - - - - - - - - - - - -(8)}$$

where

h' = distance between flange centroids

But

$f_t = 2\ f_s$ and $f_s = V/h't$, hence $f_t = \frac{2\ V}{h't}$

Substituting this value of f_t in Eq. (8)

$$M_x - F_t\ h' - \frac{Vh'}{2} = 0$$

whence

$$F_t = \frac{M_x}{h'} - \frac{V}{2} \text{ - - - - - - - - - - - - - - - (8a)}$$

Then to make $\Sigma H = 0$ on Section AB:

$$F_c = \frac{M_x}{h'} + \frac{V}{2} \text{ - - - - - - - - - - - - - - - -(9)}$$

Thus the compressive flange axial load due to bending is increased by a value equal to V/2 lbs. and the tension flange load due to bending is decreased by V/2 due to the horizontal components of the web tension field.

C7.4 General Wagner Equations for Tension Field Beams.

The approximate elementary derivation given in the previous article was for the purpose of giving the student a general idea of the influence of a complete tension field beam on the various beam stresses. The angle α is in general not 45° but depends on flange areas, beam height, stiffener spacing, etc.

The general equations derived by Wagner (Ref. 7.1) are as follows:

For beams with infinitely rigid and parallel flanges with vertical web stiffeners:

Diagonal tensile stress in web:

$$f_t = \frac{2V}{ht} \cdot \frac{1}{\sin 2\alpha} \text{ - - - - - - - - - - - (10)}$$

Axial load in tension flange:

$$F_t = \frac{M}{h'} - \frac{V}{2} \cot \alpha \text{ - - - - - - - - - - - (11)}$$

Axial load in the compression flange:

$$F_c = -\frac{M}{h'} - \frac{V}{2} \cot \alpha \text{ - - - - - - - - - - (12)}$$

Axial force in stiffeners:

$$F_{Stiff.} = -V \frac{d}{h} \tan \alpha \text{ - - - - - - - - - (13)}$$

In the above equations:

V = applied shear load
h = distance between centroids of flange-web rivets

h' = distance between centroids of flange sections
t = web thickness
d = vertical web stiffener spacing
α = angle of web buckle (see Fig. C7.10)

In deriving equations (10) to (13) Wagner assumed that the beam flanges were infinitely stiff in bending. Actually the flanges due to the lateral pull of the web tension field will act somewhat as a continuous beam over the web stiffeners as supports, as illustrated in Fig. C7.11. The deflections of the beam flanges relieves the web stress in the midportion of the panels and concentrates the web stress near the stiffeners where deflection of the flange is prevented.

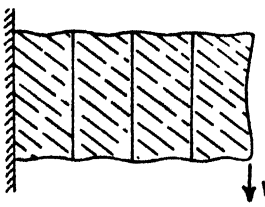


Fig. C7-11

Wagner (Ref. 7.1, Part III) has developed a correction factor R to take care of this web stress concentration due to flange deflection. This stress ratio factor is obtained from Fig. C7.12 and the following equations:

$$wd = 1.25\, d \sin\alpha \sqrt[4]{\frac{t}{(I_u + I_L)h}} \quad \text{- - - - - (14)}$$

d = stiffener spacing

I_u and I_L = moment of inertia of upper and lower beam flanges about their own neutral axis.

Wagner also has derived the following equations for determining the web buckle angle α as follows:

$$\sin^2\alpha = \sqrt{a^2 + a} - a \quad \text{- - - - - - - - - - (15)}$$

where

$$a = \frac{1 + \dfrac{ht}{A_u + A_L}}{\dfrac{dt}{A_s} - \dfrac{ht}{A_u + A_L}} \quad \text{- - - - - - - - - - (16)}$$

A_u and A_L = area of upper and lower flanges including reinforcing plates but neglecting web material.

A_s = area of stiffener

C7.5 Modified Wagner Equations for Use in Design.

The Wagner equations are too conservative for design, particularly in the web stresses and the loads in the vertical stiffeners. The shear stress carried by the web before it buckles is in many cases an appreciable part of the total resistance, as the buckled sheet normal to the diagonal compressive stresses has the ability to hold this buckling shear load after wrinkling. The load in the vertical stiffener is too conservative, since the stiffener is riveted to the web and the web is riveted to the flange; thus the web acts as a large gusset plate instead of a pin end condition as assumed in the Wagner equation.

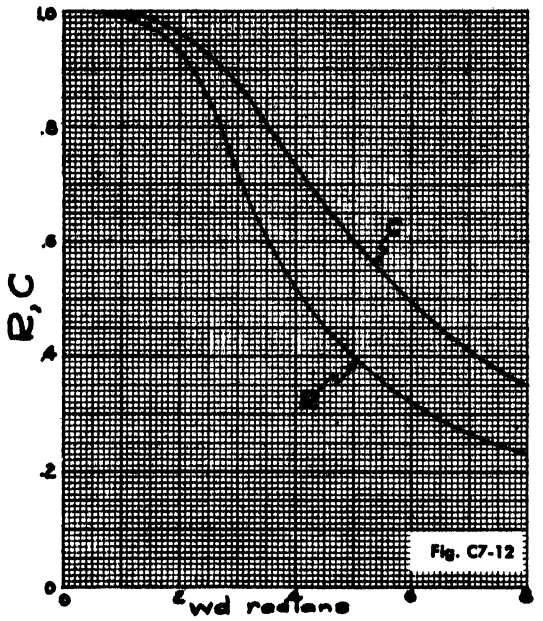


Fig. C7-12

The following general method of analysis of Wagner beams has been used by many airplane companies. Instead of assuming that the entire beam shear is taken by the web in diagonal tension, the following assumptions are made relative to the resistance for carrying the beam vertical shear.

(1) The shear strength of the beam flanges is not neglected.

(2) The shear carried by the web before it buckles, that is, as a shear resistant member is considered as an effective resistance and not neglected.

(3) The remainder of the beam shear after subtracting that carried by (1) and (2) is considered carried by the web in a buckled state in the form of a diagonal tension field.

The above assumptions apply to beams with parallel flange members. If the beam has sloping flanges, part of the beam shear will be carried by the shear component of the flange axial loads, and thus the assumptions should be applied to the net beam shear.

C7.6 Shear Carried by the Beam Flanges.

The general flexural shear flow equation is

$$q = \frac{V \int ydA}{I} = \frac{VQ}{I} \quad (\text{if } \int ydA \text{ is given symbol } Q)$$

For beam flange and web arrangements commonly used in aircraft structures the shear stresses are approximately constant over the web, that is, between the centroids of the flange-web

rivets. Using this assumption, the value Q in the above equation equals the static moment of the flange area about the neutral axis of the beam, and I equals the moment of inertia of the flange area about neutral axis. (web area is neglected).

The shear load resisted by the web alone therefore equals

$$V_w = \frac{VQh}{I} = \frac{V}{I/Qh} \quad \text{- - - - - - - - - - - - (17)}$$

where

h = effective web depth = distance between centroids of flange-web connection rivets.

The total beam shear V which equals the resistance of both web and flange, equals

$$V = \frac{V_w I}{Qh} \quad \text{- - - - - - - - - - - - - - - - (18)}$$

The difference between (17) and (18) gives the shear carried by flanges.

C7.7 Shear Load Carried by Web.

Up to the buckling stress of the web plate, the shear flow is assumed to be of constant intensity over the effective web depth. When the web buckles, it is assumed that the web maintains the diagonal critical compressive stress that produced the buckling of the plate. For further increase of shear load on the web, the entire resistance is provided by the increase in diagonal tensile stresses with no increase in the diagonal compressive stresses. In other words, for loads above the web buckling point, the web acts as a pure tension field beam. Fig. C7.13 illustrates these assumptions.

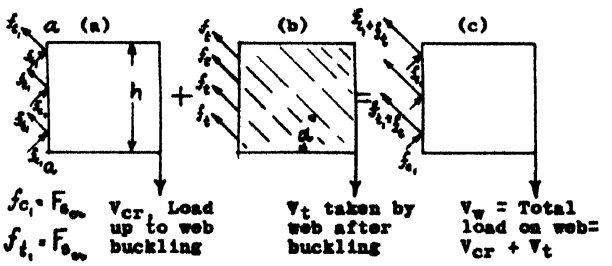


Fig. C7-13

Shear Load Carried by Web at Web Buckling Stress

Fig. (C7.13A) shows the shear resistance on the web face (aa) when the web is shear resistant. The vertical shear stresses on (aa) have been replaced by the diagonal compressive and tensile stresses. The intensity of these diagonal stresses equals the intensity of the critical shearing stress $F_{s_{cr}}$ (see Art. A4.3 of Chapter A4).

Hence the shear load carried by the web at the web buckling stress equals

$$V_{cr} = F_{s_{cr}} h t \quad \text{- - - - - - - - - - - - (19)}$$

The critical shear buckling stress is given by the following equation from Art. B2.3

$$F_{s_{cr}} = K_s E \left(\frac{t}{b}\right)^2 \quad \text{- - - - - - - - - - - (20)}$$

where K is a function of the aspect ratio a/b of the shear panel and of the edge conditions. Fig. B2.5 of Chapter B2, gives the value of K for edges simply restrained. Taking a value of K for condition, this edge condition is no doubt slightly conservative.

Shear Load Carried by Web after Buckling

Fig. (C7.13B) shows the web stress distribution that is assumed to be subjected to the web when the web shear load is increased above that which caused the web to break down into a tension field. The diagonal tensile stress f_t tends to pull the beam flanges together, and thus to bend the flanges. The diagonal tensile stress f_t for the shear resistant web does not produce such action. To obtain the maximum combined tensile stress in the web, the stress f_t must be multiplied by a concentration factor 1/R from Fig. C7.12.

Hence

$$f_{t_{(max.)}} = \left(\frac{f_t}{R} + F_{s_{cr}}\right) \quad \text{- - - - - - - - - (21)}$$

Solving for f_t

$$f_t = \left(f_{t_{(max.)}} - F_{s_{cr}}\right) R \quad \text{- - - - - - - - (22)}$$

If the web is riveted to the flanges and web stiffeners, part of the web material is cut away due to the rivet holes thus the tensile stress of equation (21) must be multiplied by a rivet correction factor $1/K_r$ to obtain the true $f_{t_{max.}}$.

Hence for riveted connections:

$$f_{t_{(max.)}} = \left(\frac{f_t}{R} + F_{s_{cr}}\right) \frac{1}{K_r} \quad \text{- - - - - - - (23)}$$

whence

$$f_t = \left(f_{t_{(max.)}} - \frac{F_{s_{cr}}}{K_r}\right) K_r R \quad \text{- - - - - (24)}$$

Where

$$K_r = \frac{\text{rivet spacing - rivet diameter}}{\text{rivet spacing}}$$

Equation (22) would apply for webs spot welded to flange members.

The vertical components of the total f_t stresses on the web effective depth (h) would thus equal the shear load V_t developed by the web after buckling.

For spot welded flange, web and stiffeners connections:

$$V_t = \left(f_{t_{max.}} - F_{s_{cr}}\right) R h t \sin\alpha \cos\alpha \quad \text{- - (25)}$$

For riveted connections:

$$V_t = \left(f_{t_{max.}} - \frac{F_{s_{cr}}}{K_r}\right) K_r R h t \sin\alpha \cos\alpha \quad \text{- (26)}$$

If $ft_{max.}$ is taken as the tensile yield point stress F_{ty} or the ultimate tensile stress F_{tu} equations (25) and (26) will give the shear load carried by the web above the buckling load when the web is stressed to the yield and ultimate tensile strengths respectively.

Thus for yield strength:

$$V_{ty} = (F_{ty} - \frac{F_{s_{cr}}}{K_r}) K_r R h t \sin\alpha \cos\alpha \quad - (27)$$

(riveted connect.)

$$V_{ty} = (F_{ty} - F_{s_{cr}}) R h t \sin\alpha \cos\alpha \quad - - - (28)$$

(Spot welded connect.)

For ultimate strength:

$$V_{tu} = (F_{tu} - \frac{F_{s_{cr}}}{K_r}) K_r R h t \sin\alpha \cos\alpha \quad - - (29)$$

(riveted connect.)

$$V_{tu} = (F_{tu} - F_{s_{cr}}) R h t \sin\alpha \cos\alpha \quad - - - (30)$$

(spot welded connect.)

The total yield shear resistance of the web equals

$$V_{w_{ty}} = (V_{cr} + V_{ty}) \quad - - - - - - - - - - - (31)$$

Total ultimate web shear resistance:

$$V_{w_{tu}} = (V_{cr} + V_{tu}) \quad - - - - - - - - - - - (32)$$

Total beam shear resistance equals equations (31) or (32) multiplied by $\frac{I}{Qh}$ (Ref. Equation 18)

hence

$$V_{yield} = \frac{I}{Qh} (V_{cr} + V_{ty}) \quad - - - - - - - (33)$$

$$V_{ult.} = \frac{1}{Qh} (V_{cr} + V_{tu}) \quad - - - - - - - - (34)$$

Substituting values from equations (27 to 30) for V_{ty} and V_{tu},

For spot welded connections:

$$V_{yield} = \frac{It}{Q}\left[F_{s_{cr}} + (F_{ty} - F_{s_{cr}}) R \sin\alpha \cos\alpha\right] \quad - (35)$$

$$V_{ult.} = \frac{It}{Q}\left[F_{s_{cr}} + (F_{tu} - F_{s_{cr}}) R \sin\alpha \cos\alpha\right] \quad - (36)$$

For riveted connections:

$$V_{yield} = \frac{It}{Q}\left[F_{s_{cr}} + (F_{ty} - \frac{F_{s_{cr}}}{K_r}) K_r R \sin\alpha \cos\alpha\right] - (37)$$

$$V_{ult.} = \frac{It}{Q}\left[F_{s_{cr}} + (F_{tu} - \frac{F_{s_{cr}}}{K_r}) K_r R \sin\alpha \cos\alpha\right] - (38)$$

C7.8 Beams with Parallel Flanges but with Oblique Web Stiffeners.

Wagner has developed equations for the condition where stiffeners are placed at an angle with the parallel flange members. (Fig. A) In this case equations (27) to (30) should be multiplied by a correction factor equal to $(1 - \tan\alpha \cot\beta)$ where β is the upright angle. For oblique stiffeners the wrinkle field angle α is equal to $\beta/2$ and the concentration factor R can be taken as unity. Hence the equations for V_{ty} and V_{tu} become as follows:

$$V_{ty} = 1/2 \ (F_{ty} - \frac{F_{s_{cr}}}{K_r}) K_r h t \frac{1 - \cos\beta}{\sin\beta} \quad - - -(38a)$$

$$V_{tu} = 1/2 \ (F_{tu} - \frac{F_{s_{cr}}}{K_r}) K_r h t \frac{1 - \cos\beta}{\sin\beta} \quad - - -(38b)$$

(For spot welded joints, omit term K_r)

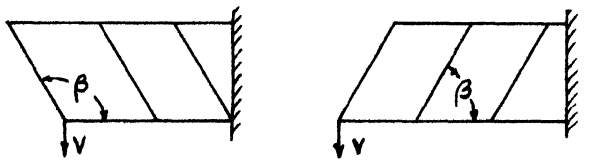


Fig. A

C7.9 Rivet Loads.

The loads on the rivets connecting the flanges to the web consists of two parts, (1) that due to the web acting as a shear resistant member subjected to stresses which cause web buckling, and(2) that due to the web tension field for web stresses above the web buckling stress.

Rivet Load At Web Buckling Stress

$$P_{x_{cr}} = \frac{V_{cr} I_F}{h I} \quad - - - - - - - - - - - - - (39)$$

where

$P_{x_{cr}}$ = load on rivet parallel to flange in #/in.
I_F = moment of inertia of flanges about beam neutral axis
I = moment of inertia of total beam section
h = distance between flange rivet centroids
V_{cr} = buckling shear strength of web, #

Rivet Loads for Tension Field Action

In Fig. C7.14 the web element (abc) is attached to the flange along line (ab). A vertical depth (bc) of 1 inch has been taken. The shearing stress on this length due to V_{tu} equals V_{tu}/h. This load represents the vertical component of the tension field, hence

$$P_t = \frac{V_{tu}}{h \sin\alpha} \quad - - - - - - - - - - - - - (40)$$

Resolving the tension load P_t into x and y components on rivet line (ab) and dividing by the length ab to get rivet loads per inch, we obtain

$$P_y = \frac{V_{tu} \sin\alpha \sin\alpha}{h \sin\alpha \cos\alpha} = \frac{V_{tu}}{h} \tan\alpha \quad - - - - (41)$$

$$P_x = \frac{V_{tu} \cos\alpha \sin\alpha}{h \sin\alpha \cos\alpha} = \frac{V_{tu}}{h} \quad - - - - - - - (42)$$

Combining the three component rivet forces as given in equations 39, 42 and 41 to obtain resultant load R on rivet.

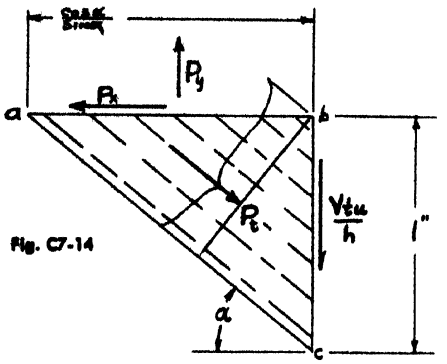


Fig. C7-14

$$P_r = \left[\left(\frac{V_{cr}\ I_F}{h\ I} + \frac{V_{tu}}{h}\right)^2 + \left(\frac{V_{tu}}{h}\tan\alpha\right)^2\right]^{1/2} \quad - - (43)$$

C7.10 Flange Loads.

The axial flange loads are due to two primary causes, namely

(1) Stresses due to primary bending of the beam by the usual flexural theory.

(2) Additional stresses produced by the web tension field.

In addition to these two primary effects, secondary bending stresses due to the bending of the flange because of the tension field are produced as illustrated in Fig. C7.11.

Stresses for Primary Bending:

$$f_b = \pm\frac{M_{cr}\ y}{I} \pm \frac{(M - M_{cr})y}{I_F} \quad - - - - - - (44)$$

where

I = moment of inertia of total section including web about neutral axis

I_F = moment of inertia of section without web about neutral axis

M_{cr} = bending moment for load which causes web buckling

M = total bending moment on section

The first term in the above equation gives the bending stresses at the point where the web breaks down into a tension field. The web is thus effective in computing the moment of inertia.I. The second term in the equation gives the bending stresses when the beam web acts as a tension field web, or in other words the buckled web is assumed ineffective in bending.

To be slightly conservative the bending stresses can be computed by the following equation which neglects the resistance of the web in bending before buckling.

$$f_b = \pm\frac{My}{I_F} \quad - - - - - - - - - - - - - - - (45)$$

The total flange loads can be calculated by equating the internal resisting couple to the external resisting couple to the external bending moment, or

$$F_c = F_t \pm \frac{M}{h'} \quad - - - - - - - - - - - - - - - (46)$$

where

F_c and F_t = total compressive and tensile flange load respectively

h' = distance between flange centroids

Equation (46) neglects the resistance of the web in bending.

Flange Axial Stresses Due to Web Tension Field

Due to the horizontal components of the diagonal tension field each flange is subjected to a compressive load equal to

$$F_c = F_t = -\frac{V_t}{2}\cot\alpha \quad - - - - - - - - - - (47)$$

(Reference see Equation (12) and general derivation when $\alpha = 45^0$ see Equation (8) and (9).

In Equation (47) V_t = shear load carried by tension field action.

Secondary Bending Stresses

For estimating the secondary bending moments on flanges due to lateral pull of web tension field, the flange can be treated as a continuous beam with spans equal to the stiffener spacing.

The component of the web diagonal tensile stresses normal to flange.

$$w_v = \frac{V_t}{h}\tan\alpha \text{ (pounds per inch)} \quad - - - (48)$$

where

V_t = shear carried by web in diagonal tension

For a continuous beam of equal spans, the moment over the supports = $1/12\ w_v\ d^2$, where d equals the stiffener spacing. The deflection of the flanges tends to relieve the pull in the center portion between stiffeners which then decreases the continuity moment over the support. Wagner (Ref. 7.1) gives a relieving factor C (See Fig. C7.12) for use with the bending moment expression.

Therefore, the secondary bending moment on flanges is

$$M_{sec} = 1/12\ C\ \frac{V_t}{h}\ d^2\tan\alpha \quad - - - - - - (49)$$

C7.11 Loads in Web Vertical Stiffeners.

No theoretical analysis which gives satisfactory results has been developed which gives the loads in the web stiffeners or loads on which to base the design of the stiffener. Some recent studies and tests on this problem have been carried out by government research agencies but such information is not available to the public. No doubt some airplane companies have carried out enough study and research on this stiffener design

question to place it upon a reasonably rational basis, but such information is usually not published.

If the web stiffeners were riveted only to the flange members, the axial load in the stiffeners tending to hold the flanges apart due to the lateral pull of the web tension field could be reasonably calculated as given by equation (13). However the stiffener is riveted in the web; thus a certain amount of the web acts with the stiffener. Tests indicate that the stress in the stiffener after the web has wrinkled is considerably greater near the middle than near the ends. The web stiffener prevents the buckled tension field from extending across the stiffener. This breaking up of the tension fields at the stiffener point no doubt places considerable torsion on the stiffener thru the medium of the web folds pulling on the rivet heads. The failure of a stiffener is therefore due to a combination of column, bending and torsional loads acting upon the stiffener. Until more definite information is available on the design of web stiffeners the following method proposed originally by Wagner (Ref. 7.1 II) which is conservative can be used in checking the strength of stiffeners.

The axial column load in the web stiffener equals

$$F_{stiff.} = - V_t \frac{d}{h} \tan \alpha \quad - - - - - - - - - \quad (50)$$

This is the same as equation (13) except V is replaced by V_t, the shear carried by the web in diagonal tension field action. Under this load Wagner considers the stiffeners as columns with elastic supports as the web tension restrains the struts from buckling out of the plane of the web. Wagner's calculations yield a reduction factor C_s which the actual length of the stiffener is multiplied by to obtain a reduced length L', or

$$L' = C_s L \quad - - - - - - - - - - - - - - - - - \quad (50a)$$

With this reduced length L', and the actual cross section of the strut, the column strength can be calculated by the methods of Chapters B1 and B5. Fig. C7.15 by Wagner shows a plot of the reduction factor C_s which is a function of the parameter as shown.

It is general practice if possible to attach stiffener to each flange by two rivets and to place the first two or three stiffener-web rivets adjacent to the flange at closer spacing than on the balance of the stiffener-web connection. To keep the web from pulling off rivet heads of stiffener rivets due to web wrinkles, round head rivets should be used.

C7.12 Beams with Non-Parallel Flanges.

In many aircraft beams the flanges are not parallel but have a slight taper. For this case equations (46) and (47) give only the horizontal components of the flange loads. The total flange forces and their vertical components can be computed from the horizontal components and the slope of the flanges. Thus from Fig. C7.15a subtracting the vertical components of the flange forces we obtain the net web shear load V_{w_n}.

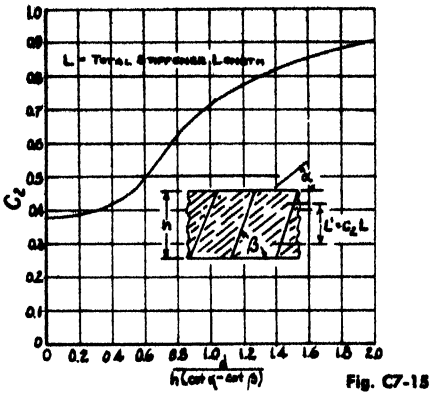


Fig. C7-15

$$V_{w_n} = V_w - (F_t \tan \theta_t + F_c \tan \theta_c) \quad - - - \quad (51)$$

where

V_{w_n} = net web shear for beam with non-parallel flanges

V_w = web shear for parallel flanges

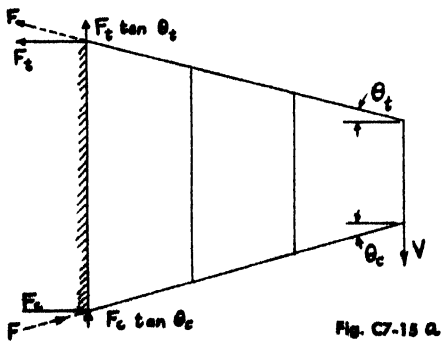


Fig. C7-15 a

C7.13 Example Problems.

Example Problem 1

Fig. C7.16 shows a cantilever beam of constant cross-section carrying a 13500# load at the free end. The beam will be strength checked for the given load.

Investigation of Web Strength

Web panel size between web stiffeners and centroid of flange rivets = 10 by 28.56.

Aspect ratio of panel = a/b = 28.56/10 = 2.856

The critical buckling shear stress is given by

$$F_{s_{cr}} = K_s E \left(\frac{t}{b}\right)^2 \text{ (see Eq. 20)}$$

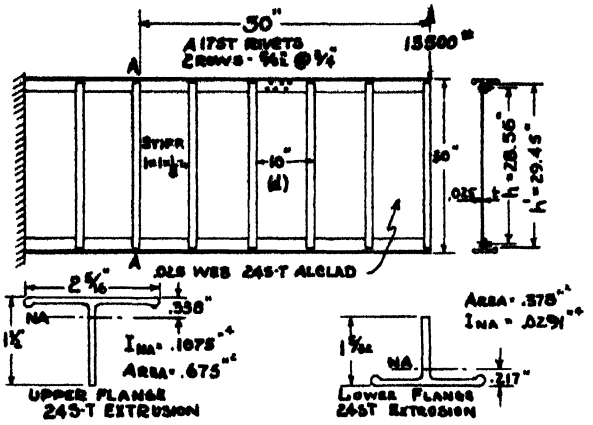
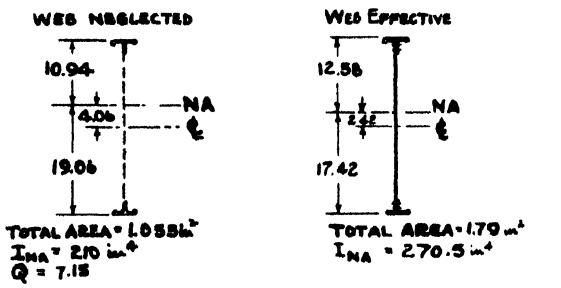


Fig. C7-16



K for panel with freely supported edges = 5.3 (Ref. Fig. B2.5)

$$F_{s_{cr}} = 5.3 \times 10{,}300{,}000 \times (.025/10)^2 = 342 \text{ psi}$$

Therefore shear load resistance developed by web up to buckling stress equals

$$V_{cr} = F_{s_{cr}}\ h\ t = 342 \times 28.56 \times .025 = 244$$

The shear strength of the web acting as a tension field after buckling is given by the following equations, when stressed to the yield point in tension

$$V_{ty} = \left(F_{ty} - \frac{F_{s_{cr}}}{K_r}\right) K_r\ R\ h\ t \sin\alpha \cos\alpha \qquad \text{(see Eq. 27)}$$

when stressed to ultimate stress in tension

$$V_{tu} = \left(F_{tu} - \frac{F_{s_{cr}}}{K_r}\right) K_r\ R\ h\ t \sin\alpha \cos\alpha \qquad \text{(see Eq. 29)}$$

Before solving these equations, the terms α, R, and K_r must be determined:

The angle of the diagonal tension field with horizontal is

$$\sin^2\alpha = \sqrt{a^2 + a} - a \qquad \text{(see Eq. 15)}$$

where

$$a = \frac{1 + \dfrac{ht}{A_u + A_L}}{\dfrac{dt}{A_s} - \dfrac{ht}{A_u + A_L}} \qquad \text{(see Eq. 16)}$$

Substituting

$$a = \frac{1 + \dfrac{28.56 \times .025}{.675 + .378}}{\dfrac{10 \times .025}{.23} - \dfrac{28.56 \times .025}{.675 + .378}} = 4.05$$

hence

$$\sin^2\alpha = \sqrt{4.05^2 + 4.05} - 4.05 = .47$$

$$\sin\alpha = .685, \quad \alpha = 43^\circ, \quad \cos\alpha = .73$$

To determine the web stress concentration factor R, we solve for term wd and use curve of Fig. C7.12.

$$wd = 1.25\ d \sin\alpha \sqrt[4]{\frac{t}{(I_u + I_L)\ h}} \qquad \text{(Ref. Eq. 14)}$$

$$wd = 1.25 \times 10 \times .685 \sqrt[4]{\frac{.025}{(.1075 + .0291)\ 28.56}} = 2.43$$

From curve Fig. C7.12, R = .86

Since the web is riveted to the flange, correction must also be made for net area of web.

$$K_r = \frac{\text{rivet spacing} - \text{rivet diameter}}{\text{rivet spacing}} = \frac{.75 - .156}{.75} = .79$$

For 24ST alclad material, F_{ty} = 37000 and F_{tu} = 56000 psi. (Ref. Chapter C1)

$$V_{ty} = \left(37000 - \frac{342}{.79}\right).79 \times .86 \times 28.56 \times .025 \times .685 \times .73$$

$$V_{ty} = (36566)\ .242 = 8840\#$$

$$V_{tu} = \left(56000 - \frac{342}{.79}\right).242 = 13450\#$$

The total shear load including strength of flanges is given by equations (33) and (34), namely

$$V_{yield} = \frac{I}{Qh}(V_{cr} + V_{ty})$$

$$V_{ult.} = \frac{I}{Qh}(V_{cr} + V_{tu}) \qquad \text{(A)}$$

From Fig. C7.16

$I_{N.A.}$ of section without web = 210 in.⁴

Q of flange about N.A. = 7.15

$$V_{yield} = \frac{210}{7.15 \times 28.56}(244 + 8840) = 9370\#$$

$$V_{ult.} = \frac{210}{7.16 \times 28.56}(244 + 13450) = 14110\#$$

The design ultimate shear load = 13500#

hence

M.S. = (14110/13500) -1 = .045

The applied shear load using a factor of safety of 1.5 is 13500/1.5 = 9000#

The yield strength is 9370#. Thus for margin of safety of yield strength over applied load, we have (9370/9000) -1 = .04.

The above results show that the beam shear resistance is proportioned as follows for a total ultimate strength of 14180#. (244/14110 x 100 = 1.7% carried by web in pure shear. (13450/14110) 100 = 95.1% carried by web as a diagonal tension field.

The remainder or 3.2% is carried by the shear strength of the flange s. This value is relatively low for this particular beam, as in general the flange may provide considerably more of the resistance. Due to the thin web thickness and the large web panels, the web buckles at a relatively low stress, thus the percent of the external shear load carried by the web at the buckling stress is quite small. The results of example problem (2) are more representative of normal conditions.

Check of Rivet Attachment - Web to Flange

The .025 - 24ST alclad web is attached to the flange member by 2 rows of 5/32 diameter A17ST rivets at 3/4 inch spacing.

The resultant load on the rivets per inch of flange is given by equation (43), namely

$$P_r = \left[\left(\frac{V_{cr}\, I_F}{h\, I} + \frac{V_{tu}}{h}\right)^2 + \left(\frac{V_{tu}}{h}\tan\alpha\right)^2\right]^{1/2} \quad -(B)$$

The web is not stressed to its ultimate tensile stress since we have 4% margin of safety. We will therefore solve equation (A) for V_{tu} using the given external shear load V = 13500#, and call this value V_t, the shear load carried by the tensile field under the given shear load of 13500#.

$$13500 = \frac{210}{7.15 \times 28.56}(244 + V_t)$$

$$13500 = 1.03\,(244 + V_t)$$

whence

V_t = 12850#, which represents V_{tu} in equation (B) for P_r

Substitute in Equation (B)

$$P_r = \left[\left(\frac{258}{28.56}\,\frac{210}{270.5} + \frac{12850}{28.56}\right)^2 + \left(\frac{12850}{28.56} \times .933\right)^2\right]^{1/2}$$

$$P_r = \left[(6 + 450)^2 + 420^2\right]^{1/2} = 624\#/\text{per inch.}$$

Load per rivet pitch of .75 inch = .75 x 624 = 468#

Single shear strength of 5/32 - A17ST rivet = 596 x .86 = 512#.

Bearing strength on 24ST alclad = .91 x 398 = 362#.

Bearing is critical and the rivet strength per rivet pitch is 2 x 362 = 724# (2 rows of rivets)

Margin of safety = (724/468) - 1 = .54

Check on Flange Stresses At Section A-A (50" from free end)

Design external bending moment = 50 x 13500 = 675,000"#.

Since V_{cr} = 244#, which is the shear load the web carries without buckling, the bending moment due to a shear of 244# will be resisted by the entire cross-section including the web. Above this value the remaining moment is resisted by the section with the web neglected in computing the moment of inertia.

Thus bending moment at web buckling load = 244 x 50 = 12200"#.

Bending moment for tension field beam = 675,000 - 12200 = 662800"#.

Bending Stresses

Upper Flange Bending Stresses:

$$f_b = -\frac{12200 \times 12.58}{270.5} - \frac{662.800 \times 10.94}{210}$$

(See Eq. 44)

$$= -567 - 34600 = -35167 \text{ psi.}$$

If the entire bending moment were assumed resisted by the flanges alone, then,

$$f_b = \frac{675000 \times 10.94}{210} = -35200 \text{ psi.}$$

Lower Flange Bending Stresses

$$f_b = \frac{-12200 \times -17.42}{270.5} + \frac{-662800 \times 19.06}{210}$$

$$= 783 + 60200 = 60980 \text{ psi.}$$

(Note: Section properties were computed without taking out one 5/32 rivet hole in vertical leg of flange Tee, thus stresses are slightly unconservative. To be on the safe side, the net section properties should be used in figuring stresses).

Average Axial Flange Loads Due To Bending

$$\text{Total Flange Load} = \frac{M}{h'} = \frac{675000}{29.45} = 22900\#$$

Upper flange $f_{c(aver.)}$ = -22900/.675 = -33900 psi.

Lower flange $f_{t(aver.)}$ = 22900/.378 = 60500 psi.

Flange Axial Loads Due to Tension Field Action

The axial load in each flange due to diagonal tension in web equals

$F_t = F_c = -.5\, V_t \cot\alpha$ (see Eq. 47)

$= -.5 \times 12850 \times 1.07 = -6860$

Average stress on upper flange

$f_c = -6860/.675 = -10{,}170$ psi.

Lower flange, $f_t = -6860/.378 = -18180$ psi.

Combined Flange Axial Stresses

Upper Flange - Extreme Fiber

f_c = -35167 - 10170 = -45337 psi.

Average stress, f_c = -33900 - 10170 = -44070 psi.

Lower Flange - Extreme Fiber

f_t = 60980 - 18180 = 42800 psi.

Average stress f_t = 60500 - 18180 = 42320 psi.

Since the tension field action is relieving on the tension flange stresses, it is recommended that only a portion of the relieving action be used in design, since the theory of semi-tension field beams as presented here is only approximate. On the compressive flange the full effect of the tension field should be used since it is additive to the primary bending stresses.

Estimation of Flange Allowable Compressive Stress

Assuming that the beam flanges are stiffened laterally by skin covering and stiffeners, the allowable compressive stress can be closely estimated by taking the computed crippling stress as the allowable. Using the methods of Chapter B5, the crippling stress for the section will be estimated.

The upper flange tee section is assumed as made up of the plate elements (1) and (2) as illustrated.

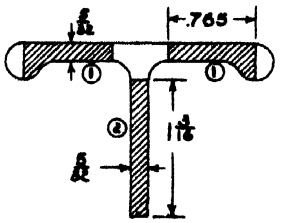


Plate element (1)

b/t = .765/.156 = 4.9

From Fig. B5.13, F_{cr} = 54,500 psi.

Plate element (2)

b/t = 1.1875/.156 = 7.6

From Fig. B5.13, F_{cr} = 40,000 psi.

Average crippling stress for section

$$F_{cs} = \frac{\Sigma F_{cr}\, b}{\Sigma b} = \frac{54500 \times .765 \times 2 + 40000 \times 1.1875}{.765 \times 2 + 1.1875}$$

F_{cs} = -48400 psi.

The average upper flange stress was -44070 against an allowable of -48400. The extreme fiber stress on upper flange is -45337 against an allowable buckling stress for plate element (1) equal to -54500 psi. Thus for primary loads the upper flange has approximately (48400/44000) -1 = .10 margin of safety. The flanges must however carry secondary bending moments due to lateral pull of tension field.

Secondary Bending Stresses

From Eq. (49)

$$M_{sec.} = 1/12\ C\ \frac{V_t}{h}\ d^2 \tan \alpha$$

From Fig. C7.12, C = .925 when wd = 2.43

whence

$$M_{sec.} = 1/12 \times .925 \times \frac{12850}{28.56} \times 10^2 \times .933 = 3230 \text{ in.lb.}$$

Secondary bending stresses on upper flange

$I_{N.A.}$ upper flange = .1075

I/y lower fiber = .1075/1.16 = .0925 I/y upper fiber = .1075/.338 = .318

$f_{b(\text{lower fiber})}$ = 3230/.0925 = 34900 psi. Compression as flange bends over the support.

$f_{b(\text{upper fiber})}$ = 3230/.318 = 10140 psi. (tension)

The combined stress on the lower fiber than would be -34900 - 44070 = -78970 psi. which is too high; thus flange is weak.

For such a large stiffener spacing, the flange should be made slightly deeper and a leg should be added to the vertical leg in order to raise the crippling stress of this relatively weak element. See Fig. e. By such re-design of the flange extrussion, sufficient strength could be obtained for the given loads without much increase in weight.

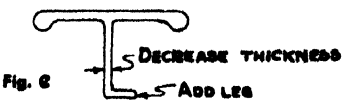


Fig. e

Secondary Bending Stresses on Lower Flange

$I/y_{\text{lower fiber}}$ = .0291/.217 = .134

$I/y_{\text{upper fiber}}$ = .0291/.939 = .031

$f_{b(\text{upper fiber})}$ = 3230/.031 = 104000 psi.

This stress added to the previous stresses due to bending of beam as a whole, greatly exceeds the ultimate tensile strength of the material. Thus a re-design would be necessary and the modification should be such as to cut down the secondary bending stresses by increasing the flange depth or by less stiffener spacing or both.

Check of Stiffener Strength

Column load in web stiffener is given in Eq. (50).

$$F_{stiff.} = -V_t \frac{d}{h} \tan \alpha$$

$$= -12850 \frac{10}{28.56} \times .933 = -4200\#$$

The reduced column length factor C_e of the web stiffener is obtained from Fig. C7.15 for a parameter of

$$\frac{d}{h\ (\cot \alpha \cot \beta)} = \frac{10}{28.56\ (\cot 40^\circ)} = .304 \text{ and}$$

gives C_e = .38

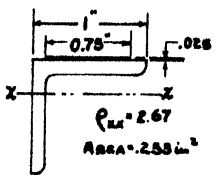
hence

L' = .38 x 28.56 = 10.8"

Assuming an effective width of web sheet equal to 30 t as acting with the 1 x 1 x 1/8 angle stiffener the radius of gyration equals .267 and the area equals .253,

hence

$L'/\rho = 10.8/.267 = 40.5$



From Fig. B1.10, the column strength for 24ST extruded material for L/ρ = 40.5 gives allowable column stress of 36000 psi.

The initial buckling stress of the angle legs can be closely estimated by method of Art. B5.2.

$$b/t \text{ of leg} = \frac{w - t/2}{t} = \frac{1 - .0625}{.125} = 7.5$$

From Fig. B5.13, F_{cr} = 40000 psi.

∴ column action is critical and allowable stress is 36000 psi.

Hence column strength = 36000 x .253 = -9100# against a stiffener load of -4200#. Thus stiffener is far overstrength.

Example Problem #2

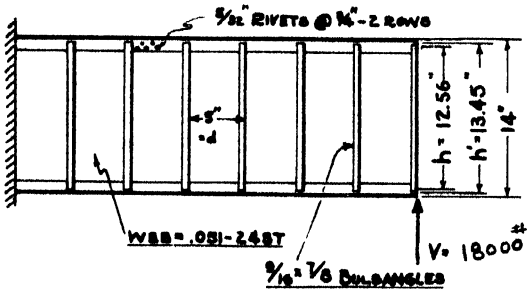


Fig. C7.17

Fig. C7.17 shows a beam with the same flanges as in example problem (1) but the beam depth is much less and the web is thicker. The web strength will be checked for a given V load = 18000#.

Solution

Web critical buckling stress,

a/b of web panel = 12.56/5 = 2.51

K_s for freely supported edges = 5.42 (Ref. B2.5).

$$F_{s_{cr}} = K_s E \left(\frac{t}{b}\right)^2$$

$$= 5.42 \times 1030000 \times \left(\frac{.051}{5}\right)^2 = 5820 \text{ psi.}$$

Shear load carried by web at buckling stress

$V_{cr} = F_{s_{cr}}\, h\, t = 5820 \times 12.56 \times .051 = 3735\#$

Determination of wrinkle angle (α)

$$a = \frac{1 + \frac{ht}{A_u + A_L}}{\frac{dt}{A_s} - \frac{ht}{A_u + A_L}}$$

A_s = .106
h = 12.56
A_u = .675
A_L = .378
I_u = .1075
I_L = .0291

Substituting

$$a = \frac{1 + \frac{12.56 \times .051}{.675 + .378}}{\frac{5 \times .051}{.106} - \frac{12.56 \times .051}{.675 + .378}} = \frac{1 + .606}{2.16 - .606} = .896$$

$$\sin^2 \alpha = \sqrt{a^2 + a} - a = \sqrt{.896^2 + .896} - .896 = .44$$

$\sin \alpha = .666 \quad \alpha = 42^\circ \quad \cos \alpha = .745$

$$wd = 1.25\, d \sin \alpha \sqrt[4]{\frac{t}{(I_u + I_L)\, h}}$$

$$wd = 1.25 \times 5 \times .666 \sqrt[4]{\frac{.051}{(.1075 + .0291)\ 12.56}} = 1.73$$

R from curve of Fig. C7.12 = .96

$$K_r = \frac{.75 - .156}{.75} = .79$$

Shear which web can carry as a tension field:

$$V_{tu} = \left(62000 - \frac{5820}{.79}\right) .79 \times .96 \times 12.56 \times .051 \times .666$$
$$\times .745 = (62000 - 7370)\ .241 = 13180\#$$

Total shear carried by beam at ultimate web strength

$$V_{ult.} = \frac{I}{Qh} (V_{cr} + V_{tu})$$

$I_t = .675 \times \overline{6.662}^2 = 30.0$

$.378 \times \overline{6.783}^2 = \frac{17.4}{47.4}$

$$\bar{y} = \frac{.675 \times 6.662 - .378 \times 6.783}{1.053}$$

$$= \frac{1.938}{1.053} = 1.84"$$

$I_{N.A.} = 47.4 - 1053 \times 1.84^2 = 43.85$ in.

$Q = .675\ (6.662 - 1.84) = 3.26$

$$V_u = \frac{43.85}{3.26 \times 12.56}\ (3735 + 13180) = 18100\#$$

Design V_u = 18000#

M.S. = 18100/18000 -1 = 0

Percent of shear strength due to flange = $\left(\frac{18100 - 16915}{18100}\right)$ 100 = 6.5

Percent of shear strength up to web buckling stress = (3735/18100) 100 = 20.6

The remainder or 72.9 percent is carried by tension field action.

The results for this typical beam show that to neglect shear strength of flanges and buckling strength of web is far too conservative.

C7.14 NACA Method of Strength Analysis of Semi-Tension Field Beams.

For a number of years the structures division of the NACA at Langley Field has been carrying on research both theoretical and experimental relative to the strength of semi-tension field beams. Ref. (13) A NACA Technical Note of 1947 summarizes most of the previous research of the NACA and presents stress analysis equations or formula with many design charts for the strength design of semi-tension field beams. The material to follow is taken almost verbatim from (Ref. 11). The student after studying the method presented in the first part of this chater should have no difficulty of understanding the design procedure as given in (Ref. 11).

Since the symbols used in the first part of this chapter do not correspond to the NACA symbols, and since the NACA figures and charts make use of the NACA symbols, it will be necessary to give the explanation and definitions of the NACA symbols.

NACA Symbols

A cross-sectional area, square inches.
E Young's modulus, KSI.
G shear modulus, KSI.
P force in KIPS.
Q static moment about neutral axis of parts of cross-section as specified by subscripts. in.^{3}
R coefficient of edge restraint.
S transverse shear force, kips.
d spacing of uprights, inches.
e distance from median plane of web to centroid of (single) upright, inches.
h depth of beam, inches.
k diagonal-tension factor.
t thickness, inches (used without subscript) signifies thickness of web).
α angle between neutral axis of beam and direction of diagonal tension, degrees.
ρ centroidal radius of gyration of cross-section of upright about axis parallel to web, inches (no sheet should be included).
σ norma stress ksi.
τ shear stress ksi.

Subscripts.

DT diagonal tension
F flange
S shear
u upright
W web
cr critical
ult ultimate
e effective

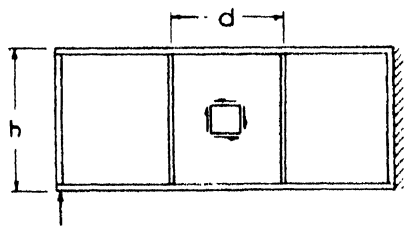
Special Combinations

P_u internal force in upright, kips.
R^* shear force on rivets per inch run kips. per inch.
R_{tot} total shear strength (in single shear) of all rivets in one upright, kips.
d_c upright spacing measured as shown in Fig. C7.20a.
h_c depth of web as measured as shown in Fig. C7.20a.
h_e depth of beam measured between centroids of flanges, inches.
h_r depth of beam measured between centroids of web to flange rivet patterns, inches.
h_u length of upright measured between centroids of upright to flange rivet patterns, inches.
k_{ss} theoretical buckling coefficient for plates with simply supported edges.
σ_o "basic" allowable stress for forced crippling of uprights.
wd flange flexibility factor $(.7d\sqrt[4]{\frac{t}{(I_c + I_T)}}\, h_e$ where I_c and I_T are moments of inertia of compression and tension flanges respectively.

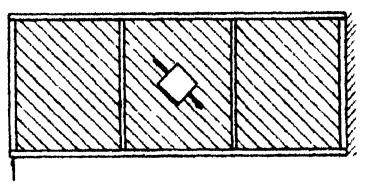
C7.15 Engineering Theory of Incomplete Diagonal Tension.

In a beam with a thin flat sheet as a web, if the external shear load is less than the buckling load for the web, then the web is in a state of pure shear at the neutral axis as indicated in Fig. C7.18 (Fig. a). If we neglect the normal stresses due to bending over the depth of the web, this shear stress arrangement can be assumed constant over the full depth of the web.

If a web is thin, it will buckle under a certain critical load and if the load is increased beyond this critical buckling value, the buckle pattern will approach a pure tension field as indicated in (b) of Fig. C7.18.



(a) Nonbuckled ("shear-resistant") web.



(b) Pure diagonal-tension web.

Fig. C7-18 - State of stress in a beam web.

In the usual practical thin web beam in aircraft construction, the state of stress in the web is intermediate between pure shear and pure diagonal tension. The engineering theory as

developed by the NACA considers that this intermediate state of incomplete diagonal tension may be based on the assumption that the total shear force in the web can be divided into two parts, a part S_S carried by pure shear and a part S_{DT} carried by pure diagonal tension.

Thus under this assumption one can write,

$S = S_S + S_{DT}$, which can be written in the form

$S_{DT} = kS$

$S_S = (1-k)S$ - - - - - - - - - - - - - - - (52)

where k is the "diagonal-tension factor" which expresses the degree to which the diagonal tension is developed by a given load. Thus the state of pure shear is measured by k = 0 and the state of pure diagonal tension by k = 1. Fig. C7.19 illustrates the stress condition for the limiting cases of k = 0 and k = 1 and for the intermediate case.

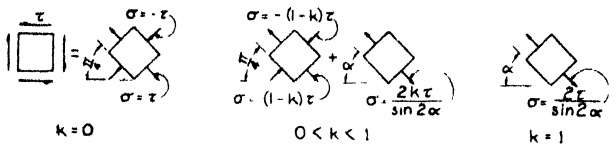


Fig. C7.19 - Resolution of web stresses at different stages of diagonal tension.

C7.16 Formulas for Stress Analysis.

Limitations of Formulas:

The NACA believes the formulas which follow will give reasonable strength predictions if normal design practices are used. The following limitations should be observed.

(1) Uprights on web stiffeners should not be too thin. $\frac{t_u}{t} > 0.6$

(2) The upright or web stiffener spacing should not be too much outside the range $0.2 < \frac{d}{h} < 1.0$

(3) The tests by NACA did not cover beams with very thin or very thick webs, hence some possibility of inconservative predictions may exist if $\frac{h}{t} > 1500$ or less than 200.

C7.17 Critical Shear Stress.

In the elastic range, the critical shear stress between two web uprights is calculated by the formula:-

$$\tau_{cr} = k_{ss} E \left(\frac{t}{d_c}\right)^2 \left[R_h + \frac{1}{2}\left(R_d - R_h\right)\left(\frac{d_c}{h_c}\right)^2\right] \quad (53)$$

where,

k_{ss} = theoretical buckling coefficient (given in Fig. C7.20 (Fig. a) for panel length of h_c and width d_c with simply supported edges.

d_c = width of sheet between uprights measured as shown in Fig. C7.20 (Fig. a).

h_c = depth of web measured as shown in Fig. C7.20.

R_h = restraint coefficient for edges of sheet along upright (See Fig. b of Fig. C7.20).

R_d = restraint coefficient for edges of sheet along flanges. (See Fig. b of Fig. C7.20).

(If $d_c > h_c$, substitute h_c for d_c; d_c for h_c; R_d for R_h; and R_h for R_d).

Curves of the critical shear stresses for plates of 24ST aluminum alloy with simply supported edges are given in Fig. C7.21. To the right of the dashed line the curves in Fig. C7.21 are plots of the theoretical equation,

$$\tau_{cr} = k_{ss} E \left(\frac{t}{d_c}\right)^2 \quad (54)$$

and may be used for most aluminum alloys. To the left of the dashed line, the curves represent straight line tangents to the theoretical curves in a nonlogarithmic plot and are valid only for 24ST.

C7.18 Loading Ratio

The loading ratio is the ratio τ/τ_{cr}, where τ is the depth-wise average or nominal shear stress.

When the depth of the flanges is small compared with the depth of the beam and the flanges are angle sections, the stress τ may be computed by the formula

$$\tau = \frac{S_w}{h_e t} \quad (55)$$

In beams with other cross-sections, the average nominal shear stress should be computed by the formula

$$\tau = \frac{S_w Q_F}{It}\left(1 + \frac{2}{3}\frac{Q_W}{Q_F}\right) \quad (56)$$

Where Q_F is the static moment about the neutral axis of the flange material and Q_W is the static moment about the neutral axis of the effective web material above the neutral axis. For the computation of I and Q the effectiveness of the web must be estimated in the first approximation. As second and final approximation, the effectiveness of the web may be taken as equal to (1 - k), where k is the diagonal-tension factor determined in the next step. Thus in computing I and Q the effective web thickness is (1 - k) t.

C7.19 Diagonal-Tension Factor k.

Having determined the loading ratio τ/τ_{cr}, the diagonal tension factor k can be read from Fig. C7.22.

C7.20 Average Stress in Upright or Web Stiffener.

The average stress over the length of the upright for a double upright (stiffener on each side of web) can be calculated by the formula,

$$\sigma_u = \frac{k\,\tau \tan\alpha}{\frac{A_u}{dt} + .05\,(1-k)} \qquad (57)$$

This equation can be evaluated with the use of Figs. C7.23 and C7.24. The stress σ_u is uniformly distributed over the cross-section of the upright until buckling of the upright begins.

Single Upright (or Web Stiffener on one side of web)

The stress σ_u for a single upright is obtained in the same manner, except that the ratio A_u/dt is replaced by A_{u_e}/dt, where

$$A_{u_e} = \frac{A_u}{1 + \left(\frac{e}{\rho}\right)^2} \qquad (58)$$

For the single upright σ_u is still an average over the length of the upright, but it applies only to the median plane of the web along the line of rivets connecting the upright to the web. In any given cross-section of the upright, the compressive stress decreases with increasing distance from the web, because the upright is a column loaded eccentrically by the web tension. Thus formulas for local crippling based on uniform distribution of stress over the cross-sections do not apply.

Maximum Stress in Upright

The stress σ_u in the upright varies from a maximum at (or near) the neutral axis of the beam to a minimum at the ends of the upright ("gusset effect"). The ratio of the maximum stress to the average stress decreases as the upright spacing or the loading ratio decreases. The empirical formula for the ratio is

$$\frac{\sigma_{u_{max.}}}{\sigma_u} = 1 + \left[\left(\frac{\sigma_{u_{max.}}}{\sigma_u}\right)_o - 1\right](1-k) \qquad (59)$$

where $\left(\frac{\sigma_{u_{max.}}}{\sigma_u}\right)_o$ is the value of the ratio when the web has just buckled. Fig. C7.25 gives the ratio.

C7.21 Angle of Diagonal Tension.

Having determined k and σ_u/τ, the angle α between the direction of the diagonal tension and the axis of the beam can be determined by the use of Fig. C7.26.

C7.22 Allowable Stresses in Uprights.

Four types of failure are conceivable.

(1) Column Failure.
(2) Forced Crippling Failure
(3) Natural Crippling Failure
(4) General elastic instability failure of web and stiffeners.

Column Failure

Column failures in the usual meaning of the word (failure due to instability, without previous bowing) are possible only in double uprights. When column bowing begins, the uprights will force the web out of its original plane. The web tensile forces will then develop components normal to the plane of the web which tend to force the uprights back. This bracing action is taken into account by using a reduced "effective" column length L_e of the upright, which is given by the following empirical formula,

$$L_e = \frac{h_u}{\sqrt{1 + k^2\,(3 - 2\frac{d}{h})}} \qquad (60)$$

The stress σ_u at which column failure takes place can be found using the standard column curve with the slenderness ratio L_e/ρ as shown.

The problem of "column" failures in a single upright has not been investigated to any extent and test results are greatly at variance with theoretical results. Two criterions are suggested for strength design, namely:-

(a) The stresses σ_u should be no greater than the column yield stress for the upright material. This accounts for the upright acting as a eccentrically loaded compression member.

(b) The stress at the centroid of the upright (which is the average stress over the cross-section) should be no greater than the allowable column stress for the slenderness ratio $h_u/2\rho$. This is an attempt to take in account a two-wave type of buckling failure that has been observed in very slender uprights.

Forced Crippling Failure

The shear buckles in the web will force buckling of the upright in a leg attached to the web, particularly if the upright leg is thinner than the web. These buckles give a lever arm to the compressive force acting in the leg and thereproduce a severe stress condition. The buckles in the attached leg will in turn induce buckling of the outstanding legs.

In single uprights the outstanding legs are relieved to a considerable extent by virtue of the fact that the compressive stress decreases with distance from the web; the allowable stresses for single uprights are therefore somewhat higher than those for double uprights. Because the forced crippling is of local nature, it is assumed to depend on the peak value $\sigma_{u_{max.}}$ of

the upright stress rather than on the average value.

The upright stress at which final collapse occurs is obtained by the following empirical method:-

(1) Compute the allowable value of $\sigma_{u_{max.}}$ for a perfectly, elastic upright material by the formula

$\sigma_o = 28\ k\ \sqrt{t_u/t}$ for single uprights- -(61a)

$\sigma_o = 25\ k\ \sqrt{t_u/t}$ for double uprights- -(61b)

(2) If σ_o exceeds the proportional limit for the upright material, use as allowable value the stress corresponding to the compressive strain σ_o/E.

(3) If $k < 0.5$ use an effective value in formula 61a or 61b given by the expression

$k_e = 0.15 + 0.7\ k$ - - - - - - - - - - -(61c)

Natural Crippling Failure

The term "natural crippling failure" is used to denote a crippling failure resulting from a compressive stress uniformly distributed over the cross-section of the upright. By this definition it can occur only in double uprights. To avoid natural crippling failure, the peak stress in the upright $\sigma_{u_{max.}}$ in the upright should be less than the crippling stress of the section for $L/\rho \rightarrow 0$. It appears that crippling failure does not appear to be a controlling factor in actual designs.

General Elastic Instability of Web and Uprights

Test experience so far has not indicated that general elastic instability need be considered in design. Apparently the web system is safe against general elastic instability if the uprights are designed to fail by column action or by forced crippling at a shear load not much less than the shear strength of the web.

C7.23 Web Design.

For design purposes, the peak value of the nominal web shear stress within a bay is taken as,

$$\tau_{max.} = \tau\ (1 + kC_1)\ (1 + kC_2) \quad - - - - - \quad (62)$$

Refer to Figs. C7.27 and C7.28 to determine values of factors C_1 and C_2. The C_1 term constitutes a correction factor to allow for the angle α of the diagonal tension field differing from 45 degrees. C_2 makes allowance for the stress concentration due to the flexibility of the beam flanges.

Allowable Value of $\tau_{max.}$

The allowable value of $\tau_{max.}$ is determined by tests and depends on the value of the diagonal-tension factor k as well as on the details of the web to flange and web to upright fastenings. Fig. C7.29 gives empirical allowable curves for two aluminum alloys. It should be noted that these curves contain an allowance for the rivet factor; inclusion of this factor in these curves is possible because tests have shown that the ultimate shear stress based on the gross section (that is, without reduction of rivet holes) is almost constant within the normal range of rivet factor ($C_R > 0.6$)

C7.24 Rivet Design.

Web to Flange Rivets

The load per inch run acting on web to flange rivets is taken as,

$$R'' = \frac{S_W}{h_R}\ (1 + 0.414\ k) \quad - - - - - - - - - \quad (63)$$

With double uprights the web to upright rivets must provide sufficient longitudinal shear strength to make the two uprights act as an integral unit until column failure occurs. The total shear strength (single shear strength of all rivets) required in an upright is

$$R_{total} = \frac{2\ \sigma_{co}\ Q\ h_u}{b\ \ L_e} \quad - - - - - - - - - \quad (64)$$

where

σ_{co} = column yield strength of upright material. (If σ_{co} is expressed in ksi, R_{total} will be in kips.)

Q = static moment of cross-section of one upright about an axis in the median plane of the web in.^{3}

b = width of outstanding leg of upright.

h_u/L_e = ratio obtainable from formula (60).

The rivets must also have sufficient tensile strength to prevent the buckled sheet from lifting off the stiffener. The necessary strength is given by the criterion,

Tensile strength per inch of rivets $\geq 0.15\ t\ \sigma_{ult.}$ - - - - - - - - - - - - - - - - (61)

where $\sigma_{ult.}$ is the tensile strength of the web.

For web to upright rivets on single uprights.

The required tensile strength is given by the tentative criterion,

Tensile strength per inch of rivets $\geq .22\ t\ \sigma_{ult}$ - - - - - - - - - - - - - - - - - - (62)

(The tensile strength of a rivet is defined as the tensile load that causes any failure; if the sheet is thin failure will consist in the pulling of the rivet through the sheet.)

No criterion for shear strength of the rivets on single uprights has been established; the criterion for tensile strength is probably adequate

to insure a satisfactory design.

The pitch of the rivets on single uprights should be small enough to prevent inter-rivet buckling of the web (or the upright leg if thinner than the web), at a compressive stress equal to $\sigma_{u_{max}}$. The pitch sould also be less than d/4 in order to justify the assumption on edge support used in the determination of τ_{cr}.

Upright to Flange Rivets

These rivets must carry the load existing between upright and beam flange. These loads are,

$$P_u = \sigma_u A_u \text{ (for double uprights)} \quad - - - \quad (63)$$

$$P_u = \sigma_u A_{u_e} \text{ (for single uprights)} \quad - - - \quad (64)$$

These formulas neglect the gusset effect (decrease of σ_u towards the ends of the upright) in order to be conservative.

C7.25 Secondary Bending Moments in Flanges.

The secondary moment in a flange, caused by the vertical component of the diagonal tension may be taken as,

$$M = \frac{1}{12} k \tau t d^2 C_s \quad - - - - - - - - - - - \quad (65)$$

where C_s is a factor given in Fig. C7.28. The moment given by this formula is the maximum moment and exists at the ends of the bay over the uprights. If C_s and k are near unity, the moment in the middle of the bay is half as large as that given by formula (65) and of opposite sign.

C7.26 Shear Stiffness of Web.

The theoretical effective shear modulus of a web G_e in partial diagonal tension is given by Fig. C7.30. This modulus is valid only in the elastic range.

C7.27 Example Problem 1. Using NACA Method.

The beam used in example problem 1 of Art. C7.13 will be checked by the NACA Method.

First check to see if given beam falls within the limitations of the NACA formulas.

From Art. C7.16:-

$\frac{t_u}{t}$ should be greater than 0.6

For our beam t_u the leg thickness of the upright is .125" and the web thickness is .025", hence .125/.025 = 5, which is greater than .6.

Also from Art. C7.16, the d/h value for the beam should fall between .2 and 1.0.

The d/h value for our beam is 10/30 = .333 which falls within the given range.

Calculation of the Critical Shear Stress (τ_{cr}).

Use will be made of Fig. C7.21,

$$\frac{d_c}{t} = \frac{10}{.025} = 400 = \frac{\text{Stiffener spacing}}{\text{Web thickness}} \text{ (See Fig. C7.20)}$$

$$\frac{h_c}{d_c}^o = \frac{27.94}{10} = 2.79, \text{ See Fig. C7.20 for } h_c.$$

Using the above values, we find from Fig. C7.21, that

$$\tau_{cr} = 370 \text{ psi.}$$

Calculation of the Loading ratio τ/τ_{cr}

From equation 55

$$\tau = \frac{S_w}{h_e t} = \frac{13500}{29.45 \times .025} = 18350 \text{ psi.}$$

where, S_w = external shear load on web.
h_e = distance between flange centroids.

Equation 55 was used because the flanges will take very little of the shear load.

Therefore the loading ratio,

$$\frac{\tau}{\tau_{cr}} = \frac{18350}{370} = 49.6$$

Calculation of diagonal-tension factor k

With τ/τ_{cr} = 49.6, we use Fig. C7.22 to find value of k = .69

Calculation of average stress in upright

Upright consists of one 1 x 1 x 1/8 24ST extruded angle section.

To obtain effective area, we use eq. 58

$$A_{u_e} = \frac{A_u}{1 + (\frac{e}{\rho})^2} = \frac{.234}{1 + (\frac{.3025}{.29})^2} = .112$$

where,

A_u = area of web upright or stiffener
e = distance from median plane of web to centroid of single upright.
ρ = centroidal radius of gyration of cross section of upright about axis parallel to web.

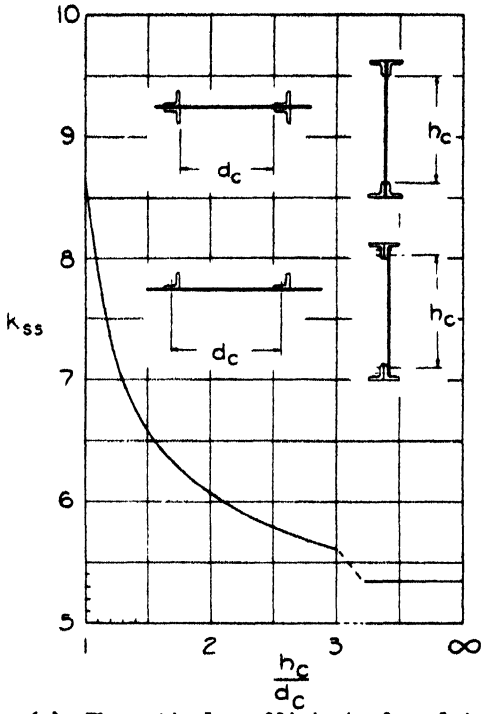
Using Fig. C7.23, with $A_{u_e}/dt = \frac{.112}{10 \times .025} =$.45 and τ/τ_{cr} = 49.6, we obtain value of σ_u/τ = .92.

Hence, σ_u = 18350 x .92 = 16900 psi, which represents the average stress over the length of the upright but applies only along the median plane of the web or along the line of rivets connecting upright to web.

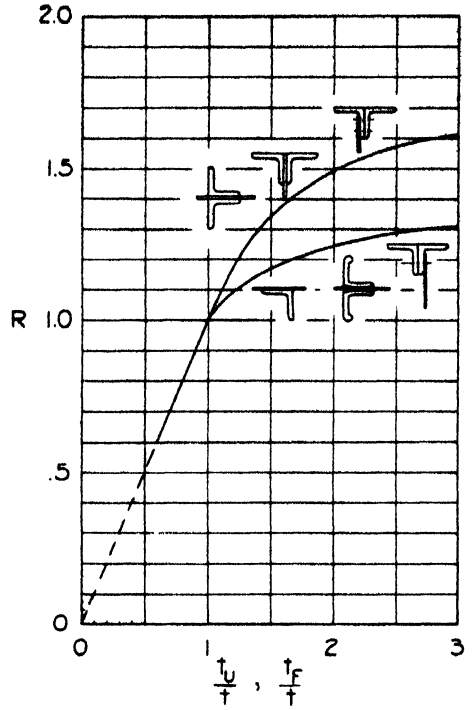
Calculation of Maximum Stress Upright

$$\text{Value of } \frac{d}{h_u} = \frac{10}{28.50} = .352$$

where, d = upright spacing
h_u = distance between centroids of upright-flange rivet connections.



(a) Theoretical coefficients for plates with simply supported edges.



(b) Empirical restraint coefficients.

Fig. C7-20 - Coefficients for calculating web buckling stress.

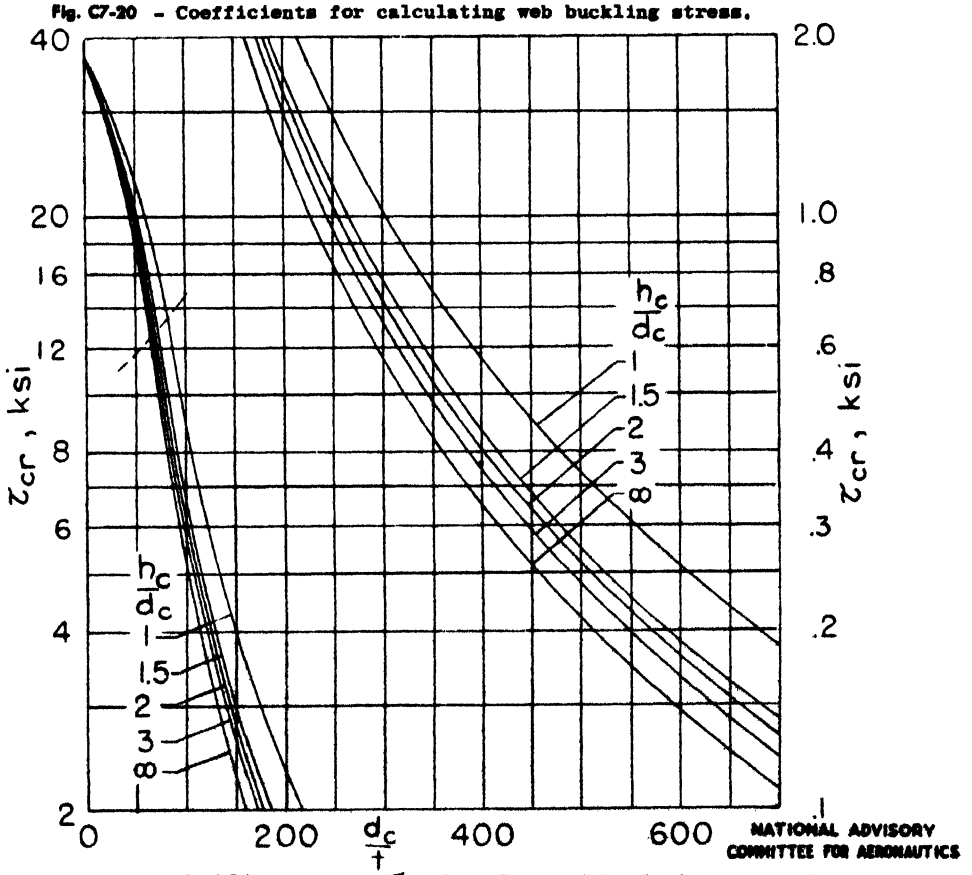


Fig. C7-21 - Buckling stresses τ_{cr} for plates with simply supported edges. E = 10,600 ksi. (To left of dashed line, curves apply only to 24ST aluminum alloy.)

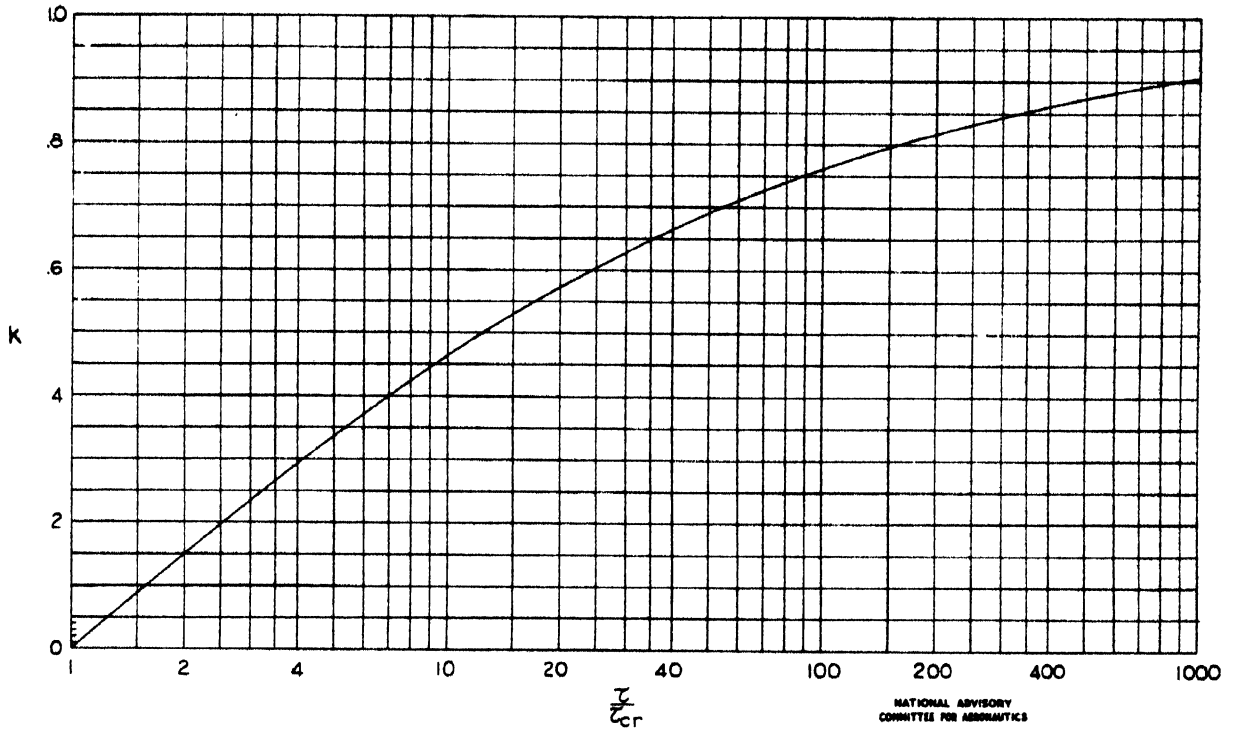


Fig. C7-22 - Diagonal-tension factor k.

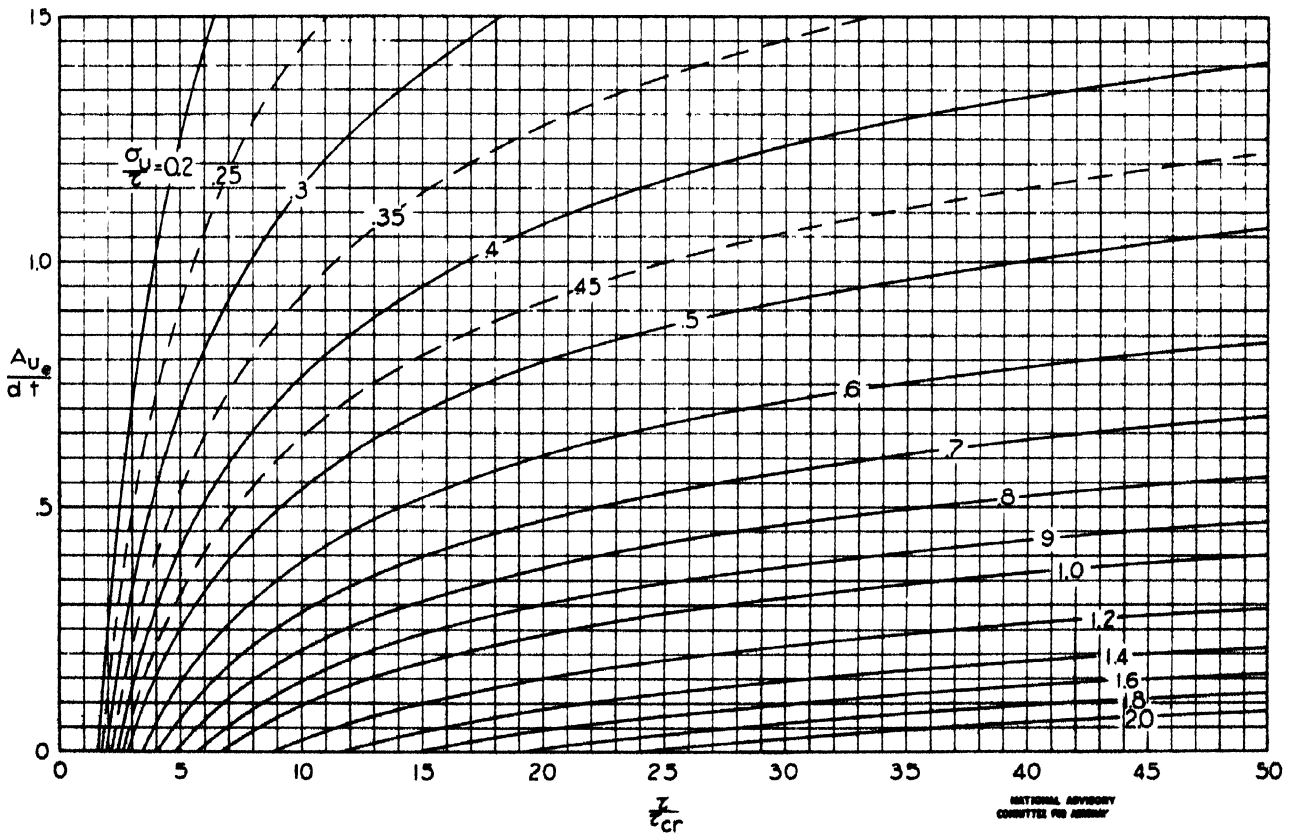


Fig. C7-23 - Diagonal-tension analysis chart (straight scale).

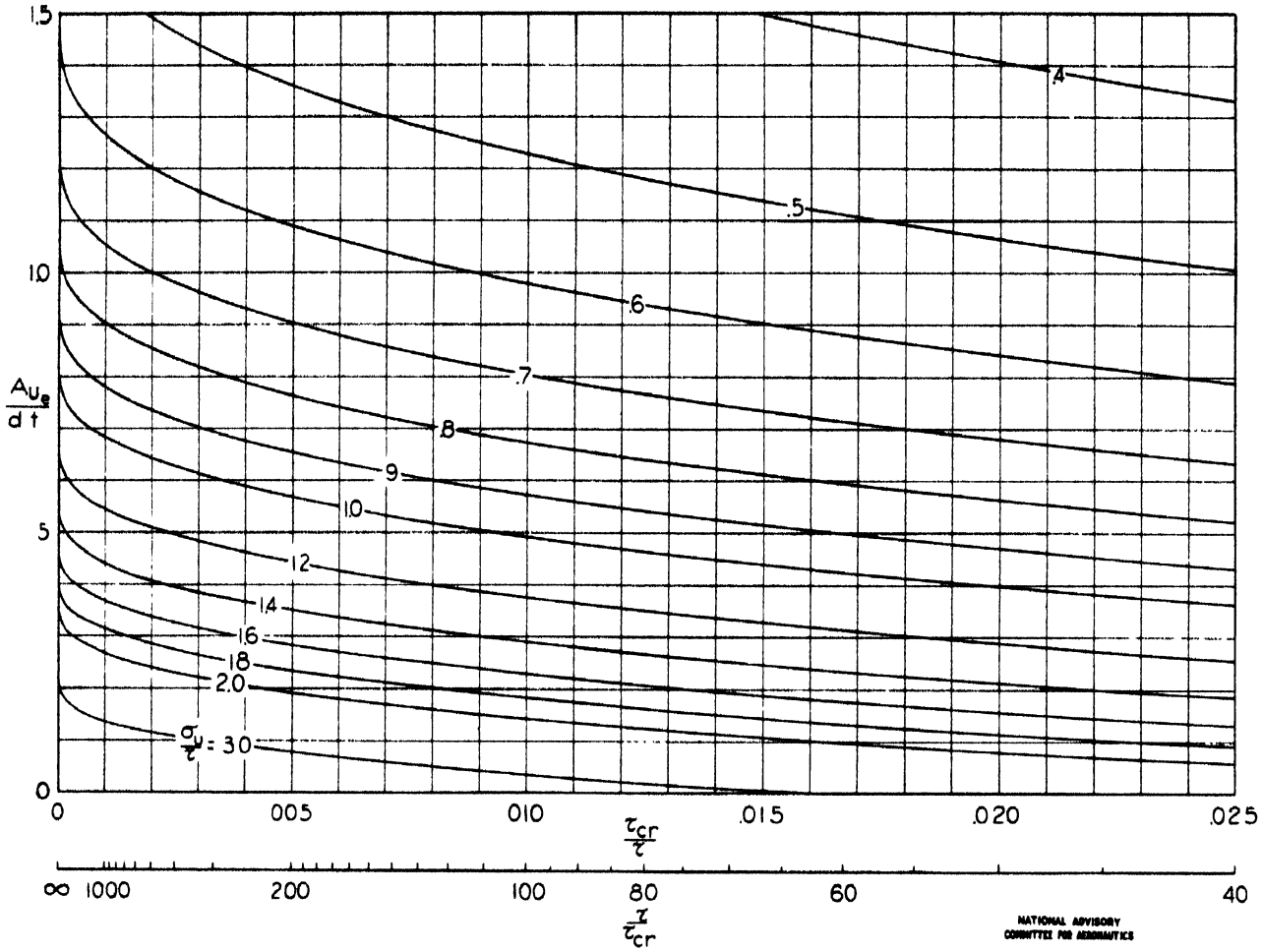


Fig. C7-24 - Diagonal-tension analysis chart (semilogarithmic scale).

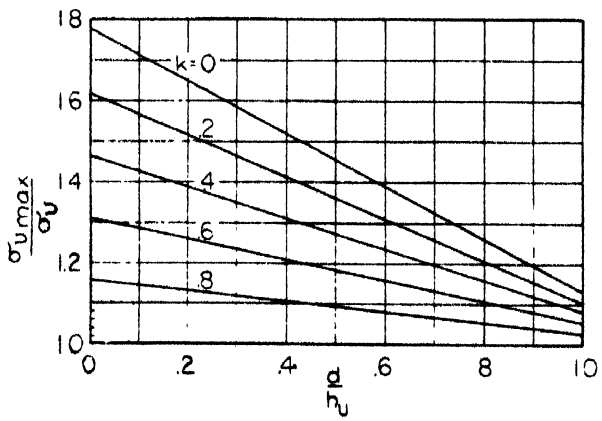


Fig. C7-25 - Ratio of maximum stress to average stress in upright.

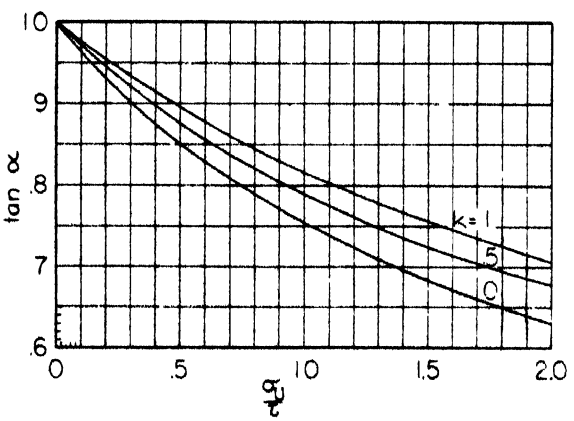


Fig. C7-26 - Graph for determining angle α.

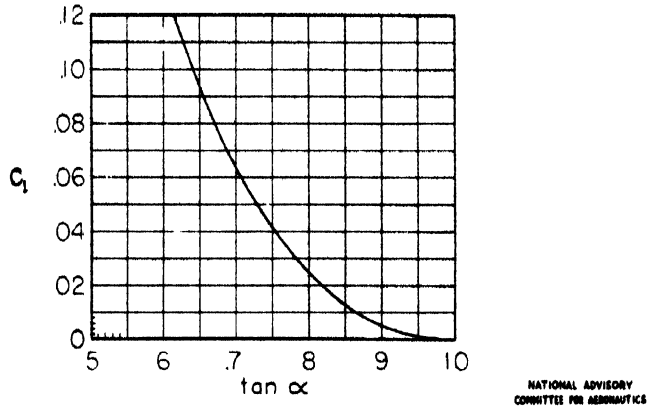


Fig. C7-27 Stress-concentration factor C_1.

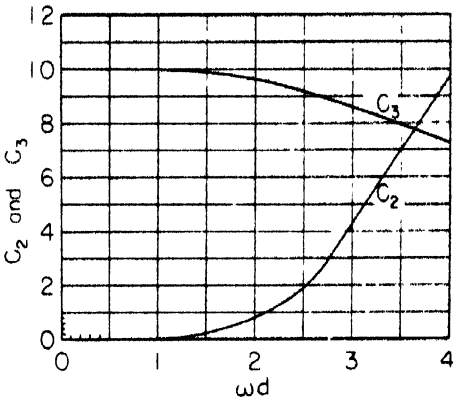
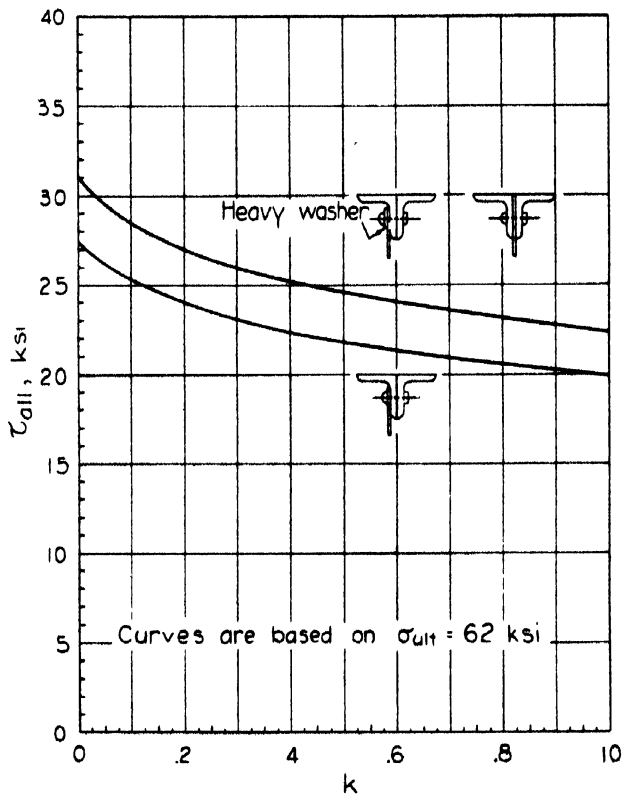
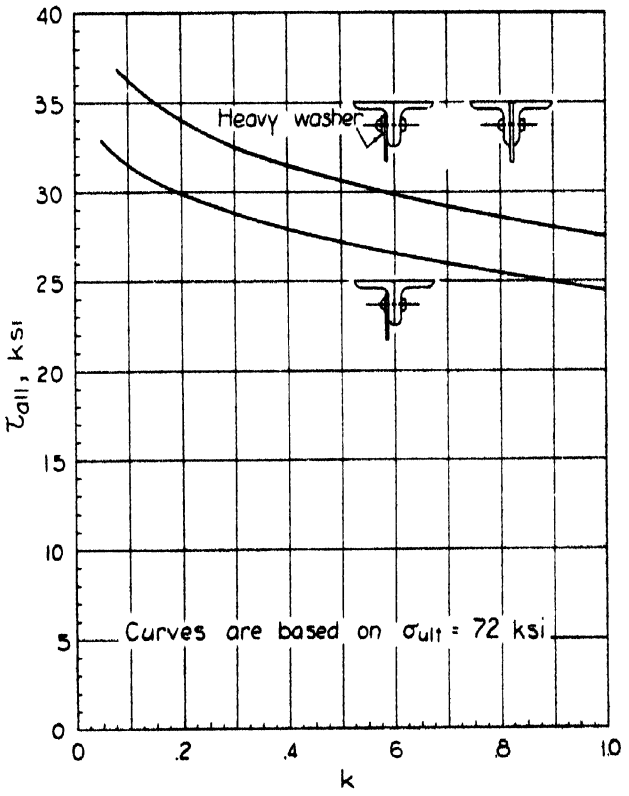


Fig. C7-28 - Stress-concentration factors C_2 and C_3.

$$\left(wd = 0.7\, d \sqrt[4]{\frac{t}{(I_C + I_T)\, h_e}}\right)$$



(a) 24ST aluminum alloy.



(b) Alclad 75ST aluminum alloy.

NATIONAL ADVISORY COMMITTEE FOR AERONAUTICS

Fig. C-7-29 Allowable values of nominal web shear stress.

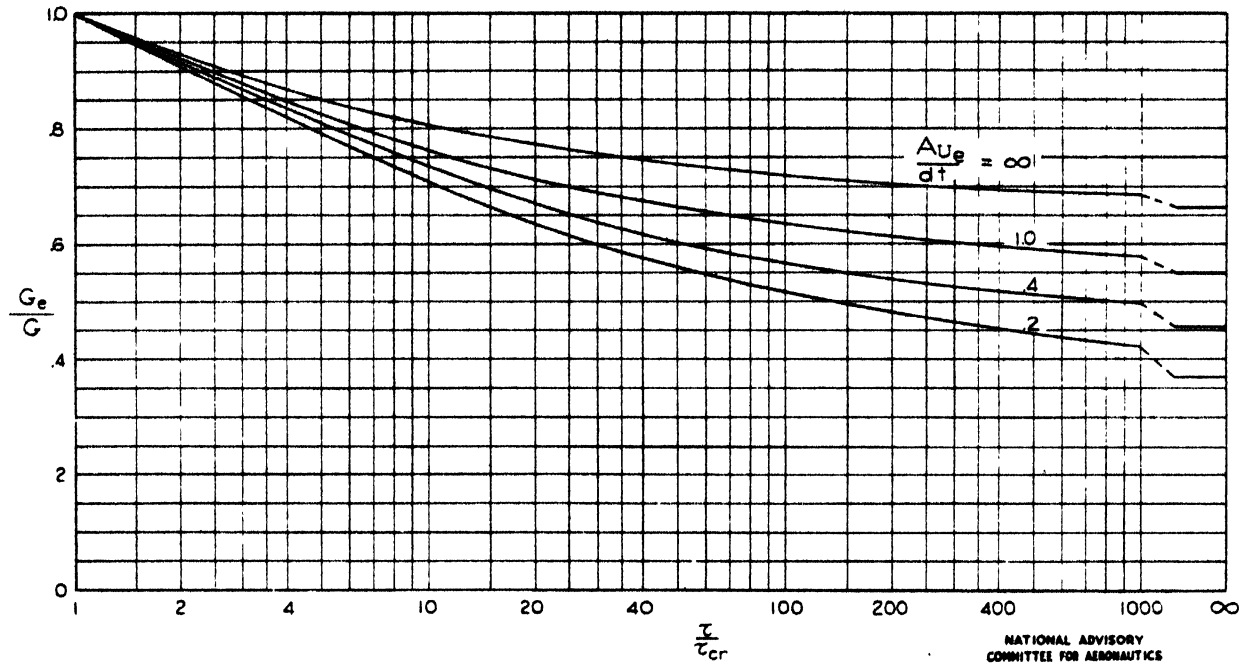


Fig. C7-30 - Effective shear modulus of diagonal-tension webs.

Using .352 as value of d/h_u and k = .69 we find from Fig. C7.25 that $\sigma_{u_{max}}/\sigma_u = 1.17$. Hence,

$$\sigma_{u_{max.}} = -16900 \times 1.17 = -19800 \text{ psi.}$$

Calculation of Diagonal Tension Angle α

From Fig. C7.26 for values of k = .69 and $\sigma_u/\tau = 16900/18350 = .92$, we obtain tan $\alpha = .815$

Calculation of Allowable Stresses For Upright

Check allowable stress for failure as a column:-

Since the design is of the single upright type, we check the following two criteria:-

(1) Stress σ_u should be no greater than the column yield stress for the upright material. The column yield stress F_{co} for 24ST material from Table C2.2 of Chapter C2 equals -50000 psi. Hence with σ_u = -16900 and allowable = -50000, the upright is far overstrength for this criterion. If we used $\sigma_{u_{max.}} = -19800$ instead of σ_u, the result would still be far overstrength.

(2) The stress at the centroid of the upright should be no greater than the allowable column stress for a slenderness ratio of $h_u/2\rho$ = 28.50/2 x .29 = 49.

The general short column equation for 24ST material equals,

$$F_c = 50000 - 421\ L/\rho$$

Substituting:-

$$F_c = 50000 - 421 \times 49 = -29300 \text{ psi.}$$

But σ_u = -16900 psi.
Hence M.S. = (29300/16900) -1 = .73

Allowable Stress for Upright for forced Crippling

The allowable crippling stress to compare against $\sigma_{u_{max.}}$ is given by formula (61a)

$$\sigma_u = 28\ k\ \sqrt{t_u/t}$$

$$= 28 \times .69 \sqrt{\frac{.125}{.025}} = -434 \text{ kips} = -43400 \text{ psi}$$

It is stated that if this value of σ_u is greater than the proportional limit of the material, than the allowable upright stress should be taken as corresponding to a compressive strain of σ_0/E = 43400/10300000 = .0042

Since the stress of 43400 is above the proportional limit of 24ST extruded material, we find from the compressive stress-strain diagram of 24ST extrusion with wall thickness less than 1/4 inch which is given in Fig. C1.5 of Chapter C1, that a stress of -37000 corresponds to a strain of .0042. Hence M.S. = (37000/19800) -1 = .86

Thus the minimum margin of safety for the upright is .73 which indicates the web stiffeners or uprights are considerably overstrength and therefore overweight and should be revised in practical design.

Check Web Design

The peak value of the nominal web shear stress within a beam bay is taken as,

$$\tau_{max.} = \tau\ (1 + k\ C_1)\ (1 + k\ C_2)$$

From Fig. C7.27 using tan α = .815, we find C_1 = .022

Using Fig. C7.28, we must find value of term

$$wd = 0.7\ d \sqrt[4]{\frac{t}{(I_c + I_T)\ h_e}}$$ before the value of C_2 can be found.

$$wd = 0.7 \times 10 \sqrt[4]{\frac{.025}{(.1075 + .0291)\ 29.45}} = 1.96$$

hence from Fig. C7.28, C_2 = .075

Substituting:-

$$\tau_{max.} = 18350(1 + .69 \times .022)\ (1 + .69 \times .075)$$
$$= 19600 \text{ psi.}$$

Allowable Web Shear Stress

From Fig. C7.29 for k = .69, the allowable τ for 24ST ($\sigma_{ult.}$ = 62000 psi.) equals 21000 psi for web without rivet washer and 23700 psi for web with rivet washer.

Assume the rivet washer type is being used, and correcting to 24ST alclad directly as the ultimate tensile strength we obtain an allowable web stress of 23700 x 56000/62000 = 21400 psi. Hence M.S. = (21400/19600) -1 = .11

Check of Rivets

Loads per inch of run web to flange rivets is given by following equation.

$$R'' = \frac{S_w}{h_r}\ (1 + 0.414\ k)$$

$$= \frac{13500}{28.50}\ (1 + 0.414 \times .69) = 610\#$$

Load per rivet pitch of 3/4 inch = .75 x 610 = 456#

These values are practically the same as by the first method of solution in Art. C7.13.

Single shear strength of 5/32 A17ST rivet = 512#. Bearing strength on .025 web = 362# (critical).

Strength per rivet pitch = 2 x 362 = 724#
M.S. = (724/456) -1 = .58

Web to Upright Rivets

The required tensile strength is given by the criterion, that the tensile strength of rivets per inch of stiffener should be greater than 0.22 to $\sigma_{ult.}$ which equals 0.22 x .025 x 62000 = 340#/inch.

In our rivet problems we have specified no web-stiffener rivets. Thus rivets should be specified that will develop 340# tension strength per inch of stiffener. The government manual ANC-5 does not give tensile strength of rivets in various sheet thicknesses, as the strength will vary with the sheet thickness. Most airplane companies have made tests to establish tension strength of rivets and thus in actual design the proper spacing should be specified to develop the tensile strength specified for single web stiffeners namely .22 t $\sigma_{ult.}$

Upright to Flange Rivets.

The web uprights are fastened to the flange both upper and lower by 1/4 dia. AN steel bolt.

The load on the upright at its ends is,
$P_u = \sigma_u\ A_{u_e}$ = 16900 x .112 = -1895#

Shear strength of 1/4 bolt = 3681
Bearing on vertical 3/32 leg of lower flange = 1.25 x 2340 = 2930# (critical).
M.S. = (2930/1895) -1 = .54
Since a 1/4" dia. rivet A17ST, F_{su} = 38 ksi has a shear strength of 1970# it could be used instead of the 1/4" bolt and the M.S. would be .04.

Check of Flange Strength

Section 50" from end is critical. Design external bending moment = 50 x 13500 = 675000"#
Diagonal tension factor = .69
Thus bending moment developed as a shear resistant beam = (1 - .69) 675000 = 209000"#

The remainder of the bending moment is developed as a pure tension field beam, or a moment of 466000"#.

Bending Stresses

Upper flange bending stresses, (extreme fiber) $f_b = -\frac{209000 \times 12.58}{270.5} - \frac{466000 \times 10.94}{210}$

$$= -9700 - 24300 = -34000 \text{ psi.}$$

Lower Flange Bending Stresses (extreme fiber)

$$f_b = -\frac{209000 \times -17.42}{270.5} + -\frac{466000 \times -19.06}{210}$$

$$= 13450 + 42400 = 55850 \text{ psi.}$$

Average axial flange loads due to Bending

As a shear resistant beam average axial flange load equals

$$\left(\frac{I - I_W}{I}\right)\ \left(\frac{M\ (1 - k)}{h_e}\right)$$

where M (1 - k) = 675000 (1 - .69) = 209000"# time of web buckling

h_e = distance between flange centroids
I = moment of inertia of entire beam section about neutral axis
I_W = moment of inertia of web about beam N.A.

Substituting

$$\text{Flange load} = \frac{209000}{29.45}\ \left(\frac{270.5 - 60.5}{270.5}\right) = \pm 5510\#$$

Average axial flange load due to bending with beam in diagonal tension state,

$$= \frac{466000}{29.45} = \pm\ 15840\#$$

Total flange average axial loads due to bending:-

Upper flange $F_c = -15840 - 5510 = -21350\#$

Lower flange $F_t = F_c = 21350\#$

Flange Axial Loads Due to Tension Field Action

$$F_F = -\frac{S_{DT}}{2} \cot \alpha$$

S_{DT} = shear load carried by diagonal tension field action = kS, where k = .69

Hence $F_F = -\frac{.69 \times 13500}{2} \times 1.11 = -5160\#$

Total Flange Average Axial Loads

Upper flange $F_c = -21350 - 5160 = -26510\#$

Lower flange $F_t = 21350 - 5160 = 16190\#$

Average stress upper flange $= \frac{-26510}{.675} = -39200$ psi.

Average stress lower flange $= \frac{16190}{.378} = 32800$ psi.

Comparing these values with the values obtained by the first method of solution we find -44000 and 42450 respectively. Thus the NACA method decreases the load on the compression flange.

Check of Flange Stresses Due to Secondary Flange Bending Moments

From Formula 65

$$M = \frac{1}{12} k \gamma t d^2 C_s$$

From Fig. C7.28, $C_s = .97$ when wd = 1.96

Hence,

$$M = \frac{1}{12} \times .69 \times 18350 \times .025 \times 10^2 \times .97 = 2560\#$$

This compares with 3210"# by the first method of solution. The flange stresses could be found as in solution method 1.

General Conclusion

The NACA method given in general gives slightly higher margins of safety.

C7.28 Problems.

(1) The beam as shown in Fig. C7.31 is subjected to a shear load of 8000# as shown. Determine the margin of safety for the given loading for the following units: (1) web, (2) web flange rivets, (3) web stiffeners. Use NACA method.

(2) Same as problem (1) but with web upright spacing = 4".

(3) Design a semi-tension field beam for the beams and loading of Fig. C7.32. Take web as 24ST with minimum thickness being .020. Web uprights and flange members to be 24ST extrusions. Rivets to be A17ST. Show calculations for at least four sections along beam length. Assume the beam braced laterally by .025 skin on top and bottom.

(4) Fig. C7.33 shows the cross-section of a single spar wing beam. Strength check the following units of the beam section. (1) web, (2) web uprights. The upright spacing is 8 inches and the design shear load on section is 35000# web material is 75ST alclad.

REFERENCES

(1) H. Wagner, "Flat Sheet Girder With Thin Metal Web"
Part I - N.A.C.A. Technical Memo. #604
Part II - N.A.C.A. Technical Memo. #605
Part III - N.A.C.A. Technical Memo. #606

(2) H. Wagner, "Structures of Thin Sheet Metal, Their Design and Construction", N.A.C.A. Memo. #490.

(3) R. Lahde and H. Wagner, "Tests for the Determination of the Stress Condition in Tension Fields". N.A.C.A. Technical Memo. #809.

(4) Paul Kuhn, "A Summary of Design Formulae for Beams Having Thin Webs in Diagonal Tension". N.A.C.A. T.N. 469.

(5) Denke, Paul H., "Strain Energy Analysis of Incomplete Tension Field Web-Stiffeners Combinations". Jr. Aero. Sci. Vol. II, No. 1 Jan. 1944.

(6) Kuhn, Paul, "Investigations on the Incompletely Developed Plane Diagonal-Tension Field". N.A.C.A. Rep. No. 697, 1940.

(7) Kuhn, Paul, and Chiarito, Patrick T., "The Strength of Plane Web Systems in Incomplete Diagonal Tension". N.A.C.A. A.R.R., Aug. 1942.

(8) Levy, Samual, Woolley, Ruth M. and Corrick, Josephine N., "Analysis of Deep Rectangular Shear Web above Buckling Load". N.A.C.A. T.N. 1009, 1946.

(9) Peterson, James P., "Strain Measurements and Strength Tests of 25 Inch Diagonal-Tension Beams with Single Uprights". N.A.C.A. A.R.R. No. L5J02A, 1945.

(10) Peterson, James P., "Strain Measurements and Strength Tests of 25 Inch Diagonal Tension Beams of 75ST Aluminum Alloy". N.A.C.A. T.N. No. 1058, 1946.

(11) Kuhn, Paul, "Ultimate Stresses Developed by 24ST Sheet in Incomplete Diagonal Tension". N.A.C.A. T.N. 833, 1941.

(12) Kuhn, Paul, and Moggio, Edwin H., "The Longitudinal Shear Strength Required in Double-Angle Columns of 24ST Aluminum Alloy". N.A.C.A. R.B. No. 3E08, 1943.

(13) Kuhn, Paul, and Peterson, James P., "Strength Analysis of Stiffened Beam Webs". N.A.C.A. T.N. 1364, 1947

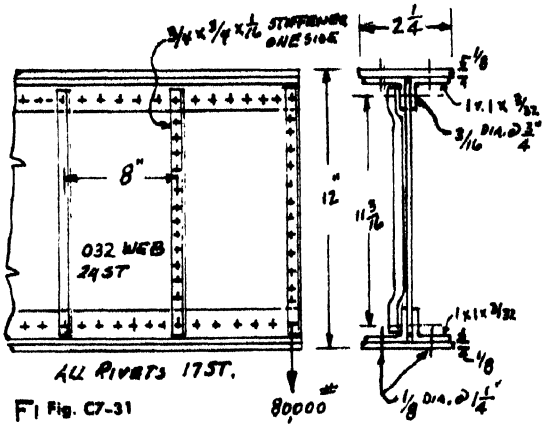
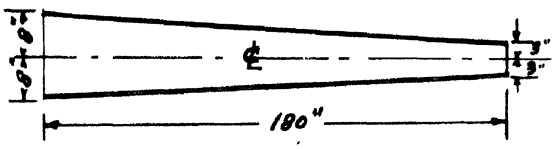


Fig. C7-31



Fig. C7-32



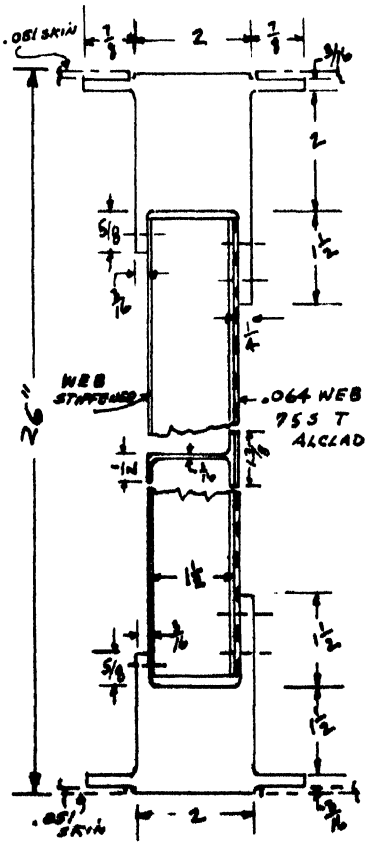


Fig. C7-33

CHAPTER C8
DESIGN OF WOOD BEAMS AND COLUMNS

C8.1 Introduction

Wood has played an important part in the structural design of airplanes. Until the development of the heat treatable aluminum alloys, wood was the most common material for the design of wing structures particularly the beams and ribs. Metals like steel and aluminum alloys are practically homogeneous and isotropic materials. Wood on the other hand is neither homogeneous or isotropic. Reference to tables C8.1 and C8.2 show that the strength properties of wood normal to the grain direction are in general considerably less than the properties parallel to the grain. Other factors which helped to produce the trend away from the use of wood in the last decade are: ready moisture adsorption which affects strength; deterioration of wood with age particularly glued connections and diminishing of the suitable supply of the right kind of wood of the proper size for the fabrication major airplane units.

To overcome these disadvantages of plain wood, considerable research has recently been carried on with wood veneers bonded with synthetic resins. In general several thin layers of wood veneers with grain directions at right angles to each other are bonded together with synthetic resin by use of heat and pressure, thus creating a wood product which approaches an isotropic condition and one which is highly impervious against atmospheric influences.

C8.2 Aircrafts Woods. General Strength Properties.

Straight grained spruce is the chief material for wing beams. For reasonable sizes and lengths it is fairly economical. Its strength weight ratio is quite favorable. Douglas fir and Oregon pine have been used to a small extent for wing beams. For beam webs and body covering, plywood made from spurce, birch and mahogany is the commonly used material. Tables C8.1 and C8.2 summarize the general strength properties of the various kinds of wood.

C8.3 Common Types of Beam Sections.

Figs. C8.1(a to k) illustrate the common types of wood beams. The solid sections of Figs. (a) and (b) are common to small airplanes with externally braced wings where the beam depths are under six inches. Beam fabrication is exceedingly simple and inexpensive and the allowable compressive strength is high due to its relatively high form factor thus for small depths it can be made practically as light as the other types of beam sections. The disadvantage of such sections is the difficulty and expense of obtaining long lengths of spruce and other woods of such large cross-sections without imperfections.

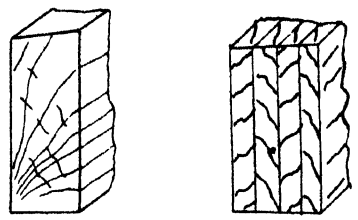


Fig. a Fig. b

Solid Beam Sections

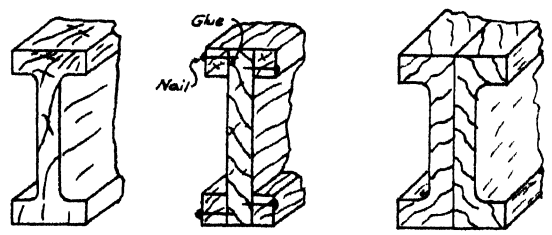
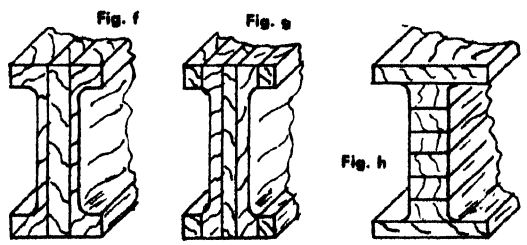


Fig. c Fig. d Fig. e

(I) Type Beam Section

Figs. c to h illustrate various types of beams of (I) cross-section. To eliminate large sizes of wood units they are built up as in Figs. (d), (g) and (h).



Figs. (i), (j) and (k) illustrate the box type of beam sections. In Figs. (i) and (j) the webs are composed of plywood. For beams over six inches these sections are generally used. The flange material is easily tapered and the plywood webs provide efficient construction from a weight standpoint.

Strength values of various woods for use in airplane design **Table C8.1** [Based on 15 per cent moisture content]

Common and botanical names	Specific gravity based on volume and weight when oven-dry	Weight at 15 per cent moisture content	Shrinkage from green to oven-dry condition: Radial	Shrinkage from green to oven-dry condition: Tangential	Static bending: Fiber stress at elastic limit [1]	Static bending: Modulus of rupture [1]	Static bending: Modulus of elasticity [2]	Static bending: Work to maximum load	Compression parallel to grain: Fiber stress at elastic limit [1] [3]	Compression parallel to grain: Maximum crushing strength [1]	Compression perpendicular to grain [4]	Shearing strength parallel to grain [5]	Hardness, side load required to embed 0.444-inch ball to one-half its diameter [6]	
	2	3	4	5	6	7	8	9	10	11	12	13	14	
HARDWOODS (BROAD LEAVED SPECIES)	Average	Moisture per cent	Lbs. per cu. ft.	Per cent	Per cent	Lbs. per sq. in.	Lbs. per sq. in.	1,000 lbs. per sq. in.	In.-lbs per cu. in.	Lbs. per sq. in.	Lbs. per sq. in.	Lbs. per sq. in.	Lbs. per sq. in.	Lbs.
Ash, black (*Fraxinus nigra*)	0.53	0.68	33	5.9	7.8	6,400	11,000	1,340	14.3	4,000	2,400	1,200	1,250	700
Ash, commercial white (*Fraxinus* sp.)[7]	.60	.66	41	6.3	8.9	8,200	14,400	1,630	16.3	5,200	3,200	1,350	1,500	1,100
Basswood (*Tilia glabra*)	.40	.56	28	6.6	9.3	5,000	8,800	1,200	6.6	3,270	1,600	730	1,050	570
Beech (*Fagus grandifolia*)	.69	.80	44	4.6	10.6	8,200	14,300	1,440	15.5	4,800	3,600	1,270	1,500	1,050
Birch (*Betula* sp.)	.65	.82	44	7.6	9.9	8,000	13,800	1,720	14.2	5,400	3,000	1,270	1,500	1,050
Cherry, black (*Prunus serotina*)	.55	.65	33	3.7	7.1	8,200	12,600	1,550	11.7	5,150	3,000	1,170	1,100	660
Cottonwood (*Populus deltoides*)	.45	.38	29	3.9	9.2	5,600	8,600	1,160	7.4	2,850	1,700	850	850	410
Elm, rock (*Ulmus racemosa*)	.68	.63	45	4.8	8.1	7,600	13,600	1,540	16.2	5,150	3,600	1,350	1,350	1,050
Gum, red (*Liquidambar styraciflua*)	.52	.46	34	5.3	9.9	7,200	11,600	1,320	10.9	4,650	3,400	1,160	1,100	660
Hickory (true hickories) (*Hicoria* sp.) [8]	.70	.71	51			10,600	18,200	1,940	27.5	6,150	4,200	1,440		
Mahogany, African (*Khaya* sp.)	.47	.42	32	4.9	5.5	7,000	10,800	1,280	8.0	4,300	2,700	1,400	900	750
Mahogany, true (*Swietenia* sp.) [9]	.51	.46	34	3.4	4.7	8,800	11,600	1,380	7.5	4,650	3,400	1,760	850	750
Maple, sugar (*Acer saccharum*)	.67	.69	44	4.8	9.9	9,800	15,600	1,600	15.7	5,650	3,800	2,170	1,450	1,270
Oak, commercial white and red [10] (*Quercus* sp.)	.68	.68	45	4.6	9.0	7,600	13,800	1,660	13.6	4,850	3,600	1,470	1,300	1,060
Poplar, yellow (*Liriodendron tulipifera*)	.43	.38	28	4.0	7.1	6,600	9,100	1,280	6.3	2,750	1,600	810	850	530
Walnut, black (*Juglans nigra*)	.56	.62	39	5.2	7.1	10,200	15,100	1,680	11.4	5,700	3,600	1,730	1,650	950
SOFTWOODS (CONIFERS)														
Cedar, incense (*Libocedrus decurrens*)	.36	.33	25	3.3	5.7	6,000	8,700	1,080	5.6	4,200	2,400	980	850	480
Cedar, Port Orford (*Chamaecyparis lawsoniana*)	.44	.40	30	4.6	6.9	7,400	11,000	1,520	8.7	4,200	2,400	1,020	760	530
Cedar, western red (*Thuja plicata*)	.34	.31	23	2.5	5.1	4,100	7,000	1,000	5.8	4,000	2,000	800	680	330
Cedar, white, northern (*Thuja occidentalis*)	.32	.30	22	2.1	4.9	4,700	6,000	700	4.9	3,040	2,000	800	610	300
Cypress, southern (*Taxodium distichum*)	.46	.43	32	3.9	6.1	7,100	10,600	1,[illegible]	7.7	4,000	2,800	1,200	730	600
Douglas fir (*Pseudotsuga taxifolia*)	.51	.45	34	5.0	7.8	8,600	11,600	1,700	8.1	5,400	2,600	1,200	910	660
Pine, Norway (*Pinus resinosa*)	.51	.46	34	4.6	7.2	8,500	11,600	1,560	8.9	5,200	2,600	1,020	970	660
Pine, sugar (*Pinus lambertiana*)	.38	.34	28	2.9	6.6	5,600	8,000	1,040	5.4	3,650	2,000	810	750	370
Pine, western white (*Pinus monticola*)	.42	.36	27	4.1	7.4	6,000	9,200	1,110	6.9	4,200	2,200	780	800	360
Pine, northern white (*Pinus strobus*)	.38	.34	26	2.2	6.0	5,000	8,700	1,140	5.2	3,040	2,000	780	680	360
Spruce (*Picea* sp.) [11]	.40	.36	27	4.1	7.4	6,200	9,400	1,200	7.8	4,000	2,000	840	750	440

[1] The average values for fiber stress at elastic limit and modulus of rupture in static bending, fiber stress at elastic limit, and maximum crushing strength in compression parallel to grain have been multiplied by 2 factors to obtain values for use in design. A statement of these factors and of the reasons for their use follows:

It was thought best in fixing upon strength values for use in design, to give some influence to the variability of wood and to the fact that a greater number of values are below the average than above it, and the most probable value (as represented by the mode of the frequency curve) was accordingly decided upon as the basis for design figures. From a study of the ratios of most probable to average values for 5 species (Sitka spruce, Douglas fir, and white ash), 0.94 was adopted as the best value of this ratio for general application to the properties in question.

The stress that wooden members can carry depends on its duration. A factor of 1.17 has been applied to test results to get values of the stress that can be sustained for a period of 5 seconds, it being assumed that the maximum load will not be maintained for a longer period.

[2] The values given are the most probable values (50 per cent of the average) of the apparent modulus of elasticity (E_c) as obtained by substituting results from tests of 2 by 2 inch beams on a 28-inch span with load at the center in the formula $E_c = Pl^3/4bd^3\delta$. The use of these values of E_c in the usual formulas will give the deflection of beams of ordinary length with but small error. For exactness in the computation of deflections of I and box beams, particularly for short spans, the formula that takes into account shear deformations (see National Advisory Committee for Aeronautics Report No. 180, Deflection of Beams with Special Reference to Shear Deformations) should be used. This formula involves E_T, the true modulus of elasticity in bending, and F, the modulus of rigidity in shear. Values of E_T may be obtained by adding 10 per cent to the values of E_c as given in the table. If the I or box beam has the grain of the web parallel to the axis of the beam, or parallel and perpendicular thereto, as in some plywood webs, the value of F may be taken as $E_T/16$ or $E_c/14.5$. If the web is of plywood with the grain at 45° to the axis of the beam, F may be taken as $E_T/5$ or $E_c/4.5$.

[3] Design values for fiber stress at elastic limit in compression parallel to grain were obtained by multiplying the values of maximum crushing strength as given in the next column by factors as follows: 0.75 for hardwoods, 0.80 for conifers. Values as given are to nearest 10 pounds.

[4] Wood does not exhibit a definite ultimate strength in compression perpendicular to grain, particularly when the load is applied over only a part of the surface, as it is at fittings. Beyond the elastic limit the load continues to increase slowly until the deformation and crushing become so severe as to seriously damage the wood in other properties. Figures in this column were obtained by applying a duration of stress factor of 1.17 (see note 1) to the average elastic limit stress and then adding 331/3 per cent to get design values comparable to those for bending, compression parallel to grain, and shear as listed in the table.

[5] Values in this column are for use in computing resistance of beams to longitudinal shear. They are obtained by multiplying average values by 0.75. This factor is used because of the variability in strength and in order that failure by shear may be less probable than failure from other causes. Furthermore, tests have shown that beams of the favorable I and box beams are so proportioned that the ultimate shearing strength is not developed and failure by shear does not occur.

[6] Includes white ash (*F. americana*), green ash (*F. lanceolata*), and blue ash (*F. quadrangulata*).

[7] Includes sweet birch (*B. lenta*) and yellow birch (*B. lutea*).

[8] Includes big-leaf shagbark hickory (*H. laciniosa*) mockernut hickory (*H. alba*), pignut hickory (*H. glabra*), and shagbark hickory (*H. ovata*).

[9] Includes material from Central America and Cuba.

[10] Includes white oak (*Q. alba*), bur oak (*Q. macrocarpa*), swamp chestnut oak (*Q. prinus*), post oak (*Q. stellata*), red oak (*Q. borealis*), southern red oak (*Q. rubra*), laurel oak (*Q. laurifolia*), water oak (*Q. nigra*), swamp red oak (*Q. pagodaefolia*), willow oak (*Q. phellos*), yellow oak (*Q. velutina*).

[11] Includes red spruce (*P. rubra*), white spruce (*P. glauca*), and Sitka spruce (*P. sitchensis*).

* Table C8.2

-Strength of 3-ply panels made of various species of wood

[All plies in any one panel are of the same thickness and of the same species, grain of successive plies at right angles; all material rotary cut, starch glue used throughout. Eight thicknesses of plywood, ranging from 1/16 inch to 1/4 inch, were tested]

Species of wood	Average specific gravity of plywood based on oven-dry weight and volume at test	Average moisture content in per cent	Column-bending modulus [8]: Parallel [1]: Number of tests	Column-bending modulus [8]: Parallel [1]: Pounds per square inch	Column-bending modulus [8]: Perpendicular [1]: Number of tests	Column-bending modulus [8]: Perpendicular [1]: Pounds per square inch	Tensile strength: Parallel [1]: Number of tests	Tensile strength: Parallel [1]: Pounds per square inch	Tensile strength: Perpendicular [1]: Number of tests	Tensile strength: Perpendicular [1]: Pounds per square inch	Splitting resistance: Number of tests	Splitting resistance: Per cent of birch [2]	Modulus of elasticity: Parallel (1,000 pounds per square inch) [1]	Modulus of elasticity: Perpendicular (1,000 pounds per square inch)
Ash, black	0.49	9.1	120	7,700	120	1,770	120	8,100	120	3,040	200	73	1,073	98
Ash, commercial white	.60	10.2	200	9,000	240	2,080	200	9,810	200	4,320	400	77	1,420	143
Basswood	.42	9.2	200	7,120	200	1,670	200	8,200	200	4,200	400	68	1,213	85
Beech	.67	8.6	120	10,200	120	2,020	120	12,000	120	7,200	200	95	2,140	167
Birch, yellow	.67	8.5	160	10,000	200	2,300	160	12,200	160	7,200	400	100	2,200	197
Cedar, Spanish	.41	13.9	118	6,400	118	1,400	118	8,300	118	2,240	200	60	1,082	84
Cherry	.56	9.1	118	10,200	118	2,020	118	9,400	118	5,000	200	80	1,697	182
Chestnut	.43	11.7	60	5,100	60	1,110	60	6,400	60	2,800	60	74	794	78
Cottonwood	.46	8.8	120	6,400	120	1,670	120	7,200	120	4,240	200	82	1,697	109
Cypress, southern	.47	10.3	58	7,600	58	1,720	58	8,200	58	4,200	120	82	1,144	91
Douglas fir	.48	8.7	180	9,400	176	1,900	174	9,200	174	4,200	360	82	1,200	120
Elm, American	.52	8.9	160	9,400	160	1,970	160	8,800	160	3,800	320	73	1,394	169
Elm, rock	.68	8.8	88	12,700	88	2,800	88	9,400	88	5,000	180	99	1,600	136
Gum, black	.54	10.6	60	8,000	60	1,600	60	8,000	60	4,200	120	85	1,272	113
Gum, red	.54	8.7	182	9,070	182	2,020	182	7,800	182	4,200	364	80	1,072	130
Gum, tupelo	.50	10.3	80	7,700	80	1,800	80	6,800	80	3,700	160	80	1,200	111
Hackberry	.54	10.7	80	8,100	80	1,800	80	8,000	80	4,200	160	84	1,704	98
Hemlock, western	.47	9.7	160	9,200	110	1,800	110	8,000	110	4,200	220	84	1,321	112
Magnolia	.50	9.9	40	9,000	40	1,940	40	10,000	40	4,200	80	88	1,704	183
Mahogany, African	.53	12.7	20	8,000	20	2,000	20	8,000	20	3,700			1,201	144
Mahogany, Philippine	.52	10.7	38	10,100	38	2,300	38	10,000	38	3,700			1,600	160
Mahogany, true	.49	11.4	36	8,000	36	1,900	36	8,000	36	3,700	40	80	1,200	120
Maple, soft	.57	8.9	182	11,500	182	2,400	182	9,000	182	4,200			1,392	117
Maple, sugar	.68	8.0	200	13,000	200	2,240	200	10,000	200	4,200	400	100	1,700	143
Oak, commercial red	.69	9.2	116	9,000	116	2,070	116	8,000	116	4,200	232	114	2,113	189
Oak, commercial white	.64	10.2	180	10,000	180	2,210	180	8,700	180	4,200	360	86	1,900	189
Pine, northern white	.43	10.2	34	7,000	40	1,770	40	7,000	40	3,700	80	86	1,348	148
Poplar, yellow	.45	9.4	160	8,000	160	1,800	160	7,200	160	3,700	320	82	1,274	91
Redwood	.41	11.2	68	7,000	68	1,800	68	7,200	68	3,700	120	86	1,104	116
Spruce, Sitka	.43	8.4	160	7,000	160	1,800	160	8,000	160	3,700	320	86	1,311	116
Sycamore	.56	9.9	160	11,000	160	2,240	160	8,800	160	4,200	320	86	1,600	166
Walnut, black	.60	9.1	116	12,000	116	2,770	116	9,200	116	4,200	232	77	1,720	141

[1] Parallel and perpendicular refer to the direction of the grain of the face relative to the direction of the application of the force.

[2] The relative splitting resistances of the various panels (Col. 12) are supposed largely on the bedding strength of the glue.

[8] May be used as modulus of rupture in pure bending.

[illegible] Probably black cherry. [illegible] Probably evergreen magnolia. [illegible] Probably Hemlock sp. [illegible] Probably tanguile. [illegible] Probably silver maple

(*From ANC-5, revision of 1940)

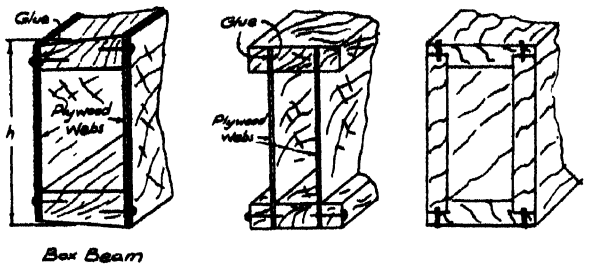


Fig. i Fig. j Fig. k

Box Type Beam Sections

C8.4 Modulus of Rupture in Bending.

Fig. C8.2 gives the allowable compressive ultimate stresses for Sitka spruce beams in bending, if the stresses are computed by the general flexure formula $f_b = My/I$. These so called allowable stresses are not the true bending stresses that exist on the critical beam sections at the time of failure, since the assumptions in the derivation of the formula assume stresses below the proportional limit of the material and that stress is directly proportional to strain, whereas the actual conditions of the wood in the failing range fall in the plastic range. However, if actual beam static tests are made and the stresses using the ultimate test loads are computed by the flexure formula, then these ficticious stresses, referred to as the modulus of rupture stress can be used in design if the flexure formula is used in calculating the design bending stresses.

The Forest Products Laboratory found that the modulus of rupture for I-beams and box sections depended primarily upon two ratios, namely t_c/h (thickness of compression flange divided by centerline depth of beam) and b'/b (thickness of web or webs divided by total width of beam), and that "form factors" based upon these ratios, when multiplied by the modulus of rupture for a standard rectangular beam specimen, gave ultimate stress values which checked closely with test results. Fig. C8.2 gives the results for Sitka spruce, the values being obtained by multiplying the modulus of rupture of 9400#/in. for a standard rectangular beam specimen by the Forest Products form factors for beams for various sections. For other woods the values obtained from this figure should be adjusted in proportion to the relative values of the modulus of rupture for solid sections, as found in Table C8.1.

In wing beam design the upper and lower flange or chord members are usually beveled due to the contour of the wing. In computing the beam section properties it is common practice to consider the section as rectangular, using a height of the equivalent beam equal to the center line depth of the actual beam, and the thickness of the chords of the equivalent beam equal to the centerline depth of the chords of the actual beam. The Forest Products Laboratory showed that this simplication in computing the beam

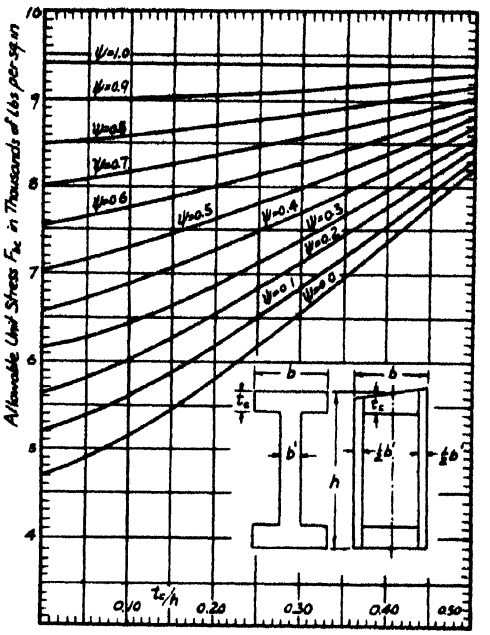


Fig. C8-2

section properties produced, negligible errors in the margin of safety.

The allowable bending compressive stresses in Fig. C8.2 are primarily for use in the design of statically determinate beams. For continuous beam they lean toward the conservative side since continuity tends to increase the ultimate strength of beams.

For the tension side the modulus of rupture should not exceed the modulus of rupture in compression for a rectangular solid section. For spruce this value is 9400#/in.^{2} which is slightly less than its ultimate tensile strength.

C8.5 Web Shear Stresses.

If beams are made of solid wood e.g. rectangular or I-sections, the allowable shear stress can be taken as the shearing strength parallel to the grain as given in the Table C8.1. Values for typical aircraft woods are:-

Sitka spruce = 750#/in.^{2}
Pine (northern white) = 640#/in.^{2}
Douglas Fir = 810#/in.^{2}
Ash (comm. white) = 1380#/in.^{2}
Birch = 1300#/in.^{2}

For 2-ply spruce or mahogany plywood having the grain of both plies at 45 degrees to the main beam axis, the allowable shearing stress can be obtained from the following formula:-

$$F_s = 960 + \frac{3140}{\sqrt[3]{C}} - 45.5\ d \quad \text{--------(1)}^*$$

* Ref. Air Corps Information Circular #587

where C = internal diaphragm or stiffener spacing in inches.

d = effective beam depth or distance between the centroids of the beam flanges in inches.

For beams with webs so constructed that plies are alternately parallel and perpendicular to the longitudinal axis of the beam the allowable shear stresses should not exceed 87.5 percent of those given by equation (1). The allowable stress should not be decreased beyond that for C = 32" spacing.

In computing the section moment of inertia for use in calculating bending stresses it is permissible to use one-half the area of 45 degree plywood webs. Some designers neglect web in computing section moment of inertia. For routed or built up I sections web area is considered fully effective in computing section properties.

C8.6 Allowable Glue Stresses.

The strength of a glued joint depends chiefly on the angle between the grain of the two pieces being joined. When the grains of both pieces are parallel, casein glue will develop the longitudinal shear strength of the wood. When the angle between the two grain directions is around 45° the joint strength is decreased around 40 percent, and when the angle is 90° the decrease in strength is 50 percent.

When 45° plywood is used as web material, the allowable glue stress between the web and the beam flanges is taken as 1/3 the strength of the flange material parallel to the grain (Ref. ANC - 5). For spruce this gives $\frac{750}{3} = 250\#/in^2$. This greatly reduced shear strength often causes difficulty in the design of box beams using plywood webs because the necessary glue area becomes the critical factor in the design of the beams. (See example problems)

Weldwood Glue

Recently the U.S. plywood Corporation has developed and placed on the market a synthetic plastic resin glue. It comes in dry powder form, mixes instantly with cold water and can be applied with a stick or brush and sets up in a few hours and it is claimed that it becomes water proof after a period of 10 days to two weeks.

Table C8.2 gives a resume of the results of static tests to determine the shear strength of weldwood glue as given in test report #17 of the Spencer-Larsen Aircraft Corporation. The grain of the glued wood was parallel to the applied line of force.

Table C8.2 Weldwood Glue Strength

Wood	Average Ultimate Shear Stress psi
Spruce to Mahogany	817
Spruce to Spruce	900
Mahogany to Mahogany	1167
Pine to Mahogany	1100

Table C8.2 (Cont'd.)
Results when soaked in sea or fresh water for 24 hours and allowed to dry 12 hours before testing.

Wood	Ult. Shear Strength psi
Spruce to Mahogany	550
Spruce to Spruce	484
Mahogany to Mahogany	884
Pine to Mahogany	634

C8.7 Calculation of Glue Shear Stresses.

The horizontal shear stress intensity is given by the familiar equation.

$$f_s = \frac{V/ydA}{Ib}$$ (See Chapter A12 for derivation)

An approximate value is given by the equation,

$$f_s = \frac{V}{db}$$, where V = shear load on section
d = distance between flange centroids
b = width of section where shear stress is desired.

Example Problem of Glue Stress Calculation

Fig. C8.3 shows a box beam section. Consider an external shear load of 2160# as acting on the section. Find the average stress on the glue between the upper flange and the webs along section A-A.

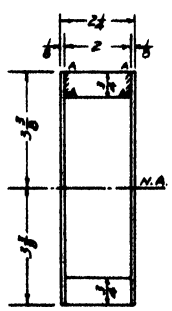


Fig. C8-3

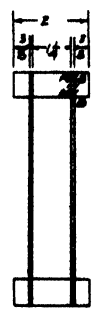


Fig. C8-4

(1) Solution using flexural shear equation

$q = \frac{V/ydA}{I}$ = horizontal shear flow in lbs. per inch

$I_{N.A.} = 30.4$ in.^{4} (includes 1/2 web area as effective)

$/ydA$ = first moment of flange area about neutral axis = 2 x .75 x 3 = 4.5

Hence longitudinal shear load per inch on glue on both sections A-A is,

$$q = \frac{2160 \times 4.5}{30.4} = 320\#/\text{inch}.$$

glue shear area $A_g = (1 \times .75)2 = 1.5$ sq. in.

Hence average glue stress $f_g = \frac{q}{A_g} = \frac{320}{1.5} = 213\#/in.^2$

(2) Solution by approximate method $f_g = \frac{V}{db}$.

d = (6.75 - .75) = 6"

Shear load per inch of beam = $q = \frac{V}{d} = \frac{2160}{6}$

= 360#

Since 1/2 of web of flange is effective in bending, the shear load on glue = $\frac{2}{2.125} \times 360 = 341\#/\text{inch}$

glue Area $A_g = (.75 \times 1)2 = 1.5$ sq. in.

Hence $f_g = 341/1.5 = 227\#/\text{in.}^2$ as compared to 213 by exact method. The discrepancy is due to approximate value of d and also to the fact that the web between flange and neutral axis has been neglected in computing d.

Fig. C8.4 shows the beam with same area but webs have been moved closer together leaving a flange portion outside of each web thus giving two glue surfaces between each web and the flange instead of one as in Fig. C8.3.

The horizontal shear load on section BB $= q = \frac{V\int ydA}{I} = \frac{2160 \times .375 \times .75 \times 3}{30.4} = 60\#/\text{in.}$

glue area on B-B = .75 x 1 = .75 " hence $f_s = \frac{60}{.75} = 80\#/\text{in.}^2$

Due to symmetry the shear flow on the flange portion between the webs will be divided between the webs, or in other words one half of the flange area between webs can be considered as loaded from each web, hence $\int ydA = .625 \times .75 \times 3 = 1.4$ and therefore the glue stress on section AA equals $f_s = \frac{2160 \times 1.4}{30.4 \times .75 \times 1} = 133\#/\text{in.}^2$

Thus the beam in Fig. C8.4 is better from a glue strength standppint.

A8.7a Problems - Wood Beams in Bending

Example Problem 1. Fig. C8.5 shows the cross section of a spruce box beam. Assuming a bending moment of 45000"# and a shear of 2800# as acting on this beam section, determine the stresses in bending and shear and margins of safety.

Solution: The first step is to compute the section properties about the neutral axis. Table C8.3 shows the detailed calculations. The properties are first calculated for reference axis 1-1 and then transferred to neutral axis.

For plywood webs, since grain is 45° with beam axis it is permissible to use only 1/2 of web area in computing section properties.

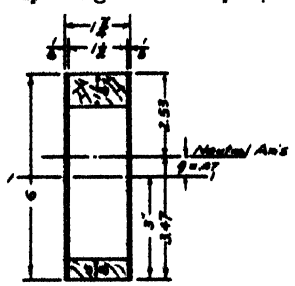


Fig. C8.5

Table C8.3

Portion	Area A	y	Ay	Ay^2	$I_o = \frac{1}{12}bd^3$	$I_{1-1} = I_o + Ay^2$
Upper Flange	1.688	2.437	4.11	10.0	0.18	10.18
Lower Flange	0.937	-2.687	-2.52	6.77	0.03	6.80
Web	0.750	0	0	0	2.25	2.25
Totals	3.375		1.59			19.23

$\bar{y} = \frac{\Sigma Ay}{\Sigma A} = \frac{1.59}{3.375} = .47"$ above 1-1 to neutral axis

$I_{N.A.} = 19.23 - 3.375 \times .47^2 = 18.48 \text{ in.}^4$

$\frac{I}{y(u)} = \frac{18.48}{2.53} = 7.30, \quad \frac{I}{y(L)} = \frac{18.48}{3.47} = 5.32$

Calculation of Stresses and Margins of Safety

Bending:-

Max bending stress upper flange $= f_b = M/I/y = \frac{45000}{7.30} = 6160\#/\text{in.}^2$ compression

$\frac{t_c}{h} = \frac{1.125}{6} = .188, \quad \frac{b'}{b} = \frac{.25}{1.75} = .143$

From allowable curves C8.2 the modulus of rupture F_{bc} for these relationships = - 6300#/in.^{2}

Hence M.S. for upper flange = $\frac{6300}{6160} - 1 = .02$

For lower flange $f_b = \frac{45000}{5.32} = 8450\#/\text{in.}^2$ tension

The allowable stress can be taken as the modulus of rupture of a solid rectangular beam in pure bending. From Table C8.1 or from Fig. C8.2 when tc/h = .5 and $\frac{b'}{b} = 1.0$, we obtain $F_{bc} = 9400\#/\text{in.}^2$

Hence M.S. of lower flange = $\frac{9400}{8450} - 1 = .11$

Shear Strength

The ultimate shear strength of spruce plywood is given closely by formula

$$F_s = 960 + \frac{3140}{\sqrt[3]{C}} - 45.5\,D$$

C is web diaphragm spacing. Take 6" for this example.

D = distance between flange centroids = 5.12"

Hence

$$F_s = 960 + \frac{3140}{\sqrt[3]{6}} - 45.5 \times 5.12 = 2450\#/\text{in.}^2$$

The maximum web stress occurs at neutral axis.

$f_s = \frac{VQ}{Ib'}$ where $Q = \int_0^{2.53} ydA = 1.125 \times 1.5 \times 1.97 = 3.32$

$.125 \times 2.53 \times 1.37 = .40$

3.72

hence $f_s = \frac{2800 \times 3.72}{18.48 \times .25} = 2250\#/\text{in.}^2$, M.S. =

$\frac{2450}{2250} - 1 = .09$

Glue Strength

The flange members are glued to the two web members. Since the lower flange has smallest thickness and therefore less glue area,

it will be more critical than upper flange.

The average horizontal shear stress on surface between webs and lower flange

$$= f_{glue} = \frac{VQ}{I \times A_g} = \frac{2800 \times .625 \times 1.5 \times 3.158}{18.48 \times 1.25} =$$

360#/in.²

where A_g = glue area = 2 x 1 x .625 = 1.25

$Q = \int ydA$ for lower flange about N.A.

The allowable stress on glued surface is based on 1/3 the allowable shearing stress parallel to the grain of the wood being used. For spruce $F_s = 750$ (See Table C8.1) ∴ allowable F_g for glued surface = 750/3 = 250#/in.

hence, $M.S. = \frac{250}{360} - 1 = -.30$

Thus, for the particular loading assumed, the critical factor is the glued joint between web and lower flange.

To eliminate the negative M.S. more glue shear surface must be provided. For example, a small triangular wood strip could be added as shown in Fig. C8.6 and glued to both flange and web. Another way to increase the glue shear of this type of box beam is illustrated in Fig. C8.7. The same amount of material is used, however, the webs are moved closer together and the flanges are composed of 3 portions, thus giving two glue surfaces on each web instead of one as in example problem. Since the width of the ear



Fig. C8-6

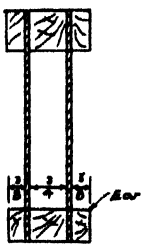


Fig. C8-7

is 3/8" or half the flange width between webs, the shear flow from web to flange will be symmetrical or each glue surface will carry same shear load. The glue shear stress in this case will be

$$f_g = 360/2 = 180, \text{ hence } M.S. = \frac{250}{180} - 1 = .39$$

The results in this example should not be taken as to mean that glue strength is always critical in this type of beam. In most cases the ratio of shear load to bending load is such as to not make glue shear stresses critical.

Example Problem 2.

Fig. C8.9 shows two beam sections of same total section area. For comparison the bending and shear strength for each beam section will be computed.

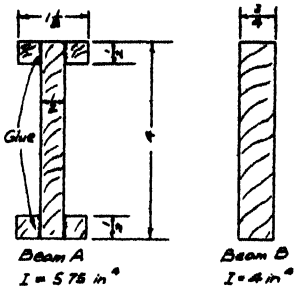


Fig. C8-9

Beam A

$$t_c/h = \frac{.5}{4} = .125$$

$$\frac{b'}{b} = \frac{.5}{1.5} = .33$$

From Fig. C8.2 allowable bending stress $F_b = 6675$

$$M = \frac{F_b I}{C} = \frac{6675 \times 5.75}{2} = 19200"\# = \text{max. moment section will develop.}$$

Allowable shear stress for spruce = 750#/in.

$$f_s = \frac{VQ}{Ib} \text{ or } V = \frac{f_s Ib}{Q} = \frac{750 \times 5.75 \times .5}{(.5 \times 1.75) + (2 \times .5 \times 1)} =$$

1150#, based on strength of web at neutral axis or midpoint of beam. The true strength of the glued joint between the web and the flange is rather questionable. If grain of both web and flange portions are parallel, the glue will develop the shear strength of spruce = 750#/in. Using this value the two glued joints on each flange will develop an external shear load,

$$V_g = \frac{f_g Ib}{Q} = \frac{750 \times 5.75 \times .5 \times 2}{.5 \times .5 \times 1.75 \times 2} = 4900\#.$$ This value provides a large margin over the shear strength of 1150# at neutral axis and can therefore take care of any variation of glue strength,

Beam B

$$t_c/h = \frac{2}{4} = .5 \quad \frac{b'}{b} = \frac{.75}{.75} = 1 \text{ hence allowable } F_b =$$

9400 and bending strength $M = \frac{9400}{2} \times 4 = 18800"\#$

shear strength $V = \frac{f_s Ib}{Q} = \frac{750 \times 4 \times .75}{2 \times .75 \times 1} = 1500\#$

The results indicate that the bending strength of each beam is practically the same, however the shear strength of beam B is considerably better.

In general for beams under 6" in depth rectangular beams are just as efficient as I-sections. For deep beams above 6" the box beam appears to better advantage, particularly so from the point of procurement of material due to large sizes required if rectangular solid beams are used.

Example Problem 3

Fig. C8-10

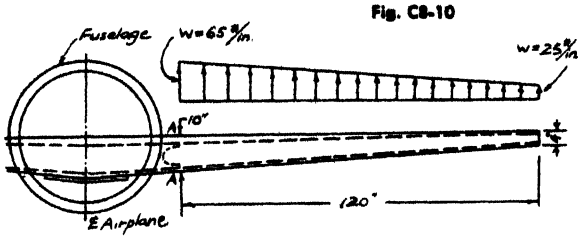


Fig. C8.10 shows a cantilever beam representative of a small wing or a large tail structure. Let it be required to determine the necessary beam section at point A-A just adjacent to fitting block at fuselage support point if beam carries the distributed load as shown.

Solution

Before stresses and allowable stresses can be found the section of the beam must be known, but the stresses depend on the beam section, thus the general procedure is to guess at a section and then check it to see if satisfactory. Since the more accurate method of calculating bending and shear stresses requires the values of the section moment of inertia which requires considerable tedious numerical calculations it is desirable to make the first guess of the beam section close enough so that very little revision will be necessary. If guesses or assumptions are made without logical background, the chances are that several revisions will be necessary before a satisfactory section is arrived at. There is no definite set of rules for making a good guess which will apply to all types and proportions of beam sections, however, if the student will think in terms of internal resisting forces and study the allowable stress chart in Fig. C8.2 he should be able to make a reasonable preliminary guess for a beam section. An effort will now be made to illustrate this conclusion. Design bending moment at beam point A-A.

$= M_A = 25 \times 120 \times 60 + 40 \times 60 \times 40 = 276000$"#

Design vertical shear.

$V_A = 120 \times 25 + 60 \times 40 = 5400$#

Since the beam is rather deep, the box type of beam as illustrated in Fig. C8.1a will be used.

Preliminary Design of Plywood Webs:-

Assume effective depth D of beam = .85h, where h is beam depth, hence D = .85 x 10 = 8.5"

The approximate horizontal component of upper and lower flange loads $= \frac{M}{D} = \frac{276000}{8.5} =$ ± 32500#. From Fig. C8.10 it is noticed that the beam tapers in depth from 10" at station A-A to 4" at beam tip, and that top flange is horizontal, thus giving a slope of the lower flange of $\frac{6}{120}$. Therefore the tension load in the bottom flange will have a vertical component which will tend to resist the external shear load, thus helping the web to carry the external shear load. Approximate net shear load on web

$= 5400 - 32500 \times \frac{6}{120} = 3775$#.

Assume the web shear resisting stress constant over the effective depth D., hence shear flow equals

$q = \frac{3775}{8.5} = 445$#/in. of web. Using a diaphragm spacing of 6", the allowable shear stress for plywood web equals,

$$F_s = 960 + \frac{3140}{\sqrt{\frac{s}{6}}} - 45.5 \times 8.5 = 2300\text{#/in.}^2$$

hence approx. web thickness $= \frac{445}{2300} = .194$". Since there are two webs, a thickness of 1/8" for each web will be assumed.

Preliminary Bending or Flange Design:-

The flanges should be reasonably thick at this section to permit tapering or decrease in flange depth as the beam tip is approached. A solid rectangular section for this depth of beam would be heavy and such large sizes of spruce would be quite expensive. Assume a beam width of 3 inches b'/b = .25/3 = .083. To obtain an area for the compression flange we need an allowable stress. Observation of Fig. C8.2 shows that F_{bc} varies between - 5800 and - 6750 for values of tc/h of .15 and .30 respectively when ψ = .083. These two values of tc/h should cover most practical designs. To obtain a preliminary area an average of these two values will be assumed or -6275#/in.^{2}. This value represents the stress for extreme or top fiber in the beam flexure formula, hence the average stress on the compression - flange will be considerably less; for example if beam was solid average stress would be 1/2 the extreme fiber stress. An average stress of .75 x -6275 = -4700 will be assumed.

Preliminary required area of upper flange

$$= \frac{M}{F_b \times D} = \frac{276000}{4700 \times 8.5} = 6.94 \text{ sq. in.}$$

$$t_c = \frac{6.94}{2.875} = 2.41\text{", use 2-7/16"}$$

(It is customary to use 1/2 of web area as effective in bending, thus effective flange width = $(3 - \frac{.25}{2}) = 2.875$")

The allowable bending tensile stress is 9400#/in.^{2}. The tension or lower flange will be less thick than the upper flange due to this higher allowable, thus an average stress of .9 times the maximum would appear more reasonable.

Preliminary required area for the tension flange equals:

$276000/(8.5 \times .9 \times 9400) = 3.84$ sq. in.

$t_t = 3.84/2.875 = 1.33$", Use 1-5/16"

Before going ahead with the accurate stress calculation involving the moment of inertia, a further check will be made of the flange thickness arrived at above, which was based on several assumed values.

For t_c = 2-7/16, $t_c/h = 2.43/10 = .243$, Fig.

C8.2 gives F_{bc} = 6375 when b'/b = .083. Fig. C8.11 shows the internal bending stress distribution assuming plane sections remain plane after bending and stress varies as strain. The average stress on the upper flange is 4457#/in.² and 8355 on the lower. The arm of the internal stress resisting couple is 8.3", hence area of compression flange = $\frac{276000}{4457 \times 8.3}$ = 7.46 sq.in.

$$t_c = \frac{7.46}{2.875} = 2.59 = \text{use } 2\text{-}5/8"$$

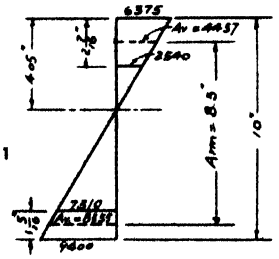


Fig. C8-11

Tension flange area = $\frac{276000}{8355 \times 8.3}$ = 3.97

$$t_t = \frac{3.97}{.2875} = 1.39 \text{ - use } 1\text{-}3/8".$$

With these preliminary flange thicknesses the moment of inertia of the section as shown in Fig. C8.12 will be computed. Table C8.4 shows the calculations. Axis 1-1 was assumed as reference axis.

Table C8.4

Portion	Area A	y	Ay	Ay^2	$I_o = \frac{1}{12} bd^3$	I_{1-1}
Upper Flange	7.50	3.687	27.50	102.00	4.60	106.60
Lower Flange	3.77	-4.312	-16.27	70.00	0.62	70.62
Web	1.25	0	0	0	10.40	10.40
Total	12.52		11.23			187.62

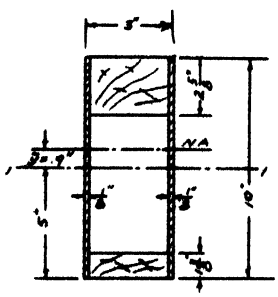


Fig. C8-12

$$\bar{y} = \frac{11.23}{12.52} = .9"$$

$$I_{N.A.} = 187.6 - 12.52 \times .9^2 = 177.5 \text{ in.}^4$$

$$\frac{I}{y_u} = \frac{177.5}{4.1} = 43.3 \qquad \frac{I}{y_L} = \frac{177.5}{5.9} = 30.1$$

Upper Flange $f_b = \frac{276000}{43.3} = -6380$#/in.²

$t_c/h = \frac{2.625}{10} = .26$ b'/b = .083 From Chart Fig. C8.2

$F_{bc} = -6500$ hence M.S. = $\frac{6500}{6380} - 1 = .01$

Lower Flange $f_b = \frac{276000}{30.1} = 9170$#/in.²

$F_{b(allow)} = 9400$, M.S. = $\frac{9400}{9170} - 1 = .02$

Thus as far as bending stresses are concerned, no revision is necessary.

Web Shear Stresses

The vertical component of the axial load in the lower flange equals the average flange stress times the flange area times the slope 6/120.

$$= \frac{9170 + 7010}{2} \times 1.37 \times 2.875 \times \frac{6}{120} = 1595\#$$

Net shear load on web = 5400 - 1595 = 3805#
The maximum shear stress occurs at neutral axis.

$$f_s = \frac{V \int ydA}{Ib} = \frac{3805 \times (3.77 \times 5.21 + 5.9 \times .125 \times 2.95)}{177.5 \times .25} =$$

1880#/in.²

The allowable shear stress F_s for 6" diaphragm spacing =

$$F_s = 960 + \frac{3140}{\sqrt[6]{6}} - 45.5 \times 8 = 2320\text{\#/in.}^2$$

$$M.S. = \frac{2320}{1880} - 1 = .24$$

Assuming the wing rib spacing is 12" and placing web diaphragms only at each rib, the above allowable stress formula would give 1965#/in.² In this case margin of safety of web would be cut to .04.

Check glue stress between webs and lower flange:-

$$f_g = \frac{V \int ydA}{I A_g} = \frac{5400 \times 3.77 \times 5.21}{177.4 \times 1.375 \times 1 \times 2} = 217\text{\#/in.}^2 \text{ (V is conservative)}$$

F_g allowable = 250 M.S. = $\frac{250}{217} - 1 = .15$

The student should design a section at two or three other points farther out on the span in order to determine the taper of the master section.

C8.8 Allowable Stresses for Combined Bending and Compression.

Combined bending and compression loads are usually produced on wing or tail surface beams when the surface is externally braced. Fig. C8.13 illustrates two common types of airplanes in which the wing beams are subjected to bending and compression loads. In cantilever surfaces axial compression is usually relatively unimportant as compared to externally braced surfaces. Fig. C8.14 illustrates several cases in which axial loads in wing beams are produced in cantilever wings.

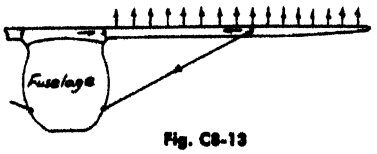


Fig. C8-13

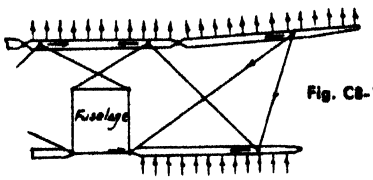


Fig. C8-13

Air loads on outer panel due to dihedral produce axial load component on center panel. Side load on landing gear produces axial load on wing beams.

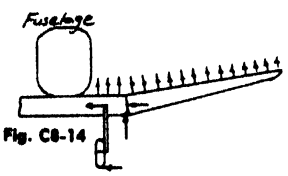


Fig. C8-14

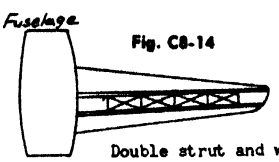


Fig. C8-14

Double strut and wire truss system for drag and torsional loads produces axial loads in beams.

(3) In the left half of the chart are two series of curves, one series is labeled with L/ρ values to which they apply and the horizontal series is unlabeled but represent the elastic limit stress values as affected by the f_b/f_t ratio of stresses. Taking as an example a value of L/ρ = 95 we interpolate value of elastic limit stress between curves at point C and follow out to its intersection with the interpolated value of L/ρ = 95 curve giving point E on chart. (L = distance between points of inflection).

(4) Draw line E D connecting the points E and D.

(5) Assume that f_b/f_t ratio is .82 for our particular section. Thus taking this value on the obscissa, project upward to line ED to locate point F. The allowable combined compressive stress is then obtained by projecting horizontally to point G.

(6) If conditions were such that L/ρ = 30, it is observed that the lowest L/ρ curve plotted is L/ρ = 50. Hence locate point H at L/ρ = 30 at lower left side of chart and draw line DH. Then project upward from the given value of f_b/f_t to give point I on line DH. Projecting horizontally to left side scale at point J we obtain the allowable combined stress.

C8.9 General Rules to be Observed in Using Fig. C8.15 and Design of Beams in General

(1) Filler blocks may be neglected in computing ρ to be used with the curves of Fig. C8.15. For beams which taper in section, an average value of ρ should be used.

The allowable combined bending and compression stress can be determined by curves of Fig. C8.15 based on the method developed by the Forest Products Laboratory. The allowable combined stress using these curves is found as follows:-

(1) Using t_c/h and b'/b for the given beam section, for example take 0.225 and 0.25 respectively, find the elastic limit in bending using the lower dashed set of curves as denoted by point "A" on Fig. C8.15, and determine the modulus of rupture on upper set of curves giving point "B".

(2) Project points A and B to the central line, which gives points C and D.

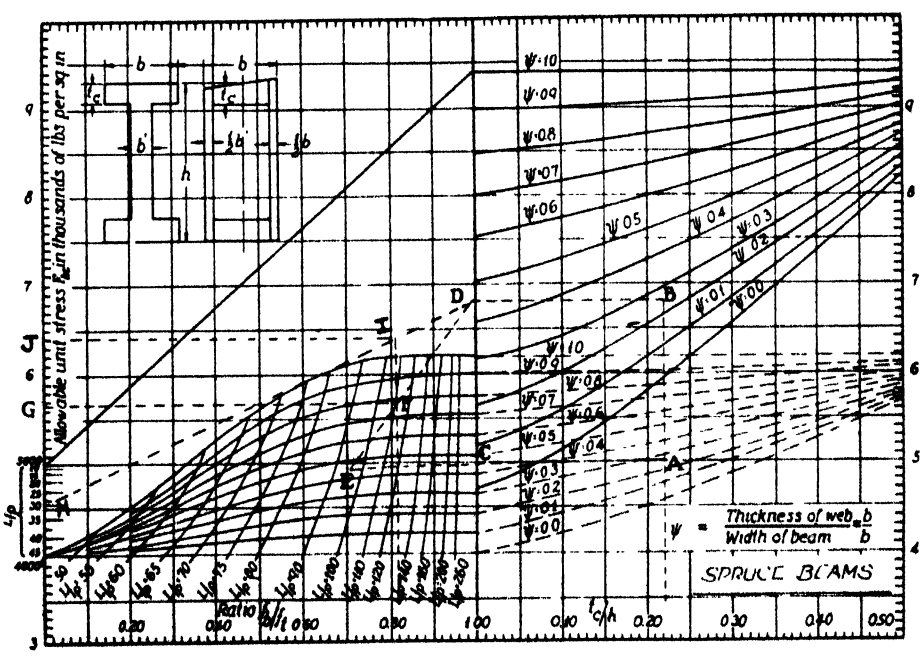


Fig. C8-15 (Ref. ANC-5)

ALLOWABLE STRESSES FOR SPRUCE SPARS

(2) In computing the modulus of rupture and the elastic limit in bending, the properties of the section being investigated should be used. Filler blocks may be included in the calculations for section properties. Allowance should be made for bolt holes in computing section properties.

(3) The slenderness ratio L/ρ should be based on the distance between the points of inflection. In general the movement of the points of inflection due to secondary moments produced by end loads times lateral deflection are not large and since the allowable stress F_b is not very sensitive to L/ρ values it is permissible to take L as distance between points of inflection due to bending under transverse loads only. For a beam carrying a uniform transverse load with end compressive loads Fig. C8.16 can be used to find exact distance between points of inflection.

Fig. C8.17 illustrates typical possible cases that might occur on a wing beam continuous over 3 spans. The end moments and transverse loading on center span are such as to produce no points of inflection.

In the outer panel for the design of span portion use column length = L_1. For design of outer strut region use column length L = 2a. For center panel for design of span portion use effective column length = L_2 or more conservative us L_3. For design in strut region use column length as L_4.

In a cantilever beam with a double internal drag truss system as illustrated in Fig. C8.14. axial stresses constant between drag truss panel points are produced. There are no points of inflection in cantilever beams and since these drag truss axial loads are relatively small compared to bending stresses due to loads in the beam direction it is usually satisfactory to use the modulus of rupture in bending and correct it by the ratio of f_b/f_t to obtain the allowable combined compressive stress.

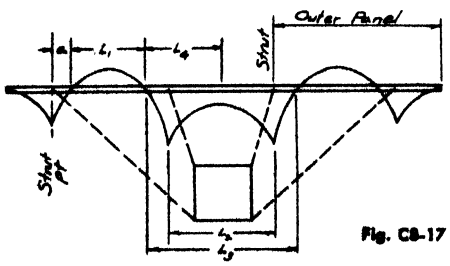


Fig. C8.17

(4) For bending and tensile axial loads, the maximum computed combined stress on the tension flange should not exceed the modulus of rupture of a solid beam in pure bending.

C8.10 Example Problem #4

To illustrate the use of the allowable stress chart Fig. C8.15 for combined bending and compressive stresses, the lower front wing beam for the biplane sketched in Fig. C8.18 will be analyzed for stresses and margins of safety. Fig. C8.19 shows the general details and dimensions of the lower front beam, a beam taken from an actual airplane. Fig. C8.20 shows the beam section in the span and at the strut point, also the properties of each section.

The lower beam is supported by a hinge fitting at point (1) and by a lift wire and interplane struts at point (2).

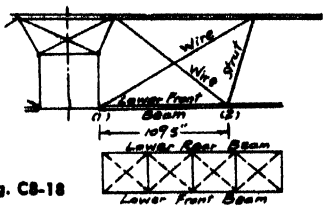


Fig. C8-18

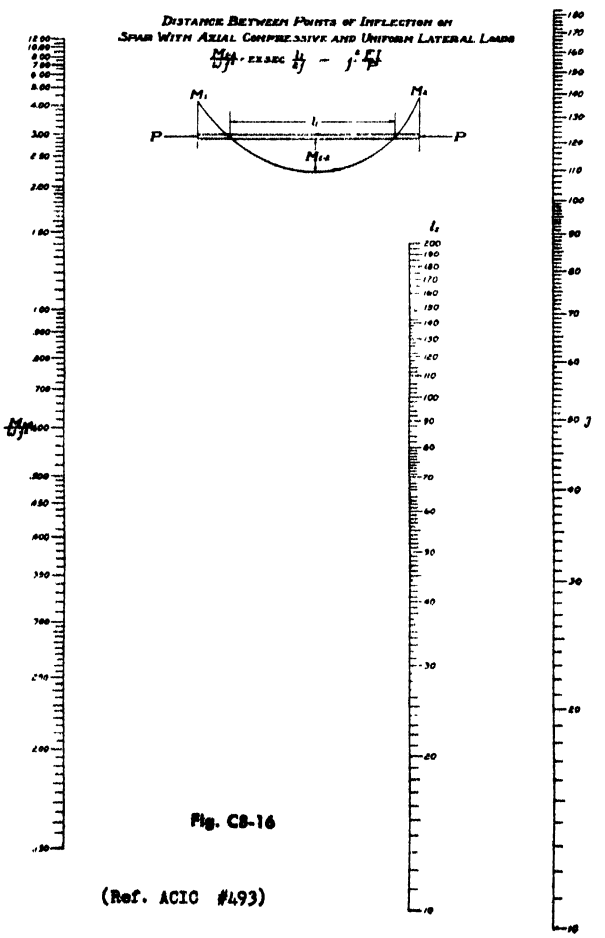


Fig. C8-16

(Ref. ACIC #493)

The beam carries a lateral distributed air load and axial loads due to lift wire, interplane and drag struts. Fig. C8.20 shows the loads on the beam for a high angle of attack condition which have been determined from a stress analysis of the wing cellule. For an inverted low angle of attack condition with negative gust the axial

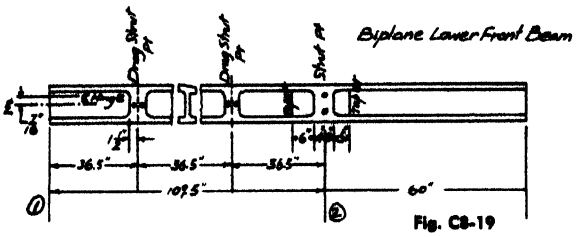


Fig. C8-19

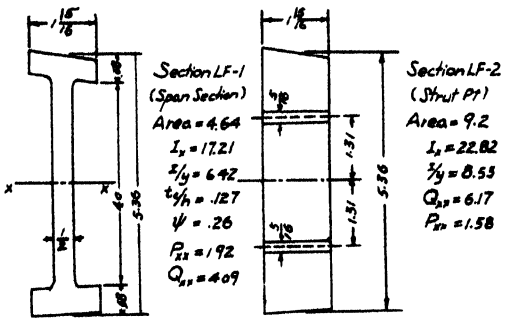


Fig. C8-20

loads on the beam would be of similar character. However, air load would act down instead of up. This fact explains why beam was made symmetrical since bending stresses are reversed in the 2 critical design conditions.

Only the H.A.A. condition will be considered in these illustrative calculations.

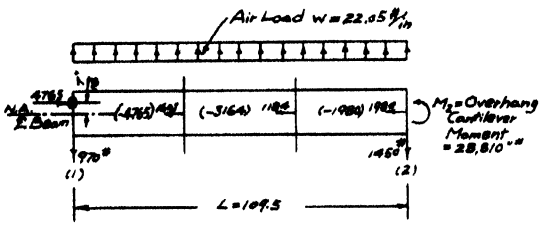


Fig. C8-20 a

Investigation of BAY Section at Point of Maximum Bending Moment

Section LF-1. I = 17.21

Bending moment at (1) due to hinge eccentricity
$= M_1 = .4375 \times 4765 = 2085"\#$

Bending moment at strut point (2) due to beam overhang
$= M_2 = 28810"\#$

The beam is subjected to a varying end load. For computing secondary moments due to axial load times lateral deflection, an average axial load will be assumed. Average axial load P =
$$\frac{(4765 + 3164 + 1980)}{3} = -3303\#$$

The point of maximum bending moment in span is given by following equation (See Chapter A10)

$$\text{Tan } \frac{x}{j} = \frac{D_2 - D_1 \cos \frac{L}{j}}{D_1 \sin \frac{L}{j}} \quad \text{----------(1)}$$

$$j = \sqrt{\frac{EI}{P}} = \sqrt{\frac{1.3 \times 10^6 \times 17.21}{3303}} = \sqrt{6775} = 82.3$$

$wj^2 = 22.05 \times 6775 = 149700$

$D_1 = M_1 - wj^2 = 2085 - 149700 = -147615$

$D_2 = M_2 - wj^2 = 28810 - 149700 = -120890$

$\frac{L}{j} = \frac{109.5}{82.3} = 1.33$

From Table A10.2 of Chapter A10

$\sin \frac{L}{j} = .9711$

$\cos \frac{L}{j} = .2385$

Subt. in (1)

$$\tan \frac{Xm}{j} = -\frac{120890 - (-147615 \times .2385)}{-147615 \times .9711} = -\frac{85690}{143500} = .598$$

$\frac{Xm}{j} = \tan^{-1} .598 = .539$, hence

$Xm = 82.3 \times .539 = 44.2"$ the distance from left end to point of max. span moment. The maximum span moment is given by the following equation (See Chapter A10)

$$M_{max.} = \frac{D_1}{\cos \frac{Xm}{j}} + wj^2$$

$\cos \frac{Xm}{j} = .8582$, hence $M_{max.} = -\frac{147615}{.8582} + 149700 = -22300"\#$

The combined compressive stress on extreme fiber due to bending and axial load = f_t

$$f_t = \frac{P}{A} - \frac{My}{I} = -\frac{3164}{4.64} - \frac{22300}{6.42} = -685 - 3475 = -4160\#/in.^2$$

$$f_b/f_t = \frac{3475}{4160} = .835$$

The column length L equals distance between points of inflection, and is determined from Fig. C8.16 where for

$\frac{M_{1-2}}{w\, j^2} = \frac{22300}{149700} = .15$ and j = 82.3, the chart gives L = 84"

Hence $\frac{L}{\rho} = \frac{84}{1.92} = 44$

Using $t_c/h = 0.127$, $\psi = 0.26$ and values of L/ρ and f_b/f_t as found above we find the allowable combined stress F_{bc} from chart of Fig. C8.15 equals $-5900\#/in.^2$

$$M.S. = \frac{5900}{4160} - 1 = .41$$ (See discussion of margin of safety Art. A10.5 of Chapter A10)

The combined stress on extreme fiber of upper flange equals $-685 + 3475 = 2790\#/in.^2$ With an allowable stress of 9400#/in. , the upper flange is not critical. For a negative acceleration condition this flange would be more critical.

Investigation of Section 35" from left end

Observation shows the axial load in the left end drag bay is -4760 against - 3164 in center bay. Thus a section just inboard of drag strut filler block may be more critical than point of maximum bending moment.

The value of the bending moment at any distance from point (1) is given by the equation (See Chapter A10)

$$M_x = D_1 \left(\tan \frac{X_m}{j} \cdot \sin X/j + \cos x/j\right) + wj^2$$

$$x = 35 \quad x/j = \frac{35}{82.3} = .425,$$

From Table A10.2 Chapter A10 $\sin x/j = .41221$, $\cos x/j = .9110$

$$M_x = -147615 \ (.598 \times .4122 + .9110) + 149700 = -20200$$

$$f_t = \frac{P}{A} - \frac{My}{I} = -\frac{4765}{4.64} - \frac{20200}{6.42} = -1028 - 4156 = -4173$$

$$f_b/f_t = \frac{3145}{4173} = .755$$

From allowable stress chart $F_{bc} = -5700$

$$M.S. = \frac{5700}{4173} - 1 = .36$$

Investigation of Section at Strut Point (2)

Ref. section LF - 2. Area = 92 I/y = 8.53

Combined compressive stress upper flange

$$f_t = -\frac{1980}{9.2} - \frac{28810}{8.53} = -215 - 3380 = -3595\#/in.^2$$

$$f_b/f_t = \frac{3380}{3595} = .94 \quad \frac{L}{\rho} = \frac{2 \times 23.5}{1.58} = 30$$

L is usually taken as twice the distance from strut point to point of inflection in the span = 23.5" in this case. For

$t_c/h = .5$ and $\psi = 10$ and the values L/ρ and f_b/f_t found above Fig. C8.15 gives allowable $F_{bc} = -9000$

$$M.S. = \frac{9000}{3595} - 1 = 1.5$$

Investigation of Section 10" Inboard of Strut Point (2)

Section LF - 1 is used at this point

The value of the bending moment at any distance x from point (1) is given by the equation.

$$M_x = D_1 \left(\tan \frac{X_m}{j} \sin \frac{X}{j} + \cos \frac{X}{j}\right) + wj^2$$

$$X = 109.5 - 10 = 99.5, \ \frac{X}{j} = \frac{99.5}{82.3} = 1.21$$

From Table A10.2 of Chapter A10.

$\sin x/j = .9356$; $\cos x/j = .3530$

Hence

$$M_x = -147615 \ (.598 \times .9356 + .3530) + 149700 = 15000"\#$$

$$f_t = -\frac{1980}{4.64} - \frac{15000}{6.42} = -425 - 2340 = -2765$$

$$f_b/f_t = \frac{2340}{2765} = .85 \quad L/\rho = 30 \quad F_{bc} \text{ from chart} = 5950$$

$$M.S. = \frac{5950}{2765} - 1 = 1.15$$

Investigation of Beam Shear Strength Strut Point (2)

$V = 1450\#$

$$f_s = \frac{VQ}{Ib} = \frac{1450 \times 6.17}{22.82 \times 1.94} = 201$$

$F_s = 750$ for spruce M.S. = 2.73

Point 10" Inboard of Strut Point (Section LF-1)

$V = 1450 - 10 \times 22.05 = 1230\#$

$$f_s = \frac{1230 \times 4.09}{17.21 \times .5} = 584, \ F_s = 750, \ M.S. = .28$$

C8.11 Shear Modull for Spruce and Spruce Plywood Webs

For finding flexural as well as torsional deflections due to web shear stresses or wall shear stresses in cellular box beams ANC-5 gives the following data for the shearing modulus.

For spruce $G = \frac{E}{15.5} = 84000\#/sq.in.$

For spruce 45^0 plywood $G = 420{,}000\#/sq.in.$

C8.12 Design of Wood Columns

The allowable stresses for solid spruce columns are given by the following formulas: (Ref. ANC 5)

Long columns -

$$F_c = \frac{13{,}000{,}000}{(L'/\rho)^2} \text{ or } P_a = \frac{13{,}000{,}000\, I}{(L')^2}$$

The critical L'/ρ value = 72

Short columns -

$F_c = 5000 - .50 \ (L'/\rho)^2$

where F_c = ultimate allowable axial compression stress in psi.

L' = effective column length = $L/\sqrt{C}$ where C is the end fixity coefficient.

ρ = least radius of gyration of cross section or about the axis which bending of column takes place.

I = moment of inertia about neutral axes.

The above formulas are plotted in Fig. C8.21

C8.13 Local Failure - Lateral Buckling

The above formulas apply only to beams of constant cross-section. They likewise do not apply to column sections with free edges that will fail by local buckling and for unconventional shapes. The column strength of such columns should be determined by tests.

The moment of inertia of wood beam about an axis normal to the transverse loading is usually considerable larger than about the other rectangular axis, thus the beam may fail by lateral buckling and thus beams should be checked for lateral strength. (See problem #5)

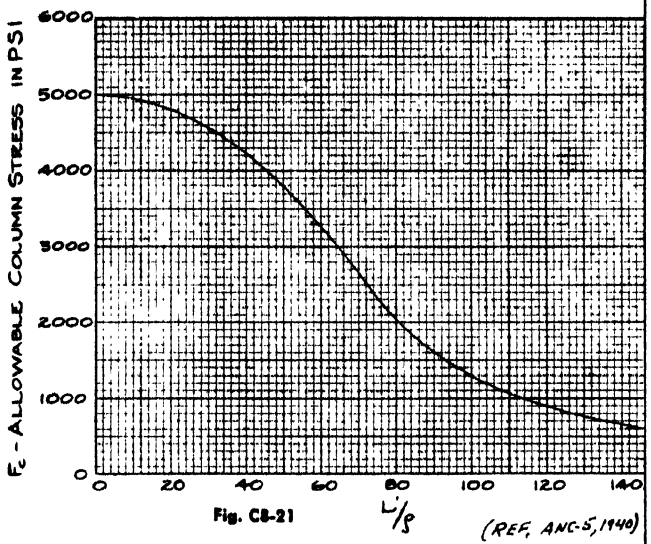


Fig. C8-21

C8.14 Example Problem #15

Fig. C8.22 shows a typical externally braced wing panel. The lift struts produce large axial compressive loads P on the front and rear wing beams between pointsAB and CD. The beams tend to bend laterally, between drag strut points as illustrated by the dashed lines. Since the beams are tied together by wing ribs they must both fail or bent laterally together. Since a metal covered leveling edge is conventional design practice this fact will add further lateral strength to beams as the loading edge skin forms a closed box section which provides additional beam strength.

The axial load P on front beam is -9233# and -9571# on the rear beam between the points AB and CD respectively. The properties of the two beam spruce sections are as follows:-

From beam: - Area = 4.64 sq.in.
I_{yy} = 0.83 in.^{4}
ρ_y = 0.42"

Rear beam: - Area = 4.29
I_{yy} = 1.22
ρ_y = 0.53

Let it be required to determine the lateral strength of the wing beams.

The free length of the beams in lateral bending will be taken as equal to the length of a drag bay or 40.37". The end fixity coefficient C will be assumed equal to 1. Considering front beam only:-

$$\frac{L'}{\rho} = \frac{40.37}{.42} = 96, \text{ hence a long column}$$

$$P_a = 13{,}000{,}000 \times \frac{.83}{40.37^2} = -6650\#$$

Considering rear beam:-

$$\frac{L'}{\rho} = \frac{40.37}{.53} = 76 \text{ (long column)}$$

$$P_a = 13{,}000{,}000 \times 1.22/(40.37)^2 = 9750\#$$

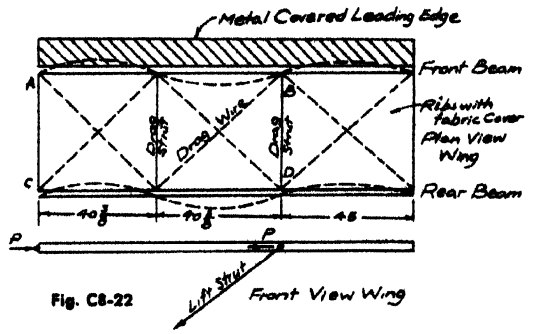


Fig. C8-22

Combined column strength = - 9750 - 6650 = -16400#
Design end loads for both beams = -9233 - 9571 = -18804#
Thus the beams appear weak in lateral column strength between drag truss joints. However, if a metal loading edge portion is used on the wing panel it is permissible to decrease the combined column load by 1/3. Thus design load
= 2/3 x -18804 = -12550# against a computed strength of - 16400# which provides a margin of safety.

C8.15 Splicing of Wood Beams

Butt joints with gluing of the end grain surfaces should not be used in members subjected to bending and tensile loads. Splices are sometimes necessary because the beam element is longer than the wood stock available. In some cases particularly plywood webs, splicing of one thickness web to another of different thickness is done to save weight. In splicing the flange members of beams the location of the splice if convenient should be near the point of inflection in order that the bending forces be limited to small value. Similarly shear splices is possible should be located in the region of low shear as an added factor of safety.

Side grain gluing can be approximated in splices by scarf joints. For splicing soft woods a scarf slope of 1 in 10 and for hardwoods 1 in 15 will produce a joint as strong in tension along the grain as the solid wood. Figs. C8.23 to 26 illustrates methods splicing wood beams as recommended by the Bureau of Air Commerce.

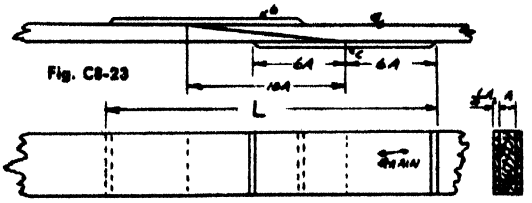


Fig. C8.23 Method of Splicing Solid or Laminated Rectangular Beams.

Fig. C8.23 illustrates the recommended method of splicing a solid or laminated rectangular beam (a) with either spruce or plywood splice plates (b). If spruce splice plates are used the grain should run horizontal or parallel to the beam.

If plywood is used the grain should run at 45°. No fittings are to be placed within the distance (L).

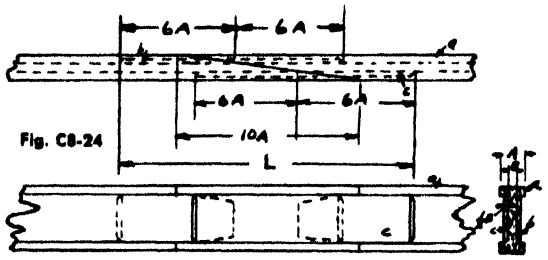


Fig. C8.24

Fig. C8.24 Method of splicing Routed (I) Section Beam.

Fig. C8.24 shows the recommended splice of a routed I section. The proportions and lengths of the reinforcing or splice plates (b) and (c) are expressed in terms of the original dimensions (A) and (B) of the I-section. No fittings are permitted within the distance (L).

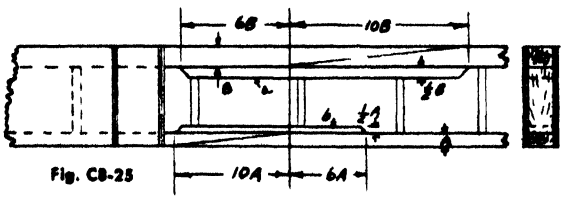


Fig. C8.25

Fig. C8.25 Method of Splicing Box Beam Flanges.

Fig. C8.25 illustrates one method of splicing the beam flanges. The spruce splice plates (a) and (b) are glued to the bottom of each flange.

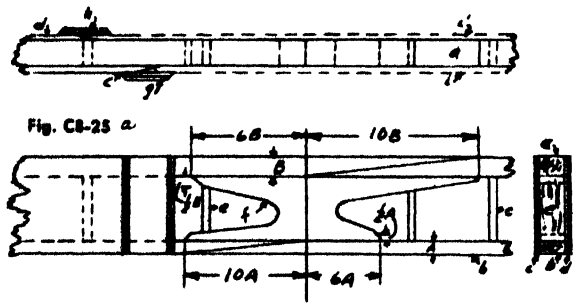


Fig. C8.25a

Fig. C8.25a Method of Splicing Box Beam Flange.

Fig. C8.25a illustrates another method of splicing the flanges of a box beam. A reinforcing block (f) is inserted between the flanges with dimensions as shown. Splices in the web should be staggered as shown at (g) and (h).

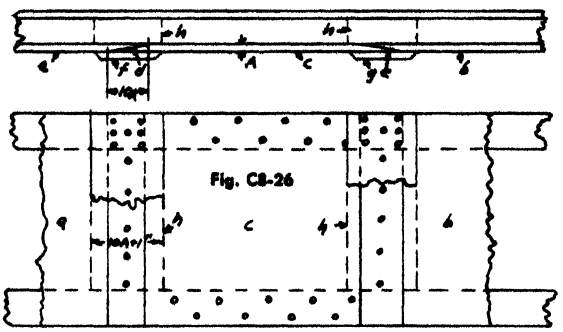


Fig. C8.26 Method of Splicing Box Beam Webs.

Fig. C8.26 illustrates the recommended method of splicing the plywood webs of a box beam. Portions (a) and (b) represent the old portions of the web and (c) represents the new inserted web portion. The scarfs between webs are located at (e) and (d). The scarf joints are covered by the cover strips (f) and (g). To strengthen the joint filler blocks (h) are used as shown.

FITTINGS

C8.16 Bolted Fittings in Wood Members.

It is common practice to use either solid steel or aluminum alloy bolts in attaching fittings to wood beams. Tests by the Forests Products Laboratory showed that hollow bolts with comparatively thin walls were little if any more efficient than solid bolts from a weight standpoint, since the allowable bearing stresses of wood on hollow bolts was reduced considerably.

Figs. C8.27 and C8.28 gives curves for the bearing strength of solid bolts on wood parallel and perpendicular to the grain respectively.

C8.17 Allowable Bearing Stresses at an Angle with the Grain.

For cases where the resultant load on a bolt acts in a direction between 0° and 90° to the grain, the allowable bolt load can be calculated from the expression:-

$$N = \frac{PQ}{P \sin^2 \theta + Q \cos^2 \theta}$$

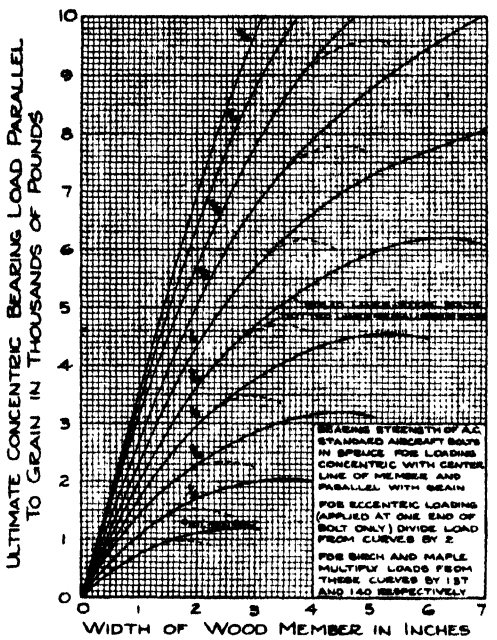
where

- N = the allowable bolt load
- P = the allowable bolt load parallel to grain using Fig. C8.27
- Q = the allowable bolt load perpendicular to grain using Fig. C8.28
- θ = angle between applied load and the direction of the grain of the wood.

C8.18 Bolt Spacing and Bolt Edge Distance.

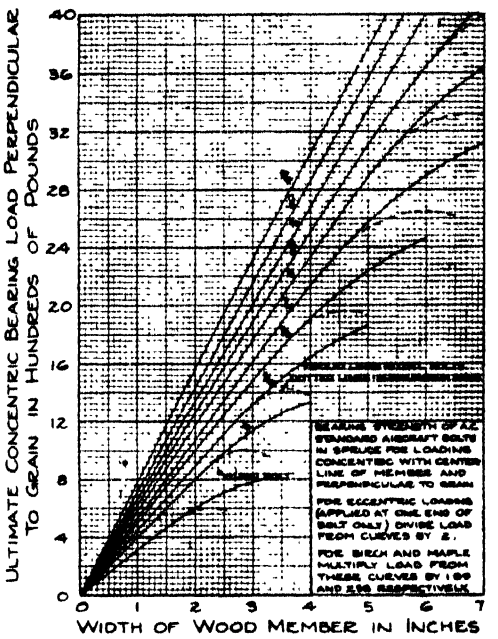
Fig. C8.29 gives curves for determining the distances between bolts and allowable distances

Fig. C8-27



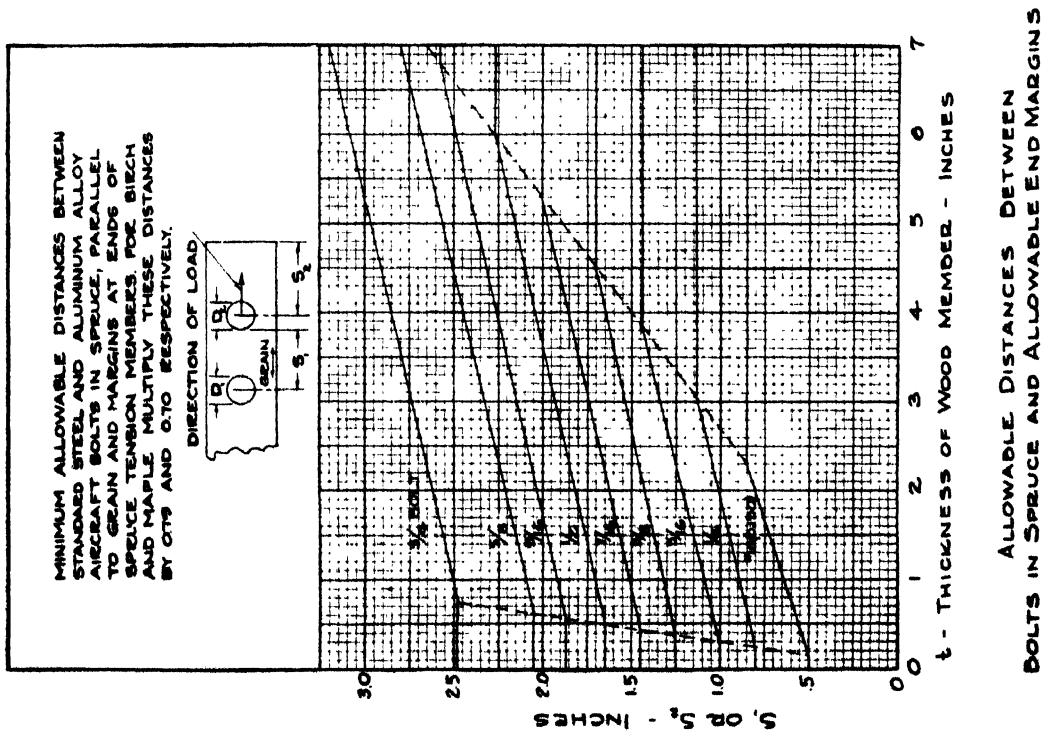
BEARING STRENGTH OF BOLTS IN WOOD - PARALLEL TO GRAIN

Fig. C8-28



BEARING STRENGTH OF BOLTS IN WOOD - PERPENDICULAR TO GRAIN

Fig. C8-29



(All Figs. on this page from ANC-5,1940)

between bolts and the edge of spruce wood members, when the bolt loads are parallel to the grain of the wood. These allowable distances were obtained by finding the length necessary for the strength of the wood in horizontal shear to develop the bearing strength of the bolt on the wood. For other woods the distances obtained from the chart may be multiplied by the factor,

$K = f_{ce}/5.33\ f_s$

where f_{ce} = allowable stress at elastic limit in compression parallel to grain

f_s = allowable shearing stress parallel to grain of material

For a joint in compression the bolt end distance should be large enough to prevent end splitting. Four bolt diameters is suggested by ANC 5.

For transverse bolt spacing ANC-5 gives the following recommendations:- The net tension area at a critical corss-section, should be at least 80 percent of the total area in bearing under all the bolts for coniferous woods, and 100 percent when hardwoods are used. The distance from the edge of a wood member to the centerline of a bolt acting parallel with the grain should be at least 1-1/2 times the bolt diameter for bolt length/bolt diameter ratios of around 5 to 6. In most cases the net area requirements at the critical section will be such that an edge margin equal to half the distance between rows will be sufficient to meet the above requirements.

For loads acting perpendicular to the grain, the distance from bolt centerline to edge of member should be at least 4 times the bolt diameter.

C8.19 Illustrative Problems.

Example Problem No. 6

Fig. C8.30 illustrates a typical flying wire connection to a wing beam. The beam is a spruce flange, plywood web box beam. In the region of the strut point, the beam is reinforced between flanges by an internal tapered spruce block and external side plates of maple 1/2 inch thick. A 1-3/4 inch diameter steel trunion transfers the two wire loads to the beam. The design wire load including a 15 percent fitting factor is 14000#. Let it be required to determine the margin of safety for bearing of trunion on wood beam, also for shear out of reinforcing blocks. In general the above joint would be subjected to another load from struts connecting the wings, however this simplified condition will illustrate bearing stresses.

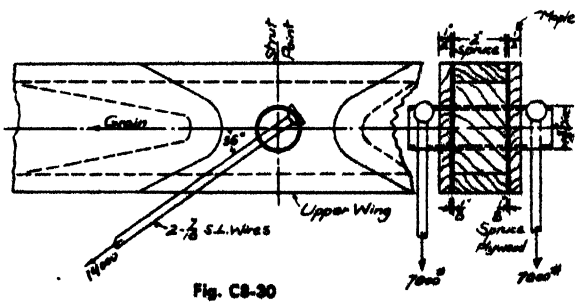


Fig. C8-30

Solution

Let P = allowable trunion load parallel to grain. The plywood web will be considered only 50% effective. The total effective spruce width = 2 + .125 = 2.125 inches, and for the maple side plates 1 inch.

Therefore, P = 1.75 x 2.125 x 50000 + 1.75 x 1 x 7500 = 31750 lbs. Since Fig. C8.27 covers only bolts up to 3/4 diameter, the allowable compressive stresses from Table C8.1 will be used, which gives 5000 for spruce and 7500 for maple.

Let Q = allowable bearing load on trunion perpendicular to grain.

Q = 1.75 x 2.125 x 840 + 1.75 x 2170 = 6940 lbs.

Let N = allowable trunion load in the direction of wire pull.

From Art. C8.17 $N = \dfrac{PQ}{P \sin^2\theta + Q\cos^2\theta}$ For

$\theta = 35^\circ$,

$N = \dfrac{31750 \times 6940}{31750 \times .571^2 + 6940 \times .619^2} = 14700$ lb.

Design fitting load = 14000, Hence M.S. =(14700/14000) - 1 = .05. This estimation of the ultimate bearing strength of trunion on beam section assumes each wood is stressed to its ultimate in bearing with no consideration regarding relative values of modulus of elasticity. Since the strains are in the plastic range at failing pressures, the above solution no doubt gives a reasonable result.

If the elastic theory holds, a solution could be made as follows:

E of spruce = 1.3×10^6 psi, and for maple E = 1.6×10^6 psi. Therefore when spruce is stressed in bearing to 5000 psi and 840 psi parallel and normal to the grain respectively, then the maple will be stressed to 1.6/1.3 = 1.23 times these values, or 6150 and 1035 psi respectively.

Hence P = 1.75 x 2.125 x 5000 + 1.75 x 1 x 6150 = 29360

Q = 1.75 x 2.125 x 840 + 1.75 x 1 x 1035 = 4920

$N = \dfrac{29360 \times .4920}{29360 \times .571^2 + 4920 \times .819^2} = 11220$ lb.

M.S. = (11220/14000) - 1 = -.20

The first result appears more reasonable since strains are in the plastic region.

Example Problem No. 7

Fig. C8.31 shows a typical drag wire-drag strut-wing beam fitting unit. The design load in the loaded drag wire including fitting factor is 3000#. Determine the margin of safety for bearing of bolts on wood beam.

Solution:- The component of wire pull parallel to beam equals 3000 cos 36°-52' = 2400# and 3000 x sin 36°-52' =1800# normal to beam. The load component parallel to beam is resisted by two bolts,

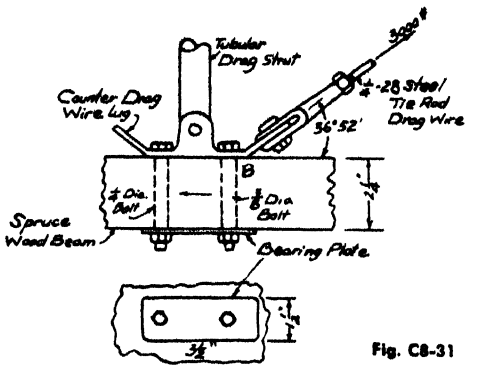


Fig. C8-31

one 3/8 and the other 1/4 inch in diameter. Since the load is applied to only one end of the bolt a triangular bearing force is applied to the wood with the maximum stress equal to twice the average. Hence the allowable bolt loads as given in Fig. C8.27 must be decreased 50 percent.

Thus bearing strength of 3/8 bolt on 2-1/4 wood width = $\frac{3200}{2}$ = 1600# and for 1/4 dia. bolt, bearing strength from Fig. C8.27 = $\frac{1800}{2}$ = 900#, giving a total allowable bolt load applied at one end of the bolts of 2500#. Hence margin of safety = $\frac{2500}{2400} - 1 = .04$.

The 1800# component of the wire pull produces a 1800# tension load in bolt B, which is resisted by the head of the bolt bearing on the bearing plate on beam which in turn transfers load in bearing to beam face. The size of the bearing plate must be such as to prevent crushing of the wood underneath the plate. The allowable bearing stress on wood perpendicular to grain = 840 psi. The approximate bearing pressure between plate and wood from load in bolt B is 1800/1.5 x 1.75 = 685 psi which is satisfactory.

Example Problem No. 8

Fig. C8.32 shows a typical end hinge fitting unit for a wood wing beam. The two loads shown are transmitted to beam by 5 - 3/8 dia. bolts. Let it be required to determine the margin of safety for bearing of bolts on wood beam.

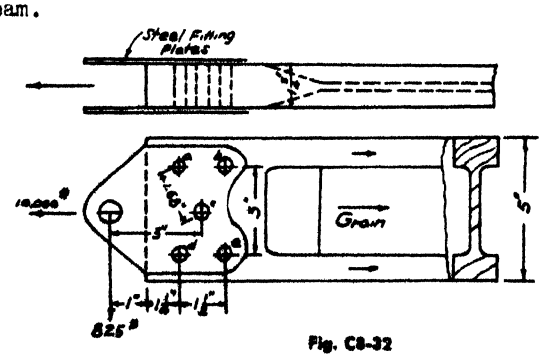


Fig. C8-32

Solution:-

Since all bolts are same size the centroid of the bolt group lies at center of bolt c. The two external loads as shown will be transferred to centroid of bolt group plus a moment of 825 x 3 = 2475"# which equals the moment of fitting loads about bolt group centroid.

Load per bolt due to horizontal load = 10000/5 = 2000#

Load per bolt due to vertical load = 825/5 = 165#

Load on each of the four bolts a, b, d, and e due to moment of 2475"# = $\frac{Mr}{\Sigma d^2} = \frac{2475 \times 1.68}{11.3}$ = 368# acting normal to radii to bolt centroid. ($\Sigma d^2 = 4 \times \overline{1.68}^2 = 11.3$) (See Chapter C4, for derivation of term $\frac{Mr}{\Sigma d^2}$). Since the moment on the joint tends to relieve the load on the bolts d and e due to 10,000# load, it is obvious that bolts a and b are critical. Fig. C8.33 shows a force polygon of the reaction of bolt a on the wood beam. The resultant load can be found graphically as shown or determined analytically as follows:-

$$\Sigma H = -2000 - 368 \times \frac{1.5}{1.68} = -2328\#$$

$$\Sigma V = -165 - 368 \times .75/1.68 = -329\#$$

Resultant load $R = \sqrt{2328^2 + 329^2} = 2350\#$

$\theta = \tan^{-1} -329/-2328 = .1417$, hence $\theta = 8^0 - 4"$

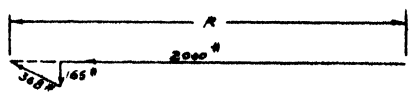


Fig. C8-33a

P = allowable bearing load parallel to grain for 3/8 bolt on 1-3/4 width wood = 2730# (From Fig. C8.27)

Q = same but perpendicular to grain = 880# (From Fig. C8.28)

Allowable bolt load equals

$$N = \frac{PQ}{P\sin^2\theta + Q\cos^2\theta} = \frac{2730 \times 880}{2730 \times .140^2 + 880 \times .990^2} = 2620\#$$

Hence margin of safety on bolt a = $\frac{2620}{2350} - 1 = .11$

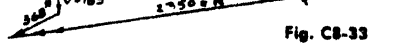


Fig. C8-33

Consider Bolt b

Fig. C8.33a shows force polygon for bolt b. It is obvious that the resultant load is less than on bolt a. Also the allowable bolt load N is larger because θ is very small.

The student should check the bolt edge distances on wood beam to see if they satisfy requirements of Fig. C8.29.

Since wood is not an isotropic material, the assumption on which the torsional resistance of the bolt group is based does not strictly hold, thus a reasonable M.S. should be maintained on the wood bearing loads.

PROBLEMS

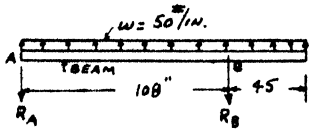


Fig. C8-34

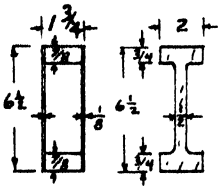


Fig. C8-35

Fig. C8-36

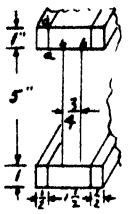


Fig. C8-37

(1) Fig. C8.34 represents a spruce box beam with cross-section as shown in Fig. C8.35. The webs are 2 plywood spruce. For the given external beam loading, determine the margin of safety in bending for points of maximum positive and negative bending moments. For a given web diaphragm spacing of 7 inches determine the margin of web for given loading. What is the margin of safety for glue strength between webs and flange?

(2) If the cross-section of the beam of Fig. C8.34 is changed to the spruce (I) section of Fig. C8.36, what is the margin of safety in bending and shear for the given loading.

(3) The spruce beam section of Fig. C8.37 is subjected to an external shear load V = 2000 lb. Determine the margin of safety for glue strength at sections (a-a) and (b-b). Also determine the maximum web shear stress and margin of safety for given shear load.

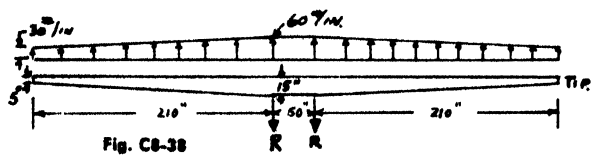


Fig. C8-38

(4) For the cantilever beam and loading of Fig. C8.38 design a box spruce beam with plywood webs for the section of maximum bending moment and shear.

(5) Fig. C8.39 illustrates a wing beam of a conventional biplane or braced monoplane. The master section of the spruce beam is shown in Fig. C8.40. The beam is subjected to the following loadings: uniform left running b beam load w = 45 lb. per inch, axial loads P = -8000 lb., P_a =-1000 lb, and P_b = -1100.

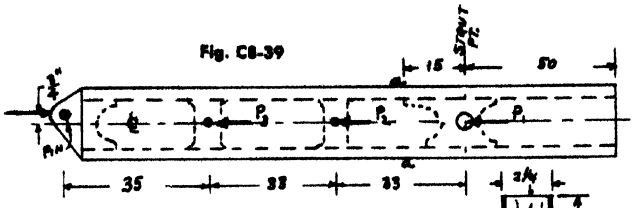


Fig. C8-39

Determine the margin of safety for the beam for the given loading at three sections, namely, point of maximum span moment, strut point and section (a-a).

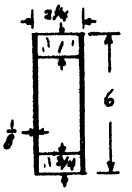


Fig. C8-40

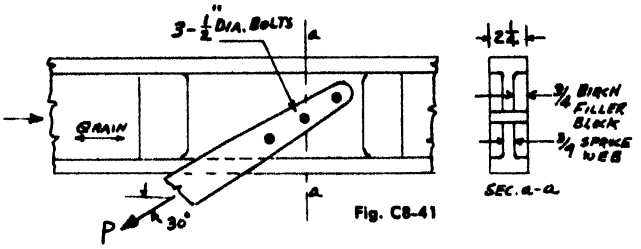


Fig. C8-41

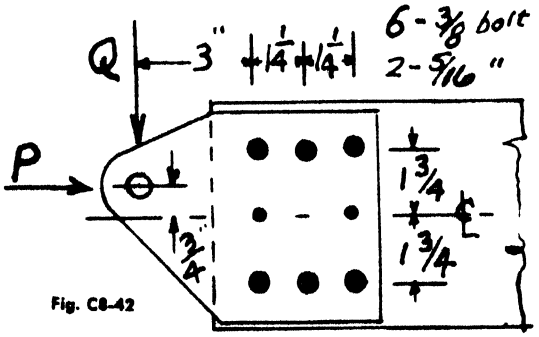


Fig. C8-42

(6) Fig. C8.41 illustrates a connection of the wing lift strut to wing beam. Find allowable load (P) in strut.

(7) Fig. C8.42 illustrates a beam end fitting. If P = 12000 lb., and V = 2000 lb., determine the approximate margin of safety of the bolted connection relative to wood strength. Beam width = 2". Material spruce.

CHAPTER C9
ANALYSIS AND DESIGN OF THE VARIOUS TYPES OF WING STRESSED-SKIN STRUCTURES

C9.1 Introduction

Methods of analyzing a stiffened cellular structure under combined axial, bending and torsional loads are being constantly revised and modified as more information derived both from experimental and theoretical research is obtained. The general methods of solution as given in this chapter are being widely used in the industry, but the stress analysis engineer should always check the latest requirements of the government agencies relative to the stress analysis procedure for a wing structure.

The student before beginning the study of this chapter should review the following chapters. (A5, A13, A14, A15 and D1). The complete stress analysis and design of a conventional wing cellular beam structure involves hundreds of engineering man-hours, involving possibly several hundred pages of calculations. The simplified example problems and discussions in this chapter however can illustrate the application of the general theory to wing analysis and design.

As discussed in chapter D1, the wing is subjected to distributed air and inertia loads and in many cases concentrated reactions or forces from other major items attached to the wing as, for example, the landing gear and power plant. The direction and location of these forces change with the various flight and landing conditions, thus a wing structure is one that will be subjected to bending in various directions as well as twisting forces and, in many conditions, axial forces are also produced. The stiffened cellular type of structure is a type of structure which is suitable for the efficient resisting of such loads. Besides being efficient in transmitting the applied loads to the supporting structures such as the fuselage or landing gear, this type of structure due to the stringers, ribs and metal covering, provides an excellent means for distributing the air pressures to the main transmitting structural units.

C9.2 General Types of Cellular Wing Structures.

The simplest type of wing structure would be a tube with an airfoil shape. This type for most materials would be far too heavy since the wall thickness required would be excessive due to the fact that the compressive buckling stresses would be low since certain regions of the airfoil contour are practically flat. Thus, in general, all types of present day wing cellular structures incorporate various spanwise stiffening elements. These spanwise elements are attached to the cell exterior and interior webs, thus forming an efficient system for resisting bending and torsional forces. Fig. C9.1 shows the various types of wing structures relative to the location of flange and web material.

In Figure C9.1, the various designs have been divided into two general classes, and are referred to as the concentrated flange type and the distributed flange type. In the concentrated flange type, the flanges in general are connected to each other by interior webs, whereas in the distributed type, the spanwise flange material is also attached to covering between internal webs or is continuous between interior webs in the form of corrugations.

All types consist of one or more closed cells which provides the torsional rigidity. To provide bending strength in any direction, at least three spanwise flange members are necessary as illustrated in Fig. (a). This assumes that the sheet metal covering buckles and is not effective in resisting bending compressive stresses. The structure and covering aft of the main structural cells is generally referred to as secondary or distributing structure as its general purpose is to transfer the air loads on this portion forward to the structural box beam. In many cases, the wing covering in this region is doped fabric. Photograph series C9.1 shows various types of wing structure which have been designed and built.

C9.3 General Considerations in the Selection of the Proper Type of Wing Structure.

In every airplane design, there is usually one or two types of wing structural layout which will provide advantages over the other various arrangements that are commonly used. The following list of factors have considerable influence on the selection of the best type of wing structural arrangement.

1. Light weight.
2. Fuselage or body arrangement which dictates method of wing-body connection.
3. Cut-outs in wing surface.
4. Folding wings.
5. Wing fuel tanks - removable and integral
6. Flutter prevention.
7. Appearance and fatigue strength of covering.
8. Ease and cost of production.

Fig. a



Fig. b



Fig. c



Concentrated Flange Type of Wing Beam.

Dashed line represents secondary structure. In many cases this portion is fabric covered.

Distributed Flange Type of Wing Beam.

Fig. d



Fig. e

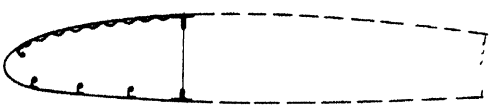


Fig. f

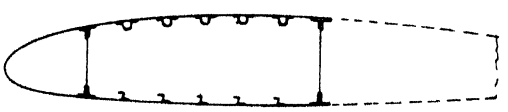


Fig. g

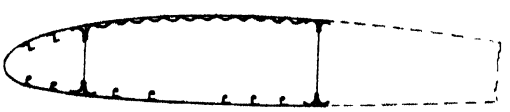


Fig. h

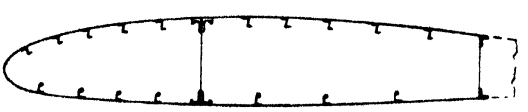


Fig. i

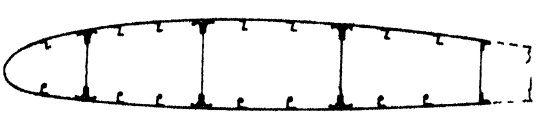


Fig. C9-1 Common Types of Wing Beam Flange Arrangement.

General Discussion of These Factors

(1) Light Weight:

The structural designer always strives for the minimum weight which is practical from a production and cost standpoint. The higher the ultimate allowable stresses, the lighter the structures. The concentrated flange type of wing structures as illustrated Fig. (a, b and c) of Fig. C9.1 permits high allowable compressive flange stresses since the flange members are stabilized by both web and covering sheet, thus eliminating column action, which permits design stresses approaching the crippling stress of the flange members. Since the flange members are few in number, the size or thickness required is relatively large, thus giving a high crippling stress. On the other hand, this type of design does not develop the effectiveness of the metal covering on the compressive side, which must be balanced against the saving in the weight of the flange members.

In the distributed type of flange arrangement (Fig. C9.1), a portion of the covering on the compression side is made effective since it is attached to closely spaced stringers or corrugations. However, the flange stringers between cell webs are supported only at rib or bulkhead points and thus suffer column action normal to the cell covering. This factor reduces the flange allowable compressive stresses since it is not practical to space wing ribs less than 12 to 18 times the flange stringer depth. Thus, if there were no other controlling factors, one could easily make calculations to determine which of the above would prove lightest. In general, if the torsional forces on the wing are small, thus requiring only a thin covering, the concentrated flange type of wing structure should prove the lightest.

In general, the flange material should be placed to give the largest moment of inertia in the Z direction, which means in general that the flange material should be placed between the 15 and 50 per cent of wing chord from the leading edge.

The secondary or distributing structure aft of the structural box beam should be made as light as possible and thus in general the farther forward the rear closing web of the box beam, the lighter the wing structure as a whole.

In the layout of the main spanwise flange members bends or changes in direction should be avoided as added weight is required in splicing or in transverse stiffeners which are necessary to change the direction of the load in the flange members. If flange members must be spliced, care should be taken not to splice them in the region of a maximum cross-section. Furthermore, in general, the smaller the number of fittings, the lighter the structure.

The detrimental action of shear distortion on the flexural stress distribution, commonly

referred to as shear lag should be given careful consideration. This question is discussed in Art. C9.16.

(2) Fuselage or Hull Arrangement:

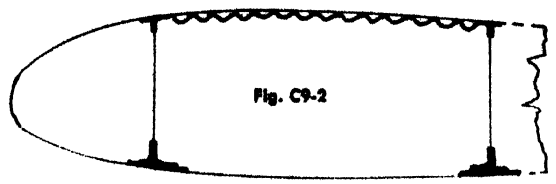
If the airplane is of the low wing or the high wing type, the entire wing structure can continue in the way of the airplane body. However, in the mid-wing type or semi-low wing type, limitations may prevent extending the entire wing through the fuselage, and some of the shear webs as well as the wing covering must be terminated at the side of the fuselage. If a distributed flange type of cell structure were used, the axial load in the flange stringers would have to be transferred to the members extending through the fuselage. To provide for this transfer of large loads requires structural weight and thus a concentrated flange type of box structure might prove the best type of structure.

(3) Cut-outs in Wing Surface:

The ideal arrangement where continuity of structure is maintained over the entire surface of the structural box is seldom obtained in actual airplane design due to cut-outs in the wing surface for such items as retractable landing gears, mail compartments and bomb and gun bays. If the distributed flange type of box beam is used, they are interrupted at each cut-out, which requires that means must be provided for drifting the flange loads around the opening, an arrangement which adds weight because conservative overlapping assumptions are usually made in the stress analysis. The additional structure and riveting to provide for the transfer of flange load around large openings adds considerably to the production cost.

For landing gears as well as many other installations, the wing cut-outs are confined to the lower surface, thus a structural arrangement as illustrated in Fig. C9.2 is quite common. The upper surface is of the distributed flange type whereas the lower flange material is concentrated at the two lower corners of the box. In the normal flying conditions, the lower surface is in tension and thus cell sheet covering between the cut-outs is equally effective in bending if shear lag influence is discounted. For negative accelerated flying conditions, the lower surface is in compression thus sheet covering between corner flanges would be ineffective in bending. However, since the load factors in these flight conditions are approximately one half the normal flight load factors, this ineffectiveness of the lower sheet in bending is usually not critical.

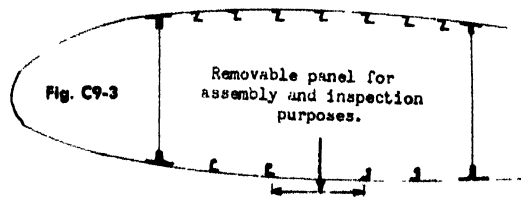
Cut-outs likewise destroy the continuity of intermediate interior shear webs of such sections as illustrated in Figs. (c and i) of Fig. C9.1, and the shear load in these interrupted webs must be transferred around the opening by



special bulkheads on each side of the cut-out. Thus, in general, it is best not to use more than two interior webs, or three for large airplanes.

In many cases, cut-outs in the leading edge are necessary due to power plant installations, landing gear wells, etc. Furthermore, in many airplanes, it is desirable to make the leading edge portion removable for inspection of the many installations which occupy this space in the portion of the wing near the fuselage. If such is the case, then an interior web should be placed in the forward portion of the cell as illustrated in Fig. b and c of Fig. C9.1.

Inspection doors for the central portion of the box beam structure are usually located on the lower side of the wing. They are usually fastened to two spanwise stringers with screws and the removable panels are effective in resisting bending and shear load. (see Fig. C9.3)



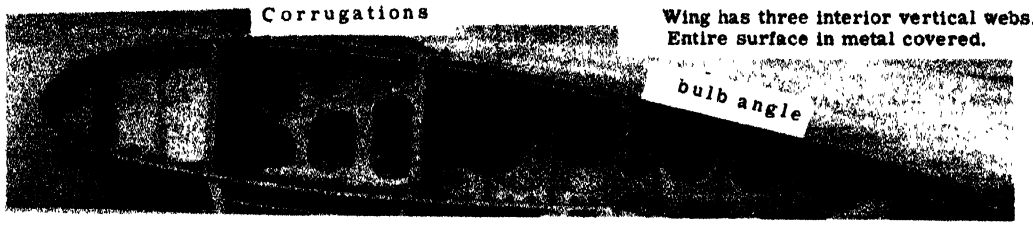
Cutouts in the wing structural box destroys the continuity of the torsional resistance of the cell and thus special consideration must be given to carrying torsional forces around the cut-out. This special problem will be discussed in detail in a later chapter.

(4) Folding-Wings:

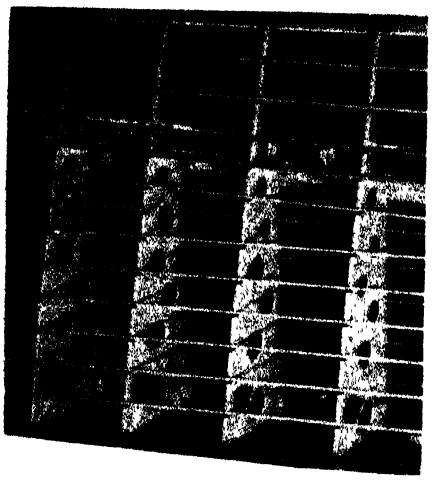
For certain airplanes, particularly Carrier based Naval airplanes, it is necessary that provision be made to fold the outer wing panels upward. This dictates definite hinge points between the outer and center wing panels. If a distributed flange type of structure is used, the flange forces must be gathered and transferred to the fitting points, thus a compromise solution consisting of a small number of spanwise members is common practice.

(5) Wing Fuel Tanks: Removal and Integral Type:

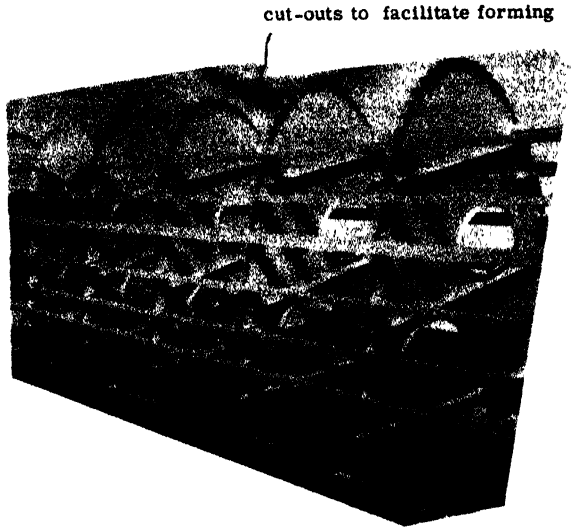
If fuel tanks are of the removable type, they are usually inserted from the lower side of the wing by means of removal panels, which are screwed to edge stiffeners and thus the continuity of the lower surface is not disturbed. Since the interior webs of a multiple web type of cell



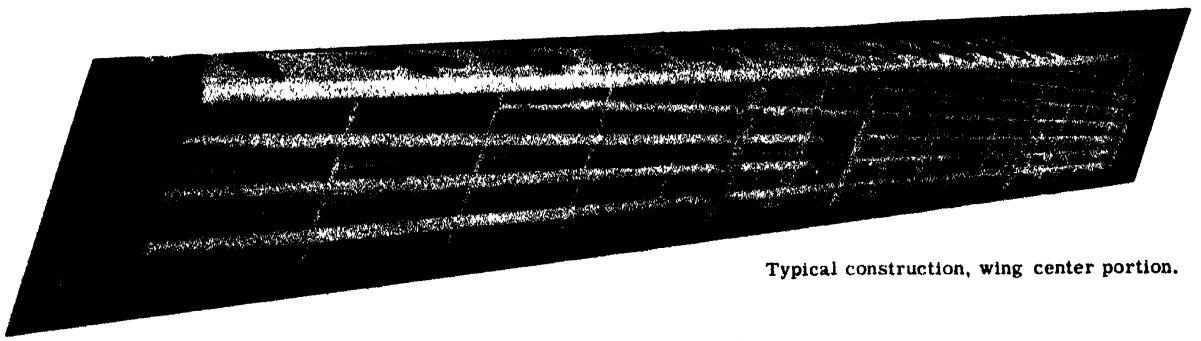
Looking inboard in wing center section of Douglas DC-2 Airplane



Typical construction, wing trailing edge portion.

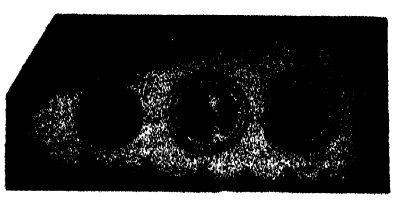


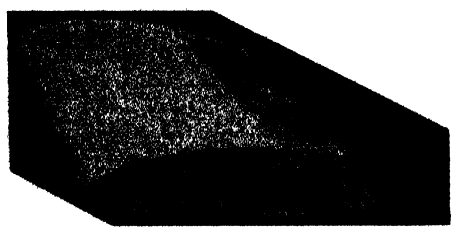
Typical construction, wing leading edge portion.



Typical construction, wing center portion.

All the above photographs by courtesy of the 'Douglas Airplane Co.





Alloy sheet steel wing construction as developed by North American Aviation.

(Photographs from Aero. Digest)

would be interrupted by the fuel tank, it is best not to use this type of cellular structure.

If the fuel tank is built integral with the wing, that is, the top and bottom covering of the wing and the interior webs form the walls of the tank, many problems involving gas tightness arise. If a distributed type of flange is used, the spanwise stringers must pass through the gas tight bulkhead at each end of the tank. This involves the difficult problem of sealing the stringer cut-outs through the tank and bulkheads. If on the other hand the stringers are cut at each bulkhead, they must be spliced or connected in some manner through the end bulkheads. This method simplifies the gas tightness problem but adds considerable weight due to splice material. As a result of these difficulties, many structural designers prefer the concentrated flange type of structure which eliminates the problem of running a large number of stringers through the fuel tanks.

(6) Wing Flutter Prevention:

With the high speeds now obtained by modern airplanes, careful attention to wing flutter prevention must be given in the structural layout and design of the wing. In general, the critical flutter speed depends to a great extent on the torsional rigidity of the wing. When the mass center of gravity moves aft of the 25 per cent of chord point, the critical flutter speed decreases, thus it is important to keep weight of the wing forward. At high speeds where "compressibility" effects become important, the torsional forces on the wing are increased, which necessitates extra skin thickness or a larger cell. Designing for flutter prevention is a highly specialized problem.

(7) Appearance and Fatigue Strength of Wing Covering:

In the concentrated flange type, particularly the one illustrated by Fig. (b) of Fig. C9.1, the upper surface covering between the wing ribs will buckle in normal flying conditions as illustrated in Fig. C9.3a because the upper surface is in compression and the wide sheet panels have a low buckling stress. Besides these compression buckles, the covering will form diagonal tension fields due to shearing forces which produce diagonal compressive stresses.

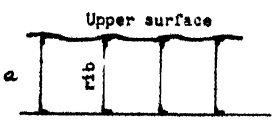


Fig. C9-3 a

If the airplane is a commercial low wing type, the formation of these wrinkle patterns is visible to the passengers and it creates in some cases a feeling of fear as it appears that the wing is being overstressed as the top skin wrinkles in various degrees as the accelerations are being changed by encountering air gusts. Consequently, for low wing airplanes it is best to add distributed spanwise members to prevent this wrinkling and buckling at such low load factors. On the lower side of a high wing monoplane, the shear stresses tend to cause the lower covering to form diagonal wrinkle patterns, but the spanwise tension stresses due to bending tend to eliminate the wrinkling, and thus under low load factors, very little evidence of wrinkling is visible and thus the concentrated flange type is satisfactory for lower wing surface.

Since the buckles on the upper surface occur at such low stresses, there is a possibility of fatigue failure of the sheet near the riveted boundaries since the magnitude of the depth of the buckles is constantly changing as the air loads are changed slightly due to gusts. Many airplanes have been built with wings similar to Fig. (b) and have given satisfactory service, so that matter of possible fatigue failure of the sheet covering due to constant flexing is only an opinionl

(8) Ease and Cost of Production:

The airplane industry has recently changed to a mass production industry and therefore the structural layout of the wing must take into account production methods. The general tendency at this time is to design the wing and body structure, so that sub-assembled of the various parts can be made, which are finally brought together to form the final assembly of the wing panel. To make this process efficient requires careful consideration in the details and layout of the wing structure. Photograph C9.2 illustrates the sub-assembly break-down of the structural parts of an airplane of a leading airplane company. Fabrication and assembly of these units permits the installation of much equipment before assembly of the units to the final assembly. (See Photograph C9.3)

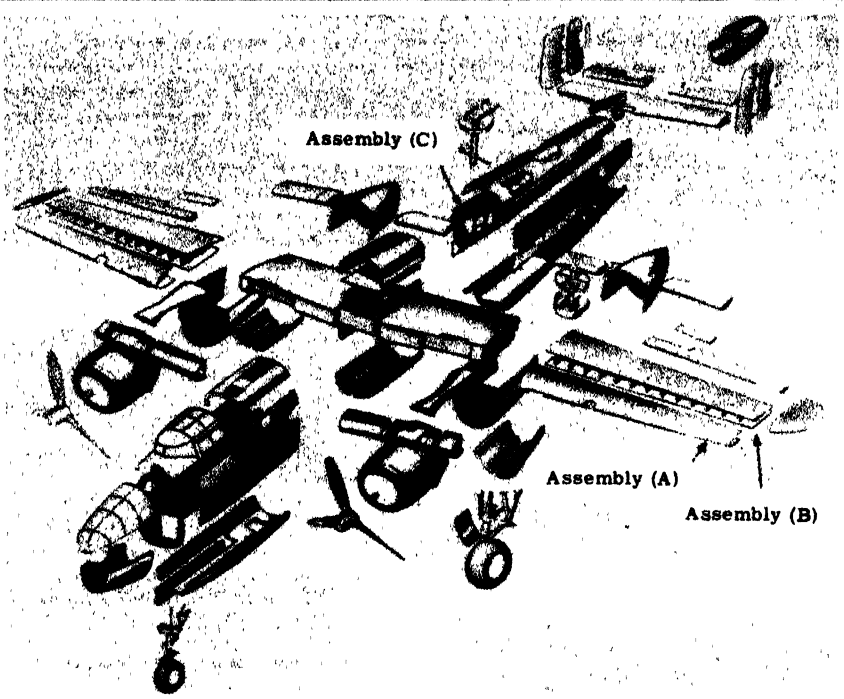
C9.4 Types of Flange Members

For the concentrated flange type of box beam, the flange in most cases is in the form of a heavy extrusion. Typical examples of this type of flange section are shown in Fig.s (g, h, i and j) of Fig. C6.2 in Chapter C6.

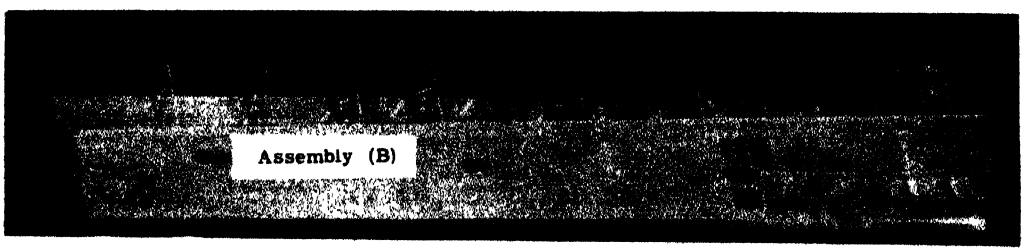
Typical stringer flange sections for the distributed flange type of box beam are illustrated in Fig. C9.4.

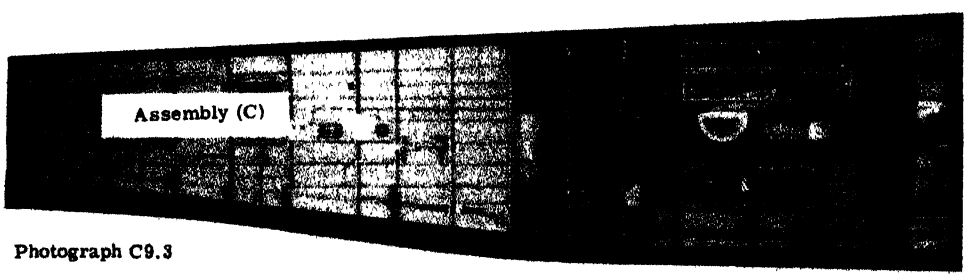
In general, the flight positive design load factors are considerable larger than the flight negative design load factors, and since positive accelerated conditions place the upper portion of the wing in compression, the critical loads for flange stringers is compression.

For strength-weight efficiency, the upper flange stringers are generally of the closed type. (Fig. C9.4). These closed sections if aluminum alloys are used can be formed from the









Photograph C9.3

Designing To Facilitate Production.

Photographs by courtesy of North American Aviation Co.

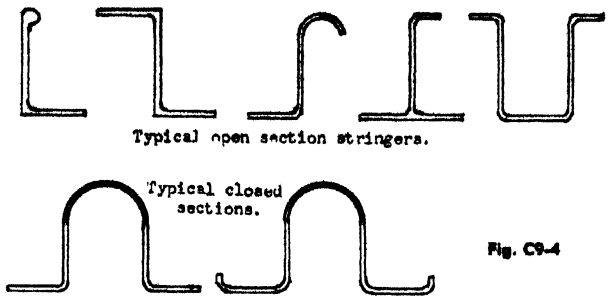


Fig. C9-4

Various types of corrugated sheet is frequently used as flange material for the upper surface of the wing.

highest strength alloys. The objection to closed sections is the possibility of corrosion between sheet covering and the interior of the stringers or corrugation which is not open to inspection. As a result, open stringer sections as illustrated in Fig. C9.4 are widely used as flange material.

In general, the lower surface of the wing in the outer wing panel is designed by tension for the normal flight attitude and then checked for the compression stresses under the lower inverted flight design load factors. In general, open section stringers have sufficient strength to give a positive margin of safety for the lower surface. In any aluminum alloy wing, if 24SRT sheet is used on bottom surface, then open stringers rolled or drawn from 24SRT sheet should be used instead of extrusions if advantage is to be taken of the high ultimate and yield strength of 24SRT sheet as compared to 24ST extruded material.

Many of the open stringer sections fail by twisting, whereas the closed sections fail as a column in bending or by local crippling. The student should refer to Chapter B6 for methods of estimating the strength of sheet-stringer units in compression.

C9.5 Web and Wall Material.

The interior webs of a box beam in general consist of flat sheets with stiffeners and are designed as Wagner or semi-tension field beams (see Chapter C7). For weight efficiency 24SRT alclad or 24SRT sheet should be used in aluminum alloy wings. The student should refer to Chapter B4 (Fig. B4.3) which explains why effective widths of sheet in compression are a function of the stress-strain relationship for the material.

General Stress Analysis Theory and Procedure.

C9.6 Optimum Cutting Planes. Structural Axes.

The question of the proper cross-section to use in the structural analysis is a confusing one because wings possess various degrees and combinations of dihedral and sweepback and the structural flange members in a wing usually do

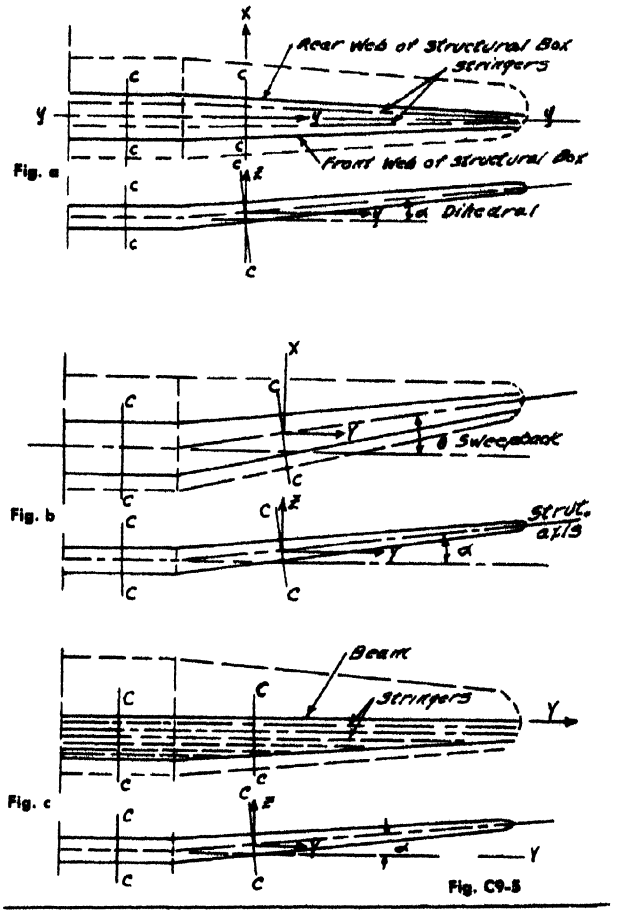


Fig. C9-5

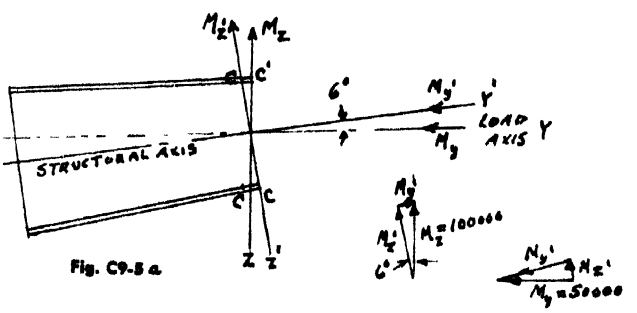


Fig. C9-5a

not run parallel to each other. In general, the section chosen for stress analysis purposes should be the one which gives the minimum cross-section.

Fig. C9.5 shows three typical wing arrangements with the outline of the structural members which make up the wing structural box. The cutting planes of sections for stress analysis purposes of the box beam as a whole are labeled (C-C). In the arrangement shown in Fig. C, all flange members run parallel except the front beam. However, since most of the flange material runs parallel, it seems logical to take the cutting plane C-C as shown and this is usually done in practical analysis. Coordinate axes which have a direction perpendicular or parallel to these

cutting planes (C-C) are generally referred to as the structural axes.

As illustrated in Chapter D1, it is common procedure to refer the applied forces and moments on the wing to a selected load axis, since the applied load analysis for the wing is usually carried out before any decision has been made as to the final interior structural arrangement. A convenient load axis as pointed out in Chapter D1 is one parallel to the Y axis. In Fig. C9.5, the structural axes for the outer wing panel structure which are normal to the cutting planes (CC) are not parallel to the Y axis and thus if applied loads and moments have been calculated with reference to a load axis parallel to Y axis, it is necessary to transform these loads and moments to the structural axes.

If the structural axis as selected and the load axis have approximately the same directions, it is not necessary to refer the loads and moments to the structural axis as the errors will be quite small, and thus the cutting planes can be taken as normal to the load axis.

The student should realize that very little error is produced if the cutting planes are not exactly perpendicular to the so-called structural axis, but appreciable errors are produced if the cutting planes are not perpendicular to the load axis. Therefore, always resolve all forces and moments with reference to coordinate axes which are normal and parallel to the selected cutting planes.

Example Problem:

Fig. C9.5a shows a portion of a tapered beam. Assume that moments M_y and M_z with reference to the beam section C'C' are known. The structural axis for the beam is normal to the section CC which makes an angle of 6° with C'C'. For moments of M_z = 100,000 and M_y = 5000 determine M_z' and M_y'.

Due to M_z = 100,000

M_z' = 100,000 x cos 6° = 99450

M_y' =-100,000 x sin 6° = -10450

Due to M_y = 50000

M_z' = 50000 x sin 6° = 5225

M_y' = 50000 x cos 6° = 49725

C9.7 Three Flange — Three Web Tapered Closed Cell Beams.

The 3-flange 3-web tapered box beam as illustrated in Fig. C9.6 is a common type of wing structural design for light airplanes and for the leading edge beams of large ailerons and wing flaps. To take bending in all directions at least three spanwise flange members are required, assuming of course that the buckling compressive strength of the thin sheet covering is exceeded under the applied loads. The three webs that connect the flange stringers provide the resistance to shearing forces, which the webs can carry in the form of diagonal tension

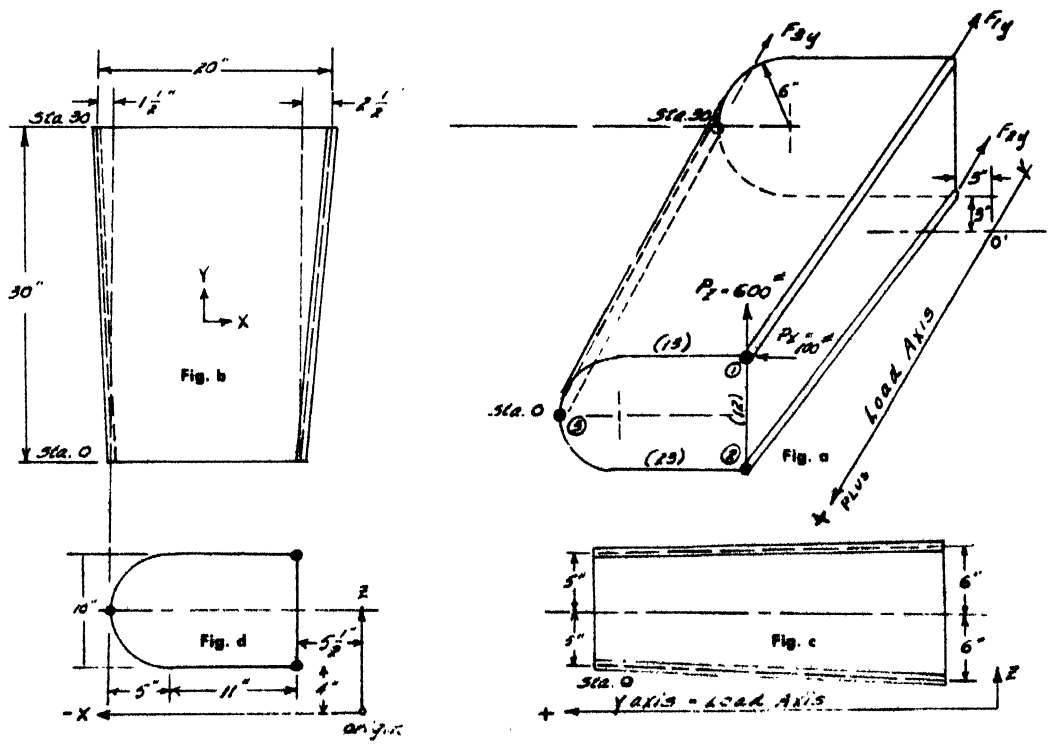


Fig. C9-6

fields if the shearing buckling stresses are exceeded. At any cross-section of the beam, there are 6 unknowns, namely the axial loads in the flange stringers which are usually referred to as the out of plane forces and the shear load in each of the three web portions which act in the plane of the cross-section. The problem is statically determinate because 6 equations are available for determining the 6 unknowns. They are:

$$\Sigma F_y = 0,\ \Sigma F_Z = 0,\ \Sigma F_X = 0,$$

$$\Sigma M_X = 0,\ \Sigma M_y = 0,\ \Sigma M_Z = 0$$

This is one great advantage of the 3-flange beam from a stress analysis view point since the loads are independent of the sectional properties and thus the usual trial and error method of design is avoided to a great extent.

The stress analysis of a 3-flange 3-web can best be explained by the solution of an example problem.

C9.8 Example Problem of 3-Flange 3-Web Tapered Web Beam.

Fig. C9.6 shows a 3-flange 3-web tapered cellular beam. External loads of P_Z = 600 and P_X = -100# are applied at station (0) as shown. The problem is to determine the flange and web loads at station 30.

Solution:

The first thing to decide upon is the direction of the cutting plane at station 30 for use in the stress analysis. Observation of the XY projection of the beam (Fig. b) shows that the slope of the leading edge flange stringer (No. 3) in the X direction is slightly different than that of the aft stringer (1) and (2). In the ZY plane (Fig. c), the taper of the cell in the Z direction is symmetrical. A cutting plane at station 30 parallel to ZX plane therefore appears reasonable.

As a reference load axis in the Y direction, the origin is taken as indicated in (Fig. d)

Solution for the Out of Plane Forces at Station 30:

The components of the flange axial loads normal to the XZ cutting plane at Station 30, can be found as follows:

The total forces in the Y direction must equal zero, hence

$$\Sigma F_y = -F_{1y} - F_{2y} - F_{3y} = 0 \quad \text{- - - - - - -(1)}$$

The reactions on the 3 stringers at station 30 have been all assumed as acting in the same direction, which is obviously incorrect, however, the resulting signs from the algebraic solution will give the true sense of the stringer loads.

The moment of all forces about reference axis X at station 30 must equal zero.

$$\Sigma M_X = 600 \times 30 + 15_{1y} + 3F_{2y} + 9F_{3y} = 0 \quad \text{- - -(2)}$$

The moments about the Z reference axis at station 30 of all forces must equal zero, or

$$\Sigma M_Z = -100 \times 30 - 23F_{3y} - 3F_{1y} - 3F_{2y} = 0 \quad \text{- -(3)}$$

Solving equations (1) and (3), F_{3y} can be found directly and equals - 150#. That is the y components of the axial reaction in stringer (3) is opposite to that assumed in (Fig. a) or compression in the stringer.

Then solving for F_{1y} and F_{2y}, we obtain:

F_{1y} = -1425# (opposite sense to that assumed)

F_{2y} = 1575 # (same sense as that assumed)

Since the angle between the Y axis and the centroidal axis of the flange members is quite small, the axial load in the flange members may be considered equal to their Y component, the error being the difference between the cosine of a small angle and unity.

In this particular example, there were no externally applied loads in the Y or axial direction. Thus the flange loads could have been determined by considering M_X and M_Z separately and then adding the results. To illustrate:

M_X = 600 x 30 = 18000"#

This moment is resisted by flange members (1) and (2) which have an effective resisting arm of 12". Hence Y component of load in (1) and (2) = 18000/12 = 1500#. (Compression in (1), tension in (2).

M_Z = -100 x 30 = -3000"#.

This moment is resisted by a beam with stringer (3) as one flange and stringers (1) and (2) as the other flange with an effective arm of 20". Y component of axial load in (3) = -3000/20 = -150#. Y component of axial load in (1) or (3) = 150/2 = 75# (tension)

Combining loads:

$F_{(1)y}$ = -1500 + 75 = -1425

$F_{(2)y}$ = 1500 + 75 = 1575

$F_{(3)y}$ = - 150 + 0 = - 150

In general, there are small externally applied axial loads due to dead weight interia loads if wing incorporates a dihedral. Wing tip auxiliary floats and landing gear reactions produce appreciable axial loads on wing in certain conditions, thus it is generally best to write the three equations (1), (2) and (3).

In Plane Components of Stringer Axial Loads:

Since the three stringers are not perpendicular to the cutting plane at station 30, components in the X and Z directions will be produced

in the plane of the cutting section. Thus, at stringer point No. 1:

F_{1X} = -1425 x 2.5/30 = -118.7#

F_{1Z} = -1425 x 1/30 = - 47.5#

At stringer point No. (2):

F_{2X} = 1575 x 2.5/30 = 131.5#

F_{2Z} = 1575 - (1/30 = - 52.5#

At stringer point No. (3):

F_{3X} = -150 x (-1.5/30) = 7.5#

F_{3Z} = 150 x 0 = 0#

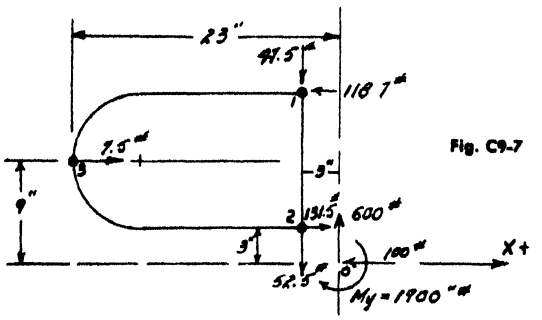


Fig. C9-7

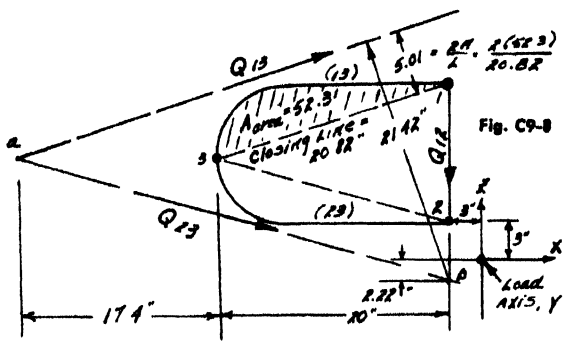


Fig. C9-8

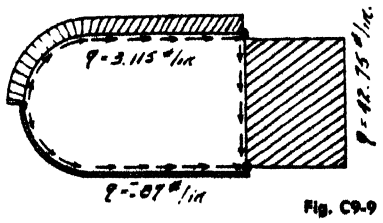


Fig. C9-9

Fig. C9.7 shows the in plane forces and couples at station 30 due to the external applied loads and the induced x and z components of the flange stringer axial loads.

The external shear due to applied loads in the Z direction equals ΣF_Z = 600#, and the shear load in the X direction equals ΣF_X = -100#. We refer these loads to the load axis Y as assumed, and these loads produce a moment M_y at station 30 of 600 x 5.5 - 100 x 14 = 3300 - 1400 = 1900"#. This couple is shown in Fig. C9.7.

The remaining in plane forces acting are the three web loads. To avoid confusion, the web resisting forces are shown separately on Fig. C9.8. Since the three flanges take all the bending stresses, the shear flow on each web portion is constant. The location and direction of the resultant shear flow force is shown by the vectors Q_{12}, Q_{13} and Q_{23} in Fig. C9.8. Since the web (1-2) is straight, the location coincides with the web. The location of the resultant shear flow vector on web portion (13), that is, between stringers (1) and (3) is parallel to the closing straight line joining the extremities at stringers (1) and (3). The length of this closing line is 20.82" (see Fig. C9.8). By the principles explained in Chapter A14 for constant shear flow webs, the resultant shear flow force is parallel to the closing line and acts at a perpendicular distance from the closing line equal to 2A/L where A is the enclosed area between web and closing line. Thus the distance to resultant shear vector equals

2 A/L = 2 x 52.3/20.82 = 5.01" (See Fig. C9.8)

The location of the resultant shear flow force on web (2-3) is located at a similar distance from the closing straight line joining stringers (2) and (3), since the web shapes are identical.

These three web shear vectors plus the known loads and moments as given in Fig. C9.7 must be in equilibrium.

Solution for Magnitudes of Resultant Shear Flow Vectors:

To find the magnitude of Q_{12} the total shear flow on the web between stringers (1) and (2), it is convenient to take moments about point (a), the point of intersection of the other two unknown vectors. Thus taking moments about point (a) of all forces in both Figs. C9.7 and C9.8, we obtain

ΣM_a = 1900 + 100 x 9 - 600 x 40.4 + 37.4 (52.5 + 47.5) - 118.7 x 6 - 131.5 x 6 + 37.4 Q_{12} = 0, hence Q_{12} = 514#

Therefore,

q_{12} = 514/12 = 42.75#/in.

To find Q_{13}, take moments about point (b), the intersection of vectors Q_{12} and Q_{23}.

ΣM_b = 1900 - 100 x 2.22 - 600 x 3 - 118.7 x 17.22 + 131.5 x 5.22 + 7.5 x 11.2 + 21.42 Q_{13} = 0

hence

Q_{13} = 65#

and

$q_{13} = 65/20.82 = 3.115\#/in.$

To find the remaining shear flow vector Q_{23}, the summation of forces in the X direction will be made.

$$\Sigma F_X = -100 - 118.7 + 131.5 + 7.5 + 65 \times 37.4/39.0 + Q_{23} (37.4/39.0) = 0$$

hence

$Q_{23} = 18.1\#$, and $q_{23} = 18.1/20.82 = .87\#/in.$

Fig. C9.9 shows the resultant shear flow pattern. The student should always check the equilibrium of the results to see if the moments in the plane of the cut section about some other moment center are zero.

Solution No. 2 for Web Shear Flow Values:

It is not necessary to deal with resultant shear flow vectors. The shear flow q per inch in each web can be found as follows:

In Fig. C9.10, the three unknowns are the three shear flows q in the three webs. The external air loads acting at the load axis (Y) and the in plane forces induced by the flange axial loads are the same as in Fig. C9.7.

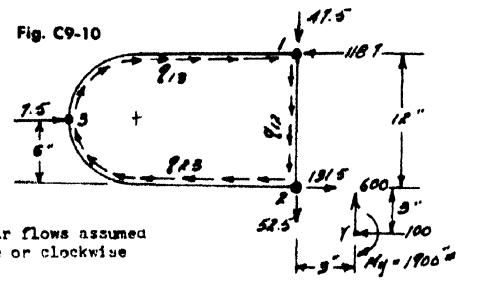
Taking moments about stringer No. 1 and equating to zero,

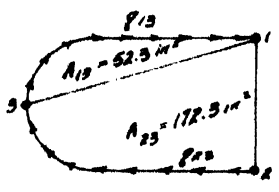
$$\Sigma M_1 = -131.5 \times 12 - 7.5 \times 6 - 600 \times 3 + 100 \times 15 + 1900 + 2 \times 52.3 \times q_{13} + 2 \times 172.3 \times q_{23} = 0 \quad \text{- - - - - - - - - -(1)}$$

or

$104.6\ q_{13} + 344.6\ q_{23} - 25 = 0$

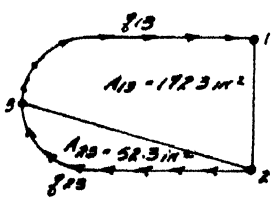
Note: The moment of the shears flows is obtained by areas in Figs. C9.11 and C9.12.





Moment of q_{13} on web 13 about point (1) equals $2A_{13}\ q_{13}$.

Moment of q_{23} on web 23 about point (1) equals $2A_{23}\ q_{23}$.



Moment of q_{13} on web 13 about point (2) equals $2A_{13}\ q_{13}$.

Moment of q_{23} about (2) equals $2A_{23}\ q_{23}$.

Taking moments about stringer (2) and equating to zero,

$$\Sigma M_2 = -118.7 \times 12 - 600 \times 3 + 7.5 \times 6 + 100 \times 3 + 1900 + 344.6\ q_{13} + 104.6\ q_{23} = 0$$

or

$344\ q_{13} + 104.6\ q_{23} - 978 = 0$ - - - - - - -(2)

Solving equations (1) and (2) for q_{13} and q_{23} gives

$q_{13} = 3.11\#/in.$, $\quad q_{23} = -.87\#/in.$

To find the remaining shear flow q_{12}, take $\Sigma F_Z = 0$, which gives

$$\Sigma F_Z = -100 + 600 + 3.11 \times 6 - .87 \times 6 - 12\ q_{12} = 0$$

hence

$q_{12} = 513.5/12 = 42.75\#/in.$

These values check the results in Fig. C9.9 as found in first method of solution.

C9.9 General Design Suggestions for 3-Flange Beam.

To save weight, two of the flange members should be placed near the deepest part of the airfoil, and the third flange member near the leading edge. The cell area should be of such size as to give sufficient torsional rigidity with ordinary skin thicknesses. In a wing beam with only 3-flange members, it is necessary to space wing ribs considerably closer than if several more spanwise stringers were used. A rib spacing of 8 to 10 inches is common practice. If a small torsional cell is used, the torsional and flexural shear stresses may require a fairly thick skin, thus giving a possibility of permanent wrinkles of the skin on the compressive bending side of the cell.

From a flutter standpoint, it is desirable to have the flexural axis of the cell near the aerodynamic load axis and furthermore the inertia axis should be near the aerodynamic axis. To obtain this result, the rear web of the cell should rarely be aft of the 30 to 35 percent of chord point from the leading edge.

In many designs, the requirements of certain installations, such as ladning gear, fuel tanks, guns, etc., will dictate the size of the cell.

Very high allowable compressive stresses can be obtained for the rear two flange members since they are stabilized in two directions, thus the allowable stresses approach the crippling stresses for the various sections. A flange section should be selected which can be tapered efficiently between root and tip chord.

Before the axial loads in the flange stringers can be found, their centroids must be known. The centroid location depends on the size of the flange which in turn is influenced by the allowable flange stresses. Thus,

considerable preliminary calculation and sketching must be done before the final load calculations can be made. In many cases, the type of skin and rib attachment effects the shape and size of the flange member.

C9.10 Allowable Web Stresses.

The rear or straight web of the beam can be designed as a semi-tension field beam using the methods of Chapter C7. The flange members attached to this web should have sufficient strength to carry the additional loads produced by the semi-tension field action of the web.

The other two webs which form the leading edge cover have a varying curvature. The allowable ultimate shear stress for this portion is highly indeterminate. Tests of several typical wing leading edge single cell beams which the writer is familiar with gave allowable stresses of around 7000 to 9000 psi. for leading edge skin thicknesses .025 to 1040 for 24ST aluminum alloy material. These values can be used in preliminary design.

The Analysis of Multiple Flange, Tapered, Single Cell Beams.

C9.11 Introduction.

The single cell, multiple flange type of beam structure is widely used in the design of wings and fuselages. Unfortunately, it is a statically indeterminate structure, and thus a method of trial and error must be used in obtaining the necessary member sizes since the stress distribution depends on the section properties, and the section properties are necessary to obtain the section stresses.

The general methods of analysis to be used in this article have been explained and illustrated in previous chapters. For various methods or equations for calculating the bending stresses in an unsymmetrical section, reference should be made to Chapter A13. For a general discussion and example problem solutions for calculating the shear flow in a tapered multiple cell beam reference should be made to (Chapter A15, Arts. A15.10 to A15.13).

In general, a stress analysis of this type of structure is first made under two broad assumptions, namely, (1) that plane sections remain plane after bending and (2) that bending stress is directly proportional to strain. The first assumption is violated near points of beam support since the cellular section is prevented from warping freely. The second assumption does not hold for stresses above the proportional limit of the materials. Since the ultimate design stresses for airplanes are usually above the proportional limit of the material, this assumption does not strictly apply. Furthermore, these assumptions neglect the effect of the shearing deformations in the webs, commonly referred to as "shear lag", which may be appreciable in certain types of wings. (See Art. C9.16). However, until stress analysts develop practical methods for dealing with stress distribution in the plastic range, and for taking care of shearing deformations, it will be necessary to use simplified approximate methods and to make allowances for the descrepancies by semi-rational methods which tend toward the conservative side.

C9.12 Summary of General Stress Analysis Equations.

All external forces and moments should be referred to rectangular axes through the centroid of the effective cross-section of the beam. In some methods of analysis, the axes in the XZ plane are taken as the principal axes for the particular section, however, since the bending stresses can be found without the use of the principal axes (see Chapter A13), it is expedient to take a convenient set of rectangular axes, such as X, Y and Z in Fig. a.

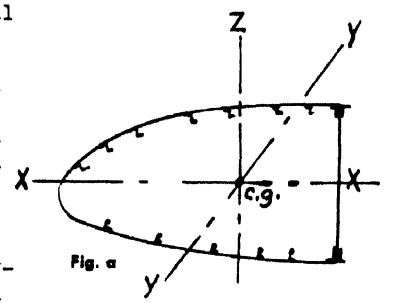


Fig. a

Longitudinal Stresses in Flange Members

The resulting external force parallel to the axis normal to thebeam section, being referred to the axis through the section centroid produces a uniform normal stress distribution over the section of

$$f_n = \frac{P}{A} \text{ - - - - - - - - - - - - - - - - - -(A)}$$

where

f_n = normal intensity of stress

P = normal load on section

A = total effective cross-sectional area

Then the total normal component of the axial load on any flange member equals

$$P_n = f_n\, a$$

where

a = effective flange area for a given member

Bending of the beam produces longitudinal stresses in the flange members. If the section properties and the external bending moments are referred to a set of centroidal rectangular axes in the plane of the section, as for example, the X and Z axes in Fig. (a), the bending longitudinal stresses can be calculated from equation (b). (See Art. A13.5)for derivation and examples of its use.)

$$f_b = -(K_2 M_Z - K_1 M_X)x - (K_2 M_X - K_1 M_Z)z \quad --(B)$$

where

f_b = bending unit stress. (plus is tension)

$K_1 = I_{XZ}/(I_X I_Z - I_{XZ}^2)$

$K_2 = I_Z/(I_X I_Z - I_{XZ}^2)$

$K_3 = I_X/(I_X I_Z - I_{XZ}^2)$

The normal component of the axial load in a flange member equals (f_b a) where (a) is the area of the flange member. Since the angle between the normal to the beam section and the centroidal axis of a stringer is generally quite small, the difference between the cosine of a small angle and unity is negligible and thus the normal component can be considered as the axial load in the stringer.

Web Stresses

The web shear stresses are statically determinate for a single cell beam once the normal load distribution for the flange material is known, which distribution can be found by equation (B). The shear stress distribution can be found from the following equations:

$$q_n = q_o + \sum_1^n \frac{\Delta P}{d} \quad ----------(C)$$

$$\Sigma T_{c.g.} = 0 \quad ----------(D)$$

For explanation of equation (C) refer to Art. A15.10. Equation (D) states that the torsional moment of all forces in the plane of the cross-section about the section centroid must be zero, which is a fact necessary for equilibrium. This moment is due to 3 sources: (1) the external applied forces, (2) the moment due to the inclination of the flange members with the cross-section, which produces in plane forces and therefore moments, and (3) the moment of the web shear forces.

The application of these equations will be illustrated by the solution of a typical single cell beam.

C9.13 Example Problems

Fig. C9.13 shows the general structural layout for a typical wing panel. This wing panel has the same dimensions as the wing on the airplane in Fig. D1.9a of Chapter D1. The wing beam consists of a vertical web on the 15 and 50 percent of chord lines, with spanwise skin stringers in between. Fig. C9.14 shows the cross-sectional body plan for the various spanwise stations. The reference load axis (Y) is located at point O' on this figure. Fig. C9.15 gives the details of the cell cross-section at the several spanwise sections. The wing portion of the front web has no spanwise stringers and in this example problem the leading edge portion will be neglected. Strictly speaking, it will take some bending and appreciable torsional resistance, however, to illustrate the solution of a single cell beam, the leading edge cell is omitted. In example problem two, the leading edge cell will be included thus making a conventional two cell tapered multiple flange beam.

Table C9.1 gives the resultant external design shears and moments all referred to the load axis at point O'. These values are approximately equal to those as computed for the airplane in Chapter D1, and which were summarized in Tables D1.10 to D1.13 of Chapter D1. However, to provide simplicity the dihedral has been omitted and the wing box beam has been so located that beam sections are normal to the assumed load axis (Y) and thus the problem of resolving moments to take care of dihedral and sweep-back angles is eliminated in this simplified problem. (See discussion in Art. C9.6)

The problem will be to determine the bending and shear stresses on the beam section at station 20, for the loads which are given in Table C9.1

Calculation of Wing Structural Section Properties

Tables C9.2 and C9.3, columns 1 to 11, give the calculations for the location of the section centroid and the moment of inertia and product of inertia about centroidal X and Z axes for wing sections at stations 20 and 47.5 respectively. All dimensions were scaled from a large drawing, such as Fig. C9.14. For the condition being analyzed, the upper surface is in compression, thus the effective flange material consists of the flange member plus a certain amount of effective sheet which has been taken as shown in Fig. C9.15. The lower surface being in tension, the skin halfway to the adjacent stringer is assumed concentrated at the centroid of the combined stringer and effective skin area. The question of proper effective skin area and procedure in design is discussed in Art. C9.19.

Translation of External Forces and Moments From Load Axis to Structural Axis.

The shears and moments as given in Table C9.1 will be referred to parallel X, Y and Z axes through the section centroid.

Consider station 20.

The location of the load axis Y at point O' with respect to the section centroid at point O is shown in Fig. C9.16.

Taking moments about point (O), the centroid of the beam section:

$$\Sigma M_{y(O)} = -390000 + 12000 \times 33.3 + 2700 \times 11.8$$
$$= 41800"\#$$

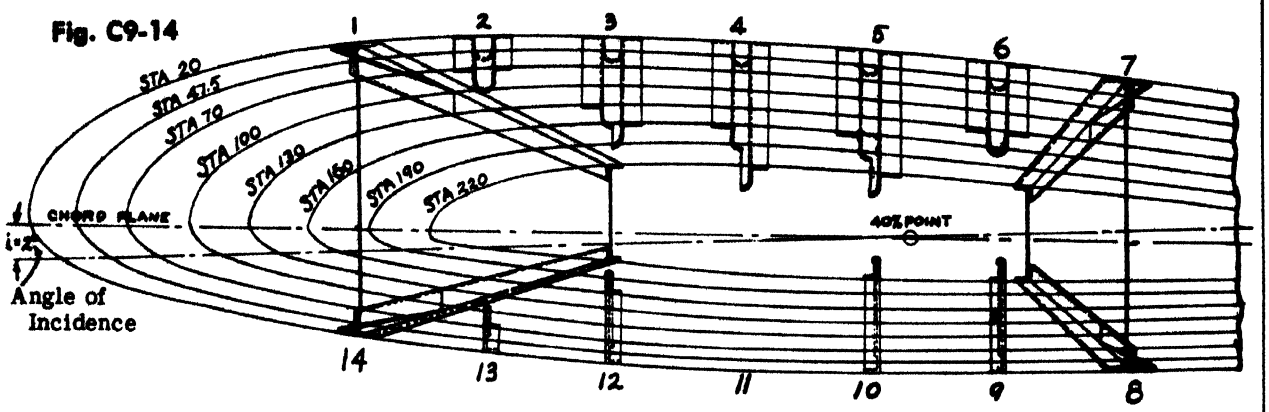
$$V_{Z_O} = 12000$$

$$V_{X_O} = -2700$$

Fig. C9.17 shows the resulting values at the section centroid.

WING BODY SECTION PLAN VIEW LOOKING INBOARD FROM TIP

Fig. C9-14



UPPER SURFACE STRINGER AND SKIN ARRANGEMENT

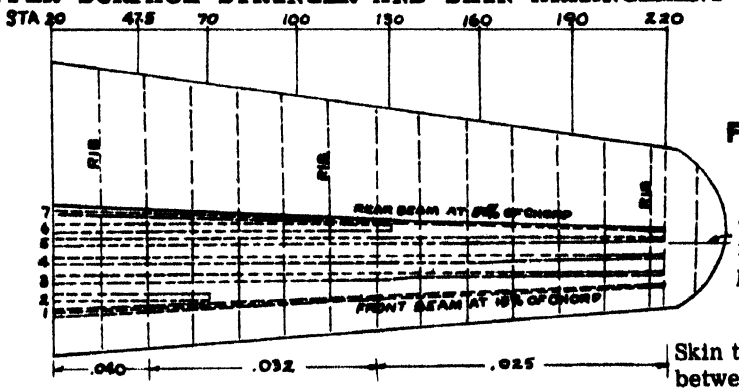


Fig. C9-13

40% of chord line is normal to airplane ZX-Plane

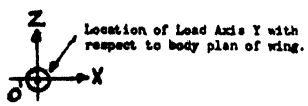


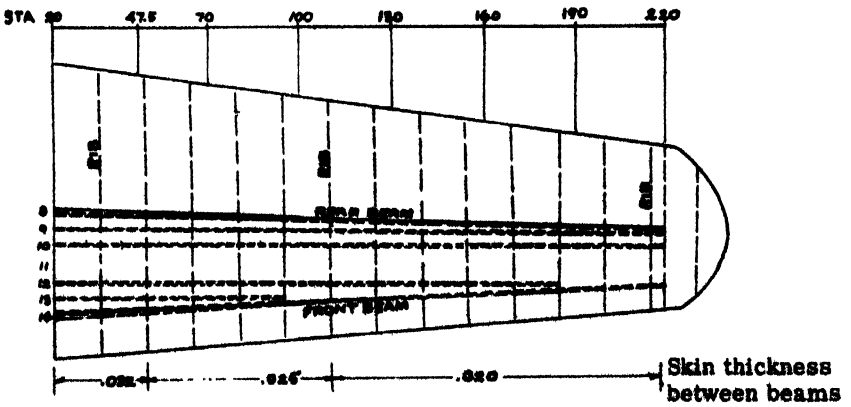
Table C9.1

Design Shears and Moments Referred to Load Axis Y. (Values are Representative of loads in a M.A.A. condition)

Station z	20	47.5	70
M_x (in.lb.)	1300000	1000000	735000
M_z "	-285000	-215000	-158000
M_y "	-390000	-375000	-324000
V_z (lb)	12000	11900	10200
V_x (lb)	-2700	-2600	-2300
P_y (lb)	0	0	0

For signs of shears and moments see Fig. D1.8a.

UPPER SURFACE STRINGER AND SKIN ARRANGEMENT



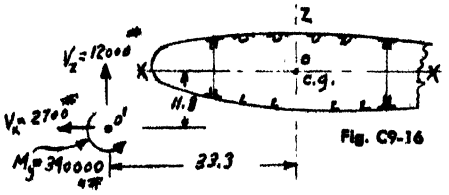


Fig. C9-16

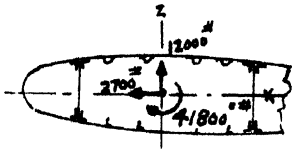


Fig. C9-17

In general, the structural axis which is normal to the beam sections is not parallel to load axis Y because of a dihedral angle and in many cases, a sweepback angle. In this case, the forces are translated to the section centroid as illustrated above and are then rotated into the plane of the cut section, making use of the dihedral and sweepback angles. If an applied axial load, P_y, should exist at the load axis O' in Fig. C9.16, in transferring it to a parallel axis through the section centroid, it would produce moments about the X and Z axes through the section c.g.

Calculation of the Bending Stresses

Station 20:

M_X = 1,300,000"# (From Table C9.1)

M_Z = -285,000"#

Station 47.5:

M_X = 1,000,000"#

M_Z = -215,000"#

Since our structural axis is parallel to the load axis Y, and since there are no applied loads along the Y axis, the magnitude of the M_X and M_Z moments about X and Z axes through the Y load axis are not changed. For the general case involving dihedral, etc., this would not be the case.

Bending stresses at station 20:

$f_b = -(K_s M_Z - K_1 M_X)x - (K_s M_X - K_1 M_Z)z$

From Table C9.2:

I_X = 230.3, I_Z = 1030, I_{XZ} = -50

$K_1 = I_{XZ}/(I_X I_Z - I_{XZ}^2) = -50/(230.3 \times 10.30 - 50^2) = -50/235500 = -.0002125$

$K_s = I_Z/235500 = 1030/235500 = .004378$

$K_s = I_X/235500 = 230.3/235500 = .00098$

Substituting in the above equation for f_b

$f_b = -\left[.00098 \times -285000 - (-.0002125 \times 1300000)\right] x - \left[.004378 \times 1{,}300{,}000 - (-.0002125 \times -285000)\right] z$

whence

$f_b = 3.3\ x - 5639\ z$

Column 12 of Table C9.2 gives the results of this equation for values of x and z in columns 10 and 11. Multiplying these bending stresses by the stringer areas, the stringer loads are given in column 13. The sum of the loads in this column should be zero since total tension must equal total compression on a section in bending.

Stresses at station 47.5:

I_X = 157.4, I_Z = 700, I_{XZ} = -35.4 (Table C9.3)

$K_1 = 35.4/(157.4 \times 700 - 35.4^2) = -35.4/108950 = -.000324$

$K_s = 700/108950 = .00643$

$K_s = 157.4/108750 = .001447$

$f_b = -\left[.001447 \times -215000 - (-.000324 \times 1{,}000{,}000)\right] x - \left[(.00643 \times 1{,}000{,}000 - (-.00324 \times -215000)\right] z$

whence

$f_b = -14.5 \times -6360\ z$

Column 12 of Table C9.3 gives the results of this equation and column 13, the total stringer loads at station 47.5.

Calculation of Shear Flow System Due to Change in Flange Loads Between Stations 20 and 47.5.

Since the value of the web shear at any point is unknown, it will be assumed as zero between stringers No. 1 and No. 14. The average shear flow under this assumption for any web portion can be calculated by the following equation:

$$q = 0 + \sum_{1}^{n} \frac{\Delta P}{27.5}$$

Table C9.4 (Column 5) gives the resulting values for q. Fig. C9.18 shows the results in graphical form for theq stresses.

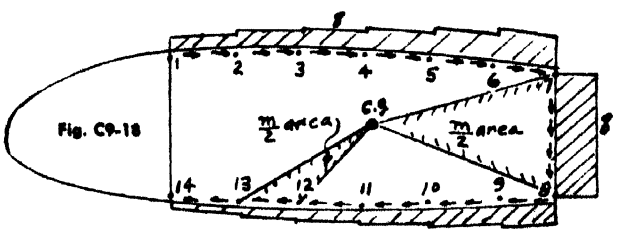
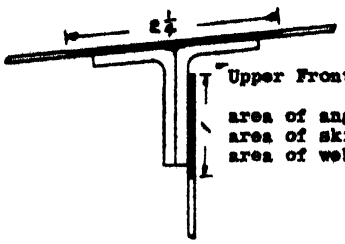
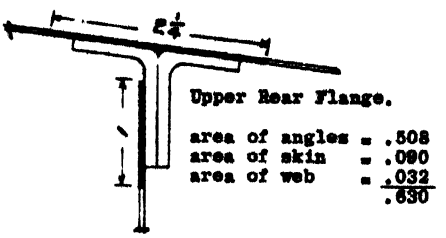


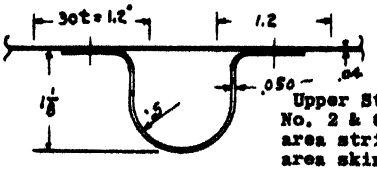
Fig. C9-18

Fig. C9.18 Flexural shear flow pattern for zero shear flow on web 1-14. The interior triangles represent the m/2 area for use in computing moment of shear flow about c.g. of section.

The moment of this shear flow system about the section centroid is given by Column 7 of Table C9.4, where m is the double area of the sectors



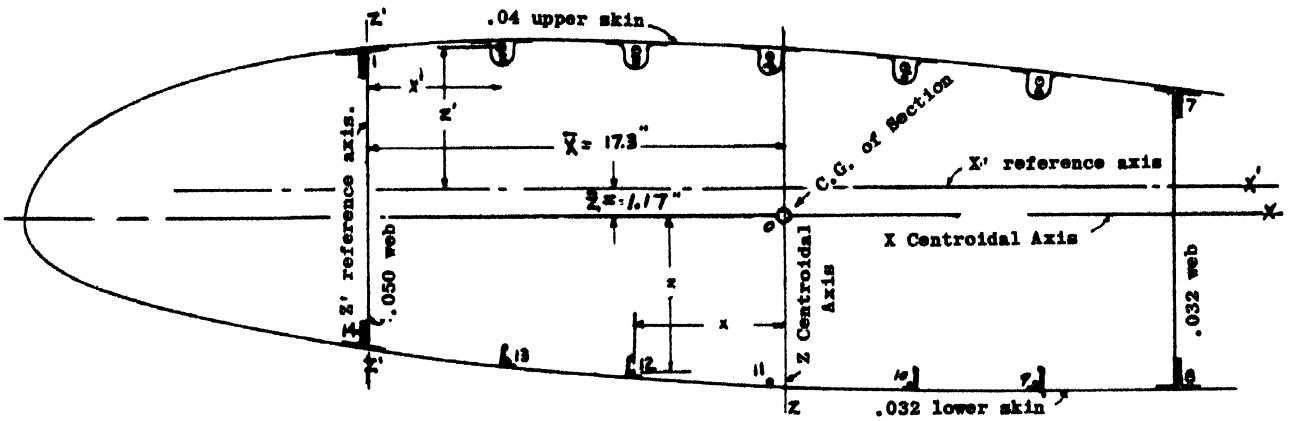


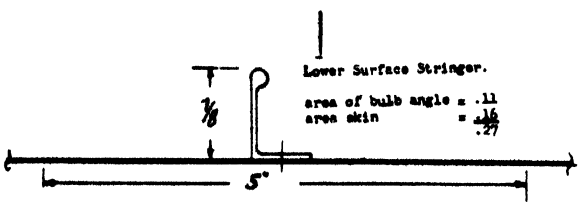


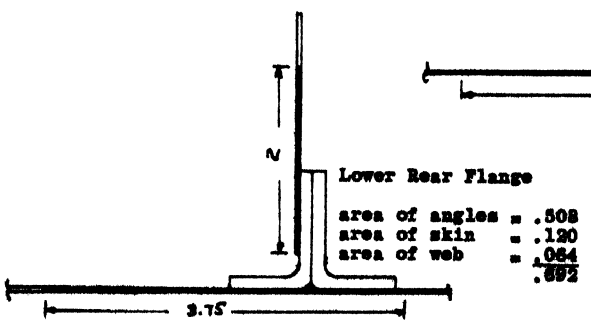
STATION 20

Upper Stringer.
No. 2 & 6 (t = .064)
area stringer = .257
area skin = .096
.353

No. 3,4 & 5(t = .050)
area stringer = .205
area skin = .096
.301







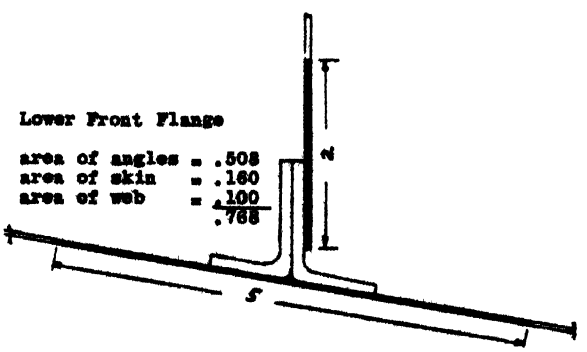


Fig. C9-15

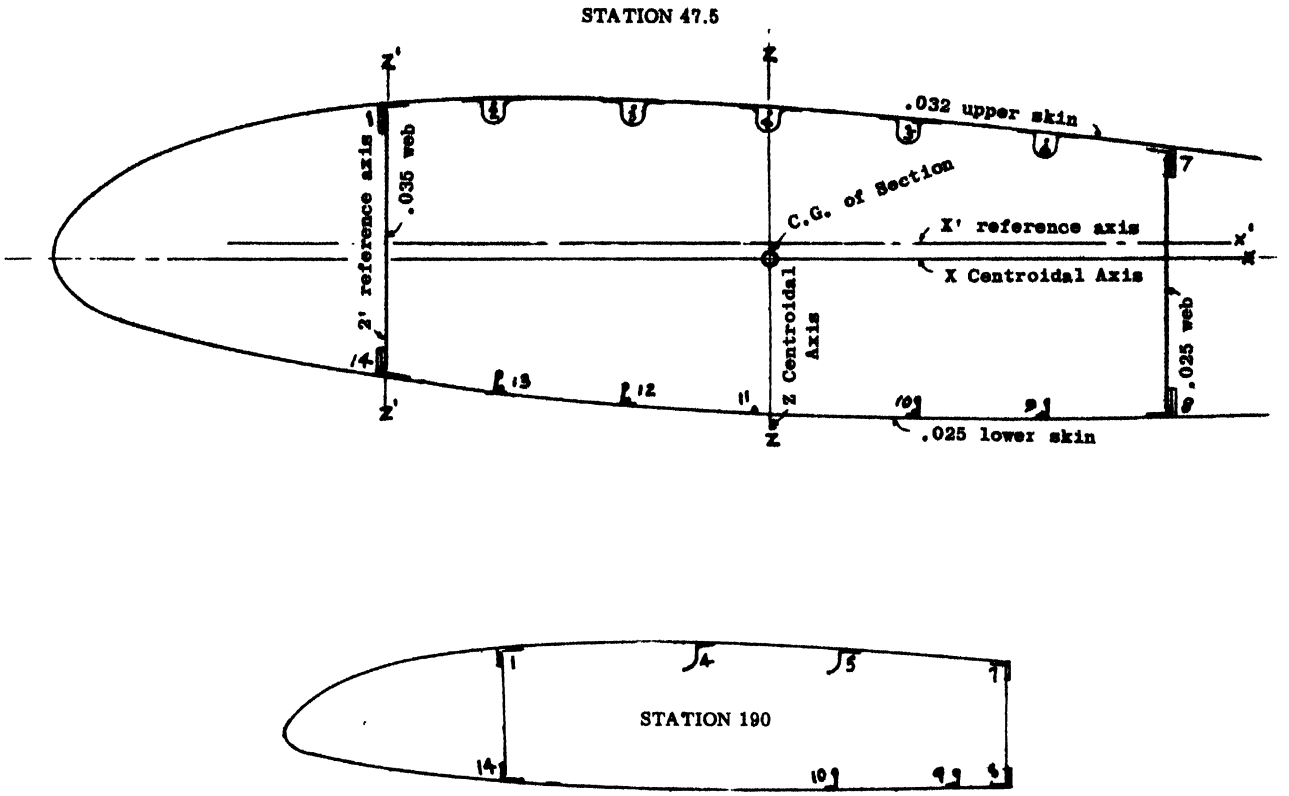


Fig. C9-15 (Continued)

Fig C9.15 shows the general details of the wing structural cross-section at three station points. The section for station (20) represents the basic section since this is the section of maximum bending moment and all other sections are derived by tapering or eliminating some of the members of the basic section. Thus, at station 190, only four of the original stringers remain and the original corner flange members have been cut down to a small angle of such size to permit riveting to web and skin.

The internal shear flow system at station 20 is found by considering the changes in axial load in the flange members between stations 20 and 47.5, hence the section properties for these two sections are required. The calculations are given in Tables C9.2 and C9.3.

The sections at stations 20 and 47.5 are broken down into 14 flange units. The area of each unit includes the area of the stringer or flange member plus the effective skin area. This combined area is then considered as concentrated at the centroid of the composite area. The effective skin on the upper or compressive side has been taken equal to 30t in width for a preliminary trial section, since the effective width depends on the stringer stress and the stringer stress depends on the section properties of the entire beam section.

Calculations will show (using the methods of Chapter B6) that the ultimate strength of the 0.51 hat-shaped stringer fabricated from 24SRT alclad and supported on wing ribs at 15 inch spacing is around -41000 psi. Using this value in the following effective width equation width equations as effective width is obtained which is close to a width of 30t which equals 1.20".

$$w = 1.7\ t\ \sqrt{E/f_{st}} = 1.7 \times .04 \sqrt{\frac{10300000}{41000}} = 1.08"$$

$$w = 1.9\ t\ \sqrt{E/f_{st}} = 1.20"$$

The resulting stresses in column 12 of Tables C9.2 and C9.3 give the information on which to base a revision of the effective widths The calculations which have been carried out for the trial section must then be repeated for the modified section.

This process is repeated for several spanwise sections in order to obtain a design which is efficient from a weight standpoint and yet not overstress any part in bending or shear.

TABLE C9.2

SECTION PROPERTIES ABOUT CENTROIDAL X AND Z AXES

Wing Section at Station 20 (Compression on upper surface)

1	2	3	4	5	6	7	8	9	10	11	12	13
Flange No.	Area A	Z'	AZ'	AZ'^2	X'	AX'	AX'^2	AX'Z'	$Z = Z' - \bar{Z}$	$X = x' - \bar{X}$	f_b	$P = f_b A$
1	.648	5.50	3.56	19.61	-0.10	-0.06	0	-0.36	6.68	-17.4	-37660	-24390
2	.353	5.90	2.08	12.30	5.65	1.99	11.30	11.78	7.08	-11.65	-39940	-14070
3	.300	5.85	1.76	10.28	11.20	3.36	37.60	19.67	7.03	- 6.10	-39620	-11890
4	.300	5.55	1.66	9.25	16.85	5.05	85.00	28.10	6.73	- 0.45	-37950	-11370
5	.300	5.05	1.52	7.65	22.40	6.72	150.50	34.00	6.23	5.10	-35115	-10510
6	.353	4.40	1.55	6.83	28.00	9.89	277.00	43.50	5.58	10.70	-31450	-11090
7	.630	3.55	2.24	7.95	35.72	23.15	826.00	80.00	4.73	18.42	-26560	-16700
8	.692	-8.40	-5.81	48.90	35.72	24.70	881.00	-208.00	-7.22	18.42	40750	28230
9	.270	-8.50	-2.30	19.55	27.80	7.50	208.00	- 64.00	-7.32	10.50	41280	11180
10	.270	-8.50	-2.30	19.55	22.60	6.10	138.00	- 52.00	-7.32	5.30	41250	11170
11	.160	-8.30	-1.33	11.05	16.70	2.67	44.60	- 22.20	-7.12	- 0.60	40100	6430
12	.27	-8.00	-2.16	17.30	10.90	2.94	32.00	- 23.50	-6.82	- 6.40	38400	10390
13	.27	-7.50	-2.02	15.20	5.60	1.51	8.45	- 11.35	-6.32	-11.7	35570	9600
14	.768	-6.50	-5.00	32.50	- 0.10	- .08	0	0.50	-5.32	-17.40	29950	23020
Σ	5.584		-6.56	238.0		96.44	2700	-163.8				0.00

$\bar{Z} = \frac{-6.56}{5.584} = -1.176$

$\bar{X} = \frac{96.44}{5.584} = 17.3$

$I_x = 238 - 5.584 \times 1.176^2 = 230.3$ in.^{4}

$I_z = 2700 - 5.584 \times 17.3^2 = 1030$ in.^{4}

$I_{xz} = -163.8 - 5.584 \times -1.176 \times 17.3 = -50$

General Notes:
See Fig. C9.15 for Section at Station 20.
Reference axes X'X' and Z'Z' are assumed as shown.
Properties are calculated with respect to these axes and transferred to the centroidal X and Z axes

$F_b = 3.3 X - 5639 Z$

TABLE C9.3

SECTION PROPERTIES ABOUT CENTROIDAL X AND Z AXES

Wing Section at Station 47.5 (Compression on upper Surface)

1	2	3	4	5	6	7	8	9	10	11	12	13
Flange No.	Area A	Z'	AZ'	AZ'^2	X'	AX'	AX'^2	AX'Z'	$Z = Z' - \bar{Z}$	$X = X' - \bar{X}$	f_b	$P = f_b A$
1	.476	5.60	3.66	14.95	- 0.10	- 0.05	0	- 0.27	6.21	-15.60	-39275	-18700
2	.318	5.83	1.80	10.80	4.40	1.40	6.16	8.16	6.44	-11.10	-40790	-12990
3	.266	5.75	1.53	8.80	10.00	2.66	26.60	15.30	6.36	- 5.50	-4025	-10710
4	.266	5.42	1.44	7.81	15.60	4.15	64.75	22.40	6.03	0.10	-38400	-10200
5	.266	4.90	1.30	6.40	21.20	5.64	120.00	27.60	5.51	5.70	-35075	- 9320
6	.318	4.30	1.37	5.88	26.70	8.50	226.50	36.60	4.91	11.20	-31360	-10000
7	.476	3.60	1.71	6.17	31.70	15.10	478.00	54.40	4.21	16.20	-27030	-12880
8	.350	-7.10	-3.93	27.90	31.70	17.51	555.00	-124.50	-6.49	16.20	41050	22770
9	.235	-7.40	-1.74	12.90	26.50	6.23	165.00	- 46.10	-6.79	11.00	43090	10140
10	.235	-7.40	1.74	12.90	21.30	5.00	107.00	- 37.18	-6.79	5.80	43180	10160
11	.135	-7.20	-0.90	6.48	15.10	1.89	28.50	- 13.60	-6.59	- 0.40	41900	5240
12	.235	-6.90	-1.62	11.20	9.60	2.26	21.70	- 15.60	-6.29	-55.90	40085	9410
13	.235	-6.25	-1.47	9.20	4.50	1.06	4.75	- 6.61	-5.84	-11.00	36060	8470
14	.605	-5.40	-3.27	17.70	- 0.10	- 0.06	0	0.33	-4.79	-15.60	30725	18600
Σ	4.61		-2.80	159.1		71.3	1804	- 79.0				0

$\bar{Z} = -2.80/4.61 = -0.61"$

$\bar{X} = 71.3/4.61 = 15.50"$

$I_x = 159.1 - 4.61 \times .61^2 = 157.4$

$I_z = 1804 - 4.61 \times 15.5^2 = 700$

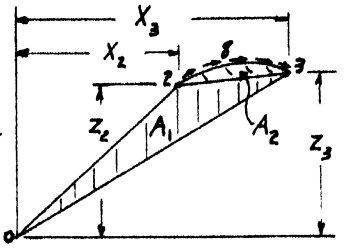
$I_{xz} = -79 - 4.61 \times -.61 \times 15.5 - 35.4$

General Notes:
See Fig. C9.15 for section at Station 47.5.
Reference axes X'X' and Z'Z' are assumed as shown.

$f_b = -14.5 X - 6360 Z$

as shown in Fig. C9.18. The double areas are listed in Column 6. These areas have been found by the use of a planimeter. The total moment of the shear flow system about the section c.g. equals the summation of Column 7 or 256060"#.

The double areas (m) can be found approximately as follows:*



The moment of the shear flow q on the web (2-3) about point O equals q times twice the area $(A_1 + A_2)$. In most cases, the area A_2 can be neglected.

By simple geometry, the area $A_1 = 1/2\ (X_3\ Z_2 - X_2\ Z_3)$. The moment of the shear flow q on web (2-3) thus equals $q\ (X_3\ Z_2 - X_2\ Z_3)$. Since values of X and Z for all flange points with reference to section (c.g.) are given in the Table C9.2, it is unnecessary to use the planimeter except for regions of sharp curvature.

Table C9.4

Calculation of Flexural Shear Flow Assuming q - zero in Web Between Flange Members (1) and (14).

(Shear values are average between stations 20 and 47.5)

1	2	3	4	5	6	7	8	9
Flange No.	P at Station 20	P at Station 47.5	$\frac{\Delta P}{27.5}$	$q = \frac{\Sigma \Delta P}{27.5}$	m sq. in.	mq	q_1	$q_r = q + q_1$
1	24390#	-18700	206.8					
				206.8	48.4	10000	-328	-121.2
2	14070	-12990	39.1					
				245.9	43.8	10780	-328	- 82.1
3	11890	-10710	42.9					
				288.8	42.0	12120	-328	- 39.2
4	11370	-10200	42.5					
				331.3	42.6	14100	-328	3.3
5	10510	- 9320	43.3					
				374.6	43.6	16340	-328	46.6
6	11090	-10000	39.6					
				414.2	42.0	17500	-328	86.2
7	16700	-12880	139.0					
				553.2	197.0	108900	-328	225.2
8	-28230	22770	-198.7					
				354.5	47.4	16800	-328	26.5
9	-11180	10140	- 37.8					
				316.7	37.2	11800	-328	- 11.3
10	-11170	10160	- 36.7					
				280.0	40.8	11420	-328	- 48.0
11	- 6430	5240	- 43.2					
				236.8	42.2	10000	-328	- 91.2
12	-10390	9410	- 35.6					
				201.2	38.0	7650	-328	-126.8
13	- 9600	8470	- 41.1					
				160.1	54.0	8650	-328	-167.9
14	-23020	18600	-160.3					
				0	204.0	0	-328	-328
1								
Total mq =						256060		

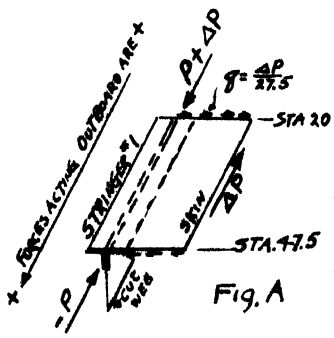


Fig. A

Notes: Cols. (2) and (3): Values from Tables C9.2 and C9.3. For signs see Fig.A
Col.6: m= double areas. See Fig. C9.18
Col.4= Col (2)+Col (3) divided by distance between stations.

*See Art. "Unit Method of Beam Analysis" by Shanley and Cozzone, Journal of Aeronautical Sciences, April 1941. The student should study this excellent article as it systemmatizes the the stress analysis procedure for wing beams.

Moments Produced by Inclination of Flange Loads With Beam Section.

Since the flange members in general are not normal to the beam sections, the flange loads have components in the Z and X directions. Columns (4) and (7) of the Table C9.5 give the values of these in plane components. The slopes dx/dy between stations 20 and 47.5 are found by scaling from Fig. C9.14. Fig. C9.19 shows these induced in plane forces as found in Table C9.5.

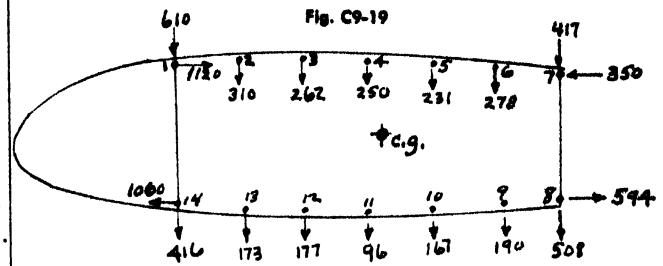


Fig. C9.19 In plane forces produced by flange axial loads.

The moments of these in plane components about the section c.g. are given in Columns (5) and (8) of Table C9.5. In general, these moments are not large.

Total Moments of All Forces About Section c.g. at Station 20:

Due to flanges = 7160 - 2224 = 4936"# (Ref. Table C9.5).

Due to assumed static shear flow = 256060"# (Ref. Table C9.4).

Due to external loads = 41800"#.

Then the total unbalanced moment = 4936 + 256060 + 41800 = 302796"#.

For equilibrium, this must be balanced by a constant shear flow q_1.

hence

$$q_1 = \frac{M}{2A} = -\frac{302796}{2 \times 461.5} = -328\#/\text{in.}$$

(Note: 461.5 = total area of cell)

The shear stresses q_1 are listed in Column (8) of Table C9.4.

The final or resultant shear flow q_r at any point therefore equals

$$q_r = q + q_1$$

The resulting values are given in Column 9 of Table C9.4. Fig. C9.20 illustrates the results graphically.

Having determined the shear flow distribution the shear stress at any point equals q/t. This stress is checked against the allowable shear stress and if revisions are necessary the calculations as illustrated must be repeated.

TABLE C9.5

IN PLANE MOMENTS ABOUT SECTION C.G. PRODUCED BY IN PLANE COMPONENTS OF FLANGE LOADS

STATION 20

1	2	3	4	5	6	7	8
Flange No.	P	$\frac{dx}{dy}$	$P_x = P\frac{dx}{dy}$	$M_{c.g.} = P_x Z$	$\frac{dz}{dy}$	$P_z = P\frac{dz}{dy}$	$M_{c.g.} = -(P_z X)$
1	-24390	-.046	1120	7480	.025	-610	-10600
2	-14070	0	0	0	.022	-310	- 3610
3	-11890	0	0	0	.022	-262	- 1600
4	-11370	0	0	0	.022	-250	- 112
5	-10510	0	0	0	.022	-231	1180
6	-11090	0	0	0	.025	-278	2970
7	-16700	.021	-350	-1660	.025	-417	7770
8	28230	.021	594	-4300	.018	-508	9350
9	11180	0	0	0	.017	-190	2000
10	11170	0	0	0	.015	-167	885
11	6430	0	0	0	.015	- 96	- 57
12	10390	0	0	0	.017	-177	-1130
13	9600	0	0	0	.018	-173	-2020
14	23020	-.046	-1060	5640	.018	-416	-7250
			Σ	7160			-2224

NOTES:
Column (2); P from Table C9.2
Column (5) and (8): Values of Z and X are found in Columns 10, 11 of Table C9.2

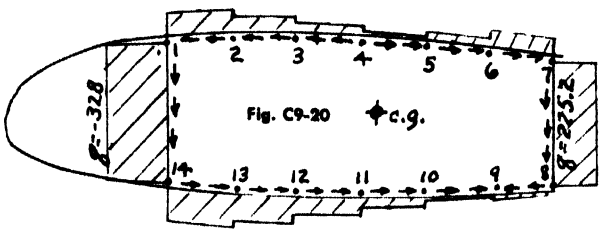


Fig. C9-20

Fig. C9.20 Final shear flow diagram. For values see Column 9 of Table C9.4.

Analysis of Two-Cell-Multiple Flange Tapered Beam.

C9.14 Introduction.

A two-cell beam is also quite common in wing structural design. (See Fig. C9.1). A two-cell structure in bending and torsion is statically indeterminate to the second degree since the shear flow at any one point in each cell is unknown. However, due to continuity between cells the angular twist of each cell must be the same, which gives the additional equation necessary for solving a two-cell beam as compared to the single cell analysis.

C9.14a Summary of Equations for Analysis of Two-Cell Beam.

The equations for the flange axial and bending stresses, the static flexural shear flow and the equilibrium of total moments are the same as for a single cell. The additional equation relates to the angular twist. Thus summarizing:

Flange axial stresses:

$$f_n = P/A \quad \text{- - - - - - - - - - - - - - - - - -(A)}$$

Flange bending stresses:

$$f_b = -(K_3 M_Z - K_1 M_X)x - (K_2 M_X - K_1 M_Z)z \quad \text{- -(B)}$$

Static flexural shear flow:

$$q_n = q_o + \sum_1^n \frac{\Delta P}{d} \quad \text{- - - - - - - - - - - - - -(C)}$$

Total moments in plane of section must equal zero.

$$\Sigma T_{c.g.} = 0 \quad \text{- - - - - - - - - - - - - - - - - -(D)}$$

The twist of each cell (1) and (2) must be equal.

$$\theta_1 = \theta_2 \quad \text{- - - - - - - - - - - - - - - - - -(E)}$$

where

$$\theta_1 = \frac{\Sigma\, q \frac{L}{t}}{2 A_1 G} \text{ (per unit length of cell 1)}$$

$$\theta_2 = \frac{\Sigma\, q \frac{L}{t}}{2 A_2 G} \text{ (per unit length of cell 2)}$$

The student should review Chapter A5, and Art. A15.8 of Chapter A15 for explanation and use of the above equations for twist.

C9.15 Example Problem -- 2 Cell Multiple Flange Tapered Beam.

To avoid repetition of similar type calculations as was used in example problem one, the bending and shear stresses will be determined at station 20 of the same structure as in example problem one, except the leading edge cell (cell No. 1) will be considered acting. Since there are no spanwise stringers in the leading edge, very little skin on the compressive side will be effective. On the tension side, the leading edge skin would be effective in resisting bending axial loads and thus the moment of inertia would be slightly different from that found in example problem 1. Since this problem is only for the purpose of illustrating the use of the equations, the leading edge skin will be neglected in computing the bending flexural stresses. With this assumption, the bending stresses and flange loads at stations 20 and 47.5 are the same as for problem 1. (See values in Column 12 and 13 of Tables C9.2 and C9.3).

Calculation of Static Shear Flow System Due to Change in Flange Loads Between Stations 20 and 47.5

Before a flexural shear flow system consistent with the flange loads can be made, a value of the shear flow at one point in each cell is necessary. For convenience, zero shear flow will be assumed as indicated in Fig. C9.21. It might be imagined that the cell webs are cut at these two points.

Shear flow assumed zero at points (a) and (b).

Fig. C9-21

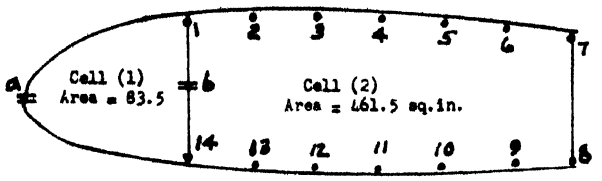


Table C9.6 (Column 5) gives the value of the static shear flow under these assumptions. The first 7 columns of this table are the same as in Table C9.4, since no stringers have been added to cell (1), and the shear q is assumed zero in cell (1).

To make the twist of each cell the same and also to make the summation of all torsional forces zero will require two unknown constant shear flows, q_1 in cell (1) and q_2 in cell (2). Thus two equations will be written, namely:

$$\theta_1 = \theta_2 \quad \text{----------(1)}$$

$$\Sigma T_{c.g.} = 0 \quad \text{----------(2)}$$

The twist θ per unit length of cell = $\Sigma \frac{qL/2AG}{t}$. The modulus of rigidity G will be assumed constant and thus will be omitted.

Consider cell (1): (Refer to Table C9.6, Columns 10 and 11)

Area of cell (1) = 83.5 sq. in.

$$\theta_1 = \frac{1}{2A_1}\left[\Sigma\, q\, L/t + \Sigma\, q_1\, L/t + \Sigma\, q_2\, L/t\right]$$

$$\theta_1 = \frac{1}{2 \times 83.5}\left[0 + 1278\, q_1 - 230\, q_2\right]$$

hence

$$\theta_1 = 7.65\, q_1 - 1.378\, q_2 \quad \text{----------(a)}$$

For cell (2):

Area of cell (2) = 461.5 sq. in.

$$\theta_2 = \frac{1}{2 \times 461.5}\left[733050 - 230\, q_1 + 2469\, q_2\right]$$

hence

$$\theta_2 = 794 - .2495\, q_1 + 2.678\, q_2 \quad \text{------(b)}$$

For continuity θ_1 must equal θ_2, hence equating (a) and (b):

$$7.899\, q_1 - 4.056\, q_2 - 794 = 0 \quad \text{-------(c)}$$

For equilibrium the summation of all moments in the plane of the cross-section about the section (c.g.) must be equal to zero, or

$$\Sigma T_{c.g.} = 0$$

The moment of the external loads about the section c.g. is the same as in Problem 1.

$$T_{\text{external forces}} = 41800\text{"\#}$$

The induced moment due to the in plane components of the flange axial loads is likewise the same as in example problem 1 (see Table C9.5).

$$T_{\text{due to flange loads}} = 4936\text{"\#}$$

The torsional moment due to the static shear flow from Column (7) of Table C9.6 equals 256060"#. The torque due to the unknown constant shear flows of q_1 and q_2 is equal to twice the enclosed area of each cell times the shear flow in that cell.

Hence

$$T_{(\text{due to } q_1 \text{ and } q_2)} = 2 \times 83.5\, q_1 + 2 \times 461.6\, q_2 = 167\, q_1 + 923\, q_2$$

TABLE C9.6

SHEAR FLOW - 2 CELL - MULTIPLE FLANGE TAPERED BEAM
(Average Shear Flow Between Stations 20 and 47.5)

1	2	3	4	5	6	7	8	9	10		11		12	13	14
									L/t		q(L/t)				
Flange No.	P at Sta. 20	P at Sta. 47.5	ΔP / 27.5	$q = i\Delta P$ / 27.5	m	mq	L (in.)	t	Cell (1)	Cell (2)	Cell (1)	Cell (2)	q_1	q_2	$q_r = q+q_1+q_2$
1	24390	-18700	206.8	206.8	48.4	10000	5.75	.04		144		29800	0	-317	-110.2
2	14070	-12990	39.1	245.9	43.8	10780	5.50	.04		137		33700	0	-317	- 71.1
3	11890	-10710	42.9	288.8	42.8	12120	5.50	.04		137		39600	0	-317	- 28.2
4	11370	-10200	42.5	331.3	42.6	14100	5.50	.04		137		45400	0	-317	14.3
5	10510	- 9320	43.3	374.6	43.6	16340	5.50	.04		137		51400	0	-317	57.6
6	11090	-10000	39.6	414.2	42.0	17500	5.50	.04		137		56700	0	-317	97.2
7	16700	-12880	139.0	553.2	197.0	108900	12.25	.032		382		211500	0	-317	236.2
8	-28230	22770	-198.7	354.5	47.4	16800	5.5	.032		172		61000	0	-317	37.5
9	-11180	10140	-37.8	316.7	37.2	11800	5.0	.032		156		49400	0	-317	0
10	-11170	10160	-36.7	280.0	40.8	11420	5.8	.032		181		50650	0	-317	- 37
11	- 6430	5240	-43.2	236.8	42.2	10000	5.8	.032		181		42900	0	-317	- 80.2
12	-10390	9410	-35.6	201.2	38.0	7650	5.3	.032		166		33400	0	-317	-115.8
13	- 9600	8470	-41.1	160.1	54.0	8650	5.5	.032		172		27600	0	-317	-156.9
14	-23020	18600	-160.3	0	204	0	11.75	.051	230	230	0	0	-62.8	-317	-254.2
1 Lead edge web				0	371		33.5	.032	1048		0		-62.8		-62.8
Sum						256060			1278	2469	0	733050			

NOTES: L = length of web sheet between flange members. Col. 4 = (Col. 2 + Col. 3)/27.5
t = web thickness.

$$\therefore \Sigma T_{c.g.} = 167\ q_1 + 923\ q_2 + 4936 + 41800 + 256060 = 0$$

or

$$167\ q_1 + 923\ q_2 + 302796 = 0 \quad -------(d)$$

Solving equations (c) and (d) for q_1 and q_2 we obtain

$q_1 = -62.8\#/in.$, $q_2 = -317\#/in.$

These values are listed in columns (12) and (13) of Table C9.6.

The final or resultant shear flow q_r at any point equals the sum of $q + q_1 + q_2$. The results are given in Column 14 of Table C9.6. Fig. C9.21 shows the resultant shear flow in graphical form.

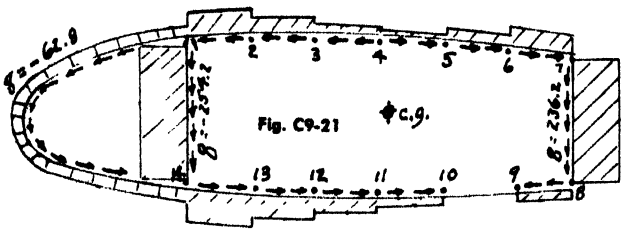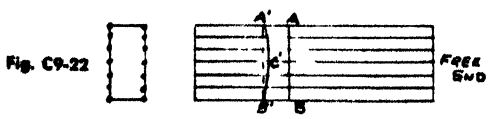


Fig. C9.21 Graphical representation of final shear flow system. See Column 14 of Table C9.6 for numerical values.

C9.16 General Discussion of Shear Lag.

The flange elements of a multiple flange beam receive or give up their axial loads due to bending though the shear in the web or sheet elements to which they are attached. This shear flow stress in the sheet elements produces a spanwise shearing deformation in the cell sheet elements. Thus instead of beam sections remaining plane sections after bending, the sheet shear deformations cause the stringers most remote from the vertical shear webs to lag back farther than those nearer the vertical shear webs. Fig. C9.22 represents a multiple flange beam. It will be supposed that a load producing compression on the top surface is acting. If plane sections remain plane a line on the top



surface (AB) would move to (A'B') when the load is applied and produces compression and therefore equal shortening of the beam flange elements. However the line may take the position (A'C'B'). Since the flange stringers nearer the center portion of the beam lag back farther, their axial deformation will be less and therefore their axial stress due to bending of the box as a whole will be less than calculated by the ordinary flexure theory which assumes that plane sections remain plane after bending. Since the total internal resisting moment must equal the external bending moment, the corner flange stringers must take more load than calculated by the flexure theory. This same reasoning applies to the tension side of the beam.

The shear lag action as illustrated in Fig. C9.22 would be representative for a box beam of constant depth and width and of uniform cross-section. However, if the beam tapers in depth and width and with most of the section area change being confined to the corner members of the stringers adjacent to the corner members, it can be shown that the shear lag influence is of minor character, since the shear flow intensity in the sheet in the center portion of the beam may change very little. No doubt in many wing structural designs corrections are made for shear lage effect which actually did not exist since a consideration of taper and spanwise distribution of flange area was not considered.*

Practical Structural Arrangement and Design to Decrease and Take Care of Shear Lag Action.

Since shear lag effect tends to decrease the bending axial loads in the flange stringers remote from the vertical shear webs and increase those for the flange members connected to the vertical web members as compared to the stresses obtained by the general beam theory, a practical thing to do for the compression side is to design the corner flange members to have a reasonably higher ultimate compressive strength than the intermediate stringers. This result is obtainable without difficulty because the corner member is restrained in two directions by the web and sheet cover, and thus suffers very little column action, whereas the skin stringers are subjected to a certain degree of solumn action over a length equal to the wing rib spacing.

Another method is to place the increase in flange area which is required as one proceeds inboard from the tip portion in the corner members, which tends to make the shear flow in the cover sheet between the corner flange members approach zero.

Since the shear flow stresses per running inch increase from a maximum at the vertical shear webs to zero in the cover sheet at some point between the corner members of the box, heavier sheet to give lower shear stresses and closer spacing of stringers nearer the corner members to prevent sheet from buckling is another practical means of decreasing shear deformation and therefor shear lag.

*See excellent paper "Unit Method of Beam Analysis" by Shanley and Cozzone. Journal of Aeronautical Sciences, April 1941.

Semi-Empirical Methods of Making Allowance For Shear Lag Influence.

Many engineers in making an analysis of a multiple distributed flange beam assume an efficiency curve for the effectiveness of the stringers in bending. Thus, if the efficiency is 1.0 for a particular unit, it is considered fully effective in bending. If it is taken as 0.8, the effective area of the particular stringer is taken as .8 of its true area and this reduced area is used in computing the beam section properties. Using the decreased section properties in the beam flexure formula produces higher stresses and therefore higher total axial load in those stringers which were not decreased by the efficiency factors. Fig. C9.23 represents a typical efficiency curve.*

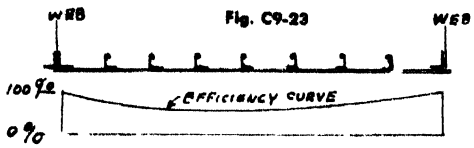


Fig. C9-23

The unknown factor is such a process is the question of what efficiency curve to chose since it might vary from an efficiency of 1.0 (zero shear lag) to a relative low efficiency for a case where thin sheet covering is used with very small corner members, wide stringer spacing and with stringers of larger sectional area concentrated near the midpoint of the cover sheet.

The above general discussion has referred to a single cell box beam. If multiple interior webs are used, shear lag influence in general becomes unimportant, since the shear flow has less distance to travel.

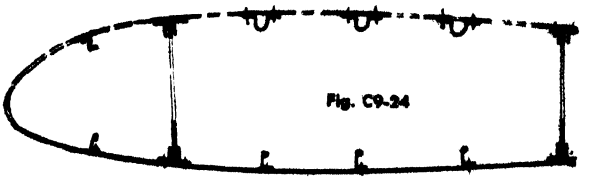
C9.17 Influence of End Restraints on Flange Longitudinal Stresses.

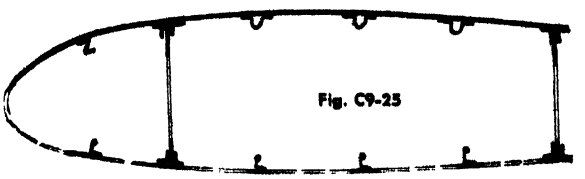
The general theory of flexure and shear flow is based on the assumption that wing sections are free to warp. At points of wing support, this assumption is definitely violated and a certain amount of the torsional moment will be resisted by the front and rear webs with their corner flange members acting as cantilever beams in bending. Thus, additional flange strength should be provided near the wing supports and extending out a distance equal to several times the wing thickness.

General Design Suggestions for Multiple Flange Beams.

C9.18 Effective Cross-section of a Cellular Wing Beam.

Fig. C9.24 shows the cross section of a distributed flange two-cell beam. For loads on the wing which tend to bend the wing upward and therefore place the upper portion in compression the effective web and skin material is represented by the black portions. For the reverse condition, that is, compression on lower side of the wing, the effective web and skin material takes the form as illustrated in Fig. C9.25.


Fig. C9-24


Fig. C9-25

The darkened sheet elements on the compressive side are referred to as the web or skin effective widths and represents the amount of sheet that can be considered to carry the same compressive stress as the adjacent stringer.

In Chapter B4, the various proposed equations for calculating the effective sheet widths were summarized and discussed. The following four equations are taken from Chapter B4.

$$w = 1.70\, t \sqrt{\frac{E}{f_{st}}} \qquad \text{----------(1)}$$

$$w = 1.90\, t \sqrt{\frac{E}{f_{st}}} \qquad \text{----------(2)}$$

$$w = 2.52\, t \sqrt{\frac{E}{f_{st}}} \qquad \text{----------(3)}$$

$$\frac{w}{b} = \sqrt[3]{\frac{f_{cr}}{f_{st}}} \qquad \text{----------(4)}$$

where

w = effective sheet width in inches

t = sheet thickness

E = modulus of elasticity

f_{st} = stringer stress

b = sheet width between stringers

Equations (1), (2) and (3) are all similar in character, the different numerical coefficient being due to the different degree of edge restraint. Equation (4) takes the compressive buckling stress f_{cr} of the sheet and the sheet width into account. Equation (1) is recommended by ANC-5, but equation (2) is widely used. Regardless of which equation is used, the sheet effective width depends on the stringer stress, and since the stringer stress depends on the beam section properties, the procedure of calculating the effective cross-sectional properties

* "A Practical Method of Allowance for Shear Lag" by Continho. Journal of Aeronautical Sciences, Oct. 1942.

of a multiple flange is a trial and error one.

C9.19 General Procedure for Obtaining Preliminary Cross-section of a Distributed Flange Beam.

There is no general procedure that will fit all conditions or portions of the wing. The general discussion which follows is for the student or beginner who is making his first attempt to design a wing cellular beam for a given set of design loads. Since the design is a trial and error method, the student in his first attempt at design is usually confused as how to begin to obtain a logical preliminary wing cross-section which should not need major revisions to be satisfactory.

1. General Structural Layout of Wing.

Before the question of size and thickness of the component parts can be considered, the general structural layout of the wing must be determined. A consideration of the eight factors which were discussed in Art. C9.3 will usually dictate what type of wing construction to use, for example, the size of the beam cell or cells the direction of the main flange or corner members and the general direction of the intermediate stringers if the distributed flange type of beam is used, the rib spacing, etc.

2. Basic Wing Structural Section (Cantilever Wing)

For the conventional cantilever wing, the maximum bending moment occurs at the fuselage or hull support point. The wing section at this point is usually referred to as the basic structural cross-section of the wing, since the member areas at all other sections are derived by decreasing or eliminating some of the material or members of the basic section. In a large proportion of the airplanes, the wing consists of a center section panel and two outer panels. In many cases, such items as powerplants, fuel tanks, baggage or bomb compartments may dictate a different structural arrangement than that required for the outer wing panel which may have different controlling design factors. In such cases, the wing can be considered as having two basic structural cross-sections, one at the fuselage support point and one at the beginning of the outer wing panel. The flange and web material are first calculated for these basic sections. The spanwise distribution of structural material is obtained by tapering or eliminating material from the basic sections.

(3) Determine Type of Flange Members and The Allowable Stresses.

The upper flange material of the wing is designed by compressive stresses, thus stringer sections should be selected which will give high allowable compressive stresses. (See Fig. C9.4 for best sections). Calculate the ultimate strength of a flat stiffener-sheet panel using several thicknesses of skin thicknesses and for a column length equal to the wing rib spacing and an end fixity of 1.5 to 2.0 (see methods as explained in Chapter B6). All calculated values should be substantiated by static tests.

Later when the definite size and shape of the corner flange members are considered, it is good practice to make the ultimate strength of these members greater than the intermediate skin stringers. (See Art. C9.16 on shear lag)

(4) Preliminary Flange Area.

With the allowable flange stresses known, the total effective flange area can be estimated. Using the largest positive bending moment about the X axis, the approximate required flange area can be calculated by equating an average internal resisting couple to the external bending moment. Thus, in Fig. C9.26, let (d) be the average resisting arm for the upper and lower flange material. Therefore, for the upper flange,

$$A_u = \frac{\text{Design } M_x}{d\ F_{st}}$$

where

F_{st} = allowable stringer compressive stress

A_u = total required upper effective flange area.

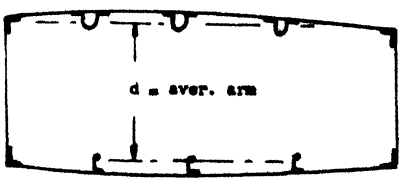


Fig. C9.26

Preliminary Lower Surface Area.

The preliminary total lower surface flange area should first be determined for the design M_x used above. Since the lower surface is in tension, the net area should be used in calculating the stresses since flange members are usually connected to skin by rivets and the skin is spliced at various intervals. In computing the moment of inertia of the beam section as a whole, the gross section is used, thus the allowable bending tensile stresses should not be taken as equal to ultimate tensile strength of the sheet and stringer material but should be reduced to take care of the net section due to rivet holes. Thus, the ultimate tensile strength should be reduced 15 to 20 percent to obtain an allowable design tension stress. For designs where shear lag may be appreciable, a further decrease should be made. Therefore, the preliminary total area for the lower surface equals

$$A_L = \frac{\text{Design } M_x}{d\ F_{tu}}$$

where

F_{tu} = 80 to 85 percent of the ultimate tensile strength of the material, if a riveted

construction is used. In general if the lower surface stringers have a fairly high allowable compressive stress, they will prove strong enough for conditions which produce negative bending moments on the wing since the flight negative load factors are approximately half the positive load factors.

(5) Preliminary Web and Skin Thicknesses.

Even though we have the approximate total upper and lower flange area as found in (4), the beam section can not be logically proportioned until approximate web and sheet thicknesses are known. The shear flow is maximum on the vertical webs of the cell, and for preliminary estimates the vertical webs can be assumed to take all the net external shear loads in the Z direction. In many cases, the wing cell is tapered in depth thus the flange members have a shear component which resists an appreciable amount of the external shear load. Therefore, the net web shear equals

$$V_{\text{net (web)}} = V_{\text{external}} - \text{total flange load} \times \text{average } \frac{dz}{dy}$$

The total approximate flange load for each surface equals M_x/d, and the approximate average slope of the flange members in the (Z) direction can be determined from the structural diagram of the wing. The net web shear load should be found for the critical load conditions. In general, it is good practice to have shear center of beam section between the 25 to 30 percent of chord point if possible. Thus, the net shear load can be referred to this arbitrarily selected shear center, resulting in a shear load plus a couple. The shear load is divided between the vertical shear webs inversely as their distance from the shear center and the couple is resisted by a constant shear flow on the cell equal to the couple divided by twice the area of the cell. With the approximate design shear flows on the vertical webs known, their thicknesses can be readily obtained. (See Chapter C7). In general, the thickness of the top and bottom cover can be assumed as one guage thickness less than the thickness vertical web.

(6) Effective Sheet Widths.

With the preliminary sheet and web thickness known, the effective sheet width acting with each stringer on the compressive side can be computed using one of the various effective width equations listed in Art. C9.17 and the allowable stress as calculated in (3). Information is now on hand to determine the number of stringers and the area of the corner flange members to give the total required area as found in (4). An approximate wing section has now been determined for use as a trial section for more accurate methods of stress analysis.

(7) Compute Bending and Shear Stresses.

With the trial section known, the section properties are computed (see Table C9.2 for example calculations). The bending and shear stresses are computed and checked against the allowable stresses. Revisions can now be made in the areas, sheet thicknesses, effective widths, etc. to give the desired results, that is, a section which will carry the loads most efficiently.

Until over-all experience is obtained in the design of wings, the student should realize that several revisions requiring a considerable amount of calculation will be required before a proper beam section is obtained.

Table A

Flange No.	Area Sta. 0	Area Sta. 120
A	.80	.15
B	.70	.15
C	.25	.10
D	.20	.10

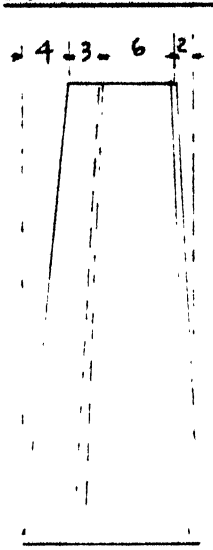
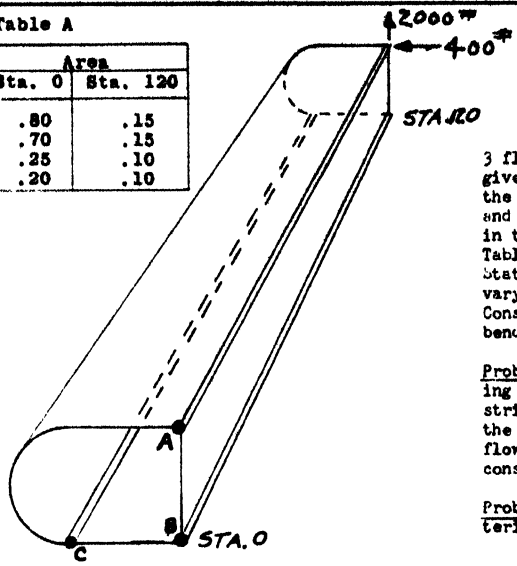
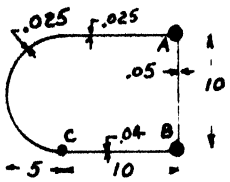
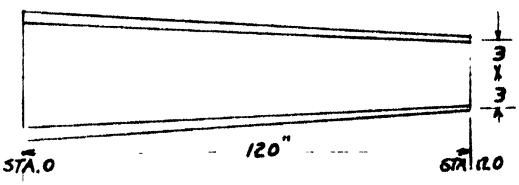
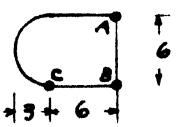


Fig. C9-27









PROBLEMS

Problem 1. Fig. C9.27 illustrates a 3 flange single cell tapered beam. For the given loads acting at station 120 determine the axial loads in the three stringers A,B and C at Sta. O. Determine the shear flow in the cell walls at Sta.O by two methods. Table A gives the area of each stringer at Stations O and 120. Assume the stringer areas vary uniformly between these end stations. Consider the cell walls as ineffective in bending.

Problem 2. Consider the same cell and loading as in Problem 1 but add an additional stringer D as shown in Fig. C9.28. Determine the axial load in the stringers and the shear flow in the walls at Station O. For simplicity consider the cell walls ineffective in bending.

Problem 3. Same as problem but add the interior web CD. See Fig. C9.29.

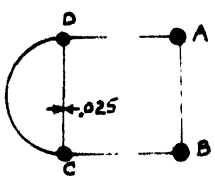
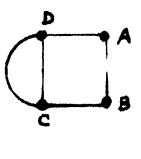


Fig. C9-29



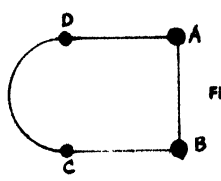


Fig. C9-28

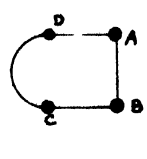


Table B

Flange No.	Area Sta.150	Area Sta.0
1	1.0	.20
2	.25	.10
3	.25	.10
4	.25	.10
5	.80	.10
6	.70	.10
7	.25	.10
8	.25	.10
9	.25	.10
10	.85	.20

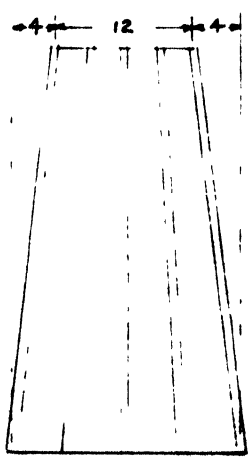
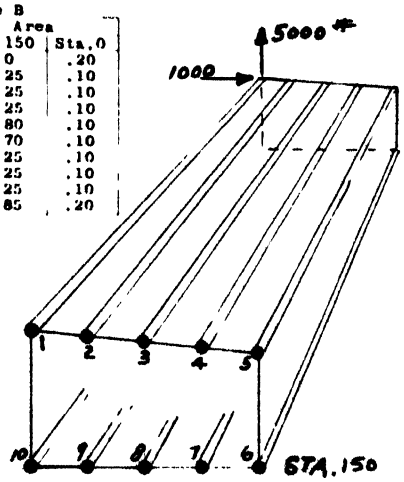


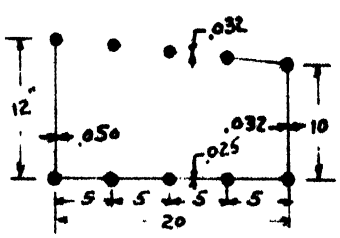
Fig. C9-30

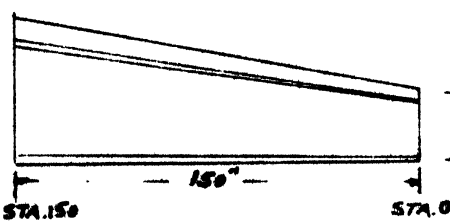


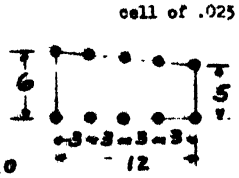
Problem 4 Fig. C9.30 shows a multiple flange single cell tapered beam. Determine the axial loads in the stringers at station 150 for the given external loading at station O. Also determine the internal shear flow system at station 150 using the average shear method between sta-150 and 125. Table B gives the flange stringer areas. Assume uniform change in stringer between stations O and 150. Assume webs not effective in bending.

Problem 5 Same as Problem 4 but add an interior web of .032 thickness connecting stringers (3) and (8).

Problem 6 Same as Problem 4 but add a circular leading edge cell of .025 wall thickness.







CHAPTER C10
ANALYSIS AND DESIGN OF METAL COVERED FUSELAGE AND HULL STRUCTURES

C10.1 Introduction.

In general, the methods for stress analyzing a fuselage or a hull are similar to those for the analysis of metal covered wings. The fuselage being composed of one cell and in most cases being symmetrical about the vertical axes is a simpler problem than a wing structure of two or more cells. The methods of analyses to be illustrated in this chapter are based on the general theory of flexure and shear flow which is presented in Chapters A5, A13, A14, and A15. Most of the general discussion of wings in Chapter C9 applies equally as well to the metal covered fuselage.

C10.2 General Types of Metal Covered Body Construction.

The stressed skin airplane body from a structural design standpoint is generally divided into two general types, namely

1. Monocoque
2. Semi-monocoque

Monocoque Types:

The "pure" monocoque type consists of a shell only. That is, there are no transverse or longitudinal stiffeners attached to the cell walls. A pure monocoque is seldom used with the present chief structural materials, namely, aluminum alloy and stainless steel, as the structure would be very inefficient from a strength-weight standpoint since the buckling strength of thin flat and curved sheets is relatively low. However, this condition is changing with the introduction of magnesium and the various forms of the so-called plastic-plywoods since sheets of these materials are much thicker than aluminum and steel alloy sheets of the same weight and buckling strength increases with thickness. With the development of these light weight materials a pure monocoque type of fuselage should become practical and efficient in the design of certain portions of the fuselage structure of small airplanes.

Modified Monocoque:

If a pure shell is reinforced by attaching transverse frames at fairly close spacing, it is sometimes referred to as a modified monocoque since no longitudinal stringers are used. The transverse frames raise the buckling strength of the shell over that of apure monocoque. For certain portions of light airplanes with no cutouts, this type of structure may prove suitable.

C10.3 Semi-Monocoque Construction.

The semi-monocoque type of construction can logically be divided into two general types, namely,

1. Concentrated flange type.
2. Distributed flange type.

Concentrated Flange Type:

This type of construction consists of either 3 or 4 longitudinal stringers attached to the shell and transverse frames at spacing considerably less than in the distributed flange type. Fig. C10.1 illustrates typical stiffener arrangements for this type of fuselage design.

Distributed Flange Type:

This type of construction consists of a relatively large number of longitudinal stiffeners which are distributed over the entire cell wall. Transverse frames are used but a considerably larger spacing than in the concentrated flange type of construction. Photograph series C10.1 illustrates this type of fuselage construction.

General Stress Analysis Theory for the Various Types of Monocoque Structures.

C10.4 Analysis of the Modified Monocoque Structure.

As explained before this structure consists of a cylindrical shell with transverse frames but no longitudinal skin stiffeners. The buckling strength of this type of structure for aluminum and steel alloy shell material can be taken as equal to the ultimate strength.

Chapter B3 summarizes most of the available theories and test data for calculating the buckling and ultimate stresses in compression, bending and torsion for unstiffened cylindrical thin-walled structures.

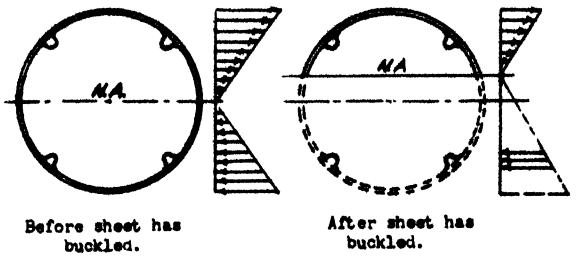
C10.5 Analysis of the Concentrated Flange Semi-Monocoque Type of Body Structure.

The depth of the cellular beam formed by the fuselage is relatively large as compared to the wing because of the requirements of space for housing the equipment and payload. Furthermore, for aerodynamic efficiency, the sectional shape is partially or entirely made from curved elements. In general, the aft portion of a fuselage or hull is subjected to relatively light loads, thus the buckling strength of the curved panels which make up the fuselage cell may be sufficient to carry a large proportion of the design load.

The buckling distortion of large curved panels falls in the category of large deflections and the tendency is for the buckles to become partially permanent, thus in general, the fuselage cell should be designed not to buckle under the applied loads, due to the possibility of the buckles becoming permanent.

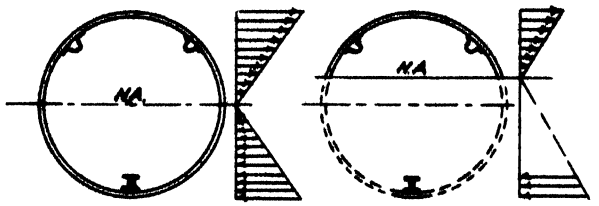
Up to the buckling strength of the curved panels which make up the cell, the bending stress distribution can be considered as following that given by the general beam theory, namely $f_b = Mz/I$, where I is the moment of inertia of the entire section. The curved panels on this type of construction will usually buckle suddenly which indicates that a change of stress distribution takes place as the structure seeks another condition of stable equilibrium. This second state of internal equilibrium permits the structure to carry a further increase in external load even though the curved sheet panels are in the buckled state. In this new state, the bending stresses are resisted by the longitudinal stiffeners plus any sheet panels which lie entirely in the bending tension zone. The buckled panels, however, can still carry shear stresses in the form of a semi-tension field beam, and this action produces secondary axial compression and bending stresses on the longitudinal stiffeners. (See Chapter C7). Fig. C10.1 illustrates the general action which experiments indicate takes place relative to internal stress distribution when cells with large curved panels and few stiffeners are loaded in bending.

Fig. C10-1
Effective Material Before and After Buckling.



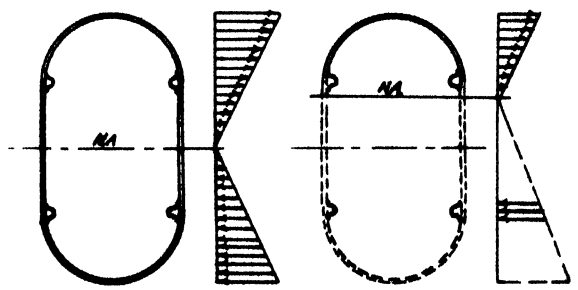
Before sheet has buckled. After sheet has buckled.

Four flange fuselage type



Before sheet has buckled. After sheet has buckled.

Three flange fuselage type.



Before sheet has buckled. After sheet has buckled.

Four flange type.

Summary of Appropriate Stress Equations

For fuselage sections symmetrical about the vertical or Z axis, the bending and shear stresses can be found by the following equations:

Axial Compression or Tension:

$$f_n = \frac{P}{A} \quad \text{----------(1)}$$

P = external normal load at section, referred to section center of gravity

A = effective area

Bending Stresses:

$$f_b = -\frac{M_y z}{I_y} - \frac{M_z y}{I_z} \quad \text{----------(2)}$$

I_y and I_z are the effective moments of inertia.

Flexural Shear Flow

For bending about Y centroidal axes:

$$q = q_o + \frac{V_z}{I_y} \Sigma a z \quad \text{----------(3)}$$

For bending about Z axis:

$$q = q_o + \frac{V_y}{I_z} \Sigma a y \quad \text{----------(4)}$$

The external shear V_z and V_y refer to the net shear, or the total shear minus the shear carried by the inclination of the flange axial stresses. Equations (3) and (4) are for beams of fairly uniform section. If section stringers and plating varies considerably longitudinally the average shear flow between adjacent stations, derived from a consideration of the ΔP flange loads, should be used, or

$$q = q_o \Sigma \frac{\Delta P}{d} \quad \text{----------(6)}$$

Torsional Shear Flow

$$q_t = \frac{T}{2A} \quad \text{-----(A = area of cell) --(7)}$$

If the fuselage material is so distributed as to make the section unsymmetrical, then the equations for unsymmetrical bending should be used. (See Chapter A15 and C9).

C10.6 Estimation of the Buckling Strength of Curved Sheet Panels.

The equations which follow are taken from Chapter B3, Arts. B11 to B.14 inclusive:

The compressive buckling stress of large curved panels can be estimated by equation 18 of Art. B3.12, which follows:

$$F_{c(cr)} = .45\ E\ t/r \quad \text{----------(8)}$$

E = modulus of elasticity

t = sheet thickness

r = radius of curvature of sheet

The buckling shear strength of large curved panels can be estimated from equation 21 of Art. B3.13, multiplied by .60 for design purposes.

$$F_{s(cr)} = \frac{E\ t^2}{(1-\mu^2)L^2}\left[2.8 + \sqrt{2.6 + 1.40\left(\sqrt{1-\mu^2}\frac{L^2}{td}\right)^{\frac{3}{2}}}\right].6$$

----------(9)

This equation is plotted in Fig. B3.8 of Chapter B3.

The buckling strength in combined bending and shear can be estimated by the following interaction equation from Art. B3.14:

$$\left(\frac{f_s}{F_s}\right)^2 + \frac{f_c}{F_c} = 1 \text{ (for compression and shear)}$$

hence

$$M.S. = \frac{2}{R_c + \sqrt{(R_c)^2 + 4\ R_s^2}} - 1 \quad \text{------(10)}$$

where

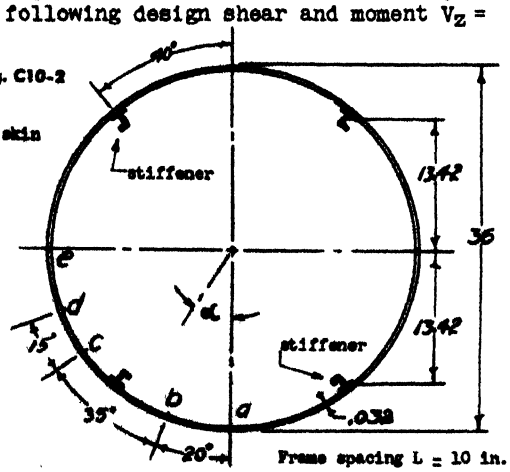
$$R_c = \frac{f_c}{F_c} \text{ and } R_s = \frac{f_s}{F_s}$$

NOTE: f_c equals the sum of the compressive stress due to bending and axial loads.

Example Problem 1.

Fig. C10.2 shows the cross-section of a fuselage section. This section is subjected to the following design shear and moment V_z = -4000# and M_y = 465,000 in. lb. These values include a factor of safety of 1.5 on the applied loads. It is required that the fuselage skin should not buckle permanently under the applied loads. Find the margin of safety under the applied loads and the final stringer compressive stress under the design loads.

Fig. C10.2



Solution

Calculation of Section Properties - All Material Effective

I_y(skin) = $\pi\ r^2\ t = \pi \times 18^2 \times .032 = 586$ in.^{4}

Stringers = $.35 \times 13.42^2 \times 4 = 256$ in.^{4}

Total I_y 842 in.^{4}

Critical Compressive Buckling Stress by Equation (8):

$F_{c(cr)} = .45\ E\ t/r = .45 \times 10{,}300{,}000 \times .032/18 =$ 8230 psi.

Critical shear buckling stress by equation (9):

$$F_{s(cr)} = \frac{10{,}300{,}000 \times .032^2}{(1-.3^2)\ 10^2}\left[2.8 + \sqrt{2.6 + 1.40\left(\sqrt{1-.3^2}\ \frac{10^2}{.032 \times 36}\right)^{3/2}}\right].6$$

= 2470 psi.

Calculation under the applied loads of the compressive and shear stress at points a, b, c, d, and e on the skin surface: (See Fig. C10.2 for location)

Applied bending $M_y = -465000/1.5 = -310{,}000$ in. lb.

Applied shear load $V_z = -4000/1.5 = -2667$#

Point (a):

$\alpha = 0^0$

$f_c = -\frac{M_y\ z}{I_y} = -310000 \times -(18)/842 = 6620$ psi.

$f_s = 0$

M.S. = (8230/6620) - 1 = .24

Point (b):

$\alpha = 20^0$

$z = 18 \cos 20^0 = 16.9$"

$f_c = 310{,}000 \times -(16.9)/842 = -6220$ psi.

$$f_s = \frac{V_z\ Q}{I_y\ t}$$

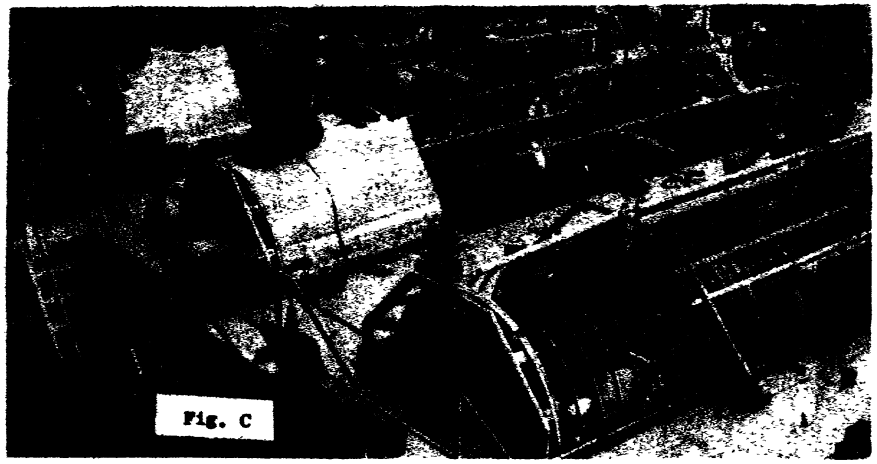
where

Q for circular arc = $r^2\ t \sin \alpha$

hence

$Q = 18^2 \times .032 \times .342 = 3.55$

$$f_s = \frac{2667 \times 3.55}{842 \times .032} = 350 \text{ psi.}$$


Fig. C

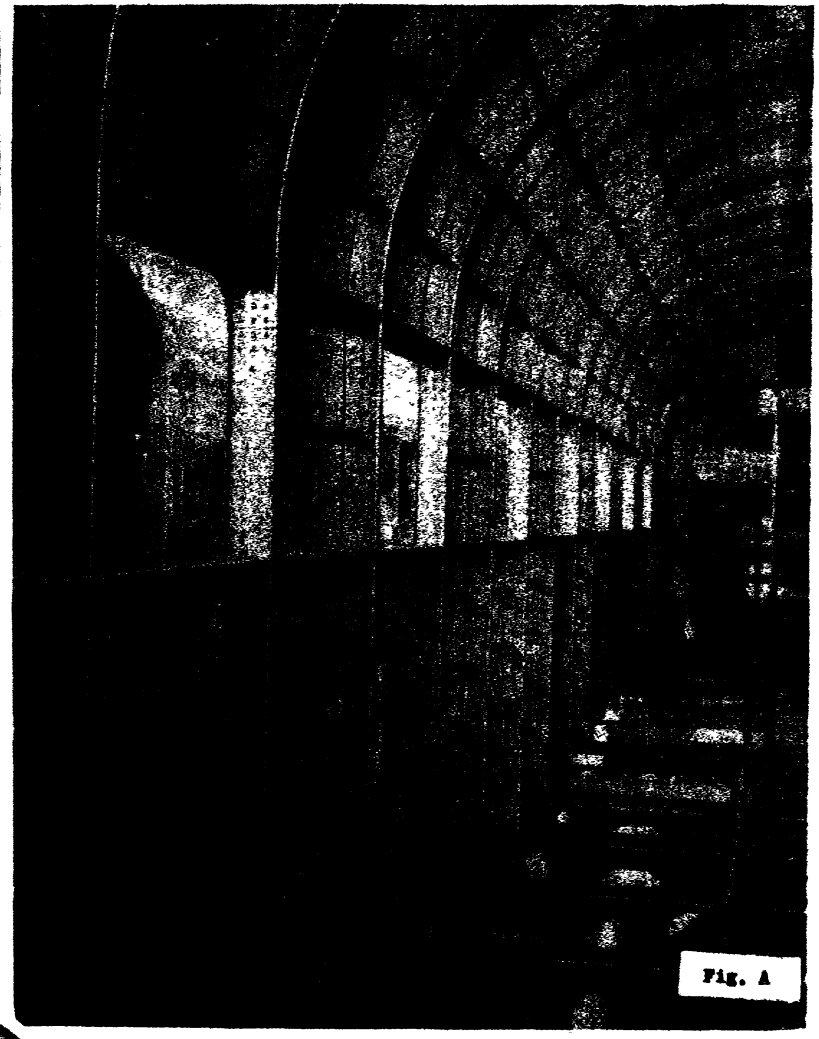

Fig. A

Fig. A shows the interior fuselage construction of the Douglas DC-2 Transport

Fig. B shows an exterior view of a fuselage portion of a large Douglas airplane. (Photographs A an B by courtesy of the Douglas Airplane Co.)

Fig. C shows a view of a portion of Boeing B-17 fuselage in the assembly jig. Note transverse and longitudional structural system. Photograph by courtesy of the Boeing Airplane Co.

Fig. D shows a view of the forward portion of the Martin B-26 fuselage. Photograph by courtesy of the Glen L Martin Co.


Fig. D


Fig. B

Stress ratios:

$R_C = f_C/F_C = 6220/8230 = .757$

$R_S = f_S/F_S = 350/2470 = .142$

$$M.S. = \frac{2}{R_C + \sqrt{R_C^2 + 4 \times R_S^2}} - 1$$

$$= \frac{2}{.757 + \sqrt{.757^2 + 4 \times .142^2}} - 1 = .28$$

Point (c):

$\alpha = 55^0$

$z = 18 \cos 55^0 = 10.3"$

$f_C = 310000 \times -10.3/842 = -3800$ psi

Q for cell skin $= r^2 t \sin \alpha = 18^2 \times .032 \times .82$

$= 8.5$

Q for flange stringer $= .35 \times 13.42 = 4.70$

Total $Q = 8.5 + 4.70 = 13.2$

$$f_S = \frac{2667 \times 13.2}{842 \times .032} = 1310 \text{ psi}$$

$R_C = 3800/8230 = .462$

$R_S = 1310/2470 = .531$

$$M.S. = \frac{2}{.462 + \sqrt{.462^2 + 4 \times .531^2}} - 1 = .23$$

Point (d):

$\alpha = 70^0$

$z = 18 \cos 70 = 6.15$

$f_C = 310000 \times -6.15/842 = -2262$

Q for cell skin $= 18^2 \times .032 \times \sin 70^0 = 9.75$

Q for stringer $= .35 \times 13.42 = 4.70$

Total $Q = 14.45$

$$f_S = \frac{2667 \times 14.45}{842 \times .032} = 1430$$

$R_C = 2262/8230 = .275$

$R_S = 1430/2470 = .58$

$$M.S. = \frac{2}{.275 + \sqrt{.275^2 + 4 \times .58^2}} - 1 = .37$$

Point (e):

$\alpha = 90^0$

$z = 0$

$f_C = 0$

$Q = 4.70 + 18^2 \times .032 \times 1 = 15.08$

$$f_S = \frac{2667 \times 15.08}{842 \times .032} = 1495$$

$M.S. = (2470/1495) - 1 = .65$

The critical margin of safety is .23 and it occurs at point (c).

Therefore, the applied bending moment and shear could be increased 23 percent before positive permanent buckling of the skin would take place which would cause a re-organization of the stress distribution.

Remaining moment to be taken after cell buckles $= -465000 + 1.23 \times 310,000 = -83000$ in. lb.

Same for shear $= -4000 + 1.23 \times 2667 = -720\#$

Calculation of New Section Properties after Sheet Has Buckled.

Fig. C10.3 shows the effective section after the sheet has buckled.

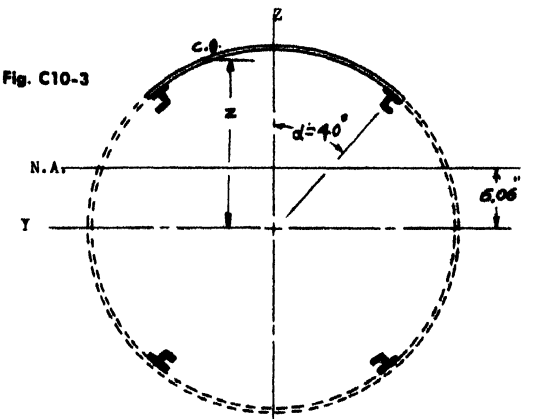
Calculation of Section Properties.

Take horizontal diameter as reference axis.

Area of effective skin $= 2 r t \alpha = (18 \times .032 \times .698)\ 2 = .806$ sq. in.

Area of four stringers $= 1.40$ sq.in.

Fig. C10-3



Effective section after buckling.

Distance from reference axis to c.g. of effective skin:

$z = r \sin \alpha/\alpha = 18 \times .643/.698 = 16.6"$

The statical moment of effective skin area about reference axis equals $za = 16.6 \times .806 = 13.4$.

Due to symmetry the statical moment of flange stringer areas about reference axis is zero. Hence, distance from reference axis to neutral axis is

$\bar{Z} = \Sigma\ za/\Sigma\ a = 13.4/(.806 + 1.40) = 6.06"$

Moment of inertia about reference axis:

Due to flange stringers $= 4 \times .35 \times \overline{13.42}^2 = 256$ in.^{4}

Due to effective skin:

$$I_y = (r^3 t\ (\alpha + \frac{\sin 2\alpha}{2})$$

$$= 18^3 \times .032\ (.698 + \frac{.985}{2}) = 222 \text{ in.}^4$$

Hence total $I_y = 222 + 256 = 478$ in.^{4}

Transferring to neutral axis:

$I_y = 478 - 2.206 \times (6.06)^2 = 393$ in.

Bending stress increase on lower flange stringers after shell buckling:

$$f_c = -\frac{M_y Z}{I_y} = \frac{-83000 \times -19.48}{393} = -4110 \text{ psi.}$$

Bending compressive stress on lower stringer before shell buckling:

$$f_c = -\frac{M_y Z}{I_y} = -\frac{1.23 \times -310000 \times -13.42}{842} =$$

-6100 psi.

Total compressive stress = $-6100 - 4100 = -10{,}210$ psi. When the skin buckles, it breaks down into a semi-tension field web. This web action produces additional end compressive loads on the flange stringers and also bending moments. (See Chapter C7). When the curved skin changes into a semi-tension field beam, it tends to straighten out between flange members, thus producing a component of load normal to the skin surface which the stringer must take as a beam with a span equal to the fuselage frame spacing. Thus, the stress of $-10{,}210$ as found above would be increased considerably when all secondary influences were considered.

The general method as illustrated above should only be used for preliminary design and for the designing of test units to obtain design information.

Analysis of the Distributed Flange Type of Semi-Monocoque.

C10.7 Introduction.

Fig. C10.4 illustrates a distributed flange type of fuselage section. Assume that external loads are applied which produce bending of the beam about the Y axis with compression on the upper portion of the cell.

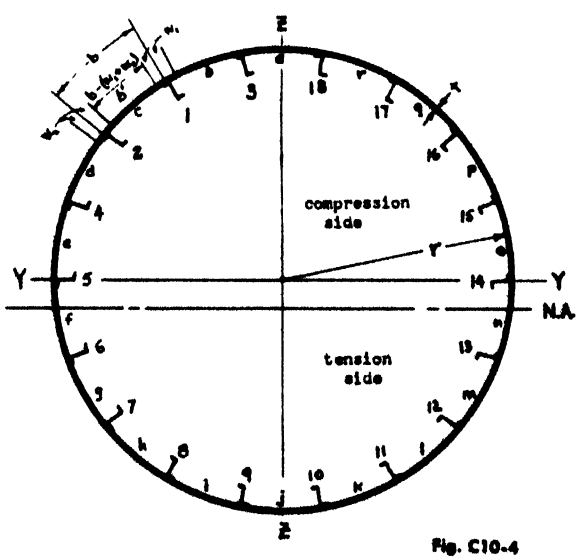


Fig. C10.4

Up to the point of buckling of the curved sheet between the skin stiffeners, all the material in the beam section can be considered fully effective and the bending stresses can be computed by the general flexure formula $f_b = Mz/Iy$, where I_y is the centroidal moment of inertia of the entire section. When a bending compression stress is reached which causes the curved sheet between stiffeners to buckle, a re-arrangement takes place in the stress distribution on the beam as a whole. Theory as well as experimental results indicate that the ultimate compressive strength of a curved sheet with edge stiffeners can be closely approximated by the following two assumptions. (See Art. B4.4 of Chapter B4):

(1) A small width of sheet w_1 on each side of the attachment line of skin to stiffener can be considered as carrying the same compressive stress as the stiffener. These effective sheet widths w_1 are shown as the blackened elements adjacent to the stiffeners on Fig. C10.4. These effective widths can be estimated by the various equations of Chapter B4. As for example,

$w = 2 w_1 = 1.7 t \sqrt{E/f_{st}}$.

(2) The remainder of the curved sheet between stiffeners, namely, $b - (w_1 + w_2)$ carries a maximum compressive stress $F_{c(cr)} = .3 E t/r$.

These sheets elements are shown by the hatched skin lengths in Fig. C10.4.

These assumptions will be used in estimating the effective bending section properties for use in computing the ultimate strength of a stiffened cell.

C10.8 Calculation of the Effective Moment of Inertia of a Stiffened Cell in Bending.

Since the sheet between the skin stiffeners buckles under a compressive stress far below the ultimate strength of the skin stiffeners, the buckled sheet is treated as an element with variable effective thickness which depends on the ratio of the buckling stress F_{cr} of the curved sheet to the bending stress f_b existing at that point for bending of the cell as a whole. Hence the effective sheet thicknesses for the curved element can be written,

$$t_e = t\ (F_{cr}/f_b)$$

or an effective area can be written

$$A_e = b' t\ (F_{cr}/f_b)$$

where b' is width of the sheet between the effective sheet widths acting with each edge stiffener.

The general idea can best be illustrated by carrying through the solution of a typical beam section.

The general idea can best be illustrated by carrying through the solution of a typical beam section.

Example Problem - Bending Stresses in a Stiffened Cell.

Let it be required to design the distributed flange material for the approximate elliptical section of Fig. C10.5. The available data is as follows:

Design bending moment about Y axis = 1600000 in.lb
Z stiffeners 1" deep and with an area of .12 sq. in. shall be used.
Ultimate compression strength for stiffeners = -32000 psi.
Skin thickness = .032.
Section to be symmetrical about center lines of section.
All material is aluminum alloy.

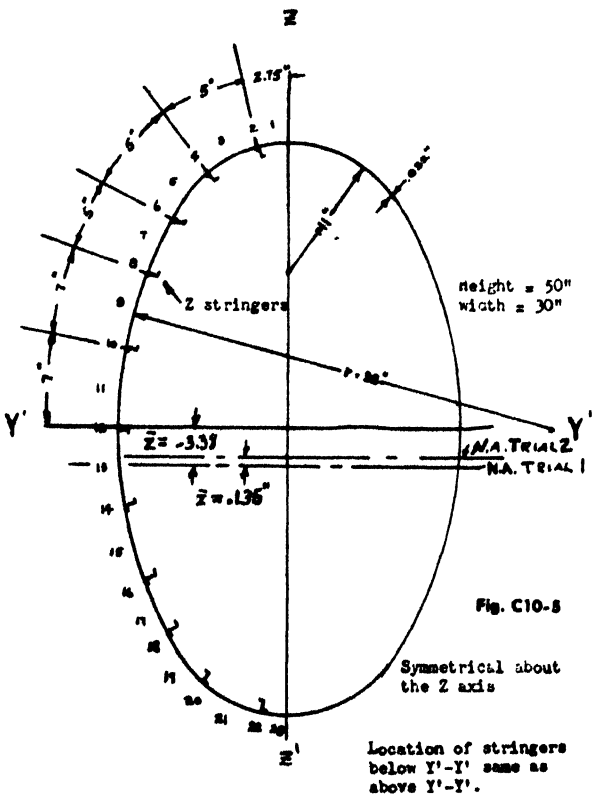


Fig. C10-5

Symmetrical about the Z axis

Location of stringers below Y'-Y' same as above Y'-Y'.

Solution:

The first thing to do is to determine approximately how many Z stringers will be required so that a cell section can be obtained to work with. Since the internal resisting moment must equal the external bending moment, one can guess at the internal resisting couple in terms of total compressive flange stress and an effective internal couple arm.

For elliptical and circular sections with distributed flange material, the approximate effective resisting arm of the internal couple can be taken as .75 times the height (h), and the average flange stress can be taken as 2/3 the maximum bending stress. Since the design allowable was given as -32000 psi, a trial total compressive flange area A_c can be solved for as follows:

$$A_c = \frac{My}{.75\,h \times .67\,F_b} = \frac{1600000}{.75 \times 50 \times .67 \times 32000} = 2.0 \text{ sq.in.}$$

For a 32000 psi compressive stress, the effective width of sheet acting with a stringer using the equation

$$w = 1.7\,t\sqrt{E/f_b} = 1.7 \times .032 \times \sqrt{10{,}300{,}000/32000} =$$

.975 inches.

which equals a width of .975/.032 = 30.5 sheet thicknesses. Since the bending stress decreases as the neutral axis is approached and since the curved sheet between the z stiffeners can carry load up to its buckling strength, a preliminary value of effective sheet equal to 40 t will be assumed acting with each stiffener. Hence, estimated area of stiffener plus effective sheet = .12 + 40 x .032² = .16 sq. in. whence,

Number of z stiffeners required = 2.00/.16 = 12.5

Fig. C10.5 shows how stringers were placed to give 12 stringers on the top half. Since the skin on the lower half is in tension and therefore fully effective, the neutral axis will be below the cell centerline and thus the two stringers on centerline will be considered part of the required 12. A section has now been obtained to work with. Whether it is satisfactory will not be known until the effective result is that the maximum stress on the upper surface should be close to 32000 psi but not over it. The procedure from this point is still a trial and error process since the effective sheet on the compressive side depends on the magnitude of the compressive bending stress which in turn is influenced by the amount of effective sheet and the buckling load carried by the curved sheet.

Using the preliminary stiffener arrangement of Fig. C10.5, Tables C10.1 and C10.2 gives the calculation of the effective moment of inertia of the section about the horizontal neutral axis, Table C10.1 deals with the stiffeners and the effective sheet elements and Table C10.2 deals with the curved buckled sheet elements.

In the trial No. 1, the following assumptions are made:

(1) A width of 30 thicknesses of skin act with each stiffener on the upper or compressive side.

(2) The area of the curved sheet between the effective sheet widths as found in (1) is modified to give an effective area by multiplying by a K factor of F_{cr}/f_b, where F_{cr} is the buckling compressive stress and f_b is the bending stress at

the center of the curved sheet element assuming 32000 at the extreme upper fiber of the beam section and zero at the horizontal centerline, with linear variation in between these points.

NOTE: Since the entire skin on the lower half is effective, a more logical assumption would be to guess at the location of the neutral axis and use a variation of f_b between the neutral axis and the extreme fiber. This approach will not be used in this example.

Due to the symmetry of the section, Tables C10.1 and C10.2 give calculations for only one half of the material, thus the results are multiplied by two. General explanatory notes are given below each table.

The results of trial No. 1 give a neutral axis 3.38" below the centerline and a moment of inertia of 1470 in.^{4}. In Trial No. 2, the effective sheet widths are based on the moment of inertia of 1470. The results of trial No. 2 give a moment of inertia of 1489 in.^{4} with a neutral axis .135" above the first location. If a third trial were used, making use of the 1489 moment of inertia, the change would be quite small since the effect of a small change in stress on the effective sheet width is negligible.

The compressive stress on stringer No. 2 using the resulting moment of inertia and neutral axis location, therefore becomes

$$f_b = \frac{Mz}{I} = \frac{-1600000 \times 27.45}{1489} = 29500 \text{ psi.}$$

against an allowable of -32000, or a margin of safety of 8 percent. Since experiment indicate that the stress distribution in such a structure does not follow the assumptions of the beam theory (see Art. C10.9) a small margin of safety is desirable.

Calculation of Shear Stress at Neutral Axis.

If the beam section as derived in Fig. C10.5 is constant longitudinally, the shear flow can be computed by the general equation

$$q = q_o + \frac{V_z}{I_{yNA}} \Sigma\, az$$

Due to symmetry of the effective material about the vertical centerline of the section, the shear flow at a point on the vertical centerline is zero. The summation of the term az between a point on the centerline at the top of the section and the neutral axis of the section is given in the table below, the values being taken from Tables C10.1 and C10.2.

Element No.	az
(1)	.021(28.28 - .13) = 0.59
(2)	.152(27.58 - .13) = 4.17
(3)	.039(27.08 - .13) = 1.05
(4)	.153(25.38 - .13) = 3.86
(5)	.022(23.68 - .13) = 0.52
(6)	.156(21.58 - .13) = 3.34
(7)	.015(19.18 - .13) = 0.28
(8)	.161(16.68 - .13) = 2.66
(9)	.031(13.48 - .13) = 0.41
(10)	.173(10.28 - .13) = 1.75
(11)	.055(6.58 - .13) = 0.35
(12)	.212(3.38 - .13) = 0.69
	Total az 19.67

thus, $q = \frac{V_z}{1489} \times 19.67 = .0132\ V_z$ #/in.

The shear stress $f_s = q/t = .0132\ V_z/.032 = .413\ V_z$

The average f_s on the section $= \frac{V_z}{2ht} = \frac{V_z}{2 \times 50 \times .032} = .312\ V_z$, where h equals the height of the cylinder.

Thus, in this shape of cylinder and material arrangement, the maximum shear stress at the neutral axis is .413/.312 = approximately 4/3 times the average shear stress. The student should remember this value as a help in the preliminary design of required skin thickness at the neutral axis.

If the cylinder section tapers, the net web shear should be used as illustrated in the example problems in Art. C10.10

C10.9 General Design Considerations.

The method as illustrated in the previous article of estimating the effective moment of inertia of a stiffened cylindrical fuselage shell is widely used. Test data on stiffened cylindrical shells in bending show that bending stresses do not follow the straight line variation as assumed in the general beam flexure formula. Shear deformation in the sheet and distortion of the cell contour between the cell transverse frames causes the actual bending stress to fall below that given by the flexure formula at the most remote element point (a), Fig. C10.6 with an increase between points (a) and (b) over that given by the beam formula. Thus, it is good practice to place a stiffener in the region of point (b) which has an ultimate compressive strength considerably greater than the adjacent stiffeners in order to carry this over which may exist.

As more information of the buckling strength of sheet panels under combined shear and compression are obtained, methods of analysis will be revised and improved.

In general, buckles in the sheet are not permanent in this type of structure until the buckling stress is exceeded several times and thus permanent wrinkling or buckling seldom occurs under the applied loads. Failure is generally due to buckling or twisting of the skin

TABLE C10.1

		TRIAL NO. 1						TRIAL NO. 2			
1	2	3	4	5	6	7	8	9	10	11	12
Flange Element No.	Area a sq.in.	Arm z'	az'	az'^{2}	z = z' − z̄	f_b = Mz/I = −1090z	Eff.skin w=1.7tVf_b	Eff.skin area = wt.	Revised Eff.area a	az	az^2
Stringers & Effective Skin 2	.15	24.2	3.63	87.8	27.58	-30020	1.0	.032	.152	4.19	115.4
4	.15	22.0	3.30	72.6	25.38	-27700	1.03	.033	.153	3.88	98.5
6	.15	18.2	2.73	49.7	21.58	-23550	1.12	.036	.156	3.36	72.4
8	.15	13.3	1.99	26.4	16.68	-18200	1.28	.041	.161	2.69	44.7
10	.15	6.9	1.04	7.2	10.28	-11200	1.66	.053	.173	1.78	18.3
12	.12	0	0	0	3.38	- 3680	2.88	.092	.212	0.72	2.4
13	.224	-3.2	-0.72	2.3	-0.18	Sheet in Tension	Skin in Tension		.226	- .04	0.7
14	.120	-6.9	-0.83	5.7	-3.52				.120	-0.42	1.5
15	.224	-10.1	-2.28	23.0	-6.72				.226	-1.52	10.2
16	.12	-13.3	-1.60	21.3	-9.92				.12	-1.19	11.8
17	.160	-15.8	-2.53	40.0	-12.42				.160	-1.99	24.7
18	.12	-18.2	-2.19	39.8	-14.82				.12	-1.78	26.4
19	.16	-20.3	-3.24	65.8	-16.92				.16	-2.70	45.6
20	.12	-22.0	-2.64	58.0	-18.62				.12	-2.24	41.6
21	.16	-23.7	-3.80	90.0	-20.32				.16	-3.25	66.0
22	.12	-24.2	-2.90	70.2	-20.82				.12	-2.50	52.1
23	.088	24.9	-2.19	54.5	-21.52				.088	-1.89	40.7
SUM = 2.49			-12.23	714.3					2.627	-2.86	673

Explanatory Notes for Table C10.1

TRIAL NO. 1

Col. 1 For numbering of stiffeners and sheet elements, see Fig. C10.5.

Col. 2 Stiffener area = .12 + 30 x .032 x .032 = .15 sq. in. For stiffeners 2, 4, 6, 8, 10. Below the centerline each stiffener is considered acting separately. The entire skin between stiffeners is considered as a unit.

Col. 3 4.5 All arms z' are measured to horizontal centerline axis.

TRIAL NO. 2

Col. 6 z = distance to neutral axis as found from results of Trial No. 1.

Col. 7 f_b = 1600000 z/1470

Col. 8 = effective width based on stress in Col. 7

TABLE C10.2

		TRIAL NO. 1										TRIAL NO. 2						
	1	2	3	4	5	6	7	8	9	10	11	12	13	14	15	16	17	18
Buckled sheet	Sheet Element No.	b'	t	r	F_{cr} = .3Ekt/r psi	Assumed f_b	Eff. Fact. K = F_{cr}/f_b	Eff. Area a = K t b'	z'	az'	az'^{2}	z = z' − z̄	f_b = Mz/I_{NA} = −1090 z	Rev. Eff. Fact. K = F_{cr}/f_b	Revised Width b'	Revised Eff Area a = K t b'	az	az^2
	1	2.27	.032	11	-9000	-31900	.282	.020	24.9	0.50	12.4	28.28	-30800	.292	2.25	.021	.59	16.7
	3	4.04	.032	11	-9000	-30300	.296	.038	23.7	0.90	21.3	27.08	-29500	.305	3.99	.039	1.06	28.7
	5	4.04	.032	24	-4510	-26000	.173	.022	20.3	0.45	9.1	23.68	-25800	.174	3.93	.022	0.52	12.3
	7	4.04	.032	38	-2600	-20200	.128	.016	15.8	0.25	3.9	19.18	-20900	.124	3.80	.015	0.29	5.5
	9	6.04	.032	38	-2600	-12900	.201	.039	10.1	0.40	4.0	13.48	-14700	.177	5.53	.031	0.42	5.7
	11	6.52	.032	38	-2600	- 4100	.63	.131	3.2	0.42	1.3	6.58	- 7200	.362	4.73	.055	0.36	2.4
TOTALS								.266		2.92	52.0	TOTALS				.183	3.24	71.3

Explanatory Notes for Table C10.2

Trial No. 1

Col. 1, 2, 3, 4 (see Fig. C10.4 for meaning of terms)

Col. 5 E = 10,300,000 for aluminum alloys

Col. 6 f_b varies as a straight line from 32000 at top of cell to zero at centerline

Col. 9 z' = distance from centroid of element to centerline axis of cell

Explanatory Notes for Table C10.2

Trial No. 2

Col. 12 z - distance to neutral axis as found in results of Trial No. 1

Col. 13 f_b = 1600000 z/1470

Col. 14 based on stress f_b of Col. 13

Results of Trial No. 1

Considering results of both Tables and multiply by 2 since only one half of cell was considered:

$\sum a$ = total effective area = (2.49 + .266)2

= 5.51 sq. in.

$\sum az' = (-12.23 + 2.92)2 = -18.62$

$\bar{z} = \sum az'/\sum a = -18.62/5.51 = -3.38"$

$I_{NA} = 2(714.3 + 52) - 5.51 \times \overline{3.38}^2 = 1470$ in.^{4}

Results of Trial No. 2

Total effective area = (2.627 + .183)2 = 5.62

$\sum az = (-2.86 + 3.24)2 = 0.76$

$\bar{z} = .76/5.62 = .135"$ above N.A. of trial 1.

$I_{NA} = 2(673 + 71.3) - 5.62 \times .135^2 = 1489$

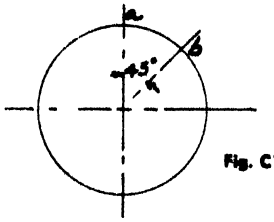


Fig. C10-6

stiffeners. From an appearance standpoint and from a fatigue standpoint, the skin panels should not buckle under a load factor of one. A reasonable margin of safety above this one load factor is desirable for initial buckling of the skin panels.

C10.10 Example Problems of Bending and Shear Flow Calculations for Tapered Sections.

The example problems which follow assume the effective cross-section of the stiffened cell, since the purpose of the example problems is to illustrate general methods of calculating shear and bending stresses. The student should realize that in actual design the effective cross-section necessitates a consideration of effective sheet widths and sheet buckling strength as was illustrated in Tables C10.1 and C10.2 which dictates a trial and error process.

Example Problem 1 - Symmetrical Tapered Section.

Fig. C10.7 shows a portion of a tapered circular stiffened cell that might be representative of the aft portion of a small fuselage. For simplicity, the 16 stringers are assumed as the only effective material. Let it be required to determine the flange bending stresses and the web shear flow system at station (0) due to the given loading at station (150).

Solution No. 1 - Solution by Considering Beam Properties at Only One Section.

If the change in longitudinal stiffener or flange material is fairly uniform this method can be used with little error in the resulting shear flow stresses.

Moment of inertia of section at station (0) about centroidal Y axis:

$$I_y = (15^2 \times .1 \times 2) + (13.86^2 + 10.61^2 + 5.74^2).1 \times 4 = 180 \text{ in.}^4$$

Table C10.3 gives the necessary calculations for determining the flange bending stresses and the net total shear load to be taken by the cell skin. Since the cell is tapered, the stiffeners have a z component, thus the stiffener axial loads help resist the external shear load. The summation of column (8) of Table C10.3 gives -333.4# for a summation for half the fuselage section.

Hence, net web shear at station 0 equals:

$$V_{web} = V_{ext.} + V_{flange} = 2000 + (2 \times -333.4)$$

$$= 1333.2\#$$

The results in this particular problem show that at station 0 the flange stiffener system resists one third of the external shear load. At station 150 the web system will resist the entire external shear load of 2000# since the load in the stiffeners is zero.

In actual design the net web shear should be used since in many cases it will decrease the sheet thickness required one guage.

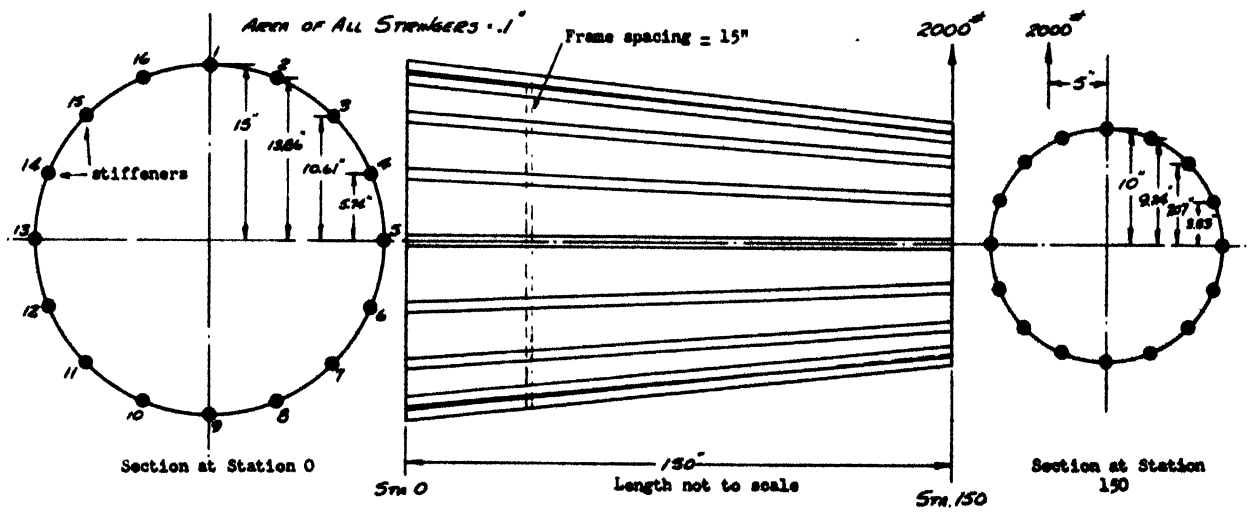


Fig. C10-7

TABLE C10.3

1	2	3	4	5	6	7	8	9
Stiffener No.	Arm z	Area a	f_b = -1667z (psi)	$P_x = f_b a$ (3)(4) lbs.	$\frac{dz}{dx}$	$\frac{dy}{dx}$	$P_z = -P_x \frac{dz}{dx}$	$P_y = -P_x \frac{dy}{dx}$
1	15	*.05	-25000	-1250	-.0333	0	-41.6	0
2	13.86	.10	-23100	-2310	-.0308	-.0127	-71.3	-29.4
3	10.61	.10	-17700	-1770	-.0236	-.0236	-41.7	-41.7
4	5.74	.10	- 9550	- 955	-.0127	-.0308	-12.1	-29.5
5	0	.10	0	0	0	-.0333	0	0
6	-5.74	.10	9550	955	.0127	-.0308	-12.1	29.5
7	-10.61	.10	17700	1770	.0236	-.0236	-41.7	41.7
8	-13.86	.10	23100	2310	.0308	-.0127	-71.3	29.4
9	-15	*.05	25000	1250	.0333	0	-41.6	0
				Shear taken by flanges =			-333.4	0

*1/2 of stiffener one is assumed acting with each half of cell.

NOTES:

Col. 4 $f_b = -Mz/Iy = -2000 \times 150 \times z/180 = -1667z$

Col. 5 Total x component of load in flange member. For practical purposes, it equals axial load in stiffeners since cosine of a small angle is practically one.

Col. 6 The slope of the stiffeners in the z and y directions can be calculated from the dimensions of the two end sections and the length of the cell. (see Fig. C10.7)

Col. 8 & 9 The in plane components of the stiffener axial loads at station 0.

Calculation of Flexural Shear Flow.

$$q = q_o + \frac{V_{z(web)} \Sigma a z}{I_y} = q_o + \frac{1333.2}{180} \Sigma az$$

$$= q_o + 7.40 \Sigma az \text{ - - - - - - - - - - - - -(A)}$$

Due to symmetry of the section about the Z axis, the flexural shear flow in the web at the centerline is zero. Therefore, q_o will be taken as zero and the summation in equation (A) will start with stiffener (1)

$q_{12} = 0 + 7.40 \times .05 \times 15 = 5.55$#/in.

$q_{23} = 5.55 + 7.40 \times .1 \times 13.86 = 15.80$

$q_{34} = 15.80 + 7.40 \times .1 \times 10.61 = 23.66$

$q_{45} = 23.66 + 7.40 \times .1 \times 5.74 = 27.91$

The torsional moment T about the centroid of the section at station (0) equals 5 x 2000 = 10000 in. lb. (clockwise when looking toward station 150). Due to the symmetry of the section at station 0, the in-plane components of the stiffener loads produce zero moment about the section centroid.

For equilibrium a constant internal shear flow q_1 is necessary to make $\Sigma M_X = 0$

$$q_1 = \frac{T}{2A} = \frac{-10000}{2 \times \pi \times 15^2} = -7.06\text{#/in.}$$

Adding the torsional shear flow q_1 to the flexural shear flow q, the following results are obtained:

$q_{12} = -7.06 + 5.55 = -1.51$#/in.

$q_{23} = -7.06 + 15.80 = 8.74$

$q_{34} = -7.06 + 23.66 = 16.60$

$q_{45} = -7.06 + 27.91 = 20.85$ etc.

Fig. C10.8 shows the results in graphical form, on the left side of the section the shears are of the same sign and therefore add together.

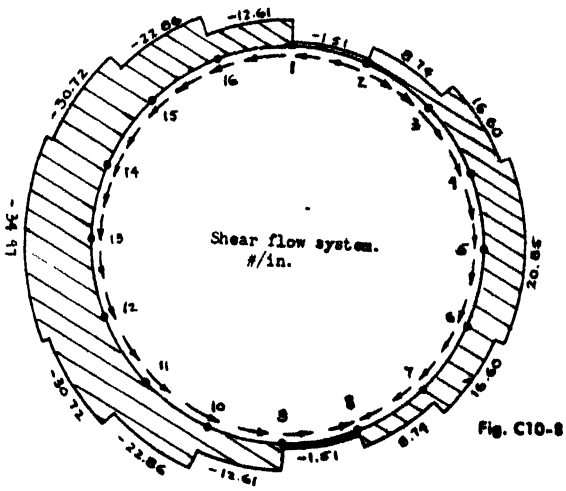


Fig. C10-8

Solution No. 2 - Shear Flow by Change in Stiffener Loads Between Adjacent Stations.

The shear flow will be calculated by considering the change in the axial load in the longitudinal stiffeners between fuselage sections at stations (0) and (30).

Fig. C10.9 shows the beam section at station 30, the stiffener areas being the same as at station 0, but the section as a whole is smaller due to the taper of the cell.

Table C10.4 gives the calculations for the flexural shear. (For general explanation of this method refer to Art. A15.10) Further explanation is given in the notes below Table C10.4.

Comparing the results of column 13 with the flexural shear flow as found by solution No. 1, we find the second solution gives a maximum shear flow of 28.95#/in. against a value of 27.91 for the first solution. The first method deals with the properties at only one section and this can include the effects of change in moment of inertia on the shear flow. The second method is recommended for design.

Since the section is symmetrical, there are no moments induced by the in-plane components of the flange forces at station 0.

The torsional shear flow forces are the same as in solution method No. 1 and these are added to the values of column 13 of Table C10.4 and give a pattern similar to Fig. C10.8.

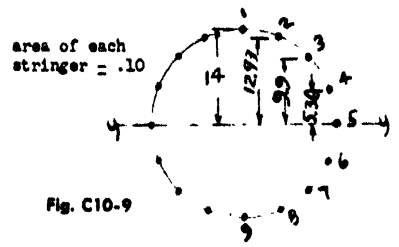


Fig. C10-9

C10.11 Bending and Shear Flow Stresses in Tapered Fuselage Cell with Flange Material Distributed Unsymmetrically.

In certain flying and landing conditions, the fuselage is subjected to side loads as well as vertical loads. Since the effective sheet and the efficiency of the curved buckled sheet depends on the flange stresses, the effective section as a whole will be unsymmetrical even though the external shape of the fuselage is symmetrical about the vertical axis. Furthermore, it is quite common for the cut-outs or openings on one side of the fuselage due to windows, hatches, doors, etc. to be different from that of the other side of the fuselage. This fact causes the longitudinal stiffeners on one side to be different from the other which produces an unsymmetrical effective cross section.

Example Problem. Unsymmetrical Tapered Section.

Fig. C10.10 shows a portion of a tapered cell with longitudinal stiffeners. For simplicity, the question of effective sheet is omitted and the stringers as shown are given such areas as to make the section unsymmetrical. The longitudinal stresses in the stiffeners and the shear flow distribution will be determined for the section at station (0), due to the given loads shown acting at station (150).

Solution No. 1 - Shear Flow by Consideration of Flange Loads at Two Sections.

Table C10.5 (Cols. 1 to 11) gives the calculation of the section properties for the fuselage section at station (0), and the similar columns of Table C10.6 gives the calculations for station (30). Explanatory notes are given below each table.

Calculation of the Flange Stresses at Stations (0) and (30)

At station (0):

The axial load F_X of 1500# acting at point (0') of the fuselage section at station (150) (see Fig. C10.10) produces bending about the Y centroidal axis at station (0), due to its arm of 7.85".

$$M_y = 4000 \times 150 + 1500 \times 7.85 = 611800"\#$$

Since the Z centroidal axis does not coincide with the centerline axis, the axial load also produces bending about the centroidal Z axis at station (0) due to the arm of 2.46".

$$M_Z = -1000 \times 150 + 1500 \times 2.46 = -146310"\#$$

In a similar manner for station (30) (see Fig. C10.11)

$$M_y = 4000 \times 120 + 1500 \times 8.10 = 492150"\#$$

$$M_Z = -1000 \times 120 + 1500 \times 2.11 = 116820"\#$$

The load $F_X = -1500\#$ is thus transferred to the centroid of stations (0) and (30).

Calculation of Flange Bending Stresses.

Station (0):

$$f_b = -(K_3 M_Z - K_1 M_y)\, y - K_2 M_y - K_1 M_Z)\, z$$

where

$$K_1 = I_{yz}/(I_y I_Z - I_{yz}^2)$$

$$K_2 = I_Z/(I_y I_Z - I_{yz}^2)$$

$$K_3 = I_y/(I_y I_Z - I_{yz}^2)$$

Substituting values from tables C10.5 and C10.6:

$$K_1 = -30.55/(641.4 \times 382.6 - 30.55^2) =$$

$$= -30.55/244670 = -.0001248$$

$$K_2 = 382.6/244670 = .00156$$

$$K_3 = 641.4/244670 = .00262$$

Substituting K values in equation for f_b:

$$f_b = -\left[.00262 \times -146310 - (-.0001248 \times 611800)\right] y$$
$$- \left[.00156 \times 611800 - (-.0001248 \times -146310)\right] z$$

whence

$$f_b = 307.0\, y - 936.1\, z \text{ (plus } f_b \text{ is tension)}$$

Station (30):

$$K_1 = -19.4/(516.6 \times 286 - 19.4^2)$$

$$= -19.4/147620 = -.0001315$$

$$K_2 = 286/147620 = .001936$$

$$K_3 = 516.6/147620 = .0035$$

$$f_b = -\left[.0035\, c\, -116800 - (-.0001315 \times 492150)\right] y$$
$$-\left[.001936 \times 492150 - (-.0001315 \times 116820)\right] z$$

whence

$$f_b = 344.3\, y - 937.7\, z$$

Column (12) in Tables C10.5 and C10.6 gives the results of solving the equations for f_b.

Since an external load of 1500# is acting normal to the sections and through the section centroids, an axial compressive stress f_c is produced on the sections. (See Columns 13). The

TABLE C10.4

1	2	3	4	5	6	7	8	9	10	11	12	13
Stiff. No.	Sta. 0 Area a sq.in.	Sta.30 Area a sq.in.	Sta.0 Arm z	Sta.30 Arm z	Sta. 0 f_b = -1667Z (psi.)	Sta.30 f_b= -1522Z (psi.)	Stiff Sta. 0 P_x = f_b a	Load Sta.30 P_x = f_b a	$\frac{\Delta P}{30}$ (lb.) in. Col.8+Col.9	Panel Taper Corr. Factor K	$\frac{\Delta PK}{30}$	Flexural Shear Flow $q = \sum\frac{\Delta PK}{30}$
1	.05	.05	15.00	14.00	-25000	-21300	1250	-1065	6.17	.935	5.76	5.76
2	.10	.10	13.86	12.93	-23100	-19700	2310	-1970	11.33	.935	10.60	16.36
3	.10	.10	10.61	9.90	-17700	-15050	1770	-1505	8.83	.935	8.25	24.61
4	.10	.10	5.74	5.36	- 9550	- 8155	955	- 815	4.65	.935	4.34	28.95
5	.10	.10	0	0	0	0	0	0	0	0	0	28.95
6	.10	.10	-5.74	-5.36	9550	8155	-955	815	-4.65	.935	-4.34	24.61
7	.10	.10	-10.61	-9.90	17700	15050	-1770	1505	-8.83	.935	-8.25	16.36
8	.10	.10	-13.86	-12.93	23100	19700	-2310	1970	-11.33	.935	-10.60	5.76
9	.05	.05	-15.00	-14.0	25000	21300	-1250	1065	-6.17	.935	-5.76	

NOTES:

Col. 6 f_b = -2000 x 150 z/180 = -1667 z

Col. 7 f_b = -2000 x 120 z/157.2 = -1522 z

Cols. 8 and 9: For signs of stiffener forces refer to Fig.A of Table C9.4 of Chapter C9 which gives a general explanation.

Col. 10 Change in axial load in each stiffener between stations 0 and 30 divided by distance between Stations. This result represents the average shear flow induced by the loading up of each stiffener between stations 0 and 30.

Col. 11 The width of a skin panel at Station 0 is 5.88" and 5.5 inches at Station 30. The shear flow on the edge of the panels at Station 0 equals (5.5/5.88) $\Delta P/30$. (See Art. A15.12 for explanation) This refinement is usually neglected and the average values as given in Col. 10 are used which are conservative.

Col. 13 Due to symetry of structure, the shear flow is zero on z axis. This shear flow at any station equals the progressive summation of the shear flow values in Col. 12.

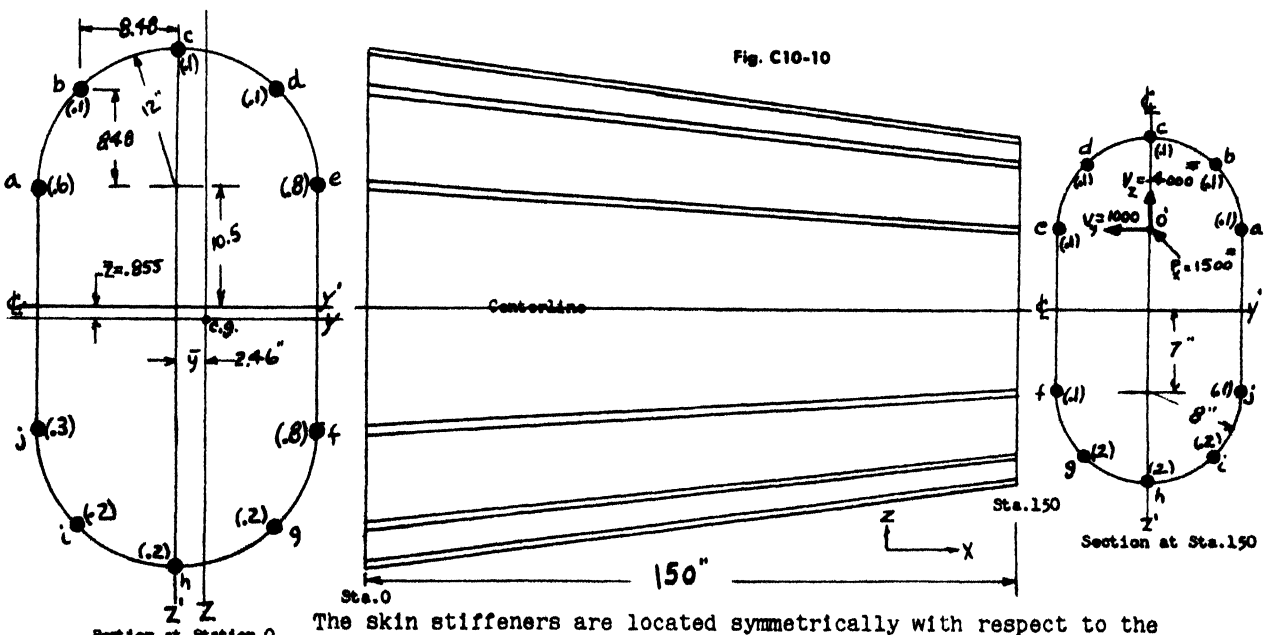


Fig. C10-10

The skin stiffeners are located symmetrically with respect to the centerline axes, however the stiffener areas as given in() on the figure are not symmetrical with these axes. It is assumed in this problem that the stiffeners taper uniformly between the values as given for stations 0 and 150 The cell would of course have interior transverse frames which are not shown on the figure.

Table C10.5

Section Properties at Sta. 0											Total Stiffener Loads at Sta. 0		
1	2	3	4	5	6	7	8	9	10	11	12	13	14
Stiff. No.	Area a	Arm z'	Arm y'	az'	az'^{2}	ay'	ay'^{2}	az'y'	z = z' − $\bar{z}$	y = y' − $\bar{y}$	f_b	$f_c = F/\Sigma a$ = -1500/3.40	P_a = a(f_b+f_c) = (2)(12+13)
a	.60	10.5	-12.00	6.30	66.20	-7.20	86.50	-75.50	11.36	-14.46	-15080	-441	-9312
b	.10	18.98	- 8.48	1.90	36.00	-0.85	7.20	-16.10	19.84	-10.94	-21960	-441	-2239
c	.10	22.50	0	2.25	50.80	0	0	0	23.36	- 2.46	-22800	-441	-2304
d	.10	18.98	8.48	1.90	36.00	0.85	7.20	16.10	19.84	6.02	-16742	-441	-1719
e	.80	10.5	12.00	8.40	88.10	9.60	115.10	100.80	11.36	9.54	- 7692	-441	-6506
f	.80	-10.5	12.00	-8.40	88.10	9.60	115.10	-100.80	-9.65	9.54	11958	-441	9216
g	.20	-18.98	8.48	-3.80	72.00	1.70	14.40	-32.30	-18.13	6.02	18798	-441	3673
h	.20	-22.50	0	-4.50	101.80	0	0	0	-21.65	-2.46	19485	-441	3809
i	.20	-18.98	-8.48	-3.80	72.00	-1.70	14.40	32.30	-18.13	-10.94	13610	-441	2634
j	.30	-10.50	-12.00	-3.15	33.10	-3.60	43.25	37.80	-9.65	-14.46	4592	-441	1246
Sum	3.40			-2.90	643.9	8.40	403.2	-37.70					-1500

Reference Axes Z' and Y' are taken as the centerline axes. (see Fig. C10.10)

Location of centroid and transfer of properties to centroidal axes.

$\bar{z}$ = -2.90/3.40 = -.855"

$\bar{y}$ = 8.40/3.40 = 2.46"

I_y = 643.9 - 3.40 x 855^2 = 641.4

I_z = 403.2 - 3.40 x 2.46^2 = 382.6

I_{zy} = -37.7 - 3.40 x 2.46 x -.855 = -30.55

General Notes:

Col. 12 f_b = 307.0y - 936.1z

Col. 14 Since the total tensile stresses equal to total compressive stresses in bending, the sum of Col. 14 should equal the external applied normal load.

Table C10.6

Section Properties at Sta. 30											Total Stiffener Loads at Sta. 30		
1	2	3	4	5	6	7	8	9	10	11	12	13	14
Stiff. No.	Area a	Arm z'	Arm y'	az'	az'^{2}	ay'	ay'^{2}	az'y'	z = z' − $\bar{z}$	y = y' − $\bar{y}$	f_b	$f_c = F/\Sigma a$ = -1500/2.98	P = a(f_b + f_c)
a	.50	9.80	-11.2	4.90	48.1	-5.60	62.8	-54.9	10.90	-13.31	-14800	-503	-7651
b	.10	17.72	- 7.92	1.77	31.4	-0.79	6.3	-14.0	18.82	-10.03	-21090	-503	-2159
c	.10	21.00	0	2.10	44.1	0	0	0	22.10	- 2.11	-21447	-503	-2195
d	.10	17.72	7.92	1.77	31.4	0.79	6.3	14.0	18.82	5.81	-15647	-503	-1615
e	.66	9.8	11.20	6.47	63.2	7.40	83.0	72.5	10.90	9.09	- 7088	-503	-5011
f	.66	-9.8	11.20	-6.47	63.2	7.40	83.0	-72.5	- 8.7	9.09	-11282	-503	7100
g	.20	-17.72	7.92	-3.54	62.8	1.58	12.6	-28.0	-16.60	5.81	-17583	-503	3416
h	.20	-21.00	0	-4.20	88.2	0	0	0	-19.90	-2.11	17943	-503	3489
i	.20	-17.72	- 7.92	-3.54	62.8	-1.58	12.6	28.0	-16.60	-10.02	12135	-503	2327
j	.26	-9.8	-11.20	-2.55	25.0	-2.92	32.6	28.6	- 8.70	-13.31	3570	-503	797
Sum	2.98			-3.29	520.2	6.28	299.2	-26.3					-1500

NOTES:

Reference Z' and Y' axes are taken as the centerline axes.

$\bar{z}$ = -3.29/2.98 = -1.10"

$\bar{y}$ = 6.28/2.98 = 2.11

I_y = 520.2 - 2.98 x 1.10^2 = 516.6

I_z = 299.2 - 2.98 x 2.11^2 = 286.0

I_{zy} = -26.3 - 2.98 x 2.11 x -1.10 = -19.4

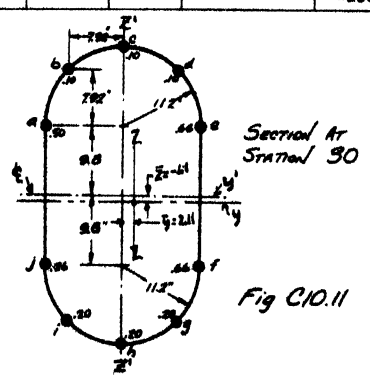


Fig C10.11

total load P_s in each stiffener equals the area of the stiffener times the combined bending and axial stresses. (see column 14 of each table).

Calculation of Flexural Shear Flow q.

Table C10.7 gives the necessary calculations to determine the shear flow at station (0) based on the change in flange loads between stations (0) and (30). The correction of the average shear due to the taper in the skin panels as was done in example problem (1), Table C10. is omitted in this solution since it tends toward the conservative side. Since the effective cross section is unsymmetrical, the value of the flexural shear flow q at any point is unknown thus a value for q at some point is assumed. In Table C10.7 the shear flow q in the web aj is assumed zero. Column (5) gives the results at other points under this assumption.

Moment of Shear Flow about Intersection of Centerline Axes

For equilibrium in the plane of the cross section at station (0), the summation of the moments in the plane of all internal and external forces must be zero. Column (7) of Table C10.7 gives the moment of the flexural shear about this point. (See notes and Fig. below Table for explanation.)

Moments Due to In Plane Components of Flange Loads.

Since the stiffeners are not normal to the section at station (0), the stiffeners has in plane components which may produce a moment about the intersection of the symmetrical axes which has been selected as a moment center. Table C10.8 gives the calculations for the in plane components and their moments about point O".

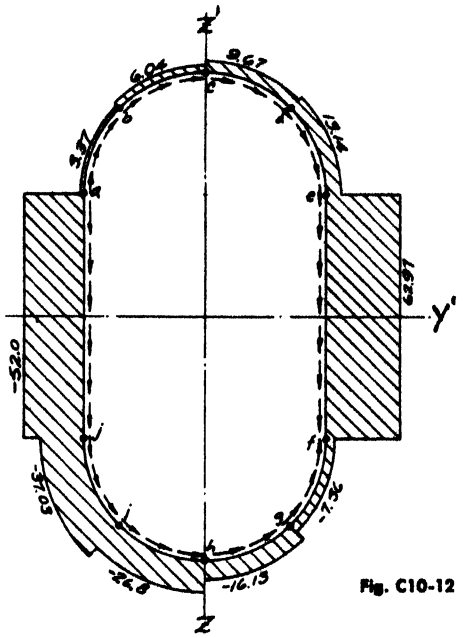


Fig. C10-12

Shear flow distribution.

TABLE C10.7

SHEAR FLOW CALCULATIONS

1	2	3	4	5	6	7	8	9
Stiff. No.	P_x at Sta.0	P_x at Sta.30	$\frac{\Delta P_x}{30}$	$q = \frac{\Delta P_x}{30}$	m sq.in.	mq	q_1	$q_r = q + q_1$
a	9312	-7651	55.37	55.37	150.04	8300	-52	3.37
b	2239	-2159	2.67	58.04	202.46	11820	-52	6.04
c	2304	-2195	3.63	61.67	202.46	12500	-52	9.67
d	1719	-1615	3.47	65.14	150.04	9780	-52	13.14
e	6506	-5011	49.83	114.97	252.0	29000	-52	62.97
f	-9216	-7100	-70.53	44.44	150.04	6660	-52	-7.56
g	-3673	3416	- 8.57	35.87	202.46	7270	-52	-16.13
h	-3809	3489	-10.67	25.20	202.46	5100	-52	-26.8
i	-2634	2327	-10.23	14.97	150.04	2240	-52	-37.03
j	-1246	797	-14.97	0	252.0	0	-52	-52.0
a					Sum	92670		

NOTES:

Col. (2) and (3) From tables C10.6 and C10.7

Col. (4) change in stiffener load between sta. 0 and 30 divided by 30", the dist. between stations.

Col. (6) m = double areas (see Fig. a).

Col. (7) mq = moment of shear flow q on each web element about 0' (Fig. a)

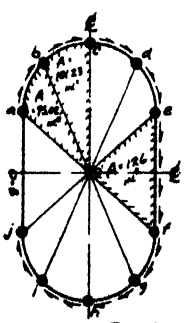


Fig a

TABLE C10.8

MOMENTS DUE TO IN PLANE COMPONENTS OF STIFFENER LOADS

1	2	3	4	5	6	7	8
Stiff.	P_x (lbs.)	$\frac{dy}{dx}$	$P_y = P_x\frac{dy}{dx}$	$M_o = P_y z'$	$\frac{dz}{dx}$	$P_z = P_x\frac{dz}{dx}$	$M_o = P_z y'$
a	-9312	.0026	248	2600	-.0233	217	-2600
b	-2239	.0188	42	798	-.0421	94	- 796
d	-2304	0	0	0	-.050	115	0
d	-1719	-.0188	32	-608	-.0421	72	610
e	-6506	-.0266	173	-1820	-.0233	152	1820
f	9216	-.0266	245	-2570	.0233	214	2560
g	3673	-.0188	69	-1310	.0421	154	1307
h	3809	0	0	0	.050	190	0
i	2634	.0188	49	930	.0421	111	-941
j	1246	.0266	33	346	.0233	29	-348
			Sum	-1634			1612

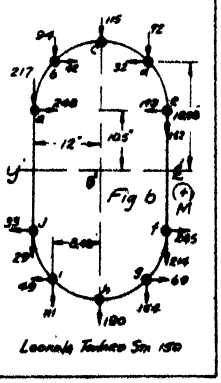
NOTES:

Col. (2) from Table C10.5

Col. (3) equal the slope of stiffeners in y and z directions. (see Fig. C10.10)

Col. (5) and (8) Values of z' and y' from Table C10.5. Fig. b shows the P_y and P_z components from Cols. (4) and (7).

Total moment about O' = -1634 + 1612 = -22"#



Moment of External Load System About Point (O').

The 1000# load at station (150) acting in the Y direction has a moment arm of 7" about the point O' of station (0).
Hence external moment = 1000 x 7 = 7000"#.

Therefore the total moment about the assumed moment center O' =

92670"# due to shear flow q
-22 due to in plane components of stiffeners.
7000 due to the external loads.
Total
=99648"# = $\Sigma M_{O'}$

Therefore for equilibrium a moment of -99646"# is required which can be provided by a constant shear flow q_1 around the cell, hence

$$q_1 = \frac{T}{2A} = \frac{-99648}{2 \times 957} = -52\#/\text{in.}$$ (957 = enclosed area of cell)

This value of q_1 is entered in column 8 of Table C10.7. The resulting shear flow in any web portion q_T equals the algebraic sum of q and q_1. (See Col. 9, Table C10.7). Fig. C10.2 shows the results in graphical form.

C10.12 Solution for the Shear Flow Considering only One Beam Section.

Since the effective cross section at station zero in the example problem is unsymmetrical, the flexural shear flow can not be obtained by the general equations for symmetrical sections as illustrated by example problem 1 of Art. C10.10. The following two methods in computing the shear flow may be used:

(1) By use of the Principal Axes.

This method is explained in detail in Articles A15.6 and A15.7 of Chapter A15.

(2) By correcting the shear loads along a given set of rectangular axes to take care of the dissymmetry of the section.

$$\text{Thus } q = \frac{V_Z'}{I_y} \Sigma\, az + \frac{V_Y'}{I_z} \Sigma\, ay$$

$$\text{where } V_Z' = \frac{V_Z - V_y \frac{I_{yz}}{I_z}}{1 - \frac{(I_{yz})^2}{I_y I_z}}$$

$$V_y' = \frac{V_y - V_z \frac{I_{yz}}{I_y}}{1 - \frac{(I_{yz})^2}{I_y I_z}}$$

V_z = external net shear load parallel to the Z axis.
V_y = external net shear load parallel to Y axis.
I_z and I_y = moment of inertia about the centroidal Z and Y axes.
I_{yz} = product of inertia about the same axes.

This method assumes a beam of constant moment of inertia. In general the fuselage is tapered in depth and width and the cross-sectional material also changes due to taper of the flange stringers and the changes in the skin thickness, thus the above method may give misleading results in certain cases of material distribution as illustrated in Arts. A15.10 of Chapter A15. Therefore the method considering the change in flange loads between two sections is recommended.

PROBLEMS

(1) The fuselage section in Fig. C10.13 is subjected to a bending moment M_y = 700,000 in. lb. and a shear load of 6000#. Determine what proportion of this loading can be carried without buckling of the curved panels. Determine the final axial stress in the three longerons under the total given loads.

(2) The fuselage section of Fig. C10.14 is subjected to a bending moment M_y = 1,100,000 in. lb. Determine the effective moment of inertia of the section under this moment.

(3) The fuselage section of Fig. C10.14 is subjected to a moment M_y = 900,000 in.lb., and a M_Z moment of 350,000 in.lbs. Determine the effective moment of inertia under this load system.

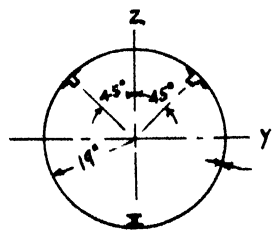


Fig. C10-13

Material: 24 ST Al.Alloy.
Frame spacing = 9 in.
Skin thickness = .040
Upper longeron area = .50 each
Lower longeron area = .70

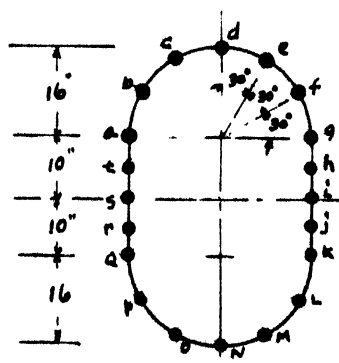
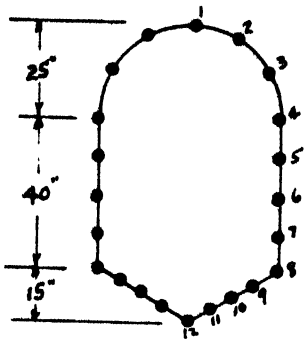


Fig. C10-14

All material 24ST
.025 skin on lower curved surface.
.040 skin on sides
.032 skin on top.
Stringer areas: a,b,c, d,e,f,g, = .15 sq.in. each.
All others are .10 each.



Bottom skin = .050
Side and top skin = .032

All stringers on each portion are equally spaced.

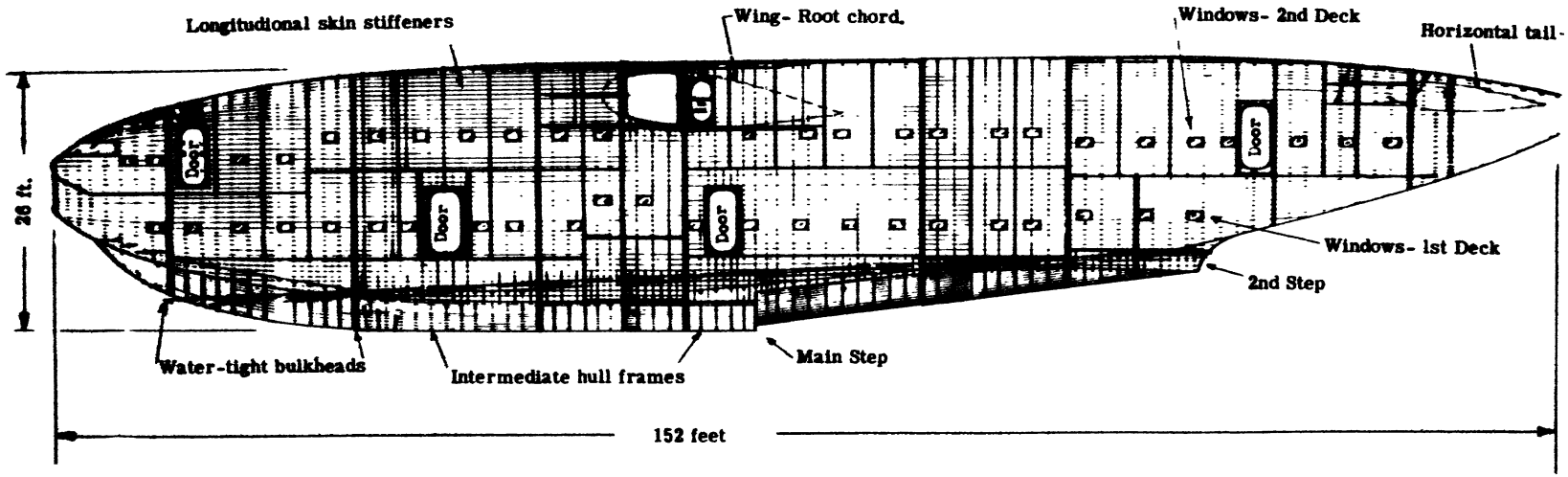
Frame spacing = 18"

Material:
Stringers -- 24ST Extru.
Sheet -- 24 ST alclad.

Fig. C10-15

(4) Fig. C10.15 shows the dimensions of a hull section. The black circles show the location of the stringers. The bottom stringers are Z sections. (For size see section No. 29 of Table C6.4 of Chapter C6). Stringers 5, 6 and 7 are bulb angles. (See section No. 3 of Table C6). The hull section is subjected to a bending moment M_y = 2,000,000 in. lbs. Select the necessary upper stringers 1 to 4 to carry this design moment and modify given stringers if necessary. Determine the allowable stress for the stringers by the methods as discussed in Chapters B5 and B6.

GENERAL STRUCTRUAL LAYOUT OF HULL STRUCTURE FOR LARGE AIRPLANE



The commercial transport airplanes of today are relatively small when compared to the airplanes which will be flying in the near future. The above diagram shows the general structural layout of a large hull as worked out by the aeronautical structural design engineers of the Sikorsky Aircraft Corp., in a study of the design of a 100 passenger long range flying boat.

In any future development of lange airplanes, the stress analyst and the structural designer will always play a very important part. New and difficult problems will always challenge the aeronautical structures engineer and no student should worry for fear that all problems will have been solved before he is ready to take his place in the industrial research and design field.

CHAPTER C11
BULKHEAD AND FRAME ANALYSIS

C11.1 General.

The wing or body of a modern airplane is essentially a stiffened thin-walled cellular structure. These structural units of the airplane are subjected to various concentrated loads of relatively large magnitude. In many cases, the wing supports the power plant, or the landing gear or floats may be attached to the wing and the wing is usually attached to the fuselage by localized fittings which produces concentrated loads or reactions on both the wing and body structure. The body usually supports the tail, and in many cases, the landing gear and power plant are attached to the body. All of these concentrated loads must be transferred into the skin of the cellular structure and the structural unit which is designed to make this transfer of load is generally referred to as a bulkhead.

In a wing structure, there are many ribs running in a chordwise direction. It is common practice to refer to ribs which are attached continuously around their perimeter to the wing skin as bulkheads. Since the chief purpose of a bulkhead is to transfer concentrated loads into the skin covering, it will usually need a flange to take bending loads and a web or truss system to transfer shear loads.

For the transfer of loads in a fuselage or hull structure, the bulkhead in most cases must be an open ring or frame since the inside of the body must be an open compartment or a series of compartments.

Thus on every airplane, there are a considerable number of bulkheads in both the wing and body structure which must be stress analyzed and designed in detail. This chapter deals with the general principles in the stress analysis of bulkheads.

Fig. C11.1 a to f shows sketches of several types of bulkheads which are typical to wing and body design.

Fig. a illustrates a bulkhead for a single cell, leading edge type of wing beam with three spanwise stringers. The flange of the bulkhead is riveted continuously to the wing skin.

Fig. b illustrates a bulkhead for a single cell beam with a distributed flange in the form of corrugations on the upper surface and bulb angles stringers on the bottom. To stiffen the flat sheet web of the bulkhead beads are pressed into the sheet.

Figs. c and d illustrate two general types of bulkheads for a wing cell confined to the midportion of the wing.

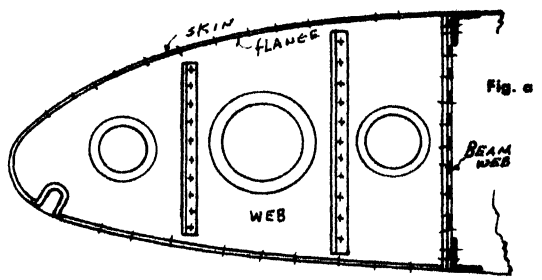


Fig. a

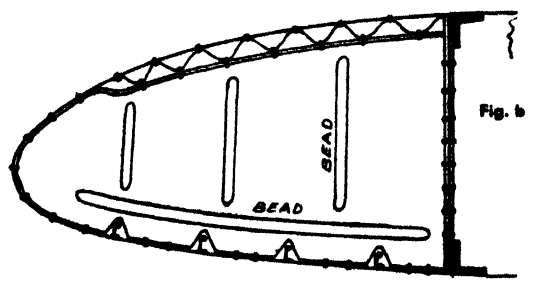


Fig. b

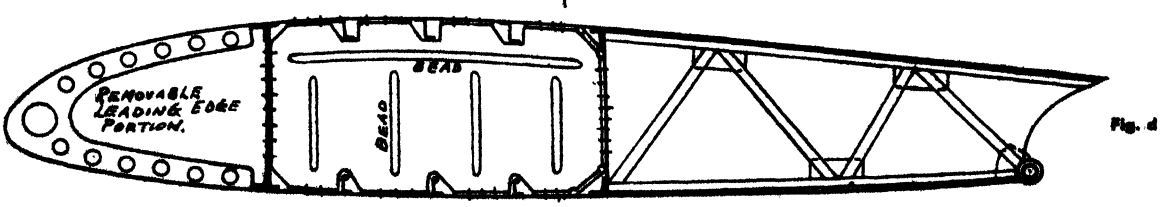


Fig. d

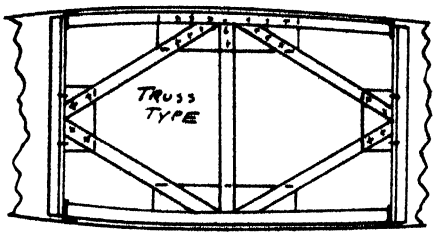


Fig. c

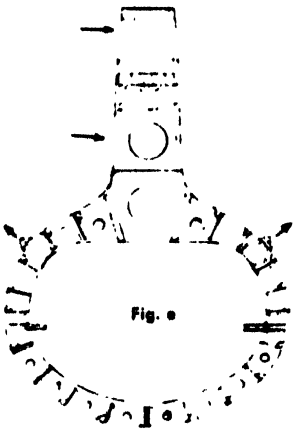


Fig. e

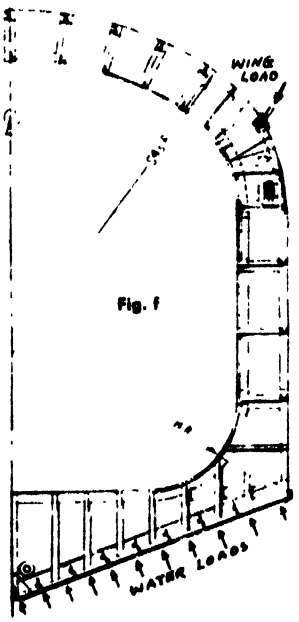


Fig. f

Fig. e illustrates a fuselage bulkhead for transfering the tail loads into the fuselage skin.

Fig. f illustrates a bulkhead for a hull which transfers the water loads and the wing reactions into the hull skin.

C11.2 Analysis of Bulkhead for 2-Flange Single Cell Beams.

Fig. C1.2 illustrates a bulkhead in a 2-flange single cell leading edge type of beam. Assume that the air-load on the trailing edge portion (not shown in the figure) produces a couple reaction P and a shear reaction R as shown. These loads are distributed to the cell walls by the bulkhead which is fastened continuously to the cell walls. Let q = shear flow per inch on bulkhead perimeter which is necessary to hold bulkhead in equilibrium under the given loads P and R.

Taking moments about some point such as (1) of all forces in the plane of the bulkhead:

$$\Sigma M_1 = -Ph + 2Aq = 0$$

hence

$$q = Ph/2A. \quad (A = \text{enclosed area of cell})$$

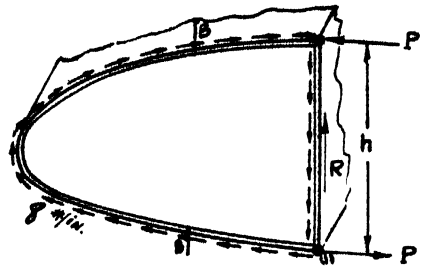


Fig. C11-2

With q known the shear and bending moment at various sections along the bulkhead can be determined. For example, consider the section at B-B in Fig. C11.2. Fig. C11.3 shows a free body of the portion forward of this section.

The bending moment at section B-B equals:

$M_B = 2qA_1$ where A_1 is the area of the shaded portion.

Let F_X equal the horizontal component of the flange load at this section.

$$F_X = M_b/a$$
$$= 2qA_1/a$$

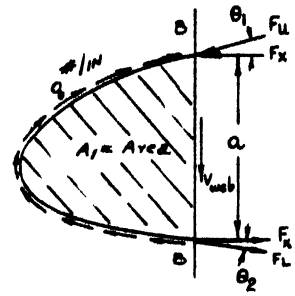


Fig. C11-3

The true upper flange load $F_U = F_X/\cos\theta_1$ and the lower flange load equals $F_L = F_X/\cos\theta_2$.

The vertical shear on the bulkhead web at B-B equals the vertical component of the shear flow q minus the vertical components of the flange loads. Hence

$$V_{web} = q\,a - F_X \tan\theta_1 - F_X \tan\theta_2$$
$$= q\,a - \frac{2\,q\,A_1}{a}(\tan\theta_1 + \tan\theta_2)$$

Illustrative Problem

The bulkhead in the leading edge portion of the wing as illustrated in Fig. C11. will be analyzed.

A distributed external load as shown will be assumed.

Solution:

The total air load aft of beam = 8 x 40/2 = 160#. The arm to its c.g. location from the beam equals 40/3 = 13.33". Hence the reactions at the beam stringer points due to the loads on the trailing edge portion equals:

P = 160 x 13.33/10 = 213.2#. (See Fig. C11.5)

Shear reaction V_r = 160#

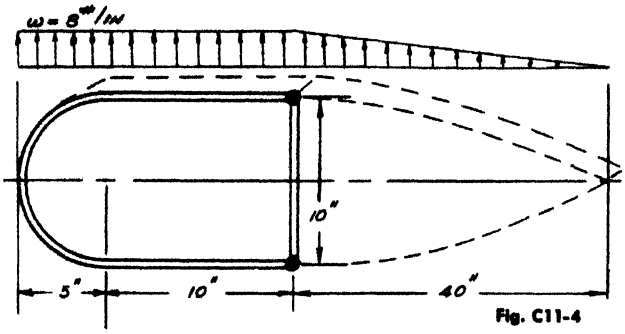


Fig. C11-4

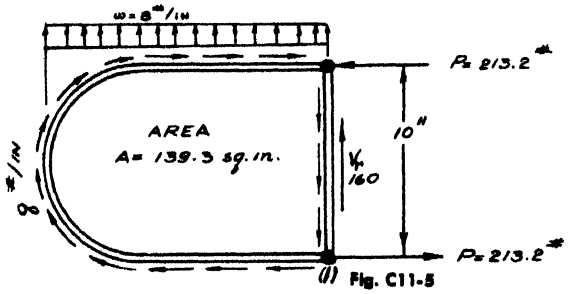


Fig. C11-5

Let q be the constant flow reaction of the cell skin on the bulkhead perimeter which is necessary to hold the bulkhead in equilibrium under the applied air loads.

Take moments about some point such as the lower stringer (1).

$\Sigma M_1 = -213.2 \times 10 + 8 \times 15 \times 7.5 + 2 \times 139.3\ q = 0$

Hence

q = 1232/278.6 = 4.42#/in.

With the applied forces on the bulkhead known, the shears and bending moments at various sections as desired can be calculated. For example, consider a section B-B 2.5" from the leading edge. Fig. C11.6.

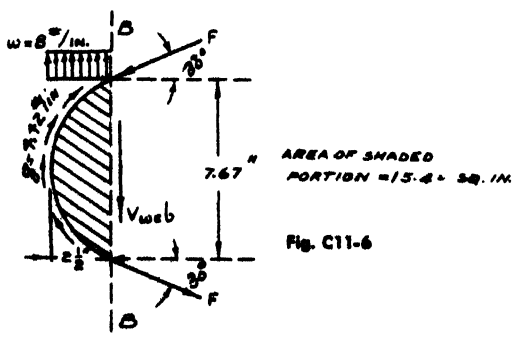


Fig. C11-6

Bending moment at section B-B =

8 x 2.5 x 1.25 + 4.42 x 2 x 15.4 = 161"#

Flange load $F = (161/7.67)\ \frac{1}{\cos 30^0} = 24.3\#$

Web shear = 4.42 x 7.67 + 8 x 2.5 - 24.3 x sin 30° x 2 = 29.4#.

In a similar manner the values of the bulkhead shears and bending moments could be determined at other actions.

C11.3 Analysis of Bulkhead for 3-Flange Single Cell Beams.

A three flange single cell beam is a very common arrangement for wings of small and medium size airplanes. Fig. C11.7 illustrates a bulkhead for a 3-flange single cell beam. The bulkhead distributes any applied loads such as a reaction from the wing flap or a reaction from a landing gear or float strut into the cell skin structure. The bulkhead flange is usually fastened continuously to the cell walls. The reaction of the cell skin on the bulkhead flange can be considered as composed of three constant flow reactions as indicated by the flow patterns q_{cb}, q_{ba} and q_{ac} in Fig. C11.7. The bulkhead is

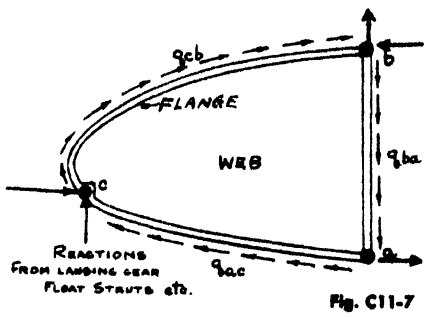


Fig. C11-7

thus held in equilibrium by these constant flow edge forces and the externally applied loads. The force system is a coplanar non-concurrent one and is statically determinate since three equations of equilibrium are available and there are 3 unknowns, namely the three constant flow reactions of the cell skin on the bulkhead flanges. Once these constant flow bulkhead reactions are determined, the shears and bending moments on the bulkhead can be found. The general analysis of such a bulkhead can best be explained by the solution of a typical problem.

Illustrative Problem.

Fig. C11.8 shows a bulkhead in a 3-flange single cell wing beam. The bulkhead must distribute the concentrated applied loads at points b and c into the cell walls. Let it be required to determine the loads in the flange and the web of the bulkhead.

Solution:

The three unknowns are q_{cb}, q_{ac}, and q_{ba}. The direction of these constant flow reactions has been assumed as shown by the arrows in Fig. C11.8.

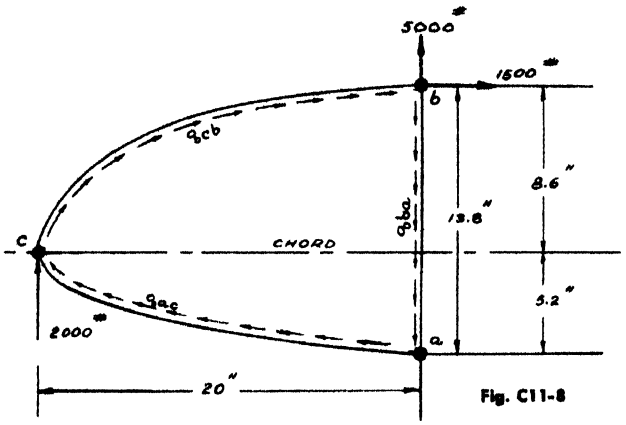


Fig. C11-8

Take moments of all forces about stringer (a) and equate to zero.

$\Sigma M_a = 1500 \times 13.8 + 2000 \times 20 + 2 \times 186 \times q_{cb} + 2 \times 19.3 \times q_{ac} = 0$ - - - - - - - - - - - - - - - -(1)

Take moments about stringer (b) and equate to zero.

$\Sigma M_b = 2000 \times 20 + 2 \times 157.3 \times q_{ac} + 2 \times 48 \times q_{cb} = 0$ -(2)

Solving equations (1) and (2) for q_{ac} and q_{cb}, we obtain

$q_{ac} = -79.8\#/in.$, $q_{cb} = -155\#/in.$

To find q_{ba} take $\Sigma F_Z = 0$

$\Sigma F_Z = 5000 + 2000 - 155 \times 8.6 - 79.8 \times 5.2 - 13.8\, q_{ba} = 0$

hence

$q_{ba} = 380.7\#/in.$ which acts in the direction that was assumed whereas the other reactions act in the reverse direction to that assumed.

In equations (1) and (2) it was necessary to find the moment of a constant flow curved force system about a selected moment center. To do this required certain enclosed areas which are illustrated in Figs. C11.9, 10 and 11.

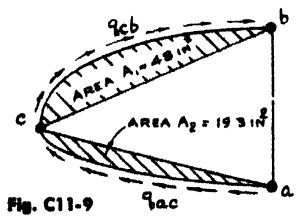


Fig. C11-9

Moment of q_{cb} about point b = $2A_1\, q_{cb}$.

Moment of q_{ac} about point a = $2A_2\, q_{ac}$.

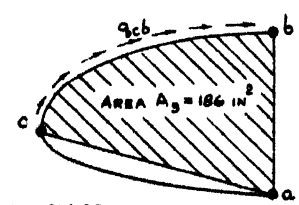


Fig. C11-10

Moment of q_{cb} about point a = $2A_3\, q_{cb}$.

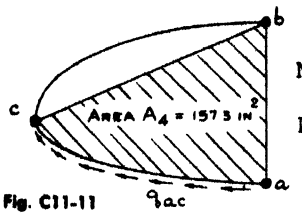


Fig. C11-11

Moment of q_{ac} about point b = $2A_4\, q_{ac}$.

Calculation of Bulkhead Flange and Web Loads.

Before the bulkhead flange can be proportioned and the thickness of the web selected, the shears and bending moments on the bulkhead at several sections should be determined. To illustrate, a section 10" from the leading edge will be considered. Fig. C11.12 shows a free body of the portion of the bulkhead forward of this section.

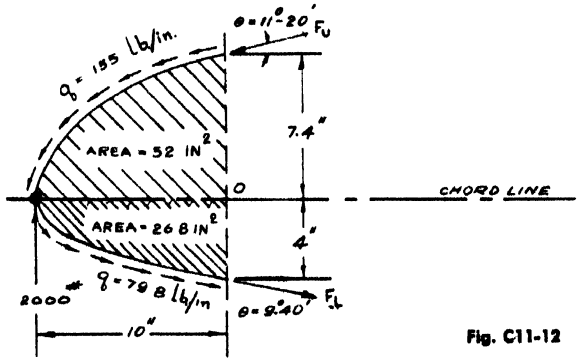


Fig. C11-12

The moment at the cut section will be referred to point (O) the intersection of the chord line with the section.

$M_O = 2000 \times 10 - 155 \times 52 \times 2 - 79.8 \times 26.8 \times 2 = -397\#\#$.

The vertical shear at (O) equals

$V_O = 2000 - 155 \times 7.4 - 79.8 \times 4 = 534\#$

The resultant horizontal thrust X_O at (O) equals

$-155 \times 10 + 79.8 \times 10 = -752\#$

Fig. C11.13 shows these resultant forces at point O.

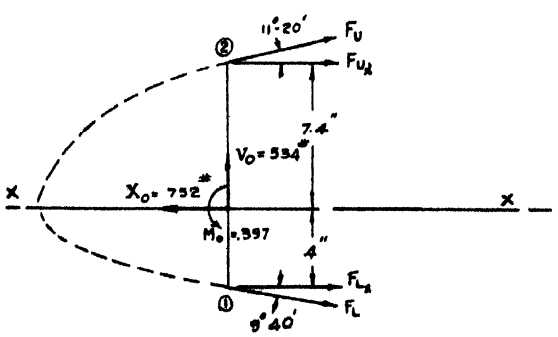


Fig. C11-13

Take moments about (1) to find Fu_X

$= 11.4\ Fu_X - 397 - 752 \times 4 = 0$, whence $F_{u_X} =$ 299#

The axial upper flange load F_u therefore equals $299/\cos 11^0 - 20' = 305\#$ tension.

Take $\Sigma F_X = 0$ to find F_{L_X}

$= -752 + 299 + F_{L_X} = 0$ whence $F_{L_X} = 453$

Therefore $F_L = 453/\cos 9^0 - 40' = 460\#$ tension

To find the web shear take $\Sigma F_Z = 0$

$V_{web} = V_0 + F_u \sin 11^0 - 20' - F_L \sin 9^0 - 40'$

$= 534 + 305 \times .196 - 460 \times .168 = 517\#$

In actual design, particularly, for bulkheads carrying large external loads, it is usually necessary to plot a complete diagram showing the variation of the flange and web loads throughout the bulkhead. Thus similar calculations to those above can be repeated at several sections from which curves may be plotted.

C11.4 Bulkhead Analysis for Single Cell Wing Beam with Multiple Stringers.

When there are more than three flange stringers in a single cell beam, there are four or more shear panels in the cell wall and thus the reactions of the cell panels on the bulkhead flange can not be found by statics as was done in the case of the 3-flange cellular beam in Article C11.3. To explain a general procedure for stress analyzing a bulkhead for a wing beam of the multiple flange type a numerical sample problem will be presented.

Fig. C11.14 illustrates a wing section consisting of four spanwise flange members. The concentrated loads acting at the four corners of the box might be representative of reactions from the engine mount or nacelle structure for an engine attached to the wing and on the rear beam, the reactions from a rib which supports the wing flap. These loads must be distributed into the walls of the wing box beam which necessitates a bulkhead. Before the bulkhead can be designed, the bending and shear forces on the bulkhead must be determined. The calculations which follow illustrate a method of procedure.

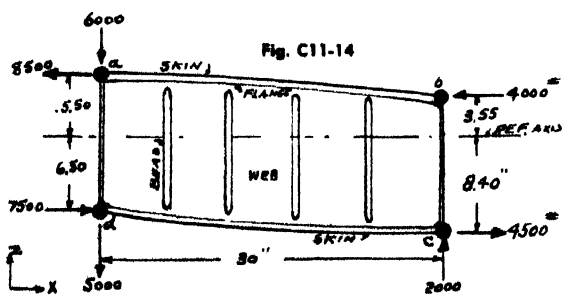


Fig. C11-14

Solution:

The z component of the applied load equals $-6000 - 5000 + 2000 = -9000\#$.

The x component equals $-8500 + 7500 - 4000 + 4500 = -500\#$.

These two resultant components are distributed to the wing cell by the bulkhead causing the wing to suffer bending and shear forces. If a section of the wing one inch long is considered, the resultant loads applied through the bulkhead produce bending moments on the wing of:

$M_X = -9000 \times 1 = -9000"\#$

$M_Z = -500 \times 1 = -500"\#$

The flexural shear flow system in the cell walls due to the above moments can be found from a consideration of the axial load in the four corner members of the box. To find these flange loads requires the use of the wing section properties. Table C11.1 gives the calculations. For simplicity in this example problem, the cell walls are considered ineffective in bending. Since the beam section is unsymmetrical, the flexure equations for the bending of unsymmetrical sections must be used.

From chapter A13, the beam flexure equation using section properties about the centroidal X and Z axes is

$f_b = -(K_s M_Z - K_i M_X)x - (K_s M_X - K_i M_Z)z$

From table C11.1, $I_X = 225.8$, $I_Z = 1310$, $I_{XZ} = -94.7$

$K_i = I_{XZ}/(I_X I_Z - I_{XZ}^2)$

$= -94.7/(225.8 \times 1310 - 94.7^2) = -94.7/286700$

$= -.00033$

$K_s = I_Z/286700 = 1310/286700 = .00456$

$K_s = I_X/286700 = 225.8/286700 = .000786$

Substituting in the equation for f_b using $M_X = -9000$ and $M_Z = -500$, we obtain

$f_b = -\left[.000786 \times -500 - (-.00033 \times -9000\right] x$

$- \left[.00456 \times -9000 - (-.00033 \times -500)\right] z$

whence

$f_b = 3.363\ x + 41.21\ z$

Columns (12) of Table C11.1 gives the results of this equation for the bending stresses in the four corner members of the box beam. Multiplying these stresses by the flange areas, the change in flange load in a length of one inch is obtained (Column 13). This change in flange load also represents the shear flow per inch of cell induced by this change in flange load. Since the value of the shear flow at any point on the cell wall due to this bending is unknown a value will be assumed at some point and then the shear flow system will follow as a summation of the ΔP changes in the flange members. In this example,

TABLE C11.1

1	2	3	4	5	6	7	8	9	10	11	12	13	14
Flange No.	Area A	z'	x'	Az'	Az'^{2}	Ax'	Ax'^{2}	Ax' z'	$z=z'-\bar{z}$	$x=x'-\bar{x}$	f_b(psi)	$\Delta P=f_bA$	$q=-\sum\Delta P$
a	2.00	5.50	0	11.00	60.5	0	0	0	6.36	-11.8	222.0	444.0	
b	1.25	3.55	30	4.43	15.72	37.50	1125	132.9	4.41	18.2	243.0	304.0	-444
c	1.15	-8.40	30	-9.66	82.20	34.50	1035	-289.8	-7.54	18.2	-249.2	-287.0	-748
d	1.70	-6.50	0	-11.04	71.90	0	0	0	-5.64	-11.8	-271.7	-461.0	-461
	6.10			-5.27	230.3	72.00	2160	-156.9					0

$\bar{z} = \sum Az'/\sum A = -5.27/6.10 = -.865"$

$\bar{x} = \sum Ax'/\sum A = 72.0/6.10 = 11.8"$

Centroidal x and z moments of inertia:

$I_x = 230.3 - 6.10 \times .865^2 = 225.8$
$I_z = 2160 - 6.10 \times 11.8^2 = 1310$
$I_{xz} = -156.9 - 610 \times -.865 \times 11.8 = -94.7$
$f_b = 3.363 x + 41.21 z$ (See Column 12)

the cell web between flange members (a) and (d) is assumed zero or it might be considered that this web is cut which leaves an open section for the beam. Column (14) of Table C11.1 gives the shear flow around the cell under this assumption. Fig. C11.15 shows the resulting forces on the bulkhead. The force system acting on the bulkhead is balanced for summation of total forces in the X and Z directions which must be zero for equilibrium of the bulkhead.

The moments of the forces in the plane of the bulkhead will now be calculated:

Taking moments about the c.g. of the beam cross section (See Fig. C11.15):

$\Sigma M_{c.g.} = -11000 \times 11.8 - 8500 \times 6.36 - 7500 \times 5.65 - 4000 \times 4.41 - 4500 \times 7.54 - 2000 \times 18.2 - 444 \times 2 \times 90 - 748 \times 2 - 108.7 - 461 \times 2 \times 99 = -648400"\#$

For equilibrium $\Sigma M_{c.g.}$ must equal zero, therefore a constant flow shear q reaction around the bulkhead perimeter is necessary which will produce a moment of 648400"#.

$$q_1 = \frac{M}{2A} \frac{648400}{2 \times 368.5} = 880\#/\text{in.}$$

(Note: 368.5 = total area of cell)

Adding this shear flow to that of Fig. C11.15, the resulting force system of Fig. C11.16 is obtained. The reactions of the beam cell walls on the bulkhead have now been determined and the bending moments and shears on the bulkhead can now be calculated.

To illustrate, consider the bulkhead section B-B which passes through the c.g. of the beam section. Fig. C11.17 shows a free body of the bulkhead portion to the left of section B-B.

Fig. C11-15

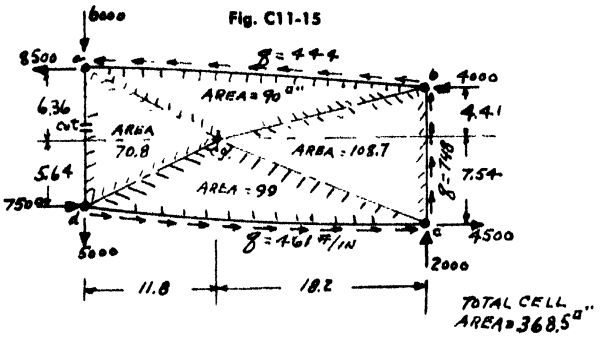
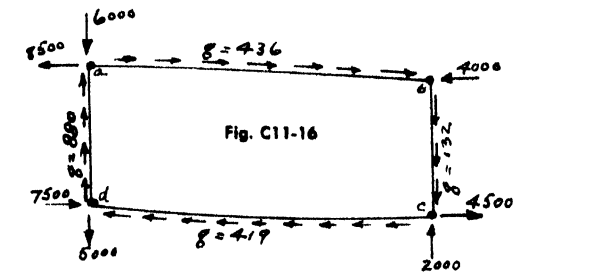


Fig. C11-16



Moments at section B-B will be referred to the point (O):

$\Sigma M_O = -11000 \times 11.8 - 8500 \times 6.36 - 7500 \times 5.64 + 436 \times 2 \times 36 + 880 \times 2 \times 70.8 + 419 \times 2 \times 38.3 = -38200"\#$

The resultant external shear force along the section B-B equals the summation of the z components of all the forces.

$V = \Sigma F_Z = -11000 + 12 \times 880 - 436 \times 0.36 + 419 \times 0.96 = -195\#.$

The resultant load normal to the section B-B equals the summation of the force components in the x direction.

$H = \Sigma F_X = -8500 + 7500 + (436 - 419)\ 11.8 = -800\#$

Fig. C11.18 shows these resultant forces referred to point (O) on section B-B. The flange loads (F) in the bulkhead and the net shear in the bulkhead web can now be found as illustrated in the previous illustrative problems. To obtain a complete picture as to the flange and web forces several sections along the bulkhead should be

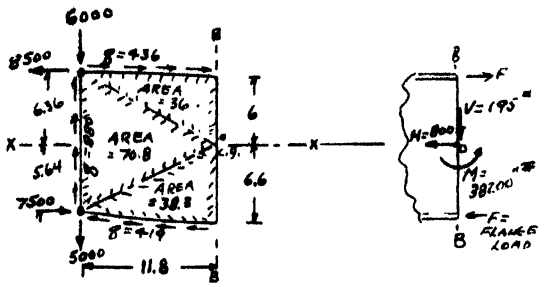


Fig. C11-17 Fig. C11-18

analyzed in order that curves of bulkhead bending moments, shears and thrusts can be drawn.

C11.5 Bulkhead Analysis For Multiple Cell Wing Structures.

In large airplanes, wing sections with three or four interior webs which divide the wing section into two or more cells, are quite common. Bulkheads for distributing large concentrated loads are of course needed regardless of the type of wing cell construction.

The general procedure as illustrated by the numerical example in Article C11.4 can be used for finding the reaction of the walls and webs on the bulkhead perimetry. The method of finding the shear flow in multiple cell beams is given in Chapters C9 and C10 and the basic theory in Chapter A15. If the student is familiar with these chapters, he should have no difficulty extending the general procedure in Art. C11.4 to bulkhead analysis for wing sections with multiple cells and a large number of spanwise stringers.

C11.5a Bulkheads Adjacent to Cut-Out in One Surface of a Box Beam.

Fig. (a) illustrates a wing box beam with a large cut out in the upper skin covering which extends entirely between the upper corner flanges of the box beam. Assume that the wing portion shown is subjected to a constant torque M_t. This torsional moment produces a constant shear flow $q = M_t/2A$ in the cell. At the cut-out in the upper surface, the shear flow q in the upper surface must be taken by the upper flange of the bulkhead. The bulkhead is held in equilibrium by three balancing shear flows q_1, q_2 and q_3 on the other three edges of the bulkhead. See Fig. b. These three forces can be determined by statics after which the shears and bending moments on the bulkhead can be determined.

To illustrate by a simple numerical problem, consider that the wing cell is subjected to a torsional moment of 100,000 in. lb. The forces acting on the bulkhead which is located adjacent to the edge of the cut-out will be determined.

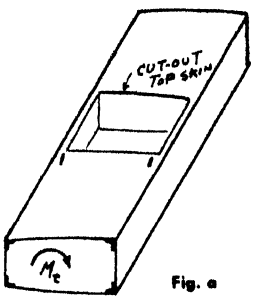


Fig. a

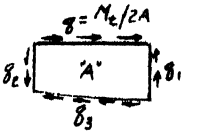


Fig. b BULKHEAD AT 1-1

Fig. (c) shows a free body of the bulkhead. The torsional shear flow in the cell walls equals $M_t/2A = 100,000/(2 \times 405.5) = 123.3\#/in$. This shear flow in the top covering is thrown off as a constant upper edge force on the bulkhead as shown in Fig. (c). The bulkhead is held in equilibrium by the shear flow reactions q_1, q_2 and q_3 on the other three edges of the bulkhead. See Fig. (c) for assumed sense of reactions.

For equilibrium $\Sigma F_X = 0$

$= 123.3 \times 29.5 - 29.5\ q_3 = 0$, hence $q_3 =$ 123.3#/in.

To find q_1, take moments around point O and equate to zero.

$\Sigma M_O = 123.3 \times 2 \times 181 + 123.3 \times 2 \times 18 - 2 \times 206.5\ q_1 = 0$

whence

$q_1 = 119\#/in.$

To find q_2, take $\Sigma F_Z = 0 = 119 \times 14 + 123.3 \times 3.4 - 10.6\ q_2 = 0$

whence

$q = 197\#/in.$

With the loads on the bulkhead known, the shears and moments on the bulkhead can be found as illustrated in the previous problems.

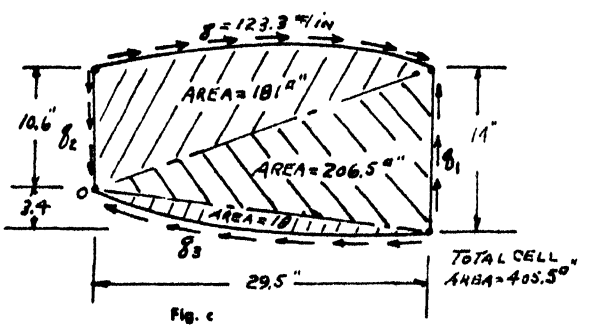


Fig. c

BULKHEAD AND FRAME ANALYSIS FOR FUSELAGE OR HULL STRUCTURES

C11.6 General.

The airplane body (fuselage or hull) is subjected to many concentrated forces of relatively large magnitude, as for example, wing reactions,

tail reactions, and in some designs, the fuselage is subjected to reactions from the power plant or landing gear. These concentrated loads on the fuselage which are usually applied through fittings must be distributed to the fuselage cell or skin covering. An internal bulkhead which is usually fastened continuously to skin covering is used to make this transfer. In many cases these bulkheads must be open rings because of interior cabin arrangements. It is common practice to refer to fuselage bulkheads which are open rings as frames, but whatever the name (bulkhead or frame), a structure must be provided to transfer the concentrated loads into the fuselage skin.

Since closed frames are statically indeterminate with respect to internal stresses, the stress analysis procedure of a fuselage or hull frame consists essentially of two steps. The first step is to determine the magnitude and distribution of the reacting skin forces on the frame which balances the externally applied loads. The second step is to analyze the frame for internal forces in resisting the applied loads (external and skin forces).

C11.7 Magnitude and Distribution of the Skin Reacting Forces on the Frame.

Fig. C11.19 illustrates a cross-section of a fuselage section of the distributed flange type. Two external loads P are applied to the fuselage as shown. To distribute these loads into the fuselage skin, an internal frame or ring is necessary as illustrated in the Fig. To hold the frame in equilibrium the external loads must be balanced by the skin reaction on the circumference of the frame. If the elementary beam theory is assumed to apply, then these reacting skin forces would be distributed according to the general flexure shear flow theory, namely

$$q = \frac{V}{I} \Sigma\, az \quad \text{(for symmetrical fuselage sections)}$$

Fig. C11.19 shows this shear distribution for a distributed flange type of fuselage structure and Fig. C11.20 shows the shear flow distribution when the fuselage flange material is concentrated into four main longerons. In this case, the shear flow is constant between the longerons.

Some structural designers contend the distribution of a large concentrated load in the fuselage skin does not follow the beam theory, and make the assumption that the resistance of the skin adjacent to the point of application is greater than that of the skin at greater distances from the load point. A triangular distribution of the skin resisting forces are illustrated in Fig. C11.21 is often used. If this is done, the shear stresses in the fuselage sheet should be checked for this distribution.

ILLUSTRATIVE PROBLEMS IN CALCULATING THE SKIN RESISTING FORCES ON A FUSELAGE FRAME SUBJECTED TO EXTERNAL LOAD CONCENTRATIONS.

Problem #1

Fig. C11.22 illustrates a cross-section of a circular fuselage. Two concentrated loads of 2000# each are applied to the fuselage frame at the points indicated. The problem is to determine the reacting shear flow forces in the fuselage skin which will balance the two externally applied loads. This fuselage section might be considered as the aft portion of a medium size fuselage and the loads are due to air loads on the horizontal tail surfaces. To make the numeri-

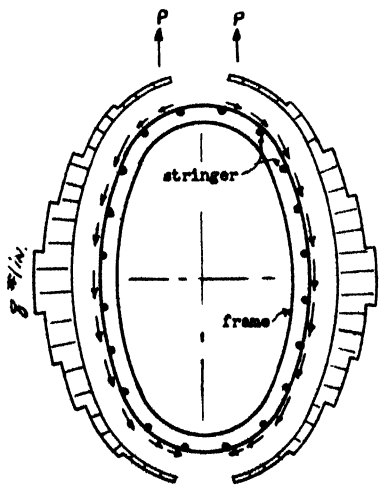


Fig. C11-19 }
Distribution of skin resisting forces on frame as per beam theory. Multiple flange type of of fuselage structure.

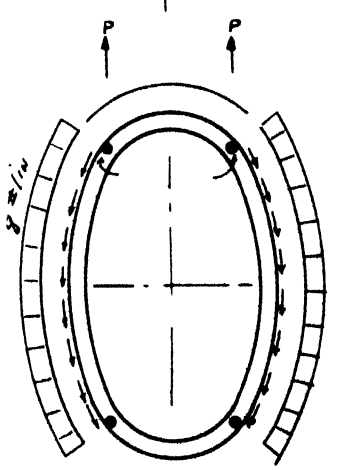


Fig. C11-20
Distribution of skin resisting forces on frame as per beam theory. Concentrated flange type of fuselage structure.

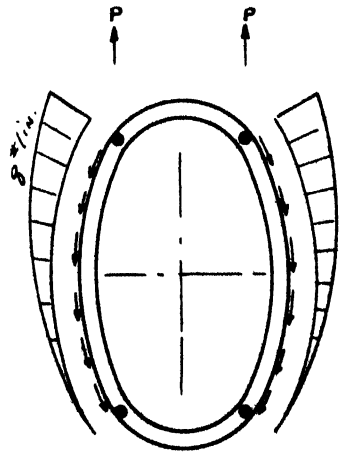


Fig. C11-21
Distribution of skin resisting forces based on a consideration of the deformation of the fuselage skin

cal calculations short the fuselage stringer arrangement has been assumed symmetrical.

Solution:

In this solution the fuselage skin resisting forces will be assumed to vary according to the general beam theory. The general flexural shear flow equation for bending about the Y axis is

$$q = q_o + \frac{V_z}{I_y} \Sigma\, az$$

In this problem, $V_z = 4000\#$

The moment of inertia I_y of the fuselage cross-section is required. In this simplified illustration, the area of each stringer plus its effective skin will be taken as .15 sq.in. The student should of course realize after studying Chapters C9 and C10 that the true effective area should be used on the compressive side and that the skin on the tension side of the fuselage is entirely effective. These facts would tend to make the effective cross-section unsymmetrical about the Y axis. Since the only purpose of this illustrative solution is to show how the frame loads are balanced, the section be assumed as symmetrical which will greatly decrease the amount of calculations required.

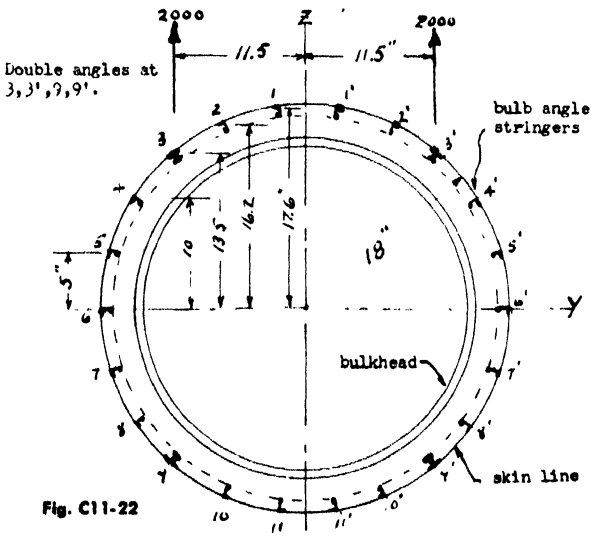


Fig. C11-22

Moment of inertia of fuselage section about Y axis which is the neutral axis under our simplified assumptions.

$$I_y = .15\ (17.6^2 + 16.2^2 + 13.5^2 + 13.5^2 + 10^2 + 5^2) = 637\ \text{in.}^4$$

Due to symmetry of effective section and external loading, the shear flow in the fuselage skin on the z axis or between stringers 1 and 1^1 and 11 or 11^1 will be zero. Thus starting with stringer (1) the shear flow in the skin resisting the external loads of 4000# can be written around the circumference of the section.

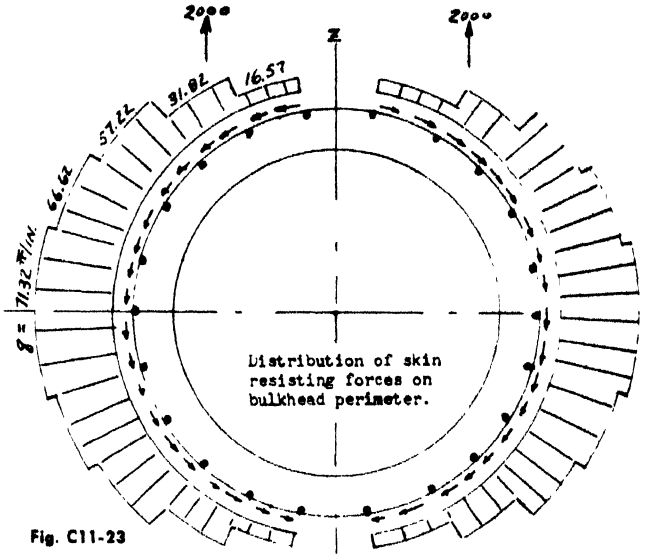


Fig. C11-23

$$q = \frac{V_z}{I_y} \Sigma\, az = \frac{4000}{637} \Sigma\, az = 6.275 \Sigma\, az$$

$q_{1-2} = 6.275 \times .15 \times 17.6 = 16.57\#/\text{in.}$

$q_{2-3} = 16.57 + 6.275 \times .15 \times 16.2 = 31.82\#/\text{in.}$

$q_{3-4} = 31.82 + 6.275 \times .30 \times 13.5 = 57.22\#/\text{in.}$

$q_{4-5} = 57.22 + 6.275 \times .15 \times 10 = 66.62\#/\text{in.}$

$q_{5-6} = 66.62 + 6.275 \times .15 \times 5 = 71.32\#/\text{in.}$

Due to symmetry of effective cross-section, the shear flow is symmetrical about the Y axis.

As a check on the above work, the summation of the z components of the shear flow on each skin panel between the stringers should equal the external load of 4000#.

ΣF_Z of skin shear flow equals the vertical projected length of each panel times the shear flow q on that panel, or

$$\Sigma F_Z = [1.4 \times 16.57 + 2.7 \times 31.82 + 3.5 \times 57.22 + 5 \times 66.62 + 5 \times 71.32]\,4 = 4000\#\ \text{(check)}$$

Fig. C11.23 shows the frame with its balanced load system. With the external loads on the frame known, the internal stresses in the frame can be determined by various methods. (See Chapter A9 and the general discussion in Art. C11.9.)

PROBLEM 2 Unsymmetrical Vertical Loading

In certain conditions in flying and landing, unsymmetrical concentrated loads are applied to the fuselage or hull structure. For example, Fig. C11.24 shows the same section and frame as was used in Problem 1. Due to an unsymmetrical load on the horizontal tail, the reactions from the tail on the fuselage are as illustrated in the figure. The total load in the z direction is still 4000# but the loads are not symmetrical

about the z axis. For analysis purposes, consider the loads as transferred to the c.g. of the section as indicated in Fig. C11.25. The moment of the two loads about the c.g. = 1500 x 11.5 - 2500 x 11.5 = -11500"#. The shear load V_Z = 4000 produces the same shear flow pattern as Fig. C11.23. To balance the moment of -11500"#, a constant shear flow q_1 around the frame is necessary.

$$q = \frac{M}{2A} \quad \frac{11500}{2 \times \pi \times 18^2} = 5.65\#/in.$$

(A = area of fuselage cross-section)

Adding this constant shear flow to that of Fig. C11.23, the resultant shear flow in the skin is illustrated in Fig. C11.26.

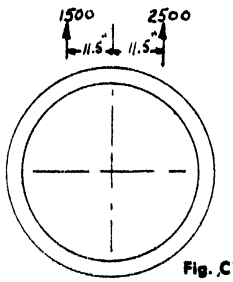


Fig. C11-24

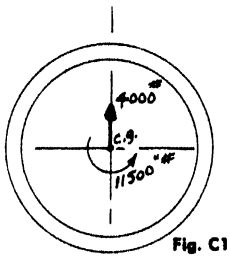


Fig. C11-25

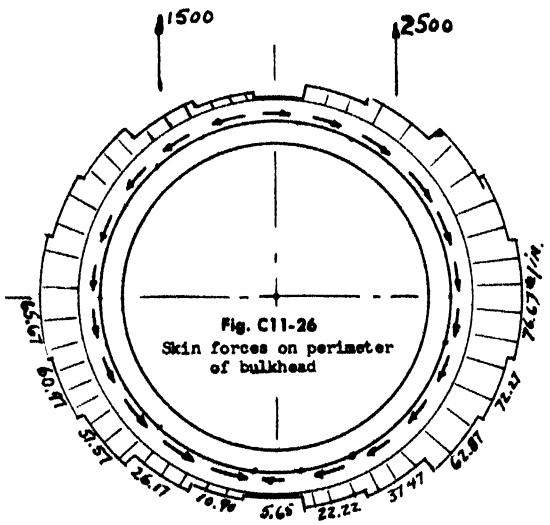


Fig. C11-26
Skin forces on perimeter of bulkhead

C11.8 Unsymmetrical Fuselage or Hull Sections.

In some cases the fuselage or hull stringers due to cut-outs, etc., may not be arranged symmetrically about the Z and Y axes. For such cases, the skin shear flow stresses can be calculated by the shear flow equations for unsymmetrical bending as given in Art. C10.12, or by the method which considers the ΔP change in axial load in the fuselage stringers due to bending of the fuselage under the applied external loads on the fuselage bulkhead or frame. This method of analysis was used for the analysis of the skin forces on the unsymmetrical wing bulkhead in Art. C11.4.

C11.9 Analysis of Fuselage Frames or Bulkheads For Internal Stresses.

After the supporting skin forces on the fuselage or hull frame have been determined, an analysis for the internal forces in the frame can be carried out. A loaded closed frame is statically indeterminate with respect to internal forces. Chapter A9 explains one method of analysis which is widely used in aircraft frame design. Since the theory is developed in Chapter A9 as well as applications of the method to the solution of typical frames problems, it is unnecessary to repeat any discussion of the theory here or its application. Once the bending moments on the frame have been determined by an elastic analysis, the shear and axial load at any section of the frame follows as a matter of statics.

If the frame of Fig. C11.23 were to be analyzed for the given loading by the elastic method of Chapter A9, the residual structure might be taken as illustrated in Fig. C11.27. The frame would be made statically determinate by cutting the frame at the top. One of the cut faces is attached to the elastic center of the frame by an inelastic bracket and the other cut face can be considered as fixed. The frame is divided into small elements and the static bending moments are calculated at the neutral axis of each of these elements. For a symmetrical frame and loading, there would be only two redundant forces at the frame elastic center and three redundants for an unsymmetrical condition of loading.

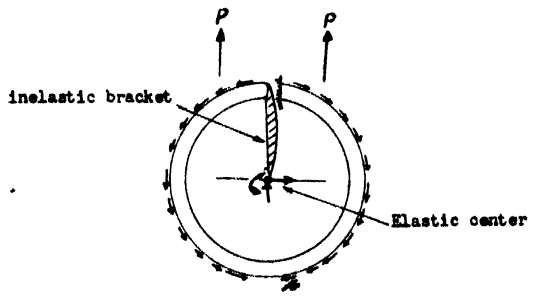


Fig. C11-27

Before an elastic analysis can be made, the section properties of the frame must be known. Thus a preliminary design or analysis must be made in order to obtain a trial frame size to use in the elastic analysis. Approximate design bending moments on the frame can be obtained by assuming points of inflection for the frame elastic axis in resisting the given loading.

The method of analysis as explained in Chapter A9 assumes that the frame deflections are not influenced by the fuselage skin and

stringers. In certain cases, the outward deflection of the frame may be considerable and this deflection will be resisted by the fuselage skin and stringers which will produce an inward force on the frame. The extent of these relieving forces is so indeterminate that it is common practice to omit their influence which tends to be conservative.

PROBLEMS

(1) In Fig. C11.28 the external bulkhead loads P_1 and P_2 equal 4000# each and P_3 equals zero. The fuselage stringer material consists of four omega sections with an area of .25 sq. in. each. Determine the skin resisting forces on the bulkhead in balancing the above loads. Neglect any effective skin in this problem.

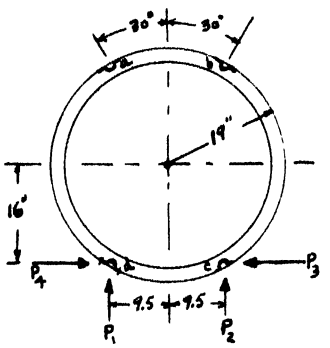


Fig. C11-28

(2) Same as problem (1) but make $P_1 = 4000\#$ and $P_2 = 6000\#$.

(3) Same as problem (1) but make $P_3 = 3000\#$.

(4) In a water landing condition the hull bulkhead of Fig. C11.29 is subjected to a normal bottom pressure of 200 lb. per in. The area of the bulb angle stringers is .11 sq. in. each and they are 7/8 in. deep. The area of the Z stringers is .18 sq. in. each and the depth 1.5 in. The area of the stringers a, b, c, d and e is .20 sq. in. each. Neglecting any effective skin determine the skin resisting forces on the bulkhead in balancing the bottom water pressures.

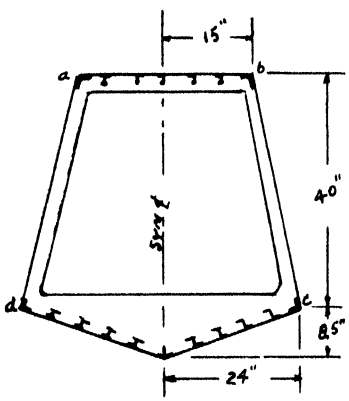


Fig. C11-29

(5) Same as problem (4) but consider that the water pressure is only acting on one side of the bottom of the bulkhead.

PART D

CHAPTER D1
THE LOADS ON THE WING

D1.1 Introduction.

Before the wing, body and tail structure can be designed, the axial and shear forces and the bending and torsional moments acting on these airplane units must be known. These design forces for flight conditions can not be found until the magnitude, location and distribution of the air loads, inertia loads and power plant loads are known. In airplane structural design, safety with minimum weight is the major criterion. This fact dictates that the information regarding the air forces on the airplane must be known quite accurately. The calculations necessary to obtain these loads are quite lengthy because of the many maneuvers to which the airplane is subjected. Consequently, most engineering departments of airplane companies set up special sections or departments, which deal almost exclusively in calculating the applied loads on the airplane. In some companies, this section is a part of the structures and stress analysis section, whereas in others it is placed under the aerodynamics section. The calculations in general require a good knowledge of aerodynamics.

The Civil Aeronautics Authority and the Army and Navy Aviation Bureaus have definite requirements as to the airplane design loads, and provide information as to the procedures to use in calculating the required results. These requirements are constantly being revised and modified, thus it does not seem wise to repeat such procedures here and thus only fundamental facts and relationships will be treated in this chapter. With this general knowledge, the student should be able to follow any of the government procedures relative to the calculation of the applied loads on the airplane.

D1.2 General Forces Acting on an Airplane.

In flying conditions, the forces acting on the airplane which must be considered in designing the airplane structure are: the air pressures and their distribution, the weight and inertia forces of the airplane, and its equipment or contents, the engine forces consisting of the propeller thrust and engine torque and gyroscopic forces for special flight maneuvers. In towed gliders, the force produced by the towing cable must be considered.

In landing conditions, the same forces as listed above for flying conditions must be considered plus the forces due to ground reactions. The air forces in a landing condition assume a minor role. In special landing conditions, as for example, the arresting of a carrier based naval plane or an assisted take-off conditions as illustrated by the catapulting of a navy seaplane the applied de-accelerating or accelerating forces must be considered.

The air pressures on the airplane are the forces produced by the resistance of the air to the passage of the airplane through it. The propeller thrust produced by the engine power is the force which pulls the airplane through the air. The engine torque forces are present but have no efficient help in propelling the airplane. The weight is a constant force which tends to draw every body toward the earth's center and is proportional to the mass of the body. The inertia forces are resistances to the forces which tend to accelerate the airplane or its elements.

D1.3 Inertia or Acceleration Forces.

For an airplane flying in a straight path with constant velocity, the vector sum of all the forces acting on the airplane will equal zero, that is, the air forces will exactly balance the engine thrust and the weight of the airplane acting toward the center of the earth.

In many flight and landing conditions, the airplane is subjected to translational as well as rotational acceleration. If the airplane velocity due to gravity or engine thrust is changed, or if the direction of the velocity is changed as for example, due to the manipulation of the control surfaces, the airplane will undergo translation and each mass element of the airplane will be subjected to a force equal to the mass of the element times the acceleration. In such cases the vector sum of the forces on the airplane is not equal to zero, but is equal to the summation of the element masses times the acceleration and the resultant of this force system will be a force acting thru the center of gravity of the airplane. If these acceleration forces are considered to act in the opposite direction, the airplane can then be considered in a state of static equilibrium. These reversed acceleration forces are referred to as the inertia forces, and this procedure is in accordance with d'Alembert's principle, which states "that every state of motion may be considered at any instant as a static of equilibrium provided opposite inertia forces are introduced".

In some conditions of flight, such as a gust on the tail, or the operations of the ailerons causing the airplane to roll, or a landing condition where the ground or water reaction does not

pass through the airplane center of gravity, the airplane is subjected to an unbalanced moment which produces angular acceleration of the airplane about its centroidal axes. Each mass element is subjected to a normal and tangential acceleration and thus each mass element is subjected to a force acting toward the c.g. of the airplane and normal to the radius arm connecting element to c.g. To place the airplane in equilibrium for stress analysis purposes, the acceleration forces are assumed acting in the opposite directions and are referred to as inertia forces.

Fig. D1.1 illustrates in general the main forces on the airplane in an accelerated flight condition. For a steady horizontal flight condition IL, ID and MI would be zero. For an accelerated flight condition, involving translation, but not angular acceleration of the airplane about its (c.g.), the inertia force M_I would be zero.

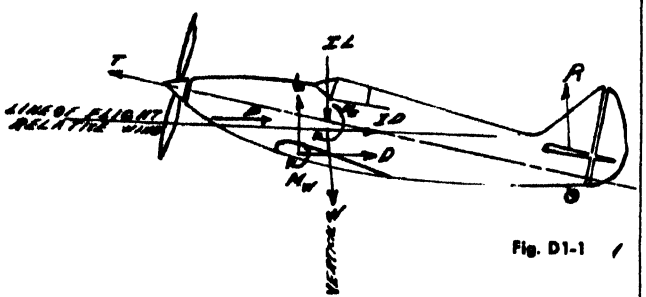


Fig. D1-1

T = engine thrust

L = wing lift

D = wing drag

P = parasite drag of airplane less wing

M_W = wing aerodynamic moment

W = weight of airplane

IL = inertia force normal to flight path

ID = inertia force parallel to flight path

M_I = inertia resisting couple

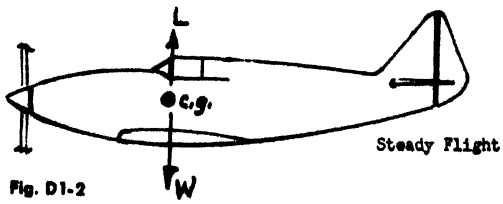
R = tail load normal to flight path

D1.4 Applied Load Factors. Design Load. Factor of Safety. Margin of Safety.

The term load factor can be defined as the numerical multiplying factor by which the forces on the airplane in steady flight are multiplied to obtain a static system of forces equivalent to the dynamic force system acting during the acceleration of the airplane. Fig. D1.2 represents the loads in steady flight where the lift L of the air forces equals the weight W of the airplane. In Fig. D1.3, the airplane is subjected to the normal acceleration (a). nL represents the external force which must be applied to the airplane to give the acceleration (a). The reversed inertia force due to this acceleration equals Wa/g. Writing the equation for the equilibrium of forces in the vertical direction, we obtain

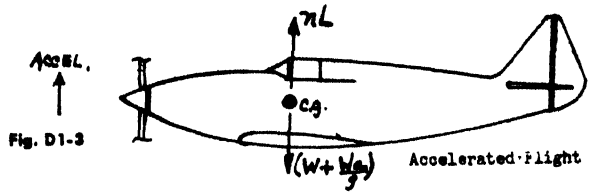
$$nL - W - Wa/g = 0 \quad \text{hence,} \quad n = 1 + a/g$$

The term a/g represents the load factor increment and n the load factor.



Steady Flight

Fig. D1-2



Accelerated Flight

Fig. D1-3

The "applied" load factor, also referred to as the "limit" load factor is the maximum load factor which the airplane is expected to be subjected in any type of maneuver. For military airplanes, these factors are determined by the Army and Navy. For pursuits and fighters, which must be highly maneuverable at all speeds, the applied load factors are relatively high. For the heavy bomber where maneuverability is secondary, the applied load factors are relatively small as compared to the pursuit airplane. The Civil Aeronautics Authority specified the load factors for all classes of airplanes. These factors are the results of many years of experience, and involve a consideration of gross weight, power loading, etc.

The airplane structure under the applied air loads should not suffer a permanent appreciable set, that is, the member stresses under the maximum applied loads should not be above the yield strength of the material.

The design flight loads are equal to the applied loads multiplied by a factor of safety. The airplane structure must take the design loads without failure, or the ultimate strength of the structure must be sufficient to carry the design loads. The usual factor of safety on the applied loads is 1.5, hence

Design loads = applied loads times 1.5.

It is customary in structural analysis to give the margin of safety of the ultimate strength of the member with respect to the design load for the member. Thus margin of safety,

$$M.S. = \frac{\text{Ultimate strength of member}}{\text{Design load for member}} - 1$$

or

$$M.S. = \frac{\text{Ultimate stress for member}}{\text{Design stress for member}} - 1$$

Thus summarizing, the structural members of the airplane must carry the stresses due to the applied loads on airplane without exceeding the yield strength of the material and must also carry a ultimate stress or load due to the design loads on airplane which are equal to the applied loads times a factor of safety.

In the design of a tension member, if the material properties are such that the ultimate tensile strength of the material is more than 1.5 times the yield strength of the material, the design of the member should be based on the applied loads and the yield strength of the member. If designed on the basis of the design loads and the ultimate strength of the material, the member would have permanent set under the applied loads.

D1.5 Aerodynamic Force Components on Wing.

For convenience, the resultant aerodynamic load at a given location on the span of a wing is usually resolved into lift and drag components, perpendicularly and parallel, respectively to the flight path and applied at the aerodynamic center and a couple about the spanwise axis. Since the airfoil characteristics are given in absolute (non-dimensional) coefficients, the lift and drag and moment components can be referred to for simplicity in coefficient form. Fig. D1.4 shows the lift and drag coefficients acting thru the aerodynamic center of the airfoil section, plus a couple M_{ac}. The moment can

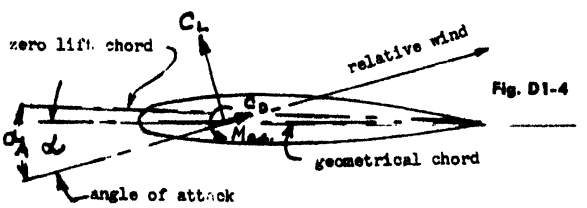


Fig. D1-4

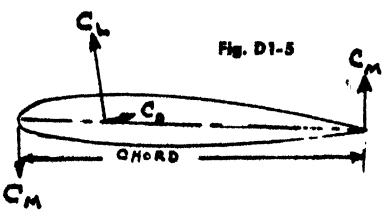


Fig. D1-5

be considered to be of the same nature as the force components if the force to which it corresponds is applied as a couple at the ends of the airfoil chord as illustrated by the coefficient C_m in Fig. D1.5.

Experiments on airfoils show that the lift and drag forces are proportional to air density (ρ), airfoil surface (S) and the square of the relative air velocity (V^2) for a given angle of attack (α) between the airfoil chord (c) and the path of the relative wind. Thus,

$$\text{Lift} = \frac{\rho}{2} C_L V^2 S \quad \text{----------(1)}$$

$$\text{Drag} = \frac{\rho}{2} C_D V^2 S \quad \text{----------(2)}$$

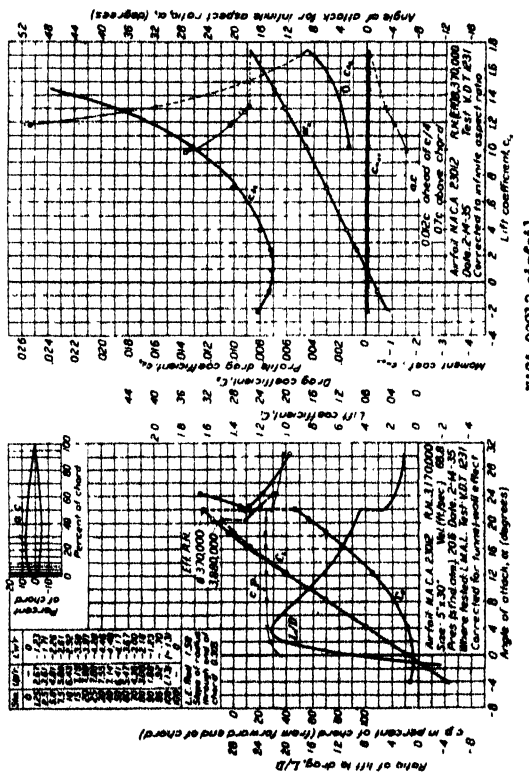
$$\text{Moment} = \frac{\rho}{2} C_M V^2 S C \quad \text{----------(3)}$$

Experiments show that for every airfoil, there is some angle of attack which will give a resultant force on the airfoil in the direction of the relative wind. This is the angle of attack of zero lift. The zero lift chord is a line in this direction through the trailing edge of the airfoil. (See Fig. D1.4). Angles measured from the zero lift chord are called absolute angles of attack (α_a).

The lift and drag components could be considered to act through the center of pressure (c.p.) for the given airfoil for the given angle of attack, however, it is more convenient to refer them to a point on the airfoil section about which the moment coefficient C_m is constant for all positive or negative angles of attack. This point is referred to as the aerodynamics center of the section. Fig. D1.6 illustrates typical curves for airfoil coefficients as determined experimentally.

D1.6 Structural Coefficients.

In certain types of wing structures such as that for an externally braced monoplane where the structure usually consists of two beams



NACA 23012 airfoil. (Ref. NACA TR 610.)

Fig. D1-6

and a drag truss, it is convenient for structural analysis purposes to resolve the aerodynamic force coefficients in the lift and drag direction into components in the beam and drag truss directions. Thus, in Fig. D1.4, if the drag truss coincided with the airfoil chord and the beams were placed normal to the chord, the resultant air forces in coefficient form in the drag truss and beam directions would be

$$C_B = C_L \cos \alpha + C_D \sin \alpha$$

$$C_C = -C_L \sin \alpha + C_D \cos \alpha$$

and the moment about the aerodynamic center is reacted by a couple with forces in the beam direction.

For monocoque, cantilever box construction, the axes for resolution of structural force components are usually taken as those which the particular investigator thinks are most convenient.

D1.6a Spanwise Distribution of Airfoil Characteristics.

Unfortunately, the spanwise distribution of the lift drag and moment coefficient are not constant, and each has a different distribution than the other. There are well-known methods for calculating this spanwise variation in the airfoil coefficients (see ANC-1, but an explanation of the methods are too lengthy to be included in this chapter. Since the conventional wing is usually tapered in plan form and since the coefficients vary spanwise, the spanwise running airloads on the wing will not follow any simple relationship and thus the calculations of shears and moments on the wing consists in resolving the variable distributed load into an equivalent system of concentrated loads on strip areas of the wing of such width as to give reasonable accuracy.

D1.7 Design Flight Conditions for Airplane Wings.

The Civil and Military Aeronautics Authorities in general issue requirements which specify the design conditions for the particular type or size of airplane. It does not seem wise here to repeat the requirements of the government publications.

Generally speaking, any airplane flight attidue can be completely defined by stating the existing values of the load factor (acceleration) and the airspeed (or more properly the dynamic pressure).

The accelerations on the airplane are produced from two causes, namely, maneuvers and air gusts. The accelerations due to the maneuvers are subject to the control of the pilot who can manipulate the controls so as not to exceed a certain acceleration. In highly maneuverable military airplanes, an accelerometer is included in the cockpit instruments as a guide for the pilot when testing or when subjecting the airplane to violent maneuvers at high speeds. For commercial airplanes the maneuver factors are placed high enough to take care of any maneuvers required in the normal operation of the given airplane. These limiting maneuver factors or accelerations are based on years of operating experience and have given satisfactory results from a safety standpoint without penalizing the airplane from a weight design standpoint.

The accelerations due to the airplane striking a gust are not under the control of the pilot, since it depends on the velocity and direction of the gust and the velocity of the airplane. From much accumulated data obtained by installing accelerometers in commercial and military airplanes and flying them in all types of weather and locations, it has been found that a gust velocity of 30 ft./sec. appears sufficient.

The speed or velocity of the airplane likewise effects the loads on the airplane. The higher the velocity the higher the aerodynamic moment about the aerodynamic center of the airfoil. Furthermore, accelerations due to gusts increase with airplane velocity, thus it is customary to place a limit on the top speed of an airplane, except in certain cases as the military pursuit airplane which may not be restricted and since the permissible maneuver factors are so high for this class of airplanes, the gust acceleration is not excessive when compared to the maneuver factors.

For commercial airplanes, the speed is usually limited to a reasonable glide speed which is sufficient to take care of normal necessary flying operations. In many cases of commercial airplane design accelerations due to gusts are critical and since gust factors increase with airplane velocity, no limitation on commercial airplane glide speeds would be detrimental from a structural weight saving standpoint.

D1.8 Gust Load Factor.

When a sharp edge gust strikes the airplane in a direction normal to the thrust line (X axis), a sudden change takes place in the wing angle of attack with no sudden change in airplane speed. The normal force coefficient (C_{Z_A}) can be assumed to vary linearly with the angle of attack. Thus in Fig. (a), let point (B) represent the normal airplane force coefficient C_{Z_A} necessary to maintain level flight with a velocity V and point (C) the value of C_{Z_A} after a sharp edged gust KU has caused a sudden change $\Delta\alpha$ in the angle of attack without change in V. The total increase in the airplane load in the Z direction can therefore be expressed by the ratio C_{Z_A} at B.

From Fig. (b) for small angles, $\Delta\alpha = KU/V$ and from Fig. (a), $\Delta C_{Z_A} = m\,\Delta\alpha$, where m = the slope

of the airplane normal force curve (C_{Z_A} per radian).

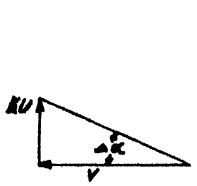


Fig. b

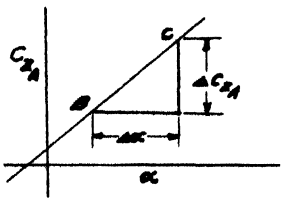


Fig. a

The load factor increment due to the gust KU can then be expressed

$$\Delta n = \frac{\Delta C_{Z_A}}{C_{Z_A}} = \left(\frac{KUm}{V}\right)\left(\frac{\rho V^2 S}{2W}\right) = \frac{KUVS_m}{575\ W} \quad -----(A)$$

where

U = gust velocity in ft./sec.

K = gust correction factor depending on wing loading (Curves for K are provided by Civil Aeronautics Authorities)

V = indicated air speed in miles per hour.

S = wing area in sq. ft.

W = gross weight of airplane

If U is taken as 30 ft/sec. and m as the change in C_{Z_A} with respect to angle of attack in absolute units per degree, equation (A) reduced to the following

$$\Delta n = \frac{3KmV}{W/S} \quad ----------(B)$$

Therefore the gust load factor n when airplane is flying in horizontal altitude equals

$$n = 1 \pm \frac{3KmV}{W/S} \quad ----------(C)$$

and when airplane is in a vertical altitude

$$n = \pm \frac{3KmV}{W/S} \quad ----------(D)$$

D1.9 Illustration of Main Design Flight Conditions. Velocity-Load Factor Diagram.

As discussed in Art. D1.7, the main design flight conditions for an airplane could be given by stating the limiting values of the acceleration and speed and in addition the maximum value of the applied gust velocity. As an illustration, the design loading requirements for a certain airplane could be stated as follows: "The proposed airplane shall be designed for applied positive and negative accelerations of + 6.0g and -3.5g respectively at all speeds from that corresponding to $CL_{max.}$ up to 1.4 times the maximum level flight speed. Furthermore, the airplane shall withstand any applied loads due to a 30 ft./sec. gust acting in any direction up to the restricted speed of 1.4 times the maximum level flight speed. A design factor of safety of 1.5 shall be used on these applied loads".

In graphical form these design requirements can be represented by plotting load factor and velocity to obtain a diagram which is generally referred to as the Velocity-acceleration diagram.* The results of the above specification would be similar to that of Fig. D1.7. Thus, the lines AB and CD represent the restricted positive and negative maneuver load factors which are limited to speeds inside line BD which is taken as 1.4 times the maximum level flight speed in this illustration. These restricted maneuver lines are terminated at points A and C by their intersection with the maximum C_L values of the airplane. At speeds between A and B, the pilot must be careful not to exceed the maneuver accelerations, since in general, it would be possible for him to manipulate the controls to exceed these values. At speeds below A and C, there need be no care of the pilot as far as loads on the airplane are concerned since a maneuver producing $C_{L_{max.}}$ would give an acceleration less than the limited values given by lines AB and CD.

The positive and negative gust accelerations due to a 30 ft./sec. gust normal to flight path are shown on Fig. D1.7. In this example diagram, a positive gust is not critical within the restricted velocity of the airplane since the gust lines intersect the line BD below the line AB. For a negative gust, the gust load factor becomes critical at velocities between F and D with a maximum acceleration as given by point E.

For airplanes which have a relatively low required maneuver factor the gust accelerations may be critical for both positive and negative accelerations. Examination of the gust equation indicates that the most lightly loaded condition (smallest gross weight) produces the highest gust load factor, thus involving only partial pay load, fuel, etc.

On the diagram, the points A and B correspond in general to what is referred to as high angle of attack (H.A.A.) and low angle of attack (L.A.A.) respectively, and points C and D the inverted (H.A.A.) and (L.A.A.) conditions respectively.

Generally speaking, if the airplane is designed for the air loads produced by the velocity and acceleration conditions at points A, B, E, F, and C, it should be safe from a structural strength standpoint if flown within the specified limits regarding velocity and acceleration.

Basically, the flight condition requirements of the Civil Aeronautics Authority, Army, and Navy are based on consideration of specified velocities and accelerations and a consideration of

*This type of diagram was originally developed by Lundquist and Rhode of the NACA and modified by others.

gusts, thus a student understanding the basic discussion above should have no difficulty understanding the design requirements of these three government agencies.

For stress analysis purposes, all speeds are expressed as indicated air speeds. The "indicated" air speed is defined as the speed which would be indicated by a perfect air-speed indicator, that is, one that would indicate true air speed at sea level under standard atmospheric conditions. The relation between the actual air speed V_a and the indicated air speed V_i is given by the equation

$$V_i = \sqrt{\frac{\rho_a}{\rho_o}}\ V_a$$

where

V_i = indicated airspeed

V_a = actual airspeed

ρ_o = standard air density at sea level

ρ_a = density of air in which V_a is attained

D1.10 Special Flight Design Conditions.

There are many other flight conditions which may be critical for certain portions of the wing or fuselage structure. Most airplanes are equipped with flaps, to decrease the landing speed and such flaps are lowered at speeds at least twice that of the minimum landing speed. Since the flapped airfoil has different values for the magnitude and location of the airfoil characteristics, the wing structure must be checked for all possible flap conditions within the specified requirement relative to maximum speed at which the flaps may be operated. Generally speaking, the flap conditions will effect only the wing portion inboard of the flap and it is usually only critical for the rear beam web or shear wall and for the top and bottom walls of the torsion box. This is due to the fact that the deflected flap moves the center of pressure considerably aft thus producing more shear load on the rear shear.wall as well as torsional moment on the conventional cantilever box metal beam.

The airplane must likewise be investigated for aileron conditions. Operation of the ailerons produce a different air load. On each side of the airplane wing which produces an angular rolling acceleration of the airplane. Furthermore, the deflected ailerons change the magnitude and location of the airfoil characteristics, thus calculations must be carried out to determine whether the loads in the aileron conditions are more critical than those for the normal flight conditions.

For angular acceleration resulting from pitching moments due to air gusts on the tail, the loads on the wing should be checked for cases where the engines are attached to the wing and are located forward of the leading edge, since large inertia reactions are produced due to the pitching acceleration.

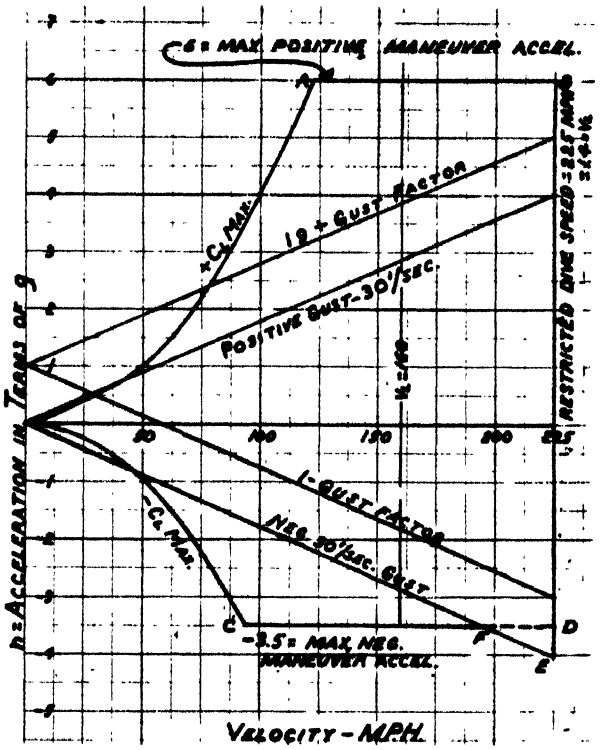


Fig. D1.7

In cases where the landing gear is attached to wing or when the fuel and engines are carried in and on the wing, the loads produced on the wing structure in a landing condition may be critical for some portions of the wing structure inboard of landing gear and engine attachment points.

D1.11 Reference Axes for Computing External Wing Shears and Moments.

In the load analysis of the normal wing, the actual procedure in calculating the wing design shears and moments may become quite confusing because the wing shape usually includes dihedral and sweepback and aerodynamically the spanwise distribution of the airfoil coefficient is variable and thus the angle of attack varies along the span. Furthermore, the load analysis for the wing is usually started long before serious consideration is given to the internal distribution of the structural material and thus any so-called elastic axes, or shear center locations are not available when the load analysis is made. Consequently, it is the practice of the structures department of most airplane companies to completely separate the load analysis

from the geometry of the internal structure by referring all shears and moments to an arbitrary selected load axis. This load axis is a straight line drawn normal to the plane of symmetry of the airplane. It is usually located at some convenient point forward and either above or below the wing. The other two axes in the plane of symmetry are most conveniently located normal and parallel to the thrust line and pass through the intersection of the load axis and the plane of symmetry, which thus locates the origin of coordinates. Fig. D1.8 illustrates such reference axis. All wing shears and moments due to air and dead weight loads are thus referred to this load axis. Later in designing and stress analyzing the internal structure of the wing, such forces can be transferred to any other axis. Fig. D1.8 illustrates the sign convention for moments about the X, Y and Z axes.

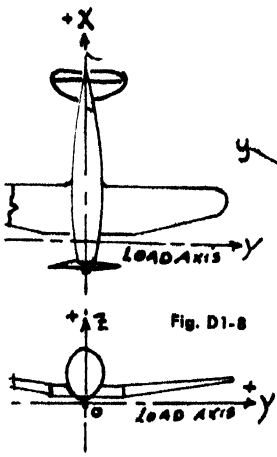


Fig. D1.8

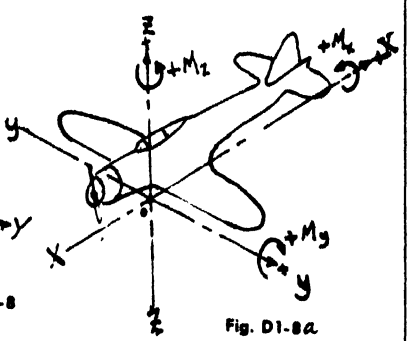


Fig. D1.8a

M_y is positive for clockwise rotation about the Y axis when looking inboard from left wing tip.

M_x is positive for clockwise rotation about the X axis when looking forward from the rear.

M_z is positive for counter-clockwise rotation about the Z axis when looking down toward airplane.

EXAMPLE PROBLEM

The Applied Loads on the Airplane in Normal Flight

D1.12 Introduction.

The determination of the applied air loads on the airplane and the resulting shears and moments on the wing is a job involving a large amount of calculation. The specified flight conditions and factors are usually given in different form by the various government agencies and the stress analysis departments of the various airplane companies usually have a different procedure of arriving at the final required result namely the external shears, bending and torsional moments on the wing. The example problem which follows is for the purpose of familiarizing the student with the general procedure so that on contact with the procedures as used by airplane companies, no difficulty should be encountered in understanding them.

D1.13 General Data and Design Specifications.

Figs. D1.9 and D1.9a shows general and dimensional data of a proposed airplane. Table D1.1 gives a weight and balance calculations for locating the airplane center of gravity.

The specifications for the normal flight applied accelerations and velocities will be assumed as follows:

(1) Maximum applied positive maneuver acceleration = 6.0.

(2) Maximum applied negative maneuver acceleration = - 2.5.

(3) Maximum dive speed to be limited to 1.3 maximum level speed. Assuming that a performance estimate for this airplane gave a high speed of 200 MPH, then limited dive velocity = 1.3 x 200 = 260 MPH.

(4) The airplane must also be designed for the loads due to a 30 ft./sec. gust from any angle up to a airplane velocity of 260 MPH.

(5) For design loads a factor of safety of 1.5 will be required.

D1.14 General Procedure.

The object of this problem is to determine the wing shears, and moments due to the air loads with respect to a convenient set of axes and for all flight design conditions. These design forces are then used by the stress analysis engineer to investigate the internal resisting forces for proportioning of the distribution and size of the internal wing structure. In Chapter C9, the results of this problem are applied to the analysis and design of the internal structure.

The general procedure in arriving at the final shears and moments will be as follows:

(1) Determine characteristics of airfoil force coefficients.

(2) Determine spanwise distribution of airfoil force coefficients.

(3) Resolve airfoil force coefficients along two convenient axes in the XZ plane at right angles of each other.

(4) Determine resultant air loads on wing in coefficient form relative to selected X, Y and Z axes.

(5) Balance airplane to find tail and airplane load coefficients.

(6) Determine total applied air loads on wing for the various design conditions.

Reference Axis

TABLE D1.1 - WEIGHT & BALANCE
Vert. (Z) arms measured from thrust line (+ is up)
Horiz. (X) arms measured from Z axis 5" forward prop. ∮ (+ is aft)

Item No.		W = Wt.#	Horiz. Arm (X) (in.)	Horiz. Moment wx	Vert. Arm (Z)	Vert. Mom. wz
1	Power Plant	1160	19	26600	0	0
2	Fuselage Group	350	113.5	39700	1	350
3	Wing Group	750	97	72750	-18	-13500
4	Tail Group	110	287	31550	24	2640
5	Surface Controls	85	127	10800	-14	- 1190
6	Electrical System	130	61	7930	4	520
7	Chassis Front	235	70	16450	-52	-12200
8	Tail Wheel Group	35	306	10700	-10	- 350
9	Furnishings	220	116	25520	5	1100
10	Radio	125	181	22600	10	1250
	Weight empty =	3140		268900		-21380
11	Pilot	200	151	30200	4	800
12	Student	200	98	19600	4	800
13	Fuel System	780	89	67600	-27	-20500
	Gross weight =	4300		376500		-40280

Calculation of C.G. locations:
Gross wt. - x = 376500/4300 = 87.5" aft of Ref. Axis
z = -40280/4300 = -9.4" below thrust line

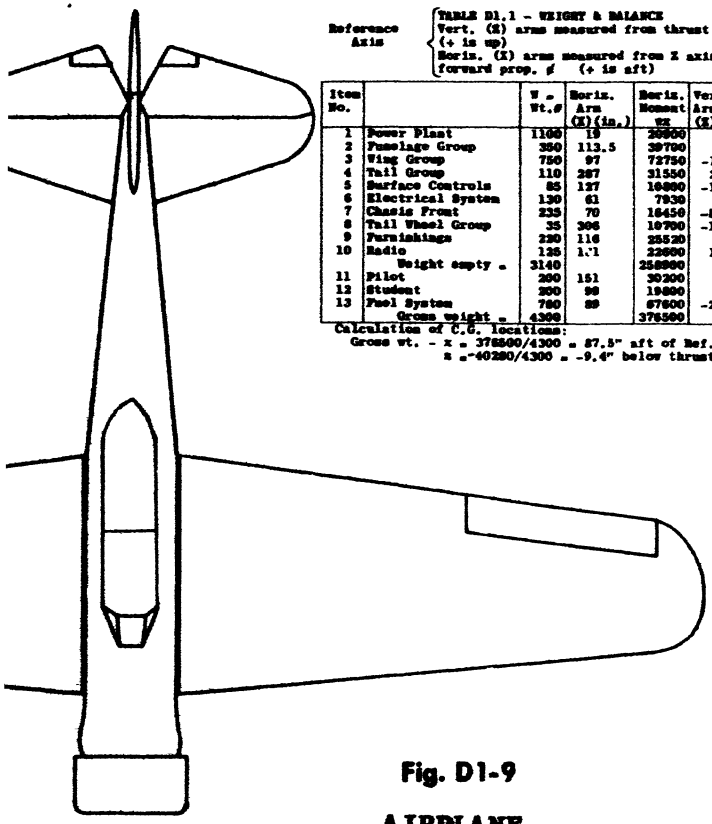
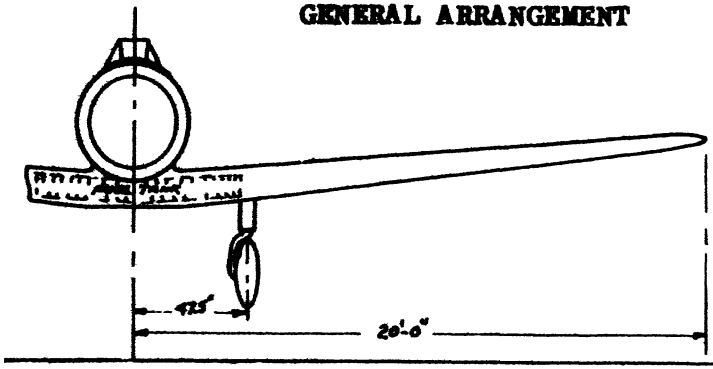
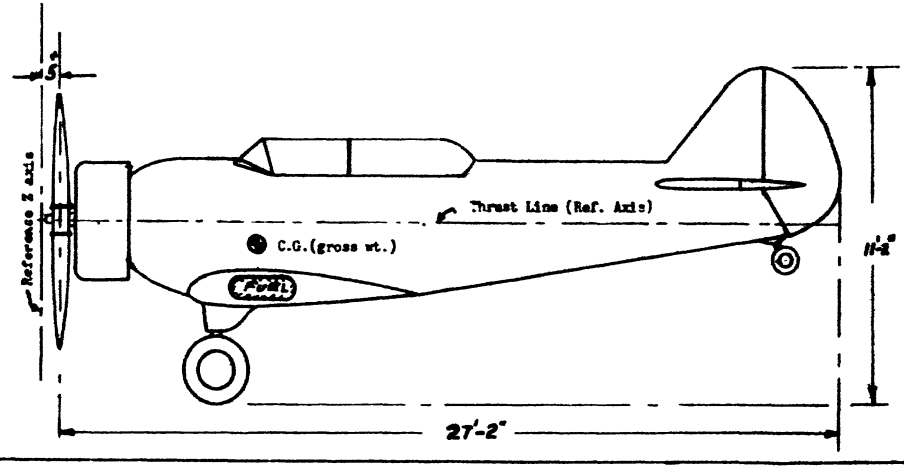


Fig. D1-9

AIRPLANE
GENERAL ARRANGEMENT





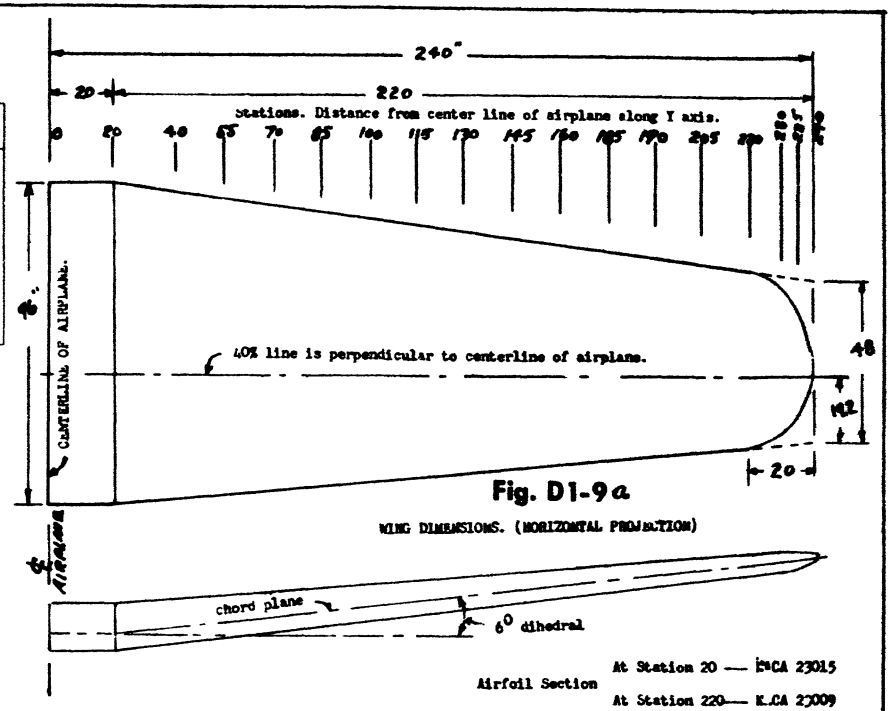


Fig. D1-9a

WING DIMENSIONS. (HORIZONTAL PROJECTION)

(7) Make unit analysis for shears and moments with respect to reference axes.

(8) By proportion using results of (6) and (7), calculate design shears and moments with respect to reference axes.

D1.15 Corrected Airfoil Characteristics.

The standard airfoil characteristics for conventional airfoils are available from NACA Reports and Technical Notes. These in general need correction to apply to a given wing which has a different aspect ratio. Considerable data is also available on corrected airfoil characteristics for wings with certain taper ratios in planform as well as wing thickness. Airfoil characteristics are also obtained by wind tunnel tests of the model of the actual wing shape to be used.

In the given wing of Fig. D1.9 the airfoil section tapers from a NACA series 23015 at wing root to a 23009 near the tip. For this simplified problem the airfoil characteristics for a 23012 airfoil will be used as the average for the wing. This would introduce very little error since the difference between the airfoil characteristics for the various thickness is not large.

Table D1.2 (Part A) gives the calculations for obtaining the corrected airfoil data. Columns 1, 2 and 3 give the airfoil characteristics for a 23012 airfoil section for a wing of infinite aspect ratio. Columns 4, 5, 6 and 7 give the corrections necessary for the aspect ratio of 6.56 which is the value for the wing in the problem. The explanation of the correction equations is given below Table D1.2 (also refer to any textbook on aerodynamics).

D1.16 Resolution of Lift and Drag Coefficients Into Components Along X and Z Axes.

It is customary in routine wing stress analysis to resolve the wind lift and drag components for the various wing angle of attacks into components along two convenient axes at right angles to each other. Frequently axes parallel to the beam webs and normal to the beam webs are selected as reference axes for resolution. In general, for semi-monocoque construction reference axes for resolution of wing forces parallel to the Z and X axes are convenient, and in this example problem the lift and drag components of the air forces will be resolved into components parallel to the X and Z axes.

Thus, in Fig. D1.10, resolving the force coefficients into components parallel to the Z and X axes:

$$C_Z = C_L \cos (\alpha - 2^0) + C_D \sin (\alpha - 2^0)$$

$$C_X = -C_L \sin (\alpha - 2^0) + C_D \cos (\alpha - 2^0)$$

Table D1.2 (Part B) gives the calculations for the Z and X components for the lift and drag coefficients for various angles of attack.

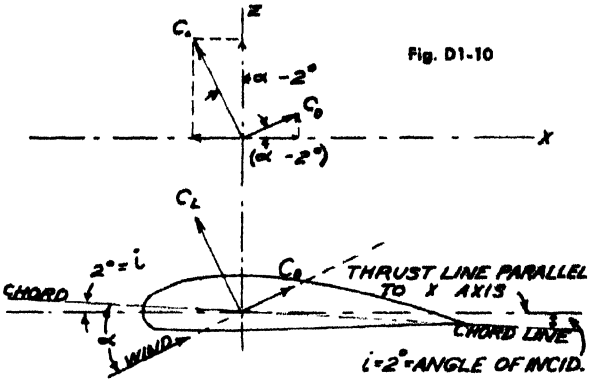


Fig. D1-10

D1.17 Spanwise Distribution of Airfoil Coefficients.

For many years it was customary to assume simplified spanwise distribution of the airfoil coefficients as illustrated in Fig. D1.11.

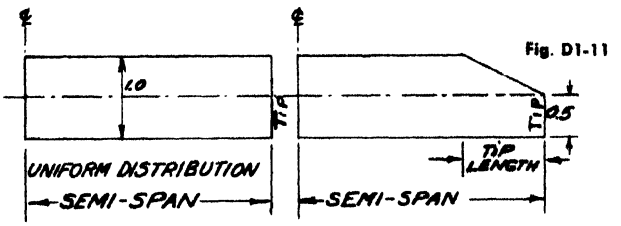


Fig. D1-11

For highly tapered wings, these arbitrary distributions prove unsafe, and thus the general procedure now usually followed is to calculate the spanwise variation of the airfoil coefficients. For convenience, the resultant aerodynamic load at a given location along the span of a wing can be resolved into a force system consisting of a lift and drag force acting normal and parallel to the flight path respectively and applied at the aerodynamic center plus a couple about the spanwise axis. The drag force may be further broken down into profile and induced drag, the profile drag being the sum of a minimum and an additional profile drag. The curves of distribution along the span of lift, moment and the three component drags are different in general. For stress analysis purposes simplifying assumptions on some of the component distributions are sometimes made, since the effect on the wing shears and moments would not be appreciable.

The detailed explanation and recommended procedures for calculating the spanwise distribution of the airfoil coefficients is given in government publication ANC-5[1] "Spanwise Air-Load Distribution". Space does not permit the explanation and illustration of the general procedure, since the above publication contains some 200 pages.

TABLE D1.2
Calculation of Corrected Airfoil Characteristics and the Components of the Force Coefficients Along the E and X Axes.

PART A	1	C_L Infinite AR	1.627	1.567	1.490	1.319	1.135	.935	.730	.525	.323	.120	0	.090	- .226	- .539	- .844	- 1.135
	2	α_o Infinite AR	16.2	16.1	14.0	12.0	10.0	8.0	6.0	4.0	2.0	0	-1.1	-2.0	-3.3	-6.4	-9.4	-12.5
	3	C_{D_o} Infinite AR	.0390	.0310	.0262	.0194	.0148	.0123	.0109	.0098	.0088	.0086	.0087	.0088	.0093	.0109	.0135	.0195
	4	$\Delta\alpha$ = 2.78 C_L	4.5	4.4	4.1	3.7	3.2	2.6	2.0	1.5	.9	.3	0	- .3	- .6	-1.5	- 2.3	- 3.2
	5	α = (2) + (4)	20.7	19.5	18.1	15.7	13.2	10.6	8.0	5.5	2.9	.3	-1.1	-2.3	-3.9	-7.9	-11.7	-15.7
	6	ΔC_D = .0485 C_L^2	.1284	.1191	.1077	.0843	.0625	.0424	.0256	.0134	.0051	.0007	0	.0004	.0025	.0141	.0348	.0625
	7	C_D = (3) + (6)	.1674	.1501	.1339	.1037	.0773	.0547	.0365	.0232	.0139	.0093	.0087	.0092	.0118	.0250	.0481	.0820
	8	Cos (α -i) = cos (5)-2°)	.947	.954	.960	.971	.981	.987	.995	.998	.999	.999	.998	.997	.995	.985	.971	.952
	9	sin (α -i) = sin (5)-2°)	.3210	.3010	.2775	.237	.1943	.1496	.1045	.061	.0157	-.0297	-.0541	-.075	-.1028	-.1720	-.237	-.304
PART B	10	C_{L_E} = (1) x (8) x.995	1.532	1.488	1.422	1.273	1.108	.918	.722	.521	.321	.119	0	-.0894	-.224	-.528	-.816	-1.075
	11	C_{D_E} = (7) x (9) x .995	.0534	.045	.0369	.0245	.0149	.0082	.0038	.0014	.0002	-.0003	- .0005	-.0007	-.0012	-.0043	-.0113	- .0248
	12	C_{L_X} = -(1)x (9)	- .5220	-.4710	-.4135	-.3125	-.2206	-.1400	-.0763	-.0320	-.0051	.0036	0	-.0068	-.0232	-.0927	-.2000	- .3450
	13	C_{D_X} = (7) x (8)	.1586	.1431	.1285	.1006	.0759	.0540	.0363	.0232	.0139	.0093	.0087	.0092	.0117	.0246	.0467	.0780

Explanatory Notes:

(4) $R = \frac{b^2}{S} = \frac{(480)^2}{35048} = 6.56$

$\Delta\alpha = 18.24\ K\ C_L$, $K = \frac{1}{R} = \frac{1}{6.56}$

$\Delta\alpha = \frac{18.24}{6.56}\ C_L = 2.78\ C_L$

(6) and (7)

$C_D = C_{D_o} + \Delta C_{D_i}$

$\Delta C_{D_i} = \frac{C_L^2}{\pi R} \quad \frac{C_L^2}{\pi 6.56} - .0485\ C_L^2$

A plote of the coefficients in the above Table is given in Fig. D1.16.

(8) and (9)

Angle of incidence = 2° = i
Angle between geometric chord and Z.L.C. = 1.1°

(10) Approximate effective Z component of C_L and C_D due to dihedral of outer panel θ =-6°

$$\left[\frac{P_L \text{ outer panel}}{P_L \text{ total}} \cos\theta + \frac{P_L \text{ center panel}}{P_L \text{ total}}\right] C_L =$$

$$\left[\frac{15604}{17524} \cos\theta + \frac{1920}{17524}\right] C_L = .995\ C_L$$

(11) Drag correction for dihedral angle, θ

$$\left[\frac{P_D \text{ outer panel}}{P_D \text{ total}} \cos\theta + \frac{P_D \text{ center panel}}{P_D \text{ total}}\right] C_D =$$

$$\left[\frac{15406}{17556} \cos\theta + \frac{2150}{17556}\right] C_D = .995\ C_D$$

The purpose of this example problem is to give the student a general over-all picture as to how the design wing shears and moments are arrived at and therefore the tedious process of calculating the spanwise distributions will not be gone into, but the following assumptions will be made.

(1) The spanwise distribution of the moment coefficient will be assumed constant.

(2) The spanwise distribution of lift (C_L) and drag (C_D) will be assumed as that shown by the curves of Fig. D1.12. In general, these curves represent approximately the actual distribution for this particular wing.

D1.18 Resultant Wing Forces in X and Z Directions Referred to Arbitrary Y Load Axis. Magnitude of Resultant Aerodynamic Wing Moment About Spanwise (Y) Axis.

For stress analysis purposes it is customary to consider the accelerated airplane in a static condition of equilibrium by reversing the inertia forces. In general the resultant of the air forces does not pass thru the center of gravity of the airplane, thus requiring a tail load for equilibrium. To find the tail load coefficient as well as the relation between the airplane and wing coefficients, it is necessary to know the direction and location of the resultant air forces.

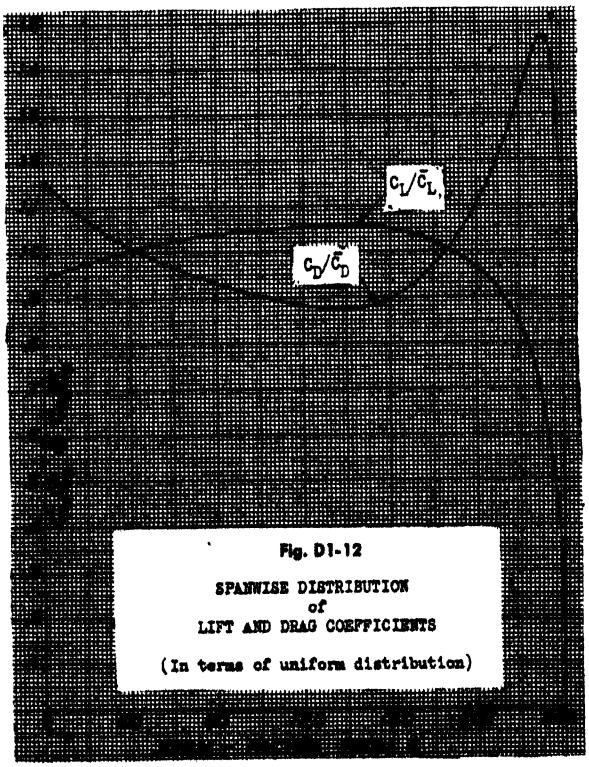


Fig. D1-12

SPANWISE DISTRIBUTION
of
LIFT AND DRAG COEFFICIENTS

(In terms of uniform distribution)

In this example problem, the resultant air force on a wing strip element will be resolved into components parallel to the X and Z axes at the aerodynamic center (a.c.) of the airfoil strip elements plus a couple about the aerodynamic center. In Article D1.17, the spanwise variation of the wing moment coefficient ($C_{M_{a.c.}}$) was assumed as constant. To find the total aerodynamic wing moment, it is convenient to find the mean aerodynamic chord (M.A.C.). Table D1.3 gives the calculations for determining the (M.A.C.) for constant spanwise variation of moment coefficient. The horizontal projected area of the semi-span has been divided into 19 strips bounded by the station numbers as listed in column (1) of Table D1.3. Due to the curvature in planform of the wing tip, the strip widths near the tip are decreased to obtain reasonable accuracy. The results of the Table D1.3 give the length of the (M.A.C.) as 77 inches.

TABLE D1.3

Determination of Mean Chord

1	2	3	4	5	6	7
Dist. from ℄ along Y Axis = y	Chord C	C^2	C^2 ave.	Δ y Strip Width	Area x chord = $\Delta y C^2$ ave. = a·c	$\sum$a·c
240	0	0	0	0	0	0
235	33.8	1142	571	5	2855	2855
230	45.0	2025	1584	5	7920	10775
220	52.3	2735	2380	10	23800	34575
205	55.6	3090	2913	15	43650	78225
190	58.9	3470	3280	15	49700	127925
175	62.1	3860	3665	15	55000	182925
160	65.4	4280	4070	15	61000	243925
145	68.7	4730	4505	15	67600	311525
130	72.0	5184	4957	15	74350	385875
115	75.3	5670	5427	15	81400	467275
100	78.5	6160	5915	15	88750	556025
85	81.8	6700	6430	15	96400	652425
70	85.1	7250	6975	15	104600	757025
55	88.4	7820	7535	15	113000	870025
47.5	90.1	8110	7965	7.5	59750	929775
40	91.7	8410	8260	7.5	62000	991775
20	96.0	9220	8815	20	176300	1168075
0	96.0	9220	9220	20	184400	1352475

$\sum$a = area of semi-wing = 17524 sq. in. (Horiz. projection)

Mean aerodynamic chord M.A.C. = $\frac{\sum a \cdot c}{\sum a} = \frac{1352475}{17524} = 77'' =$ M.A.C.

In Art. D1.17, the spanwise distribution of the lift coefficient (C_L) and the drag coefficient (C_D) was assumed as that given by the curves of Fig. D1.12. Since the distributions are different the resultant force coefficients in the Z and X directions will be determined for each spanwise distribution. Tables D1.4 and D1.5 give the calculations. The resoltuion of the X and Z components of the air forces is made with respect to a convenient (Y) load axis, taken forward and below the wing as shown in Fig. D1.13 and D1.14, which also shows the X and Z reference axes. The air forces as explained before act thru the aerodynamic center (a.c.) of the airfoil section. Fig. D1.13 shows the location of the (a.c.) for positive angle of attack conditions. The equations below Fig. D1.14 give the distances from the (a.c.) to the reference load axis Y. Tables D1.4 and D1.5 give only the calculations for the

TABLE D1.4

Centroids of C_{L_z} and C_{L_x} Forces

1	2	3	4	5	6	7	8	9	10	11	12	13	14	15	16	17	18
Sta. Dist. from c Along Y axis = y	Chord Length	$C_z = C_x \frac{C_L}{C_L}$ from Fig. D1.12	CC_z (2)(3)	(CC_z)ave.	Dist. between Station Δy	$\Sigma C_z = \Delta y(CC_z)$ave. (5)(6)	$y\,CC_z$ (1) (4)	(yCC_z)ave.	$\Sigma C_z y = \Delta y(yCC_z)$ave. (6) (9)	x = dist. of a.c. aft of Y axis	x CC_z (11) x (4)	(xCC_z)ave.	$\Sigma C_z x = \Delta y(xCC_z)$ave. (6) (13)	Z = dist. of a.c. above Y axis	ZCC_z (4) (15)	(ZCC_z)ave.	$\Sigma C_z Z = \Delta y(ZCC_z)$ave. (6) (17)
240	0	0	0	0	0	0	0	0	0	0	0	0	0	0	0	0	0
235	33.8	.524	17.7	8.85	5.0	45	4160	2080	10400	37.00	655	328	1640	36.28	642	321	1605
230	45.0	.677	30.45	24.08	5.0	121	7010	5585	27925	34.00	952	803	4015	35.83	976	809	4045
220	52.3	.840	43.9	37.18	10.0	372	9610	8340	83400	31.40	1330	1141	11410	34.95	1530	1253	12530
205	55.6	.942	52.4	48.15	15.0	723	10750	10210	153150	30.86	1610	1470	22050	33.63	1760	1645	24670
190	58.9	.995	58.5	55.45	15.0	830	11110	10930	163950	30.31	1775	1692	25380	31.79	1865	1812	27180
175	62.1	1.033	64.2	61.35	15.0	921	11230	11175	167555	29.80	1900	1837	27555	30.98	1985	1925	28880
160	65.4	1.050	68.7	66.45	15.0	991	11000	11105	166570	29.25	2000	1950	29250	29.63	2035	2010	30150
145	68.7	1.058	72.7	70.70	15.0	1061	10530	10765	161475	28.70	2075	2037	30550	28.31	2055	2045	30680
130	72.0	1.056	76.0	74.35	15.0	1115	9880	10205	153075	28.17	2120	2097	31450	26.98	2051	2053	30790
115	75.3	1.053	79.25	77.63	15.0	1162	9120	9500	142500	27.62	2180	2150	32250	25.66	2040	2046	30690
110	78.5	1.049	82.4	80.83	15.0	1212	8240	8680	130200	27.10	2220	2200	33000	24.33	2000	2020	30300
85	81.8	1.040	85.0	83.70	15.0	1255	7220	7730	115950	26.74	2245	2232	33480	23.00	1955	1977	29640
70	85.1	1.032	88.0	86.50	15.0	1300	6160	6690	100350	26.01	2275	2260	33900	21.68	1905	1980	29700
55	88.4	1.020	90.1	89.05	15.0	1338	4950	5555	83320	25.48	2285	2280	34200	20.35	1835	1870	28050
47.5	90.1	1.010	91.0	90.05	7.5	680	4320	4635	34720	25.20	2290	2287	17150	19.68	1790	1813	13600
40	91.7	1.000	91.7	91.35	7.5	686	3670	3995	30000	24.92	2282	2286	17150	19.02	1745	1767	13250
20	96.0	.978	93.9	92.80	20.0	1861	1878	2774	55480	24.20	2280	2281	45620	17.22	1620	1683	33660
0	96.0	.947	91.0	92.45	20.0	1851	0	939	18780	24.22	2203	2241	44820	15.98	1405	1513	30260
						17524			1798860				474870				429680

A = 1/2 of projected wing area = 17524 sq.in.

Aver. Wing force coefficient $C_{L_x} = \frac{\text{Col. 7}}{A} = \frac{17524}{17524} = C_{L_x} = C_{L_z}$

Centroids of C_{L_z} and C_{L_x} forces:-

$\bar{y} = \frac{\text{Col. 10}}{A} = \frac{1798800}{17524} = 102.7"$, $\bar{x} = \frac{\text{Col. 14}}{A} = \frac{474870}{17524} = 27.1"$, $\bar{Z} = \frac{\text{Col.18}}{A} = \frac{429680}{17524} = 24.5"$

Moment of C_{L_z} and C_{L_x} about reference axis Y:-

$M_y = -27.1\ C_{L_z} + 24.5\ C_{L_x}$

TABLE D1.5

Centroids of C_{D_z} and C_{D_x} Forces

1	2	3	4	5	6	7	8	9	10	11	12	13	14	15	16	17	18
Sta. Dist. from c Along Y axis = y	Chord Length	$C_z = C_x \frac{C_x}{C_D}$ from Fig. D1.12	CC_x or CC_x (2)(3)	(CC_z)ave	Dist. between Station Δy	$\Sigma C_z = \Delta y(CC_z)$ave. (5)(6)	$y\,CC_z$ (1) (4)	(yCC_z)ave.	$\Sigma C_z y = \Delta y(yCC_z)$ave. (6) (9)	X = dist. of a.c. aft of Y axis	X CC_z (11) x (4)	(xCC_z)ave.	$\Sigma C_z x = \Delta y(xCC_z)$ave. (6) (13)	Z = dist. of a.c. above Y axis	ZCC_x (4) (15)	(ZCC_x)ave.	$\Sigma C_x Z = \Delta y(ZCC_x)$ave.. (6) (17)
240	0	0	0	0	0	0	0	0	0	0	0	0	0	0	0	0	0
235	33.8	1.41	47.6	23.8	5.0	119	11190	5595	27970	37.00	1762	881	4405	36.28	1750	875	4375
230	45.0	1.47	66.1	56.95	5.0	280	15220	13205	66030	34.00	2244	2003	10015	35.83	2368	2059	10295
220	52.3	1.335	69.7	67.90	10.0	679	15390	15305	153050	31.40	2190	2217	22170	34.95	2436	2402	24020
205	55.6	1.153	64.0	66.85	15.0	1002	13110	14250	213750	30.86	1978	2084	31260	33.63	2155	2295	34425
190	58.9	1.026	60.5	62.30	15.0	935	11500	12305	184570	30.31	1833	1905	28570	31.79	1922	2038	30570
175	62.1	.947	58.8	59.65	15.0	894	10300	10900	163500	29.80	1752	1792	26880	30.98	1823	1872	28080
160	65.4	.896	58.5	58.65	15.0	829	9360	9830	147450	29.25	1711	1732	25980	29.63	1732	1778	26670
145	68.7	.876	60.2	59.35	15.0	890	8720	9040	135600	28.70	1727	1719	25780	28.31	1702	1717	25755
130	72.0	.877	63.1	61.65	15.0	925	8200	8460	126900	28.17	1778	1752	26280	26.98	1702	1702	25530
115	75.3	.887	66.7	64.90	15.0	973	7660	7930	119080	27.62	1843	1810	27150	25.66	1710	1706	25590
100	78.5	.905	71.0	68.85	15.0	1032	7100	7380	110700	27.10	1922	1882	28230	24.33	1725	1718	25770
85	81.8	.924	75.6	73.30	15.0	1099	6430	6765	101470	26.74	2020	1971	29570	23.00	1740	1732	25980
70	85.1	.946	80.5	78.05	15.0	1170	5635	5032	90480	26.01	2096	2058	30870	21.68	1745	1743	26145
55	88.4	.974	86.0	83.25	15.0	1248	4725	5180	77700	25.48	2192	2144	32160	20.35	1750	1747	26205
47.5	90.1	.988	89.0	87.50	7.5	655	4230	4477	33600	25.20	2241	2216	16600	19.68	1751	1750	13130
40	91.7	1.01	92.5	90.75	7.5	680	3700	3965	29800	24.92	2304	2272	17000	19.02	1760	1756	13200
20	96.0	1.07	102.9	97.70	20.0	1954	2058	2879	57580	24.20	2490	2397	47940	17.22	1771	1765	35300
0	96.0	1.159	111.1	107.0	20.0	2140	0	1029	20580	24.22	2700	2595	51900	15.98	1780	1775	35500
						17524			1859810				482760				436540

A = 1/2 projected wing area = 17524 sq.in.

Aver. wing force coeff. $C_{D_x} = \frac{\text{Col. 7}}{A} = \frac{17524}{17524}$ $C_{D_x} = C_{D_z}$

Centroids of C_{D_z} and C_{D_x} forces:-

$y = \frac{\text{Col. 10}}{\text{Col. 7}} = \frac{1859810}{17524} = 106"$, $x = \frac{\text{Col.14}}{\text{Col. 7}} = \frac{482760}{17524} = 27.5"$, $z = \frac{\text{Col.18}}{\text{Col. 7}} = \frac{436540}{17524} = 24.82"$

Moment about Y axis: $M_y = 27.5\ C_{D_z} + 24.82\ C_{D_x}$

(a.c.) locations for positive angles of attack. Similar calculations should be made for the (a.c.) locations for negative angles of attack. To minimize the amount of calculations, the (a.c.) location for negative conditions will be assumed the same as given in Fig. D1.13, since the purpose of this example problem is only to give the student a general overall picture of the problem of finding the flight loads on the airplane. Tables D1.4 and 5 are self-explanatory.

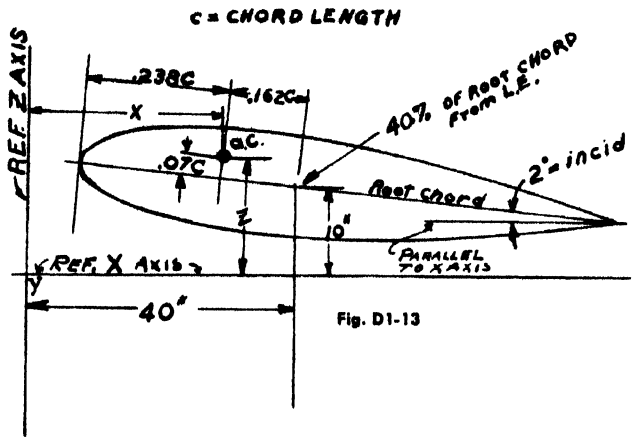


Fig. D1-13

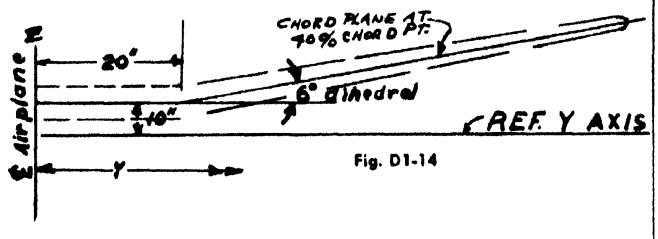


Fig. D1-14

$x = 40 - (.162C)\cos 2^0 + (.07C)\sin 2^0 = 40 - .1643C$

$z = 10 + (y \tan 6^0 - 20 \times \tan 6^0) + (.162C)\sin 2^0 + (.07C)\cos 2^0 = 7.9 + .105y + .00555C + .07C$

But from the geometry of the planform in Fig. D1.9a, the chord length C between stations 20 and 220 can be expressed $C = 100.4 - .218y$

hence

$z = 7.9 + .105y + 7.58 - .0165y$

which gives $z = 15.48 + .0885y$

D1.19 Balancing the Airplane. Solving for Tail and Airplane Load Coefficients.

In the previous article the resultant air loads on the wing in coefficient form for the lift and drag spanwise distributions were found by acting thru the reference load axis (Y), plus a moment about the Y axis. The airplane as a whole is subjected to other flight forces, such tail load, engine thrust and parasite drag of the fuselage. These forces together with the reversed inertia forces form a force system in static equilibrium.

Fig. D1.15 shows the load on the airplane in coefficient form. The resultant wing loads in the Z and X directions as found in Table D1.4 and 5 are shown acting thru the Y reference axis which is perpendicular to the X and Z plane at the intersection of reference axes X and Z. The moments of the X and Z force components about the load axis (Y) as taken from Tables D1.4 and 5 are also shown. The other forces as shown on Fig. D1.15 are the wing aerodynamic moment $C_{M(a.c.)}$, the engine thrust T, the fuselage parasite drag C_p and the normal tail load C_t. For simplicity, it is usually better to assume a power off condition and treat the engine forces as a separate item in later investigations. In

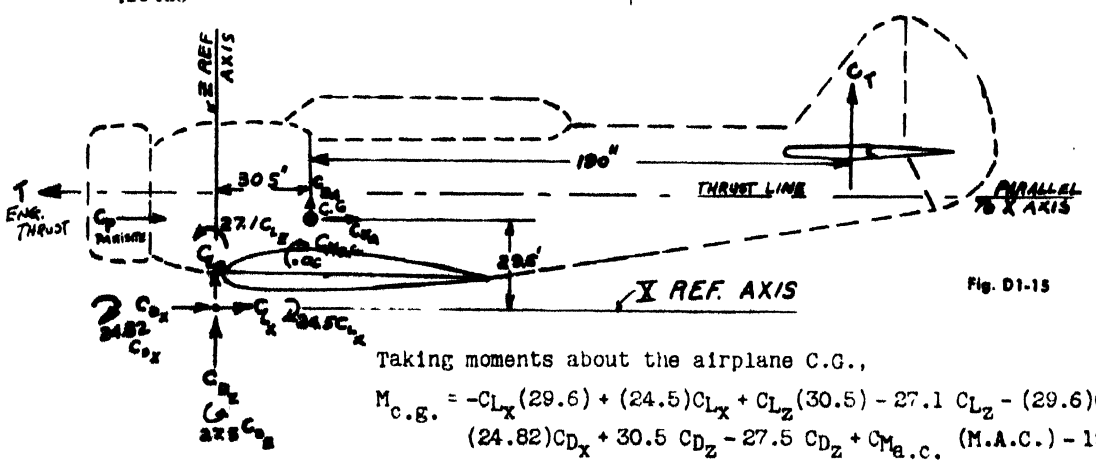


Fig. D1-15

Taking moments about the airplane C.G.,

$$M_{c.g.} = -C_{L_X}(29.6) + (24.5)C_{L_X} + C_{L_Z}(30.5) - 27.1\ C_{L_Z} - (29.6)C_{D_X} + (24.82)C_{D_X} + 30.5\ C_{D_Z} - 27.5\ C_{D_Z} + C_{M_{a.c.}}\ (M.A.C.) - 190\ C_t = 0$$

Solving for C_t using M.A.C. = 77 (see Table D1.3)

$$C_t = -.0269\ C_{L_X} + .0177\ C_{L_Z} - .0251\ C_{D_X} + .0156\ C_{D_Z} + .405\ C_{M_{a.c.}}$$

TABLE D1.6

Determination of Tail Load Coefficient C_T and Airplane Coefficient C_{Z_A}

$$C_T = -.0269\ C_{L_X} + .0177\ C_{L_A} - .0251\ C_{D_X} + .0156\ C_{D_Z} + .405\ C_{M_{a.c.}}$$

1	2	3	4	5	6	7	8	9	10	11	12
C_L	C_{L_X}	$-.0269C_{L_X}$	C_{L_Z}	$.0177C_{L_Z}$	C_{D_X}	$-.0251C_{D_X}$	C_{D_Z}	$.0156C_{D_Z}$	$.405\ C_{M_{a.c.}}$	C_T	C_{Z_A}
1.627	.5220	-.0140	1.532	.02715	.1586	-.00398	.0534	.000834	-.00364	.00636	1.592
1.567	.4710	-.01267	1.488	.02635	.1431	-.003595	.0450	.000702	-.00364	.00710	1.541
1.490	.4135	-.0111	1.422	.02520	.1285	-.003221	.0369	.000575	-.00364	.00781	1.467
1.319	.3125	-.00830	1.273	.02255	.1006	-.002521	.0245	.000382	-.00364	.00847	1.306
1.135	.2206	-.00593	1.108	.01960	.0759	-.00190	.0149	.000232	-.00364	.00836	1.131
0.935	.1400	-.00376	0.918	.01620	.0540	-.001351	.0082	.0001278	-.00364	.00758	.934
0.730	.0763	-.00205	0.722	.01275	.0363	-.000910	.0036	.0000593	-.00364	.00621	.732
0.525	.0320	-.000860	0.521	.00922	.0232	-.000582	.0014	.0000218	-.00364	.00416	.527
0.323	.0001	-.000137	0.321	.00568	.0139	-.000349	.0002	.00000312	-.00364	.00156	.323
0.120	-.0036	-.0000968	0.119	.002105	.0093	-.000233	-.0002	-.00000312	-.00364	-.00187	.117
0	0	0	0	0	.0087	-.000218	-.0005	-.00000780	-.00364	-.00387	- .004
-0.090	.0068	-.000182	-.0894	-.001528	.0092	-.000230	-.0007	-.0000109	-.00364	-.00564	- .096
-0.226	.0232	-.000624	-.224	-.00396	.0117	-.000294	-.0012	-.0000187	-.00364	-.00854	-..234
-0.539	.0927	-.002485	-.528	-.00935	.0246	-.000617	-.0043	-.000067	-.00364	-.01616	- .549
-0.844	.2000	-.00538	-.816	-.01441	.0467	-.001170	-.0113	-.000176	-.00364	-.02478	- .852
-1.135	.3450	-.00928	-1.075	-.01901	.0780	-.00195	-.0248	-.000387	-.00364	-.03427	-1.134

Values in columns (1), (2), (4), (6) and (C) taken from Table D1.2.

Col. 11 = Cols. 3 + 5 + 7 + 9 + 10

Col. 12 = $C_{Z_A} = C_t + C_{L_Z} + C_{D_Z}$ = Cols. 11 + 4 + 8

Col. 10 = $C_{M_{a.c.}} = -.009$

SPECIAL NOTE:
The sign of C_{L_X} in col. 2 should be opposite to that shown. Hence values in col. 3 have opposite sign. This error causes values in columns 11 and 12 to be slightly incorrect. To correct this error would cause all the numerical calculations in the following pages to change slightly. Thus the error is not corrected as it is felt the general procedure in calculating the aerodynamic loads is provided regardless of the unfortunate error in Table D1.6.

general, the fuselage parasite resistance for this type of airplane can be assumed to act thru the center of gravity of the airplane. For airplane arrangements where this assumption is obviously far off, the fuselage drag can of course be calculated and applied along the proper line. In Fig. D1.15, the engine thrust is omitted and the fuselage drag has been taken as acting through the airplane (c.g.). To find the tail load coefficient C_t, moments are taken about the airplane (c.g.). The equation is given below Fig. D1.15. Table D1.6 gives the solution of the equation for C_t for the various values of C_L, as well as for the normal airplane coefficient C_Z. Fig. D1.16 shows a plot of the various coefficients as taken from Tables D1.2 and D1.6.

D1.20 Calculation of Applied Wing Loads (Maneuver and Gust).

The coefficient curves of Fig. D1.16 give sufficient data for calculating the wing and tail loads for the various flight conditions.

Condition 1. - High Angle of Attack Condition.

From Fig. D1.16 maximum value of $C_L = 1.6$ which gives a corresponding value of 1.562 for C_{Z_A}.

The specifications as assumed require a positive maneuver acceleration of n = 6.

From elementary aerodynamics,

$$n = .002558\ C_{Z_A}\ V^2\ S/W$$

or

$$V = \sqrt{\frac{391\ n\ W/S}{C_{Z_A}}}$$

where

S = wing area = 243.5 sq. ft.

V = velocity, MPH.

W = gross weight = 4300#.

W/S = 17.66

Solving for V,

$$V = \sqrt{\frac{391 \times 6 \times 17.66}{1.562}} = 162.8 \text{ MPH.}$$

Dynamic pressure times wing area = $1/2\ \rho\ V^2\ S$

= .002558 x 162.8 x 243.5 = 16480.

From the curves of Fig. D1.16, for $C_L = 1.6$, the following wing force coefficients are obtained. Multiplying these coefficients by the dynamic pressure times wing area or by 16480, the total applied loads on the wing in the Z and X directions due to the wing lift and drag forces are obtained.

$C_{L_X} = -.498$, $L_X = -.498 \times 16480 = -8215\#$

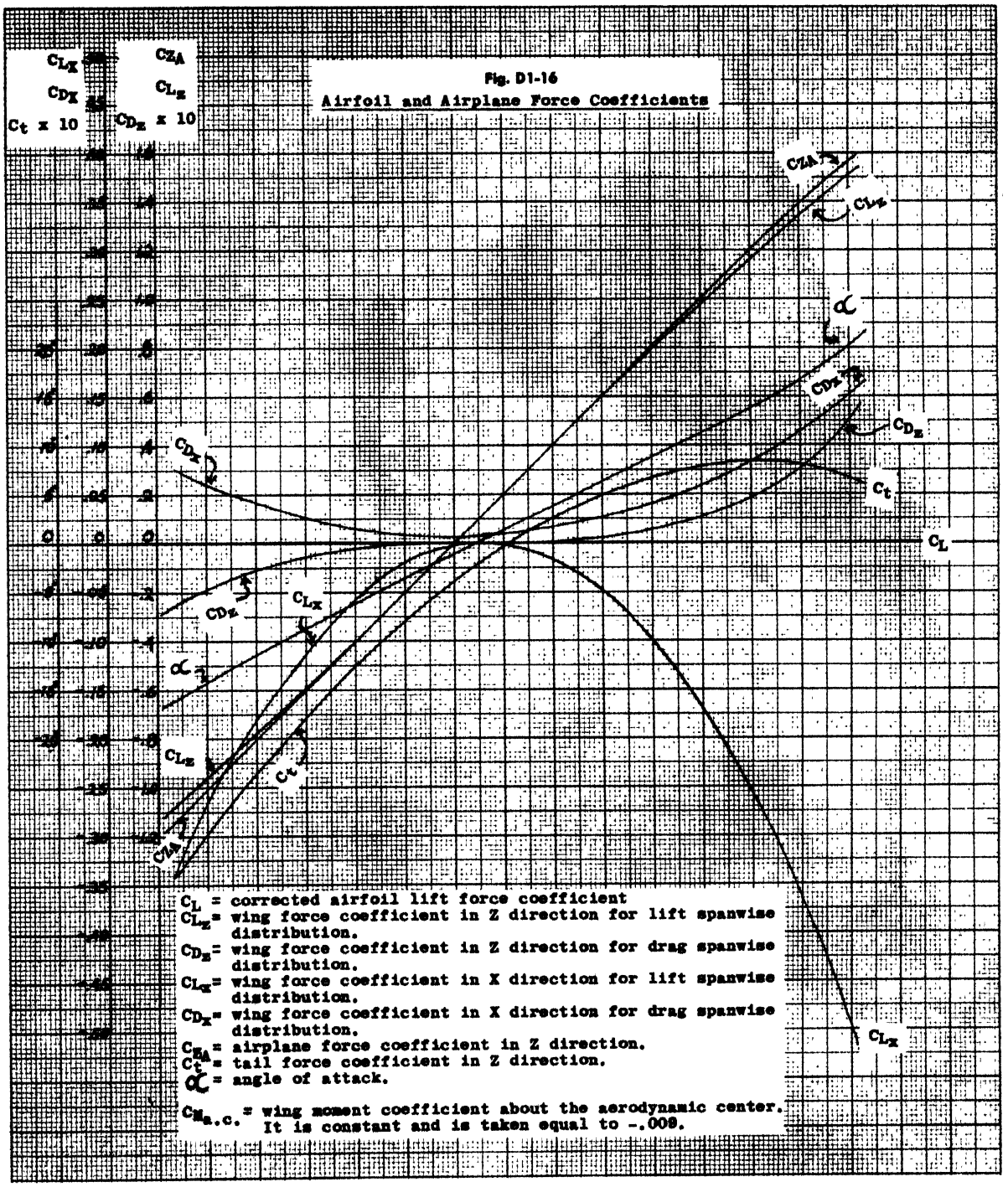


Fig. D1-16
Airfoil and Airplane Force Coefficients

C_L = corrected airfoil lift force coefficient
C_{L_Z} = wing force coefficient in Z direction for lift spanwise distribution.
C_{D_Z} = wing force coefficient in Z direction for drag spanwise distribution.
C_{L_X} = wing force coefficient in X direction for lift spanwise distribution.
C_{D_X} = wing force coefficient in X direction for drag spanwise distribution.
C_{Z_A} = airplane force coefficient in Z direction.
C_t = tail force coefficient in Z direction.
α = angle of attack.

$C_{M_{a.c.}}$ = wing moment coefficient about the aerodynamic center. It is constant and is taken equal to -.009.

C_{L_Z} = 1.510, L_Z = 1.51 x 16480 = 24850#

C_{D_X} = 0.151, D_X = .151 x 16480 = 2480#

C_{D_Z} = .049, D_Z = .049 x 16480 = 805#

C_T = .0067, T_Z = .0067 x 16480 = 110#

Wing Aerodynamic Moment

The moment coefficient for this wing ($C_{M_{a.c.}}$) = -.009. The length of the mean aerodynamic chord as found in Table D1.3 equals 77" = (d).

The total wing aerodynamic moment is given by the following equation,

$$M = 1/2\ \rho\ V^2\ C_{M_{a.c.}}\ d\ S$$

$$= .002558 \times \overline{162.8}^2\ (-.009\ 77 \times 243.5 =$$

-11330"#

The total air loads in the Z direction as found above must be balanced by the airplane inertia loads in the Z direction.

Airloads = $L_Z + D_Z + T_Z$ = 24850 + 805 + 110 = 25765#.

The specified airplane acceleration for this condition was 6, thus the inertia Z forces equal 6 x 4300 (gross weight) = 25800#, which checks within the accuracy of plotting, etc.

Condition 2. - Low Angle of Attack Condition.

From the specifications V restricted is 260 MPH with a maneuver acceleration n = 6.

With velocity and acceleration known, the normal airplane coefficient C_{Z_A} can be calculated.

$$C_{Z_A} = \frac{391\ n\ W/S}{V^2} = \frac{391 \times 6 \times 17.66}{260^2} = .611$$

$$1/2\ \rho\ S\ V^2 = .002558 \times 2435 \times 260^2 = 42150$$

From Fig. D1.16 for C_{Z_A} = .611, the following values for the various wing coefficients are obtained, which multiplied by 42150 give the total wing loads.

C_{L_X} = -.047, L_X = -.046 x 42150 = -1940#

C_{L_Z} = .605, L_Z = .605 x 42150 = 25500#

C_{D_X} = .0275, D_X = .0275 x 42150 = 1160#

C_{D_Z} = .002, D_Z = .002 x 42150 = 84#

C_T = .0052, T_Z = .0052 x 42150 = 220#

Wing aerodynamic moment M = .002558 x 260^2 (-.009) 77 x 243.5 = -29200"#.

Condition 3. - Inverted Low Angle of Attack Condition.

From the specifications V = 260 and maximum maneuver acceleration is limited to n = -2.5.

Hence, $C_{Z_A} = \frac{391\ (-2.5)\ 17.66}{260} = -.255$

$1/2\ \rho\ V^2\ S = .002558 \times 243.5 \times 260^2 = 42150$

From Fig. D1.16

C_{L_X} = -.026, L_X = -.026 x 42150 = -1100#

C_{L_Z} = -.244, L_Z = -.243 x 42150 = -10300#

C_{D_X} = .012, D_X = .012 x 42150 = 505#

C_{D_Z} = -.0018, D_Z = -.0018 x 42150 = -76#

C_T = -.0092, T_Z = -.0087 x 42150 = -366#

Wing aerodynamic moment load = -29200"# (same as for condition (2) since velocity is same.

Condition 4. - Inverted High Angle of Attack Condition.

From the curves of Fig. D1.16, the value of C_{Z_A} for the maximum negative value of C_L equals -1.133. The restricted maneuver acceleration n is -2.5. For n = 2.5 and C_{Z_A} = -1.133, the velocity V can be calculated.

$$V = \sqrt{\frac{391\ n\ W/S}{C_{Z_A}}} = \sqrt{\frac{391\ (-2.5)\ 17.66}{-1.133}} = 122.3\ \text{MPH}$$

$1/2\ \rho\ V^2\ S = .002558 \times 1233^2 \times 243.5 = 9500.$

From Fig. D1.16 for C_{Z_A} = -1.1133,

C_{L_X} = -.345, L_X = .345 x 9500 = -3280#

C_{L_Z} = -1.075, L_Z = -1.075 x 9500 = -10,210#

C_{D_X} = .078, D_X = .078 x 9500 = 740#

C_{D_Z} = -.025, D_Z = -.025 x 9500 = -238#

C_T = -.0346, T_Z = -.0346 x 9500 = -328#

Wing aerodynamic moment load = .002558 x 123.3^2 (-.009) 77 x 2435 = -6500"#.

Gust Accelerations and Applied Loads.

The equation for acceleration due to a 30 ft./sec. gust normal to thrust line is,

$$n = 1 \pm \frac{3\ K\ m\ V}{W/S}$$

where

n = gust load factor.

K = wing loading factor. It is 1 for this airplane.

$$m = \frac{dC_{Z_A}}{d\alpha} = .088\ \text{(From Figl D1.16)}$$

V = velocity in MPH.

Condition 5. - Positive Gust. V = 260 MPH. Horizontal Altitude.

$$n = 1 + \frac{3\ K\ m\ V}{W/S} = 1 + \frac{3 \times 1 \times .088 \times 260}{17.66} = 4.88$$

load factors.

This is less than the design maneuver factor of n = 6 at this velocity, thus a positive gust

condition is not as critical as the positive maneuver conditions.

Condition 6. - Negative Gust. V = 260 MPH. Vertical or Dive Attitude.

$$n = -\frac{3\,K\,m\,V}{W/S} = -\frac{3 \times 1 \times .088 \times 260}{17.66} = -3.88 \text{ load factor}$$

This is more than the restricted negative maneuver factor of -2.5 accelerations at 260 MPH and thus a negative gust at the limiting velocity is more critical than condition (3).

Solving for C_{Z_A},

$$C_{Z_A} = \frac{391\ (-3.88)\ 17.66}{260} = -.396$$

From Fig. D1.16, $C_{Z_A} = -.396$

$C_{L_X} = -.053$, $L_X = -.053 \times 42150 = -2240\#$

$C_{L_Z} = -.382$, $L_Z = -.382 \times 42150 = -16100\#$

$C_{D_X} = -.017$, $D_X = .017 \times 42150 = 716\#$

$C_{D_Z} = -.0025$, $D_Z = -.0025 \times 42150 = -105\#$

$C_T = -.0120$, $T_Z = -.0120 \times 42150 = -506\#$

Wing aerodynamic moment = 29200"# same as for conditions 2 and 3 since velocity is same.

D1.21 Applied Load Factor - Velocity Diagram.

In graphical form the applied design conditions can be repeated by plotting velocity load factor as illustrated in Fig. D1.17. The lines AB and DF are determined by the value of the restricted maneuver load factors, namely 6 and -2.5 respectively. The extremities B and F are determined by the restricted dive or glide speed of 1.3 times the high level speed of 200 MPH = 260 MPH = 260 MPH. The points A and D are determined by the velocity required when flying at C_{Z_A} maximum to give the restricted maneuver load factors. The curved lines OA, and OD represent the relation between velocity and load-factor when flying at maximum C_{Z_A}.

From a maneuver standpoint, the critical normal flight conditions for loads on the wing would be represented points A, B, F and D on Fig. D1.17. The load factors produced by a 30 ft./sec. gust at various velocities up to 260 MPH is shown by the straight sloping lines which represent the plot of the equation n = 3 K m V S/W. For a positive gust, the gust line falls below the maneuver line AB and thus is not critical. For a negative gust when flying in a vertical attitude, the gust line cuts the negative maneuver load factor line DF at E with a maximum value at C. Thus, for velocities above point E, the negative gust condition is more critical than the specified maneuver load factors. The airplane therefore should be investigated and designed to take the loads indicated by the conditions at points A, B, D, E and C on the diagram.

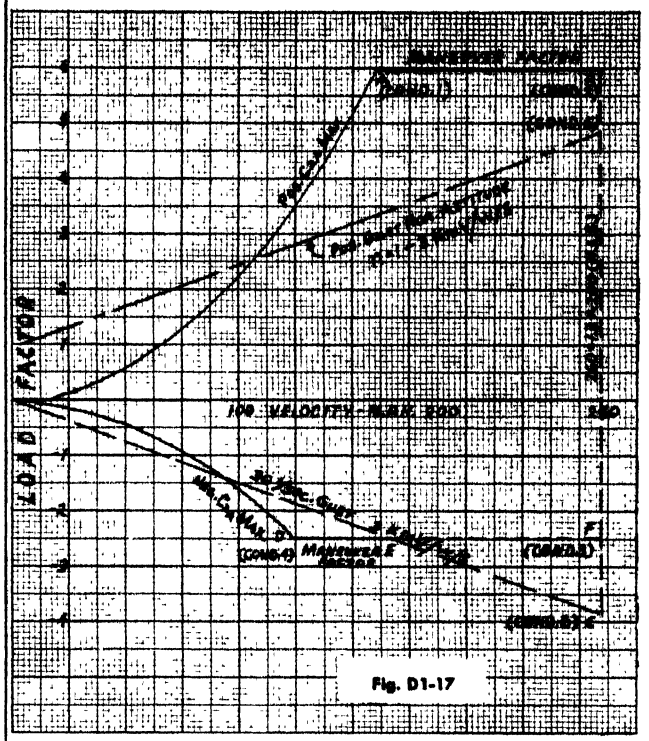


Fig. D1-17

Since the magnitude of the gust load factors vary inversely as the wing loading (W/S), the lightly loaded conditions of the airplane (small fuel and payload) will give higher load factors and may prove critical in some cases. Therefore, in actual design, this fact must be considered.

The loads represented by this velocity-load factor diagram (Fig. D1.17) are applied loads. For the design of members, the applied loads are multiplied by a factor of safety,which in general is 1.5.

Velocity-load factor diagrams can also be drawn for flight conditions where the wing flaps or ailerons are operated. In general, the principles are the same, the chief difference being the changed airfoil characteristics due to the deflected surfaces.

D1.22 Calculation of Wing Shears, Bending and Torsional Moments, Unit Analysis.

In article D1.20, the total applied wing air loads were determined for the various flight conditions. In addition, there are inertia resisting loads. In the various flight conditions, the magnitude, direction and location of the loads change thus it usually saves considerable time if a unit load analysis is made, and this is the usual procedure in the load analysis for actual airplane analysis, and thus this procedure will be carried out in this example problem.

In balancing the airplane in Art. D1.19, the wing air loads, were referred to a convenient set of reference X, Z and Y axes (See Fig. D1.15).

For simplicity, the wing shears and moments will be referred to these axes. Later when the design of the internal wing structure is considered, these forces relative to the selected reference axes can be transferred or referred to any other set of axes if desirable.

In Tables D1.4 and D1.5, column No. 7 gives the area of each wing strip times the spanwise, distribution factor of the lift and drag forces respectively. The summation of these columns gives the projected area of each semi-wing or 17524 sq. in. For simplicity, unit air loads of 17524 lbs. acting on the semi-wing will be selected for the unit analysis. This procedure will make it possible to use many of the numerical values in Tables D1.4 and D1.5 in the unit analysis to follow.

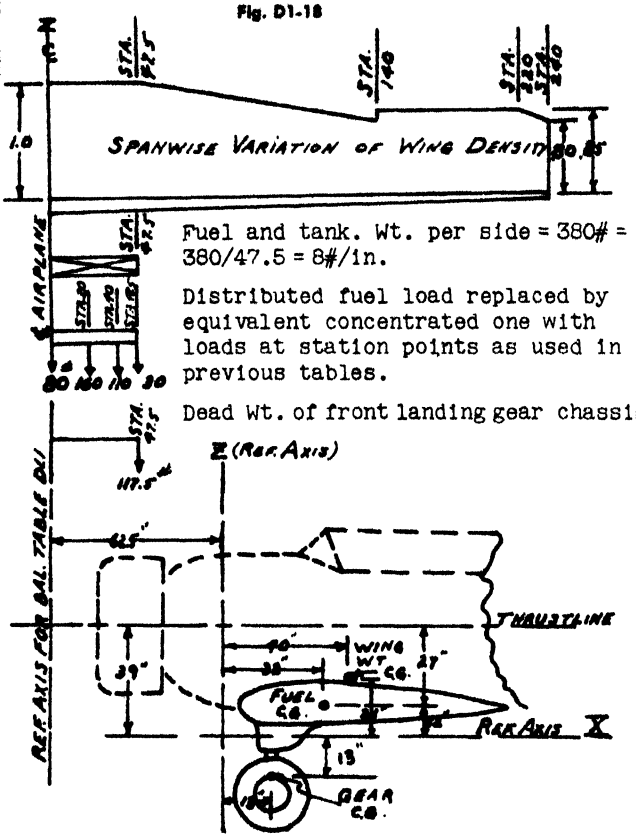
Tables D1.7 and D1.8 give the necessary calculations for determining the shears and moments with respect to the reference axes due to unit loads for spanwise distribution of both the lift and drag forces. The student should refer to article A6.7 of Chapter A6 for review of shears and bending moments for cantilever beams with varying distributed loads.

D1.23 Unit Dead Weight Analysis for Wing Shears and Moments.

Since the design load factors in the Z and X directions change with the various flight conditions, it is convenient to make a unit analysis, usually for one load factor, which is equivalent to the weight of the airplane. The wing weight is usually broken down into the wing panel weights which represents a distributed type of load plus any concentrated installations placed inside the wing or attached to it, as for example, fuel, landing gear, engine installations, wing floats, etc.

The spanwise distribution of the wing weight is usually based on experience and data accumulated from previous designs of similar types of airplanes and from semi-rational formulas which consider such items as load factor, aspect ratio, taper ratio, etc. Fig. D1.18 gives the spanwise weight distribution as assumed for this example problem. The figure also shows the location and magnitude of the fuel and landing gear loads.

Fig. D1-18



Fuel and tank. Wt. per side = 380# = 380/47.5 = 8#/in.

Distributed fuel load replaced by equivalent concentrated one with loads at station points as used in previous tables.

Dead Wt. of front landing gear chassis

The distributed fuel load has been replaced by the equivalent system composed of 4 concentrated loads as shown. The weights and their center of gravity locations are obtained from the weight and balance data in Table D1.1.

Table D1.9 gives the calculations for determining the dead weight shears and moments with respect to the reference axes.

D1.24 Applied Wing Shears and Moments.

With the unit analysis completed as given in Tables D1.7, 8 and 9, the applied wing shears and moments for the total applied loads as found in Art. D1.20 follow as a matter of proportion of some numerical factor times the values in the unit solution.

Tables D1.10 and D1.11 give the calculations for the applied wing shears in the Z and X directions for two design flight conditions, namely condition 1 and condition 4. The multiplying factor is given at the head of each column.

Tables D1.12 and D1.13 give the calculations for the moments about the three reference axes X, Y and Z, for the same two flight conditions. Similar tables for the shears and moments should be made up for the other two critical conditions. The student should realize that the moments M_y are not the true torsional moments on the wing but only the moment about the assumed location of

the Y axis. With the shears and moments known for one set of axes, they can be referred to any other desired set that may be required in the stress analysis of the wing as illustrated in Chapter C9.

The values given in Tables D1.10 to 13 are applied loads and should be multiplied by a factor of safety which is usually 1.5.

The simplified problem which has been presented has dealt only with the symmetrical, normal wing flight conditions. In the actual design of an airplane, many other conditions must be investigated as for example, the conditions when the wing flaps are deflected and the operation of the ailerons which produces a rolling acceleration on the airplane.

For the portion of the wing between the landing gear and the fuselage support, investigation must be carried out as to the loads on the wing in the landing condition, since the reaction to the dead weight inertia loads is provided by the landing gear.

The load analysis for the airplane wing involves several hundred hours of work and is a subject on which a complete textbook could be written consequently the analysis as given in this chapter can only be of simplified character.

Problem.

To give the student practice, it is suggested that the instructor change the weight and balance data of Table D1.1 to give a different c.g. location, and also change the airfoil section and let the student carry the problem through with this revised data.

References:

Before starting the load analysis of any actual commercial airplane, the latest requirements of the Civil Aeronautics Authorities should be reviewed in detail. For Army and Navy airplanes the design regulations and specifications as issued by these agencies should be studied carefully.

TABLE D1.7

Wing Shears and Moments (M_X, M_Z, M_y, V_X, V_Z) For Unit Lift Loads

Unit Wing Loads 17524# on half wing acting in Z direction (up)
17524# on half wing acting in X direction (aft)

1 Sta. = Dist. y from ℄	2 Strip Load $\Delta P_Z = \Delta P_X$	3 Δy = Dist. between Sta.	4 Shear $V_Z = \Sigma\Delta P_Z$ or $V_X = \Sigma\Delta P_X$	5 $V_X \Delta y$ or $V_Z \Delta y$	6 $P_Z \frac{\Delta y}{2}$ or $P_X \frac{\Delta y}{2}$	7 M'	8 B. Moment M_X or M_Z	9 ΔP_Z X in. lbs.	10 Torque = $M_y = \Sigma \Delta P_Z$ X	11 ΔP_X Z	12 Torque = $M_y = \Sigma\Delta P_X$ Z
240			0	0			0		0		
	45	5									
235			45	0	112	0	112	-1640	- 1640	1605	1605
	121	5									
230			166	225	302	112	639	-4015	- 5655	4045	5650
	372	10									
220			538	1660	1860	639	4165	-11410	- 17065	12530	18180
	723	15									
205			1261	8070	5422	4165	17657	-22050	- 39115	24670	42850
	830	15									
190			2091	18915	6225	17657	42797	-25380	- 64495	27180	70030
	921	15									
175			3012	31366	6907	42797	81064	-27555	- 92050	28880	98910
	991	15									
160			4003	45180	7432	81064	133676	-29250	-121300	30150	129060
	1061	15									
145			5064	60050	7957	133676	201683	-30550	-151850	30680	159740
	1115	15									
130			6179	75960	8362	201683	286005	-31450	-183340	30790	190530
	1162	15									
115			7341	92680	8715	286005	387400	-33250	-215550	30690	221220
	1212	15									
100			8553	110120	9080	387400	506600	-33000	-248550	30300	251520
	1255	15									
85			9808	128300	9412	506600	644312	-33480	-282030	29640	281160
	1300	15									
70			11108	147120	9750	644312	801182	-33900	-315930	29700	310860
	1338	15									
55			12446	166620	10030	801182	977832	-34200	-350130	28050	338910
	680	7.5									
47.5			13126	93300	2550	977832	1073602	-17150	-367280	13600	352510
	686	7.5									
40			13812	98500	2570	1073682	1174752	-17150	-384430	13250	365760
	1861	20									
20			15673	276240	18610	1174752	1469602	-45820	-430050	33800	399420
	1851	20									
0			17524	313460	18510	1469602	1801572	-44820	-474870	30260	429680

Column No. (2) = Column 7 from Table D1.4
(5) = (4) preceding x (3)
(6) = (2) x (3) x 1/2
(7) = (8) preceding
(8) = (5) + (6) + (7)
(9) = column (14) from Table D1.4
(11) = Column (18) from Table D1.4.

TABLE D1.8

Unit Wing Loads 17524# on half wing acting in Z direction (up)
17524# on half wing acting in X direction (aft)

1 Sta. = Dist. y from ℄	2 Strip Load $\Delta P_Z = \Delta P_X$	3 Δy = Dist. Between Sta.	4 Shear $V_Z = \Sigma\Delta P_Z$ or $V_X = \Sigma\Delta P_X$	5 $V_X \Delta y$ or $V_Z \Delta y$	6 $P_Z \frac{\Delta y}{2}$ or $P_X \frac{\Delta y}{2}$	7 M'	8 B. Moment M_X or M_Z	9 ΔP_Z X in. lbs.	10 Torque = $M_y = \Sigma\Delta P_Z$ X	11 ΔP_X Z	12 Torque = $M_y = \Sigma\Delta P_X$ Z
240			0				0				
	119	5									
235			119	0	297	0	297	-4405	-4405	4375	4375
	280	5									
230			399	595	700	297	1592	-10015	-14420	10295	14670
	679	10									
220			1078	3990	3395	1592	8977	-22170	-36590	24020	38690
	1002	15									
205			2080	16170	7510	8977	32657	-31360	-67850	34425	73115
	935	15									
190			3015	31200	7020	32657	70877	-28570	-96420	30570	103685
	884	15									
175			3900	45720	6720	70877	123317	-26880	-123300	28080	131765
	879	15									
160			4788	58640	6610	123317	188567	-25980	-149280	25878	158435
	890	15									
145			5678	71820	6675	188567	267062	-25785	-175065	25755	184190
	925	15									
130			6603	85170	6940	267062	359172	-26280	-201340	25530	209720
	975	15									
115			7576	99050	7300	359172	465522	-27150	-228490	25590	235310
	1032	15									
100			8608	113640	7745	465522	586907	-28230	-256720	25770	261080
	1099	15									
85			9707	129120	8240	586907	724267	-29570	-286290	25980	287060
	1170	15									
70			10877	145610	8775	724267	878652	-30870	-317160	26145	313205
	1248	15									
55			12125	163150	9360	878652	1051162	-32190	-349350	26205	339410
	652	7.5									
47.5			12780	91000	2460	1051162	1144622	-16660	-366020	13130	352540
	680	7.5									
40			13460	95900	2550	1144622	1243072	-17000	-383020	13200	365740
	1954	20									
20			15414	269200	19540	1243072	1531672	-47940	-430960	35300	401040
	2140	20									
0			17554	308280	21400	1531672	1861352	-51900	-482760	38500	439540

Column No. (2) = Column (7) from Table D1.5
(5) = (4) preceding x (3)
(6) = (2) x (3) x 1/2
(7) = (8) preceding
(8) = (5) + (6) + (7)
(9) = Column (14) from Table D1.5
(11) = Column (18) from Table D1.5

TABLE D1.9

DEAD WEIGHT UNIT ANALYSIS FOR WING SHEARS AND MOMENTS

(M_X, M_Z, M_y, V_Z, V_X)

Load Factor = 1. Weight acting down and aft

1	2	3	4	5	6	7	8	9	10	11	12	13	14	15	16	17	18
Sta. x Dist. y from $\frac{\ell}{2}$	From Fig.D1-18 Span-wise Weight Dist. Factor	Chord	(2)x(3)	(4) Ave.	Δy	(5)x(6)	w	$V_n = \Sigma w$	$V \Delta y$	$w \frac{\Delta Y}{2}$	M'	M_X or M_Z	wx	Torque M_y = Σ wx	z	wz	Torque M_y = Σ wz
240	.8	0	0	0	0			0	0	0	0	0	0	0	0	0	0
				13.78	5	69	-1.6						64		33.3		
235	.8125	33.8	27.45					-1.6	0	-4.0	0	-4.0		64		53	53
				32.28	5	162	-3.8						152		33.0		
230	.825	45.0	37.10					-5.4	-8.0	-9.5	-4.0	-21.5		216		126	179
				40.78	10	408	-9.6						384		32.5		
220	.850	52.3	44.45					-15.0	-54.0	-48	-21.5	-123.5		600		312	491
				45.85	15	688	-16.2						648		31.8		
205	.850	55.6	47.25					-31.2	-225	-121.5	-123.5	-470		1248		515	1006
				49.08	15	736	-17.3						702		30.0		
190	.850	58.9	50.90					-48.5	-468	-139.8	-470	-1068		1950		520	1526
				51.85	15	778	-18.4						736		28.9		
175	.850	62.1	52.80					-66.9	-728	-138.0	-1068	-1934		2686		502	2028
				54.18	15	814	-20.7						828		27.5		
160	.850	65.4	55.55					-87.6	-1003	-155.2	-1934	-3092		3514		569	2597
				56.98	15	855	-20.2						808		26.0		
145	.850	68.7	58.40					-107.8	-1214	-151.5	-3092	-4457		4322		527	3124
				58.80	15	881	-19.1						764		24.5		
130	.822	72.0	59.20					-126.9	-1607	-143.2	-4457	-6218		5086		468	3592
				61.75	15	926	-21.8						872		23.1		
115	.854	75.3	64.30					-148.7	-1903	-163.5	-6218	-8284		5958		505	4097
				66.95	15	1004	-23.7						948		21.6		
100	.887	78.5	69.60					-172.4	-2231	-176.0	-8284	-10693		6906		512	4609
				72.35	15	1085	-25.6						1024		20.0		
85	.919	81.8	75.10					-198.0	-2586	-192.0	-10693	-13471		7930		512	5121
				78.05	15	1171	-27.6						1104		18.6		
70	.951	85.1	81.00					-225.6	-2970	-207.0	-13471	-16648		9034		512	5633
				84.05	15	1261	-29.7						1188		17.2		
55	.984	88.4	87.10					-255.3	-3384	-233.0	-16648	-20255		10222		510	6143
				88.55	7.5	664	-15.6						624		16.1		
+47.5	1.000	90.0	90.0					-270.9	-1910	- 58.5	-20255	-22223		10846		251	6394
	Landing gear			0			-117.5						1526	12374	-13.0	-1527	4867
	Fuel			0			-30.0						960		13.7	411	
-47.5	1.000	90.0	90.00					-418.4			-22223	-22223		13334			5278
				90.85	7.5	682	-16.0						640		15.3	245	
+40	1.000	91.7	91.70					-434.4	-3140	- 60.0	-22223	-25423		13974			5523
	Fuel			0			-110						3520		13.0	1435	
-40	1.000	91.7	91.70					-544.4			-25423	-25423		17494			6958
				93.86	20	1877	-43.0						1720		14.1	607	
+20	1.000	96.0	96.00					-587.4	10888	-430.0	-25423	-36741		19214			7565
	Fuel			9			-160						5120		11.6	1860	
-20	1.000	96.0	96.00					-747.4			-36741	-36741		24334			9425
				96.0	20	1920	-45.0						1800		13.0	585	
0	1.000	96.0	96.00					-792.4	14948	-450.0	-36741	-52139		26134			10011
	Fuel			0			-80.0						2560		10.9	875	
0	1.000	96.0	96.00				Σw =	872.4			-52139	-52139		28694			10886
						15981		872.5	Check								

Check of Σ wx = 28644 (Col. 15)
From Fig.
wing wt. = (750/2) 40 = 15000
fuel wt. = (760/2) 32 = 12160
F. land. gear = (235/2)13 = 1527
28687

Check of Σ wz = 10886 (Col. 18)
From Fig.
wing wt. = (750/2) 21 = 7875
fuel wt. = (760/2) 12 = 4560
L. gear = (235/2) 13 = 1827
10908

Notes:- Values in () refer to column numbers.
(8) = $\frac{(7)}{(7)}$ times total weight of semi-wing = $\frac{\text{Col (7) } 375}{15981}$
(10) = (9) preceding times(6)
(11) = (8) (6) x .5
(12) = (13) preceding
(13) = (10)+(11)+(12)
(14) = wx = (8)x, where x = 40" for wing structure
x = 13" for landing gear
x = 32" for fuel
(16) = z = (y-20) tan 6° + 10
z = -13" for gear and 12" for fuel.

TABLE D1.10

WING SHEAR LOADS V_Z AND V_X

CONDITION 1. H.A.A.

n_z = 6.0, C_{Z_A} = 1.562, V = 162.8 MPH

Applied wing loads:- L_Z = 24850 lbs., L_X = -8215, D_Z = 805, D_X = 2480.

1	2	3	4	5	6	7	8	9
Sta. Dist. y from ℄	V_{Z_L} = $(\frac{24850}{35048})$ Col.4 of Table D1.7	V_{X_L} = $(\frac{-8215}{35048})$ Col.4 of Table D1.7	V_{Z_D} = $(\frac{805}{35048})$ Col.4 of Table D1.8	V_{X_D} = $(\frac{2480}{35048})$ Col.4 of Table D1.8	V_Z(dead wt.) = 6 (Col. 9) of Table D1.9	V_X(dead wt.) = $(\frac{5735}{4300})$ Col.9 of Table D1.9	V_Z = (2)+(4)+(6)	V_X = (3)+(5)+(7)
240	0	0	0	0	0	0	0	0
235	32	-10.6	2.7	8.4	-9.6	2.1	25.1	-0.1
230	118	-39	9.2	28.2	-32.4	7.2	94.8	-3.6
220	382	-126	24.8	76.4	-90.0	20.0	316.8	-29.6
205	895	-296	47.7	147	-187	41.6	745.7	-107.4
190	1480	-489	69.2	213	-288	64.6	1263	-211.4
175	2135	-705	89.6	276	-401	89.3	1824	-339.7
160	2858	-944	110	338	-526	116.8	2442	-489.2
145	3590	-1187	131	402	-646	144	3075	-641
130	4375	-1447	152	468	-761	169	3786	-810
115	5200	-1718	174	536	-891	198	4483	-984
100	6065	-2003	198	610	-1033	230	5230	-1163
85	6950	-2297	223	687	-1188	264	5985	-1348
70	7890	-2603	249	768	-1350	300	6789	-1535
55	8825	-2915	278	857	-1530	340	7573	-1718
+ 47.5	9320	-3080	294	905	-1628	361	7986	-1814
- 47.5	9320	-3080	294	905	-2510	557	7104	-1618
40	9800	-3240	309	952	-2600	579	7509	-1709
40	9800	-3240	309	952	-3265	726	6844	-1562
20	11100	-3670	354	1090	-3520	783	7934	-1797
20	11100	-3670	354	1090	-4490	995	6964	-1585
0	12420	-4100	403	1240	-5240	1160	7583	-1700

TABLE D1.11

WING SHEAR LOADS V_Z AND V_X

CONDITION 4 INVERTED H.A.A.

Applied Wing Loads:- L_Z = -10210 L_X = -3280 D_Z = -238 D_X = 740

1	2	3	4	5	6	7	8	9
Sta. Dist. y from ℄ Airplane	V_{Z_L} = $(\frac{-10210}{35048})$Col.4 of Table D1.7	V_{X_L} = $(\frac{-3280}{35048})$Col.4 of Table D1.7	V_{Z_D} = $(\frac{-238}{35048})$Col.4 of Table D1.8	V_{A_D} = $(\frac{740}{35048})$Col.4 of Table D1.8	V_Z(dead wt.) = -2.5 (Col.9 of Table D1.9	V_X = $(\frac{2540}{4300})$Col.9 of Table D1.9	V_Z (2)+(4)+(6)	V_X (3)+(5)+(7)
240	0	0	0	0	0	0	0	0
235	-13.1	- 4.21	-0.8	2.51	4.0	.944	-9.9	- .76
230	-48.3	-15.5	-2.7	8.4	13.5	3.19	-37.5	-3.9
220	-157	-50.3	-7.3	22.75	37.5	8.85	-126.8	-18.7
205	-367	-118	-14.1	43.9	78.0	18.4	-303.1	-56.0
190	-609	-195.5	-20.4	63.7	121	28.6	-508.4	-103.2
175	-875	-282	-26.8	82.5	167	39.5	-735	-160.0
160	-1166	-375	-32.5	101	219	51.8	-979	-222
145	-1473	-474	-38.5	119.8	269	63.5	-1243	-291
130	-1800	-578	-44.9	139.5	317	74.8	-1528	-364
115	-2140	-687	-51.4	160	372	87.6	-1819	-439
100	-2495	-807	-58.4	181.8	431	102	-2122	-523
85	-2860	-925	-65.9	205	496	117	-2431	-603
70	-3250	-1045	-73.5	229.6	563	133	-2761	-682
55	-3620	-1165	-82.2	256	637	151	-3065	-758
+ 47.5	-3820	-1230	-86.5	270	677	160	-3230	-800
- 47.5	-3820	-1230	-86.5	270	1045	247	-2862	-713
40	-4025	-1292	-91.3	284	1085	256	-3031	-752
40	-4025	-1292	-91.3	284	1360	321	-2756	-687
20	-4560	-1465	-105	326	1465	347	-3200	-792
20	-4560	-1465	-105	326	1865	441	-2800	-698
0	-5100	-1640	-119	371	1975	468	-3244	-801

TABLE D1.12

APPLIED MOMENTS ON WING. (M_x, M_z, M_y)

CONDITION1. H.A.A.

n_z = 6 C_z = 1.562 V = 162.8 MPH

Total Applied Wing Loads: L_Z = 24850#, L_X = -8215#, D_Z = 805#, D_X = 2480#, $M_{a.c.}$ = -11330"#

1	2	3	4	5	6	7	8	9	10	11	12	13	14	15	16	17
	Moment about X Ref. Axis				Moments about Z Ref. Axis						Moments about Y Ref. Axis					
Sta. Dist. from ℄	M_{Z_L} = $(\frac{24850}{35048})$ Col. 8 of Table D1.7	M_{Z_D} = $(\frac{805}{35048})$ Col. 8 of Table D.8	M_Z (dead wt.) (6) Col.13 of Table D1.9	M_X total = (2)+(3)+(4)	M_{Z_L} = $(\frac{68215}{35048})$ Col. 8 of Table D1.7	M_{Z_D} = $(\frac{2480}{35048})$ Col. 8 of Table D1.8	M_Z (dead wt.) $(\frac{5375}{4300})$ Col. 8 of Table D1.9	M_Z total = (6)+(7)+(8)	Due to L_Z $(\frac{24850}{35048})$ Col. 10 of Table D1.7	Due to L_X $(\frac{-8215}{35048})$ Col. 12 of Table D1.7	Due to D_Z $(\frac{805}{35048})$ Col. 10 of Table D1.8	Due to D_X $(\frac{2480}{35048})$ Col. 12 of Table D1.8	Z Inertia Forces (6) Col. 15 of Table D1.9	X Inertia Forces $(\frac{5735}{4300})$ Col. 18 of Table D1.9	Wing Aero Moment $(\frac{-11330}{1352475x2})$ Col. 7 of Table D1.3	Total M_y = Cols. 10 to 16 Inclusive
240	0	0	-0	0	0	0	0	0	0	0	0	0	0	0	0	0
235	79	7	-24	62	-26	21	5	0	-1161	-376	-101	309	384	68	-12	-889
230	452	37	-129	360	-150	113	27	-10	-4060	-1323	-331	1037	1297	229	-45	-3136
220	2950	206	-741	2415	-975	635	154	-186	-12060	-4260	-840	2736	3600	626	-145	-10343
205	12500	752	-2820	10432	-4135	2310	588	-1237	-27700	-10040	-1560	5170	7500	1283	-327	-25674
190	30300	1830	-6410	25520	-10000	5010	1335	-3655	-45600	-16400	-2220	7330	11700	1945	-536	-43781
175	57500	2837	-11600	48737	-19000	8740	2416	-7844	-65200	-23170	-2835	9300	16120	2590	-715	-63910
160	94500	4340	-18540	80300	-31250	13350	3860	-14040	-86000	-30200	-3430	11200	21070	3312	-1020	-85070
145	142700	6140	-26800	122040	-47150	18880	5560	-22710	-107500	-37400	-4025	13000	25920	3995	-1305	-107415
130	202200	8250	-37300	173150	-67000	25400	7770	-33830	-129800	-44600	-4625	14800	30500	4580	-1615	-130780
115	274000	10700	-49350	235350	-90700	33000	10360	-47340	-152500	-51860	-5260	16640	35700	5525	-1960	-153955
100	358000	13500	-64100	307400	-118800	41600	13370	-63830	-176000	-58900	-5900	18450	41750	5875	-2330	-177055
85	455000	16680	-80750	390930	-151000	51300	16800	-82900	-199800	-65900	-6590	20320	47600	6540	-2730	-200580
70	567000	20200	-99300	487900	-187800	62100	20800	-104900	-224000	-72900	-7290	22150	54200	7190	-3170	-223820
55	691000	24170	-121500	593670	-229000	74500	25330	-129170	-248000	-79400	-8030	24000	61370	7840	-3650	-245870
47.5	760000	26300	-127300	659000	-252000	81100	27800	-143100	-260000	-82600	-8410	24950	65000	8520	-3890	-255430
													80000	7050		-242900
40	832000	28800	152700	707900	-275000	88000	31800	-155200	-272500	-85300	-8800	25800	83700	7460	-4150	-254090
													105000	8800		-231450
20	1040000	35200	218500	856700	-344000	108500	45900	-189600	-304500	-93500	-9900	28400	115200	10100	-4890	-259090
													146000	12550		-225840
0	1278000	42800	312200	1008600	-423000	131800	65200	-226000	-336000	-100800	-111000	30800	172000	14500	-5665	-236300

TABLE D1.13

APPLIED MOMENTS ON WING (M_x, M_z, M_y)

CONDITION 4. INVERTED H.A.A.

n_Z = -2.5 C_{Z_A} = -1.133 V = 123.3 MPH

Total Applied Wing Loads: L_Z = -10210#, L_M = -3280#, D_Z = -238#, D_A = 740#, $M_{a.c.}$ = -6500"#

1	2	3	4	5	6	7	8	9	10	11	12	13	14	15	16	17
	Moments about X Ref. Axis (M_X)				Moments about Z Ref. Axis = (M_Z)						Moments about Y Ref. Axis = (M_y)					
Sta. Dist. from ℄ (9)	M_{X_L} = $(\frac{10210}{35048})$ Col. 8 of Table D1.7	M_{X_D} = $(\frac{-238}{35048})$ Col. 8 of Table D1.8	M_X(dead wt.) =(2.5) Col. 13 of Table D1.9	M_X = (2)+(3)+(4)	M_{Z_L} = $(\frac{-3280}{35048})$ Col. 8 of Table D1.7	M_{Z_D} = $(\frac{740}{35048})$ Col. 8 of Table D1.8	M_Z(dead wt.) =$(\frac{2540}{4300})$ Col. 13 of Table D1.9	M_Z = (6)+(7)+(8)	Due to L_Z $(\frac{-10210}{35048})$ Col. 10 of Table D1.7	Due to L_S $(\frac{-3280}{35048})$ Col. 12 of Table D1.7	Due to D_Z $(\frac{-238}{35048})$ Col. 10 of Table D1.8	Due to D_Z $(\frac{740}{35048})$ Col. 12 of Table D1.8	Z Inertia Forces (-2.5) Col. 15 of Table D1.9	X inertia Forces $(\frac{2540}{4300})$ Col. 8 of Table D1.9	Wing Aero Moments $(\frac{-6500}{2704950})$ Col. 7 of Table D1.3	Total M_y = Col. 10 to 16 Inclusive
240	0	0	0	0	0	0	0	0	0	0	0	0	0	0	0	0
235	-33	-2.0	10	-25	-10.5	6.3	2.4	-1.8	478	-150	29.9	92.4	-160	31.3	-6.9	314.7
230	-186	-10.8	53.7	-143.1	-59.7	33.6	12.7	-13.4	1650	-529	98	309.5	-540	105.8	-25.9	1068.4
220	-1212	-61.0	308.5	-964.5	-389	189.5	73.0	-126.5	4970	-1700	248	817	-1500	290	-83	4042
205	-5150	-221.9	1175	-4196.9	-1650	690	278	-682	11400	-4010	460	1544	-3120	594	-188	6670
190	-12480	-481	2665	-10296	-4010	1496	631	-1883	18800	-6550	654	2190	-4870	901	-307	10818
175	-23650	-837	4840	-19647	-7590	2605	1142	-3843	26850	-9250	838	2780	-6720	1200	-439	15259
160	-39000	-1280	7730	-32550	-12500	3980	1825	-6695	35400	-12100	1015	3350	-8780	1530	-585	19830
145	-58800	-1810	11130	-49480	-19000	5640	2635	-10725	44200	-14930	1190	3895	-10810	1846	-748	24643
130	-83400	-2420	15540	-70280	-26750	7580	3680	-15490	53500	-17800	1365	4420	-12710	2120	-926	28775
115	-112900	-3160	20700	-95360	-36200	9830	4890	-21480	62800	-20650	1550	4960	-12900	2420	-1124	35056
100	-147700	-3980	26700	-124980	-47400	12300	6310	-28790	72500	-23500	1740	5510	-17290	2720	-1337	40343
85	-187800	-4920	33600	-159120	-60200	15290	7950	-36960	82200	-26300	1945	6060	-19800	3025	-1569	45561
70	-233500	-5960	41600	-197860	-75000	18550	9840	-46610	92000	-29050	2150	6610	-22600	3320	-1820	50610
55	-285000	-7140	50600	-241540	-91500	22200	11980	-57320	102200	-31700	2370	7170	-25550	3620	-2090	56020
47.5	-315500	-7770	55600	-267670	-100800	24200	13150	-62450	107000	-33000	2480	7440	-271100	3780	-2235	58363
40	-342000	-8450	63600	-286850	-110000	26250	15030	-68970	112000	-34200	2600	7710	-33400 -34900 -43700	3120 3260 3900	-2385	51405 54085 55425
20	-428000	-10400	91700	-346700	-137200	32350	21700	-83150	125200	-37300	2925	8470	-48100 -58400	4465 5560	-2810	62840 63645
0	-528000	-12640	130500	-408140	-168700	39300	30800	-98600	138300	-40100	3280	9210	-74200	6420	-3250	39660

CHAPTER D2
THE LOADS ON THE BODY

D2.1 Introduction.

The body of an airplane acts essentially as a beam and in some conditions of flight or landing as a beam column which may be also subjected to twisting or torsional forces. Thus to design an airplane body requires a complete picture of the shearing, bending, twisting and axial forces which may be encountered in flight or landing. In the load analysis for wings, the direct air forces are the major forces. For the body, load analysis the direct air pressures are secondary, the major forces being of a concentrated nature in the form of loads or reactions from units attached to the body, as the power plant, wing, landing gear, tail, etc. In addition, since the body usually serves as the load carrying medium, important forces are produced on the body in resisting the inertia forces of the weight of the interior equipment, installations, pay load, etc.

As in the case of the wing, a large part of the load analysis can be made without much consideration as to the structural analysis of the body. The load analysis of an airplane body involves a large amount of calculation, and thus the treatment in this chapter must be of a simplified nature, and is presented chiefly for the purpose of showing the student in general how the problem of load analysis for an airplane body is approached.

D2.2 Design Conditions and Design Weights.

The airplane body must be designed to withstand all loads from specified flight conditions for both maneuver and gust conditions. Since accelerations due to air gusts vary inversely as the airplane weight, it is customary to analyze or check the body for a light load condition for flight conditions. In general, the design weights are specified by the government agencies. For landing conditions, however, the normal gross weight is used since it would be more critical than a lightly loaded condition.

The general design conditions which are usually investigated in the design of the body are as follows:

Flight Conditions:

H.A.A.	(High angle of attack)
L.A.A.	(Low angle of attack)
I.L.A.A.	(Inverted low angle of attack)
I.H.A.A.	(Inverted high angle of attack)

The above conditions generally assume only translational acceleration. In addition, it is sometimes specified that the forces due to a certain angular acceleration of the airplane about the airplane c.g. must be considered.

The body is usually required to withstand special tail loads both symmetrical and unsymmetrical which may be produced by air gusts, engine forces, etc. Also, the body should be checked for forces due to unsymmetrical air loads on the wing.

Landing Conditions:

In general, the body is investigated for the following landing conditions. The detailed requirements for each condition are given in the government specifications for both military and commercial airplanes.

Landplanes:
- Level landing.
- Level landing with side load.
- Three point landing.
- Three point landing with ground loop.
- Nose over or turn over condition.
- Arresting. (usually for only Navy Carrier based airplanes)

Seaplanes or Boats:
- Step landing with and without angular acceleration.
- Bow landing.
- Stern landing.
- Two wave landing.
- Beaching conditions.
- Catapulting conditions (Navy airplanes)

Special Conditions or Forces:
- Towing of airplane
- Body supercharging.

D2.3 Body Weight and Balance Distribution.

The resisting inertia forces due to the dead weight of the body and its contents plays an important part in the load analysis for the airplane body. When the initial aerodynamic and general layout and arrangement of the airplane is made, it is necessary that a complete weight and balance estimate of the airplane be made. This estimate is usually made by an engineer from the weight control section of the engineering department who has had experience in estimating the weight and distribution of airplane units. This estimate which is presented in report from gives the weights and (c.g.) locations of all major airplane

units or installations as well as for many of the minor units which make up these major airplane assemblies or installations. This weight and balance report forms the basis for the dead weight inertia load analysis which forms an important part in the load analysis of the airplane body. The use of this weight and balance estimate will be illustrated in the example problem to follow later.

D2.4 Load Analysis. Unit Analysis.

Due to the many design conditions such as those listed in Art. D2.2, the general procedure in the load analysis of an airplane body is to base it on a series of unit analyses. The loads for any particular design condition then follows as a certain combination of the unit results with the proper multiplying factors. A simplified example problem follows which illustrates this unit method of approach.

D2.5 Example Problem on Applied Loads on Fuselage.

To illustrate the general procedure in calculating the design shears and moments on the airplane body, the calculations for the airplane of Example Problem 1 in Chapter D1 will be carried out. (Refer to Fig. D1.9, Table D1.1 and the general flight specifications as given in Art. D1.13.

Solution:

Weight and Balance of Body Items:

Table D1.1 of Chapter D1 gives the weight and balance for the complete airplane. Table D2.1 gives the weight and balance calculations for all items attached to fuselage or carried in the fuselage, except the wing and the units attached to the wing or enclosed in the wing as the landing gear and fuel.

TABLE D2.1

WEIGHT AND BALANCE OF AIRPLANE LESS WING GROUP AND INSTALLATIONS IN AND ON WING

Ref. Axes: Z equal arm from thrust line. + is up. X is distance from Z Ref. Axis 5" forward of propeller. + is aft.

	Item	Name	Weight w	Horiz. Arm x	Horiz. Mom. wx	Vert. Arm z	Vert. Mom. wz
Wt. empty	1	Powerplant group	1100	19	20900	0	0
	2	Fuselage group	350	113.5	39700	1	350
	4	Tail group	110	287	31550	24	2640
	5	Surface controls	85	127	10800	-14	-1190
	6	Electrical system	130	61	7930	4	520
	8	Tail wheel group	35	306	10700	-10	- 350
	9	Furnishings	220	116	25520	5	1100
	10	Radio	125	181	22600	10	1250
		Weight empty =	2155		169700		4320
Useful load	11	Pilot	200	151	30200	4	800
	12	Student	200	99	19800	4	800
		Gross weight = Σ	2555	Σ	219700	Σ	5920

Empty $\bar{x} = \frac{169700}{2155} = 78.7"$ $\bar{z} = \frac{4320}{2155} = 2.00"$

With useful load $\bar{x} = \frac{219700}{2555} = 86.0"$ $\bar{z} = \frac{5920}{2555} = 2.32"$

Weight Distribution:

In order to obtain a close approximation to the true shears and moments on the fuselage due to the dead weight inertia loads, it is necessary to distribute the weights of the various items as given in Table D2.1. Fig. D2.1 shows a side view of the airplane with the center of gravity locations of the weight items of Table D2.1 indicated by the (+) signs. In the various design conditions, the direction of the weight inertia forces changes, thus it is convenient and customary to resolve the inertia forces into X and Z components. Thus, in Fig. D2.2, the weights as given in Table D2.1 are assumed acting in the Z direction through their (c.g.) locations. The loads as shown would not give a true picture as to the shears and moments along the fuselage, thus these loads should be distributed in a manner which should simulate the axial weight distribution. In most weight and balance reports, the weight items are broken down into considerable more detail than that shown in Table D2.1, which makes the weight distribution more evident. The person making the weight distribution should study the inboard profile drawing of the airplane which shows the general arrangement of all the installations and equipment. Furthermore, he should study the overall structural arrangement as to its possible influence on fuselage weight distribution. The whole process involves considerable common sense if a good approximation to the weight distribution is to be obtained. Fortunately the large dead weight loads, such as the power plant, tails, etc. are definitely located thus small errors in the distribution of the minor distributed weights does not change the overall shears and moments an appreciable amount.

In order to obtain reasonable accuracy, the fuselage or body is divided into a series of stations or sections. In Fig. D2.1, the sections selected are designed as stations which represent the distance from the Z reference axis. The general problem is to distribute the concentrated loads as shown in Fig. D2.2 into an equivalent system acting at the various fuselage station points.

Obviously, if a weight item from Table D2.1, represents a concentrated load such as a pilot, student, radio, etc., the weight can be distributed to adjacent station points inversely as the distance of the weight (c.g.) from these adjacent stations. However, for a weight item such as the fuselage structure (Item 2 of Table D2.1) whose c.g. location causes it to fall between stations 80 and 120 of Fig. D2.2, it would obviously be wrong to distribute this weight only to the two adjacent stations since the weight of 350# is for the entire fuselage. This weight item of 350# should thus be distributed to all station points. The controlling requirement on this distribution is that the moment of the distributed system about the reference axes must equal the moment of the original weight about the same axes. Fig. D2.3 shows how the dead weight of 350# was distributed to the various station points considering the weights to be acting in the Z direction.

Table D2.2 shows the results of this station point weight distribution for the weight items of Table D2.1. The values in the horizontal rows opposite each weight item shows the distribution to the various fuselage stations. The summation of the weights in each vertical column at each station point as given in the third horizontal row from the bottom of the table gives the final station point weight. These weights are shown in Fig. D2.4 for weights acting in the Z direction. The moment of each total station load about the Z axis is given in the second horizontal row from the bottom of Table D2.2. The summation of the moments in this row must equal the total wx moments of Table D2.1 or 219700"#. This check is shown in the last vertical column of Table D2.2.

The distributed system must also be distributed in the Z or vertical direction in such a manner as to have the same resultant c.g. location as the original weight system which is illustrated in Fig. D2.5. Fig. D2.6 illustrates how the fuselage weight distributed system as shown in Fig. D2.3 is distributed in the vertical direction at the various station points so that the moment of this system about the X axis is equal to that of the original fuselage weight of 350#. For convenience, these distributed fuselage weights can be transferred to the X axis plus a moment as shown in Fig. D2.7.

Table D2.2 shows the vertical distribution of the various items at the various station points. The bottom horizontal row gives the moment about the X axes of the loads at each station point, which equals the individual loads times their Z distances. The summation of the values in this horizontal row must equal the total wz moment of Table D2.1. This check is shown at the bottom of the last vertical column. Fig. D2.8 shows the results as given in Table D2.2 for the weight distribution in the X direction.

D2.6 Unit Analysis for Fuselage Shears and Moments.

Since there are many flight and landing conditions, considerable time can be saved if a unit analysis is made for the fuselage shears, axial and bending forces. The design values in general then follow as a summation of the values in the unit analysis times a proper multiplication factor.

The loads on the fuselage in general consists of tail loads, engine loads, wing reactions, landing gear reactions if attached to fuselage and inertia forces due to the airplane acceleration which may be due to both translational and angular acceleration of the airplane. For simplicity, these loads can be resolved into components parallel to the Z and X axes.

To illustrate the unit analysis procedure, a unit analysis for our example problem will be carried out for the following unit conditions:

(1) Unit acceleration or load factor in Z direction.

(2) Unit acceleration or load factor in X direction.

(3) Unit tail load normal to X axis.

Unit analyses are alse usually carried out for engine thrust and engine torque, side load on tail and angular acceleration, but to keep the example calculations from becoming too lengthy only the above 3 unit conditions will be carried out in detail. The others will be discussed in detail in later paragraphs.

Solution for Unit Load Factor in Z Direction.

Fig. D2.8a shows the dead weight loads acting in the Z direction as taken from Table D2.2 or Fig. D2.4. The wing is attached to the fuselage at stations 73 and 116 as shown on Fig. D2.8a. The fittings at these points are assumed as designed to cause all the drag or reaction in the X direction to be taken off entirely at the front fitting on station 73.

To place the fuselage in equilibrium, the wing reaction will be calculated:

$$\Sigma F_X = 0,\ R_H + 0 = 0,\ \text{hence } R_H = 0$$

$$\Sigma M_{\text{station } 0} = 219700 - 116\ R_R - 73\ R_F = 0 \quad -(A)$$

(Note: 219700 from Table D2.1)

TABLE D2.2
PANEL POINT WEIGHT DISTRIBUTION
(Monocoque Type of Fuselage)

Item No.	Name	Wt. W	Station No. = distance x from Ref. o Axis: 11 w	11 z	50 w	50 z	80 w	80 z	120 w	120 z	170 w	170 z	200 w	200 z	230 w	230 z	280 w	280 z	290 w	290 z	315 w	315 z	
1	Powerplant group	1100	874	0	226	0																	1100
2	Fuselage group	350	19	1	80	-4	78	-3	85	8	82	6	30	1	10	1	10	1	6	0.5			350
3	Tail group	110															11	34	99	34			110
4	Surface controls	88							73	-14	15	-14											88
5	Electrical system	130			82	4	48	4															130
6	Tail wheel group	88																	13	-10	28	-10	88
7	Furnishings	350					78	5	100	5	44	5											350
8	Radio	135									78	10	44	10									135
9	Pilot	200							76	4	124	4											200
10	Student	200					105	4	95	4													200
	Total W	3555	893	.02	388	.02	307	2.47	409	1.67	311	5.3	76	6.48	10	1.0	21	1396	118		22	-10	3555
	Horizontal Moment = Σwx =		98230		19800		24580		49100		52800		10200		2300		5460		24200	15.1	6930		219700
	Vertical Moment = Σwz =		19		8		759		682		1650		480		10		374		2249		-250		5630

x = distance of station from a reference axis which is 8" forward of propeller.
z = distance above or below thrust line or X axis.

WEIGHT DISTRIBUTION TO FUSELAGE STATIONS

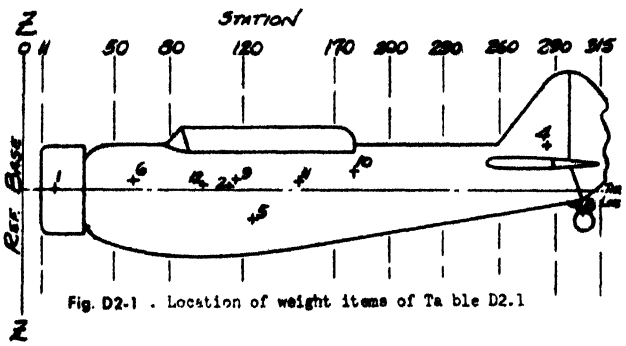


Fig. D2-1 . Location of weight items of Ta ble D2.1

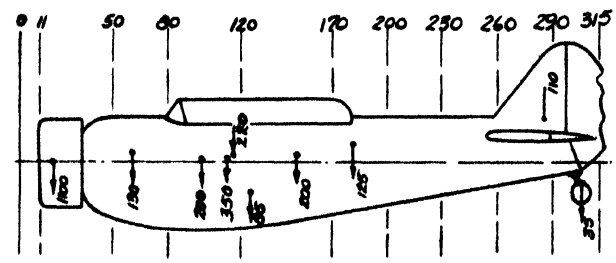


Fig. D2-2 Weight items of Table D2.1 acting in Z direction.

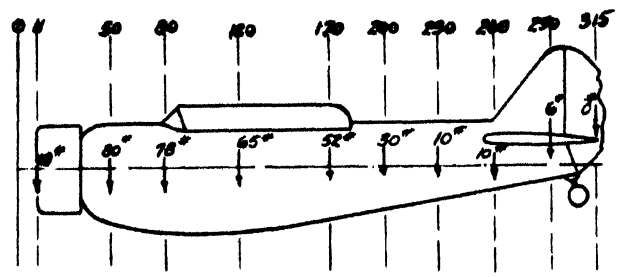


Fig. D2-3 Results of fuselage weight distribution to stations.

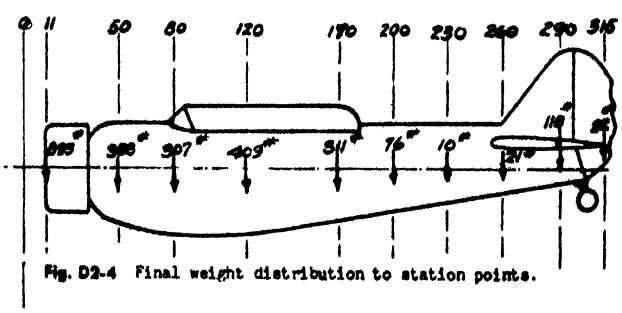


Fig. D2-4 Final weight distribution to station points.

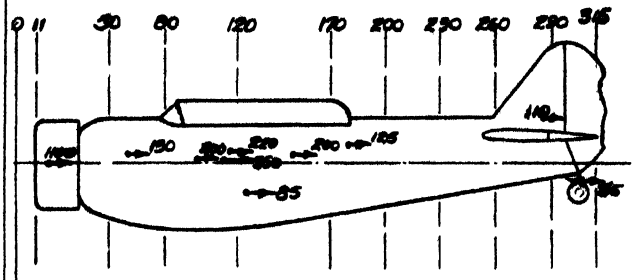


Fig. D2-5 Weight items from Table D2.1 acting in X direction.

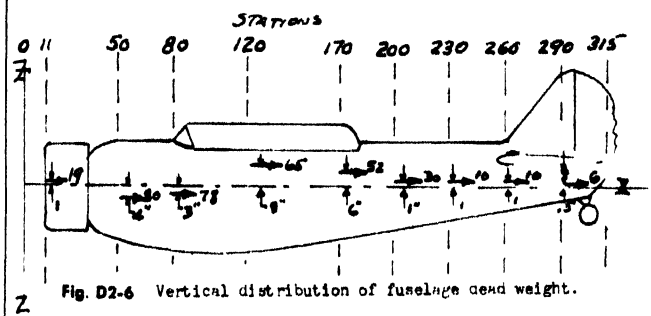


Fig. D2-6 Vertical distribution of fuselage dead weight.

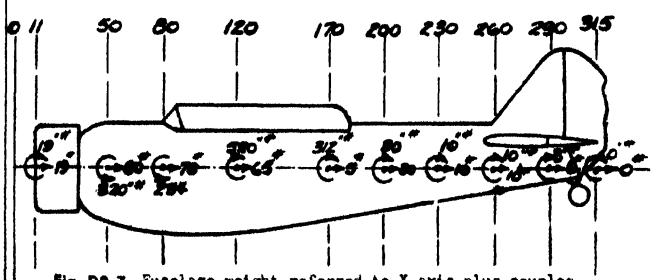


Fig. D2-7 Fuselage weight referred to X axis plus couples.

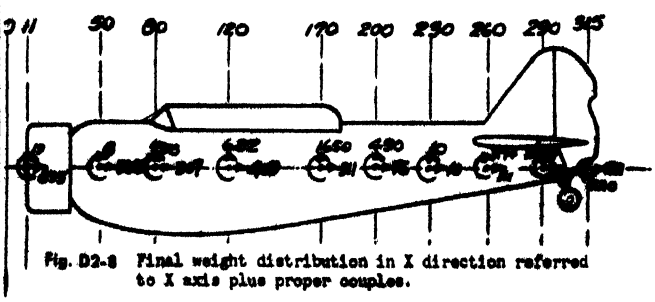


Fig. D2-8 Final weight distribution in X direction referred to X axis plus proper couples.

$\Sigma F_Z = -2555 + R_F + R_R = 0$ - - - - - - - - - -(B)

Solving equations (A) and (B) for R_F and R_R:

$R_F = 1780\#$, $R_R = 775\#$

Table D2.3 gives the calculations for the fuselage shears and bending moments at the various station points.

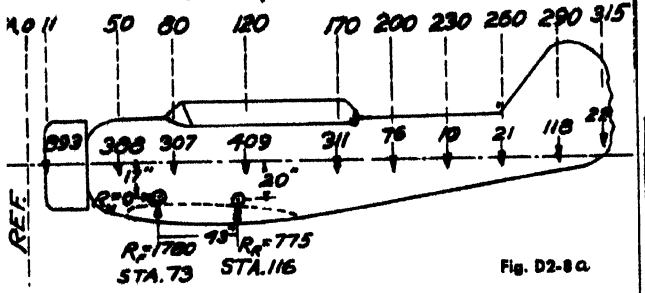


Fig. D2-8a

TABLE D2.3
FUSELAGE SHEARS AND MOMENTS FOR ONE LOAD FACTOR IN Z DIRECTION
(Dead Weight Acting Down)

1 Sta. No.	2 Load or Reaction w	3 V=shear = Σ w (lbs.)	4 Δx = Dist. between stations	5 $\Delta M = V\Delta x$	6 Moment $M = \Sigma \Delta M$ (in. lbs.)
315 +	0	0			
−	- 22	22	25	0	0
290 +	0	22			
−	-118	140	30	-550	-550
260 +	0	140			
−	- 21	161	30	-4200	-4750
230 +	0	161			
−	- 10	171	30	-4830	-9580
200 +	0	171			
−	- 76	247	30	-5130	-14710
170 +	0	247			
−	-311	558	50	-7410	-22120
120 +	0	558			
−	-409	967	4	-27900	-50020
116 +	0	967			
−	775	192	36	-3868	-53888
80 +	0	192			
−	-307	499	7	-6912	-60800
73 +	0	499			
−	1780	-1281	23	-3493	-64290
50 +	388	-1281			
−	0	- 893	39	-29463	-34827
11 +	893	- 893			
−	0	0		34827	0

(3) Up on left and down on right side of a section is positive shear.
(6) Tension in upper fuselage portion is negative bending moment.
(1) + refers to aft side of station.
- refers to forward side of station.

Solution for Unit Load Factor in X Direction.

Fig. D2.9 shows the panel point dead weight distribution for loads acting in the X direction and aft, as taken from Table D2.2 or Fig. D2.8. To place the fuselage in equilibrium the wing reactions at points (A) and (B) will be calculated.

$\Sigma F_X = 2555 - R_H = 0$, hence $R_H = 2555\#$ (forward)

Take moments about point (A)

$\Sigma M_A = 2555 \times 17 + 5920 - 43\ R_R = 0$, hence $R_R = 1147.8$ (up)

(5920 equals the sum of the couples from Table D2.2).

$\Sigma F_Z = 1147.8 - R_F = 0$, hence $R_F = 1147.8\#$ (down)

Table D2.4 gives the calculations for the shears, moments and axial loads for the loading of Fig. D2.9.

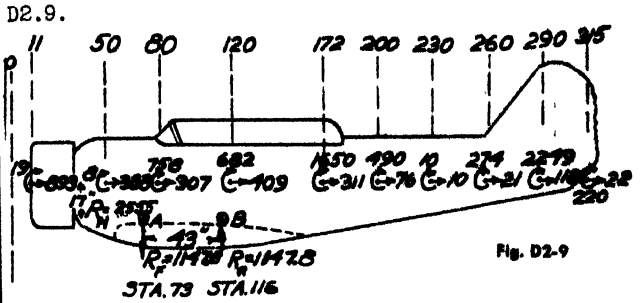


Fig. D2-9

TABLE D2.4
FUSELAGE SHEARS, MOMENTS & AXIAL LOADS FOR ONE LOAD FACTOR IN X DIRECTION
Inertia Loads Acting Aft

1 Sta.	2 W_X = load in X Dir.	3 W_Z = load in Z Dir.	4 $P_X = \Sigma W_X$ = Axial Load	5 $V = \Sigma W_Z$ = Shear	6 ΔM_1 = Couple Moment	7 ΔX = Dist. between Station	8 ΔM_2 = V_X	9 $M = \Sigma \Delta M_1 + \Sigma \Delta M_2$
315 +	0		0		0			0
−	22	0	22	0	220	25	0	220
290 +	0		22		0			220
−	118	0	140	0	-2949	30	0	-2029
260 +	0		140		0			-2029
−	21	0	161	0	- 274	30	0	-2303
230 +	0		161		0			-2303
−	10	0	171	0	- 10	30	0	-2313
200 +	0		171		0			-2313
−	76	0	247	0	- 490	30	0	-2803
170 +	0		247		0			-2803
−	311	0	558	0	-1650	50	0	-4453
120 +	0		558		0			-4453
−	409	0	967	0	- 682	4	0	-5135
116 +	0	0	967				0	-5135
−	0	1147.8	967	-1147.8	0	36	41320	36185
80 +	0	0	967	-1147.8			0	36185
−	307	0	1274	-1147.8	- 758	7	8035	43462
73 +	0	0	1274	-1147.8	0		0	43462
−	2555	-1147.8	-1281	0	-43435*	23	0	27
50 +	388	00	-1281	0	8		0	27
−	0		- 893		0	39		19
11 +	893	0	- 893	0	19		0	19
−	0		0		0			0

* = 17 x (2555) = 43435
+ refers to aft side of station.
Col. 1 - refers to forward side of station.
P_X is plus for tension in fuselage.

Solution for Unit Horizontal Tail Load.

The fuselage shears and moments will be computed for a unit tail load of 100 lb. on the tail acting in the Z direction, with balancing reactions at the wing attachment points. The center of pressure on the horizontal tail is at station 277.5. Fig. D2.10 shows the fuselage loading. To find wing reactions at (A) and (B):

$\Sigma M_A = 100 \times (277.5 - 73) - 43\ R_R = 0$, hence $R_R =$ 475.6# (up)

$\Sigma F_Z = -100 + 475.6 - R_F = 0$, hence $R_F = 375.6\#$ (down)

Table D2.5 gives the detailed calculations for the shears and moments at the various stations points.

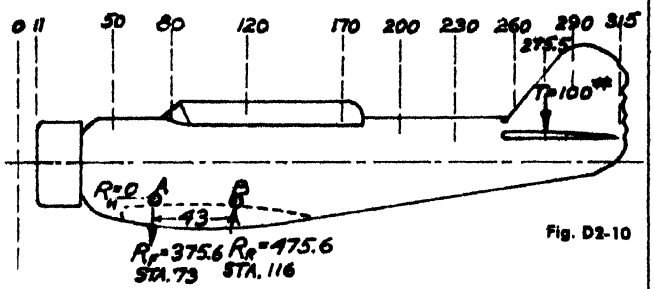


Fig. D2-10

TABLE D2.5

FUSELAGE SHEARS & MOMENTS FOR UNIT HORIZONTAL TAIL LOAD IN Z DIRECTION
(Load Acting Down)

1 Sta.	2 Load or Reaction w lbs.	3 V = shear = $\sum$ w lbs.	4 Δ X = dist. between stations	5 ΔM = VΔ x	6 Moment M = $\sum \Delta$ M in. lbs.
315 +	0	0			0
-	0	0	25	0	0
290 +	0	0			0
-	0	0	12.5	0	0
272.5 +	0	0			0
-	-100	100	17.5	-1750	-1750
260 +	0	100			-1750
-	0	100	30	-3000	-4750
230 +	0	100			-4750
-	0	100	30	-3000	-7750
200 +	0	100			-7750
-	0	100	30	-3000	-10750
170 +	0	100			-10750
-	0	100	50	-5000	-15750
120 +	0	100			-15750
-	0	100	4	- 400	-16150
116 +	0	100			-16150
-	475.6	-375.6	36	13521	- 2629
80 +	0	-375.6			- 2629
-	0	-375.6	7	2629	0
73 +	0	-375.6			0
-	-375.6	0	23		0
50 +	0	0			0
-	0	0	39		0
11 +	0	0			0
-	0	0			0

Calculations of Applied Fuselage Shears, Moments and Axial Loads.

Using the results of the unit solutions as given in Tables D2.3, 4 and 5, the applied values for flight conditions in general follow as a matter of proportion and addition. To illustrate, the applied fuselage shears, moments and axial loads will be calculated for one of the flight conditions as worked out in detail in Chapter D1.

Flight Condition 1. High Angle of Attack (H.A.A.)

From Page 7 of Chapter D1.

Applied load factor in Z direction = -6.0 (down)

Applied load factor in X direction = (8215 - 2480)/4300 = 1.333 (aft)

Applied tail load = 110# (up)

With the Z and X load factors and the tail load known, Table D2.6 can be filled in as illustrated. In a similar manner the values for the other flight conditions can be found, the difference being a new set of multiplying factors, since the applied loads are different.

TABLE D2.6

APPLIED FUSELAGE SHEARS, MOMENTS & AXIAL LOADS FOR FLIGHT CONDITION 1. (H.A.A.)

1 Sta.	2 V_z for Z Load Factor (lbs.)	3 V_z for X Load Factor (lbs.)	4 V_z for Tail Load	5 App. Shear V_z	6 M for Z Load Factor in.lbs.	7 M for X Load Factor in.lbs.	8 M for Tail Load in.lbs.	9 App. Mom. M in.lbs.	10 Axial Load P_x (lbs.)
315 +	0	0	0	0	0	0	0	0	0
-	132	0	0	132	0	284	0	0	29.3
290 +	132	0	0	132	-3300	284	0	-3016	29.3
-	840	0	0	840	-21000	-2710	0	-23710	186.8
260 +	840	0	0	840	-21000	-2710	1625	-24085	186.8
-	968	0	-110	858	-24200	-3075	1925	-27350	215
230 +	968	0	-110	858	-57480	-3075	5280	-55335	215
-	1026	0	-110	916	-57480	-3280	5280	-55480	228
200 +	1026	0	-110	916	-88360	-3080	8540	-82810	228
-	1482	0	-110	1372	-88360	-3740	8540	-83560	330
170 +	1482	0	-110	1372	-132730	-3740	11830	-124640	330
-	3348	0	-110	3238	-132730	-9681	11830	-130581	745
120 +	3348	0	-110	3238	-300120	-6068	17320	-288868	745
-	5262	0	-110	5152	-300120	-6860	17320	-288860	1290
116 +	5262	0	-110	5152	-323328	-6860	17770	-312408	1290
-	1152	-1530	413	-413	-323328	-6860	17770	-312408	1290
80 +	1152	-1530	413	-413	-364800	48200	2910	-313690	1290
-	2994	-1530	413	1877	-364800	47250	2910	-314640	1700
73 +	2994	-1530	413	1877	-385740	57900	0	-327840	1700
-	7686	0	0	-7686	-385740	38	0	-385704	-1710
50 +	-7686	0	0	-7686	-208842	38	0	-208926	-1710
-	-5358	0	0	-5358	-208842	25	0	-208937	-1190
11 +	-5358	0	0	-5358	0	25	0	25	-1190
-	0	0	0	0	0	0	0	0	0

NOTES: (Moments & axial loads are referred to the thrust line)

Col. 2 - 6 x values in column 3 of Table D2.3.
Col. 3 - 1.333 x values in column 5 of Table D2.4.
Col. 4 - -1.10 x values in column 3 of Table D2.5.
Col. 5 - column (1) + column (2) + column (3).
Col. 6 - 6 x values in column 6 of Table D2.3.
Col. 7 - 1.333 x values in column 9 of Table D2.4.
Col. 8 - 1.10 x values in column 6 of Table D2.5.
Col. 9 - columns (6) + (7) + (8).
Col. 10 - 1.333 x values in column (4) of Table D2.4.

D2.7 Example of Fuselage Shears and Moments for Landing Conditions.

Fig. D2.10 a illustrates the airplane in a level landing condition. The ground reaction is assumed to pass the center of landing gear wheel and c.g. of airplane. The fuselage shears, moments and axial loads are required when the vertical ultimate load factor is 7. (gross weight = 4300#).

Solution:

The vertical or Z component of the ground reaction R is specified as 7 load factors which equals 7 x 4300 = 30100#. One half of this is acting on each wheel.

The horizontal or X component of R is 30100 tan 23° = 425 x 30100 = 12800# and acting aft.

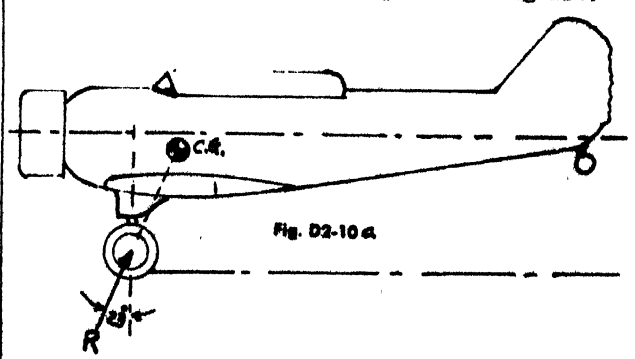


Fig. D2-10 a

The horizontal load factor on airplane equals 12800/4300 = 2.98.

The resistance to these X and Z components of the ground reaction R is provided by the inertia forces of the airplane in the X and Z directionss

Tables D2.3 and D2.4 show the fuselage shears, moments and axial loads for inertia loads due to one load factor in the Z and X directions respectively. Thus to obtain the fuselage forces for this given landing condition, it is only necessary to multiply the values in these two tables by the proper factor and add the results.

Thus fuselage forces due to vertical load factor of 7 would equal 7 times the values in columns (3) of Table D2.3 to obtain shear and 7 times column 6 to obtain bending moment.

Likewise the forces due to the 2.98 load factor in X direction would equal (-2.98) times the values in columns (4), (5) and (9) of Table D2.4 to obtain axial loads, shears and bending moments respectively.

The final or true forces would be the algebraic sum of these results.

Landing with Angular Acceleration

In a level landing condition, it is sometimes specified that the horizontal component of the ground reaction must be a certain proportion of the vertical component, which causes the line of action of the ground reaction R in Fig. D2.10a to not pass thru the c.g. of the airplane, which creates an external pitching moment on the airplane. This moment is usually balanced the inertia forces due to the angular acceleration produced by the unbalanced moment about the c.g. The shears and moments on the fuselage due to this external moment could be found as explained in Art. D2.9.

D2.8 Inertia Loads Due to Angular Acceleration.

In some of the flying conditions, it is sometimes specified that the airplane must be subjected to an angular acceleration as well as translational acceleration. This angular acceleration of the airplane produces inertia forces which must be calculated if the airplane is to be treated as a body in static equilibrium. In some cases, a tail loads due to a gust on the tail is specified which produces a moment about the airplane c.g. which produces angular acceleration of the airplane. In certain landing conditions, the ground forces due not pass through the airplane c.g. thus producing a moment about the c.g. which for stress analysis purposes is balanced by inertia forces.

Moment of Inertia of Airplane

The calculation of the moment of inertia of an airplane about the center of gravity axes was explained on page A3.5 of Chapter A3. A detailed example solution was given in detail in Table 6A of Chapter A3. The general equations for the moments of inertia of the airplane about the reference axes are:

$$I_y = \Sigma\, wx^2 + \Sigma\, wz^2 + \Sigma\, \Delta\, I_y$$

$$I_x = \Sigma\, wy^2 + \Sigma\, wz^2 + \Sigma\, \Delta\, I_x$$

$$I_z = \Sigma\, wy^2 + \Sigma\, wx^2 + \Sigma\, \Delta\, I_z$$

The last term in each of the above equations represents the moment of inertia of each weight item about its own centroidal axes parallel to the reference axes.

D2.9 Solution for Inertia Loads Due to Unit 100,000 In. Lbs. Pitching Moment.

To illustrate the general procedure of determining the balancing inertia loads when the airplane is subjected to an unbalanced moment about the c.g., an analysis will be made for a unit 100,000 in. lb. moment. Table D2.7 gives the necessary calculations.

From kinetics:

Pitching angular acceleration $\alpha = \frac{M_y}{I_y} g$

(rad/sec.^{2})

where

M_y = unbalanced external pitching moment about c.g. of airplane.

I_y = pitching moment of inertia of airplane about airplane c.g.

The tangential inertia force F for a mass w/g due to an angular acceleration α equals,

$$F = \frac{w}{g} r\alpha \text{ , but } \alpha = \frac{M_y}{I_y} g$$

hence

$F = \frac{M_y}{I_y} w\, r$, where r is the distance from the weight w to the airplane c.g.

It is convenient to treat the inertia force F as resolved into two components F_x and F_z

hence

$$F_z = \frac{M_y}{I_y} w\, x_c \quad \text{----------(1)}$$

$$F_x = \frac{M_y}{I_y} w\, z_c \quad \text{----------(2)}$$

From Table D2.7, $I_y = 16097600$

M_y was assumed as 100,000

hence

$$F_z = \frac{100000}{16097600} w\, x_c = .00621\, w\, x_c$$

$$F_x = .00621\, w\, z_c$$

where z_c and x_c are the z and x distances of the

weight w to the airplane c.g.

Columns No. 9 and 10 of Table D2.7 gives the values of these inertia components. Fig. D2.11 shows these inertia loads applied to the fuselage. The reactions at wing attachment points should be computed and then a table of fuselage shears, moments and axial loads should be made up. This unit table could then be used for all conditions involving angular acceleration of the airplane.

It should be realized that the inertia resisting loads in Table D2.7 are only approximately, since the moment of inertia neglects the centroidal moment of inertia of the big items, such as the power plant, wing, etc. The example is only for the purpose of illustrating the general procedure of determining the inertia resisting loads due to angular acceleration. The same general procedure can be followed in considering unbalanced external moments about the Z and X axes, commonly referred to as yawing and rolling moments.

TABLE D2.7

BALANCING INERTIA FORCES FOR UNIT 100,000 IN.LB. MOMENT

ABOUT Y AXIS THROUGH AIRPLANE C.G. (PITCHING MOMENT)

1	2	3	4	5	6	7	8	9	10
Fuselage Panel Sta. No.	Sta. Wt. w	Arm Z	Arm X	Arm Z_c	Arm X_c	$x_c^2+z_c^2$	$I_y = w(Z_c^2+X_c^2)$	Inert. Force F_z	Inert. Force F_x
11	893	.02	11	9.42	-76.5	5949	5300000	-426	-52.1
50	388	.02	50	9.42	-37.5	1494	580000	-90.6	-22.6
80	307	2.47	80	11.87	- 7.5	197	60500	-14.3	-22.6
120	409	1.47	120	11.07	32.5	1182	484000	82.5	-28.2
170	311	5.30	170	14.70	82.5	7016	2180000	159.0	-24.4
200	76	6.45	200	15.85	112.50	12950	985000	53.2	- 7.5
230	10	1.00	230	10.40	142.50	20460	204600	8.9	- 0.6
260	21	13.06	260	22.48	172.50	30270	635900	22.5	- 2.9
290	118	10.10	290	28.50	202.50	31085	3670000	146.3	-20.9
315	22	-10.0	315	- 0.6	227.50	51800	1140000	31.2	- 0.1
Wing	750	-18	97	- 8.6	9.50	164	123000	44.3	40.2
Front Chassis	235	-52	70	-42.6	-17.50	2120	498000	-25.6	62.3
Fuel	760	-27	89	-17.6	1.50	312	237600	7.1	83.2
						I_y =	18097600		

Columns (2), (3), & (4) Taken from Table D1.1 of Chapter D1.
Column (5) $Z_c = Z - 9.4$ { See Table D1.1 for c.g. location
Column (6) $X_c = X - 87.5$
Column (9) $F_z = .00621\ wz_c$
Column (10) $F = .00621\ wz_c$

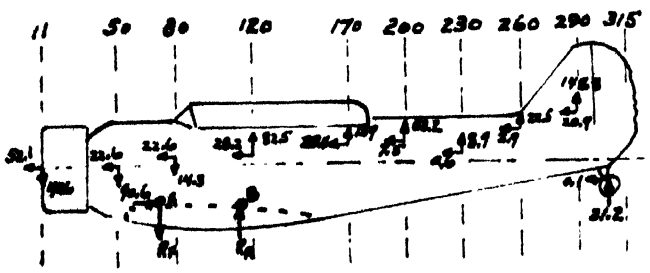


Fig. D2-11

D2.10 General Procedure for Trussed Type of Fuselage Construction.

For many airplanes a welded tubular truss structure is used instead of the semi-monocoque type of structure. Instead of finding shears, bending moments and axial loads on the body as a whole as is done with the shell type of fuselage, it is conventional practice to distribute all loads to the truss panel points and then solve for the axial loads in the trussed structure by the usual graphical stress polygen as explained in Chapter A2. The general procedure of distributing the loads for a truss type of fuselage can be explained best by carrying truss type of fuselage through a simplified example problem. The same airplane as used in previous example will be used. (Refer to Table D2.1)

Fig. D2.12 shows the side view of a tubular truss which has been adapted to the given airplane. The fuselage proper extends from panel point 1U to 11U. The engine mount structure is designated by the dashed lines in the panel (BU, 1U, BL, 1L). Table D2.8 repeats the items of Table D2.1 with their weights and center of gravity location. The circles adjacent to the item numbers on the truss of Fig. D2.12 show the c.g. locations. The general problem is to distribute these 12 concentrated loads to the truss panel points in a manner which will simulate closely the actual distribution.

Methods of Distributing a Weight to Truss Panel Points.

For atruss with vertical members, a load falling within a truss panel can be proportioned to the four panel joints as follows:

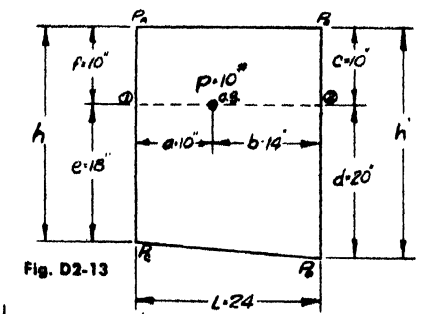
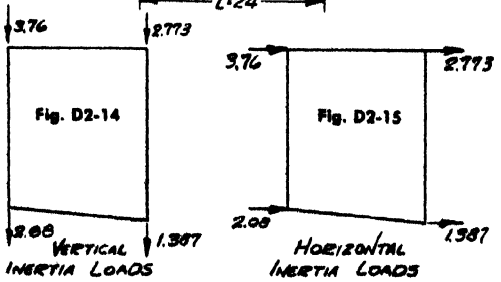


Fig. D2-13



In Fig. D2.13 the weight P = 10# with its center of gravity location is shown. It is desired to replace this 10 lbs. weight by an equivalent system acting at the four joints of the panel. Consider the weights as acting normal to the panel and consider it first as supported by an imaginary beam (1) (2). The reaction at points (1) and (2) are:

$P_1 = Pb/L = 10 \times 14/24 = 5.84\#$

$P_2 = Pa/L = 10 \times 10/24 = 4.16\#$

Loads P_1 and P_2 are now considered as loads acting on beams P_A P_C and P_B P_D respectively.

Hence

$P_A = P_1\ e/h = 5.84 \times 18/28 = 3.76\#$

$P_C = P_1\ f/h = 5.84 \times 10/28 = 2.08\#$

$P_B = P_2\ d/h' = 4.16 \times 20/30 = 2.773\#$

$P_D = P_2\ c/h' = 4.16 \times 10/30 = 1.387\#$

Fig. D2.14shows the resulting panel point distribution for inertia loads in the vertical direction and Fig. D2.15 for inertia loads in the horizontal direction.

As a check on the panel point distribution, the algebraic sum of the panel point loads must equal the original load, and the moment of the panel point loads about any two rectangular axes must equal the moment of the original load about these axes. Convenient axes would be those through the (c.g.) of the original weight which requires that the moments of the panel point loads must then equal zero.

For a truss panel determined by a triangle as in the conventional Warren type of truss, a weight falling inside of the triangular panel is distributed to the 3 corners of the panel. For example, in Fig. D2.16, the weight P = 10# will be replaced by an equivalent system, acting at the 3 panel joint. First, consider the load P as carried by an imaginary beam resting on points (1) and (2), then,

$P_1 = P\ b/L = 10 \times 8/14 = 5.71\#$

$P_2 = P\ a/L = 10 \times 6/14 = 4.29\#$

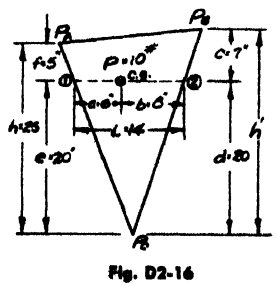


Fig. D2-16

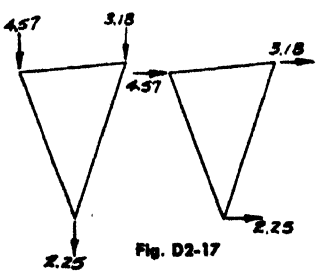


Fig. D2-17

The loads P and P are then reacted at points A and C and B and C respectively. Thus, for load P

$P_A = P_1\ e/h = 5.71 \times 20/25 = 4.57\#$

$P_C = P_1\ f/h = 5.71 \times 5/25 = 1.14\#$

For load P

$P_B = P_2\ d/h' = 4.29 \times 20/27 = 3.18\#$

$P_C = P_2\ c/h' = 4.29 \times 7/27 = 1.11\#$

The total load at C = 1.14 + 1.11 = 2.25#

Fig. D2.17 shows the results for vertical and horizontal inertia forces.

There are various other methods of distributing a load to adjacent panel points. Fig. D2.18 illustrates a graphical variation. The (c.g.) of the weight P is as shown.

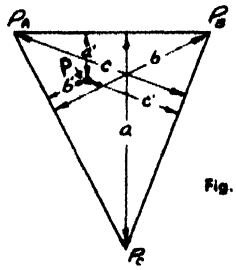


Fig. D2-18

Perpendiculars are dropped from point P to each of the three sides and from each panel joint to the opposite side of the triangle. Then the distributed weights or loads to the panel joints are

$P_A = P\ c'/c$, $P_B = P\ b'/b$, $P_C = P\ a'/a$

Distribution of Weights to Fuselage Truss Panel Points for Example Problem.

Table D2.8 shows the results of the weight distribution to the various truss panel points. This table is typical of the work that is required in the load analysis of the fuselage truss of an actual stress analysis problem. To illustrate how the distributed panel point weights as given in the table were obtained, part of the procedure as used will be given in detail.

Consider Item No. 10 (Radio)

Weight = 125#

c.g. location given by x = 181" and z = 10" (Table D2.8 columns 1, 2, 3).

Fig. D2.19 shows the location of the (c.g.) of the radio weight with respect to the truss triangular panel (5U, 6U, 7D).

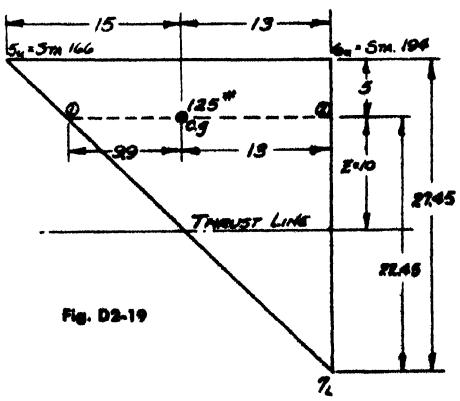


Fig. D2-19

The load is first determined to points (1) and (2).

$P_1 = 125 \times 13/22.9 = 71\#$

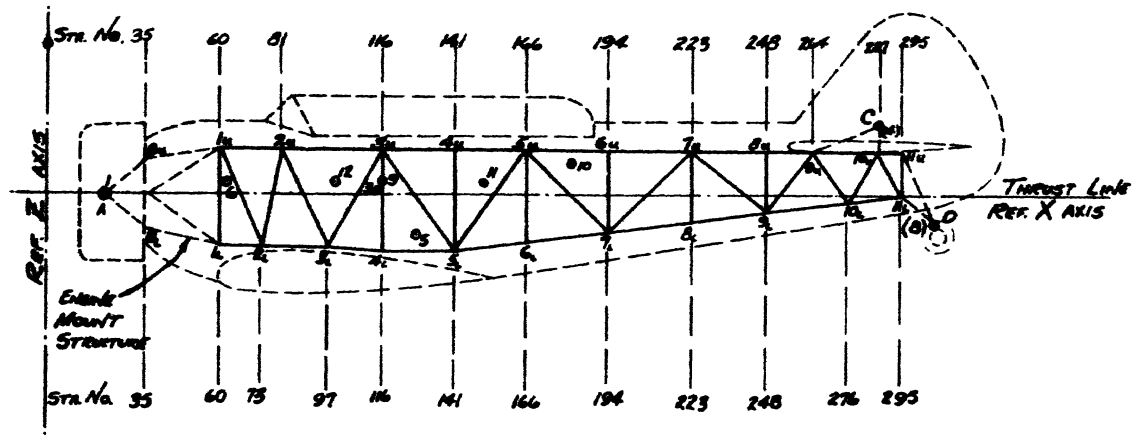


Fig. D2-12

TABLE D2.8

DISTRIBUTION OF WEIGHTS TO FUSELAGE TRUSS PANEL POINTS.

Col. No.	Item No.	Name	1 Panel Points Wt. w	2 arm x	3 z = z₀ − 335	4 A	5 B$_u$	6 B$_l$	7 1$_u$	8 1$_l$	9 2$_l$	10 2$_u$	11 3$_l$	12 3$_u$	13 4$_l$	14 4$_u$	15 5$_l$	16 5$_u$	17 6$_l$	18 6$_u$	19 7$_l$	20 7$_u$	21 8$_l$	22 8$_u$	23 9$_l$	24 9$_u$	25 10$_l$	26 10$_u$	27 11$_l$	28 11$_u$	29 C	30 D	31 Total
			19	35	35	60	60	75	81	97	116	116	141	141	166	166	194	194	223	223	248	248	264	276	287	295	287		287	295			
			0	13	13	15	17	17	15	17	15	19	15	19	15	15.9	15	13.45	15	8.88	15	5.8	15	2.98	19	0	15	24	10				
1	1	Power pl. gr.	1110	19	0	1109																									1109		
2	2	Fuselage gr.	1000	115.5	0		43.69	21.69	49.16	33.6	11.6	21.6	28.6	22.34	8.89	16.74	16.64	13.74	14.46	11.04	11.86	7.76	10.24	2.66	8.68	5.33	5.91	2.25	1.46				200
3	3	Fuel gr.	1100	287	24																									110		110	
4	4	Engine Unit	1100	287	24						12.4	1.8	18.3	1.1	8.9	3.1	26.4	0.8	7.2			0.75	1.25			0.43	0.17	2.4					85
5	5	Misc. Equ.	150	61	6				88.3	34.7	16.0																					139	
6	6	Fuel Sy.	35	288	19																										35	35	
7	7	Furnishings	200	116	5							41.28	41.0	88.46		27.34	26.34	17.78														200	
8	10	Cargo	130	185	10													88.1		44.3	28.7											130	
9	11	Pilot	200	115	4											81.2	38.8	51.5	28.5													200	
10	12	Payload	200	88	4							59.7	48.9	71.4																		200	
11		Total	5235			1109	43.69	21.69	137.46	34.3	24.0	122.58	108.90	181.30	17.79	128.28	109.06	141.92	50.16	55.34	34.66	8.51	11.49	2.66	8.68	5.76	8.08	4.65	1.46	0	110	35	2856
12	Mom. of wt. moments =					36865	1521	735	7520	5285	2680	10978	15300	18710	2852	18100	15210	23550	8220	10680	6730	1897	2560	800	2155	1620	1678	1335	421	0	31850	10780	219780
13	Mom. of wt. moments =					0	565	-273	1880	-991	-576	1864	-2667	2420	-336	1924	-2055	2125	-798	826	-432	128	-102	40	-50	87	-18	70	0	0	2840	-380	5920

* Includes oil plus tank = 75 lb.
Engine mount structure = 25 lb.

P_a = 125 x 9.9/22.9 = 54#

P_a is now distributed between panel joints 6U and 7L and P_1 between 5U and 7L.

For load P_a

P_{6U} = 54 x 22.45/27.45 = 44.2#

P_{7U} = 54 x 5/27.45 = 9.8#

for load P_1

P_{5U} = 71 x 22.45/27,45 = 58.1#

P_{7U} = 71 x 5/27.45 = 12.9#

Total P_{7L} = 12.9 + 9.8 = 22.7

Figs. a and b show the resulting panel joint loads acting in vertical and horizontal direction.

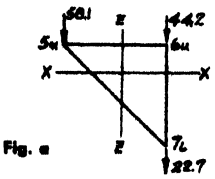


Fig. a

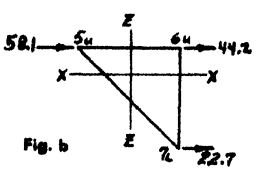


Fig. b

Before entering the results in Table D2.8, the distributed results should be checked.

Summation of panel joint loads = 58.1 + 44.2 + 22.7 = 125#.

The moment of the panel joint loads about X and X axes thru the (c.g.) of the original weight must equal zero.

ΣM_X = (58.1 + 44.2) 5 - 22.7 x 22.45 = 511 - 510 = 1. This is within the accuracy of calculations since loads are carried to only one decimal place).

ΣM_Z = (-58.1 x 15 + (44.2 + 22.7) 13 = -871 + 870 = 0.

The student should always check the distribution of each weight item before entering the results in the composite distribution table such as Table D2.8 in order to avoid the trouble of searching for errors later on.

The three panel point loads of 58.1, 44.2, and 22.7 are entered in Table D2.8 opposite Item No. 10 and under the proper panel joints 5U, 6U and 7L respectively.

In Table D2.8 it should be noticed that the distributed weights at each panel due to the various weight items are added to give the total joint load as shown in horizontal row 11 of the table. These total joint loads are then multiplied by the joint (X) and (Z) arms to give the horizontal and vertical moments as listed in horizontal rows 12 and 13 of the Table. Furthermore, summations are made of all the values in the horizontal rows of the Table which are given in column 31 of the Table. It should be noticed that the total weights total horizontal moments, and total vertical moments of 2555, 219700 and 5920 respectively as given in column 31 equal the values in the original weight and balance diagram for the fuselage as given in Table D2.1.

Distribution of Dead Weight of Fuselage to Truss Panel Points.

The total fuselage group is listed as one weight, namely 350 lbs. This weight must be distributed throughout the length of the fuselage in a manner which should approximate closely the actual weight distribution. This distribution to a great extent is left to the judgment of the computor who should base his judgment on a study of the inboard profile drawing of the airplane. The weight and balance estimate which is available for an actual airplane is given in for greater detail than that of Table D2.1 which will therefore assist him in making a logical panel point weight distribution. This discussion also applies to such items as surface controls and furnishings which are actually scattered over a considerable length of the fuselage and not concentrated at a point as Table D2.1 would seem to indicate.

To illustrate, the general procedure, the fuselage dead weight item No. 2 of 350# will be distributed to the truss panel point. The controlling requirement in the distribution is that the (c.g.) of the distributed system will coincide with the given c.g. for the fuselage weight.

Fig. D2.20 shows the weight distribution that has been selected after several trial and error approaches. The fuselage group according to note on Table D2.8 contains the weight of the oil and oil tank (75#) and engine mount (25#). The cowling and supports between stations B and 1U is assumed to weight 15#, thus making a total of 115#. This is taken as the total weight between these two points with a (c.g.) location of 46" from reference z axes. (See Fig. D2.20). The heavy portion of the fuselage installation is between stations 60 and 166. The fuselage structure is heaviest in this region due to member loads and due to the supports and braces for many of the interior installations in this region. The cockpit enclosure adds weight and it is assumed that the fuselage covering in this region consists of removable metal panels for accessibility to interior installations. The aft portion of the fuselage (station 166-295) is considered as fabric covered. The weight per running inch between stations 60 and 295 is therefore taken as shown in Fig. D2.20.. As mentioned before the usual weight and balance estimate as provided by the weight control section of the engineering department provides more detailed information on the weight breakdown, which together with a study of the inboard profile drawing of the airplane would give the stress man considerable more data on which to base his fuselage weight distribution. This example problem isonly for the purpose of illustrating the general procedure.

The total weight in Fig. D2.20 is 350# and the moment about the reference z axes will equal 39700"#, which is the value as given in Table D2.1 for item No. 2. The next step is to re-

place this running load by an equivalent concentrated system, the forces of which equal the running load between the fuselage panel points. Fig. D2.21 shows the running load divided into segments. The weight of each one of these segments is then computed and its horizontal (c.g.) location. Fig. D2.21 shows the results. The c.g. locations are rapidly calculated by the use of Table 4 of Chapter A3.

This resulting concentrated load system must also have a total moment about the thrust line as the original weight of 350#, which equals 350"# (Table D2.1) since the c.g. is 1" above thrust line. Fig. D2.23 shows the vertical location of the various concentrated forces which will give a total moment of 350 in. lb. about thrust line. These locations must also be based on a logical consideration of the actual conditions.

The single item of 350# has now been replaced by a distributed concentrated equivalent system with a weight distributed between each truss station. These loads can now be distributed to the fuselage panel joints by the general methods previously explained. The results are shown in Table D2.8 in the horizontal row opposite item No. 2. To assist, the student in checking these values, the results of four individual panel distributions are shown in Fig. D2.24. The student should check a few of these panel results in order to obtain a complete understanding of the procedure.

External Applied Groups.

The fuselage proper extends from station 1U to 11U. The center of gravity of the power plant installation is at point (A) of Fig. D2.12 and the c.g. of the weight of the tail wheel group and the tail group is located at points (D) and (C) respectively. One convenient method of handling the dead weight of these external groups is to connect them to the fuselage structure by a phantom truss structure which is considered as part of the fuselage truss in drawing the stress polygon. In the distribution process in Table D2.8, these external groups have been considered as applied at their c.g. and attached to the fuselage by a phantom truss. Another method sometimes used is to transfer these external loads to the fuselage attachment points, which involves replacing the load by a load plus a proper couple.

Fuselage Truss Loadings for Unit Truss Loadings.

As was explained and carried out in the example load calculations on the shell type or semi-monocoque fuselage, it is customary procedure to find the axial stress in the members of the fuselage trusses for several unit conditions. The true or total stresses in any member for a particular flying or landing condition then follow as a matter of a multiplication and addition of the results for the various unit solutions.

Fig. D2.25 shows the truss loading for a unit load factor of 2.0 in the z direction. The panel point truss loads as shown are taken directly from horizontal row number 11 of Table D2.8. These loads are for the complete airplane and since a fuselage truss structure is composed of 2 side trusses only one half of the panel loads in Table D2.8 should be shown on truss for one load factor. Thus, using the total loads as shown on one side truss represents a load factor of two on the airplane. Fig. D2.26 shows the side truss loading for a load factor of two in the X direction. The same loads as shown in Fig. D2.25 are now shown acting in the horizontal direction. Fig. D2.26 shows the truss loading for a unit 100# tail load in the z direction. The reactions for these unit conditions is provided by the wing at the wing attachment points (2L and 4L). These reactions are computed for the various unit conditions, which places the fuselage side truss in equilibrium. A graphical stress polygon is then drawn for each unit condition which gives the axial load in each truss member under each unit loading. The true member axial stress for a particular design flying condition then follows as the result of multiplying the results of each unit condition by a certain factor and adding the results algebraically as was done in Table D2.6 when illustrating the procedure for a shell type fuselage.

For landing conditions, a unit analysis is usually made for a unit load on tail or nose wheel in the Z and X directions. Likewise a unit analysis is usually made for a unit angular acceleration of airplane about c.g. which is balanced by rotational inertia resisting forces. All of these conditions make use of the panel point weight distribution as given in Table D2.8.

TABLE D2.9
WEIGHT & BALANCE

x arms from line 10" forward of propeller, + is aft.
z arms from thrust line, + is up.

Item	Name	Wt. w	Arm x	Moment wx	Arm z	Moment wz
1	Engine group & prop.	1400	32.2	45100	0.34	476
2	Wing group	480	86.0	41300	-13.0	-6240
3	Tail group (less fin)	68	246.1	16730	12.4	843
4	Fin	13	240.5	3881	31.0	372
5	Fuselage	380	115.4	43800	1.4	532
6	Landing gear for *	280	70.0	19600	-18.0	-5040
7	Tail wheel group	35	287	9000	- 4.0	- 140
8	Arresting gear group	20	202	4040	- 6.7	- 134
9	Fuel system	850	79.3	67400	- 3.0	-2550
10	Oil system	90	55.0	4950	10.0	900
11	Radio group	105	153.0	16080	3.0	315
12	Oxygen Equipment	20	150.0	3000	5.0	100
13	Life raft	30	172.0	5160	20.0	600
14	Gun installation	360	95.0	34200	10.7	3860
15	Pilot & furnishings	280	137.0	38400	4.8	1342
16	Miscellaneous furnishings	53	78.5	4080	-1.1	- 57
	TOTALS =	4462		355727		-4821

*Landing gear retracted. $\bar{x}$ = 355727/4462 = 79.6"
z = -4821/4462 = -1.08"

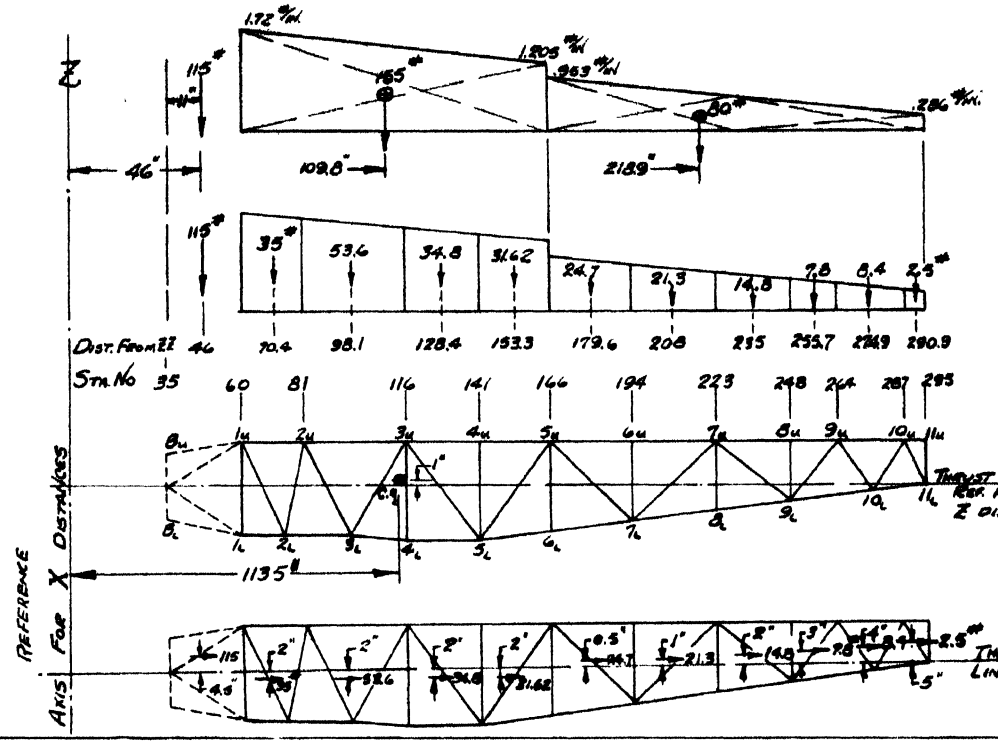


Fig. D2-20

Fig. D2-21

Fig. D2-22

Fig. D2-23

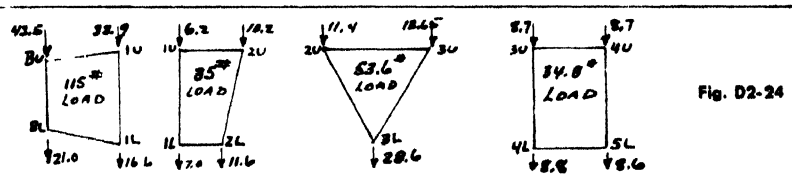


Fig. D2-24

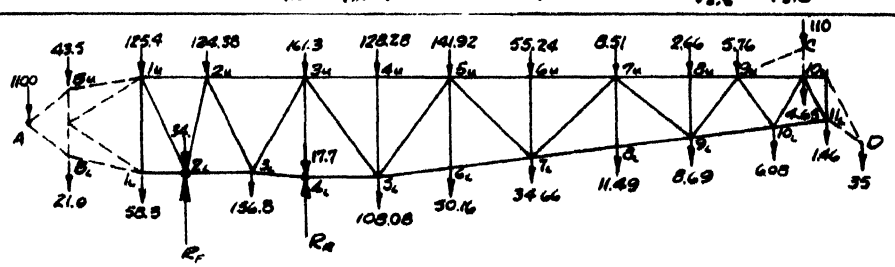


Fig. D2-25

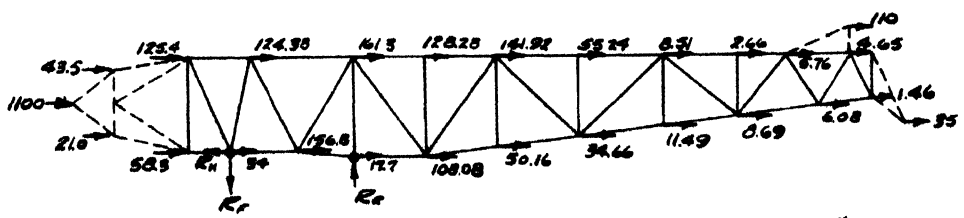


Fig. D2-26

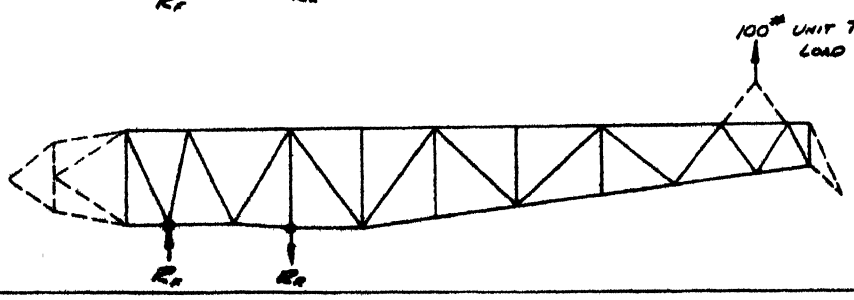


Fig. D2-27

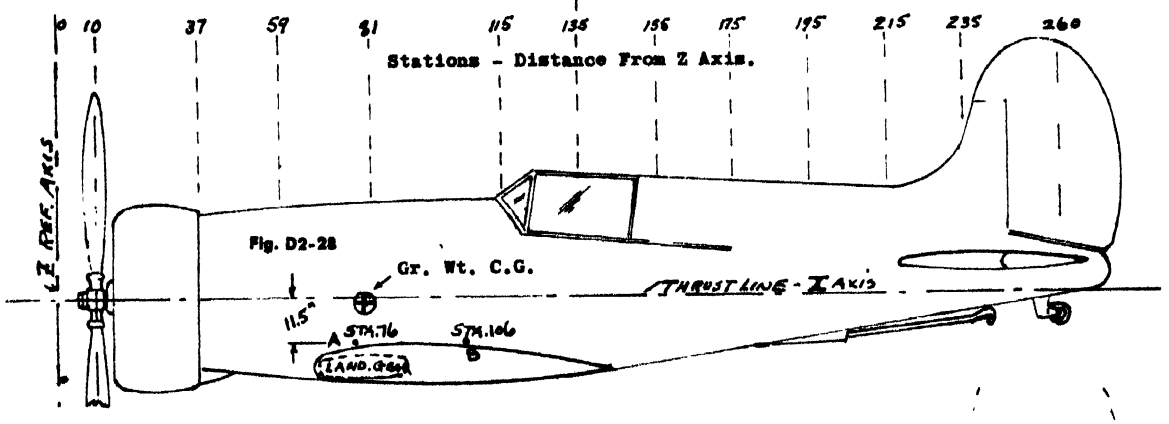
Problem 1. Fig. D2.28 shows the side view of a low wing single seater military airplane. A simplified weight and balance scheduled is given in Table D2.9. Make up a dead weight panel point distribution Table similar to Table D2.2 using the station points as indicated on Fig. D2.28. With airplane supported at points A and B compute shears, moments and axial loads on fuselage for unit load factors in the X and Z directions. Landing gear is located on the wing.

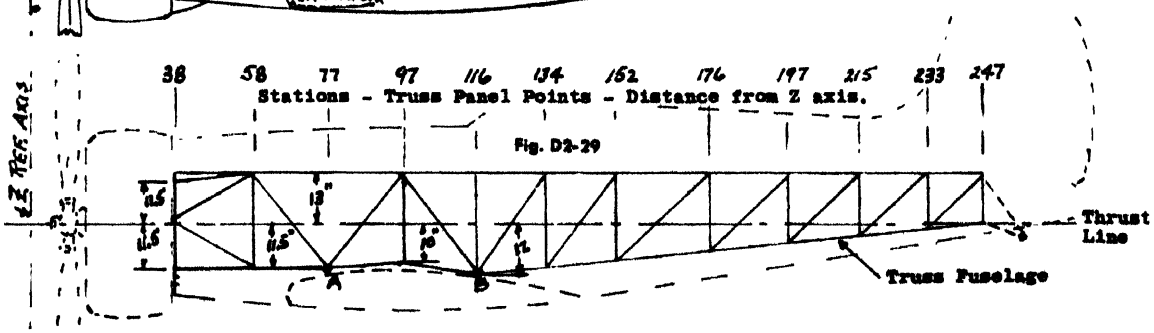
Problem 2. Instead of a semi-monocoque type of fuselage a tubular truss type is used as illustrated in Fig. D2.29. Make up a dead weight truss panel point distribution Table similar to Table D2.8.

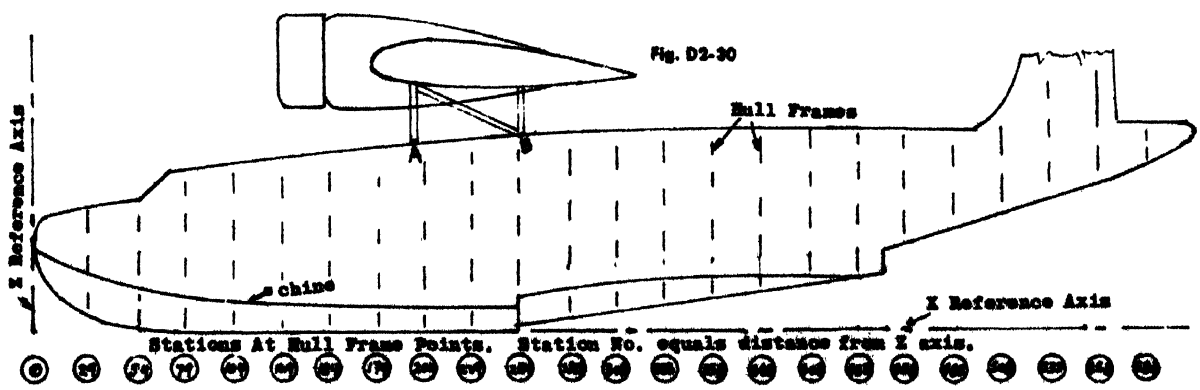
Problem 3. Fig. D2.30 shows the hull of a twin engine boat. A simplified weight and balance schedule for body items only is given in Table D2.10 Make up a dead weight panel point distribution Table using stations at hull frame locations. For flight conditions assuming hull supported at points A and B, compute hull shears, moments and axial loads for dead weight unit load factors in X and Z directions. Refer moments due to X forces to the X reference axis.

TABLE D2.10
WEIGHT & BALANCE OF BODY ITEMS
(See Fig. D2.30 for Ref. Axes)

Item	Name	Wt. w	Arm x	Moment wx	Arm z	Moment wz
1	Hull struct.	2200	210	462000	55	121000
2	Crew (2)	340	76	25840	53	18020
3	Steward (1)	170	110	18700	48	8160
4	Passengers (3)	510	238	121380	49	24930
5	Passengers (3)	510	276	140760	51	26010
6	Passengers (3)	510	316	161160	54	27540
7	Passengers (2)	340	356	121040	56	19040
8	Passengers (2)	340	387	131580	60	20400
9	Passengers (2)	340	432	146880	60	20400
10	Baggage	347	130	45110	50	17350
11	Flooring	185	216	39960	23	4255
12	Furnishings between Station 120 and 400	700	260	18200 0	40	28000
13	Tail group	280	563	157700	145	40600
	TOTALS =	6772#		1754110		435705







PARTIAL LIST OF ANSWERS TO PROBLEMS

CHAPTER A1

ART. A1.13a

(1) P_1 = 2300#; P_2 = 2850#
(2) P_2 = 137#
(3) Load on pulley pin = 318#. Load on x face of bracket = 252#, y face = 194#
(4) R_A = 4850# parallel to AE. R_C = 2600# acting at angle of 30.6° with horizontal.

ART. A1.14a

(1) R_1 = 183#; R_2 = 13#
(2) R (front wheel) = 12768#; on both rear wheels, 13616# each.
(3) R_1 = 44#; R_2 = 206#

ART. A1.15a

(1) BC = -4870#
(3) C_{HOR} = 1050#
(4) D_P = 865#
(5) BC = -810#; AB = -123#
(6) EB = 2570, FC = -7950, Horizontal reaction at D = 2600#

ART. A1.18

(4) R_A = 10; R_B = 90#; R_C = 30; R_D = 70
(5) OC = 1000#
(6) Cable pull = 1200#; Reaction at C = 150#; D = 750#

CHAPTER A2

ART. A2.4a

(1) EB = 692; AB = 1442; AE = -2884
(2) ah = -2630; ab = 1713; bh = 800; c1 = -400; d1 = 525; ij = -3080
(3) BC = -4233; AJ = 2533; EF = 2533; DG = 0; DF = 0
(4) Wires HF, DH, CJ, AK are acting. AC = 10540; CJ = 6710; JH = -5292
(5) d = -600; a = 867 Refer to Page A2.18.
(6) AB = 5000; BO = -2500; DC = -3354; AD = 5640
(7) FC = 3415; BC = -1340; AG = 3700; CD = 1000
(8) AB = 5333; KJ = -3085; KB = -3300
(9) a = 3100; b = 1678; C = -1678
(10) (a) No. No member stresses can be statically computed.
(b) Stable but not statically determinate. Stresses in members EF and ED can be determined statically.
(c) No. Yes.
(11) All members except those in panel abcd can be found by statics. Truss statically indeterminate to first degree or one too many members.

CHAPTER A3

ART. A3.76

(1) I = 66 in.⁴
(2) I_X = .026 in.⁴ I_Z = .018 in.⁴
(3) I = 0.417 in.⁴
(4) I_h = 60.8 in.⁴ I_V = 192 in.⁴

ART. A3.14

(1) Ø = 24°, I_{x_p} = 15.6 in.⁴, I_{z_p} = 2.78 in.⁴
(3) (a) I_{x_p} = 54.9 in.⁴, I_{y_p} = 141 in.⁴
(b) I_{x_p} = 53.4 in.⁴, I_{y_p} = 142.1 in.⁴
(4) I_{x_p} = 74.5 in.⁴, I_{y_p} = 10.0 in.⁴
(5) I_{x_p} = 118 in.⁴, I_{y_p} = 246.2 in.⁴
(6) I_{x_p} = 812 in.⁴, I_{y_p} = 1210 in.⁴

CHAPTER A5

ART. A5.15

(1) f_s = 4270 psi; f_s = 3420 psi
(3) q for large cell = -159.6 lb./in.; q for small cell = -149.6 lb./in.; θ = 0.0118 rad.
(4) q = -156.2 lb./in.; θ = 0.118 rad.
(5) q large cell = 182.7 lb./in.; q middle cell = 180.5; q for curved wall cell = 112.8 lb./in. θ = 0.0151 rad.
(6) q large cell = 181.7 lb./in.; q for curved cell = 113.1; θ = 0.0151 rad.
(6) q = 168.6 lb./in. θ = 0.0161 rad.

CHAPTER A6

ART. A6.8

(1) $V_{max.}$ = +350#; $M_{max.}$ = -20500"#.
(2) $V_{max.}$ = -2720#; $M_{max.}$ = -52000"#
(3) $V_{max.}$ = -720#; $M_{max.}$ = -17600"#
(6) V = .07812 X^2 + 31.25 X; M = 15.62 X^2 + .02604 X^3

CHAPTER A7

ART. A7.18

(1) δ_V = .0246"; δ_h = -.0047"
(2) δ_C = .0104"
(6) δ_C = -0.15 in.
(7) δ_B = 0.483 x 10^{-3} in.
(8) δ_{C_V} = +0.026 in.; δ_{C_H} = +0.077; δ_{D_V} = -0.0094; δ_{D_H} = +0.0184.
(9) δ_{C_H} = 0.0692 in. to right. δ_{B_H} = 0.1277" to right.
(10) δ_{D_V} = 0.505 in. down.
(11) δ_{A_V} = +0.085 in.; δ_{A_H} = 0.0036 in.; δ_{B_V} = 0.062; δ_{B_H} = 0.0079 in.
(13) α_A = -0.00666 Rad.; δ_A = -1.515 in.; α_B = +0.0144 rad.; δ_B = -1.11 in.
(14) δ_A = +0.08 in.; δ_E = +0.07 in.; α_C = -0.002 rad.
(15) α_B = +0.105 rad.; δ_C = +1.03 in.
(16) δ_C = 8550/EI; δ_D = 6075/EI; α_D = 1575/EI
(17) α_A = 24350/EI; δ_A = -414300/EI
(18) M_A = M_B = 750"#
(21) δ_V = -$PR^3\pi/4EI$; δ_H = $PR^3/2EI$; α = PR^2/EI
(22) $\delta_V = -\frac{PR^3}{EI}\left(1+\frac{\pi}{4}\right)$; $\alpha_A = \frac{PR^2}{EI}$
(23) δ_V = .0104"

CHAPTER A8

ART. A8.10

(1) AB = -2500; BC = -2500; CD = 2500; AD = 2500; AC = -3500; BD = 3500
(2) AB = -785; BC = 615: BD = 148
(3) BF = -3290; CE = -930
(4) AB = -749; BC = 526; DB = 276; EB = -80
(5) BD = 3100#
(6) AB = 1093#
(7) BD = 465#; CE = 2170#
(9) AB = 7183#; BC = 7415#

CHAPTER A10

ART. A10.7

(1) $M_{max.}$ = 13500"#; M side level only = 5250"#; y = -1.51"
(3) M = -23400"#
(4) M = -294700"#
(5) M = 15800"#

CHAPTER A11

ART. A11.15

(1) M_B = -2000; M_C = -1614; M_D = 0
(6) M_A = 600; M_B = 900
(7) M_A = 705; M_B = 0
(8) M_A = 0; M_B = 333
(9) M_{BA} = -205"#; M_{BC} = -190; M_{BD} = -145
(14) M_C = -1073"#; R_B = 513#; R_C = +327#
(15) M_A = 1100"#; M_B = 6800; M_C = 7700; M_D = 2900
(16) M_A = 526"#; M_B = 281"#; M_C = 882"#
(17) M_{BC} = -2150 ft.lb.; M_{CB} = -2120 ft.lb.; M_{DC} = -2630 ft.lb.; M_{CF} = -130 ft.lb.
(18) M_{BA} = -1700"#; M_{BC} = -2610"#; M_C = -1000; M_D = 500"#
(19) M_A = -101.1 ft. kips; M_B = -22.7 ft. kips.
(20) (a) 10.8 ft. above A; (b) 11.4 ft. above A; (c) 12.5 ft. above A

ART. A11.19

(2) q_1 = -290; q_2 = -341; q_3 = -204
(3) q_1 = 78.4; q_2 = 103.7;

CHAPTER A12

ART. A12.5

(1) $V_{max.}$ = 405#; $M_{max.}$ = 6480"#; $f_{b_{max.\ comp.}}$ = 516 psi; $f_{s_{max.}}$ = 173 psi
(2) $V_{max.}$ = 11600#; $M_{max.}$ = 1,665,000"#

CHAPTER A13

ART. A13.9

(2) f_B = -15200 psi.
(3) A = -8450 psi; B = -10340 psi; C = -11220; F = 8890 psi.
(4) A = 9930 psi; B = 11800 psi; F = -16020 psi
(5) At point (1) f = -19635 psi; point (7) f = -6440; point (14) f = 9300 psi.

CHAPTER A14

ART. A14.10

(1) Shear center located 0.544" to left of centerline of 2" length side for section in Fig. A14.27 For Fig. A14.29, shear center located 4.50" to left of vertical web. Assumees stringer material concentrated at skin line.
(3) 17.3" below bottom side on vertical symmetrical axis.
(6) 3.94" to left of Y_b axis; 21.2" below X_p axis
(7) q = 17.25"/in.
(8) M_o = 13140"#. Resultant is 224# located 58.7" from point O.
(9) e = 17.8"
(10) e_{x_p} = -7.27"; e_{y_p} = 27.11"

CHAPTER A15

ART. A15.10

(1) Fig. 15.49. q_{ab} = -9.42#/in.; q for curved wall = 1.69#/in.
(2) Fig. 15.51. q_{ab} = -16.85#/in.; q_{bc} = 11.87; q_{ac} = -2.42.
Fig. 15.52. q for vertical web = 24.53#/in. q for lower web = 14.46 and q for curved web = -11.24#/in.
(3) q at upper left hand corner = 33#/in., q at upper right hand corner = -29.5#/in. Shear center located 14.4" to right from left side of box.
(4) q in left side vertical web = 3.41#/in. q for right vertical web = -6.59#/in. The shear center is located at point 6.85" to right of left side of box.
(5) q_{ac} = -13.63#/in.; q_{ab} = 16.37; q_{bc} = -3.63
(6) q_{ab} = 5.64#/in.; q in each curved wall = 2.18#/in.
(7) $q_{aa'}$ = 26.9#/in.; q_{bc} = -13.1; q_{dc} = -12.9#/in. Shear center is 1.2" to left of cc'.
(8) q_{ab} = 17.84; q_{dea} = 30.9; q_{bfc} = -3.55
(9) q_{ab} = 21.48#/in.; q_{bc} = 32.13; q_{dc} = -30.37
(10) q_{ab} = 6.62"/in.; q_{bc} = 0.34; q_{cd} = 80.34; $q_{a'da}$ = -17.70
(11) q_{ab} = -51.2; q_{cd} = 28.6; q_{ef} = 14.2; $q_{ff'}$ = 46.5; $q_{a'oa}$ = -34.0

CHAPTER B2

ART B2.8

(1) P_c = 185#
(2) P_c = 1660#
(3) P_c = 2960#
(4) P = 500#; P = 1000#
(5) Sheet will not buckle. M.S. = .08
(6) M.S. = .16

CHAPTER C2

PAGE C2.17

(3) Top longeron = 1-1/4 - .065
(7a) 3-3/4 - .065; (7b) 4-1/2 - .083; (7c) 3-3/4 - .065
(8) AC = 2-3/4 - .058 24ST. S.L.

CHAPTER C3

ART. C3.11

(1) 1-5/8 - .049 tube.
(3) Far understrength. Check 1-3/8 - .058 for strength
(6) 1-3/4 - .049; M.S. = .12
(7) 1-1/4 - .049; M.S. = .08
(8) 3/4 - .049; M.S. = 3.27; θ = 4.8 degrees
(9) M.S. = .04
(10) M.S. = -.015
(11) M.S. = .22
(12) M.S. = .18

CHAPTER C4

ART. C4.25

(1) Shear out is critical. M.S. = .04 on edge distance.
(2) Bolt shear is critical
(3) Shear out critical. M.S. = 0.29
(6) Lower right hand bolt is critical. Bolt load is 4860#
(11) Either top bolt is critical; tension load on bolt = 2927#, shear load = 1950#
(12) Upper right hand rivet is critical. Resultant load on this rivet is 2065#

INDEX

Aircraft Rivets. C4.2
Aircraft Nuts. C4.12
Air Loads, Applied . . .A2.15
Analysis,Bulkhead. . . .C11.2
Analysis, Frame. C11.1
Analysis, Strength . . .C7.13
Analysis, Stress C7.14
Angle Sections B5.1
Applied Air Loads. . . .A2.15
Area Moments A7.15
Auxiliary Phantom Members. A2.8
Axes, Inclined A3.10
Axes of Symmetry A3.9
Axial Load A11.20

Beam, Cantilever A6.4
Beam,Fixed End Moments. A7.15
Beam, Flange C9.24
Beam Sections. C8.1
Beam, Tapered. C9.20
Beam, Unsymmetrical. . .A15.9
Beam, Web. C9.9
Beams, Cell. C9.12
Beams, Deflection of . . A7.5
A7.13
Beams, Metal C6.1
Beams and Trusses, Deflections of A7.1
Beams, Wood. C8.1
C8.5
Bending. C3.1
Bending and Compression. C3.8
Bending and Torsion. . .C3.10
C3.13
Bending Forces A6.1
Bending Modulus. C3.1
Bending Moment A6.3
Bending Strength C3.6
Bending Stress A13.1
C7.7
C7.10
Bending, Unsymmetrical .A13.1
Bolt Fitting C4.14
Bolts. C4.7
Box Beams, Flange. . . . A15.11
Bulkhead, Analysis . . .C11.2
Bushings C4.13

Cantilever Bar A9.2
Cell Beams C9.12
Cellular Structures. . . C9.1
Center of Gravity, Centroids. A3.1
Centroids, Center of Gravity. A3.1
Charts, Column C2.2
Closed Sections. B5.10
Column Buckling. B1.2
Column Charts. C2.2
Column Curves. C2.2
Column Design. C2.3
Column Failure B1.1
Column Load, Critical. . B1.2
Column Members, Beam . .A10.1
Column Theory. B1.1
Columns. B1.1
C2.15
C8.1
Columns, Long. C2.1
Columns, Long and Short. B1.3
Columns, Short C2.1
Columns with Thin Walls. B5.1
Columns, Wood. C8.12
Combined Loadings. . . . C3.1
Compression, Bending . . C3.8
Compressive Strength, Ultimate B4.1
Compressive Strengths. . B6.1
Conductivity C1.1
Corrugated Shapes. . . .B6.11
Corrugations B6.11
Crippling Stress B5.10
B5.12
Crippling Stresses . . . B5.1
Cross Sections, Column Theory B1.1
Curved Sheet, Flat . . . B4.1
Curves, Column C2.2
Curves, Stress-Modulus . C1.6
Cylindrical Bars, Torsion of A7.9

Deflection, Torsional. .A15.3
Deflections. A5.1
Deflections, Reciprocal.A7.25
Density. C1.1
Design, Column C2.3
Design, Metal Beams. . . C7.1
Displacement, Angular. . A7.3
A7.6

Elastic Weight A9.2
Equilibrium, Principles of A1.1
Equilibrium, Stress. . . A4.5

Factor k C7.15
Failure, Instability . . C2.3
Failure, Loads C3.8
Fitting, Bolt. C4.14
Fittings C8.14
Fittings, Joints C5.1
Fixed End Moments. A11.3
Flange Beam. C9.24
Flat and Curved Sheet. . B4.1
Flexure, Formulas. . . .A12.4

Flow Shear C10.11
Flow Systems A5.3
Force System A1.4
A1.10
Force System, Non-Coplanar A1.10
Frame Analysis C11.1
Frame, Hull. A9.12
Frames A9.9
Frames, Rings and. . . . A9.1
Funicular Polygon. . . . A1.3
Fuselage, Metal Covered.C10.1
Fuselage Reactions . . .A2.13
A2.15
Fuselage Shears. D2.3
D2.6

Gravity, Center of Centroids. A3.1
Glue Stresses. C8.4

Hull Structure C10.1

Inertia, Mass Moments of A3.2
Inertia, Moment of . . . A3.1
D2.7
Inertia, Polar Moment. . A3.1
Instability Failure. . . C2.3
Internal Forces, Redundant. A9.3
Internal Work. A7.22

Joints A2.1
Joints and Fittings. . . C5.1

Lift Load, Beam. A2.15
Linear Deflection Virtual Work A7.8
Load A10.1
Load, Axial. A11.20
Load, Critical Column. . B1.2
Loadings, Combined . . . C3.1
Loadings, Single Span. .A10.2
Loadings, Truss. D2.12
Loads, Failure C3.8
Loads, Wing D1.1
Long Columns C2.1
Longeron C2.11
Lugs, Tension. C4.13

Margins, Safety. C4.1
Material, Web. C9.7
Members, Tension C2.1
C2.3
Metal Beams. C6.1
Metal Beams Design . . . C7.1
Metal Covered Fuselage .C10.1
Method; Distribution, Moment A11.1
Modulus, Bending C3.1
Modulus, Torsional . . . C3.7
Mohr's Circle, Principal Stresses A4.3
Moment Diagram A6.3
Moment Diagrams. A6.2
Moment; Distribution Method A11.1
Moment of Inertia. . . . A3.1
D2.7
Moment, Maximum Bending. A6.3
Moment, Polar Inertia. . A3.1
Moments, Area. A7.15
Moments, Method. A2.2
Moments, Principal of. . A1.2
Multiple-Cell. A5.4

Neutral Axis Location. .A12.1
Nuts, Aircraft C4.12

Operations Table . . . A11.30

Parallel Axis Theorem. . A3.1
A3.9
Polar Moment, Inertia . . A3.1
Polygon, Funicular . . . A1.3
Principal Axes A3.10
Principles of Equilibrium. A1.1
Principles of Moments. . A1.2
Principal Stresses, Mohr's Circle. A4.3
Product of Inertia . . . A3.9

Radius of Gyration . . . A3.1
Reactions, Fuselage. . .A2.13
A2.15
Redundant Internal Forces A9.3
Rings and Frames A9.1
Rivet Spacing. B6.7
Rivets C4.4
C4.5
Rivets, Aircraft C4.2
Rods, Tie. C4.13
Round Tubes. C2.1

Safety Margins C4.1
Section Properties of Areas. A3.2
Sections, Angle. B5.1
Sections, Beam C8.1
Sections, Cell-Closed. . A5.3
Sections, Solid. C2.15
Shaft, Cylindrical . . . A5.1
Shapes, Corrugated . . .B6.11
Shear. A6.1
Shear, Beam. A6.1
Shear Center A14.1
Shear, Flexural. A7.22
Shear Flow A14.1
A15.18
C10.11
Shear Lag. C9.22
Shear Load C7.5
Shear Stresses C6.7
C8.3
Shear, Torsional A5.7
Shear, Web C9.11
Shears A2.3
Shears, Method A2.3
Sheet, Flat and Curved . B4.1
Shears, Fuselage D2.3
D2.6
Shears, Wing D1.18
Short Columns. B1.3
C2.1
Solid Sections C2.15
Spacing, Rivet B6.7
Splices. C4.22
Spot Welding C5.6
Stiffener Strains. . . . B6.8
Stiffeners B6.6
Strain C1.1
Strain Energy. A7.22
Strains, Stiffener . . . B6.8
Strength, Analysis . . .C7.13
Strength, Bending. . . . C3.6
Strength, Compressive. . B4.4
Stress Analysis. C7.14
Stress, Combined Equations. A4.2
Strengths, Compressive . B6.1
Stress, Components of. . A4.3
Stress, Crippling. . . .B5.12
Stress Distribution. . . A5.4
A12.2
Stress Intensities, Varying. A4.5
Stress-Modulus Curves. . C1.6
Stressed-Skin Structures C9.1
Stresses A13.2
C1.1
C7.11
C8.8
Stresses, Bending. . . . C7.7
C7.10
Stresses, Comprehensive. A4.1
Stresses, Crippling. . . B5.1
Stresses, Glue C8.4
Stresses, Principal. . . A4.1
Stresses, Shear. C6.7
C8.3
Stresses, Torsional. . . A5.5
Structures, Cellular . . C9.1
Structure, Hull. C10.1
Structures, Stressed-Skin C9.1
Symbols, Stress. A4.1
Systems, Force A1.4

Tapered Beam C9.20
Tension, Axial A7.22
Tension-Field. C7.1
Tension Lugs C4.13

Tension Members. C2.1
C2.3
Tie Rods C4.13
Torsion, Bending C3.10
C3.13
Torsion Formula. A5.1
Torsional Deflection . . A5.1
A15.3
Torsional Modulus. . . . C3.7
Torsional Moment A5.3
Torsional Stresses . . . A5.2
Truss Deflection A7.16
Truss, Drag. A2.11
Truss Loadings D2.12
Truss Stress A2.1
Trusses, Beams
Deflections of A7.1
Trusses, Deflections of. A7.1
Trusses, Determinate
and Indeterminate. . . A2.1
Trusses, Indeterminate . A8.1
Trusses, Parallel Chord. A2.4
Tubes, Round C2.1

Unsymmetrical Bending. .A13.1

Web Beam C9.9
Web Material C9.7
Web Shear. C9.11
Web Shear Flow A15.18
Web, Tapered A15.20
Weight, Moment A9.2
Welding. C5.1
C5.4
Welding, Spot. C5.6
Wing, Loads. D1.1
Wing Shears. D1.18
Wood Beams C8.1
C8.5
Wood Columns C8.12